MOBILE SATCOM COMES OF AGE

IMSC '95

Proceedings of the fourth International Mobile Satellite Conference 1995

Ottawa, Canada
June 6-8, 1995

Industry Canada
Industrie Canada

CRC
Communications Research Centre
Centre de recherches sur les communications

NASA
National Aeronautics and Space Administration

JPL
Jet Propulsion Laboratory
California Institute of Technology

JPL 95-12
CRC-CP-95-001

IMSC '95

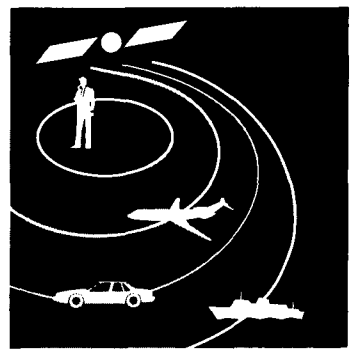

Proceedings of the fourth International Mobile Satellite Conference 1995

Ottawa, Canada June 6-8, 1995

Cataloguing Data

International Mobile Satellite Conference (4th : 1995 : Ottawa, Canada)

Proceedings of the Fourth International Mobile Satellite Conference, IMSC '95, Ottawa, Canada, June 6-8, 1995
Co-sponsored by the Communications Research Centre, Canada
and the Jet Propulsion Laboratory, USA,
compiled by J. R. Rigley and P. Estabrook,
edited by D. H. M. Reekie.

598 pages including appendix

ISBN 0-662-23028-0
Catalogue no C2-264/1995E

1. Artificial satellites in telecommunications-Congresses.
2. Mobile communication systems-Congresses. I. Rigley, J. R. II. Estabrook, P.
III. Communications Research Centre (Canada). IV. Canada. Industry Canada.
V. United States. National Aeronautics and Space Administration.

TK5104 621.38/0422

JPL catalog number: 95-12
CRC catalogue number: CP-95-001

Additional copies of this book can be obtained, subject to availability,
at no charge, as follows:

In Canada send requests to:
Communications Research Centre-VPCS
Re publication: CRC-CP-95-001
3701 Carling Avenue
P.O. Box 11490, Station H
Ottawa, Ontario, Canada
K2H 8S2

In the US and elsewhere, send requests to:
Space Communications Program
Jet Propulsion Laboratory
Re publication: JPL Publication 95-12
4800 Oak Grove Drive, MS 161-260
Pasadena, California, USA 91109

Tel: 818-354-7421
Fax: 818-393-4643

Printed in Canada

Industry Canada / Industrie Canada

CRC Communications Research Centre / Centre de recherches sur les communications

NASA National Aeronautics and Space Administration

JPL Jet Propulsion Laboratory
California Institute of Technology

Proceedings of the fourth

International Mobile Satellite Conference 1995

Ottawa, Canada
June 6-8, 1995

Co-sponsored by the
Communications Research Centre, Canada
and the Jet Propulsion Laboratory, USA

Compiled by:

J. R. Rigley,
Technical Committee Co-Chairman, CRC

P. Estabrook,
Technical Committee Co-Chairman, JPL

Edited by:

D. H. M. Reekie, CRC

IMSC '95 STEERING COMMITTEE

Jack Rigley
Communications
Research Centre

Dr. Polly Estabrook
Jet Propulsion Laboratory

The IMSC '95 Steering Committee wishes to thank the Session and Panel Organizers listed in the final program, who gave considerable time and effort in setting up the detailed structure. The Co-Chairs Bob Huck and Dr. Stephen Townes are thanked for their support and guidance. Special thanks should also go to Dr. William Rafferty, JPL, who was Co-Chair until April 1995. The Organizing Committee are thanked for their hard work to ensure a successful conference.

IMSC '95 ORGANIZING COMMITTEE

The IMSC Organizing Committee shown at an informal working meeting are, left to right, front; *Hélène Lamadeleine*, Golden Planners; *Jack Rigley*, Technical Co-Chair; *Debbie Kemp*, Conference Logistics; *Hugh Reekie*, Conference Proceedings Editor; back *Louise Casavant*, Creative Visual Services; *Beatrice Baker*, Publicity Coordinator; *Phil Ecclestone*, *Amanda Greenhalgh*, Golden Planners, (Exhibits and Registration); *Lynell Wight*, Conference Records Manager; *Debora Morton*, Production Coordinator and *Roberta Gal*, Creative Visual Services. Debora Morton and Golden Planners are contractors, all others are CRC employees.

A MESSAGE FROM THE IMSC '95 CO-CHAIRMEN

Bob Huck
Communications
Research Centre

Dr. Stephen Townes
Jet Propulsion Laboratory

With this our fourth International Mobile Satellite Conference it is interesting to reflect on the evolution of mobile satellite communications since our first IMSC conference in Pasadena in 1988.

The mobile satellite communications industry was still very young in 1988 and most development activity was centered in government sponsored research labs. Mobile services existed for only a relatively few maritime vessels. Seven years later, services to aeronautical and land mobile users are common. More powerful satellites in geostationary orbit and an expanding market, particularly in North America, will soon mean much lower cost terminals, attracting an even greater number of users and a variety of applications not yet foreseen. Today we are pleased to acknowledge the successful launch and deployment of AMSC's first satellite, certainly a milestone in mobile satellite communications history

In 1988, nine year old Inmarsat was just starting to emerge from it's first generation of satellites; it is now on the verge of launching a constellation of third generation satellites and has spun-off an affiliate to create a global satellite-based personal communications system. At our first IMSC conference there was no mention of Inmarsat P, Iridium, Globalstar, Odyssey, Ellipsat or Teledesic, names which now dominate any discussion of mobile satellite communications.

Our theme this year, *Mobile Satcom Comes of Age,* is meant to indicate a level of maturity, but not an end to development. If there is one thing to be learned from our short history, it is that mobile satellite communications will continue to be a fascinating enterprise, one which combines complex scientific challenge with heart-stopping business adventure.

On behalf of both our organizations, NASA/Jet Propulsion Laboratory and Industry Canada's Communications Research Centre, we welcome you to Ottawa and hope you enjoy the exchange of ideas, the camaraderie of your colleagues and the beauty of this city.

Session Index

Modulation, Coding and Multiple Access

1

Session Chairman: **Bob Lyons,** Calian Communications Systems, Canada
Session Organizer: **John Lodge,** Communications Research Centre, Canada

Topic Introduction: Modulation, coding, and multiple access are at the heart of the physical layer design of a mobile satellite system. No single set of choices is optimal for all conceivable transmission scenarios and service offerings; consequently, a broad range of techniques are of interest to mobile satellite system designers.

This session begins with a paper proposing techniques appropriate for low data rate transmission, with possible applications including paging and low capacity packet data. Next are two papers that address the issue of implementing high performance modem equipment, at a low cost. The fourth paper discusses the Globalstar system, with emphasis on multiple access issues. The session wraps up with a paper on the interesting (and sometimes controversial) topic of spread spectrum multiple access for mobile satellite communications.

Low Bitrate System Design in the Presence of Phase Noise

Hans-Christian Haugli
VISTAR TELECOMMUNICATIONS INC.
Suite 1410, 427 Laurier Avenue West
Ottawa, K1G 3J4, Ontario, Canada
Phone: + 1 613 230 4969
E-mail: haugli@vistar.ca

1. ABSTRACT

There are a number of interesting mobile satellite applications that require the transmission of short packets of data. In the design of such systems one of the challenges is often to minimize the transmitted power to reduce cost, which implies using power efficient low bitrate modulation and coding methods.

PSK systems can be very power efficient, but at low bitrates the carrier recovery circuits can be sensitive to oscillator phase noise.

In this paper we address the problem of determining the lowest bitrate that can be supported using PSK for a given level of system phase noise. The classical formulas are reviewed, and a method is derived to calculate the minimum C/N_0 required to recover the carrier for CW, BPSK and QPSK signals for a given phase noise level.

2. THE CLASSICAL FORMULAS

In a well designed demodulator, the acquisition threshold is usually determined by the carrier recovery algorithm. Here a model based on a Phase Locked Loop (PLL) as shown in Figure 1. is assumed This model has been extensively studied in the past and the basic formulas are fairly simple. In some cases it is possible to improve the performance using sophisticated algorithms, and the bounds calculated here are conservative and provides the system designer with some margin.

Gardner's book [1] is a classical reference on PLLs and is the main source of the formulas used in this paper.

2.1 Noise intermodulation loss

The input PSK signal is filtered using a matched filter and passed through a non-linearity to generate a discrete spectral line at N times the input frequency which the PLL locks to. The effective carrier to noise density (C/N_0) at the PLL input is reduced by noise intermodulation products also generated by the non-linearity. The net C/N_0 is given by:

$$C/N_{0pll}=CN_0 / N^2L_N \quad \text{(i)}$$

CN_0 is the signal input C/N_0

N is the order of the non-linearity
N=1 for CW
N=2 for BPSK
N=4 for QPSK

L_N is the self noise intermodulation loss and is given by:

$$L_1= 1 \quad \text{(ii)}$$
$$L_2= 1+1/2\ SN_i \quad \text{(iii)}$$
$$L_4=1+9/SN_i+6/SN_i^2+3/2SN_i^3 \quad \text{(iv)}$$

SN_i is the input signal to noise ratio

For a non-sampled matched filter the SN_i is given by:

$$SN_i=CN_0/BPS=E_S/N_0 \quad \text{(v)}$$

BPS is the channel bitrate in bit/s
E_S/N_0 is the symbol energy per bit/noise density

For the popular half rate convolutional FEC a bit error rate of 10^{-5} is achieved at an E_S/N_0 of around 1.5 dB.

2.2 PLL thermal noise phase variance

The PLL will lock onto the spectral line at the non-linearity output. The phase variance due to thermal noise is given by:

$$\sigma_n^2=N^2 B_l L_N/CN_0 \quad \text{(vi)}$$

B_l is the PLL one sided noise bandwidth

The phase variance at frequency divider output is reduced N^2 times as long as the loop is not cycle slipping.

2.3 System phase noise spectrum

The system total phase noise is the sum of the individual contributions from the terminal, the satellite and the satellite earth station. The single sided system phase noise power (normalized relative to the carrier in a 1 Hz bandwidth) can be approximated by the following formulae [2]:

$$G_i(f)=k_a/f^3 + k_b/f^2 + k_c \quad \text{(vii)}$$

f is the offset frequency from the carrier in Hz

The coefficients (k_a, k_b, k_c) are usually derived from measurements or specifications using standard curve fit methods.

The frequency at the PLL input is N times the input frequency, this increases the phase noise N^2 times.

$$G(N, f) = N^2 G_i(f) \quad \text{(viii)}$$

2.4 PLL phase noise variance

The PLL tracks the phase noise inside the loop bandwidth. In Reference [2] it is shown that the residual phase variance is given by (ix):

$$\sigma_p^2 = \int G(N,f)\ (\omega/\omega_n)^4/(1+(\omega/\omega_n)^4)\ d\omega$$

ω= $2\pi f$
ω_n is the natural loop frequency
ω_n=1.89 B_l for a second order PLL with a damping of 0.7

In [2] it is shown that for a phase noise spectrum given by (vii) the residual phase variance for a second order PLL with damping factor of 0.7 is given by (x):

$$\sigma_p^2 = N^2 (8.71\ k_a/B_l^2 + 3.7\ k_b/B_l + k_c\ W)$$

W is the matched filter noise bandwidth, which is approximately equal to the symbol rate.

2.5 Minimum total phase variance

It can be seen that the phase variance due to thermal noise is minimized for small loop bandwidths (B_l). The phase variance due to phase noise is however, minimized for large loop bandwidths.

The optimum loop bandwidth (B_l) minimizes the total phase variance σ_t^2.

$$\sigma_t^2 = \sigma_n^2 + \sigma_p^2 \qquad \text{(xi)}$$

We first determine the derivative with respect to B_l for (xi). The optimum B_l is calculated by setting the derivative to zero.

$$N^2 (L_N/CN_0 - 17.4\ k_a/B_l^3 - 3.7 k_b/B_l^2) = 0$$

To simplify the mathematics it is assumed that the contributions from the k_b and k_c factors can be neglected:

$$k_a/k_b >> 0.42\ B_l \qquad \text{(xii)}$$

$$k_a/k_c >> 0.11\ W\ B_l^2 \qquad \text{(xiii)}$$

These assumptions are reasonable in practical systems. It is now easy to show that the optimum loop bandwidth is given by:

$$B_l = (17.4\ k_a\ CN_0/L_N)^{1/3} \qquad \text{(xiv)}$$

The total phase variance can be derived by substituting the optimum B_l in (vi) and (x). The minimum total variance is given by:

$$\sigma_t^2 = 3.9\ N^2\ k_a^{1/3}\ (L_N/CN_0)^{2/3} \qquad \text{(xv)}$$

It turns out that for the optimum B_l, the phase variance due to thermal noise is twice the phase variance caused by phase noise. If we assume that the phase variance due to the k_b and k_c terms are identical and contribute in total together less than 10% of the total variance given in (xv), then the maximum values can be calculated to be as follows:

$$k_b = 0.36\ k_a/Bl \qquad \text{(xvi)}$$

$$k_c = 1.36\ k_a/W\ B_l^2 \qquad \text{(xvii)}$$

2.6 Minimum C/N_0

A PLL will normally not cycle slip when the total phase variance is less than 0.25 rad^2. At this threshold the corresponding recovered carrier phase jitter is less than 15 degrees, and the demodulation loss does not exceed 0.3 dB. The minimum C/N_0 required to track the thermal and phase noise is given by:

$$CN_{0min} = 62\ N^3\ k_a^{1/2}\ L_N \qquad \text{(xviii)}$$

2.7 Maximum phase noise level for given C/N_0

In some situations we need to determine the maximum allowable system phase noise level. We can determine the k_a coefficient by re-arranging (xviii):

$$k_a=CN_0^2/3800\ N^6L_N^2 \qquad \text{(xix)}$$

3. REAL LIFE EXAMPLES

In this section we look at two different problems that a satellite system designer may encounter. The formulas derived in the previous sections are used to determine the minimum C/N_0 required for a system and thereby the minimum bitrate. In the second example we assume that a certain C/N_0 is available, and calculate the maximum allowable phase noise level.

3.1 Calculation of minimum C/N_0

The typical total system phase noise in a domestic mobile satellite system can be approximated as follows:

$$G_i(f)=2.2/f^3+0.039/f^2+2.8\ 10^{-7}$$

The task at hand is to determine the lowest possible bitrate for a BPSK system using half rate FEC.

For a convolutional half rate code we need an E_S/N_0 of around 2 dB (1.6 power ratio). The noise intermodulation loss is calculated as follows:

$$L_2=1+1/(2\ 1.6)=1.32$$

The threshold carrier to noise density is then calculated as follows (xviii):

$$CN_0=62\ 2^3\ 2.2^{1/2}\ 1.32=29.9\ \text{dBHz}$$

The symbol rate can the be determined as follows:

$$BPS=CN_0/E_S/N_0=29.9-2.0=617\ \text{bit/s}$$

The optimum B_l can be calculated as follows (xiv):

$$B_l=(17.4\ 2.2\ 971/\ 1.32)^{1/3}=30.4\ \text{Hz}$$

The final task is to verify that the contributions to the variance by the other phase noise coefficients is insignificant:

$$k_b<0.36\ k_a/Bl=0.026$$

The actual value of k_b is 0.039, hence the phase variance is underestimated by around 8%.

$$k_c<1.36\ k_a/W\ B_l^2=1.36\ 2.2/617\ 30.4^2$$
$$k_c<5.3\ 10^{-6}$$

The actual value of k_c is $2.8\ 10^{-7}$ which results in a negligible phase variance contribution.

3.2 Maximum phase noise level

This example corresponds to the Inmarsat-C system, which is a global satellite data system operating at 1200 symbol/s. The link budget provides a C/N_0 of 33 dBHz for this coded BPSK system. In this section the phase noise requirements will be determined.
The noise intermodulation loss is calculated as follows ($E_S/N_0=2.2$ dB):

L_2=1+1/2 1.66= 1.30

Next we calculate the first phase curve coefficient k_a (xix):

ka= $2000^2/3800\ 2^6\ 1.3^2$= 9.7

The optimum loop bandwidth can now be calculated:

B_l=(17.4 9.7 2000/ 1.30)$^{1/3}$= 64 Hz

The maximum values of k_b and k_c can be calculated using (xvi) and (xvii):

k_b=0.36 k_a/Bl =0.36 9.7/64 = 0.05
k_c=1.36 k_a/W B_l^2 = 1.36 9.7/1200 64^2
k_c= 2.7 10^{-6}

The phase noise floor determined by the k_c coefficient corresponds to a noise floor level of -55.7 dBc/Hz. This corresponds to a phase noise floor 22.7 dB below the thermal noise floor. In an operational system several thousands transmitter can operate simultaneously within one band and the system phase noise specification should be at least 30 dB more stringent. A resonable specification would be to require the phase noise floor to be about 85 dB below the carrier. The required system phase noise mask is then as follows:

$G_i(f)=9.7/f^3+0.05/f^2+3\ 10^{-9}$

4. CONCLUSIONS

Often a satellite system designer needs to quickly calculate system design limits to verify a system concept. In this paper we have shown that phase noise calculations do not have to be complex or difficult. By using some of the classical PLL formulas some new equations have been derived that can be used to calculate the C/N_0 threshold or the maximum phase noise level for a given C/N_0.

5. REFERENCES

[1] **F. Gardner**, *Phaselock Techniques*, Wiley, 1976

[2] **J. Spilker**, *Digital Communications by Satellite*, Prentice Hall, 1973

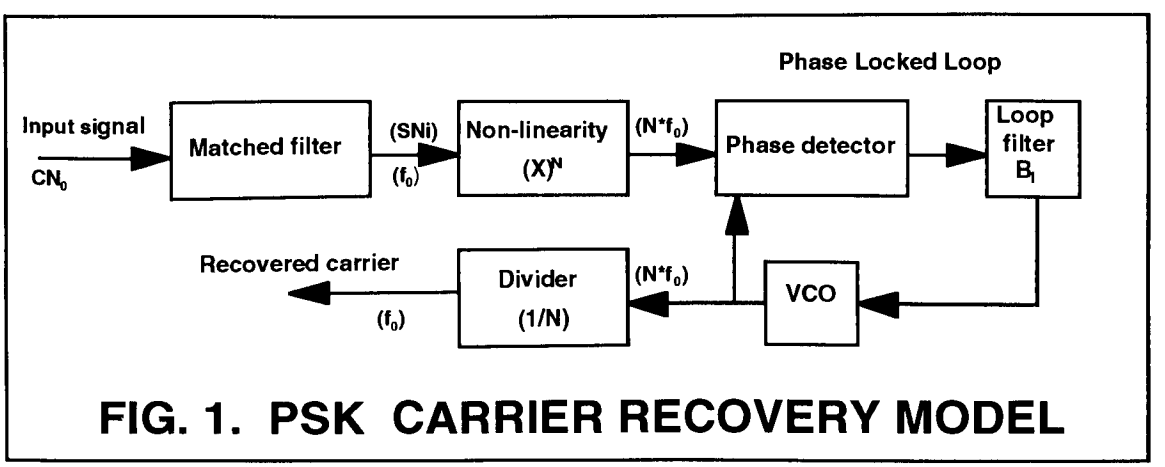

FIG. 1. PSK CARRIER RECOVERY MODEL

An Efficient Software Implementation of a Variable Rate Modem

Ramesh Mantha*, Andrew Hunt*, and Stewart Crozier**

*Gemtronic Engineering Ltd., 210-39 Robertson Rd., Nepean, Ontario, Canada, K2H 8R2, ph: 613-726-0236, fax: 613-726-0433

**Communications Research Centre, 3701 Carling Ave., P.O. Box 11490, Station H, Ottawa, Ontario, Canada, K2H 8S2, ph: 613-998-9262, fax: 613-990-0316

ABSTRACT

This paper describes the software implementation of the baseband portion of a variable rate modem. The modem can handle arbitrary symbol rates with a fixed input/output sample rate. This approach reduces hardware complexity related to external clock generation circuitry, offers complete flexibility in the selection of symbol rates, and conveniently accommodates symbol timing and symbol rate corrections.

1. INTRODUCTION

The key requirement of a variable rate modem is the ability to convert data at some arbitrary number of samples per symbol to an integer number of samples per symbol and vice versa. This translation operation is done through the combination of a rate generating time accumulator and the transmit pulse shaping and receive matched filtering operations. This process is independent of the many other modem characteristics, such as modulation scheme, decision process and timing, frequency and phase estimation algorithms. These other modem functions will not be discussed here. The pulse shaping and matched filter used in this implementation is a 60% rolloff root raised cosine filter which spans 5 symbol periods.

There are three key elements involved in the implementation of the variable rate modulator. First, a time reference must be maintained that relates the output sample rate to the input sample rate. This is realized using a 32 bit time accumulator. The second requirement is a means of sampling the impulse response of the desired transmit filter taps. Finally, since small lookup tables can introduce unacceptable timing jitter and related spectral spurs outside the transmit band of interest, a mechanism for reducing this distortion is required. The spectral spurs can be reduced to acceptable levels by linearly interpolating between two closely time spaced filter output calculations.

The demodulator can also handle arbitrary symbol rates by using a 32 bit time accumulator to relate the input sample rate to the desired output sample rate. The average rate of accumulator overflow corresponds to the desired output sample rate. The output rate is typically an integer multiple of the symbol rate to accommodate downstream processing requirements, such as symbol timing estimation. On each accumulator overflow, a matched filter output value is computed. Timing jitter is corrected through the use of a bank of matched filters, with each filter having a slightly different delay. For each requested symbol rate, the filter bank is automatically generated from a single stored matched filter response.

The time accumulator approach naturally accommodates symbol timing and symbol rate corrections. Symbol timing is changed by adjusting the time accumulator. The symbol rate is changed by adjusting the time increment value. Other advantages of this method include the capability of changing the modem symbol rate without the hardware complexity of changing the external clocking of the analog to digital converters (ADCs) and digital to analog converters (DACs) for receive and transmit sampling. Any arbitrary rate can be selected within the limits of the available processing power and rapid, on the fly, rate changes are possible.

II. VARIABLE RATE MODULATOR

The block diagram shown in Figure 1 portrays the overall structure of the variable-rate modulator. The modulator receives data from an external source at some arbitrary rate, governed by the *input data clock*. After processing, the modulator sends samples to the DACs at another rate set by the *output sample clock*. These two rates are completely independent, allowing the use of a single output sample clock regardless of the input data rate. Of course, the output sample rate dictates the highest frequency that can be output, and this in turn imposes a limit on the maximum attainable data rate.

Algorithm

The following pseudo-code illustrates the concept behind the variable-rate modulator. The actual implementation differs somewhat since it has been optimized for processing efficiency. Variable names printed in italics refer to complex quantities.

Initialization:

```
tinc=SamplePeriod/SymbolPeriod
tacc=0
```

For every output sample:

```
tacc=tacc+tinc
if(tacc≥1)
      tacc=tacc-1
      Shift symbols in buffer.
      Get new symbol.
Total=0
t=tacc
for Index=1 to NumTaps
      Total=Total+Symbols[Index]*f(t)
      t=t+1
OutputToDac(Total)
```

Emulating a continuous-time f(t)

The impulse response f(t) returns the value of the pulse-shaping filter's time response at the point given as an argument. Since it would be computationally intensive to calculate these values in real-time, it is necessary to use a lookup table. A simple table lookup, however, will give poor performance unless a very large table is used. To solve this problem, a linear interpolation is made between the two closest values stored in the table.

In implementation, the linear interpolation is not performed for every filter tap lookup. Instead, a filter output is first calculated based on rounding down the time values to the closest entries in the table. Then, another output value is calculated based on rounding up the time values to the closest entries in the table. These filter taps are easily picked off if the filter is stored with an integer number of samples per symbol period. Finally, a single linear interpolation between the two filter output values is performed based on where the true time lies in relation to the two output samples. This method is mathematically equivalent to interpolating the taps but is much more efficient.

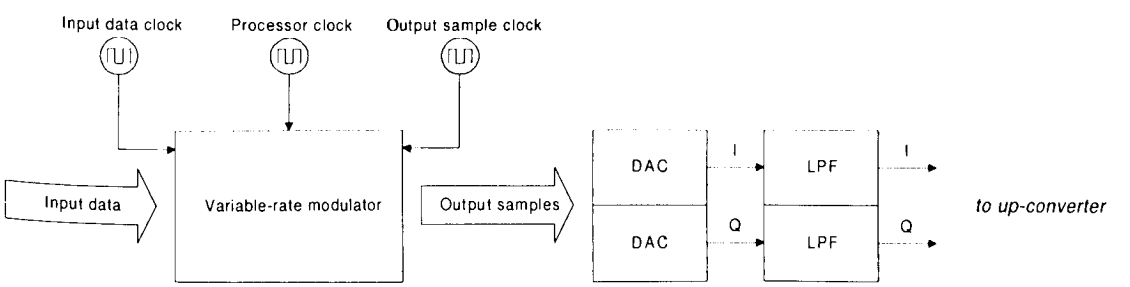

Figure 1 **Overall modulator structure**

Implementation

Figure 2 depicts some details of the variable-rate modulator. Two filtering operations are performed on the input data for each output sample. The filter outputs are then combined by a linear interpolator before being sent to the DAC. The filtering operations and the interpolation are both affected by the time accumulator. It is incremented every sample period and keeps track of time relative to the input symbol rate. This time reference is used in the selection of filters from the filter bank, and to provide weighting coefficients for the linear interpolator.

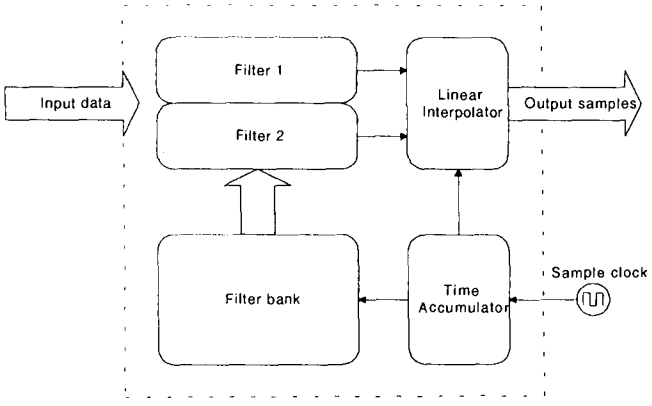

Figure 2 Detailed modulator operation

The variable-rate modulator concept described above has been implemented on an Analog Devices ADSP2101 processor, a low-cost 16-bit fixed-point digital signal processor (DSP). DSPs are designed to perform efficient finite impulse response (FIR) filtering. The modulation method implemented was quadrature phase shift keying (QPSK). The processing requirements of the modulator total to an average of less than 50 cycles per complex output sample. For an output sample rate of 48 kHz, the modulator therefore requires only 15% of a 16 million instructions per second (MIPS) DSP. The impulse response lookup table spans 5 symbol periods, with 64 samples per symbol. This means that only 321 words of storage are used, which is a very reasonable memory requirement. (The extra storage word is used to make possible certain code optimizations).

Performance

If only a simple table-lookup approach (without interpolation) was used to implement the variable-rate modulator, the output spectrum would be of rather poor quality. Timing jitter causes degradation of the transmit spectrum. This is shown in Figure 3. Adding the interpolation feature, however, improves the spectrum dramatically, as shown in Figure 4.

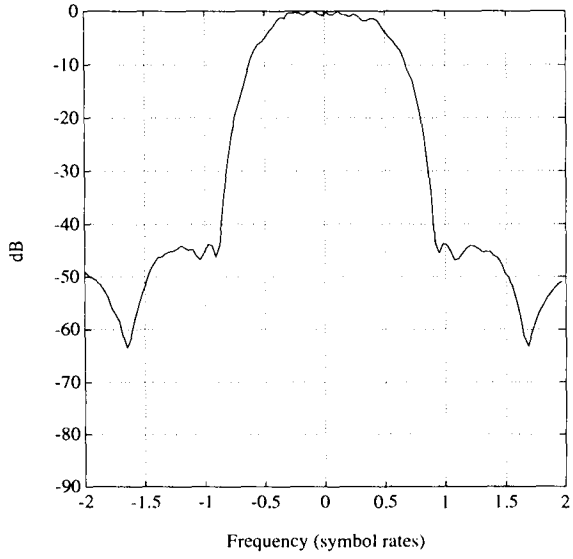

Figure 3 Transmit spectrum without interpolation

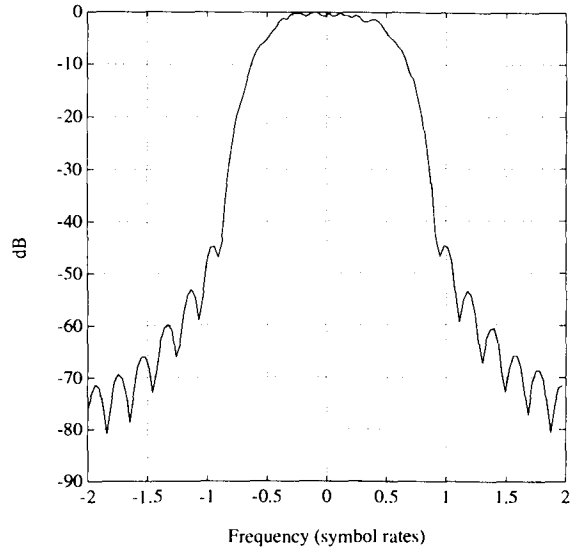

Figure 4 Transmit spectrum with interpolation

III. VARIABLE RATE DEMODULATOR

The demodulator portion of the variable rate modem can handle any arbitrary symbol rate with a fixed input sample rate. In order to do this, the receiver must convert the input sample stream entering at an arbitrary number of samples per symbol to an integer number of samples per symbol after matched filtering. This is achieved by incrementing a 32-bit time accumulator with a specific increment value on each sampling interval. The increment value is selected such that the time accumulator overflows at the desired rate. The operation of the variable rate receiver is depicted in figure 5.

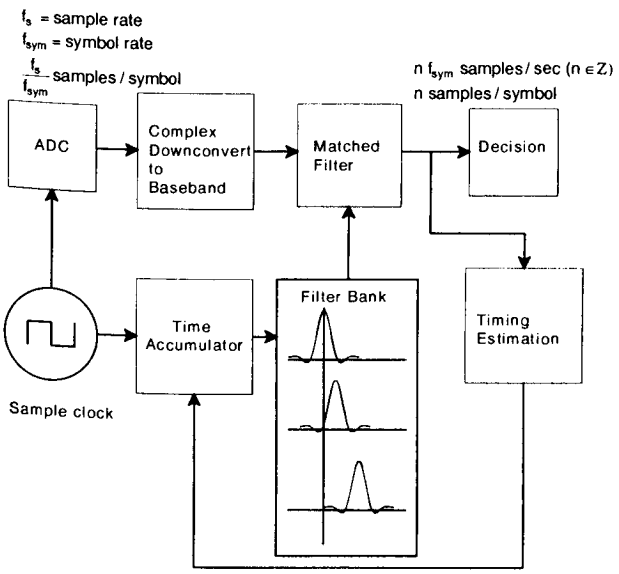

Figure 5 **Overall demodulator structure**

Samples from the ADC are only processed when there is a time accumulator overflow. The increment value added to the time accumulator is a function of the desired overflow rate and the input sampling rate. The overflow rate of the time accumulator is typically an integer multiple of the symbol rate. This multiple is selected based on the requirements of the downstream processing algorithms of the demodulator, such as timing or frequency estimation, with typical values being one, two or four samples per symbol.

The accuracy of the average overflow rate of the time accumulator is tied to the accuracy and precision of the input sample clock. Assuming an ideal input sample clock, the average overflow rate will be as desired to within the limitations of the 32 bit accuracy of the time accumulator. Practically, this means that the overflow rate will have an accuracy on the order of 10^{-10} with respect to the input sample clock, which is more than adequate for most applications.

Each time accumulator overflow triggers a matched filter calculation. If only a single filter were used, its output would have timing accurate to within a sample period. Instead, a bank of matched filters, each with the same magnitude frequency response but with a different delay, is used to provide finer timing accuracy. This usage of a bank of filters is similar to traditional approaches of obtaining fine timing accuracy with a fixed rate. The residual value in the time accumulator after an overflow is proportional to the required fine timing correction and is used to derive an index into the filter bank. The filter selected, based on this index, will have a delay that corrects timing to within the resolution of the filter bank.

The timing resolution is determined by the resolution of the matched filter bank. The filter bank has delays spanning ±½ a sample period. Therefore, the number of filters in the filter bank determines the fraction of a sample period to which timing can be adjusted. The matched filters in the bank will always be a fixed number of symbol periods in length. Since the number of input samples per symbol decreases with increased symbol rate, the filters will have fewer taps at higher rates.

In order to maintain a constant timing resolution relative to the symbol rate, there must be more filters in the filter bank when higher symbol rates are required. However, since each filter has fewer taps at higher symbol rates, the overall number of taps required for the filter bank remains approximately constant regardless of symbol rate. This means that the memory requirements for the filter bank is constant.

Unlike the modulator, the number of filters, the number of taps per filter and the filter coefficients are a function of the symbol rate. However, only a single matched filter response, specifically the one used in the modulator, need be permanently stored. For each requested symbol rate, the filter bank can be generated from the single stored filter in a manner similar to the interpolation procedure used in the variable rate modulator. This computation typically takes less than 1 ms, allowing for rapid, on the fly changes in the symbol rate.

Timing Correction

The time accumulator approach naturally accommodates symbol timing and symbol rate corrections. A symbol timing adjustment is implemented through a one time

addition to the time accumulator while the symbol rate can be adjusted by changing the increment value. The overflows of the time accumulator automatically give correct timing to within a sample period. The filter bank then reduces the timing error to the resolution of the filter bank. This means of timing correction is completely independent of the algorithm used to determine the timing error.

It is worth noting the differences in timing error between the variable rate demodulator and a traditional fixed rate demodulator with an integer number of samples per symbol. In both cases, the timing error is determined by the resolution of the bank of matched filters. However, in the fixed rate case, the timing error will be constant while in the variable rate case, the timing error will vary due to the possibility of different time accumulator overflow values. The fluctuating overflow values result when the input number of samples per output sample is a non integer value. The maximum timing error in the variable rate case will be no worse than in the fixed rate case, assuming both methods have similar filter bank resolutions.

Implementation and Performance

The demodulator was implemented on an ADSP2101 fixed point DSP, running concurrently with the modulator. For an input sample rate of 48 kHz and an output rate of 2 times the symbol rate, the variable rate matched filtering component of the demodulator uses 15% of the processing power of the 16 MIPS version of the ADSP2101 DSP. This processor usage is constant, regardless of the symbol rate. The processor usage is a function of the sample rate and will decrease if the sample rate is lowered.

The performance of the variable rate matched filter with various numbers of filters in the filter bank is shown in figure 6. The spectra are of the signal after matched filtering, with filter banks containing n=2, 4, 8, and 16 filters. In this example, the symbol rate was 5926 symbols/sec and the sample rate was 48 kHz. There were approximately 8.1 input samples per symbol. The overall timing resolution in each case was therefore [1/(8.1*n)] of a symbol period. Since the timing error must be less than one half the timing resolution, the maximum timing error is equal to [1/(8.1*2*n)] of a symbol period. The worst case in the example, where n=2, has a maximum timing error of about 1/32 of a symbol period. Note that at higher data rates, a filter bank with more filters but fewer taps per filter would be required to achieve a comparable timing error. In this case, the total number of taps in the filter bank would remain the same.

The noise level of each spectrum is an indication of the distortion that results from timing error jitter. The required quality of this spectrum is a function of the desired bit error performance of the demodulator. Any distortion down more than 40 dB has a negligible impact on bit error performance. Therefore in this particular example, a filter bank with two filters would be sufficient to give acceptable performance.

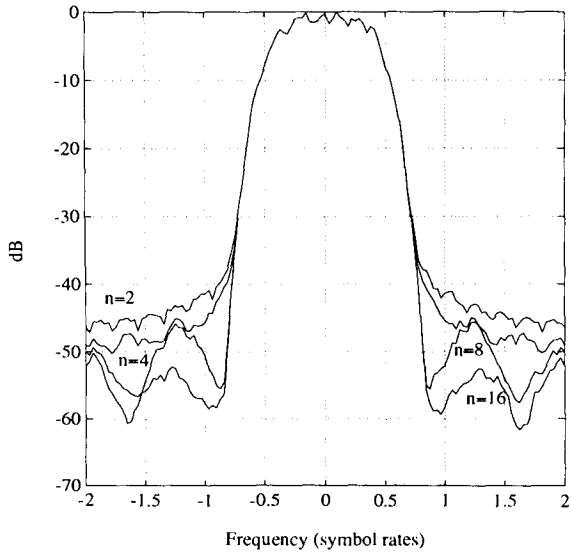

Figure 6 **Receive spectrum after matched filtering with n filters in bank**

IV. Conclusions

This paper has presented the implementation of a variable rate modem. The variable rate is achieved through a rate generating time accumulator combined with an interpolating pulse shaping filter and matched filter. A key feature is the ability to operate at arbitrary symbol rates with a constant input and output sample rate. In addition, the flexibility of the variable rate feature provides the ability to implement real-time rate changes, without external hardware modifications. The algorithms are not processor intensive and have very low memory requirements. These attributes make the algorithms appropriate for implementation on a low cost, fixed point digital signal processor.

Biographical Notes

Ramesh Mantha is currently with the Communications Research Centre.

Design of an Anti-Rician-Fading Modem for Mobile Satellite Communication Systems

Toshiharu Kojima, Fumio Ishizu, Makoto Miyake, Keishi Murakami and Tadashi Fujino

Communication Systems Laboratory, Mitsubishi Electric Corp.

5-1-1 Ofuna, Kamakura City 247, Japan

Phone:+81-467-41-2451 Fax:+81-467-41-2487

Abstract: To design a demodulator applicable to mobile satellite communication systems using differential phase shift keying modulation, we have developed key technologies including an anti-Rician-fading demodulation scheme, an initial acquisition scheme, automatic gain control (AGC), automatic frequency control (AFC), and bit timing recovery (BTR). Using these technologies, we have developed one-chip digital signal processor (DSP) modem for mobile terminal, which is compact, of light weight, and of low power consumption. Results of performance test show that the developed DSP modem achieves good performance in terms of bit error ratio in mobile satellite communication environment, i.e., Rician fading channel. It is also shown that the initial acquisition scheme acquires received signal rapidly even if the carrier-to-noise power ratio (CNR) of the received signal is considerably low.

I. INTRODUCTION

Recently, mobile satellite communication systems using the geostationary satellites have been gathering much attention, since they can provide low-cost mobile communication services with wide coverage. In mobile satellite communication systems, the propagation path is generally modeled by a Rician fading channel. Therefore, the first problem in mobile satellite communication systems is to overcome the effect of Rician fading. Secondly, carrier frequency offset is caused in received signal by use of higher frequency band and Doppler shift due to movement of mobile terminal. In the low bit rate applications such as voice services in single channel per carrier (SCPC) communications, the amount of the carrier frequency offset is often comparable to modulation signal rate. Demodulator has to achieve rapid acquisition of the received signal with such relatively large frequency offset. Rapid signal acquisition is especially important, when the system employs the voice activation technique to increase channel capacity. Finally, it is required from the practical viewpoint to develop mobile terminals that are compact, of light weight, and of low power consumption.

To overcome these problems and to design a demodulator applicable to mobile satellite communication systems using differential phase shift keying (DPSK) modulation, we have developed key technologies of a novel anti-Rician-fading demodulation scheme[1],[2] based on multiple differential detection technique and a novel initial acquisition scheme detecting a non-modulated part of the received signal. Although multiple differential detection schemes have been investigated as bit error ratio (BER) performance improvement method of the conventional differential detection scheme in additive white Gaussian noise (AWGN) channel[3],[4] mainly, they are also useful in Rician fading channel[2],[5]. In addition, to cope with blockage and shadowing, we have also developed technologies for demodulator including AGC, AFC and BTR. These technologies make it possible to achieve rapid resynchronization after blockage or shadowing. All developed technologies are based on digital signal processing, and are easily implemented either by LSI or by DSP. Using these key technologies, we have developed one-chip DSP modem for mobile terminals.

In this paper, we concentrate on the anti-Rician-fading scheme and the initial acquisition scheme. We also describe the configuration of the demodulator part of the developed DSP modem. Finally, we show the results of performance test of the DSP modem, which demonstrate the feasibility of developed technologies including the following:

1. BER performance of conventional differential detection is improved in Rician fading channel by the anti-Rician-fading demodulation scheme.

2. The initial acquisition scheme acquires non-modulated signal rapidly, even in the low CNR environment with relatively large carrier frequency offset.

II. COMMUNICATION SYSTEM MODEL

Fig.1 shows a communication system model using DPSK modulation. In this paper, unless otherwise indicated, the addition and subtraction on phase are calculated in modulo 2π in the range $[-\pi, \pi)$. In the modulator, an M-ary transmitted symbol $a_i \in \{0,1,\cdots,M-1\}$ at symbol time i is Gray mapped to a transmitted differential phase $\Delta\theta_i \in S$, where $S = \{2m\pi / M; m = 0,1,\cdots,M-1\}$ is the set of transmitted

differential phases. Then, a transmitted signal phase θ_i is generated by the differential encoding $\theta_i = \theta_{i-1} + \Delta\theta_i$. The differential MPSK signal $s_i = \sqrt{E_s}\exp(-j\theta_i)$ is transmitted, where E_s denotes the signal energy per symbol: $E_s = (\log_2 M)E_b$, and E_b is the energy per bit. In the channel, the transmitted signal s_i is affected by Rician fading and AWGN with single-sided noise power spectral density N_0, resulting in the received signal r_i. The demodulator estimates the transmitted differential phase sequence $\{\Delta\theta_i\}$ from the received signal sequence $\{r_i\}$. Finally, based on each value of the estimated differential phase sequence, the demodulated symbol $\hat{a}_i \in \{0,1,\cdots,M-1\}$ is produced.

III. KEY TECHNOLOGIES

3.1 Anti-Rician-fading demodulation scheme

As an anti-Rician-fading demodulator scheme, we have developed a novel demodulation scheme[1],[2] based on multiple differential detection technique. We call this scheme "multiple differential phase detection (MDPD) scheme" in this paper, since it has a feature that only phase information of received signal is required in its algorithm. A differential phase detection signal is produced by subtracting the phase of the received signal delayed by n symbol duration from the phase of the current received signal (called "n-symbol differential detection signal" in this paper). It is known that n-symbol differential detection signal constitutes a convolutional code of 1-symbol differential detection signal[3]. Using this property, MDPD scheme employs Viterbi algorithm to estimate the transmitted differential phase sequence from $1,\cdots,N(\geq 2)$-symbol differential detection signals.

Fig.2 shows an example of basic configuration of MDPD scheme in the case of $N = 3$. In this configuration, the 1-symbol differential detector produces the 1-symbol differential detection signal $\theta_{(1)i}$:

$$\theta_{(1)i} = \theta_{(0)i} - \theta_{(0)i-1} \tag{1}$$

where $\theta_{(0)i}$ denotes the phase of the received signal r_i. Then, the $n(=2,\cdots,N)$-symbol differential detection signals $\theta_{(n)i}$ are successively generated from the 1-symbol differential detection signal $\theta_{(1)i}$ by the following recurrent formula:

$$\theta_{(n)i} = \theta_{(n-1)i} + \theta_{(1)i-n+1} \tag{2}$$

Let us define the differential phase symbol Θ_i by the set of the $1,\cdots,N$-symbol differential detection signals,

$$\Theta_i = \left(\theta_{(1)i},\cdots,\theta_{(N)i}\right) \tag{3}$$

Note that Θ_i is a type of systematic convolutional code of the 1-symbol differential detection signal with constraint length equal to N.

The differential phase symbol Θ_i is supplied to a sequence estimator based on Viterbi algorithm, which is called "Viterbi estimator" in this paper. The trellis diagram used in the Viterbi estimator has M^{N-1} kind of states that are a combination of elements of the set S over $(N-1)$ symbols, and each state has M incoming branches and M outgoing branches. The Viterbi estimator generates branch metrics from the differential phase symbol Θ_i. In MDPD scheme, branch metric calculation can be simplified by using the absolute function instead of the cosine function without perceptible performance degradation. Namely, in the case of state transition from a state $\Phi_{i-1} = (\phi_{i-N+1},\cdots,\phi_{i-1})$ $(\phi_i \in S)$ at time $(i-1)$ to a state $\Phi_i = (\phi_{i-N+2},\cdots,\phi_i)$ at time i, the branch metric $\lambda(\Phi_{i-1},\Phi_i)$ can be calculated by a simple formula[2]

$$\lambda(\Phi_{i-1},\Phi_i) = \sum_{n=1}^{N}\left|\theta_{(n)i} - \sum_{k=0}^{n-1}\phi_{i-k}\right| \tag{4}$$

Then, the add-compare-select (ACS) operation is executed on each state using the branch metrics defined by Eq.(4), and the path metrics are updated. The result of each ACS operation is represented by a trellis connection signal that takes on a value of an element of the set S, and is stored in the path memory of the Viterbi estimator. Finally, the contents of the path memory for the surviving path having the minimum path metric, corresponding to the maximum likelihood, are produced from the Viterbi estimator, as the estimated differential phase sequence $\{\Delta\hat{\theta}_i\}$.

Features of MDPD scheme are as follows:

1. MDPD scheme improves BER performance of conventional differential detection scheme both in AWGN channel and in Rician fading channel[2].

2. MDPD scheme can achieve rapid synchronization, since it does not require carrier recovery function.

3. MDPD scheme can be easily implemented, since the signal processing of MDPD scheme only requires addition and subtraction when branch metrics defined by Eq.(4) is used.

3.2 SST type MDPD scheme

To simplify the signal processing further, a signal processing technique corresponding to the scarce state transition (SST) type Viterbi decoding[6] can be applied to

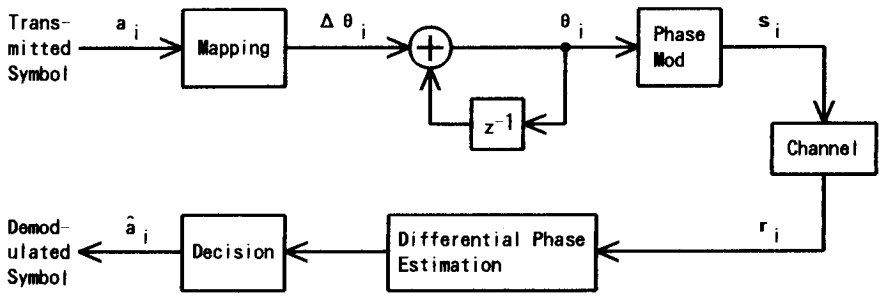

Fig. 1 Communication system model.

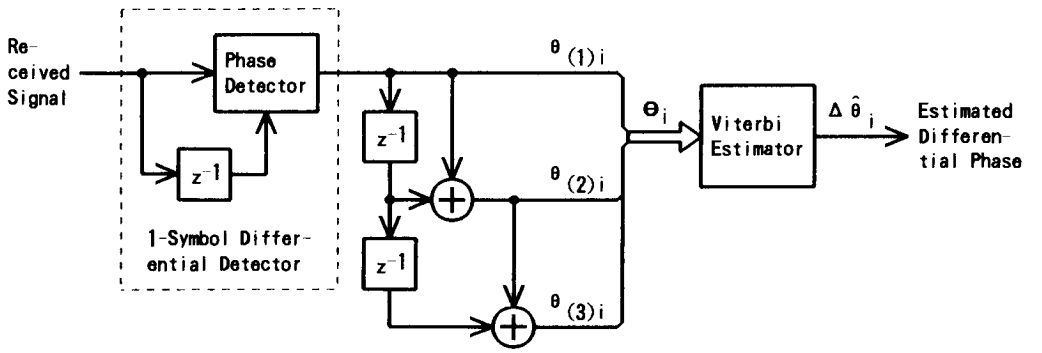

Fig. 2 Basic configuration of MDPD scheme with N=3.

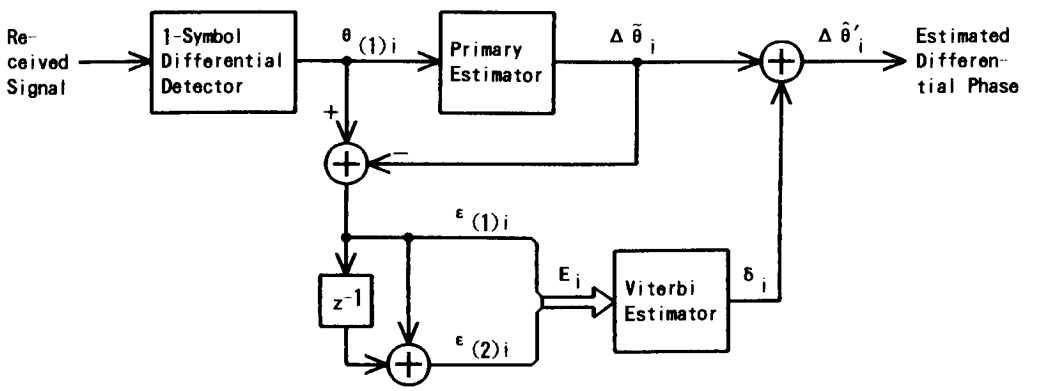

Fig. 3 Configuration of MDPD scheme — SST type with N=2.

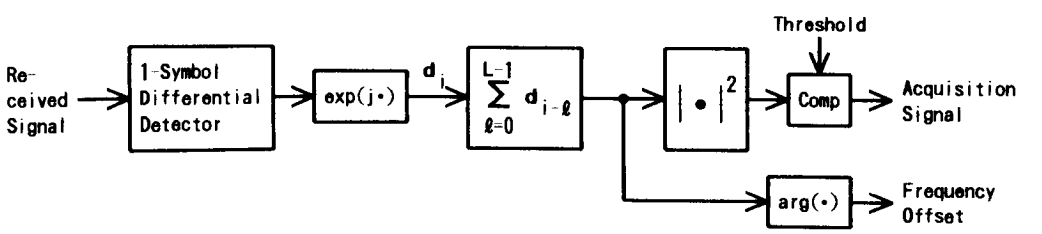

Fig. 4 Configuration of the initial acquisition scheme.

MDPD scheme[1],[2]. Fig.3 shows an example of this configuration in the case of $N=2$. In the following, the configuration in Fig.2 is called "basic type", and that in Fig.3 is called "SST type".

In Fig.3, the 1-symbol differential detection signal $\theta_{(1)i}$ is supplied to the primary estimator. Based on the estimation method of the conventional differential detection scheme[7], the primary estimator generates $\Delta\tilde{\theta}_i \in S$ minimizing $\left|\theta_{(1)i} - \Delta\tilde{\theta}_i\right|$ as the primary estimated value of the transmitted differential phase $\Delta\theta_i$. Then, by subtracting the primary estimated value $\Delta\tilde{\theta}_i$ from the 1-symbol differential detection signal $\theta_{(1)i}$, the first residual signal $\varepsilon_{(1)i}$ is produced. That is,

$$\varepsilon_{(1)i} = \theta_{(1)i} - \Delta\tilde{\theta}_i \tag{5}$$

Using the first residual signal $\varepsilon_{(1)i}$, the $n(=2,\cdots,N)$-th residual signals are successively generated by the following recurrence formula corresponding to Eq.(2):

$$\varepsilon_{(n)i} = \varepsilon_{(n-1)i} + \varepsilon_{(1)i-n+1} \tag{6}$$

The residual symbol $E_i = \left(\varepsilon_{(1)i},\cdots,\varepsilon_{(N)i}\right)$ composed of the first to N-th residual signals is supplied to the Viterbi estimator. In the same way as in the basic type, the branch metric with the state transition from a state Φ_{i-1} to a state Φ_i is given by:

$$\lambda'\left(\Phi_{i-1},\Phi_i\right) = \sum_{n=1}^{N}\left|\varepsilon_{(n)i} - \sum_{k=0}^{n-1}\phi_{i-k}\right| \tag{7}$$

Finally, by adding the primary estimated sequence $\left\{\Delta\tilde{\theta}_i\right\}$ produced by the primary estimator and the error sequence $\left\{\delta_i\right\}$ produced by the Viterbi estimator, the estimated differential phase sequence $\left\{\Delta\hat{\theta}'_i\right\}$ is produced. That is,

$$\Delta\hat{\theta}'_i = \Delta\tilde{\theta}_i + \delta_i \tag{8}$$

As shown in [2], BER performance of the SST type is identical with that of the basic type.

In the SST type, the surviving path having the minimum path metric concentrates around all-zero state[2]. Using this feature of "likelihood concentration" in the SST type Viterbi decoding[6], the states of the trellis diagram can be reduced without performance degradation. When this state reduction method is employed, the trellis diagram used in the Viterbi estimator only requires 3^{N-1} states composed of 3 phases $\{0, 2\pi/M, 2(M-1)\pi/M\}$, independent of the number of signal phases M[2]. Therefore, the effect of the state reduction increases, as M and N increase. We have also confirmed that by introducing SST type signal processing to the multiple-symbol differential detection proposed in [4], its signal processing can be simplified without performance degradation.

Since state reduction of the Viterbi estimator causes hardware size reduction and/or computational complexity reduction, the SST type MDPD scheme with the state reduction method can be more easily implemented than the basic type. For example, in the case of differential 8PSK modulation with the configuration of $N=4$, it is difficult to implement the basic type having 512 states, but the SST type with the state reduction method has only 27 states and can be easily implemented. In addition, when MDPD scheme is to be implemented by DSP, the SST type can achieve higher bit rate operation than the basic type, since less computational complexity owing to the state reduction method enhances the signal processing speed remarkably.

3.3 Initial acquisition scheme

We have developed a novel initial acquisition scheme detecting non-modulated part of the received signal with relatively large carrier frequency offset. Carrier frequency offset Δf rotates the received signal vector. Namely, if there is no AWGN and fading, the received signal r_i is represented by

$$r_i = \sqrt{E_s}\exp\left\{-j\left(\Delta\theta + 2\pi\Delta fiT + \varphi\right)\right\} \tag{9}$$

where T is the symbol duration, and φ is a constant initial phase. In this case, the 1-symbol differential detection signal $\theta_{(1)i}$ has a constant phase shift. That is,

$$\theta_{(1)i} = \Delta\theta_i + 2\pi\Delta fT \tag{10}$$

Consequently, when non-modulated signal is received, i.e., $\Delta\theta_i = 0$, the 1-symbol differential detection signal $\theta_{(1)i}$ takes on a constant value of $2\pi\Delta fT$. The developed initial acquisition scheme uses this factor.

Fig.4 shows the configuration of the initial acquisition scheme. In Fig.4, a unit vector $d_i = \exp\left(j\theta_{(1)i}\right)$ is produced from the 1-symbol differential detection signal $\theta_{(1)i}$. Then, the unit vector d_i is accumulated over L symbols successively, resulting in the accumulated vector D_i. That is,

$$D_i = \sum_{l=0}^{L-1} d_{i-l} = \sum_{l=0}^{L-1}\exp\left(-j\theta_{(1)i-l}\right) \tag{11}$$

When non-modulated signal is received, the expectation value of the length of the accumulated vector D_i is equal to L, independent of the carrier frequency offset Δf. On the other hand, if no signal or modulated signal is received, the expectation value is equal to zero. Based on this characteristic, the initial acquisition scheme compares the

square of the length of the accumulated vector D_i with the predetermined threshold T_h in the range $0 < T_h < L^2$, and the acquisition signal is sent out if $|D_i|^2 > T_h$. In addition, when the non-modulated signal is received, the expectation value of the argument of the accumulated vector D_i is equal to $2\pi\Delta fT$. Therefore, the argument of the accumulated vector D_i is sent out as the estimated value of the frequency offset simultaneously with the acquisition signal. Thus, the initial acquisition scheme not only detects the non-modulated signal but also estimates the carrier frequency offset. Features of this initial acquisition scheme are as follows:

1. This scheme can be easily implemented, since the signal processing of this scheme requires only addition and subtraction essentially.

2. Since the unit (i.e., hard limited) vector d_i is used in this scheme, the predetermined threshold T_h is invariable, independent of the received signal power or CNR.

3. This scheme can essentially detect the frequency offset Δf in the range $|\Delta fT| < 0.5$. Namely, the frequency offset less than half the symbol rate can be detected.

IV. DSP MODEM

We have also developed key technologies including AGC, AFC and BTR based on digital signal processing. Using these technologies, we have developed one-chip DSP modem. Major parameters of the DSP modem are as follows:

1. Modulation : Differential QPSK
2. Bit rate : 6750 bit per second
3. Demodulation : SST type MDPD scheme (N=3)

4.1 Configuration of the demodulator part

Fig.5 shows the block diagram of the demodulator part of the DSP modem. Major parts of the demodulator part are as follows:

1. Baseband converter and square-root Nyquist filter part

In this part, the IF signal received through the down converter and the variable gain amplifier for AGC is sampled asynchronously at the rate of 4 times the IF carrier frequency. The sampled IF signal is converted to the quasi-coherent detection signal by means of serial-to-parallel converting and finite impulse response (FIR) filtering. The quasi-coherent detection signal is resampled asynchronously at the rate of 4 times the symbol rate, and is filtered by square-root Nyquist filter using FIR transversal filtering method, resulting in the baseband received signal.

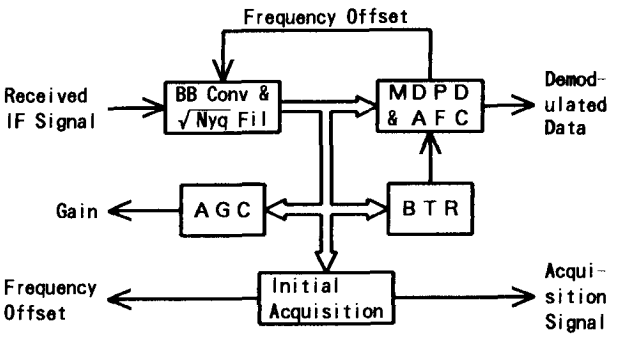

Fig. 5 Block diagram of demodulator part of the DSP modem

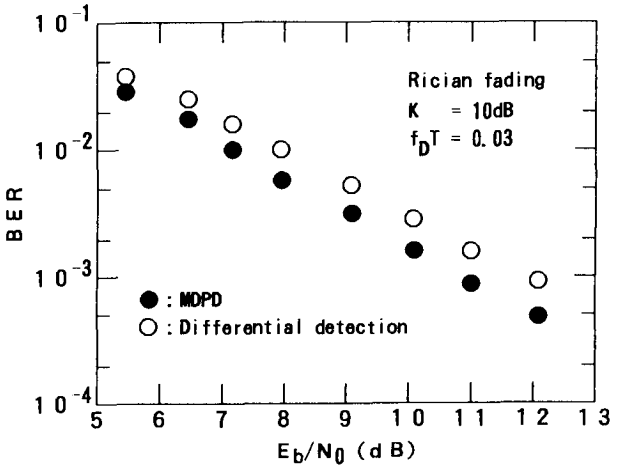

Fig. 6 BER performance of the DSP modem

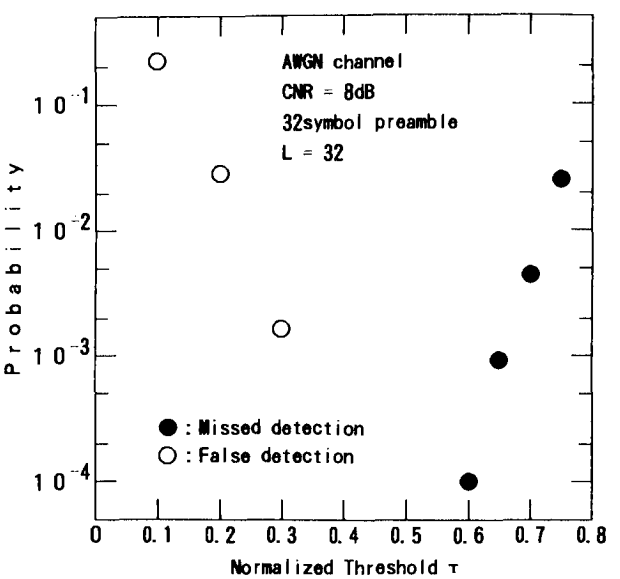

Fig. 7 Initial acquisition performance of the DSP modem

2. AGC part

This part executes the developed digital AGC processing, and generates the gain value to control the long term average of envelope of the baseband received signal constantly. By employing a random walk filter, the digital AGC processing is simplified. The generated gain value is successively supplied to the variable gain amplifier.

3. Initial acquisition part

This part executes the signal processing of the developed initial acquisition scheme using argument of the baseband received signal. When this part supplies the initial acquisition signal to the transmission control part, it also supplies the estimated value of the carrier frequency offset to the local oscillator in the down converter to cancel carrier frequency offset (initial AFC).

4. BTR part

This part executes the developed digital BTR processing based on the square-low detector and tank-limiter method with feed forward control and interpolation. Namely, the baseband received signal is squared, and digital tank-limiter employing discrete Fourier transform (DFT) processing extracts the clock signal from the squared signal. Feed forward control makes it possible to achieve rapid clock synchronization and resynchronization after blockage or shadowing, and interpolation reduces the sampling rate.

5. MDPD and AFC part

This part generates the demodulated data by executing the SST type MDPD processing using the argument of the baseband received signal. This part also generates estimated value of the carrier frequency offset caused after the initial AFC by accumulating the first residual signal used in the SST type MDPD processing. The estimated value of the carrier frequency offset is supplied to the baseband converter and square-root Nyquist filter part to cancel the frequency offset by rotating the resampled quasi-coherent detection signal before square-root Nyquist filtering (tracking AFC).

4.2 Performance of the demodulator part

Fig.6 shows the BER performance of the DSP modem in Rician fading channel with the K=10dB and $f_D T = 0.03$, where K is the power ratio of the direct-path component to the multipath component of the received signal, and f_D is the maximum Doppler frequency of the multipath component. It is confirmed from Fig.6 that the MDPD scheme improves BER performance of the conventional differential detection scheme by more than 1dB even under fast Rician fading of $f_D T = 0.03$ expected in mobile satellite communication systems.

Fig.7 shows the initial acquisition performance of the DSP modem in AWGN channel with CNR=8dB and carrier frequency offset of 0.3 times the symbol rate. In Fig.7, the missed detection probability of non-modulated preamble of 32 symbols and the false detection probability of random modulated signal are plotted as functions of the normalized threshold $\tau = T_h / L^2$ with accumulation length of $L = 32$. It is confirmed from Fig.7 that by setting $\tau = 0.6$, the missed detection probability can be suppressed to less than 1% with the false detection probability negligibly small even in the low CNR environment of 8dB with relatively large carrier frequency offset of $\Delta fT = 0.3$ and relatively short accumulation length of $L = 32$. It is also confirmed that other functions including AGC, AFC and BTR achieve expected performance.

V. CONCLUSIONS

We have developed key technologies for demodulator applicable to mobile satellite communication systems using DPSK modulation. Using these technologies, we have developed one-chip DSP modem achieving good performance.

Acknowledgment: The authors wish to express their thanks to T. Yamauchi and M. Murotani of Mitsubishi Electric Corporation for their support and encouragement.

REFERENCES

[1] **T. Kojima, M. Miyake and T. Fujino,** *Differential detection schemes using MLSE on phase sequence*, in Proc. 1991 IEICE Fall Conf., 1991, pp. B-234, *in Japanese.*

[2] **T. Kojima, M. Miyake and T. Fujino,** *Differential detection scheme for DPSK using phase sequence estimation*, Trans. IEICE B-II, vol. J76-B-II, pp. 783-792, Oct. 1993, *in Japanese.*

[3] **S. Samejima, K. Enomoto and Y. Watanabe,** *Differential PSK system with nonredundant error correction*, IEEE J. Select. Areas Commun., vol. SAC-1, pp. 74-81, Jan. 1983.

[4] **D. Divsalar and M.K. Simon,** *Multiple-symbol differential detection of MPSK*, IEEE Trans. Commun., vol. COM-38, pp. 300-308, March 1990.

[5] **J. Yang and K. Feher,** *An improved π/4-QPSK with nonredundant error correction for satellite mobile broadcasting*, IEEE Trans. Broadcast., vol. BC-37, pp. 9-16, March 1991.

[6] **S. Kubota, T. Kohri and S. Kato,** *A SST (scarce state transition) type Viterbi decoder*, Trans. IEICE B, vol. J68-B, pp. 38-45, Jan. 1985, *in Japanese.*

[7] **W.C. Lindsey and M.K. Simon,** *Telecommunication systems engineering*, Englewood Cliffs, NJ: Prentice-Hall, 1973, ch.5, pp. 246-252.

Concept and Implementation of the Globalstar Mobile Satellite System

Joel Schindall
Globalstar L.P.
3200 Zanker Road
P. O. Box 640670, San Jose, California, 95164-0670, USA
Tel: 408-473-6201 Fax: 408-473-5040

ABSTRACT

Globalstar is a satellite-based mobile communications system which provides quality wireless communications (voice and/or data) anywhere in the world except the polar regions.

The Globalstar system concept is based upon technological advancements in Low Earth Orbit (LEO) satellite technology and in cellular telephone technology, including the commercial application of Code Division Multiple Access (CDMA) technologies.

The Globalstar system uses elements of CDMA and Frequency Division Multiple Access (FDMA), combined with satellite Multiple Beam Antenna (MBA) technology and advanced variable-rate vocoder technology to arrive at one of the most efficient modulation and multiple access systems ever proposed for a satellite communications system. The technology used in Globalstar includes the following techniques in obtaining high spectral efficiency and affordable cost per channel:

1. CDMA modulation with efficient power control.
2. High efficiency vocoder with voice activity factor
3. Spot beam antenna for increased gain and frequency reuse
4. Weighted satellite antenna gain for broad geographic coverage
5. Multisatellite user links (diversity) to enhance communications reliability
6. Soft hand-off between beams and satellites.

Initial launch is scheduled in 1997 and the system is scheduled to be operational in 1998. The Globalstar system utilizes frequencies in L-, S- and C-bands which have the potential to offer worldwide availability with authorization by the appropriate regulatory agencies.

Full text of the paper is in the Appendix page A-11

Adaptive Data Rate SSMA System for Personal and Mobile Satellite Communications

Tetsushi IKEGAMI, Takashi TAKAHASHI, Yoshiya ARAKAKI and Hiromitsu WAKANA

Communications Research Laboratory,
Ministry of Posts and Telecommunications
893-1 Hirai, Kashima, Ibaraki 314 JAPAN
Telephone: +81-299-84-7125
Fax: +81-299-84-7158
e-mail: ikegami@crl.go.jp

ABSTRACT

An adaptive data rate SSMA system is proposed for mobile and personal multimedia satellite communications without the aid of system control earth stations. This system has a constant occupied bandwidth and has variable data rates and processing gains to mitigate communication link impairments such as fading, rain attenuation and interference as well as to handle variable data rate on demand.

Proof of concept hardware for 6MHz bandwidth transponder is developed, that uses offset-QPSK and MSK for direct sequence spread spectrum modulation and handle data rates of 4k to 64kbps. The RS-422 data interface, low rate voice and H.261 video codecs are installed. The receiver is designed with coherent matched filter technique to achieve fast code acquisition, AFC and coherent detection with minimum hardware losses in a single matched filter circuit. This receiver structure facilitates variable data rate on demand during a call.

This paper shows the outline of the proposed system and the performance of the prototype equipment.

1. INTRODUCTION

Spread spectrum (SS) multiple access systems are widely studied for possible candidates of the future mobile and personal communication systems[1]. In these studies, mobile satellite communication systems for public networks usually utilize a pilot SS signal which is transmitted from base earth station for code synchronization, and the systems are centrally controlled by network coordination stations.

On the other hand, random access capability of the SS system without coordination stations is very attractive for personal and mobile satellite communication systems. Moreover, a distributed system which handles one-hop communication links between small earth stations is also attractive for personal and multimedia communications in private or non-profit networks[2].

We propose a variable data rate spread spectrum multiple access(SSMA) system for mobile and personal satellite communications and develop a prototype hardware system. The proposed system can be operated without coordination stations nor pilot signals. This paper deals with the proposed SSMA system and shows the outline of the proof of concept earth station developed. SSMA field tests are scheduled at S-band(2.1/2.2GHz) and O-band(38/43GHz) with ETS-VI satellite[3] as well as Ka-band(21/31GHz) and Q-band(43/47GHz) with COMETS satellite[4].

2. VARIABLE DATA RATE SSMA SYSTEM

Mobile satellite communication systems for public networks generally use a pilot SS signal for code synchronization and consist of mobile earth stations, central base earth stations and some coordination stations. In these systems, communications between mobile users need two-hop links for billing, i.e., base station

must relay the call between mobile users. The use of a pilot SS signal remarkably helps the code synchronization process of mobile stations whereas it sacrifices little transmitted total power from base stations.

On the other hand, the SS system has an advantage of random access capability without the aid of coordination station. This advantage is attractive for distributed personal and mobile multimedia satellite communication systems with user-to-user one-hop links. Multimedia communications in which various amounts of data should be transmitted for video, text and audio transmission, need variable data rate transmission systems. SS technique is capable of variable data rate systems, because various channels that handle different data rates can co-exist in the same SS bandwidth, and receiver implementation for variable data rate system is relatively easy.

As a result of the study mentioned above, we propose a variable data rate SSMA system for one-hop multimedia mobile and personal satellite communications. Figure 1 shows a concept of the system.

This system utilizes a constant spreading bandwidth and a fixed PN code length. In order to obtain necessary link margins at appropriate data rates, fading and rain attenuation can be compensated for by changing data rate and transmitting power. Appropriate data rate and quality on demand can be achieved whenever communication link is kept. Compared with the frequency division system, the advantage of the constant occupied bandwidth system is the adaptability of data rate variation during a call and maintaining minimal hardware complexities.

However, Automatic Frequency Control (AFC) at the receiving earth station is mandatory for one-hop system without the aid of network coordination station nor pilot signal. Necessary frequency range for AFC is around 10kHz in geostationary satellite systems at L-band (1.5/1.6GHz) and tends to 100kHz in low earth orbit satellite systems at S-band (2GHz) frequencies. Synchronization for code and carrier should be firm under fading and low C/N conditions which is a typical condition of mobile satellite communication channel.

Coherent matched filter (CMF) receiver[4][5] is suitable for this system. The CMF realize receiver AFC and coherent detection without the aid of pilot SS signal. The CMF technique makes it possible to recover a carrier and to demodulate data coherently from low S/N SS signals in fading channels. In a CMF receiver, two correlators for spreading code are inserted into both I and Q arm filters of the Costas loop demodulator.

3. PROTOTYPE HARDWARE

A prototype system for 6 MHz bandwidth transponder is developed for a scale model of 36 to 72MHz bandwidth standard transponders based on the proposals mentioned above. Figure 2 shows an overview of a prototype terminal. This prototype hardware consists of several circuit boards and installed in a standard rack bay to be easily modified the detailed circuit during a field test with real satellite channels.

Table 1 summarizes a general specification of the prototype system.

Both offset-QPSK and MSK direct sequence spread spectrum systems are examined for non-linear effect of HPAs of earth stations and transponders. Spreading sequence is chosen from augmented Gold code or arbitrary code of length 1024. The use of longer sequences for user identification is under study. Spreading code clock and bandwidth are fixed at 4.3Mbps and about 6MHz, respectively which corresponds to available transponder bandwidth of ETS-VI. Data rate is variable on demand and ranges from 4kbps to 64kbps. Rate 1/2 convolutional FEC code and Viterbi decoder are utilized for error protection of data. Data rate is changed during a call in accordance with the performance monitor output. Data rate can be also changed upon request at both transmitter and receiver sides whenever the link is established.

RS-422 data port is available for multimedia communication via workstations or PCs. Also installed are an H.261 video codec for TV conference and low rate voice

codecs. Ranging function is installed to measure the range between two earth stations via a satellite.

Signal format is designed as a fixed frame structure of 120 ms length as in Fig. 3. It consists of unique word (UW) for synchronization of data, data rate indicator bits, variable data rate status bits, and information bit stream. Except for the information bit stream, operating bit rate is 8.5kbps. Within an information bit stream of 112.94 ms, 960 to 15360 bits of data (including rate 1/2 FEC and overhead) run on 8.5kbps to 136kbps respectively.

Figure 4 shows a major block diagram of the receiver. The receiver is designed with coherent matched filter technique with multibit quantized digital correlators. It performs code synchronization, AFC and coherent detection of data in a single circuit. Range for AFC is +/-60kHz which corresponds to frequency drift of low earth orbit satellite system at S-band frequency. Correlation process for MSK is similar to OQPSK. It uses a quadrature detection scheme, correlators are inserted in both I and Q arms. The tap coefficient for reference spreading code is 1 bit, i.e., reference PN code pulse shape is rectangular, whereas true matched pulse for MSK-SS should be a raised cosine shape. This reduces the hardware size remarkably with a little mismatch loss.

Bit error rate performance is measured in the IF loop back mode. Figure 5 and 6 show bit error rate versus C/N_0 in MSK-SS mode. It should be noted that in MSK-SS mode, hardware loss is only about 1dB. Initial acquisition time including AFC over +/-60kHz is found to be about 2 second at average when C/N_0 is greater than 43 dBHz.

4. CONCLUSIONS

An adaptive data rate SSMA system is proposed for mobile and personal multi-media satellite communications without the aid of system control earth stations. This system has a constant occupied bandwidth and has variable data rates and processing gains to mitigate communication link impairments such as fading, rain attenuation and interference as well as to handle variable data rate on demand.

Proof of concept hardware for 6MHz bandwidth transponder is developed, that uses offset-QPSK and MSK for direct sequence spread spectrum modulation and handle data rates of 4k to 64kbps. The RS-422 data interface, low rate voice and H.261 video codecs are installed. The receiver is designed with coherent matched filter technique to achieve fast code acquisition, AFC and coherent detection with minimum hardware losses in a single matched filter circuit. This receiver structure facilitates variable data rate on demand during a call.

The loop back test performance of the prototype equipment is found to be feasible for personal and mobile satellite applications. SSMA field tests at S-band and O-band frequencies are scheduled in Spring this year with ETS-VI satellite and result will be described at the conference site.

The author would like to thank members of Toshiba Corporation for their help in development of the hardware.

REFERENCES

[1] Special Issue on Future PCS Technologies, IEEE Trans. VT-43, 3, Aug. 1994.

[2] H. Wakana, T. Ikegami, S. Yamamoto, N. Hamamoto, "An Overview of ETS-V/PARTNERS Project", ICT'95, Bali, Apr. 1995.

[3] H. Kitahara, T. Itoh, C. Harada, Y. Matsumoto, H. Kohata, "The ETS-VI Satellite", 15th AIAA Int. Satellite Com. System Conf., pp.1095-1101, San Diego, 1994.

[4] S. Ohmori, S. Isobe, M. Takeuchi, H. Naito, "Advanced Mobile Satellite Communications Using COMETS Satellite in MM-wave and Ka-band", IMSC'93, pp.549-553, Pasadena, June 1993.

[5] T. Ikegami, R. Suzuki, N. Hamamoto, N. Sato, "Experiments on a Coherent Matched Filter Receiver for Spread Spectrum Mobile Satellite Communications", IEICE Trans., Vol.E74, No.5, pp.1130-1136, May 1991.

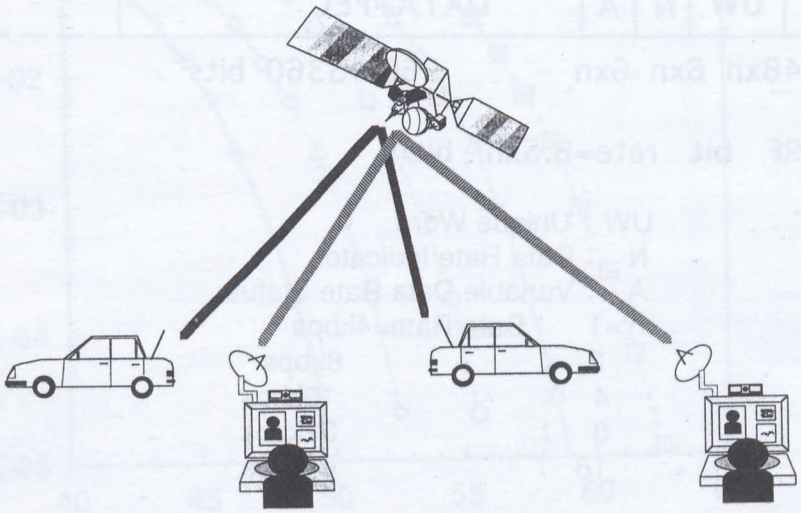

Fig. 1 System concept for variable data rate
SSMA satellite communications

Table 1 Major specification of hardware

IF Frequency	70 MHz
Modulation	DS-OQPSK, DS-MSK
Spreading code	Augmented Gold code or arbitrary, 1024 chips
Code clock	4.352 Mbps
Data Rate	Variable, adaptive or on demand 4, 8, 16, 32, 64kbps
Demodulation	Coherent Matched Filter, coherent detection
Matched Filter	Digital correlater, 2048 stages
Data Terminal	RS-422 I/F, H.261 Video codec (64 kbps), Voice codecs (4.8k, 9.6kbps)
AFC range	+/-60 kHz

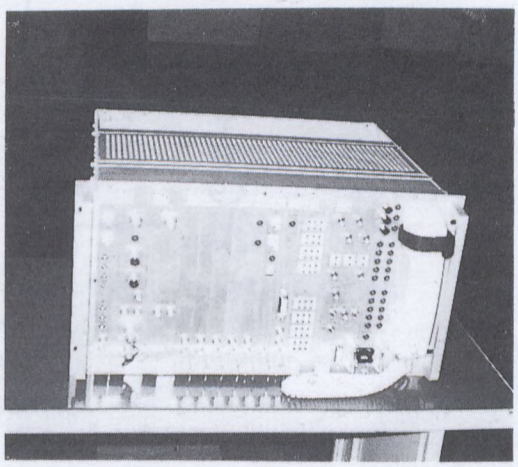

Fig. 2 Prototype terminal

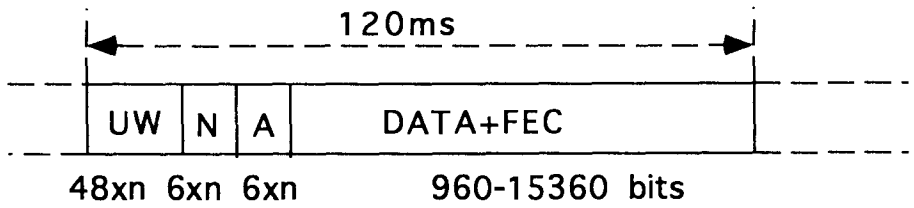

RF bit rate=8.5xn bit/s

UW : Unique Word
N : Data Rate Indicator
A : Variable Data Rate Status
n=1 : Data Rate=4kbps
2 : 8kbps
4 : 16kbps
8 : 32kbps
16 : 64kbps

Fig. 3 Signal frame format

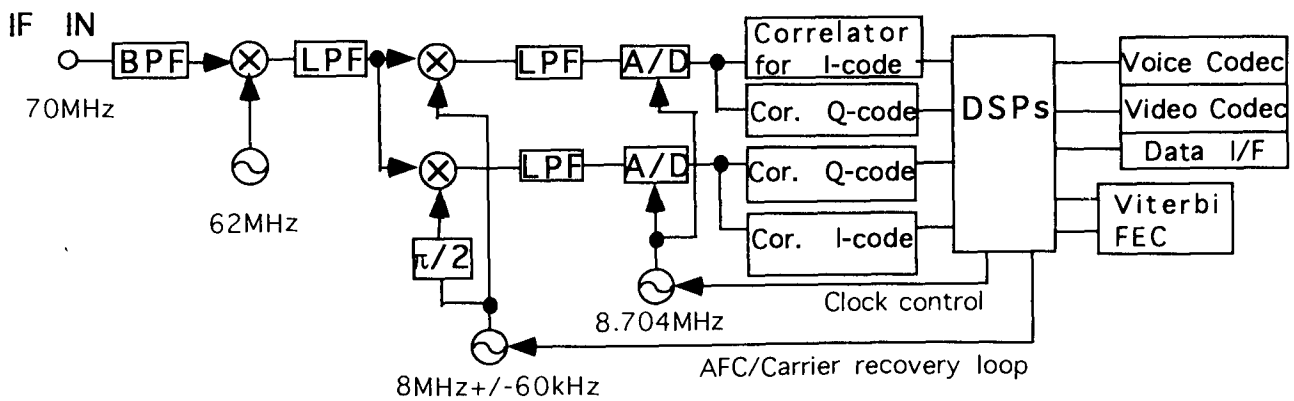

Fig. 4 Block diagram of receiver

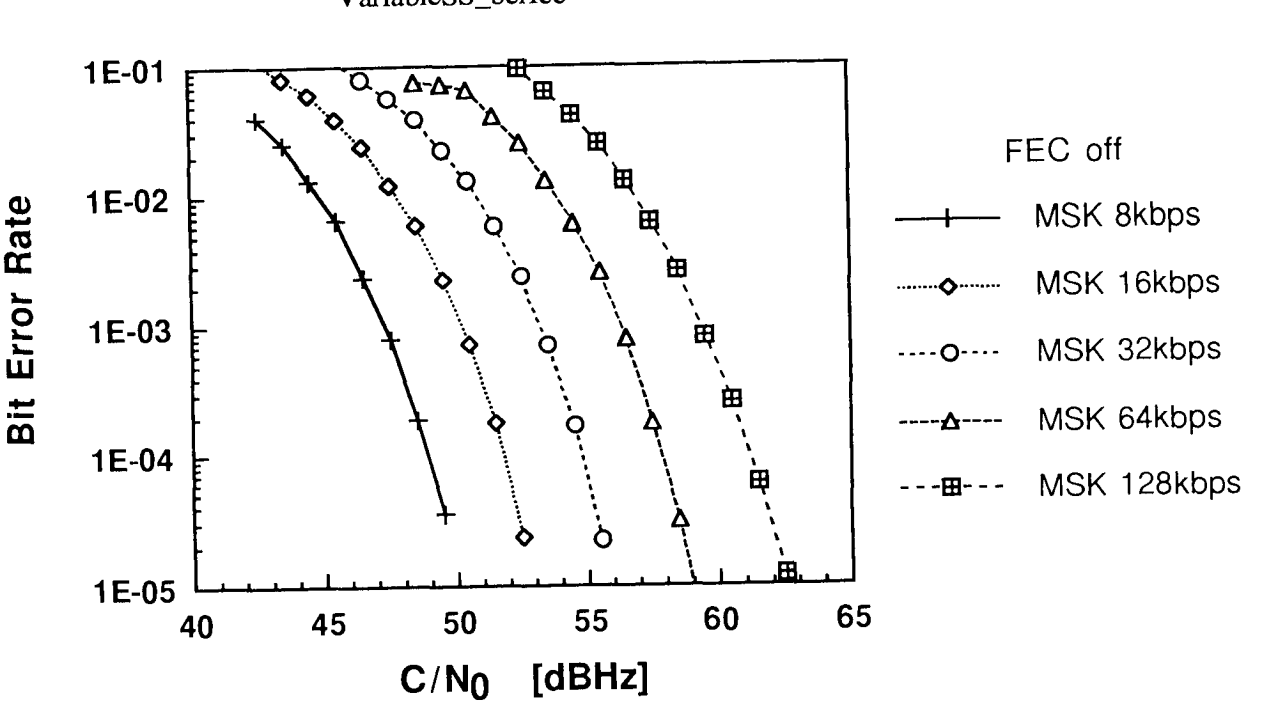

Fig. 5 Bit Error Rate performance
IF loop back, FEC off

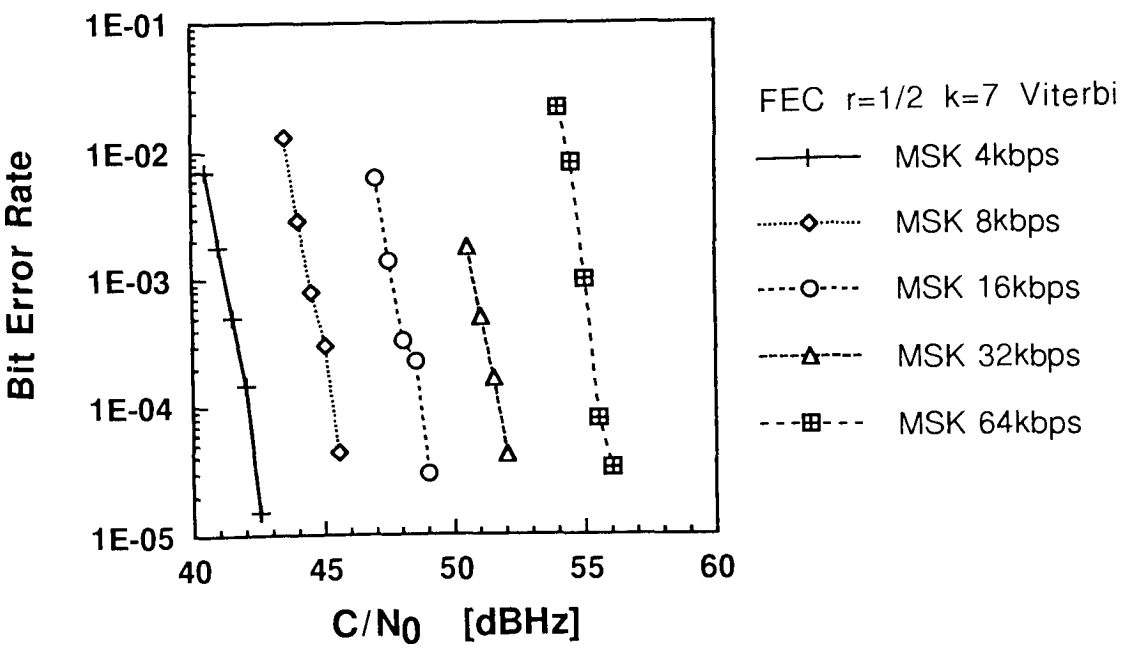

Fig. 6 Bit Error Rate performance
IF loop back, FEC on

Hybrid Networks - I

Session Chairman: **Mala Laurin,** Motorola Satellite Communications, USA
Session Organizer: **Polly Estabrook,** Jet Prolpulsion Laboratory, USA

Topic Introduction: This session is the first of two sessions exploring the challenges facing the integration of satellite and terrestrial networks. In this session, topics such as intersystem call delivery and call handoff are discussed. The first paper presents methods used to determine the location of mobile users; it discusses strategies to enable user handoff between satellite beams as well as between satellites. The second paper details several user terminal location algorithms and evaluates their performance with a LEO satellite system similar to IRIDIUM® . The third paper examines several traffic sharing algorithms to enable intersystem call handoff and presents the resultant user grade of service attainable over a range of traffic loads. The fourth paper compares the threshold power level at which intersystem call handoff is required when soft and hard handoff strategies are utilized. The fifth and last paper discusses issues in user mobility management in hybrid networks supported by an Intelligent Network architecture.

Mobility Management in Satellite Networks

Gary A. Johanson
Westinghouse Electric Corporation
Mobile Communications Department
P.O. Box 746, MS 8665
Baltimore, MD 21203, USA
Phone: +1-410-765-9045 FAX: +1-410-765-9745

ABSTRACT

This paper addresses the methods used or proposed for use in multi-beam and/or multi-satellite networks designed to provide Mobile Satellite Services (MSS). Specific topics include beam crossover in the North American Mobile Satellite (MSAT) system as well as registration and live call hand-off for a multi-regional geosynchronous (GEO) satellite based system and a global coverage Low Earth Orbiting (LEO) system. In the MSAT system, the individual satellite beams cover very large geographic areas so the need for live call hand-off was not anticipated. This paper discusses the methods used to keep track of the beam location of the users so that incoming call announcements or other messages may be directed to them. Proposed new GEO systems with large numbers of beams will provide much smaller geographic coverage in individual beams and thus the need arises to keep track of the user's location as well as to provide live call hand-off as the user traverses from beam to beam. This situation also occurs in proposed LEO systems where the problems are worsened by the need for satellite to satellite hand-off as well as beam to beam hand-off within a single satellite. The paper discusses methods to accomplish these hand-offs and proposes system architectures to address the various hand-off scenarios.

INTRODUCTION

This section begins by describing the functions required for mobility management by using the familiar terrestrial cellular system as an example. Then mobility management in satellite networks is introduced including the special topic of hybrid satellite/terrestrial cellular networks.

Mobility Management

Mobility management is a system of functions and protocols that allow mobile terminals to roam freely about the network and communicate at will. In standard "wireline" networks, a telephone directory number is associated with a particular physical pair of wires that leads to a specific telephone instrument. In this case, no mobility management is required since the system is all physically connected. This system works very well when the parties wishing to communicate can be near these instruments. This is not always possible. Telephone networks using wireline connections are most often limited by the economics of running physical wiring to everyone in the area who wishes to communicate. This becomes a very large expense when rural areas with sparse populations are considered where it may cost more that $10,000 to connect one rural customer - a sum not likely to be recovered quickly by subscription fees. Mobility management is required when the telephone instrument is allowed to move about unencumbered by physical connections to wires. Cellular telephone networks are examples of systems where mobility management is needed. In these systems, every mobile phone has a home. This is called the Home Location Register (HLR). Each of these mobile phones has a Mobile Identification Number (MIN) that is used to locate the phone. This is the phone's directory or telephone number. When someone dials this number, say from a "wireline" phone, the terrestrial network directs this call to the location of the HLR. If the mobile phone is in touch with the HLR directly, the call is connected right away. The mobile phone can move, however, and is often not in contact with the part of the system that contains the HLR. As the mobile phone moves about, it is continually coming into contact and subsequently losing contact with various "cells". These cells are provided by radio transceivers that are connected into the mobile switching centers that serve a given area. Each time a new cell is entered, the mobile

phone and mobile switching center (MSC) communicate so that the MSC can immediately find the mobile phone if a call comes in for it. Once the mobile phone moves outside of the mobile switching center area that contains its HLR, then it must activate a function of mobility management known as the Visiting Location Register (VLR). MSCs are connected to each other and communicate via signaling channels. When a mobile phone enters into the territory of a MSC that does not contain its HLR, it identifies itself to that system which reads the mobile phone's MIN. The MSC decodes the MIN and contacts the appropriate HLR and tells it via the signaling channel that a mobile with that MIN has entered its territory and that a VLR has been set up. Now if a call comes through for that mobile, it will still be directed to the HLR first, but the HLR will then divert the call to the MSC that has set up the VLR because that is where the mobile phone is now located. You can see how the mobile phone can always be contacted as long as it is in range of a MSC that contains its HLR or one that has agreed to handle VLRs for the MSC containing its HLR. Another important aspect of mobility management is the live call hand-off. This allows a call that is in progress to continue as the mobile phone moves out of coverage of one cell and into the coverage of another. This can be done between adjacent cells within the same or even different MSCs. Cellular networks are economically constrained like wireline networks in that it is very expensive to build out cellular coverage into rural areas with sparse populations requiring infrequent communications. Satellite networks can overcome some of the financial difficulties of terrestrial wireline and mobile networks since they are capable of covering vast areas from a single point. Satellite networks can also have mobility management requirements which will be discussed next.

Mobility Management in Satellite Networks

A satellite network as defined in this paper consists of a single or multiple cooperating satellites providing communications services to Mobile Terminals (MT). Of course, some satellite terminals do not need to be mobile and for them mobility management has not been required. This situation is about to change with the introduction of Low Earth Orbiting Satellite Systems described later. A familiar system utilizing mobility management is the INMARSAT system which has divided the globe into regions (very much like very large cell sites in a terrestrial cellular network). Another is the North American MSAT system which is described in this paper. Mobility management has three major functions:

- Roaming Call Origination
- Extended Call Delivery, and
- Live Call Hand-off.

Roaming call origination allows the MT to make calls whenever it is in contact with the satellite. This is a situation similar to the mobile phone as it can always originate calls through the mobile switching center that it is connected to.

Extended call delivery allows an incoming call to be directed to the MT. This is not a problem in some regional networks such as the Mobilesat® system in Australia and the Movisat system in Mexico as their satellites have only a single beam covering the entire region. The INMARSAT system has many satellites and many regions. Similarly, the MSAT system will have many beams dividing the region. Again the situation is similar to the cellular networks in that a MT will notify the system control center that it has acquired the signal from a new area (region/beam). The satellite control center will mark the new location in its database so it will know where to find the MT when a call comes in.

Live call hand-off allows a call in progress to continue when a MT travels between regions or beams. Since the regions and beams cover very large distances, this function was not designed into the INMARSAT or MSAT systems since the call duration's were expected to be minutes but it would take hours or days to enter into another region. This situation is also about to change as described below.

Mobility Management in Hybrid Terrestrial/Satellite Networks

The MSAT system offers the special case of cellular interoperability as it provides roaming call origination and extended call delivery to specially equipped MTs whether they are in contact with the cellular network or the satellite system. Such MTs may be homed on either system and a VLR will be set up when the other is visited. Live call hand-off is supported when operating strictly within the cellular network and is not provided when operating strictly within the satellite network as described above. In the MSAT system, live call hand-off is also supported between cellular and satellite systems in the direction of cellular to satellite only. Once a call is transferred to the satellite system, it stays there until the call is terminated. There is no provision to return the ongoing call to the cellular network.

The remainder of the paper discusses how the MSAT system recognizes that a MT has moved into the coverage of another beam than the one in which it registered followed by how mobility management could be provided by a large multi-region geosynchronous satellite system or by a Low Earth Orbiting Satellite System.

MSAT SYSTEM

The first generation MSAT system uses one or more satellites to cover North America. The satellite design provides six beams. The first four beams divide up the majority of the territory and cover the East, East/Central, West/Central, and Western regions of the United States and Canada. The fifth beam covers the states of Alaska and Hawaii while the sixth covers the southern reaches of North America including the Caribbean. A MT may move freely about any of these regions and communicate as well as have incoming calls directed to it as described below.

Terminal Registration and Movement

Once a MT has been commissioned into the system, it may move about freely making and receiving calls while in any part of North America as long as it has line of sight visibility to the satellite. During commissioning, the MT was assigned to a particular beam as its home region/beam (East, East/Central, etc.). The MT is also loaded with information about the other beams. When a MT is first activated, it searches for the forward broadcast channel assigned to its home beam. If that channel is found, it need do nothing as the system will assume that the MT is in its home beam. After the MT has verified that its database is up to date, it will allow incoming or outgoing calls. If the MT subsequently loses or cannot find its home beam upon power-up, it will look into its database and begin searching for the broadcast channels for the other beams. When it finds one, the MT signals the control center that it has crossed over into the coverage of a different beam. That beam then becomes the MT's new home beam and calls will be directed to it there. This is all fairly simple as the MT does not have to register unless it moves a great distance which will not happen very often. Other parts of the World are proposing networks that also cover very large regions but with smaller beam sizes or rapidly moving satellites. This brings on more difficult registration and hand-off situations which will be discussed next.

MULTI-REGIONAL GEOSYNCHRONOUS SYSTEM

This type of system is being proposed for large regions that cross many political borders. Two systems are in the planning stages. One is proposed to cover from China in the North to India and then Eastward to cover all the rest of Asia through Indonesia. Another plans to cover Africa, the Mid-East, and India. These systems are characterized by very large satellites, many spot beams (at least in one case greater than 200), a large space-deployable antenna, and very high capacity compared to MSAT. These systems also plan to offer voice service directly to users with hand-held transceivers. These two systems are proposed by separate organizations which may not offer interoperability so that when the user leaves the service area of one system, he may not be able to continue to use his phone. Still, with these two systems operating along with those planning to go into service soon in North America and Australia, a very large portion of globe will have additional mobile satellite service. With hundreds of spot beams per satellite, the earth coverage within any one beam will be much smaller than it is with MSAT. Therefore, the system designers must consider what type of mobility management will be required. The difficulties of operating across many political borders adds to the complexity. This section discusses several aspects of mobility management for this type of system: User Location, User Movement within an "Operating" Region, User Movement Outside of a Home Operating Region, and Beam to Beam Hand-off.

User Location

The location method used for this system may be almost as simple as that used on MSAT. The User Terminal (UT) would search for the home beam frequency and then one from an internal database list if the home frequency is not found. The UT must then decode the broadcast information being received to determine what region is being received since it is likely that the satellite system will reuse frequencies in geographically separate beams. If the UT finds it is anywhere except where it last registered, it would access the control center via a signaling channel and re-register itself. It is possible at this point that the UT has entered a region that does not have an operating agreement with its home region and thus service would be denied. If this is to be the case, a more precise method of position location may be required such as would be available through the use of the Global Positioning Satellite (GPS) service. With GPS, service could be offered or denied even within the same satellite beam due to border crossings but this would increase the amount of call processing that would

be required at each call setup. Once the UT has been located, it may be moved about freely or powered off/on without having to use satellite and control center resources as long as it stays within the same satellite beam. In this case, UT location is much like MT location in the MSAT system.

User Movement within an "Operating" Region

An operating region may be a very small country or a very large area covering several cooperating countries. It is characterized by having a single service supplier that registers UTs, provides mobile satellite services, and collects revenue from the calls made. A large country like China may have several operating regions. If an operating region has only one satellite beam, then mobility management within the region is not required. It is possible, however, that a very small region or country may be better served by partnering with a larger region with which it has a cooperative telecommunications agreement since the installation and operation of an entire ground segment for a small region may be too expensive. Here the small region would become a sub-region of the larger operating region and would operate under the mobility management rules of the larger region. In such a case calls to or from UTs within the region would be terminated at the larger region's ground station and would be trunked terrestrially from and to the smaller region. An interesting exception could be UT to UT calls that would originate and terminate within the same small region. This may not even require transmission through the large region's gateway as the satellite may be able to route UT to UT calls itself using on-board processing. A large operating region may require several ground entry points called "gateways". The regions then begin to look like cellular telephone systems with multiple cell sites as far as mobility management is concerned. As UTs move about the region and even into beams covered by ground stations not holding their "Home Location Register" information, a beam change entry could be made in the database at the operating center in the home region that would allow extended call delivery to the ground station and satellite beam where the UT was last registered. If the region was very large and the UT had to be reached via or wished to make calls through another ground switching point, a VLR would be set up for more efficient processing of call information. This architecture may be extended to UTs moving between operating regions.

Movement Outside of a Home Operating Region

As long as the regions have cooperative operating agreements, a UT may make or receive calls while away from the coverage of the home region. Registration information would be passed to the "visited" region which would set up a VLR for that UT. If the UT subsequently moved to a third region or back home, the first VLR would automatically be canceled by the HLR like function at the UTs home. Setting up these agreements between regions may be difficult if they are between countries not used to working together and thus may require some positive form of geolocation (such as GPS as discussed above) to be used at each call setup in order to police the revenue flow. This will add to the cost of these systems if necessary.

The UT can now move freely throughout the satellite's coverage area and make or receive calls. Once a call is in progress, the third area of mobility management comes into play - hand-off.

Beam to Beam Hand-off

As beam area coverage becomes smaller, the system designer must consider whether or not live call hand-off will be supported within the system. If required, it will add considerably to the complexity of the system and to its overall cost. Live call hand-off, to be useful, must be seamless. That is, the user must not be aware that a hand-off is taking place and will accept only the briefest of call interruptions when the hand-off actually takes place. Call hand-off is one of the most difficult portions of mobility management to address. This is especially true in the mobile satellite system where there are considerably longer delays in signal paths than in terrestrial systems. This situation would be particularly burdensome in a UT to UT call via a processing satellite. Virtually all of the hand-off decision making would have to be in the UT itself as the signals would not be accessible at the ground control center. As was discussed in the beginning of the paper, the MSAT system designers chose not to include this requirement on that system. The choice may not be so easy in the future as technology allows the satellite beam spot size to shrink even more. The next section discusses LEO satellite systems where live call hand-off is not an issue - it must be designed into the system from the start!

LOW EARTH ORBITING SYSTEM

Several LEO systems are proposed to provide global or virtually global communications capability within the next few years. Rather than discuss a particular system, this paper addresses the generic mobility management problems faced by them. Also, the methods suggested here are not tied to any particular access scheme. The LEO providers are contemplating two access schemes: Time Division Multiple Access (TDMA) and Code Division Multiple Access. GEO providers are currently considering TDMA and Single Channel Per Carrier access.

LEO System Description

The generic LEO system has the characteristic of satellites that are moving rapidly relative to the User Terminals (UTs) they are communicating with. This is in contrast to the GEO system discussed above where the satellites relative position is changing much more slowly. What this means to mobility management is that it is very likely that during a given call, the communications link to the UT will have to be switched between beams on the same satellite or may have to be switched between satellites. The LEO system is similar, again, to the terrestrial cellular telephone networks where the users are moving rapidly relative to the cell sites and must be handed-off between them. Here the beams of the satellites are moving rapidly across the ground and the UTs appear not to move. It is really the same situation. Some LEO systems help solve this problem by mechanically or electronically "steering" their beams so that they maintain a fixed location on the earth. Since the satellites continue to move, the ability to maintain this beam steering is limited and hand-offs will eventually be required or calls will be dropped. Location and registration in LEO systems may be handled in a manner similar to the GEO systems. The major difference is that the UT will search for the characteristic signal from its home ground station rather than its home beam since the beams are moving. The real difficulty with LEOs is in the hand-off process. When not in a call, the UT can afford some delay as it acquires the signal from a new beam. This is not desirable, however, because this happens quite often and the UT is effectively out of service during this time. Two cases are discussed: hand-offs within the same satellite and between satellites.

Beam to Beam Hand-offs Within a Single Satellite

As the satellite communications beam moves across the earth's surface, the UT will begin to loose the communications signal. Before this happens, the call must be switched to the next beam. Since it is possible that the transmit and receive frequencies at the UT may be one GHz apart, the communications channel may not be reciprocal meaning that the path to the UT and the path from the UT will not act the same. Then the UT itself should participate in the hand-off process. We call this a mobile assisted hand-off. The UT will likely be outfitted with dual receivers. One to process the communications in the current beam and one to search for and acquire the next. An alternative to this would be a precisely timed signal such that the UT could switch or be switched remotely at just the right moment. This could be accomplished at the expense of a more complicated ground processing facility and would work during a call but not between them when the UT is not transmitting.

With dual receivers at the UT, the second receiver would search for the signal from the next beam, would acquire it, and would begin processing it. When the signal quality was as good as or better that that from the operational beam, the UT would switch itself if not in a call or would notify the control center (via in-band signaling) that a new beam could/should be used. In addition, when in a call, the second receiver associated with the call at the ground control center would be waiting for the signals sent from the UT. When found, the ground station would use the better of the two signals (or coherently combine them) and may use the information to switch the transmitter for that call to the adjacent beam. This situation works well within the same satellite and using the same ground control center. When switching between satellites, additional considerations come into play.

Beam to Beam Hand-offs Between Satellites

Two satellites in view may have large differences in relative velocity and in path delay. The differences in velocity cause differential Doppler shifts that can be compensated for to some extent at the ground control center. The path delay differences must be compensated for by signal buffering. This could be accomplished at the ground control center also during any given call. After these effects are accounted for, the process for satellite to satellite hand-off becomes similar to beam to beam hand-off within the same satellite as discussed above.

The system designer can make very good use of a system that has enough satellite coverage to have two satellites in view of the user terminals for most of the time. This situation could be exploited to allow communications to

continue when the path to one of the satellites is blocked by a building or terrain. This would most likely be implemented using soft hand-off techniques for fast response and user comfort.

An additional complication that the system designer has to think about is the possibility of hand-off simultaneously between satellites and between ground control centers. This is a situation requiring further study and may not be needed in all cases but if needed, the system designer would do well to study what is being done in cellular telephone systems in order to reduce the amount of new engineering that has to be done.

SUMMARY AND RECOMMENDATIONS

This paper has shown that mobility management in satellite networks faces many of the same issues as in cellular telephone networks. Also, there has been in the industry a desire to offer cellular interoperability as a feature of new mobile satellite systems. In recent work at Westinghouse, this issue has received extensive study with the conclusion that today, the best choice for designing a new mobile satellite system's mobility management functions would be to start with the Global System for Mobility (GSM) standards now in place and build on them. The GSM standards body is currently working on augmenting the standards to include a satellite capable terminal. This bodes well for the industry since it offers the hope that future mobile satellite systems and terminals could be built to a standard set of protocols thereby reducing the cost to the consumer.

A UT Positioning Approach for Dynamic Satellite Constellations

W.Zhao, R.Tafazolli, B.G.Evans
Mobile Communication Research Group
Centre for Satellite Engineering Research (CSER)
University of Surrey, Guildford, Surrey, GU2 5XH U.K.
Tel: +44-483-259808 Fax: +44-483-259504

Abstract - In this paper, we discuss a new positioning scheme which is thought to be applicable for dynamic satellite constellations. We begin with the introduction of our filter model which is based on stochastic process and filtering theory. Then, simulation results of the technique are presented based on a LEO constellation and some of the IRIDIUM system parameters. Performance of this algorithm is investigated under various noise conditions. Finally, several applications of this UT positioning algorithm are discussed.

INTRODUCTION

Satellite system will play an important role in the future global communication system. User terminal(UT) location information is a key factor both for mobility management, mobile terminated call, and even for handover. Much attention has been paid to UT positioning scheme in recent years. It is considered that the more accurate is the UT's position, the less signalling transmission is required through network. An efficient signalling load can only be achieved through reduced positioning uncertainty. Positioning algorithm analysed in this paper is based on delay and Doppler shift which can be measured in a ground station during a call for each active UT. The combination of these parameters can be used to determine the UT's position. In the process of calculating a UT position, some assumptions had to be made. Firstly, we assumed the user's movement is negligible compared with that of satellite; Secondly, a satellite moves along its true orbit and no deviation for this orbit is assumed. Finally, surface of the earth is a perfect sphere and no uneven surface is assumed.

1. Positioning scenarios

Suppose at the beginning of the calculation, satellite is at position '**S**' and it is moving in the direction ***v***. We establish a right-handed rectangular three dimensional co-ordinate system which centred at the earth's centre '**O**' in following way: The **z**-axis passes through initial satellite position(t=0), (**y**,**z**) plane is the satellite orbit plane and the x-axis completes a right-handed co-ordinate system. This is shown in Figure-1. Suppose the user terminal is at position-**P**, then '**θ**' is the angle between satellite moving direction and line '**SP**'. The angle between line '**SO**' and z-axis is defined as 'γ' which is an available value for the network at any time. Distance '**SO**' is constant value ***R+H***(***R***: radius of the earth, ***H***: altitude of the satellite). By measuring Doppler shift ***fd1*** and delay ***td*** from **S** to **P** on network side, UT's position expressed by ***(x,y,z)*** can be determined in this three dimensional co-ordinate system. The measurement and calculation are conducted by the network and no signalling exchange with the active UT is necessary.

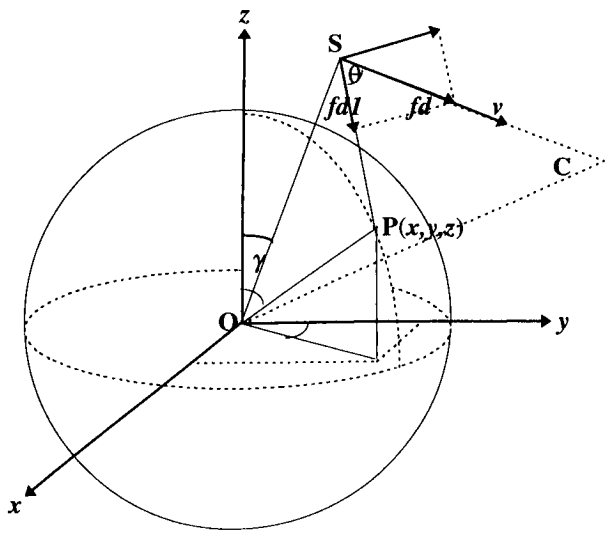

Figure-1 Relation between satellite and UT

Doppler shift:
According to the moving speed and direction for each satellite, Doppler shift magnitude along its moving direction ***v*** can be calculated at any time by network, this is identified by ***fd*** in Figure-1. During a call, the Doppler shift component along the direction of the line '**SP**' can be measured by network, which is identified by ***fd1***. Relation between ***fd*** and ***fd1*** can be expressed by Equation-1.

$$fd1 = fd \cdot \cos\theta \qquad \text{<Equation-1>}$$

Delay:
Delay (or distance) from a UT to satellite can be measured all the time during a call. If UT's position is (***x,y,z***), satellite position is (x_S, y_S, z_S) which is expressed by

Equation-2, relation between ***td*** and UT position can be expressed by Equation-3(***c*** is the velocity of light).

$$x_S = 0$$

$$y_S = (R+H)\cdot\sin\gamma \qquad \text{<Equation-2>}$$

$$z_S = (R+H)\cdot\cos\gamma$$

$$(x-x_S)^2 + (y-y_S)^2 + (z-z_S)^2 = (c\cdot td)^2$$

< Equation-3>

UT position:

In order to get UT position, some other factors have to be used. The UT is supposed to be located on a perfect round sphere with a radius ***R***, this is expressed by Equation-4.

$$x^2 + y^2 + z^2 = R^2 \qquad \text{<Equation-4>}$$

The other factor is the relation between θ and position **'S'**, **'P'** and **'C'**(extended from **'S'** along the direction ***v*** with length ***R+H***).

$$\cos\theta = \cos(SP_x)\cos(SC_x) + \cos(SP_y)\cos(SC_y) + \cos(SP_z)\cos(SC_z)$$

<Equation-5>

In Equation-5, $\cos(SP_x), \cos(SC_x)$ are direction cosine of line **'SP'** and **'SC'** along ***x*** axis. These direction cosine can be expressed by Equation-6. For direction cosine along ***y*** and ***z*** axis, similar expressions apply.

$$\cos(SP_x) = \frac{x - x_S}{\sqrt{(x-x_S)^2 + (y-y_S)^2 + (z-z_S)^2}}$$

$$\cos(SC_x) = \frac{x - x_C}{\sqrt{(x-x_C)^2 + (y-y_C)^2 + (z-z_C)^2}}$$

<Equation-6>

Co-ordinate of point $\mathbf{C}(x_C, y_C, z_C)$ is expressed in Equation-7.

$$x_C = 0$$

$$y_C = \sqrt{2}(R+H)\sin(\gamma + \frac{\pi}{4}) \qquad \text{<Equation-7>}$$

$$z_C = \sqrt{2}(R+H)\cos(\gamma + \frac{\pi}{4})$$

Finally, UT position (***x,y,z***) can be obtained by combining Equations 1-7. For a stationary terminal, its co-ordinate (***x,y,z***) should be determined using ***td*** and ***fd1***. It is reasonable that the solution is not unique. But this uncertainty can be eliminated if the network knows through which spotbeam the active UT is communicating.

2. Measurement and evaluation

2.1 Uncertainty with single sample

During a call, samples are taken with time interval τ at $t_0, t_1, \cdots t_k \cdots t_{N-1}$, $t_k \in [t_a, t_b]$, k=0,1···N-1. τ is determined by different system. If the active UT is stationary and samples of Doppler shift and delay are accurate enough, each pair of samples will result in the same UT position according to the algorithm mentioned before. In the real situation, these measurements are generally contaminated with noise caused by the electronic and mechanical components of the measurement device. The accuracy for UT position is greatly influenced by measurement noise so that produced position P_k at each sampling time t_k (k=0,1,...N-1) is variable.

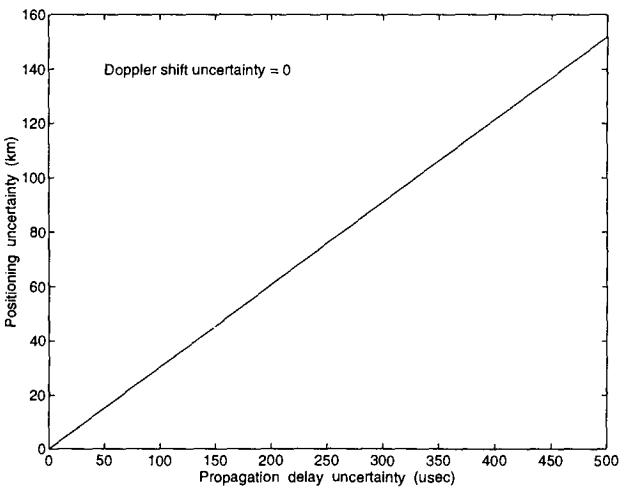

Figure-2: Positioning uncertainty vs. delay uncertainty

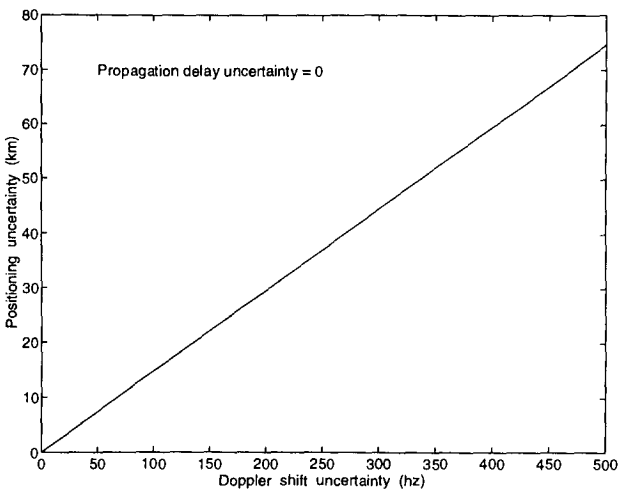

Figure-3: Positioning uncertainty vs. Doppler shift uncertainty

Figure-2 and Figure-3 have shown the positioning uncertainty along with the changes of measurement error both for delay and Doppler shift. From these figures we can see that uncertainty obtained from each single sample is quite large. Thus eliminating UT positioning uncertainty from noisy measurement is one of our major task in this paper.

2.2 Uncertainty for average position

Since a number of samples can be obtained during a call, and since the active UT is supposed to be stationary, one reasonable solution is to decrease uncertainty by averaging those positions calculated from each samples. If the measurement noise for delay and Doppler shift is zero mean, finally obtained position should tend to true value if the number of samples is large enough. Figure-4 shows some results obtained from average position. In obtaining Figure-4, UT position components on x, y and z axis are calculated separately for each pair of samples. Mean value $\overline{P(x,y,z)}$ is obtained for each component by averaging all the results(e.g. $x_0 \cdots x_{N-1}$, $y_0 \cdots y_{N-1}$, $z_0 \cdots z_{N-1}$). Positioning uncertainty is obtained by calculating distance between true position $P(x,y,z)$ and average position $\overline{P(x,y,z)}$.

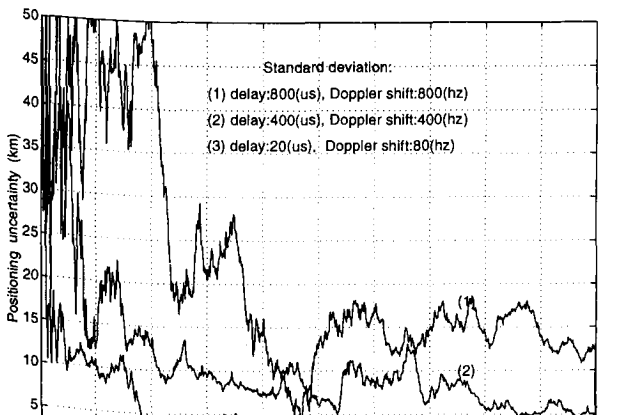

Figure-4
Positioning uncertainty by average samples

From Figure-4, positioning uncertainty decreases along with the increase of sampling number; Standard deviations for delay and Doppler shift measurement have great influence on these results; The rate of change of uncertainty tends to be constant after sample number is around 600-800. Two problems for this algorithm exist: First of all, resulted positioning uncertainty is not stable even though the sampling number is already very large. This can be seen from the fluctuation for each curve in Figure-4. Because of this fluctuation, the maximum uncertainty is determined by the peak in each curve(e.g. for the curve (3), average uncertainty is around 2km after 600 samples, but maximum value can be as high as 4km). The reason for this fluctuation comes from the fact that we consider all samples having the same importance even though some of them have very large deviation. Another problem is large amount of memories needed in this algorithm. From the beginning of a call, each measurement sample has to be stored for later calculation. For a ground station which processes hundreds of calls at the same time, large memory is required. In the next section, we demonstrate that these problems can be avoided if a Kalman filter is used to eliminate measurement noise.

3. UT positioning with Kalman filter

It has been foreseen that a Kalman filter is helpful in getting accurate position with reasonable number of samples. This section will discuss this technique in details.

3.1 Kalman filtering theory

The problem of determining the state of a system from noisy measurements is called noise filtering, and is the main subject of Kalman filtering theory[6][7]. First of all, we define the filtering problem and Kalman filtering procedure in the context of the mathematical model used in this paper. This is shown in Appendix.

For a dynamic satellite system, our target is to calculate accurate UT position by using the Kalman filter, with reasonable number of samples(delay and Doppler shift) as input. In order to achieve this, several steps have to be followed: Selecting parameters to represent system state; Establishing system model; Establishing filtering scheme.

3.2 Filtering scheme for LEO system

According to <A-3>, a linear mathematical expression is necessary in order to make use of Kalman filter. This means the relationship between system states at different sampling time should be linear. For a dynamic system like a LEO satellite constellation, a large number of parameters can be chosen to represent system state, but only part of them result in linear expression. In this paper, we choose relative position and relative velocity between satellite and UT as system states. This results in a linear expression and hence the calculations can be greatly simplified.

Each system state has three components (x,y,z) in a three dimensional co-ordinate system. These three components can be produced separately by using three filters with each of them working along one direction(x, y and z axis). This means each time after obtaining samples of delay and Doppler shift, we input them into these three filters and get output about system state(relative position and relative velocity, one dimension from each filter). Finally, UT position can be obtained from this relative position (since satellite position is an available knowledge all the time). In most cases, after each step of iteration, the new position will be more accurate comparing with the original one. Following is detailed introduction about system modelling and filtering results.

3.2.1 System modelling

Assuming we have a disturbance-free satellite orbit. Then satellite position $\vec{r}_s$, velocity $\vec{v}_s$ and acceleration $\vec{a}_s$ can be expressed by Equation-8.

$$\vec{r}_s = x_s \cdot i + y_s \cdot j + z_s \cdot k$$

$$\vec{v}_s = \frac{d\vec{r}_s}{dt} = v_x \cdot i + v_y \cdot j + v_z \cdot k \qquad \text{<Equation-8>}$$

$$\vec{a}_s = \frac{d\vec{v}_s}{dt} = a_x \cdot i + a_y \cdot j + a_z \cdot k$$

If we establish our three dimensional co-ordinate according to Figure-1, each component in $\vec{r}_s$ can be expressed by Equation-9 with angular velocity ω and initial angle θ_0.

$$x_s = 0$$

$$y_s = (R+H)\cdot\sin(\omega t + \theta_0) \qquad \text{<Equation-9>}$$

$$z_s = (R+H)\cdot\cos(\omega t + \theta_0)$$

For a user terminal at position $\vec{r}(x, y, z)$, we establish system model in x-axis as follow:

Defining a 2×1 vector $\vec{e}$, its two components are relative position and relative velocity between satellite and stationary UT.

$$\vec{e}^{\,T} = [\vec{r}_s - \vec{r}, \vec{v}_s] \qquad \text{<Equation-10>}$$

Then, we have:

$$\dot{\vec{e}} = \begin{bmatrix} 0 & 1 \\ 0 & 0 \end{bmatrix} \cdot \vec{e} + \begin{bmatrix} 0 \\ \vec{a}_s \end{bmatrix} \qquad \text{<Equation-11>}$$

It is easy to verify that the state transition matrix of this system is:

$$\varphi(t,\tau) = \begin{bmatrix} 1 & t-\tau \\ 0 & 1 \end{bmatrix}$$

so that

$$\vec{e}(t) = \varphi(t,\tau)\cdot\vec{e}(\tau) + \int_{\tau}^{t} \begin{bmatrix} 1 & t-s \\ 0 & 1 \end{bmatrix} \begin{bmatrix} 0 \\ \vec{a}_s \end{bmatrix} ds$$

Finally, we have

$$\vec{e}(t+1) = \begin{bmatrix} 1 & 1 \\ 0 & 1 \end{bmatrix} \cdot \vec{e}(t) + \int_{t}^{t+1} \begin{bmatrix} 1 & t+1-s \\ 0 & 1 \end{bmatrix} \begin{bmatrix} 0 \\ \vec{a}_s \end{bmatrix} ds$$

<Equation-12>

For each dimension (**x,y,z**), we have a similar expression as Equation-12. Taking x-dimension as example, we have

$$e_x(t+1) = \begin{bmatrix} 1 & 1 \\ 0 & 1 \end{bmatrix} \cdot e_x(t) + \int_{t}^{t+1} \begin{bmatrix} 1 & t+1-s \\ 0 & 1 \end{bmatrix} \begin{bmatrix} 0 \\ a_x \end{bmatrix} ds$$

<Equation-13>

Comparing Equation-13 with <A-3>, we find a linear dynamic system model has been established. Because we are considering a disturbance-free satellite orbit, $\Gamma(k)$ becomes zero.

Now we obtain the relative position ($\vec{r}_s - \vec{r}$) and relative velocity $\vec{v}_s$ between UT and satellite in each dimension, they are calculated from delay and Doppler shift measurement which are contaminated with noise.

If we take scalar measurement (relative position only), in x-dimension we have

$$y_t = [1 \quad 0]\cdot e_x(t) + v_t \qquad \text{<Equation-14>}$$

This is our system measurement expression with $M(t) = [1 \quad 0]$ in <A-3>. Because our original measurement is not relative position, a translation from delay and Doppler shift to relative position is necessary.

Finally, we obtained a dynamic system model in x-dimension expressed by Equation-13 and 14. For y and z-dimensions, we have similar expressions. A Kalman filter can be used directly into these three system models.

3.2.2 Positioning result

Some results have been given in this section. We define positioning uncertainty by calculating distance between simulated position(based on output of each Kalman filter in each dimension) and true position. During these simulations, we compare filtering results with Figure-4. We establish the relation between positioning uncertainty and measurement error standard deviation for delay and Doppler shift; Relation between positioning uncertainty and filter's iteration time.

Filtering result is shown in Figure-5 and 6. In these graphs, positioning uncertainty is calculated along with the increase of iteration number. Different standard deviations for delay and Doppler shift have been selected.

From these graphs, we have:

(1) Positioning uncertainty from output of a Kalman filter is smaller than averaging position shown in Figure-4. Comparing Figure-5 with Figure-4, their uncertainties converge to zero in a similar way, but fluctuations in Figure-5 have been eliminated. By eliminating those fluctuations, positioning uncertainty can be decreased by more than 2km after 600 steps of iterations. This has been shown in Figure-6.

(2) From Figure-6, if standard deviations for delay and Doppler shift are not too high, positioning uncertainty can be as small as 1km after 1000 steps of iterations. For IRIDIUM system, considering the worst case, only one pair of samples can be taken for each frame, then 1000 samples take 90 seconds. If 10 pairs of samples can be collected in each frame, 1000 samples take only 9

seconds. This is especially useful for handover purpose, because a UT may need handover to other beam soon after a call set-up.

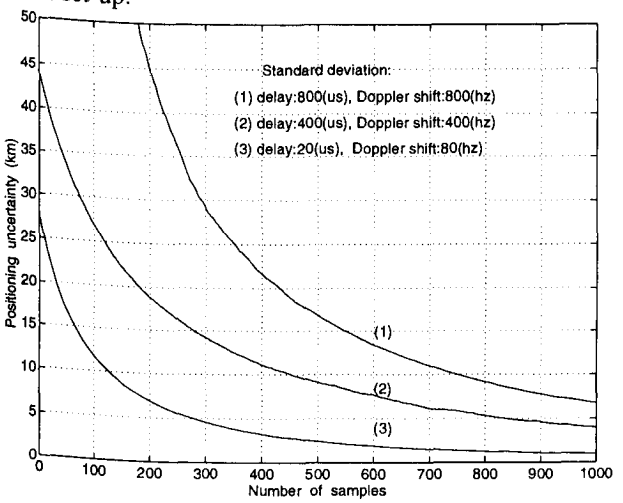

Figure-5
Filtering results for different deviations

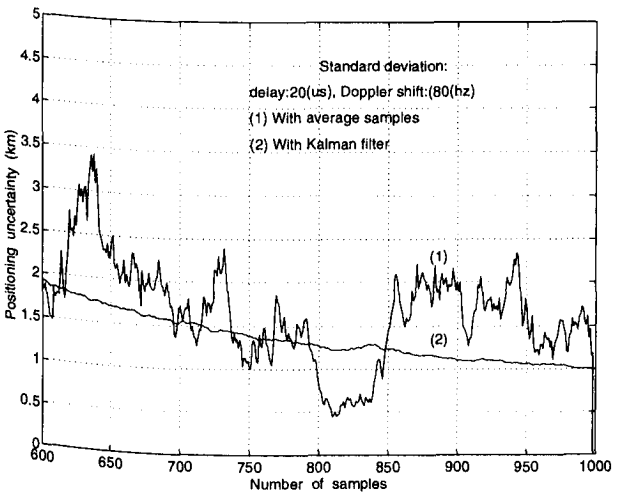

Figure-6
Result comparison (with and without Kalman filter)

4. Application for in-call positioning algorithm

In-call positioning algorithm can find its applications in several areas, most of them concentrate on handover process. We introduce these applications in this section.

4.1 Handover reliability

A handover is forced to be terminated if power level on current channel goes down before a new channel is allocated to this active UT. As is mentioned in [1][2][3], the handover termination rate or handover failure rate is determined by traffic channel capacity, channel allocation scheme and queuing scheme for handover. The larger of a satellite channel capacity, the smaller of the handover failure rate; A dynamic channel allocation scheme with handover having higher priority over call set-up is helpful in reducing handover failure rate in the price of higher call set-up blocking rate[3]; A lower handover failure rate can be achieved further if a handover which can not be served by the network immediately is queued[2]. Apart from above factors, another important factor to influence the handover failure rate is UT's position inside a spotbeam or satellite footprint. If a handover is detected to be necessary because of radio power reason, duration for this UT to remain inside the same beam is changeable in terms of its position, this has been shown in Figure-7.

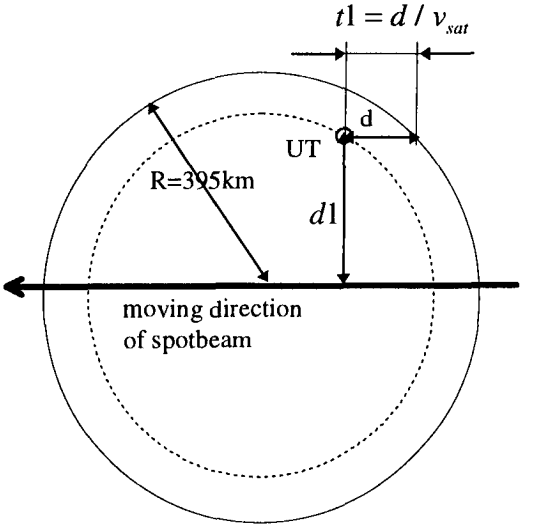

Figure-7 UT position inside a spotbeam

In Figure-7, **t1** is the remaining time for a UT to be under the same beam after it has detected a handover. **d1** is the distance from this UT to the track of that beam's centre. It is apparent to see that **t1** is a function of **d1**. Selecting the outer beam in IRIDIUM as an example(diameter is 790km), suppose **t1**(**d1**=0) is 8s(this figure is determined by specific handover criteria). The value of **t1** in terms of different **d1** inside the same beam is shown in Figure-8.

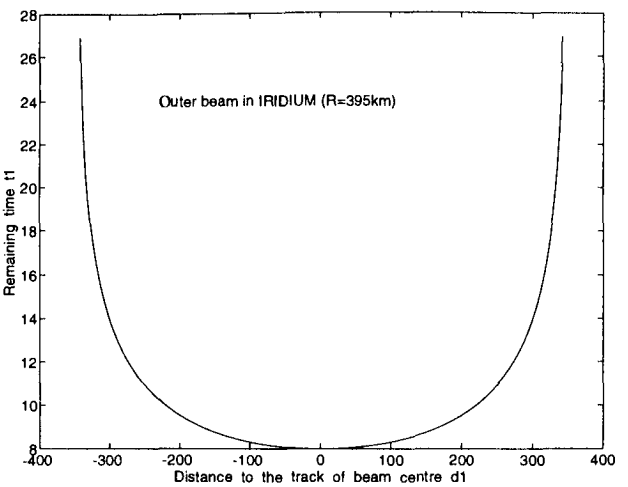

Figure-8 Time to use current link

From Figure-8, after a handover detection, some users will remain inside the same beam as long as 25s, some others only 8s. If we use handover scheme adopted in [2] (a handover is queued if traffic channel is not available), those handovers whose queuing delay is longer than **t1** in Figure-7 and 8 are dropped. Thus, a handover failure rate is directly influenced by its position inside a beam. As a result, it is a reasonable consideration to allocate those handovers which have smaller **t1** value with higher priority. The smaller of positioning uncertainty, the lower of handover failure rate. Related simulation results are not included in this paper.

4.2 Handover signalling overhead

Another application is to reduce signalling exchange specifically designed for handover. For any handover protocol, radio link measurement result(power level or bit error rate) should be transmitted either from network to a user terminal(for a mobile controlled handover or a network assisted handover) or from a user terminal to network(for a mobile assisted handover or a network controlled handover) during a call. This signalling exchange is compulsory throughout a call even though there is no handover during this call. These unnecessary signalling exchanges have greatly increased network signalling load and no system by now(existing system or proposed system) seems to have already overcome this problem. One solution for this problem is to co-ordinate handover protocol with user terminal's position. If the network has the UT's positioning knowledge all the time during a call, signalling exchange can be avoided if the UT is far away from spot beam boundary and thus handover probability is low. When it identifies some UTs are approaching the boundary of a spot, signalling exchange can be started or a handover even can be initiated by network because network knows the suitable handover time and target spotbeam number. Working in this way, large amount of signalling exchanges about measurement result can be avoided.

4.3 Handover between different segment

Another application is during a handover between different segment in a terrestrial and satellite integrated system. It has been identified that UT position is important when handover from spot to cell[8]. After it has been determined a handover to terrestrial cell is necessary, satellite network should contact a specific terrestrial BS in which area the UT is moving. In this case, providing satellite network with a UT's exact position is helpful in finding the target terrestrial BS.

5. Conclusion

An in call user terminal positioning algorithm has been presented in this paper for dynamic satellite constellations. IRIDIUM system has been taken as prototype. UT position can be determined from delay and Doppler shift measurement by a serving ground station. Due to measurement noise, resulted positioning uncertainty can be very large. The proposed UT positioning technique employs a Kalman filter to eliminate measurement noise and resulted uncertainty has been compared with another filtering algorithm: making average for all samples. Through computer simulation, it has been shown that the proposed algorithm achieves better performance than making average of samples in terms of positioning uncertainty and storage memory requirement. In particular, in the case of LEO satellite system like IRIDIUM, around 1.5km uncertainty can be achieved within reasonable duration. This will bring a great reduction for handover failure rate and signalling exchange during handover. Thus this positioning algorithm is of great importance for a dynamic satellite system which has large number of handovers. In the last section, a general outline has been given for positioning applications in several areas, performance for each application has been left for further investigation.

Appendix

Consider a discrete stochastic dynamic system described by a stochastic vector difference equation:

$$x_{k+1} = \varphi(x_k, t_{k+1}, t_k) + \Gamma(x_k, t_k)\omega_{k+1}, \quad k = 0,1.... \qquad \text{<A-1>}$$

where the state at t_k is x_k, an n-vector; φ is an n-vector function, Γ is n×r, and $\{\omega_k, k = 1,2....\}$ is an r-vector, white Gaussian sequence, $\omega_k \sim N(0, Q_k)$. The distribution of the initial condition x_0 is assumed given, and x_0 is independent of $\{\omega_k\}$. Let discrete, noisy, m-vector measurements y_k be given by

$$y_k = h(x_k, t_k) + v_k, \qquad k = 1,2.... \qquad \text{<A-2>}$$

where h is an m-vector function and $\{v_k, k = 1,2,...\}$ is an m-vector, white Gaussian sequence, $v_k \sim N(0, R_k)$, $R_k > 0$. For simplicity, $\{\omega_k\}$ and $\{v_k\}$ are assumed to be independent, and $\{\omega_k\}$ is independent of x_0. For a dynamic system expressed by <A-1>, each measurement y_k corresponds to a system state vector x_k. By processing each measurement y_k step by step with a Kalman filter, system state x_k can be estimated more and more accurately[6].

More specifically, we simplify <A-1> by considering a linear dynamic system expressed by <A-3>.

$$x_{k+1} = \varphi(k+1, k)x_k + \Gamma(k)\omega_{k+1}$$
$$y_k = M(k)x_k + v_k$$

with

$$\varepsilon\{\omega_k\}=0, \qquad \varepsilon\{\omega_k \omega_l{}^T\}=Q(k)\delta_{kl},$$

$$\varepsilon\{v_k\}=0, \qquad \varepsilon\{v_k v_l{}^T\}=R(k)\delta_{kl}, \quad R(k)>0 \qquad \text{<A-3>}$$

With each new measurement sample y_{k+1}, system state estimation $\hat{x}(k+1)$ can be obtained according to following procedures:

(1) Store the filter state $[\hat{x}(k/k), P(k/k)]$;

(2) Compute the predicted state

$$\hat{x}(k+1/k)=\varphi(k+1,k)\hat{x}(k/k);$$

(3) Compute the predicted error covariance matrix

$$P(k+1/k)=\varphi(k+1/k)P(k/k)\varphi^T(k+1,k) + \Gamma(k)Q(k+1)\Gamma^T(k);$$

(4) Compute the filter gain matrix

$$K(k+1)=P(k+1/k)M^T(k+1)\times \left[M(k+1)P(k+1/k)M^T(k+1)+R(k+1)\right]^{-1};$$

(5) Process the measurement y_{k+1}

$$\hat{x}(k+1/k+1)=\hat{x}(k+1/k)+K(k+1)\cdot \left[y_{k+1}-M(k+1)\hat{x}(k+1/k)\right];$$

(6) Compute the new error covariance matrix

$$P(k+1/k+1)=\left[I-K(k+1)M(k+1)\right]\cdot P(k+1/k);$$

(7) Set $k=k+1$, and return to step (1).

Repeat step (1) to step (7) for each measurement y_{k+1}, system state estimation $\hat{x}(k+1)$ will converge to its true value $x(k+1)$ if k is large enough.

REFERENCES

1. **Enrico Del Re, Romano Fantacci and Giovanni Giambene,** "Performance Analysis of a Dynamic Channel Allocation Technique for Satellite Mobile Cellular Network", International Journal of Satellite Communications, Vol 12, 25-32(1994)

2. **Sirin Tekinay, Bijan Jabbari,** "A Measurement-Based Prioritisation Scheme for Handovers in Mobile Cellular Network", IEEE Journal on Selected Areas in Communications. Vol 10. No. 8. Ocy. 1992

3. **Daehyoung Hong and Stepen S. Rappaport,** "Traffic Model and Performance Analysis for Cellular Mobile Radio Telephone Systems with Prioritised and Nonprioritized Handoff Procedures", IEEE Trans. on Vehicular Technology. Vol. VT-35, No. 3. Aug. 1986

4. **Ming Zhang and Tak-Shing P. Yum,** "Comparisons of Channel-Assignment Strategies in Cellular Mobile Telephone Systems", IEEE Trans. on Vehicular Technology. Vol. 38. No. 4. Nov. 1989

5. **David Everitt, David Manfield,** "Performance Analysis of Cellular Mobile Communication Systems with Dynamic Channel Assignment", IEEE Journal on Selected Areas in Communications. Vol. 7. No. 8. Oct. 1989

6. **Andrew H. Jazwinski,** "Stochastic Processes and Filtering Theory". Vol 64 in Mathematics in Science and Engineering, Academic Press, 1970

7. **Andrew P.Sage, James L.Melsa,** "Estimation Theory with Applications to Communications and Control". Robert E.Krieger Publishing Company, Malabar, Florida, 1971

8. **W.Zhao, R.Tafazolli, B.Evans,** "Handover Signalling Analysis in the GSM and Satellite Integrated System".

Traffic Sharing Algorithms for Hybrid Mobile Networks

S. Arcand
DCEEM,
National Defense HQ
Ottawa, Canada
simon@sce.carleton.ca

K. M. S. Murthy
Adv. Tech. & Networks,
VISTAR Telecomm. Inc.
Ottawa, Canada
murthy@vistar.ca

R. Hafez
Dept. Systems &
Computer Eng,
Carleton University,
hafez@sce.carleton.ca

Abstract

In a hybrid (terrestrial+satellite) mobile personal communications networks environment, a large size satellite footprint (supercell) overlays on a large number of smaller size, contiguous terrestrial cells. We assume that the users have either a terrestrial only single mode terminal (SMT) or a terrestrial/satellite dual mode terminal (DMT) and the ratio of DMT to the total terminals is defined γ. It is assumed that the call assignments to and handovers between terrestrial cells and satellite supercells take place in a dynamic fashion when necessary. The objectives of this paper are two-fold, (i) to propose and define a class of traffic sharing algorithms to manage terrestrial and satellite network resources efficiently by handling call handovers dynamically, and (ii) to analyze and evaluate the algorithms by maximizing the traffic load handling capability (defined in erl/cell) over a wide range of terminal ratios (γ) given an acceptable range of blocking probabilities. Two of the algorithms (G & S) in the proposed class perform extremely well for a wide range of γ.

1 - INTRODUCTION

If the objective of mobile personal communications is to serve anyone and anywhere (ubiquitous), then the evolution of hybrid (terrestrial + satellite) networks becomes essential to meet such a requirement. Terrestrial based Cellular and evolving PCS systems are designed to address medium to high capacity needs of urban and suburban mobility users. While technically feasible, the economics of these systems becomes less and less attractive as the coverage area increases (to cover rural & remote areas) and associated traffic decreases. On the other hand the satellite based global and regional systems can provide services to wide area, low traffic, high mobility services. Although technically possible, the currently proposed satellite systems alone cannot meet the needs of high capacity urban mobile users both from the capacity and cost points of view. Most of the proposed low earth orbit systems entertain high frequency reuse compared to conventional geostationary systems, but it is not high enough to meet the capacity needs of the urban users. Further, the usage of satellite systems for indoor and intra-premise access services would not only have to overcome severe technical difficulties but would also be unattractive from an economical point of view.

The concept of integrated satellite-terrestrial network for provision of mobile personal communication services (PCS) has been proposed previously **[1]**. An alternate low bit rate(LBR) structure to suitable for evolving PCS network and a mechanism to transport the LBR traffic through an ISDN network has been proposed in **[2]**. The transmission performance (the delay, voice quality) of interconnected systems (cascaded channels) had been studied for twelve different configurations hybrid networks involving Cellular, PCS, PSTN and satellite systems. In the case of satellite systems, both Ku-band (Anik C) and Ka-band (Olympus) systems were used for testing and comparison **[3,4]**. The general traffic management strategies including call setup & handover procedures for a satellite /GSM hybrid system were discussed in **[5]**. The handoff criterion based on channel fading and its effect were discussed in **[6]**. The traffic analysis of micro cellular systems with hierarchical macro cell overlay has been studied in **[7]**.

Another important question in a hybrid network environment is how to maintain a high level of network efficiency* in the presence of a rather arbitrarily growing population of single mode terminals (SMT) and dual (satellite/terrestrial) mode terminals (DMT). The primary objective of this paper is to propose and study a class of traffic sharing algorithms which perform extremely well over a wide range of DMT, SMT terminal ratios (γ). Two algorithms (G & S) which perform extremely well for a given blocking probability and for a wide range of γ have been identified. This paper presents a brief description of the class of proposed algorithms and their performance for two special cases. Detailed mathematical representation of the algorithms and a rigorous analysis of their performance are dealt with in **[8]**. In this paper, section 2 describes the system and traffic models, section 3 defines the class of algorithms including the recommended algorithms G & S, and the performance these algorithms are briefly discussed and compared in section 4.

* The network efficiency is defined as the load supported by the network (erlangs/cell) for a specified acceptable level of grade of service, e.g. blocking probability & call dropping probability.

2 SYSTEM DEFINITION

2.1 System Model

The schematic of a hybrid system illustrating a large size satellite beam (called supernal) overlaid on a large number of contiguous terrestrial cells is shown in **Fig. 1**. Each user is equipped with either a "terrestrial-only" SMT system or a DMT. It is assumed that no user is equipped with a "satellite-only" SMT, although some DMT users are outside the coverage of the terrestrial system will have to use "satellite-only" access. Within the coverage region, the ratio of DMT to total terminals (γ) is assumed to vary from 0 to 1 and is uniform amongst all cells.

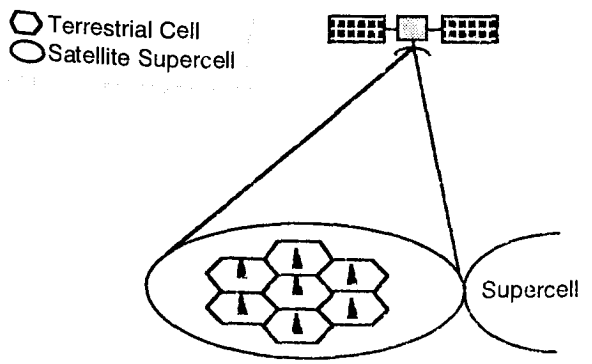

Fig. 1 Hybrid System Schematic Illustrating Cell Overlay

From the point of view of access availability, we can assume that the overlay region shown in **Fig. 1** is divided into three zones: (i) the first served by "terrestrial-only" systems, (ii) the second served by both systems, and (iii) the third served by satellite-only system. There will not be a sharp boundary between theses zones. The first zone could be considered to be consisting of indoor & intra-premise accesses. Although the satellite beam covers this zone, direct satellite access is considered neither viable nor desirable. Therefore the DMT terminals in this zone will operate in the SMT mode. In zone two, the SMTs & DMTs can access either systems or engage in mutual call handoffs based on some rules (defined in algorithms). Further, in zone 3, it is assumed that the DMTs operate in a "satellite-only" mode as there are no "satellite-only" SMT present in the system. Both satellite & terrestrial systems are connected to PSTN.

Satellite footprint is assumed to have a number of stationary beams(supercells), handovers between supercells are not considered in this paper. The terrestrial system is divided into contiguous cells with one base station per cell. There is a clear boundary between cells and from an offered traffic point of view, all cells are identical, although their physical size may differ. Offered traffic is independent between cells.

When the DMT is covered by both systems, it chooses an option as per the traffic sharing algorithm. These algorithms assume that before call setup (or handoff) the DMT can sense the number of busy channels on each system. This is the only criterion used to make the decision. In this study, we assume that the choice is made by the DMT in accordance with the algorithm. If a channel request made by a DMT for call setup (or handoff) is denied by the system first chosen, the DMT requests a channel from the other system before the call is declared blocked (or dropped).

2.2 Traffic Model

The user population generates calls with a Poisson arrival process at a call arrival rate λ per cell per unit time. Call duration has a negative exponential distribution with mean μ. The user population is assumed infinite. Blocked calls are cleared. The mobility model suggested in **[9]** is used. A SMT can establish a connection with only the terrestrial system. If all channels inside the cell are occupied at call setup (or cellular boundary crossing), the call is blocked (or dropped). DMT calls may be handed off between the two systems whether terminals are mobile or not and a hand-off request is either accepted or blocked. Hand-off requests are not queued at the mobile switching center. A guard channel is reserved for these inter-cell hand-offs. For the purpose of eliminating any confusion with "soft guard channel", which we will define later, and to emphasize that this guard channel is assigned exclusively to hand-off requests caused by movement of terminals, it is called "hard guard channel".

3 ALGORITHMS DEFINITION

For the purpose of analysis the traffic sharing algorithms are divided into **two categories**, viz., those dealing with (i) intra-cell terminal mobility, and (ii) inter-cell terminal mobility. In the next section, we shall define seven algorithms for Case I and four algorithms for Case II.

The **first case** assumes stationary or quasi-stationary terminals or, equivalently, mobile terminals that do not cross inter-cell boundaries. Since calls cannot be dropped, only the blocking probability is used to determine the grade of service. Calls that were not blocked upon setup are allowed to continue until completed by the user. They can stay assigned to the same channel throughout their duration or, depending on the algorithm, they can be handed off between terrestrial and satellite systems.

The **second case** deals with inter-cell terminal mobility and assumes that the terminals roam between terrestrial cells. Only movement between terrestrial cells is considered. Since the size of the satellite super-cell (i.e. beam footprint) is large compared to the relatively short distance traveled by a mobile terminal during a call, the received power level may not vary enough to trigger a inter-supercell hand-off request. Also, the density of call hand-off requests between supercells is very is very low compared to those between cell & supercell within a supercell. Nevertheless such a assumption does not affect the comparative performance of different algorithms described below.

3.1 Case I : Intra-Cell Mobility

Seven algorithms are proposed and defined for the case of the intra-cell mobility. The sets of algebraic equations describing the algorithms have not been included for brevity. As a general rule, a DMT tries to set up a new call with the

terrestrial system. If the terrestrial system is saturated (or near saturation depending on the algorithm) the SMT tries to set up a new call with the satellite. The first four algorithms (A to D) do not support inter-system hand-off: a connection with one system lasts from call setup to call completion. With algorithms E, F and G, the initiation or completion of a call may cause the inter-system hand-off of a different call being processed within the same cell. Algorithm E supports such hand-offs at call completion only, F at call setup only, and G at call setup and call completion.

Algorithm A : A new call from a SMT takes a terrestrial channel if there is at least one free; otherwise it is blocked. A new call from a DMT takes a terrestrial channel if there is at least one free. If all terrestrial channels are busy, it takes a satellite channel if there is at least one free; otherwise the call is blocked. There are no inter-system hand-offs.

Algorithm B : Here we consider the soft guard channel concept. DMTs try a connection with the satellite even if one terrestrial channel is still free. This channel is a guard channel since it is reserved for SMTs. However, DMTs may use it upon call setup if no satellite channel is free at the time. That is, a new call from a SMT takes a terrestrial channel if there is at least one free; otherwise it is blocked. A new call from a DMT takes a terrestrial channel if there is more than one free or if all satellite channels are busy. If one terrestrial channel or none is free, the call takes a satellite channel if there is at least one free. If all terrestrial and satellite channels are busy, the call is blocked. There are no inter-system hand-offs.

Algorithm C : A new call from a SMT takes a terrestrial channel if there is at least one free; otherwise it is blocked. A new call from a DMT takes a terrestrial channel if there is more than two free or if all satellite channels are busy. If two terrestrial channels or less are free, the call takes a satellite channel if there is at least one free. If all terrestrial and satellite channels are busy, the call is blocked. There are no inter-system hand-offs.

Algorithm D : A new call from a SMT takes a terrestrial channel if there is at least one free; otherwise it is blocked. A new call from a DMT takes a satellite channel with a probability equal to mt/nt. If all terrestrial and satellite channels are busy, the call is blocked. There are no inter-system hand-offs.

Algorithm E : This algorithm implements the "satellite avoidance" measure where DMTs use the satellite as a last resort only. A new call from a SMT takes a terrestrial channel if there is at least one free; otherwise it is blocked. A new call from a DMT takes a terrestrial channel if there is at least one free. If all terrestrial channels are busy, it takes a satellite channel if there is at least one free; otherwise the call is blocked. If a DMT is using a satellite channel, as soon as a terrestrial channel is released by the completion of a different call, the DMT call is handed off to this terrestrial channel.

Algorithm F : This algorithm includes an inter-system hand-off to strengthen the soft guard channel. Strengthening means increasing the probability that this guard channel is free for SMT calls while maximizing the use of the all other terrestrial channels. This hand-off occurs when a SMT requests the last terrestrial channel with a new call. If this occurs when at least one of these terrestrial channels was occupied by a DMT, then the SMT takes the last terrestrial channel and one DMT is immediately handed off from the terrestrial system to the satellite. The terrestrial channel thus freed assumes the role of soft guard channel. The channel capture occurs before the hand-off of the DMT call. Therefore, even if the hand-off protocol is lengthy (several handshakes exchanged over a satellite link), the SMT call setup is not unnecessarily delayed.

Formally described, a new call from a SMT takes a terrestrial channel if there is at least one free; otherwise it is blocked. A new call from a DMT takes a terrestrial channel if there is more than one free or if all satellite channels are busy. If one terrestrial channels or less is free, the call takes a satellite channel. If all terrestrial and satellite channels are busy, the call is blocked. If one and only one terrestrial channel is free and at least one of the busy terrestrial channels is occupied by a DMT, a new call attempt by a SMT will capture the last terrestrial channel and will be followed by a hand-off of the DMT call from the terrestrial system to the satellite.

Algorithm G : Algorithm G is similar to algorithm F with two additional hand-off processes implemented on channel release to further strengthen the soft guard channel. A new call from a SMT takes a terrestrial channel if there is at least one free; otherwise it is blocked. A new call from a DMT takes a terrestrial channel if there is more than one free or if all satellite channels are busy. If one terrestrial channels or none is free, the call takes a satellite channel. If all terrestrial and satellite channels are busy, the call is blocked. If one and only one terrestrial channel is free and at least one of the busy terrestrial channels is occupied by a DMT, a new call attempt by a SMT captures the last terrestrial channel and is followed by a hand-off of the DMT call from the terrestrial system to the satellite. If all terrestrial channels and all satellite channels are busy and a DMT completes a call on a satellite channel, a different DMT call is automatically handed off from the terrestrial system to the satellite. If a DMT is using a satellite channel, as soon as a terrestrial channel is released by the completion of a different call, the DMT call is handed off to this terrestrial channel.

3.2 Case II : Inter-Cell Mobility

Of the seven algorithms examined in the previous chapter, four prove interesting. These four algorithms (B, E, F and G) are modified to cater for the mobility of terminals and reduce the resulting call drop probability. Their new versions are algorithms P, Q, R and S respectively. All algorithms have a hard guard channel, reserved exclusively for inter-cell hand-offs. When only one hard guard channel is free in the terrestrial system, a SMT new call is blocked.

Algorithm P : A new call from a SMT takes a terrestrial channel if there are at least two free; otherwise it is blocked. If at least one terrestrial channel is free and a SMT using a

terrestrial channel in a adjacent cell enters the cell of interest, this SMT takes a terrestrial channel; if all terrestrial channels are busy in the new cell, the call is dropped. A new call from a DMT takes a terrestrial channel if there is more than one free. If one and only one terrestrial channel is free, the call takes a satellite channel. If all satellite channels are busy and one terrestrial channel or none is free, the call is blocked. If at least one terrestrial channel is free and a DMT using a terrestrial channel from an adjacent cell enters the cell of interest, this DMT takes a terrestrial channel; if all terrestrial channels are busy in the new cell and at least one satellite channel is free, this DMT takes a satellite channel; if all terrestrial and all satellite channels are busy, the call is dropped. There is no inter-system hand-off.

Algorithm Q : A new call from a SMT takes a terrestrial channel if there are at least two free; otherwise it is blocked. If at least one terrestrial channel is free and a SMT using a terrestrial channel from an adjacent cell enters the cell of interest, this SMT takes a terrestrial channel; if all terrestrial channels are busy in the new cell, the call is dropped. A new call from a DMT takes a terrestrial channel. If one and only one terrestrial channel is free, the call takes a satellite channel if there is at least one free. If all satellite channels are busy and one terrestrial channel or less is free, the call is blocked. If at least one terrestrial channel is free and a DMT using a terrestrial channel from an adjacent cell enters the cell of interest, this DMT takes a terrestrial channel; if all terrestrial channels are busy in the new cell and at least one satellite channel is free, this DMT takes a satellite channel; if all terrestrial and all satellite channels are busy, the call is dropped. If a DMT is using a satellite channel and one and only one terrestrial channel is free, as soon as another terrestrial channel is released by the completion of a different call, the DMT call is handed off to this terrestrial channel.

Algorithm R : A new call from a SMT takes a terrestrial channel if there are at least two free; otherwise it is blocked. If at least one terrestrial channel is free and a SMT using a terrestrial channel from an adjacent cell enters the cell of interest, this SMT takes a terrestrial channel; if all terrestrial channels are busy in the new cell, the call is dropped. A new call from a DMT takes a terrestrial channel if there is more than one free. If one and only one terrestrial channel is free, the call takes a satellite channel. If all satellite channels are busy and one terrestrial channel or less is free, the call is blocked. If at least one terrestrial channel is free and a DMT using a terrestrial channel in a previous cell enters the cell of interest, this DMT takes a terrestrial channel; if all terrestrial channels are busy in the new cell and at least one satellite channel is free, this DMT takes a satellite channel; if all terrestrial and all satellite channels are busy, the call is dropped. If one and only one terrestrial channel is free and at least one of the busy terrestrial channels is occupied by a DMT, a new call attempt by a SMT captures the last terrestrial channel and is followed by a hand-off of the DMT call from the terrestrial to the satellite system.

Algorithm S : A new call from a SMT takes a terrestrial channel if there are at least two free; otherwise it is blocked. If at least one terrestrial channel is free and a SMT using a terrestrial channel from an system cell enters the cell of interest, this SMT takes a terrestrial channel; if all terrestrial channels are busy in the new cell, the call is dropped. A new call from a DMT takes a terrestrial channel if there is more than one free. If one and only one terrestrial channels is free, the call takes a satellite channel. If all satellite channels are busy and one terrestrial channel or none is free, the call is blocked. If at least one terrestrial channel is free and a DMT using a terrestrial channel from an system cell enters the cell of interest, this DMT takes a terrestrial channel; if all terrestrial channels are busy in the new cell and at least one satellite channel is free, this DMT takes a satellite channel; if all terrestrial and all satellite channels are busy, the call is dropped. If one and only one terrestrial channel is free and at least one of the busy terrestrial channels is occupied by a DMT, a new call attempt by a SMT captures the last terrestrial channel and is followed by a hand-off of the DMT call from the terrestrial system to the satellite. If all terrestrial channels and all satellite channels are busy and a DMT completes a call on a satellite channel, a different DMT call is automatically handed off from the terrestrial system to the satellite. If a DMT is using a satellite channel and one and only one terrestrial channel is free, as soon as another terrestrial channel is released by the completion of a different call, the DMT call is handed off to this terrestrial channel.

4 PERFORMANCE ANALYSIS

To study the performance of algorithms (Case I & II), a combined analytical and simulation methodology was used. The combined approach consists of an initial mathematical analysis and a sequence of Monte-Carlo simulations. This approach was necessary due to the magnitude of the network under study. Mathematical analysis is performed on an individual cell, conditioned on the number of satellite channels available to that cell only. The conditional statistics obtained in the analysis are then used in a simulation conducted on a cluster of 1024 terrestrial cells overlaid with one satellite beam. The results of the simulation include the number of satellite channels occupied by each cell and eliminates the condition imposed previously. The net result is the beam-wide probability of blocking and probability of call dropping. Finally, a weighted average of blocking probability and call dropping probability gives the grade of service.

4.1 Case I Algorithms Results (Intra-Cell)

We are looking for the algorithm that supports maximum load for a wide range of γ values. Here the offered load is termed "supported load". It is defined as the traffic load per cell for which the blocking probability equals 0.01.

Fig. 2 shows the traffic load supported by **algorithm A** for a DMT proportion varying between γ=0 and γ=1. As γ increases but stays small, the demand for satellite channels is well below the number available for the complete beam. The blocking probability for DMTs is negligible and only SMTs suffer blocking. When γ approaches unity, there is a higher probability that all satellite channels are occupied the DMT blocking probability is no longer negligible and has a greater weight in the overall blocking probability Pb.

Therefore it becomes the limiting factor in the determination of the supporting load whose reflex point occur around γ=0.8 and decreasing slope beyond γ=0.8.

For γ=0 the supported load of **algorithm B** is the same as with algorithm A, since SMTs do not use either algorithm. As γ increases, the supported load increases again, but faster than with algorithm A. This is explained by the effort made by algorithm B to keep the soft guard channel free for a future SMT call, therefore reducing the blocking probability for SMTs. For γ>0.6, the probability that all satellite channels are busy becomes important. As γ approaches unity, algorithm B supports a lower traffic load than algorithm A. Cells are more likely to use satellite channels, even if they have some terrestrial channels free. The greater demand on satellite channels increases the probability that all channels (both terrestrial and satellite) in a particular cell are occupied. Consequently these cells deny service to other cells that are already using all their terrestrial channels.

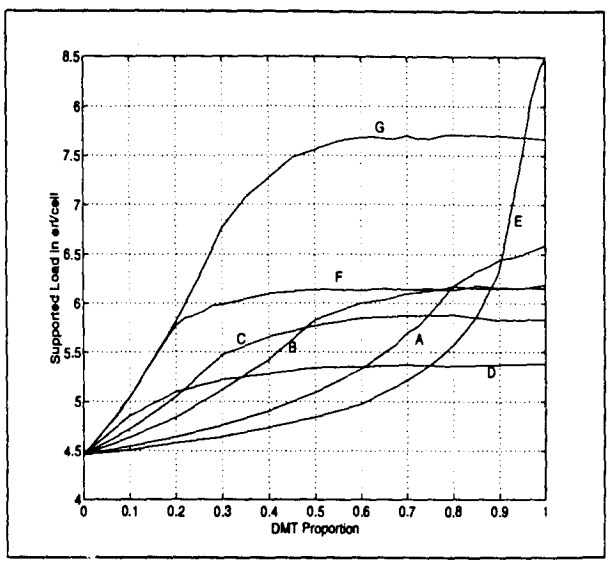

Fig. 2 Performance of Algorithms A-G at Blocking Probability = 0.01

Algorithm C performs even better than algorithm B for low DMT proportions. However the improvement from algorithm B to C is not as marked as from A to B. Also the plateau is lower at approximately 5.8 erl/cell because of the greater demand for satellite channels. As was expected, **algorithm D** takes advantage of the satellite capacity at very low DMT ratios, but the probability that all satellite channels are occupied is higher than with the other three algorithms and the supported load reaches a plateau at only 5.3 erl/cell. **Algorithm E** supports a very large load when the DMT proportion is close to unity. However, for γ<0.75, it performs worst than any other algorithms.

There is a marked improvement for small DMT proportions with **algorithm F**. Two important observations are the steep slope for γ<0.2 and the fact that the supported load is the same as with algorithm B when γ approaches unity. They are explained as follows. For a small γ, DMTs offer a very small load to the satellite. Consequently the probability that all satellite channels are occupied is negligible. The satellite is under saturated and DMTs are almost guaranteed to be assigned a free satellite channel when required, i.e. when SMT request a terrestrial channel. Therefore, the joint probability that all terrestrial channel are occupied and one of the nt terminals is a DMT is also negligible. SMTs have virtually the whole terrestrial system to themselves. The second observation pertains to the coincidence of algorithms B and F for high DMT proportions. For γ>0.8, satellite channels are in high demand from the many DMTs and there is a high probability that they are all occupied and the inter-system hand-off unique to algorithm F cannot be implemented. Algorithm F without this hand-off process is like algorithm B.

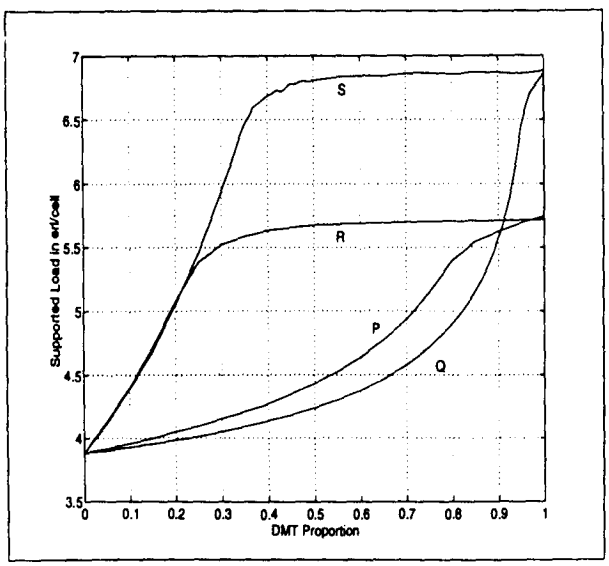

Fig 3 Performance of Algorithms P - S for the Grade of Service = 0.002

Algorithm G performs much better than most other algorithms. For γ < 0.95, algorithm G performs better than any other algorithms. For 0.4<γ<0.9, the improvement in supported load exceeds 1 erl/cell over the next best algorithm(F). The same steep slope for small values of γ as with algorithm F is present and it continues well after algorithm F reaches its plateau. Only for γ>0.95, does algorithm E offer a better performance. A logical explanation is the effort made by algorithm G to keep one terrestrial channel free for SMTs, while these SMTs account for less than 0.05 of all terminals in the cells.

4.2 Case II Results (Inter-Cell)

Fig. 3 illustrates the supported load for each of the four algorithms of Case II. As expected, since these algorithms are based on corresponding algorithms of Case I, there are striking similarities between the curves in **Figs 2** and **3**, especially when curves are compared on a one-to-one basis (B with P; E with Q; F with R; G with S). Some similarities also apply to more than one curve in each group. For instance, algorithms R and S coincide for

$\gamma<0.2$ and exhibit a steep slope, in the same manner as algorithms F and G do. Algorithms P and R share the same supported loads at $\gamma=1$, for the same reason that B and F share the same plateau. A three dimensional plot shown in **Fig. 4** illustrates the grade of service for different traffic loads for different DMT radios (γ) for algorithm P.

There are a few noticeable differences. For instance, the absolute value of the supported loads is lower in the mobile terminal scenario. This is due to the difference in the performance measurement (blocking probability counts for only 0.1 of the grade of service in Case II scenarios). The main difference however is the **absolute superiority of algorithm S** over the complete range of DMT proportions, unlike algorithm G which does not perform as well as E for $0.95<\gamma<1$. The use of a hard guard channel for all algorithms in the mobile scenario prevents algorithm Q from overtaking S even when the DMT proportion approaches $\gamma=1$.

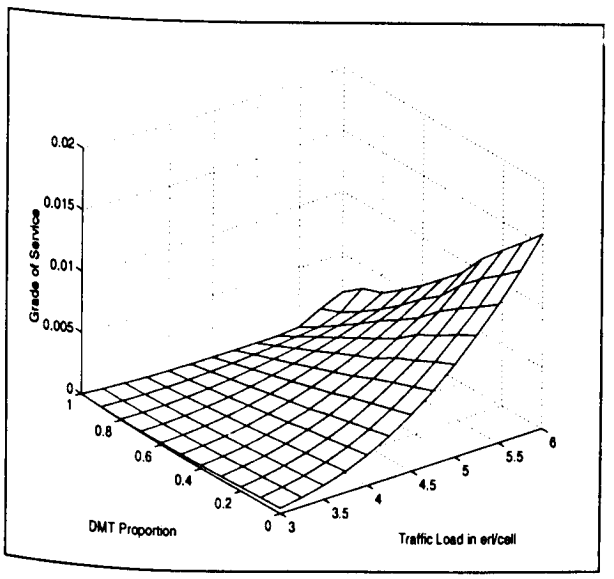

Fig. 4 Grade of Service vs. Traffic Load for Different γ for Algorithm P.

5 CONCLUSION

We have defined a class of traffic sharing algorithms for integrated terrestrial-satellite mobile personal communications network. The users were assumed to have either a terrestrial-only single mode terminal or a terrestrial - satellite dual mode terminal. No constraint was introduced on the ratio of DMT & SMT terminals. The class algorithms were proposed and their performance was evaluated. The grade of service was based on the blocking probability and call dropping probability. Both probabilities were computed by a combined method of analysis and Monte Carlo simulation.

It was found that the algorithms which allow inter-system hand-offs (e.g. algorithms G & S) normally perform better than the others. The key aspect of the algorithms which performance better than others is that existing DMT users, even while not crossing a cell boundary, could be shifted between systems to accommodate a SMT users when the associated system capacity reaches near saturation.

The best performance is reached when DMTs use a soft guard channel on the terrestrial system and take every possible measure to exploit it, such as combining it with the hard guard channel required to reduce the call dropping probability. When such a strategy is employed, DMTs use the terrestrial system to its maximum potential without creating a prohibitive SMT blocking probability. In such an instance, the supported load is increased by as much as 57% for certain DMT proportions.

6 ACKNOWLEDGEMENT

One of the authors acknowledge the support from NSERC for this work.

7 REFERENCES

[1] K.M.S.Murthy,"Hybrid Networks for Personal Communications : Proposed Architecutres and Planned Experiments" Workshop on Adv. Net. and Tech. Concepts for Mobile, Micro, and Pers. Com., JPL, Pasedena, **May 30-31, 1991**,

[2] K.M.S.Murthy, "Internetworking ISDN and PCN in a Satellite Environment : Alternate Rate Structures" Proc. AIAA's 14th Intnl. Com. Sat. Sys. Conf. **Mar.22-26, 1992**, pp 240-247

[3] K.M.S.Murthy, "Personal Communications Using Hybrid Radio/Satellite Networks : Ku/Ka-Band Experimental Results", Proc. Int. Conf. on Dig. Sat. Com.. (ICDSC), **May 1992**, pp 435-442

[4] K.M.S.Murthy, etal, "Personal Communication Trials Using Ku & Ka band Satellite Systems", Proc. Intl. Conf. Selected Topics in Wireless Com., Vancouver, **June 25-26, 1992**, pp 250-253

[5] E. Del Re, etal, "Traffic Management Strategies in an Integrated Satellite-Cellular Network for Mobile Services", Proc. of IEEE ICUPC, Ottawa, 12-15 **Oct., 1993**, pp839-843

[6] J.P. Castro, "Hand-off Techniques in Universal Mobile Communications", Proc. of IEEE ICUPC, Ottawa, 12-15 **Oct., 1993**, pp844-848

[7] S.S.Rappaport, etal, "Microcellular Communication Systems with Hierarchical Macrocell Overlays : Traffic Performance Models & Analysis", Proc. IEEE, vol 82, **Sep. 1994**, pp1383-1397

[8] S. Arcand,"Load Sharing in an Integrated Satellite - Terrestrial Cellular Network", M. Eng. Thesis, Carleton University, Ottawa, April 1995

[9] G.J.Foschini,etal, "Channel Cost of Mobility", IEEE Trans. Veh. Tech.,VT-42, **Nov.1993**, pp414-424

Increasing Cellular Coverage Within Integrated Terrestrial/Satellite Mobile Networks

Jonathan P. Castro, Telecommunications Laboratory,
Swiss Federal Institute of Technology, CH-1015 Lausanne, Switzerland
Phone/Fax: +41 21 634 66 05

ABSTRACT

When applying the hierarchical cellular concept, the satellite acts as giant umbrella cell covering a region with some terrestrial cells. If a mobile terminal traversing the region arrives to the border-line or limits of a regular cellular ground service, network transition occurs and the satellite system continues the mobile coverage. To adequately assess the boundaries of service of a mobile satellite system an a cellular network within an integrated environment, this paper provides an optimized scheme to predict when a network transition may be necessary. Under the assumption of a classified propagation phenomenon and Lognormal shadowing, the study applies an analytical approach to estimate the location of a mobile terminal based on a reception of the signal strength emitted by a base station.

Keywords: Coverage, Cellular, Shadowing, PCS, mobile, satellite, terrestrial.

INTRODUCTION

Some recent cellular network specifications, which could be extrapolated to hybrid systems when satellites are involved, imply that base station (BS) transitions are best handled by selecting the server for which the carrier-to-noise interference plus noise is maximum (C/I + N) or the one with the minimum bit error rate (BER). However, this is not accurate when bit rates are pushed higher, because the BER is not a simple function of the (C/I + N), it is also a function of the delay spread. Thus, even if it is true that speech quality improves uniformly as bit error probability decreases, the subjective quality of digital speech vs. bit error probability tends to be rather binary in character. This means that below a certain error probability the quality is unnoticeable from zero errors, while above the error probability limit the speech becomes very quickly unacceptable. Therefore, here we propose an alternative scheme that uses the link or fade margin instead a BER threshold as a key information to base network transitions.

Background

Full availability of global access for personal communications services (PCS) will depend on the level of coordination achieved by the integration of terrestrial and spatial mobile networks. An initial type of integration will most likely be the transparent inter-operability of the terrestrial and the satellite BSs through a multi-mode mobile station (MS) operating at least in two frequency ranges. If the goal is to integrate the newer mobile satellite systems (MSS) with established terrestrial mobile systems like GSM, it would be ideal not to modify the GSM network at all and design the MSS to minimize costs. Although this approach may be logical expectation of present network operators and some GSM investors, it is not practical because it may impose unnecessary burden on the MSS design. We say unnecessary, since GSM for example is willing to coordinate the integration process with a flexible and progressive participation.

In the context of multi-spot satellites we expect that each beam projects a satellite cell covering none or many GSM cells depending on the region where the projection falls. More details and the terminology of these arrangements are described in references [1]-[3]. Thus, in a hybrid (GSM + Satellite) environment, the BS_{GSM} serve terrestrial GSM cells and the BS_{SAT} serve satellite cells. If we use the MAGSS-14 constellation [4]-[5] as a medium earth orbit (MEO) satellite system for example, we will have 37 beams per satellite, each beam covering a zone radius of 930 km. Hence, our satellite system under consideration would have S spots with N BS_{SAT}, where each BS_{SAT} can be connected to any spot, and certain BS_{SAT} may serve M satellite cells. The mobile switching centers (MSCs) controlling the different BS_{GSM} and BS_{SAT} are strategically located and may serve both types of base stations.

Since most of the principals of cell selection and reselection had been already introduced in [1] and [2], in this study we will concentrate on the *soft handoff* aspects to successfully pass from the terrestrial to the satellite system and vice versa. In a soft handoff scheme mobile units in transition between one cell and its neighbor transmit to and receive the same signal from both base stations simultaneously. When spread spectrum techniques with universal frequency reuse and a Rake receiver in the mobile unit are employed, the two signals may be isolated and aligned both in time and phase to reinforce one another on the forward link. While on the reverse link, MCSs will evaluate which base station is receiving the stronger (i.e., better signal replica) and decide in its favor [6].

The rest of the paper is distributed as follows: the 2nd section presents the mobile environment while discussing hard/soft-handoff, the 3rd section outlines the fading model, the 4th section introduces some simulation results based on experimental data, and the 5th section provides conclusions.

THE MOBILE ENVIRONMENT

Generally a mobile satellite channel is approximated by a Rician distribution with a ratio of specular to diffuse component k = 10 dB, and a Lognormal distributed

shadowing process affecting the direct path with a mean value = -7.5 dB and standard deviation of 3 dB [7]. However, universal terminals for global PCS will comprise basically all environments as it was described in [1]. But within a hybrid integrated mobile system, active transition from one system to another will be primarily in heavily shadowed areas. Therefore, the propagation attenuation in this transition region following [6] can be modeled as the product of the μth power of distance and a Lognormal component representing shadowing losses. These imply slowly varying fluctuations for all users in motion and affects to both reverse and forward links. Furthermore, in the light of the four state model presented in [1], the Lognormal shadowing corresponding to suburban or hilly, or dispersed forest area in the vicinity of a urbanized region will be the borderline for full satellite coverage ends or begins. Thus, whenever Lognormal type attenuations are present network transition signalization will be intensive. Then for a user at distant r from a base station (BS_{GSM} or BS_{SAT}) the attenuation α is proportional to

$$\alpha(r,\zeta) = r^{\mu}\, 10^{\zeta/10}$$

$$10\log\alpha(r,\zeta) = 10\mu \log r + \zeta \qquad \text{(dB)} \qquad (1)$$

where ζ is the dB attenuation due to shadowing, with zero mean and standard deviation σ.

Cell Coverage and Handoff

As the MS comes in contact with multiple type of base stations (i.e., BS_{GSM} & BS_{SAT}) the corresponding MSC will begin to gather information about the propagation characteristics the mobile unit goes through. In principal, if a MS traverses rural areas it will be in contact primarily with a BS_{SAT}; however, as it approaches a suburban or a large metropolis the two types of base stations will be present. The information provided by the MS will include in particular the power levels and fade durations discriminating environmental states [1]. Thus all the comparisons made by the MSC will be on the basis of received power and the fade durations (e.g., the shadowing effects).

Hard-Handoff Considerations: Hard handoff may occur exactly at the boundary between the satellite cell and the nearest neighbor terrestrial mobile cell. Then the relative attenuation from the mobile user at the boundary to either base station (i.e, BS_{SAT} & BS_{GSM}) at distance r_i is given as

$$10\log\alpha(r_i,\zeta_i) = 10\mu \log r_i + \zeta_i \qquad i = 0,1, \quad (2)$$

where r_i are normalized distances to the base stations, and ζ_i are the corresponding normal shadowing with zero mean and standard deviation σ. In the absence of shadowing, the minimum power required from the MS's transmitter to overcame background noise is simply proportional to $10\mu\log r$. Nevertheless, the random component due to shadowing, ζ, must have the minimum power increased to guarantee consistent acceptable performance. In the case of the satellite would mean clear path transmission conditions with certain percentage of non-service availability i.e., $1-P_{out}$, where P_{out} is the outage probability in Viterbis's [6] terminology. In propagation terms, a fade margin γ dB must be added to the transmitted power to combat signal degradation. Since the desired performance during shadowing events are achieved when ($\zeta < \gamma$), we can predict the outage probability (i.e., the time where performance is not achieved) by the following formulation:

$$P_{out} = \Pr(\zeta > \gamma) = \frac{1}{\sqrt{2\pi}\sigma}\int_{\gamma}^{\infty} e^{-\zeta^2/2\sigma^2}\, d\zeta$$

$$= Q\left(\frac{\gamma}{\sigma}\right) \qquad \text{where} \qquad (3)$$

$$Q(y) = \int_{y}^{\infty} e^{-x^2/2}/\sqrt{2\pi} = \int_{-\infty}^{-y} e^{-x^2/2}/\sqrt{2\pi}$$

However, it should be noted that handoff right at the cell boundaries is not realistic, and more than that, it is undesirable because this can lead to the well known "*ping-pong*" effect where the user could be passed back and forth several times from the satellite base station to the terrestrial base station and vice versa, while network transition is about to occur. Therefore, in practical (BS_{GSM} to BS_{SAT}) hard handoff implementation, the handoff would occur only after the BSS power is reduced to the lowest supportable value below the expected cell boundary threshold level; which generally happen when the user has moved a certain distance away from the service boundary. Thus, if the ratio of this distance to the cell radius is $\rho > 1$ (i.e., distance from the or nearest BS_{GSM} cell to the satellite cell or BS_{SAT}) the outage probability P_{out} for a given fade margin γ is given by

$$P_{out} = \Pr(10\mu\log\rho + \zeta > \gamma)$$

$$= Q\left(\frac{\gamma - 10\mu\log\rho}{\sigma}\right) \qquad (4a)$$

$$\gamma = 10\mu\log\rho + 10.3. \qquad (4b)$$

The idea is to maximize the coverage extension by the terrestrial system before it passes control the satellite system. However, the contrary may be desired when control is to be passed from the satellite to the terrestrial system. But since the ratio of a satellite cell will be sufficiently high in relation to a regular terrestrial cell, the hard handoff configuration for network transition does not seem to be feasible. Hence, we will next consider the soft handoff as the most ideal approach.

Soft Handoff Options: Soft handoff occurs primarily throughout a range of distances from the two base stations. Thus, at any given time or for any given frame or packet, the better of the two base station receptions will be utilized by the MSC. In terms of attenuation, the one with lesser attenuation will be selected. Since any analysis of inter-cell interference involves comparison of propagation losses among two or more stations, there is a dependence of the

propagation losses to two different base stations from a mobile user. Therefore, if we assume a joint Gaussian probability density for losses to two or more base stations; we can then equivalently express the random component of the loss as the *sum* of a component in the near field of the user, which is common to all base stations, and a component which pertains solely to the receiving base station being independent from one base station to another [6]; and express the random component of the dB loss for the ith base station (i = 0, 1, 2, ...) as

$$\xi_i = a\xi_0 + b\xi_i \qquad \text{where} \quad a^2 + b^2 = 1 \qquad (5)$$

Then the outage probability P_{out} expressed in terms of the independent variables ξ_0, ξ_1 is given by

$$P_{out} = \Pr\left\{Min\left[10\mu\log r_0 + b\xi_0, 10\mu\log r_1 + b\xi_1\right]\right\}$$
$$> \gamma - a\xi$$
$$= \frac{1}{\sqrt{2\pi}}\int_{-\infty}^{\infty} e^{-x^2/2} Q\left(\frac{\gamma - 10\mu\log r_0 + ax}{b\sigma}\right) \qquad (6)$$
$$Q\left(\frac{\gamma - 10\mu\log r_1 + ax}{b\sigma}\right) dx$$

where the mobile is assumed to be either in cell *0* (e.g., BS_{SAT} cell) or *1* (e.g., BS_{GSM} cell), so that either, $r_0 \le 1$, $r_1 \ge 1$ or $r_0 \ge 1$, $r_1 \le 1$. When the mobile is exactly in the cell border, $r_0 = r_1 = 1$, the P_{out} representing the worst case is

$$P_{out} = \frac{1}{\sqrt{2\pi}}\int_{-\infty}^{\infty} e^{-x^2/2}\left[Q\left(\frac{\gamma + ax}{b\sigma}\right)\right]^2 dx \qquad (7)$$

For values $a = b = 1/\sqrt{2}$ and $\sigma = 8$ dBm the authors in [6] find by numerical means that for outage probability $P_{out} = 0.1$, the fade margin $\gamma_{soft} = 6.2$ dB while $\gamma_{hard} = 10.3$ dB. This is a clear improvement of about 4 dB. Therefore, if we are to use fade margins as one criteria for network transition events, it seems logical to use the soft-handoff rather than the hard-handoff approach.

As indicated earlier, in the universal PCS concept [1], statistically the signal transition for network change will have primarily a Log-normal/Rayleigh type distribution, as it passes from acceptable to non-acceptable signal reception. The analytical processes of this transition will be presented in the next section.

FADING ANALYSIS

Since in the preceding section we have established the principals of network transition in terms of distance with relation to the BSs , we can now analyze the fade duration effects at an established fade margin. The fade margins are defined according to different propagation environments presented in [1]. The degree of fading effect can be evaluated by observing how it reduces the information reliability of the network, and determining how many times a *transmission unit* needs to be transmitted to have a successful transmission. But before discussing the fading events and the fading model we will describe the frame structure of the GSM system, which provided the *transmission unit*.

The GSM Frame Structure

- The unit of transmission is burst of finite time.
- Burst are sent in time and frequency windows called slots.
- Slots are positioned every 200 KHz and recur in time every 0.577 or 15/26 ms.
- The time unit of time slot is the Burst Period (BP). Figure 1 illustrates the a burst unit.

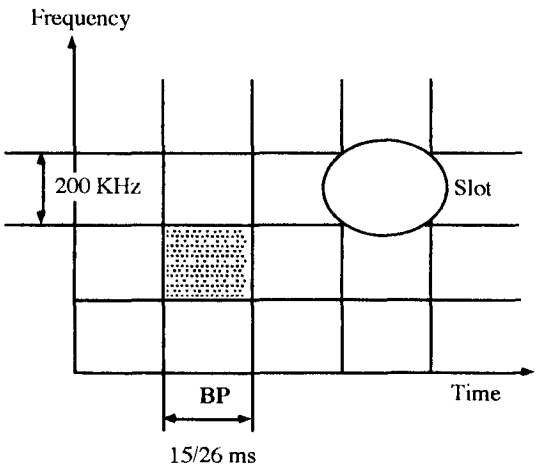

Figure 1. A slot in time and frequency

By definition a frame is succession of n slots, thus the TDMA frame is represented by a succession of 8 consecutive slots. Figure 2 illustrates the GSM frame hierarchy. In this hierarchy the,

- the "26 TDMA frame multiframes" corresponds to a succession of 26 TDMA frames equivalent to 26 x 8 BP or simply 120 ms cycle when related to the traffic channel definitions (TACH/F and TACH/H, see the appendix for a description of the different GSM channels).
- Likewise, the "51 TDMA frame multiframes" as a succession of 51 TDMA frames corresponds to the 51 x 8 BP cycle in the definition of the TACH/8 and that of the common channels.
- The "superframe" as a succession of 51 x 26 TDMA frames is equivalent to 6.12 seconds and it corresponds to the smallest cycle for which the organization channel is repeated (e.g., SACCH).
- Finally, the "hyperframe" corresponding to the numbering period, is 2048 x 51 26 x 8 BP long, which is exactly 12533.760 seconds, or 3 hours 28 minutes, 53 seconds, and 760 ms. As a multiple of all the foregoing cited cycles, it is the smallest cycle for frequency hopping and for ciphering.

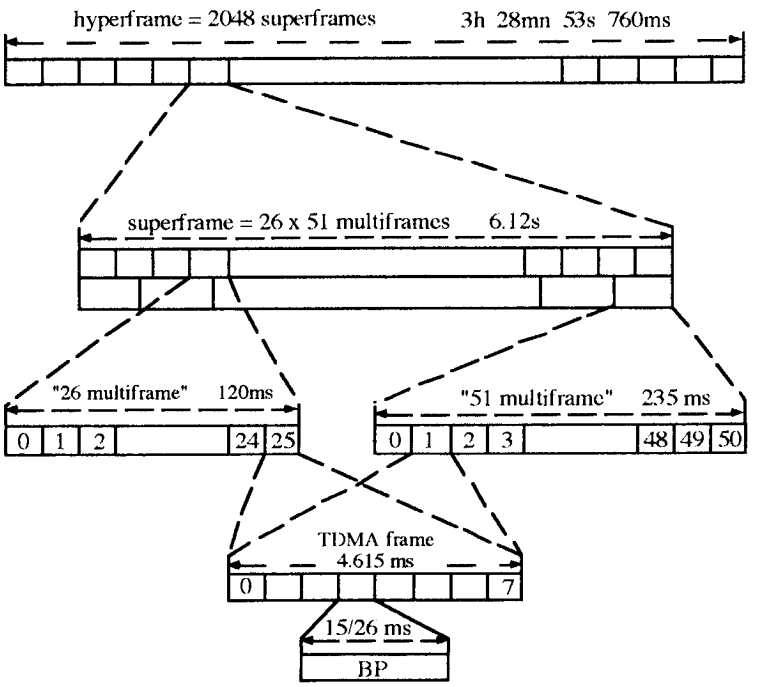

Figure 2. GSM Hierarchy of frames

Fading Model

When considering only the signal transition under influence of Log-normal/Rayleigh type distribution, passing from acceptable to non-acceptable reception conditions, the fading characteristic of the channel can be modeled by observing the evolution of the signal power level in a given time. If the time axis is divided into a set of equal length intervals, chosen according to the slot duration of the signaling channel described in the preceding subsection, the channel state can then be associated with each time slot following the two state Markov chain [9]-[11]. This would imply that when the Markov chain is in good state, at least a BP, but most likely a TDMA frame can be successfully transmitted. However, if the chain is in the bad state, even a single burst or a BP will be corrupted. The chain also implies that will be a transition from the good state to the bad state and vice versa with a probability P_{gb} and P_{bg} respectively. Figure 3, which as discussed in [9], illustrates the transition process.

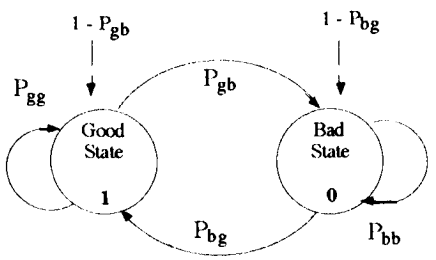

Figure 3. The channel states

Then the state transition probabilities are given by the following matrix:

$$P = \begin{bmatrix} 1 - P_{gb} & P_{gb} \\ P_{bg} & 1 - P_{bg} \end{bmatrix}, \qquad (8)$$

where P_{gb} and P_{bg} can be obtained from experimental measurements by determining the mean time spent by the channel under either good or bad state. Analytically, the mean times and the transition parameters P_{gb} and P_{bg} of the model are related by the geometric distribution as follows:

$$S_{good} = 0P_{gb} + 1\left(1 - P_{gb}\right)P_{gb} + 2\left(1 - P_{gb}\right)^2 P_{gb} + \ldots = P_{gb}\sum_{i=1}^{\infty} i\left(1 - P_{gb}\right)^i = \frac{1 - P_{gb}}{P_{gb}} \qquad (9)$$

$$S_{bad} = 0P_{bg} + 1\left(1 - P_{bg}\right)P_{bg} + 2\left(1 - P_{bg}\right)^2 P_{bg} + \ldots = P_{bg}\sum_{i=1}^{\infty} i\left(1 - P_{bg}\right)^i = \frac{1 - P_{bg}}{P_{bg}} \qquad (10)$$

S_{good} and S_{bad}, in the context of our study are formulated in terms of the number of TDMA frames or burst periods. The probability of remaining in good state P_G, or bad state P_B during a given transmission period, observed under stationary conditions may be expressed as follows:

$$P_{gb}P_G = P_{bg}P_B \quad \text{and} \quad P_G + P_B = 1\ , \qquad (11)$$

from which the simplified[1] state probabilities are formulated as

$$P_G = \frac{P_{bg}}{P_{gb} + P_{bg}} \text{ and } P_B = \frac{P_{gb}}{P_{gb} + P_{bg}} \quad (12)$$

From the preceding equations using experimental data we can calculate the probabilities and the time in which a channel remains in the good state. For example Figure 4, illustrates the change of the transition parameters for duration periods equivalent to GSM multiframe TDMA illustrated in Figure 2, that would allow us to estimate the state probabilities.

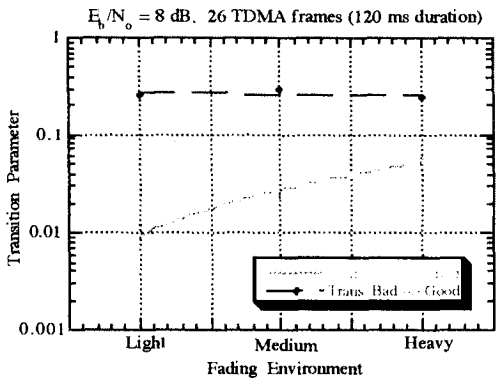

Figure 4 Transition Parameters, from extrapolated experimental data [11]

It is clear that in the channel is not in good state it is under the effects of fading. So if we measure the fading time and couple it with the Soft-handoff mechanism presented in section 2, we can certainly predict the network transitions events in mobile system such as GSM.

CELL TRANSITION EXAMPLES

In the context of the mobility management (MM) there are several options for determining the MS's position [12]. Among them the GPS[2] technique, although it can increase network dependency, it offers an ideal performance for MM because in most cases will reduce the signaling exchange. Therefore for all practical purposes at this time, we will assume that the localization of a MS in relation to the cell radius is done through GPS. Then the goal is to reduce the uncertainty area (Figure 5) to the minimum, in order to define the cell transition distance. We should notice here the presence of two types of cells, the satellite cell (big hexagon) resulting from the projection of a beam, and the regular GSM cell (small hexagon).

The MS measures the distance between the actual position and the last reported one, which is kept in memory. Thus, when the distance between the MS and the centre of the uncertainty area reaches the value of R_u, it request position update. The maximum value of R_u can be defined according to the transmission and motion characteristics, such as propagation conditions and speed. In a global system, some regions like metropolitan, urban or semi-urban areas will have a regular terrestrial mobile network such as GSM, while other areas like rural or developing regions will be primarily covered by satellite services.

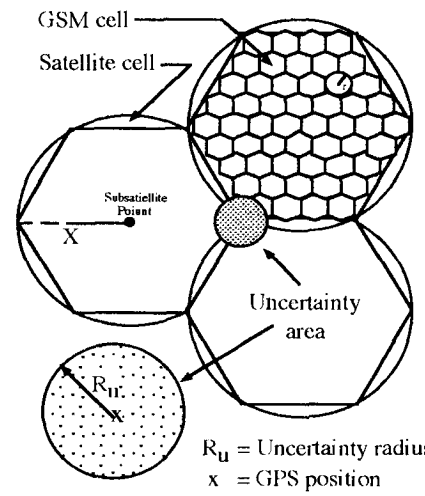

Figure 5 Network transition regions

Therefore, as a MS approaches or leaves a zone with a GSM type system, network transition procedures will be expected. This idea does not preclude the event, that system transition may occur at any given time if network conditions demand it. From the Lognormal shadowing model described in section 2, the spread of propagation, which varies with distance besides geographical influence, can be measured by a single value, the standard deviation σ (dB); which depending on the environment [1] may vary from 2-to-10 dB. Assuming typical GSM cell sizes of 5-10 km for urban to semi-urban areas, we will next estimate the outage probability based in equations (4) and (6). The idea is to maximize the GSM coverage before the MS is served by a satellite cell. Thus, we may emphasize *GSM to satellite network transition* and assume that, satellite to GSM transition is done as soon as the MS linked to a satellite cell perceives a corresponding[3] GSM cell service.

If we estimate 90% of the time coverage around the GSM-type cell boundary as it was done in [6], then according to equation (4a), the required transmission power of equation (4b), a shadowing margin ζ = 10.3 and standard deviation σ = 8 dB, the outage probability P_{out} = 0.102. Now, to estimate the handoff power levels to pass from the GSM network to the satellite system, we vary $\rho = [r + \delta] \div r$, where δ is the distance beyond the boundary of cell with radius r. These power levels are illustrated in Figure 6. In this figure we see that as we increase the relative distance beyond the cell boundary, the handoff transmission margin

[1] A detailed formulation taken into account the statistical degradation of the satellite channel, has been presented in [9]

[2] Global Positioning System

[3] Best power levels are not the only factors, network and capacity correspondence should also be considered.

also increases. In the case of the soft handoff technique, the power margins are about 30 to 40 % lower than at hard handoff.

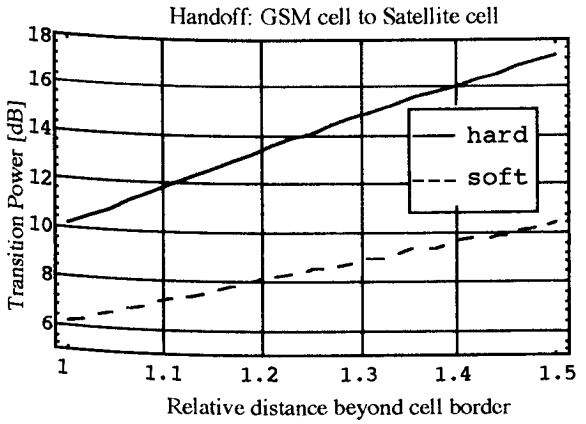

Figure 6. Network transfer power level vs. distance away from the current cell border.

To determine the relative distance beyond the cell border in the satellite side, we use the radius of the uncertainty region. Thus, $\rho = [R_u + \delta] \div R_u$. Other variables used are: $\sigma = 3$ dB, $\zeta = 7.5$ dB. These values imply better signal conditions before a satellite to GSM transition occurs. Although this may not always be the case, the general scenario will be that the MS being served by the satellite approaches a highly shadowed area from a rural or semi-rural region. Figure 7 illustrates the transition power levels from the satellite cell side. Once again, the soft handoff technique requires lower power margins.

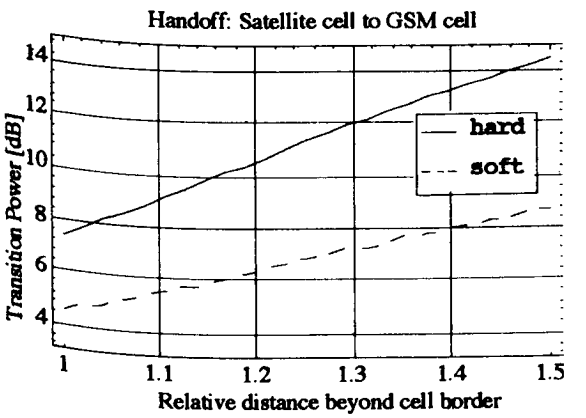

Figure 7 Transition from Satellite to GSM

CONCLUSIONS

In order to quantify the power levels at the moment of transition from a terrestrial to space mobile network and vice versa (e.g., GSM-to-satellite, satellite-to-GSM), in this brief study we have applied the hard and soft handoff techniques. From the adaptation of these techniques, it appears that the soft handoff allows the maximization of the terrestrial system service and thereby increases the coverage area before a network transfer takes place. The technique also shows a good alternative method to balance the traditional means of evaluating the signal quality at the cell borders based on the BER. Because, after all before we calculate the BER we can in apriori already know the evolution of the signal in the cell environment.

REFERENCES

[1] J.P. Castro, " Integrating 3th Generation Mobile Networks," Internal Report EPFL-TCOM 94-1, Feb. 1994.

[2] F. Delli Priscolli and F. Muratore, "Assessment of a public mobile satellite system compatible with the GSM Cellular network," Int. Journal of Satellite Comm., vol. 12, pp. 13-24, Jan.-Feb. 1994.

[3] E. Del Re, R. Fantacci and G. Giambene, "Performance Analysis of a Dynamic Channel Allocation Technique for Satellite Mobile Cellular Networks," Int. Journal of Satellite Comm., vol. 12, pp. 25-32, Jan.-Feb. 1994.

[4] J. Benedicto, J. Fortuny & P. Rastrilla, "MAGSS14: A Medium-Altitude Global Mobile Satellite System for Personal Communications at L-band," ESA Journal, vol. 16, pp. 119-125, 1992.

[5] C. Cullen et al., "Network and Common Channel Signaling Aspects of Dynamic Satellite Constellations," Int. Journal of Satellite Comm., vol. 12, pp. 125-134, Jan.-Feb. 1994.

[6] A. J. Viterbi et al., "Soft Handoff Extends CDMA Cell Coverage and Increases Reverse Link Capacity," Proc. 1994 International Zurich Seminar on Digital Communications, Zurich, Switzerland, pp. 541-551, March 1994.

[7] J.S. Butterworth, "Propagation measurements for land mobile satellites systems at 1542 MHz," Commun. Res. Cen, Tech. Note no. 723, Dep. Commun., Canada, Aug. 1984.

[8] M. Mouly and M-B. Pautet, "The GSM System for Mobile Communications," © 1992 M. Mouly and M-B.Pautet, pp. 342-346.

[9] J.P. Castro, "Statistical Observations of Data Transmission Over Land Mobile Satellite Channels," IEEE Journal on Select. Areas in Comm., vol. 10, no. 8, pp. 1227-1235, Oct. 1992.

[10] Lutz E. et al., "The Land Mobile Satellite Communications Channel- Recording, Statistics and Channel Model," IEEE Trans. on Veh. Tech., vol. 40, no. 2, pp. 375-385, May 1990.

[11] M.J. Miller et al., "Satellite Communications Mobile and Fixed Services," Kluwer academic publishers, P.O. Box 322, 3300 AH Dordrecht, The Netherlands, pp. 325-328, 1993.

[12] M. Denis et all. "A proposed Mobility Management Techniques for Resonant Mobile Satellite Constellations," COST 227 Proj. Doc. No 227TD(94)02, Noordwijk, The Netherlands 27-28 Jan. 1994.

An Approach to Efficient Mobility Management in Intelligent Networks

K. M. S. Murthy
Advanced Technology & Networks,
VISTAR Telecommunications Inc.
427 Laurier Ave West, Room 1410
Ottawa, Ontario, K1G 3J4, Canada
e-mail : murthy@vistar.ca
Phone 613-230-4327 Fax 613-230-4940

ABSTRACT

Providing personal communication systems supporting full mobility require intelligent networks for tracking mobile users and facilitating outgoing and incoming calls over different physical and network environments. In realizing the intelligent network functionalities, databases play a major role. Currently proposed network architectures envision using the SS7-based signaling network for linking these DBs and also for interconnecting DBs with switches.

If the network has to support ubiquitous, seamless mobile services, then it has to support additionally mobile application parts, viz., mobile origination calls, mobile destination calls, mobile location updates and inter-switch handovers. These functions will generate significant amount of data and require them to be transferred between databases (HLR, VLR) and switches (MSCs) very efficiently.

In the future, the users (fixed or mobile) may use and communicate with sophisticated CPEs (e.g. multimedia, multipoint and multisession calls) which may require complex signaling functions. This will generate volumness service handling data and require efficient transfer of these message between databases and switches. Consequently, the network providers would be able to add new services and capabilities to their networks incrementally, quickly and cost-effectively.

Full text of the paper is in the Appendix page A-17

Spacecraft Technology

Session Chairman: **Thomas Brackey,**
Hughes Space & Communications Systems, USA
Session Organizer: **Allan Maclatchy,** Communications Research Centre, Canada

Topic Introduction: Spacecraft Technology is evolving at an ever faster rate. As satellite communications develop, the need for more and more advanced spacecraft designs is necessary to meet the demands of innovative applications. The papers in this session describe a number of divergent subjects under the general heading of Spacecraft Technology. The first two papers address passive intermodulation (PIM), a particularly challenging problem in the design of communications satellites. The next two papers, on specific on-board component developments, are especially relevant to Personal Satellite Communications applications. These are followed by papers describing a demonstration of laser communications; a paper on the test support facilities for mobile satellites; and finally a paper on the IRIDIUM advanced satellite system.

A Study of Secondary Electron Emission Effects for Suppressing Passive Intermodulation Interference in High Power Communication Satellites

Renato G. Bosisio and Yansheng Xu
Poly-Grames Research Center, Département de Génie Électrique et de Génie Informatique, École Polytechnique de Montréal, C. P. 6079, succ. Centre-ville, Montreal, Québec , Canada H3C 3A7 Tel.514-340-4654 FAX 514-340-5892

ABSTRACT

In this paper a study of secondary electron emission effects for suppressing passive intermodulation interference in high power communications satellites is studied. The test facility is described and the test results are provided. The effects of environmental factors on the secondary emission coefficient are given. It is found out that certain refractory compounds are very promissing in eliminating some of the passive intermodulation in satellite communications.

INTRODUCTION

It is well-known that one of the major problems in the design of modern satellite communication systems is to eliminate passive intermodulation (PIM) interference [1]. An important source of PIM appears to be multipactor or microdischarge phenomena. These effects are quite complicated and they depend on various factors such as surface conditions, vacuum, temperature and so forth. Therefore, it is important to study the basic phenomenon - secondary electron emission to make clear the conditions of multipactor effects and try to find means of suppressing them. To this purpose we shall describe an apparatus suitable for this measurement and provide useful measurement results on the secondary electron emission coefficients of various materials and surfaces.

DESCRIPTION OF TEST APPARATUS

The features of our measurement apparatus are:

1. The apparatus is demountable, thus permitting the test of many samples with the same vacuum envelope,

2. It permits accurate measurements for different incidence angle of the primary electron beam, since the impinging electrons are part of a filamentary beam with a trajectory divergence of less than 6 degrees at the surface of the sample,

3. The sample can be baked out and degassed just prior to measurements or even during the course of performing measurements,

4. It is possible to make accurate comparison of the secondary electron emission coefficients of two different surfaces. This is performed by testing the two surfaces within the same vacuum envelope and using the same primary electron beam.

The schematic diagram of measuring apparatus is shown in Fig. 1. The test apparatus is placed inside a bell jar. An

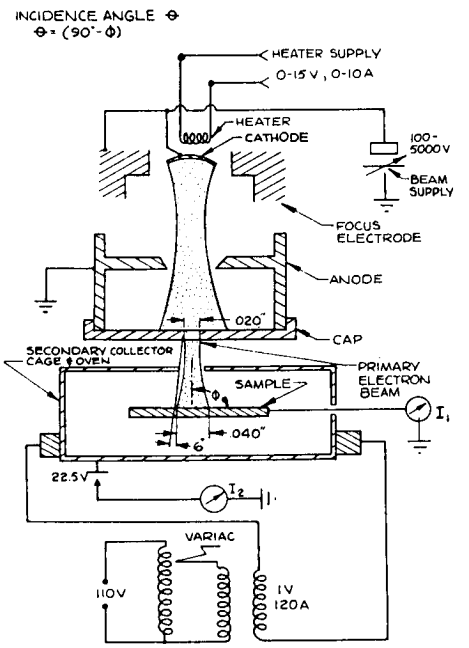

Fig. 1. The schematic diagram of measuring apparatus

oil diffusion pump backed with the usual mechanical pump is used to exhaust the bell jar down to high vacuum. The pressure inside the bell jar is about 2×10^{-6} Torr. Two methods for baking out the test sample are available. The first method consists of heating the sample by radiation from a surrounding molybdenum oven, which also serves as a secondary electron collector cage (see Fig. 1). Typical bakeout schedules for degassing the samples are 450° C for 10 hours or more. The maximum temperature of the sample can reach 600° C. The second method for degas-

sing the sample is achieved by passing an AC current of several hundred amperes through the sample base to raise the sample surface temperature. It is not possible to vary the incident angle of the primary electrons by using this heating method. Typical bakeout schedules for this method of heating are 900° C for 30 minutes. The maximum temperature of the sample may reach 1600° C.

The angle of incidence of the primary electrons is varied from outside the vacuum envelope. The magnetic flux lines from a permanent magnet outside the bell jar are coupled to a cold rolled steel bar inside the vacuum envelope. A rotation of the permanent magnet results in a rotation of the shaft assembly attached to the steel bar inside the vacuum envelope. The test sample fixed to this shaft assembly rotates and the angle of incidence of the primary electron beam on the sample is altered. The sample has a free 360 degree rotational movement so that both surfaces can be tested within the same vacuum envelope. The angle of incidence of both surfaces can be varied continuously between 0 and 90 degrees. By this way the two surfaces can be compared within the same environmental conditions, such as pressure, temperature, bakeout, etc.

The sample is biased to 22.5 volts negative with respect to the secondary electron collector cage (see Fig. 1). The curents I_1 and I_2 are read when a voltage is applied by the beam supply. The secondary emission coefficient for electrons of energy eV is simply calculated from the formula $d = I_2/I_1 + I_2$. The interception of the primary electron beam by the collector cage cannot occur since the hole in the cage through which the beam passes is much larger than the beam diameter and the beam divergence is only 6 degrees.

MEASUREMENT RESULTS

First of all, a study is devoted to the effects on the secondary electron emission coefficients of environmental factors such as gassiness, temperature and angle of incidence. Several samples made from OFHC copper, tungsten, molybdenum, vanadium carbide, niobium carbide and so forth have been tested. Fig. 2 shows the different secondary emission coefficients for an OFHC copper sample under different gassiness conditions for normal incidence. It is found out that though the temperature-time factors for bakeout are quite different, the secondary emission coefficients differ only by a few per cent. It is interesting to note that at higher primary electron energies (greater than 1000 ev) the secondary emission coefficients for the two surfaces are identical. This means that variable gassiness conditions will affect the secondary electron emission in the low primary electron energy range (less than 1000 eV) and have little effect at the high primary electron energy ranges. On the contrary, as shown in Fig. 3, these same two samples have considerably different secondary electron emission coefficients for 60 degree incidence angle

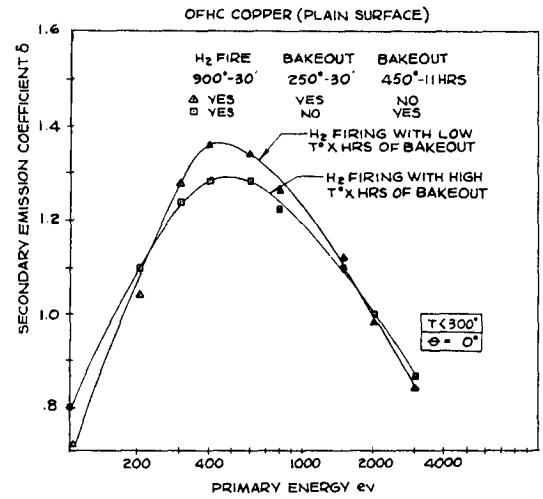

Fig. 2. Effects of gassiness on secondary electron emission at normal incidence

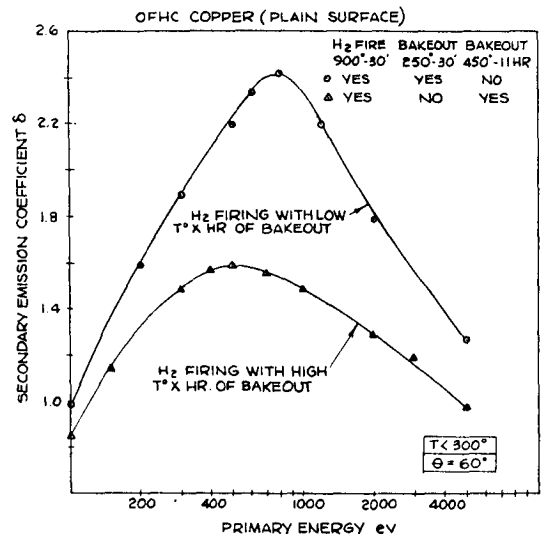

Fig. 3. Effects of gassiness on secondary electron emission at oblique incidence

of the primary electron beam. These differences may achieve as high as 50 per cent and cover the full range of the primary electron energies. From this we can conclude that oblique incidence makes the effects of surface conditions much more evident than normal incidence. Fig. 4 shows the results obtained from a surface which reabsorbs gases after the bakeout process. It is observed that gas reabsorption after bakeout can increase the secondary electron emission value by 10 per cent. It is also found out that this effect is saturated only 8 hours after bakeout.

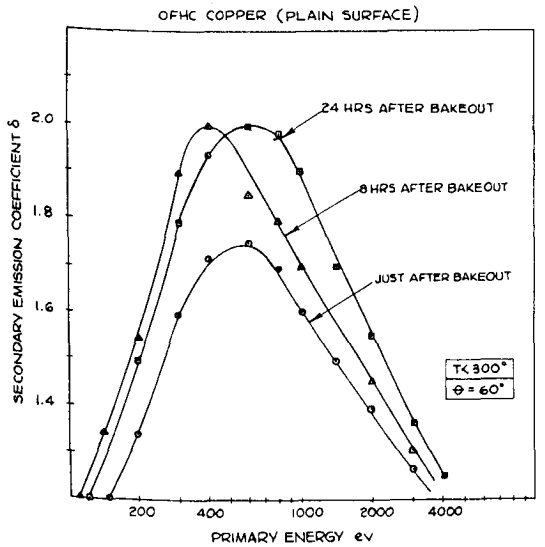

Fig. 4. Effects of reabsorption of gases after bakeout

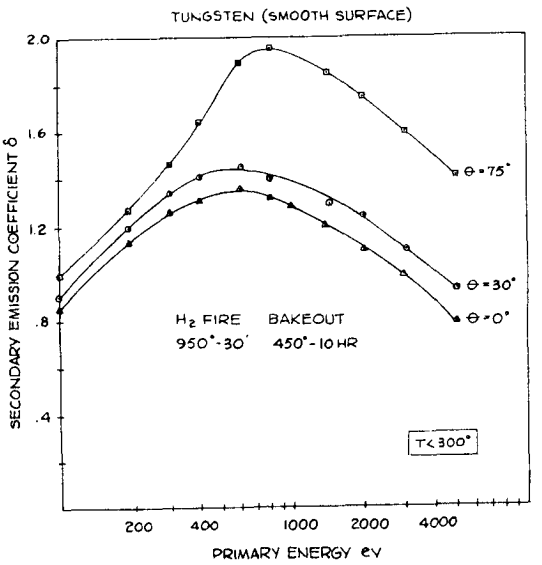

Fig. 5. Effects of incident angle on a smooth surface

The effects of incident angle of the primary electrons on the secondary electron emission coefficient are shown in Figs. 5 and 6. It is observed that oblique incidence (75 degrees) can increase the secondary electron emission by 40 per cent over normal incidence for a smooth tungsten surface (Fig.5). A similar experiment with the roughened back side of the same plate shows that the secondary electron emission coefficients increase is less than 7 per cent. These two surfaces were measured within the same vacuum envelope, and these results were repeatable. It is noted that surface roughening does not change the secondary electron emission appreciably for normal incidence. The secondary electron emission decreases appreciably only in cases of oblique incidence after surface roughening. Therefore, the effects of incident angle can be reduced significantly by roughening the surface finish.

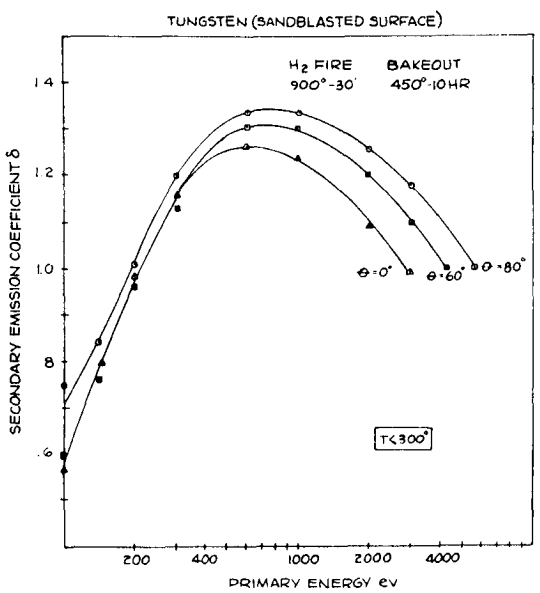

Fig. 6. Effects of incident angle on a rough surface

Some surfaces reputed to be secondary electron emission suppressors were then measured, such as soot surfaces and so forth. It was found that at low temperatures some of these surfaces are very good secondary emission suppressors, but are unstable at high temperatures probably due to carbon diffusion. Therefore, it remains an important task to obtain stable secondary emission suppressors for surfaces submitted to low or elevated temperatures near satellite antennas.

To this end, measurement of refractory compounds is also performed. It is observed that for the refractory compounds vanadium carbide, niobium carbide and tantalum carbide the maximun secondary emission yield is less than unity. They are thermally stable up to 1600° C. The results of vanadium carbide are shown in Fig. 7. It is observed that the maximum value of the secondary electron emission coefficient is less than 0.8 before and after bake out at 1600° C for 15 minutes. Thus, this surface produces a low secondary electron emission coefficient and maintains high thermal stability.

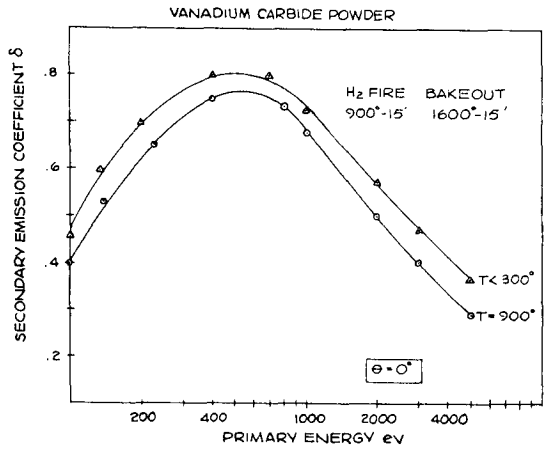

Fig. 7. Temperature effects of Vanadium Carbide

CONCLUSION

An apparatus used for measuring the secondary electron emission coefficient is introduced. The effects of environmental factors on the secondary emission coefficient are studied and some refractory compounds are found to be very effective in suppressing this emission at high temperatures and stable. It is expected the proposed apparatus and test results will find significant applications in the study of the passive intermodulation in satellite communications.

REFERENCES

1. C. F. Hoeber, D. L. Pollard and R. R. Nicholas, "Passive intermodulation product generation in high power communication satellites" Communication Satellite Systems Conference, San Diego, March 1986, pp.361-374.

2. R. G. Bosisio, "Secondary electron emission suppression", Thesis.

MSAT PIM and Multipactor Test Program

Y. Patenaude, S. Richard, F. Ménard, E. Amyotte, C. K. Mok
SPAR Aerospace Ltd, 21025 Trans-Canada Hwy, Ste-Anne-de-Bellevue
Québec, Canada, H9X 3R2, Phone: 514-457-2150, FAX: 514-457-2724

ABSTRACT

The MSAT satellite system will provide telephone, fax and low data rate communication services to mobile users throughout North America. The space segment of the MSAT system must supply high radiated power densities on the ground to allow communication with small mobile terminals. Therefore, the high power handling requirement (multipactor, PIM and thermal dissipation) are very important performance parameters for mobile satellite communication systems.

Large separate transmit and receive L-Band deployable reflectors are used on MSAT to reduce the risk of PIM. In addition, PIM and multipactor avoidance were major design drivers for the L-Band high power transmit output network and antenna. This paper provides an overview of the designs selected and the extensive qualification and verification program undertaken on MSAT to meet the challenging PIM and multipactor requirements. The test campaigns at component, sub-system and system levels and the associated test results are presented. The manufacturing and assembly approaches taken to allow the PIM and Multipactor to be met are also briefly described.

INTRODUCTION

The MSAT satellite system provides communication services (telephone, fax and low rate data) at L-Band to sea, land and air mobile terminals throughout north America including the Gulf-of-Mexico, Puerto-Rico and Hawaii. Spar had a leading role in defining system requirements and has been responsible for the satellite payload design, integration and test.

The payload required a high power L-Band antenna and repeater output section to enable communication with mobile terminals. An extensive qualification program was needed to support the design of antenna and repeater units and assemblies that met the stringent high power requirements. This paper describes the high power test setups and it summarizes the measurements performed for the development qualification and acceptance testing of the L-Band high power transmit antenna and repeater units (transmit feed assembly, Output Hybrid Matrix (OHM), Isolator, T-switch and coaxial cables). Emphasis will be given to the tests performed to verify the PIM, multipactor and high power performance of the L-Band Transmit feed assembly.

PERFORMANCE REQUIREMENTS

The geostationary L-Band satellite antenna subsystems must offer high gain in order to maximize the EIRP on the ground and to ensure adequate transponder sensitivity. The high gain requirement stems from the need to communicate with small mobile earth terminals which have limited output power and antenna gain. As a result, the operating power level of the transmit antenna is fairly high. The power handling problem is compounded by the fact that the receive signal EIRP from the earth mobile station is very low. This renders the transponder vulnerable to PIM products and consequently results in very stringent PIM specification.

DESIGN CONSIDERATIONS

The risk of system interference due to PIM has become a major design driver on the MSAT payload. The decision to use separate transmit and receive antennas was made early in the program. Although this provides a significant decoupling between the transmit and receive paths, PIM remained a major design requirement for the transmit antenna due to the very high transponder gain. The MSAT L-Band transmit antenna subsystem is shown in Figure 1 and described in [1].

In order to further reduce the risk of system interference due to PIM, it was also decided to incorporate a high rejection output bandpass filter as far as possible in the high power L-Band output section so as to minimize the number of PIM critical units. On the MSAT payload, some of the L-Band transmit feed components (the cup dipole array, the Beam Forming Network (BFN), the output bandpass filters and the honeycomb support panel) were very critical units from a PIM standpoint. The design and performance of the L-Band feed assemblies are presented in [2].

In addition to the L-Band transmit feed components, all the units, structures and thermal hardware exposed to high RF

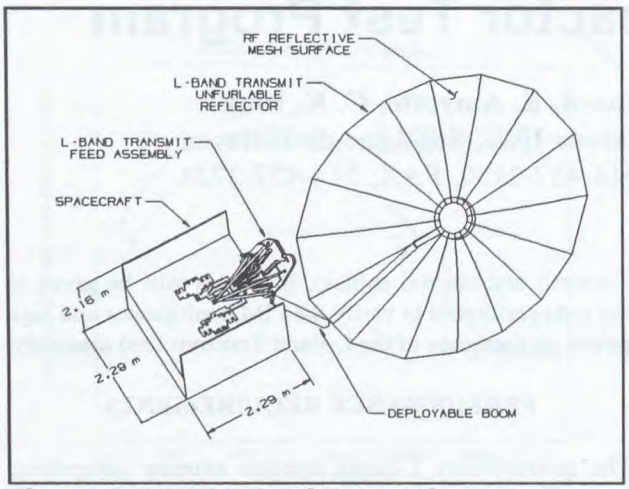

Figure 1. MSAT L-Band Transmit Antenna

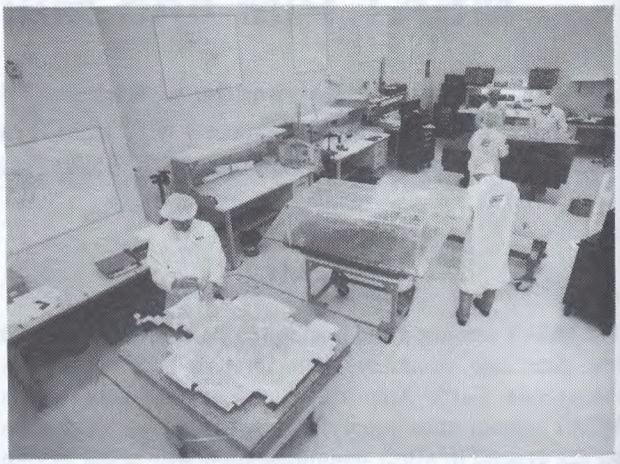

Figure 2 Assembly Room for PIM Critical Units

energy on the transmit antenna side of the spacecraft have required special precautions to ensure that the payload PIM requirements are met. Whenever possible, the potential PIM sources were eliminated or reduced to negligible levels. The PIM sources that could not be eliminated were shielded from the high flux density radiated by the L-Band transmit feed array.

SPECIAL PRECAUTIONS

The workmanship is of the utmost importance for the PIM and multipactor performance of high power units. Spar has taken numerous measures to ensure that the quality of the workmanship will enable the PIM and multipactor high power requirements to be met. All the personnel involved in the design, fabrication, assembly, test, inspection and quality assurance of PIM critical hardware were trained and provided with continuous technical support.

Special processes were developed for the fabrication of non-metallic parts which are susceptible to contamination. A new electro-plating process was used. New approaches for handling, protecting and storing parts were developped. A dedicated assembly, integration and test room with limited access was established for the L-Band high power assemblies (Figure 2). Special tools for assembly and inspection were developed. All the parts of high power units and assemblies were subjected to thorough inspections throughout the manufacturing, assembly and test phases.

PASSIVE INTERMODULATION

PIM Test Setup

Since MSAT uses separate transmit and receive antennas at L-Band, only the radiated PIM from the Tx antenna and bus hardware is of concern. Consequently, all the PIM tests were conducted in radiating mode. The PIM test setup consists of two low spurious signal synthesizers used to generate the 2 pure transmit test tones. Using two high power amplifiers (250W), the two tones are amplified. A Tx-Tx diplexer is used to combined the two high power carriers in a low loss fashion. The test carriers are then routed to one port of the DUT which is placed into an RF transparent thermal enclosure inside an anechoic chamber to perform PIM tests. The two tones test is more stringent than a real traffic situation.

The PIM signals generated by the DUT are monitored using a receive probe in front of the radiating assembly under test. The measured signal is filtered and amplified using high rejection bandpass filter (Rx filter) and low noise amplifier in cascade. This removed the Tx carriers and the PIM these carriers might have generated in the monitoring line. The signals are divided in two channel using a 3 dB hybrid. Two different PIM order can be monitored simultaneously. The 7^{th} order was the lowest order that had to meet the PIM requirements. However, for debugging reasons, the 5^{th} order signals were monitored at times The PIM signals are detected using highly stable spectrum analyzers.

A new state-of-the-art thermal PIM test chamber was designed, manufactured and qualified for the acceptance testing of the large MSAT L-Band feed assembly and associated feed thermal blankets. The new PIM test chamber is shown in Figure 3. The thermal enclosure can accommodate test articles up to 3.5 m long by 3.2 m large by 2.1 m high. The thermal enclosure allows testing of DUTs over a temperature range from -65°C to +110°C. The PIM test chamber is built inside an RF shielded

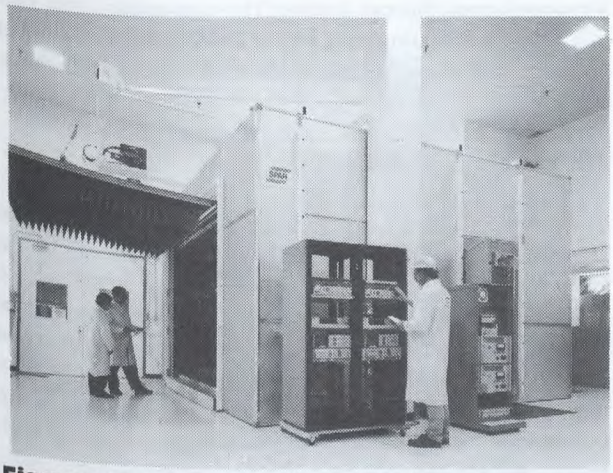

Figure 3. New SPAR PIM Test Chamber

enclosure that provides a noise free environment which allows measurements down to the sensitivity of the low noise amplifier (-155 dBm).

PIM Test Plan

An extensive PIM test development program was undertaken to ensure a PIM free antenna feed design and qualify all the fabrication, assembly and inspection processes. The exercise started with a single element breadboard feed model assembly which consisted of a high power transmission TEM-line section, a transmit bandpass filter, a short BFN section and a cup dipole radiator. This simple assembly was used to qualify all the basic components, all the various materials and all the interfaces comprised in the transmit feed. The breadboard feed model was upgraded to include all the different changes as the flight feed mechanical and electrical design evolved over an 18 month period.

After the feed design was finalized and fully qualified to meet the PIM requirements, an engineering model was manufactured, assembled and tested. The EM, representing one of the six antenna beams, consisted of an array of 5 cup dipoles, a BFN section, a bandpass filter, a section of high power TEM-line and a honeycomb aluminum support panel. The EM feed was used to qualify the design at a larger scale. It was also used to finalize the feed thermal blanket design and all the low PIM grounding scheme developed for MSAT.

The two transmit feeds were tested at partial assembly level to provide an early verification of the flight hardware. Each acceptance PIM test consisted of 3 thermal cycles for each of the 6 beams for a total of 18 thermal cycles per partial feed assembly. Since PIM is a very critical performance parameter and is highly dependent on the quality of the workmanship, it was decided to perform this intermediate thermal PIM test before final feed integration. It is clearly much easier to resolve any problem on a smaller assembly.

The complete protoflight and flight feed assemblies were subjected to thermal PIM testing through the acceptance test program at pre- and post-environment levels. Again for the complete feed assemblies, each of the six antenna beams were tested over 3 thermal cycles for a cumulative total of 36 thermal cycles for each feed assembly.

PIM testing was performed at spacecraft level in order to assess the overall satellite PIM performance. To support this test, a qualification test setup was put together to qualify the large anechoic chamber of the David Florida Laboratory of the Canadian Space Agency. Two full scale PIM free mock-up reflectors (Tx/Rx) and a PIM free mock-up spacecraft bus were built to perform that qualification test. The engineering model feed was used in various configurations in order to simulate the radiation patterns of the 6 transmit antenna beams.

The spacecraft level PIM tests were done using the flight model Tx reflector and a mockup Rx reflector together with the satellite configured in a configuration that included all the PIM critical hardware (Figure 4). The Rx reflector was replaced by a mock-up since it was established that it was submitted to a very low RF power density and, hence, was not a PIM concern . Non-metallic

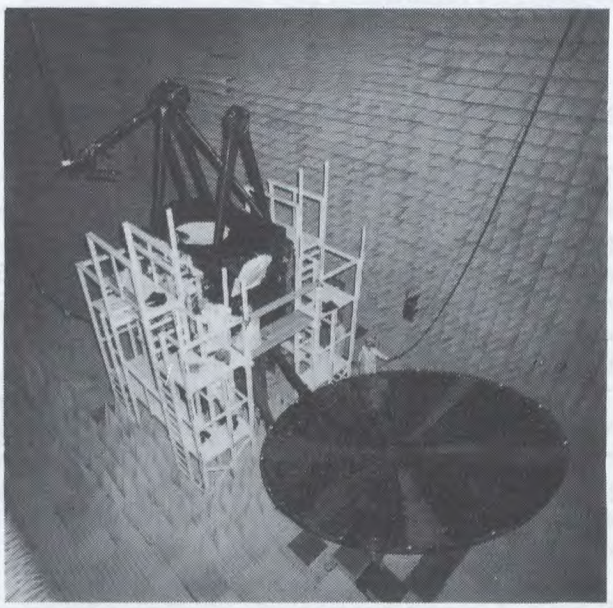

Figure 4. Spacecraft Level PIM Test

test supports were used to eliminate the risk of PIM and minimize the RF blockage between the Tx and Rx sides of the spacecraft. An elaborate wooden scaffold was used to provide easy access to any part of the satellite at any time during the PIM test.

Measured PIM Performance

As previously mentioned, the breadboard feed model was used for the validation of the L-Band transmit feed design. The objective of the breadboard level PIM testing was to eliminate all PIM sources above the noise floor of the measurement system. No PIM signals above the test setup average noise floor of -155 dBm was measured for the engineering model feed over the qualification temperature range of -45 to +110^{oC}. The engineering model testing confirmed the feed design as well as the quality of the workmanship.

In general, for the final acceptance thermal PIM tests performed on the complete feed assembly, no PIM signals above the average test setup noise floor of -155 dBm were observed. In a few cases, a worst case level of -135 dBm was measured throughout the entire acceptance test program.

Thermal PIM testing of the complete spacecraft was not practical and, thus, the spacecraft level test was performed at ambient temperature. No PIM was measured above the transponder receive noise floor during the final integrated spacecraft testing. Therefore, the overall MSAT L-Band payload PIM requirements have been met with margin.

MULTIPACTOR

Multipactor Requirements and Component Design

The design objective for the L-band components was to achieve a multipactor threshold at least 3 dB above the peak operating power. For that purpose, multipactor analyses were part of the design process for each high power component. This generally involved performing numerical analyses of the components in order to determine the internal field levels at the operating peak power. The levels were then compared with known multipactor threshold fields. This provided a margin estimate for each component. Because of tight mass constraints, it was not possible to systematically oversize the components to achieve large multipactor margins. The optimum component sizes needed to be determined.

Because of the complex nature of multipactor, all margins were confirmed through testing. The pass criteria was 3 dB margin over operating peak power for acceptance testing of actual flight components, and 4 dB for qualification models.

Multipactor Test Setups

The setups fall in two categories, namely resonant ring and straight line. The preferred configuration is the straight line since it yields slightly more accurate results by allowing a better control of the VSWR seen by the component under test. This configuration can also accommodate one-port and lossy multi-port devices which is not possible with a resonant ring. The advantage of the ring however is the power gain which reduces the requirements on the high power source. Both types of setups have been used successfully in this program. Figures 5 and 6 respectively show the TEM-line resonant ring (large size square coaxial assembly) and the instrumentation used for multipactor testing.

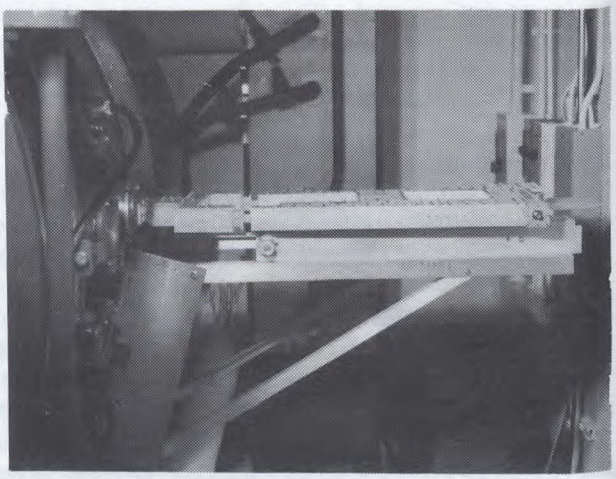

Figure 5. Multipactor Resonant Ring

The peak test levels were achieved through amplitude modulation of high power CW sources or by using a combination of CW and high power pulse sources. A number of detection methods have been used, including transmission and reflection phase measurements as well as electron migration detection.

The tests were conducted at the qualification temperature (hot case) in hard vacuum, slightly above the average operating power in order to reproduce the operating thermal gradient. The tests typically lasted 2 to 24 hours. In some cases, longer duration tests were carried out, up to a maximum of 170 hours.

Figure 6. Multipactor Test Setup

Test component

EQM versions of the following components were tested:

- high power air stripline isolator
- coaxial cable
- coaxial T-switch
- 8x4 TEM-line output hybrid matrix (OHM)

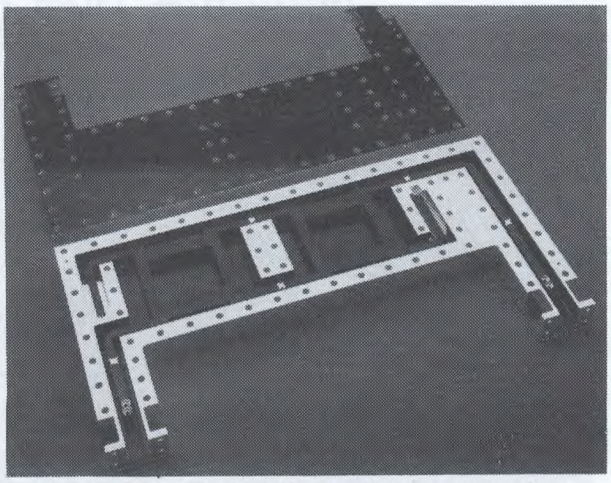

Figure 7. High Power Branch-Line Coupler

- high power interconnecting TEM-line
- coaxial cavity bandpass filter
- TEM-line beam forming network (BFN)
- cup dipole

In addition, every flight models of the isolators and T-switches were tested at reduced peak power levels.

The OHM and BFN are highly integrated assemblies which consist mostly of a network of branch-line couplers, bends and feed-throughs. It is very difficult to measure the multipactor threshold of such embedded components. For

Table 1 Operating and Multipactor Test Power Levels

COMPONENT	OPERATING POWER LEVEL (PEAK POWER) [W]	QUALIFICATION TEST LEVEL (AVG./PEAK) [W]	FLIGHT MODEL ACCEPTANCE TEST LEVEL (PEAK POWER) [W]
HIGH POWER ISOLATOR	125	50/300	250
COAXIAL CABLE	125	50/300	-
T-SWITCH	125	50/300	190
8X4 TEM-LINE OUTPUT HYBRID MATRIX (OHM) COMPONENTS	540	230/1360	-
HIGH POWER INTER-CONNECTING TEM-LINE	540	230/1360	-
COAXIAL CAVITY BANDPASS FILTER	525	225/1320	-
TEM-LINE BEAM FORMING NETWORK (BFN) COMPONENTS	500	210/1250	-
CUP DIPOLE	380	165/960	-

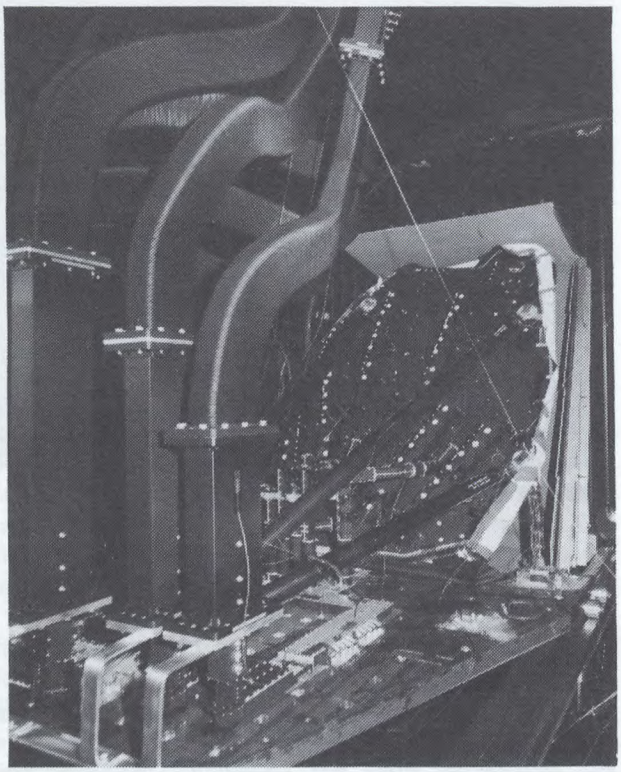

Figure 8. L-Band Tx Feed High Power Test

these assemblies, the qualification testing was therefore performed on identical separate components which were fabricated especially for the test, i.e. separate couplers,bends and feed-throughs. Figure 7 illustrates such a branch-line coupler.

Multipactor Test Results

Table 1 provides the operating peak power levels for each component, as well as the multipactor test power levels. The 3 and 4 dB margin objectives were met in general. Due to the relatively low margins however, it was necessary to observe special handling and manufacturing procedures in order to avoid contamination and the associated multipactor threshold reduction.

Transmit Feed High Power TVAC Test

A high power handling/multipactor test was performed on the complete Tx feed assembly. The test was conducted in a thermal vacuum chamber with the feed radiating inside an RF absorbing enclosure (Figure 8). The RF test consisted in monitoring changes in return loss performance and observing any evidence of multipaction while radiating high power through the Tx feed. The average power used in any of the 6 beams during return loss checks was 315 Watts. The return loss was continuously monitored over one complete thermal cycle (+110°C to -45°C). Each beam port was monitored for a period of 20 minutes at each temperature plateau. The maximum return loss variations met the test requirements. Furthermore, the variations were gradual with no abrupt changes in return loss which confirmed the mechanical stability of the feed assembly over temperature and at high power. For multipactor, the tests were performed during the hot plateaus with 309 Watts average and 600 Watts peak. There were no multipactor events recorded during the test.

CONCLUSION

The development and qualification of the high power MSAT payload components and assemblies represent an important technical challenge. A comprehensive PIM and multipactor qualification program was undertaken to support the hardware design. State-of-the-art test facilities were developed to support this qualification program. A substantial quality improvement program was also undertaken to ensure very high workmanship quality. This approach has led to very successful acceptance test campaigns at subsystems as well as at complete spacecraft level.

REFERENCES

[1] Y.Patenaude, E.Amyotte, P.Ilott, F.Ménard, S.Gupta, C.Mok, *MSAT L-Band Antenna Subsystems*, presented at the 15th International Communication Satellite Systems Conference, San Diego, U.S.A., February 27 - March 3, 1994.

[2] S.Richard, K.N.Patel, Y.Patenaude, J.P.Langevin, J.Wang, *M-SAT L-Band Antenna Feed Arrays*, presented at the 15th International Communications Satellite Systems, San Diego, U.S.A., February 27 - March 3, 1994.

Applications of Multi Port Amplifier to Personal Satellite Communications

Shunichiro Egami

Mitsubishi Electric Corporation
325, Kamimachiya, Kamakura, 247, Japan
Tel: 81-467-47-2138 Fax:81-467-47-2087

Abstract

In personal satellite communications, satellite antenna beam becomes narrow, and number of beams will be thirty to more than one hundred. This paper shows that Multi Port Amplifier[1] is most suitable to multiple beam transmitter for personal communications satellite. It was shown that the single beam coverage area(cell) diameter is determined by personal earth station(PES) eirp, uplink C/No and uplink frequency band[2]. Required number of cells for European or North American regional coverage at FPLMTS uplink frequency band is shown as around 32. It was shown that 32 beams systems will be easily implemented by using 2 set of 16-port MPA. Redundancy to SSPA failure is considered by increasing number of SSPAs. Actual configuration for 16-port MPA are briefly shown. The presented configuration will be easy to implement and the most economical solution.

Introduction

In mobile satellite communications, it is necessary to use multiple beam satellite antenna in order to communicate by small mobile terminals. Although high gain narrow beam satellite antenna enables use of small eirp mobile terminals, sub-dividing of coverage area to large number of small cells cause system design problems. To alleviate these problems, author proposed multiple Hybrid transmitter in 1987[1], which is recently called Multi Port Amplifier. Since author proposed MPA in May 1987 issue of the IEEE Journal on Selected Areas in Communications[1], the idea seems affected multiple beam mobile satellite systems appeared after that. Proposed concept affected Immarsat-3 5-beams transmitter[3], AMSC/MSAT 6-beams transmitter[4/5] and Nstar 4-beams transmitter design[6]. All these satellites will be launched this year. This paper considers application of MPA to personal mobile satellite communications systems.

Merit of Using MPA.

Satellite antenna gain can be increased by using large number of narrow beams, which enables use of small earth stations. Therefore, next generation mobile satellite systems will use large number of multiple beams by which hand-held terminals with small transmitting power can be used.

However, dividing single service area to multiple cells will cause difficulties which do not exist in single beam systems. Traffic in each beam will significantly change necessitating much higher transmitting power corresponding to peak load in the beam. If fixed transmitting power are assumed to each beam corresponding to the peak load, efficiency of using satellite power will be significantly degraded. This is the reason why MPA is proposed. MPA enables power sharing among beams by which efficiently utilizing limited satellite total transmitting power.

In multiple beam mobile satellite communications, required transmitting power to each beam will vary corresponding to the varying traffic in the beam. This will necessitate flexible power transmitter for each beam. The multiple beam transmitter which has these functions are multiple beam phased array and MPA. Simplicity of implementation and low cost are why MPA is used in many multiple beam mobile satellite systems.

MPA can also be used in multiple beam fixed satellite systems. By applying MPA, fixed satellite communications systems can increase number of beams as desired.

High G/T and high eirp enabled by large number of narrow beam coverage will allow use of extremely small earth stations and will also allow to increase total transmitting capacity of the satellite significantly.

Personal Satellite Communications Requirements [2]

Personal earth station(PES) will have omni directional antenna which enables communications without knowing direction of the satellite. This means PES antenna gain is around 0dB, which is not depend on frequency. If transmitting power is assumed to be about 0.5W , eirp of PES will be around -3 dBW. If PES eirp is represented by $eirp_{PES}$ and satellite altitude is represented by H, then, up link power flux density at satellite is represented by

$$PFD=eirp_{PES}\,(1/4\,\pi\,H^2) \qquad (1)$$

If satellite antenna diameter is represented by D and aperture efficiency is represented by η , then effective aperture of satellite antenna is represented by

$$A_{eff}=\eta\,\pi\,(D/2)^2 \qquad (2)$$

Satellite receiving power C when PES is at the beam center can be obtained by

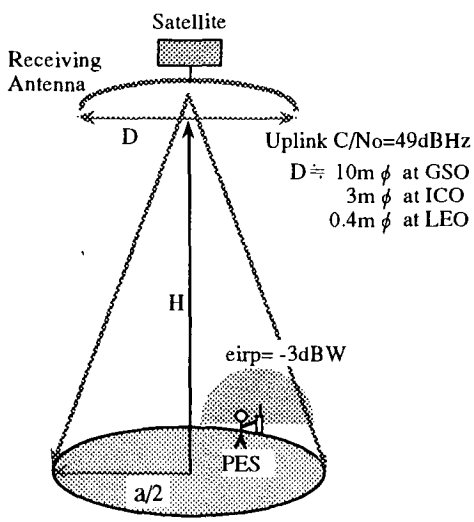

Up Link Beam Coverage Area (Cell)

Fig.1 Up link beam coverage(cell) concept

$$C=PFD*A_{eff} \qquad (3).$$

If PES is at the beam edge where antenna gain is 3dB lower than peak, receiving power C will be given by

$$C=0.5*PFD*A_{eff} \qquad (4).$$

Receiving noise density is given by $N_0=kT_S$ if satellite system noise temperature is given by T_S. Then, beam edge uplink $C/N_{0,UP}$ is given by the following frequency independent equation.

$$C/N_{0,up}=(\eta/32)(eirp_{PES}/kT_S)(D/H)^2 \qquad (5)$$

This means that if "$eirp_{PES}/kT_S$" were given by some fixed value, uplink C/N_0 is solely dependent on D/H.

In order to obtain some fixed uplink C/N_0, satellite antenna diameter D must be proportional to satellite altitude H.

If $eirp_{PES}$=-3dBW, T_S=600K, η =50% and beam edge C/N_0=49dBHz, then antenna diameter D is determined by satellite altitude as shown in Table 1.

Table 1 Required satellite antenna diameter

Satellite Type			GSO	ICO	LEO
Satellite Altitude	(H)	km	36,000	10,370	1,389
Sat. Ant. Ap. Eff.	(η)	%		50	
Sat. Sys. Noise Temp.	(Ts)	K		600	
PES eirp		dBW		-3	
Beam Edge Uplink C/No		dBHz		49	
Satellite Ant. Diameter	(D)	m	10.43	3.01	0.40

These requirement for satellite antenna diameter are frequency independent. On the other hand, uplink 3dB beamwidth θ is approximately given by (λ :wave length)

$$\theta=70\,\lambda/D \qquad (6).$$

Then, satellite antena beam coverage area(cell) diameter "a" at nadir is given by

$$a=2H\,Tan(\theta/2)\fallingdotseq H\,\theta \qquad (7).$$

Using Eq.5 and 6 cell diameter is given by the following equation.

$$a=(\pi\,70/180)\,\lambda\,SQRT\{(\eta\,eirp_{PES}/32kT_S)/(C/N_{0,up})\} \qquad (8)$$

The cell diameter is not dependent on the satellite altitude, but dependent on uplink frequency. Table 2 shows cell diameter for several uplink frequency band.

Table 2 Required cell diameter vs. uplink frequency band

Uplink Frequency		GHz	1.66	2.01	2.69
Sat.Ant.Ap.Eff	(η)	%		50	
Sat. Sys.N.Temp.	(Ts)	K		600	
PES eirp		dBW		-3	
Beam Edge Uplink C/No		dBHz		49	
Cell Diameter at Nadir (a)		km	761	629	470

Required Number of Beams for Major Regional Coverage

Cell diameter necessary to support personal satellite communications is given in Table 2. This is the fundamental requirement which does not depend on satellite altitude. The cell diameter shown in Table 2 is at nadir. Actually, more wider area can be covered on the earth if beam covers earth aslant. In order to obtain earth coverage image, cell pattern on North America is shown in Fig.2. Frequency is 2.01GHz, FPLMTS satellite up link frequency band. The number of beams(cells) for this regional coverage example is 32. It will be understood, if personal satellite communications are intended at 2.01 GHz band, 32 beams will be approximately enough to cover North America.

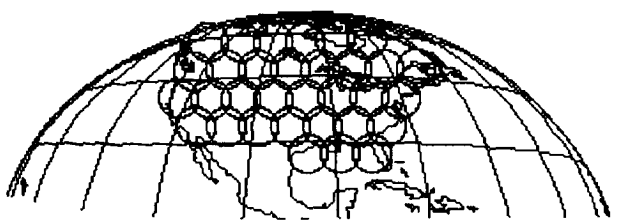

Fig.2 32 beams North America coverage which support personal satellite communications at 2.01GHz
Beam diameter is 629km ϕ at nadir.

The same coverage is considered on Europe. Fig. 3 shows 32 beams coverage example on Europe at 2.01 GHz.

From these coverage examples, it seems reasonable to cover major regional area by approximately 32 beams if uplink frequency is at 2.01 GHz band.

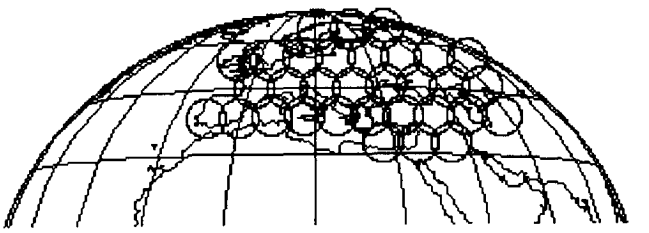

Fig.3 32 beams European coverage which support personal satellite communications at 2.01GHz
Beam diameter is 629km ϕ at nadir.

Basic Configuration of MPA

Fig.1 shows basic constituent of MPA, which is 2-port MPA. This is well known balanced amplifier. Using 2 set of 2-port MPA and another 2 pair of Hybrids, 4-port MPA can be assembled as shown in Fig.5

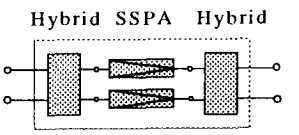

Fig.4 Basic Constituent of MPA

Similarly, using 2 set of 4-port MPA and another 2 pair of Hybrids, 8-port MPA can be assembled as shown in Fig.6. Basic configuration of MPA have number of port equal to 2,4,8, , 2^n (n=1~) and the same number of SSPAs.

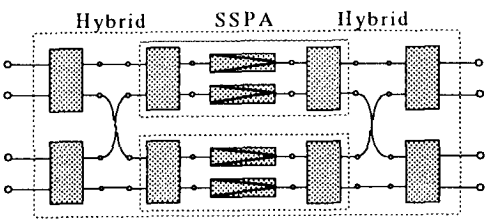

Fig.5 4-port MPA or 4-SSPA Block

Since Hybrid is a low Q circuit, its loss is small if it was designed by low loss transmission line. Thus, output combining loss will be made small by using Hybrid with low loss transmission line and low loss cables. Fig.6 shows 8-SSPA MPA for 8-beams configuration. Any number of beams smaller than 8 can be accommodated by not using unnecessary ports.

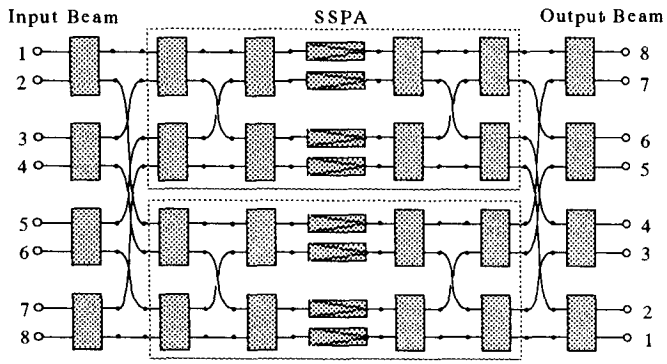

Fig.6 8-port MPA for 8-beam transmitter

Effect of Phase and Amplitude Error

In order to have enough isolation between ports, SSPA and connecting cables must have equal gain and electrical length. Also, input and output Hybrid must have minimal phase and amplitude error. If amplitude and phase mean variation at each SSPA port is represented by Δ and δ respectively, then, isolation at the isolated port are approximately given by the following equation for N-port MPA.

$$P_{iso}/P_{out} = (\Delta^2 + \delta^2)/N \qquad (9)$$

For combined output, these amplitude and phase error have minimal effect. Mean amplitude and phase error are important because it affects isolation at the isolated ports. As understood from above equation, it is better to select MPA configuration with large number of N, using large number of SSPA.

Amplitude and phase error occurs at input and output multi-port hybrid and each SSPAs. Therefore, in actual cases, amplitude and phase error of input and output multi port Hybrid at each SSPA port can be compensated by selecting amplitude and phase error of each SSPA.

Redundancy Consideration

In actual implementation, reliability considering SSPAs failure become necessary. One SSPA failure in N SSPAs will decrease output power at the output port by the following equation.

$$P_{-1}/P_0 = ((N-1)/N)^2 \qquad (10)$$

On the other hand, one SSPA failure in N SSPAs will degrade isolation at the isolated port approximately by the following equation.

$$P_{-1,ISO}/P_0 = (1/N)^2 \qquad (11)$$

One method of SSPA redundancy is to implement a redundant SSPA which can be switched from failed SSPA without changing electrical length . This will complicate SSPA interconnection to multi-port Hybrid. Especially, to improve isolation among beams, it is better to use large number of SSPAs. If large number of SSPAs is used, implementing redundant SSPAs become difficult.

Another method is simply increasing number of SSPAs. If number of SSPAs is larger, effect of single SSPA failure become small. Decrease of combined output power by one of 8 SSPA failure and 2 of 16 SSPA are same. Isolation at worst port decrease to $(1/8)^2$ in one failure in 8 SSPA . However, 2 random failure in 16 SSPA will evenly distribute isolation around $2*(1/16)^2$. Therefore, increase of the number of SSPA is considered most practical method to implement redundancy to SSPA failures. Number of SSPAs can be increased to 8,16,32, 64, 2^n. 16 to 32 will be practical number of SSPAs. Figure 7 shows method of increasing number of SSPA by dividing 1 SSPA to two half power SSPA. By this method, 4-port 4-SSPA MPA in Fig.5 changes to 4-port 8-SSPA MPA. N is increased from 2 to 3. By using this kind of method, it will become unnecessary to implement redundant SSPAs to number of SSPAs.

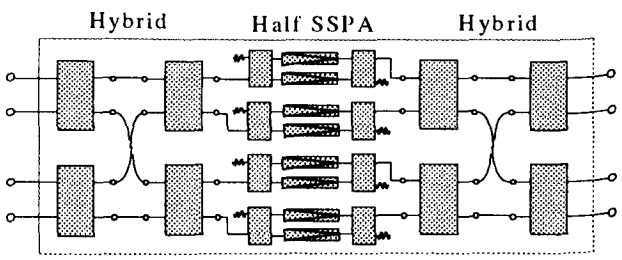

Fig.7 Increasing number of SSPAs by implementing Half SSPA

MPA Configuration for Personal Satellite Communications

Required number of up link beams will be determined by the required coverage area and the required nadir cell diameter as stated in the former section. If down link beams pattern are assumed to be similar to up link beams, required number of down link beams is same as uplink beams. The number of down link beams determines configuration of MPA as a multiple beam transmitter. Although number of SSPAs is limited to 2^n (n=1~), where n is equal to necessary stage of Hybrid, MPA can be used for any number beams if it is smaller than 2^n. Maximum number of ports is equal to the number of SSPAs and number of ports can be decreased by not using unnecessary ports[1].

As estimated in the former section, if required number of beams is around 32, transmitter section will be made by fully using 32-SSPA MPA or 2 set of 16 SSPA MPA or 4 set of 8-SSPA MPA. MPA configuration will be determined by requirement for beam isolation and peak traffic concentration considering hardware complication, output loss and redundancy capability. 32-port 32-SSPA MPA will have better isolation, better power concentration capability and better redundancy performances. But it is necessary to use rather complicated 5 stage Hybrid circuit and a little higher output loss. Also, power handling capability must be higher because total 32 SSPA power may concentrate in any one of the output port. From this hardware consideration, it is better to use two set of 16-port 16-SSPA MPA which use 4 stage Hybrid.

Proposed configuration is shown in Fig.9. If 10W SSPAs are used, total transmitting power, which can be concentrated in any port, will be 160W. By increasing set of this 16- port MPA, it can be applied to the system with more than 32 beams.

Basic constituents of 4 stage Hybrid is one block of 4-port Hybrids. This 4-port block will be easily made by air suspended line or by waveguide. SSPA will consist of 4 sets of the 4-port SSPA block. Since output section must endure concentration of high power, output 4-port hybrid section must be designed to have high power capability. Use of low loss 4-port Hybrid, band pass filter and multiple beam feed will results high power capability in output section. For inter connection of 4 blocks of 4-port SSPA and 4-port output Hybrid will be made by using low loss equal length flexible cables.

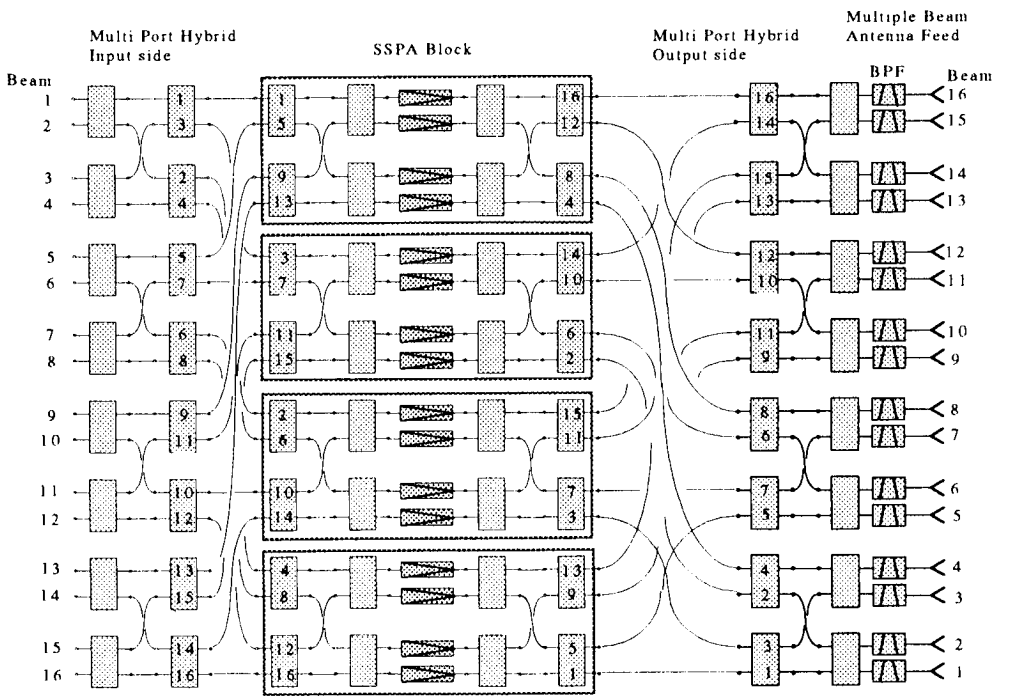

Fig.9 16 port 16 SSPA MPA with high power output Hybrid and multiple beam antenna feed.

Forward Link Block Diagram

Figure 9 shows conceptual block diagram of 32 beams forward link. Accommodation of more than 32 beams will also be possible by implementing more than 2 sets of 16-port MPA. In case of GSO, feeder link will be able to use frequency band allocated to Fixed Satellite Service.

In principle, it is possible to allocate full bandwidth allocated to Mobile Satellite Service to all beams. In this ideal case, if allocated bandwidth is 30MHz, required feeder link bandwidth will be 30MHz*32=960MHz. In actual cases, it will not be necessary to assume full bandwidth to all beams. Frequency re-use will be maximally performed when channel frequency is assigned by control earth station.

Future Application of MPA

Utilizing of MPA enables power sharing among large number of beams. In principle, this will erase restriction on the number of beams to be implemented in the multiple beam systems. In the future, MPA will be applied in high capacity, high frequency re-use systems with more than hundreds beams.

Conclusion

Personal satellite communication systems require large number of beams. It was shown that required cell diameter which support handheld terminals is about 600km at 2.0 GHz. By this cell size, North American or European regional coverage can be made by about 32 beams. For these requirements, use of 2 set of 16-port 16-SSPA MPA configuration was proposed. MPA consists of number of 4-SSPA block and 4-port Hybrid which are easy to make. For easy and low cost approach to multiple beam transmitters, MPA will be most advantageous and effective.

References

[1] S.Egami and M.Kawai,"An Adaptive Multiple Beam System Concept" IEEE Journal on Selected Areas in Communications", pp630-636, Vol.SAC-5, No.4, May 1987.

[2] S.Egami, "Satellite Link Requirements in Personal Satellite Communications", Space Communications, No.12 1994, pp105-114, IOS Press, Dec. 1994.

[3] A.Howell,G.V.Kinal,"Inmarsat's Third Generation Space Segment"AIAA 14th Int.Comm.Sat.Sys. Conf. pp92~ 100, March 1992.

[4] D.J.Whalen,G.Churan,"The American Mobile Satellite Corporation Space Segment" AIAA 14th Int. Comm. Sat.Sys. Conf. pp394-404, March 1992.

[5] S.Hatzigeogiou, G.Turgeon, S.Jarvis, L.Gilbert, S.StPierre, K.Patel, G.Brassard, N. Whittaker, "MSAT Hybrid Matrix Power Amplifier Subsystem", AIAA 15th Int.Comm .Sat.Sys. Conf. , pp542-552, March 1994.

[6]K.Nakagawa,M.Minomo, M. Tanaka, T.Itanami , "N-Star: Communication Satellite for Japanese Domestic Use", AIAA 14th Int.Comm.Sat.Sys. Conf. pp1129-1134, March 1994.

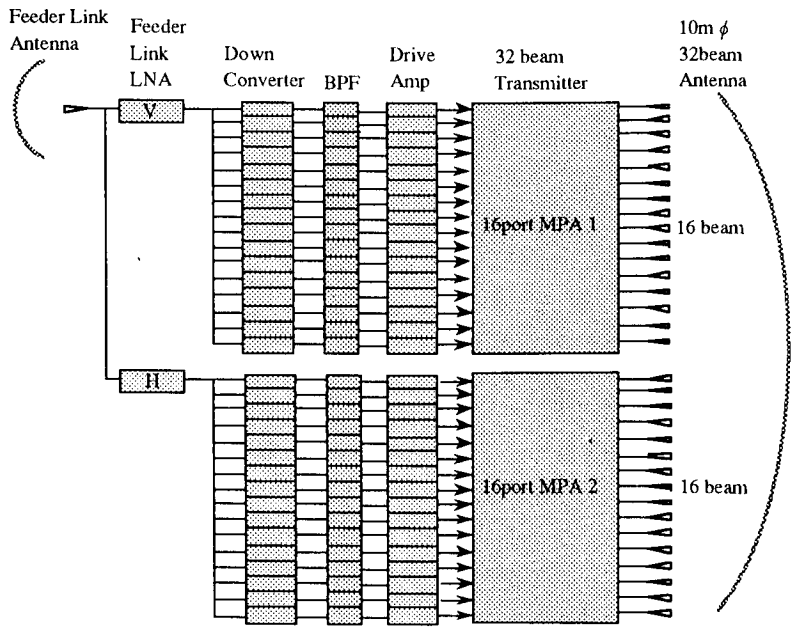

Fig.10 Forward link conceptual block diagram

New Developments for SAW Channelization for Mobile Satellite Payloads

R.C. Peach and P. Mabson
COM DEV Ltd
155 Sheldon Drive, Cambridge, Ontario, Canada N1R 7H6
Phone: 519-622-2300 Fax: 519-622-1691

ABSTRACT

The use of SAW technology in mobile communication payloads is becoming widely accepted by the industry since being pioneered by Inmarsat for its third generation of satellites. This paper presents new developments in this area, including broadband processors of the Inmarsat 3 type, and the use of SAW filters at L-band. It is demonstrated that SAW processors have considerable potential for increasing the capacity of future communications payloads, while allowing fully transparent operation without any restriction on traffic type or modulation format. In addition to the evolutionary development of Inmarsat type processors, new SAW applications have also emerged recently. Therefore, despite the rapid changes in the industry, it is predicted that SAW processing has a strong future in satellite communications.

INTRODUCTION

A number of current geostationary L-band mobile satellites, notably Inmarsat 3, EMS and Artemis, use surface acoustic wave (SAW) filters for narrowband channelization and routing [1]. The high selectivity of the SAW filters provides very efficient use of the extremely limited available spectrum. In the case of Artemis, SAW transversal filters with 900 kHz bandwidths and only 100 kHz transition widths have been successfully developed at COM DEV.

There have, however, been some radical developments in the mobile communications market since these programmes were initiated. For the hand-held terminal market, interest is now focussed on low earth orbit (LEO) satellite constellations such as Iridium and Globalstar, and on medium earth orbit (MEO) constellations such as Odyssey. These systems use either L-band or a combination of L and S-band user links, and are mostly based on CDMA techniques. Iridium is an exception in this regard; it employs a combination of FDMA and TDMA. Other even more ambitious systems such as Teledesic propose to provide higher data rate communications at Ka-band. In this case, small antennas would be used that could be mounted either on buildings or vehicles.

The fixed satellite service market is also undergoing major changes. Traditional point to point communications between major population centres are rapidly being converted to optical fibre, and operators are now looking to provide a far greater number of narrowband links, principally to areas that are not well served by existing terrestrial infrastructure. To this end, proposed satellites have more beams, higher EIRPs, and greater inter- beam connectivity; users will then only require small low cost ground terminals. These trends are being accelerated by data compression techniques, which are forcing operators to lease comparatively narrow bandwidths (6-9 MHz).

There is therefore a general blurring of the distinctions between mobile and fixed satellite services. The markets for all system operators are in the sparsely populated areas, the mobile or semi-mobile users, and the developing countries with limited infrastructures. Point to multi-point (broadcast) communications are also a natural application for satellite systems. Numerous services will be available in the future, covering a wide range of data and bit error rates, and requiring ground equipment ranging from hand-held terminals to VSATs.

These developments in satellite communications have significantly modified the market for SAW devices; the market has not necessarily diminished, but it has changed radically from that envisaged five years ago. In general, SAW devices perform functions that can also be performed by digital processing. Digital is usually preferred if it is competitive in mass and power, and the breakpoint between the technologies is determined by the system bandwidth; at present, digital would almost certainly be used for bandwidths below 10 MHz. The channelization of a 34 MHz band by SAW filters, as employed by Inmarsat 3, will therefore soon be within range of digital technology, and it is not anticipated that such applications have much potential for SAW in the future. Inmarsat did consider a hybrid SAW CFT/digital implementation for its new Inmarsat P system, but

ultimately opted for an all digital approach.

In the future, the principal application for channelization with contiguous SAW filter banks will be in broad band systems [2]. These normally operate at C or Ku-band, and serve the high quality, high data rate end of the market. Given current trends towards greater connectivity and narrower bandwidth leases, SAW channelization has considerable merit. The rationale for such SAW based systems and their possible effects on data traffic are discussed in this paper.

Although systems such as Iridium, Globalstar, and Odyssey use very narrow bandwidths, with mostly CDMA traffic, they do have significant applications for SAW devices. Globalstar uses a bank of SAW filters, implemented directly at L-band, to reduce the system noise bandwidth over low traffic areas, and reduce power consumption. Examples of prototype Globalstar filters are described in this paper. Odyssey also uses large numbers of SAW filters. In this case, the feeder link spectrum from the base station (Ka-band) is channelized into 5.5 MHz segments by a bank of 52 SAW filters. The channels are then routed to their appropriate spot beams, where they are shared amongst users on a CDMA basis.

Future applications for SAW devices in space therefore include:

- channelization and routing in broad band systems,
- feeder link frequency division in mobile systems,
- special applications, such as noise bandwidth control.

APPLICATION OF SAW CHANNELIZATION

In current SAW based systems, such as Inmarsat 3, the satellite links the mobile user to the base station, and hence to the terrestrial network, rather than providing a direct link to another mobile user. This principle is also used in the newer hand-held systems. The systems currently under consideration for SAW channelization use a different model, with multiple zone beams and direct links between users. The number of zone beams would typically be between 4 and 10, with up to 500 MHz of bandwidth available in each. This has the advantages of giving the user much higher EIRP than would be available with hemi-beams, and also of enhancing frequency reuse. The satellite must however provide flexible traffic routing between zones, and must therefore support a high degree of connectivity. In addition, as the number of beams increases, available power rather than bandwidth may limit the number of transponders per beam.

In traditional broad band systems, transponder bandwidths have been between 36 and 72 MHz. However, in the future much of the traffic will be from VSAT users requiring only small bandwidths of 9 MHz or less. In a multi-beam system this gives numerous partially utilized transponders, thus reducing the effective capacity of the system. SAW filters can provide much finer channelization of the band than traditional cavity filters, and can eliminate this inefficiency.

A typical N beam system would have a demultiplexer for each input beam that would divide the band (500 MHz) into 36-72 MHz channels. Each set of corresponding channels from different uplink beams would then be cross coupled by an NxN switch matrix; any uplink channel could then map into its corresponding channel on the downlink. The purpose of a SAW processor is to replace some of NxN switch matrices and their associated IMUX filters. The processor would still provide full connectivity, but would do it on a sub-channel basis.

The structure of a typical SAW processor is illustrated in Figure 1 [3], which shows a four sub-channel, four beam system. For a system with 36 MHz channel widths, the sub-channels would be 9 MHz wide. For each input beam the sub-channels are independently routed to any output, where they are combined before being fed into the high power amplifiers (HPAs) and hence to the output multiplexers. This type of processor is very similar to that employed on Inmarsat 3, with the exception of the filter bandwidths. It is however much simplified, and would in general only employ a single local oscillator for all frequency conversions (not shown in figure 1).

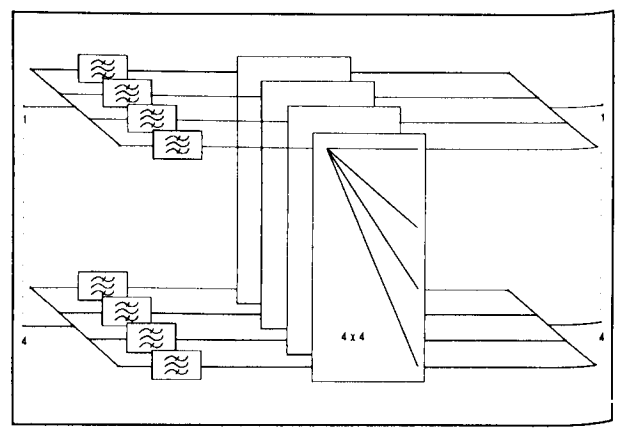

Figure 1: Four Beam, Four Sub-Channel SAW Processor Functional Diagram

The advantages of using sub-channelization can be demonstrated by quite simple arguments. First, there are several conditions that must be satisfied for sub-channelization to be beneficial:

- Fractional transponder leases must be employed.
- The satellite must have multiple beams with a high degree of connectivity between beams.
- The system must be operating at near to its bandwidth capacity.

The first two of these conditions are satisfied in virtually all systems currently under development. This is dictated both by the changes in traffic patterns, and by the need to provide high EIRPs. The third condition assumes that bandwidth capacity is a limiting factor, which is likely to be the case after a few years of operation.

If the satellite has N beams, and 1/n (n integral) is the smallest fraction of a transponder that can be leased, then, in a simple traffic model, it may be assumed that on each uplink the probability of the traffic destined for a given downlink requiring a fractional number of transponders is (n-1)/n. For a system without sub-channelization, the average number of partially utilized transponders per uplink would therefore be N*(1-1/n). On the average a partially used transponder would only be 50% occupied, giving an average loss of 0.5*N*(1-1/n) transponders as compared to a system with n-way sub-channelization. It can therefore be concluded that:

Average gain in capacity per uplink = 0.5*N*(1-1/n)

~ 0.5*N transponders;

Number of channels per uplink to be sub-channelize = 0.5*N*(1-1/n)

~ 0.5*N;

Relative gain in capacity per uplink = 0.5*N*(1-1/n)/NT

~ 0.5*N/NT, where NT is the total number of channels in the uplink.

It is clear from this argument that it is not appropriate to sub-channelize all channels. If a transponder is fully occupied with traffic for a single downlink then sub-channelization produces no advantage; it is only used to manage the remaining fractional transponder traffic. Typically, the number of transponders sub-channelized in each beam would be 0.5*N, and each of these would, on average, be twice as efficient as a conventional transponder. In effect, the 0.5*N sub-channelized transponders are equivalent to N normal transponders, but without the need for additional HPAs. For systems with large numbers of beams, and high interconnectivity, the capacity increase may therefore be very substantial. In the case of a 10 beam system, for example, 5 transponders per beam could be sub-channelized and would be the equivalent of 10 conventional transponders per beam. If, say, the system had 8 transponders per beam, sub-channelization would increase capacity by 0.5*5/8 = 31%. The use of this method is therefore very appropriate given the current trends in the industry.

It should also be noted that the capacity increase is only weakly dependent on n for n >= 4. Therefore, dividing the channel by more than a factor of four produces little advantage relative to the increased hardware complexity, even though the sub-channel bandwidth might then be greater than the minimum lease.

PROTOTYPE PROCESSOR ARCHITECTURE

Figure 2 shows the architecture of an experimental broadband SAW processor currently being developed at COM DEV; for simplicity, redundancy is omitted in the figure. The basic structure is very similar to that of the Inmarsat 3 processor, but with significant simplifications. The prototype assumes a four beam system, but the architecture can easily be extended to accommodate more beams.

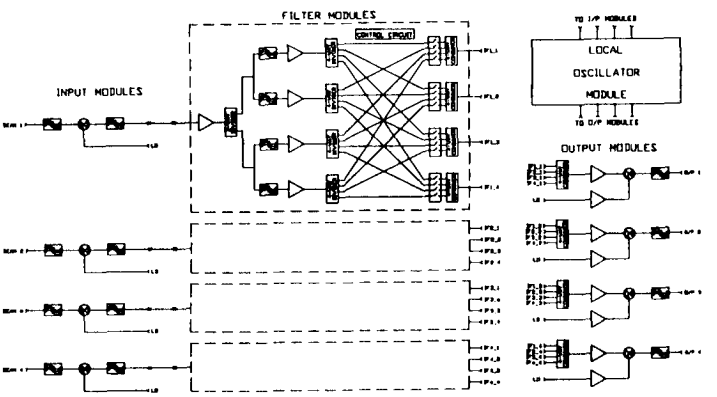

Figure 2: Simplified Schematic For Prototype SAW Processor

Each input signal is fed into the input module where it is downconverted from Ku or C-band by a common LO.

The input mixer is preceded by a bandpass filter that provides image rejection, and also limits the input noise bandwidth. A lowpass filter is placed after the mixer to remove LO leakage before the signal is fed into the filter module.

The filter modules operate entirely at IF, 350 MHz in this case, and contain all the channelization and routing functions. The channelization is accomplished by a bank of contiguously combined SAW filters whose outputs are then routed via a GaAs FET switch matrix to the output modules; this switch matrix differs from that used on Inmarsat 3 in that broadcast mode operation for each sub-channel is supported. The selectivity of the system is determined entirely by the SAW filter bank; and the processor would not normally be preceded by a separate IMUX filter.

Each beam has a corresponding output module that combines the appropriate switch matrix outputs from each filter module. The output module also contains the RF upconversion, and the output filtering that removes the LO leakage and image signals prior to the HPAs.

In this processor, a single LO signal is used for all up and down conversions. This means that the RF channel frequencies are the same for all inputs and outputs. By using multiple LOs, different frequency channels from different beams could be cross coupled. However, in most cases, this is not particularly beneficial, and it increases the problems with spurious generation within the processor. In a full system, several such processors would be employed, one for each sub-channelized channel. The processors would only differ in the frequencies of the LOs and of the RF filters. Virtually all of the modules, and the filter modules in particular, would therefore be standardized.

In many applications each processor would serve a fixed RF channel, and there would be no requirement to vary the LO frequency. However, the frequency of the LO synthesizer can easily be varied to provide a processor with variable channel frequency in addition to variable bandwidth. This principle has already been successfully demonstrated in an L-band programmable SAW filter module developed by COM DEV for the European Space Agency. This unit operated in the frequency range 1525-1559 MHz, and was programmable in centre frequency with a resolution of 125 kHz; it used a four channel contiguously combined SAW filterbank, allowing the bandwidth to be varied continuously between 0.25 MHz and 2 MHz in 0.25 MHz steps, and giving a maximum bandwidth of 3.25 MHz.

Unlike conventional filters and switches, a SAW processor adds noticeable amounts of noise and intermodulation products to the signal traffic. It may therefore be a significant contributor to the overall system budgets. For low signal powers the system C/N ratio may be degraded, and at high powers the C/I ratio may be affected. Given the predicted noise figures and two tone intermodulation levels for the prototype processor, it is estimated that the C/I and C/N ratios would both be greater than 35 dB for a typical range of signal levels. The noise contributions, while not negligible, are therefore comparatively insignificant in an overall link budget.

SAW Filterbank Performance

Reference [1] discusses the design and tradeoffs associated with the Inmarsat 3 filters. These considerations also apply in this case; the principal differences being centre frequency and bandwidth. The prototype filter bank developed for the new SAW processor also uses the method of contiguous combining developed for Inmarsat 3. This method, sometimes called bandwidth switchable SAW filtering (BSSF) [1][3], allows adjacent filters to add together to form a single continuous response without any amplitude or phase distortions in the crossover region (guard band). BSSF is particularly beneficial in this case, because it recovers guard bands, and allows the processor to handle traffic of up to the full bandwidth of the processor.

It was noted in [1] that the manufacturing sensitivity of the devices increases rapidly with frequency, and that higher IF frequencies must be balanced against reduced selectivity. Inmarsat 3 employs 200 kHz guard bands and a 160 kHz IF frequency; for the new processor the centre frequency has been raised to 350 MHz and the guard band increased to 1 MHz. However, given the much wider system bandwidth, these guard bands are comparatively insignificant.

The prototype filterbank employs four 9 MHz bandwidth filters with 1 MHz transitions. As on Inmarsat 3, quartz substrates have been employed on account of their temperature stability; though in this application, other materials such as lithium tantalate could also be used. Figure 3 shows the response of filter 2, and Figure 4 shows the contiguously combined response of all four filters; Figures 5 and 6 show the combined passband amplitude and phase responses respectively. Further improvements in filter performance are certainly possible, but the initial results clearly show the selectivity that can be achieved, combined with flat amplitude and phase responses.

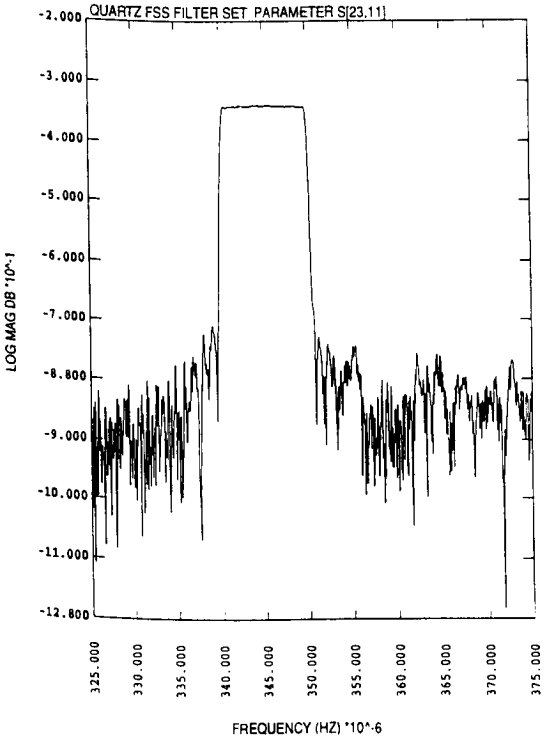

Figure 3: SAW Processor Filterbank Filter 2 Frequency Response

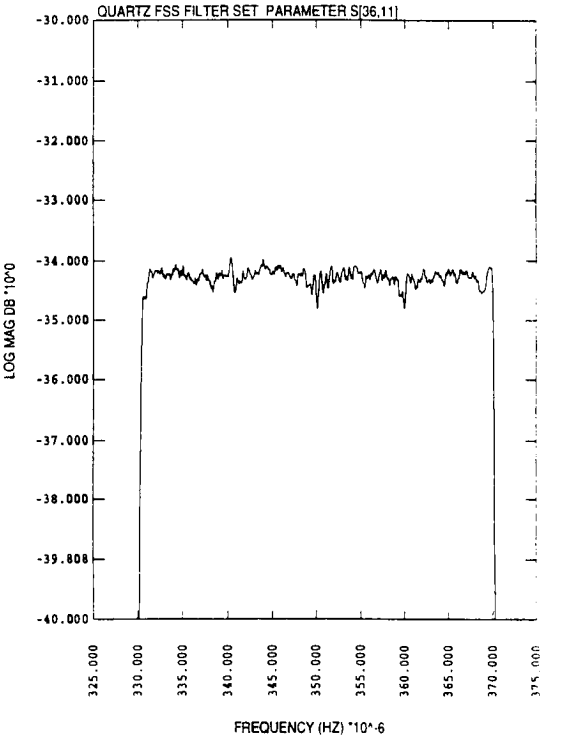

Figure 5: SAW Processor Combined Filterbank Passband Amplitude Response

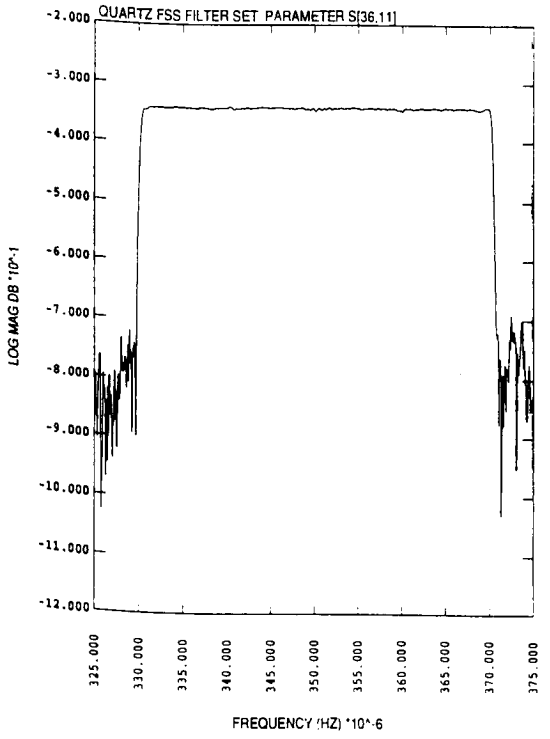

Figure 4: SAW Processor Combined Filterbank Frequency Response

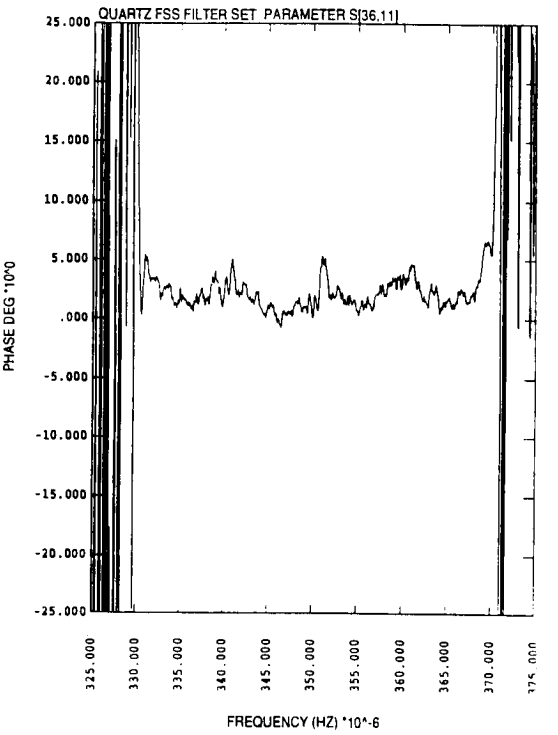

Figure 6: SAW Processor Combined Filterbank Passband Phase Response

Amplitude ripples of a few tenths of a dB and phase ripples of a few degrees are fairly typical in SAW filters. However, unlike the slow variations associated with traditional filters, these variations are in the form of very rapid sinusoidal ripples. The possible effect of such variations on signal traffic has been the subject of considerable debate. But all existing evidence indicates that they are relatively harmless [2].

The in-band characteristics of SAW filters, including the ripples due to spurious echoes, can be described by an echo model; this is the basic argument underlying all existing analyses. An impulse response of the form:

$$h(t) = d(t)+a*d(t+T)+a*d(t-T),$$

where d(t) is a delta function and 'a' is the echo amplitude, gives a frequency response

$$H(\omega) = 1+2*a*\cos(\omega T)$$

corresponding to the passband ripple $20*\log((1+2*a)/(1-2*a))$ dB. With the worst case assumption that an echo bit adds destructively with a wanted signal bit, the bit energy degradation is $20*\log(1-a)$ dB. From this it can be inferred that:

E/N degradation (dB) = 0.25 x passband ripple (dB).

A passband ripple of 0.4 dB would therefore degrade bit energy to noise density ratio by 0.1 dB, which is negligible.

Studies on the effects of SAW filters on analogue traffic also show that there is little degradation. Virtually all future traffic will however be digital, and studies on analogue traffic are now of relatively little importance.

Work is currently in progress, in conjunction with INTELSAT, to verify these conclusions using hardware simulation.

Other Applications of SAW To Mobile Communications

As noted in the introduction, processors of the Inmarsat 3 type are by no means the only application of SAW to mobile communications. The Globalstar system, like Iridium and Odyssey, uses the 1610 - 1626.5 MHz band for the user uplink. Over highly populated areas all of this bandwidth is required, but over the ocean, for example, a much reduced bandwidth will suffice. Globalstar uses a bank of four SAW filters, implemented directly at 1.6 GHz, to vary the input bandwidth between 16.5 MHz and 2.7 MHz in accordance with demand. This minimizes the input noise power, where in this case 'noise' includes signals from rival systems. In high traffic areas the full bandwidth is required, and the power requirements cause the satellite batteries to be depleted; but in a low traffic region power can be conserved, allowing the batteries to recharge, and balancing the power budget over the period of the orbit. Sixteen of these SAW filter banks are used on each Globalstar satellite, one per spot beam. The high selectivity and small size and mass of the SAW filters are therefore exploited to balance the satellite power equation; which is a vital but very unexpected application.

Figures 7 and 8 show the experimental responses of two prototype Globalstar 1.6 GHz filters developed at COM DEV. The transition bandwidth is 5 MHz, and this is obtained with a quartz substrate only a few millimeters in length; the SAW transducers employed electrode widths of 0.45 μm. This demonstrates the potential of SAW devices at L-band and possibly at S-band also; although the price for such high frequency operation is lower selectivity than that obtained at 350 or 160 MHz.

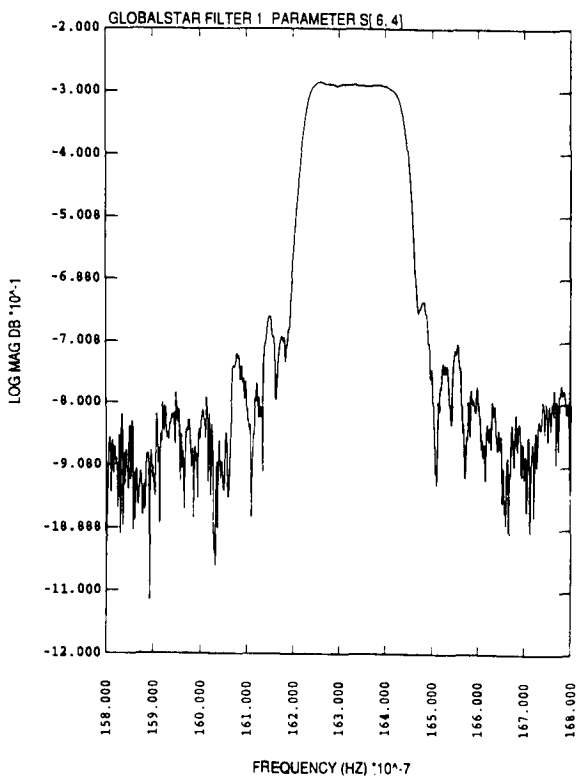

Figure 7: Globalstar Prototype 16.5 MHz Filter Response

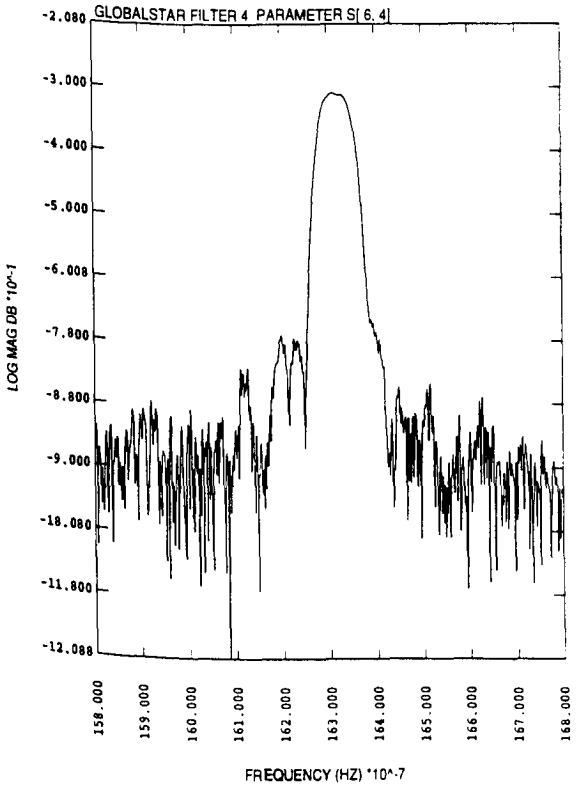

Figure 8: Globalstar Prototype 2.7 MHz Filter Response

SAW filters for the Odyssey system are at a much earlier phase of development. However, a filterbank of 52 SAW filters, each with a 5.5 MHz bandwidth and 1 MHz transitions, is required to channelize the feeder link spectrum; these filters operate at IF frequencies ranging from 316.125 to 596.625 MHz. The channels are allocated among 32(or 37) spot beams, and each channel is shared between users on a CDMA basis. This approach removes the need for the very high selectivity filters used on Inmarsat 3 or Artemis, but replaces it with an equally demanding requirement for a broad band high selectivity filter bank.

The use of SAW chirp Fourier transform (CFT) processors for frequency channelization has been a topic of considerable interest in recent years [4], usually as part of a hybrid SAW/digital system. However, now that Inmarsat has opted for an all digital system for the Inmarsat P programme, the future of the method is uncertain; it may however still find application for broad band channelization.

CONCLUSIONS

The predicted applications for SAW filters in mobile communications have changed dramatically in recent years. It appeared at one time that Inmarsat 3 type systems would be the model for a considerable number of future satellites; however, for L-band communications, interest is now focussed on LEO and MEO satellite constellations mostly employing CDMA. In addition, there is a general convergence in the industry, and a loss of distinction between fixed and mobile communication systems.

It is now predicted that the principal application for SAW based systems is not for low data rate, low quality traffic, but rather for high data rate, low bit error rate (BER) traffic. Typical users would employ VSATs and require bandwidths of up to 9 MHz. The technology developed for Inmarsat 3 is still broadly applicable to this application, but it requires processors with different bandwidths, different operating frequencies, and different switch matrix configurations.

In addition to SAW based processors for channelization and routing, other applications have emerged, some of them quite unforeseen. This includes major applications on both Globalstar and Odyssey. On balance therefore the prospects for SAW in satellite systems seem reasonably good. However, the market is clearly changing rapidly, and SAW suppliers must be able to respond quickly with new products if they are to exploit the available opportunities.

REFERENCES

[1] R. Peach, N. Miller and M. Lee, "SAW Based Systems for Mobile Communications Satellites", Proc. International Mobile Satellite Conference, pp53-58, 1993.

[2] R. Peach, F.Z. Bi, and B. Van Osch, "The Application of Surface Acoustic Wave Filters to Communications Satellite Design", Proc. 15th AIAA International Communications Satellite Systems Conference, pp707-715, 1994.

[3] H. Shinonaga and Y. Ito, "SS/FDMA System for Digital Transmission", Proc. 7th International Conference on Digital Satellite Communications, Munich, Germany, 12-14 May 1986.

[4] P.M. Bakken and A. Ronnekleiv, "SAW Based Chirp Fourier Transform and its Application to Analogue On-board Signal Processing", International Journal of Satellite Communications, vol. 7, 4, pp 283-293, 1989.

Laser Communication Demonstration System (LCDS) and Future Mobile Satellite Services

Chien-Chung Chen, Michael D. Wilhelm, and James R. Lesh
Jet Propulsion Laboratory, California Institute of Technology
4800 Oak Grove Drive, Pasadena, CA 91109
Phone (818)-354-3855, Fax: (818)393-6142

ABSTRACT

The Laser Communications Demonstration System (LCDS) is a proposed in-orbit demonstration of high data rate laser communications technology conceived jointly by NASA and U. S. industry. The program objectives are to stimulate industry development and to demonstrate the readiness of high data rate optical communications in Earth orbit. For future global satellite communication systems using intersatellite links, laser communications technology can offer reduced mass and power requirements and higher channel bandwidths without regulatory constraints. As currently envisioned, LCDS will consist of one or two orbiting laser communications terminals capable of demonstrating high data rate (greater than 750Mbps) transmission in a dynamic space environment. Two study teams led by Motorola and Ball Aerospace are currently in the process of conducting a Phase A/B mission definition study of LCDS under contracts with JPL/NASA. The studies consist of future application survey, concept and requirements definition, and a point design of the laser communications flight demonstration. It is planned that a single demonstration system will be developed based on the study results. The Phase A/B study is expected to be completed by the coming June, and the current results of the study are presented in this paper.

INTRODUCTION

The market for satellite services world-wide is expected to grow significantly in the next decade. This growth is fueled partly by the emergence of global mobile satellite services. These mobile services combine the advantages of universal coverage and wide bandwidth with reliable services for the increasingly mobile world. This potential of providing global interconnect will enable companies to cost-effectively transmit data (fax, email, voice, and other electronic data interchange) around the world, including under-developed nations and rural areas. Furthermore, these services permit users to access satellite transponders on demand and hence can significantly reduce the cost to end users for satellite services. The mobile satellite industry is expected to be a multi-billion dollar industry in the coming years (possibly $6.5 billion by the end of 1995 and to $17 billion by 2003[1]). Shown in Table 1 is a partial list of global mobile satellite services currently under development. The growth of global mobile services has led to an increasing demand on bandwidth and frequency allocation. Furthermore, it has led to a renewed interest in high data rate intersatellite links as a method of routing information between satellites.

A high data rate intersatellite link (ISL) is an important technology for future global mobile satellite services. ISLs experience neither transmission fades nor multipath, and can maintain effective link margin with a lower power requirement than ground-based routing. The use of intersatellite links can permit global data distribution without multiple hops through ground stations. Additionally, with the short propagation delay to a LEO orbit, it is envisioned that a LEO satellite network using lasercom technology can be part of a global information network that provides seamless interconnect capability with terrestrial fiber optic networks. This application would provide complete transparency for delay-sensitive ground-based computer communications protocols. ISLs can also be applicable in long-haul services to eliminate double-hop connections between destination points. Another possible application for ISL is to connect cluster satellites to enhance capacity, and to permit the use of smaller, modular, low cost, and low risk satellite designs.

Two of the most ambitious Mobile systems (Iridium™ and Teledesic™) will rely on ISLs to provide global coverage. The Iridium constellation has 66 satellites in 6 orbital planes, with 4 crosslinks on each satellite (front, back, and two in adjacent orbits). The Teledesic constellation has 21 orbital planes with 40 satellites each for a total of 840 LEO satellites and 8 crosslink connections from each satellite. Each satellite in the constellation will communicate and route network traffic to provide direct and practical routing between users throughout the world, and provide a substantial redundancy that can continue to support traffic flow in the event of degradation to one of the satellites. Because of the large number of satellites and consequently the number of crosslink terminals (264 for Iridium and 6720 for Teledesic), minimizing the mass and power of the

Name	Altitude/# orbital planes	Total # satellites	Mass per satellite	Intersatellite Links	Services Offered	System Cost
MSAT	GEO/1	2	2500	No	voice, data, fax	$500 million
Globalstar	1400km/8	48	250	No	voice, data, FAX, paging, RDSS	$1.8 billion
Iridium	780/6	66	700	Yes	voice, data, Fax, paging, RDSS	$3.4 billion
Odyssey	10400km/3	12	1900	No	voice, data, Fax, paging, RDSS	$1.3 billion
Project-21	10355/2	10	1960	Maybe	voice, data, fax, paging, navigation	$1-2 billion
Teledesic	700/21	840	750	Yes	broadband services	$9 billion

Table 1. Mobile satellite services currently under consideration.

crosslink terminal is mandatory for these systems. For example, the baseline Teledesic satellite has allocated only 144 kg for its communications payload[2]. This includes 8 crosslink terminals and the main mission antenna. Similarly, the Iridium system has baselined 165.1 kg for its communications payload[3], including the four crosslink terminals and four gateway moveable antennas. The large number of crosslinks per satellite can also impose constraints on the size of the antenna as it affects the spacecraft packaging and the size of the launch fairing.

Lasercom technology, with its mass, power, and size advantages, can provide a viable solution to these needs. Additionally, laser-based ISLs are not susceptible to radio-frequency interference (RFI), and no frequency allocation or bandwidth constraints exist for the optical frequencies. Furthermore, because the laser terminals can transmit and receive on the same wavelength, all satellites in the constellation can be made identical. This interchangeability of lasercom terminals and satellites is another factor that will minimize the cost for these commercial ventures (an advantage that can not be provided by RF).

Despite the relative advantages offered by the lasercom technology for intersatellite applications, potential users have been slow to embrace the technology. This is in part because past development efforts were conducted before the technology is ready. More importantly, there have been concerns about the perceived difficulties in establishing an optical link between moving platforms. To address these concerns and to gain user acceptance of the technology, a functioning demonstration under a relevant operating environment has been regarded as a critical step. A successful demonstration can address the user concern by validating mutual acquisition and accurate beam pointing from space platforms with vibrational spectra representative of future user spacecraft. A space-based demonstration can also validate the design, performance, and operating lifetime of the terminal under high vacuum, radiation, and space debris environments similar to the expected user conditions and in the presence of bright sunlight.

LCDS PROGRAM OVERVIEW

The Laser Communications Demonstration System (LCDS) is a joint NASA-U.S. Industry program to demonstrate high data rate lasercom technology under a dynamic orbital environment. The objectives of the LCDS program are to:

(a) Identify the user base and potential applications for lasercom technology,

(b) Demonstrate lasercom technology in a relevant operating environment envisioned for future users. This demonstration should be derived from and traceable to future applications. Furthermore, it is essential that the demonstration be successful and timely.

(c) Facilitate development of industry base for lasercom technology

LCDS will consist of one or two orbiting laser communications terminals capable of demonstrating high data rate (greater than 750 Mbps) transmission in a dynamic space environment. Two industry teams, one led by Motorola Inc. with participation by Martin Marietta Technologies Inc., and the other led by Ball Corp. with participation from Thermotrex, Comsat Laboratory, Astroterra, Laser Diode Systems Corp., and Daedalian Technologies, have been selected for the Phase A/B Mission Definition study to define an in-orbit demonstration of lasercom technology with a goal of demonstrating at least 750 Mbps data rate.

The Phase A/B Mission Definition study includes the following task areas:

Application	LEO-GEO	LEO-LEO	LEO-Ground
32GHz	46 cm LEO aperture, 75lbs, 95W 4.9 m GEO aperture,110 lbs, 55W	38 cm aperture, 80 lbs, 80 W	46 cm aperture, 65 lbs, 45 W 5 m ground aperture
60 GHz	46 cm LEO aperture, 75lbs, 80W 4.9 m GEO aperture,110lbs, 60W	38 cm aperture, 80 lbs, 75 W	N/A
Optical	18 cm LEO aperture,55 lbs, 90W 30 cm GEO aperture,60 lbs, 75W	16.5 cm aperture, 22 lbs, 25 W	16.5 cm aperture, 22 lbs, 25 W 1 m ground aperture

Table 2. Comparison of RF versus optical for selected applications

(a) Application Survey: Identify future commercial and government space applications to identify areas where lasercom is applicable, cost effective, and competitive.

(b) Demonstration Design: This includes the development of the demonstration objectives and concept based on the assessment of future markets, definition of the demonstration system and subsystem requirements, point design of the demonstration, and assessment of the technologies required for the demonstration. Also included in this task are the definition of the mission operations concept, and assessments of the launch vehicle and host spacecraft.

(c) Development of a life cycle cost estimate and Phase C/D program development plan.

The Phase A/B studies is expected to be completed by the coming June, and JPL is in the process of preparing a consolidated program plan for submission to NASA.

COMPARISON OF RF AND LASERCOM SOLUTIONS TO ISL

The application surveys conducted under LCDS indicated, as expected, that most future applications for lasercom will be for high data rate intersatellite links, with a majority of the links operating at medium (2000-6000km) range, although a few demanding applications will require crosslinks over the geosynchronous arc (e.g. TDRSS follow-on, etc.). Based on the application survey, a comparison of RF and Lasercom ISLs was conducted.

The technical merit of laser ISLs is derived principally from the highly collimated optical signal, and hence a greatly increased transmit power efficiency compared to conventional microwave systems. The improved power efficiency can lead to a terminal design with greatly reduced size, mass and power requirements. By virtue of shorter wavelength and higher operating frequency, a lasercom system also offers wider information bandwidth. Furthermore, lasercom systems are not susceptible to radio frequency interference and are not subject to frequency or bandwidth regulation. The combination of these advantages makes lasercom highly attractive for ISL applications.

Comparisons of ISL implementations using optical and RF technologies were conducted under the LCDS activity for both LEO-LEO and LEO-GEO crosslinks. RF technologies for 30, 60, and 90 GHz ISLs were assessed and projected for a 1999 deployment date. Shown in Table 2 is a summary of RF system performance and comparable lasercom system designs for a 750 Mbps link. 90 GHz ISLs were not included because of its relatively immature technology status for the 1999 time frame. For the LEO-GEO link, the RF LEO terminal is assumed to have a modest antenna size (0.45 m) with a 55% antenna efficiency and a transmit power of 25W with 1.5 dB circuit loss. The GEO terminal has a 4.88m aperture mesh antenna and an uncooled MMIC InP HEMT front end with a noise figure of 1.5dB. The expected antenna noise temperature of 230K results in an overall system noise temperature of 350K. In addition, there is an assumed 1.0 dB receiver circuit loss, and a 5.6 dB coding gain. For the LEO-LEO link with a deep space background, the antenna temperature is assumed to be 10K, resulting in a system noise temperature of 130K. The antenna diameter is scaled to 38 cm to provide a 3 dB link margin.

It is seen in Table 2 that a lasercom ISL requires substantially less mass and power compared to the RF solutions for the LEO-LEO and LEO-ground links. Furthermore, lasercom technology offers large growth potential as the data rate can be improved easily by increasing the transmit power or reducing the beam divergence.

In addition to size, mass, and power, lasercom ISLs can also have potential cost advantages over RF links. Because of the high complexity of the laser ISL, it has previously been thought that only the most demanding users such as the military can "afford" lasercom systems. However, the recent emergence of large constellation

Demonstration	Topics
Acquisition and Tracking	• Initial Acquisition • Track and Communicate • Reacquisition
Data Communications	• Random and burst errors • Near sun performance
Life and Operational Reliability	• Design reliability • Laser lifetime • Laser wavelength drift • Orbital Environment issues, including thermal loading, optical contamination, space debris, high vacuum, and radiation.

Table 3. Performances to be demonstrated in-orbit by LCDS.

LEO mobile satellite systems such as Iridium™ and Teledesic™ have redefined the potential markets for intersatellite links. Each of these constellations will require a large number of crosslinks to channel data and status information between satellites. With the large number of terminals, design to unit production cost (DTUPC) processes will be adopted to lower the cost of the lasercom terminal. Cost assessments conducted under the LCDS study indicated that lasercom is not only competitive in the demanding LEO-GEO or GEO-GEO links, but also for the high volume LEO-LEO links.

In addition to intersatellite links, lasercom technology can also be applicable for space-to-ground data return. The rapidly expanding commercial market for high-resolution remote sensing will require large amounts of image data to be transmitted from sensor satellites to data processing and distribution sites, or directly to end users. A space-to-ground link can also be part of an integrated global network that provides high rate data distribution and seamless interconnect with the terrestrial fiber optics networks. However, until the development of a ground infrastructure to support weather diversity reception, space to ground links will be limited to non-real-time data transmission and relay as the availability of an optical link through inclement weather is severely limited.

DEMONSTRATION OBJECTIVES

Based on the characteristics (range, data rate, background condition, etc.) of the identified applications, the LCDS demonstration concepts were developed to support an on-orbit experiment to demonstrate and validate all aspects of a 750 Mbps link. Specific technical objectives of the demonstration include

Demonstrate link performance in a relevant environment:

The primary objective of LCDS is to demonstrate lasercom technology in an operating environment similar to that of the projected applications. The demonstration must also address any user concerns regarding the readiness of the technology. The link performance characteristics to be demonstrated are summarized in Table 3, and include the following

Acquisition and Tracking: Spatial acquisition and fine tracking of a narrow optical signal has long been regarded as the most difficult aspect of lasercom system implementation. This is because, even though a lasercom system derives most of its performance advantages by virtue of a narrow transmit beamwidth, the narrow beamwidth also imposes stringent demands on signal acquisition and beam pointing. To acquire such beams, a beacon signal from the intended receiver must be acquired and tracked by the transmitting terminal. This problem is complicated by the fact that the platform onto which the lasercom system is mounted will experience random vibrations due to on-board mechanical noise. The magnitude of the noise is typically larger than the transmit beamwidth. Furthermore, in order to compensate for the relative motion of the spacecraft, the transmit signal needs to be pointed ahead of the apparent position of the receiver. This point-ahead angle is also typically comparable to, or larger than the transmit beamwidth. Demonstration of the acquisition, tracking, and subsequent beam pointing functions must be conducted under realistic range, power, and platform vibration conditions. Effective demonstration of the spatial acquisition and tracking is a critical step in gaining user confidence in the technology.

Data Communications: Efficient modulation and reception of data in the presence of optical background conditions similar to future applications need to be validated in a space environment. Effective handling of the burst errors introduced by the platform jitter environment also needs to be demonstrated. Additional issues include demonstration of effective transmit-receive isolation and data handling/protocol related to routing of a 750 Mbps data stream.

Life and Operational Reliability: This includes the demonstration of effective designs to provide suitable lifetime and reliability of the communications terminal. Issues to be considered include the design reliability and scalability to future mission needs, and the impact of an orbital environment on the performance of a lasercom system.

Demonstrate Design Viabilities

In addition to the link performance, LCDS will also demonstrate that a lasercom terminal can be designed with system size, weight, and power allocation that are competitive with existing or projected RF technology, while achieving the desired performance objectives. Additionally, the demonstration will show that the cost of developing and fielding the lasercom technology, including the recurring and non-recurring engineering costs, is competitive with potential RF solutions. The design will also minimize technical risk by requiring minimum technology development.

Collect In-Space Performance Data

The demonstration will collect sufficient data over its on-orbit lifetime to confidently validate the communications system performance. This data will be used to support the specification, design, and manufacturing of operational systems. Data obtained should provide for the resolution of any observed anomalies and performance deficiencies during the demonstration and supply the basis for assessing performance and design margins. Performance data collected from the demonstration will be used to validate prediction models for the lasercom link and will permit scaling of the design to different operating regimes.

DEMONSTRATION CONCEPTS

The LCDS demonstration concepts were developed to meet the demonstration objectives, and to provide a low risk demonstration that provides high confidence in achieving the basic goals. In developing each concept, options were examined and compared in a number of areas, including scalability to future applications, technology maturity, cost, and performance. The latter includes the range, geometry, and data rate. Starting with the prime objectives of validating a 750 Mbps link under conditions similar to those identified by the application survey, alternatives concepts were developed and ranked. Two different concepts were proposed by the two contractor teams. These concepts are summarized in Table 4 and described as follows:

Ball Concept: The Ball team proposed the use of a single spacecraft/lasercom terminal in a geosynchronous transfer orbit (GTO) and companion aircraft/ground terminals to achieve a wide range of demonstrations. With the spacecraft in GTO, link demonstrations can be conducted from LEO to Ground/Air and GEO to Ground/Air. The difference in range permits a single demonstration to validate a wide range of link applications.

Motorola Concept: The Motorola team proposed to develop a space-to-space demonstration in which satellites in different orbital planes will establish data communications at an intended rate of 750Mbps (plus necessary data framing overhead). This demonstration concept permits direct validation of link performance under an orbital environment similar to that of LEO-network applications.

TECHNOLOGY READINESS

Lasercom technology, with its significant past investment, is ready for operational use. Assessments of critical technologies for LCDS were conducted during the Mission Definition Study, and concluded that the demonstration can be supported by existing technology with minimum development effort. A number of previous lasercom development programs, most notably

Parameters	Ball concept	Motorola Concept
# spacecraft	1 in GTO	2 in different orbital planes
Orbit	350/35,256 km 28.5 degree inclination 10.5 hr period	700 km circular Angle between orbital planes =8-32 degrees
Data Rate	1 Gbps LEO-Air, Air-LEO 1 Gbps GEO-Air, Air-GEO 1 Gbps GEO-Ground 10 Mbps Ground-GEO	760.88 Mbps
Range	up to 2,500 km for LEO-ground/Air links >30,000 km for GEO-Air/Ground link	1000-5000km
Space terminal	Volume: 110cm x 57cm x 52cm Mass: < 50kg	Volume: 30cm x 30 cm x 24cm Mass: 12 kg

Table 4. Summary of demonstration concepts

the Laser Communication System (LCS) have led to space qualification of many components and subsystem technologies, including detectors, pointing, acquisition and tracking electronics, gimbals, encoders, motors, mechanisms, optical elements and coating, and communication system high speed electronics. Risk mitigation requirements for these components and subsystems are minimal.

For communications electronics, the major area of user concern is the laser diode lifetime and high data rate modulation driver. The current concepts of LCDS employ laser diode master oscillator power amplifier (LD-MOPA) with higher power output (0.6-1W average) as the transmit signal source. These devices are commercially available with a NASA Technology Readiness Level of 5. However, they have not been qualified for space operation, and lifetime and high bandwidth modulation characteristics have not yet been fully demonstrated. Fortunately, suitable alternate exists for the LD-MOPA technology by combining the outputs of several high power laser diodes (SDL 5430s). These diffraction-limited, high power laser diodes have previously been developed to deliver an average power of 150mW with an MTBF in excess of 500,000 hours. Large signal modulation bandwidth in excess of 1GHz has also been demonstrated. Suitable power combining schemes have been demonstrated in previous development programs (FEWS/BSTS). Furthermore, high speed electronics required for driving the laser diodes have also been developed and are commercially available.

For the spatial acquisition, pointing, and tracking subsystem, the major area of concern is the control system and mechanism needed to achieve fine pointing in the presence of platform-induced disturbances. High bandwidth beam steering mechanisms have been developed that exhibit control bandwidths in excess of 2 kHz. Alternatively, the required control bandwidth can be substantially decreased by employing suitable vibration isolation mechanisms. Both techniques have been validated by ground-based testing, and precision beam pointing and tracking have been demonstrated in space (RME).

CONCLUSIONS

The development of LCDS is directly applicable to future commercial mobile satellite systems that require high bandwidth intersatellite crosslinks. The small size, mass, and power of the lasercom technology makes it ideally suitable for application in satellites constellations with small spacecrafts (e.g. Iridium™ and Teledesic™). In addition to the commercial applications, the development of LCDS is also relevant to NASA's strategic function on space communications by providing a technology capable of improving the data relay services and reducing cost. Furthermore, as a technology with high commercial potential, development of the LCDS can stimulating commercialization so that future NASA and government needs can be met more economically.

Successful completion of the LCDS can validate the technology readiness for the relevant applications, and can lead to fast insertion of the technology into future operations. Furthermore, the flight demonstration can provide important design and performance data for scaling the technology to other, more ambitious applications.

ACKNOWLEDGMENTS

The research described in this report was carried out by the Jet Propulsion Laboratory, California Institute of Technology, under contract with the National Aeronautics and Space Administration.

---

[1] Leslie Taylor Associates, Satellite News, May 30, 1994.

[2] FCC Application of Teledesic for Low Earth Orbit Satellite System in the Domestic and International Fixed Satellite Services, March 1994.

[3] FCC Application of Iridium for a Low Earth Orbit Mobile Satellite System, December 1990.

David Florida Laboratory Support for Mobile Satellite Communications

JEAN-GUY DUMOULIN AND ROLF MAMEN
DAVID FLORIDA LABORATORY, CANADIAN SPACE AGENCY
3701 CARLING AVENUE, OTTAWA, ON, CANADA K2H 8S2
TELEPHONE (*613*) 998-2491 FAX (*613*) 993-6103

ABSTRACT

The comprehensive integration and environmental (including RF) test facilities of the Canadian Space Agency's David Florida Laboratory (CSA)(DFL) were used extensively for the MSAT Program. Following a description of the facilities, the paper outlines their application to the qualification of the two MSAT satellites following an overview of the test plan. Particular emphasis is given to passive intermodulation measurement (PIM) demands, which for the MSAT satellites, contributed to the need to extend the anechoic chamber. The extended chamber was also used for an EMC test and SAR signature test of the RADARSAT satellite.

The DFL's facilities are being used for additional aspects of mobile satellite communications. One shielded anechoic Extra High Frequency (EHF) chamber and associated test equipment are employed predominantly for measuring the performance of the IRIDIUM satellites' Engineering Model Gateway Moveable Antennas (EM)(GMA). Other chambers are used for testing aeronautical antennas on behalf of Inmarsat. Still others combine thermal and PIM testing.

The paper concludes with a review of the test requirements of evolving satcom missions such as Inmarsat Aero-1.

INTRODUCTION

Opened in 1972, the DFL is Canada's world-class national facility for satellite assembly, integration, and test. The DFL has supported a number of major Programs and Projects over the years including the Canadian telecommunications satellite Hermes, the CanadArm remote manipulator, Brazilsat S1 and S2, the European Space Agency's Olympus, and Telesat Canada's Aniks C, D, and E. Currently, testing is underway for the MSAT and RADARSAT satellites. This paper will discuss some of the test capabilities at the DFL with special emphasis on the current Programs in particular the method used to measure the L-Band PIM performance of the large anechoic chamber in preparation for the MSAT satellites PIM tests in this facility. Calibration results are presented. Also briefly discussed is the design of the EHF Test Facility as this test facility was built to meet the stringent test requirements of IRIDIUM's EM GMA.

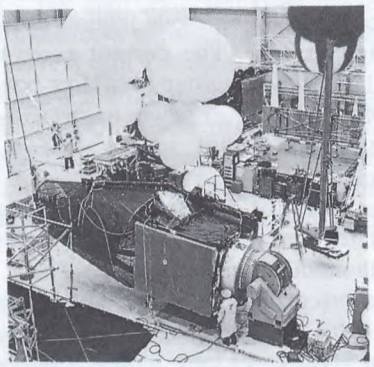

Figure 1: DFL's Highbay 3 Satellite Integration Area

Figure 2: DFL's 7 m x 10 m Thermal Vacuum Chamber

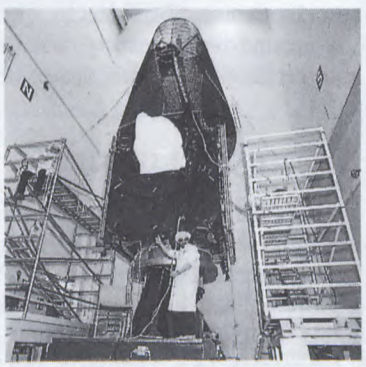

Figure 3: DFL's 178 kN Vibration Test Fixture

DFL Environmental Test Facilities

The extensive services offered by the DFL include: three large clean rooms (2,100 sq m of total available highbay space) suitably equipped for the assembly and integration of satellites and other space hardware (see Figure 1); a range of thermal vacuum chambers and an infrared testing system for verifying the thermal design and workmanship of satellite (see Figure 2); and vibration plus modal analysis and static load testing equipment for qualifying the structural aspects (see Figure 3).

The class 100,000 cleanroom facilities include capabilities for satellite mass properties measurement and spin balance. Antennas and RF payloads may be evaluated using the DFL's anechoic chambers, shielded rooms, and antenna ranges. Various environmental and RF facilities were modified to satisfy the test requirements of the MSAT and RADARSAT Programs.

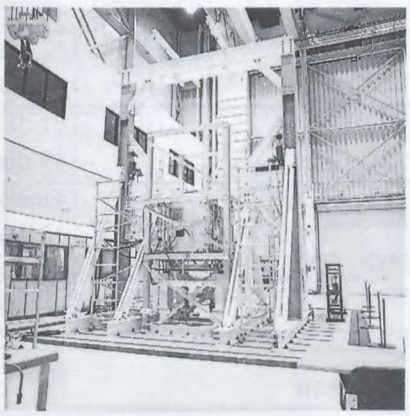

Figure 4: The DFL's Static Load Test System

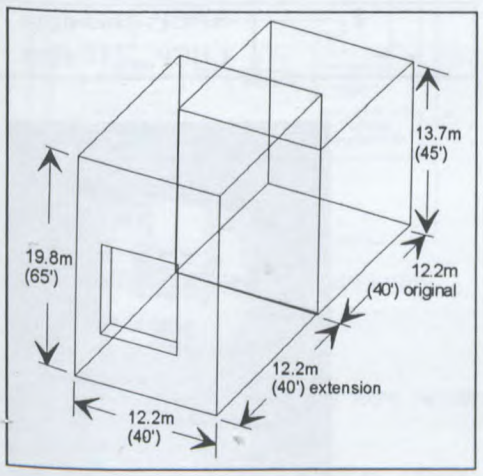

Figure 5: The DFL's Anechoic Chamber Expansion

Facility Modifications To Meet RADARSAT And MSAT Test Requirements

During 1990 to 1993, the CSA procured upgrades to the DFL to support the MSAT and RADARSAT Programs:

1) Static Load Test Facility

This facility was installed in Highbay 3 on the seismic mass (see Figure 4). It consisted of a system of computer controlled hydraulic actuators which subjected the RADARSAT satellite structural model to lateral and longitudinal static forces. These forces simulated the forces induced by acceleration during the launch phase. Applied forces were measured by load cells at each actuator. Deflections were monitored by LVDTs (linear variable differential transformers) and strain gauges. These tests verified the ability of the satellite structure to survive the quasi-steady-state forces induced during launch. These tests also served to check the structural math model.

2) Modal Test System

The RADARSAT satellite structural model was also subjected to modal testing using a new modal test facility which was also installed on the seismic mass in Highbay 3. The vibration modes that were predicted by the structural math model, were verified by using an LMS vibration controller and an array of vibration exciters and accelerometers.

3) Vibration Controller

A new LMS controller system, used for RADARSAT and MSAT testing, was procured to drive the existing 40K vibration shaker at the DFL. This system supports more channels of instrumentation and provides more precise control than its predecessor.

4) RF Anechoic Chamber Expansion

The existing large RF anechoic chamber at the DFL was enlarged to more than double its previous size in order to accommodate the then future satellite Programs such as MSAT and RADARSAT. The new dimensions of 12 m wide, 24 m long, and 20 m high, permitted the RADARSAT satellite to be set up in the chamber with the 15 m SAR antenna fully deployed and also to deploy the two MSAT reflectors in the chamber. The extension was lined with sheet metal and RF-absorbing foam cones. A new control room was also set up adjacent to the anechoic chamber.

5) Data Acquisition System

A new data acquisition system, based on 486-based PCs, was set up throughout the DFL to support testing. It was used for the RADARSAT Program during static load, modal, and Thermal Vacuum (TVAC) testing, and it was used for the MSAT Program during TVAC testing.

CALIBRATION OF ANECHOIC CHAMBER TO MEET MSAT PIM TEST

During the calibration, the two mock-up L-Band reflectors were placed in the anechoic chamber according to their nominal location on each side of the MSAT satellite. The test setup for the PIM calibration of the chamber consisted of three phases:

First Phase: Transmit (TX) and receive (RX) reflectors, satellite stand, scaffolds, and a mock-up satellite (only feed fixture and aft portion of the East wall). The EM RHCP (right hand circularly polarized) and the LHCP (left hand circularly polarized) RX probes were mounted adjacent to the TX EM Feed.

Second Phase: Setup remained the same as above except that the two RX probes were moved and aimed at the RX Reflector.

Third Phase: Added three new satellite mock-up walls.

Test blankets were custom made and installed around the TX Feed and RX probes.

The "Air-Knives" (coolers) were installed off the scaffolds. A fourth RHCP RX "debugging" probe was added. It was placed in the satellite plane of symmetry underneath the satellite and aimed at the center of the TX Reflector (see Figure 6).

The two first test phases consisted of four PIM tests (one PIM measurement for each TX Feed position), and the last test phase consisted of only two TX Feed positions. Each PIM measurement consisted of monitoring the setup for PIM for at least 60 minutes and then taking a 5 minute measurement with a controlled PIM source in front of the TX Feed.

During the monitoring period, the PIM levels were recorded on both strip chart paper as well as on spectrum analyzer plots. For this calibration, the TX Feed was required to be rotated in four positions since it had fewer feed elements than that of the MSAT flight TX Feed, thus generating only one beam.

This test, with the four TX Feed positions, simulated most of the L-Band illumination of the test chamber and test setup by the six downlink beams and therefore the most potential PIM sources were checked. The chamber was verified by injecting two amplified carriers in the EM feed and filter assembly on the TX side. PIM was measured on the RX side by two probes (LHCP and RHCP).

TX Carrier Frequencies: 1527 MHz and 1560 MHz, 300 watts per carrier

PIM RX Frequencies: 5th Order = 1626 MHz, 7th Order = 1659 MHz

TABLE 1: TEST RESULTS, PIM CHAMBER CALIBRATION

PHASE I

TX Feed Position	PIM Levels 7TH ORDER
1	RHCP: -140 dBm LHCP: -140 dBm
2	RHCP -139 dBm LHCP: -134 dBm
3	RHCP: -140 dBm LHCP: -137 dBm
PIM SOURCE	RHCP: -62.5 to -53.0 dBm LHCP: -62.5 to -53.7 dBm

PHASE II

TX Feed Position	PIM Levels 7TH ORDER
1	RHCP: -141 dBm LHCP: -140 dBm
2	RHCP: -142 dBm LHCP: -140 dBm
3	RHCP: -141 dBm LHCP: -139 dBm
4	RHCP: -141 dBm LHCP: -140 dBm
PIM SOURCE	RHCP: -93 to -61 dBm LHCP: -99 to -87 dBm

PHASE III

TX Feed Position	PIM Levels 5TH ORDER
2	RHCP: -142 dBm LHCP: -140 dBm
4	RHCP: -143 dBm LHCP: -141 dBm

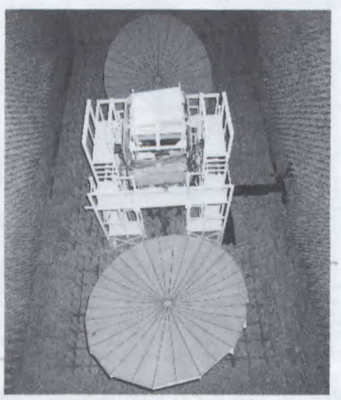

Figure 6: The MSAT satellite in the Anechoic Chamber

EHF TEST FACILITY

The EHF Facility is located in Highbay 2 (see Figure 7). The Aerotech Model 330ART Azimuth and Roll Positioner System orients the antenna-under-test with a pointing accuracy of 0.0025 degrees. Depending on the data sampling rate required, the Aerotech positioners are capable of a maximum measurement scan speed of approximately 7 RPM.

The EHF Test Facility is primarily used for spherical near-field antenna measurements using the Hewlett-Packard (HP) 8530A Network Analyzer/Receiver System. The Spherical Near-Field Antenna Measurement System is a combined hardware and software package which enables near-field radiation patterns to be acquired, and, with subsequent data processing, antenna radiation characteristics can be derived at arbitrary ranges. The HP 8360 Series Synthesizers provide signal generation from 10 MHz to 50 GHz. Automated control for data acquisition and processing is provided by the HP coprocessor, the Cemtech Pentium PC, and the 386-based PC computer systems.

The EHF Facility was used to measure the RF properties of the IRIDIUM satellites' EM GMA, and to calibrate Standard Gain Horn Antennas in the 19 GHz to 30 GHz frequency band. This work was performed for COM DEV Ltd., located in Cambridge ON, CANADA. The GMA is a dual reflector antenna. It provides coverage within a cone shaped at approximately 126 degrees.

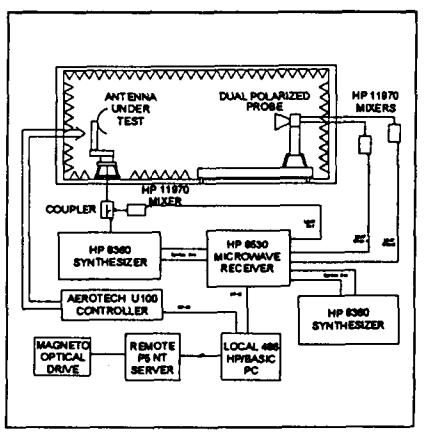

Figure 7: The DFL's EHF Test Facility

CONCLUSION

The MSAT and RADARSAT satellites were successfully tested at the DFL.

The Anechoic Chamber PIM calibration results have shown that the DFL facility met the requirements for the MSAT satellite-level PIM test, and the test was successful.

ACKNOWLEDGMENTS

The authors would like to express their gratitude to Mr. Russ Alexander of the RADARSAT Office and Mr. Yves Patenaude of SPAR Aerospace for their technical contribution to this paper.

IRIDIUM® - a Lockheed Transition to Commercial Space

Thomas N. Tadano
Director of Iridium® Bus Program
Lockheed Missiles and Space Company

Abstract. At Lockheed Missiles & Space Company, the IRIDIUM® commercial space program is dramatically revolutionizing spacecraft development and manufacturing processes to reduce cost while maintaining quality and reliability.

THE IRIDIUM® SYSTEM–AN OVERIEW

By 1998, Motorola's IRIDIUM® global personal communications system will provide mobile telecommunications services to anyone, at any time, anywhere in the world. Through a revolutionary network of 66 low-Earth-orbiting satellites, IRIDIUM® will provide 100-percent global coverage to its customers, allowing seamless communications services that can transform a pocket-sized telephone into a full-fledged, global, wireless workstation capable of voice, page, fax, and data transmissions, even if the subscriber's location is unknown.

The IRIDIUM® network of satellites will orbit approximately 420 nautical miles above the Earth's surface. The constellation will include six orbital planes, with 11 operational satellites and one on-orbit spare per plane. Compared with geostationary communications satellites 22,300 nautical miles above the Earth, the low orbit of the IRIDIUM® satellites will allow communications to low-power, hand units on the ground with negligible time delay.

Through its intersatellite links, the system will cover the vast portions of the world where telecommunications networks cannot be economically justified, and also will serve polar and ocean areas. Furthermore, by being able to hand off a call from satellites in the same or adjacent orbiting planes, IRIDIUM® will allow a user to maintain a call indefinitely, preventing calls from dropping, which occurs on systems in which the satellites are not linked.

The technological implications of this project are immense. Business travelers can be connected to their home offices from remote sites or from a skyborne airplane flying outside a cellular range. Governments and other organizations operating in undeveloped areas will have access to vital, even life-saving, communications capabilities. The IRIDIUM® system will be virtually impervious to earthquakes, floods, hurricanes, and other natural disasters, and it will not be affected by weather and damage to local telephone systems and power lines, making it an important asset to disaster-relief operations. Portable handsets can be air-dropped to aid disaster-relief efforts anywhere in the world.

IRIDIUM® will bring a new dimension of capability to the commercial, rural, and mobile sectors by providing service that is portable, universal, and reliable. Motorola is the prime contractor and creator of the original system concept.

THE LOCKHEED IRIDIUM® PROJECT AND CHALLENGES

On July 19, 1993, Motorola Satellite Communications Division awarded Lockheed Missiles & Space Company (LMSC) a contract valued at more than $700 million to design, develop, and manufacture 125 satellite buses for the IRIDIUM® system, including the electrical power subsystem, attitude control subsystem, propellant subsystems, and solar arrays. (A satellite bus is the satellite less the payload. It provides power, attitude control, and propulsion for the payload.) Lockheed also will provide systems engineering, satellite vehicle assembly, and integration and test services.

This contract represents the single largest commercial space endeavor ever undertaken by LMSC, long recognized as one of the nation's premier defense and aerospace contractors, and it understandably has presented some unique production challenges. In what is perhaps the most remark-able aspect of its work, LMSC ultimately will produce up to four satellites a month, an unheard-of feat in an era when some large satellites take years to produce. LMSC's satellite assembly line will be an impressive example of the space company's capabilities to compete in the commercial marketplace.

The challenges are numerous, but it is significant that none of them is a technology-development challenge. To a large extent, this is because LMSC is using off-the-shelf or modified off-the-shelf technology. Some of the more notable challenges are to complete the bus design in one year, complete qualification in 18 months, and, as mentioned above, achieve peak production rates of one bus per week. The first flight bus must be delivered 27 months after contract go-ahead. (The first IRIDIUM® launch is planned for the second half of 1996, just three years after contract go-ahead, and the system is expected to be fully operational by early 1998.)

Achieving the targeted production rates offers the largest challenge. Aerospace companies traditionally can take up to five years to develop satellites, which generally are larger and more complex than the IRIDIUM® bus and are manufactured at rates of only one or two per year. The existing paradigm was unacceptable for IRIDIUM®; it had to be broken and new processes established. Lockheed began by reducing the cycle time.

CYCLE-TIME REDUCTION THROUGH PRODUCTION REORGANIZATION

Reduction in cycle time (completing the work in less time) is the single most significant factor in reducing program costs and meeting schedules. To effect these reductions, LMSC decided to move beyond the traditional program management methods used for producing the older, larger systems. Lockheed sought a proactive means to change the workplace culture, which was seen as the primary obstacle. Comprehensive changes in the organizational structure and operation were the result.

For the larger and more complex space systems, programs have been organized by functions. Figure 1 is an example of a program organized by functions, or stove pipes. These functional groups reside in separate areas under the direction of their respective

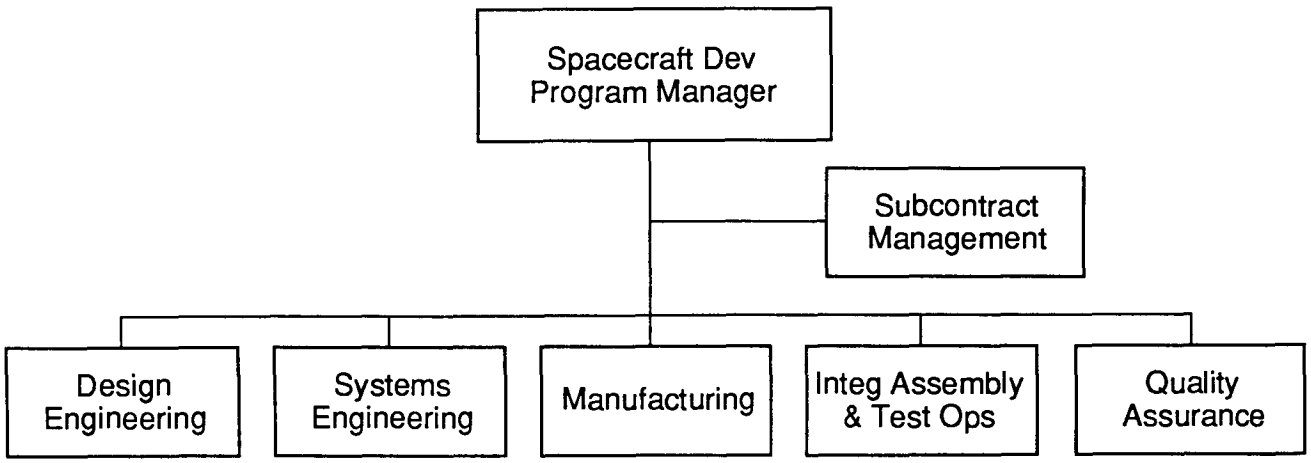

Figure 1. Organization by Function

managers, potentially creating various types of barriers, both physical and operational.

For example, a design could not be released to the manufacturing floor unless all functional groups signed off on it, and resolution of conflicts among the groups could be costly, both in time and money. Furthermore, commentary on the design was made serially, and designs were iterated several times before an agreement was reached. Even then, the final design might not be optimum for manufacturing. Historically, the problems inherent in the function-oriented organization have been considered a significant production challenge.

Lockheed met the challenge by organizing the IRIDIUM® Bus Program by product, using Integrated Product Development (IPD) teams. Although IPD is a relatively new term in aerospace manufacturing, the concept itself is not new; it has evolved to meet the changing needs of a changing industry.

Lockheed colocated the IPD team members and supplied them with the latest tools to maximize efficiency and institute concurrent engineering. Concurrent engineering allows all members of the team to participate in the design process simultaneously. The result is that designs can be completed much more quickly, often meeting manufacturing requirements on the first effort.

Figure 2 depicts a program organized by products and IPD teams. Each of the key functional groups is represented on the team, and team members are colocated.

With concurrent engineering and access to the latest tools, the Lockheed IRIDIUM® Bus Program has achieved significant reductions in cycle time in all development areas. For example, the Application Special Integrated Circuit (ASIC) electronics development cycle time was reduced by a factor of eight and achieved a phenomenal efficiency rating of 80 transistors per hour. Furthermore, all ASICs worked the first time, a testament to the capability of the latest simulation tools. Overall, electronic boxes were designed in one-third the time of any previous effort.

For the bus structure, which is made of composite materials and required special manufacturing tooling, the team produced quality hardware in record time. The initial tool try hardware, which normally is scrapped, turned out to be acceptable for flight hardware.

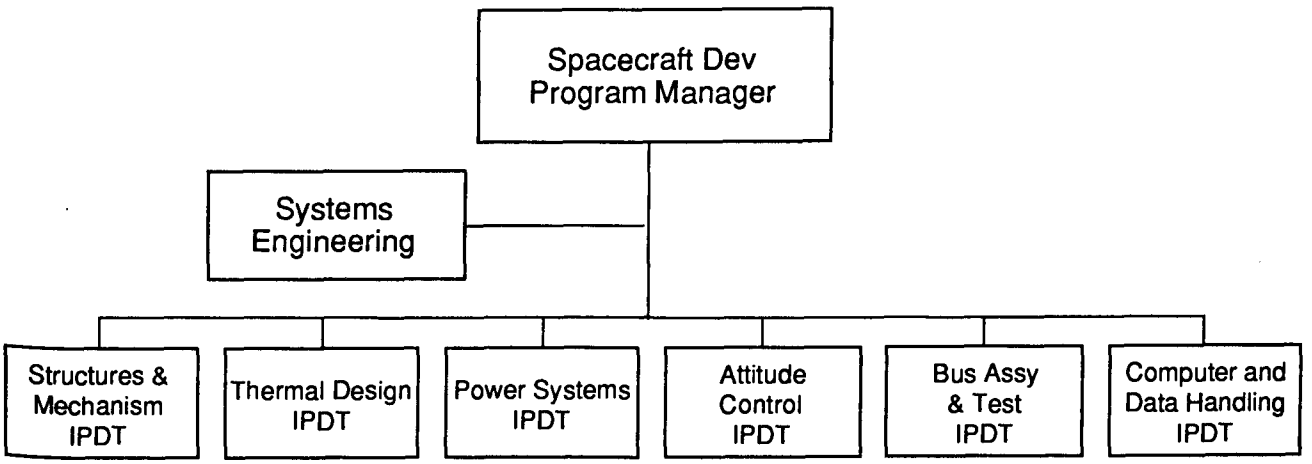

Figure 2. Organization by Product

Finally, the bus design was assigned a single part number and will be launched, as a single unit of off-the-shelf hardware, on three different international boosters. As traditional satellite designs can comprise hundreds of part numbers, each customized to a specific launch, this was a major feat. It could not have been possible under earlier satellite-manufacturing management systems.

DESIGN FOR MANUFACTURING AND QUALITY

The IRIDIUM® Bus program must meet the one-bus-per-week production rate. Because this will not be possible with high defect rates, high quality is critical to the program. Lockheed believes that quality cannot be *inspected* into the hardware; it must be must be *designed* in. With that in mind, an all-out campaign was initiated to deploy a Design for Manufacturability (DFM) initiative to all program personnel, including suppliers. The DFM manual provides advanced statistical tools for design which, in effect, reduces reject rates and establishes methods for controlling processes. Manufacturing personnel, through a simple performance measurement system, can easily determine when processes are starting to get out of control. In most cases, the problem can easily be corrected before rejects occur, eliminating the need for downstream inspection.

Dramatic results were achieved with these DFM tools. By using the design of the experiment tool, the Battery Radiator IPD team determined that the process parameters produce robust welds on the heat pipe end-caps. This produced better than 6-sigma results (3.4 defects per million opportunities as defined by Motorola's 6-Sigma Initiative).

Similar results also were reported by the solar cell and battery suppliers on some of their critical processes. One supplier, Starsys Research, using the Design for Assembly (DFA) techniques, produced the first interchangeable and reusable release mechanism in the industry.

Application of these tools has helped to produce robust products with repeatable and reproducible features. The DFM tools also have been instrumental in enabling the IRIDIUM® Bus Program to achieve simple, producible designs capable of meeting the one-bus-per-week production rate.

PARTNERSHIPS FOR SUCCESS

The traditional customer-contractor and -subcontractor relationships have been replaced on the IRIDIUM® program by a partnership or team relationship. The three major space vehicle associates (Motorola Communications Satellite Division, LMSC, and Raytheon) are also investors in IRIDIUM®, which creates an additional incentive to succeed. Lockheed believes this partnership approach is likely to become more routine on future commercial space ventures.

On the IRIDIUM® Bus Program, partners are not always selected for having the lowest bid, but for being best-in-class, thereby minimizing risk to the program. Suppliers and vendors are being developed and strengthened as long-term partners. Quality surveys identify a supplier's strengths and weaknesses and focus on a continuous-improvement program approach.

This partnership approach has been immensly helpful in breaking down barriers that might otherwise impede the critical flow of information and communication, providing seamless operation that eliminates ambiguity and helps reduce cycle time.

REQUIREMENTS MANAGEMENT AND COST CONTAINMENT

Much of the success in cost containment on the IRIDIUM® Bus Program can be directly attributed to requirements management. Extraordinary emphasis is placed on having firm, unambiguous requirements at contract signing. That tactic is now paying dividends. To-be-determined (TBD) and to-be-resolved (TBR) requirements are delegated to minor interface requirements, which poses a lower risk of affecting cost.

Requirements creep and over-design are also cost drivers. Requirements creep can come from the customer's "wish list" or from the design engineer's desire to have a conservative (excessive built-in margin) design. In the past, government programs have pushed designers to achieve the best performance possible and the most conservative design at the expense of cost and weight. *However, on a fixed-price program with tight schedules, cultural change is necessary to recognize when a design meets the requirement and to stop designing when the design is good enough.*

Understanding impacts to mass, power, production cycle-time, and cost has helped the designers optimize the designs. Concurrent engineering through IPD teams, program metrics, and the Design to Unit Product Cost initiatives are the tools used to maintain design balance.

STREAMLINING PROCUREMENT

In the past, it often took weeks to order a part after it was identified by the design engineer. On the IRIDIUM® program it takes two to three days on average to place the same order. The procurement process has been streamlined by colocating the buyer and parts engineer with the design engineers and eliminating non-value-added signature requirements.

The cost of these parts is 50 percent of that of the equivalent military part because of volume buys and elimination of unnecessary inspections and paperwork. Most of the parts come off the same production line. The commercial parts database and price breakthroughs are also being shared among the major partners, saving time and money.

BENEFITS FOR THE FUTURE

The IRIDIUM® Bus Program has successfully implemented numerous new initiatives and streamlined processes that will benefit future programs at LMSC. Cycle-time reduction, designing for manufacturability, process control for quality, organizing by IPD teams, and design-to-unit production costs are some of the key process improvements successfully employed on the program. Government agencies tasked with acquisition reform have shown keen interest in the cost-cutting processes developed on the IRIDIUM® Bus Program. Many of these streamlined processes are now being proposed on new government projects.

The visions and technologies of LMSC's F-Sat (Frugal Satellite) and Small-Sat development programs were a springboard for the IRIDIUM® bus team. Synergism among these programs has helped to produce a whole family of low-cost satellite buses to fulfill any mission imaginable.

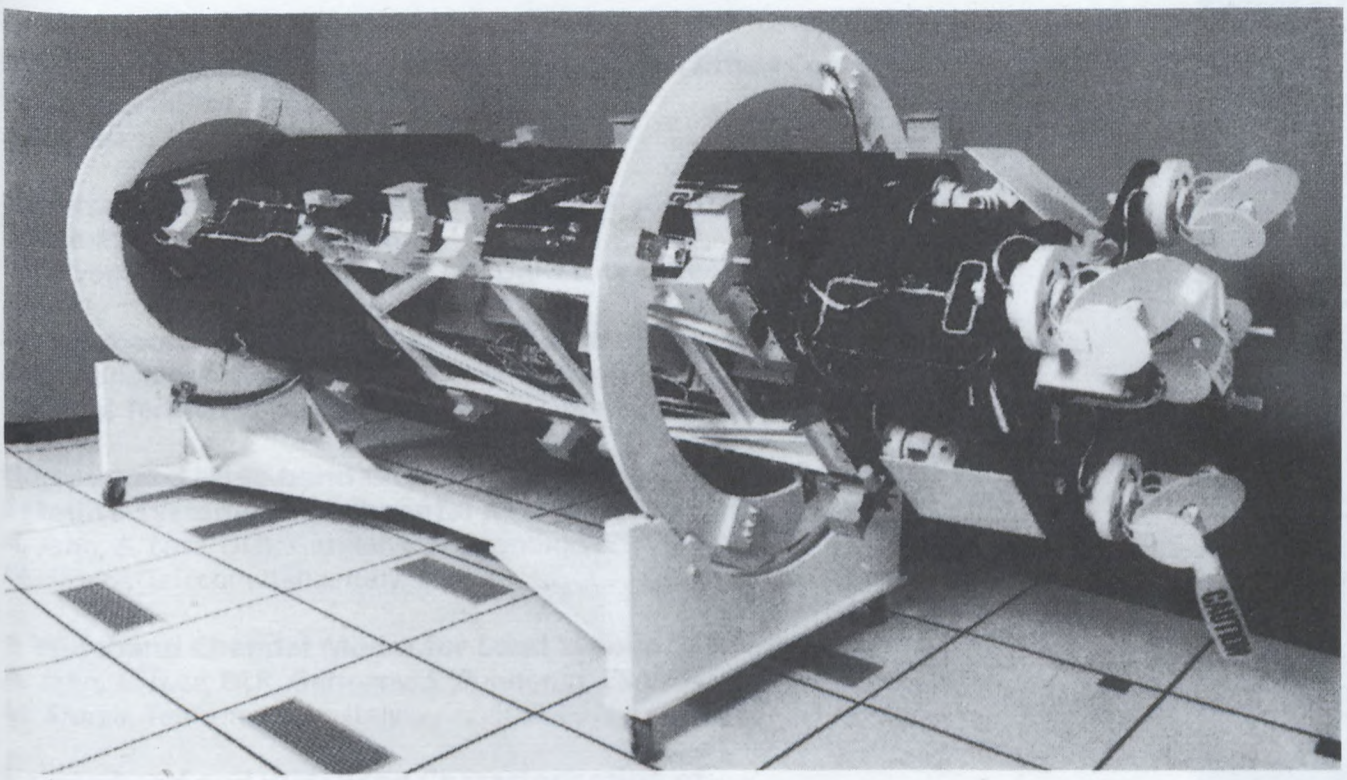

Mockup of Iridium® Spacecraft prior to Main Mission Antenna and Solar Array Installation.

Propagation

Session Chairman: **Wolfhard Vogel,** University of Texas, USA
Session Organizer: **Faramaz Davarian**, Jet Propulsion Laboratory, USA

Topic Introduction: Predictions of radiowave propagation effects are needed for the planning of mobile/personal satellite systems. Although several propagation effects are present in mobile satellite channels, signal attenuation by tree shadowing and blockage is the biggest impediment for the design of a reliable Earth-space link. Moreover, atmospheric effects such as gaseous and rain attenuation, which are negligible at L- and S-band frequencies, pose an additional challenge to the system planner at the Ka-band. There are also other channel anomalies that cannot be neglected. Examples are multipath effects, depolarization loss, delay-spread effects in wideband channels, harmful interference in multisatellite and multiple-beam systems, and more.

This session begins with a review of the available prediction models in the Recommendations of the International Communications Union. The review presentation is followed by eight papers that address a variety of topics of interest. These topics include attenuation due to tree shadowing, propagation effects for narrowband and wideband systems, and the propagation issues of the 20/30 GHz band. In summary, this session offers a wealth of propagation data and prediction models that can be used for the planning and design of mobile satellite systems.

cont'd

ITU Recommendations Regarding Propagation Effects on Mobile-satellite Links

F. Davarian
Jet Propulsion Laboratory
California Institute of Technology
4800 Oak Grove Drive
Pasadena, CA 91109, USA
Phone: 818-354-4820 FAX: 818-393-0096

ABSTRACT

To predict the effect of radiowave propagation on mobile-satellite links, the International Telecommunication Union (ITU) offers three Recommendations. These Recommendations have been developed by the participants of ITU Study Groups to enable service planners and design engineers of mobile-satellite systems to characterize the mobile-satellite link. This paper briefly reviews the structure of the ITU, its Study Groups, and its contributions to propagation modeling. The shortcomings of some of these models are examined and means to overcome them have been pointed out. The protocol for participation in ITU Study Groups is very briefly discussed.

INTRODUCTION

Impairments rising from radiowave propagation in mobile-satellite links can significantly limit the performance of a communication system. Consequently, system planners strive for the prediction of propagation effects to reduce the risk associated with mobile communications. To assess the mobile-satellite channel, major propagation experiments were first launched in the eighties with continuing work to date. Past efforts have resulted in a number of prediction models, enabling system engineers to evaluate the propagation channel in mobile-satellite systems.

For the users of propagation data, two major sources of information are the NASA Reference Publications 1274 [1] and ITU-R Recommendations [2]. In this paper the latter source will be examined.

INTERNATIONAL TELECOMMUNICATION UNION

The ITU is an intergovernmental organization that any sovereign state may join. The member states, usually represented by their telecommunication agencies, are constitutional members with certain obligations and rights. These members pay for the expenses of the ITU and vote for the changes in the structure and the charter of the union. Other organizations, such as service providers, manufacturers, and scientific institutes, may be admitted through their national administrations to certain ITU activities but cannot vote.

The objectives of the ITU are as follows:

- maintain and extend international cooperation for improvement and rational use of telecommunications;
- promote the development of technical facilities and their most efficient operation with a view to improve the efficiency of telecommunication services and increase their usefulness to the public;
- harmonize telecommunication-related efforts of member nations.

The ITU achieves its goals via three functions: 1) standardization of

telecommunications, 2) regulation of radio communications, and 3) development of telecommunications. These functions are carried out by the three Sectors of Telecommunication Standardization, Radiocommunication, and Development. Each Sector is headed by a director, and the union is headed by its secretary general, who is the legal representative of the ITU.

Figure 1 shows the structure of the ITU. As shown in Figure 1, the plenipotentiary conference is the ultimate policy-making body of the union. Since propagation work is conducted in the Radiocommunication Sector, the next section will examine this sector of the ITU.

ITU RADIOCOMMUNICATION SECTOR

The ITU Radiocommunication Sector (ITU-R) deals with matters concerning radio communications, including the regulation of radio communications. Technical work is performed in Study Groups. Each Study Group deals with a specific area of Radiocommunication (propagation, interference, spectrum sharing, mobile communications, broadcasting, science services, and many more). The primary products of Study Groups are ITU-R Recommendations. These Recommendations are tools that can be used for design, specification, and calculation of telecommunication systems and system parameters.

In most countries active in ITU-R, a national ITU-R committee has been established. For example, the U.S. National Committee of the ITU-R functions as a federal advisory committee to the Department of State. It coordinates and reviews the submissions made by the United States to the meetings of ITU-R.

Study Group members are delegates sent by their administrations. Other organizations can also participate by sending their experts as participants if their organization has been admitted by their ITU-R National Committee. In the United States, National Committee membership is open to anyone with a knowledge and interest in telecommunication matters. A written request or application to the particular U.S. Study Group chairperson is sufficient to establish membership.

A Study Group's agenda usually includes a complex set of issues. Therefore, each Study Group is divided into Working Parties, each of which attends to a specific area of work. Such Working Parties may further split into Task Groups, Focus Teams, Ad Hoc Groups, and so on.

Propagation is the purview of Study Group 3, and presently it consists of four Working Parties. Issues related to mobile-satellite propagation are studied by Working Party M, chaired by Mr. Martin Hall[1]. The U.S. Study Group 3 delegation is chaired by Mr. Eldon Haakinson[2].

ITU-R RECOMMENDATIONS FOR THE PREDICTION OF PROPAGATION EFFECTS ON MOBILE-SATELLITE LINKS

ITU-R offers three Recommendations for the prediction of propagation effects in maritime, land, and aeronautical mobile-satellite links. These Recommendations are numbered 680, 681, and 682, respectively.

Recommendation 680

This Recommendation deals with propagation effects on maritime mobile-satellite links, and it consists of four areas:

- Tropospheric effects
- Ionospheric effects
- Fading due to sea reflection

[1] Mr. Hall's address: Rutherford Appleton Laboratory, Chilton, Didcot, OXON OX11 0QX, UK

[2] Mr. Haakinson's address: ITS, U.S. Department of Commerce, 325 Broadway, Boulder, CO 80303, USA

- Interference from adjacent satellite systems

The Tropospheric Effects Section refers the user to Recommendation 618, the basic slant path impairment text for fixed satellite services, of the ITU-R. The Ionospheric Section discusses scintillation and Faraday rotation, and a reference is made to Recommendation 531. Topics such as fade depth, fade duration, and spectrum spreading due to multipath are discussed in the Sea Reflection Section. The models provided in this section are valid for frequencies 1–2 GHz. Finally a method for calculating signal to interference power ratio in multiple satellite systems is given in the last section.

Recommendation 681

The main contribution of Recommendation 681 is in providing five important prediction methods for land mobile-satellite applications:

1. Empirical roadside shadowing
2. Attenuation frequency scaling
3. Fade duration distribution
4. Non-fade duration distribution
5. Fading due to multipath

All the above models have been empirically derived. The first model enables the user to predict the effect of roadside tree shadowing on the mobile-satellite link. The model accepts path elevation angle and percentage of link availability as input parameters and outputs fade depth. This model is valid for a frequency of 1.5 GHz.

The second model provides a simple equation for extending the range of the Roadside Shadowing Model to 0.8–2.7 GHz. The input to this model is fade depth at frequency f_1, and the output is fade depth at frequency f_2, at the same probability level.

The third model provides a method of calculating fade duration statistics in land mobile-satellite systems. This method applies only to a 5-dB fade threshold and cases of moderate to extreme shadowing. Although measurements have shown a moderate dependence on elevation angle, no dependence on elevation angle is yet given in this model. The fourth model provides an estimate of non-fade statistics, again restricted to a 5-dB fade threshold.

The fifth model includes two methods of predicting fading due to multipath, one in a mountain environment and the other in a roadside tree environment. Clear line of site is assumed in both these methods.

All five of the models of Recommendation 681 are rather restricted due to limited experimental data and the difficulty of adequately describing the mobile terminal environment. These models will be refined in the future as more measurements become available.

Another important shortcoming of Recommendation 681 is that it does not sufficiently treat non-geostationary applications. The above models were developed using data from geostationary spacecraft. Hence subtleties such as dependence on elevation angle, which is an important parameter in non-geostationary systems, are not treated adequately. Study Group 3 members are currently working toward the improvement and expansion of Recommendation 681 models. It is expected that the following enhancements will be provided in the near future:

- A more rigorous description of the environment
- Expanded range of model applicability (frequency, elevation angle, fade value, and percentage)
- Models valid for all orbital configurations (GEO, LEO, HEO, and MEO)
- Diversity models (satellite diversity, antenna diversity, etc.)

Recommendation 682

This Recommendation consists mainly of prediction models and data on the effect

of ground reflections in aeronautical links. Fade statistics due to sea reflections as a function of the path elevation angle can be computed. Also coherence bandwidth as a function of aircraft altitude is given for low elevation angles. Data are also provided on the effect of land reflections. The data provided in this Recommendation have been taken at frequencies between 1 and 2 GHz.

CONTRIBUTIONS TO STUDY GROUP 3

Study Group 3 solicits contributions in the form of input documents from its members. These input documents may propose modifications and amendments to the existing Recommendations, propose new Recommendations, or may provide signal measurements (propagation data). The subject matter of the input documents is loosely confined to Study programs established by Study Group 3 in response to questions posed by Radio Conferences, the Study Group itself, or other Study Groups.

For the purposes of model development and testing, Study Group 3 maintains a Data Bank of propagation measurements. As mentioned earlier, Recommendations 680, 681, and 682 have notable shortcomings due to the scarcity of data. Therefore, it is very important that this Data Bank is regularly supplied with new data to allow the enhancement of mobile-satellite models. Study Group 3 has developed a simple format for supplying data to its Data Bank. For every study area, a single-page table is available for entering data. For example, land mobile-satellite data (Recommendation 681) are provided using the table shown in Figure 2.

Each table is looked after by a volunteer table keeper. For example the author of this paper maintains the table shown in Figure 2. The Data Bank, which is the collection of all the tables in an electronic form, has a volunteer custodian, Mr. Bertram Arbesser-Rastburg of the European Space Agency. Supplying data to Study Group 3 is, therefore, straightforward. A table is filled out and provided to the Study Group as an input document. The table keeper of the supplied information will review the data for validity and clarity and will enter them in the data base. As a matter of courtesy, it is recommended that an electronic version of the table also be provided so that the table keeper is relieved from key punching the information into the computer.

Blank copies of Study Group 3 data tables can be obtained from the Radiocommunication Bureau in Geneva by sending a message to Mr. Kevin Hughes, counsellor (e-mail: kevin.hughes@itu.arcom.ch). Mr. Hughes can also provide the Data Bank.

UPDATE

In its most recent meeting, January 1995, WP 3M proposed a few changes to Recommendation 681. Examples of these changes include the extension of the Roadside Shadowing Model to 3 GHz, and the introduction of an approximate method to extend the range of the same model to non-geostationary applications.

ACKNOWLEDGMENT

The research conducted for this paper was funded by the Jet Propulsion Laboratory, California Institute of Technology, under a contract with the National Aeronautics and Space Administration.

REFERENCES

1. J. Goldhirsh and W. Vogel, *Propagation Effects for Land Mobile Satellite Systems: Overview of Experimental and Modeling Results,* NASA Reference Publication 1274, Feb. 1992.

2. *1992 CCIR Recommendations, RPN Series, Propagation in Non-Ionized Media,* ITU, Geneva, Switzerland, Oct. 1992.

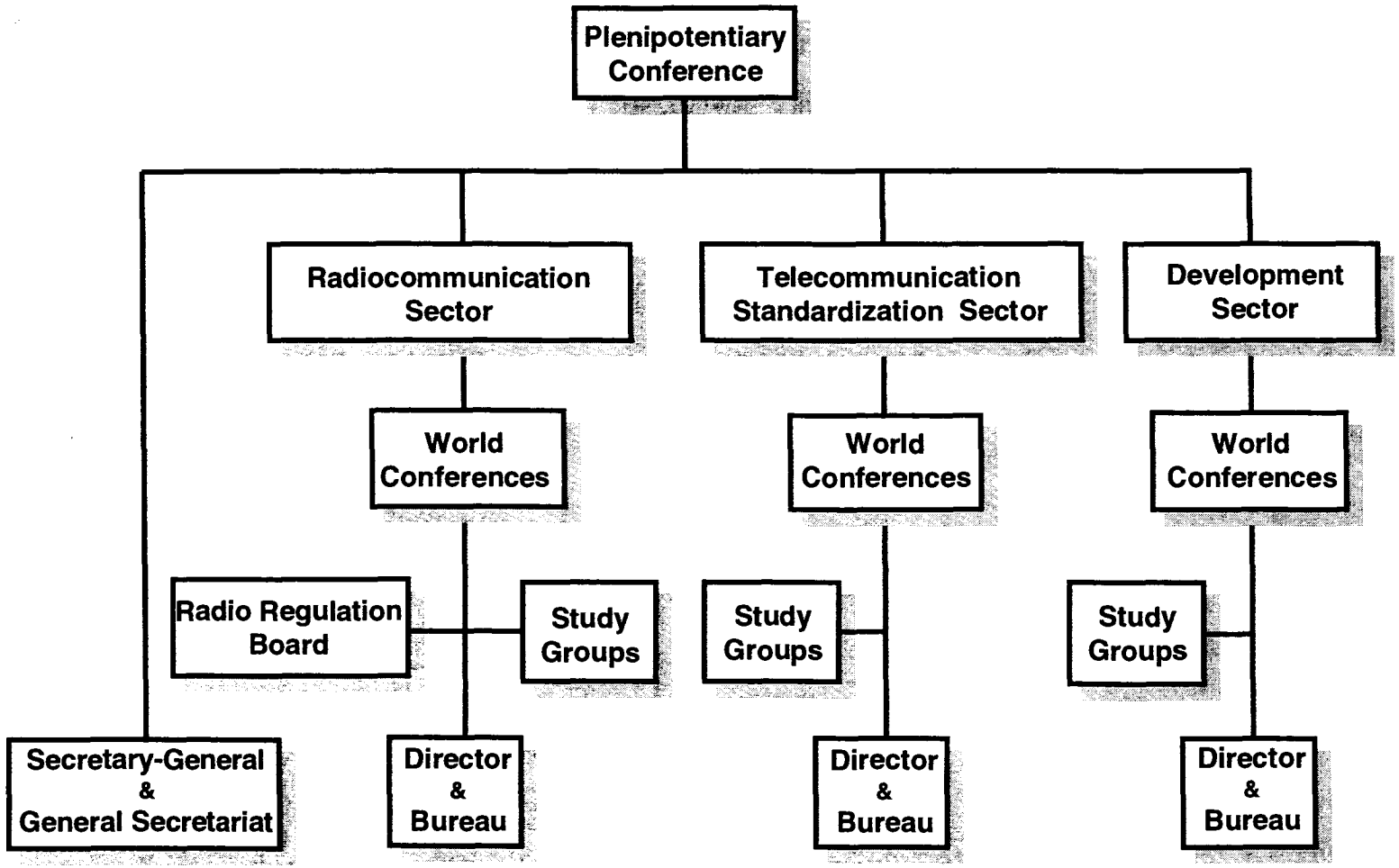

Figure 1. The Organizational Structure of the International Telecommunications Union

Station number
TX frequency (GHz)
TX polarization (L/C)
TX polarization tilt φ_p(deg)
RX average elevation angle
RX CCIR rain zone
Signal source (transmitter on i.e: Satellite, helicopter, aeroplane, balloon, tower
If satellite: satellite name
orbital position (deg) E
TX antenna gain towards mobile (dBi)
Mobile station
RX area name
RX country (1)
RX average latitude (-90..+90) (deg)
RX average longitude (0..360) (deg) E
Average velocity of vehicle (km/h)

RX average altitude amsl h_{gr} (m)
RX antenna height ag h_r (m)
RX antenna type
RX 3 dB beamwidth in Az Θ_{ras} (deg)
RX 3 dB beamwidth in El Θ_{rel} (deg)
RX antenna gain (dBi)
RX antenna diameter D (m)
RX radome (Y/N)
RX polarization (L/C)
RX polarization tilt φ_p(deg)
RX multipath reduction (Y/N)
RX dynamic range (dB)
RX minimum signal-to-noise ratio (dB)
RX integration time (s)
RX bandwidth (Hz)
Data sampling interval (s)
Calibration interval (days)
Data resolution (dB)
Measurement: Exp Nr.
Start date (yyyy.mm.dd)
End date (yyyy.mm.dd)
Duration of measurement in this environment (h)
Season
Environment
Land mobile terrain type (2)
Building type
Vegetation type
Surface Condition (wet, dry, snow)

Table a:
Fade depth (dB relative to LOS) exceeded and XPD (dB) NOT exceeded for percentage of time

% time	0.1	1.0	5.0	10.0	30.0	50.0	90.0	99.0	99.9
A									
XPD									

able b:
Fade duration reported in seconds or meters (s/m)
Fade duration (s or m) NOT exceeded for percentage of locations at given fade levels(sec)

% Loc	0.1	1.0	5.0	10.0	30.0	50.0	90.0	99.0	99.9
0 dB									
2 dB									
5 dB									
10 dB									

References:

Comments:
(1) See § 6.1 for list of country codes.
(2) Environment types for land mobile: DU: dense urban, UR: urban, SU: suburban, RU: rural, WD: wooded, OP: open, HI: hilly, MO: mountainous, WA: water.

Figure 2. Data Table for Land Mobile Satellite Links (narrow band statistics)

Simultaneous Measurements of L- and S-Band Tree Shadowing for Space-Earth Communications

Wolfhard J. Vogel, Geoffrey W. Torrence, and Hsin P. Lin
Electrical Engineering Research Laboratory
The University of Texas at Austin
Austin, Texas 78758, USA
Phone: +1-512-471-8608 FAX: +1-512-471-8609, e-mail: Wolf_Vogel@mail.utexas.edu

ABSTRACT

We present results from simultaneous L- and S-Band slant-path fade measurements through trees. One circularly-polarized antenna was used at each end of the dual-frequency link to provide information on the correlation of tree shadowing at 1620 and 2500 MHz. Fades were measured laterally in the shadow region with 5 cm spacing. Fade differences between L- and S-Band had a normal distribution with low means and standard deviations from 5.2 to 7.5 dB. Spatial variations occurred with periods larger than 1~2 wavelengths. Swept measurements over 160 MHz spans showed that the stdv. of power as function of frequency increased from ~1 to ~6 dB at locations with mean fades of 4 and 20 dB, respectively. At a 5 dB fade, the central 90% of fade slopes were within a range of 0.7 (1.9) dB/MHz at L- (S-) Band.

INTRODUCTION

Propagation effects in the LEO bands such as tree shadowing, terrain multipath, and obstacle blockage impose random variations on signal strengths at the satellite and may require mitigation. To assess possible mitigation, we present results from simultaneous L- and S-Band propagation measurements through several trees.

Multi-frequency propagation measurements of roadside tree fading have previously been reported for UHF and L-Band [1,2] and at UHF, L-Band and S-Band [3]. They used separate receiving antennas in each band for statistical comparisons of power received at two frequencies. This experiment differs in two key aspects. It used one aperture at both ends of the dual-frequency transmission link and fixed-frequency or swept-cw modes, for measuring the temporal, spatial, and frequency structure of the received power at L- and S-Band. In addition, data were obtained for co-polarized and cross-polarized reception, although consecutively.

EXPERIMENTAL SETUP

The measurement system consists of a dual-frequency sweeping transceiver located in a van, a 20 m crank-up transmitter tower mounted it, and a wired remote receiving antenna (RHCP or LHCP), filter, and preamplifier on a linear positioner. Signals at L- and S-Band are generated as upper and lower sideband mixing products of a stable 2055 MHz oscillator combined with a tracking generator. Both antennas are wideband, cavity-backed conical spirals. The system can be operated in two modes: (1) constant cw-tone mode for measuring time series data and (2) swept cw-tone mode for measuring the frequency variability of the channel. The antennas have a 3 dB beamwidth of about 90° in both bands. Received signals are converted to 2 and 6 kHz audio signals and fed to a 16 bit A/D data acquisition board. The final IF, which contains both L- and S-Band signals, is sampled at a 51.2 kHz rate. All signal processing is done digitally.

Mode 1 output is a time series with a 0.01 s sampling rate. Mode 2 processing results in frequency spectra over 160 MHz with about 1 MHz resolution obtained in 0.1 s. The advantage of this dual-frequency system implementation is that it allows making simultaneous dual-band measurements through shared antennas with a single-channel receiver. A positioner holds the receiving antenna on a computer-controlled linear motion arm. The motion can be along any direction and over a range of 80 cm.

MEASUREMENT DETAILS

Measurements were made through three different trees, a Pecan (*carya illinoensis*), a Cottonwood (*populus deltoides*), and a Loblolly Pine (*pinus taeda*)while the deciduous trees were still in leaf. All trees had heights in the range from 9 to 12 m, maximum crown diameters of 6 to 10 m, and trunk diameters of 0.25 to 0.38 m. The receiver positioner was placed on the opposite side of the tree and moved along a horizontal arc centered on the tower base such that the propagation path would initially be clear of obstructions and subsequently, after moving laterally, pass through the tree crown. The path elevation angle was 30° for the Pecan, 23° for the Cottonwood, and 20° for the Pine tree.

Mode 2 (swept-cw; frequency spectrum) data were obtained in 5 cm steps over 13 m for the Pecan and Pine and over 10.5 m for the Cottonwood. After completing a measurement set with one receiving antenna, the set was repeated with the opposite receiving polarization. All results are presented relative to the co-polarized clear-path level.

RESULTS

Time Variability

Time series were measured to verify that variations observed during a 0.1 s Mode 2 frequency sweep are due to changes with frequency, not to time. Observed power level changes are due to short term variations in the propagation medium, mainly wind-induced swaying of tree branches also motion of multipath scatterers such as trees, people, or cars near the antennas but off the direct path. The median autocorrelation of all Pine tree time series at a lag of 0.1 s exceeded 0.96 at both frequencies for the co-polarization and 0.91 for the cross-polarization. Therefore, the system's sweep rate of 2000 MHz/s was sufficiently fast to ensure that frequency variability as opposed to time variability was measured with Mode 2 frequency sweeps.

Space Variability

Figure 1 shows the spatial variation of co-polarized power levels received at 1618 and 2492 as a function of position in the shadow of the Pecan tree. The Pine was the only free-standing tree and power levels at both ends of the horizontal scan assumed the clear-path value. For the Pecan and Cottonwood, the crowns of other trees were intercepted by the line-of-sight path towards the end of each scan. There is a macroscopic correlation between power levels at the two frequencies, i.e., both L- and S-Band are attenuated by the intervening tree, with 5 to 20 dB being typical values. On a finer distance scale, however, there are many deviations from equality. Co-polar fades at the two frequencies occupy a similar range for the Pecan and Pine, but fades for the Cottonwood tend to be deeper at S-Band than at L-Band. The differences between the received power levels at 1618 and 2492 MHz are summarized in Table 1.

Table 1: Summary of L-Band Minus S-Band Difference Power

Difference Power	Polari-zation	Avg (dB)	STD (dB)
PECAN	Co	1.0	5.6
C'WOOD	Co	5.4	5.2
PINE	Co	0.4	7.1
PECAN	Cross	-0.2	7.5
C'WOOD	Cross	-0.5	6.3
PINE	Cross	-0.8	7.2

The co-polarized power level difference for the Pine tree, plotted in Figure 2, ranges from a maximum of 25 dB to a minimum of less than -25 dB over the 13 m span of the measurement and varies quite rapidly with position. Cumulative distributions of the co-polarized power difference are given in Figure 3.; corresponding cross-polar normal probability plots of power differences are nearly indistinguishable by tree-type and exhibit much more normal behavior.

To assess the sensitivity of the power level to horizontal motion, the percentage of power variations faster than a given spatial frequency has been calculated. This information is needed to design a stable power control loop. The power of the spatial variations for all trees decreases exponentially with spatial frequency: 50% is at

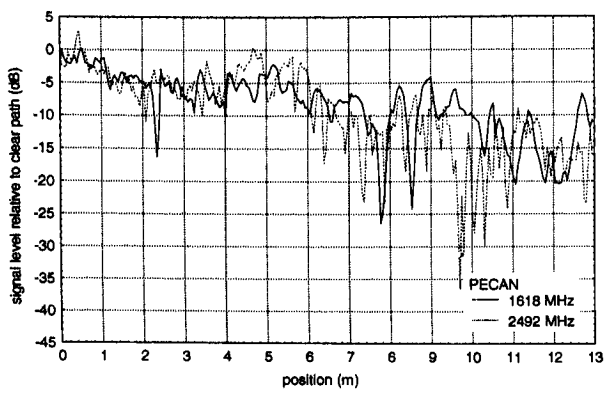

Figure 1: Co-polarized signal levels received at 1618 MHz (solid) and 2491 MHz (dashed) versus position in the shadow of a Pecan tree.

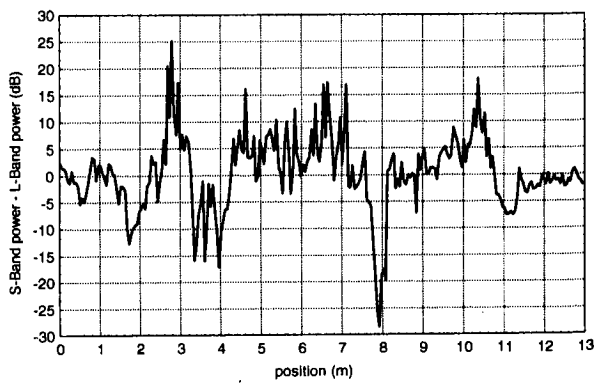

Figure 2: Example of the S-Band minus L-Band received power difference versus position for the pine tree in the co-polarization.

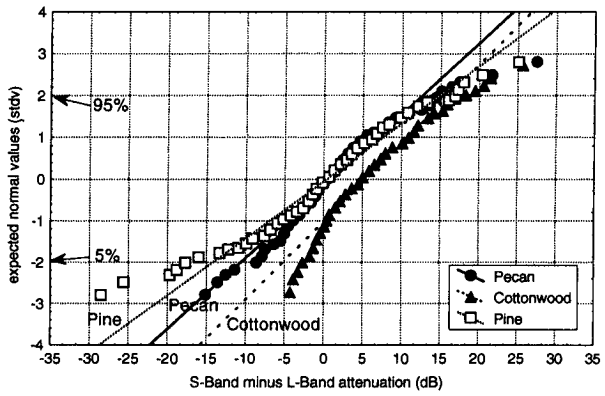

Figure 3: Probability plot of the difference between S-Band and L-Band co-polarized attenuation for the three trees.

a frequency below about 0.2 λ^{-1}, 90% below about 1 λ^{-1}. Our measurement of the spatial spectrum is high-frequency limited by the electrical antenna diameter (nearly equal at the two frequencies).

Frequency Variability

Similarly to the spatial variations, rapid changes with frequency occur only when the power level is reduced into the range of diffusely scattered power, which for land-mobile satellite scenarios is about 15 to 20 dB below the direct power level. Both co- and cross-polarized signals show similar characteristics. A close-up view of the frequency selectivity of tree-fading (Pine) for the allocated mobile satellite service bands from 1600 to 1626.5 MHz (upper panel) and 2483.5 to 2500 MHz has been plotted in Figure 4 to illustrate that at low fade levels only limited frequency selectivity is exhibited. The standard deviation of the frequency variations depended somewhat on the mean level. There is appreciable scatter; when the co-polarized mean level is reduced to -4 dB, the standard deviation σ is near 1 dB. For the cross-polarization, at a mean of near -20 dB, σ tends to saturate near 6 dB, as would be expected for a Rayleigh scattering process, for which σ=5.57 dB.

Another indicator for frequency variability is the fade slope vs. frequency, defined by

$$fadeslope = \frac{dS}{dF} \text{ (dB/MHz)} \qquad (1)$$

where dS is the change in received co-polarized power over the measurement frequency resolution dF. Regression coefficients for the standard deviation of the fade slope as a function of the mean signal level have been derived using

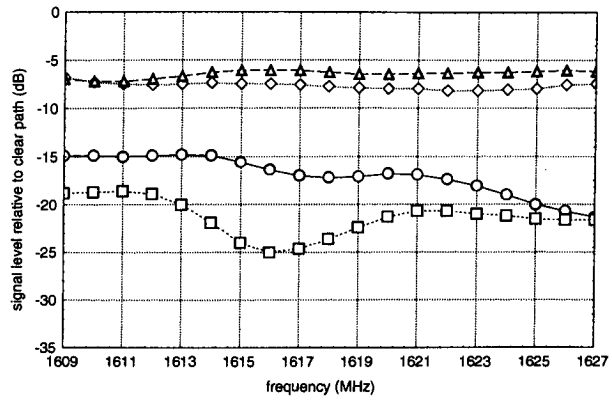

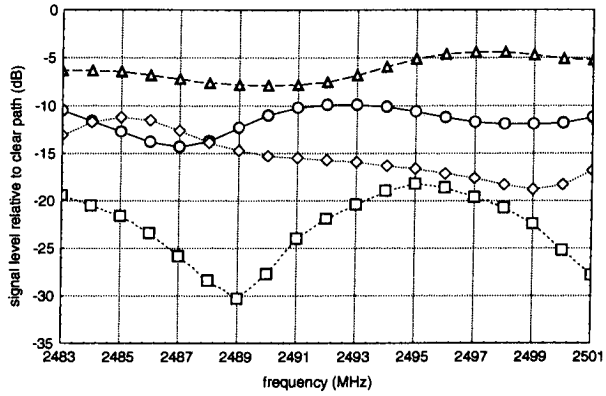

Figure 4: A close-up view of the frequency selectivity of tree fading (Pine tree shown) in the allocated mobile satellite service bands from 1600 to 1626.5 (upper panel) and 2483.5 to 1500 MHz (lower panel). .

The range of the fade slope increases with diminishing signal level. For a 5 (10) dB faded signal at L-Band the central 90% of the fade slopes (±1.96 Std. Dev.) are within a 0.7 (1.0) dB/MHz range, compared to a 1.9 (2.9) dB/MHz range at S-Band. All fade slopes were tested for normality using the Kolmogorov-Smirnov procedure and for most a hypothesis of normality could not be rejected. Probability plots of L- and S-Band fade slopes for selected Pine tree measurements with mean signal levels of -5, -10, -15, and -20 dB are shown in Figure 5.

CONCLUSIONS

We have observed the time, space, and frequency domain structures of L- and S-Band simulated satellite power levels after slant-angle propagation through three representative trees. Our findings are:

1. Power level variations at L-Band are not correlated with those measured simultaneously at S-Band in any of the domains and spatial averages of power levels

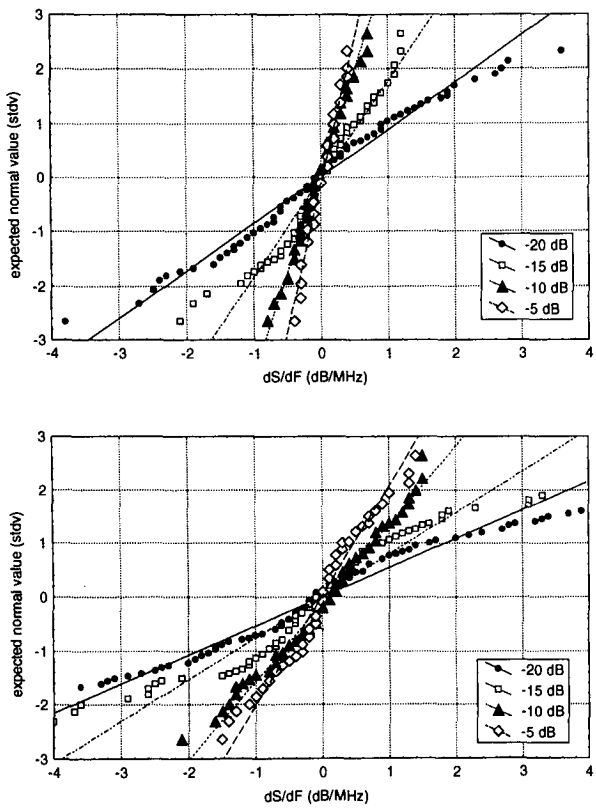

Figure 5: Probability plots of co-polarized fade slopes for the Pine tree exhibit near-normal behavior at L-Band (top) and S-Band (bottom).

are only weakly correlated. This means that uplink power control based on downlink power measurements will be difficult to implement.

2. Time variations are slow if there is little wind and the receiver is stationary; i.e., for satellite communications systems with fade margins less than about 15 dB, time variations of mobile terminal power at the satellite, therefore, will be spatial variations converted to time variations primarily by user- and secondarily by satellite-motion.

3. Power level variability in the three domains increases with increasing attenuation, because as the direct signal is reduced, multipath scattering has a greater effect.

4. Power levels as a function of location measured with a cross-polarized receiving antenna were in the mean 15 to 20 dB below the co-polarized clear-path level and more variable than the co-polarized signal. These characteristics were independent of position with respect to the tree.

5. The fade slope with frequency, measured in dB/MHz, was found to be normally distributed with zero mean and standard deviation increasing with fade level. At moderate fade levels fading is essentially flat and little can be gained from frequency diversity mitigation techniques.

ACKNOWLEDGMENT

This effort was supported jointly by Loral Aerospace Corporation and JPL under Contract JPL 956520, via the JPL Technology Affiliates Program, coordinated by the JPL Commercialization Office. We appreciate Dr. G. Xu's help with the signal processing algorithms.

REFERENCES

[1] **Vogel, W. J. and U. S. Hong,** "Measurement and modeling of land lobile satellite propagation at UHF and L-Band," IEEE Transactions on Antennas and Propagation, Vol. 36, No. 5, May 1988

[2] **Goldhirsh, J. and W. J. Vogel,** "Mobile satellite system fade statistics for shadowing and multipath from roadside trees at UHF and L band," IEEE Transactions on Antennas and Propagation, Vol. 37, No. 4, April 1989

[3] **Bundrock, A. and R. Harvey,** "Propagation measurements for an Australian land mobile-satellite system," *Proc. of International Mobile Satellite Conference*, Pasadena, California, pp. 119-124, May 1988

[4] **Goldhirsh, J. and W. J. Vogel,** "Propagation effects for land mobile satellite systems: overview of experimental and modeling results," *NASA Reference Publication 1274*, February 1992

[5] **Vogel, W. J. and G. W. Torrence,** "Propagation measurements for satellite radio reception inside buildings," *IEEE Transactions on Antennas and Propagation*, Vol. 41, No. 7, July 1993

Narrowband Land Mobile Satellite Channel Modeling

A.G. Kanatas, E.C. Kanderakis, P. Constantinou

National Technical University of Athens
Mobile Communications Laboratory
42 Patission Str, Athens, Greece
Phone: +30-1-3811877 FAX: +30-1-3647704

ABSTRACT

The subject of this paper is the development of a generalized analog model for the narrowband Land Mobile Satellite Channel (LMSC). It is based on the model proposed by Lutz [1], the 3-dimensional scaterring model of Aulin [2] and the multipath interference simulation method proposed by Jakes [3]. Statistical tests of the simulated data show excellent agreement with the expected distributions whereas the power spectrum predicted by Aulin is duplicated in a discrete manner.

I. INTRODUCTION

The importance of the LMS channel characterisation stems from the need of system engineers in designing and optimising the LMS Systems performance. Signal degradation caused by attenuation and multipath from the vicinity of the mobile has to be accurately calculated in order to allow for the necessary link margins. The time varying behavior of the channel has to be investigated for the selection of the modulation scheme, the multiple access scheme, the error protection methods, the carrier recovery and bit synchronization to be used.

Lutz etal.[1] has proposed an analog model for the land mobile satellite channel. The transmitted signal is deteriorated by multiplicative fading and additive white Gaussian noise. The fading process is switched between Rician fading representing time intervals with unshadowed signal coming directly from the satellite and Rayleigh/Lognormal fading which represents shadowed intervals. For urban environments this process can be produced by a method proposed by Jakes [3] for multipath interference simulation.

As an alternative a generalized method can be used instead of Jakes'. The new method is based on the model of Aulin [2] for multipath interference. Aulin assumed that the component waves of multipath propagation arriving at the mobile do not necessarily travel in a horizontal direction as it was supposed to be by Jakes. He introduced a new angle of arrival for the component waves on the vertical plane. So the model can be characterized as 3-dimensional and the generalization of Jakes' method which uses the new angle is a 3-dimensional multipath simulator. The new simulator provides a discrete approximation to the power spectrum as it was predicted by Aulin.

Section II of this paper reviews Lutz's model and how it is revised at its base. The model for the multipath signal and method for multipath interference simulation is presented in section III and the power spectrum is provided. In part A of the section IV we present some statistical tests for the generated distributions, whereas in part B of the same section we quote the power spectrum estimates with the discrete Fourier transform for the Rayleigh channel. In part C of section IV waveforms of the channel are presented for various combinations of the model's parametres. These are the mean durations of Rayleigh/Lognormal and Rician states, the Rician factor, and the mean μ, and variance σ of the Lognormal distribution.

II. THE ANALOG MODEL

Figure 1 shows a block diagram of the analog model proposed by Lutz [1]. s(t) is the transmitted signal and e(t) is the signal received by the mobile receiver. The two states are characterized as good and bad state respectively. The switching process can be simulated by a Markoff model with two states. The transition probabilities p_{gb} and p_{bg} are related directly to the mean durations of the good and bad states in bits D_g, D_b respectively as follows:

$$D_g = 1/p_{gb} \quad \text{and} \quad D_b = 1/p_{bg} \qquad (1)$$

The above model with multiplicative fading can be applied only to narrowband Land Mobile Satellite systems, where the coherence bandwidth (about 100 Khz) [1] of the channel is larger than the signal's bandwidth.

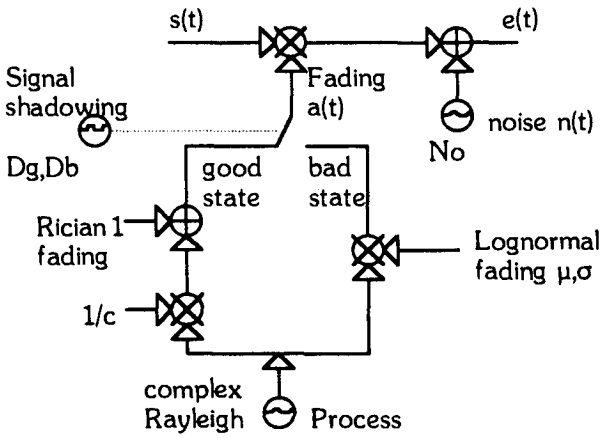

Figure 1 : The LMS Channel Analog Model

For the bad state the mean signal power is chosen according to its Lognormal probability density function and kept constant during the bad state. The Rician channel is produced by attenuating the power calculated by the Rayleigh process to 1/c and then adding the constant 1. That means that the Rayleigh process must be normalized to power 1 since c is the Rician factor representing the ratio of the power of the direct component to the power of the multipath signal.

The complex Rayleigh process is a statistical description of the multipath interference phenomenon present in urban environments due to the superposition of various waves scattered by the surrounding objects.

III. THE MODEL FOR THE MULTIPATH SIGNAL

We assume that a static transmitter (geostationary satellite) sends an unmodulated sinusoidal wave with a carrier frequency of ω_c. If a mobile receiver has no line of

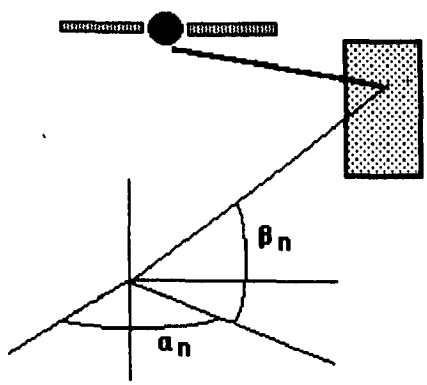

Figure 2 : Multipath Propagation Geometry

sight contact with the transmitter then the electric field around it is a superposition of N plane waves arriving each with an angle α_n on the horizontal plane and an angle β_n on the vertical plane as shown in figure 2. Each component wave has a power of c_n^2 and a phase shift of ϕ_n. The parametres α_n, β_n, c_n, and ϕ_n are all random and statistically independent. The angles ϕ_n and α_n are assumed to be uniformly distributed between 0 and 2π. The angle β_n has a probability density function of $p(\beta)$ which takes zero values outside the interval $[-\beta_m,\beta_m]$, where $\beta_m \leq \pi/2$. In addition:

$$E\{c_n^2\} = \frac{E_0^2}{N} \tag{2}$$

where E_0^2 is a positive constant expressing the mean power of the signal received. The electric field at a point (x_0,y_0,z_0) can be written as:

$$E(t) = \sum_{n=1}^{N} E_n(t) \tag{3}$$

where

$$E_n(t) = c_n \cos[\omega_c t - \frac{2\pi}{\lambda}(x_0 \cos\alpha_n \cos\beta_n + y_0 \sin\alpha_n \cos\beta_n + z_0 \sin\beta_n) + \varphi_n] \tag{4}$$

The electric field can be written in the form:

$$E(t) = T_c(t)\cos(\omega_c t) - T_s(t)\sin(\omega_c t) \tag{5}$$

where T_c (t) and T_s (t) are the in-phase and quadrature components.

With the above assumptions Aulin [2] has shown that $T_C(t)$ and $T_S(t)$ are independent Gaussian random processes having zero means and equal variances and that the autocorrelation function of the field can be written:

$$R(\tau)=A(\tau)\cos(\omega_C\tau) \tag{6}$$

where

$$A(\tau) = \frac{E_0^2}{2}\int_{-\beta_m}^{\beta_m} J_0\left(\frac{2\pi u\tau}{\lambda}\cos\beta\right)p(\beta)d\beta \tag{7}$$

is the common autocorrelation function of $T_C(t)$ and $T_S(t)$, J_0 is the Bessel function of zero order and first kind, and u the velocity of the mobile. The pdf of angle β is given either by [2]

$$p(\beta) = \begin{cases} \dfrac{\cos\beta}{2\sin\beta_m}, & |\beta| \leq \beta_m \leq \dfrac{\pi}{2} \\ 0, & \text{elsewhere} \end{cases} \tag{8}$$

or by [4]

$$p(\beta) = \begin{cases} \frac{\pi}{4\beta_m}\cos\left(\frac{\pi}{2}\cdot\frac{\beta}{\beta_m}\right) & , |\beta| \le |\beta_m| \le \frac{\pi}{2} \\ 0 & , \text{elsewhere} \end{cases} \quad (9)$$

The Fourier transforms of $A(\tau)$ when $p(\beta)$ is given by (8) or (9) respectively are shown graphically in figure 3 for the case β_m=45. f_m is the maximum Doppler shift experienced by the carrier frequency, equal to u/λ.

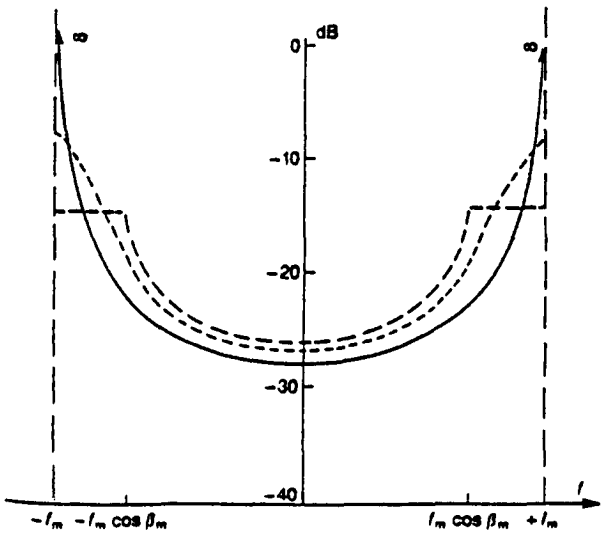

Figure 3 : Power Spectrum
——— $p(\beta) = \delta(\beta)$ (2-D Model)
----- $p(\beta)$ given by (8)
- - - - $p(\beta)$ given by (9)

Finally it can be shown that the envelope:

$$r(t) = \sqrt{T_c^2(t) + T_s^2(t)} \quad (10)$$

of the field is Rayleigh distributed with a mean power of $\alpha(0)$ and that the phase:

$$\varphi(t) = \tan^{-1}\frac{T_s(t)}{T_c(t)} \quad (11)$$

is uniformly distributed in the interval $[0,2\pi]$.

Therefore the multipath signal is a random process that can be described by its statistical properties. To simulate that signal a pseudo-random function of time is composed, that has the same statistical properties with the theoretical case when time averages are applied. The angles of arrival will no longer be random. We assume that for each angle α_n on the horizontal plane there are K incoming waves each with an angle of β_k k=1,2,...,K on the vertical plane. So there are exactly N·K incoming waves. The angles α_n are selected out of the interval $[0,2\pi]$ in a uniform manner so that $\alpha_n = 2\pi n/N$, n=1,2,...,N. The angles β_k are also selected uniformly out of $[-\beta_m,\beta_m]$

$$\beta_k = -\beta_m + \frac{2k-1}{K}\beta_m, \quad k = 1,2,...,K \quad (12)$$

In Aulin's model α_n is uniformly distributed in $[0,2\pi]$ while β_k has a probability density function of $p(\beta)$. Since we assume that α_n's and β_k's take certain discrete values there must be a corresponding factor c_{nk} for each pair of α_n and β_k which represents the fraction of the total signal power that comes from a solid angle around the direction determined by the two angles. The power density must be the product $p(\alpha_n)p(\beta_k)$ so that

$$c_{nk}^2 = E_0^2 p(\alpha_n)p(\beta_k)d\alpha_n d\beta_k, \quad n=1,2,...,N \quad k=1,2,...,K$$

where $p(\alpha_n) = 1/2\pi$, $d\alpha_n = 2\pi/N$ and $d\beta_k = 2\beta_m/K$ and we finally have:

$$c_{nk}^2 = \frac{E_0^2}{N}\cdot\frac{2\beta_m}{K}p(\beta_k) \quad (13)$$

The electric field near the mobile can be written as:

$$E(t) = \mathrm{Re}\left\{T(t)e^{i\omega_c t}\right\} \quad (14)$$

where

$$T(t) = \sum_{k=1}^{K}\sum_{n=1}^{N} c_{nk}\, e^{i(\omega_m t\cos\alpha_n\cos\beta_k + \varphi_{nk})} \quad (15)$$

and φ_{nk}'s are independent random variables uniformly distributed throughout 0 to 2π. We adopt the complex form for the field because it will ease the computations. Observing the symmetries of α_n and β_k we let N/2 be an odd integer and K be an even integer. Then using (13), equation (15) can be rewritten in the form:

$$T(t) = \sqrt{2}E_0\sqrt{\frac{2\beta_m}{KN}}\sum_{k=1}^{K/2}\sqrt{p(\beta_k)}\cdot$$
$$\left\{\sqrt{2}\sum_{n=1}^{N_0}\left[e^{i(\omega_m t\cos\alpha_n\cos\beta_k+\varphi_{nk})} + e^{-i(\omega_m t\cos\alpha_n\cos\beta_k+\varphi_{-nk})}\right] + e^{i(\omega_m t\cos\beta_k+\varphi_{0k})} + e^{-i(\omega_m t\cos\beta_k+\varphi_{-0k})}\right\} \quad (16)$$

where $N_0 = 0.5(N/2-1)$.

According to the central limit theorem T(t) is a complex Gaussian random process when N_0 and K approach infinity. In fact T(t) is approximately Gaussian for rather small values of N_0 and K. More restrictions to the values of N_0 and K will be put by demanding that a good approximation of the power spectrum is provided.

The autocorrelation function of the field as given by equations (15) and (16) can be computed analytically to give:

$$R(\tau) = \frac{2\mathcal{E}_m}{K}\frac{E_0^2}{N}\sum_{k=1}^{K/2} p(\theta_k)\cdot\{4\sum_{n=1}^{N_0}[\cos(\omega_m\tau\cos\alpha_n\cos\theta_k)] + 2\cos(\omega_m\tau\cos\theta_k)\}\cdot\cos(\omega_c\tau) \quad (17)$$

In Aulin's [2] model the autocorrelation function was given by equations (6) and (7). Given that the bessel function can be defined as:

$$J_0(x) = \frac{2}{\pi}\int_0^{\pi/2}\cos(x\cos\alpha)d\alpha \quad (18)$$

we conclude that (17) is a discrete approximation to $R(\tau)$ as given by (6) and (7) because the double sum in (17) approximates the double integral. In fact for an approximation with 8 significant digits and with $\omega_m\tau$ ranging from 0 to 15, N_0 must equal 8 (N=34) and K must have a value of about 8000.

Therefore the Fourier transform of (17) is a discrete approximation to the power spectrum predicted by Aulin. However this is still the power spectrum of a random process. The pseudo-random signal that can be used as the basis of a software simulation and has the same power spectrum (squared magnitude of its Fourier transform) as the one given by (17) is:

$$y(t)=T_c(t)\cos(\omega_c t)-T_s(t)\sin(\omega_c t) \quad (19)$$

where

$$T_c(t) = \sum_{k=1}^{K/2}\sqrt{p(\theta_k)}\cdot\{\sqrt{2}\sum_{n=1}^{N_0}[\cos\varphi_n\cos(\omega_m t\cos\alpha_n\cos\theta_k)] + \cos\varphi_N\cos(\omega_m t\cos\theta_k)\}$$

$$T_s(t) = \sum_{k=1}^{K/2}\sqrt{p(\theta_k)}\cdot\{\sqrt{2}\sum_{n=1}^{N_0}[\sin\varphi_n\cos(\omega_m t\cos\alpha_n\cos\theta_k)] + \sin\varphi_N\cos(\omega_m t\cos\theta_k)\} \quad (20)$$

The RF power spectrum of y(t) is the same as the Fourier transform of (17) because of the trigonometric relationships $\cos^2\phi_n+\sin^2\phi_n=1$, $n=1,2,...,N_0$ and $\cos^2\phi_N+\sin^2\phi_N=1$. Of course ϕ_n's and ϕ_N of (20) are not random. Their values must satisfy the pseudo-randomness conditions for the envelope and phase. Given that $T_c(t)$ and $T_s(t)$ as given by (25) are approximately zero mean Gaussian random processes then the envelope will be Rayleigh and the phase will be uniform if

$$<T_c^2(t)>=<T_s^2(t)> \quad \text{and} \quad <T_c(t)T_s(t)>=0 \quad (21)$$

where the symbol <.> denotes time average. It can be shown that for $\phi_n=\pi n/N_0$, $n=1,2,...,N_0$ and $\phi_N=\pi/4$, we have:

$$<T_c^2(t)>=\left(\frac{N_0}{2}+\frac{1}{4}\right)\sum_{k=1}^{K/2}p(\beta_k)$$
$$<T_s^2(t)>=\left(\frac{N_0}{2}+\frac{1}{4}\right)\sum_{k=1}^{K/2}p(\beta_k) \quad (22)$$
$$<T_c(t)T_s(t)>=\frac{1}{4}\sum_{k=1}^{K/2}p(\beta_k)$$

The first condition of (21) is satisfied and the second is approximated because the mean value of the product $T_c(t)T_s(t)$ as given by (22) is much less than the mean square values for $N_0=8$. A block diagram of the simulator based on equations (20) is shown in figure 4.

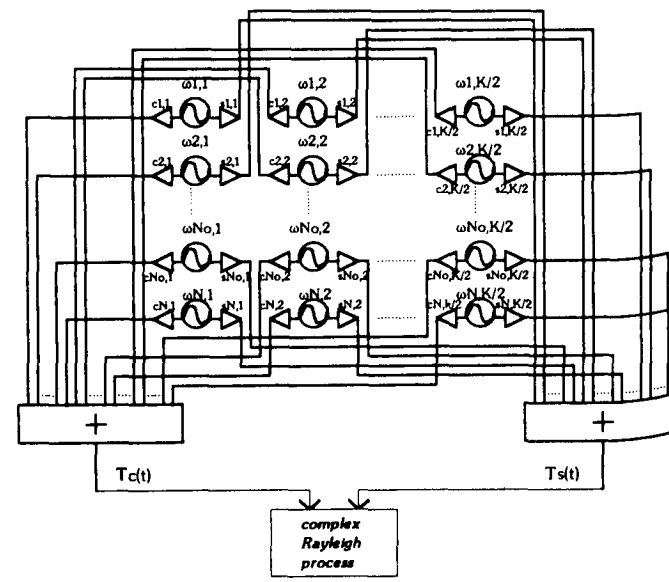

Figure 4 : The 3-dimensional Multipath Simulator

The $\omega_{i,j}$, $c_{i,j}$, $s_{i,j}$ are given by the equations:

$$\omega_{n,k} = \omega_m \cos\alpha_n \cos\beta_k, \quad \omega_{N,k} = \omega_m \cos\beta_k$$

$$c_{n,k} = \sqrt{p(\beta_k)}\sqrt{2}\cos\varphi_n, \quad s_{n,k} = \sqrt{p(\beta_k)}\sqrt{2}\sin\varphi_n$$

$$c_{N,k} = \sqrt{p(\beta_k)}\cos\varphi_N, \quad s_{N,k} = \sqrt{p(\beta_k)}\sin\varphi_N$$

with n=1,2,...,N_0 and k=1,2,...,K/2.

IV. RESULTS

A. Statistical Tests

To test the validity of the statistical hypothesis that the envelope and phase of the basis process are Rayleigh and uniformly respectively distributed, we have applied the Kolmogoroff_Smirnov distribution test to the simulated data for different values of the parameter β_m and for the two functions $p(\beta)$ mentioned.

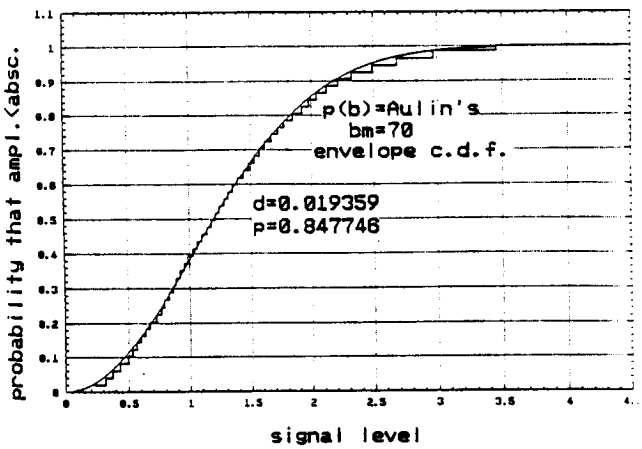

a) Envelope

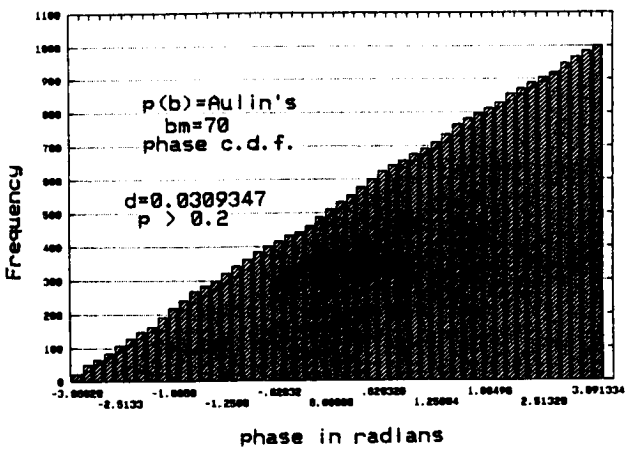

b) Phase

Figure 5: Expected and simulated distributions .
——— Expected, ⎽⎽⌐‾ Simulated

The results were satisfactory in all cases. Results for β_m=70 degrees and for Áulin's $p(\beta)$ are shown in figures 5a, 5b. The test uses 1000 samples (complex) of the simulated signal with a sampling rate of $2f_m$. We should note that the value of the criterion d must be less than 0.0429 with a significance level of 0.05. The p value is the maximum significance level for which the hypothesis is not rejected.

B. The Simulated Spectrum

Results from the application of the FFT to 1024 samples of the complex Rayleigh process, are shown in figures 6a, 6b, 6c, for three different cases. 1024 points are not enough to distinguish 36000 (N_0*K/2+K/2) frequencies and as we can see there are only 9 peaks (the positive). Each peak corresponds to 4000 sinusoids but as we approach the centre the peaks get higher because the same number of frequencies is depicted on a narrower area.

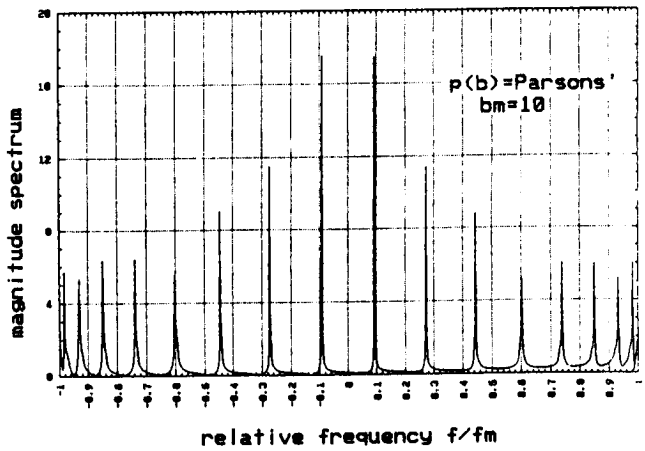

a)

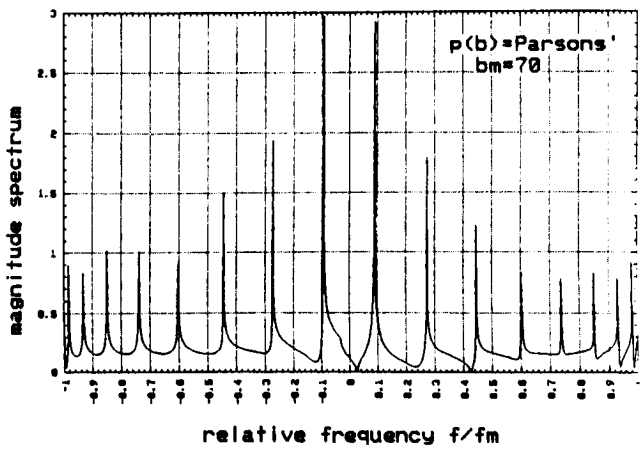

b)

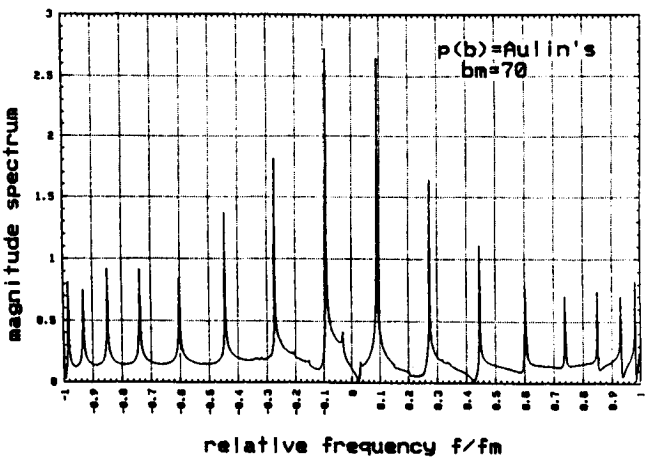

c)

Figure 6: Magnitude Spectrum of the Rayleigh process.

Any increase of β_m shortens all peaks, widening their bases and transfers power towards the central frequency. A comparison between spectrums with equal β_m's and different p(β) functions shows that there are a lot of very small peaks between the large ones for p(β) given by (8) while there are no such peaks for p(β) given by (9). This is due to the fact that Aulin's p(β) although discontinuous falls less rapidly in the open interval $(-\beta_m,\beta_m)$ [4].

C. Output Waveforms

In Figures 7a, 7b, waveforms of the process a(t) are given for a short distance for two different cases. The values of the parametres for the cases are given at table I. In all cases f_c is kept constant to 1.54 GHz and u to 50 Km/h. The bit rate is 9.6 Kbits/sec.

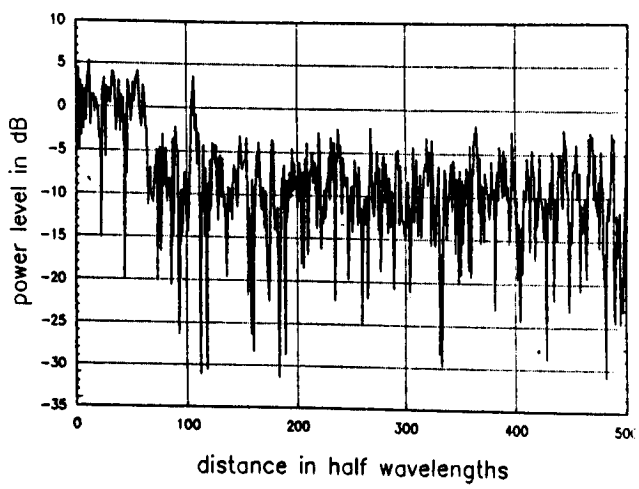

a)

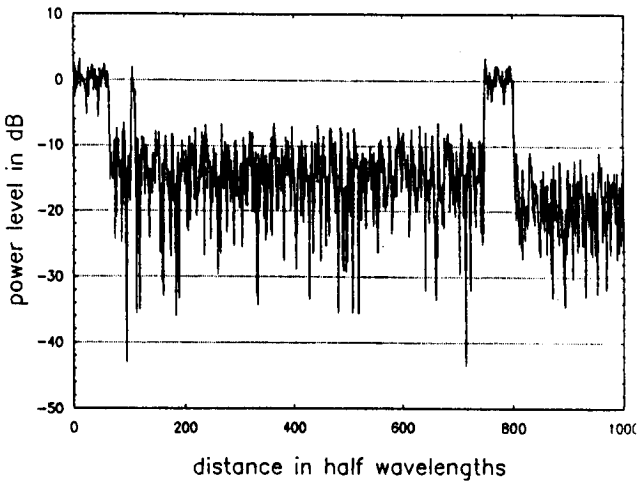

b)

Figure 7: Power level of the simulated process a(t). 0dB is the Line-Of-Sight level.

TABLE I

Fig	D_{min}	D_{max}	c (dB)	μ (dB)	σ (dB)
7a	8	33	5.5	-10	3.7
7b	16	29	11.0	-15.4	5.4

V. CONCLUSIONS

This paper presents a generalised simulation model for the LMS channel. A 3-dimensional multipath simulator is developed in order to compensate for the loss of accuracy when neglecting non horizontally travelling waves in urban environments. The simulation results verify the use of the model in designing the LMS link.

REFERENCES

[1] **E. Lutz, D. Cygan, M. Dippold, F. Dolainsky, and W. Papke**, "*The land mobile satellite communication channel-recording, statistics and channel model.* " IEEE Trans. Veh. Technol., vol. 40, pp. 375-385, May 1991.

[2] **Tor Aulin**, "*A Modified Model for the Fading Signal at a Mobile Radio Channel* ", IEEE Trans. Veh. Technol., vol. VT-28, No. 3, Aug. 1979.

[3] **W. C. Jakes et al.**, *Microwave Mobile Communications.* New York: Wiley, 1974.

[4] **D. Parsons**, *The Mobile Radio Propagation Channel* London: Pentech Press, 1992.

[5] **A. Papoulis**, *Probability, Random Variables, and Stoehastic Processes.* New York: McGraw Hill,1991.

Narrow- and Wide-band Channel Characterization for Land Mobile Satellite Systems: Experimental Results at L-Band

Axel Jahn* Sergio Buonomo† Mario Sforza‡ Erich Lutz*

* DLR
Institute for Communications Technology
P.O. Box 1116
82230 Wessling, Germany
Tel: +49 8153 28-2847
Fax: +49 8153 28-1442
E-mail: Axel.Jahn@dlr.de

† ESA/ESTEC, XE
Keplerlaan 1
2200 AG Nordwijk
The Netherlands
Tel: +31 1719 8-5328
Fax: +31 1719 8-4999
E-mail: napoli@xe.estec.esa.de

‡ Telecom Italia
Space Division - Telespacio
Via Tiburtina, 965
00156 Rome, Italy
Tel: +39 6 4079-6375
Fax: +39 6 4079-3624
formerly with ESA/ESTEC

ABSTRACT

The results of an airborne measurement campaign aimed at the characterization of the mobile satellite link are presented in this paper. The experimental tests were carried out at 1.8 GHz. The objective of the campaign was to obtain results applicable to all proposed satellite constellations: LEO, HEO, and GEO. Therefore, the measurements were performed for elevation angles from 10 deg...80 deg using a light aircraft. A set of different environments and operational scenarios have been investigated, typically for handheld and car-mounted applications.

We present a survey of wide- and narrowband results for a wide range of elevation angles and environments. For the wideband characterization, the power delay profiles of the channel impulse response are presented and discussed. Figures for the delay spread versus elevation and for the carrier-to-multipath ratio versus time are also given. The narrowband behaviour of the channel is described by power series.

1 INTRODUCTION

Several system alternatives are being considered for provision of mobile and personal satellite services in the near future. Many proposals adopt non-geostationary satellite constellations, so that the channel characteristics are not stationary. Furthermore, multiple access techniques under consideration range from narrowband to wideband (e.g. CDMA) solutions. Finally, due to the requirement of being virtually global, a satellite system should provide service in a wide range of environmental conditions.

Propagation measurements have previously been made by several organisations, for LEO , MEO, HEO, and GEO systems. Aircraft and helicopters have been used to simulate satellites in a wide range of elevation angles and environments [1, 2, 3, 4]. Some wideband channel measurements have been performed [5] but results are available to a limited extent. DLR has performed a measurement campaign aiming at the channel characteristics of LMS systems [6]. The purpose of the campaign was twofold:

1. to perform narrowband measurements in order to extend a channel database with a wide range of elevation angles.
2. to investigate the wideband characteristics of the land-mobile satellite channel.

The campaigns were performed at L-band (1820 MHz). This paper will concentrate on the presentation of selected results. The work described here has been performed under ESA contract No. 141742 [7].

2 MEASUREMENT SETUP

A measurement system has been set up with a transmitter part carried by aircraft and a receiver part in a van. The transmitter radiated a test signal.

The following campaigns were conducted:

1. **Narrowband** measurements.
   An aircraft transmitted a CW signal. Two antennas picked up the signal and fed it to two channel sounders. Thus, antenna diversity experiments could be performed. An RHCP drooping dipole antenna for the handheld and a car-roof mounted RHCP antenna have been used. The receiver has a dynamic range of 40 dB and a filter bandwidth of 1 kHz.
2. **Wideband** measurements.
   The aircraft transmitted a spread spectrum signal using a pseudo noise bit sequence with a bandwidth of 30 MHz. This corresponds to a spatial resolution of 10 m. An RHCP handheld antenna and a car-roof mounted RHCP antenna were used.

The sampling rate corresponds to 15.6 impulse responses per second.

The measurement setup has been described previously in more detail in [6, 7]. Here, the environments and the operational scenarios are listed, too.

3 Narrowband Results

The narrowband LMS channel behaviour shall be demonstrated using Figs. 1 and 2 as two examples for the urban LMS channel. In Fig. 1 the situation is given for quasi-fixed users, i.e. a handheld terminal (upper graph) and a standing van (lower graph) whereas in Fig. 2 the user is driving. Here, one can compare the performance between the in-car handheld antenna and a car-roof mounted antenna. For the low elevation angles between 10 and 30 deg, shadowing is the major effect. In shadowed conditions the channel attenuation is 20...30 dB. In both operational scenarios, standing and driving, the car-roof mounted antenna gets the better channel. The handheld terminal suffers from head shadowing and worse line-of-sight (LOS) conditions (since the antenna on the roof of our van has a higher height of $\approx$ 2.3 m). Two-path fading caused by specular reflections is affecting the handheld but not the car-roof mounted antenna. Fades from specular reflections have a depth ranging from 3 ...9 dB. Comparing the signal during the driving run, the handheld in-car antenna seems to have an attenuation of 3...10 dB with respect to the roof antenna in LOS conditions.

Cumulative distributions can be derived from the power values. From the CDFs one can easily take link margins for a required grade of service. In Fig. 3 values for the required link margin are given for two grades of service, 95% and 98%, in urban and suburban environment. In these environments we expect a large percentage of shadowing. This will increases the average link margin. Moderate link margins of 6...10 dB appear for higher elevation angles above 50 deg. For low elevations, the required link margins will exceed reasonable values by far. Satellite diversity will be of great benefit in such shadowed environments.

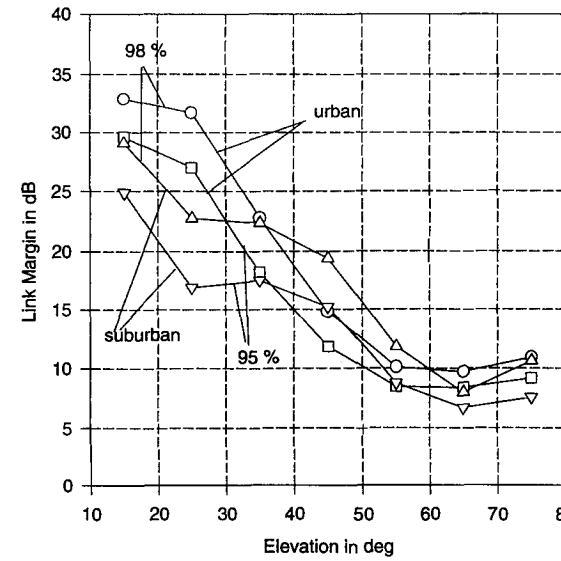

Figure 3. Link margin versus elevation angle for urban and suburban environment. RHCP handheld.

4 Wideband Results

The wideband results are presented as channel impulse responses $h(t, \tau)$ (sometimes also referred to as the time-delay system function). The delay of an echo is denoted by τ with respect to the propagation delay of the direct path. Fig. 4 show the impulse responses of the wideband LMS channel for different environments and elevation angles.

Common to all environments is that echoes appear in general with small delays, usually smaller than 600 nsec (corresponding to a detour of 200 m). The echoes are attenuated by 10...30 dB. The environment is mainly characterized by shadowing of the direct path and the number and attenuation of echoes. It is also obvious that the power of echoes with small delays decreases exponentially versus delay (note the logarithmical scale). Fig. 4 (a) and (b) show a handheld in a rural environment, standing on a provincial road. At 15 deg elevation the user is shadowed by trees. At 55 deg elevation, the user has line-of-sight (LOS) conditions most of the time. About 3-5 echoes can be detected with delays up to 300 nsec and an echo attenuation of 15-25 dB. In the mountainous environment, (c) and (d), we can find echoes with longer detours and a higher echo power. In the standing scenario, the echo delay is stationary, the number of echoes depend only on the azimuth angle of the satellite whereas in driving conditions the echo delay is changing monotonously (cf. (d) and (e)) since the receiver approaches to, or departs from the reflector. The urban environment is again characterized by fewer echoes. On a highway (f) the traffic in front of and behind the receiver yields good reflectors. Thus, many echoes can be detected. These echoes have usually short delays.

Although the measurement equipment was able to measure delays of 15 μsec, the figures show power delay profiles for delays up to 2 μsec since most of the echoes appear in the close vicinity of the receiver. Fig. 5 shows

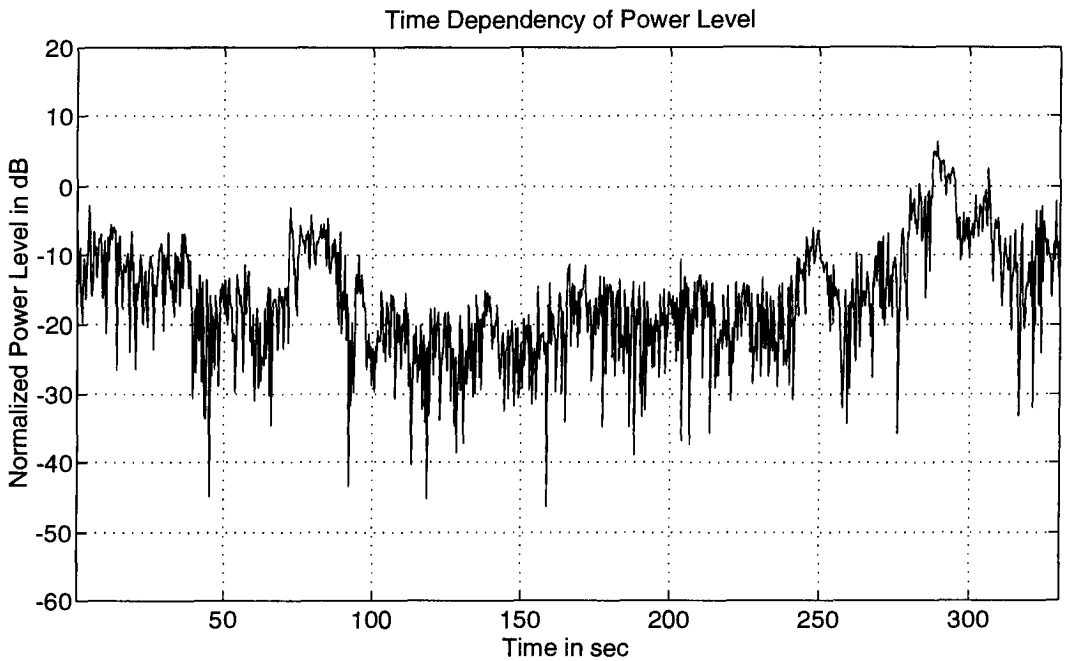

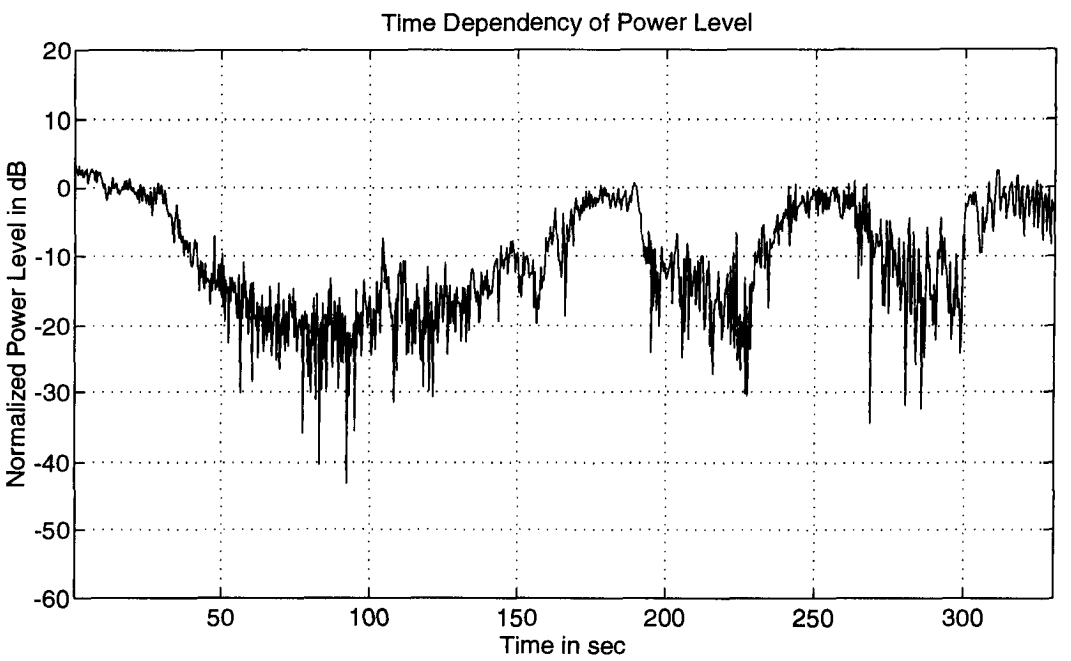

Filename	:	GNU10RRC	Location	:	Germany
Environment	:	urban	Elevation Angle	:	10-20 deg
Azimuth Angle	:	0-60 deg	Receiver	:	narrowband
Scenario 1	:	handheld, random user	Scenario 2	:	car roof-mounted, standing

Figure 1. Power series.
Upper graph: handheld
Lower figure: car-roof mounted, standing

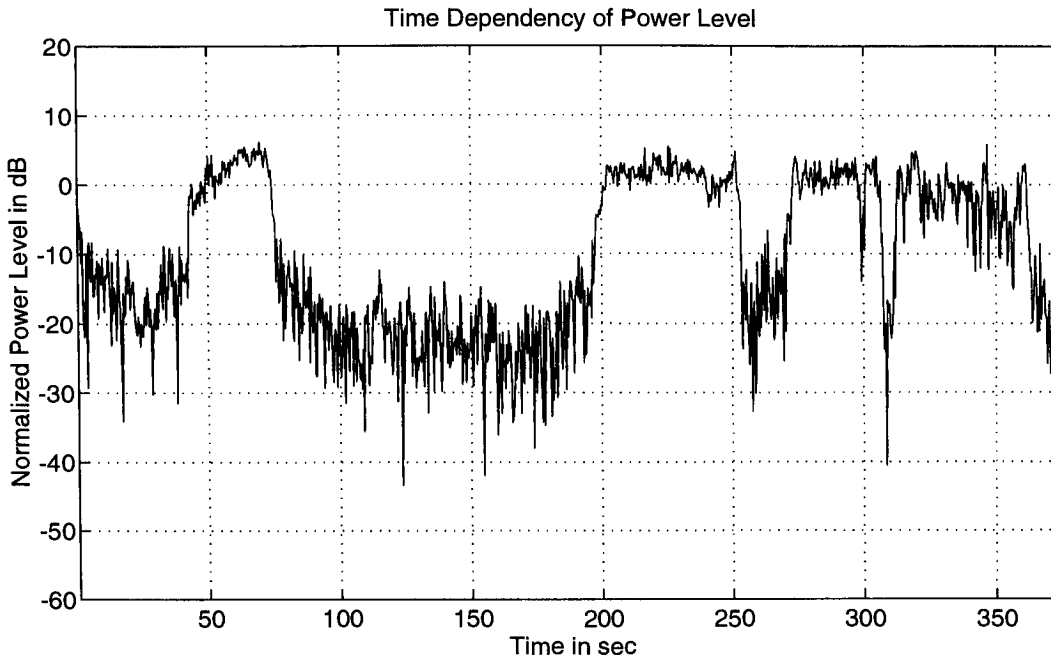

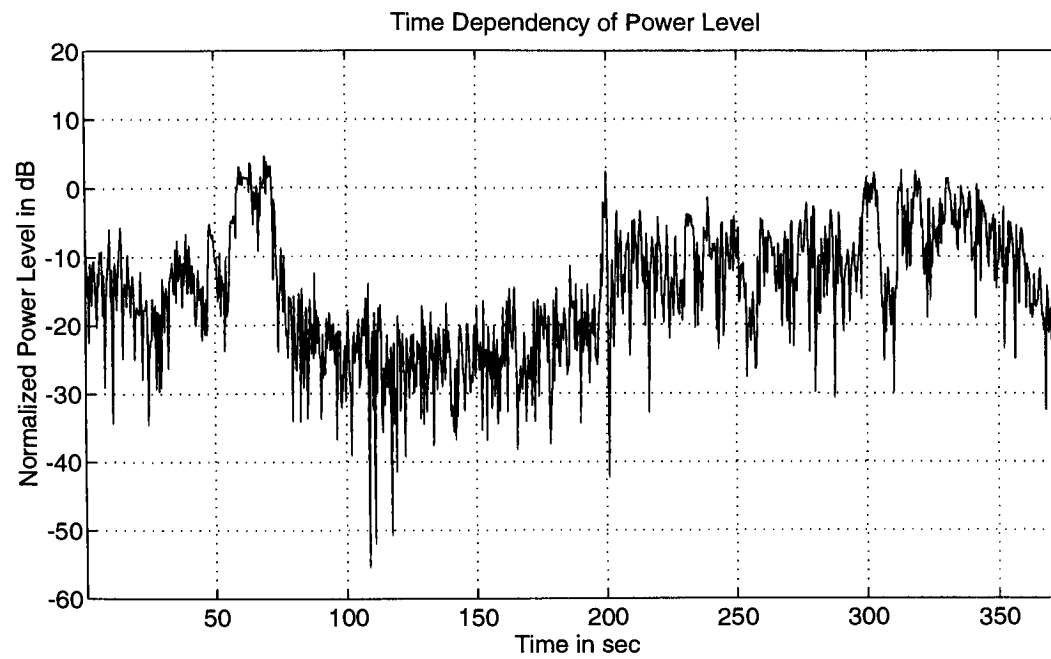

Filename	:	GNU20RDI	Location	:	Germany
Environment	:	urban	Elevation Angle	:	20-30 deg
Azimuth Angle	:	0-60 deg	Receiver	:	narrowband
Scenario 1	:	car roof-mounted, driving	Scenario 2	:	handheld, in-car, driving

Figure 2. Power series.
Upper graph: car-roof-mounted, driving
Lower figure: handheld in-car, driving

a) provincial road, handheld, 15 deg elevation

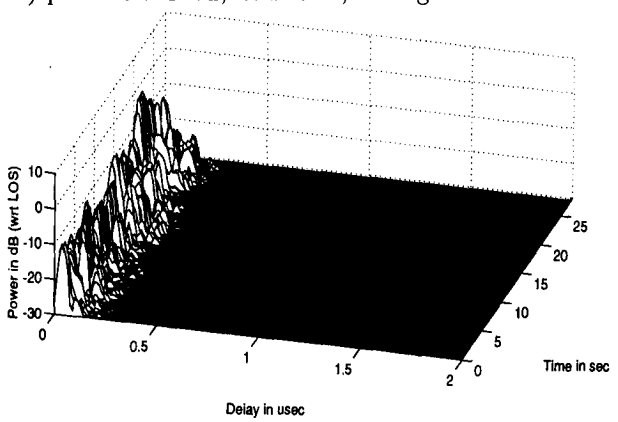

b) provincial road, handheld, 55 deg elevation

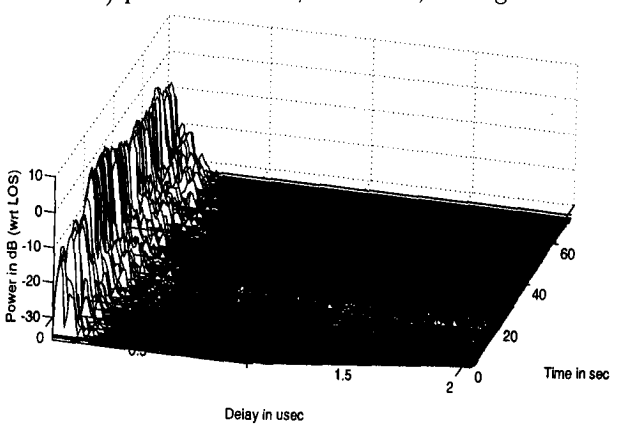

c) mountainous, handheld, 35 deg elevation

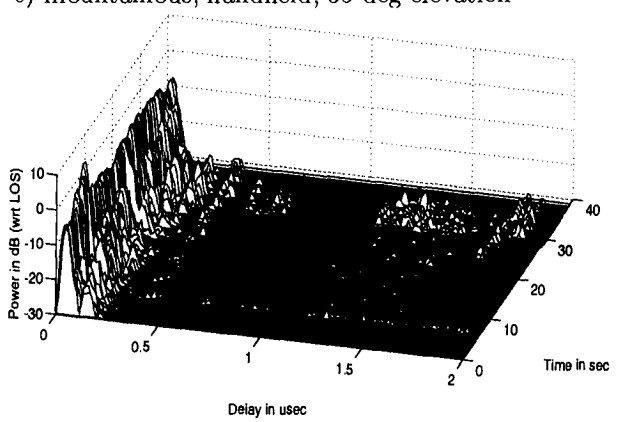

d) mountainous, car driving, 55 deg elevation

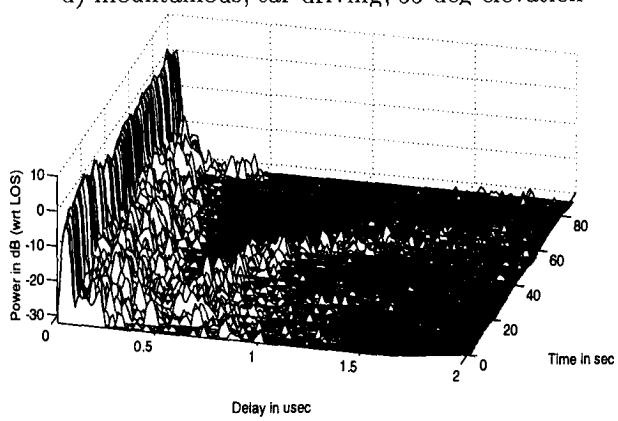

e) urban, car driving, 15 deg elevation

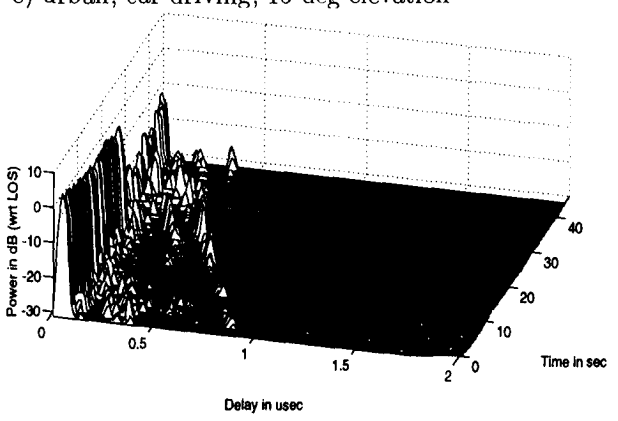

f) highway, car driving, 65 deg elevation

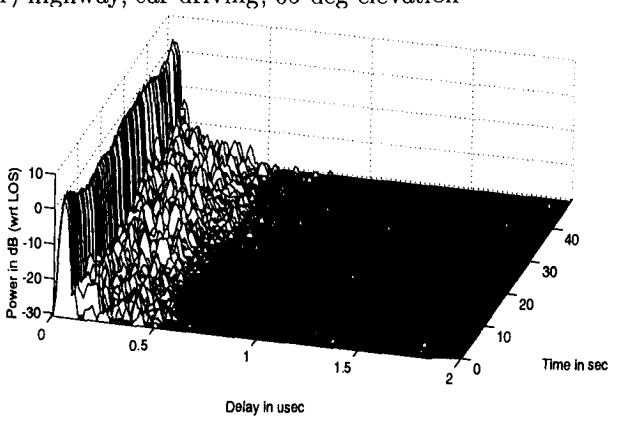

Figure 4. Power delay profiles for various environments.

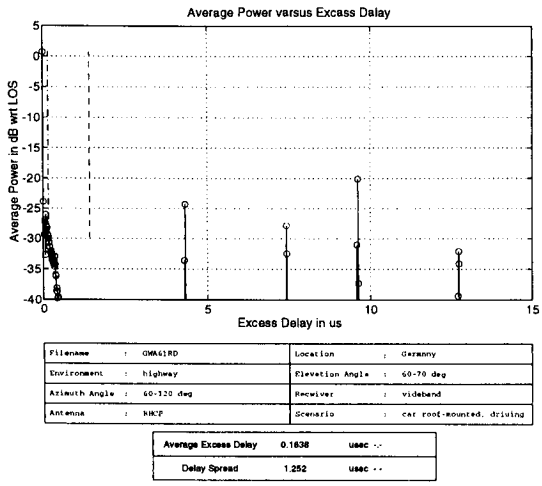

Figure 5. Average power delay profile.

the full scale of one highway run with many echoes. The delay power profile was averaged over time. The number of echoes with long delays is quite small compared to the near echoes, but with reasonable power if existing. The different power statistics of echoes with long and short delays can be seen easily. The power of near echoes is decreasing exponentially. This is not valid for echoes with long delays.

In Fig. 6 the delay spread is presented versus elevation. For higher elevation angles the spread tends to decrease (except for the urban environment). Values range mainly from 500 nsec to 2 μsec.

The carrier-to-multipath ratio C/M is one interesting measures that can be derived directly from the power delay profile since one can distinguish between the power of the direct path and the echo power. Its time behaviour is important for the design of receivers. The C/M is calculated by

$$C/M = \frac{A_d^2}{2\sigma^2} = \frac{A_d^2}{\sum_{i=1}^{n} |c_i^2|}$$

with the power of the direct path A_d^2 and the power of the multipath $2\sigma^2$ or n discrete echoes with complex amplitudes $c_i, i = 1 \ldots n$. The C/M is often referred to as the *Rice-factor*. The C/M is plotted in Fig. 7 for a highway environment. The values range from 10...25 dB.

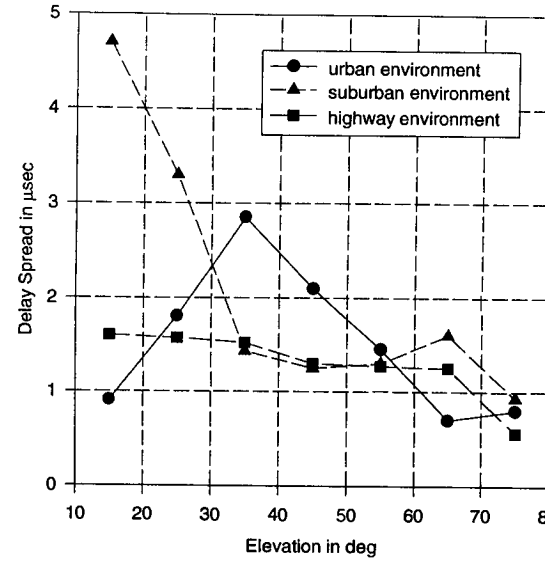

Figure 6. Delay spread versus elevation angle. RHCP handheld.

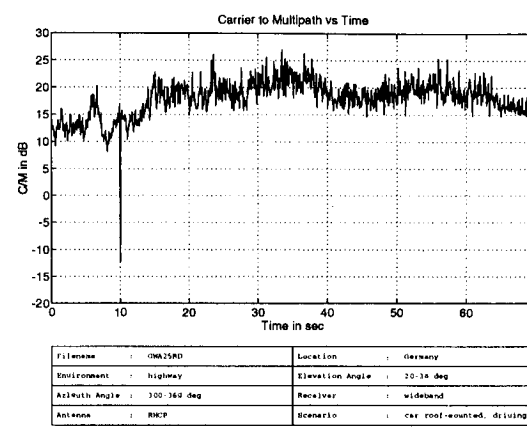

Figure 7. Carrier-to-multipath ratio versus time.

5 Conclusions

In this paper we have presented narrowband and wideband results from a measurement campaign aiming at LMS channels for non-geostationary satellite systems.

The channel characteristics of LMS channels are mainly influenced by shadowing. For high elevation angles, moderate link margins can be provided to overcome fading effects. For low elevation angles the required link margins will increase drastically.

The measured data agree with the narrowband models currently used at ESA. Further studies based on the results of the measurement campaign are available to the authors.

The wideband properties of the LMS channel are characterized by few echoes with small delays, usually less than 600 nsec. The echoes are strongly attenuated by 10...15 dB. The delay spread tends to decrease for higher elevation angles.

REFERENCES

[1] Faramaz Davarian. Earth-satellite propagation research. *IEEE Communications Magazine*, April:74–79, 1994.

[2] Julius Goldhirsch and Wolfhard J. Vogel. Mobile satellite propagation measurements from UHF to K-band. In *Proc. 15th AIAA Intern. Commun. Satellite Systems Conf.*, pages 913–920, 1994.

[3] Erich Lutz, Daniel Cygan, Michael Dippold, Frank Dolainsky, and Wolfgang Papke. The land mobile satellite communication channel — recording, statistics and channel model. *IEEE Trans. Vehicular Technology*, 40:375–386, 1991.

[4] Gulraiz Butt, Barry G. Evans, and Madhavendra Richharia. Narrowband channel statistics from multiband propagation measurements applicable to high elevation angle land-mobile satellite systems. *IEEE J. Selected Areas in Communications*, 10:1219–1226, 1992.

[5] Norbert Kleiner and Wolfhard J. Vogel. Impact of propagation impairments on optimal personal communication systems. In *Workshop Adelaide, Australia*, Nov 1992.

[6] Axel Jahn and Erich Lutz. DLR channel measurement programme for low earth orbit satellite systems. In *Proc. Int. Conf. on Universal Personal Communications ICUPC'94*, pages 423–429, San Diego, 1994.

[7] Axel Jahn. Propagation data and channel model for LMS systems. *Final Report, ESA Purchase Order 141742*, DLR, Institute for Communications Technology, 1994.

A Wideband Channel Model for Land Mobile Satellite Systems

Axel Jahn* Sergio Buonomo† Mario Sforza‡ Erich Lutz*

* DLR
Institute for Communications Technology
P.O. Box 1116
82230 Wessling, Germany
Tel: +49 8153 28-2847
Fax: +49 8153 28-1442
E-mail: Axel.Jahn@dlr.de

† ESA/ESTEC, XE
Keplerlaan 1
2200 AG Nordwijk
The Netherlands
Tel: +31 1719 8-5328
Fax: +31 1719 8-4999
E-mail: napoli@xe.estec.esa.de

‡ Telecom Italia
Space Division - Telespacio
Via Tiburtina, 965
00156 Rome, Italy
Tel: +39 6 4079-6375
Fax: +39 6 4079-3624
formerly with ESA/ESTEC

ABSTRACT

A wideband channel model for Land Mobile Satellite (LMS) services is presented which characterizes the time-varying transmission channel between a satellite and a mobile user terminal. The channel model statistic parameters are the results of fitting procedures to measured data. The data used for fitting have a time resolution of 33 ns corresponding to a bandwidth of 30 MHz.

Thus, the model is capable to characterize the channel behaviour for a wide range of services e.g., voice transmission, digital audio broadcasting (DAB), and spread spectrum modulation schemes. The model is presented for different environments and scenarios. The model is derived for a quasi-mobile user with handheld terminal being in two different environments: rural and urban. The parameters needed for the description are a) the number of echoes, b) the distribution of the echo power, and c) the distribution of the echo delay. It is shown that the direct path follows a Rician distribution whereas the reflected paths are Rayleigh/lognormal distributed. The parameters are given for an elevation angle of 25 deg.

1 INTRODUCTION

The effects of the land-mobile satellite channel play a big role in design and development of satellite-based communications networks. For design and engineering of the mobile user link, channel models are widely used to investigate and simulate appropriate transmission schemes. A couple of narrowband channel models are known from the literature for LMS channels [1, 2, 3, 4]. Theses models already cope with varying elevation angles for systems with non-geostationary orbits. Future systems will also employ broadband broadcast services (ESA DAB program) and very high transmission rates, eg. CDMA systems. For such systems, the narrowband characteristics are not sufficient anymore. Some wideband channel measurements have been performed [5] but results are available to a limited extent. Thus, DLR performed a measurement campaign aiming at the wideband channel characteristics of LMS systems [6, 7]. The channel impulse response was measured using a pseudo noise bit sequence with a bandwidth of 30 MHz. This corresponds to a spatial resolution of 10 m. RHCP drooping dipole antennas have been used as handhelds and car roof-mounted. The sampling rate corresponds to 15.6 impulse responses per second.

Fig. 1 shows an example of the measured impulse profiles. Using such measurements, a wideband model for the LMS channel was derived and its parameters have been fitted with the measured data.

The work described in this paper was performed under ESA contract 141742 [8].

2 MODEL DEFINITION

The model starts from a physical background: a signal is transmitted in many directions. Different reflectors R_k cause echoes with a delay $\Delta\tau_k$ and a round-trip detour $\Delta s_k = c_0 \Delta\tau_k$. All reflected components of the signal superimpose at the receiver input. Echoes with different delays can be resolved when the difference of the delay is larger than the corresponding receiver system bandwidth $\Delta\tau_k - \Delta\tau_l > 1/B$.

The received signal is time-variant when the physical geometry changes. The measurements proved that the channel is quasi-stationary with correlation duration of $\geq$ 100 msec. Since echoes are expected with a maximum delay less than 100 msec, the channel is also stationary for the duration of the impulse response. Due to the physical separation of the reflectors we can also assume that signals with different delays will be uncorrelated. Such a channel is called WSSUS (wide-sense stationary with uncorrelated scatterers).

Bello [9] has developed a general description for time-variant and frequency-selective systems. The relation between the transmitted signal $x(t)$ and the received si-

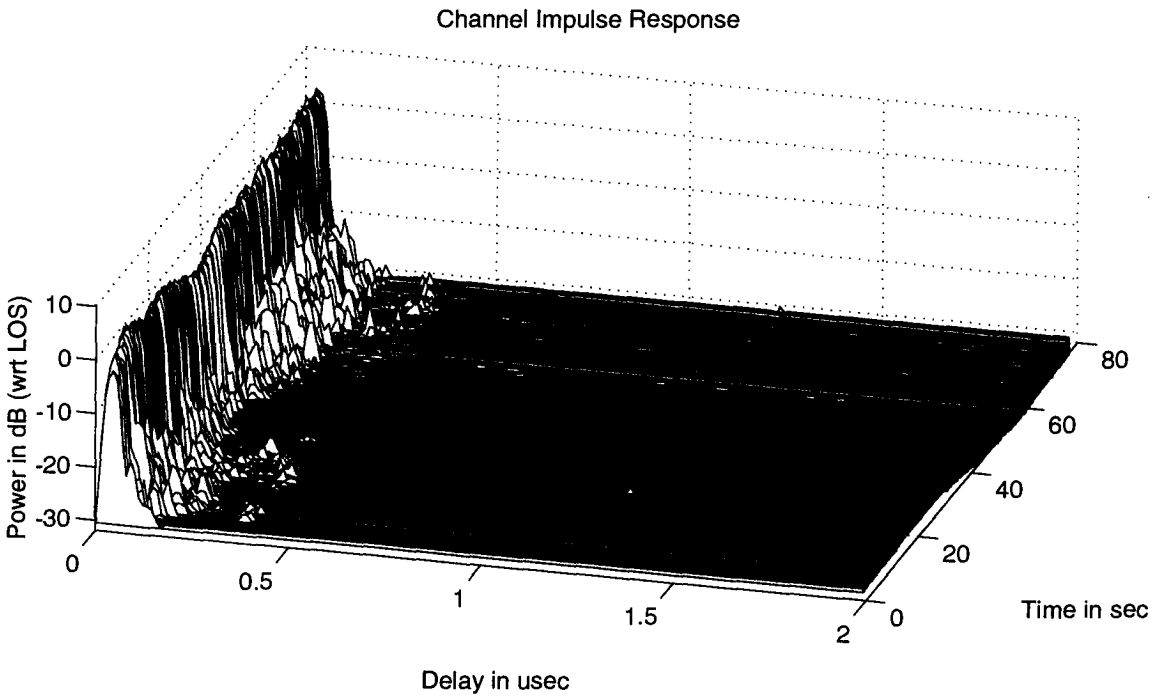

Figure 1: Example for measured channel impulse responses; suburban environment; 25 deg elevation; RHCP handheld.

gnal $y(t) = x(t) * h(t, \tau)$ is called the time-delay system function $h(t, \tau)$ whereas τ denotes the delay. Using the time-delay system function, three other equivalent system functions can be deducted to describe the transmission channel in the time and frequency domain and to derive important properties of the channel.

With the WSSUS assumption, the wideband channel can be modelled as filter structure with delay taps, see Fig. 2.

The complex impulse response of the satellite wideband channel can now be expressed as a sum of $k = 1 \ldots N$ echoes $E_k(t)$ having delays $\tau_1(t)$ and $\tau_k(t) = \tau_1(t) + \Delta\tau_k(t)$, $k = 2 \ldots N$:

$$h(\tau, t) = \sum_{k=1}^{N} E_k(t) \cdot \delta(\tau - \tau_k(t)) . \qquad (1)$$

The amplitude of each echo is complex, i.e. it can be expressed by:

$$E_k(t) = a_k(t) \cdot e^{j\phi_k(t)} . \qquad (2)$$

The measurement equipment unfortunately did not provide information on the phase of the received signals. Thus, the phase $\phi_k(t)$ has to be assumed as uniformly distributed in $[0, 2\pi)$. This simplification is valid for the WSSUS channel since in the WSSUS there is no correlation among scatterers with different geometrical distances.

The results in Fig. 1 and other measurements (cf. [7]) show that the channel impulse response can be divided into three parts with different behaviour. Fig. 3 shows the definition of the regions of the impulse responses.

An impulse response with N echoes is divided into three regions:

1. the *direct path* a_0: the amplitude statistics of the direct path have to be modelled according to the shadowing. It can be expected that the probability function will differ from LOS when shadowing is present.

2. N_n *near echoes* in the close vicinity of the receiver with delays $0 \ldots \tau_e$ ($\tau_e \approx 600$ nsec (200 m)). Most of the echoes will appear in this delay interval. The echoes seem to have an exponential decrease of the mean echo power.

$$S(\tau) = \mathcal{E}(a_\tau) = E_u \, e^{-\Delta \tau} \qquad (3)$$

where the gradient Δ is defined according

$$\Delta = \frac{1}{\tau_e} \log(\frac{E_u}{E_l}) . \qquad (4)$$

3. $N_f = N - N_n - 1$ *far echoes* with delays $> \tau_e$ (≈ 600 nsec). Only a few echoes with long delays could be observed. The amplitudes of the

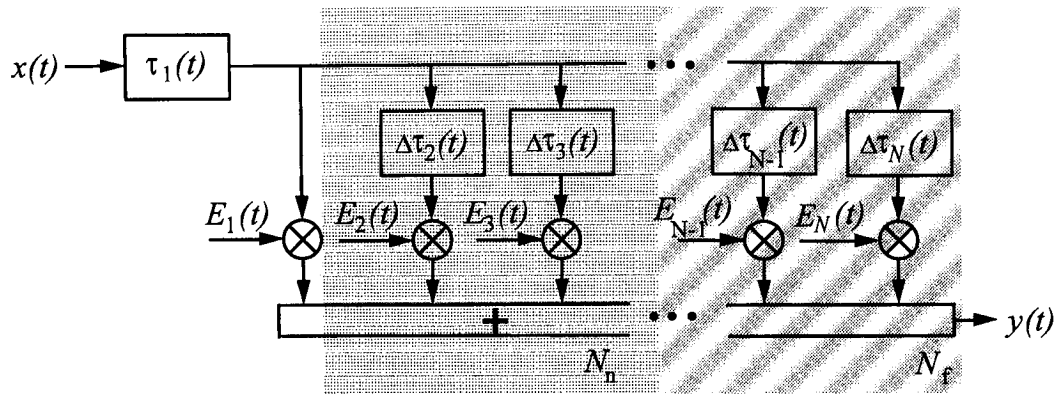

Figure 2: Tap structure of the wideband LMS channel.

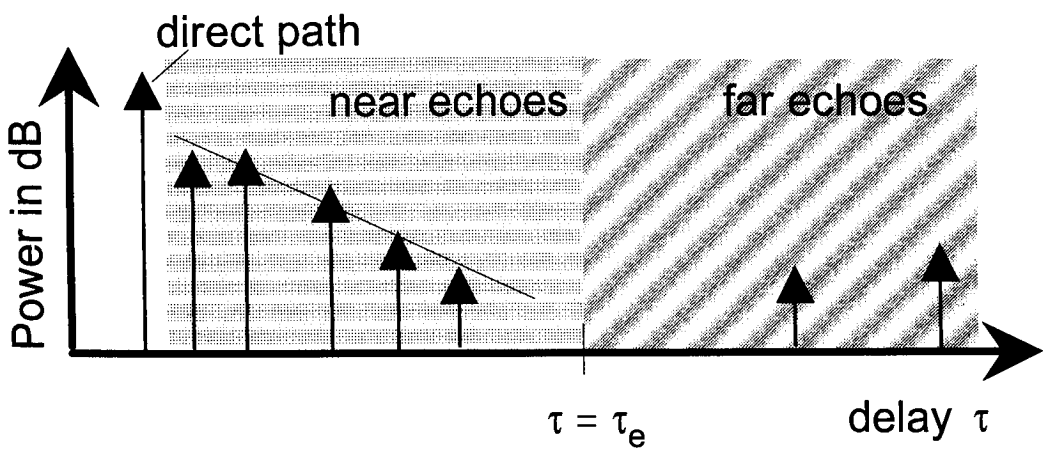

Figure 3: Definition of three regions for the echo characteristics.

far echoes don't show an exponential behaviour but this could be also due to the limited 30-dB-dynamic range of the measurement equipment.

3 Model Parameters

The following parameters must be determined for the channel model for the specific environments under investigation:

1. the amplitude of the direct path a_1 for shadowed and LOS conditions.
2. the number of echoes with short delays N_n.
3. the number of echoes with long delays N_f.
4. the distribution of the echo delays.
5. the parameters of the exponential decrease E_u, E_l, and τ_e.
6. the statistics of the echo amplitudes a_k.

The parameters have been fitted with data from the measurements. In the next section the fit equations are given.

3.1 Fit Equations

A signal amplitude A with uncorrelated additive Gaussian noise variables x, y in Inphase and Quadrature direction can be expressed by

$$s(t) = (A+x)\sin(\omega t) - y\sin(\omega t) = \rho\cos(\omega t + \phi)\,, \quad (5)$$

with signal envelope $\rho = \sqrt{(A+x)^2+y^2}$ and phase $\phi = \arctan\frac{y}{A+x}$.

The power of the signal is $z = \rho^2 = (A+x)^2 + y^2$. The noise power is $\sigma^2 = \bar{x^2} = \bar{y^2}, \bar{xy} = 0$.

The signal-to-noise ratio SNR (equivalent to the carrier-to-multipath ratio) is defined as

$$\gamma = \frac{A^2}{2\sigma^2}. \quad (6)$$

The Rice distribution for the signal envelope ρ is defined as

$$P_\rho(\rho) = \frac{\rho}{\sigma^2} I_0(\frac{A\rho}{\sigma^2}) \exp(-\frac{\rho^2+A^2}{2\sigma^2})\,. \quad (7)$$

For $A = 0$, the Rayleigh distribution is given by

$$P_\rho(\rho) = \frac{\rho}{\sigma^2} \exp(-\frac{\rho^2}{2\sigma^2})\,. \quad (8)$$

The same equations can also be denoted for the signal power z. For Rician signals, the distribution

$$P_z(z) = \frac{1}{2\sigma^2} I_0(\frac{A\sqrt{z}}{\sigma^2}) \exp(-\frac{z+A^2}{2\sigma^2}) \quad (9)$$

follows for the power z of the signal. The power distribution of a Rayleigh signal follows an exponential decrease

$$P_z(z) = \frac{1}{2\sigma^2} \exp(-\frac{z}{2\sigma^2})\,, \quad (10)$$

with the expected value $2\sigma^2$ for the power of $s(t)$.

A slow shadowing process results in a time-varying short-term mean received power S_0 for which sometimes a lognormal distribution is assumed:

$$p_{LN}(S_0) = \frac{10}{\sqrt{2\pi}\,\sigma\,\ln 10} * \frac{1}{S_0} \exp\left(-\frac{(10\log S_0 - \mu)^2}{2\sigma^2}\right). \quad (11)$$

Here μ is the mean power level decrease (in decibel) and σ^2 is the variance of the power level (in dB) due to shadowing. Note that the dimension of σ^2 is dB^2 and it is referred to as *dB-spread*.

An exponential distribution for a number x of events (e.g., number of echoes) can be described by

$$P(x) = N * \frac{1}{\Delta} \exp(-\frac{x}{\Delta}), \quad (12)$$

whereas N is a constant factor to the expected value $1/\Delta$.

3.2 Numeric Values

Parameter fits have been performed for many environments. In this article we will give numbers for two environments: urban and rural for an elevation angle of 25 deg.

As one example for the fits, Fig. 4 shows the Rayleigh distribution of the power of near echoes for a fixed delay interval (the mean power is decreasing exponentially versus delay).

Most of the fits showed very good confidence values with the data. Thus, the selected distributions can be applied to characterize the statistics of the related parameters. Some fits have reasonable spreads. In this case, files with more data should be investigated in order to obtain a better confidence interval.

A general rule is that

- the number of near echoes can be described by a Ricean peak. The Ricean distribution avoids negative events. Note that the Ricean distribution yields for $A/\sigma >> 1$ a Gaussian. The mean value of near echoes depends on the environment. Value range from 1-2 echoes in an open environment up to 10-20 echoes in an urban.
- the number of far echoes seems to decrease exponentially.
- the delay of near echoes seems also to decrease exponentially. Note that near echoes occur in a delay interval of 600 nsec.

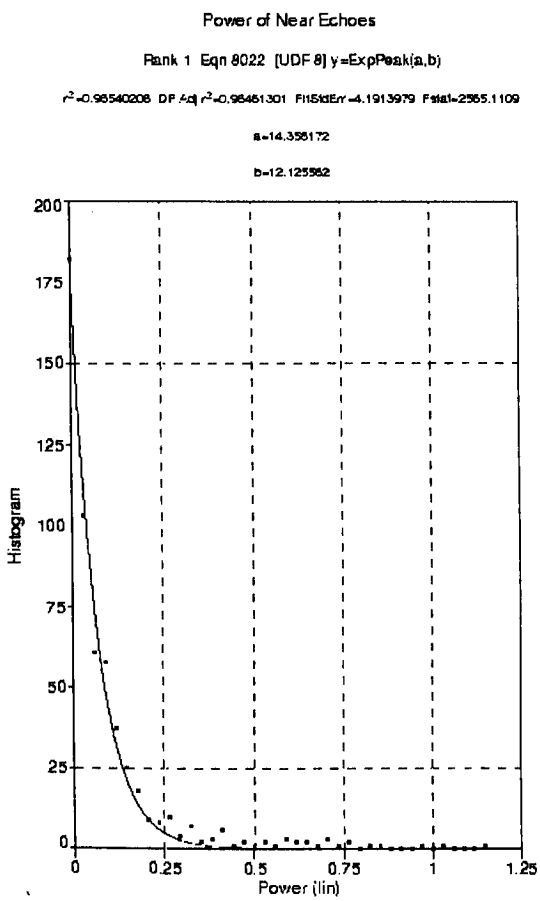

Figure 4: Fit: Power of near echoes. Urban environment, 25 deg. A Rayleigh distribution with exponential decrease of the mean power is adopted.

- the delay of far echoes can be described by a uniform distribution.
- the power of far echoes is lognormal-distributed.
- the power of near echoes follows a Rayleigh-distribution. That implies that the mean power of near echoes shows an exponential decrease.
- the power characteristics of the direct path depend on the user environment. For good line-of-sight conditions a Ricean distribution can be adopted whereas for shadowing conditions Rayleigh and/or lognormal fit very well.

Table 1 shows a summary of parameters for the wideband channel model for two selected environments.

4 Long Term Modelling

The modelling of the wideband channel so far gives impulse responses. The time-delay function will be unchanged as long the channel is stationary. After the channel correlation time, the parameters must be determined again. For a continuous-time simulation, the statistical time-dependance among the profiles must be known. A short- and long-term modification should extent the model for that. In what follows here, only an idea can be given how the correlation among the profiles can be modelled.

Short-term fluctuations of the echoes are caused by changing phase relations between signals with the same delay. Thus, constructive or destructive interference occurs and the signal magnitude varies. A short-term description in general has a spatial correlation of 40λ.

Long-term variations of the echoes are mainly determined by the lifetime of the echoes. The direct path is affected by obstacles whereas the echoes are affected by the presence of reflectors.

Three effects influence the wideband channel:

1. the operational scenario (user behaviour, user movement); mainly the direct path suffers from shadowing or blockage.
2. the change of the foreground environment (traffic); echoes with delays up to 500 nsec are affected.
3. the change of the background environment (aircraft/satellite motion); the movement has to be scaled to the actual satellite constellation. Mainly echoes with long delays are influenced.

The short-term effects can be modelled with correlation coefficients for subsequent echoes. The long-term modelling must distinguish among the three effects identified above. Birth-Death processes should

Parameter	Distribution		
Urban environment, 25 deg, random user			
No of near echoes	Ricean	$A = 10.5$	$\sigma = 2.1$
No of far echoes	exponential	$N = 718$	$\Delta = 1.033$
Delay of near echoes	exponential	$N = 106\mu$sec	$\Delta = 0.17/\mu$sec
Delay of far echoes	uniform	[600 nsec, 15μsec]	
Power of far echoes	lognormal	$\mu = -32$ dB	$\sigma = 2.2$ dB
Mean power of near echoes	exponential	$P = -34$ dB	$1.2 * 10^{-4}/\mu$sec
Power of direct path, unshad.	Ricean	$A = 1.22$	$\sigma = 0.3$
Power of direct path, shad.	Rayleigh	$\sigma^2 = -10.8$ dB	
Provincial road environment, 25 deg, random user			
No of near echoes	Ricean	$A = 1.7$	$\sigma = -0.3$
No of far echoes	exponential	$N = 570$	$\Delta = 2.186$
Delay of near echoes	exponential	$N = 230/\mu$sec	$\Delta = 0.32/\mu$sec
Delay of far echoes	uniform	[600 nsec, 15μsec]	
Power of far echoes	lognormal	$\mu = -31$ dB	$\sigma = 2.1$ dB
Mean power of near echoes	exponential	$P = -29$ dB	37/nsec
Power of direct path, shad.	Rayleigh	$\sigma^2 = -10.7$ dB	

Table 1: Parameters for the wideband channel model.

control the generation and lifetime of echoes. The model parameters have to be changed according to this generation process.

As a first step for the lifetime of shadowing in the direct path, the values of the shadowing probability A in [2] can be taken.

5 Conclusions

A wideband channel model for LMS services was derived. The model has three sections: the direct path, echoes with small delays and echoes with far delays. The parameters of the model have been fitted for selected environments.

Actually, parameter fits for more environments and more elevation angles are performed. The long term modelling is under investigation and the correlation coefficients among different echoes will be modelled. The results will be published in future publications.

References

[1] Faramaz Davarian. Earth-satellite propagation research. *IEEE Communications Magazine*, April:74–79, 1994.

[2] Erich Lutz, Daniel Cygan, Michael Dippold, Frank Dolainsky, and Wolfgang Papke. The land mobile satellite communication channel — recording, statistics and channel model. *IEEE Trans. Vehicular Technology*, 40:375–386, 1991.

[3] Chun Loo. A statistical model for a land mobile satellite link. *IEEE Trans. Vehicular Technology*, 34:122–127, 1985.

[4] Branka Vucetic and Jun Du. Channel modeling and simulation in satellite mobile communication systems. *IEEE J. Selected Areas in Communications*, 10:1209–1218, 1992.

[5] Norbert Kleiner and Wolfhard J. Vogel. Impact of propagation impairments on optimal personal communication systems. In *Workshop Adelaide, Australia*, page Nov 1992.

[6] Axel Jahn and Erich Lutz. DLR channel measurement programme for low earth orbit satellite systems. In *Proc. Int. Conf. on Universal Personal Communications ICUPC'94*, pages 423–429, San Diego, 1994.

[7] Axel Jahn, Mario Sforza, Sergio Buonomo, and Erich Lutz. Narrow- and wideband channel characterization for land mobile satellite systems: Experimental results at L-band. In *Proc. Int. Mobile Satellite Conference IMSC'95*, 1995.

[8] Axel Jahn. Propagation data and channel model for LMS systems. *Final Report, ESA Purchase Order 141742*, DLR, Institute for Communications Technology, 1994.

[9] Philip A. Bello. Characterization of randomly time-variant linear channels. *IEEE Trans. Communications Systems*, Dec.:360–393, 1963.

Narrowband and Wideband Characterisation of Satellite Mobile/PCN Channel

G.Butt , M.A.N.Parks, B.G.Evans
Centre for Satellite Engineering Research (CSER), University of Surrey
Guildford, Surrey GU2 5XH, UK
Fax: (+44) 1483 259504
e-mail: g.butt@ee.surrey.ac.uk

Abstract

This paper presents models characterising satellite mobile channel. Statistical narrowband models based on the CSER high elevation angle channel measurement campaign are reported. Such models are understood to be useful for communication system simulations. It has been shown from the modelling results that for the mobile satellite links at high elevation angles line-of-sight (LOS) signal is available most of the time, even under the heavy shadowing conditions. Wideband measurement campaign which CSER is about to undertake, and subsequently the modelling approach to be adopted is also discussed. It is noted that a wideband channel model is expected to provide a useful tool in investigating CDMA applications.

Introduction

Propagation channel plays an important role in the overall design of any mobile communication system, even more so for a satellite-based mobile system. Shadowing of the line-of-sight (LOS) signal and multipath reception are the most significant issues of concern to system designers. Estimation of additional link margin, necessary for low gain low directivity mobile terminal, to provide reasonable service availability is usually a first step towards understanding the propagation impairments. Satellite-mobile link quality to a great extent is determined by the propagation channel characteristics. The propagation channel characteristics most significantly depend upon the immediate environment surrounding a mobile. Signal amplitude variations of the order of several dBs may be experienced mainly due to the obstruction of the line-of-sight (LOS) path between a satellite and a mobile over a relatively short duration of time. This effect is known as 'shadowing'. In general, mobile terminal is not capable of discriminating between the LOS signal and its various reflected replicas. This causes degradation in the received signal due to 'multipath'. For broadband systems, the differential delays of different incoming replicas cause further problems and therefore distort the signal.

Currently due to widespread interest in the satellite personal communication networks (S-PCNs), it becomes increasingly important to carefully examine the typical channel conditions for such a system design. Unfortunately channel conditions for S-PCN could be significantly different from conventional mobile satellite channel. In fact propagation considerations would influence the choice of satellite constellation, which in turn effects almost all aspects of a S-PCN; choice of multiple access scheme, modulation, channel coding, power control and signalling requirements are a few most important to mention.

Narrowband Channel Models

CSER undertook narrowband channel measurements during 1991/92 with the aim to characterise mobile satellite channel at high elevation angles (above 60°). Such an exercise was an attempt to fill the gaps left over from other studies in the channel characterisation, in particular for systems such as ARCHIMEDES. Simultaneous channel measurements were made at L, S and K_u-band frequencies, and under a variety of channel conditions (physical environments). Details of the measurement campaign, results and empirical models have been reported in the literature previously [1] [2] [3]. Data has further been analysed to generate statistical model of the channel.

Statistical Channel Models

Statistical channel models are particularly useful for communication system simulations and should provide a more 'comprehensive' understanding of the nature of a communication link. Previously reported statistical models, as in [4] [5], mainly describe the channel at lower elevation angles. These models understandably suggest shadowing as a major problem. At lower elevation angles it may be expected that the LOS signal would frequently suffer from blockages due to various natural and man-made obstructions in the surrounding environment. As the elevation angle increases, LOS signal should suffer less and less blockage. Therefore the statistical behaviour of the received signal, $p(r)$, may then be modelled using Rice probability density function.

$$p(r) = \frac{r}{\sigma^2}.e^{-\left[\frac{(r^2+d^2)}{2\sigma^2}\right]}.I_o\left(\frac{rd}{\sigma^2}\right) \qquad (1)$$

r is the instantaneous received signal amplitude, σ^2 is the diffused signal power and d id the amplitude of the LOS signal. It is obvious that the Rice factor (ratio of the power in the LOS to the power in the diffused component) can be used to characterise various channel conditions.

It has been found that at high elevation angles the channel (amplitude) variations are Rician distributed with reduced problems from road-side obstacle shadowing. Figure 1 illustrates model fits at the L-band frequency for a measurement run during phase-II of the campaign (Spring '92) in the 'suburban' environment at 60° (fig. 1a) and 80° (fig. 1b). For the same stretch of the measurement route, the simultaneously measured channel responses at S-band are shown in figure 2.

It is important to note two obvious features in the L-band case. Due to the reduced shadowing problem at the high elevation angles the channel is purely Rician as opposed to Rayleigh and/or Log-normal, typically for terrestrial mobile and in many instances (at low elevations) for satellite mobile scenarios. Also the channel improves when the elevation angle is increased; Rice factor increases from 12 dB at 60° to 20 dB at 80°. Such a behaviour is consistent with the common understanding of the mobile satellite channel. Also for the S-band, the channel variations are still Rician distributed but evidently more dominated by the multipath effect. Figure 3 shows the L-band fade duration distributions at 60°, for thresholds at 3 and 7 dBs. The curves indicate 50% of the fades shorter than 5ms. Similarly S-band fade duration distributions are shown in figure 4.

For the 'wooded' environment, characterised as potentially heavy shadowing conditions for a typical mobile terminal, the models for the L-band channel characteristics at 60° and 80° are shown in figure 5. Due to more frequent shadowing problems, the channel is no longer purely Rician distributed at 60°. However, it could be reasonably modelled using Nakagami-*m* distribution, given as

$$p(r) = \frac{2}{\Gamma(m)}\left(\frac{m}{\Omega}\right)^m r^{2m-1} e^{\left(-\frac{m}{\Omega}r^2\right)} \qquad (2)$$

An *m*-factor of 1.5 (fig.5a) indicates that the channel is not Rayleigh distributed either. On the other hand, at 80° the channel is very close the one being Rician distributed with the Rice factor of 9.2 dB. Again a clear improvement in the channel response is demonstrated with the increase in the path elevation angle. Also the influence of the mobile surrounding environment clearly reveals itself. The corresponding fade duration distributions in the wooded environment are illustrated in figure 6.

It is important to note that most of the above discussion is applicable to what is now more commonly termed as 'vehicular-mounted' mobile-satellite channel. The nature and operation of a personal communication terminal is different from a vehicular (or transportable) terminal and therefore necessitates channel characterisation accordingly. At present very little information is available in the public domain regarding the satellite hand-held channel. Reference [6] contains some details of the propagation measurements carried out for the Iridium system, one of the planned satellite personal communication networks. It is reported that large fade margins are required even in the LOS conditions to support adequate link quality. This may be due to a combination of reasons such as moving satellite, closeness to human body etc.

Wideband Channel Model

Wideband measurements primarily provide information on the excess time delays of the signal replicas echoed across the 'channel'. The information can be processed to extract the coherence bandwidth of the channel. Knowledge of such parameters is important in engineering signal formats to avoid distortion. Excess time delays can cause inter-symbol interference in digital systems which can either be handled by choosing suitable transmission rates or appropriate receiver architectures. Very little data is available on wideband characterisation of either vehicular based or hand-held satellite channels. Some wideband trials carried out in connection with the Iridium program [6] suggest that the delay spread for echoes arriving at the receiver are in order of less than 0.25 μs, thus indicating no serious problems associated with excess delays in a personal communication channel. Similar results have been reported by a recent wideband campaign carried out by DLR [7]. Small delay spreads may be attributed to the higher path elevation angles involved in such links. Similar conclusions can be made for vehicular based mobile channels as well.

CSER is about to launch a wideband propagation campaign, under an ESTEC contract. Investigations on excess delays and other wideband parameters at L and S bands will be carried out. Following the narrowband measurements, again a helicopter in parallel flight paths will be used as an alternative platform to transmit simultaneous dual-wideband signals simulating a satellite source. The wideband sounder has been designed and implemented based on *swept time-delay cross-correlation (STDCC)* principle. The delay resolution of the sounder is

fixed at 0.1μsec (10 MHz chip rate), whilst the maximum unambiguous delay can be set to one of the four values, 12.7μsec, 25.5μsec, 51.1μsec and 102.3μsec. The facility to select the maximum unambiguous delay for any measurement run has been built in view of the campaign to be carried out in a variety of channel conditions such as urban, suburban, open, lightly and heavily wooded environments. Measurements will also cover the full range of elevation angles i.e, 15° - 80° in each environment. In addition, the campaign is expected to address both vehicular-mounted mobile and hand-held type channels.

The trials arrangement has been tested for proper operation in the field. Figure 7 shows the line-of-sight correlation functions, averaged over 50 profiles, obtained during the pseudo-runs. With the transmitting arrangement mounted in the second floor window of a campus building, 200m away in a campus car park the mobile laboratory travelled at about 5/6 kph. This has also been confirmed by the off-line processing of the data. Some preliminary results from the wideband campaign will be available for presentation at the conference.

The wideband data will be used to construct what is termed as a 'Tapped Delay Line' wideband channel model, as depicted in figure 8. This type of model is believed to be most suitable for communication system simulation purposes such as CDMA performance evaluations.

Conclusion

The paper discusses various aspects of mobile satellite propagation channel. It outlines CSER activities in modelling the narrowband characteristics, and wideband measurements, of the channel. A dual-wideband measurement campaign, using a helicopter as an alternative platform, is about to be carried out which should result in obtaining the wideband statistics of the channel as well as a tapped delay line type model for system simulations.

Acknowledgements

ESTEC/ESA funding for the wideband channel measurement campaign is gratefully acknowledged.

REFERENCES

[1] G.Butt et.al.," Narrowband Channel Statistics from Multiband Propagation Measurements Applicable to High Elevation Angle Land Mobile Satellite Systems", IEEE J-SAC, SAC-10(8), vol.10, no.8, October 1992, pp.1219-1226

[2] G.Butt et.al.," Results of Multiband (L, S, Ku band) Propagation Measurements for High Elevation Angle Land Mobile Satellite Channels", Proceedings of International Conference on Antennas and Propagation ICAP '93, Edinburgh, March 1993

[3] M.A.N.Parks et.al.," Empirical Models Applicable to Land Mobile Satellite System Propagation Channel Modelling", IEE Colloquium on Communications Simulation and Modelling Techniques, 28 September 1993, Digest no.1993/139

[4] C.Loo et.al.," Measurements and Modelling of Land Mobile Satellite Signal Statistics", IEEE 36th Vehicular Technology Conference, May 1986

[5] E.Lutz et.al.," The Land Mobile Satellite Communication Channel - Recording, Statistics, and Channel Models", IEEE Transactions on Vehicular Technology, vol.40, no.2, May 1992, pp.375-385

[6] N.Kleiner, W.J.Vogel," Impact of Propagation Impairments on Optimal Personal Mobile Satellite Communication System Design", November 1992, Australia

[7] G.E.Corazza et.al, " Channel Characterisation for Mobile Satellite Communications", EMPS'94, Italy, October 1994

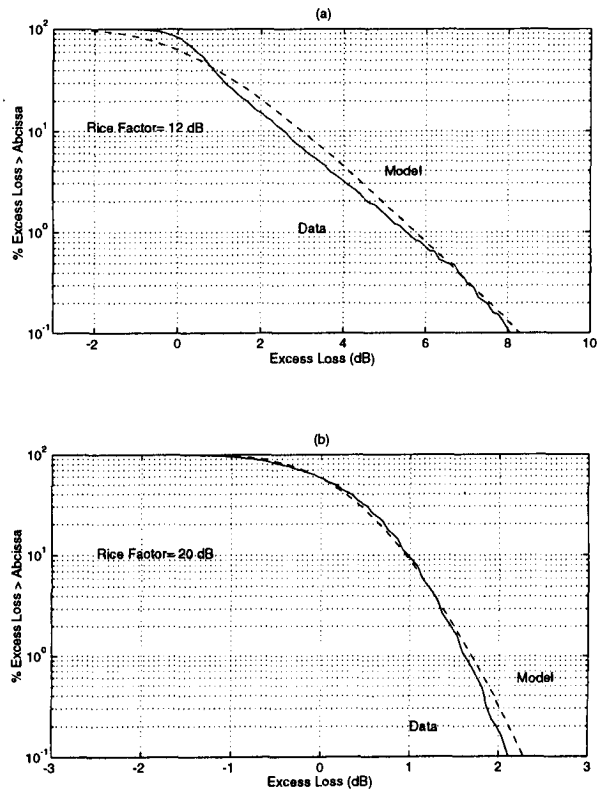

Figure 1: Models for L-band channel data
Suburban - Spring '92 (a) 60° (b) 80°

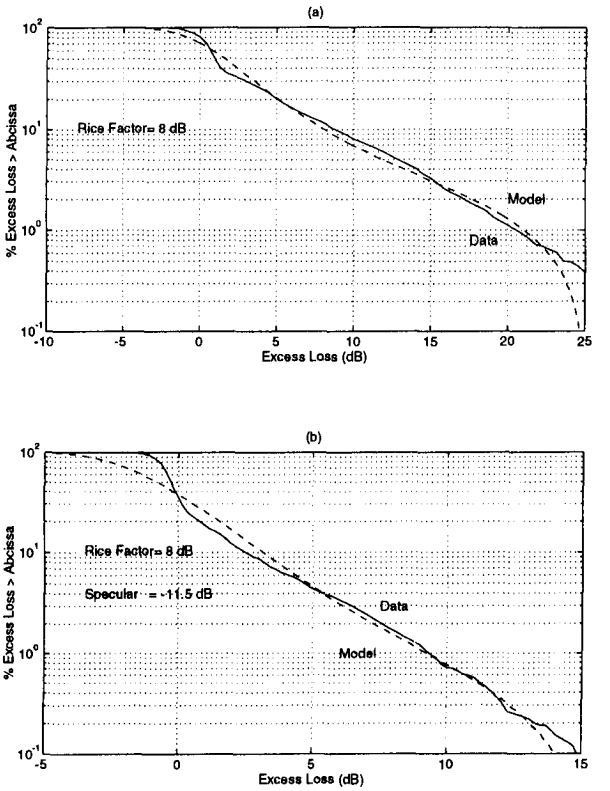

Figure 2: Models for S-band channel data
Suburban - Spring '92 - (a) 60° (b) 80°

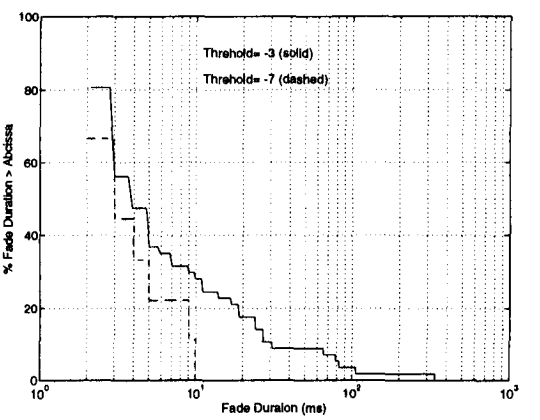

Figure 3: L-band Fade Duration Distributions
Suburban - Spring '92 - 60°

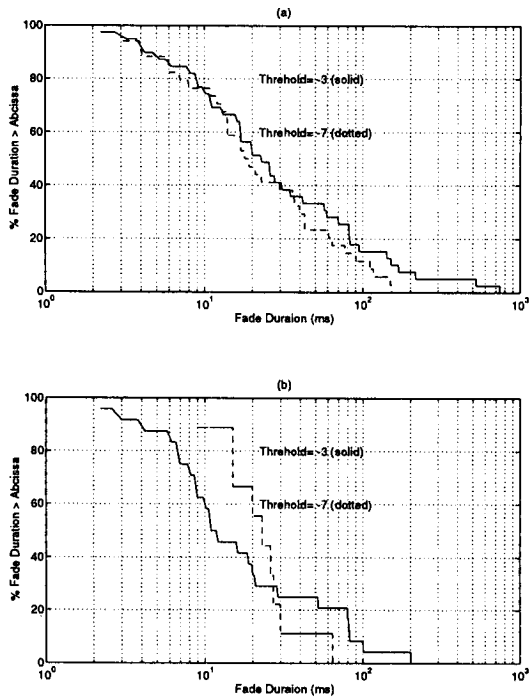

Figure 4: S-band Fade Duration Distributions
Suburban - Spring '92 (a) 60° (b) 80°

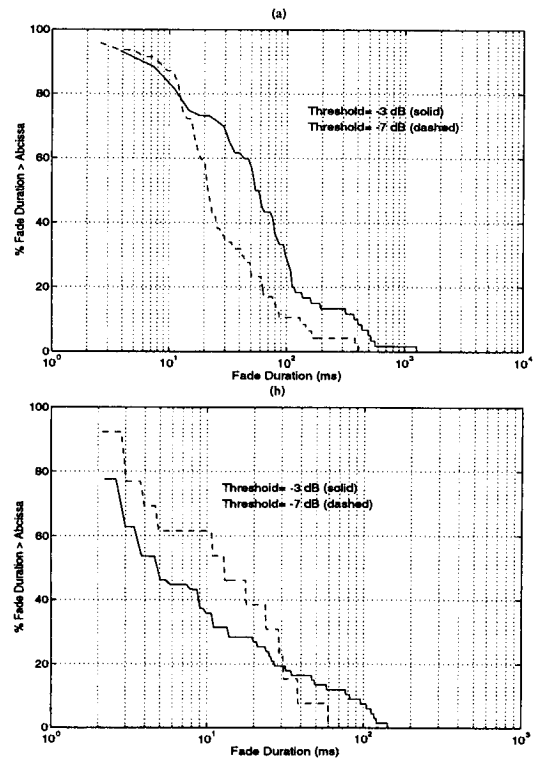

Figure 6: L-band Fade Duration Distributions
Wooded - Spring '92 (a) 60° (b) 80°

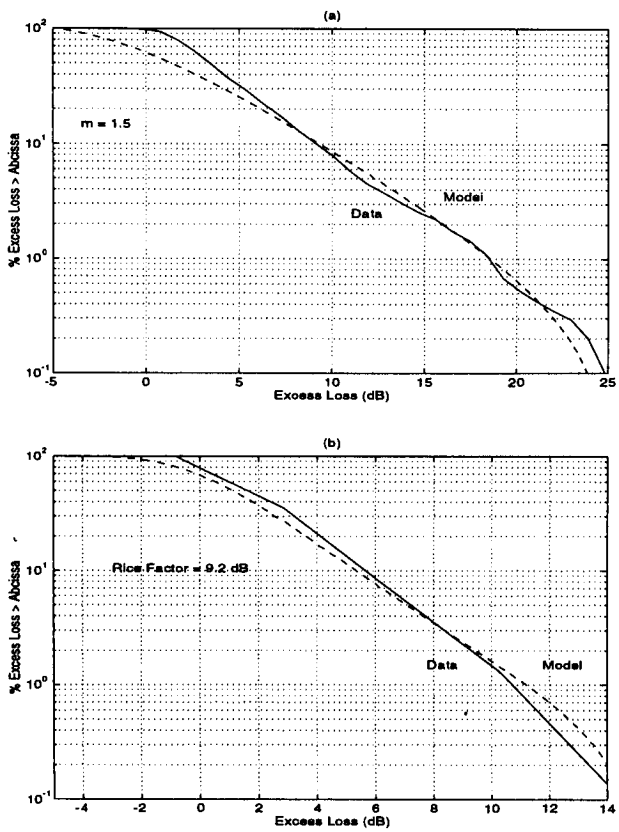

Figure 5: Models for L-band channel data
Wooded - Spring '92 (a) 60° (b) 80°

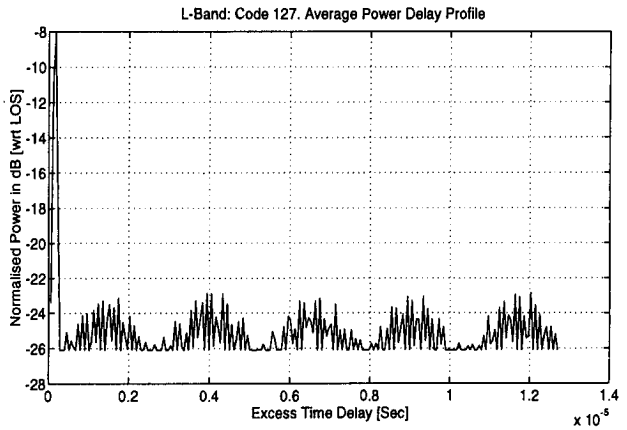

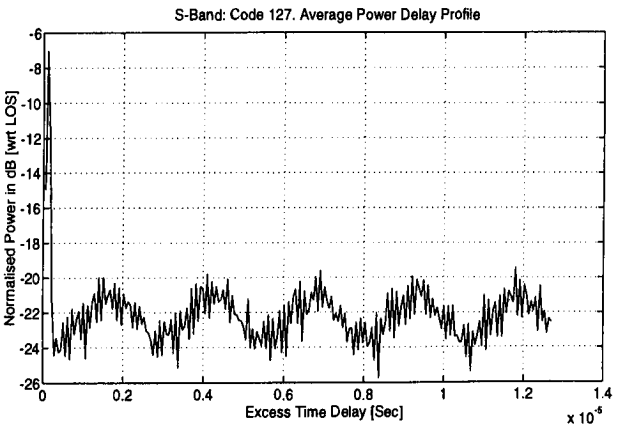

Figure 7: LOS Average Power Delay Profile

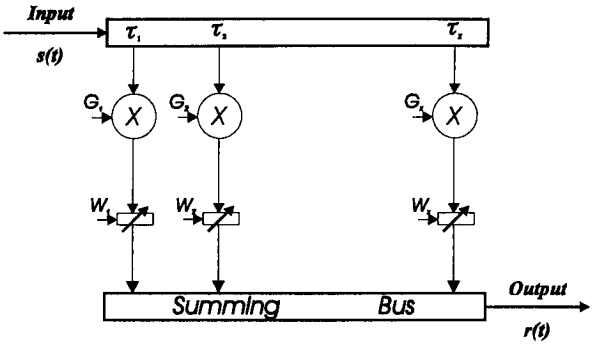

Figure 8: Typical Tapped Delay Line type wideband channel simulator

Land Mobile Satellite Narrowband Propagation Campaign at Ka-Band

[1]F. Murr, [2]B. Arbesser-Rastburg, [2]S. Buonomo

[1]Joanneum Research IAS, A-8010 Graz, Austria
[2]ESA-ESTEC/XEP, NL-2200 AG Noordwijk, The Netherlands

ABSTRACT

This paper gives a short description of the equipment used, lists the activities of the experimental campaign and presents the first statistical evaluation of the recorded data. Due to the restricted size of the document only few results are reported, additional information can be found in [1].

INTRODUCTION

The aim of the propagation campaign with a mobile beacon terminal is to study the possible use of the Ka-band (20/30 GHz) for mobile communication and to investigate the shadowing component of the mobile propagation channel. For this purpose the European Space Agency equipped a van with a beacon receiver, a data acquisition system and a video system and commissioned the measurement campaign in the following environments:

- open rural
- tree-shadowed
- suburban
- urban
- mixed (a composition of the previous four items)

The campaign used the 18.7 GHz propagation payload of Italsat F1 as a source [2]. The resulting elevation angle was between 30° and 35° while the azimuth angle was chosen to be 0°, 45° and 90° respectively.

THE MOBILE TERMINAL

The Land Mobile Beacon Terminal (LMBT) was specified by ESA and built by RESCOM (Denmark) [3,4]. A Mercedes van was modified to host the antenna system, the receiving equipment and the data acquisition system. Additionally, a video system was installed to monitor the environment.

Antenna System

The receiving antenna is a high gain cassegrain system with a 3 dB-beamwidth of 2.4°. This narrow beam antenna needs careful tracking of the satellite in mobile conditions to keep the received power constant. The tracking of the antenna was realised by a dual-gyro stabilisation system. The gyro system is fast enough to avoid mispointing during normal driving conditions. Even at high speeds of 80 to 90 km/h, the residual error due to the inertia of the antenna platform is less than 0.3 dB.

Beacon receiver

The received signal at 18.7 GHz is down converted in several steps and then fed to an orthogonal detector with adjustable detection bandwidth and sample rate. The in-phase and quadrature components delivered by the detector output are linearly dependent on the received field strength at the antenna input. Though designed as a dual channel receiving system (for the OLYMPUS dual polarisation 20 Ghz beacon), only the copolar signal component has been measured. The sample rate was kept constant at 1kHz for all measurements during the LMS campaign. The frequency shift due to the Doppler effect when driving the LMBT towards or from the satellite was corrected by tuning the LO frequency of the IF down converter. The value to be corrected (up to 900 Hz at 50 km/h) is derived from the van speed and the driving direction with respect to the satellite. A fast PLL (phase lock loop) provided low recapture times after loss of lock, typically less 0.1 seconds at 50 km/h. The overall error in measuring the fade level is less 1 dB, were an error of 0.5 dB for the gyro drift is included. The typical duration of a measurement run was 12 to 15 minutes; the error due to gyro drift was generally less than 0.3 dB for all runs and even this residual error was corrected in the data processing phase.

Data Acquisition and Video System

The received signal components (I and Q values sampled at rate of 1kHz), the information on van speed and driving direction, the error signals from the gyro system and general system status information are stored directly on an EXABYTE tape drive. To give an impression on the environment and on the obstacles causing shadowing on the line of sight path two cameras are mounted in the LMBT.

One is mounted on the antenna platform looking towards the satellite, the other one is mounted above the dash board looking into the driving direction. The signal from both cameras is fed into a video mixer and recorded on a video tape. The direction to the satellite is indicated by a computer generated cross-hair superimposed onto the video image.

CAMPAIGN PLANNING

In the planning phase specific homogeneous environments have been identified in four European countries:

- The Netherlands (open, suburban)
- France (tree-shadowed, open, mixed)
- Germany (urban, suburban, tree-shadowed)
- Austria (mixed, suburban, tree-shadowed)

For each environment three different orientations of the driving route with respect to the satellite direction, i.e. 0°, 45° and 90°, were investigated. The minimum duration of the run was defined as 10 minutes and the average van speed was approximately 30 km/h in non-urban areas and approximately 20 km/h in urban areas. The following environments were chosen:

- Open environment

The typical *open area* can be described as a flat area without any obstruction of the LOS. In The Netherlands, the open area was interrupted in one case by pylon of wind power generator and in another case by single trees around farm houses. The measurements in France and Austria were made in clear open environment.

- Tree shadowed environment

Tree-shadowed environments can either be wooded regions or tree-lined roads. In France the deciduous tree forests around Colmar (Alsace) were selected for the measurements. At measurement time (in spring) the foliage was just starting to develop. In Germany the measurements were carried out in dense needle-tree forests whereas in Austria alleys with cherry and horse chestnut trees in full foliage were chosen.

- Suburban environment

Suburban environment is characterised by low building density, single trees and small gardens or parks. The average building height is 1 to 3 three storeys and severe obstructions by underpasses are rare. Measurements in suburban areas were performed in small towns in The Netherlands, in modern suburbs around Munich and in rural villages in Austria.

- Urban environment

Urban environment is characterised by high building density. Most of the buildings are more than 3 storeys high. Mobile measurements were performed only in Munich as this town was providing a sufficient homogeneous environment at the required minimum length of roads.

- Mixed Environment

A *mixed* environment is a combination of all four previously described environments. Areas with such characteristics have been found in France (Strasbourg), in Germany (Munich) and in Austria (Vienna).

Organisation of LMS-measurements

Basically, all measurements have been performed at clear sky conditions or at least at constant weather conditions. In order to be able to exclude single shadowing effects which are of unknown origin for each environment and for any of the three orientations at least two consecutive measurement runs covering a minimum time period of 10 minutes of useful data was performed. Each route was used in both directions. The undisturbed line-of-sight (LOS) reference level was established before and after each run. In case of attenuation by rain or heavy clouds the LMS measurements were halted and repeated at better meteorological conditions. In total data from some 160 runs have been collected of which 140 have been analysed.

DATA ANALYSIS

Data processing

From in-phase and quadrature component (I and Q) the power level and the phase were calculated and stored for further processing. Then the data were inspected and if they met the general acceptance criteria, were screened for necessary corrections. One important effect is caused by the gyration of the satellite. This gyration results in an amplitude modulated signal with a very stable period of 7:30 minutes and a magnitude of 0.2 to 1 dB, depending on the site location within the beam contour. Another effect is a single cloud drifting through the receiving path and causing additional attenuation of 0.2 to 1.5 dB. Both effects have been removed where possible. During LOS reference measurements, scintillation were sometime observed with peak-to-peak values between 1 and to 2.5 dB. The cleaned data files has been clipped to obtain only the pure LMS part of a measurement run.

Statistical analysis

First order statistics include cumulative distribution function (CDF) and probability density function (PDF). The classes of o.5 dB were chosen from -35 dB to +5 dB. In case of loss of lock the signal level dropped to -45 to -55 dB, i.e. the measured power level was mainly determined by the receiver noise.

Second order analysis includes level crossing rate (LCR), cumulative fade duration (CFD), cumulative connection time (CCT), timeshare of fade (TSoF). This analysis was done for values from -45 dB to +5 dB in 1.0 dB steps. The scan for fade time, fade counts, connection time and connection counts was performed by a quasi-logarithmic scale for the time classes, e.g. classes of 1, 2, 4, 6, 8, 10, 20, .. 100, 200, ..., 1000, ..., 100000ms were applied to investigate fades and connections.

RESULTS

Open environment

As expected, the results showed no angular dependency for the shadowing effect in open environment. As the receiving antenna is quite narrow (i.e. the 3 dB-beam width is 2.4°) no multipath effect was observed. In rare cases, e.g. when passing the wind power generators and their rotating metallic blades, short spikes on the received signal due to multipath were seen.

Suburban environment

The roads in the suburbs of The Netherlands are narrow (~5m) and the houses are relatively near to the roadside (2 to 4m) whereas in Germany the roads were about 6 m wide and buildings were set back by about 5 to 7 m from the road. This is reflected by the more severe shadowing situation at 90° in The Netherlands, see Fig.1 and 2.

Tree-shadowed environment

The comparison of the two different types of forests (leaf trees and needle trees) reveals interesting details. At an orientation of 0° the bushy leaf trees where branches are reaching across the road cause much more shadowing than the tall but slim pine trees, see Figs.3 and 4. The leaf trees show only very little difference in shadowing at angles between 45° and 90° orientation, but much less attenuation compared to pine trees. The remarkable difference in shadowing between 45° and 90° in the needle tree forest is mainly caused by gaps in the tree line, which provide visibility to the satellite between two trees at an orientation orthogonal to the road. At 45 degrees azimuth, the gaps between the trees are obstructed.

On alleys with tree-shadowing by single trees the impact of the azimuth angle on the received signal is less pronounced, however, the height and the diameter of the trees plays an important role.

Urban environment

The most severe shadowing has, as expected, been found in urban area with its total blockage over long time periods. The shadowing at 0° orientation is moderate and mainly determined by road signs, underpasses and overhead street lights. Between 0° and 45° orientation the shadowing of the received signal increases considerably, whereas at 90° open roads at intersections provided better conditions than at 45°, similar to the tree-shadowed situation. This effect can also be seen from the LCR statistics in Figs.5 and 6.

Note: The fade duration and the connections are expressed in terms of time (seconds) instead in terms of length (m). To obtain comparable statistics the average speed was kept as constant as possible for all runs. Usually, a van speed of 23 to 25 km/h was used. Possible stops at traffic lights, the duration was in the range of a few seconds up to 60 or 70 seconds, could influence the statistics as always the full length of a LMS run was analysed. Thus, measurements in urban area with high traffic were mainly made in the morning or evening hours with less traffic density. This allowed to minimise the number of long stops and improved the possibility to compare statistics of different sites. For all statistics presented in this paper the worse case, i.e. the measurements on the road side closer to the satellite, has been investigated. The difference is usually quite remarkable.

CONCLUSION

Measurements using a high gain antenna on a van have been made in several land mobile environments to see how well the currently existing prediction algorithms predict the shadowing of the direct line-of-sight path at different path orientation while the model validation efforts are still on going, some preliminary conclusion can be drawn from the statistical results. At an elevation angle of 30 to 35 degrees open and suburban environments would allow Ka-band land mobile satellite communications services with a manageable margin. However, for urban and wooded regions a reasonable link can only be maintained when the road is leading straight towards or away from the satellite which is an impractical assumption for a commercial service. Comparison with L-band data shows, that in urban conditions at L-band (where, with a broad beam antenna

diffracted and reflected multipath components are picked up) the first order statistics are comparable with Ka-band statistics from suburban areas. Further analysis will relates the video images to the RF signal received. It is expected that measurements using only a video camera can produce useful statistics at all elevation angles.

REFERENCES

[1] **Joanneum Research**, *Land Mobile Satellite Narrowband Propagation Campaign at Ka-band*, Final Report W.O. #4, ESTEC Contract 9949/92/NL, January 1995.

[2] **A. Paraboni, B. Giannone**, *Information for the participation to the ITALSAT Propagation Experiment*, Politecnico di Milano Report 91.032, 1991.

[3] **RESCOM A/S** *Land Mobile Terminal*, Final Report ESA Contract 9896 ESA RPT CR(X) 3835,1994.

[4] **M. Sforza, S. Buonomo, B. Arbesser-Rastburg**, *Channel Characterisation for future Ka-band Mobile Satellite Systems*, Proc. NAPEX XVIII, JPL 94-19, August 1994, pp. 105-116.

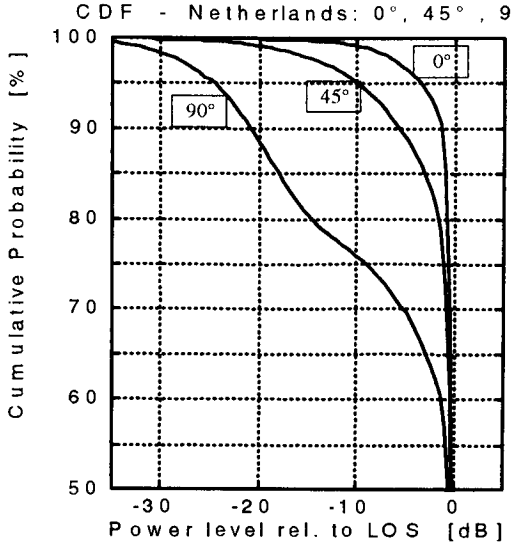

Figure 1: Suburban environment - CDF

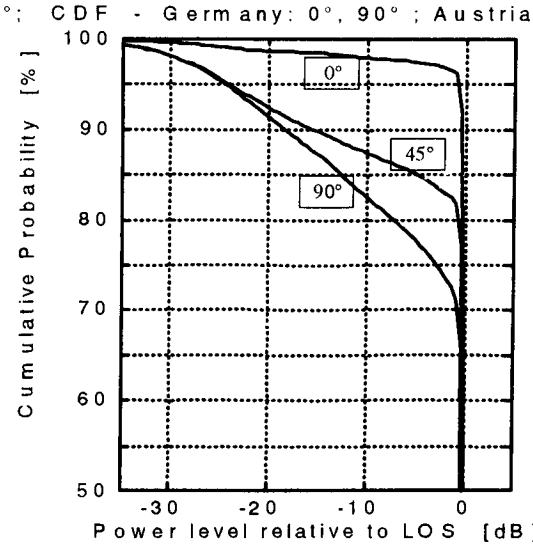

Figure 2: Suburban environment - CDF

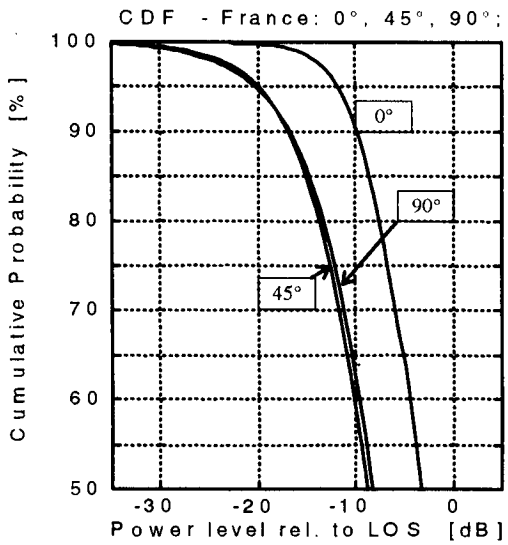

Figure 3: Tree-shadowed environment - CDF

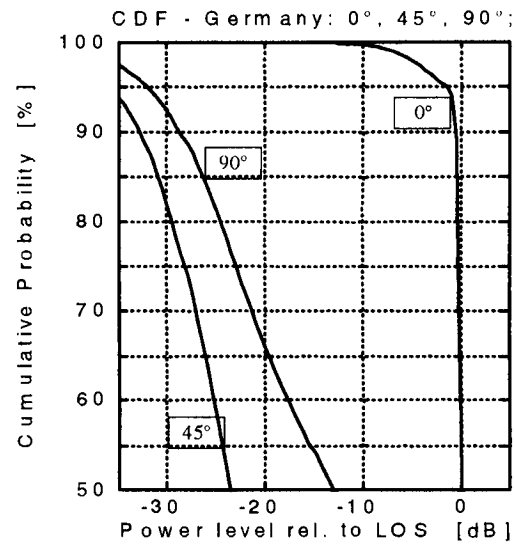

Figure 4: Tree-shadowed environment - CDF

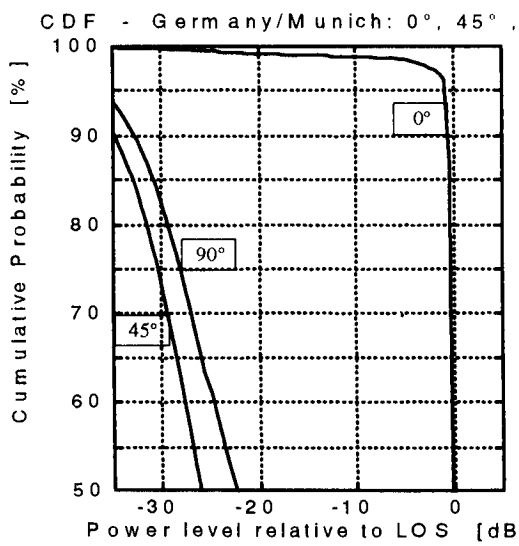

Figure 5: Urban environment - CDF

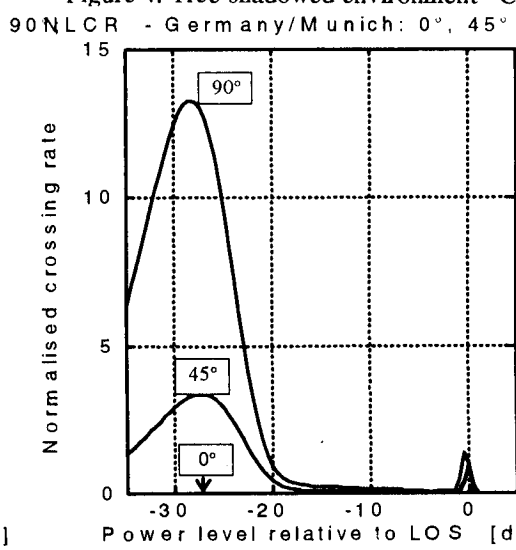

Figure 6: Urban environment - NLCR

K/Ka-band Channel Characterization for Mobile Satellite Systems

Deborah S. Pinck
JPL
4800 Oak Grove Drive, MlS 161-241
Pasadena, CA 91109
Phone: (818) 3548041
Fax: (818) 393"4643
e-mail: pinck@zorba.jpl.nasa.gov

Michael D. Rice
Department of Electrical/Computer Engineering
Brigham Young University
Provo, Utah 84602
Phone: (801) 378 4469
Fax: (801) 37&6586
e-mail: mdr@ee.bye.edu

ABSTRACT

Mobile satellite systems allow truly ubiquitous wireless communications to users anywhere and anytime. NASA's Advanced Communications Technology Satellite (ACTS) provides an ideal space-based platform for the measurement of K/Ka band propagation characteristics in a land mobile satellite application. Field tests conducted in Southern California during the first seven months of 1994 using JPL's ACTS Mobile Terminal (AMT) provided channel characterization data for the K/Ka-band link. A pilot tone was transmitted from a fixed station in Cleveland, Ohio through the satellite and downlinked at 20 GHz in the Southern California spot beam. The AMT was equipped with a narrow beam, high gain antenna which tracked the satellite in azimuth for a fixed elevation angle (46 degrees for this case). The field tests were conducted in three basic environments: clear line-of-sight (LOS) highways, lightly shadowed suburban, and heavily shadowed suburban. Preliminary results of these field tests indicate very little multipath for rural environments and for clear LOS links (as expected with a narrow beam antenna). Deep fades were experienced in shadowed areas, especially those where tree canopies covered the road.

Full text of the paper is in the Appendix page A-3

Satellite Ka-Band Propagation Measurements in Florida

Henry Helmken*, Rudolf Henning**

*Florida Atlantic University
777 West Glades Road
Boca Raton, Florida 33431
Phone: 407-367-3452 FAX:407-367-2336
**University of South Florida
4202 Fowler Ave
Tampa, Florida 33620
Phone: 813-974-4782 FAX: 813-974-5250

ABSTRACT

Commercial growth of interactive, high data rate communication systems is expected to focus on the use of the Ka-band (20/30 GHz) radio spectrum. The ability to form narrow spot beams and the attendant small diameter antennas are attractive features to designers of mobile aeronautical and ground based satellite communication systems. However, Ka-band is strongly affected by weather, particularly rain, and hence systems designs may require a significant link margin for reliable operations. Perhaps the most stressing area in North America, weatherwise, is the Florida sub-tropical climatic region. As part of the NASA Advanced Communications Technology Satellite (ACTS) propagation measurements program, beacon and radiometer data have been recorded since December 1993 at the University of South Florida (USF), Tampa, Florida.

INTRODUCTION

NASA's Advanced Communications Technology Satellite (ACTS) was developed to foster the creation and validation of communication technology as it expands into the millimeter region.[1] At Ka-band frequencies, reliable signal transmission system design depends heavily on validated channel models and propagation statistics. Several proposed global mobile communication systems (Iridium, Teledesic etc.) have Ka-band link components and both ground mobile and aeronautical testing is being carried out via the AMT program at JPL. The Space Communications Technology Center headquartered at Florida Atlantic University (FAU) is a NASA sponsored Center for the Commercial Development of Space (CCDS) and is developing systems for digital satellite communication of voice, data and video via Ka-band and thus is very dependent on accurate propagation information.

ACTS PROPAGATION TERMINALS

The ACTS satellite was launched in September 1993 and currently has a lifetime expectancy to 1999. The satellite has a Baseband Processor (BBP) mode for T1 TDMA data streams and a Microwave Switch Matrix (MSM) mode for operation as a wideband (to 1 GHz) transponder [1]. Two highly stable beacons at 20.185 and 27.5 GHz have been operational since October 1993. Both beacons are currently connected to transmit vertical polarization.

NASA, via the Lewis Research Center, has established the ACTS propagation measurements program. Based on experience with the OLYMPUS propagation measurements program, seven identical receiving terminals were constructed and have been strategically placed at sites in North America

LOCATION	ACTS Elev.	ITU-R Rain Zone
Vancouver, B.C.	30	D
Ft. Collins, CO	43	E
Fairbanks, AL	9	C
Clarksburg, MD	39	K
Las Cruces, NM	51	E
Norman,OK	49	M
Tampa, FL	52	N

Table 1: Experiment Sites

(Table 1). Terminals have a 1.2 m aperture antenna and measure both beacon signal strength and broadband radiometer sky noise temperature. Signal strengths are measured with a digital receiver; measurement resolution is 0.01 dB and the dynamic range exceeds 30 dB. The terminals simultaneously record both beacon and radiometer data at a 1 Hz sampling rate. For scintillation studies, short term sampling can be increased to 20 Hz. Atmospheric factors such as water vapor, humidity, rain rate, pressure, temperature along with general housekeeping data are simultaneously recorded. Greenwich Mean Time (GMT) is used by all stations to facilitate data comparison. Raw and processed data from all sites is archived at the data depository located at the University of Texas at Austin, TX. Common automatic data preprocessing is being developed however the analysis in the present paper is based on semi-automatic hand processing. This analysis is preliminary since calibration procedures changed during the year and a completely consistent set of calibration procedures is still being formulated. Experimenter workshops are held on a bi-annual basis which review calibration procedures, results and insure uniformity of analysis procedures [2].

FLORIDA PROPAGATION TERMINAL

The ACTS Propagation Terminal (APT) established by NASA at the University of South Florida in Tampa supports both the ACTS propagation program and the CCDS mission. A second, transportable receive-only terminal has been constructed and will be used in upcoming site diversity experiments.

Preliminary analysis has been made of the first nine months of data. This period of time encompasses both a relatively dry winter season (Dec 1993 to May 1994) and the wet, rainy summer season (June 1994 - August 1994). Results have focused on generating Cumulative Distribution Functions (CDF) distributions. Information in these distributions present the percent of time during which atmospheric loss exceeds a specified level. For purposes of providing information for power control algorithms, relative correlation comparisons such as Beacon 20 GHz vis-a-vis Radiometer 20 GHz are being studied. Comparisons were also made to the CCIR and Global prediction models using a JPL-developed propagation program [3]. Initial interest has also focused on the occurrence of deep (>10 dB) fades since this is of particular interest to system designers.

In the absence of a beacon tone, radiometer measurements may be the simplest method to track deep fades and apply power compensation algorithms. Of particular interest is both the short and long term correlation of measured beacon fade with radiometer sky temperature measurement.

System calibration is a critical issue and is currently in the final revision process. In the initial program stages, the system was periodically calibrated with hot and cold loads. The cold load was hood lined with radar absorbing material, cooled to liquid Nitrogen temperature and placed over the feed horn. Even though the calibration was done rapid-

ly, some water crystallization in the hood due to Florida's high humidity may have contributed significantly to an observed error buildup. This procedure was subsequently abandoned.

A semi-automatic hand editing program was used to do the initial preprocessing of the data. Diurnal variation is removed via a curve fitting routine. Each second of data was screened and marked as good or bad. Bad data consisted of artifacts, anomalous level jumps, system outage, operation in a non-calibrated mode or data taken during calibration cycles. A staggered 30 second calibration is made every 15 minute by switching in a noise diode on each channel.

FADE DISTRIBUTIONS

Figure 1 is an example of a 20/27 GHz fade event which exceeded the dynamic range (30 dB) of the system. The periodic signal dropouts are the noise diode calibration intervals which have been marked as bad by the pre-processing software. Individual fade events are culled out and subjected to an analysis for fade depths, fade duration and fade rate. One particular phenomenon observed in the Tampa area is the effect of morning ground fog. Even though the terminal sits atop a five story building and has a 52 degree elevation angle to ACTS, the effects are quite noticeable in the data.

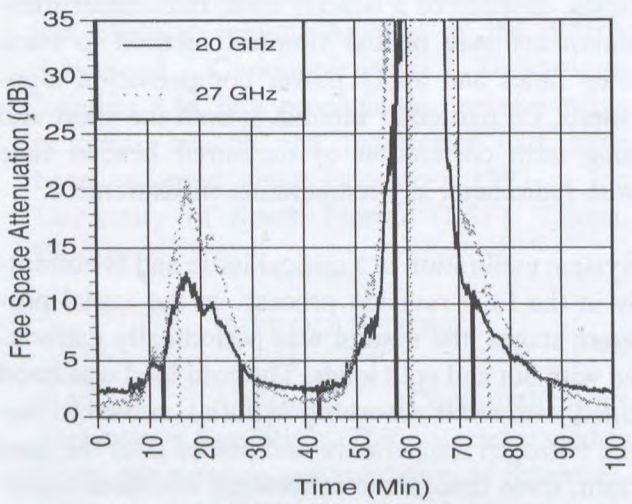

Figure 1 20/27 GHz Fade Comparison

This may be of particular concern to LEO systems which require reliable communication links at very low elevation angles.

Typical of what will become available are the statistics of the observed fades seen in the Summer of 1994. Shown in Figures 2 & 3 are the percentage of total time a fade exceeds the abscissa attenuation value and in Figures 4 & 5 the average fade duration for the abscissa attenuation values. During the summer, fades exceeding 10 dB and lasting several minutes occur almost 1% of the time. Since sub-tropical and tropical rain activity is fairly localized, this data underscores the value of having diverse terminal sites when high reliability is to be achieved[4].

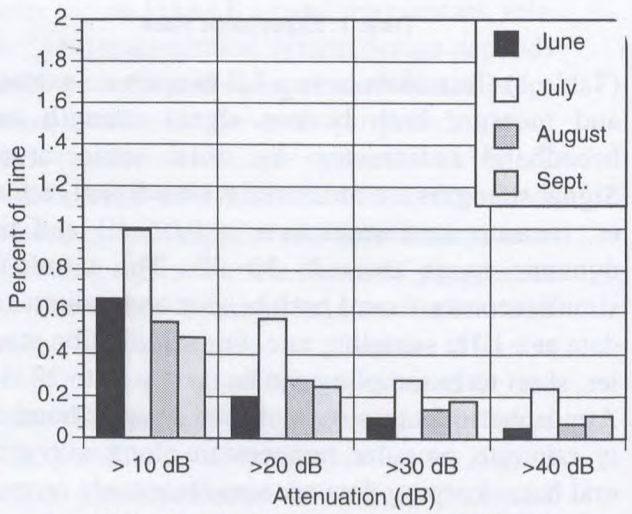

Figure 2 20.185 GHz Summer Fade Statistics

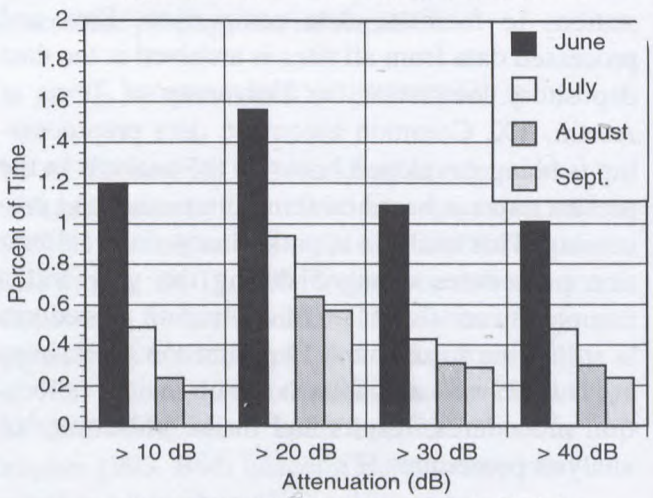

Figure 3 27.5 GHz Summer Fade Statistics

BEACON RADIOMETER CORRELATIONS

Beacon and radiometer data is processed on a 24 hour day to day basis. Long term diurnal averages are made during clear times which in turn aid in subsequent daily fits, especially during periods of weather activity. For small fades (< 10 dB), the beacon and radiometer data track well. On both short (seconds) and long (minutes), the amplitudes of beacon and radiometer signal correlate well.

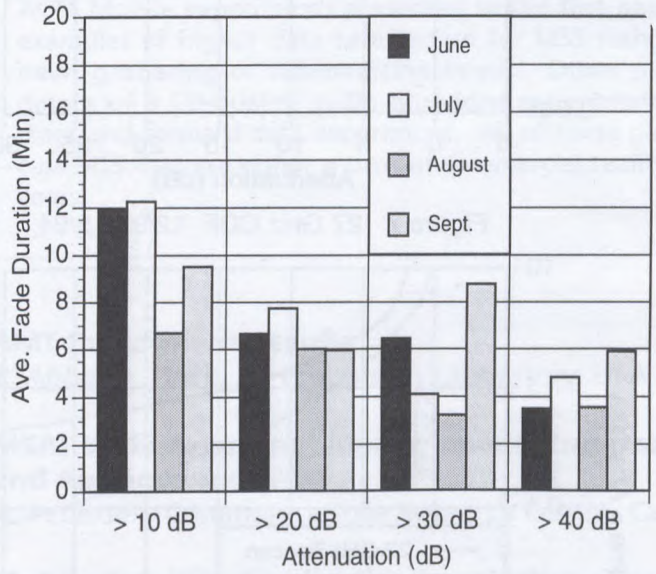

Figure 4 20 GHz - AVERAGE FADE DURATION

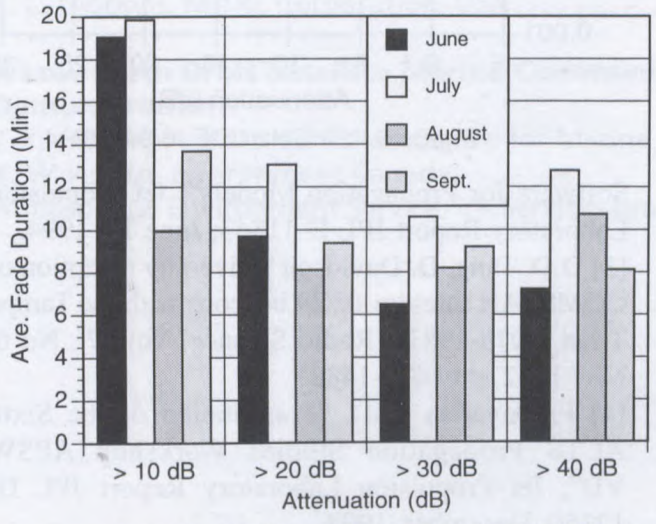

Figure 5 27 GHz AVERAGE FADE DURATION

CUMULATIVE DISTRIBUTIONS

One of the major ACTS Propagation Campaign products will be multi-year CDF's of fade statistics. This data will either validate existing global prediction models or lead to their revision. Figures 6 and 7 compare our first six months of 20 GHz and 27 GHz data (Dec - May) to predictions of the proposed CCIR model and agree reasonably well. However when summer only data (June - August) is considered, as shown in Figures 8 and 9, significant departure from CCIR prediction is seen. This may reflect the attempt to characterize Florida with a single rain region (N) which may be an oversimplification. The sub-tropical region may require more that one rain region specification depending upon the time of year.

CONCLUSIONS

The ACTS propagation measurements program has been accumulating data since December, 1993 at its sub-tropical site at USF in Tampa, Florida. Initial results are felt to be representative but not final, since complete calibration and analysis procedures are not fully in place. Data from the period June 1994 to August 1994, the Florida rainy season, exhibited numerous deep fades. For approximately 1% of the period, fades greater than 10 dB and of several minutes duration were observed. Fades of this magnitude are beyond the ability of forward error codes and illustrate the value of site diversity. The proposed CCIR model may be adequate for a yearly average but special consideration should be given to these intense rainy seasons. Radiometer data tracks beacon fade data well and offers the possibility of providing an input to signal power control algorithms in cases where there is an absence of beacon signals. The results presented here are based on a nine month analysis. The propagation program will hopefully continue for the entire lifetime of ACTS, another 4 years and thus should generate a good statistical

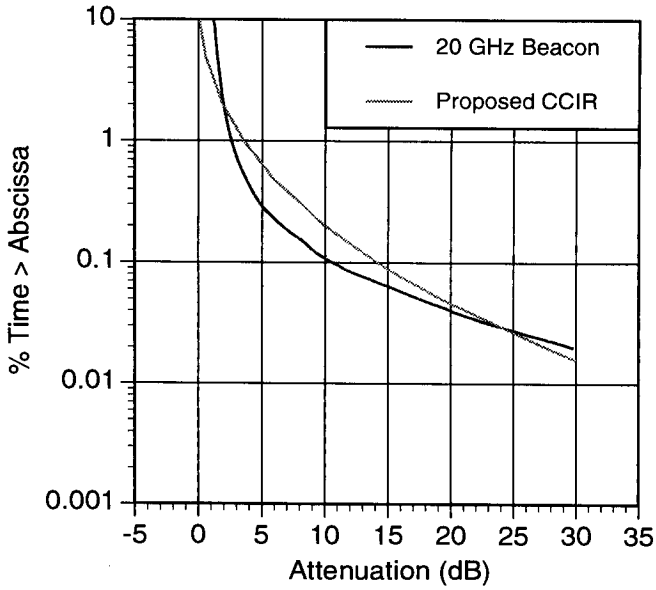

Figure 6 20 GHz CDF 12/93 - 5/94

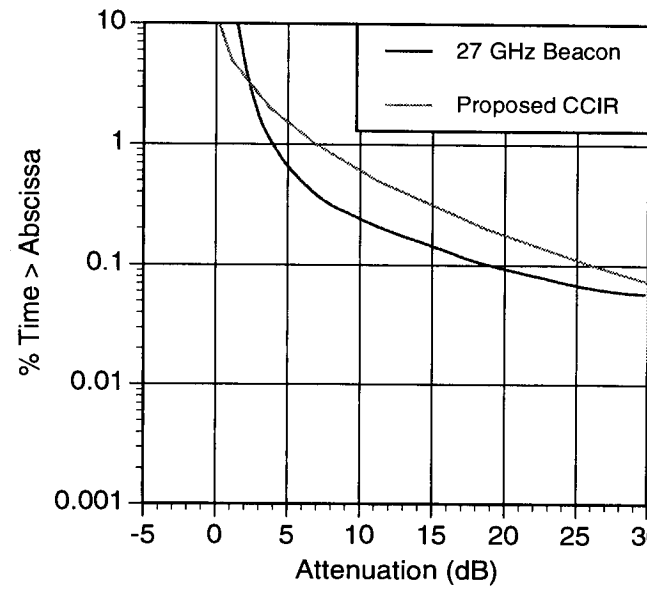

Figure 7 27 GHz CDF 12/93 - 5/94

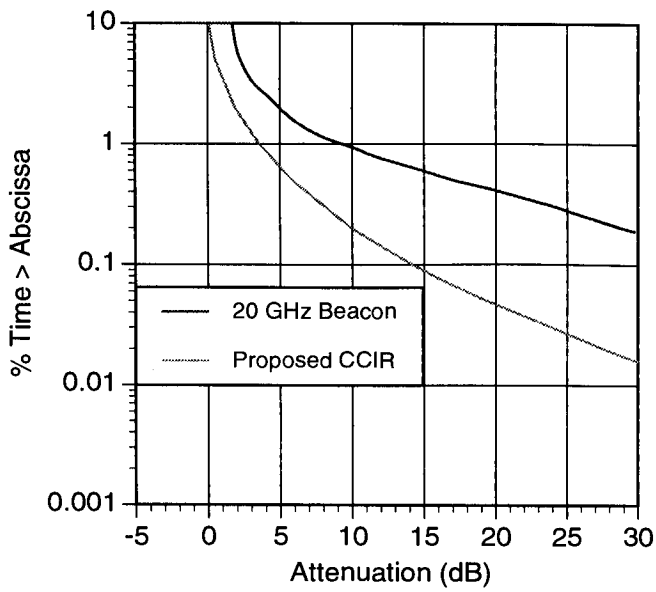

Figure 8 20 GHz CDF 6/94 - 8/94

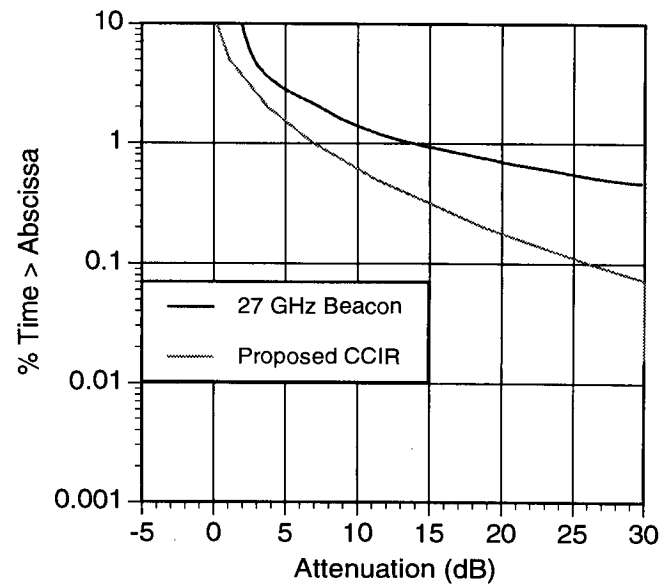

Figure 9 27 GHz CDF 6/94 - 8/94

basis for designing K/Ka band systems for sub-tropical regions, such as Florida

REFERENCES

[1] D.L. Wright, J.R. Balombin, P.J. Sohn, "Advanced Communications Technology Satellite (ACTS) and Potential System Applications", Proc. IEEE, July 1990, pp. 1165-1175

[2] A. Kantak, K. Suwitra, C. Le, "Database Software for Propagation Models", Jet Propulsion Laboratory Report JPL D-11843, June 15, 1994.

[3] D.D. Tang, D. Davidson "Diversity reception of COMSTAR satellite 19/29 beacons with the Tampa Triad, 1978-1981", Radio Science, Vol 17., No 6. Nov 1982, pp 1477-1488

[4] F. Davarian (Ed), "Presentation of the Sixth ACTS Propagation Studies Workshop (APSW VI)", Jet Propulsion Laboratory Report JPL D-12350, December, 1994.

Applications and Experiments - I

Session Chairman: **Bill Meder,** ORBCOMM, Canada
Session Organizer: **Brian Abbe**, Jet Propulsion Laboratory, USA

Topic Introduction: Current commercial mobile satellite systems provide mainly voice and dataservices. As mobile satellite services (MSS) have become more widely accepted, it is anticipated that new applications for MSS will be sought. The collection of papers presented in this session detail various experiments and demonstrations that ultimately could lead to many of these new application services. Through the ACTS Mobile experiments presented in the first paper of this session, one sees many examples of higher data rate service for MSS such as compressed video for satellite news gathering or telemedicine needs. Other papers in this session provide the details of a CD-quality audio broadcast experiment and a Low Earth Orbiting (LEO) store-and-forward data experiment. All of these papers presented in this session discuss MSS that are either a current commercial reality or potentially could be in a few years.

AMT Experiment Results

Mr. Brian S. Abbe and Ms. Deborah S. Pinck
Jet Propulsion Laboratory
California Institute of Technology
M.S. 238-420
4800 Oak Grove Drive
Pasadena, California 91109
Voice: (818) 354-3887 FAX: (818) 354-6825
e-mail: abbe@bvd.jpl.nasa.gov

ABSTRACT

The Advanced Communications Technology Satellite (ACTS) Mobile Terminal (AMT) experiments have provided a terminal technology testbed for the evaluation of K- and Ka-band mobile satellite communications (satcom). Such a system could prove to be highly beneficial for many different commerical and government mobile satcom users. Combining ACTS' highly concentrated spotbeams with the smaller, higher-gain Ka-band antenna technology, results in a system design that can support a much higher throughput capacity than today's commercial configurations. To date, experiments in such diverse areas as emergency medical applications, enhanced Personal Communication Services (PCS), disaster recovery assistance, military applications, and general voice and data services have already been evaluated. Other applications that will be evaluated over the next year include telemedicine, ISDN, and television network return feed. Baseline AMT performance results will be presented, including Bit Error Rate (BER) curves and mobile propagation data characterizing the K- and Ka-band mobile satcom channel. In addition, observations from many of the application-specific experiments will also be provided.

INTRODUCTION

Throughout the eighties NASA, through JPL, has been involved in the development and demonstration of system concepts and high risk technologies to enable the introduction of commercial mobile satellite services (MSS). This initial effort occurred at L-band (1.5 GHz), and currently commercial L-band MSS are available through a host of U.S. and international companies. It is expected that the present allocation for L-band MSS will become saturated by the turn of the century. In view of this, and the already existing non-MSS frequency allocations at other bands (C-, X-, and Ku-bands for example), NASA and JPL have focused on K- and Ka-bands for further expansion of MSS.

K- and Ka-bands have outstanding potential for higher data rate communications and more highly diversified MSS for a number of reasons. Unlike L-band, K- and Ka-bands have a significant amount of bandwidth (500 MHz at each K- and Ka-bands) already allocated for MSS services. Moreover, these higher frequencies can support antenna designs that while physically smaller than their L-band counterparts, can provide higher gain, often 10 dB or more. K- and Ka-bands, therefore, are excellent candidates for the pursuit of higher capacity services for commercial users (i.e., compressed video). However, satellite communication system design at these higher frequencies poses significant technical challenges including: a young technology with lossy RF components, significant rain attenuation effects, potentially large frequency uncertainties, and large Doppler shifts due to vehicular motion.

NASA has provided a platform for the initial evaluation and exploitation of K- and Ka-bands through their development of the ACTS. JPL's goal, through the use of ACTS and the development of the AMT, is to overcome these technical challenges with a system architecture and components that will exploit the potential benefits of such a migration from L-band. The final phase of this effort has been and continues to be the transfer of such technologies to interested groups within U.S. industry. By

directly involving U.S. industry in these experiments, NASA hopes to expedite the commercialization of this technology.

The remainder of this paper provides a brief description of the ground terminal equipment and it's baseline performance in a series of internal JPL experiments. Furthermore, an explanation of the various experiments with U.S. industry that have been conducted or are in the process of being planned will be presented. Finally, the experiment results to date will be provided.

AMT DESCRIPTION

The complete technical details and architecture of this terminal can be found in [1]. The AMT can be broken down into two broad divisions, namely, the baseband and microwave processors. The baseband processor consists of a speech codec, a modem, and a terminal controller (TC). Also included as part of this setup, strictly for experimental purposes, is a Data Acquisition System (DAS). The elements of the microwave processor are: the IF Converter (IFC), the RF Converter (RFC), the antenna controller, and the antenna.

The TC is the "brain" of the terminal. It contains the algorithms that translate the satcom protocol into operational procedures and interfaces to all of the other terminal subsystems. The TC is also responsible for providing the user with a system monitoring capability, and a variety of test functions during experimentation, such as bit stream generation and bit error rate (BER) calculations.

Two different modems have been used as part of the AMT. The baseline AMT modem, that was designed in-house, implements a simple yet robust DPSK scheme with rate 1/2 convolutional coding and interleaving. The performance specification for this modem is for a BER of 10^{-3} at an E_b/N_0 of 7 dB in AWGN. Further capabilities have been built into this modem to compensate for frequency offsets of up to 10 kHz with an additional performance degradation of only 0.5 dB. This modem is operational at 2.4, 4.8, and 9.6 kbps. The second modem that has been utilized as part of this setup is a commercially developed satcom modem that includes such features as coherent BPSK with convolutional coding, concatenated coding (Reed-Solomon), and interleaving. The performance specification for this modem is for a BER of 10^{-6} at an E_b/N_0 of 5 dB in AWGN. This modem is operational at data rates ranging from 9.6 kbps to 2.048 Mbps.

The vehicle antenna is the critical K-/Ka-band technology item in the microwave processor. The design of this antenna called for a "passive" elliptical reflector-type antenna to be used in conjunction with a separate high powered amplifier. Complete with a spherical radome, it stands approximately 5 inches in height, and is approximately 8 inches in diameter at its base. This antenna is fully tracking in azimuth, while manually positioned in elevation to one of five distinct settings.[1] Combined with a 10 W TWTA, this antenna system provides at least 32 dBW transmit EIRP on boresight. The 3 dB beamwidth is 12° in azimuth and 18° in elevation. Receive specifications for this antenna have been set at -5 dB/°K, once again on boresight.

The antenna pointing system enables the antenna to track the satellite for all practical land-mobile vehicle maneuvers. The antenna is mated to a simple, yet robust, mechanical steering system. A scheme wherein the antenna is smoothly dithered about its boresight by about a degree at a rate of 2 Hz is used. The pilot signal strength is measured through this dithering process, and is used to compliment the inertial rate sensor's information. This information allows the antenna to track the satellite while experiencing a shadowing event of up to 10 seconds in duration.

Preceding (or following) the antenna, the RFC converts an IF signal around 3.373 GHz to (from) 30 (20) GHz for transmit (receive) purposes. The IFC translates signals between 3.373 GHz and a lower 70 MHz IF at the output (input) of (to) the modem. A key function of the IFC is pilot tracking and Doppler compensation (for the return communications link).

[1] These five settings allow for complete elevation coverage for the continental United States.

AMT BASELINE TEST RESULTS

BER Results

The initial baseline AMT tests collected fall into two categories: (1) terminal performance characterization (utilizing the baseline AMT modem) and (2) mobile satcom K- and Ka-band propagation characterization. Complete details of these tests can be found in [2]. The single best method for determining the terminal's performance were accomplished through a series of stationary BER tests. The test setup for the baseline system performance is provided in Figure 1. A set of baseline BER tests were performed from the fixed terminal (FT) to the mobile terminal (MT). PN sequence data was transmitted from the FT's Terminal Controller (TC) and a final BER was determined at the MT's counterpart. The E_b/N_o value was determined by the E_b/N_o box prior to and after the actual transmission of the PN sequence, once again using an unmodulated data signal. These two values were then averaged for the test run. This test was performed for all three of the lower operational data rates of the AMT (2.4/4.8/9.6 kbps). Four different E_b/N_o values were recorded for each data rate corresponding to final BER values ranging between approximately 10^{-5} and 10^{-1}. Several test conditions were established at the beginning and maintained throughout these tests to ensure consistent results. They are as follows: (1) the van was stationary, (2) the van's engine was turned off to minimize external noise sources (3) the power used in operating the terminal was supplied by the AC generator, (4) the mobile terminal's antenna pointing was accomplished in the manual mode to minimize any sources of error due to pointing (dithering), and (5) no pilot signal was transmitted to minimize the effects of intermodulation on-board the satellite.

The results of these BER tests for 9.6 kbps, 4.8 kbps, and 2.4 kbps are provided in Figures 2, 3, and 4, respectively. For comparison purposes, the pre-satellite test results, which utilized a satellite simulator, have also been included. These are listed as Xlator in the figures. Both of these results agree to within experimental error (0.25 dB or less) with each other. For terminal operation at a 9.6 kbps data rate, an E_b/N_o of 6.8 dB is required to achieve a BER of 10^{-3}. For the 4.8 and 2.4 kbps cases, this performance level is achieved for an E_b/N_o level of 6.7 and 8.5 dB, respectively. The significantly larger E_b/N_o requirement for the 2.4 kbps case can be attributed to higher sensitivity to system frequency offsets at this data rate.[2]

Propagation Test Results

The objectives of the mobile propagation experiments were to measure and analyze the fading characteristics of the K- and Ka-band channel. The analysis involved examining multipath, shadowing and blockage effects. Field tests were conducted in various environments; results presented here include 1) rural freeway runs free of obstructions except for occasional overpasses and 2) shadowed suburban runs with occasional obstructions from buildings, utility poles, and trees. Additional information on the propagation test results can be found in [3].

Data from the first category, that is rural freeway runs, was collected on Interstate 210 between California State Highway 2 and California State Highway 118. This is 15 mile east-west span. A map of this route is provided in Figure 5. The bolded path was the experimental route. A representative time series of the pilot power transmitted by the fixed station and received the AMT is shown in Figure 6. The statistics of the shadowing/fading are summarized by a histogram of the cumulative distribution of the pilot power received at the AMT. The histogram of the run shown in Figure 6 is provided in Figure 7. It can be seen that the 1% fade level for the 20 GHz channel is 1dB. This is typical for a clear line-of-sight (LOS) channel.

Data from the second category, that is a shadowed suburban run, was collected on the roads the circle the Rose Bowl in Pasadena, California. A map of this route is provided in Figure 8. The bolded path was the experimental route. The road is surrounded by rolling hills with substantial amounts of foliage. Figure 9 shows the time series for a test run around the Rose

[2] Residual frequency offsets in this particular system setup have been calculated to be several kHz in a worst case scenario.

Bowl. The statistics of the shadowing/fading are summarized by the histogram in Figure 10 where it is seen that the 1% fade level for the 20 GHz channel is 25dB. This corresponds to a moderately shadowed suburban environment.

The shape of each histogram is typical for mobile satellite channels. The slope from the reference level to 2-3 dB below is steep and consistent with a Ricean characteristic. A transition region, or "knee" (at 3-5 dB fade levels) precedes a less steep curve for deeper fades. This shallow curve is characteristic of heavy shadowing. These characteristic curves have also been observed on other K-band propagation experiments [4].

AMT EXPERIMENTS

As part of the ACTS Experiments Program, JPL has been given the task of seeking out useful applications for K- and Ka-band mobile satcom and to further demonstrate these capabilities through ACTS and the AMT. To date, twelve different experimenters involving several different government agencies, U.S. industrial interests, and academia have been officially approved to experiment with ACTS and the AMT by NASA Headquarters and the ACTS Project Office at NASA LeRC. The experiments period began in December 1993 and will continue for at least two years through November 1995. A summary of the mobile experiments is presented in Table 1. Many other experiments are still in the formative stage. Applications-oriented experiments and demonstrations in such areas as emergency medicine, personal communications (PCOMM), disastery recovery, military communications, telemedicine, direct broadcast, and satellite news gathering (SNG), have been or will be demonstrated.

It is clear that these applications for mobile satcom will result in a better overall quality of service within their respective fields. In fact, some of these applications could be offered with current commercial mobile satcom systems. The ACTS/AMT experiments that were conducted in emergency medicine and personal communications [5] could be supported today with existing commercial service (e.g., Inmarsat, AMSC) as they are low-bandwidth services. These experiments were conducted strictly to investigate the viability of offering these services via satellite. Other experiments would require an ACTS-like (higher capacity) K- and Ka-band system to fulfill their needs. Further explanations on aeronautical mobile applications for K- and Ka-band may be found in [6]. The remainder of this section will focus on the satellite news gathering and telemedicine experiments.

NBC SNG Experiment

Current communication capabilities for mobile satellite news-gathering are limited to cellular telephone service (where available). Furthermore, while communications can typically be expanded to include video capabilities once the SNG van is stationary, the setup is rather large and unwieldy. Utilizing ACTS and the AMT, a series of experiments and demonstrations were accomplished which overcame both of these deficiencies. A picture of the experimental van parked side by side with a typical operational SNG van is provided in Figure 11 (the experimental van is the one on the left). Note the tremendous size difference between the two vehicles' antennas. In addition, there is effectively no setup time required for the AMT.

Full-duplex compressed video communications at data rates up to 768 kbps, both fixed and mobile, was established between an experimental van located in the greater Los Angeles area and a fixed station located at NASA LeRC in Cleveland, Ohio. The communications link was further enhanced by terrestrially connecting (via a fractional T1 data line) the fixed station with NBC New Headquarters, New York. Two different types of video codecs were used in this experiment: ABL's VT2C and NEC's VisuaLinks 5000EX. Both of these video codecs worked well under the conditions that were experienced over the mobile satcom link.

University of Washington Medical Center Telemedicine Experiment

Vast regions of the United States do not have access to recent advances in medical technology. This particular experiment will link rural America to these technologies by connecting them to metropolitan areas and

research hospitals associated with many universities. Specifically, the University of Washington Medical Center, known for their capabilities and advances in radiology, will be linked to various locations throughout the northwestern United States via ACTS and the AMT. This experiment is scheduled to take place during the summer of 1995. The data rates that are targeted for this experiment are 64 kbps and 128 kbps. The NEC VisuaLinks 5000EX will be utilized. One particular objective for these tests to evaluate is the quality of a transmitted 64 kbps or 128 kbps still image for reliable medical diagnosis. Medical applications such as X-Rays, Magnetic Resonance Images (MRI's), and Computed Tomographies (CT's) will be evaluated.

SUMMARY

The development of ACTS and the AMT have been an excellent proof-of-concept technology testbed for K- and Ka-band mobile satcom. Through this work, many advancements have been made in the area of mobile satcom (i.e., several high gain, directional, tracking antenna schemes, a novel Doppler estimation and correction algorithm, etc.). Initial tests with the AMT suggest that this terminal's performance meets or exceeds that expected of the initial design. Through these developments, and the influx of experimenters with this equipment, it is hoped that NASA and JPL are contributing to the U.S. industrial community's technological advantage in this highly competitive field.

REFERENCES

[1] Dessouky, K. and Jedrey, T., "The ACTS Mobile Terminal (AMT)," Proceedings of the 14th AIAA Conference, March 22-26, 1992, Washington, D.C.

[2] Personal Experiment Notes, December 6, 1993.

[3] Rice, M. and Pinck, D., "K-Band Mobile Satellite Propagation Characteristics Using ACTS, URSI, Boulder, Colorado, January 1995.

[4] J. Goldhirsh and W. Vogel, "ACTS Mobile Propagation Campaign," Proceedings of the 18th NASA Propagation Experimenters Meeting, ppg. 135-150, Vancouver, British Columbia, June 1994.

[5] Pinck, D., Tong, L., McAuley, A., Kramer, M., "Satellite-Enhanced Personal Communications Experiment," International Mobile Satellite Conference 1995, June 6- 8, Ottawa, Canada.

[6] Agan, M.J. and Densmore, A.C., " ACTS Broadband Aeronautical Terminal," International Mobile Satellite Conference 1995, June 6 - 8, Ottawa, Canada.

ACKNOWLEDGEMENTS

The research described in this paper was carried out by the Jet Propulsion Laboratory, California Institute of Technology, under contract with the National Aeronautics and Space Administration.

Table 1 ACTS Mobile Experiments Summary

EXPERIMENT	PRINCIPAL INVESTIGATORS
Land-Mobile, Phase I	JPL
Emergency Medical	EMSAT Corporation
Secure Land-Mobile, Phase I	NCS
Comm-on-the-Move	U.S.. Army CECOM
Aero-X	NASA LeRC
Satellite/Terrestrial PCN	Bellcore
Satellite News Gathering	NBC
High Quality Audio Broadcast	CBS Radio, CCS
Telemedicine	Univ. of Washington Medical Center
Land-Mobile, Phase II	JPL
Secure Land Mobile, Phase II	NCS, JPL
Unmanned Ground Vehicle	ARPA

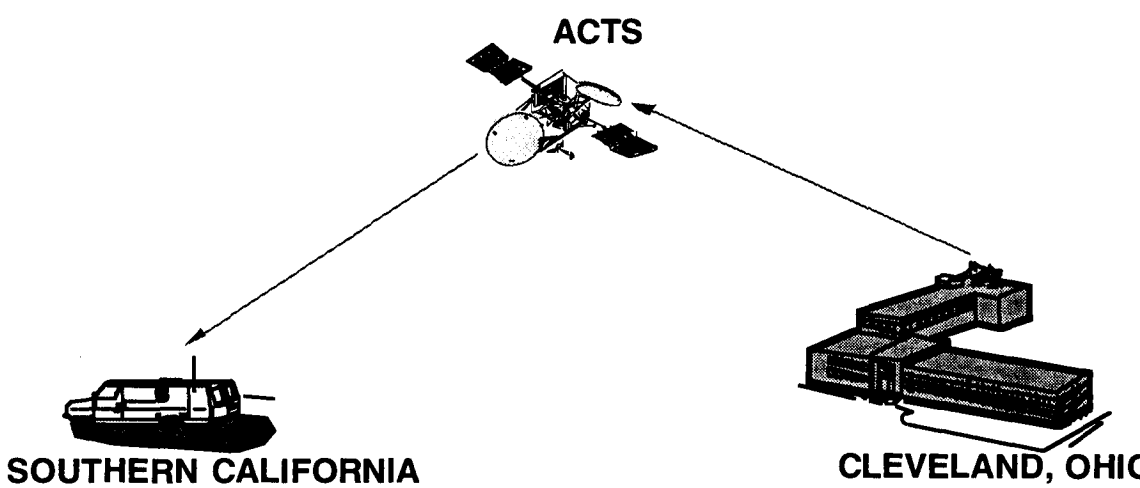

Figure 1 Baseline AMT System Performance Test Configuration

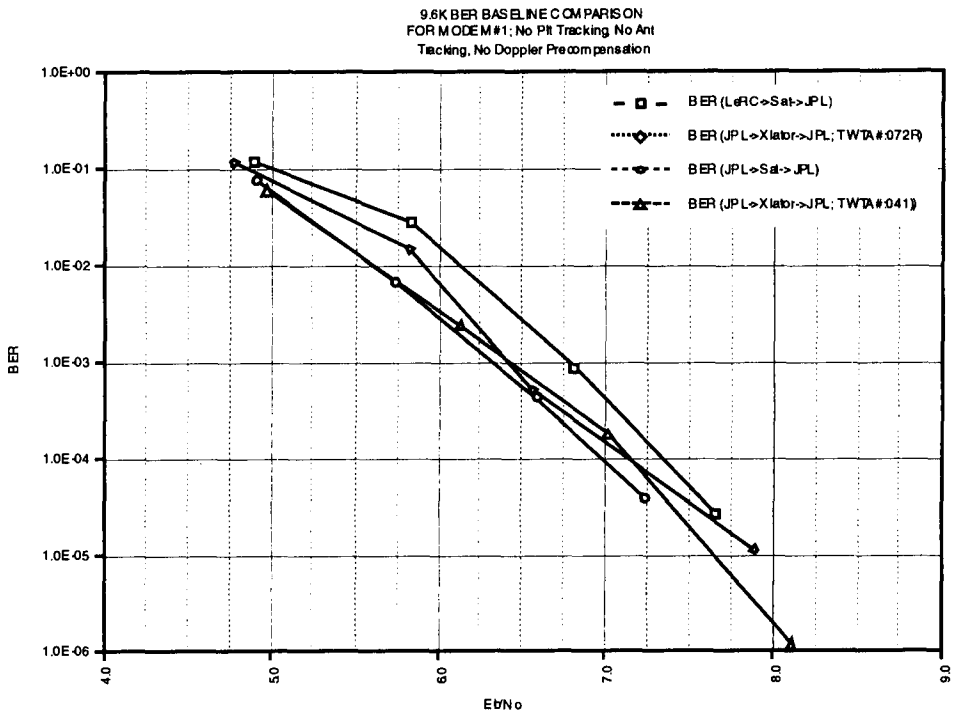

Figure 2 9.6 kbps BER Test Results

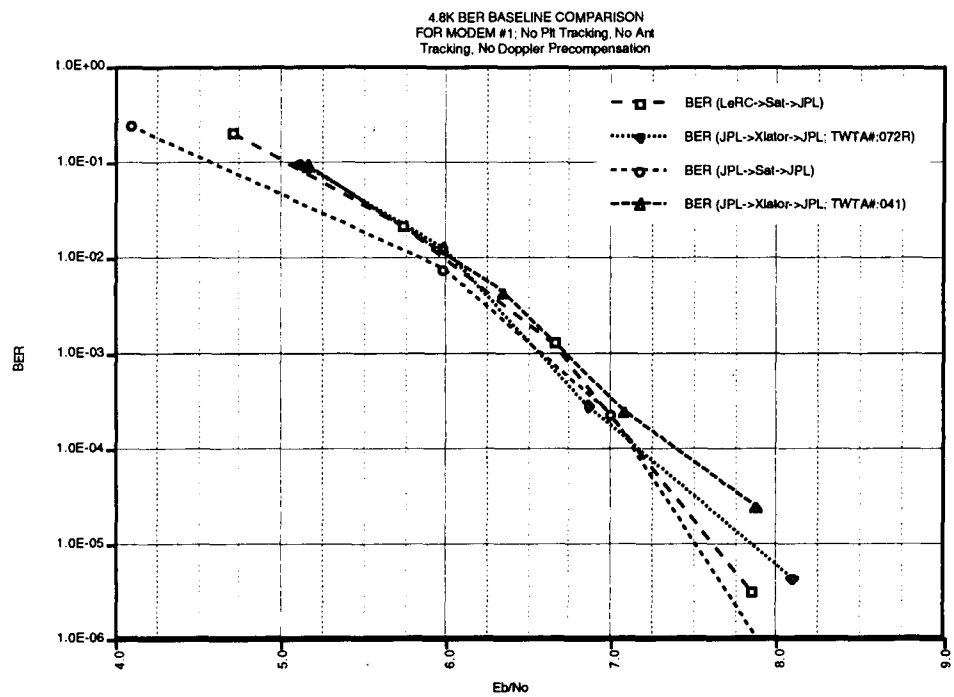

Figure 3 4.8 kbps BER Test Results

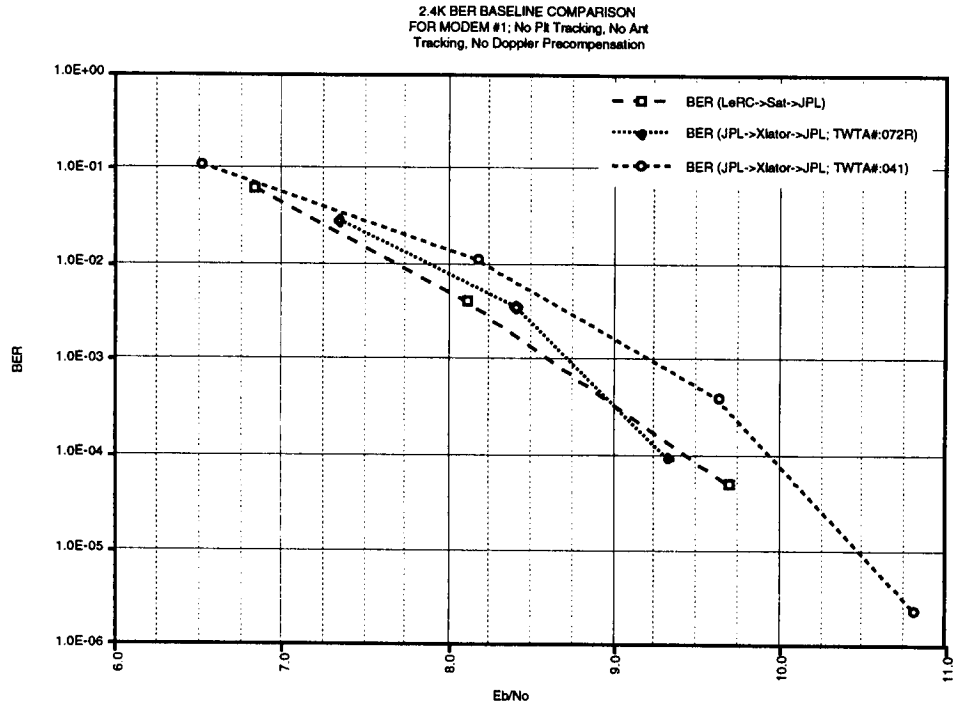

Figure 4 2.4 kbps BER Test Results

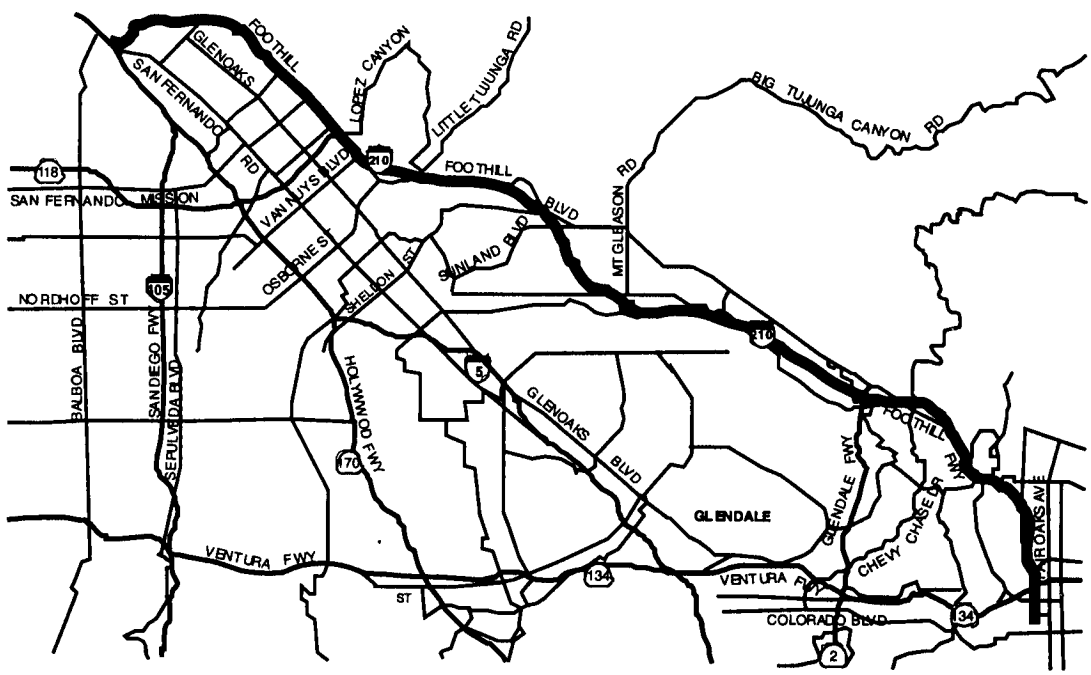

Figure 5 Interstate Propagation Test Route

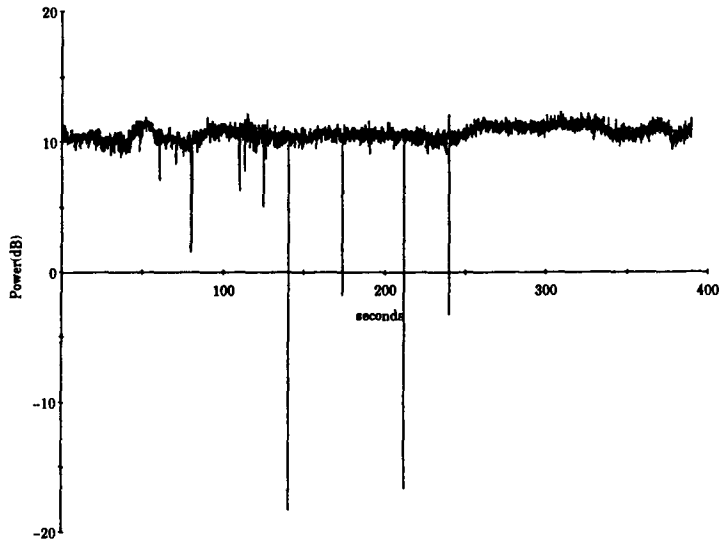

Figure 6 Typical Propagation Data from Interstate Test Route

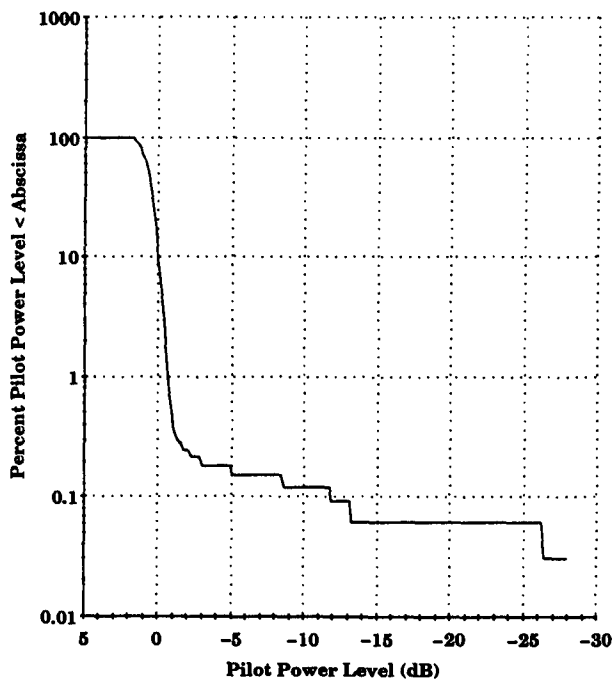

Figure 7 Interstate Test Route Cumulative Fade Distribution

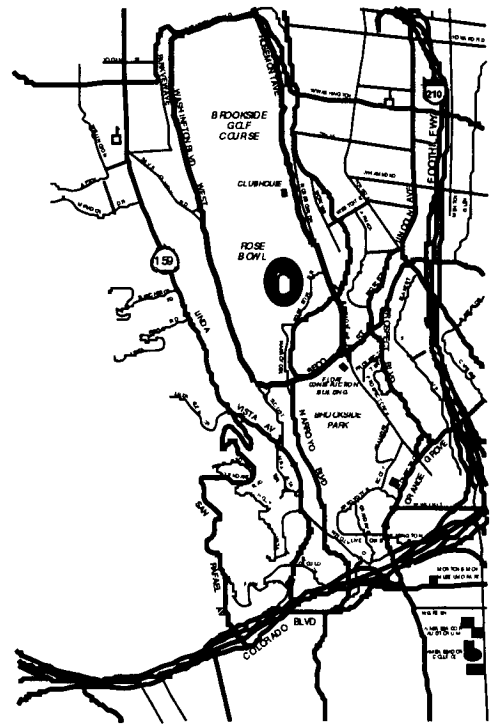

Figure 8 Surface Street Test Route

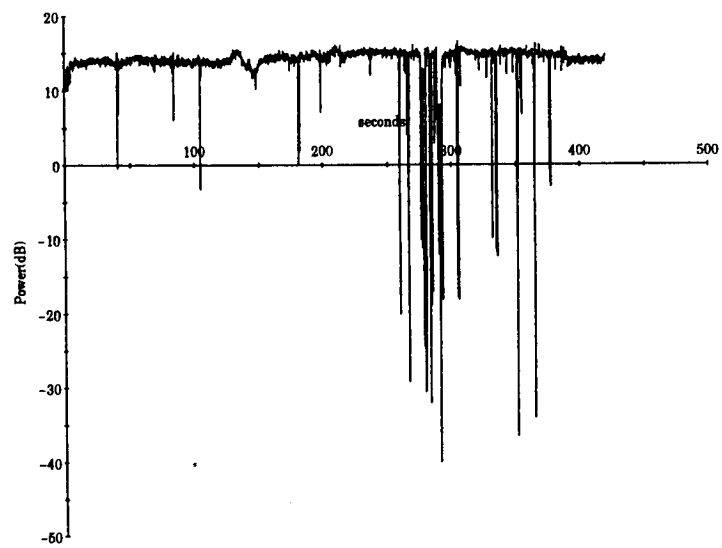

Figure 9 Typical Propagation Data from Surface Street Test Route

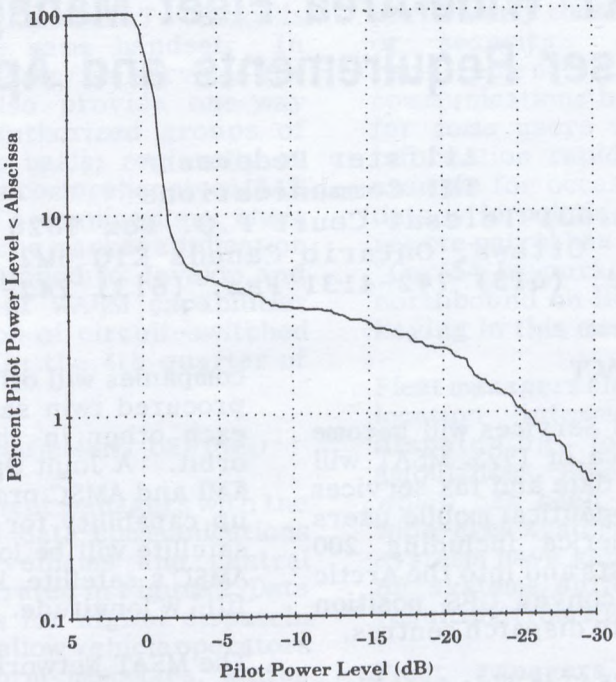

Figure 10 Surface Street Test Route Cumulative Fade Distribution

Figure 11 Antenna Size Comparison Between SNG Van of Today and Tomorrow

MSAT Wide-Area Fleet Management: End-User Requirements and Applications

Allister Pedersen*
TMI Communications
1601 Telesat Court P.O. Box 9826
Ottawa, Ontario Canada K1G 5M2
Phone: (613) 742-4131 Fax: (613) 742-4100

ABSTRACT

MSAT™ (Mobile SATellite) Services will become a reality in North America in 1995. MSAT will provide wide-area voice, data and fax services to land, marine and aeronautical mobile users anywhere in North America including 200 nautical miles off the coasts and into the Arctic waters. MSAT will also convey GPS position information from mobiles to dispatch centres.

One broad application of MSAT is Wide Area Fleet Management (WAFM). This paper defines WAFM, outlines end-user requirements and identifies potential applications of MSAT WAFM. The paper draws from information obtained in several pre-MSAT WAFM field trials in land, marine and aeronautical mobile environments. The paper concludes with an outline of the potential benefits of MSAT WAFM.

INTRODUCTION

In the late 1960's, the Government of Canada commenced work on the MSAT program at the Communications Research Centre (CRC) in Ottawa. The CRC-led project also involved cooperation with NASA in the United States. In 1988 the lead for the MSAT project moved from government to the private sector. TMI Communications, a BCE Inc. business, is the Canadian MSAT Network™ operator now working with authorized service providers to deliver MSAT services for government (federal, provincial, municipal) and private sector end-users located throughout North America, Central America and the Caribbean.

MSAT NETWORK

TMI Communications and Company, Limited Partnership (TMI) is the designated MSAT Network operator in Canada. American Mobile Satellite Corporation (AMSC) is the mobile satcom operator in the United States. The two companies will offer similar services and have procured twin satellites that will be close to each other in the geosynchronous satellite orbit. A Joint Operating Agreement between TMI and AMSC provides restoration and back-up capability for each satellite. TMI's MSAT satellite will be located at 106.5° W longitude; AMSC's satellite, known as AMSC-1, will be at 101° W longitude.

The MSAT Network provided by TMI offers an unprecedented range of wireless digital voice and data communications services covering Canada, the United States, Central America, the Caribbean and off-shore coastal regions. The network consists of a geostationary satellite and a central control and switching facility. Subscribers access the network using compact, feature-rich mobile, fixed and portable radios called MSAT Communicators™ [1,2,3]

TMI manages the satellite's large pool of approximately 1800 demand-assigned 6.4 kbps digital communications channels, as well as voice and data switches in the control and switching facility. These switches manage calls and provide interconnection with the public switched telephone network (PSTN), public packet switched data networks (PSDN) and private networks. Figure 1 shows the MSAT Network.

Generic Service Offerings

The Network supports the following five types of narrow band communications:

- Telephone calls
- Group voice calls (dispatch radio similar to trunk radio [4])
- Fax calls
- Circuit-switched data calls
- Packet switched data calls.

One option is dual-mode MSAT/cellular operation whereby cellular and MSAT voice calls can be made using the same handset. In addition to 2-way voice/data/fax services the MSAT Network can also provide one-way broadcast services to authorized groups of mobiles on a geographic basis; regionally or continent-wide. With this comprehensive MSAT Network offering, TMI Communications, their Service Providers and niche market application developers are well positioned to develop and deliver a broad range of WAFM capabilities following the introduction of circuit-switched voice and data services in the 4th quarter of 1995.

WIDE AREA FLEET MANAGEMENT DEFINED

MSAT WAFM will provide fleet managers with the capability for voice and data communications between a fleet(s) of vehicles and central dispatch centres as illustrated in Figure 2. Data communications provides for digital dispatch. Data communications will allow vehicle operators to compile and send form messages, status codes, emergency alerts and free-form text messages. It will also be possible to interface MSAT Communicators with GPS receivers and vehicle status monitoring systems.

The transmission from mobiles of status codes and GPS position reports will allow dispatchers to select, either manually or automatically, the most appropriate mobile needed for a specific task from the perspective of location and status of all vehicles in the fleet or sub-fleet. The transmission of emergency alerts provides for increased safety of mobile personnel and improved monitoring of high value cargo.

END-USER REQUIREMENTS

General Requirements

There is strong interest in MSAT WAFM from a broad range of users in the commercial and government sectors embracing the land, marine and aeronautical mobile communities.

Government and commercial fleet managers are increasingly moving towards digital data communications from the traditional analog voice dispatch and fleet management systems. End-users require wide-area "seamless" fleet management where wide-area for some users may be defined as all of North America. While many fleets are moving away from inefficient analog voice dispatch systems to full digital data dispatch, some organizations insist on having both voice and data capabilities, particularly those involved with public safety or security. Most fleet management requirements are satisfied by data communications but optional voice is essential for some users with a requirement to pass information rapidly and easily. An obvious example for occasional voice in preference to data is in policing where a single officer on a remote patrol has an obvious preference to say "Car 54 in pursuit of a late model...heading northbound on Hwy 97 at 120 ..." rather than keying in this message on a keypad.

Fleet managers also require status and position location information whether they are dispatching long-haul trucks or air ambulances. Fleet managers want reliability which has been difficult to achieve in some wide-area systems where VHF/UHF terrestrial systems have gaps in their coverage or where HF systems suffer from reliability problems resulting from HF propagation variations.

Fleet managers want the full range of capabilities available with "intelligent" digital dispatch systems. Dispatchers want the capability to specify the number of re-tries if a message doesn't get through on the first attempt and/or the opportunity to be notified within a certain period of time if the message is not automatically or manually acknowledged.

Requirements in the Mobile

In order to acquire mobile status information fleet managers want the capability to interface the MSAT Communicator or transceiver with on-board vehicle information systems. Such systems might be an on-board computer in a long haul tractor unit that monitors RPM, speed and trailer temperature in a refrigerated trailer. Or the onboard system might be a flight management system in an aircraft.

In addition to acquiring status information automatically, fleet managers require mobile systems that allow vehicle operators to easily select and transmit a variety of user-defined status codes that indicate the status of the vehicle, e.g., "fully loaded-in transit", and also the driver status, e.g., "out of vehicle".

Dispatch Centre Requirements

Fleet managers are becoming more knowledgeable and more demanding as digital fleet management capabilities expand in the existing terrestrial and satcom infrastructures.

Dispatchers are demanding much more than the simple presentation of data from fleets. Dispatchers want systems that provide some value-added. Rather than simply having a list of truck locations, status, and available capacity they want systems that will manage all of this information. When an order comes in for a pickup they want a system that will respond to a query that states, "Identify the closest available tractor/trailer heading West through Winnipeg to Vancouver that has 500 kg capacity in a refrigerated trailer".

Text-only dispatch systems will satisfy many end-user requirements but graphics-based dispatch systems that display the locations of mobiles overlaid on a geographic map display are increasingly in demand. In some applications "one picture (graphic) is worth a thousand words". Forest-fire fighting is one application where graphics displays would be beneficial. The graphics display would show the location of all MSAT fleet members including water bombers, spotter aircraft and aircraft involved in evacuations of threatened communities. Other MSAT fleet members displayed on the graphics display might be transportable terminals at "fixed" sites and land mobiles providing support. The graphic display could illustrate the perimeters of the fire, hot spots and areas that have been water-bombed. Dispatchers want the capability to display the historical track of mobiles for selected intervals. This applies to applications as diverse as displaying the tracks of search and rescue vessels and snowplowing in remote areas.

End-users also want dispatch systems that can provide information to or accept information from other in-house management information systems. An example would be an MSAT WAFM system that provides information to a fleet management maintenance system. The MSAT WAFM could provide information on the number of kilometres driven or hours flown to a maintenance database that in turn notifies the dispatcher and/or vehicle operator that maintenance is required within so many kilometres or hours of service.

Special Requirements

Some special requirements have been identified by potential users of MSAT WAFM. Some end-users require the capability to have different position reporting intervals for individual mobiles within a fleet and the capability to modify position reporting intervals "on-the-fly" for individual mobiles. Other fleet managers (e.g., rescue organizations) may want the capability to "establish a fleet" for the duration of a Search and Rescue (SAR) incident that includes members of its usual operational fleet and other ships/aircraft that are MSAT-equipped and able to participate in the SAR incident. Some end-users want their MSAT WAFM dispatch centre to provide "emergency notification" when regularly scheduled position reports are not received.

The standard positioning service associated with GPS (100 meters horizontal accuracy) is more than adequate for most applications. Some marine and aeronautical users may however require accuracies in the order of 1 to 10 meters. This requirement could be met by using the MSAT Network for the dissemination of correction factors (and integrity information), in other words WADGPS (Wide Area Differential GPS).

POTENTIAL APPLICATIONS

MSAT WAFM has applications in the land mobile community for courier companies, public safety agencies and even remote school bus fleets. Marine and aeronautical fleet management applications include the tow-boat industry, fishing vessels, ferries and general aviation.

Trucking

Potentially the largest market for MSAT WAFM is trucking. Depending on the operators, the application may range from regional fleet management requiring simple digital dispatch to fleets requiring seamless North American coverage and the full range of communications options; voice, data, fax and position location. Simple digital dispatch would satisfy commercial requirements most of the time. The voice option provides the trucker with the opportunity to enter into a discussion with dispatch about complex maintenance problems or contact his family using the alternate account billing option for personal use of the MSAT Communicator. Systems may be stand alone or may be integrated with other corporate MIS systems for maintenance and tracking of shipments for shippers and consignees.

Courier Fleets

Courier fleets operating beyond the range of terrestrial fleet management radio systems are ideal candidates for MSAT WAFM. Wide-area mobile satcom fleet management provides the

opportunity for digital dispatch, vehicle tracking and emergency reporting through the use of a panic button. Modern digital dispatch systems such as the Ultimateast Data Communications FLAG™ (Fleet Locating and Graphics) system used in pre-MSAT trials allows fleet managers to assign vehicles to routes. FLAG dispatch can convert GPS-based position reports from lat/long format to position reports referenced to cities or other reference points along routes to which each vehicle is assigned. The dispatch system can be configured to initiate audible and visual alarms when regularly scheduled position reports are not received or to raise an alarm when an emergency coded message is received. These support tools provide benefits for armoured vehicles engaged in the transport of high value cargo or in hazardous goods.

Marine Fleets

Potential end-users of MSAT WAFM in the maritime community include tugs, passenger ferries, cargo ferries, coastal freighters, fishing companies and government fleets for policing, fishery patrols and coast guard activities.

Federal government applications are perhaps the most varied and complex of all those in the maritime sector. Within the government sector search and rescue (SAR) provides the most demanding and potentially one of the most beneficial applications.

Search and Rescue

Marine SAR is primarily undertaken by Canadian Coast Guard vessels with support as required from RCMP, Fisheries and Oceans, DND and any other vessel that may be in a position to lend support. Coordination and management of a major offshore SAR incident could involve significant benefits under a scenario where all offshore government vessels are MSAT-equipped and utilizing MSAT WAFM.

In terms of the initial response by the RCC (Rescue Coordination Centre), the RCC could immediately determine the locations of all government vessels in the immediate area, assuming a cooperative arrangement where the RCC has access to position reports from all government vessels. (Ideally the RCC could also be provided with the positions of all MSAT-equipped vessels; government and commercial vessels alike. Commercial fishermen may initially express concerns about confidentiality of their fishing spots but MSAT-equipped fishing vessels could be major beneficiaries of improvements in SAR).

For the duration of a specific SAR incident, a "SAR fleet" could be identified and tasked directly by the RCC providing a high level of coordination and sharing of information among members of the SAR fleet. For those vessels that participate in various forms of grid searches, the position reporting intervals could be increased from the relatively infrequent reporting intervals for daily operational activities to frequent position reporting that would provide the RCC with one single, accurate, combined graphic picture of the overall area searched when all position reports are displayed for a specific duration.

Aeronautical

Discussions with prospective aeronautical users of the MSAT Network identify aircraft location as one of the single most important requirements. This has been identified as a priority by provincial air ambulance operators, provincial ministries of natural resources and helicopter companies. A pre-MSAT aeronautical mobile data trial [5] with the Ontario Ministry of Natural Resources identified the pre-MSAT flight following service as a significant improvement over their existing flight following system involving voice calls every 30 minutes. In some cases aircraft would have to climb from a working altitude of 500' to 6,000' before a communications link could be established. Approximately 50% of the flying by the Ontario Ministry of Natural Resources is undertaken at altitudes of 500' and the automated pre-MSAT flight following trial provided the dispatch centre with more frequent position reporting and more accurate position reporting with fewer resources. The flight following can be implemented with only one central dispatch centre, with minimal or no ongoing involvement of a dispatcher and without any involvement of flight deck crew and no requirement to climb to a "communications altitude".

Operators of helicopter fleets look to MSAT for position information as well but also as an opportunity to file daily billings from aircraft which may be away from a base and telecommunications services for weeks or more at a time. Without Wide Area Fleet Management, valuable time is often lost when mechanical problems develop and there is no ability to contact the company base until a relay is

established with an overflying aircraft or a search effort is launched.

Rural School Bus Fleets

It is not uncommon these days for urban bus fleets to be equipped with terrestrial-based fleet management systems ranging from straightforward voice dispatch systems to digital dispatch systems offering position location. In rural areas of Canada some school busses operate on long rural routes unserved by radio systems. In some cases rural school busses without 2-way radio communications are cancelled when there is extreme cold. While not a fleet management application in the traditional sense, an MSAT-equipped rural school bus would have the capability for emergency communications and the transfer of position location information. While safety benefits would be significant, the ongoing operating costs would be low with minimal requirement to use the system on a daily basis.

BENEFITS OF MSAT WAFM

The benefits of MSAT Services in particular over all other existing services are:

-the improved North America-wide coverage
-the comprehensive range of service offerings that include not only circuit-switched data and packet-switched data but also telephone, one to many dispatch radio, fax and cellular from a single mobile radio installation.

In general MSAT WAFM provides the opportunity for:

-better coverage
-decreased operating and maintenance costs
-increased communications security by using data instead of voice
-high reliability and availability
-improved fleet response time
-minimal investment because TMI Communications owns and manages the network
-increased safety

REFERENCES

[1] **R. Martinson,** *Enhanced Performance of the Westinghouse Series 1000 Mobile Satellite Telephone System,* presented at IMSC '95, Ottawa, Canada, June 6-8, 1995.

[2] **T. Fuji, M. Tsuchiya, Y. Isota and K. Aoki,** *Design and Performance of Mobile Terminals for the North American MSAT Network,* presented at IMSC '95, Ottawa, Canada, June 6-8, 1995.

[3] **C. Sutherland and J.T. Sydor,** *MSAT Aeronautical Mobile Satellite Communications Terminal Development,* presented at IMSC '95, Ottawa, Canada, June 6-8, 1995.

[4] * **J.W. Jones,** *Specialized Mobile Radio Spans the Continent:The Reach of MSAT Trunked Radio,* presented at IMSC '95, Ottawa, Canada, June 6-8, 1995.

[5] **A.V. Pedersen,** *Canadian Aeronautical Mobile Data Trials,* Proceedings of International Mobile Satellite Conference 1993, pp.219-224

The services and capabilities described here are available once the MSAT Network becomes fully operational. Capabilities are subject to change.

*The author is on secondment from Industry Canada, Communications Research Centre.

* Ref [4] J.W. Jones is now entitled MSAT Broadcast Voice Services, and is to be found on page 401
Ref [1] R. E. Martinson: paper is to be found on page 359
Ref [3] C. A. Sutherland: paper is to be found on page 256

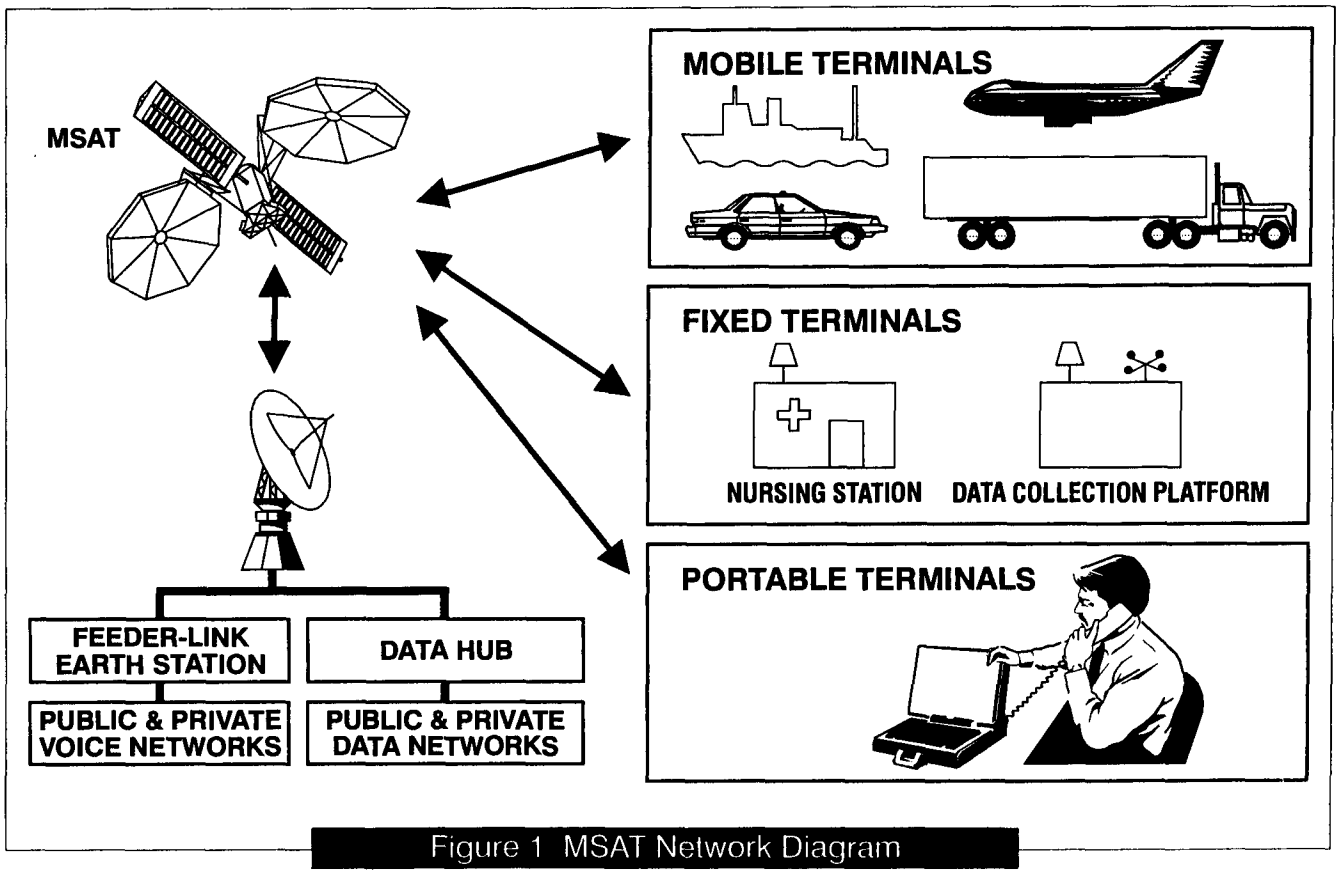

Figure 1 MSAT Network Diagram

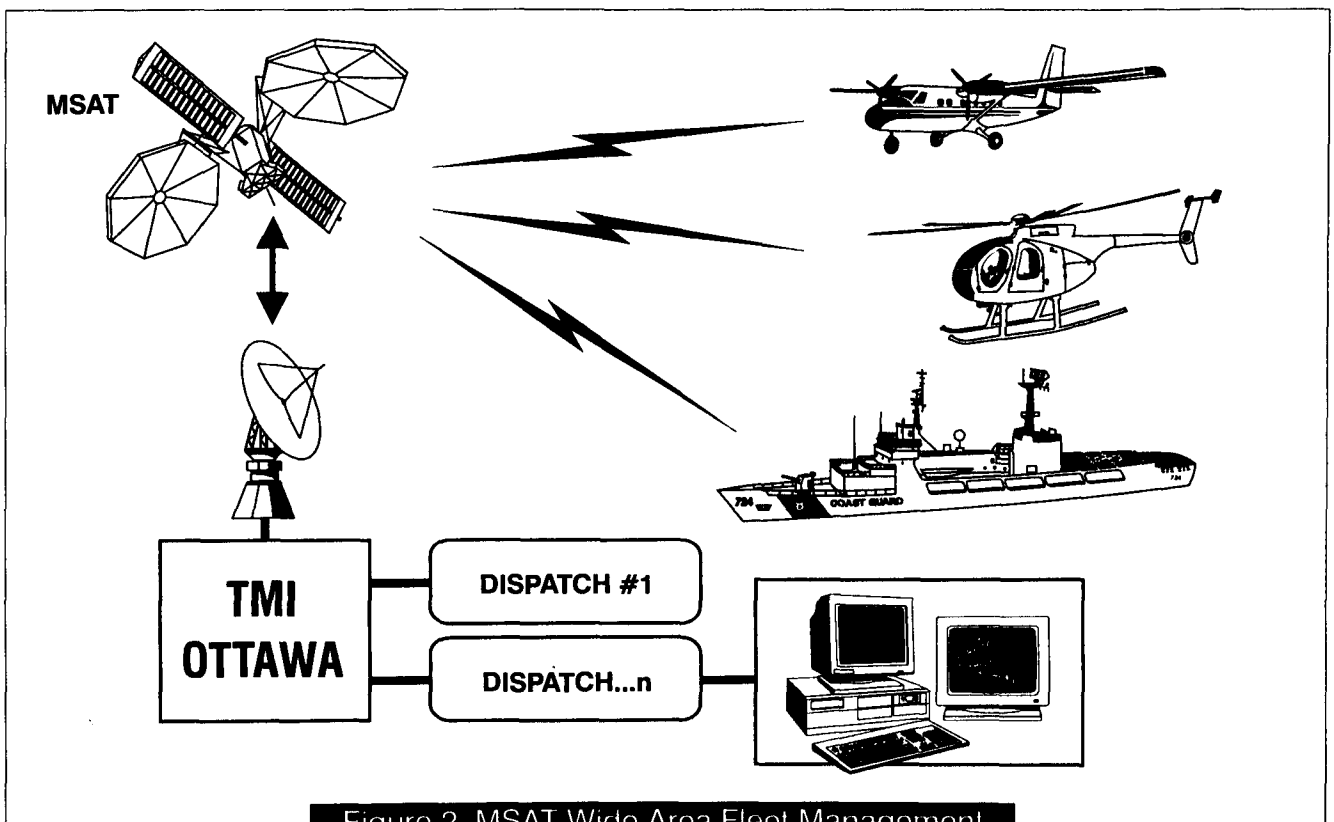

Figure 2 MSAT Wide Area Fleet Management

Mobile Satellite Service Communications Tests using a NASA Satellite

Katherine H. Chambers
NASA
Code OX
Washington, DC 20546
(202) 358-4830 FAX-(202) 358-3525

Louis A. Koschmeder
Stanford Telecom
1761 Business Center Drive
Reston, VA 22090
(703) 438-7919 FAX-(703)438-8112

James E. Hollansworth
NASA Lewis Research Center
Code 5610
Cleveland, OH 44135
(216) 433-3458 FAX-(216) 433-8705

Jack O'Neill
NIALL Enterprises, Inc.
329 Liberty Street
Belmont, WI 53510
(608) 762-5327 FAX-(608) 342-1254

Robert E. Jones
NASA Lewis Research Center
Code 5650
Cleveland, OH 44135
(216) 433-3457 FAX-(216) 433-8705

Richard C. Gibbons
MITRE Corporation
6305 Ivy Lane, Suite 500
Greenbelt, MD 20770
(301) 901-9268 FAX-(301) 901-9209

ABSTRACT

Emerging applications of commercial mobile satellite communications include satellite delivery of compact disc (CD) quality radio to car drivers who can select their favorite programming as they drive any distance; transmission of current air traffic data to aircraft; and handheld communication of data and images from any remote corner of the world. Experiments with the enabling technologies and tests and demonstrations of these concepts are being conducted before the first satellite is launched by utilizing an existing NASA spacecraft.

INTRODUCTION

NASA is providing use of its Tracking and Data Relay Satellite (TDRS) to industry, government and universities active in the satellite communications industry free of charge to perform measurements, experiment with their technology, and demonstrate their innovative commercial system concepts. CD Radio, Inc. of Washington, DC in partnership with NASA's Lewis Research Center (LeRC) has embarked on a test program using TDRS to demonstrate spatial diversity techniques. These tests support commercial development of a new satellite direct broadcast national radio service called Satellite Radio. Goddard Space Flight Center, (GSFC) through Stanford Telecommunications, Inc. has developed and tested prototype, low-power, compact, portable terminals which, although not yet miniaturized, demonstrate handheld portable satellite communications from almost anywhere in the world, including Antarctica. NIALL Enterprises, Inc. and the University of Wisconsin are pursuing satellite distribution of real time air traffic data to aircraft and are using TDRS to test their digital satellite data auxiliary interface. A Very High Rate Data Modem (VHDRM) and telepathology techniques are also expected to be tested via TDRS in the near term. These systems and their TDRS experiments are described in the paper. The experiment opportunity is also described.

DIGITAL AUDIO RADIO PROGRAM

Systems Concept

NASA is committed to providing technology development enabling the introduction of new commercial applications for communications satellites. The Digital Audio Radio (DAR) Program is an effort between The National Aeronautics and Space Administration's Lewis Research Center (LERC) and the United States Information Agency/Voice of America (VOA Office of Engineering) designed to provide technology definition and development for a new direct-to-listener satellite sound broadcasting service. Major program efforts are being directed toward frequency planning, hardware and service development, service demonstration, and experimentation with new satellite receiver technology.

Evolution of digital and mobile satellite communications technologies has enhanced the potential quality and availability of a DAR service well beyond original expectations. By its nature, a DAR satellite system can be very flexible in its antenna coverage area (e.g. from approximately 100,000 square miles using a 1 degree spot beam, to 1,000,000 square miles using a 3 degree spot beam, depending upon the desired broadcast area to be reached with the necessary power flux density). DAR will be able to offer audio signals with various levels of sound quality, ranging from robust AM quality, through FM monophonic and stereo quality, to CD quality. DAR digital signals will be able to reach a variety of radio receiver types (fixed, portable, and mobile) in various environments (indoor/outdoor, rural, urban, and suburban). Studies have shown that DAR systems can provide an economical cost per broadcast-channel-hour for wide area coverage. As the potential quality and availability of a direct-to-listener satellite radio service have evolved, so has recognition of the desirability of such a service. The 1992 World Administrative Radio Conference (WARC-92) has established new frequency allocations for the DAR

Service. The Federal Communications Commission has recently affirmed the U.S. portion of that allocation.

DAR offers listeners and service originators many benefits not previously available in the audio broadcast medium. Satellites can broadcast on a single channel to a national, regional, or continental audience. Wider coverage presents new opportunities for audience access to a variety of types of programming. Such programming might include educational, cultural, national, or target audience-oriented broadcasts which may not be economically attractive to offer in any other way. Commercial radio broadcasting has not seen a more dramatic possibility for change since the introduction of FM stereo broadcasting.

Currently, there are four satellite DAR systems filed in the United States. The proponents are: (1) American Mobile Radio Corporation, (2) CD Radio, Inc., (3) Digital Satellite Broadcasting Corporation, and (4) Primosphere Limited Partnership. It is expected that the FCC will begin licensing activity for DAR service mid to late 1995.

DAR Tests And Demonstration

Private industry (CD Radio, Inc., AT&T, USA Digital and Eureka 147 [the European Broadcasting Union entry]) and VOA/JPL have conducted a number of demonstrations and experiments throughout the world since WARC-92. These experiments and demonstrations have been delivered via satellite-only at S-band, terrestrial-only at existing AM and FM and satellite/ terrestrial-only at Ku-band and S-band. It is expected that this effort will continue well into the future. Satellite demonstrations and experiments using the NASA Tracking and Data Relay Satellite System have been conducted or are in the planning stages for the following metropolitan areas in the western hemisphere. They are:

1. Propagation Testing, - Austin, TX
2. Demonstrations and Testing - Pasadena, CA
3. Propagation/Diversity Testing - Washington, DC CD Radio, Inc.
4. Demonstrations - Brasilia, Brazil
5. Demonstrations - Toronto, Canada
6 Planned Demonstration - IMSC '95 Meeting - Ottawa, Canada
7. Planned Demonstration - ACTS Results Conference - Cleveland, OH
8. Planned Testing - EIA Field Tests - San Francisco, CA

The Electronic Industries Association Consumers Electronic Group (EIA/CEG) has established an extensive Digital Audio Radio Laboratory at NASA's Lewis Research Center in Cleveland, Ohio. The test plan outlines two phases of receiver testing to be conducted. Phase 1 is the Laboratory Testing being conducted at NASA's Lewis Research Center, and Phase 2 is the Field Testing to be conducted in the San Francisco area.

Results of these tests will be presented to the FCC to help in establishing U.S. standards for DAR services. The same results will then be introduced in the international ITU form for establishment of international DAR standards.

LOW POWER, COMPACT PORTABLE TERMINALS

Stanford Telecom under contract to GSFC has leveraged technology from the NASA Advanced Systems Program and developed portable terminals which communicate with the NASA TDRSS. Physically, the terminals consist of a transmitter unit and a receiver unit. The units are designed to communicate with the Multiple Access (MA) Services of the TDRSS. The transmitter frequency is 2287.5 MHz for MA Return Link Service. The TDRS MA Forward Link Service frequency is 2106.4 MHz. The TDRSS phased array provides earth coverage and is capable of supporting a large number of simultaneous random transmissions from widely distributed geographic locations.

Salient features of the transmitter include:

- Programmable data rates up to 4.8 kbps
- Fixed RF output power of 1.0 Watt
- Rate 1/2 convolutional coding
- Small patch antenna of 3 inch diameter with boresight gain of 6.8 dB and 80° beamwidth
- Programmable PN (Gold) codes of 2047 length
- Integrated COTS 8 channel GPS receiver
- RS-232 user data interface for PC interface
- Operation for up to 2 hours using self contained camcorder battery

Testing of the transmitter unit has demonstrated success in transmitting both ASCII text and binary image data formatted in packets at rates up to 4.8 kbps. These tests have been conducted from GSFC, through windows at the STel offices in Reston, VA, and from the roof of NASA Headquarters in Washington, DC. All data transmissions were accomplished with less than 10^{-5} bit-error rate (BER). No errors were detected in the transmitted data during actual testing. Testing was conducted through the NASA TDRSS White Sands Ground Terminal (WSGT) using the TDRS F-6 spacecraft at 46°W. All data including the formatting, capture and processing has been verified through the GSFC Packet Processing Facility. Additional link margin was evident during each of these tests. Two of the transmitter units were taken to the Antarctic for tests in December, 1994. Tests were successful with antenna elevations as low as 3 degrees above the horizon.

The receiver development has been able to take advantage of the NASA Advanced Systems Program. Receiver units have been successfully tested with the TDRSS. Features of the receiver include;

- Programmable data rates up to 4.8 kbps
- Rate 1/2 Viterbi decoding
- Programmable PN (Gold) codes of 1,023 length G/T ~ -20 dB/K
- PN carrier acquisition in less than 5 seconds
- BER less than 10^{-5}

- Small patch antenna of 3 inch diameter with boresight gain of 6.8 dB and 80° beamwidth

Currently, numerous applications exist for this type of portable, low power communication. Several government agencies have expressed interest in the technology represented. Applications include science and technology, economic benefit, law enforcement, and rapid detection and reaction to emergencies. Examples include monitoring of nuclear sites, wildlife tracking with radio collars, monitoring /tracking of ships and tankers in coastal areas, search and rescue of hikers and others in remote areas, unmanned automatic science and/or weather data collection from land and water, and rapid deployment of mobile networks to react to emergency situations.

REAL TIME AIR TRAFFIC DATA TO A LOFTED AIRCRAFT

Concept

NIALL Enterprises Inc. and the University of Wisconsin, Platteville are using TDRSS to test new technology to broadcast air traffic control radar data to a lofted aircraft via satellite. In this concept, this data is utilized to generate an air traffic situation display on an in flight moving map as an aid to the pilot in locating nearby aircraft.

TDRS Experiment

Live air traffic control radar data is to be gathered at the Federal Aviation Administrations Chicago Center in Aurora, Illinois. NIALL will access the real time data at that location, deliver it to White Sands Complex on a dial-up telco circuit where it will be handed off to the uplink equipment provided by NASA's Jet Propulsion Laboratory (JPL). The JPL equipment interfaces directly with the Second TDRSS Ground Terminal (STGT) equipment on site.

From STGT the data is uplinked to the TDRS and will be transmitted by the TDRS to NIALL's test Piper Malibu aircraft in flight over southern Wisconsin within the subject radar scan. The receive equipment on the test aircraft is also provided by JPL, with the exception of one of the antennas to be used and the display computer. The computer uses the received data to generate an air traffic situation display on a moving map typically used for inflight navigation. With the test aircraft at the center of the display, the proximate air traffic is also seen on the graphic presentation and used as an aid to the pilot to locate neighboring planes that might create a conflict with the planned flight path.

Support for this experiment will be entirely provided at the White Sands Complex and requires no special equipment beyond the JPL provided interface which has been used in previous Digital Audio Broadcasting (DAB) field trial experiments. The TDRSS high gain single access antenna transmits at a frequency in the 2025 - 2110 MHz band at an information data rate of 10 kbps and a total transmitted data rate of 160 kpbs.

The preliminary tests will be accomplished in one week, allowing two days for ground testing and final aircraft rigging and three days for the actual flight tests with the satellite link. The initial tests are scheduled for spring 1995 with a more comprehensive test and demonstration program expected to follow. Details on the test results are available by contacting the author, J. O'Neill, directly at the IMSC '95 conference or at the phone number provided.

Successfully "piggybacking" this data on a Digital Audio Radio Service frequency in the future should provide cost advantages to the user and data provider as well as increase the speed of implementing this new technology. This applies to Air Traffic Services as well as to other real-time data services to aviation and other users.

VERY HIGH DATA RATE MODEM EXPERIMENT

Introduction

The Space Electronics Division of NASA LeRC has maintained an ongoing technology development program to advance the state of the art of critical components and subsystems of digital satellite communications systems. In the future, integrated data including voice and video will support multiple-gigabit-per-second throughput utilizing hybrid satellite links. Increasingly higher performance, very high-data-rate-modems for ground-to-ground, space-to-ground, and inter satellite links will be required to enable or enhance the operational flexibility, reliability, and cost efficiency of future communications systems. This can result in reduced development risk and cost for both government and commercial applications in the near and distant future. In addition, the most efficient usage of the available electromagnetic spectrum for data transmission is a concern now, and will continue to increase in priority in the future as the spectrum resource becomes even more crowded.

Background

In response to these issues, the Digital Systems Technology Branch of the Space Electronics Division has sustained ongoing in-house investigations and contractual developments of modulation and coding technologies. The technology development contract for the VHDRM contract (NAS3-26393) awarded to Hughes Space and Communications was one initiative responding to such investigations and projected needs for development of high data rate modem technology. The VHDRM concept uses digitally shaped quadrature phase shift keying (QPSK) modulation with a truncated Nyquist response raised cosine waveform. The waveform is then passed through an anti-aliasing and bandlimiting filter resulting in the final signal that is then modulated and transmitted. This approach helps in achieving bandwidth efficient modulation approaching 2 bits per second per Hertz. The VHDRM also has a requirement for clock and carrier acquisition within 1000 symbol times. This feature will enable the VHDRM to be used in burst data applications. In the TDRS experiment opportunity, the VHDRM

contract hardware deliverable will be demonstrated over an actual satellite link.

VHDRM Program Objectives

The objectives of the VHDRM program were to (1) develop a demonstration model of a self-contained, fast acquisition, high data rate modem that could be used in ground-to-ground satellite data transmission applications; and (2) to establish a database and clear path to a flight-qualifiable VHDRM that could be used in space-to-ground or space-to-space satellite applications.

TDRS Experiment Objectives

One objective of the VHDRM TDRS experiment will be to demonstrate successful transmission of 400 Mbps of data through an existing 225-MHz-bandwidth TDRSS link, using QPSK modulation. This would represent a one third increase in data capacity over the standard 225-MHz link with minimal implementation loss and modem complexity increase. Work is also in progress on 8-PSK modulation and coding that meets 2 bits per second per Hertz. Another objective of the experiment will be to demonstrate the fast clock and carrier acquisition capability of the VHDRM, validating the concept for its use as a fast-acquisition modem for burst data applications.

TDRS Experiment Approach

The VHDRM MOST experiment will be performed using a combination of proof-of-concept hardware deliverables resulting from the technology development contract and off-the shelf hardware. The VHDRM proof-of-concept hardware will consist of three 19-in. standard-mount chassis in a half rack. There will also be a separate half rack of special test equipment consisting of a frequency converter, an off-the-shelf bit error rate test set, and a personal computer for control. The system is currently being developed and is expected to be completed in the third quarter of fiscal year 1995.

The VHDRM MOST experiment will require access to the Second TDRS Ground Terminal K-band, single access return (KSAR) link in a loop-back configuration to support 225-MHz bandwidth in the uplink and downlink. The experiment will interface directly to the 370-MHz intermediate frequency port of the KSA-1 upconverter on the K-band single-access-forward (KSAF) link and the 370-MHz intermediate-frequency port of the KSA-1 downconverter of the KSAR link.

Concluding Remarks

The VHDRM TDRS experiment intends to demonstrate successful transmission of 400 Mbps of data through an existing 225-MHz-bandwidth TDRSS link. This demonstration would illustrate a definite increase in state-of-the-art data transmission capabilities while utilizing the widely accepted QPSK modulation format and limiting complexity increase. The techniques, tested and demonstrated in this experiment, should be enabling to future satellite system designers and manufacturers. Test data will be available from the author, R. E. Jones. Members of the NASA LeRC MOST Experiment team include: R. E. Jones, T. Bizon, M. Kifle, H. Kim, M. Vanderaar* and D. Mortensen*. (* NYMA Inc.)

TELEPATHOLOGY DEMONSTRATION

The purpose of this demonstration is to determine the required video resolution for telepathology using a geostationary satellite delivery system. Telepathology allows a pathologist to diagnose slides remotely. The effectiveness of such a procedure will depend on the transmitted video spatial and temporal resolution. The amount of dynamic resolution will be determined by the transmission bandwidth. TDRSS has a wide bandwidth (225 MHz) in its high data rate channel. Using conventional QPSK this channel can support 300 Mbps. MITRE intends to determine the required resolution for various pathologic slides using microscopic workstations with variable rate HDTV cameras, a variable rate Modem (5 - 650 Mbps), TDRSS and a pathologic work station equipped with a high resolution monitor.

The current HDTV system under development (the "Grand Alliance") will use a video data rate around 20 Mbps and is confined to a 6 MHz terrestrial channel. Since the HDTV source signal is around 1000 Mbps, this requires a compression ratio of 50 to 1. While this may be acceptable for commercial HDTV it may not be for telepathology. Several pathologists will be asked to diagnose different categories of slides using the microscopes directly and after data compression using satellite delivery. These experiments have been performed before but with a fixed resolution [1]. The subjective determination of the dynamic video resolution threshold for telepathology is believed to be new. This information will be used to determine the required channel bandwidth for satellite (and other) delivery systems for telepathology applications.

Description

The tests to be performed will progress in the following stages:

A. Direct Microscope Observation by Pathologists
B. Modem Back/Back Tests (20, 90, 140, 300, 650 Mbps)
C. TDRSS Satellite Simulator Tests (20, 90, 140, 300 Mbps)
D. TDRSS Tests (20, 90, 140, 300 Mbps)

Case A is the performance baseline. Case B will degrade these results depending on the data rate and the quality of the Modem. MITRE has borrowed a high speed, variable rate Modem from Motorola which is capable of rates between 5 and 650 Mbps. Case C allows an exhaustive series of tests in a controlled environment at MITRE in Reston, VA. MITRE has developed and validated a hardware testbed of TDRSS. The highest data rate that can be supported on TDRSS using QPSK is 300 Mbps.

Finally, the same tests will be repeated on TDRSS using NASA facilities at Reston, VA. (Case D)

MITRE has had discussions with pathologists and the HDTV equipment vendors. MITRE hopes that an agreement can be reached between NASA, MITRE, the HDTV vendors and with pathologists that would allow the indicated tests. MITRE is in the process of seeking funding for this project.

Plan

Microscope and pathologic workstations for the tests will be assembled in MITRE facilities at Reston, VA. A formal test plan and experimental design will be generated to ensure reliability of the test cases. Tests will be conducted by pathologists for cases A, B, C and D and results compared under the varying resolution conditions.

The test plan will follow procedures already established [1]. Receiver-operating characteristic techniques will be used to objectively measure observer performance. Pathologists will render diagnosis on a set of pathological specimens. To directly compare performance with light microscopy (A) and with video microscopy (B, C and D), each pathologist will review the selected cases twice, once in A and once in D at different diagnostic sessions. A counter-balanced experimental design will be used in which the pathologists will see half the cases with light microscopy (A) and half with video microscopy (D) in part 1 and will see each case in the opposite viewing condition in part 2.

Preliminary video microscopy tests in B and C will determine the expected performance on TDRSS. Tests performed at 650 Mbps in B are expected to be almost identical to Case A [1]. The other data rates should show additional degradation. The TDRSS satellite simulator tests at 300 Mbps will be used to determine the series of telepathic tests to be demonstrated on TDRSS. The tests will be conducted over a period of two months.

TDRSS Demonstration

An objective series of tests will determine the video S/N and realized resolution for all four tests cases and the results will be compared. The pathologists will again be asked to subjectively evaluate the required resolution (data rate) in order to accurately diagnose pathologic slides. Depending on the preliminary subjective evaluation the scope of the required tests on TDRSS will be considered. If need be, the prior tests could be repeated. The demonstration is expected to occur over a period of one month.

Expected Results

It is expected that the 650 Mbps case and perhaps the 300 Mbps case will achieve results that are similar to the HDTV case considered in the reference. The reference study used a Sony Model SHR-10 video camera (1050 scan lines) mounted on a microscope and the images were displayed on a Sony Trinitron 950 line monitor. The 300 Mbps case requires 4 to 1 compression which is possible to achieve using lossless compression. On the other hand, the use of the current HDTV terrestrial standard requires a data rate around 20 Mbps. This standard would no doubt yield inferior performance but would be universally available. It is possible that a 20 Mbps data rate would yield satisfactory results in say 90 percent of the routine cases but that higher data rates are required for the more challenging cases.

[1]. R. S. Weinstein et all, "Progress in Telepathology: System Implementation and Testing," Advances in Pathology and Laboratory Medicine, vol. 6 ©1993 Mosley-Year Book, Inc.

EXPERIMENT OPPORTUNITY

NASA continues to provide an opportunity to conduct experiments and demonstrations of satellite communications technology using TDRSS (Figure 1). In addition to those experiments described in this paper, many proposals have been submitted. Experiment proposals are still welcome. Others wishing to use the TDRSS for experiments should submit a proposal detailing the nature of the experiment, the TDRSS resources, time required, as well as other pertinent information. Arrangement for use of the TDRSS and other NASA resources by a private organization are covered by a Space Act Agreement. These resources will be made available free of charge for approved experiments and demonstrations. Interested parties will be responsible for providing experiment unique equipment external to the TDRSS interface, and personnel to operate experiment equipment, as well as costs associated with any modifications to systems at the White Sands Complex (WSC) or GSFC. If requested, NASA will protect any proprietary data generated. NASA has a time limited authorization to offer this opportunity due to spectrum limitations.

Experiments will be using resources and services which routinely support NASA spacecraft missions. Scheduling is on a best efforts basis. Subject to specific agreement, NASA will make available for approved experiments any of the following:

- access to the TDRS spacecraft S and/or Ku-band return link (see tables);
- access to the TDRS spacecraft forward link via an IF interface at WSGT/STGT;
- baseband access through NASCOM to TDRSS forward/return link services at WSC or the GSFC SOC as appropriate;
- access to appropriate NASA facilities and physical space for experimenter provided equipment and personnel during the conduct of the experiment;
- access to any readily available TDRSS measurement data pertinent to the experimentation;
- resources to permit the scheduling of agreed upon TDRSS services for the purposes of experimentation;
- technical support related to service scheduling;

- Space Network and associated ground system operations as required and agreed upon in support of the experiment or demonstration;
- technical/engineering assistance associated with discrete interfaces and data handling elements;
- technical/engineering assistance associated with frequency management and authorization.

The MOST Experiment Program is sponsored by the NASA Office of Space Communications (Code O), located at NASA Headquarters in Washington, DC. Project management has been assigned to GSFC in Greenbelt, MD. Additional information can be obtained by contacting any of the NASA authors. The opportunity announcement and proposal guidelines can be obtained by contacting the Project Manager, Arthur H. Jackson at 301-286-9058 or (FAX) 301-286-1723.

TDRS Payload RF Parameters

TDRS Service	Polarization	EOL EIRP min	EOL G/T min	3 dB Contour
Multiple Access (Phased Array)	LHCP	≥ 34 dBW	≥ + 0.5	2500 km
S-band High Gain Single Access	RHCP or LHCP Selectable	≥ 37.5 / 43.6 / 46.1 (low, norm, high)	≥ + 8.5	1155
K-band High Gain Single Acss	RHCP or LHCP Selectable	> 40.5 / 46.5 / 48.5 (low, norm, high)	≥ + 23.8	175

TDRS Payload Frequency Plan

TDRS Service	Link	Center or Band	Bandwidth(S805	5Data Rate (max)
MA Forward	Receive from TDRS	2106.4 MHz	6 MHz	10 kbps
MA Return	Transmit to TDRS	2287.5 MHz	6 MHz	50 kbps
SSA Forward	Receive from TDRS	2025-2110 MHz	20 MHz	300 kbps
SSA Return	Transmit to TDRS	2285-2290 MHz	10 MHz	12 Mbps
KSA Forward	Receive from TDRS	13.775 MHz	50 MHz	25 Mbps
KSA Return	Transmit to TDRS	15.0034 MHz	225/212 MHz	300 Mbps

Figure 1 Experiment Architecture

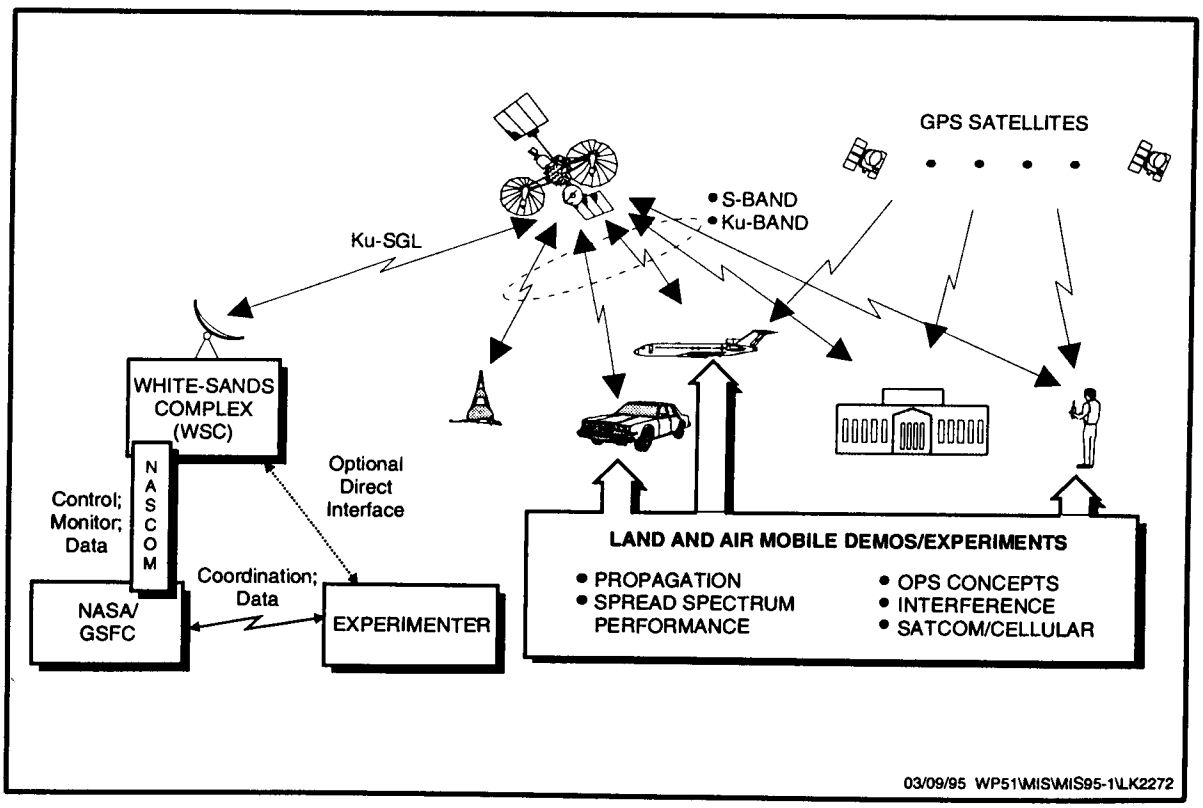

A Low Earth Orbit Satellite Marine Communication System Demonstration

T. Keith Elms[1], Kenneth A. Butt[1], and Ken W. Asmus[2]

[1] Canadian Centre for Marine Communications
P.O. Box 8454, 155 Ridge Rd., St. John's, Newfoundland, Canada A1B 3N9
Tel. (709)579-4872 Fax. (709)579-0495

[2] Environment Canada, Atmospheric Environment Service, Ice Services Branch
3rd Floor, 373 Sussex Drive, Ottawa, Ontario, Canada, K1A 0H3
Tel. (613)996-5236 Fax. (613)996-4218

ABSTRACT

An application of Low Earth Orbit (LEO) satellite communications technology was investigated during a joint Canadian/American scientific expedition to the north pole in the summer of 1994. The Canadian ice breaker involved, was equipped with a store-and-forward LEO satellite terminal which was linked to a ground station in St. John's, Newfoundland, via the near-polar-orbiting satellite, HealthSat-1. The objective was to evaluate the performance of such a system while providing an alternate means of communications in the far north.

The system performed well, given its inherent limitations. All 151 attempts to send data files to the ship were successful. Only two (2) of the 35 attempts to send files from the ship were unsuccessful. The files ranged in size from 0.1 to 60 Kbytes. In the high arctic, above 80° north, this system often provided the only practical means of data communications. This experiment demonstrated the potential of such a system for not-real-time communications with remote and/or mobile stations, and highlighted the many issues involved.

This paper describes the project objectives, system configuration and experimental procedure used, related technical issues, trial results, future work, and conclusions.

INTRODUCTION

A recent experiment was conducted by the Canadian Centre for Marine Communications (CCMC), in cooperation with the Telemedicine Centre of Memorial University of Newfoundland, to investigate an application of Low Earth Orbit satellite (LEOSat) communications in the marine environment. The goals were to demonstrate the potential of such a system as a low cost marine communications alternative and to further explore the technical issues related to transferring digital data files (<100 Kbytes each) to an offshore vessel.

The work was carried out in conjunction with Arctic Ocean Section 1994 (AOS '94), where on August 22/94, the Canadian Coast Guard icebreaker Louis S. St-Laurent and the US Coast Guard ice breaker POLAR SEA reached the geographic north pole.

EXPERIMENTAL PROCEDURE

Data file Transfer

The types of files transmitted to the ship ranged from ERS-1 satellite imagery (1 Mbyte uncompressed) to ASCII text messages (<10 Kbytes). Files were routed from the Ice Centre in Ottawa, to CCMC (via internet-FTP) and manually loaded onto the ground station terminal, to await the next satellite pass. The ERS-1 SAR files were panelized (divided into smaller files of 25 Kbytes or less) prior to transmission. The ship terminal operator would check the terminal regularly and remove any files received. Files were also transmitted from the ship on an "as required" basis and relayed via internet once received at the ground station.

Received Signal Strength Logging

A data recording system was implemented which enabled sampling of the received signal level during two (2) optimally selected satellite passes each day. The stored data, voltage versus time (UTC), could eventually be used to create a plot of received signal level (dBW) versus satellite elevation angle for each selected satellite pass.

SYSTEM DESCRIPTION

The system used for this experiment consisted of three (3) parts: the shipboard terminal, the ground station terminal, and the satellite link.

Shipboard Terminal

The LEOSat shipboard terminal was located in the chart room adjacent to the bridge and the radio room, with the antennas installed on the railing above the bridge on the port side (see figure 1).

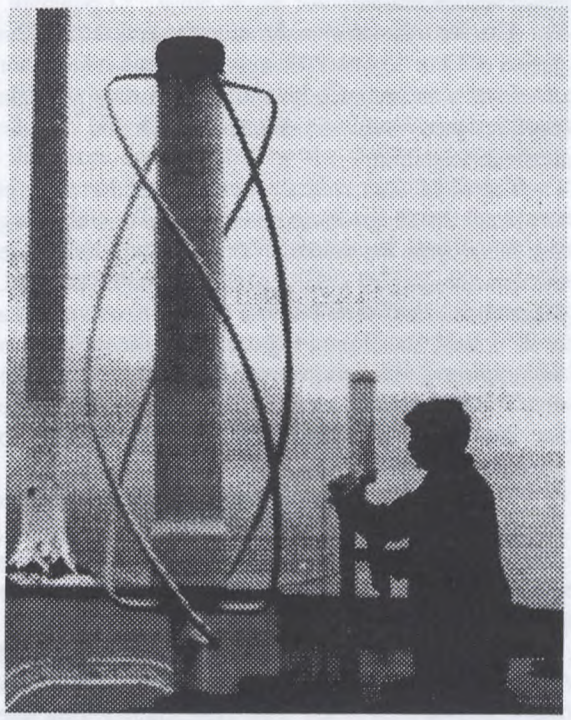

Figure 1 - Shipboard Antenna Installation

Ideally the antennas would have been installed on the mast, allowing a 360° unobstructed view of the horizon, but this would have subjected them to extreme vibration and greater risk of damage.

The shipboard system was configured by CCMC (see figure 2). In this application, quadrifilar helix (Q-helix) antennas (Satellite Data Systems QH148RH VHF and QH 435RH UHF) were used for their combined performance and robustness. Their maximum gain (3dBi) is at zenith, with a 140°, 3 dB beamwidth. The low angle performance of these antennas was not ideal since the satellite is below 30° for the majority of the period that it is visible to a fixed observer. However, the low angle sensitivity does assist with grazing multipath signal rejection. Low antenna gain was compensated for by signal amplification on both receive and transmit. On the transmit side, a 3W single channel radio (Kantronics D4-10) fed a 150W high power amplifier and the VHF Q-helix antenna (max. gain 3 dBi). On the receive side, the UHF Q-helix (max. gain 3 dBi) fed two low noise amplifiers (LNA) in series (approx. 16 dB gain each) and the single channel radio (Kantronics dvr 2-2).

The terminal equipment was specified to meet the vibration, motion, and environmental tolerance requirements of northern marine operations. All Equipment in the chart room was secured with metal brackets and rubber cushioning. The transmit antenna was reinforced with PVC tubing by CCMC, and the receive antenna was sealed in PVC tubing with end caps and filled with low dielectric foam by the manufacturer.

A second PC and data acquisition card enabled the AGC (Automatic Gain Control) level of the receive radio to be sampled and recorded during selected satellite passes.

Ground Station Terminal

The ground station terminal is located at CCMC in St. John's, NF. Primarily it consists of a pair of mechanically steered Yagi style antennas (12 dBi, M^2 Enterprises 149CP26 VHF and 429CP26 UHF), one 16 dBi preamp on the receive side, a VHF\UHF transceiver (45W, Kenwood TS-790A), tracking controller, Terminal Node Controller (TNC)/modem, and PC.

Satellite Link

HealthSat-1 (UoSat-3 or UO-14) was built by Surrey Satellite Technology Limited (Centre for Satellite Engineering Research, University of Surrey, U.K.) and launched in 1990. At the time of this demonstration, HealthSat-1 was being used by SatelLife, a not-for-profit health aid organization which operates Healthnet, a LEO satellite communications service linking medical centres in Africa with Europe and the USA. The Telemedicine Centre at Memorial University acts as Healthnet's North American gateway.

Transponder: The transponder on HealthSat-1 operates at Mode-J (digital) frequencies (uplink 145 MHz, downlink 435 MHz). The satellite links are 9600-baud FSK using FM ground station equipment. The system is controlled by an 8 MHz, 80C186

microprocessor with 4 Mbytes of RAM [1].

Visibility: HealthSat-1 operates in a near polar orbit (altitude 800 km). Therefore, the number of satellite passes seen per day depends on the observer's latitude. For example, the CCMC station (47°35'N, 52°44'W) would see approximately eight (8) passes per day, whereas a ship at the north pole would see approximately fifteen (15). The maximum elevation angle of these passes varies significantly, from merely grazing the horizon to near zenith. The overall access window at the pole (15% of the day) was much greater than at the ground station (7% of the day). At the CCMC location, approximately half of the passes are high enough for practical use. At the north pole, all passes reach a peak elevation angle of approximately 35°. With the Q-helix antennas on the ship optimized for higher elevation angles, the link quality was not maximized for the majority of the satellite visibility.

Path Loss Variation: The distance to the satellite, from a fixed observer, ranges from 3300 km at the horizon to 800 km at zenith. Therefore, the free space path loss ranges from approximately 155 dB at the horizon to approximately 143 dB at zenith. The satellite antenna partially compensates for this variation with its toroidal radiation pattern (lowest gain at nadir). Ideally the radiation pattern of the earth station antenna should have mirrored that of the satellite antenna to maximize performance for the majority of any given pass.

Other Losses: The attitude, or alignment with respect to the earth's center, of HealthSat-1 is known to be unstable and can vary by as much as 40°. The transmit power level of satellite varies significantly (1 to 6 watts) depending on the level of battery charge and the bus temperature.

DATA ANALYSIS

Data File Transfer Results

Data file transfer between the ship and CCMC was conducted on a regular basis between July 27 and September 2, 1994. During the 38 days, approximately 1.7 Mbytes of data were transferred (in 184 files), much of which was compressed prior to transmission. The total uncompressed volume was approximately 10.5 Mbytes.

To Ship: Greater than 99% of the total raw (uncompressed) data transferred, was destined for the ship. All of the 151 attempts to transmit files were successful. These files ranged in size from 0.1 to 60 Kbytes. The average transmission period was 11.5 hours. The minimum period was 0.5 hours; the maximum was 79.2 hours.

From Ship: There were 35 attempts to transmit files to CCMC. Of these, 33 were successful. These files (ASCII text only) ranged in size from 0.5 to 6 Kbytes. The average transmission period was 11.5 hours. The minimum period was 0.5 hours; the maximum was 35.5 hours.

The files transfer results should be qualified as follows:

1) All file transmissions were in response to the real data requirements of the users. Therefore, the total amount of data sent did not represent absolute performance limits.

2) The file transmission durations stated, refer to the period of time between file upload initiation (whether or not it was completely uploaded during a single satellite pass) and download completion at the destination station.

3) Each LEOSat terminal was configured to attempt to upload the file(s) in its queue before downloading any file(s) from the satellite. This sequence can cause the downloading of a particular file(s) to be delayed. Since the CCMC terminal had large amounts of data in its upload queue on a regular basis, files sent from the ship would experience additional delays. Often the CCMC terminal remained in PG (upload) mode for the entire satellite pass, not attempting to download any files.

4) The CCMC terminal competed with other North American LEOSat stations for access to HealthSat-1, and was often shut out of the two (2) available channels. This reduced the ground station's satellite access time and therefore throughput.

5) The performance of the ship station was limited by the reduced antenna gain at low angles. This was particularly true near the north pole where all satellite passes have a peak elevation angle of only 35°. In addition to this, the compromise in antenna placement, further reduced performance due to shadowing by the ships superstructure.

6) There are software problems which may cause the terminals to lock up. The CCMC station was operated seven (7) days per week but usually not manned outside of normal business hours. Therefore, any overnight system lockups would not be resolved until the following morning, adding as much as 12 hours to transmission times.

Received Signal Level Measurement Results

Fifty-six (56) received signal level data sets were recorded, for selected satellite passes, and plotted as

signal level versus satellite elevation angle. Interpretation of the signal level profiles was difficult due to the number of factors which affected received signal strength. Due to attitude instability, the satellite can rotate around its z-axis slowly (once every 10 - 15 minutes) such that the satellite antenna null (actually a series of nulls) may appear at any point during a pass, or not at all. The satellite transmit power level could vary by as much as 7 dB. The degree to which the radiation pattern of the ship's receive antenna was affected by the surrounding superstructure was unknown. There is a ripple component on the radiation patterns of downlink antennas (3 - 6 dB on the satellite transmit antenna). The multipath due to the constantly varying look angle to the satellite would create a constantly varying signal, even in the absence of all other contributing factors [2]. Figure 3 and 4, both show satellite passes that were unobstructed by the ship's superstructure. It appears that the more rapid variation (likely due to multipath effects) is superimposed upon the slower variation, due to the combination of antenna patterns and path loss variation. The null of the satellite antenna is not clearly evident in either of these plots, indicating significant satellite off-pointing. These figures illustrate the degree of signal fading associated with the use LEO satellites and low gain, non-tracking antennas in an environment where multipath is severe [3].

DISCUSSION

The weather conditions during this cruise were essentially benign (temp. -5° to +2°C), with few icing occurrences, and did not affect external equipment. Vibration was constant and often extreme. There was no hardware damage or failure, no problem with system software or ship's power, and no apparent evidence of Radio Frequency Interference (RFI) from the ship's transmitters. An operational system could be adversely affected by these factors, however.

When possible, the system was monitored during satellite passes. The digital carrier detection (DCD) was not always constant even at high elevation angles, although, solid detection didn't always ensure successful data transfer. The file transfer rate appeared, at times, to be better during low elevation passes. Hence, the system appeared to be more efficient when near the pole where all passes were below 35°. Small text files seemed to transfer quickly and reliably. Larger files (i.e. the 25 Kbyte subdivided ERS-1 files) sometimes took more than one pass to be completely transferred.

Technical constraints limited throughput to about 100 Kbytes/day of data. This proved to be satisfactory for this project as the intent was to demonstrate the feasibility of using LEO's for data transmission to vessels. All the system users, including the Radio and the Electronics Officers, were impressed with the overall performance and ease of operation. The ship station did not experience any of the possible system lockup conditions. In essence, the LEOSat system performed well.

Seamless connection to a server on one or both ends of the satellite link would allow remote and/or mobile stations to have reliable, inexpensive access to worldwide E-mail. This, along with improving the operating software reliability, could enable continuous operation and automatic routing of files. This approach however, due to bandwidth and transponder restrictions, would eventually restrict the practical data file size as the user base expanded. Therefore, the greatest potential application for this type of store-and-forward technology appears to be in the low cost transfer of high data volumes, globally, to large common use groups.

FUTURE WORK

As a result of this experimental research, CCMC recommends that future work with this technology should include the following:

- Improve on the current operating software to enhance reliability and performance.
- Develop a seamless connection to a server on one or both ends of the satellite link.
- Investigate compact, robust, non-tracking, circularly polarized antennas optimized for elevation angles below 30°.
- Research shipboard antenna spatial diversity, intelligent antenna switching and digital processing techniques.
- Develop an inexpensive integrated terminal which would incorporate the transceiver, modem/TNC, and power supply.
- Conduct a demonstration with various marine data products utilizing a common user broadcast data access protocol. Emphasize data products having highly repetitive transmission schedules and market requirements that are unique to the marine environment. Use satellite technology that uses the maximum power and bandwidth under WARC '92 approved RF spectrum allocations.
- Examine the technical viability and cost of a small constellation of more than one LEO satellite to address the requirements for specific file transfer times, system capability and reliability for commercial acceptance.

CONCLUSIONS

This experiment is among the first uses of a LEO satellite (LEOSat) terminal in a mobile marine environment. Overall, the system performed well, given the limits of the technology. The ship station experienced no technical problems throughout the entire experiment.

In total, 184 files were successfully transferred over the satellite link and two (2) files were unsuccessful. File transfer times varied between 0.5 and 79.2 hours. This variation is attributed to the factors outlined in the Data Analysis section.

The system performance was limited by ship structural shadowing, multipath fading, and the unstable attitude (alignment) and varying transmit power level of HealthSat-1. There were often significant variations in the received signal level for satellite passes of similar elevation and ship orientation. Therefore, increased satellite attitude stability and transmit power level, as found in the latest technology, would improve reliability.

This experiment demonstrated that a LEOSat system can provide a communications alternative in regions of operation where other approaches, such as terrestrial HF radio or geostationary satellites communications, have proven to be either unreliable or unusable. At times during the expedition, the LEOSat system was the only practical data communications available to the ship.

Existing improved technology and access protocols, and system optimization can significantly improve the functionality and performance of LEOSat systems for marine operations.

ACKNOWLEDGEMENTS

This project was made possible through the support of SatelLife of the USA, which provided the satellite link through HealthSat-1; the Canadian Coast Guard of Transport Canada, which provided financial and onboard technical/operating assistance; and the Ice Services of Environment Canada, which provided financial and field data collection assistance. The analysis of the received signal level data was assisted by Mark Allery, Surrey Satellite Technology Limited, Centre for Satellite Engineering Research, University of Surrey, U.K.

REFERENCES

[1] Martin Davidoff, *The Satellite Experimenter's Handbook*, Newington, CT: The American Radio Relay League, 1990, appendix B, pp. B11-B13.

[2] R.M. Allnut, A. Dissanayake, C. Zaks, and K.T. Lin, *A Study of Satellite Motion-Induced Multipath Phenomena*, in Proceedings of the International Mobile Satellite Conference, Pasadena, California, 1993, pp. 337-342.

[3] Mark Allery, Surrey Satellite Technology Limited, extracted from correspondence between Oct. 28/94 and Feb. 14/95.

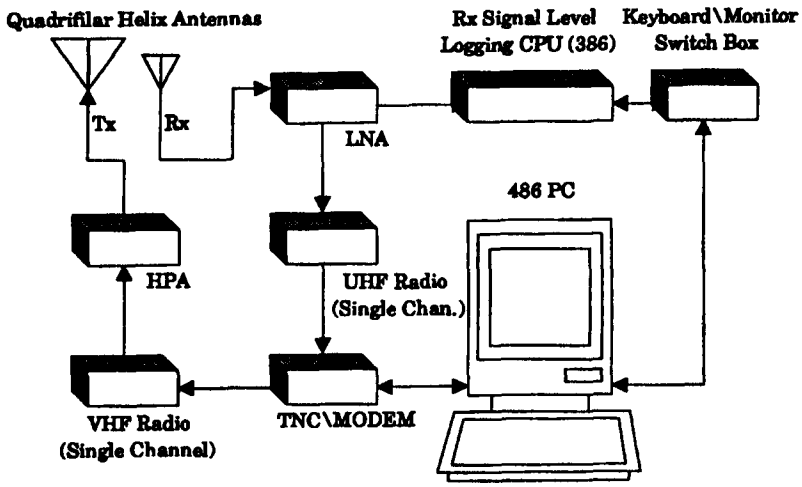

Figure 2 - Block Diagram of Shipboard Terminal

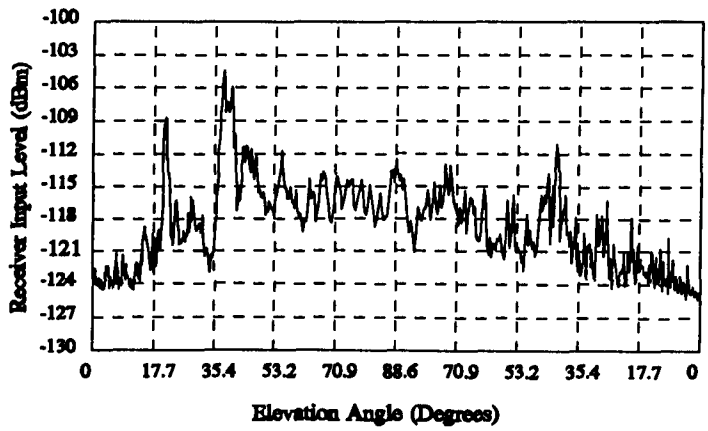

Figure 3 - Example 1 of Receive Signal Level Variation

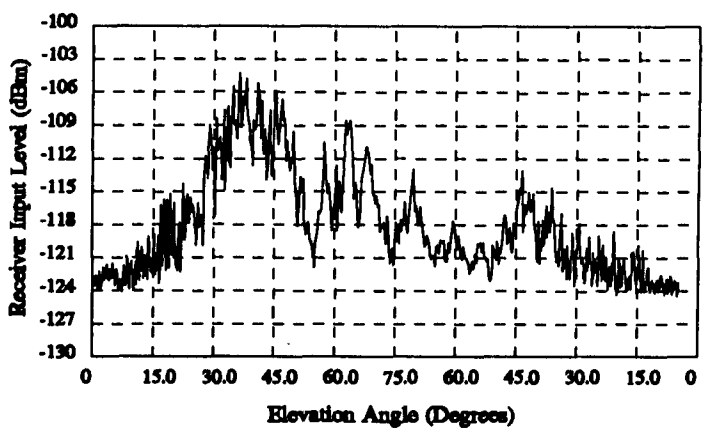

Figure 4 - Example 2 of Receive Signal Level Variation

Advanced System Concepts & Analysis

Session Chairman: **Edward Ashford**, European Space Agency, The Netherlands
Session Organizer: **Ted Hayes,** Communications Research Centre, Canada

Topic Introduction: Compared to the conservative growth of satellite communications systems in the past, the growth during the next few years is expected to be unprecedented. This growth is being driven both by the expansion of the traditional fixed-satellite services, particularly in the Asia-Pacific region, and by the introduction of several new systems providing mobile-satellite services. In addition, there is a number of advanced system concepts being proposed for a variety of new services including personal, residential and mobile communications. This session includes presentations which describe some of these advanced system concepts which are being developed to provide future mobile services. More than half of the papers discuss concepts which employ constellations of satellites in non-geostationary orbits. The session should provide the participant with an overview of some of the emerging advanced system concepts, applications and technologies. Topics covered during the session include: Low-Earth Orbit (LEO) systems, LEO systems designed to provide non-uniform coverage, new applications for mobile satellite systems, inter-system interference-analysis and satellite antenna design trade-offs.

cont'd

The GEMnet Global Data Communication

Byung K. Yi,
Richard Chitty,
Dave Walters,
and
Regan Howard

CTA Commercial Systems, Inc.,
6116 Executive BLVD.,
Rockville, MD 20852
Phone:301-816-1327 Fax:301-816-1426

Abstract

The GEMnet™ (Global Electronics Messaage network) will provide global digital data communications anywhere in the world at any time for minimum cost. GEMnet™ is an end-to-end Non-Voice Non-Geostationary Mobile Satellite (NVNG) (sometimes dubbed "Little LEO") System which consists of a constellation of 38 low Earth orbiting small satellites and a ground segment. The GEMnet™ ground segment will consist of subscriber user terminals, gateway stations, a Network Operational Center(NOC), and a backbone network interconnecting the NOC and gateways. This paper will describe the GEMnet™ system concept including ground and space segments, system heritage, data communication services, and protocols.

Introduction

Following the 1992 World Administrative Radio Conference (WARC' 92), the US FCC adopted a Little LEO MSS spectrum allocation in the bands 137 to 138 MHz, 148 to 149.9 MHz, and 400.15 to 401 MHz to provide low-rate data communication services. [1] Three organizations (Orbcomm, Starsys, and VITA) filed applications for the first round process. Orbcomm recently received a license to construct and launch 36 satellites while the Starsys and VITA are still pending. In the meantime, the FCC entertained submissions for a second round filing. There were seven applicants, of which five were new and two of which were modifications or amendments of first round filings. CTA Commercial Systems is one of the second round applicants. Over the past ten years CTA has developed twenty one small satellites, and has designed and built twelve ground stations for command and control of LEO satellites. The company's satellite programs, including the MACSAT communications satellites, and Microsat satellite program, have made CTA a pioneer in the creation of store and forward communication satellite systems. GEMnet™, the global two-way data communication system CTA has filed for Round 2, will start service in 1997.

System description

The GEMnet™ system is a cost-effective, global two way data communication service, using a constellation of small, low-Earth orbiting satellites and a ground communication network. [2] The GEMnet™ system architecture is depicted in Figure 1.

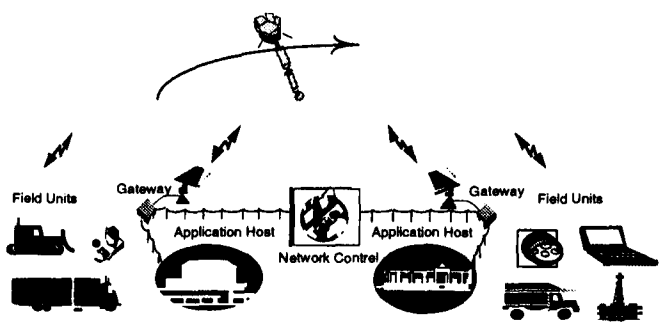

Fig. 1 The GEMnet™ system architecture

The GEMnet™ constellation will consist of thirty-eight satellites in low-Earth orbit and two on-ground spares. Specifically, the space segment

Specifically, the space segment constellation consists of four planes of eight satellites in 50° inclined (circular) orbit and one plane of six satellites, in a polar (circular) orbits to provide not only optimal coverage in the areas where demand is likely to be greatest ,but also global coverage. The footprints of the GEMnet™ constellation are shown in Figure 2.

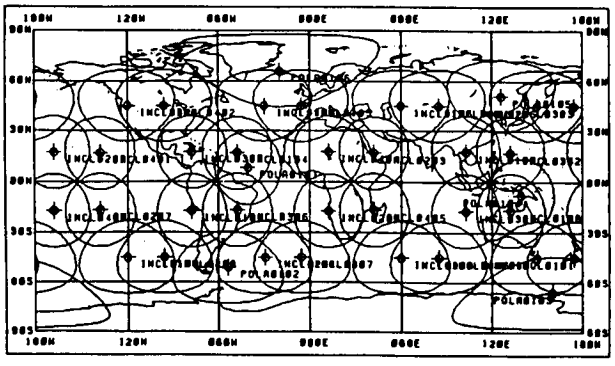

Fig. 2 The typical foot prints of the GEMnet™ constellation

All spacecraft altitudes are 1000 km. (540 nautical miles) circular. The satellites will weigh approximately 100 lb. (45.2 kg.) and have an operational life of 5-7 years. The total orbit peak power requirement is 100 watts. The spacecraft mass and power budget are listed in Table 1, and Table 2 respectively.

	Subsystem Mass Budgets (kg)
Structure & Cables	8.0
C&DH	2.0
Thermal Control	1.0
Attitude Control	3.0
Propulsion	7.0
Power	12.0
Communications	7.2
Contingency (15%)	5.0
S/C Mass	45.2

Table 1 The spacecraft mass budget

The GEMnet™ ground segment will consist of subscriber field units (user terminals), gateway stations in the United States and worldwide, a Network Operations Center (NOC) and a terrestrial network of dedicated links. The number and location of gateway stations will depend upon market demand. Three gateways will be located in the United States. The NOC will perform control and management of the entire system, including TT&C functions via the gateway stations. The GEMnet™ system supports a variety of data collection and personal communication services, such as E-mail. The GEMnet™ user will communicate directly with the satellites which, in turn, will interconnect with the local or global gateway stations for purposes of routing messages to or from the user. For example, data collected from containers and mobile assets will be routed for processing to a central business office.

	Peak Power (W)	Orbit Avg. (WHr)
Communications Payload		
Packet Switch	5.0	8.8
148 MHz Rcvr	7.0	6.1
137 MHz Xmtr	50.0	43.8
400 MHz Xmtr	20.0	11.2
Payload Subtotal	76.0	104.0
Engineering Housekeeping		
C&DH	2.0	3.5
Attitude Control	5.0	8.8
Power	5.0	8.8
Harness	2.0	3.5
GPS Receiver	4.0	7.0
Housekeeping Subtotal	18.0	31.5
Total Required Power	100.0	101.4

Table 2 The spacecraft power budget

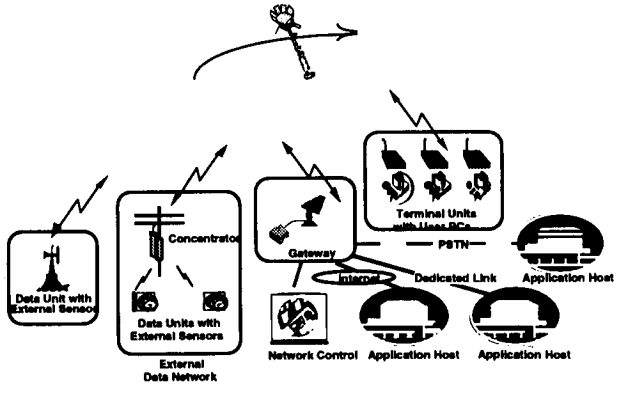

Figure 3. The GEMnet™ ground system concept.

In the case of E-mail, the message would be routed to the ultimate recipient via the Internet, Public Switched Telephone Network (PSTN) or dedicated links. The GEMnet™ ground system concept is shown in Figure 3.

Description of Services

Six major services that GEMnet™ will initially address were identified. These are: (1) asset tracking and monitoring (GEMtrack); (2) utility/meter reading (GEMread); (3) E-mail (GEMmail); (4) global paging (GEMpage); and (5) buoy/environmental sensor reading (GEMsense);and (6) direct-to-home communications services. In general terms, two different classes of data formats will be implemented for the services identified. These two classes are E-mail data message and short data packet which are similar to HDLC data format.

GEMnet™ access and protocol description

For each GEMnet™ satellite, the uplinks will be configured with one signaling channel and a supporting set of data channels using FDM. The uplink in the 148 MHz band of the existing commercial spectrum will consist of eleven uplink data channels operating at 2.4 or 4.8 kbps with one of those channels reserved as the signaling channel.

Access to the GEMnet™ satellites on the uplink signaling channel may be obtained using a modified reservation ALOHA protocol or a polling protocol. The modified reservation ALOHA protocol uses the order channel to accept requests for users time slots in the subsequent frame time. This method is primarily used to support E-mail and paging applications that have essentially bursty access characteristics and larger message sizes. Those applications that allow pre-determined scheduling will be serviced by the polling protocol that will permit large numbers of subscriber field units with small data messages to access the satellite. Polling access will be employed for applications like utility monitoring and transportation asset tracking.

The GEMnet™ satellites will provide both access methods over intervals of typically five to ten second in order to service
both random and polled applications within the same footprint.

Using dynamic channel assignment on the uplink band, each satellite will continually scan the uplink frequencies to determine the available channels and broadcast the frequency assignment to the subscriber field units. The subscriber field units will track the appropriate subscriber-satellite downlink carrier to compensate for Doppler shift.

Subscriber field units transmit data to the spacecraft either by requesting an uplink data channel via the subscriber uplink signaling channel or by being commanded via one of the signaling downlink channels. If the subscriber field units are requesting service or the message is short (< 32 bytes approximately), the unit can send the message on the random access signaling channel. If the message is longer, the unit will send a reservation request to the satellite. Then the satellite will examine the activity on the uplink bands, select an available clear channel, and send a channel assignment to the subscriber field unit on the downlink channel.

When the subscriber field unit is being polled to initiate a transmission, the satellite will transmit an assignment message for the unit via the appropriate subscriber downlink channel. This message will specify the uplink data channel and time offset from the signaling channel synchronization signal for transmission. The satellite may also issue group commands requesting a group of subscriber field units to respond. However, in this case the subscriber field units must respond on the signaling channel either sending the response message or requesting a data channel.

During data transmission, the packetized data will use an HDLC format. Packet lengths can vary from 12 to 512 bytes excluding overhead to accommodate different applications. It is expected that packet lengths will be fixed within each application. Furthermore, each subscriber unit is identified with an unique address which supports the required group addressing schemes that will allow the polled access approach to be effective. The optimum packet length for a given propagation delay and 10^{-5} bit error rate is 256 bytes.

Throughput Analysis

We have performed a throughput analysis for the modified reservation ALOHA protocol and short message polling protocol. The throughput of the polling protocol, which is the function of bit error rate and ratio between propagation delay, and transmission time, is deterministic. We will discuss only the reservation ALOHA in this paper. The throughput analysis for store and forward data communications with reservation ALOHA multiple access has been performed for a subset of the satellite constellation. The characteristics of the store and forward satellite operations in NVNG allocated spectral bands are; 1) the message arrival rate is modeled as a delta function at time zero with some constant amplitude instead of a Poisson distribution with constant average arrival rate (the coverage foot print, shown in Figure 4, is large enough to cover a continent and every terminal will have accumulated data ready to transmit to the satellite as soon as it comes in view), 2) for a single unit transmitting on a single frequency, the satellite access is restricted to a total of 9 seconds over a 15 minute period, 3) the minimum burst interval is 15 seconds, and 4) the maximum burst length is 450 ms. Items 2), 3) and 4) are issued as part of FCC regulations Footnote US323. This traffic model can be explained by the following analogy.

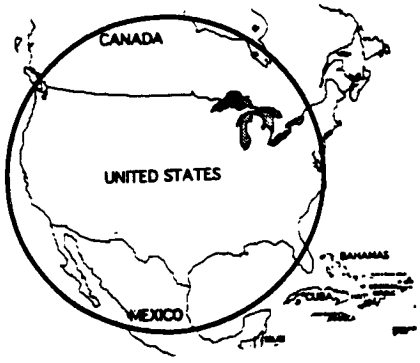

Figure 4 Typical Footprint

We throw n balls randomly into v boxes and if any boxes contain one ball then the ball is removed from system, and we continue the experiment until last ball is removed from the system. The number of experiments, n ,and v are equal to the required number of frames to service all the messages, total number of messages outstanding, and number of reservation ALOHA contention slots respectively. Our interest is to calculate the average number of frames required for n messages with different packet sizes and different access protocols. The exact solution including the upper bound and lower bounds for the average number of frames required are not analytically tractable. Instead we performed a Monte Carlo analysis for three cases; 1) one packet per message with a persistent protocol. The persistent protocol is such that any message involved in a collision will contend in next time frame. 2) an average 4 packets per message with a first come and first serve access protocol which blocks packets more of than the maximum the number of packets allowed in one time frame. 3) an average 4 packets per message complying with Footnote US323 which does not allow the transmission of packets in consecutive 10 seconds frames. In this case, the message with more than one packet has to contend for the channel on alternate frames. The throughput analysis results for 32 reservation slots and 14 data frames are shown in Figure 5. The results apparently shows that for 24 frames (4 minutes of satellite connection period) can

support 45 users which comply the US 323 rules.

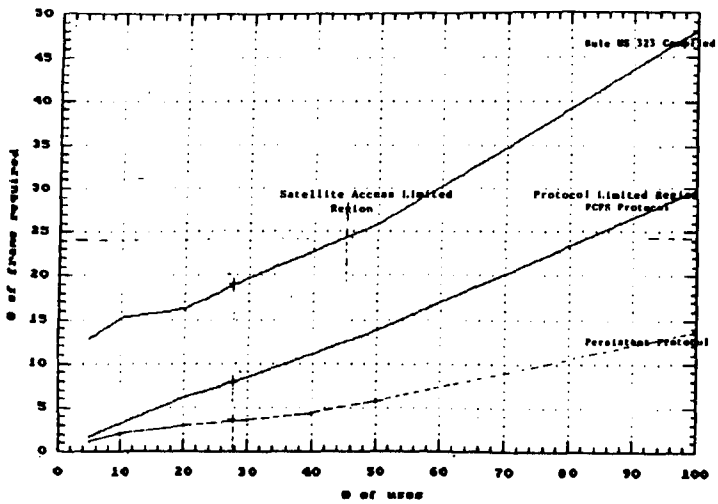

Figure 5 The results of throughput analysis

Spectrum Plan and Interference Analysis

The GEMnet™ system will use frequency bands that have been allocated to the NVNG MSS. These are: 148-150.05 MHz for the subscriber/satellite uplink and gateway/satellite uplink (feeder link); 137-138 MHz for the satellite/subscriber downlink; and 400.15-401 MHz for the satellite/gateway downlink (feeder link). The prime considerations in selection of these spectral bands were the ground subscribers terminal cost and environmental interference.
Low-cost, compact, hand-held or truck-mounted terminals will be rugged, low-power, easy to interface, and have a near omni-directional antenna gain pattern. For fixed transmitter and receiver antenna gains, which is the case of the little LEO communication scenario, the received power is :

$$P_r = (\frac{c}{4\pi Rf})^2 G_r G_t P_t \qquad (1)$$

where:
c = speed of light
R = range
f = carrier frequency
G_r = receiver antenna gain
G_t = transmitter antenna gain
P_t = transmitter power.
The received power is anti-square proportional to frequency. Two times higher frequency means 4 times of transmitter power requirement. Another upper bounding limitation is Doppler shift which is proportional to the carrier frequency. The lower bounding limitation of the operating carrier frequency for the little LEO applications are due to man-made and natural interference caused by industrial machinery, automobiles, and magnetosphere noise. These interference sources are too high below 100 MHz to have reasonable operational margin for the hand-held power and bandwidth limited subscriber terminal. This is why the operational frequencies of the little LEO bands are bounded between 100 M Hz to 500 M Hz.

Communication system

The GEMnet™ space-ground communications links, shown in Figure 6, consist of links for Subscriber Field Unit access and Gateway access.

The GEMnet™ System will employ four (4) types of simplex communications links which will be used for subscriber-satellite and gateway-satellite communications. The links are:

- Subscriber-Satellite Uplink
- Subscriber-Satellite Downlink
- Gateway-Satellite Uplink
- Gateway-Satellite Downlink.

Table 3 summarizes the characteristics of the GEMnet™ System RF links.
All GEMnet™ System links are designed for a 10^{-5} bit error rate with a required 7 dB E_b/N_o after consideration of coding gain.
These links will use differentially encoded offset-QPSK (OQPSK) modulation filtered for excess bandwidth and a rate 7/8, constraint length 7, convolutional code.

	Subscriber/ Sat. Uplink	Sat./ Subscriber Downlink	Gateway/ Sat.Up link	Sat./ Gateway Downlink
Band(MHz)	148-150.05	137-138	148-149.9	400.15-401
Number Signaling +Data Channels (Sat.)	11	1	1	1
Number Channels (System)	dynamic channel allocation	9	1	3
Channel Data Rate (bps)	4,800 2,400	19,200	50,000	50,000
Signal Bandwidth (Hz)	4,100 2,100	16,400	42,800	42,800
Frequency Stability (Hz)	±1,500	±200	±200	±200
Doppler Shift (Hz)	±3,700	±3,400	±3,700	±9,800
Channel Bandwidth (Hz)	10,000	25,000	50,000	60,000
Emission Designator (Hz)	10K0G1D	25K0G7D 25K0F7D	50K0G7D	60K0G7D
Transmit Polarization	Linear, vertical	RHCP & LHCP	RHCP	RHCP

Table 3 GEMnet™ link Characteristics

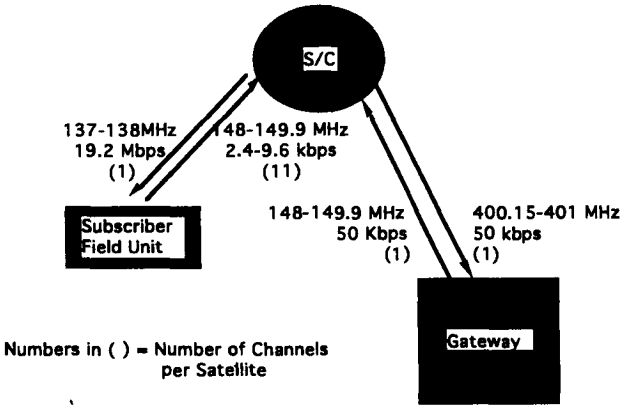

Figure 6 Communication link overview

Conclusions

GEMnet™ will provide low cost, effective, global digital mobile data communication services between remotely dispersed and highly unstructured communication nodes not currently being served. The combination of LEO satellites, efficient modulation and multiple access protocols, spectrum sharing methodologies, and advances in personal communication systems allow us to introduce the "gem" of the modern mobile data communication.

References

[1]C.M. Rush, "How WARC '92 will affect mobile services", IEEE Communication Magazine, October, 1992.
[2]Application of CTA before the Federal Communication Commission, Nov., 1995.

A LEO Concept for Millimeter Wave Satellite Communication

A. H. Jackson
Code 504
NASA GSFC
Greenbelt, Maryland 20771
301-286-9058

P. Christopher
Stanford Telecommunications, Inc.
Reston, Virginia 22090
703-438-8017

ABSTRACT

A conceptual 60 satellite LEO constellation for millimeter wave communication is discussed. It could be launched in segments, with the first 30 satellites providing high elevation angles for all time in the Northern latitudes between Miami and Thule. The second set of 30 satellites would complete the worldwide coverage with emphasis on high ground elevation angles in the densely populated temperate zones. Full earth searches for all time are used to generate probability density functions for elevation angle. The density functions are used to derive optimum frequencies for random elevation systems. The 55 degree average elevation angle and 14 degree standard deviation are seen to be acceptable for 0.997 rain availability in Washington, DC for the 40 to 47 GHz region. The 40 to 47 GHz region is nearly optimum, if 0.99 rain availability is acceptable.

1.0 BACKGROUND

Millimeter wavelengths extend from 30 to 300 GHz. Millimeter wavelength frequencies have been known (1) to have quantitative advantages in many satellite communication applications. Reference (1) showed optimum frequencies in the 14-17 GHz, 30-40 GHz, and 90 GHz regions. The actual optimum frequencies depended on many things, including the ground elevation angles. High elevation angles allowed higher frequencies. The millimeter wavelength regions of intense interest now include the NASA Advanced Communication Satellite (ACTS) 30 GHz region and the Milstar 44 GHz band. Key developments associated with these nationally important projects have allowed objections to millimeter wave communication to fade gradually during the past two years.

We emphasize the 40-47 GHz region for possible mobile satellite communication for several reasons. Important developments which are coalescing in 1995 include

(a) Current FCC activity in allocating massive spectral regions for frequencies greater than 40 GHz.
(b) Ongoing Milstar and ACTS transmitter and receiver developments.
(c) Japanese commercial success at 30 GHz during the past decade.
(d) Current Japanese research at 47 GHz (2).

Prior analysis has shown that elevation angles greater than 30 degrees are required for reasonably reliable millimeter wave communication. This is clearly more stringent than many existing satellite systems provide. Geosynchronous satellites may provide high elevation for some of the temperate region between 30 to 50 degrees North. The inclined, elliptic 12 hour Soviet Molniya satellites of the mid sixties provided high elevation angles (3) for the entire region from 30-70 degrees North. Low Earth Orbiting satellites (LEOs) also offer the possibility of high elevation angles in the entire temperate region, as recent descriptions of the 840 satellite Teledesic system (4) concept have indicated. We describe a 60 satellite LEO system concept for high elevation angles in the temperate regions where intense communication traffic occurs. Worldwide coverage would be available, but only modest elevations would be available near the equator.

We begin the discussion with propagation analysis, and a new result for integrated oxygen attenuation on ground-satellite paths. Propagation losses are seen to increase monotonically with frequency, but the antenna gain is shown to effectively counteract propagation loss in some 'optimum' frequency bands. The optimum frequency section indicates striking advantages for high ground elevation angles. A LEO system is then described to fulfill these demands for high elevation angles. Probability density functions (pdf's) for elevation angle are shown as a function of latitude to indicate worldwide coverage. The question of optimum frequencies for LEO systems is resolved by integrating a net loss function over the elevation pdf. The 40-47 GHz region will be found to be close to optimum for a Washington, D.C. climate region. We close with a discussion of FCC interest in the millimeter wavelength region and the opportunities which would appear with millimeter development.

2.0 PROPAGATION ANALYSIS AND FREQUENCY OPTIMIZATION

This section briefly treats gaseous attenuation and rain attenuation before indicating solutions for optimum frequencies. Gaseous attenuation relies heavily on the World War II results of J. H. Van Vleck (5) and the more recent oxygen attenuation corrections due to H. Liebe (6). A new integrated Liebe-Van Vleck oxygen attenuation equation is shown. Rain attenuation results result from a Crane rain model (7) with a rain height shown by Ippolito (8).

Since 1960, a heavy emphasis has been placed on atmospheric attenuation as a function of frequency. Early observers noted that both gaseous and rain attenuation increased steadily up to the water vapor absorption line (22.2 GHz), and then increased even more sharply. These early efforts also used very conservative rain attenuation estimates. The Defense Communications Agency attempted to observe 10E-4 rain outage probability in the mid sixties. This assumption led to prohibitive rain attenuation for a number of conditions. Satellite communication frequencies were strongly influenced by these observations and were limited to 6 GHz for many applications. Some hints began to appear that rain attenuation may not be as bad as it at first appeared, but these suggestions were dismissed because few space-ground attenuation measurements existed. A key Bell Labs sun tracker experiment occurred in 1969 (9) which showed modest attenuation even in the millimeter wave region. This bellwether experiment was largely ignored. Massive rain observations had to be collected by R. K. Crane before many engineers would consider frequencies greater than 6 GHz.

Gaseous attenuation at sea level was carefully described by J. H. Van Vleck. A convenient form of the Van Vleck oxygen attenuation was shown by Bean and Dutton (5). A closed form integration of the Van Vleck oxygen equation over an exponential pressure profile has yielded:

$$A_{o_1} = \frac{.34}{\lambda^2}\left(\frac{-H_o}{\sin E}\right)\left[\frac{1}{2K_1}\ln\left(\frac{(\frac{1}{\lambda})^2}{(\frac{1}{\lambda})^2+K_1v_1^2}\right)+\frac{1}{2K_2}\ln\left(\frac{(2+\frac{1}{\lambda})^2}{v_1^2K_2^2+(2+\frac{1}{\lambda})^2}\right)+\frac{1}{2K_2}\ln\left(\frac{(2-\frac{1}{\lambda})^2}{(2-\frac{1}{\lambda})^2+K_2^2v_1^2}\right)\right] \quad (2\text{-}1)$$

dB, total oxygen attenuation (1 GHz < f < 50 GHz)

where

K_1 = 0.018
K_2 = 0.049
λ = wavelength in cm

E = elevation angle, radians
Ho = oxygen scale height, km (typically 7 or 8 km)
v_1 = $\exp(-h_1/H_0)$
h_1 = height of ground reflection point above sea level, km

More recently, Liebe (6) has shown results which imply that the line width K2 of equation 2-1 should be more accurately represented as 0.0274 cm-1. We use Liebe's recent results for linewidth and again seek a closed form result because the attenuation calculations must be used repeatedly in later calculations. We also integrate over exponential pressure and temperature profiles for a more accurate closed form than found above (2-1). Integrated oxygen attenuation is found with the aid of Mathematica and may be called an integrated Liebe-Van Vleck oxygen attenuation.

The integration result is long, and is listed here in Fortran form to save space.

```
AO2 = 0.68*(1. *H0*K1*TR1*Log(Tmin) +
    0.5*H0*K2*TR1*Log(Tmin) - 0.25*H0*K2*TR1*Log(Tmin*
*2) - 0.25*H0*K1*TR1*Log((-1 + 2*L)**2*Tmin**2) -
   0.25*H0*K1*TR1*Log((1 + 2*L)**2*Tmin**2))/
   (K1*K2*L**2*Tmin) -
   0.68*(1. *H0*K1*TR1*Log(Tmin + DEL*w1) +
   0.5*H0*K2*TR1*Log(Tmin + DEL*w1) -
   0.25*H0*K2*TR1*Log(Tmin**2 + 2*DEL*Tmin*w1 +
      DEL**2*w1**2 + K1**2*L**2*TR1**2*w1**2) -
   0.25*H0*K1*TR1*Log(Tmin**2 - 4*L*Tmin**2 +
      4*L**2*Tmin**2 + 2*DEL*Tmin*w1 - 8* DEL*L*Tmin*w1+
      8*DEL*L**2*Tmin*w1 + DEL**2*w1**2 -
      4*DEL**2*L*w1**2 + 4*DEL**2*L**2*w1**2 +
      K2**2*L**2*TR1**2*w1**2) -
   0.25*H0*K1*TR1*Log(Tmin**2 + 4*L*Tmin**2 +
      4*L**2*Tmin**2 + 2*DEL*Tmin*w1 + 8*DEL*L*Tmin*w1+
      8*DEL*L**2*Tmin*w1 + DEL**2*w1**2 +
      4*DEL**2*L*w1**2 + 4*DEL**2*L**2*w1**2 +
      K2**2*L**2*TR1**2*w1**2))/(K1*K2*L**2*Tmin)
```

dB, Oxygen Attenuation (2-2)

where

Tmin = minimum atmospheric temperature (210K, representatively)
TR1 = reference temperature = 293K
DEL = Surface Temperature - Tmin (83K for temperate regions)
WI = Exp [h_i/H_o]
h_i = altitude of ground station above sea level, km
L = Fortran form for λ, cm.

The combined attenuation effects of oxygen, water vapor, and light rainfall for the Washington, D.C. area may be represented as Figure 2-1. The water vapor resonance is

included as the hump at 22.2 GHz and the oxygen resonance is indicated at 60 GHz. This total attenuation (dB) through the troposphere has led engineers to stay at low frequencies if at all possible. A higher rainfall rate (9.2 mm/hr) is used in Figure 2-2 to include 99.7% of rainfall attenuation possibilities in Washington, D.C. Some communication engineers consider 99.7% rainfall availability to be a reasonable performance target.

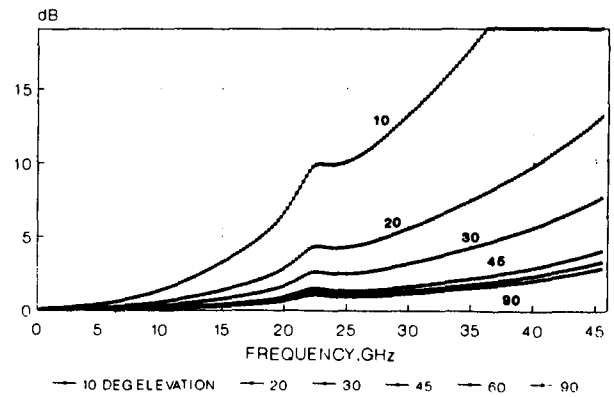

Figure 2-1. Attenuation, Washington, D.C. P=0.99 3.0 MM/HR Rainrate RHO=7.75 G/M^3

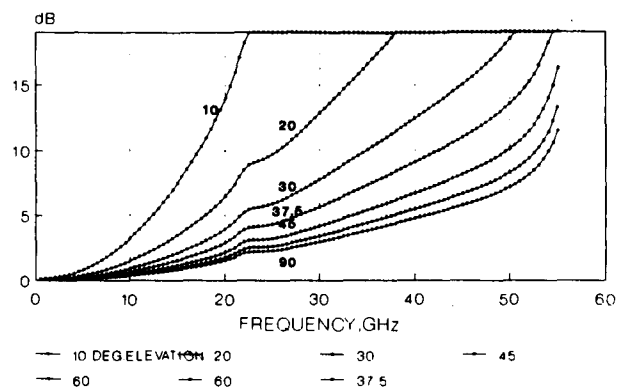

Figure 2-2. Attenuation at Washington, D.C. P=0.997 9.27 MM/HR Rainrate RHO=7.75 G/M^3

Frequency Optimization

Results like Figures 2-1 and 2-2 have retarded the advance of satellite communication frequencies. The actual power transfer between the satellite and ground receiver, as shown by the link equations, contains both the transmitter and receiver antenna gains. A net frequency squared advantage exists if directional antennas are present at both ends of the link. Indeed, other frequency advantages may exist (1) but we include only the F^2 advantage. Gain may be subtracted from loss, as in Figure 2-3, to give new results which may be compared with Figure 2-1. The new ordinate is :"Net Loss" in dB. Net Loss omits some constants because we are interested in loss minima rather than absolute values. Figure 2-3 shows a Net Loss minimum at 16 GHz for a 10 degree elevation system and 43 GHz at 45 degrees. These frequencies may be referred to as optimum frequencies for the respective elevations. Figure 2-4 refers to an interesting communication example with a 9.2 mm/hr rain rate in Washington. It indicates an optimum frequency at 36 GHz for 45 degree elevation. These optimum frequencies refer to constant elevation angles. The relation of these results to variable elevation satellite systems will be shown at the end of the paper.

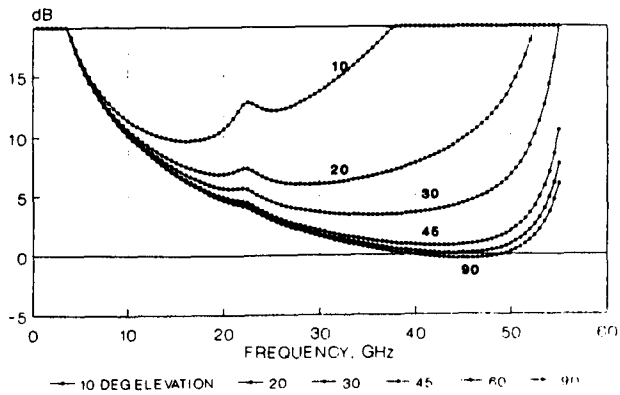

Figure 2-3. Net Loss at Washington, D.C. P=0.99 3 MM/HR RHO=7.75 G/M^3

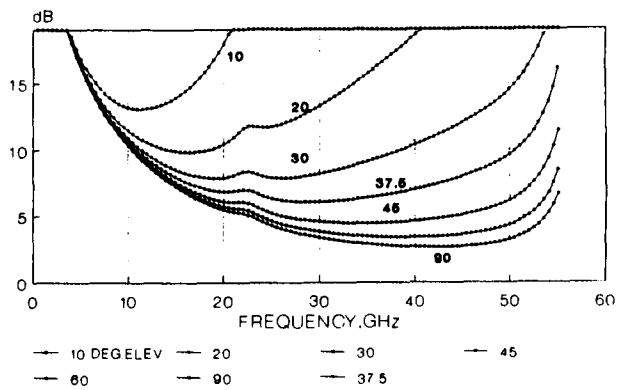

Figure 2-4. Net Loss at Washington, D.C. P=0.997 9.27 MM/HR RHO=7.75 G/M^3

3.0 A LEO SYSTEM FOR HIGH ELEVATION ANGLES

A special orbital effort is required to fulfill the high elevation angles needed by millimeter wave communications. LEO's offer the possibility of high elevation angles in the intense communication regions of the temperate zone, but we attempt to avoid the large number of LEO's suggested by the Teledesic system. The

excellent coverage of the Soviet Molniya series for the Northern Hemisphere showed a fundamental advantage of elliptical orbits. Their stable apogees can be placed over the temperate latitudes and a major part of their orbits can be used for communication. Figure 3-1 shows a snapshot (11) of an inclined, elliptic 2 hour system of 30 satellites with stringent 30 degree elevation angle coverage contours. Every satellite is paired with a sister at 60° East & West for easy crosslinks. Appendix A lists the orbital elements. The argument of perigee is chosen to give good coverage between 30 to 70 degrees North. This surprisingly large region is referred to as a temperate zone here, but it is really intended to imply a high communications intensity zone. The region near 70 North is of interest to the North Atlantic air traffic routes.

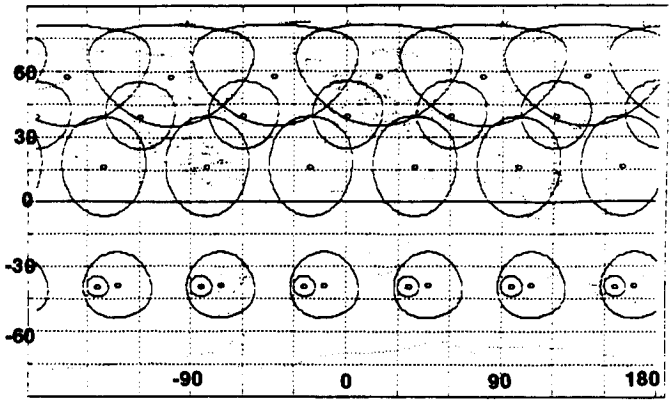

Figure 3-1. 30 Inclined, Elliptic Satellites at Epoch 30° Elevation Contours 2 Hr orbits, I =63.43°, w_p=45°, perigee=350 km

A blowup of Figure 3-1 would show a failure to meet 30 degrees elevation at El Paso (32N, -106E) at the epoch time. Of more concern is the fact that the satellites are moving and a thorough search for all time and area must occur before an adequate description of elevation angle statistics is available. We use the method of osculating elements (11) and the extensive, thorough search methods of (12) to find the elevation probability density function for 24 snapshots as a function of latitude (Figure 3-2). A clear failure to meet 30 degrees elevation angle is seen at 30 degrees North in Figure 3-2. A pdf of the entire temperate region is generated separately and will be used later for frequency optimization.

The second set of 30 satellites is chosen to complement the first set. Figure 3-3 indicates a snapshot of the 60 satellite constellation at the time of epoch. The 30 degree contours cover the earth except for intermittent regions between 20 South and 20 North. The coverage for all time remains a question. A full earth search for all time yields Figure 3-4.

The mean elevation angle for high latitudes is seen to approach 55 degrees and very little possibility is seen for elevation less than 20 degrees at the equator. The probability of such a low equatorial elevation is actually zero at the equator but it is not clear from the figure.

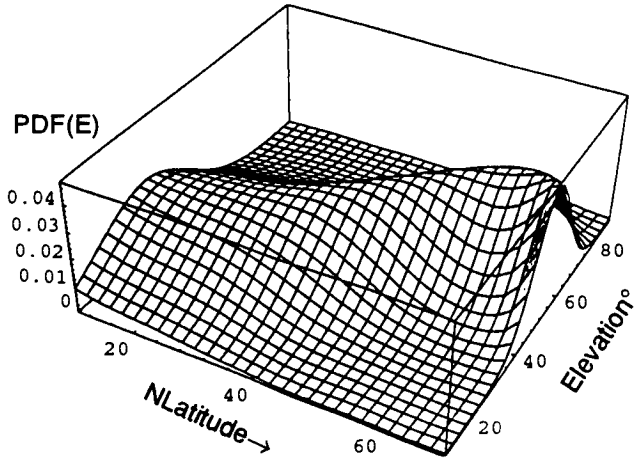

Figure 3-2. Elevation PDF vs NLatitude (30 sats.)

Elevation pdf's are crucial to estimating optimal frequency for a LEO system. The method is outlined in Section 4.

4.0 OPTIMUM FREQUENCIES FOR RANDOM ELEVATION SYSTEMS

Section 2 indicated optimum frequencies for constant elevation angles in the Washington, D.C. area. It was helpful enough to recognize that elevation angles should be higher than most conceptual satellite systems offer for an effective use of the millimeter wave band. The implementation with LEO's, however, in Section 3 implied that an infinite number of possibilities existed for elevation angles. Even a limited area such as the temperate region demanded an elevation pdf.

The net loss as a function of both frequency and elevation may be represented as a power series in two variables. With the aid of Mathematica, a plot of the function f(F, EI) is shown in Figure 4-1. Every elevation angle has a different net loss function, as was also seen in the net loss figures of Section 2. It is possible to integrate f(F, EI) over a good approximation of a Gaussian density (Appendix B) to yield a function g(F) for net loss in a random elevation system.

$$g(F) = \int_0^{\pi/2} f(F, EI)\, \rho(E)\, dE \qquad (4\text{-}1)$$

The result is a general function of elevation mean and standard deviation. The general result may be used in future applications for other satellite constellations.

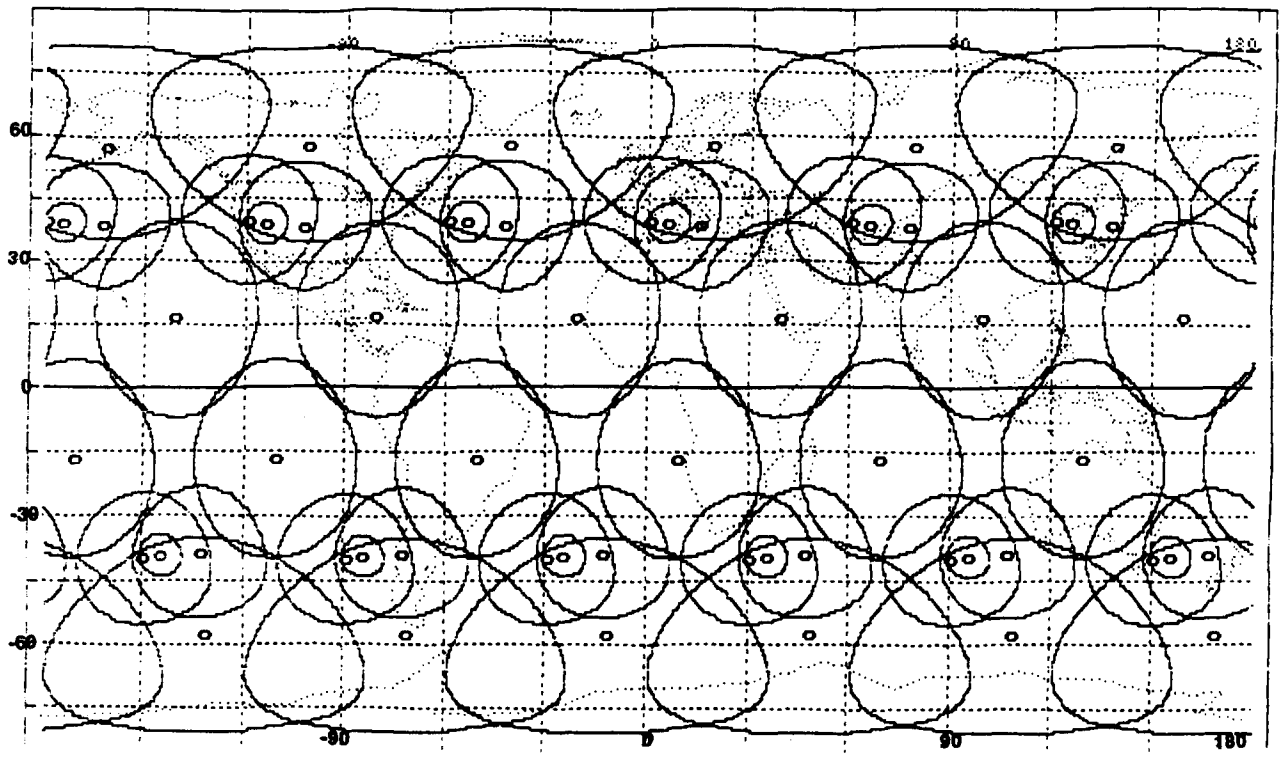

Figure 3-3. 60 Inclined, Elliptic Satellites at Epoch.
30° Elevation Contours

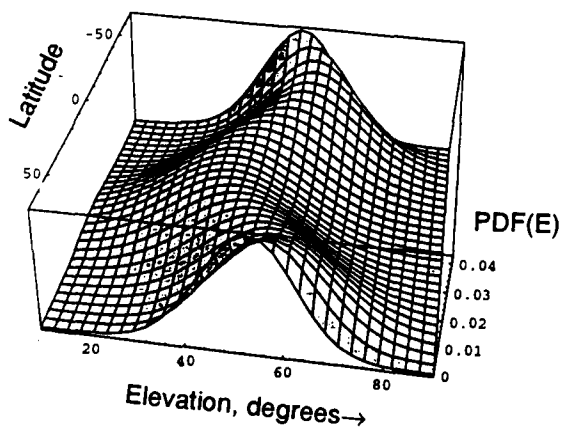

Figure 3-4. Elevation PDF vs NLatitude
(60 sats., wp=-45)

The mean and standard deviation for the 60 satellite system are 54.0 and 14.5 degrees, respectively. The raised Cosine approximation which Psychrometrika (13) has found useful may be seen in Figure 4-2. It cuts off the tails at 2.76 standard deviations. This is fortunate in this case because no elevation angles are actually observed below 20 degrees. Even this approximation allows some unrealistically low elevation angles. When the mean and standard deviation are substituted into the general result, the net loss function g(F) is found and is shown as Figure 4-3. An optimum frequency is seen near 33 GHz with 4.88 dB net loss. Net loss is barely higher (5.0 dB) at 41 GHz. Net loss then increases another 0.24 dB at 45 GHz, but net loss is still within 0.5 dB of the optimum value at 46 GHz. Even 47 GHz may not be a cause for concern except for the net loss slope. A one GHz band at 47 GHz may have discernable pulse shape variation due to the differential loss across the band.

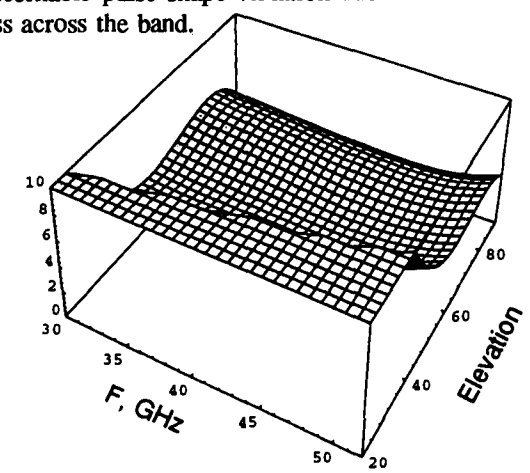

Figure 4-1. Net Loss (dB) vs F, E; 0.997

Optimum frequency shifts upward to 44 GHz if a modest 0.99 availability is allowed. The entire 38-47 GHz region would then be seen to be nearly optimum (Figure 4-4).

The federal Communication Commission has allocated generous spectral regions for mobile satellite communication (Table 4-1). The allocations indicate a startling similarity to the optimum frequencies. Licensing arrangements are expected to become even more favorable after a pending 1995 FCC action.

Table 4-1. Frequency Bands for Mobile-Satellite

		39 40 41 42 43 44 45 46 47
Uplink	Government	(435) (47)
	Non-Gov.	45.5 (47)
Downlink	Government	(39.5) (40.5)
	Non-Gov.	

02/10/95 MIS215\PC7205

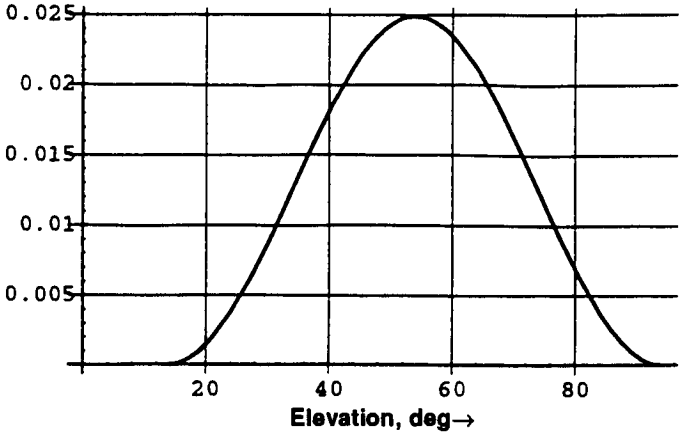

Figure 4-2. PDF (Elevation) for Temperate Zone (60 sats)

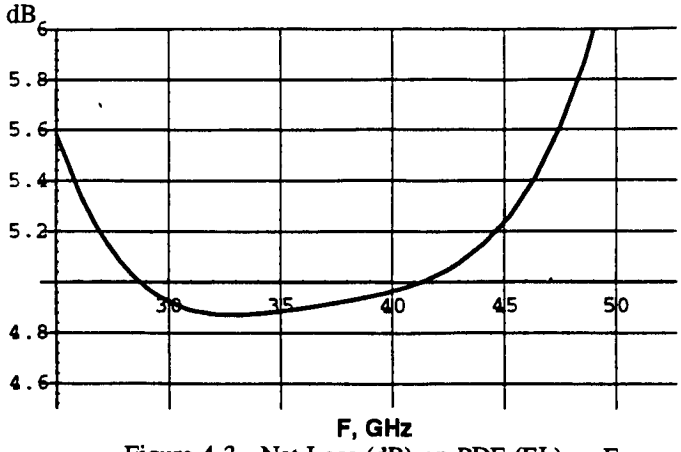

Figure 4-3. Net Loss (dB) on PDF (EL) vs F, GHZ p=0.997

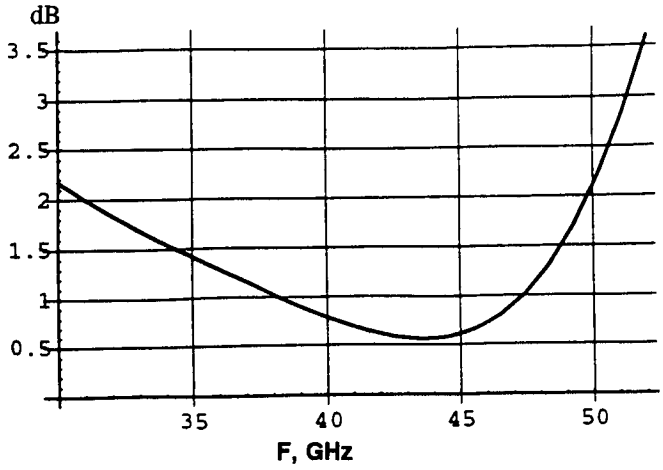

Figure 4-4. Integrated LEO Net Loss, dB Temperate Zone P=0.99

5.0 CONCLUSIONS

We have described a conceptual 60 satellite LEO system which offers high elevation angles for millimeter wave communications in the key world communication areas. The elevation angle pdf was nearly optimum for 40-45 GHz frequencies from Miami to Thule. The 47 GHz region has attractive millimeter wave communication possibilities in the temperate zone of the Northern Hemisphere.

We developed two new results specifically to analyze the LEO concept. The first was a closed form equation for integrated Liebe-Van Vleck oxygen attenuation. An equation for net loss in a random elevation angle LEO system was also developed.

The mobile station is obliged to have a directional antenna and the ability to point it to take advantage of millimeter wave capabilities. Directional capabilities are beginning to appear for the disadvantaged user, as seen with the success of RCA DirecTV. The vast expansion of mobile radio spectrum implied by the further opening of the region over 40 GHz implies many opportunities. Video transmission may be considered. CDMA would have the benefits of both spectral allocation and high elevation angles to avoid the 'near-far' problem. All forms of modulation would benefit from the lack of shadowing implicit in a high elevation system.

It is difficult to overemphasize the importance of millimeter wave satellite communications. Teledesic Corporation has recognized this with their wideband communication concept and video delivery to homes in a wide area. The 9 billion dollar pricetag was ridiculed, but the president of Sony Corporation (14) noted that it would cost 16 billion to wire up California with fiberoptic cable. Of

course, Teledesic is intended to cover much more than California. This leaves the clear implication that satellites might replace an important fiber optic application. The fiber optic/satellite controversy would then have come full circle since the mid eighties.

ACKNOWLEDGEMENTS

W. T. Brandon of the Mitre Corporation and E. Bedrosian of the RAND Corporation recognized the potential cost effectiveness of low altitude satellites in the mid seventies. They offered launch strategies to overcome objections to the difficulties of massive deployment.

J. Wesdock of Stanford Telecommunications, Inc. observed that L band severely constricts CDMA performance. He further developed a mobile-satellite concept at 28 GHz. Vickie Granberg and Sherri Clauson coped with long equations and finessed them into columns. They also introduced legibility into the reduced figures.

SELECTED REFERENCES

[1] A. K. Kamal and P. F. Christopher, "Communications at Millimeter Wavelengths", Proc. ICC, June 1981, Denver, CO.

[2] NASA/NSF Panel Report on Satellite Communications Systems and Technology, Vol I. Analytical Chapters, ITRI, July 1993. These comparisons of U.S. and international satellite technology were presented in early February 1993.

[3] Dorothy C. Rogers, P. Christopher, "Satellite Orbits to Relieve Ionospheric Scintillation", Proc. of Ionospheric Effects Symposium, April 1981.

[4] Edmund L. Andrews, "A Satellite System is Planned to Link Most of the Globe", N.Y. Times, March 21, 1994.

[5] B. R. Bean and E. J. Dutton, "Radio Meteorology", NBS Monograph 92, U.S. Department of Commerce, 1966, pp. 270-274.

[6] H. J. Liebe, P. W. Rosenkranz, and G. A. Hufford, "Atmospheric 60 GHz Oxygen Spectrum: New Laboratory Measurements and Line Parameters", J. Quantum Spectroscopy and Radiative Transfer, Vol. 48, No. 516, pp. 629-643, 1992.

[7] R. K. Crane, "Prediction of Attenuation by Rain", IEEE Transactions on Communications, Vol. Com-28, No. 9, September 1980.

[8] L. J. Ippolito, R. D. Kaul, and R. G. Wallace, "Propagation Effects Handbook for Satellite Systems Design", NASA Reference Publication 1082 (second edition), December 1981.

[9] R. W. Wilson, "Sun Tracker Measurements of Attenuation by Rain at 16 and 30 GHz", B. S. T. J., Vol. 48, No. 5, pp. 1383-1404, May-June 1969.

[10] Francesco Linsilata, Bruce Gribble, Barry Gribble, "SGAT User's Manual", Stanford Telecom Report, Reston, VA., 1988.

[11] A. H. Jackson, et al, "Optimum Satellite Relay Positions", Proc. of NASA GSFC Flight Mechanics Symposium, Publication 3265, May 1994.

[12] P. Christopher, W. W. Wu, "Krypton; A Low Cost Satellite Communication Concept", Proc. of National Telemetry Conference, Ashburn, VA., June, 1992.

[13] D. H. Raab, et al, "A Cosine Approximation to the Normal Distribution", Psychrometrika, Vol. 26, December 1961.

[14] John J. Keller, "McCaw-Gates Satellite Plan Draws Skeptical Reviews", Wall Street Journal, March 22, 1994.

[15] S. Wolfram, "Mathematica, A System for Doing Mathematics by Computer", Second Edition, Addison Wesley, 1991.

APPENDIX A: ORBITAL ELEMENTS FOR A MILLIMETER WAVE LEO SYSTEM

Elements are chosen for a 350 km perigee and a lifetime on the order of 10 years. Elements are listed as semimajor axis (km), eccentricity, right ascension; argument of perigee; mean anomaly; and inclination.

Table 1a. Two Hour Orbits for N. Hemisphere with Sister Satellites Spaced 60°E, 60°W for ISL's

A	e	Ω	Wp	MA	I	Comment
8059.0	.1651396	0	-45	0	63.435	Satellite 1
8059.0	.1651396	12	-45	144	63.435	Satellite 2
(successive satellites with 12° Ω increments, (144° MA increments)						⋮
8059.0	.1651396	348	-45	576	63.435	30

Table 1b. Two Hour Orbits to Complete Worldwide Coverage

A	e	Ω	Wp	MA	I	Comment
8059.0	.1651396	6	135	72	63.435	Satellite 31
8059.0	.1651396	18	135	216	63.435	Satellite 32
(successive satellites with 12° Ω increments, (144° MA increments)						⋮
8059.0	.1651396	354	135	288	63.435	60

APPENDIX B: NET LOSS FOR A RANDOM ELEVATION SYSTEM

We seek a solution to the equation

$$g(F) = \int_0^{\pi/2} f(F, E)\, \rho(E)\, dE \qquad \text{(B-1)}$$

where f(F, E) is net loss as a function of Frequency and Elevation. The net loss chosen here is representative of 0.99 availability in Washington, D.C.

$$f(F,E) = 115.033 - 0.89422\,E + 0.0239618\,E^2 - 0.000257479\,E^3 + 8.00353\,10^{-7}\,E^4 - 10.9092\,F - 0.00823157\,E\,F + 0.000156356\,E^2\,F + 0.460541\,F^2 - 0.000191151\,E\,F^2 - 0.00840929\,F^3 + 0.0000590047\,F^4 \quad \text{dB} \qquad \text{(B-2)}$$

The function may be visualized as Figure B-1

The minimum of f(F,E) is difficult to see. A contour plot (Figure B-2) shows a near-minimum at 45 GHz and 60°.

Raab (13) has introduced a convenient approximation to a Gaussian pdf. If p(E) is Gaussian [M, σ],

$$\rho(E) \approx \frac{1.14}{2\pi\sigma}\left[1+\cos\frac{1.14}{\sigma}(E-M)\right] \qquad \text{(B-3)}$$

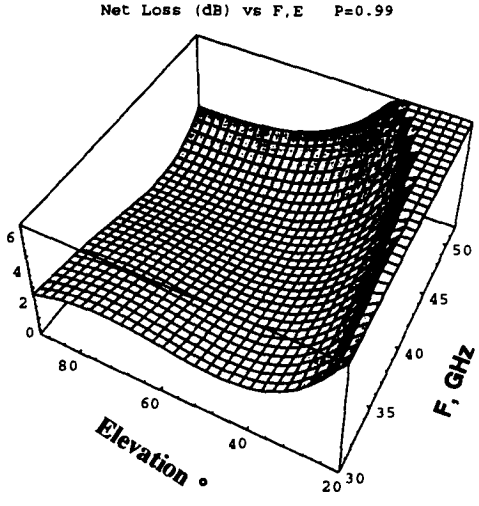

Figure B-1. Bivariate Net Loss

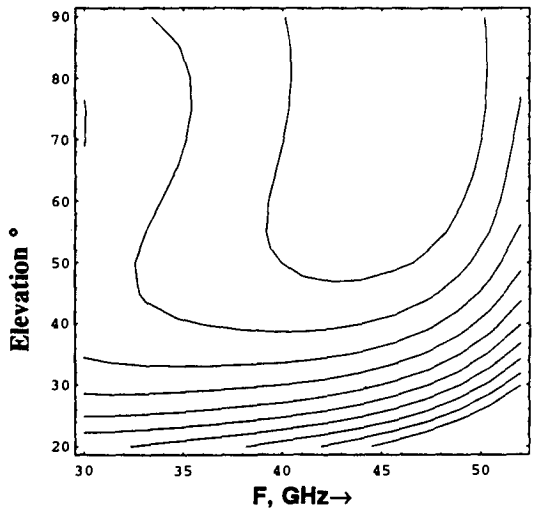

Figure B-2. Net Loss Contours

Mathematica allows (B-1) to be completed in a long closed form as follows (with M = mean, SD = standard deviation). Reference (15) is helpful for symbolic operations.

The net loss for 0.99 availability may be found as a general function of frequency (GHz), mean (MU) and standard deviation (SD) of elevation angle:

$$\text{Net Loss} = 7.54192\,10^{-8}\,(1.52524\,10^9 - 1.44647\,10^8\,F + 6.10642\,10^6\,F^2 - 111501.F^3 + 782.356\,F^4 - 1.18567\,10^7\,MU - 109144.F\,MU - 2534.51\,F^2\,MU + 317714.MU^2 + 2073.16\,F\,MU^2 - 3413.97\,MU^3 + 10.612\,MU^4 + 315335.SD^2 + 2057.63\,F\,SD^2 - 10165.2\,MU\,SD^2 + 63.1955\,MU^2\,SD^2 + 25.1541\,SD^4) \text{ dB} \qquad \text{(B-4)}$$

This general result (B-4) is the second new result we require in order to find optimum frequencies for random elevation systems.

The result for the 60 satellite system may be visualized as Figure 4-4. The optimum frequency approaches 44 GHz.

The value of a general result, such as equation (B-3), is that it may be applied to other LEO systems. A low elevation LEO system, with 25° average elevation, may be represented as Figure B-3. The optimum frequency is seen to drop to 29 GHz. The net loss is also on the order of 7dB higher than Figure 4-4.

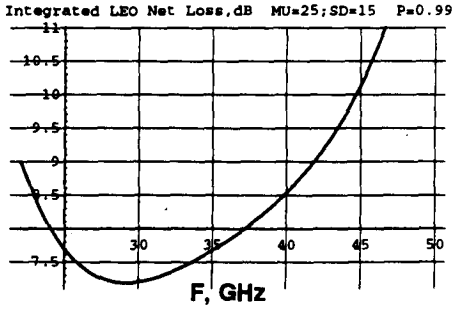

Figure B-3. Net Loss for Low Elevation System

The NUONCE Engine for LEO Networks

Martin W. Lo and Polly Estabrook
Jet Propulsion Laboratory
California Institute of Technology
4800 Oak Grove Dr., Mail Stop 301-142
Pasadena, CA, 91109, USA
Phone: 818-354-7169 FAX: 818-393-9900
mwl@trantor.jpl.nasa.gov

ABSTRACT

Typical LEO networks use constellations which provide a uniform coverage. However, the demand for telecom service is dynamic and unevenly distributed around the world. We examine a more efficient and cost effective design by matching the satellite coverage with the cyclical demand for service around the world. Our approach is to use a non-uniform satellite distribution for the network. We have named this constellation design NUONCE for Non-Uniform Optimal Network Communications Engine.

INTRODUCTION

On July 26, 1963, the Syncom satellite was successfully launched into orbit and became the world's first geosynchronous communications satellite. This joint venture of the Hughes Aircraft Co. with NASA revolutionized the telecommunications world. These satellites have affected every aspect of our lives and changed the way we live. Today, a new revolution in the world of satellite communications is in the making: the Low Earth Orbit (LEO) satellite communications networks. The April 18, 1994 issue of Space News [1] lists no less than 12 companies with proposed global networks. Teledesic Corp. leads the pack with a network of nearly 1000 satellites. This April, Orbital Communications Corp. is scheduled to launch the first two of its 36 Orbcomm data communications satellites.

Typical LEO networks use uniformly distributed constellations to provide uniform coverage. These networks tend to use circular orbits with almost identical altitudes, evenly spaced in the orbit planes. The resulting constellation is usually highly symmetrical. However, the demand for telecommunications service is dynamic and highly non-uniform. This is because the users are unevenly distributed on the continents which cover only a quarter of the earth. Furthermore, there is a bimodal diurnal cycle in the demand for services due to the business day. This suggests that perhaps a dynamic non-uniformly distributed network is more efficient.

We have named this constellation design NUONCE, the Non-Uniform Optimal Network Communications Engine. Such a network would require fewer satellites and may reduce the capital overlay required to the benefit of both industry and consumers alike. The NUONCE constellation may also provide a good phased implementation strategy. Since the network is non-uniform to begin with, the routing, traffic management and operations are designed to function accordingly. The early sparse phase could target certain limited markets. As the demand increases, additional satellites could be added to the network. This enables an adaptive and evolving network with greater flexibility than a fixed uniform constellation both in the implementation and the resource management. Of course, this would demand a more carefully thought out telecom design that would permit migration from one configuration to another.

GOAL

Our goal in this paper is to consider some orbital design strategies to help the satcom system designer to come up with a non-uniform constellation. Specifically, we want to find constellations which will spend most of the time in the day side where the demand for telecom service is highest.

CONVENTIONS AND COORDINATES

Frequently, the right picture will suggest the solution to a seemingly difficult geometric problem. In this case, the right picture is provided through the use of rotating coordinate systems. Fig. 1 below shows the equatorial plane of the earth as viewed from above the north pole. Assume at time 0 the sun is in the direction of the y-axis at the top of the figure. In earth-centered inertial coordinates, the sun moves roughly 1° per day counter-clockwise. Thus 1 day after time 0, the sun will no longer point in the y-direction but will be in roughly 1° to the left of the y-axis. However, if we let our coordinate system rotate counter-clockwise to match the apparent motion of the sun, we then have the sun always fixed in the y-direction. We will adopt this rotating coordinate system in the following discussion. The reason this coordinate system is useful for our problem is because we want to find orbits which linger on the sun-side as stated in the goal above.

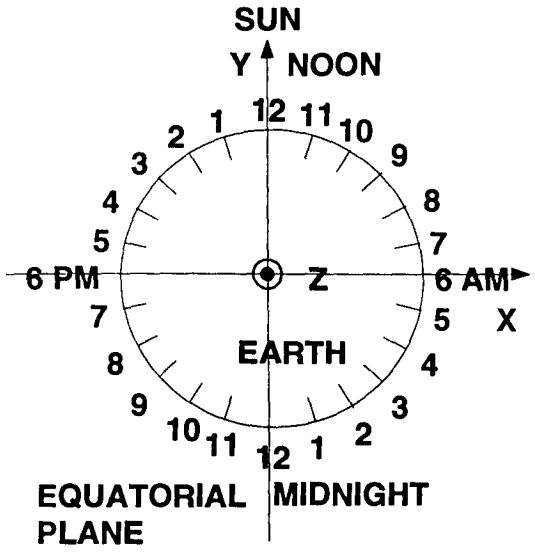

Figure 1. Rotating Coordinate System

We now define some conventions to be adopted for the discussion in this paper. Note in Figure 1, we have marked the different longitudes with their local times. We define the "day side" to be 6 AM to 6 PM going counter clockwise. This is the top half of Figure 1; the bottom half is the "night side".

To simplify the discussion, unless otherwise noted, we assume the orbit of earth is circular and that the equator coincides with the ecliptic. However, we do include the first order effects of the earth's equatorial bulge which cannot be ignored for LEOs. For this discussion, we define a LEO to be an orbit with altitude under 2000 km, a MEO (Medium Earth Orbit) to be an orbit with altitude under 16763 km (6 hour period), a HEO (Highly Elliptical Orbit) to be an orbit with eccentricity greater than 0.1.

CIRCULAR VS. ELLIPTICAL ORBITS

In order to quantify the performance of an orbit, we define a metric called the Day Side Fraction. This fraction is the ratio of the amount of time a satellite spends in the day side of an orbit divided by the orbit period. For example, the day side fraction of circular orbits is 0.5.

Let us look at a typical circular LEO at 200 km altitude and 85° inclination with a period of about 1.5 hours. Figure 2 is a plot of 4 satellites clustered together in this orbit. But, clearly the cluster will spend just as much time in the day side as in the night side. So an uneven distribution of satellites in this orbit does not seem to help our cause. In fact, given a satellite in any circular LEO about the earth, it will always spend equal time in both the day side and the night side.

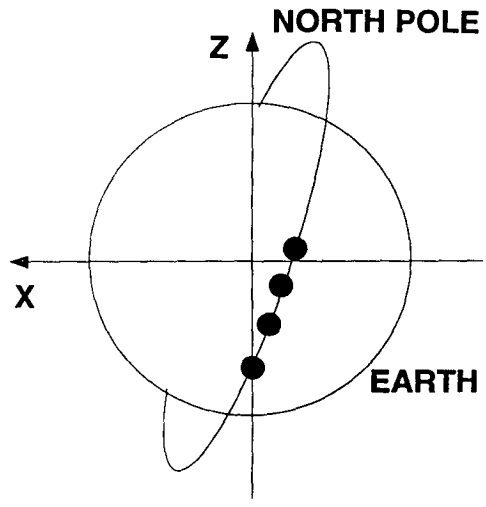

Figure 2. Four Satellite Cluster in a Circular LEO Orbit

This suggests using elliptical orbits. Figure 3 shows the fraction of time per orbit a satellite is in the day side as a function of orbit eccentricity. For this calculation, we assume the perigee is placed at the equator. Thus the apogee is also on the equator. Figure 4 shows what this means geometrically. For a given orbit plane and eccentricity, this orientation provides the greatest day side fraction for an orbit. For example, a Molniya orbit has e=0.75 which yields a day-side fraction of 93%. This means it spends 93% of each orbit on the day side. But, with a period of 12 hours, the Molniya orbit is a HEO. What about elliptical LEOs?

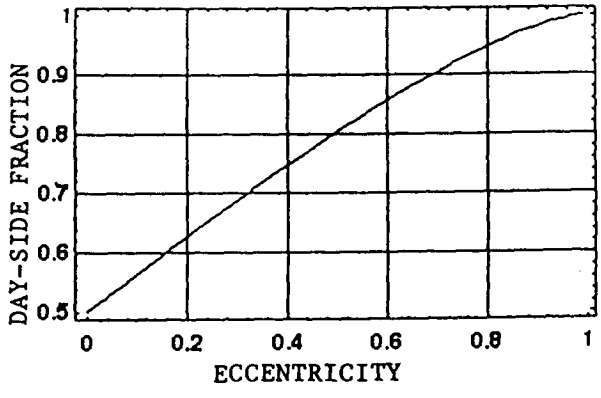

Figure 3. Day Side Fraction vs. Eccentricity

In the range we are considering (altitude < 2000 km), what are the most eccentric elliptical orbits we can consider? Since the altitude is restricted to be less than 2000 km, this means the apogee must be less than 2000 km. The perigee can vary from 200 to 2000 km. Table 1. below lists a few of these orbits, their eccentricities, and day-side fraction.

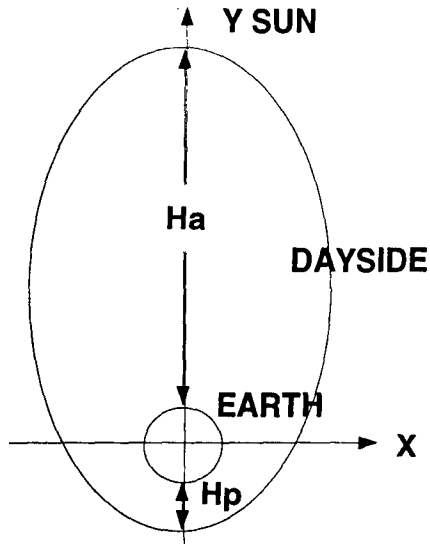

Figure 4. Geometry of Day Side Fraction

Hp/Ha (km)	Ecc.	Fraction	Minutes
200/1000	0.0573	0.5364	3.5
300/1000	0.0498	0.5317	3.1
400/1000	0.0424	0.5270	2.7
450/1000	0.0387	0.5246	2.4
475/1000	0.0369	0.5235	2.3
500/1000	0.0351	0.5223	2.2
200/2000	0.1204	0.5764	8.2
300/2000	0.1129	0.5717	7.8
400/2000	0.1056	0.5671	7.3
450/2000	0.1019	0.5645	7.1
475/2000	0.1001	0.5636	7.0
500/2000	0.0983	0.5625	6.9

Table 1. The Day-Side Fraction of Selected LEOs

Hp/Ha are the perigee and apogee altitudes of the orbit. Ecc is the eccentricity of the orbit. Fraction is the Day-Side Fraction and the resulting extra time spent on the day side per orbit is the last column. Realistically, in order to avoid drag decay of the orbit, the perigee should be around 500 km. Thus the 500/2000 case is the most eccentric orbit to be used in a LEO. This provides a maximum of about 7 minutes of extra time on the day side for an orbit period of 108 minutes. If we drop the apogee altitude to 1000 km, the 500/1000 case yields a 2 minute advantage on the day side for an orbit period of 100 minutes. Thus elliptical orbits will increase the day-side portion of the orbit. Even a small savings of a few per cent is significant when the stakes are high.

Unfortunately, this is not the entire story. The equatorial bulge of the earth introduces other challenges. The dominant term of the perturbation in the geopotential with coefficient J2 causes the orbit planes to precess about the poles. This is called "nodal precession" because the precession is defined by the motion of the orbit node where the satellite first crosses the equatorial plane into the northern celestial sphere. J2 also causes the line connecting the perigee and the apogee to rotate within the orbit plane about the orbit normal vector. This is called "apsidal rotation". We note that apsidal rotation does not affect a circular orbit since it has no apogee or perigee.

To first order, these perturbations are governed by the orbit semimajor axis, eccentricity, and inclination. For the LEO elliptical orbit at 85° inclination with 500 km perigee height and 2000 km apogee height, the nodal precession is -0.47°/day and the apsidal rotation is -2.6°/day. For the same elliptical orbit at the lower inclination of 28.5°, the nodal precession is -4.8 °/day and the apsidal rotation is 7.8 °/day. Thus, for the 28.5° orbit, the apogee will have moved 180° in less than a month. So if it started in the day side, it will now be in the night side.

This can be fixed by using orbit planes at the critical inclination of ±63.43° where the rotation of the perigee is eliminated. However, there remains the precession of the node. At critical inclination, the nodal regression of the 500/1000 LEO elliptical orbit is still -2.4°/day. In 150 days, the orbit plane will have precessed 360° around the equator. Thus we are unable to force the orbit planes to remain in their time slot. Fortunately, sun-synchronous orbits (see next section) solve this problem.

Alternatively, we should mention that both the nodal precession and the apsidal rotation can be fixed by propulsive maneuvers. But this requires a lot of orbit maintenance which is expensive both in the fuel and operational costs. However, new technology using continuous low thrust and autonomous control may provide answers to these problems in the near future. But, for this discussion, we do not consider this kind of technology although the orbit design strategy described in this paper is equally valid and compatible with the new technology.

SUN-SYNCHRONOUS ORBITS

Sun-synchronous orbits are those orbits whose nodal precession rates exactly match the orbital motion of the earth around the sun. The orbit plane maintains a near constant geometry with respect to the sun. Sun-syncronicity is determined by three orbit parameters: semimajor axis, inclination, and eccentricity, and requires inclinations greater than 90°. Now each orbit still goes through the full 24 hours of time zones during one revolution and it has the interesting property that it always passes the same latitude

at the same local mean time. For example, we want an orbit over New York City (41° latitude) at 10 AM. Figure 5 [2] below is a plot of the local mean time as a function of the satellite nadir latitude in an orbit centered on NYC at 10 AM. Note that the variation of the local mean time for this orbit is fairly narrow. From -50° to 50° latitude, the variation of the local mean time is just 1 hour. Figure 6 is a plot of the orbit over earth as viewed from the sun. This geometry will remain fairly constant over time.

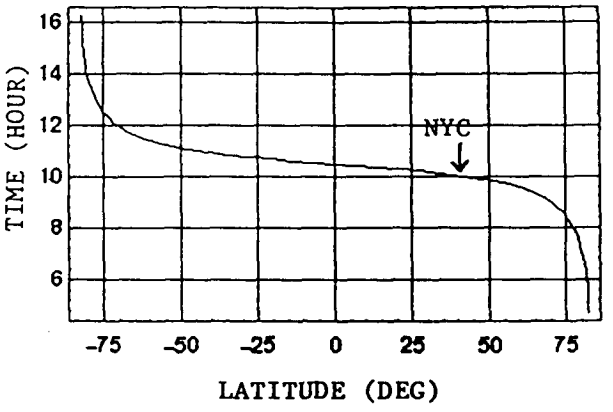

Figure 5. Local Mean Time of 10 AM Orbit Over NYC

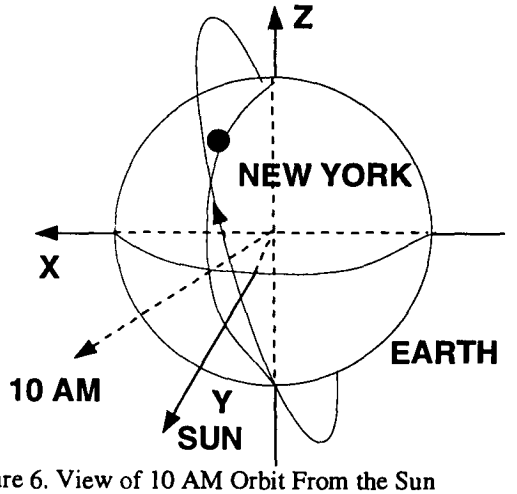

Figure 6. View of 10 AM Orbit From the Sun

This suggests we can use sun-synchronous orbits to optimize the day side coverage as follows. Suppose we want to cover New York City and we expect the heaviest traffic over New York to be from 9 AM to 3 PM. Let us start with a Walker constellation of circular orbits as an example of a uniformly distributed constellation and change it into a NUONCE constellation. The Walker design has all satellites at the same altitude and inclination [3] where the satellites are spaced evenly within each orbit plane and the planes are evenly spaced around the equator. The phasing of when the satellites cross the equator in adjacent planes is also the same for all orbit planes. The aim of the Walker constellation is for continuous global coverage. But, the aim of the NUONCE constellation is to maximize coverage of high demand regions over day time. For our satcom example, suppose a sun-synchronous Walker design requires an orbit plane every 15° (1 hour) apart with 6 satellites per orbit. This requires 12 planes with 72 satellites total. Figure 7 below is a schematic diagram of this design. The lines around the clock represent orbit planes with nodal crossings at the time indicated. For simplicity, the inclination is not represented.

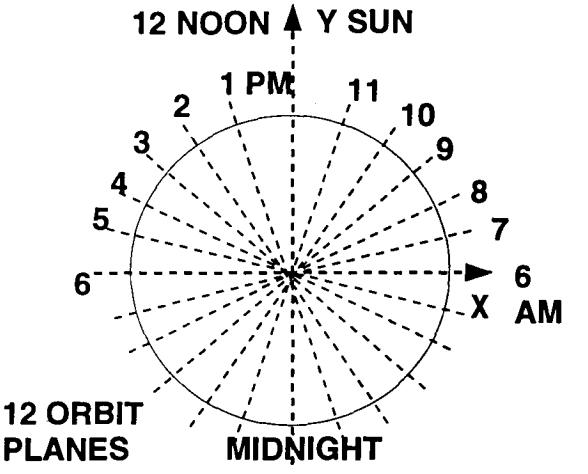

Figure 7. Diagram of Walker Constellation

Since the usage from 6 AM to 9 AM and 3 PM to 6 PM will be low, perhaps just a single plane at 6 PM with 4 satellites is sufficient to handle the traffic. Also, at 12 Noon, there will be less demand due to the lunch hour. So the 12 PM plane may be removed. The resulting constellation has 7 planes with 40 satellites total. Figure 8 below is a schematic diagram of this design. This shows a dramatic reduction of 32 satellites. Of course, this is just an example to illustrate the approach without the detail analysis verifying whether the real coverage demand has been met.

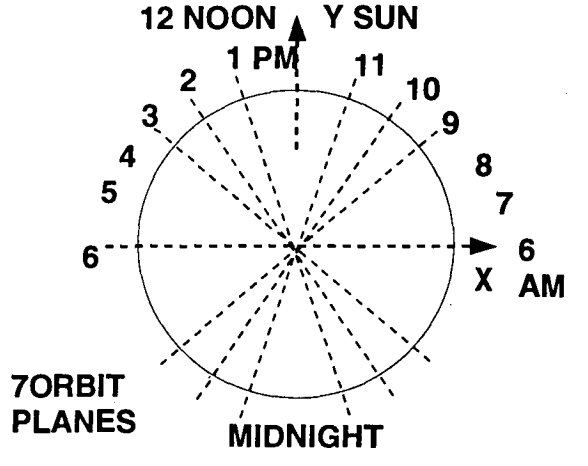

Figure 8. Diagram of NUONCE Constellation

NON-UNIFORM STRATEGY

Now that we have discussed circular orbits, elliptical orbits, critically inclined orbits, and sun-synchronous orbits, we can put the pieces together to formulate a non-uniform satcom orbit design strategy. Recall the aim for our NUONCE constellation is to optimize day-side coverage. This can be achieved by using the following guidelines:

1. Use sun-synchronous orbits (inc. > 90°) so that one can control the local time passage at specific latitudes.

2. Concentrate the orbit planes with specific longitudes in time zones of highest usage demands.

3. Evenly space the satellites within each plane. In planes over regions and time zones of high demand, increase the number of satellites. In planes over regions and time zones of low demand, decrease the number of satellites.

4. Use elliptical orbits where possible. Place the apogee over the latitude of a region of high demand at the peak hours.

5. Use critical inclination to control the apsidal rotation in elliptical orbits. Critically inclined sun-synchronous orbits exist only at the inclination of 116.57° (-63.43°).

USING HEO

What about using elliptical orbits to take advantage of all the extra capacity wasted on the night side? For our 500/2000 km LEO elliptical orbit, the sun-synchronous inclination is 100.46° and the apsidal rotation rate is still a hefty -2.3°/day. Thus, we need to use critically inclined sun-synchronous orbits. But this would bring us out of the LEO realm since a circular sun-synchronous orbit has an altitude of 3438 km.

Suppose we want an elliptical orbit with 70% day side coverage per orbit. From Figure 3 we see that this requires an eccentricity of 0.32. A sun-synchronous orbit with this eccentricity at critical inclination will require a semimajor axis of 10441 km. This gives a perigee/apogee altitude of 722 km/ 7404 km with a 3 hour period. The apogee is fixed by the critical inclination and the orbit plane follows the sun synchronously as designed. Clearly, this provides much better day-side coverage than a circular LEO if time is the only consideration. This is in fact like the HEO orbit selected by Ellipso as part of its constellation design.

CONCLUSION

The observations of this paper suggest that uniform circular LEO constellations are not optimal for the day-side coverage. However, a non-uniform distribution which does not use sun-synchronous orbits will not provide good coverage of the day side due to the precession of the orbit plane and the rotation of the apogee. Similarly, although an elliptical orbit can increase the coverage on the day-side. its apogee must somehow be fixed on the day-side.

Using sun-synchronous orbits, the day-side coverage can be optimized by concentrating the orbit planes in the time zones with the heaviest traffic. This can be achieved with circular LEOs. By using critically inclined sun-synchronous HEOs, the day-side fraction of the coverage can be increased significantly to 70% or more.

This paper provides guidelines to assist in the orbit design process to ensure maximum coverage on the day side. More detailed analysis is required, but the NUONCE constellation concept clearly provides better coverage than a uniform constellation. These conclusions address only the geometric coverage issue and do not take into consideration other important issues such as the telecom design, spacecraft design, impact on operations, and launch cost which will impose other constraints on the constellation design.

ACKNOWLEDGMENTS

This paper presents the result of research carried out at the Jet Propulsion Laboratory, California Institute of Technology under contract with the National Aeronautics and Space Administration. The authors wish to thank Dr. Johnny H. Kwok, Jess Fordyce, Larry Bright, and James Stephens of JPL for their helpful comments and discussions in reviewing this work, and Mark Garcia for performing several simulations in support of this work.

REFERENCES

[1] Space News, pp. 1, April 18, 1994.

[2] J. R. Wertz (ed.), "Spacecraft Attitude Determination and Control", D. Reidel Publishing Company, 1980, pp. 68-69.

[3] J. G. Walker, "Circular Orbit Patterns Providing Whole Earth Coverage", Royal Aircraft Establishment Technical Report 70211, November 1970.

Air Traffic Management System Design Using Satellite Based Geo-Positioning and Communications Assets

Phil Horkin, Motorola Government and Space Technology Group
2501 S. Price Road, Chandler, AZ 85248-2899 USA
Phone: 602-732-2313 FAX: 602-732-2598

ABSTRACT

The current FAA and ICAO FANS vision of Air Traffic Management will transition the functions of Communications, Navigation, and Surveillance to satellite based assets in the 21st century. Fundamental to widespread acceptance of this vision is a geo-positioning system that can provide worldwide access with best case differential GPS performance, but without the associated problems. A robust communications capability linking-up aircraft and towers to meet the voice and data requirements is also essential.

The current GPS constellation does not provide continuous global coverage with a sufficient number of satellites to meet the precision landing requirements as set by the world community. Periodic loss of the minimum number of satellites in view creates an integrity problem, which prevents GPS from becoming the primary system for navigation. Furthermore, there is reluctance on the part of many countries to depend on assets like GPS and GLONASS which are controlled by military communities.

This paper addresses these concerns and provides a system solving the key issues associated with navigation, automatic dependent surveillance, and flexible communications. It contains an independent GPS-like navigation system with 27 satellites providing global coverage with a minimum of six in view at all times. Robust communications is provided by a network of TDMA/FDMA communications payloads contained on these satellites. This network can support simultaneous communications for up to 30,000 links, nearly enough to simultaneously support three times the current global fleet of jumbo air passenger aircraft. All of the required hardware is directly traceable to existing designs.

INTRODUCTION

The FAA and ICAO have been developing a Future Air Navigation System (FANS) concept [1] that uses an augmented form of the GPS constellation to provide navigation, precision landing and surveillance functions for Air Traffic Management (ATM). Differential GPS enhanced through a Wide Area Augmentation System (WAAS) [3] which corrects for propagation path disturbances would provide both the navigation function for the aircraft, and also the Automatic Dependent Surveillance (ADS) function, replacing fixed radar sites. Communications is included in this concept for voice and data using satellite links. It is widely recognized by both the FAA and the international community that the current (un-augmented) GPS constellation is inadequate due primarily to an insufficient number of satellites, and the inability to quickly correct for failed satellites.

The existing GPS constellation, while developed for military purposes, does not provide enough satellites in view at any instant to provide a sufficiently good differential navigation solution, while also providing redundancy needed for integrity purposes. There are frequent periods where less than six are in view at a time. Four are required to provide three dimensions and time, a fifth to determine that a bad satellite is included in the group, and a sixth to determine which one is bad. Failure to solve this problem will prevent the FANS concept to become the primary system of choice. A further problem of the existing system is the long time required to repair the constellation when a failure occurs (switch in a redundant payload, or satellite) which places the aircraft and its passengers in danger. Also, there is a period everyday when the satellites line-up just the wrong way causing the navigation solution (GDOP) to blow up, significantly degrading performance. The international community has also been reluctant to adopt the use of a DoD system for which they have no control.

Communications between multiple aircraft, and between aircraft and towers is planned using evolutionary satellite based systems. A robust communications architecture must be developed for high capacity, low duty cycle burst communications. The development of new communications payload architecture's providing a large number of relatively narrowband adaptive channels has been a major developmental issue. Globally, there are currently over

11,700 commercial jetliners (plus many smaller private planes) that must be linked in a constellation that can provide hand-offs as the aircraft fly between regions. Communications are also required to relay aircraft navigation and other data to a master control facility within air regions as well as relaying differential corrections. The differential corrections from several tens to hundreds of wide area reference stations (part of the WAAS concept) [3] must be relayed back to a master station, and in turn, the master station must broadcast the correction map or algorithm to all of the aircraft in the region.

SYSTEM DESCRIPTION

The system to be described herein overcomes most of the obstacles faced by the use of the current infrastructure for air traffic management. The constellation is selected based upon requirements for air navigation, and its attendant integrity and timeliness required for precision landings. A robust communications system is included to provide worldwide interconnectivity between aircraft and towers. It is also utilized for automatic dependent surveillance, the autonomous reporting of aircraft position, tail number, and telemetry information back to a centralized processing facility. These features will be described below.

Constellation

The satellite constellation is configured using a Walker delta arrangement of satellites at approximately geosynchronous altitude and in near polar orbits, and augmented with 3 geostationary satellites. The Walker delta configuration consists of 4 planes of satellites equally spaced in longitude, and containing 6 satellites per plane, again equally spaced within each plane. The phasing of satellites between planes is nominally offset by one-half the in-plane separation. An illustration of this arrangement is shown in the figure below.

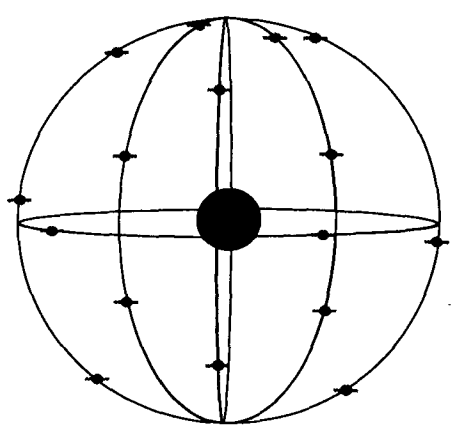

Orbital Arrangement of Satellites on Front of Orbital Sphere

The design of the orbital configuration was driven by the aviation need to simultaneously view six satellites. The GPS constellation provides six in view part of the time, but drops to five or four which can create a disaster for precision (automatic) landings. Extremely high integrity and availability are required to ensure that safe landings are possible even when a satellite fails, or the geometry is momentarily in a disadvantageous configuration.

Navigation receivers to be used by the FAA for use in their WAAS (Wide Area Augmentation System) Program [3] use a receiver autonomous integrity monitoring (RAIM) algorithm to determine that either all received GPS (or GPS-like) signals are within acceptable tolerance, or if there is one failed, or out of specification, it can be uniquely identified and ignored. Four good signals are required for an acceptable solution. Good system integrity is achieved with six in view since this is the minimum number that can *both* determine that one is bad, *and* identify which one.

The orbital configuration presented here provides 100 percent visibility to six satellites minimum at any aircraft location with a viewing elevation angle above 12 degrees from the local horizontal. While other systems such as GPS have to operate down to low elevation angles such as 5 degrees in order to provide coverage, this proves to be a problem during precision approaches where ground multi-path can degrade performance. This system is less vulnerable to these problems.

System Architecture

The overall architecture includes the twenty-seven satellites just described each carrying a communications and navigation payload. A satellite control facility (SCF) is used to coordinate the activities of the satellites, provide orbit maintenance, telemetry processing, and clock updates. While tracking antennas used at the SCF cannot connect to all satellites simultaneously, the SCF can indirectly connect to all as a network is formed using crosslinks between satellites and their neighbors both in-plane and cross-plane.

Other parts of the ground infrastructure (not required to be co-located with the SCF) include a processing facility, a wide area master station, and wide area reference stations (which are intentionally scattered to collect differential corrections for the navigation signals). These functions are all associated with the navigation and surveillance aspects of the system. While operating as a differential GPS type system, the ground infrastructure is used to provide the spatially separated differential monitoring sites, central

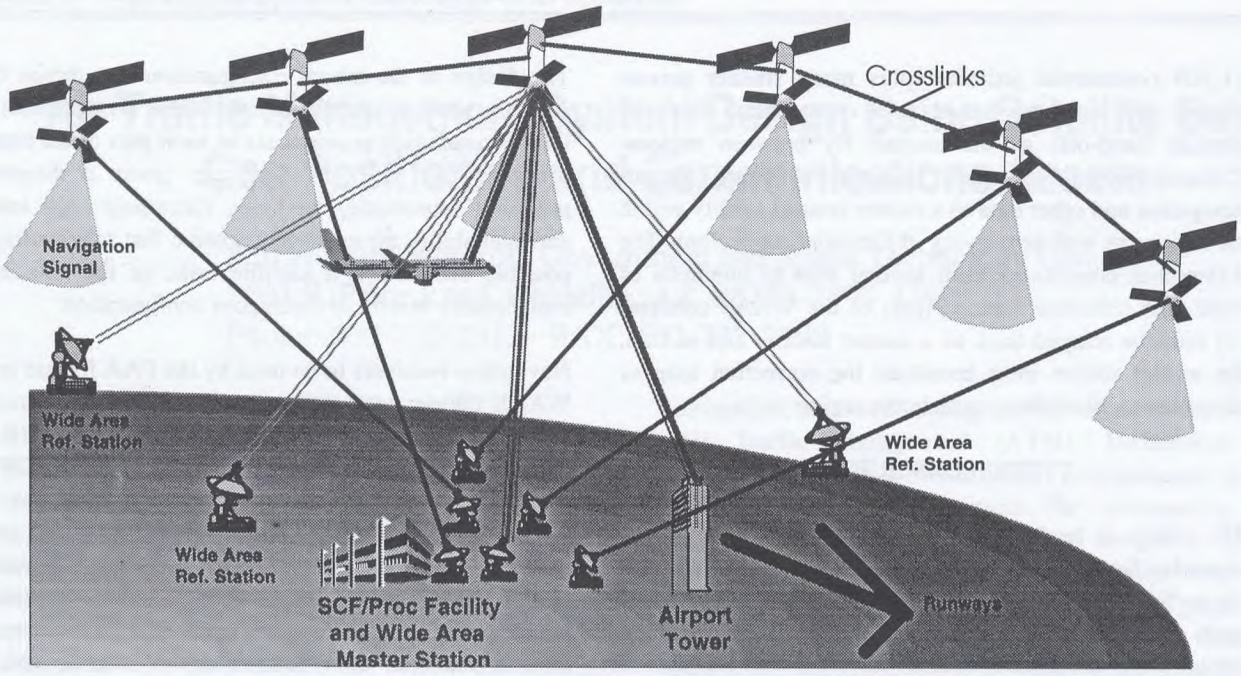

System Architecture

processing function, and the collection of surveillance signals for the ADS function.

Aircraft and towers are the primary users of this system. A description of how these elements operate together is described under the heading Operations Concept. The figure above illustrates the overall architecture.

Operations Concept

The operations concept is divided into two major functions, navigation and communications. Navigation will be described first. This system operates much as the GPS system, broadcasting PRN sequences which are correlated by receivers to determine pseudo-ranges to each satellite. Further analysis of the pseudo-ranges leads to position in three dimensions and time. This system utilizes unused codes chosen to minimize the cross-correlation interference. Unlike GPS, this concept designs-in differential corrections as part of the architecture rather than as an afterthought. The method for correcting the signals will be described later.

The aircraft will all carry a GPS-like receiver, one that includes both the original codes used on L1 (the C/A code frequency) and the additional codes used here. Upon receipt of the signals, the receiver-processor computes nominal position, and continually updates this. An additional processing function strips-off the differential corrections signal encoded on the L1 signal, and improves the navigation result. By using a receiver that is compatible with the existing GPS codes, operational compatibility is maintained, providing further graceful degradation. These receivers also continuously implement the RAIM algorithm to ensure that the best possible solution is achieved.

The navigation signal is used for enroute planning as well as providing the surveillance function. The surveillance function is analogous to current radars that track the motion of aircraft inside selected air space regions such as in the US. This navigation data along with tail number and other aircraft telemetry is relayed to airport towers and specialized processing facilities using the communications payload. These new facilities (the function could be located in major air traffic control centers) are able to track the progress of all aircraft in the global fleet, and provide enroute changes to optimize flight plans for fuel consumption, flight time, weather conditions, etc. Improved navigation accuracy and timeliness, especially over the large oceans will allow reductions in aircraft separation and provide more altitude flexibility.

The communications provided by the satellite-based system affords global connectivity between any combination of aircraft, towers, and air traffic control personnel. The links provide two-way networking of both data, such as the ADS function just described, alerts, and voice communications using a highly efficient packet switched TDMA/FDMA (time division multiple access/frequency division multiple access) architecture. The combination of the navigation, surveillance, and communications functions included in this concept can theoretically allow landings and take-offs at airports without towers or personnel with the same degree of confidence afforded at manned sites.

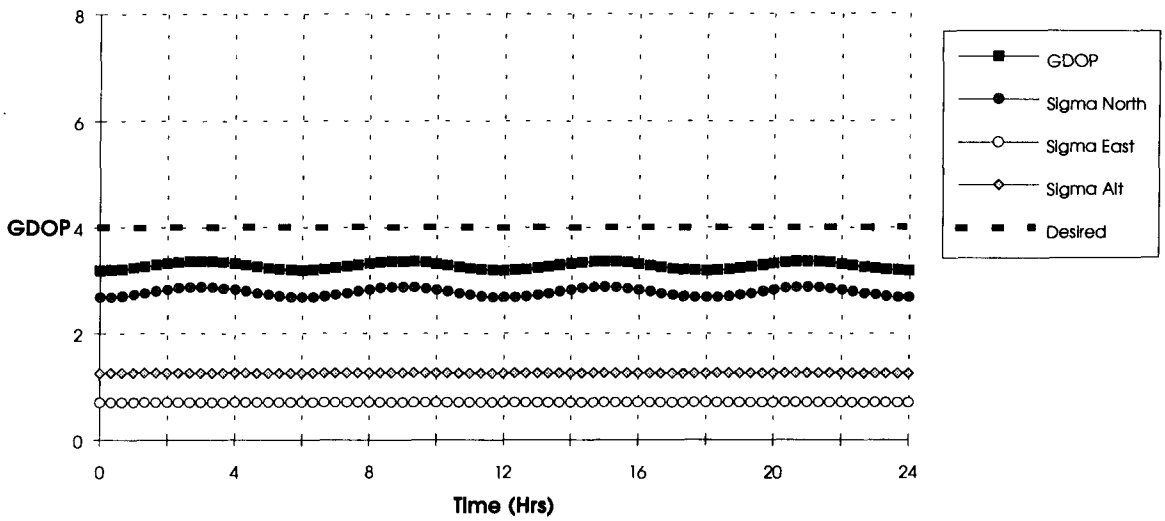

GDOP Results Six Satellites In View

Differential Corrections

The differential corrections approach is identical to those commonly in use today as modified by the FAA's specification FAA-E-2892. Wide area reference stations located broadly around areas which require improved navigation accuracy are precisely surveyed, and each contain a navigation receiver. In the US for example, 20-30 such sites would be required. Each site receives L1 and L2 navigation signals (L2 occasionally broadcasting the same C/A code structure with the unused codes) and computes its own location. These computed locations are compared to the known surveyed results, and error signals are formed for both the L1 and L2 frequencies.

The error signals (offsets) are relayed to a central processing facility (wide area master station) where the global data base is gathered. A correction map is produced, and a correction algorithm is linked through the satellites to all of the users using the FAA-E-2892 format. The data instructs a user on how to correct his computed position based upon the global corrections map. This "map" is updated frequently, so all users have current data.

The GDOP (geometric dilution of precision) results for a similar configuration (six satellites optimized for regional coverage) is presented in the plot at the top of this page. Comparing these results to GPS, one notes that there are no spikes, or sudden discontinuities in performance when satellite geometry becomes unfavorable. Even for scenarios with a failed satellite, i.e. one is determined bad by the RAIM algorithm and not used in the computations, the system gracefully degrades in performance. The altitude error from this simulation shows an error component running just over 1, or a resultant uncertainty of perhaps 1-1.3 meters.

Communications Heritage

A single communications architectural design provides all of the functions required to fully implements the FANS concept and has roots in the ACTS Program. The ACTS (Advanced Communications Technology Satellite) [2] Program developed the first multibeam TDMA system (dubbed a switchboard in the sky) beginning in 1984 and became operational two years ago. This first space-based packet switched communications system led to the development of an enhanced multi-beam TDMA/FDMA configuration for use in a personal communications system.

The addition of the FDMA format to the existing TDMA design creates a very spatially and spectrally efficient modulation format for use in applications such as personal communications as well as air traffic management. Users are geographically diverse, and this allows frequency re-use in separate beams, multiplying the actual spectrum in use to achieve a higher effective equivalent spectrum. Our current design provides several dozen overlapping beams in which users may simultaneously communicate using an order wire assigned time and frequency channel.

Routing of signals between users (aircraft, towers, control stations, etc.) is accomplished using header data at the start of packets. The satellite operates in a fully autonomous fashion, reading the destination information from each user, and switching between beams and satellite crosslinks on the fly. A functional flow diagram of this configuration is shown on the following diagram.

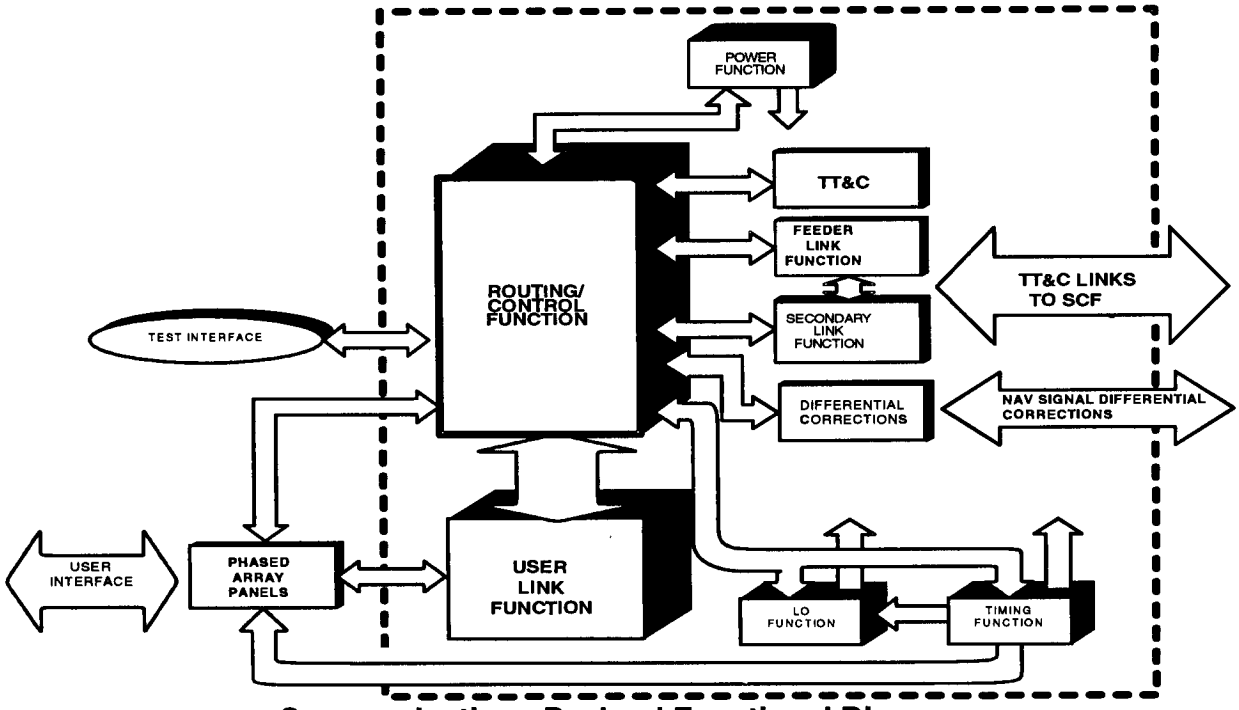

Communications Payload Functional Diagram

Aircraft Equipment

The equipment carried by the aircraft to be compatible with this system will need to be changed. Currently, aircraft do not routinely use GPS for navigation, but an increasing number are beginning to use it for secondary navigation. There are a few FAA certified aircraft GPS receivers, and these will require updating to include the new codes, and to perform the differential corrections processing. The communications equipment carried by aircraft operate on standards dating back 30-50 years, and use VHF push to talk voice. This equipment will need to be made dual compatible to support a transitional period. The new equipment (TDMA/FDMA) will also have to be linked to an on-board computer and the navigation receiver/processor. Data on aircraft parameters, i.e. position, tail number, fuel status, and so forth will be automatically collected and transponded to towers and control facilities. Crew members will not have to be burdened with this repetitive chore. Voice communications

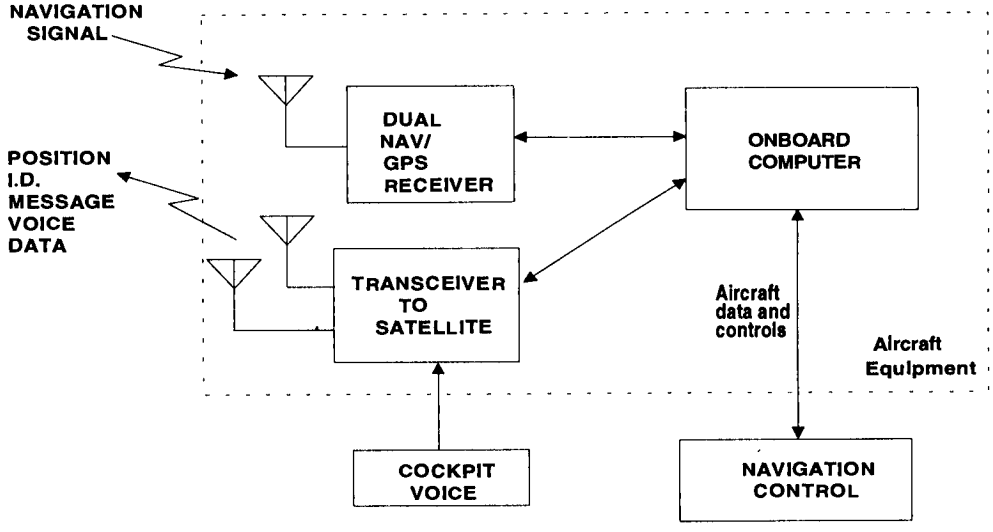

Aircraft Equipment

can still be supported as required with an automatic communications set-up procedure.

Spacecraft Concept

A pictorial drawing of a candidate spacecraft concept based upon modifications to an existing design is shown if the figure. Two sun-tracking solar arrays are used to provide adequate prime power on this three axis stabilized spacecraft. Horizon sensors and star trackers are used to sense vehicle orientation, while a three axis momentum wheel is used to provide control. Small thrusters are used for orbit maintenance as well as de-saturating the wheels.

The spacecraft uses a variety of antennas to perform the dual navigation and communications functions. Two small hemispherical antennas are used by the TT&C subsystem for orbit insertion. A higher gain TT&C antenna is used for mission operations. The navigation signal is broadcast by an array of helical antennas providing greater than full earth coverage. ATM traffic to the users is accomplished using three multi-beam phased array panels parallel to the local horizontal.

The electronics is contained in the mid-section of the spacecraft. Both the communications electronics and the navigation subsystem along with vehicle support subsystems are housed jointly for an efficient packaging approach. This layout provides for easy access during integration and test of the vehicle.

Summary

A new concept has been presented that solves most of the issues created by weaknesses in the GPS constellation design and creates an architecture suitable for a global FANS. Worldwide navigation is available from this system with best case differential GPS performance and a minimum of six satellites in view at all times. Integrity is thus assured.

Substantial margin is built into the architecture in the areas of coverage (elevation angle), communications capacity, and availability. Migration towards an internationally owned and operated constellation is made possible by eliminating DoD functions from this new architecture. A transition to inter-operability of this concept and the existing infrastructure is technically possible. Existing and mature low cost technology is fully available to support the development of this new FANS compatible air traffic management system.

REFERENCES

[1] *FAA Strategic Plan*, Appendix: Future System Concept, Washington D.C., March 8, 1994, pp. 67-89

[2] **Donald H. Martin**, *Communication Satellites 1958-1992*, Los Angeles: The Aerospace Corporation, December 31, 1991, pp. 41-44

[3] GPS Implementation Plan for Air Navigation and Landing, Washington D.C., August 1994, pp. 3-18

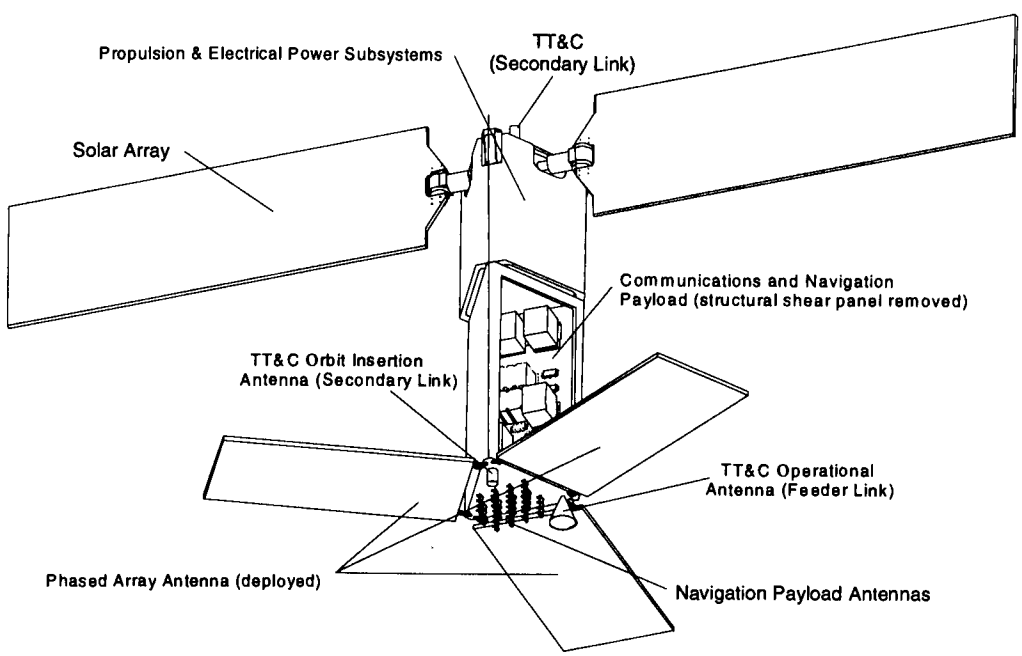

Spacecraft Concept

Global Tracking and Inventory of Military Hardware via LEO Satellite: A System Approach and Likely Scenario

David Bell, Polly Estabrook and Richard Romer
Jet Propulsion Laboratory
California Institute of Technology
4800 Oak Grove Drive
Pasadena, Ca, USA 91109
Telephone: (818) 354-3828
dbell@qmail.jpl.nasa.gov, polly@zorba.jpl.nasa.gov

Abstract - A system for global inventory control of electronically tagged military hardware is achievable using a LEO satellite constellation. An equipment Tag can communicate directly to the satellite with a power of 5 watts or less at a data rate of 2400 to 50,000 bps. As examples, two proposed commercial LEO systems, IRIDIUM and ORBCOMM, are both capable of providing global coverage but with dramatically different telecom capacities. Investigation of these two LEO systems as applied to the Tag scenario provides insight into satellite design trade-offs, constellation trade-offs and signal dynamics that effect the performance of a satellite-based global inventory control system.

1.0 Introduction

1.1 Study Goals

The goal of this study was to verify the feasibility and performance of direct Tag-satellite communication as applied to global inventory control of military hardware. Two commercial LEO systems were used as example satellite support scenarios. The investigation culminated with the estimation of temporal coverage and telecom capacity provided to potential military hot spots.

1.2 Satellite-Tag System Goals

The military employs Tags on equipment to help automate inventory control, speed access to inventory and provide automated tracking of valuable or sensitive material. Initial systems used bar codes and readers. Current systems now under development include an RF Tag with 2-way capability and a capacity of 128,000 bytes of information. A single interrogation unit can cover an area up to two acres, access any single unit or multiple units, read current information, update information and locate the device within a radius of 15 to 20 feet. While these new systems are limited to a range of several hundred feet, the desire is to be able track equipment in a theater of operation that may be scattered over hundreds of miles and equipment in transit to the theater of operations. The idea proposed is to augment existing remote inventory control with direct Tag-to-Satellite communications. A constellation of Low Earth Orbit, LEO, satellites would pass sufficiently low over equipment to allow two way communications to a Tag equipped with an omni-directional antenna and limited to 5 watts RF transmit power. There are several applicable commercial LEO satellite networks currently under development that could accomplish the task of providing true global connectivity to tagged military equipment.

This operational scenario is depicted in Figure 1 where a logistics support person is shown as using a computer to send (and receive) messages to (and from) a Tag. Tags will be placed on equipment containers that are shipped and stored around the world. The computer messages are envisaged as utilizing the Internet or private line to link the user with a satellite hub station. Messages are reformatted at the hub station to conform to the satellite and Tag system protocols. These messages are then transmitted to the Tag via the appropriate satellite in a constellation of satellites providing global coverage.

1.3 LEO System Models

In this study two types of Low Earth Orbiting (LEO) satellites are examined for use in closing the link to the Tag: an IRIDIUM satellite and an ORBCOMM satellite. IRIDIUM and ORBCOMM satellites were chosen for two reasons; (1) to represent operation with a satellite from the 'Big' LEO category (IRIDIUM) and from the 'Little' LEO category (ORBCOMM) and (2) to investigate Tag operation and performance with satellites systems likely to offer global coverage in the near future.

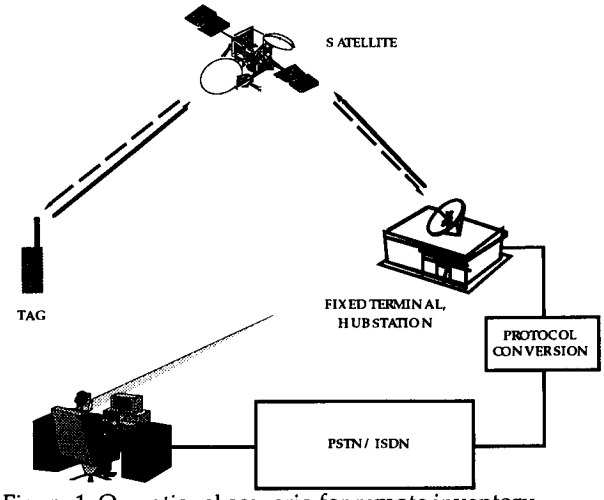

Figure 1. Operational scenario for remote inventory tracking using satellite communications to link materiel Tags with a logistics support personnel.

Using these two candidate LEO systems, additional study goals were to investigate LEO satellite systems' coverage of the Earth and their applicability to global Tag operations and provide insight into satellite design trade-offs, constellation trade-offs and signal dynamics that effect the performance of a satellite-based global inventory control system.

Analytical and trade-off analysis performed in this section were based on LEO satellite system parameters found in references 1, 2, 3, and 4.

1.4 Tag Operating Environment and Constraints

Tags will be placed on equipment containers that are shipped and stored around the world. Shipping times may be on the order of several months and storage times may exceed several years. Tags must be able to operate for years off battery power possibly augmented by solar cells. RF power output will be limited to about 5 watts peak and the antenna must be omni-directional to accommodate random orientations. The link must have sufficient margin to accommodate some shadowing and multipath as the Tag may at times be obscured from a line-of-sight link to the satellite. Link budgets in appendix A of this paper show that both the IRIDIUM and ORBCOMM systems can close the link while providing 15 dB of signal shadowing margin.

Tags will be in motion at times, but this motion will be dwarfed by the relative motion of the LEO satellites that communicate with the Tags. Hence both Tags and satellites must accommodate Doppler shifts of the transmit and receive frequencies due to the physical dynamics of the link.

No specific requirements exists for unintentional or intentional interference. Error correction coding and link margin must be sufficient to combat unintentional interference and special techniques, not covered in this analysis, would be necessary to combat intentional interferers. Security may be achieved by currently available digital encryption techniques.

2.0 LEO Satellite System Characteristics

2.1 IRIDIUM

IRIDIUM was originally developed and marketed by the Motorola Corporation. Under current organization, the IRIDIUM system will be funded and managed by the private international corporation, Iridium, Inc. which includes investors from the U.S., Canada, South America, Asia, India, Russia, Europe and the Middle East. The system is being marketed as a global satellite based personal communications system, providing near toll quality two-way voice, paging, data, geo-location and FAX services.

Global coverage is provided by 66 satellites placed in polar LEO orbits. Communications is Time Division Multiple Access, TDMA. Uplink and downlink frequencies are identical and channels are allocated in the 1610-1626.5 MHz L-band range. 50 kbps uplink and downlink data bursts are time-interleaved and thus with appropriate data buffering the users have the perception of lower rate, 4800 bps voice or 2400 bps data, full-duplex communications.

Subscriber units will include hand-held, portable and mobile versions that will be offered in a dual-mode configuration that will work with terrestrial cellular networks and the new IRIDIUM satellite network.

2.2 ORBCOMM

ORBCOMM is a LEO satellite communications system proposed by Orbital Communications Corporation a wholly owned subsidiary of Orbital Sciences Corporation. ORBCOMM has secured license agreements with service providers in Argentina, Brazil, Canada, Columbia, Ecuador, Guatemala, Honduras, Mexico, Panama and Uruguay.

The developers have proposed a tier set of communication and position location services. Two way communications services are emphasized for accidents, search and rescue, and emergency medical units. Data acquisition services are emphasized for monitoring of remote environment test sites and utilities vehicles. The monitoring service provides a one-way data retrieval and position monitoring with the option for occasional transmission to the remote unit.

Based on ORBCOMM's 1990 FCC filing their satellite constellation is comprised of 20 satellites in circular LEO orbits at an altitude of 970 km. (*More Recent FCC Filings propose a different satellite constellation of 36 satellites orbiting at an altitude of 775 km. This analysis is based on the earlier filings*). Uplink from the user is a 2400 bps QPSK signal at 148 MHz. Downlink to the user is a 4800 bps BPSK signal at 137 MHz.

ORBCOMM has proposed different classes of user terminals, including portable, mobile and hand held units. The simplest units will have fixed transmit and receive channels which will restrict access to satellites in a single orbit plane and thus reduce coverage by 1/3. More advanced terminals add frequency agility to the transmitter and to the receiver. Position determination service and hardware is optional.

3.0 Satellite Network and Satellite Dynamics

The IRIDIUM Satellite constellation consists of 66 satellites divided into 6 polar orbit planes spaced 31.6° apart. Each plane has 11 satellites equally spaced around the orbit with the orbit positions in adjacent orbit planes staggered. The satellites have an orbital altitude of 785 km, with an inclination of 86.4° and a nearly circular path. The resulting orbital period is approximately 101 minutes.

IRIDIUM assumes that the ground user will be able to communicate with the spacecraft if it appears at least 7°-10° above the horizon. Given this minimum elevation angle of 7°-10° and the low 785 km altitude of the spacecraft we find that at any instant the spacecraft can communicate to any user within an area below it on the earth roughly 4170-4650 km in diameter. Figure 2 depicts the scenario.

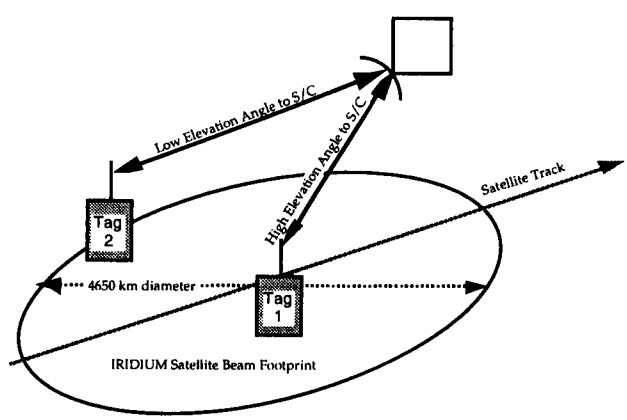

Figure 2: Users on outskirts of coverage see spacecraft only briefly at low elevation angles.

Users on the outskirts of this footprint only see the spacecraft for a brief instant as it rises above 10° elevation angle. Users directly under the path of IRIDIUM see the spacecraft above 10° elevation for about 10 minutes, which corresponds to the maximum pass time for any user.

The ORBCOMM full constellation consists of 20 satellites in circular LEO orbits at an altitude of 970 km. The resulting orbital period is about 104 minutes. Eighteen of the satellites form the primary constellation and are partitioned into 3 orbit planes equally spaced 120° apart in longitude and inclined between 40 and 60 degrees. Exact orbit inclination will be determined after further technical and market research. Within a plane, the 6 satellites are equally spaced around the orbit path. This primary constellation is designed to favor coverage to the equatorial and temperate latitudes. Two additional satellites in orthogonal polar orbits and 180° out of phase provide coverage to latitudes above 70° north or south. Coverage gaps of one to two minutes will occur in the lower latitudes and coverage to the northern latitudes is in 14 minute intervals separated by 30 minute gaps.

ORBCOMM assumes a minimum elevation angle of 5° which results in a maximum slant range of 3135 km and a beam coverage circle 5600 km in diameter. Maximum pass time is about 15 minutes and decreases as the satellites ground track diverges from the user's location.

3.0 Global Coverage

The rotation period of the Earth is much slower than the orbit time of the IRIDIUM spacecraft. This results in a single spacecraft covering a different ground swath on every orbit. In one day an IRIDIUM spacecraft completes 14.3 orbits. If we integrate the full 66 satellite constellation coverage over 1 day we get the coverage vs. user latitude plot shown in figure 3. In general, coverage increases for increasing latitude. This is a feature of any near polar low earth orbit. On every orbit each IRIDIUM satellite visits the poles but on each orbit only a fraction of the lower latitudes can be covered. Coverage values at all latitudes exceed 24 hours per day. This means that at times, there is more than one satellite visible. A coverage time of more than 48 hours per day says that there are on average, 2 or more satellites visible to the ground user during the entire day. This is true for users above 55° north or south latitude.

Similar results for the 20 satellite ORBCOMM constellation are also shown in figure 3. (Note the different minimum elevation angle assumption). The main constellation, with orbits inclined at 50°, enhances coverage in the lower to middle latitudes. Coverage falls off at higher latitudes and would in fact be zero above 75° if the two polar orbiters were eliminated. It is important to note that for latitudes below 40°, the ORBCOMM constellation provides nearly the same temporal coverage as does IRIDIUM but with only 1/3 the number of satellites. This is because the orbit inclination of 50° in general is better than a near polar orbit for providing coverage to lower latitudes. Above 40° latitude the IRIDIUM constellation is a better performer in part because of the better high latitude coverage afforded by polar orbiting satellites. Reasons for using a larger number of satellites in near polar orbit include IRIDIUM's desires, (1) to provide > 99% temporal coverage to virtually 100% of the globe, (2) to provide traffic capacity high enough to meet expected user demands.

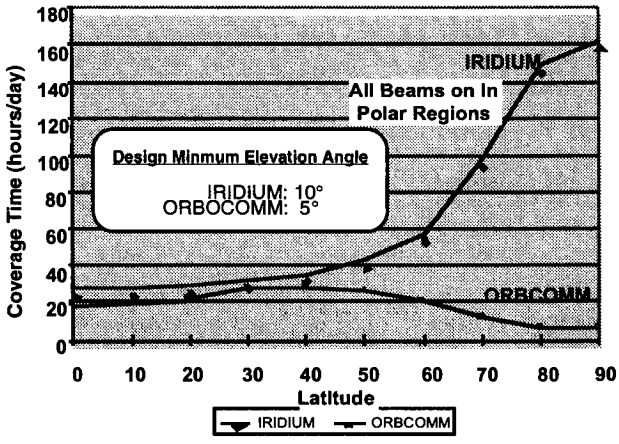

Figure 3: IRIDIUM vs. ORBCOMM: full constellation coverage vs. user latitude.

Normally, the IRIDIUM system turns off overlapping beams in the polar regions so actual polar coverage is lower than the maximum value shown.

4.0 Global Telecom Capacity

A single IRIDIUM satellite sees a ground swath up to 4650 km wide on the earth below. For IRIDIUM the roughly circular coverage is divided into 48 spot beams as depicted in figure 5. The diameter of each spot beam is about 600 km. As the spacecraft moves the user is passed to adjacent beams approximately once a minute. Adjacent spots use different frequencies, but non-adjacent spots can re-use the frequency already used by another spot. In fact the allocated frequency is divided into 12 sub-bands and each sub-band is reused 4 times on a single satellite.

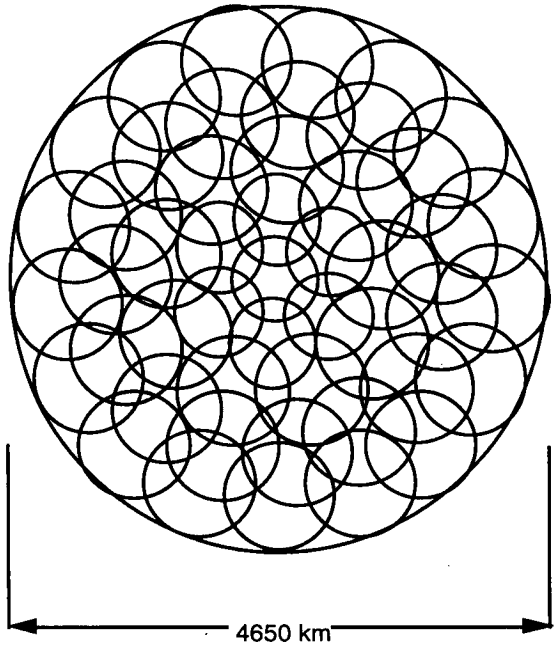

Figure 5. IRIDIUM 48 spot beam antenna pattern.

With 48 spot beams per satellite and 66 satellites, a total of 3168 beams are available to cover the globe. At high latitudes, spacecraft orbits cross and coverage overlap between satellites increases. Some of the outer beams on each satellite are not used at high northern or southern latitudes. The result is that 2150 spot beams are active at any instance to cover the globe and a global frequency reuse factor of 2150/12 ≈ 180 is achieved. Motorola states that 59 beams will cover the lower 48 states, CONUS, for a frequency reuse of 59/12 ≈ 5. The system is designed for each spot beam to support 80 channels; 80*59 = 4720 channel for CONUS and 80*2150 = 172000 channels worldwide. Each Channel will support 4 TDMA Full Duplex Users. Two user modes are available, 4800 bps compressed voice or 2400 bps data. If data links are used, it may be possible to split the channel usage into 4 uplinks and 4 downlinks for a total of 8 users per channel.

Table 1 summarizes the global telecom capacity for the two systems. Calculations are based on system descriptions given in [1], [2] and [3]. In the case of IRIDIUM it is not completely clear from the documentation available how the data and voice services differ in format and quality.

System	IRIDIUM		ORBCOMM	
	Uplink	Down-link	Uplink	Down-link
Single Sat				
# Spot Beams/Sat.	48	48	1	1
Freq. Reuse/Sat.	x4	x4	x1	x1
# Chan/ Sat.	48*80=3840	48*80=3840	21	18
Data Rate/Chan	19200 kbps voice or 9600 kbps data i.e. 4 users	19200 kbps voice or 9600 kbps data i.e. 4 users	2.4 kbps	4.8 kbps
bps/Sat.	73.7 Mbps voice or 36.9 Mbps data	73.7 Mbps voice or 36.9 Mbps data	48 kbps	86.4 kbps
Global				
# Spot Beams	2150	2150	20	20
# Channels	172000	172000	420	360
bps Global Max	3.3 Gbps data or 1.7 Gbps voice	3.3 Gbps data or 1.7 Gbps voice	1.0 Mbps	1.7 Mbps

Table 1: Global Telecom Capacity Comparison

A compact high gain spacecraft antenna operating in the ORBCOMM UHF band is not feasible and thus a much simpler single beam antenna is proposed. The result is lower antenna gain and no possibility of frequency reuse per spacecraft. Although not completely clear from the reference material, it appears that each satellite is capable of handling 21 uplinks at 2400 bps and 18 downlinks at 4800 bps. (Note that the individual satellite uplink capacity is well below the uplink frequency allocation which allows 74 channels total, see table 4 and page 4-10 of reference 2. That is, a single satellite is not capable of using the entire uplink allocation). Focusing on the uplink channels as they apply most to the data retrieval scenarios envisioned by ORBCOMM, at any one time there are a maximum of 20 satellites x 21 channels/sat. = 420 channels worldwide. This is a factor of 400 less than IRIDIUM. The last row of Table 1 shows that after scaling for data rate differences, the ratio of IRIDIUM to ORBCOMM global telecom capacity is between 1000:1 and 3000:1.

5.0 Single User Coverage Dynamics

5.1 Pass Duration and Elevation Angle vs. Time

This section considers the single satellite, single pass coverage provided to a user located in Goldstone California, 35.43° North Latitude, 116.89° West Longitude, the U.S. site for JPL's deep space antennas. This location is used as an example only to give the reader a feeling for the link geometry and dynamics. In general, for a polar orbit satellite, coverage increases with increasing latitude

Figures 4 show IRIDIUM Elevation Angle to the spacecraft vs. time for a near overhead pass. Recalling that the minimum elevation angle for IRIDIUM is 10°, the useful pass time is seen to be 10 minutes.

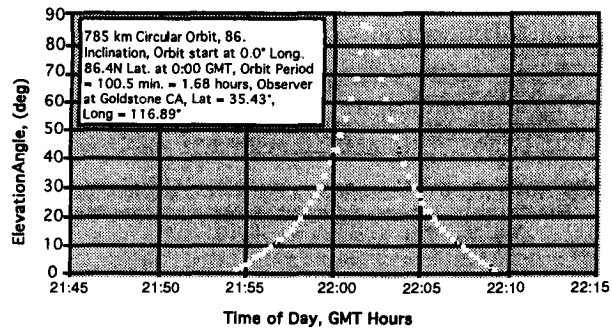

Figure 4: Goldstone, Ca. pass elevation angle to IRIDIUM vs. time.

Figure 5 shows a similar plot for an ORBCOMM satellite. ORBCOMM minimal elevation angle is 5° and thus the useful pass time is 15 minutes. The longer time is the combined result of ORBCOMM's higher orbit altitude and lower minimum elevation angle.

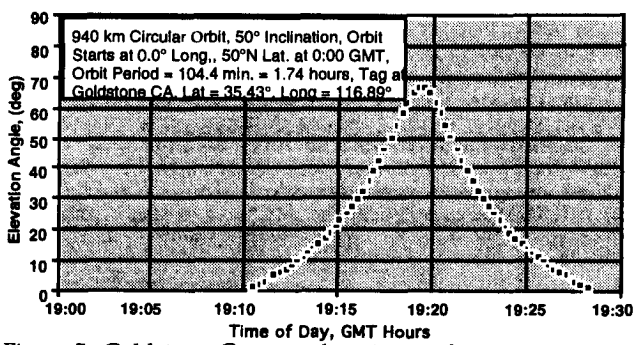

Figure 5: Goldstone, Ca. pass elevation angle to ORBCOMM vs. time.

Figure 6 shows how constellation coverage time to our Goldstone user varies with minimum elevation angle. In general, if lower elevation angles are allowed, the user's view period of any satellite increases and in particular is extended around the times of satellite rise and set. In addition, the ground swath covered is larger allowing a single satellite to cover more area per pass.

On the other hand, allowing lower elevation angles has some negative impacts. For lower elevation angles, slant range to the spacecraft increases in turn increasing the required signal power needed to communicate. At lower angles the possibility of signal blockage increases and interference from signal reflections, i.e. multipath, also increases. Link power again must be pushed up to cover these additional link impairments.

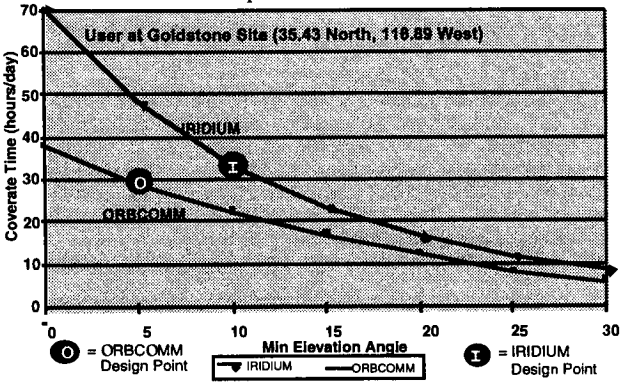

Figure 6: IRIDIUM vs. ORBCOMM: single satellite average coverage per day vs. minimum elevation angle.

System designers must trade off, number of satellites, orbit parameters, coverage times, link power requirements and link continuity requirements when choosing a minimum elevation angle. In addition the type of user must be considered. For example, if we designed a LEO satellite system to communicate with aircraft we would not have to worry about blockage. Multipath would vary as the reflection coefficient of the earth below varied. For small elevation angles and aircraft heights above about 10 km, the reflection from the Earth is reduced by its curvature and thus we could specify a very low elevation angle. For a system primarily used for maritime communications, blockage would be almost nil, but multipath reflection from the sea could impair communications somewhat at all elevation angles. For a land mobile system, signal blockage in heavy foliage or urban terrains will be significant at low elevation angles. In these situations even 10 - 15 dB fade margins will not eliminate frequent signal interruptions. There is no simple formula to solve these complex trade offs. System designers use models of the satellite constellations and links to investigate different options and to optimize performance based on the desired set of services and coverage. The ORBCOMM and IRIDIUM examples show us that these, "optimized," designs can result in very different satellite systems.

5.2 S/C to Tag Range Variations

Figures 7 shows Range to the IRIDIUM spacecraft vs. time for the same near overhead pass used in figure 5. Range varies from a maximum of about 2574 km for 7° elevation angle down to 785 km for the IRIDIUM spacecraft directly overhead. Since link capacity varies inversely as the square of the distance we can say that the link capacity at minimum range is about 10 dB more than at maximum range. To compensate for this variable space loss, the gain of the IRIDIUM antenna is tapered so that the gain for spot beams at the perimeter is 7.5 dB higher than the gain for the center spot beam. The result is a signal power between user and Spacecraft that is much less dependent on the range and elevation angle.

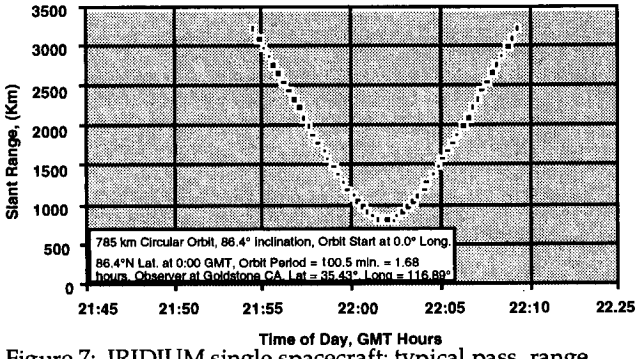

Figure 7: IRIDIUM single spacecraft: typical pass, range vs. time.

Figure 8 shows Range to the spacecraft vs. time for the same ORBCOMM pass used in figure 6. Range varies from a maximum of about 3135 km for 5° elevation angle down to 1000 km for the spacecraft nearly overhead. The link margin at minimum range is about 10 dB more than at maximum range. ORBCOMM's filings with the FCC in 1990 did not propose a scheme to compensate for this variation.

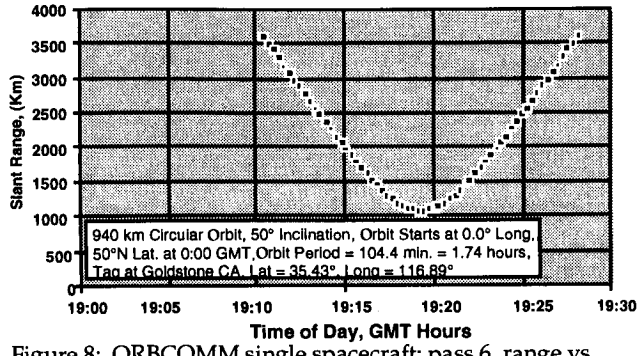

Figure 8: ORBCOMM single spacecraft: pass 6, range vs. time.

5.3 Doppler Dynamics

Figures 9 shows the Doppler Shift vs. time as seen by the IRIDIUM system user receiving a 1620 MHz transmission from the spacecraft for the same pass used in figures 5 and 7. When the Spacecraft comes over the horizon, the Doppler shift is at a positive maximum of 36 kHz. When the elevation angle reaches 10° the Doppler shift is still near maximum at 35 kHz. Over a full pass the user sees a Doppler shift ranging from +35 kHz to - 35 kHz. Maximum Doppler Rate is over 300 Hz/sec. Hence a user unit must handle these large Doppler Shifts and high Doppler rates. In their FCC filing, IRIDIUM has indicated that some form

of Doppler compensation would be used but they were not specific.

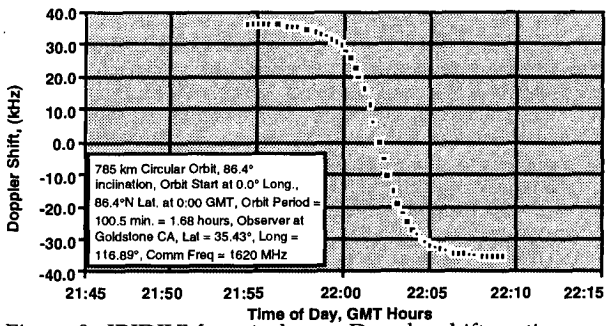

Figure 9: IRIDIUM: typical pass, Doppler shift vs. time.

Figures 10 shows Doppler shift vs. time as seen by an ORBCOMM system user receiving a 137.3 MHz transmission from the spacecraft for the same pass used in figures 8 and 10. Over a full pass the user sees a Doppler shift ranging from +2.8 kHz to -2.8 kHz. Maximum Doppler Rate is over 25 Hz/sec. No Doppler compensation techniques were described in the references.

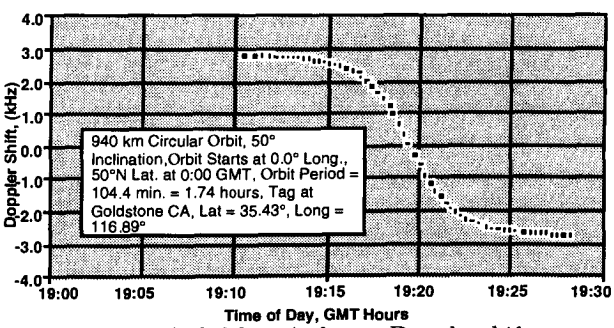

Figure 10: ORBCOMM: typical pass, Doppler shift vs. time.

6.0 Strategic Military Use

As stated previously, the military is particularly interested in tracking hardware in route to and in the theater of operations. Three example regions were considered, (1) North and South Korea, 124°-130° East Longitude and 34°-42° North Latitude (500,000 km^2); (2) Persian Gulf with parts of adjacent Iran, Iraq, Saudi Arabia and Kuwait, 44°-56° East Longitude and 24°-32° North Latitude, (1,000,000 km^2); and (3) Bosnia with parts of Eastern Croatia, 115.5°-19.5° East Longitude and 43°-45.5° North Latitude, (90,000 km^2). Based on IRIDIUM and ORBCOMM coverage results shown in figure 3 and telecom capacity figures given in table 1 coverage and telecom capacity estimates for each of these critical areas were calculated. Table 2 gives a point by point comparison of IRIDIUM and ORBCOMM based approaches.

It is immediately apparent the IRIDIUM system provides far better coverage of the example critical areas. The ratio of data capacity of the two systems is somewhere between 1000:1 and 3000:1. Increased capacity can be achieved with the ORBCOMM system if one assumes that all resources of any ORBCOMM satellite that can be seen from the region of interest are dedicated to the purpose of military Tag communications.

	IRIDIUM	ORBCOMM
Region and Extent	**Temporal Coverage by Full Satellite Constellation**	
Korea 500,000 km^2	34 hours/day	28 hours/day
Persian Gulf 1,000,000 km^2	30 hours/day	25 hours/day
Bosnia 90,000 km^2	39 hours/day	27 hours/day
Sat. Beam Dia.	490 km to 930 km	5600 km
	Avg. Number of Beams Covering the Region	
Korea	2.4	0.024
Persian Gulf	4.4	0.040
Bosnia	0.48	0.0040
	Average Channel Capacity if Satellite Usage is based on Area Serviced	
Korea	**768 2-Way Users** @ 4800 bps voice or @ 2400 bps data 3.7 Mbps Voice or 1.8 Mbps Data	**0.5 Uplink Users** @ 2400 bps 1200 bps **0.4 Downlink Users** @ 4800 bps 1920 bps
Persian Gulf	**1830 2-Way Users** 8.8 Mbps Voice 4.4 Mbps Data 2-way	**0.8 Uplink Users** @ 2400 bps 1920 bps **0.7 Downlink Users** @ 4800 bps 3360 bps
Bosnia	**246 2-Way Users** 1.2 Mbps Voice 2-way 0.6 Mbps Data 2-way	**0.08 Uplink Users** @ 2400 bps 120 bps **0.07 Downlink Users** @ 4800 bps 192 bps

Table 2: Example Coverage and Telecom Capacity for Militarily Significant Areas

Korea	Persian Gulf	Bosnia
25 Uplink Users @ 2400 bps 60 kbps	**21 Uplink** Users @ 2400 bps 50 kbps	**23 Uplink** Users @ 2400 bps 55 kbps
22 Downlink Users @ 4800 bps 106 kbps	**18 Downlink** Users @ 4800 bps 86 kbps	**20 Downlink** Users @ 4800 bps 96 kbps

Table 3: Average Channel Capacity and Throughput Provided By the ORBCOMM Constellation to Critical Areas Assuming That All of a Satellite's Resources are Dedicated to Tag Communications When the Satellite is in View of the Region.

In this case the average number of beams covering the region from the ORBCOMM constellation is roughly equal to the average number of satellites in view. The Channel capacity for ORBCOMM in this case is given in Table 3. The ratio of data capacity of the two systems for this assumption is a more respectable 10:1 to 100:1 depending on the region and data type assumptions.

7.0 Other Issues and Summary

Detailed link design, signal outage due to blockage, Scintillation effects, unintentional interference and general satellite ground equipment trade-offs are some of the topics not covered in this paper due to space limitation. These are covered in the parent study [5]. Appendix A contains link budgets for IRIDIUM and ORBCOMM Tag communications. In our summary we cover the analysis described in this paper and key points covered only in [5].

We have proposed in brief a system approach to provide global tracking of electronically tagged military hardware. Two candidate global LEO satellite systems, IRIDIUM and ORBCOMM were analyzed as to their ability to provide coverage and telecom capacity globally and to specific "hot" spots. The following important findings were made.

1) Tag hardware limited to a 0 dBi omni-directional antenna and 5 watts of power is sufficient for robust link performance with LEO satellite systems. Data rates of 2400 to 50,000 bps can be achieved with path loss margin of 15 dB providing global coverage and good temporal coverage, (see appendix A and [5]).

2) Selection of the number of satellites and their orbits can result in quite different coverage of the Earth. System designers can tailor the spacecraft constellation to prefer users at certain latitudes over others. ORBCOMM has demonstrated this. Their 20 satellite constellation provides essentially the same temporal coverage to all latitudes below 40° that the IRIDIUM system does but with 1/3 the number of satellites. Because of its polar orbits, IRIDIUM provides better service to far north and far south latitudes.

3) IRIDIUM's use of L-band frequencies enables the implementation of the high gain multiple beam spacecraft antenna in a reasonably small package. This in turn enables higher data rate service, the reuse of limited satellite frequency spectrum and the support of many more users. Combined with the larger number of satellites, the result is an upper limit on telecom capacity for IRIDIUM that is 3000 times greater than ORBCOMM's global telecom capacity. On the other hand, the multi-beam spacecraft antenna and greater number of satellites makes the IRIDIUM system and satellites more costly. These higher costs are amortized over a much larger user base. The lower 137 to 148 MHz operating frequencies of ORBCOMM do not lend themselves to implementation of a compact, high gain spacecraft antenna.

Additional points from [5]:

4) IRIDIUM uses identical frequency and channelization for uplink and downlink. The communication is only one-way at a time, or time-duplex. But, using a burst transmission rate of 50 kbps which is 10 times faster than the data rate of 4800 bps needed for compressed digitized voice, the IRIDIUM user terminals are capable of rapidly switching between receive and transmit modes, buffering the data and presenting it to the user as if it were a continuous 2-way or full duplex link. This feature of using only one set of frequencies for both uplink and downlink can simplify the user hardware in at least two ways. First, the range of frequencies that the RF components must operate over is minimized and makes their design less complex and allows them to pass more RF power, (less losses), in both the transmit and receive direction. Second, half-duplex operation eliminates the need for a diplexer, thus reducing mass, cost and RF losses again.

5) For all mobile systems, the inclusion of path margin is essential to combat shadowing and multipath signal fades. In reference [5] it is estimated that a 15 dB margin chosen by IRIDIUM should be sufficient to provide protection against greater than 95% of all shadowing and multipath fade conditions. The same 15 dB margin used by ORBCOMM is harder to evaluate. In particular amplitude scintillations at UHF frequencies can at times and in places exceed 10 dB peak-to-peak during severe solar activity. UHF ionospheric group delay effects can also limit the radio navigation or satellite ranging accuracy. These degradations are particularly important at high latitudes and in the equatorial regions and are worse during local night time than during the day. Hence, system performance may on occasion be adversely affected in these places and times. Additionally, man-made interference and galactic background noise at UHF frequencies can be much greater than receiver thermal noise, especially in populated areas.

7) Tag location on equipment or containers can impact link availability. For a Tag placed on the side of a container, the container itself will shade the Tag from a view of half of the sky, thus reducing the line-of-sight communications time by 50%. If sufficient path margin exists, the shadowed link may still be possible. If not, the side mounted Tag has 1/2 the link availability time of a Tag mounted on top of a container. A worse scenario is the same container with side mounted Tag stacked close to a second container. The second container effectively shades the Tag from nearly all of the remaining part of the sky. Line-of-sight communications would be possible only when a satellite passed directly overhead and could see down into the gap between the two containers. Again, the point of these two examples is to emphasize the impact of Tag and equipment positioning on link quality and/or availability.

8.0 Acknowledgments

This paper was based on satellite systems studies [5] carried out at the Jet Propulsion Laboratory, California Institute of Technology and sponsored by the Naval facilities Engineering Services Center, Port Hueneme, CA through an agreement with the National Aeronautics and Space Administration.

9.0 References

1) **W. Ciesluk, et. al., "Survey of the Mobile Satellite Communications Industry,"** MITRE Technical Report 92B0000059, April 1992.

2) W. Ciesluk, et. al., **"An Evaluation of Selected Mobile Satellite Communications Systems and Their Environment,"** MITRE Technical Report 92B0000060, April 1992.

3) L. Gaffney, et. al., **"A Reevaluation of Selected Mobile Satellite Communications Systems: Ellipso, Globalstar, IRIDIUM and Odyssey,"** MITRE Technical Report 93B0000157, February 1994.

4) T. C. Jedrey and R. P. Romer, "**Survey of Commercial Mobile Satellite Services (MSS),**" Prepared by Jet Propulsion Laboratories under contract to Naval Facilities engineering Services Center, JPL Document D-11669, March 21, 1994.

5) D. Bell, P. Estabrook and R. Romer, "Satellite to Tag Communications Link Analysis," For Naval Facilities Engineering Services Center, September 23, 1994.

Appendix A. Detailed Link Budgets for IRIDIUM and ORBCOMM

Iridium Downlink to Tag			Tag Uplink to Iridium		
iridum Xmit Power, Watts	3.5	Watts	Tag Xmit Power, Watts	5.0	Watts
Iridum Xmit Power, dBm	35.4	dBm	Tag Xmit Power, dbm	37.0	dBm
Iridum Ckt. Loss	-2.1	dB	Xmit Ckt. Loss	-0.7	dB
iridum Antenna Gain	24.3	dBi	Tag Antenna Gain	0.0	dBi
EIRP	57.6	dBm	EIRP	36.3	dBm
Orbit Altitude, km	785.0	km	Orbit Altitude, km	785.0	km
Elevation Angle to S/C	10.0	degrees	Elevation Angle to S/C	10.0	degrees
Range to S/C, km	2336.0	km	Range to S/C, km	2336.0	km
Comm Frequency	1620.0	MHz	Comm Frequency	1620.0	MHz
Free Space Loss	-164.0	dB	Free Space Loss	-164.0	dB
Atm+Pol Loss	-0.8	dB	Atm+Pol Loss	-0.8	dB
Tag Antenna Gain	0.0	dBi	S/C Antenna Gain	23.9	dBi
Carrier Power	-107.2	dBm	Carrier Power	-104.6	dBm
Tag Noise Figure	0.9	db	S/C Noise Figure w/loss	2.4	dB
Antenna Circuit Loss	-0.7	dB	Antenna Circuit Loss	Incl. Above	dB
Antenna Circuit Loss	120.0	K	Antenna Noise Temp	290.0	K
System Noise Temp	249.2	K	System Noise Temp	504.0	K
Noise Bandwidth	31.5	Khz	Noise Bandwidth	31.5	KHz
Noise Power	-129.7	dBm	Noise Power	-126.6	dBm
Tag G/T	-24.0	dB K	S/C G/T	-3.1	dB K
C/N	22.5	dB	C/N	22.0	dB
Eb/No Req (1E-5Ber)	5.8	dB	Eb/No Req (1E-5BER)	5.8	dB
Implementation Loss	0.5	dB	Implementation Loss	0.5	dB
Coded Channel Data Rate	50.0	kbps	Coded Channel Data Rate	50.0	kbps
Code Rate	0.75		Code Rate	0.75	
Uncoded Data Rate	37.5	kbps	Uncoded Data Rate	37.5	kbps
Uncoded Data Rate	45.7	dB-bps	Uncoded Data Rate	47.7	dB-bps
Pd/ (No+Io) Required	52.0	dB/Hz	Pd/(No+Io) Required	52.0	dB/Hz
Pd/(N+I) Requred	7.1	dB	Pd/(N+I) Required	7.1	dB
C/I (Specification)	18.0	dB	C/I (Specification)	18.0	dB
Reg C/N	7.4	dB	C/N Required	7.4	dB
Margin for Shadow	15.1	dB	Margin for Shadow	14.6	dB

Table A-1 IRIDIUM - Tag Link Budgets

ORBCOMM Downlink to Tag			ORBCOMM Downlink to Tag		
5/C Xmit Power, Watts	10.0	Watts	Tag Xmit Power, Watts	5.0	Watts
S/C Xmit Power, dBm	40.0	dBm	Tag Xmit Power, dBm	37.0	dBm
S/C Ckt. Loss	-0.5	dBi	Xmit Ckt. Loss	-0.7	dB
S/C Antenna Gain	7.0	dB	Tag Antenna Gain	0.0	dBi
EIRP	46.5	dBm	EIRP	36.3	dBm
Orbit Altitude, km	970.0	km	Orbit Altitude, km	970.0	km
Elevation Angle to S/C	5.0	degrees	Elevation Angle to S/C	5.0	degrees
Range to S/C, km	3135	km	Range to S/C, km	3135.0	km
Comm Frequency	137.3	MHz	Comm Frequency	148.0	MHz
Free Space Loss	-145.1	dB	Free Space Loss	-145.8	dB
Atm+Pol Loss	-7.1	dB	Atm+Pol Loss	-7.1	dB
Tag Antenna Gain	0.0	dBi	S/C Antenna Gain	6.5	dBi
Carrier Power	-105.7	dBm	Carrier Power	-110.1	dBm
Tag Noise Figure	0.8	dB	S/C Noise Figure	0.8	dB
Antenna Circuit Loss	-0.7	dB	Antenna Circuit Loss	0.5	dB
Antenna Noise Temp	700.0	K	Antenna Noise Temp	700.0	K
System Noise Temp	819.6	K	System Noise Temp	801.2	K
Noise Bandwidth	31.5	KHz	Noise Bandwidth	31.5	KHz
Noise Power	-124.5	dBm	Noise Power	-124.6	dBm
Tag G/T	-29.1	dB K	S/C G/T	-22.5	dB K
C/N	18.8	dB	C/N	14.5	dB
Eb/No Req (1E-05BER)	10.0	dB	Eb/No Req (1E-05BER)	10.0	dB
Implementation Loss	1.5	dB	Implementation Loss	1.5	dB
Coded Channel Data Rate	4.8	kbps	Coded Channel Data Rate	2.4	kbps
Code Rate	1.00		Code Rate	1.00	
Uncoded Data Rate	4.8	kbps	Uncoded Data Rate	2.4	kbps
Uncoded Data Rate	36.8	dB-bps	Uncoded Data Rate	33.8	dB-bps
Pd/ (No+Io) Required	48.3	dB/Hz	Pd/(No+Io) Required	45.3	dB/Hz
Pd/(N+I) Requred	3.3	dB	Pd/(N+I) Required	0.3	dB
C/I (Spec.)	40.0	dB	C/I (Spec.)	40.0	dB
Reg C/N	3.3	dB	C/N Required	0.3	dB
Margin for Shadow	15.4	dB	Margin for Shadowing	14.2	dB

Table A-2 ORBCOMM - Tag Link Budgets

Architecture of the TELEDESIC Satellite System

Mark A. Sturza
Teledesic Corporation
2300 Carillon Point
Kirkland, Washington 98033
(818) 907-1302 fax (818) 907-1357

ABSTRACT

There is a significant worldwide demand for broadband communications capacity. Teledesic plans to meet this demand using a constellation of 924 low-Earth orbit (LEO) satellites operating in Ka-band (30/20 GHz). The Teledesic network will provide "fiber-like" service quality, including low transmission delay, high data rates, and low bit error rates, to fixed and mobile users around the world starting in 2001.

INTRODUCTION

Teledesic was founded in June 1990. Its principle shareholders are Craig McCaw, founder of McCaw Cellular Communications, the world's largest wireless communications company, and Bill Gates, founder of Microsoft, the world's largest computer software company.

"Teledesic seeks to organize a broad, cooperative effort to bring affordable access to advanced information services to rural and remote parts of the world that would not be economic to serve thorough traditional wireline means." [1]

"Today, the cost to bring modern communications to poor and remote areas is so high that many of the world's people cannot participate in our global community. Forcing people to migrate into increasingly congested urban areas in search of opportunity is economically and environmentally unsound. All of the world can benefit from efforts to expand access to information technologies." [2]

The solution is a satellite-based broadband network whose service cost in rural, remote areas is comparable to that of wireline networks in advanced urban areas. Such a network can provide a variety of services including multimedia conferencing, video conferencing, videotelephony, distance learning, and voice. It will allow people to live and work in areas based on family, community, and quality of life.

The global scope of the Teledesic network embraces a wide range of service needs. Local partners will determine products and prices and provide sales and service in host countries. Teledesic will not market service directly to users. Rather, it will provide an open network for service provides in host countries. Teledesic will not manufacture satellites or terminals. Its goal is to provide the highest quality communications services at the lowest cost.

Wireline broadband (fiber) networks in advanced urban areas will drive demand for global access to broadband applications. Advanced information services are increasingly essential to education, health care, government, and economic development. Continued decrease in the price/performance ratio of microprocessors and computer memory will increase the demand for transmission of information. Video and high-resolution graphics require high data rates.

Most of the worlds population will never get access to advanced digital applications through terrestrial means. The majority of the world does not even have access to basic voice service. Most areas that are not now wired never will be wired. Increasingly, wireless cellular will be the access technology of first choice in rural and remote areas. Cellular is limited to narrowband applications and most existing wireline networks will not support advanced digital applications.

Teledesic will provide seamless compatibility with terrestrial broadband (fiber) networks. Future broadband applications and data protocols will not be designed to accommodate the delays of geostationary satellites. Users will want one network for all applications.

The Teledesic network will be complementary to terrestrial wireless networks. It will be a broadband overlay for narrowband cellular systems, backbone infrastructure for cell site interconnect, and backhaul for

long distance and international connections. The aggregation of voice channels requires low-delay broadband capability.

Teledesic will provide a global wide-area network, a seamless, advanced, digital broadband network. It will fill in missing and problematic links everywhere, facilitating economic and social development in rural and remote areas.

Teledesic will supply instant infrastructure, providing rapid availability of advanced "fiber-like" services to almost 100% of the world's population. System capacity is not rigidly dedicated to particular end users or locations.

The cost of the Teledesic network will be $9 billion. This is a fraction of what will be spent on installing fiber in just the United States. It is less then the $15 billion that will be spent just to lay fiber for interactive TV in California [3]. Teledesic plans to initiate service in 2001.

DESIGN CONSIDERATIONS

Some of the key design drivers of the Teledesic Network are:

- High data rate (broadband) fixed and mobile service
- Continuous global coverage
- Fiber-like delay
- Bit error rates less than 10^{-10}
- Mitigate effects of rain attenuation and blockage
- Rapid network repair
- Geodesic (mesh) network interconnect

The broadband service requirement drives Ka-band operation. No lower frequency bands are available to support a broadband satellite-based network. The Teledesic satellite uplinks operate in the 30 GHz band and the downlinks operate in the 20 GHz band.

Fiber-like delay requires a low-Earth orbit (LEO) constellation. Geostationary (GEO) satellites introduce a minimum 500 msec round-trip transmission delay. Medium-Earth orbit (MEO) constellations introduce a minimum 133 msec round-trip transmission delay. The round trip transmission delay for a LEO constellation is typically less than 20 msec.

The practical altitude range for LEO constellations is 500 km to 1400 km. Below 500 km, atmospheric drag significantly shortens the satellites lifetime in orbit. Above 1400 km, the Van Allen radiation belt makes radiation hardening of the satellite prohibitively expensive.

Continuous global coverage requires a constellation with a near-polar inclination angle. Rapid network repair requires that the satellites in each orbital plane are decoupled from those in other orbital planes. This allows for the inclusion of active spare satellites in each plane. When a satellite fails, the remaining satellites in the plane spread out to close the resulting gap.

Ka-band communications links are subject to severe rain fading (Figure 1). This effect is reduced as the Earth terminal to satellite elevation angle is increased. The Teledesic constellation is designed to operate with an Earth terminal elevation mask angle of 40° to provide rain availability of 99.9% over most of the United States.

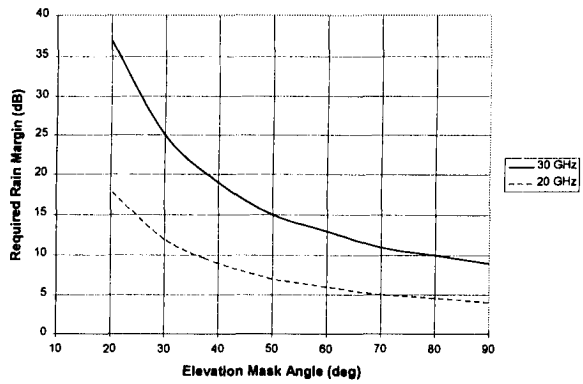

Figure 1. Required Rain Margin (Region D2, 99.9% Availability)

The Teledesic constellation [4] is organized into 21 circular orbit planes that are staggered in altitude between 695 and 705 km. Each plane contains a minimum of 40 operational satellites plus up to four on-orbit spares spaced evenly around the orbit. The orbit planes are at a sun-synchronous inclination (approximately 98.16°), which keeps them at a constant angle relative to the sun. The ascending nodes of adjacent orbit planes are spaced at 9.5° around the Equator (Figure 2).

Satellites in adjacent planes travel in the same direction except at the constellation "seams", where ascending and descending portions of the orbits overlap. The orbital parameters are shown in Table 1.

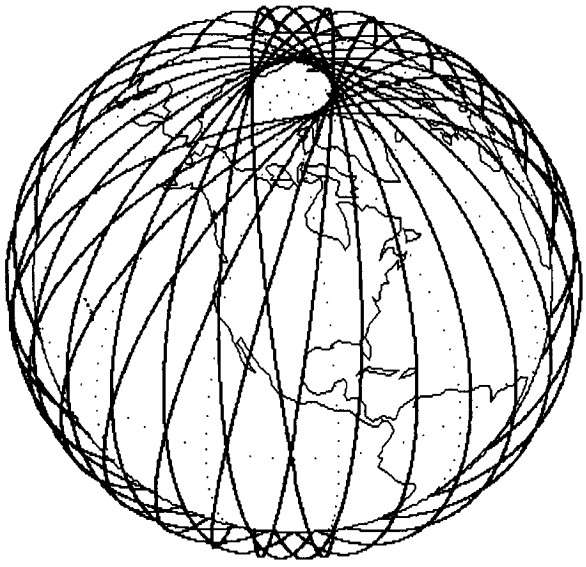

Figure 2. Teledesic Orbits

Table 1. Constellation Parameters

Total Number of Satellites	840
Number of Planes	21
Number of Satellites Per Plane	40
Satellite Altitude	695 to 705 km
Eccentricity	0.00118
Inclination Angle	98.142° to 98.182°
Inter-Plane Spacing	9.5°
Intra-Plane Satellite Spacing	9°
Inter-Plane Satellite Phasing	Random
Earth Terminal Elevation Mask Angle	40°

SYSTEM DESIGN

The system design is described in Teledesic's FCC application [4] and amendment [5]. The network (Figure 3) uses fast packet switching technology based on Asynchronous Transfer Mode (ATM) developments. Each satellite in the constellation is a node in the fast packet switch network, and has intersatellite communication links with eight neighboring satellites. This interconnection arrangement forms a non-hierarchical geodesic network that is tolerant to faults and local congestion.

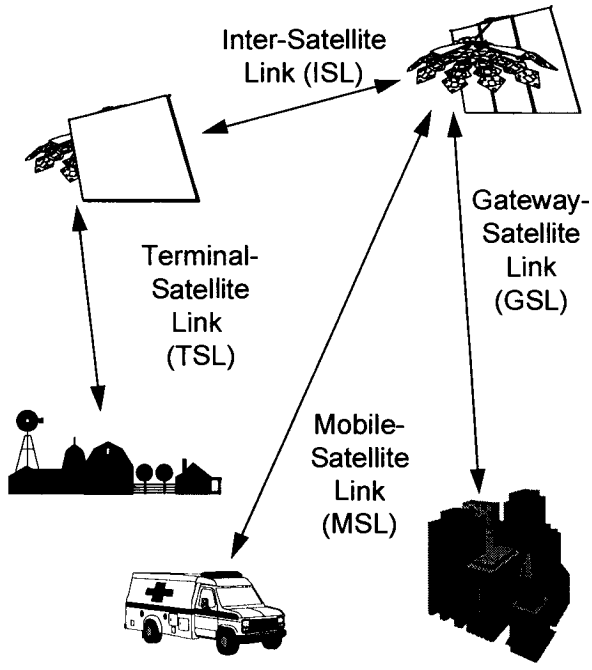

Figure 3. The Teledesic Network

All communication is treated identically within the network as streams of short fixed-length packets. Each packet contains a header that includes address and sequence information, an error-control section used to verify the integrity of the header, and a payload section that carries the digitally-encoded video, voice, or data. Conversion to and from the packet format takes place in the terminals. Fast packet switching technology is ideally suited for the dynamic nature of a LEO network.

The network uses a "connectionless" protocol. Packets of the same connection may follow different paths through the network. Each node independently routes the packet along the path that currently offers the least expected delay to its destination, see Figure 4. The required packets are buffered, and if necessary resequenced, at the destination terminal to eliminate the effect of timing variations. Teledesic has performed extensive and detailed simulation of the network and adaptive routing algorithm to verify that they meet Teledesic's network delay and delay variability requirements.

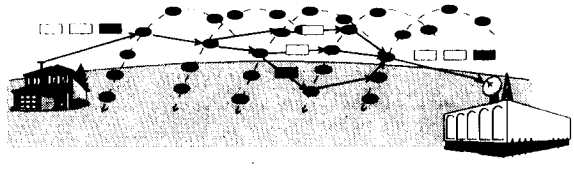

Figure 4. Distributed Adaptive Routing Algorithm

Earth Fixed Cells

The Teledesic Network uses an Earth-fixed cell design to minimize hand-offs. The Earth's surface is mapped into a fixed grid of approximately 20,000 "supercells". Each supercell is a square 160 Km on each side and is divided into 9 cells as shown in Figure 5.

Supercells are arranged in bands parallel to the Equator. There are approximately 250 supercells in the band at the Equator, and the number per band decreases with increasing latitude. Since the number of supercells per band is not constant, the "north-south" supercell borders in adjacent bands are not aligned.

A satellite footprint encompasses a maximum of 64 supercells, or 576 cells. The actual number of cells for which a satellite is responsible varies by satellite with its orbital position and its distance from adjacent satellites. In general, the satellite closest to the center of a supercell has coverage responsibility. As a satellite passes over, it steers its antenna beams to the fixed cell locations within its footprint. This beam steering compensates for the satellite's motion as well as the Earth's rotation. This concept is illustrated in Figure 6.

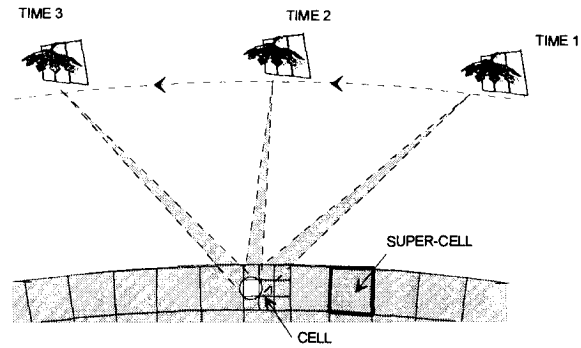

Figure 5. Beam Steering

Channel resources (frequencies and time slots) are associated with each cell and are managed by the current "serving" satellite. As long as a terminal remains within the same Earth-fixed cell, it maintains the same channel assignment for the duration of a call, regardless of how many satellites and beams are involved. Channel reassignments become the exception rather than the normal case, thus eliminating much of the frequency management and hand-off overhead.

A database contained in each satellite defines the type of service allowed within each Earth-fixed cell. Small fixed cells allow Teledesic to avoid interference to or from specific geographic areas and to contour service areas to national boundaries. This would be difficult to accomplish with large cells or cells that move with the satellite.

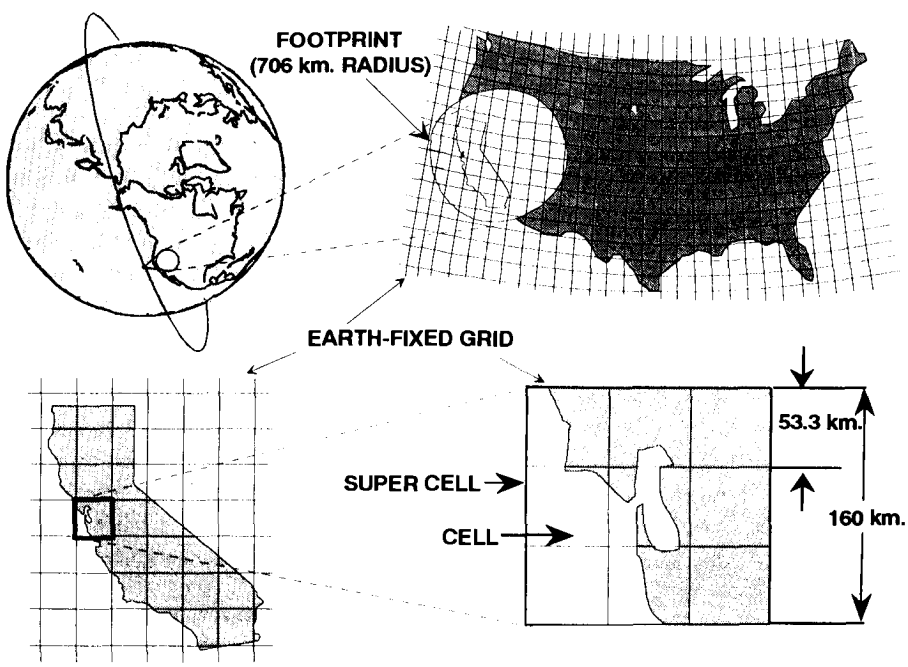

Figure 6. Earth Fixed Cells

Multiple Access

Teledesic uses a combination of space, time, and frequency division multiple access to ensure efficient spectrum utilization (Figure 7). At any instant of time each fixed supercell is served by one of 64 transmit and one of 64 receive beams on one of the Teledesic satellites. The scanning beam scans the 9 cells within the supercell with a 23.111 msec scan cycle. Each scanning beam supports 1440 16-Kbps channels. FDMA is used for the uplinks and asynchronous TDMA (ATDMA) for the downlinks.

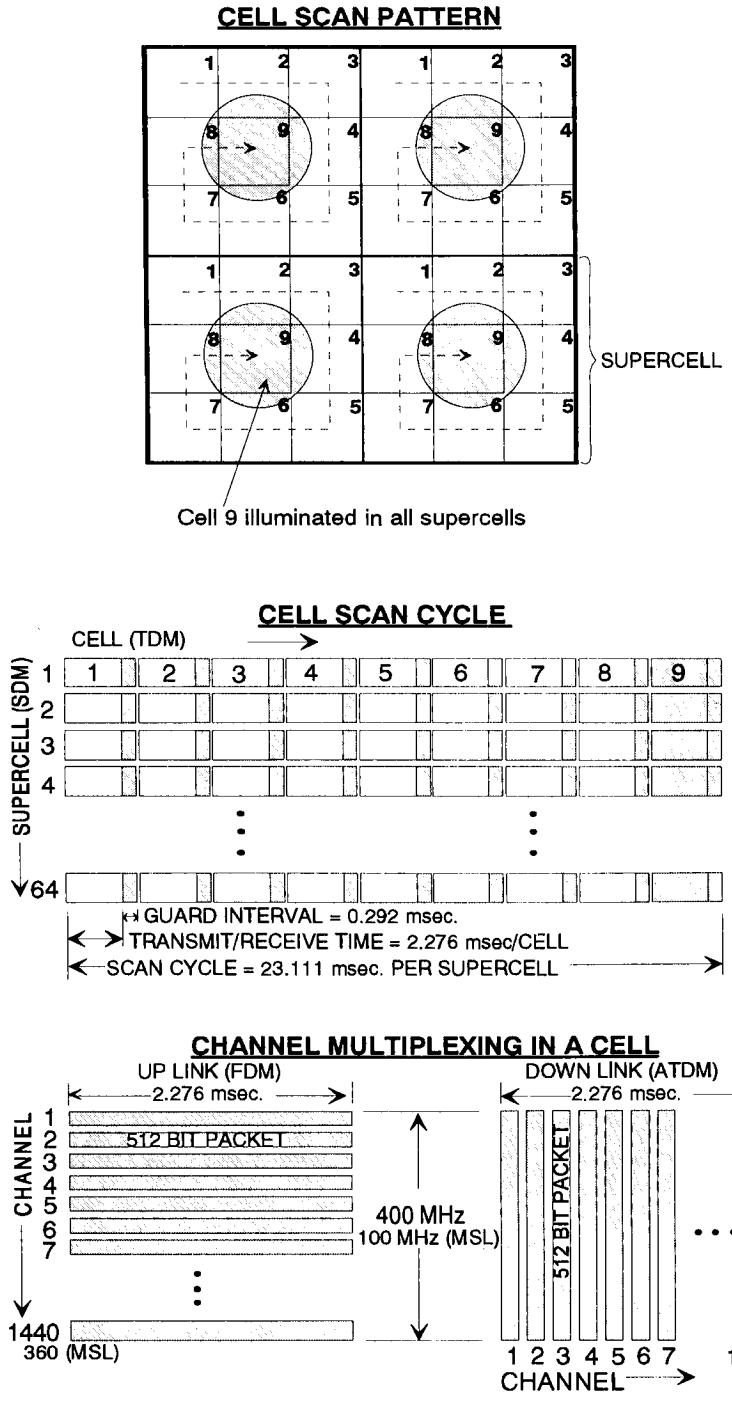

Figure 7. Standard & Mobile Terminal Multiple Access

Satellite transmissions are timed to ensure that all supercells receives transmissions at the same time. Terminal transmissions are also timed to ensure that transmissions from the same numbered cell in all supercells in its coverage area reach that satellite at the same time. Physical separation and a checkerboard pattern of left and right circular polarization eliminate interference between cells scanned at the same time in adjacent supercells. Guard time intervals eliminate overlap between signals received from time-consecutive cells.

On the uplink, each active terminal is assigned one or more frequency slots for the call's duration and can send one packet per slot each scan period (23.111 msec). The number of slots assigned to a terminal determines its maximum available transmission rate. One slot corresponds to a Standard Terminal's or Mobile Terminal's 16 Kbps basic channel with its associated 2 Kbps signaling and control channel. A total of 1440 slots per cell scan interval are available for Standard Terminals, or 360 slots per cell scan interval for Mobile Terminals, or some combination.

The terminal downlink uses the packet's header rather than a fixed assignment of time slots to address terminals. During each cell's scan interval the satellite transmits a series of packets addressed to terminals within that cell. Packets are delimited by a unique bit pattern, and a terminal selects those addressed to it by examining each packet's address field. A Standard Terminal or Mobile Terminal operating at 16 Kbps requires one packet per scan interval. The downlink capacity is 1440 packets per cell per scan interval. The satellite transmits only as long as it takes to send the packets queued for a cell.

The combination of Earth-fixed cells and multiple access methods results in very efficient use of spectrum. The

Teledesic system will reuse its spectrum over 350 times in the continental U.S. and 20,000 times across the Earth's surface.

COMMUNICATIONS LINKS AND TERMINALS

All of the Teledesic communications links transport data, video, and voice as fixed-length 512 bit packets. The links are encrypted to guard against eavesdropping. Terminals perform the encryption/decryption and conversion to and from the packet format.

The uplinks use dynamic power control of the RF transmitters so that the minimum amount of power is used to carry out the desired communication. Minimum transmit power is used for clear sky conditions; transmit power is increased to compensate for rain.

The Teledesic Network supports a family of subscriber terminals providing on-demand data rates from 16 Kbps up to 2.048 Mbps (E1), and for special applications from 155.52 Mbps (OC-3) up to 1.24416 Gbps (OC-24). This allows a flexible, efficient match between system resources and subscriber requirements.

Standard Terminals include both fixed-site and transportable configurations. Mobile Terminals include maritime, aviation, and land mobile configurations. All configurations operate at multiples of the 16 Kbps basic channel payload rate up to 2.048 Mbps (the equivalent of 128 basic channels). These terminals use antennas with diameters from 16 cm [8 cm for Mobile Terminals] to 1.8 m as determined by the terminal's maximum transmit channel rate, climatic region, and availability requirements. Their average transmit power varies from less than 0.01 W to 4.7 W depending on antenna diameter, transmit channel rate, and climatic conditions. All data rates, up to the full 2.048 Mbps, can be supported with an average transmit power of 0.3 W by suitable choice of antenna size.

Within its service area each satellite can support a combination of terminals with a total throughput equivalent to over 100,000 simultaneous basic channels.

The Network also supports a smaller number of fixed-site GigaLink Terminals that operate at the OC-3 rate (155.52 Mbps) and multiples of that rate up to OC-24 (1.24416 Gbps). Antennas for these terminals range in size from 28 cm to 1.6 m as determined by the terminal's maximum channel rate, climatic region and availability requirements. Transmit power varies from 1 W to 49 W depending on antenna diameter, data rate, and climatic conditions. Antenna site-diversity can be used to reduce the probability of rain outage in situations where this is a problem.

GigaLink Terminals provide gateway connections to public networks and to Teledesic support and data base systems, as well as to privately owned networks and high-rate terminals. Each satellite can support up to sixteen GigaLink terminals within its service area.

Intersatellite Links (ISLs) operate in the 60 GHz band. They interconnect each satellite with its eight neighbor satellites. Each ISL operates at the OC-3 rate, and multiples of that rate up to OC-24 depending upon the instantaneous capacity requirement.

SATELLITES

The Teledesic satellites are specifically designed to take advantage of the economies that result from high volume production and launch. All satellites are identical and use technologies and components that allow a high degree of automation for both production and test. To minimize launch cost and the deployment interval, the satellites are designed to be compatible with over twenty existing international launch systems, and to be stacked so that multiple satellites can be launched on a single vehicle. Individual satellites, the constellation as a whole is designed to operate with a high degree of autonomy.

The on-orbit configuration of the Teledesic satellite, Figure 8, resembles a flower with eight "petals" and a large boom-mounted square solar array. The deployed satellite is 12 m in diameter and the solar array is 12 m

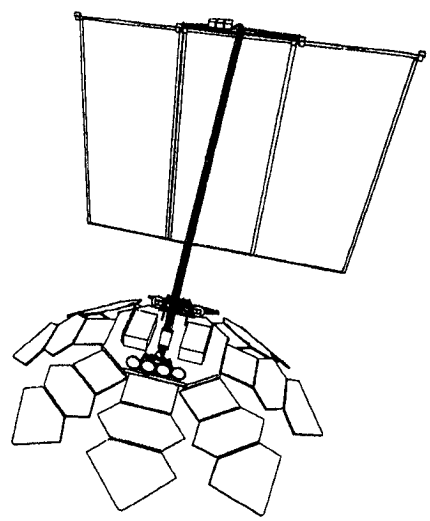

Figure 8. Teledesic Satellite

on each side. Each petal consists of three large panels containing the phase-array antennas. The octagonal baseplate also supports eight pairs of intersatellite link antennas, the two satellite bus structures that house the engineering subsystem components, and propulsion thrusters. A third satellite bus structure, containing power equipment and additional propulsion thrusters, is mounted at the end of the solar array boom. The solar array is articulated to point to the sun.

COMMUNICATIONS PAYLOAD

A functional block diagram of the communications payload is shown in Figure 9. The heart of the payload is the fast packet switch (FPS). It routes packets to and from the Scanning Beam (SB), GSL, and ISL transmitters and receivers. The FPS is essentially non-blocking with very low packet delay, and a throughput in excess of 5 Gbps.

The SB subsystem supports the Standard Terminal links and the Mobile Terminal links. It consists of 64 transmit channels and 64 independent receive channels plus spares. The transmitters are time shared between the Standard Terminals and the Mobile Terminals, and the receivers are shared by frequency division.

ACKNOWLEDGMENTS

The author wishes to thank David Patterson, Dr. James Stuart, Russ Daggatt, Tren Griffin, David Montanaro, and the other members of the Teledesic team for their contributions to this paper.

REFERENCES

[1] *Teledesic Company Overview*

[2] **Craig O. McCaw**, *Remarks at G-7 Information Society Conference*, Brussels, Belgium, February 24, 1995.

[3] **George Gilder**, "*TELECOSM: Ethersphere*", Forbes ASAP, 10 October 1994, pp. 133-148.

[4] *Application of Teledesic Corporation for a Low Earth Orbit ("LEO") Satellite System in the Fixed Satellite Service ("FSS")*, 21 March 1994.

[5] *Amendment of Application of Teledesic Corporation for Authority to Construct, Launch, and Operate a Low Earth Orbit Satellite System in the Domestic and International Fixed Satellite Service*, 30 December 1994.

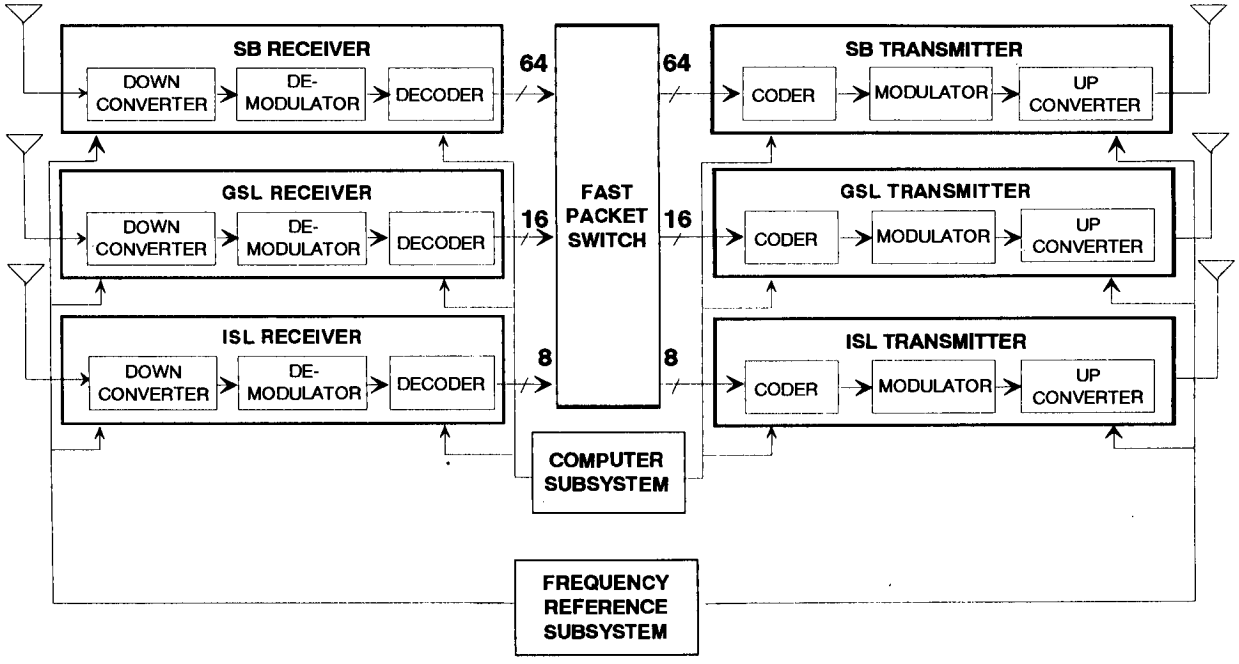

Figure 9. Communications Payload

Mobile Satellite Business Networks: A Part of the European Mobile System

M.L de Mateo* A. Jongejans* C. Loisy*
C. Van Himbeeck** J.P. Marchal**
A. Borella*** M. Sartori***

* European Space Agency
Keplerlaan 1
2200 AG Noordwijk
The Netherlands
Tel.: 31-1719-84582
Fax: 31-1719-84596
email: mdemateo@estec.esa.nl

** Sait Systems
Ch. de Ruisbroek 66
B-1190 Brussels
Belgium
Tel.: 32-2-3705349
Fax: 32-2-3322890

*** Fiar
Via Montefeltro, 8
20156 Milan
Italy
Tel.: 39-2-35790.355
Fax: 39-2-33400981

Abstract

The European Space Agency (ESA) is presently procuring an L-band payload EMS, to be embarked on the ITALSAT-2 satellite due for launch in early 1996, in order to promote a regional European mobile system ([1]). One of the Land Mobile Communication systems supported by EMS is the MSBN (Mobile Satellite Business Network) voice and data system which will offer the services of a business network on a seamless European coverage. This paper will first recall the characteristics of the MSBN system, which is based on quasi-synchronized CDMA (Code Division Multiple Access) techniques in both directions, and then describe the CDMA receivers implementation. Main validation test results will also be reported confirming predicted performances.

1. INTRODUCTION:

The present MSBN definition is the result of many detailed studies including market surveys, and in-depth technical evaluation. Market research has shown that there is a definite market for satellite-based private business networks providing voice/data communications. It must of course be remembered that, in Europe, this market, although significant in terms of economic turnover for satellite operators, may remain a niche market compared to the one addressable by terrestrial systems such as GSM.

The rate of penetration of this potential market will depend very much upon the adaptation of the system to the market requirements. Previous studies have demonstrated that a decentralized network architecture based on direct access to the satellite through Ku-band VSAT hub-stations provides the optimum configuration. This corresponds to the concept of Mobile Satellite Business Network (MSBN). The basic configuration of a MSBN system consists of a star shaped network composed of a Fixed Earth Station (FES) or hub station, a fleet of Mobile Earth Stations (MES's), a Network Management Station (NMS) or control station, and a dedicated satellite channel.

The initial development work on MSBN was completed in October 94; one FES and one NMS manufactured by SAIT (Belgium) and two MES's developed by FIAR (Italy) were delivered to ESA for tests and demonstration, using the Inmarsat-II satellite. The development included the implementation of a dedicated protocol for voice and data transfer.

This paper is divided into five sections:

Section 2 includes a general description of the MSBN system concept. In Section 3, the fixed

(FES) and mobile (MES) earth stations are described. Main validation test results are reported in Section 4, confirming predicted performances. Overall conclusions are drawn in Section 5.

2. DESCRIPTION OF THE MSBN SYSTEM:

A typical application of the MSBN concept (fleet management) is shown in Figure 1. The fixed user (fleet dispatcher) has direct access to his own fleet of mobiles through the satellite transponder. The FES is a VSAT station which operates at Ku-band frequencies, while the MES operates in the 1.5/1.6 Ghz frequency band (or L-band). The overall system is controlled by a Network Management Station (NMS) which has the capability to transmit and receive in both frequency bands (Ku and L).

The MSBN system uses quasi-synchronized CDMA techniques in both directions over the satellite link ([2]). The choice of CDMA, while eventually also easing the coordination with other satellite systems, is particularly suited for the PMR (Private Mobile Radio) concept since independent networks share a common bandwidth resource (typically 1 MHz) without the need for inter-network coordination.

In the basic scenario, a star shaped network operates one satellite channel consisting of a pair of carriers (one Forward Common Carrier (FCC), and one Return Common Carrier (RCC)). This Common Channel allows to transport part of the network load and also to control additional auxiliary channels for the remainder of the traffic. In this way, the system allows for a modular growth of the communication capabilities of the network through the addition of auxiliary channels. Besides, a FES may be shared by two or more fixed users with low traffic in order to reduce costs.

An important novelty of the system is the synchronization scheme, specifically for the MES-to-FES link, which allows a larger channel capacity and therefore higher spectral efficiency due to the drastic reduction in self-noise which is achieved through synchronizing the epochs of the CDMA sequences. In order to implement the synchronization, two Reference Carriers (one for the forward link (FRC) and one for the return link (RRC)) are broadcast by the NMS and used as reference. All signals transmitted by the FES's or MES's are thus synchronized at chip, bit and frame level with respect to these reference signals (FRC and RRC respectively).

The link characteristics of MSBN are summarized in Table 1.

3. DESCRIPTION OF THE FIXED (FES/NMS) AND MOBILE (MES) EARTH STATIONS:

Although MSBN was designed to be operated on Ku/L band transponders (e.g. EMS), the planning of the MSBN validation was not compatible with the availability of EMS in orbit and required initial usage of existing C/L satellite transponders. To this end, the prototype fixed earth stations (FES/NMS) were designed to allow access to these C/L band transponders through existing C-band earth stations.

3.1 NMS Functional Description:

The NMS accomplishes the following functions:

- Generation and locking of the FRC signal to a local reference.
- Broadcast of the SIT[1] (System Information Table) data on the FRC.
- Generation of the RRC signal.

The FRC is continuously transmitted by the NMS and received by all MES's & FES's. The transmission is from C- to L-band. The FRC transmit frequency at C-band is controlled by the NMS in order to keep the transponded carrier at L-band at the nominal value. The control loop is internal to the NMS and compares the signal received at L-band with a local reference. The FRC allows to perform the frequency and code phase control of all Forward Link Carriers.

The RRC is continuously transmitted by the NMS and received by all the FES's. The transmission is from L- to C-band. The RRC is used as a reference for the power and code phase control of all Return Link Carriers.

3.2 FES Functional Description:

The FES performs the following functions:

- Generation and locking of the FCC to the received FRC.

[1] The SIT is continuously broadcast by the NMS on the FRC to all networks. It contains information on which networks are active and on the FCC/RCC code pair used by the active networks.

- Reception and locking of the RCC to the received RRC.

The FCC (or RCC) is transmitted by one FES (or MES) at a time; the transmission in both cases is not continuous and takes place in bursts. The FCC/RCC carries data (or voice) information, including signalling data.

The FCC transmit frequency at C-band and chip timing are controlled by the FES in order to keep both parameters aligned with those of the FRC. The control loops are internal to the FES and compare the two signals received at L-band.
In a similar manner, the RCC chip timing is aligned with that of the RRC to better than ± 0.1 chip. A long control loop involving the transmitting MES and the FES, compares the signals received at C-band. The control information is sent by the FES to the MES at time intervals as part of the signalling.

3.3 NMS/FES Prototype Implementation:

The FES is composed of an RF rack, a VME rack, a FES gateway PC, a local MMI (Man Machine Interface) PC, a microphone and a loudspeaker. The FES VME rack contains a VME300 real time processor, a synthesiser board, a FC-C/FAC (Forward Auxiliary Carrier[2]) modulator, a vocoder, a fast acquisition unit and the FRC, FCC, RRC, RCC and RAC (Return Auxiliary Channel[3]) demodulators. The fast acquisition unit can be connected to any of the demodulators to speed up the acquisition process.

In order to cope with the shared FES situation, the FES can be configured to operate either in local or remote mode (see Figure 2). In the remote configuration, the MMI and Vocoder Unit are located in the operator premises and linked via modems to the FES; in this case, the voice is coded (analysed) at the source and sent to the FES digitally. In so doing, the PSTN connection does not induce further voice quality degradation.

The MSBN operator can communicate via a user graphical interface (MMI) with his fleet of MES's. Via this MMI, he can send and receive Datagrams (short messages). He can also initiate broadcast messages, set-up a call or receive an incoming call. At a later stage, fax and real time data services will be added.

The Network Management Station (NMS) is also composed of an RF rack (same as for the FES), a VME rack and a P.C. which can be operated locally or via modem. Its structure is very similar to the one of the FES.

3.4 MES Description:

The MES architecture is shown in Figure 3 and consists of the following subsystems: Antenna and Tracking Processor, RF Front-end, Below Roof Equipment (BRE) and Terminal Equipment.

The Antenna Subsystem has been developed by the VTT Research Centre of Finland and contains the radiating element, the azimuth pointing mechanism with the stepper motor and the Tracking processor.
The radiating elements is an array of two OTAs (One Turn Antenna). Two phase shifters are part of the feed network and allow the switching between two beams in order to perform a step tracking function. An angular velocity sensor is used as an aid which detects vehicle course changes in maintaining satellite pointing.
All the software procedures concerning the satellite acquisition and tracking are resident in the Tracking Processor board and are supported by the MES FCC demodulator. A serial line at 9600 bps interconnects the Antenna Subsystem to the BRE and a specific set of monitoring, command and data messages have been defined in order to allow the implementation of the acquisition and tracking routines under the supervision of the Terminal Processor.

The L-band front-end performs all the amplification and conversion functions and consists of the SSPA and Upconverter, the LNA and Downconverter and the Diplexer. The Receive chain is composed of an LNA and a Downconversion stage to the first IF frequency of 138 MHz. The transmit side performs the Upconversion of the signal from the IF frequency of 239.5 MHz to L-band and then a class-C amplifier provides the required output power. The diplexer is integrated in the unit and provides the required isolation between the Transmit and Receive chains for duplex operation.

The BRE performs all the IF and baseband processing and supports the user and auxiliary in-

[2] this carrier is similar to the FCC; it carries mainly traffic information. A particular network can operate many FAC's.
[3] this carrier is paired with the FAC.

terfaces. The IF signal received at 138 MHz is amplified, filtered and then downconverted to the frequency of 1.734 MHz at the demodulator input. The demodulator board includes two distinct demodulation chains, processing the FRC and FCC respectively. The timing/frequency synchronization function (including signal re-acquisition) is performed solely by the FRC demodulator; since both FCC and FRC are quasi-synchronous, the FCC demodulator which is slaved to the FRC one operates with minimum acquisition delay. In this way, the MES receiver complexity is minimised. Frame synchronization, decommutation, Viterbi and Reed-Solomon decoding are also performed in the demodulator board. The transmit data are encoded according to the convolutional and RS algorithms. The data frames are spread by the selected RCC CDMA code and passed to the modulator at an IF of 239.5 MHz. The analog voice signal is provided directly to the Vocoder. The voice data are then passed to the CPU for frame formatting and spreading. The signalling frames are also included in the voice data stream (whenever a signalling frame has to be transmitted, one vocoder frame is suppressed and replaced with the signalling frame).

The BRE includes all the necessary means to implement the return link synchronization. The RCC CDMA code phase is adjustable via a dedicated DDS oscillator. The terminal includes a Doppler Estimator (based on Doppler measurements performed on the received FRC), in order to compensate for the Doppler effect encountered by the RCC signal on the return path. The output power is adjustable in a range of 4 dB. The frequency stability of the transmit chain is directly determined by the performances of the MES OCXO which offers a stability of $1*10^{-7}$/month including temperature variation and aging. The OCXO can be remotely calibrated by sending appropriate commands to the MES on the FCC.

The Terminal Equipment is equipped with a telephone handset with PTT button. A hand-free device can also be connected to the terminal. Data messages and all the monitor and control functions can be handled by a dedicated User Terminal or a Lap-top PC. A Group-3 standard fax machine can be connected to the terminal, and two auxiliary interfaces are available to connect on-board equipment.

Technical specifications of the MES equipment are listed in Table 2.

4. SYSTEM TESTING AND VALIDATION:

4.1 System validation:

The first session of MSBN global testing took place in September 94. The main objective of the test was the verification of the compatibility between the FES, NMS and MES at both physical and protocol levels.

For this purpose, these initial tests were carried out in a configuration where the MES was fixed. The physical links between the NMS, FES and MES were successfully established; this included the NMS generation and FES/MES reception of the Reference Carriers (FRC, RRC), the activation of the various NMS/FES synchronization loops, and, the transmission and reception of the SIT data broadcast on FRC. The compatibility at protocol level between the various stations was further verified.

The verification of the following functions was achieved:

1. Silent Broadcast (SB), from the FES to the MES's using FCC.
2. Polling of MES's by the FES.
3. Broadcast of Datagram from the FES to MES's.
4. End to end Datagram from FES to MES and in the other direction.
5. Real time voice call from FES to MES.
6. Real time voice call from MES to FES.
7. Real time voice call from FES to MES (and in the other direction) using an auxiliary channel (FAC/RAC), while polling is being in operation on the common channel (FCC/RCC).

It is to be noted that tests (5) to (7) included the remote synchronization of the MES (return link synchronization), which implies an accurate chip phase adjustement of the MES transmitted signal using commands sent by the FES at time intervals over the FCC, in such a way that the RCC is being kept (quasi) synchronous (i.e. with less than $\pm$ 0.1 chip error) with the RRC.

4.2. Test set-up:

The Inmarsat-II Atlantic East satellite was used for the tests, access on the fixed side being obtained through the Fucino Earth Station of

Telespazio (Italy) where the NMS and FES as well as the MES were installed.

The test set-up was such as to allow, besides the local operation of the FES in Fucino, a remote mode of operation from another site in Belgium, emulating an identical Man Machine Interface; the remote control was operated through modems on PSTN connections.

4.3 Achievements so-far:

The tests described above were successfully performed between September and December 94, using either local or remote control.

Hundreds of Datagrams and voice calls were successfully transmitted without any malfunction. The various parameters of the polling function and the SIT update were verified. The Silent Broadcast interleaved with polling or voice call sessions was successfully tested. The voice quality was generally judget excellent. Test speakers could even be identified through the received speech.

4.4 Future outlook:

The initial functional validation in fixed environment is to be supplemented by field trials in mobile environment aiming at evaluating the overall system performance and usability under operational conditions. At the time of printing, these tests have not yet been performed.

It is to be noted though that extensive field testing of the autopointing MES antenna have already taken place ([3]).

The field testing in mobile environment are expected to provide, beyond the final system design validation, the tool to experimentally adjust link budget margins as a function of the propagation environment (open, foliage, obstacles, built-up areas etc...) and of the required grade of service.

5. CONCLUSIONS:

The developed equipment, both mobile and fixed, and the system validation tests have already allowed to verify the general validity of the MSB-N system concept. Further field testing in various mobile environments is still required in order to fine-tune system parameters.

Depending on the comtemplated applications and specifically whether truly mobile (i.e. vehicle mounted) or portable MES's are to be used, equipment parameters may in the future evolve from those which have been tested to date.

Typically, the gain of the mobile antenna could be lowered and consequently its dimensions significantly reduced alleviating the installation requirements on the smaller vehicles.

The availability of the EMS payload on Italsat II in 1996 will allow to demonstrate the capabilities offered by MSBN based mobile communication systems, specifically in the area of Private Networks (Private Mobile Radios) due to the flexibility of satellite access on the fixed side (Ku band) and, as a consequence, the capability to tailor network architecture and operations to specific user requirements.

The next step in equipment development will indeed be based on the detailed requirements of specific potential users who are unlikely to be adequately served (both in terms of technical performances and utilisation costs) by the competing systems in existence today and likely to offer extensive geographical coverage, i.e. the extensions of public telephony networks provided either through terrestrial based cellular systems or satellites with worldwide coverage.

It is indeed expected that a number of potential customers who require integral geographical coverage over rather large areas and high service availability[4] will be better served by tailored private networks with multiple satellite feeder link access implemented through satellites like EMS with optimized regional coverage.

References

[1] A. Jongejans et al., *"The European Mobile System"*, Proceedings of the IMSC'93, June 16-18, 1993, Pasadena, California.

[2] R. de Gaudenzi, C. Elia and R. Viola, *"Bandlimited Quasi-Synchronous CDMA: A Novel Satellite Access Technique for Mobile and Personal Communication Systems"*, IEEE Journal on Selected Areas in Communications, vol. 10, n.2, February 92

[3] J. Aurinsalo et al., *"Steerable L-band antennas for land mobile terminals"*, Proceedings of the Vehicular Technology Conference (VTC'94).

[4] typically mobile patrols of emergency services.

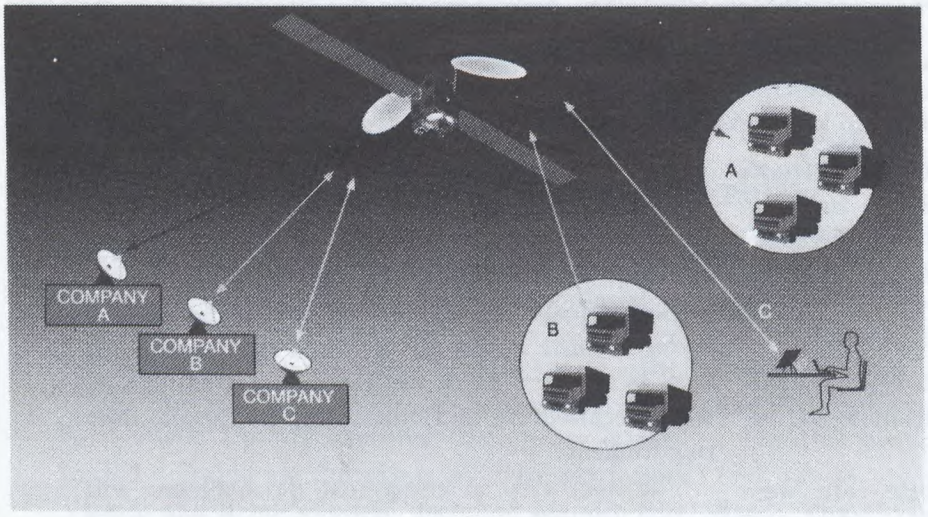

Figure 1: An Overview of the MSBN system concept.

- L-band mobile link
- Both links use CDMA Quasi-Synchronized
- DS-QPSK at 867 Kchip/s
- Real Time Voice at 6.4 Kbit/s (including FEC)
- Real Time Data at 2.4 Kbit/s (excluding FEC)
- Other Services: data messaging, voice messaging and telefax.
- Convolutional and Block coding (Reed-Solomon).
- Steered mobile antenna with 11 dB gain ([3])
- 10 W max transmit RF power (power control)

Table 1: MSBN Link Characteristics.

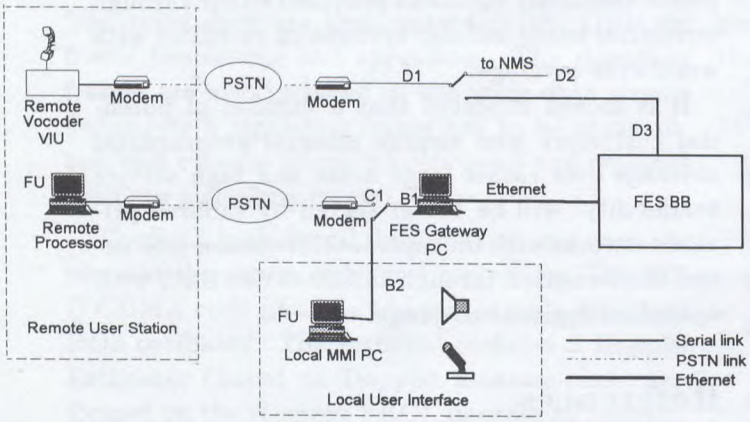

Figure 2: FES Local/remote configuration

Technical Specification	
Frequency range receive	: 1530.0 to 1559.0 MHz
Frequency range transmit	: 1631.5 to 1660.5 MHz
TX nominal output power level	: 12 dBW
G/T	: -13dB/°K
Frequency Tuning	: 5 KHz grid
Antenna	
Coverage in elevation	: 15 to 45 degrees
Coverage in azimuth	: full 360 degrees
Gain	: >11.5 dB (Tx), >=10.5 dB (Rx)
Polarization(for early trials)	: RHCP
Power handling	: > 20 W
Mean acquisition time	: <= 13 sec
Maximum angular speed to maintain tracking	: 30 deg/sec
Mechanical	
Antenna	: diameter 420 mm , heigh 205 mm
L-band front end	: 250*113*110 mm
IDU	: 350*156*95mm
Power supply	: +24Vdc

Table 2: MES technical specifications

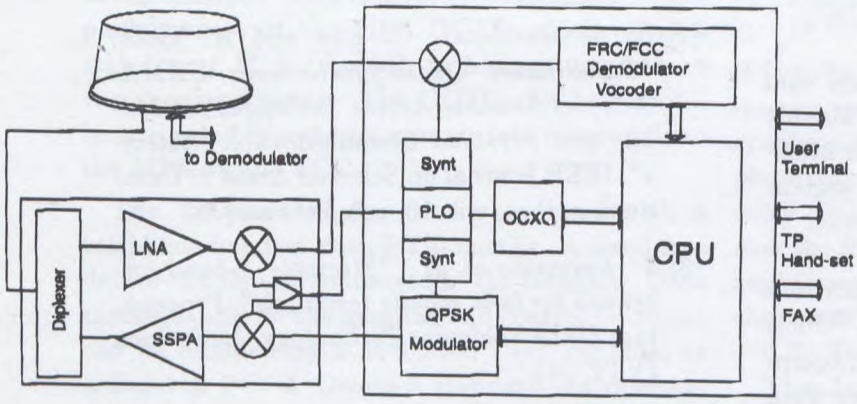

Figure 3: MES Terminal Block Diagram

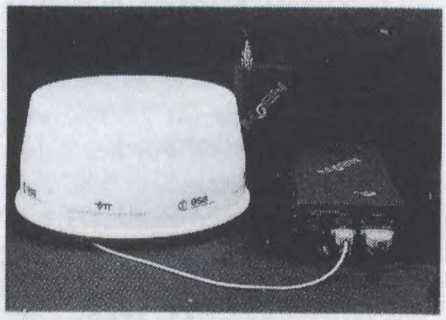

Figure 4: A MSBN mobile terminal

Ka-Band Geostationary Satellite Spacing Requirements And Access Schemes

Mario Caron and Daniel J. Hindson

Communications Research Centre
3701 Carling Avenue, P.O.Box 11490, Station H,
Ottawa, Ontario, Canada K2H 8S2
Phone : 613-998-2864, Fax : 613-990-0316, E-Mail : mario.caron@crc.doc.ca

ABSTRACT

Geostationary satellite systems for wideband personal communications applications have been proposed [1,2]. This paper looks at the geostationary satellite spacing requirement to meet the ITU-R sharing criterion for FDMA and CDMA access schemes. CDMA capacity equation is first developed. Then the basis for the interference analysis between two systems with an overlapping coverage area is developed for the cases of identical and different access schemes and for bandwidth and power limited systems. An example of an interference analysis between two systems is fully carried out. The paper also points out the inherent problems when comparing systems with different access schemes. It is found that under certain scenarios, CDMA can allow a closer spacing between satellites.

1.0 INTRODUCTION

At the World Administrative Radio Conference (WARC) in 1992, the Mobile Satellite Service (MSS) frequency bands 19.7-20.2 GHz (space-to-Earth) and 29.5-30.0 GHz (Earth-to-Space) were raised from secondary to co-primary status with the Fixed Satellite Service (FSS) so that a single satellite could provide both services and thus be more efficient. The satellite systems proposed in these frequency bands [1,2] plan to provide services to terminals using very small antennas. Because these terminals create more interference to (and are more prone to interference from) adjacent satellite systems, there were some concerns about the required orbital spacing for such hybrid systems.

This paper addresses this concern by looking at the satellite spacing requirement for two identical multi-service satellite systems with co-coverage. The analysis is carried out for both frequency division multiple access (FDMA) and code division multiple access (CDMA) schemes. The latter has been proposed in a number of MSS systems [3] due to its ability to operate under strong interference levels and its low level of interference power to adjacent systems.

In the next section, we briefly review the capacity of CDMA networks. Section 3.0 defines the acceptable level of interference assumed in this paper and derives the equations relating the carrier to interference power ratio (C/I) to the basic system parameters for both CDMA and FDMA access schemes. Section 4.0 relates the discrimination factor between two systems to the satellite spacing while Section 5.0 presents a system level approach to the interference analysis problem and provides some qualitative results. In Section 6.0 we derive a more formal interference analysis where the acceptable level of interference is related to the discrimination factor between two satellite systems under identical or different access schemes. Section 7.0 presents results through two examples while Section 8.0 concludes this paper.

2.0 CDMA CAPACITY

Consider a network of M users in an asynchronous CDMA satellite system using binary phase shift keying (BPSK) as the modulation. Each of the M users appears to any single user as a source of interference so that the received effective noise power density (N_o^{eff}) is given by :

$$N_o^{eff} = (M-1)\,E_c + N_o \qquad (1)$$

where E_c is the energy per chip and N_o is the thermal noise power density. The effective energy per bit to noise density (E_b/N_o^{eff}) is then :

$$\frac{E_b}{N_o^{eff}} = \frac{E_b}{(M-1)\,E_c + N_o} = \frac{E_b/N_o}{1 + \frac{(M-1)}{G_{ss}}\frac{E_b}{N_o}} \qquad (2)$$

where G_{SS} is the spreading factor (i.e. chip rate over the data rate). The ratio $(M-1)/G_{ss}$ is referred to as the CDMA loading factor.

Using eq. (2) and isolating E_b/N_O the single user required energy per bit to noise density ratio, we get:

$$\frac{E_b}{N_o} = \frac{E_b/N_o^{eff}}{1 - \frac{(M-1)}{G_{ss}}E_b/N_o^{eff}} \qquad (3)$$

3.0 SHARING CRITERION

The single entry interference criterion set by the ITU for FSS digital links is a 6 % increase in the thermal noise power [4]. Beyond that level, system coordination is re-

quired to get ITU approval. The 6 % increase in thermal noise power can be seen for FDMA as a carrier to interference power ratio (C/I) of 12.2 dB **above** the required C/N_{th} where N_{th} is the thermal noise power in the system. For CDMA, the effective noise power is given by:

$$N^{eff} = N_o B_{rf} + C(M-1) + I$$

where B_{rf} is the spread bandwidth, C is the user power and I the interference power from external systems. After several manipulations, one gets the following expression for the C/I in a CDMA system :

$$\frac{C}{I} = \frac{E_b/N_o^{eff}[N_o/I_o + 1]}{G_{ss}\left[1 - \frac{E_b}{N_o^{eff}}\left(\frac{M-1}{G_{ss}}\right)\right]} \qquad (4)$$

where N_o/I_o is set to 6% to meet the sharing criterion. In the following we derive the discrimination factor required for the case where CDMA interferes into another CDMA system or with an FDMA system such that the sharing criterion is met.

4.0 SATELLITE SPACING AND DISCRIMINATION FACTOR

The discrimination factor between two satellite systems is a combination of the losses from the wanted terminal being off-boresight to the interfering satellite and the interfering satellite being off-boresight from the wanted terminal. However because we assume in this paper two identical systems with co-coverage, there is no satellite off-boresight loss and the discrimination is then essentially provided by the terminal antenna off-boresight loss. The relationship between the antenna off-boresight angle and the satellite spacing is not very difficult to derive. Let us say that for satellite spacing of interest (i.e. less than 10°) and for terminal latitudes less than around 60°, the difference between the terminal off-boresight angle and the satellite spacing is within ±0.5°. So in this paper we assume that the off-boresight angle is effectively the satellite spacing.

In order to find the terminal off-boresight angle related to a given discrimination factor, one can use the radiation patterns suggested in [5] or a measured pattern.

5.0 SYSTEM APPROACH

5.1 IDENTICAL ACCESS SCHEMES

For identical co-coverage and co-located satellite systems based on the same access schemes, it is possible to derive some intuitive results. If we note that for CDMA systems the interference appears as additive white Gaussian noise, then the capacity is reduced by a factor proportional to the antenna discrimination toward the interfering satellite. Accordingly we have a graceful degradation of system capacity with CDMA as the amount of interference increases.

For an FDMA system and without frequency coordination, the capacity of both systems is reduced by 50 % for a discrimination level less than the minimum required to meet the sharing criterion. With frequency coordination though the total capacity of the two FDMA systems may be more than the two CDMA systems for a given discrimination factor. This is better illustrated using a graph. Figure 1 shows an example where the FDMA system is 1.5 times more spectrum efficient than the CDMA system but both systems have equal power efficiency. Because of the improved FDMA spectrum efficiency over CDMA, more FDMA channels can be packed over the same bandwidth. Thus with no discrimination between the two FDMA systems and with frequency coordination, 75 % of the capacity of each system can be accommodated. As the discrimination factor increases to the minimum required, the total FDMA capacity goes from 75 % to 100 % for each system. As we can see, there is a zone of operation* where the FDMA system can be better than the CDMA system **if** frequency assignments are coordinated. Without frequency coordination, we see that CDMA outperforms FDMA and offers a graceful degradation. In addition, as

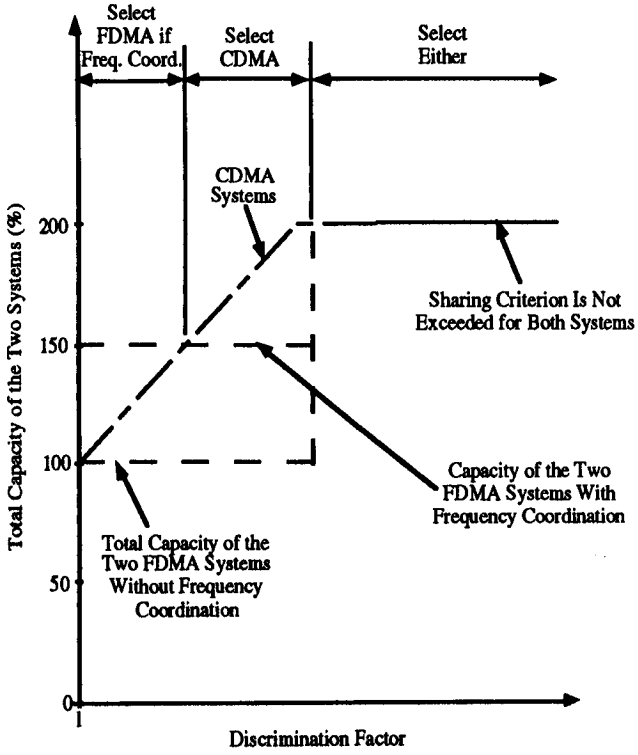

Figure 1 : Generic Decision Graph Based on Capacity for Two Identical Systems with CDMA and FDMA being Equally Power-Efficient

* This figure is not to scale and effects are exaggerated for the ease of illustration.

shown in the figure, we would expect CDMA systems to reach their maximum capacity with less discrimination between systems than for FDMA systems because of its robustness to interference.

The cross-over point where FDMA with frequency coordination offers more capacity than CDMA is obviously different under different assumptions. The case depicted in that figure is for two systems with equal power efficiency and we would expect the CDMA systems to need less discrimination to reach their respective 100 % capacity. If CDMA is made more power efficient than FDMA (i.e. single user E_b/N_o is less than the FDMA one), then the actual point where it reaches the 200 % capacity will be moved left relative to where it is in Figure 1 shrinking further the zone where FDMA with frequency coordination exceeds CDMA. The reverse effect occurs when the CDMA system is less power efficient than FDMA. Similarly if FDMA is made less spectrum efficient than the system depicted in Figure 1, the zone where FDMA with frequency coordination outperforms CDMA is narrowed down. Essentially it is a matter of power and spectrum efficiency trade-off.

Note that Figure 1 is a simplified scenario. It was used to simply illustrate the general behavior for systems based on FDMA and CDMA.

5.2 DIFFERENT ACCESS SCHEMES

For different access schemes, we can intuitively say that we would expect a CDMA system to cause less interference to a FDMA system and to be more robust to interference. So we would expect a wanted system to require less discrimination against an interfering CDMA system than from an interfering FDMA system. In addition, we expect a wanted CDMA system to be more tolerant to interference than an FDMA system.

6.0 INTERFERENCE ANALYSIS

6.1 CDMA INTO CDMA

In this section we are interested in looking at the interference between two co-located identical systems based on CDMA with co-coverage. The acceptable interference power* is bounded to 6% of the thermal noise power (N_oB_{rf}) and is given by :

$$I = \frac{C_{CDMA}\,M}{D} = \frac{E_b}{G_{ss}} B_{rf} \frac{M}{D}$$

where D is the discrimination factor between the two systems. Upper-bounding and re-arranging, we get :

$$\frac{E_b}{G_{ss}} B_{rf} \frac{M}{D} \le 6\,\%\, N_o\, B_{rf} \quad \text{or} \quad \left\{\frac{E_b}{N_o}\right\}_{CDMA} \le 6\,\% \frac{G_{ss}}{M} D$$

and the minimum required discrimination factor is thus :

$$D \ge \left\{\frac{E_b}{N_o}\right\}_{CDMA} - 10 \log\left\{ 0.06 \frac{G_{ss}}{M} \right\} \quad \text{dB} \quad (5)$$

where $\left\{\frac{E_b}{N_o}\right\}_{CDMA}$ is the design single user E_b/N_O for the CDMA system.

6.2 FDMA INTO FDMA

Here again we are interested in two identical co-located systems with co-coverage based this time on FDMA. Without frequency coordination the required minimum discrimination factor is :

$$D \ge 12.2 + C/N_{th} = 12.2 + E_b/N_O \quad \text{dB} \quad (6)$$

6.3 CDMA INTO FDMA

This time we consider two co-located systems with co-coverage but the wanted system is based on FDMA while the interfering system is based on CDMA. The allowable interference power is bounded by :

$$\frac{M}{D} \frac{C_{CDMA}}{B_{rf}} B_{FDMA} \le 6\,\%\, N_O\, B_{FDMA}$$

Noting that :

$$\frac{M}{D} \frac{C_{CDMA}}{B_{rf}} B_{FDMA} = \frac{M}{D\, G_{ss}} \{E_b\}_{CDMA} B_{FDMA}$$

where B_{FDMA} is the FDMA system channel bandwidth (including filtering but excluding guard bands), and $\{E_b\}_{CDMA}$ is the energy per information bit on the CDMA system; we get after re-arranging:

$$\left\{\frac{E_b}{N_o}\right\}_{CDMA} \le 6\,\% \frac{G_{ss}}{M} D$$

and : $D \ge \left\{\frac{E_b}{N_o}\right\}_{CDMA} - 10 \log\left\{ 0.06 \frac{G_{ss}}{M} \right\}$ dB (7)

6.4 FDMA INTO CDMA

Again we consider two co-located systems with co-coverage but the wanted system is based on CDMA while the interfering system is based on FDMA. The allowable interference power is given by :

* Path loss differential between the two satellites is neglected in the following discussion.

$$I = \frac{C_{FDMA}\, M}{D} \quad \text{where} \quad \mathcal{M} = \begin{cases} \left\lfloor \frac{B_{rf}}{W_{FDMA}} \right\rfloor & \text{BW limited} \\ \left\lfloor \frac{P_{total}}{C_{FDMA}} \right\rfloor & \text{power limited} \end{cases}$$

with P_{total} being the total RF power available, W_{FDMA} is the FDMA system channel bandwidth **including** guard bands and $\lfloor x \rfloor$ denotes the nearest integer less than or equal to x. Re-arranging the above equation, we get :

$$\left.\frac{C}{N_o}\right|_{CDMA} \leq 6\% \frac{B_{rf}}{\mathcal{M}} D$$

Expressed in terms of E_b/N_o we get the wanted system receiving the interfering signal with an E_b/N_o bounded by :

$$\left.\frac{E_b}{N_o}\right|_{FDMA} \leq 6\% \frac{B_{rf}}{\mathcal{M}} \frac{D}{R_b} = 6\% \frac{G_{ss}}{\mathcal{M}} D$$

Note that this assumes that the data rate R_b is the same in both systems. If $\left\{\frac{E_b}{N_o}\right\}_{FDMA}$ is the design E_b/N_o for the FDMA system, then the minimum required discrimination factor is :

$$D \geq \left\{\frac{E_b}{N_o}\right\}_{FDMA} - 10 \log \left\{ 0.06 \frac{G_{ss}}{M} \right\} \text{ dB} \qquad (8)$$

6.5 OVERALL RESULTS FOR DIFFERENT ACCESS SCHEMES

It is noteworthy that the required discrimination factors to meet the sharing criterion as derived earlier for different access schemes have the same form. Indeed we have shown that :

$$D \geq \left\{\frac{E_b}{N_o}\right\}_{interf} - 10 \log \left\{ 0.06 \frac{G_{ss}}{M_i} \right\} \text{ dB} \qquad (9)$$

where $\left\{\frac{E_b}{N_o}\right\}_{interf}$ is the design E_b/N_o for the interference system and M_i is the number of users in the interfering system. The number of users allowable is determined by the available bandwidth or power on the system. If we consider that the interfering system has up to the same bandwidth and power as the wanted system that supports M users, then we have :

$$M_i = \begin{cases} \frac{M}{\mathcal{E}} & \text{for BW Limited} \\ \text{antilog}\left([E_b/N_o]_{wanted} - [E_b/N_o]_{interf} + 10 \log M \right) & \text{for Power Limited} \end{cases} \qquad (10)$$

where $\mathcal{E}$ is the spectrum efficiency factor of the wanted system relative to the interfering system. Note that the above equation for the bandwidth limited case when CDMA interferes on FDMA is confusing because the CDMA required bandwidth is not related to the number of users in the network but is a design parameter. Indeed once the CDMA system is designed for a given maximum number of users, its bandwidth requirement is set. However the above equation for the bandwidth limited case can result in the number of interfering users being less than the actual maximum number of users that the interfering CDMA system is designed for. This can be seen as a CDMA system that is over designed. In order to make the results fair to CDMA we can do two things. First we can assume that there is an additional discrimination to the interfering system such that it appears to the wanted system as having only M_i users in the interference power sense. Another way to get the same result is to increase M_i to the designed maximum number of users and to increase proportionally the number of users in the wanted system. Both approaches lead to the same results.

7.0 EXAMPLES

7.1 LOW POWER EFFICIENCY

Let us consider an example of two networks. The first network is based on CDMA with BPSK modulation and with rate 1/2 constraint length 7 Viterbi decoding error correction coding. The required theoretical E_b/N_o^{eff} for 3-bit soft-decision decoding is 4.5 dB for a bit error rate (BER) of 10^{-5} [6] which corresponds to a single user E_b/N_o of 9.4 dB for a loading factor of 0.24. An equivalent FDMA system also based on BPSK but with no coding to preserve its spectrum efficiency would require an E_b/N_o of 9.5 dB for the same BER making both systems equally power efficient. For this example, a 20 user CDMA system would then require a total bandwidth of 79 (=19/0.24) times the information bandwidth.

For an FDMA system, the bandwidth requirement is a function of the filtering and guard band between channels. For typical BPSK systems a roll-off factor of 40 % can be assumed. The guard band can be specified based on the terminal oscillator stability. Assuming a 1 ppm oscillator stability at 30 GHz, we get a frequency offset of 30 kHz such that a minimum 60 kHz channel spacing is required. Table 1 shows the channel bandwidth requirement for two data rates: 64 and 256 kbps. The total bandwidth for 20 users is then 50 times the information rate at 64 kbps and 33 times at 256 kbps. The spectrum efficiency of CDMA is 0.24* and for FDMA it is 0.4 at 64 kbps and 0.61 at 256 kbps. In both cases FDMA is more bandwidth efficient than CDMA for the same power efficiency in this example.

* In the following we assume that the CDMA loading factor is its spectrum efficiency. This is valid because M-1≈M.

Table 1 : Bandwidth Requirements for an FDMA System Including Filter Spreading and Channel Guard Band.

Parameters	Data Rate of 64 kbps	Data Rate of 256 kbps
Filter Roll-Off (%)	40	40
Minimum Bandwidth Including Filter Spreading (kHz)	89.6	358.4
Channel Guard Band (kHz)	60	60
Total Bandwidth Required (kHz)	159.6	418.4
Bandwidth Required in Multiple of Data Rate	2.50	1.63

Using eq. (10) we find for CDMA interfering on FDMA in the bandwidth limited case for the 64 kbps data rate that $\varepsilon = 0.40/0.24 = 1.67$ and $M_i=12$ while for FDMA on CDMA with bandwidth limitation we have $\varepsilon=0.24/0.40=0.6$ to get $M_i=33$. As we can see the number of users can exceed the total capacity initially assumed for the interfering system. One way to look at this is to consider the case where more than one interfering system is present and the total effective number of users is given by M_i.

For power limited systems, we can again use eq. (10) to find that $M_i=20$ for both CDMA into FDMA and FDMA into CDMA scenarios because both systems are equally power efficient. Table 2 shows the results for the required discrimination factor and the equivalent satellite spacing for a ground terminal with a 30 cm antenna diameter and a radiation pattern model as described in [5] and plotted in Figure 2. As expected the worst case occurs for FDMA interfering on FDMA and all other results agree with our general expectation. The CDMA into CDMA shows an advantage of 6.1 dB over the FDMA into FDMA case. In the FDMA into CDMA case with bandwidth limitation, we see that 66 % more users can be supported over the same bandwidth under FDMA. This ratio is essentially the spectrum efficiency ratio of 1.67 (=0.4/0.24). So this is showing that CDMA is more robust by 3.8 dB than FDMA even though the interference power is increased. In the case of CDMA into FDMA with bandwidth limitation, the better FDMA spectrum efficiency essentially makes the result equivalent to the power limited case.

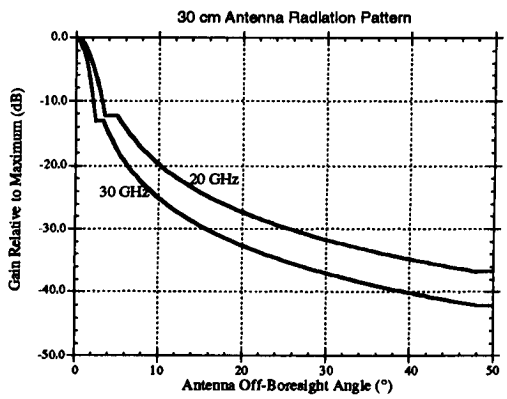

Figure 2 : Terminal Antenna Radiation Pattern [5].

Table 2 : Discrimination Factor and Satellite Spacing for Low Power Efficiency Systems and a 30 cm Dish Antenna.

Scenario	Discrimination Factor (dB)	Capacity of CDMA/FDMA	Sat. Spacing (°) @ 20 GHz	Sat. Spacing (°) @ 30 GHz
CDMA into CDMA	15.6	20/na	6.8	4.2
FDMA into CDMA - power limited	15.6	20/20	6.8	4.2
CDMA into FDMA - power limited	15.6	20/20	6.8	4.2
FDMA into FDMA	21.7	na/20	11.7	7.3
FDMA into CDMA - BW limited	17.9	20/33	8.4	5.2
CDMA into FDMA - BW limited	15.8*	12/20	6.9	4.3

na : not applicable
* Includes an additional factor of 10log(20/12).

Table 3 : Discrimination Factor and Satellite Spacing for Improved Power Efficiency Systems and a 30 cm Dish Antenna.

Scenario	Discrimination Factor (dB)	Capacity of CDMA/FDMA	Sat. Spacing (°) @ 20 GHz	Sat. Spacing (°) @ 30 GHz
CDMA into CDMA	11.2	20/na	3.3	2.2
FDMA into CDMA - power limited	11.2	20/22	3.3	2.2
CDMA into FDMA - power limited	10.7	18/20	3.3	2.2
FDMA into FDMA	16.7	na/20	7.6	4.7
FDMA into CDMA - BW limited	10.8	20/33	3.3	2.2
CDMA into FDMA - BW limited	13.4*	12/20	5.6	3.4

na : not applicable
* Includes an additional factor of 10log(20/12).

7.2 IMPROVED POWER EFFICIENCY

So far we have considered FDMA systems with no coding. This is not really fair because in practice FDMA systems will be relying on some coding to improve their power efficiency. If a rate 1/2 coding (k=7) with Viterbi decoding is also considered for the FDMA system, then the FDMA into FDMA required discrimination factor would be decreased by 2 dB to take into account the 5 dB coding gain and the 3 dB increase in bandwidth. We can also use a QPSK modulation for the FDMA system to improve its spectral efficiency. Note that the use of QPSK on CDMA does not change its spectral efficiency. The FDMA channel bandwidth is thus still 2.5 times the data rate (for 64 kbps) and the spectrum efficiency is 0.40.

For CDMA a rate 1/2 coding scheme was assumed but we could add more coding. Let us assume that up to 2 dB additional gain can be obtained. Then the required E_b/N_o^{eff} is 2.5 dB and we will assume that the loading factor is maintained at 0.24 resulting in an E_b/N_o of 4.9 dB (almost as power efficient as the FDMA system). Then the spreading factor for a 20 user system is 79 as before.

The required discrimination factor to meet the sharing criterion is shown in Table 3. Noting that the FDMA system is almost as power efficient as the CDMA system and we would expect the results to be (on a relative scale) comparable to the one in the previous example where equal power efficiency was assumed. This is in fact what we get.

8.0 CONCLUSION

After a basic review of spread spectrum systems, system equations are derived. An interference analysis of CDMA and FDMA systems is carried out and the discrimination factor required to meet the sharing criterion is derived. The discrimination factor is then related to the satellite spacing and ground terminal off-boresight angles. Two examples of FDMA and CDMA systems with identical capacities are compared in terms of their discrimination factor requirements. The comparison highlights the power limitation of satellite systems by looking at the required energy per information bit to thermal noise power density (E_b/N_O) for both systems. It is shown that for equally power efficient and identical CDMA and FDMA systems, CDMA allows for closer satellite spacing than FDMA at the cost of spectral efficiency. Typical results for a 30 cm terminal dish antenna would allow twice as many CDMA based satellites as FDMA based satellites. The study did not address explicitly the bandwidth requirements for feeder links of repeater satellites but for systems with large number of beams as in [1,2], this should be a concern for CDMA systems. In fact, it is possible that the feeder link bandwidth requirements for such a repeater satellite might defeat the CDMA advantage stated above.

Furthermore no comparison was done on the implementation of CDMA on-board demodulators for regenerative satellites and that should be taken into account before selecting the access scheme.

All the results of the interference analysis are expressed in terms of required discrimination factor between systems. If the systems do not have co-coverage or have different transmit powers, the procedure can easily take into account the required increase or decrease in discrimination factor. The interference analysis method used in this paper was developed for inter-system interference analysis but it can easily be applied to the case of intra-system interference analysis for multiple beam systems.

During the analysis, a major concern was the meaning of the sharing criterion when applied to CDMA systems. In this report a 6 % increase in thermal noise power has been assumed for the analysis but there is no general agreement on this interpretation of the sharing criterion for CDMA systems. Indeed because CDMA systems can be designed to support more interference, a 6 % increase in total (thermal plus self noise) noise power is sometimes preferred. Given that the sharing criterion was developed initially for analog channels, we think it would be useful to re-visit this sharing criterion definition and to use a better performance measure for digital links such as the degradation in E_b/N_O or bit error rate.

9.0 REFERENCES

[1] C. Black, P.J. Garland, S. Irani, P. Takats, *Flexible On-Board Processing for a Multi-Service Environment*, 15th AIAA International Communications Satellite Systems Conference, Feb. 28-Mar 3, 1994, AIAA-94-1102-CP.

[2] *Application of Hughes Communications Galaxy Inc., before the Federal Communications Commission for SPACEWAY : A Global Network of Ka-Band Fixed Communications Satellites*, July 26, 1994.

[3] Manuta Lou, editor, *Big LEO Revolution*, Satellite Communications, March 1995, pp. 33-40.

[4] *Frequency Sharing Between Networks of the Fixed-Satellite Service*, Report 455-5, in *Reports of the CCIR,1990, Annex to Volume IV-Part 1, Fixed-Satellite Service*, Geneva, 1990

[5] *Radiation Diagrams of Antennas for Earth Stations in the Fixed-Satellite Service for use in Interference Studies and for the Determination of a Design Objective*, Report 391-6, Annex I in *Reports of the CCIR, 1990, Annex to Volume IV-Part 1, Fixed-Satellite Service*, Geneva, 1990

[6] V.K Bhargava, D. Haccoun, R. Matyas, P. Nuspl, *Digital Communications by Satellite : Modulation, Multiple Access and Coding*, John Wiley & Sons, Toronto, 1981, chap. 12.

Alternative Beam Configuration For A Canadian Ka-Band Satellite System

Daniel J. Hindson and Mario Caron

Satellite Systems and Technologies Directorate
Communications Research Centre
3701 Carling Avenue, P.O.Box 11490, Station H
Ottawa, Ontario, Canada K2H 8S2
tel. (613) 998-2861, fax (613) 990-0316, email: dan.hindson@crc.doc.ca

ABSTRACT

Satellite systems operating in the Ka-band have been proposed to offer wide band personal communications services to fixed earth terminals employing small aperture antennas as well as to mobile terminals. This requirement to service a small aperture antenna leads to a satellite system utilizing small spot beams. The traditional approach is to cover the service area with uniform spot beams which have been sized to provide a given grade of service at the worst location over the service area and to place them in a honeycomb pattern. In the lower frequency bands this approach leads to a fairly uniform grade of service over the service area due to the minimal effects of rain on the signals. At Ka-band, however, the effects of rain are quite significant. Using this approach over a large service area (e.g. Canada) where the geographic distribution of rain impairment varies significantly yields an inefficient use of satellite resources to provide a uniform grade of service. An alternative approach is to cover the service area using more than one spot beam size in effect linking the spot beam size to the severity of the rain effects in a region.

This paper demonstrates how for a Canadian Ka-band satellite system, that the use of two spot beam sizes can provide a more uniform grade of service across the country as well as reduce the satellite payload complexity over a design utilizing a single spot beam size.

INTRODUCTION

In 1994 the Canadian government announced funding for an advanced satellite communications program (ASC) [1]. A geostationary satellite being studied is to provide advanced personal communications services to both Ka-band fixed terminals employing small aperture antennas and mobile terminals. The requirement to service small aperture earth terminals leads to a payload design utilizing small spot beams. The traditional approach to covering a service area with spot beams has been to define the beam size based on the minimum grade of service for the worst case location over the service area and then to place the beams in a honeycomb pattern. This leads to designs such as those in [2,3].

The present ASC payload concept also includes an advanced VSAT system at Ku-band. To accommodate the use of Ku-band an existing Canadian Ku-band orbital slot is to be used. At present Canada has filed for the 114.9°W orbital location.

In a previous study the optimal orbital location for a Ka-band satellite covering Canada had been determined to be around 92.5°W [4]. This was based on the distribution of rain fade margins required across the country. Moving west to 114.9°W causes the rain margin required in the southeast of Canada to be greatly increased. Additionally the southeast has the worst rain environment for fades in Canada. These two facts compound to cause the rain fade margin in southeastern Canada to be significantly higher than the rest of the country.

In this paper we first describe the methodology of determining the satellite and terminal requirements necessary to meet a given grade of service (GOS) over the service area (assumed to be Canada in this paper).We then look at the combined effect on the satellite and terminal of the use of small equal-sized spot beams to cover a service area with large propagation margin variations. A proposed scheme of using different sized spot beams is then presented which produces a more uniform GOS over the service area. The impact on the satellite payload of using this alternate scheme is then presented and conclusions about the merit of this approach are reached.

METHODOLOGY

In this section the methodology used to determine the effect on the satellite and terminal of providing a given GOS across Canada is presented. The GOS is defined as a percentage of time that a terminal at a given location will be able to maintain a communications link with a maximum bit error rate.

A program was developed in-house to analyze the effects of the use of spot beams and propagation impairments. The program calculates the spacecraft effective gain towards a grid of satellite roll/pitch points spaced at 0.1° covering

Canada. The location of the boresights of the spot beams in the satellite's roll/pitch coordinate system and the beam's boresight gains are inputs into the program. For each grid point the gain from each beam was calculated using:

$$G_{ij} = Gb_i - 3\left[\frac{d_{ij}}{d_{i\text{-}3\,dB}}\right]^2 \text{ dB} \qquad (1)$$

Where: G_{ij} is the i^{th} spot beam's gain toward the point j, Gb_i is spot beam i's boresight gain, d_{ij} is the angular distance from the i^{th} spot beam's boresight to the point j, and $d_{i\text{-}3dB}$ is the i^{th} spot beam's -3 dB beam radius. The maximum gain, over all spot beams, towards point j was then stored ($Gmax_j$). The program then calculated the rain margin, atmospheric absorption and spreading loss toward each point on the grid from the satellite at both the uplink and downlink frequencies. The rain margin and atmospheric absorption were calculated using the method outlined in [3]. The rain margin calculations were performed for an availability of 99.75%. This leads to an overall link availability of 99.5% when a regenerative satellite is assumed. The composite satellite gain towards the grid point (G_s) was then calculated as:

$$G_s = Gmax_j - L_R - L_A - L_S \qquad (2)$$

Where: $Gmax_j$ is the maximum satellite antenna gain towards the grid point j, L_R is the rain fade margin, L_A is the atmospheric absorption loss, and L_S is the spreading loss. The G_s for a specific location (e.g. Windsor) was then extracted from the data and saved as the reference value. This reference value was then subtracted from the data resulting in the composite satellite gain relative to the reference location.

If we now consider the ground terminal, one would like to have a common terminal type to provide a particular service. This is desirable in order to reduce the terminal costs through economies of scale but is also a requirement for mobile services. It is reasonable then to assume that for a particular service that the terminals will have the same EIRP and G/T. For this analysis we assume that the EIRP and G/T of the terminal have been sized to provide a link with the desired availability for the reference location we have chosen. Then the composite satellite gain relative to the reference location can be thought of as the excess EIRP of the terminal to provide the same availability at other locations on the uplink, and the excess G/T on the downlink. Alternatively on the downlink instead of excess terminal G/T we could see this as excess satellite EIRP. In an ideal system both the excess terminal and satellite EIRPs would be zero over the full service area. This would indicate a uniform GOS and a maximized use of terminal and spacecraft resources. Any excess EIRP can then be looked upon as an overdesign to meet the GOS objectives and thus is an inefficiency measure.

EQUAL-SIZED SPOT BEAMS

In Figure 1 we show a hypothetical satellite coverage of Canada from the 114.9°W geostationary slot. In this case Canada is covered with 57 0.5° spot beams. This is similar to the coverage discussed in [2]. The program discussed above was run using this beam configuration for a 30 GHz uplink case with a 99.75% availability requirement and using Windsor, Ontario, as the reference location. Windsor was chosen because it is the worst case location in terms of rain fade margin requirements in the highly populated areas of Canada. The results were overlaid on a map of Canada as viewed from the 114.9°W orbital slot, are shown in Figure 2. In this figure we can see high excess terminal EIRPs in the North and West of Canada. Most of this region has more than 6 dB excess EIRP. In Southeastern Canada, however, the excess EIRP is minimal. Based on these results it was deduced that the North and West of Canada could be covered using larger spot beams than the Southeast.

TWO SPOT BEAM SIZE ANALYSIS

Since the equal-sized spot beam analysis showed excess terminal EIRPs in the order of 6 dB in the North and West it was decided to double the spot beam size used to cover these areas. Figure 3 shows the beam configuration chosen. It has reduced the number of beams down to 23 (13 1.0° and 10 0.5°). The GOS analysis software was run using this beam configuration for a 99.75% availability at 30 GHz with Windsor as the reference location. The results of this analysis are shown in Figure 4. Examining this figure, it is apparent that the regions of high excess terminal EIRP have been much reduced compared to the equal-sized spot beam case. A few areas require extra terminal EIRP, notably Southern Manitoba and Northern Quebec. These regions could be covered adequately with a slightly altered beam set. In this analysis, beams formed by single feeds have been assumed. If triplet feeds were used, the beam cross-over regions would have increased gain. This could enable the use of even larger spot beams in the North and West.

The downlink was analyzed using the beam configuration of Figure 3 and assuming a 99.75% availability requirement at 20 GHz with Windsor as the reference location. The results of this analysis are shown in Figure 5. From this figure it can be seen that in the cross-over regions of the 1.0° beams an increase in the satellite EIRP between 0 and 3 dB is required over that used for the reference location. On examination of the numerical results it was found that a satellite EIRP increase of approximately 2 dB is required. This EIRP deficit will have to be made up by using larger power amplifiers on the 1.0° spot beams.

PAYLOAD COMPARISON

This section examines the effect on the satellite payload of using two spot beam sizes over the equal-sized spot beam approach. This discussion is based on the Ka-band portion of the payload design described in [2] and shown in Figure 6.

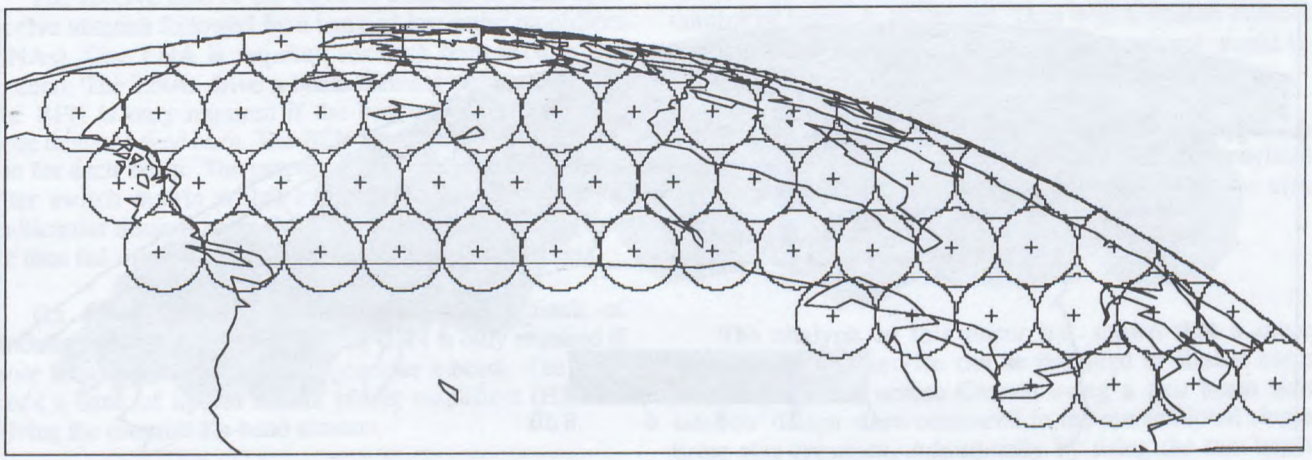

Figure 1 Single Spot Beam Size Beam Layout Over Canada From 114.9°W

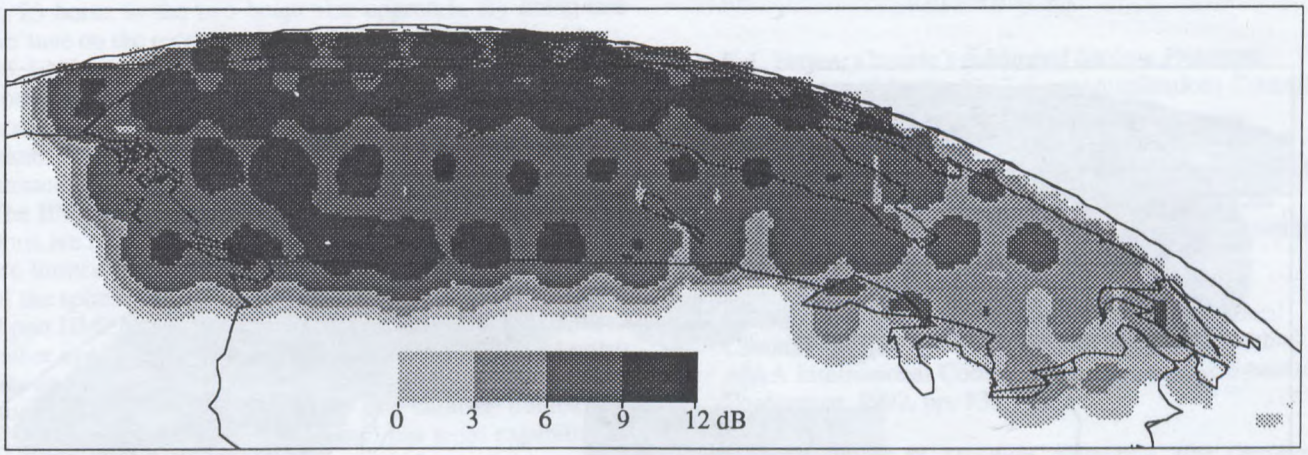

Figure 2 Single Spot Beam Size Excess Terminal EIRP at 30 GHz 99.75% Availability

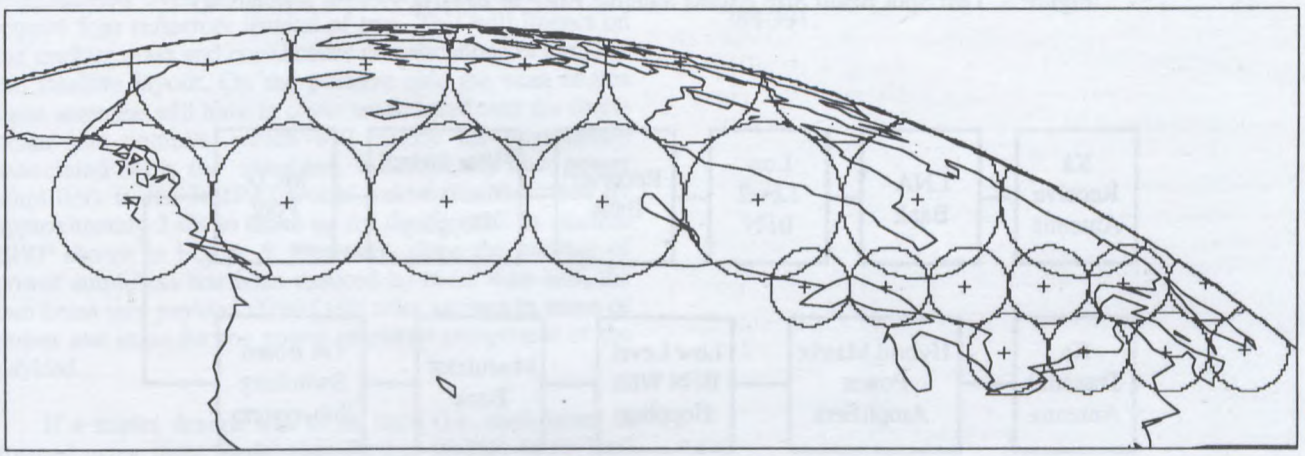

Figure 3 Two Spot Beam Size Beam Layout Over Canada From 114.9°W

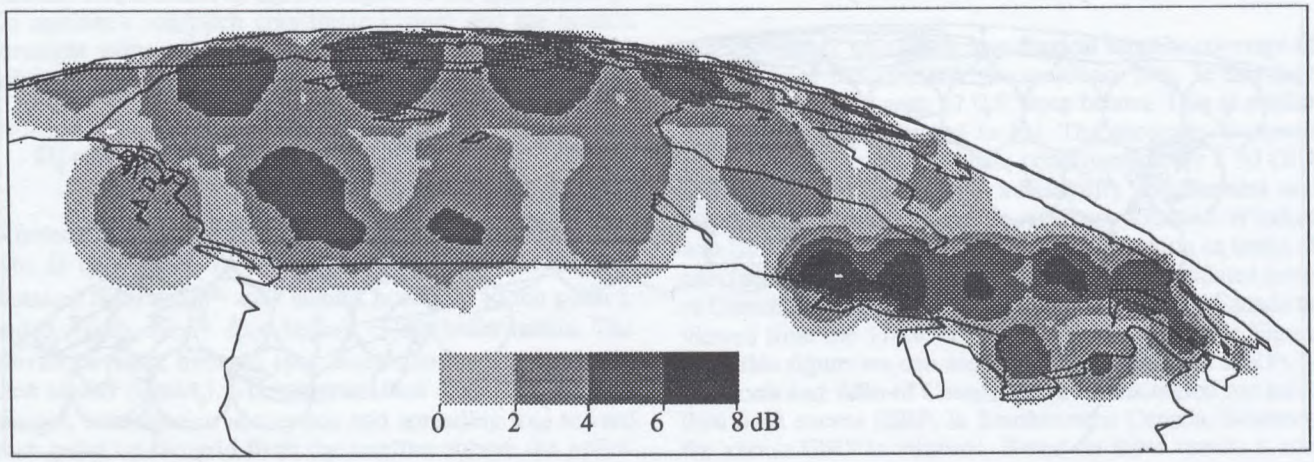

Figure 4 Two Spot Beam Size Excess Terminal EIRP at 30 GHz 99.75% Availability

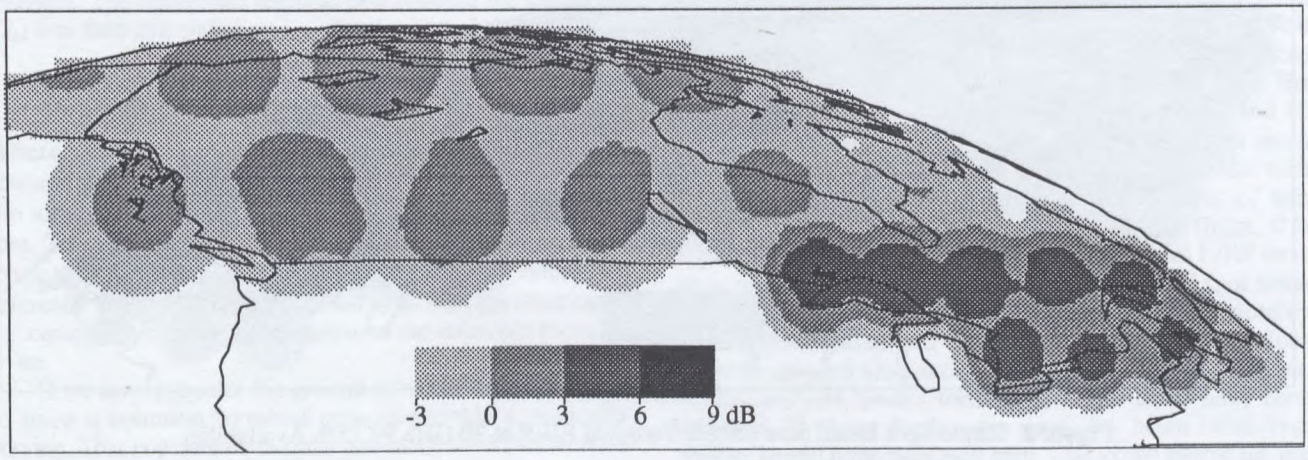

Figure 5 Two Spot Beam Size Excess Satellite EIRP at 20 GHz 99.75% Availability

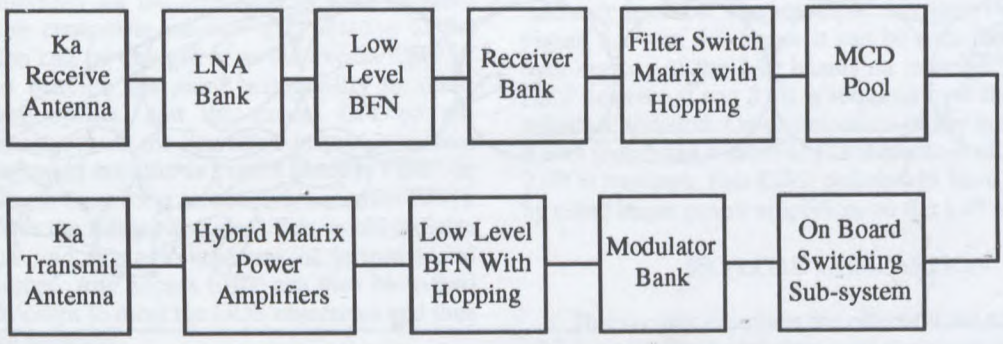

Figure 6 Ka-Band Satellite Payload Block Diagram After [2]

The receive side of the payload consists of a Ka-band receive antenna followed by a bank of low noise amplifiers (LNAs). One LNA is required for each horn used in the antenna. The LNAs drive a beam forming network (BFN). The BFN is only required if the beams are formed using more than one feed horn. The BFN feeds a bank of receivers, one for each beam. The output of the receivers are fed to a filter switch matrix which switches beams to a bank of multicarrier demodulators (MCDs). The demodulated signals are then fed to an on-board switch which performs routing.

On the transmit side of the payload a bank of modulators drive a BFN. Again this BFN is only required if more than one horn is used to generate a beam. The BFN feeds a bank of hybrid matrix power amplifiers (HMPA) driving the transmit Ka-band antenna.

If we consider the single horn per beam approach (i.e. the receive and transmit BFNs are not required), then we are going from 57 horns in the equal-sized spot beam approach to 23 horns in the two beam size approach. By doing this we save on the receive side: 35 feed horns, 35 receive filters, 35 LNAs, and 35 receivers. We also reduce the FSM complexity significantly by reducing its number of input ports by 35. The MCD and on-board switch remain the same. On the transmit side we save: 35 feed elements, 35 transmit filters, and 35 high power amplifiers in the HMPA. The HMPA complexity is further reduced since now only 23 ports are required as opposed to 57 ports. Generally HMPAs are limited to 8 port designs due to the increase complexity of the splitting and combining networks beyond this size. If 8 port HMPAs are assumed then only 3 HMPAs are required rather than 8. This reduction in the number of HMPAs also has an impact on the payload flexibility since it defines the number of power pools. With the smaller number of HMPAs the two beam size payload has more capability in distributing the payload RF power over the service area.

The two beam size payload however has some extra requirements over the single beam size approach. It will require four reflectors instead of two. This will impact on the satellite mass and could cause complications in terms of the satellite layout. On the positive side the scan angles these antennae will have to cover are reduced over the single beam size antenna, which will reduce the scan losses associated with the antennae. Additionally the power amplifiers in the HMPAs would have to be increased by approximately 2 dB to make up for the shortfall in satellite EIRP shown in Figure 5. However, since the number of power amplifiers has been reduced by more than half, the two beam size payload should still offer savings in terms of power and mass for the power amplifier component of the payload.

If a triplet design was to be used (i.e. each beam is formed using three feeds) then further savings in payload hardware could be realized with the two beam size approach. The main savings would be in the receive and transmit BFNs. The BFNs complexity and size are related to the number of beams to be formed. Thus with a smaller number of beams the BFNs complexity, mass, and volume would be reduced.

Overall it can be seen that using the two beam approach should provide significant savings in terms of payload complexity, mass, and power over a single beam size design.

CONCLUSIONS

The analysis in this paper has shown that a more uniform grade of service can be provided to similar earth terminals located across Canada using a two beam size satellite design when compared to the conventional single beam size approach. Additionally by using the two beam size approach significant reduction in the payload complexity, mass, and power can be achieved.

REFERENCES

[1] **E.J. Hayes**, *Canada's Advanced Satcom Program*, Proceedings of the Pacific Telecommunications Council 17th Annual Conference, 1995, pp. 24-29.

[2] **C. Black, et al**, *Flexible On-Board Processing For A Multi-Service Environment*, Proceedings of the 15th AIAA International Communications Satellite Systems Conference, 1994, pp. 1250-1260.

[3] **L.C. Palmer, et al**, *20/30 GHz Satellite Personal Communications Networks*, Proceedings of the 14th AIAA International Communications Satellite Systems Conference, 1992, pp. 739-741.

[4] **M. Caron and D. Hindson**, *Selecting The Optimal Orbit Location For A Canadian EHF Communications Satellite*, Proceedings of the 1994 Canadian Conference On Electrical and Computer Engineering, 1994, pp. 388-391.

System and Antenna Design Considerations for Highly Elliptical Orbits as Applied to the Proposed Archimedes Constellation

C. Paynter and M. Cuchanski

Spar Aerospace Ltd

21025 TransCanada Highway
Ste-Anne-de-Bellevue, Quebec, H9X 3R2, Canada
tel (514) 457 2150 fax (514) 457 2724

ABSTRACT

The paper discusses various aspects of the system design for a satellite in a highly elliptical inclined orbit, and presents a number of antenna design options for the proposed Archimedes mission. A satellite constellation was studied for the provision of multi media communication services in the L and S Band for northern latitudes. The inclined elliptical orbit would allow coverage of Europe, America, and East Asia. Using Canada and North America as the baseline coverage area, this paper addresses system considerations such as the satellite configuration and pointing, beam configuration, and requirements for antennas. A trade-off is performed among several antenna candidates including a direct radiating array, a focal-fed reflector, and a single reflector imaging system. Antenna geometry, performance, and beam-forming methods are described. The impact of the designs on the antenna deployment is discussed.

COVERAGE CHARACTERISTICS DURING ACTIVE ORBIT ARC

The proposed Archimedes spacecraft travels in an inclined highly elliptical orbit with a period of 8 hours, an eccentricity of 0.63, an apogee altitude of 26737 km, and an inclination of 63.3 degrees. The active orbit arc is a 4-hour period centred on the apogee, during which the spacecraft is almost stationary when viewed from northern latitudes (its ground track has a nearly constant longitude). The constellation consists of six satellites spaced 60 degrees apart and phased at 4 hour intervals. A satellite entering the active arc takes over the communications traffic from another satellite in the adjacent orbital plane (handover 1); and when exiting the active arc, the satellite passes on the traffic to the following satellite, (handover 2). During a 24-hour period, one satellite can service successively three zones spaced 120 degrees in longitude: Europe, North America, and East Asia. Relative to a geostationary orbit, the inclined elliptical orbit provides the advantage of a high elevation angle of a ground station situated in a northern latitude, typically between 40 and 90 degrees for most of the coverage area.

Two key parameters are a function of the orbit time: the propagation path losses and the shape of the coverage area, *viz.* the size, position, and orientation. The path loss is reduced by about 2.3 dB from the apogee to a handover point as a result of a decrease in the spacecraft altitude. The path loss at the edge of coverage relative to the path loss at the nadir depends on both the spacecraft attitude and the diameter of the coverage area. For the rim of the earth, the relative path loss varies from 1.7 dB at the apogee to 2.1 dB at the handover. For the 40-degrees elevation circle, the path loss decreases to 0.6 dB at the apogee and 0.8 dB at the handover. The Canada and USA coverage areas are actually only about 30 to 40% of the area of the 40-degrees circle, and consequently the path loss variation across the coverage area is small, about 0.2 dB.

An example of variations in the extent and location of the coverage area with orbit time is given in Figure 1, which shows the outlines of Canada and the USA at the handover 1, the

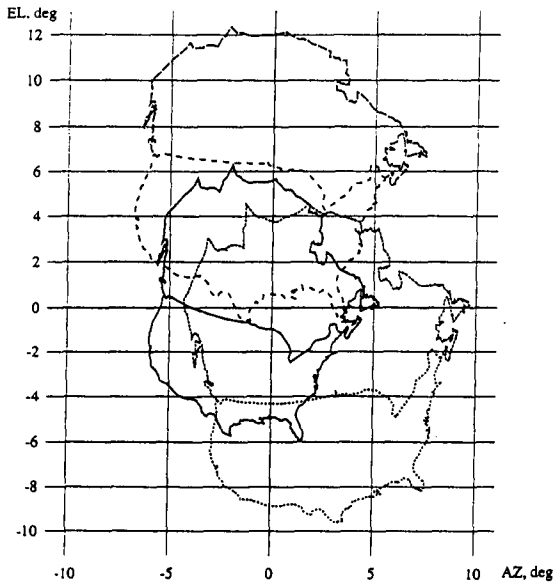

Figure 1 Canada & USA at Handover 1 & 2 and Apogee, Boresight at Nadir.

apogee, and the handover 2. The yiewing co-ordinates frame is pointed at the nadir and has another axis in the plane containing the satellite and the earth north axis. The displacement of the coverage area relative to the nadir varies during the active arc and reaches 7 to 9 degrees at its maximum. The ratio of the coverage area at the handover to the area at the apogee is about 1.9 dB for Canada and US combined coverage, while for Canada only the ratio is 2.1 dB. To minimise the effective (composite) coverage area and the associated scan losses, we need to point the antenna (or actually the spacecraft if we are assuming a fixed-mounted antenna) towards the centre of the coverage area rather than the nadir. This will necessitate a continuous and dynamic control of the spacecraft attitude throughout the active orbit arc. The required range of boresight adjustment is about +-1.5 degrees East-West (pitch) and +-4.5 degrees North-South (roll). With the antenna continuously re-pointed towards an optimum boresight, the antenna design problem is simplified to providing a multibeam coverage for a composite overlapped area. An example of such a composite coverage is shown in Figure 2; a comparison with the maps of Figure 1 clearly demonstrates the effectiveness of boresight re-pointing in minimising the total area and the scan angles.

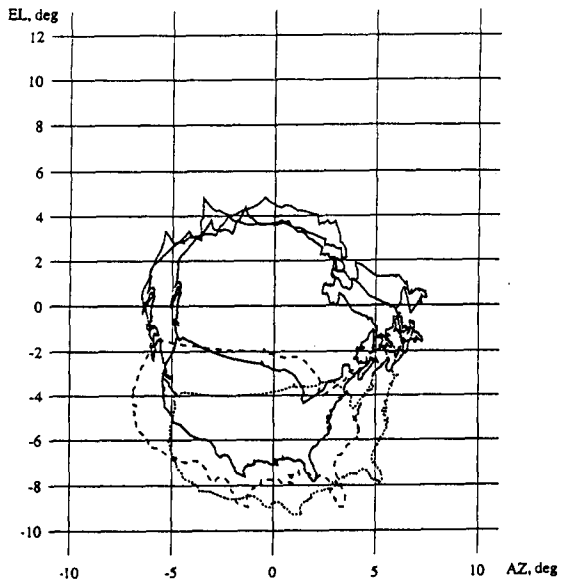

Figure 2 Composite Coverage with Boresight at Canada Centre

ANTENNA BEAMWIDTH AND GAIN LEVEL AT EDGE OF COVERAGE

The variation of the coverage size as function of the orbit time appears to require that the antenna be equipped with a beam zooming capability. Zooming would greatly increase the antenna complexity and cost. Our preferred approach is to take advantage of a reduced path loss at the handover relative to the apogee to design the antenna as a passive self-compensating system which will maintain constant signal level at the edge of coverage, from the apogee to the handover. Conditions for such a system are derived to define the appropriate edge-of-coverage beamwidths and levels below peak. For a simple pencil beam, the beam power pattern at the apogee can be approximated as $Pa(T) = K * T*T$, where K = -3 dB, and T is the angle normalised with respect to half the 3-dB beamwidth. The beam power pattern at the handover is $Ph(T) = Pa(T) + L$, where L is the path loss reduction at the

handover (2.3 dB). For a self-compensating system we must have Pa(Ta) = Ph(Th), where Ta and Th are the edge-of-coverage angles at the apogee and the handover, respectively. The ratio Th / Ta = R can be estimated from the change of the coverage area size from handover to the apogee (R*R = 2.0 dB, or R = 1.259). Solving for Ta we obtain Ta = sqrt(-L / (K * (R*R - 1)). Hence the edge-of-coverage angles and gain levels below peak are:

apogee: Ta = 1.145, Pa = -3.9 dB
handover: Th = 1.441, Ph = -6.2 dB + 2.3 dB

It is well known that in order to maximise the edge-of-coverage gain of a pencil beam, the edge-of-coverage level should be set at approximately 4 dB below the beam peak, with the edge-of-coverage angle equal to the 4-dB beamwidth. Our solution for the edge of coverage angle has thus the additional benefit of providing the optimum gain. The level at the handover is 6.2 dB below peak, which may cause concerns about the gain slope (S) at the edge of coverage. However, since the gain slope is given by S(T) = -2 * K * T (or S = -24 * actual angle / (3-dB beamwidth)**2), Sh / Sa = R = 1.259, that is the gain slope at the handover is only 26% larger than the gain slope at the apogee.

ANTENNA DESIGN CONSIDERATIONS

Independently of a hardware implementation, two types of antennas have been analysed, mainly differing in the permissible aperture size:

1. non-deployable antennas with a maximum diameter of about 3 meters as enforced by the launch vehicle envelope,
2. large deployable antennas with an aperture diameter of 5 to 10 meters.

The 3-meter antennas provide an adequate gain performance and are relatively simple. However, they produce wide beams with a gentle roll off and sidelobe levels of about 23 to 25 dB below peak. Therefore the 3-meter antennas are unsuitable for mission scenarios requiring very low interference levels over a nearby region. The 5 to 10 meter antennas achieve much better gain, narrow beams with sharp roll off, and can ensure low sidelobes, 30 to 35 dB, over neighbouring areas. The minimum angular separation between a coverage area and a sidelobe isolation area is about 1.5 times the 3-dB beamwidth of a spot beam, and hence is inversely proportional to the aperture diameter. With closely spaced coverage regions, large apertures would be required to keep the sidelobe interference in the adjacent area to a low level.

Two beam configuration options have been considered:

1. a small number of steerable beams with full control of position and possibly shape synthesis capability, and
2. a stationary, circularly symmetric pattern of beams with beam position control via switching.

The steerable beam formation consists of 4 circular high gain spots and one shaped beam. The stationary beam layout is produced by either 7, 13, or 19 beams. A choice of either steerable or fixed beam configuration is a critical factor in the determination of a feasible antenna candidate. In particular, it determines the beamforming network: for steerable beams, a power divider/combiner with variable phase shifters for an array or a reconfigurable network with variable attenuators and phase shifters for a focal-fed reflector; for fixed beams, a simple corporate power divider, a Butler matrix, a Blass matrix, or a Rotman lens.

DIRECT RADIATING ARRAY

For the non-deployable DRA option, two nominal aperture diameters were used: 280 cm and 300 cm. For each aperture diameter, arrays with 37, 48, and 61 elements were designed. Radiation patterns were computed for two values of the element aperture efficiency, 95% and 100%, for an on-axis beam and a beam scanned 8 degrees off axis. The peak directivity ranged from 31.4 dB for the 280 cm array to 32.1 dB for the 300 cm array. The scan loss at 8 degrees varied from about 0.9 dB for the 37-element array to 0.5 dB for the 61-element array. The edge of coverage is defined as 3.9 dB below peak at the apogee, and 6.2 dB at the handover, resulting in edge-of-coverage directivity of 27.5 dB (280 cm) or 28.2 dB (300 cm) for the on-axis

beam. The corresponding beamwidths are 5.6 degrees or 5.2 degrees (apogee), and 6.9 degrees or 6.4 degrees (handover). The grating lobe for the 300 cm, 37-element array is situated 31 degrees off axis for the non-scanned beam, and 22.7 degrees off axis for a beam scanned 8 degrees. For comparison, the edge of the earth is at 11.1 degrees off nadir at the apogee, and 13.8 degrees off nadir at the handover; with the antenna boresight centred on Canada, the grating lobe is just outside the earth disk. For the 48 and 61 element arrays the closest grating lobe positions are 27.2 and 31.9 degrees off axis, respectively. The sidelobe level, determined by the aperture distribution selected for the array (radially tapered parabolic, with edge taper of -10 dB), is virtually the same in all cases, about 23 dB below beam peak.

A stationary, rotationally symmetric 7-beam system can be created using the above DRA, with beams selected via switching. For the 300 cm array for instance, the beam spacing is 4.5 degrees and the crossover beamwidth is 5.2 degrees. For this system, the beam spacing is fixed, thus obviating the need for variable phase shifters and simplifying the beamforming network, for which a lightweight Rotman lens could be used. The 7-beam system can cover Canada or Canada & US combined with service for nearly 100% of the area.

A 5.2 meter, 127-element deployable DRA was also designed to form a steerable beam system consisting of four high gain spots serving southern Canada and one wider elliptical beam for the northern region. The 3.9-dB beamwidth of the spots is 3.5 degrees, the ellipse is 8.5 by 5.0 degrees. The peak directivity of the spots is 35.6 dB, that of the elliptical beam is 29.6 dB. The edge-of-coverage directivity for the high gain spots is 31.3 dB including scan losses. Thanks to a highly tapered illumination (parabolic-squared distribution with an edge taper of -18 dB), the sidelobe levels are about 36 dB below peak. Except in the immediate vicinity of the beam, this design is therefore able to provide good sidelobe isolation. It requires, however, a beamformer with variable phase shifters for beam steering and beam shape synthesis.

FOCAL-FED REFLECTOR DESIGN

For the focal-fed offset parabolic reflector designs, the aperture sizes ranged from 2.6 to 7 meters. Three beamforming methods were considered:

1. single feed per beam
2. triplet feed cluster per beam, with one or two shared feeds per cluster
3. feed array with a reconfigurable low-level feed network

When using a single feed per beam, the spacing between feeds corresponds to the spacing between beams and is a function of the reflector geometry. If the beams are closely spaced, this puts a severe restriction on the physical size of the feed. Small feed sizes result in high spillover losses, of the order of 2 to 3 dB. To improve spillover efficiency, endfire feeds such as helices can be used, occupying a relatively small space in the feed plane but providing a large effective aperture. However, an endfire feed cannot be too long, for both electrical and mechanical reasons (mutual coupling, bandwidth, stability, reflector blockage), resulting in upper values of achievable aperture efficiency of about 100% to 120%. The beam pattern is fixed in position, with beam control achieved only via switching. The performance achievable with a reflector fed by singlets is inferior to that of a comparable size DRA, mainly due to spillover losses.

A triplet feed offers a good alternative to an endfire element without the need for extremely high aperture efficiencies of the elements. Successive feed clusters can be overlapped, thus increasing the effective aperture of the cluster, and permitting closer beam spacing. Spillover loss is reduced, usually to about 1 dB or less, and the tapered reflector aperture illumination results in sidelobe levels of about 24 dB.

The overlapping triplet feed clusters require a beam forming network. For an active antenna, the beamforming is best done using a low power level beam former. The outputs from the low level beamformer can then be fed into a multi-matrix parallel hybrid matrix amplifier. Instead of Butler matrices, a Blass matrix or a Rotman lens can also be used.

Successive triplets can share either 1 or 2 feeds. When 1 feed per triplet is shared, any given feed element is connected to at most three triplets, and the beam spacing corresponds to the inter-element spacing. When 2 feeds per triplet are shared, a feed element is connected to six triplets. The beam spacing is either 1.0 or 0.527 times the value corresponding to the element spacing, thus resulting in an increased beam overlap. With 1 shared feed per triplet, there exist empty gaps at the triple crossover points between beams, where the minimum gain values occur. The system with 2 shared feeds per triplet places additional beams over the gaps, increasing the number of beams over the coverage area, decreasing the beam spacing, and providing a more uniform gain. Both the beam position control and the edge of coverage gain is improved, the latter by nearly 1.0 dB. Furthermore, the system with the two shared elements has a ratio of the number of beams to the number of elements greater than unity, in contrast to the system with one shared element, where the ratio is typically 0.6 to 0.8 dB. Hence the use of the feed array area is more efficient.

A large diameter focal-fed reflector with a multi-feed reconfigurable array is capable to synthesise either a spot or a shaped beam at a desired location, with low sidelobes (27 to 33 dB) over a nearby region. Very good gain performance is achievable, depending on the angular area of the synthesised beam. The geometry, feed element characteristics, beam shaping, and sidelobe isolation performance are all very similar to the well-known Intelsat Hemi-Zone C-Band antennas. However, a major difference is that the antenna proposed for the Archimedes mission is an active system, and that the beam forming would be achieved in a low-level BFN. Such a low-level BFN would be realised using a microwave integrated circuit technology. We shall give an example of the scale of miniaturisation possible, for a 37-element feed array. The key element of the BFN is a module consisting of a 1-to-8 power divider, variable attenuators and phase shifters. Five of these modules would be used in this case to form a beam. The size of the module is approximately 3.0 x 3.0 x 0.25 cm, allowing very compact and low mass packaging for the entire BFN. This concept of a large reflector with an active reconfigurable feed has tremendous performance advantages in terms of gain, sidelobe isolation, beam flexibility, and an in-orbit control. However, the deployment problems for a 7 to 10 meter reflector will have to be addressed, including a 37-element feed array with a diameter of nearly 2 meters. An example of synthesised beam is given in Figure 3.

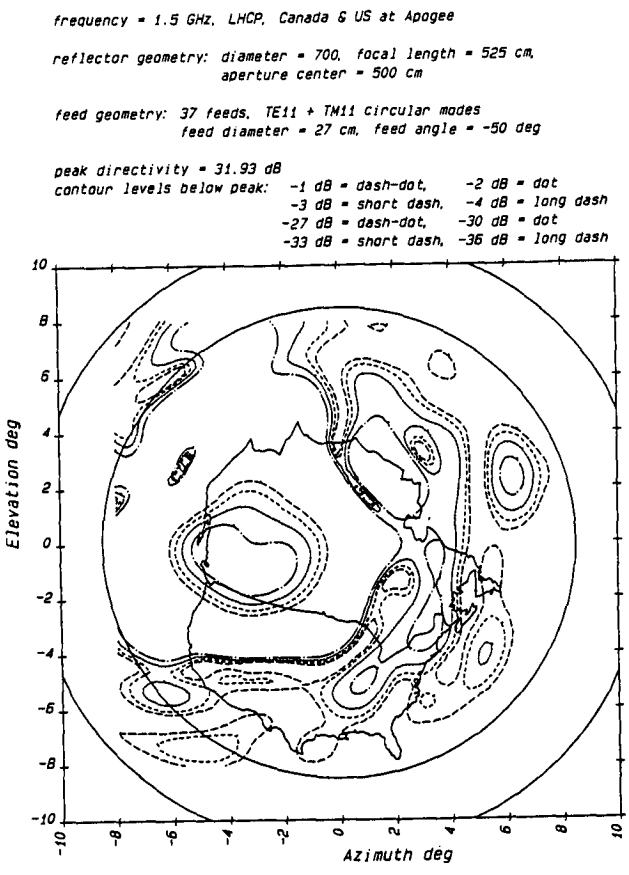

Figure 3 Reflector with Reconfigurable Feed Array

SINGLE IMAGING REFLECTOR

The single imaging reflector combines the features of a phased array and a reflector antenna. The reflector is an offset hyperboloid, with the array in a defocused, near-field position displaced towards the reflector. The phased array radiates a spherical wave which can be scanned over the reflector, producing a scanned secondary beam. The reflector must be

oversized to avoid spillover losses. We explored the performance of a reflector with a diameter of 7 meters, focal length of 5 meters, and a feed array consisting of 19 elements, with an overall diameter of 1.4 meters. Four reflector surfaces were tried, with hyperboloid magnifications of 10, 15, 20, and 25. For each reflector surface shape, a position of the feed array (amount of defocusing towards the reflector) was determined to maximise the gain of the non-scanned beam.

As shown in Figure 4, the major problem with the single imaging reflector system is the limited scan range, about half of what is needed for the Archimedes mission, beam distortion, and a rapid rise in sidelobe levels with scan. It is not entirely clear whether this is an inherent characteristic of the SIR optics, or whether the antenna geometry could be further optimised (for instance by finding a better location for the feed array to minimise scan losses). The scan performance can also be improved by synthesising an appropriate excitation for the phased array for each scan direction instead of merely imposing a linear phase slope. These possibilities are somewhat speculative at the moment and further work would be required to assess the suitability of an SIR. Unless the problems discussed above are solved, the poor scan performance of the SIR design appears to preclude its use for the Archimedes mission.

CONCLUSIONS

The performance and suitability of several antenna candidates has been evaluated relative to the requirements and constraints of the Archimedes mission. For a non-deployable antenna with a maximum diameter of about 3 meters, a direct radiating array is the best candidate both in terms of gain performance and beam flexibility. If a fixed beam layout is a viable option, then a focal-fed reflector fed by triplets with 2 shared elements provides similar edge-of-coverage gain. For operational scenarios requiring high gain, sharp beam roll off, and low sidelobes, the preferred solution is a large, offset parabolic reflector with an active, reconfigurable feed array.

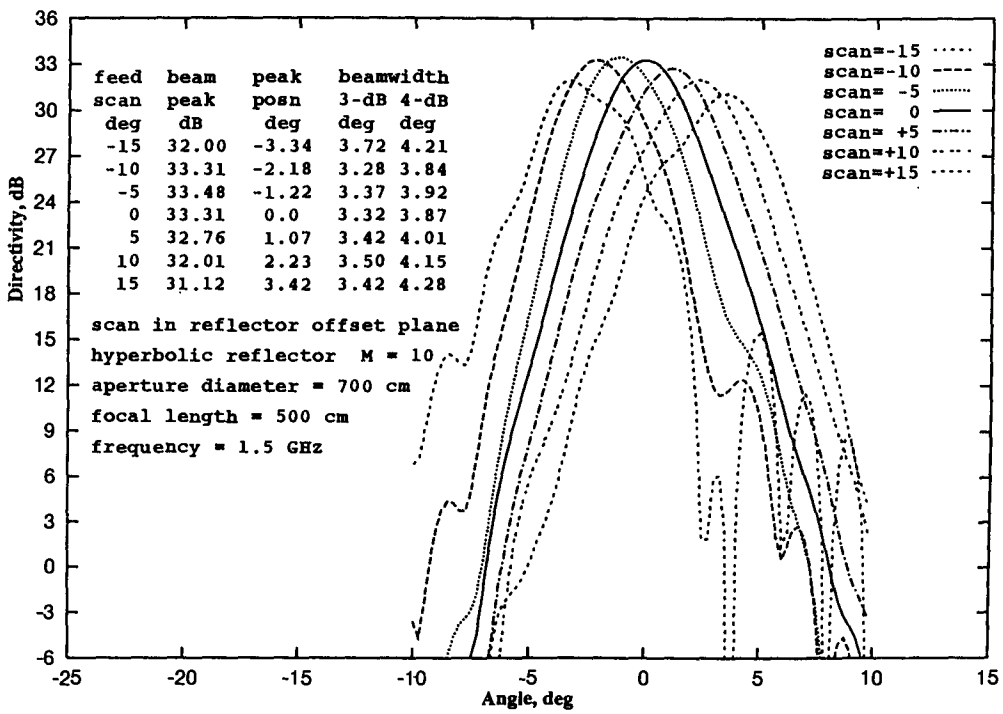

Figure 4 Scanned Patterns of Single Imaging Reflector.

Aeronautical Mobile Satellite Communications

Session Chairman: **Elizabeth Young,** Consultant, USA
Session Organizer: **Martin Agan,** Jet Propulsion Laboratory, USA

Topic Introduction: Aeronautical mobile satellite communications is an area that has seen considerable growth in the recent past, and through continued technological innovation offers much future potential. Aeronautical satcom users range from commercial airlines to general aviation aircraft. User requirements encompass both high bandwidth (video and multimedia) and low bandwidth (voice, data, fax) applications. The papers in this session highlight this broad range of users and applications, their present and future needs, and the systems and technologies that are being developed to meet these needs. Aeronautical satcom utilizing LEO and GEO satellites are addressed. This session should offer insight into the current challenges being encountered in the drive to expand aeronautical satcom system capabilities at a reasonable cost.

con't.

Evolution of the INMARSAT Aeronautical System: Service, System, and Business Considerations

Jay R Sengupta
Manager, Aeronautical System Development
INMARSAT, 99 City Road, London, UK EC1Y 1AX
Tel: +44 171 728 1000 Fax: +44 171 728 1044

ABSTRACT

A market-driven approach was adopted to develop enhancements to the Inmarsat-Aeronautical system, to address the requirements of potential new market segments. An evolutionary approach and well differentiated product/service portfolio was required, to minimize system upgrade costs and market penetration, respectively. The evolved system definition serves to minimize equipment cost/size/mass for short/medium range aircraft, by reducing the antenna gain requirement and relaxing the performance requirements for non safety-related communications. A validation programme involving simulation, laboratory tests, over-satellite tests and flight trials is being conducted to confirm the system definition. Extensive market research has been conducted to determine user requirements and to quantify market demand for future Inmarsat Aero-I AES, using sophisticated computer assisted survey techniques.

BACKGROUND

In response to user and industry demands, in November 1993 Inmarsat decided to embark on a commercial and technical assessment program to determine the feasibility of evolution of the Inmarsat-Aeronautical mobile satellite communications system. These investigations were conducted under the auspices of a joint Inmarsat-Industry group, during a one-year period concluding in February 1995.

The imminent availability of Inmarsat's third generation satellites, equipped with focused spot beam service link capability in addition to the earth coverage global beam, as well as recent advances in mobile satellite communications systems technologies especially in the area of low-rate voice encoding algorithms, offered the potential to evolve the Inmarsat-Aero system. The primary objective of the evolved system would be to make satcom services attractive to aircraft types beyond the current installed base of long-haul airliners and large business jets. It was clear that a market-driven approach had to be followed, in order to ensure that the evolved system would satisfy user requirements in the most cost effective manner.

Firstly, a survey was conducted by means of interviews with selected aircraft operators and manufacturers in the target new market segments. These user requirements were used to determine the technical goals for the evolved system definition, to be satisfied by either an evolution of the existing high-gain aircraft earth station (Aero-H AES) or the development of a proposed new intermediate-gain (Aero-I) AES. Having developed a strawman system definition and based upon feedback from potential vendors of Aero-H and Aero-I AES equipment, regarding the planned characteristics of their respective products, a market demand assessment was carried out. The demand assessment was performed on the basis of conjoint analysis technique, to determine the likelihood of aircraft owners to purchase and install the proposed new Aero-I AES equipment. This was further supplemented with an updated survey of airline passenger telecom service usage trends. Prior to finalization, all novel aspects of the evolved system definition were validated by means of computer simulations, as well as laboratory tests with prototype units.

USER REQUIREMENTS

The proposed evolution of the Inmarsat-Aero system has been guided by a user requirements assessment. Such a market-driven approach would serve to ensure that the developed products and services would be responsive to the stated needs and requirements of the users in the target markets for Inmarsat's aeronautical services.

The potential markets for an Aero-I product could be broadly categorized into the following segments :

- short-haul commercial aircraft
- commuter/turbo-prop aircraft
- corporate aircraft

A focused survey of representative users within each of the above market segments, was carried out to determine the actual requirements for satcom services. The intent of the survey was to determine basic service needs, and hence did not suggest the possibility of a new Aero-I AES product to fulfill those needs.

The major findings of the survey are listed below:

(a) Satcom service was deemed to be desirable for all the target market segements above, except the commuter/turbo-prop aircraft where the demand for any sort of telecommunications facility was marginal. However, even the commuter/turbo-prop aircraft operators stated that telecommunications services would be installed if it became a competitive priority;

(b) Passenger telecom services were considered to be the major requirement for users in these market segments. Telephony and telefax were stated to be the most important services. Data communications services for passengers was felt to be useful, but not of primary importance;

(c) Cockpit (safety-related) communications was generally not felt to be important or useful, perhaps since these aircraft typically operated in regions where there is adequate coverage from terrestrial systems for air-traffic control and airline operational communications. The operators of the heavy/medium corporate jets were an exception, since they require satcom ATS services over the long-haul routes;

(d) Operators of light-jets and turbo-prop corporate aircraft stated that AES equipment prices should be well below $100,000, in order for satcom to be an afforable service option. Operators of short-haul commercial and large-jet corporate aircraft appeared to be less sensitive to equipment prices, although they would obviously avail of the lowest market prices;

(e) Users in all market segments stated the need for (end-user) telephone/telefax services to be about US$ 5.00/US$ 6.00 per minute, although corporate aircraft users appear to be less concerned;

(f) There was a requirement for AES equipment to be configurable to multi-channel capability, for all except the light-jet corporate aircraft. The weight of the avionics would also be a constraint for the light-jet corporate aircraft, with a target of about 20 kg net weight.

SYSTEM DEFINITION

Design Objectives

The primary design objectives for the evolved Inmarsat-Aeronautical system were to:

(a) ensure backward compatibility with the currently operational system, in order to facilitate the transparent introduction of the new evolved system functions;

(b) ensure an evolutionary approach to the definition of the new system features, in order to minimize the development costs to upgrade existing AES/GES products to the evolved standards;

(c) satisfy the requirements of the existing and potential new Inmarsat-Aeronautical system users, determined by means of extensive market research by independent consultants.

Basic Technology Drivers

The fundamental technology drivers for the changes to the Inmarsat-Aero system are:

(a) the imminent availability of Inmarsat-3 satellites, affording an increased satellite G/T for the mobile service L-band uplink; and,

(b) recent improvements in low-rate voice encoding algorithms and DSP implementations.

It should be noted that the currently operational Inmarsat-Aero system has the necessary flexibility to accomodate evolutionary changes of this type, without impacting on-going operations.

Major Enhancements to System Definition

The major enhancements to the system definition are identified below:

(a) definition of a new reduced-rate SCPC voice channel (C-channel) with O-QPSK modulation, operating at 8.4 kbit/s and with rate 2/3 FEC; this would serve to reduce space segment resource requirements per channel, by a reduction in the channel bandwidth from 17.5 kHz to 5 kHz;

(b) adoption of the Improved MultiBand Excitation (IMBE) voice encoding algorithm, operating at an aggregate rate of 4.8 kbit/s; the performance of the $IMBE_{tm}$ algorithm in an aeronautical environment, was found to be equivalent to or better than the currently operational 9.6kbps Linear Predictive Coding (LPC) algorithm;

(c) adoption of channel availability and channel blocking (GOS) performance objectives for aeronautical non-safety services, of 90% (under worst case fading and edge of coverage) and 10% (during the peak traffic in busy hour) respectively; these reduced performance requirements would facilitate reductions in AES EIRP requirements and space segment resource requirements per traffic unit;

(d) definition of new AES type, with an intermediate gain antenna of 6 dBi (G/T = -19 dB/K), termed the *Aero-I AES*; the chosen antenna gain was deemed to be optimal for voice service operation within Inmarsat-3 spot beam coverage, while being compatible with the light-jet/turbo-prop corporate aircraft types;

(e) definition of signalling system and ACSE enhancements to introduce the new channel and AES types, while ensuring full backward compatibility with the currently operation system; backward compatibility would ensure that the enhanced AES and GES functions can be introduced transparently into the system without causing disruption to operational traffic.

(f) adaptation of the Inmarsat-Aero Terminal Interface Function (TIF), which provides the telefax and voice-band data modem interface for the C-channels, is currently being adapted to operate on the new reduced-rate C-channel. The retention of this function for the new reduced-rate channel was essential, in order to ensure a common telefax/data interface for all C-channel types.

Relaxations to AES Performance Requirements

During the course of the System Evolution Studies, attention had been focused on identifying those AES technical requirements which currently result in increased equipment costs, ie. cost drivers. Several cost drivers were identified, but only the following relaxations could be made without compromizing system objectives :

(a) reduction of maximum AES EIRP requirement by 3 dB (to 22.5 dBW), making it feasible to use a 20W HPA for single channel installations;

(b) pairing of receive/transmit C-channel frequencies, ie., with fixed frequency offset, making possible the use of single synthesizor for a C-channel pair.

The issue of relaxation of AES transmit phase noise performance is still under investigation, by means of testing of the acquisition and tracking capability of the installed C-channel modems at Ground Earth Stations. Such relaxation could be beneficial to AES installations in high vibration environments (eg. helicopters), or alternatively allow the use of less expensive reference oscillators.

SERVICE DIFFERENTIATION

The market positioning of the Aero-I AES product was considered to be of prime importance. It was intended to differentiate the product and service capabilities of Aero-I AES sufficiently from the other AES types, in order to avoid any impact on the well developed Aero-H AES market.

Aero-I Product Differentiation

Requests from several airlines operating medium/short haul aircraft indicated that there was sufficient interest for an affordable satcom service in this market sector. Furthermore, the success of satcoms in the business aircraft market, had also stimulated significant interest in the lower-end business aircraft market. At the same time, the migration of satcoms to this segment of the commercial and

	AERO-H	AERO-I	AERO-L
Telephony	9.6/4.8 kbps	4.8 kbps	n/a
Telefax	4.8/2.4 kbps	2.4 kbps	n/a
Cct Data	9.6/4.8 kbps	4.8 kbps	n/a
Pkt Data	< 10.5 kbps	< 4.8 kbps	< 1.2 kbps
Channels	1-6 typical	1-4 typical	1
Mass	80-120 kg	20-50 kg	60 kg
Price	$250-$350K	$50-100K	$100K
Coverage	Global/Spot Voice/Data	Global Data Spot Voice	Global/Spot Data

Aero-I AES Product Positioning

business aviation market was a natural progression and would result in increased communication traffic.

The current Aero-H AES type was determined not to be satisfactory in addressing the entire commercial short/medium haul airline and medium/light weight business jet markets. It was too large, too heavy and too costly to be considered by potential customers. The figure below shows the Aero-I product as compared to the Aero-H and Aero-L products currently serving the aeronautical market

Aero-I AES Market Position

The commercial aircraft satcom market is currently segmented in two dimensions: size of aircraft requiring satcom service and the satcom services required for each of these market segments. In the chart below, the commercial aircraft market has been grouped into long/medium haul commercial aircraft, medium/short haul commercial aircraft, short haul commercial aircraft and commuter aircraft. There is a considerable overlap in the types of aircraft in each category, reflecting the various ways aircraft are used on different route sectors. On this same chart, the business aircraft have been segmented into heavy jets, light jets and turbo-props.

The Inmarsat satcom product range shown on this chart includes Aero-H AES (4.8Kbps and 9.6Kbps codec versions) and Aero-I AES (4.8Kbps codec). The Aero-H product range covers all long/medium haul commercial aircraft, short/medium haul commercial aircraft and heavy corporate jets. While the Aero-H AES has had excellent success in penetrating the long/medium haul market, it has had very little penetration in the medium/short haul market. This is due to the size, weight and cost limitations of the product.

The Aero-I and Aero-H AESs overlap in the medium/short haul commercial market but, because it was designed to specifically address the requirements of this market, the former is expected to have excellent market penetration. Although, Aero-I will negatively impact the future of Aero-H in this market, the impact would be limited since Aero-H has had limited success in this market anyway.

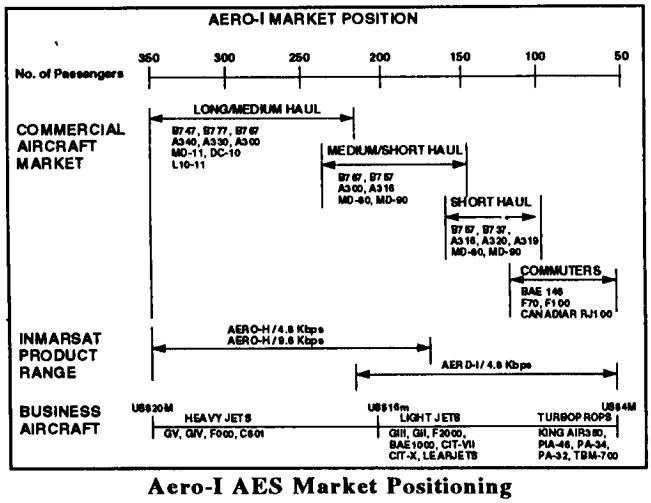

Aero-I AES Market Positioning

In the corporate aircraft market area, the Aero-H/Aero-I product positioning is much more clear. The heavy corporate jets have opted for the Aero-H AES, because there is a requirement for full functionality (telephone, facsimile, data and cockpit datalink). On the other hand, the light corporate jets and turbo-prop aircraft would prefer the Aero-I AES for its size, weight and cost advantages; the restricted service coverage area of the Aero-I AES would be acceptable to such aircraft, which would typically operate within the planned spot-beam footprints of the Inmarsat-3 satellites.

At the low end of the heavy jets and high end of the light jets, the decision between Aero-H and Aero-I will be based upon whether the aircraft will require cockpit satcom datalink provided by Aero-H or passenger services only (telephone, facsimile and data), which can be provided by Aero-I. In this market, Aero-I will not have a negative impact on Aero-H since the lower end of this corporate market sector would not install Aero-H due to its high cost, size and weight.

The Aero-I product has been carefully positioned to address the requirements of the market below long/medium haul commercial aircraft and low-end heavy commercial jets and smaller aircraft. The utilisation of Aero-I for aircraft not requiring global coverage for voice service provides a natural separation between Aero-H and Aero-I markets

MARKET RESEARCH

The total size of the addressable market for the Aero-I AES product has been deermined, based on data from commercially available databases with forecasts of aircraft production volumes. The cummulative aircraft population derived therefrom, excludes the following :

- aircraft flying in domestic US and Canadian airspace, due to coverage by terrestrial air-ground telephone systems;
- retirements of older aircraft being put out of service.

The assessment of demand for the Aero-I AES products and services was conducted by means of *conjoint analysis* market research techniques. The research was carried out using a computer assisted personal interview (CAPI) method which collected background material of relevance to the

research and conducted two experiments. The airlines selected represented all major geographic regions, with the exception of North America and Africa; the major corporate jet manufacturers in North America and Europe were surveyed.

Market Size	1996	1999	2002
Commercial Jets	3062	3410	3604
Commuter Jets	501	677	834
Corporate Jets	1366	1804	2164
Total	4930	5892	6602

Aero-I AES Addressable Market Size

Experiment 1

In this experiment. respondents were asked to imagine they were considering purchasing a satellite based telephone system for their planned aircraft fleet in 5 years time. The basic interview method was to repeatedly vary the attributes of the satcom product/service as outlined below, and ask the respondent to continually make a choice between 2 alternative combinations :

- passenger comms, with and without upgrade path for safety-related comms, services
- AES equipment price varied in the range $60K-$125K, dependent on number of installed channels
- service coverage area varied between 60%-100% of of carrier's operational route network
- telephone call charge range: $3.5-$8.5 per min.

Experiment 2

In this experiment, respondents were asked to make choices between a satellite and terrestrial based communications systems. As background information, each respondent was informed of the proportion of his carrier's route-miles which could be expected to be contained within the service coverage areas of terrestrial air-ground communications systems, within the next 5 years. The basic interview method was to repeatedly vary the equipment cost and telecoms usage charges within the bounds indicated below for each system, and to ask the respondent to allocate proportions of his aircraft fleet to be equipped for the 3 alternative system choices :

Global Coverage Satellite System - $400K-$600K installed equipment price; $3-$6 per min telecoms charge;

Spot-Beam Satellite System - $60K-$125K installed equipment price; $5-$8 per min telecoms charge;

Terrestrial Based System - $80K-$120K installed equipment price; $3-$5 per min telecoms charge.

There are, of course, substantial variations between the choices made by different carriers, due to differences in their respective route structures, aircraft fleet composition and financial positions. In aggregate, however, the results have clearly indicated that the Aero-I AES operating within the Inmarsat-3 satellite spot beam coverage areas, would have the largest market share in the target new market segments.

FIELD TRIALS PLAN

Ground and flight trials of prototype Aero-I AES equipment is planned to be undertaken during 1995. The purpose of these trials would be to confirm the proper operation of Aero-I AES in the real system. Specifically, tests will be conducted to validate the performance of the new C-channel and voice codec, as well as the new intermediate gain aircraft antenna.

Flight tests are planned to cover operation at low satellite elevation angles and over sea, to test the performance of the system at the extreme propagation conditions. These trials will be useful to validate the performance of critical system functions, such as the operation of the dynamic power control, as well as the service quality for telephone and telefax services.

REFERENCES

[1] *INMARSAT Aeronautical System Definition Manual*, Inmarsat, London, UK.

[2] *INMARSAT Aeronautical SDM Change Proposal 76*, Inmarsat, London, UK.

[3] *Market Potential for Inmarsat-I*, International Air Transport Association (IATA) Surveys, London, UK.

Aeronautical Satellite Data Link System (SDLS) for high-density Air-Traffic areas

Alain DELRIEU, Claude LOISY, Philip CLINCH, Philippe BENHAIM

Centre d'Etudes de la Navigation Aérienne, Athis-Mons, FR, fax +33 1 60 48 70 20
European Space Agency, ESTEC, NL, fax: + 31-1719-84598
Europe Aerospace Consultancy, Sceaux, FR. Fax: + 33-1-43 50 70 48
ALCATEL-ESPACE, Toulouse, FR; fax : +33-61 19 61 69

ABSTRACT

The European Space Agency has recently commissioned a study to investigate the feasibility of a low-cost aeronautical Satellite Data Link System (SDLS) to provide for the needs of Air Traffic Services, i.e. safety-related communications over continental areas with high air-traffic density. This study is placed in today's context which sees the first generation of Aeronautical Mobile Satellite System (AMSS) being gradually but restrictively put into service in oceanic airspaces with low air-traffic density.

This paper first discusses the case of ATS dedicated versus mixed (ATS and commercial) Comms service provision and identifies the specific ATS comms requirements context. Specific emphasis is put on the ICAO (International Civil Aviation Organisation) standardisation framework for both the ATN (Aeronautical Telecommunication Network) and the SSR (Secondary Surveillance Radar) Mode S *specific services.*

An architectural system and network design for a future SDLS is then proposed, such as to meet the ATS comms requirements within the realm of existing technologies.

To minimize development risk and cost, consideration is given to re-use the ESA-developed Land Mobile Communication Technology, known as MSBN (Mobile Satellite Business Network) featuring distinct subnetworks. It is particularly suited to an ATM (Air Traffic Management) decentralized architecture made of independent ATC (Air Traffic Control) Centers.

Finally the study follow-on phase is introduced, which is intended to cover system design and development leading to a demonstration programme, as a first step towards proposals for international standardization and acceptance

INTRODUCTION

Satellite based communication systems have now been under consideration for use by Civil Aviation for over two decades, but have failed so-far to materialize on a significant scale. Consecutive to their development of a worldwide public telecommunication service (telephony, telex) in the framework of the Maritime Mobile Satellite Service (MMSS), INMARSAT (The International Maritime Satellite Organization) further promoted the development, under the Aeronautical Mobile Satellite Service (AMSS), of a system offering passenger public correspondence services as well as cockpit air-ground data. By end July 94, 111 aircraft worldwide had a commissioned Aeronautical Earth Station (AES) for data service.

Looking today into the future of ATM systems, air-ground datalinks are undoubtedly going to play a key role. It is unclear, however, what the relative shares of the three communication media currently contemplated for these required datalinks will be; namely: the VHF, the SSR mode S and the Satellite. The present paper aims to evaluate the potentialities of Satellite Communication Systems in providing flight-safety air-ground exchanges as required for Air Traffic Services (ATS) world-wide and particularly in high density air-traffic continental airspaces. Prominent among ATS comms applications will be the provision of automated Aircraft Position Reporting (APR) to extend the reach of radar surveillance to neighboring airspaces, with an equivalent surveillance quality of service, in terms of info rate and availability; APR is the "specific services" equivalent to the ICAO-defined concept of ADS (Automatic Dependant Surveillance).

The European Space Agency (ESA) has recently awarded a study contract to an industrial consortium to analyze the technical and economic feasibility of an ATS-dedicated SDLS offering a quality of service for dependability and transmission delay commensurate with the need of high density air-traffic areas. ALCATEL-ESPACE is leading this consortium which includes AEROSPATIALE, Europe Aerospace Consultancy and CENA-SOFREAVIA of France, RACAL RESEARCH of UK and SAINCO of Spain.

Section 2 of this paper deals with the aeronautical communication requirements context. Section 3 presents a possible SDLS system implementation. The re-use of

ESA-developed MSBN Land Mobile comms technology is introduced in section 4. Finally a study follow-on programme focused on a demonstrations and evaluation programme through field trials is outlined in section 5.

2 AIRGROUND COMMS REQUIREMENTS CONTEXT

The first generation AMSS was not primarily conceived to optimally provide for the ATS functionalities, since its basic system architecture is that of a public telephony system. Therefore one can logically expect the design of a future system, dedicated to ATS, to far better accomodate ATS's very specific and demanding requirements .*Why ATS only*? The different types of air ground communications that ICAO distinguishes in a decreasing order of priority in relation to safety of flight, are:

a) ATS
b) Aircraft Operations Communication (AOC)
c) Airline Administrative Communication (AAC)
d) Aeronautical Passenger Communication (APC)

The easy-to-understand desire of airlines owners to minimize avionics costs by seeking equipment capable of offering all the above-defined services should be balanced with considerations of the need for efficient and dependable ATS comms, yet at an affordable cost. Although mixing requirements and services has been the approach so far for the implementation of the first AMSS systems targeted at trans-oceanic traffic on long-haul carriers, its generalisation to a datalink system intended to serve all aircraft in all airspaces has serious limitations. *Safety of flight* on one hand and *commercial communications* on the other, tend to have rather opposite requirement profiles:

- *Availability* and *grade of service* are dominant for safety-related services, cost having a lower priority; it is exactly the opposite for commercial services.
- *Bandwidth requirements* are and will remain low for safety-related services, they are order of magnitudes higher for public telephony and fax and will likely further increase with the introduction of new services. A poor grade of ATS comms capability resulting from mixed services systems may deter ATM upgrading and lead to ATC (Air Traffic Control) penalties, in terms of delay and high ATC users' charges, which may ultimately offset short term savings on avionics .

ATS COMMs capacity requirement sizing An assumption on the required communications capacity and on the associated transmission delays has been established on the basis of review of references [1] and [2]. This assumption is summarized in Table 1 which presents the European ATS datalink requirement context irrespective of the choice of comms system used. In this table maximum average bits per second, in terms of actual information bits, have been assessed on the basis of the European average flight duration of 1.3 hours [3]. It is worth noting that in both the up and down link directions (as viewed by the a/c) the bit capacity requirement is well under 50 bps. A similar assessment has been made for the North American context in [4], which points out to the same indication. Capacity sizing should also consider the Peak Instantaneous Aircraft Count (PIAC) to be served over continental areas. The PIAC estimates shown below have been established on the basis of EUROCONTROL Central Route Charging Office data for the peak of year 1991 and a multiplying factor reflecting projected Air Traffic growth (quoted from a European Commission study on the future European ATM System) up to year 2010:

Phases of flight//PIAC for year	1991	2000	2010
Taking-off &Climb in TMA	160	240	350
Rest of Climb, En-route Cruise & start of Descent	1280	1900	2800
Descent & Landing in TMA	160	240	350
Total	1600	2400	3500

Table 1: ATS Air-Ground data-exchange requirements

A-G data exchange service 1.3 Hr flight duration	D/L bits	U/L bits	Freq.	Xfr delay/ TRA(1) sec
Pre-depature Clearance	60	500	1	15//30
Oceanic and/or Sector pre-entry Clearance	60	800	8	15//30
Frequency Change Clearance	60	60	10	5//10
Other Tactical Clearance	60	60	25	5//10
Conditional Clearance	60	180	3	15//30
Coupling of A/C and GND Flight PLN at A/C log-in	1200	60	1	15//30
Trajectory Negociation, initial	1200	1200	3	15//30
Trajectory Modification, in-flight	450	450	15	15//30
Airport terminal Information (ATIS)	60	3000	3	60//90
Terminal Area Forecast(TAF)/METAR	60	3000	6	60//90
NOTAM	60	3000	6	60//90
METEO/NowCast	350	1500	15	30//60
Navigation database consultation	90	3000	6	30//60
Traffic Information	60	240	15	5//10
ADS or A/C Position Reporting (APR,) (2)	80		936	1//2
Downlinking of Airborne Parameters (DAP)(3)	80	40	468	5//10
METEO Hazard Report	120		10	5//10
Access to FMS-entered PLN (flight Plan)	1150	60	3	15//30
Average bps:	29,7	27,3		

Notes:(1) Technical Receipt Acknowledge; max Transfer delay and/or TRA is for 90%//99.9 % of times
(2) basic ADS : same as APR, assumed to be every 5sec
(3):U/L para. request: assumed every 10 sec.,
DAP incl. MTO routine observ. report (wind, temp..)

Open Communication Network Architecture: The ICAO Aeronautical Telecommunications Network (ATN) Panel is currently producing an ICAO ATN standard for aeronautical data communications. The International Standards Organization (ISO) has developed an Open System Interconnection (OSI) model to logically separate the functions implemented in a data communications system. The ATN standard specifies the use of OSI compatible ISO protocols. Accordingly the future SDLS will have to comply with the ATN standards wherever practical and economical. Indeed, the interest is now well recognized, to also provide *non-ATN specific services*, which take advantage of unique characteristics of the currently contemplated comms (e.g. Broadcast for satellite and VHF datalink).

ATN-compliant Service Requirements: The ATN standard specifies a protocol for the interconnection of air-ground communications systems with a terrestrial data network. This is the ISO 8473 "Connectionless Network Protocol" (CLNP) , often referred to as the ATN protocol. The ATN standard specifies that ATS application systems are to transmit messages over the ATN in the CLNP format. It also specifies the format of the addresses to be used in the CLNP messages to address ATS application systems. The interconnection between air-ground and terrestrial data networks is processed by an ISO 8473 Intermediate System (IS).
The CLNP IS entities access the currently contemplated ATN subnetworks (VHF Datalink, SSR Mode S and AMSS) using the protocol specified in ISO 8208 "X.25 Packet Layer Protocol" through a separate ISO 8208 Data Terminal Equipment (DTE). The subnetworks are required to provide an ISO 8208 virtual circuit with the DTE linked to a CLNP IS in a system on the ground. The SDLS will be required to accept the same interface with an ISO 8208 DTE function in the ATN avionics and to provide an ISO 8208 virtual circuit between CLNP IS entities in airborne and ground systems.The SDLS GES would need to be connected to a ground CLNP IS via a terrestrial X.25 network and to be capable of switching ISO 8208 packets messages between the SDLS link and X.25 virtual circuits to the CLNP IS.

Random versus polling accesses: The current data-only AMSS features a "random" access function whereby a "call channel", i.e. a fixed capacity in the satellite link return direction is dedicated to this function and shared among the mobiles in a "Random Access" mode. Due to the fast increasing probability of collisions when the rate of randomly initiated calls increases, the usable capacity of a random access channel tends to be limited to typically 10 to 15% of its full capacity. Therefore, and if efficiency is to be preserved, this technique can only be used, if the amount of traffic corresponding to the call function is kept very small compared to the overall traffic, otherwise system overloads occurs In the specific case of data-only AMSS (which has a minimum transmission rate of 600bps) this qualitative assessment was numerically confirmed recently [5] by the computer modelling of its comms traffic, assuming a load of 50 aircraft per GES, which shows:
a) Close to saturation, the AMSS practical capacity is limited to 30 (respectively 55) bps per a/c , with one open ATN-specified SVC (Switched Vitual Circuit (SVC) and assuming that the X25 packetized transmission mode favors short (respectively long) data packet
b) at 55 (effective) bps, the uplink and downlink transfer delays in seconds turn out to be :

Xfer delay(s)	Average	Std dev.	Max
Uplink	4.0	5.7	100
Downlink	5.5	2.6	45.1

The wide ranging variability in the AMSS X25 datalink transfer delays is an obvious deterrent to its application to high density traffic areas

By contrast in a *polling scheme* all mobiles a priori likely to require transmission capacity are individually addressed in a sequential manner and invited to transmit their data in individualised time windows. This removes the risk of collision, but is of course inefficient if mobiles are polled whenever they have nothing to transmit. Therefore polling is most attractive for sequential interrogation where it is known in advance that a reply will be supplied. The typical case of optimum usage is the systematic mobile's position reporting on request of the network *central* station. Requests corresponding to rather infrequent transmissions, and with a level of urgency compatible with poll time intervals, can be forwarded to central station more efficiently than through pure random access. Indeed, the next position report can also be used to carry a piggy-backed "transmission request message" signalling downlink request. For the more common cases, efficiency through delay avoidance is done sorting out requests according to pre-assigned message priorities and allocating distinct random access capacity to assigned priority levels.

ATN -compliant vs non- ATN specific services
Communication efficiency is the key consideration for any mobile communication system, which for reason of cost cannot afford high gain antenna and have to make do with low-gain omnidirectionals, and therefore with optimized link budget margins. It follows that, when designing link protocols, the need for maximum efficiency must always be a top priority. Accordingly, the loading factor of the link, taking into consideration the useful transmission data only, must constantly remain as close as possible to 100 % of the provided capacity. This can be achieved through a centralised satelllite network architecture where the central station is always master

and mobiles are slaves- It is therefore clear that indiscriminate use of the complete stack of ATN/OSI layered protocols with associated "hefty" transmission overheads, which would be deemed generally adequate for the ground part of ATN, would create major difficulties in the mobile satellite network due to the low link capacity. Accordingly the dividing line between *ATN compliant* and *non-ATN specific services* is to be drawn between those applications for which data transmission delay is not critical but data integrity is, and those for which short delays and high refresh rate is critical. Aircraft Position Reporting (APR) or downlinking of airborne parameters (DAP) belong to this latter category. Exchange of flight plan data between the on-board and ground ATM computers is an example of the former.

ICAO standardized specific services : The SDLS capability to support aircraft position reporting with refresh rates of few seconds, associated with the selected polling scheme for communicating with mobiles, is analogous to SSR Mode S datalink, whereby an aircraft is interrogated every 4 to 10 seconds, for identity confirmation, height, access to on-board parameters, and/or to set up a two way exchange of data. And as new system acceptance is made easier by use of established standards, it is logical to design SDLS *specific services* formats and protocol for compatibility with those defined by ICAO for Mode S specific services. [6]

ATS comms quality of service requirement .
Quality of service reflects several attributes. Of prime importance are service availability, data integrity and guaranteed transmission time. In the case of this last attribute a further consideration needs to be made in the case of "manual" handling of the data at either end, i.e. if for instance an ATC officer is awaiting confirmation that a tactical clearance message he has issued is correctly received aboard the intended aircraft within a set time - given that the aircrew might take an unspecified time to act upon this clearance, or even to actually acknowledge receipt. In such a case the requirement for a set transmission time is superseded by that of receiving a Technical Receipt Acknowledge (TRA) within a specified time period. The question is open at this point in time whether TRA downlinking within a short time, at variable and unpredictable intervals and over a low capacity datalink system, is compatible with the ATN/OSI multi protocol layers implementation, or whether one will need to cut through these layers to implement TRA as a specific service, within the SDLS MAC (Medium Access Control) layer.

Data integrity is a matter of adequate link budget margin which requires implementation of forward error correcting coding techniques.

Service availability is also a key issue. A performance figure not lower than that required for the availability of surveillance data from radars is a reasonable objective. This has a significant impact on the system design in terms of required provision of hot redundant satellite link and of selecting a suitable RF channel type of access permitting instantaneous switchover from one satellite signal path to the other, and at minimum AES cost.

Emergency voice communication
For the purpose of offering an emergency voice communication service of interest to Europe's neighboring areas not well served by terrestrial comms, the future SDLS will incorporate technical provisions of real time, full duplex "cockpit voice" capability. In order to preserve the AES cost effectiveness it will be assumed that (a) the capacity required for voice transmission is equivalent to that required by 30 aircraft for data transmission at 50 bps and (b) voice transmission supersedes that of data

3. SDLS POSSIBLE SYSTEM IMPLEMENTATION

A reasonable assumption in terms of SDLS suitable network architecture may be to derive it from that of the present Civil Aviation decentralised architecture which allows for the local management of the communication resources at the ATCCs. This architecture favours the most critical communications, i.e. those which take place directly between the aircraft and the regulating ATM entity on ground (e.g. aircraft position reports and tactical Pilot to Controller communication). It also ensures an adequate availability level of communication resources as priorities can be managed in real time according to the prevailing traffic situation. Each ATCC would manage an SDLS local network by polling aircraft in its control responsibility area for position reporting and "piggy-backed " transmission of data using the scheme as defined in section 2 above. Indeed the polling list can be managed or modified in real time upon initiative of the ATM authority to cope with unforeseen situations. These local networks would interface at the local ATCCs with the ATN ground infrastructure to achieve full connectivity. Finally a decentralized architecture allows each ATCC to possess its own access to satellite(s), via its own GES, assumed to be of a VSAT type (see section below), which, by minimizing the chain of equipment needed within the ground infrastructure, yields the best dependability performance overall .

Space segment considerations: Some preliminary assumptions must be made, having regard to economical considerations, in order to limit the analysis to the most probable scenarios:
a) an aeronautical service providing ATS cannot, on economical grounds, afford an independent dedicated constellation of satellites. As a minimum, satellite platforms must be shared with other missions
b) although a communication system for ATS ought to be dedicated, for the reasons given in section 2., this system

could share parts of communication payloads with other mobile services, in so far as the required bandwidth and power would be reserved for exclusive use by the ATS system. This would still allow sharing of satellite platforms and of expensive parts of the communication payload (e.g. antenna)
As regards the feeder link (satellite to GES) design and bearing in mind the objective of a decentralised network architecture with distributed satellite access, a frequency band ought to be selected which allows the use of VSAT type earth stations (e.g. Ku band)

Satellite Link organization
The basic satellite link organisation could rely on the classical full duplex arrangement using Time Division Multiplex (TDM) for the ground to air and the associated Time Division Multiple Access (TDMA) for the air to ground direction. Moreover, separate satellite networks would share the bandwidth in the satellite by using "orthogonal spreading sequences" according to a Code Division Multiple Access (CDMA) scheme. CDMA provides, in this case, a number of advantages over FDMA, having regards to:
- efficient accomodation of low traffic networks
-protection against interference
- provision of "dual link" (see below)
- reduction in AES costs

The service availability requirements will dictate hot redundant satellite links.This could be organised, in the ground to air direction, in such a way that each aircraft would permanently receive its data from the ATCC through two satellites simultaneously. The required protocol would have to share the data between the two links such as to ensure that the unexpected loss of one link (e.g. failure of one satellite) although reducing by half the instantaneously available capacity would maintain minimum communication with all aircraft, making use of adequate priority schemes.
In the air to ground direction, an appropriate scheme would be that aircraft transmission is picked up in parallel by the the two satellites. This scheme could offer continuity of service irrespective of where the failure actually takes place:
- within seconds for ground equipment through automatic switch-over to redundant equipment
- and within minutes for the activation of the spare units aboard satellites. However, a half rate service (in terms of overall capacity) would remain available during failure, and no action would be required on-board aircraft to restore full service, once a spare satellite transponder takes over - in particular no aircraft antenna re-pointing or new log-in procedure would be needed, as is the case with today's AMSS.

Aeronautical Earth Stations:.The ESA system contemplated in the SDLS study should be designed for compatiblibility with the AES characteristics as specified by ICAO for data-only AMSS:
- omni. antenna with a min G/Tof -26 dB/K
- EIRP(effect. isotropic radiated Power) of 13.5 dBW
These AESs would be compatible with both a spotbeam and global earth coverage type of space segment (e.g. Inmarsat III and II respectively)

Ground Eath Stations: As introduced above, the use of a Ku-band feeder link makes it possible to locate GESs directly at the ATCCs, with antenna size of typically 1.8 m diameter and thus providing direct access to the satellites. One antenna per satellite would be needed, not including provisions for redundancy and site diversity (having regard to atmospheric losses associated with rainfall).

System capacity: The overall capacity would be dependent on the performance levels of the space segment, namely the size of the global/spot beams used to provide the coverage . The following table gives an assessment of the achievable capacity per MHz of bandwidth.

Service area	oceanic	continental
Satellite coverage	Global beam (INMARSAT 2)	Spotbeam (INMARSAT 3)
Time intervals for APR	30 to 60s	5 to 10 s
Data rate for APR	1.7 to 3.3 bps	8 to 10 bps
Overall data rate per aircraft (A/C)	25 bps	50 bps
A/C in a coverage area, per MHz	1200	1200

Taking into account the peak instanteneous aircraft count projections, the whole of continental Europe could be served, up to year 2010, with 3 Mhz of bandwidth assuming an unique European size spot beam. The potential system capacity, would improve with narrower spotbeams owing to the frequency re-use capability in non-overlapping areas of coverage .

SDLS emergency voice service The SDLS CDMA scheme can support transmission of either 2 kbps for data at high integrity or voice signals digitized at 2.4 kbps and targeted for emergency use . Voice signals will be processed by advanced vocoding techniques to achieve 2400 bps. Implementation of this service will require to reserve one CDMA code, within each MHz of L band, out of possible 40, in asynchronous CDMA.

4. RE-USE OF LAND MOBILE COMMS TECHNOLOGY TOWARDS SDLS DESIGN

MSBN development programme :In 1991 ESA started a programme called MSBN (Mobile Satellite Business Network) aiming to provide the Transport Industry with an effective satellite communication system capable of meeting the communication requirements associated with management of vehicle fleets over Europe. The basic services provided are real time voice (telephony) and data transfer, with other applications including data messaging, voice messaging and fax. Contracts were placed with Industry for the procurement of prototype fixed and mobile earth Stations. Equipment is now close to factory acceptance testing and system experimentation using a satellite will start shortly. Two experimental satellite payloads known as EMS and LLM are under development by European Industry to be flown respectively on ITALSAT 2 and ARTEMIS in 1996 and 1997 respectively. They will offer communication capacity at L-band using Ku-band feeder links and will be used, among other applications, to field-test MSBN

AES preliminary cost estimates: The modem section of the AES has already been developped for the MSBN programme - for which the Agency has funded the development of an ASIC chip, implementing this modem part. As a result associated costing elements are well defined. Concerning the RF front end (antenna, diplexer, HPA, LNA), a study is presently on-going, also under support from ESA, at Racal Avionics Limited of UK which is expected to produce reliable recurrent cost data.

5. PLANNED DEMONSTRATION PROGRAMME

Assuming a successful outcome of the on-going SDLS feasibility study, a detailed system design phase is expected to follow which would include the implementation of a limited scale demonstration system. Performance evaluation programme will feature in-flight demonstrations using satellites and the aviation community would be given the opportunity to critically assess SDLS , through field trials, in comparison with other means of surveillance and communication (SSR Mode S, VHF datalink and AMSS). The satellite L-band payloads to be used are expected to be ITALSAT 2 EMS and ARTEMIS LLM.

The AES prototype to be developed for this demonstration programme would at a minimum allow a demonstration of Aircraft Position Reporting, downlinking of a limited set of airborne parameters , aircrew access to ATC ground databases and limited Controller Pilot two-way datalink . The current SDLS study will determine a practical way of implementing the AES on several aircraft types without incurring significant hardware and software changes between different aircraft fittings. Implementation involving a standalone PC with a built-in GPS receiver to provide APR as well as means of simulating data application processes, will be explored.

The prototype GES and associated Controller's HMI (Human Machine Interface) would support the above defined air-ground exchanges as well as an interconnection to the experimental ATN platform available at CENA's (Centre d'Etudes de la Navigation Aérienne) premises for ATN integration and other comms (e.g. VHF datalink) inter-operability testing.

6. CONCLUSION

A preliminary characterization of a suitable Satellite Communication System aimed at providing ATS safety-related communications as a "primary means" to a majority of civilian aircraft has been attempted. It suggests that the required technical basis, in terms of concepts and technology is readily available. Accordingly a feasibility study has been recently commissionned by ESA to confirm the SDLS technical and economical merits, in comparison to the other communication systems currently contemplated - SSR Mode S, VHF datalink and data-only AMSS. Depending on the results of this study, a demonstration and evaluation programme should be implementated to assess performances through field trials and as a first step towards international standardization and acceptance

REFERENCES

[1] PHARE: Air-ground data exchange study, S3, Internal PHARE/EUROCONTROL document, August 1994

[2] WP on initial applications for air-ground data communication. EUROCONTROL/ODT/IP/001 22/4/1994

[3] EUROCONTROL EATCHIP Phase 1 report Volume 1, level 3, Objective 3 "Airspace Management" , dated August 1991

[4] "Capacity as a consideration for providing Aeronautical Mobile Satellite Air Traffic Services in the U.S. Domestic Airspece", Curtis A. Shively, Mitre Corporation, IEEE AES Magazine, June 1992

[5] EUROCONTROL/CENA AMSS and Mode S Performances comparison, EUROCONTROL/CENA R94024 Report, June 3rd 1994

[6] Mode S Specific Services Manual , Attachment 1 to SICASP/5 report, Montreal 1993

MSAT Aeronautical Mobile Satellite Communications Terminal Development

C. A. Sutherland,
CAL Corporation
1050 Morrison Drive
Ottawa, Ontario, Canada K2H 8K7
Phone: 613-820-8280 FAX: 613-820-8314

J. T. Sydor,
Communications Research Centre
3701 Carling Avenue, P.O. Box 11490, Station 'H'
Ottawa, Ontario, Canada K2H 8S2
Phone: 613-998-2388 FAX: 613-990-0316

Abstract

CAL has undertaken the development of a new aeronautical mobile terminal for the North American MSAT market. The terminal is to meet the MSAT standard and is aimed in particular at the 300,000 general aviation and business aircraft in North America. The terminals are therefore relatively low cost and small in size when compared to those currently being produced for larger airline aircraft.

The terminal incorporates a top mounted mechanical steered antenna and a unique antenna steering subsystem. An overview of the terminal design is presented.

Introduction

TMI Communications and American Mobile Satellite Corporation are jointly establishing the MSAT mobile satellite service to provide voice, FAX and data services for North America. Although aimed primarily at land mobile users, MSAT will also serve other classes of terminals, including aeronautical. This paper describes an aeronautical MSAT terminal currently under development at CAL Corporation, in collaboration with American Mobile Satellite Corporation and the Canadian Communications Research Centre (CRC).

Land mobile terminals under development for the MSAT market have received significant investment to enable the cost expectations of the marketplace to be met. It was therefore logical to base CAL's aero terminal on the use of land mobile terminal hardware to the greatest extent possible. This terminal uses a Transceiver Unit (TU) and Antenna Electronics Unit (AEU) from Westinghouse Electric Corporation (WEC) in conjunction with a specially developed antenna and Beam Steering Unit (BSU). The result is an aeronautical terminal which can be purchased and installed for a fraction of the cost of existing satcom terminals while providing excellent voice quality plus FAX and data services.

Challenges to be Overcome

The aeronautical application presented some significant challenges. The antenna had to deal with motion in three axes, and yet had more severe size and weight constraints than its land mobile counterpart. For the initial product offering, it was also decided to target a G/T of -15 dB/K for the primary coverage area, higher than the medium gain land mobile specification, to permit lower user charges. A second version will offer a different tradeoff by providing an even more compact antenna suitable for the smallest aircraft.

In addition to the antenna differences, it was necessary to address beam steering, Doppler correction, distance of transceiver from antenna, environmental conditions, EMC, supply voltage, and certification and installation issues. CAL's approach to some of these matters is described in more detail in the following sections.

Antenna Design

The aeronautical antenna must be steered in both azimuth and elevation in order to minimize the size required to provide the required gain of approximately 11 dBic. The height of the radome is more critical than either of the other dimensions, so a horizontal array of highly shortened helical elements was chosen. This antenna was based on a design created at CRC and flight proven in the Ontario Air Ambulance Service on a Cessna Citation. CAL's modifications were based on optimization using an enhanced version of the Numerical Electromagnetics Code, NEC-2s from Lawrence Livermore Laboratories, and changes in construction to permit repeatable manufacturing at low cost.

A common ground screen is shared by the elements and rotates with them in both axes. The antenna base plate and the aircraft fuselage form a larger, fixed ground screen, and the complex interaction between this and the rotating screen results in significant changes in pattern with elevation. One effect of this is that the gain peak does not always lie in the same direction as the mechanical orientation of the antenna. In particular, no benefit is obtained by steering the antenna below an elevation of twenty degrees, even for operation with the satellite at ten degrees elevation. A look-up table is used optimize the beam steering in the presence of these effects.

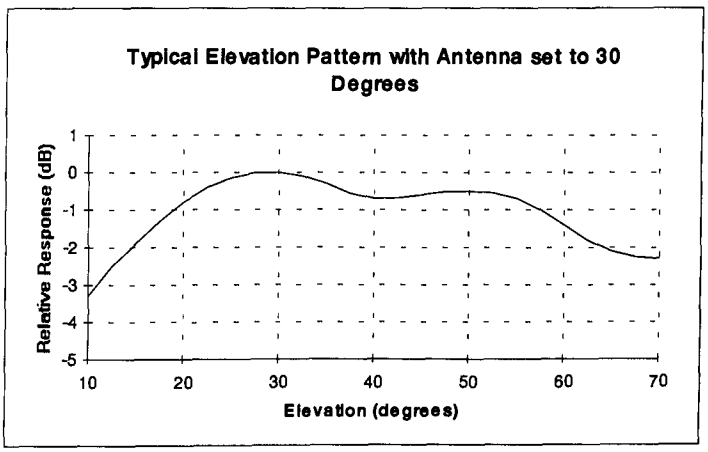

Figure 1: Typical Elevation Pattern for the Highly Shortened Helix Array

Figure 1 shows a typical pattern plot for the prototype array.

Radome design

The radome is approximately 5.5" high by 12" wide by 24" long, and uses a "beaver tail" design for low drag. Conventional fibreglass construction was found adequate for a radome of this size, and was adopted in favour of a more complex sandwich construction for its low cost. Protection from direct lightning strikes is provided by segmented metal diverter strips. A rain ablative coating is used to minimize erosion of the outer surface.

Five ranges of fuselage diameter have been identified, ranging from 58" to 146", and radome models will be available for each of these sizes. These diameters include the following aircraft: Beechcraft, Canadair (all models), Cessna Citation (all models), Falcon (all models), Raytheon RBU 800 and RBJ 1000 (a.k.a. BAe-800 or HS-125), Gulfstream II and III, and Learjet (all models). With the exception of the installation kit, the radome is the only item which must incorporate detailed differences to suit specific aircraft.

Beam Steering Unit

One design goal in this development was to make the antenna BSU independent of the aircraft's navigational system and other avionics. This is attractive because it reduces the installation time and cost and mitigates a number of flight safety concerns that arise whenever new avionics are installed on aircraft.

The BSU uses received signal strength measurement derived by the communications subsystem of the terminal as an indicator of successful antenna orientation. Aircraft attitude and position information is provided respectively by a geomagnetic field sensor and a GPS receiver built into the terminal. Used singly or together, these subsystems provide information cues that are used to deduce the state of aircraft motion. Redundancy is built into the BSU, so that if one of the cues is not available, effective tracking is still achievable using what remains.

The BSU code runs in a TMS 320C31 digital signal processor (DSP). The DSP samples the magnetic field sensors and conducts the integration and processing of the field strength and GPS information. Motors which control the antenna are actuated by the DSP in response to any changes in the orientation of the aircraft. Figure 2 shows the signal processing features that are necessary to maintain the antenna steering functions assigned to the BSU.

Acquisition and Geomagnetic Sensing

On activation the terminal must find the signalling channel emanating from the satellite and communicate over the corresponding return channel in order to log into the mobile satellite call processing system. At the same time the BSU must determine the direction of the direct satellite signal so that acquisition and log on can be undertaken.

While the aircraft is on the ground the received signal will likely be corrupted by multipath conditions which will cause wide signal strength variations. It becomes impossible to confidently determine the mean signal strength without integrating the measurements over a number of seconds, during which time an aircraft can make a significant orientation change. Reflections produce numerous signal paths, each having a different direction, making it impossible to identify the direct path which is necessary if effective bi-directional communications are to be made with the satellite. To compound these problems, the communications subsystem of the terminal itself may be searching in frequency, testing various signalling channels for robustness.

One way to resolve the multipath problem is to provide information regarding the orientation of the antenna with respect to the magnetic north. This is done using a geomagnetic field sensor capable of resolving the magnetic field in three dimensions. This sensor has been used in

previous mobile aeronautical satellite terminals developed by CRC [1]. The device is highly robust and uses adaptive electronics which mitigate the effect of magnetic field perturbations caused by the host aircraft. It is capable of resolving the geomagnetic field vector inclination and declination angles to an accuracy of approximately ± 2 degrees.

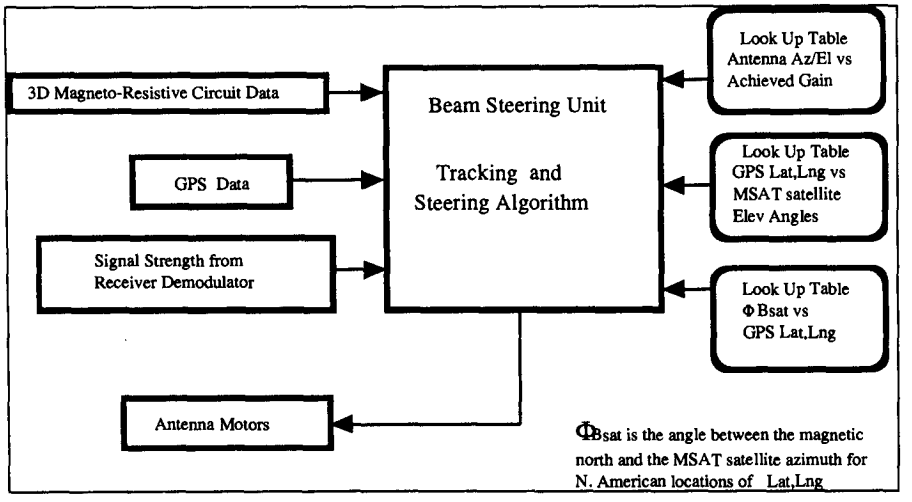

Figure 2: Beam Steering Unit System Organization

To achieve fast acquisition the BSU must find and use the angle between the magnetic north and the orientation of the antenna toward the satellite. This angle (Φ_{Bsat}) is determined by the BSU during flight and has the characteristic of being unique to the geographical location of the aircraft, changing slowly as the aircraft traverses the North American continent. By knowing Φ_{Bsat} before the terminal is turned off, it is possible to determine the antenna pointing angle to the satellite when the terminal is reactivated by determining the direction of magnetic north and adding Φ_{Bsat}. One makes the assumption here that the terminal is reactivated in the same geographical location that it was deactivated. However, even if a significant geographical displacement does occur before reactivation, there are other cues and procedures which can be employed, albeit with a resulting extension in acquisition time.

The magnetic sensor is capable of providing accurate readings of the magnetic declination and inclination angles more than 30 times a second. Using these it is possible to quickly determine changes in orientation of the aircraft. This is done to maintain tracking while the aircraft manoeuvres on the ground, through an environment that can have significant multipath and signal fading. In essence, the tracking being undertaken under these circumstances is solely dependent on magnetic field sensing, with signal strength information being used only to augment the tracking decisions. The geomagnetic sensor, because of its ability to resolve the magnetic field vector in three dimensions, is also able to determine any significant tilt in the aircraft, as would be the case when the aircraft takes off.

Dynamic Tracking and GPS

The BSU is also provided with geographical position information by a GPS processor. In flight GPS is used to augment the steering decisions made by the BSU. By determining geographical location, it is possible for instance, to accurately determine elevation angle to the satellite, which narrows the search range of the antenna to azimuth angles only.

GPS provides a position fix every second. With this it is possible to determine the velocity of the aircraft and determine if there have been any changes in the heading. Heading and other orientation changes of the aircraft are also detected by the magnetic sensor. Using the magnetic sensing system alone, orientation changes to the aircraft can be resolved to ± 8 degrees. Using the GPS information the accuracy of the orientation change estimate is to within ± 4 degrees.

The estimated roll and heading changes of the aircraft are used to drive a series of spherical axis transformation functions which generate new antenna pointing angles. Figure 3 shows the changes in the satellite and magnetic field orientation vector angles due to and aircraft making a 90 degree port turn having a peak roll of 28 degrees.

Doppler Correction

The MSAT land mobile terminal is not required to make Doppler corrections and therefore does not have sufficient frequency stability to permit direct measurement of the Doppler offset. It was deemed impractical to provide an external high stability reference for this purpose, so it became necessary to provide an independent measure of the motion of the terminal in relation to the satellite. Larger systems often rely on the aircraft's navigational system, but the absence of standardized interfaces in smaller aircraft, or sometimes the complete lack of an inertial system, dictated a different approach. A GPS receiver was selected as the most effective way to provide the required information. The location of the aircraft is used together with a

knowledge of which satellite is in use to define the geometry, and the aircraft velocity is used to calculate the radial velocity with respect to the satellite, and hence the Doppler shift. The terminal uses this information to assist acquisition and tracking of the received channels, and also to correct the transmitted signal to within the required limits.

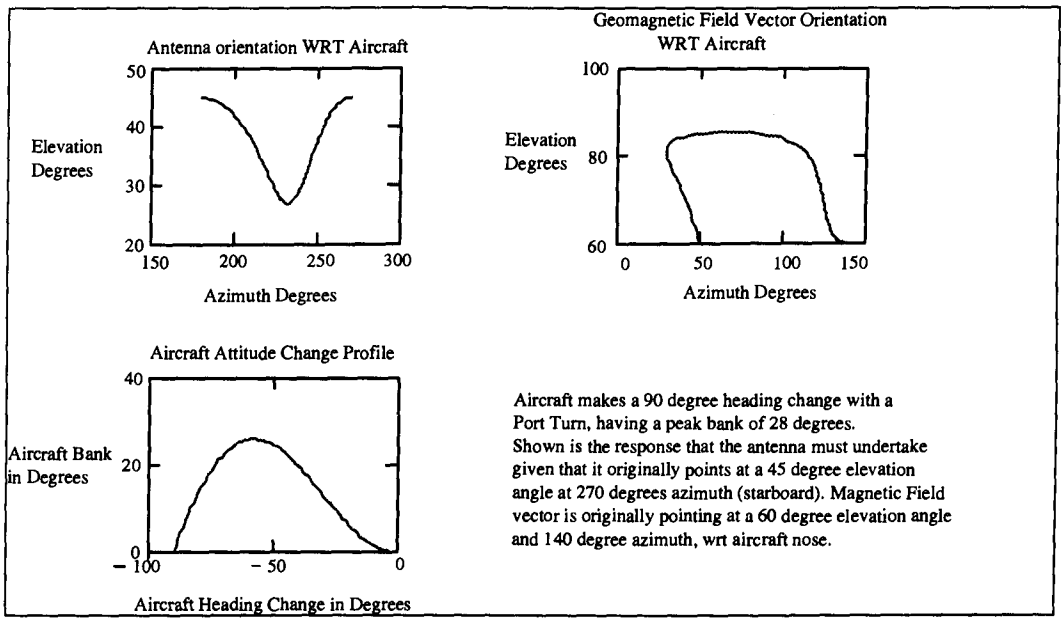

Figure 3: Magnetic Field and Antenna Pointing Vector Changes due to Aircraft Motion

GPS Compatibility

The L-band satcom transmitter is capable of interfering with GPS reception in two distinct ways. Firstly, its output spectrum includes noise which lies within the GPS band centred on 1575.42 MHz, and the level of this noise must be well below the wanted signal level at the GPS receiving antenna. Secondly, the satcom transmission in the band 1626.5 to 1660.5 MHz may be strong enough to saturate either the GPS low noise amplifier or the front end of the receiver, reducing sensitivity and possibly preventing proper GPS reception. These phenomena may affect both the GPS receiver which forms part of this terminal, and any other GPS receiver on the same aircraft or an adjacent one.

Broadband Transmitter Noise

In order to avoid problems with a co-located GPS receiver, the terminal's EIRP in the band 1565 to 1585 MHz is specified as -155 dBc/4KHz. Fortunately, the WEC land mobile terminal has an excellent performance in this regard, and little extra filtering was needed to meet this specification.

Saturation of GPS by Satcom Transmission

This problem cannot be solved by the design of the terminal since it is caused by the wanted transmission. It must be controlled by a combination of antenna separation and filtering at the appropriate stage in the GPS receive chain. Attention to the compression points of the RF stages in the GPS receiver may also be necessary.

For the GPS receiver within the CAL terminal, heavy filtering has been incorporated both at the input and output of the GPS LNA. It is hoped that this will permit the GPS antenna to be located within the main radome, leading to simpler installation than with a separate antenna. However, this has not been confirmed at the time of writing.

The situation with other GPS receivers on a particular aircraft is dependent on several factors such as whether an active or passive antenna is used, antenna location, and receiver characteristics. It depends also on whether disruption of GPS reception during satcom operation is considered acceptable. These issues will be addressed at installation time

DO160C Environment

DO160C [2] defines a broad range of environmental conditions relating both to the susceptibility of the equipment, and also to its possible effect on other equipment and the airframe. This is the standard to which the terminal must be tested in order to satisfy the regulatory agencies who must certify the equipment and its installation. In addition to the usual temperature, altitude, humidity, shock and vibration, there are stringent requirements for EMC as well as exposure to some devastating supply fluctuations and lightning induced transients. In the case of the antenna, there is also the need to withstand exposure to a range of fluids, a water jet, sand and dust, and to avoid compromising the safety of the aircraft in the event of a lightning strike.

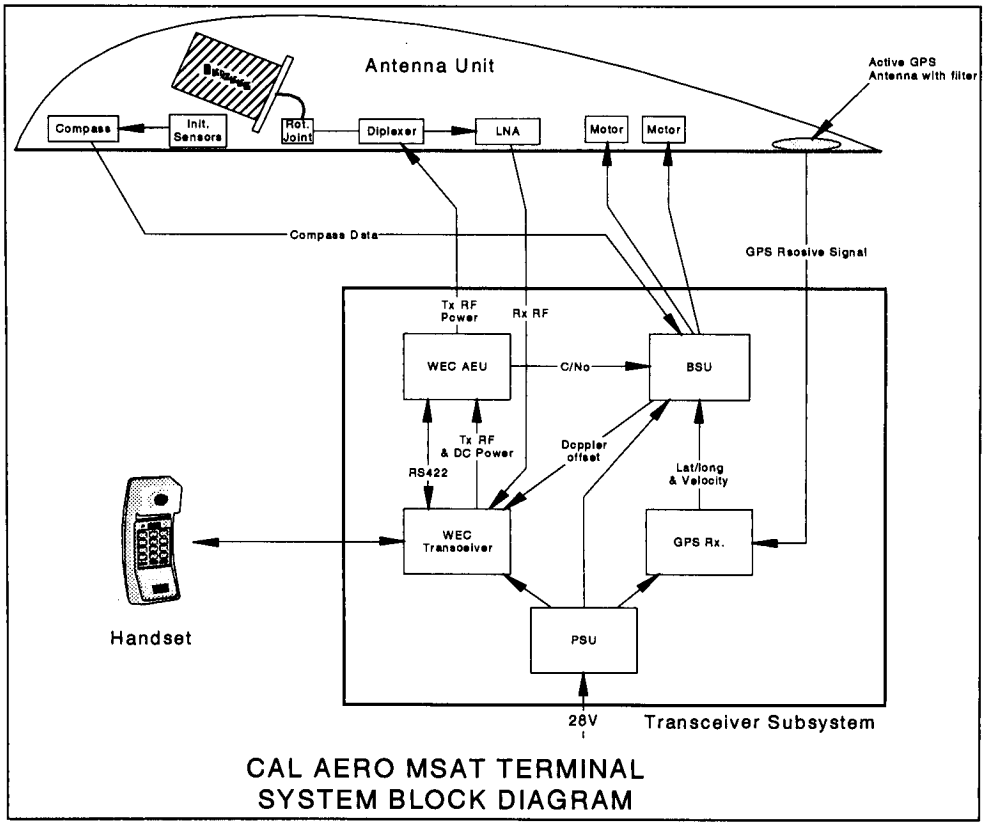

Figure 4: System Block Diagram

The EMC requirements and lightning-induced transients have led to the use of a shielded enclosure for the Transceiver Subsystem, having filters and transient protection devices at every external interface. All wiring between the AU and the Transceiver Subsystem is shielded, and RS-422, a balanced signalling format, is used for serial digital communication.

Installation Philosophy

Simplicity of installation was one of the dominant considerations during the design of the system. As mentioned previously, there is no dependence on any navigational systems in the aircraft, so the only electrical interface with the aircraft systems is the 28 volt DC power input, which enters at the Transceiver Subsystem.

Connectors are used where wiring passes through the fuselage skin, making it easy to install the antenna, and to remove it should this ever be necessary. Its light weight (8 lb.) and small size make it easy for one person to handle while making the connections and installing the fasteners.

The Transceiver Subsystem is housed in an ARINC style enclosure which is readily installed in an avionics bay or other convenient location. The relatively stringent EMC categories chosen for certification of this equipment give considerable flexibility in siting it in a small and crowded aircraft.

Terminal Architecture

Figure 4 shows a block diagram of the CAL aeronautical MSAT terminal. The two major subsystems are shown, together with the handset and the interconnecting cables. The central role of the BSU in controlling several aspects of terminal operation is apparent.

Despite the appearance of complexity, the system is compact and relatively lightweight, and is expected to achieve wide acceptance by the general aviation community.

References

[1] **J. Sydor and M. Dufour,** *Aeronautical Satellite Antenna Steering Using Magnetic Field Sensing,* IMSC '93 Conference Proceedings. JPL Publication 93-009, pp. 593-598.

[2] *Environmental Conditions and Test Procedures for Airborne Equipment,* RTCA/DO–160C, December 1989

Computer Simulation and Performance Assessment of the Packet-Data Service of the Aeronautical Mobile Satellite Service (AMSS)

Wassim Ferzali, Vassilis Zacharakis, Triveni Upadhyay
Mayflower Communications Company, Inc. 80 Main street, Reading, MA 01867, USA.
Tel: 617-942-2666, Fax: 617-942-2403

and

Dennis Weed, Gregory Burke
Federal Aviation Administration
800 Independence Ave, S.W., Washington DC, 20591, USA.

Abstract

The ICAO Aeronautical Mobile Communications Panel (AMCP) completed the drafting of the Aeronautical Mobile Satellite Service (AMSS) Standards and Recommended Practices (SARPs) and the associated Guidance Material and submitted these documents to ICAO Air Navigation Commission (ANC) for ratification in May 1994. This effort, encompassed an extensive, multi-national SARPs validation. As part of this activity, the US Federal Aviation Administration (FAA) sponsored an effort to validate the SARPs via computer simulation. This paper provides a description of this effort. Specifically, it describes: (1) the approach selected for the creation of a high-fidelity AMSS computer model; (2) the test traffic generation scenarios, and (3) the resultant AMSS performance assessment. More recently, the AMSS computer model was also used to provide AMSS performance statistics in support of the RTCA standardization activities. This paper describes this effort as well.

Introduction

The ICAO AMCP/Working Group A (WG-A) had the responsibility to develop and validate the AMSS SARPs. The SARPs validation effort encompassed several methods, such as: test and demonstration, manufacturer's data collection, analysis, and computer simulation. This paper focuses on the computer simulation aspect of the validation effort. WG-A identified computer simulation as a primary method for the validation of the draft SARPs. In this regard, the US Federal Aviation Administration sponsored an effort to develop an extensive computer model for AMSS and to derive simulation results that directly support the validation of certain aspects of the AMSS SARPs. Three main objectives for the AMSS computer simulations were identified: (1) protocol specifications correctness check, (2) protocols implementability check, and (3) performance testing and verification. This paper focuses on the third objective.

The AMSS SARPs and the associated Guidance Material (GM) contain performance parameters relating to packet-mode data transmission and circuit-mode call establishment. The objective of the AMSS computer simulation was to verify that such performance parameters could be attained under the assumed nominal traffic loading.

RTCA Inc., a standardization organization for civil aviation systems and electronics, is active in the development of several AMSS related standards. The ICAO AMSS SARPs computer model was also instrumental in providing performance statistics data to RTCA activity. The data provided to RTCA focused on the packet-data services of AMSS and was of larger scope than the data that supported the SARPs and GM validation (it provided results for all data message length and at various levels of message priority.)

In the following, we first give an overview of the AMSS followed by a brief description of the AMSS simulation model, and then we present the simulation results.

AMSS Overview

AMSS is a satellite-based, mobile communications network that caters to the aviation users data and voice communication needs. It has been selected by ICAO as one of the air-ground communication links for the ICAO FANS Global CNS concept. Currently, near SARPs compliant AMSS is provided via the Inmarsat aeronautical service and the Civil Aviation Authorities are gearing to adopt the system as part of their ATC services.

Communications within AMSS are accomplished between a mobile unit, called the Aircraft Earth Station (AES), and a fixed ground station, called the Ground Earth Station (GES), through a geostationary satellite. Four types of channels are defined; namely, the P, R, T, and C channels. From the AES three types of channels are applicable: the R, T and C channels. The slotted Aloha R and the TDMA T channel support packet-switched transmission of users data. The R channel is accessed by the AES on a random basis for the transmission of signaling and short user data messages. The T channel is accessed by the AES for the transmission of long user data messages upon request for TDMA slots and receipt of slot reservations from the GES. The single user, single carrier C channel support the circuit-switched voice communications.

The packet-switched data communication from the GES is supported by the time division multiplexed P channel. A set of P, R, and T channels is assigned by the GES to the AES during the AES log-on procedure. Multiple R and T channels could be supported within a given set. A set of two C channels, one to transmit and one to receive, are assigned to an AES by the GES upon request to establish a voice call. The C channel format provides for a sub-band signaling channel.

The AMSS is specified in the SARPs via different layers and functions. For the packet-switched data services three layers are specified, in accordance with the ISO OSI Model: the Physical, Link, Link Layer, and Subnetwork layers. Three distinct functions are specified for the Subnetwork layer: (1) the Subnetwork access (SNAc) function, specified as the ISO 8208 DCE, (2) the Interworking Function (IWF), and (3) Satellite Subnetwork Dependent sub-layer (SSND). The SSND implements a connection-oriented protocol that establishes, and monitors the operations of multiple virtual connections between an AES/GES pair for packet transmission. For the Link Layer, three distinct protocols are specified for the transmission of data packets: the P channel, the R channel, and T channel protocols. In addition, a T channel reservation protocol for the request and assignment of T channel TDMA slots and a sub-band C channel protocol to handling signaling over the C channel sub-band are specified as part of the Link Layer protocol suite. All Link layer protocols, except for the sub-band C channel protocol, implement a Reliable Link Service (RLS) with selective ARQ schemes for data packet error correction employing the 16-bit CCITT CRC. The physical layer specifies the channel formats, modulations, FEC, interleaving, etc., associated with each channel.

The processing of the outgoing and incoming voice calls at the AES and the GES is specified as a separate entity, the circuit-mode services. This entity uses the Link Layer resources to exchange signaling information pertinent to a particular call between the AES and the GES. The Link Layer resources used are the P channel protocol, the R channel protocol, and the sub-band C channel protocol. Furthermore, the circuit-mode services procedures interface with external telephony networks through an interworking interface comprising a standardized set of interworking telephony events (CCITT Recommendations Q.601 to Q.608).

Management of the data and voice communications between an AES and a GES is specified as two separate entities: the AES management functions and the GES management functions. The procedures performed by the AES and GES management functions are: log-on, log-off, satellite-to-satellite and GES-to-GES handover, channel reassignment, system table broadcast, selective channel release, and log-on verification.

Simulation Model Description

The AMSS computer model development encompassed implementations of the various AMSS protocols and functions and the capability to vary the configuration of the system, such as the number of mobile users, ground stations, number of inbound and outbound channels, channel rates, etc. The model was created with the Optimized Network simulation tool (OPNET), developed by MIL-3 Inc.

Model Description

The AMSS computer models provide the capability to simulate the AMSS incorporating many AESs and GESs with varying simulation attributes. Each AES and GES in the AMSS model contains the following:

- Physical Layer Model
- Link Layer Model
- Subnetwork Layer Model
- Circuit-mode Services Model
- AES/GES Management Model
- Traffic Generation Capabilities

The following provides a brief description of the modules listed above:

Physical Layer Model. The Physical Layer model is intended to account for the features of the Physical Layer that have direct impact on the operation of the Link Layer, e.g., channel rates, transmission and propagation delays, information bit error rate (BER), slotted Aloha operation. Therefor, it does not simulate any RF parameters, modulation/coding schemes or signal filtering. The Physical Layer model encompasses simulation of the various in-bound and out-bound channel format, namely the P, R, and T channels. For all the channels, the transmission delays are accounted for by taking into

consideration the respective channel frame formats, the associated framing overhead, and the assigned channel rates. A one-way propagation delay of 270 ms is observed. Since the Physical Layer model does not operate at the "bit" level, the impact of the SARPs specified channel BER, which is set at 10^{-5} after forward error correction (FEC) for all the channels, is translated to a link layer Signal Unit (SU) error rate at which SUs from the transmitted SUs stream are discarded. This SU error rate is derived taking into consideration the theoretical error detection capability of the SARPs-specified 16-bit CCITT CRC and the bit length of the SUs. Furthermore, for the slotted-aloha R channel, SUs collision and subsequent deletion are modeled.

Link Layer Model. The Link Layer model fully implements all the link layer protocols specified in the SARPs; namely: the P, R, T, and sub-band C channel protocols. In addition, the model contains a T channel TDMA slot assignment algorithm at the GES that could handle reservation assignments on up to 4 independent TDMA T channels, simultaneously. The link layer model could support several P, R and T channel sets per GES at various channel rates. An instance of the sub-band C channel protocol model is enabled with the establishment of each C channel associated with a voice call and subsequently disabled when the voice call is cleared.

Subnetwork Layer Model. The Subnetwork Layer model fully implements the SARPs specified SSND and IW functions. At the GES an SSND instance is created for each AES that logs on during a simulation run. The SSND model incorporates all the specified functionality: e.g., connection establishment, reset and release, etc. The IW model has the capability to interface with several DCEs, either at the AES or the GES. A simplified DCE model is implemented. The DCE model may request the establishment of up to the maximum allowable connections between a given AES/GES pair.

Circuit-mode Services Model. All four state machines specified to handle the incoming and outgoing voice calls at the GES and the AES are modeled. The model interfaces at the AES and the GES with an interworking modules implemented to induce interworking events into the model. Upon the establishment of a call, a sub-band C channel protocol is engaged to handle the transmission of the appropriate SUs.

AES and GES Management Models. All the functions specified for the AES and the GES management were implemented as part of the AES and GES management models. The models interface with all other models pertinent to the AES and the GES for connectivity information and other specified functionality. The models also interface, at the AES and the GES, with specific user modules. The user modules were implemented to induce user commands into either the AES or the GES management models, such as commands to log-on, log-off, or handover the AES, and commands to execute a channel reassignment for the AES.

Traffic Generation Capabilities. Separate modules are implemented in order to induce user data packets and voice calls traffic into an AMSS simulation. The traffic generation capability consist of functions and procedures that are designed to virtually create any traffic profile for a given AES and GES in the simulation.

Other Capabilities. Several simulation attributes defined to customize an AMSS model for the user specifications can be set by the user. Sample of such attributes is given below:

- Bit error rates on the P, R, T and C channels
- Channel rates for the P, R and T channels
- The number of P channels supported by the GES
- The number of R and T channels per P channel
- Number of GESs and AESs in a given simulation
- Traffic generation rate per AES per priority for packet data
- Call generation frequency and call duration for voice calls
- Number of established SVC's per AES/GES pair
- Log-on time for each AES and the duration of the log-on session

Simulation Results

Numerous simulation runs were executed under varying scenarios in order to collect simulation results pertinent to the AMSS SARPs packet data service validation and the RTCA DO-215, "Guidance on Aeronautical Mobile Satellite Service End-to-End System Performance"

Simulation Scenarios

The following simulation configuration parameters were used to collect the results reported in this paper:

Channel configuration: One P channel, one T channel, and a variable number of R channels.

Channel occupancy levels: 60-70 % P channel, 60-70 % T channel, and 15-20 % R channel.

Different approaches were used for the traffic model in the collection of data for AMSS SARPs validation and the collection of data for the RTCA standards. For the AMSS SARPs, data traffic was generated as follows: At the lowest (0) and the highest (14) data priorities, user data packets are generated with fixed length of 128 octets. At all other priorities, user data packets are generated with a uniformly distributed length at a maximum of 128 octets. The

generated user data packet interarrival times are exponentially distributed with average values selected such that the desired channel occupancy levels are attained.

For the RTCA DO-215 simulation runs, a traffic model based on anticipated traffic for the near term operation of the AMSS was used. This traffic model was developed with major input by ARINC, Inc. for the RTCA SC-165 dealing with the AMSS standards. In the ARINC traffic model user data packets are generated in accordance with specified interarrival time and length distributions at various user data priorities.

Packet-Data Performance Parameters

Data service performance specifications are provided in terms of selected parameters in the AMSS SARPs and the RTCA DO-215. In the SARPs, the performance specifications are given for packets of 128 octets in AMSS user data. The mean and 95 percentile (95%) of the AMSS delay for such packets, in the from-aircraft and to-aircraft directions, at the lowest and highest AMSS data priorities are specified. The expected throughput for data services is given in the AMSS Guidance Material (GM). Throughput is the speed of service performance parameter for the transfer of multiple data packets. The throughput is specified in the GM as a minimum expected value in bits per second (bits/s) on the basis of the transfer of multiple of 128-octet long data messages, per a given AMSS user, for the lowest and highest message priorities.

In the RTCA DO-215, AMSS delay performance for packet service is specified in terms of the latency, mean and 95% delays, in both the from-aircraft and to-aircraft-directions, for the flight safety data category. In the AMSS SARPs, the flight safety data is assigned priority 11. The latency delay represents the expected delay for unloaded channels, whereas, the mean and 95% delays are specified for the loaded channels. The RTCA DO-215 delay specifications are given for a various message lengths, unlike the AMSS SARPs delay specifications which are given in terms of only 128-octet long user messages.

Simulation Results

Simulation results were collected for the specified AMSS SARPs and GM, and the RTCA DO-215 performance parameters described above. The simulation results for the AMSS SARPs delay specifications are given in Table 1. The simulation results for the RTCA DO-215 delay specifications are given in Figures 1-4, in graphical format.

As for the throughput parameter specified in the AMSS GM, it is determined in the simulation as the user bits received per second at a given destination based on the receipt of the last 9 of 10 user data packets of length 128 octets each. The subject 10 packets are generated and enqueued to be transmitted to the destination at the same instant of time. The reported throughput is computed in accordance with the following equation:

$$\text{Throughput (b/s)} = \frac{(N-1) * 128 * 8}{T_2 - T_1}$$

where N =10, T_1 is the time of receipt of the first packet of the subject N packets, and T_2 is the time of receipt of the last packet of the subject N packets. The simulation results for the AMSS throughput specification are given in Table 2 below.

Comments and Observations

The simulation results indicate that the AMSS SARPs delay and throughput specifications and the RTCA DO-215 delay specifications could be met, with conservative margins. Further comments are provided as follows:

Effect of priority in the from-aircraft direction. From the simulation results for the AMSS SARPs delay performance given in Table 1, we observe that the delay in the from-aircraft direction is not very dependent on the message priority, exemplified in the results for the highest and lowest message priorities. This is inherent to the current operation of AMSS. For the transmission of short packets (< 34 octets), the AESs vie for access of the R channel resources randomly, with no prioritization among the active AESs. For longer packets transmitted on the TDMA T channel, which is the case here, the ground station T channel slot assignment algorithm handles the AES slot request on a first-come first-serve basis, disregarding the priority of the messages. Although prioritization is observed within the same AES, these R and T channel operations minimize the effect of prioritization for multiple aircraft communications. Means to enhance the effect of message priority in this case would be either to enforce the assignment of the aircraft reservation request in accordance to the priority of the message for which T channel slots reservation are being requested, or to restrict the usage of a given T channel to message of the desired priority when multiple T channels are in operation. The first remedy would result in a more complicated T channel assignment algorithm than the currently used algorithm, whereas, the latter remedy may result in inadequate loading of the specialized T channel. In either case, the AMSS SARPs does not enforce the usage of any scheme, as long as the SARPs specified performance parameters are met, which seems to the case. However, in the future, enhanced service might be needed which may require improved delay performance, at which time these issues might come to play.

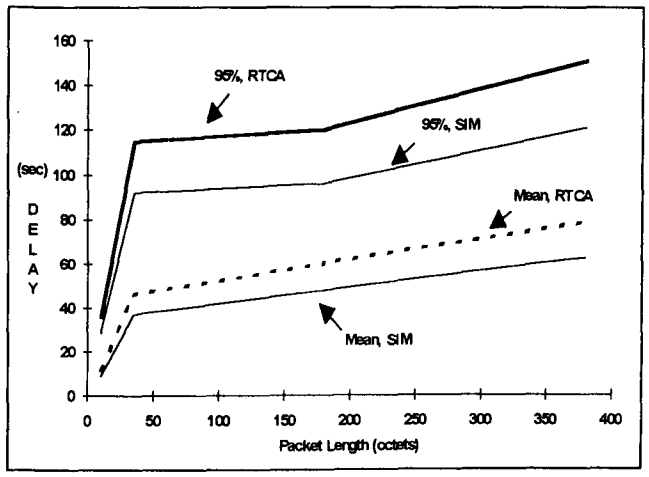

Figure 1- RTCA DO-215 Delay Specifications Vs Simulation results in the From-Aircraft Direction, Mean and 95%. 600 bps Channel rates

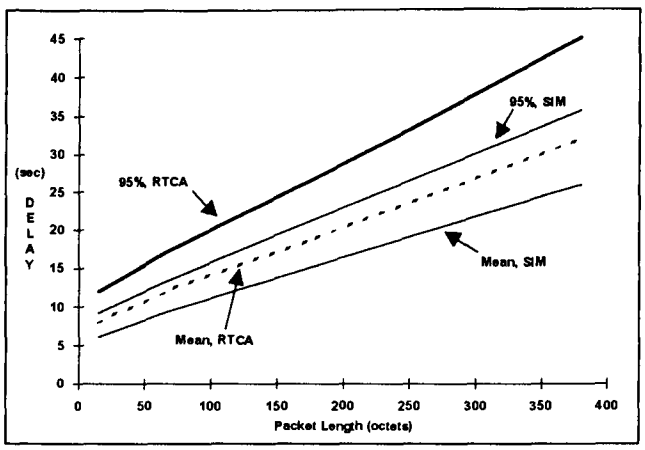

Figure 2- RTCA DO-215 Delay Specifications Vs Simulation results in the To-Aircraft direction, Mean and 95%, 600 bps Channel rates.

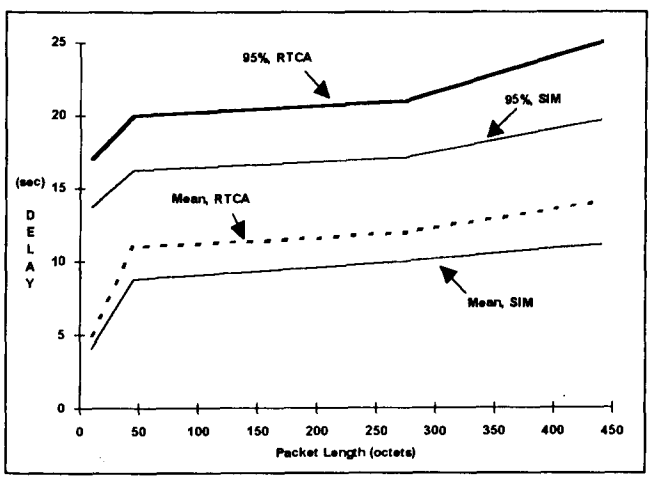

Figure 3- RTCA DO-215 Delay Specifications Vs Simulation results in the From-Aircraft direction, Mean and 95%, 10.5 kbps Channel rates.

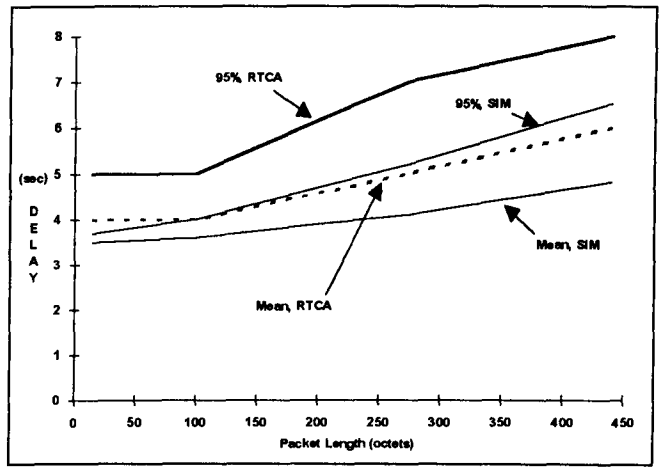

Figure 4- RTCA DO-215 Delay Specifications Vs Simulation results in the To-Aircraft direction, Mean and 95%., 10.5 kbps Channel rates.

R/T channel boundaries. In the from aircraft direction sudden variations in the delay are due to the fact that short messages are transmitted on the R channel and longer messages are transmitted on the T channel in AMSS. The message length at which the R to T channel switching occurs is 34 octets into the AMSS Link Layer. The R and the T channel exhibit a different delay performance. Furthermore, even in the T channel region, further sudden jumps are observed due to the T channel burst assignment by the GES, where multiple burst with interburst gaps are assigned for messages at preselected message boundaries. In the plots in Figures 1 an 3, sudden jumps in the delay statistics are not sharp due to insufficient data close to the preselected boundaries.

CONCLUSION

In this paper we summarized the results of a multi-year effort sponsored by the US Federal Aviation Administration (FAA) to assess the performance of the Aeronautical Mobile Satellite Service (AMSS). This effort provided vital input to the development and validation of the ICAO AMSS Standards and Recommended Practices (SARPs) Guidance Material, and the RTCA DO-215. As part of the future work, this simulation effort is being expanded to incorporate models of the Aeronautical Telecommunications Network (ATN) in order to assess the implications of the observed delay statistics on the definition and operation of the anticipated data link ATC applications, such as the Automatic Dependent Surveillance (ADS) application.

ACKNOWLEDGMENT

The authors would like to acknowledge the effort of the members of the US AMSS SARPs Team and RTCA SC-165 who in several ways either supported this effort, or

reviewed the results. In particular we would like to acknowledge the following individuals: Dr. Duncan Cox, Mr. Don Dement, Mr. Brian Hung, Mr. Yaroslav Kaminsky, Mr. Frank Mackowick, Mr. Andy Pickens, and Mr. Walt Scales.

REFERENCES

1- RTCA DO-215, "Guidance on Aeronautical Mobile Satellite Service (AMSS) End-to-End System Performance", and associated change #1.

2- Draft ICAO AMSS SARPs as approved by AMCP/3 on April, 1994.

Table 1- AMSS SARPs Delay Specifications Vs Simulation Results.
(Channel Loading: 70-73% P and T channels, 12-14% R channel)
(Delays are given in Seconds)

Channel Rates [bits/s] (all Channels)		FROM AIRCRAFT				TO AIRCRAFT			
		Highest Priority		Lowest[1] Priority		Highest Priority		Lowest Priority	
		Mean Delay	95% Delay	Mean Delay	95% Delay	Mean Delay	95% Delay	Mean Delay	95% Delay
600	SARPs	40	80	-	-	12	15	40	110
	SIM	*39*	*74*	*46*	*98*	*10*	*15*	*36*	*96*
1200	SARPs	30	65	-	-	8	9	25	60
	SIM	*25*	*48*	27	53	*7*	*9*	*19*	*50*
2400	SARPs	15	35	-	-	5	6	12	30
	SIM	*12*	*21*	*14*	*27*	*5*	*6*	*10*	*22*
4800[2]	SARPs	13	30	-	-	4	5	7	20
	SIM	*8*	*15*	*10*	*18*	*4*	*5*	*7*	*15*
10500	SARPs	13	30	-	-	4	4	5	10
	SIM	*7*	*15*	*9*	*18*	*2*	*3*	*4*	*7*

1- Delay specification for the lowest-priority from-aircraft traffic is not included in the AMSS SARPs
2- P channel at 4800 bits/s, and T and R channels at 10500 bits/s

Table 2- AMSS Guidance Material (GM) Throughput Specifications Vs Simulation Results.
(Channel Loading: 65-70% P and T channels, 14-16% R channel)
(Delays are given in Seconds)

Channel Rates [bits/s] (all Channels)		FROM AIRCRAFT THROUGHPUT[1,2] [bits/s]		TO AIRCRAFT THROUGHPUT[1,2] [bits/s]	
		Highest Priority	Lowest Priority	Highest Priority	Lowest Priority
600	GM	35	30	70	35
	SIM	*53*	*47*	*80*	*42*
1200	GM	100	80	130	70
	SIM	*121*	*109*	*136*	*78*
2400	GM	300	275	150	90
	SIM	*350*	*325*	*157*	*98*
4800[3]	GM	500	475	160	110
	SIM	*597*	*578*	*172*	*118*
10500	GM	500	500	165	115
	SIM	*587*	*569*	*165*	*122*

1- The simulation (SIM) results represent the throughput averaged over several experiments
2- The Guidance Material Throughput Specification are provided as minimum expected values.
3- P channel at 4800 bits/s, and T and R channels at 10500 bits/s

Satellite Communications Provisions on NASA Ames Instrumented Aircraft Platforms for Earth Science Research/Applications

L. Shameson, J.A. Brass, J.J. Hanratty, A.C. Roberts, S.S. Wegener
NASA Ames Research Center
Moffett Field, California 94035-1000, USA
Phone: 415-604-6185 FAX: 415-604-4680

ABSTRACT

Earth science activities at NASA Ames are research in atmospheric and ecosystem science, development of remote sensing and in situ sampling instruments, and their integration into scientific research platform aircraft. The use of satellite communications can greatly extend the capability of these agency research platform aircraft. Current projects and plans involve satellite links on the Perseus UAV and the ER-2 via TDRSS and a proposed experiment on the NASA Advanced Communications Technology Satellite.

Provisions for data links on the Perseus research platform, via TDRSS S-band multiple access service, have been developed and are being tested. Test flights at Dryden are planned to demonstrate successful end-to-end data transfer. A Unisys Corp. airborne satcom STARLink system is being integrated into an Ames ER-2 aircraft. This equipment will support multiple data rates up to 43 Mb/s each via the TDRSS Ku-band single access service. The first flight mission for this high-rate link is planned for August 1995. Ames and JPL have proposed an ACTS experiment to use real-time satellite communications to improve wildfire research campaigns. Researchers and fire management teams making use of instrumented aircraft platforms at a prescribed burn site will be able to communicate with experts at Ames, the U.S. Forest Service, and emergency response agencies.

INTRODUCTION

Sensing the winds of war and noting the world speed records established by the new Messerschmitt and Heinkel airplanes in early 1939, Dr. Joseph S. Ames Chairman of The National Advisory Committee on Aeronautics (NACA) urged and finally succeeded in setting up a new NACA aeronautical laboratory at Moffett Field in California to augment the NACA Langley laboratory in Virginia.

Construction of the 7x10-foot and the 16-foot wind tunnels began in 1940; ground was broken for the full-scale 40x80-foot wind tunnel in 1942, and for the 1x3-foot supersonic wind tunnel in 1945. These facilities provided experimental interaction with the theoretical research activities in aerodynamics being carried out at NACA Ames; by 1945, a High-Speed Research Division joined the earlier Flight Research and Full-Scale Divisions.

In October 1957, Sputnik achieved earth orbit! The public shock engendered by this event (and the advice of NACA, the President's Science Advisory Council, and the Bureau of the Budget), resulted in the establishment of NASA as a civilian agency; NACA Ames became the NASA Ames Research Center with the intent to enter the space arena.

HISTORY OF AMES SATELLITE COMMUNICATIONS ENDEAVORS and EARTH SCIENCE PLATFORM AIRCRAFT [Refs. 1, 2, 4]

Ames' first space program was the continuation of the Pioneer Project which had been initiated by ARPA. Pioneer 1, 2, & 5 had been developed by the Space Technology Labs (STL); while Pioneer 3 and 4 had been developed by the Jet Propulsion Labs (JPL). Ames became the project manager of Pioneers 6 thru 11, with TRW (the former STL) as the prime contractor and JPL providing tracking services. Pioneer 10 transmitted images of Jupiter in 1973, Saturn in 1976 and Pluto in 1987; Pioneer 11 viewed Saturn in 1979 with even greater clarity.

Like television's pink battery-driven bunny, the Pioneer spacecraft keep on going and going; at a recent Smallsat conference at Utah, I reminisced with TRW engineers who had built the spacecraft after they had asked about current operations.

Space and Satellite Communications

Pioneer 9, launched in 1968, had provided the first demonstration of convolutional error-correcting coding to extend the communications capability of deep space missions. JPL had already been working with block coding, so Ames pursued the newer convolutional coding schemes. The initial success on Pioneer 9 led to more sophisticated units on Pioneers 10/11. Henry Lum designed the spacecraft encoder which included a

25-bit shift register, and Larry Hofman wrote the ground station sequential decoding software based on the Fano algorithm; 3 dB coding gain was achieved [Refs. 2, 3].

Ames had experiments on the NASA Advanced Technology Satellites ATS-1,3 in the mid-'60s, as well as on the ATS-6 and the CTS Hermes in the mid-'70s. The VHF transponders on ATS-1,3 were intended to demonstrate satellite mobile communication with ships at sea; Skip Gross at Ames was able to exchange messages with Jaques Cousteau near Antarctica. Larry Hofman and Dale Lumb worked with Norman Abramson at the University of Hawaii to connect its computers to the Arpanet node at Ames via packet broadcast through ATS-3. Ames researchers developed an experiment to demonstrate delivery of health care services to remote areas in Alaska via ATS-6 [Refs. 2, 4].

The 1976 CTS Hermes experiment on curriculum sharing between Stanford University in Palo Alto and Carleton University in Ottawa made use of video picture compression technology provided by Ames researchers. Loss of signal synchronization and mismatches between the academic traditions at the different institutions were among the technical and cultural problems encountered [Ref. 5].

My first job at Ames in 1984 was to look at the feasibility of extending an experimental DEA ATS satellite communication system covering the western hemisphere to also cover the Pacific rim "golden triangle." The system was based on the old ATS-1 and ATS-3 satellites operating at VHF, portable alphanumeric suitcase ground terminals developed by General Electric, and larger VHF base-stations; the extension would have needed a relay station in Hawaii. Tests through both the ATS-3 and the ATS-1 indicated that special provisions would be needed to accommodate the edge-of-coverage operation and the hard-limiting nature of the ATS-1; its low fuel reserve, however, made it impractical to pursue further use of the ATS-1 link.

NASA Ames Instrumented Platform Aircraft

We now return to the early '70s to pick up the thread of the earth observation aircraft platforms. In 1969, when construction of Space Sciences Research Laboratory begun, there already existed airborne medium altitude research laboratories on the Convair 990 and 340 aircraft stationed at Ames; by 1971, these were augmented by the high altitude U-2 aircraft which arrived at Ames together with Marty Knudsen, their pilot and future chief of the Airborne Missions and Applications Division (which later evolved into the Flight Operations Directorate).

The transition into the '70s was marked by uncertainties resulting from the post-Apollo downsizing. In reaction to rumors that Ames might be closed and to an actual upcoming Reduction-in-Force, the Ames Director Hans Mark reorganized and lobbied; one result was that in 1972 Ames became the lead Center for earth observation aircraft.

The medium altitude C-990 "Galileo" aircraft became very active in many cooperative research missions on weather and resource surveys: wildlife migration patterns, ice floe measurements, archeological surveys of Mayan ruins, and monsoon behavior in the Indian Ocean. Its mission was abruptly ended in April 1973, when it collided with a Navy P-3 reconnaissance aircraft while both were making landing approaches to the Moffett Field runway. In 1974, Galileo II resumed the work of its predecessor.

The high altitude U-2s were also active. In 1973, they flew observation missions that produced the first accurate land usage map for the whole state of Arizona. In the following year, they were used to measure flood damage along the Mississippi and in California's Sacramento and Feather River basins; the U-2 also surveyed melon infestation in the California's Imperial Valley. In 1976, U-2s supported California State agencies in following forest fires burning uncontrolled in the northern part of the state; this experience was to be recalled in the Yellowstone fires of 1988 and the Oakland Hills fire of 1992.

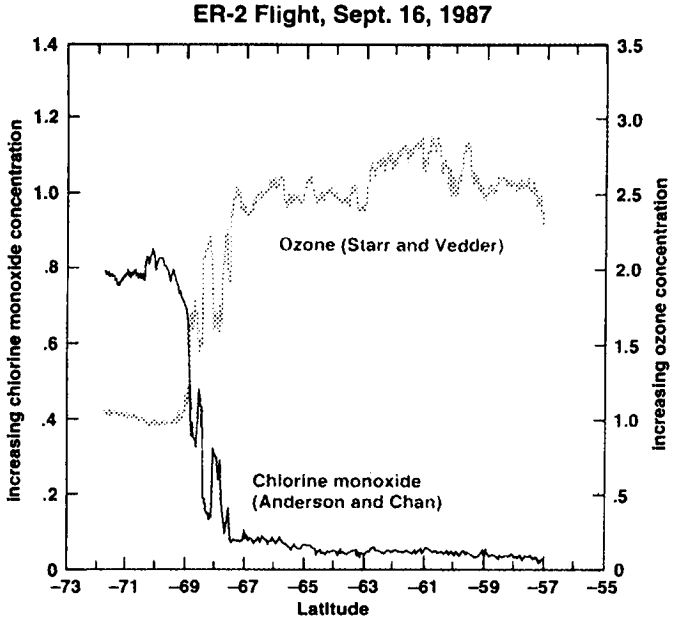

Figure 1. Results of Airborne Antarctic Ozone Experiment

In 1975, the Atmospheric Experiments Branch was created within the Space Sciences Division; this resulted in the extended use of the Ames U-2 instrumented aircraft to perform in situ sampling measurements in addition to their remote sensing capabilities. In 1977, a U-2 and the Lear Jet were deployed at

the Panama Canal Zone to study how halocarbons carried from low altitudes into stratosphere and how they might influence ozone balance. This work led to extensive future Arctic and Antarctic campaigns to determine the extent of ozone depletion and to demonstrate the role of halocarbons the depletion process (see Figure 1).

In 1980, a U-2 sampled the plume of the Mount St. Helens volcanic eruption as part of the Aerosol Climate Effects (ACE) study; years later a similar campaign was conducted for the Mount Pinetubo eruption. During the mid-1980's, the original U-2 aircraft at Ames were replaced by three ER-2 aircraft; these were a larger version of the U-2 with increased payload capabilities to enhance their ability to carry out international research programs.

CURRENT ACTIVITIES and PLANS

The current activities in atmospheric and ecosystem scientific research at the NASA Ames Research Center includes the development of remote sensing and in situ sampling instruments and their integration onto the platform aircraft. Current projects and plans involve satellite links on the Perseus Unmanned Aircraft Vehicle (UAV) >SPELL OUT< and the ER-2 via the Tracking and Data Relay Satellite System (TDRSS). We also have proposed an experiment on the NASA Advanced Communications Technology Satellite (ACTS),together with Marty Agan and the Communications Research Section at JPL.

TDRSS Satellite Communications Provisions for Perseus

Precursors to this project were the studies conducted internally and by Stanford Telecom [Refs. 6,7]. In July 1994 NASA's Environmental Research and Sensor Technology (ERAST) program funded Ames Research Center (ARC) to demonstrate a Tracking and Data Relay Satellite System (TDRSS) communication capability on Aurora Flight Sciences Corporation's Perseus Remotely Piloted Aircraft (RPA). This project was a joint effort between ARC, Goddard Space Flight Center (GSFC), Dryden Flight Research Center (DFRC) and Aurora. ARC provided overall project management, a Telemetry Interface Data System (TIDS) previously developed by ARC for Perseus with ERAST funding and a pseudo experiment consisting of a wire impactor, a set of crosshairs on an actuator controlled arm that was swung out from and back into the Perseus payload fairing to trap airborne particles on the exposed crosshairs. GSFC provided a TDRSS Transponder and Transponder Interface Electronics (TIE), power amplifier and diplexor, S-Band antenna and TDRSS scheduling. DFRC provided the flight range and Science Project Operations Center (SPOC) facilities. Aurora provided the RPA and flight support personnel.

In the first phase of this project, Perseus would fly at 10,000 feet with flight control provided by Aurora via Perseus's established UHF radio link. Figure 2 indicates the system configuration. The pseudo experiment would send aircraft and wire impactor status information to TIDS and TIDS would forward this information to the TIE. The TIE would format and transmit this information at 9.6 baud through the TDRSS/NASA Communication network (NASCOM) to the SPOC. At the SPOC the received telemetry data would be unblocked, saved to hard disk, and displayed. The SPOC also had the capability to send commands via NASCOM/TDRSS, at 250 or 500 bits per second, for control of the Transponder, the TIDS or the pseudo experiment. Due to Perseus unavailability during the December 1994 time frame this demonstration flight did not take place.

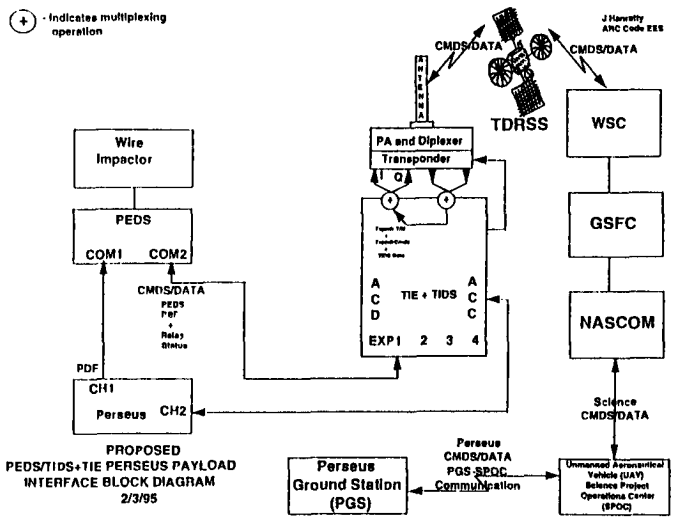

Figure 2

The second phase of the Perseus/TDRSS demonstration project began in January 1995. During the project's second phase the scrubbed December 1994 flight will be conducted in the May 1995 time frame. In addition, the TIE and TIDS (TIE + TIDS) electronics will be combined into one unit, the ability of Perseus to communicate with the TIE + TIDS as a means of flying Perseus via TDRSS will be added, documentation for a procurement package of an S-Band antenna which will provide 57.6 baud TDRSS communication capability will be generated and a second set of test flights will be conducted in the September 1995 time frame.

TDRSS STARLink Communications for the ER-2

The STARLink architecture is made up of three major elements; 1) the Airborne element, 2) the Tracking Data and Relay Satellite (TDRS) elements, and 3) the ground station distribution center at Ames Research Center (See Figure 3).

Figure 1 - STARLink Elements

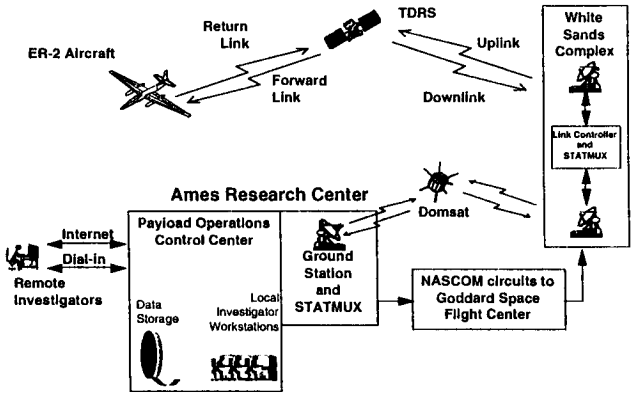

Figure 3

The Airborne element consists of an Airborne Data Recorder (ADR) used as temporary buffer and storage for digital data channels from onboard experiments. The ADR interfaces to the Airborne Modem Assembly (AMA). The AMA provides multiplexing and demultiplexing of the various channels, modulates the aggregate Return Link I and Q channels, and demodulates the forward link channels. Both the return and forward link Intermediate Frequency of 1700 MHz are passed to the Transceiver group for conversion and amplification to the TDRSS Ku-band frequencies. The Return Link is transmitted to the satellite via a 400 watt traveling wave tube amplifier and a 30-inch steerable parabolic antenna.

The TDRS element consist of the TDRS cluster and the designated Second TDRS Ground Station (STGT). The Ku-band Single Access (KSA) transponder of the TDRS is utilized to receive the ER-2 RF return link of 274 Mbit/s and to relay the RF energy to one of the three designated STGT antennas at the White Sands Complex. The signal is then routed to the RF Baseband equipment where it is demodulated and converted. The aggregate 137 Mbit/s channels are demultiplexed by the link controller into a combination of 42 Mbit/s, 21 Mbit/s, 6 Mbit/s, and 1.5 Mbit/s channels. A combined 48 Mbit/s (4 channels) is routed to the WSC Statistical Multiplexer and to an existing Domestic Satellite earth station node for transmission to Ames Research Center.

The ground station distribution center at Ames allows investigators to use telephone modems, Internet or a private Local Area Network (LAN) to access their data. This distribution center will also coordinate all command link activity through the wide or local area networks and back to the aircraft. All the multiplexing and demultiplexing activity is performed in this control center. The ground station also performs all the necessary scheduling and coordination activity with the TDRSS Network Control Center at Goddard, both in advance of the mission and during flight operations.

A full discussion of the Ames ER-2 STARlink data return link is given in this IMSC '95 conference in the paper by C.J. Hashem of Unisys Systems and Andy Roberts of NASA Ames. [Ref. 8].

The Ames/JPL Proposed ACTS Experiment

The proposed Advance Communications Technology Satellite (ACTS) Experiment on Wildfire Research and Assessment builds upon 1) our experience in wildfire and urban fire assessment, 2) the Ames aircraft platforms for remote sensor and in situ measurement instruments, 3) Ames' long tradition in satellite communications experiments, and 4) JPL's resources and expertise in the field of mobile and personal satellite communications. The mobile land and aeronautical satellite communications equipment developed by JPL in connection with the ACTS program is discussed in this IMSC '95 conference in JPL papers by Marty Agan & A. Densmore [Refs. 9, 10].

Globally, 8680 Teragrams (~1 million tons) of dry biomass are burned per year, mostly due to human activity; this produces 3500 Tg Carbon in the form of CO2 (40% of the total). Since 1980, CO2 emissions from fossil fuel combustion have leveled off, but the CO2 atmospheric concentration data measured at Mauna Loa has kept rising - biomass burning is suspected as a possible cause. CO, tropospheric O3, and other trace gases and particular emissions are also associated with biomass burning [Ref. 11].

In the United States alone, over 130,000 wildland fires occur each year. The consequences are devastating: from the generation of greenhouse gases and atmospheric pollution to destruction of homes, ecosystems, and lives. Globally, wildfires recur annually over vast areas of savanna. In the Llanos of Orinoco, Venezuela, individual fires have spread over 8000,000 hectares; and in the Brazilian Cerrado, over 200 million acres burns at an interval of one to four years (B. Diaz, personal communication). These large fires in rural areas destroy many homes, disrupt commerce, and close down airports due to the smoke.

Environmental effects of fire are dramatic in the local area and also have regional and global implications. Fires have been shown to contribute to climate change and to loss of species and biodiversity [Ref. 12]. Research has shown that fires produce greenhouse gases, ozone depleting gases, and massive amounts of aerosols - all affecting the climate and ecosystem health.

The remote sensing and in situ measurements and data analyses of wildfire activity, combustion/emission factors, will lead

to a better understanding of wildfires in chaparral biomes; hopefully, this will improve assessments of regional impacts, as well as possible global effects on atmospheric trace gases and ozone.

Perhaps 2 million years ago man overcame the natural fear common to all primates and other animals and learned to use wildfires. Today, since wildfire frequency and intensity are inversely related, prescribed burning is one of the methods used in fire management. The disaster assessment/management goal of the proposed experiment is to serve as a demonstration of satellite communications applied to the needs of a wildfire campaign. We have proposed to work with the Office of Emergency Services (OES), the Federal/State Incident Command Centers (ICCs), the Federal Emergency Management Administration (FEMA), the California Department of Forestry, and other local resource agencies to demonstrate the rapid movement of data to all agencies involved in disaster management.

The experience gained from merging remote sensing and mobile satellite communications used in the management and assessment phase of the prescribed burn experiment can lead to their application in real-life wildfire situations (see Figure 4). Also, the experience gained from this proposed experiment will, hopefully, contribute to a more effective long-term policy of wildfire management, and to improved coordination procedures in more general emergency situations such as hurricanes, floods, volcano eruptions, and oil spills.

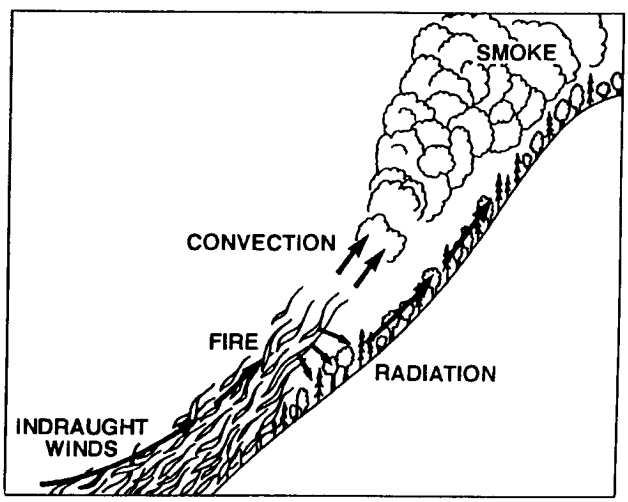

Figure 4. Sketch and of an Uphill Chaparral Fire (from Biswell) [Ref. 13].

The fire research and assessment activity will take place during a prescribed burn at a Southern California chaparral type ecosystem [Ref. 14]. Measurements will include:

- Remote Sensing Imagery - satellite AVHRR, aircraft AIRDAS
- Aircraft Sun Photometer - radiance, optical depth
- Sample Analysis - trace gases, smoke particles, ozone
- Fire Character - flame and soil temperatures, total energy release rate

These measurements will be used to calibrate the remote sensing data, to determine emission factors and combustion efficiencies, and to determine the general relationship between the extent of biomass burning and concentrations of trace gases, smoke particles, and tropospheric ozone. The results for the flaming and smoldering phases of the prescribed burn will be compared.

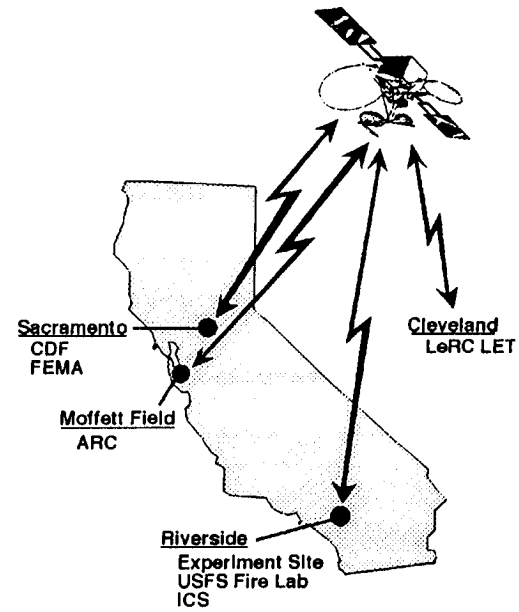

Figure 5. Proposed ACTS Links between Burn and Agency Sites

The commercial/experimental communications services will be greatly augmented (or backed-up) by three classes of ACTS communications links:

- 9.6 kb/s mobile telephony/data service
- 64 kb/s to 1.54 Mb/s image data ground uplinks
- 64 to 112 kb/s image data aircraft uplinks

The image data uplinks from the prescribed burn site will be relayed by the ACTS to researchers and disaster assessment managers at agency sites as shown in Figure 5. This "telepresence" can enable experts at the U.S Forest Service, FEMA, OES, and the California Department of Forestry to direct and/or monitor various phases of the activities at the remote prescribed-fire site.

FUTURE TRENDS for the AMES INSTRUMENTED AIRCRAFT PLATFORMS

These are indeed exciting times for satellite communications. An optical fiber infrastructure has forced satellite and other wireless technologies to become more competitive; image compression technology has enabled the long awaited direct broadcast of television; reduced path loss from LEO constellations promise direct hand-held telephone terminals and new Personal Communication Services; innovative MEO and GEO approaches offer competition to LEO.

Direct telephony and personal communications will certainly be applicable to earth science "ground truth" research campaigns, especially in remote areas. However, higher data rates (and larger terminal equipment) are associated with instrumented research aircraft and the aero-mobile satellite communications services they will use. With this in mind, we take a look at the anticipated future satcom offerings.

The American Mobile Satellite Corporation's MSAT, a GEO system, is scheduled for launch in spring of 1995. The MSAT is intended for land, maritime and aero mobile voice and 9.6 kb/s data services for North America and adjacent ocean/air space; it is not intended for higher data rates or for global coverage. The INMARSAT-P or Project 21, on the other hand, is designed to provide voice and data services over a global coverage; however its data rate will be only 2.4 kb/s. Other planned commercial LEO and MEO systems such as Motorola's Iridium, Loral's Globalstar, or TRW's Odyssey operating at L-band will not exceed 9.6 kb/s. To obtain appreciably higher data rates with a planned commercial mobile satellite system, one must wait for the turn-of-the-century Teledesic System having 840 LEO satellites operating at Ka-band; Teledesic promises 16 kb/s voice/data and 1.5 Mb/s video/data services.

While future Ka-band commercial operations via the Teledesic system are ambitious and problematical, the new NASA TDRSS satellites recently contracted to be built by Hughes will include new Ka-band transponders in addition to the S-band and Ku-band operations on the current TDRSS. Thus, any Ames instrumented research aircraft platforms participating in ACTS experiments at Ka-band would be able to transition to operations through the new TDRSS.

This paper has depicted the synergy between research in earth science, instrumented aircraft platforms, and satellite communications. This synergy is but one of several similar fruitful research collaborations at Ames: astrophysics and airborne telescopes; life science and the space station; distributed computation and aerodynamics. We recall how the successful "small step for mankind" onto the surface of the Moon was followed by a post-Apollo restructuring of NASA. Today, the successful "winning of the Cold War" has resulted in new proposals to restructure the Agency. Though costs must indeed be reduced, great care should be taken to preserve the partnerships which have taken decades to build and have been so fruitful. These synergies between advanced technologies and scientific research could be broken-up in a sudden rush to restructure without considering what would be lost.

REFERENCES and BIBLIOGRAPHY

[1] E.A. Muenger, Searching the Horizon - A History of Ames Research Center 1940-1976, NASA SP-4304, 1985.

[2] Larry Hofman, informal conversation

[3] D.R. Lumb and L.B. Hofman, "An Efficient Coding System for Deep Space Probes with Specific Application to Pioneer Missions", NASA TN D-4105, August 1967.

[4] Skip Gross, informal conversation

[5] L.B. Hofman and D.A. George, "Curriculum Sharing by Digital TV using Hermes," Hermes Symposium, Ottawa, Canada, October 1977.

[6] L. Shameson, "Satellite Relay of Aircraft Science and Command Data for Atmospheric Telescience Missions", Technical Note, NASA Ames Research Center, June 1991.

[7] Stanford Telecom, "TDRSS Support Study for NASA Aircraft," Status Review, July 1993.

[8] C.J. Hashem and A. Roberts, "Satellite Telemetry and Return Link (STARLink)," IMSC '95, June 6-8, Ottawa.

[9] M. Agan and A. Densmore, "The ACTS Broadband Aeronautical Terminal," IMSC '95, June 6-8, Ottawa.

[10] B.S. Abbe, M.J. Agan, and T.C. Jedrey, "ACTS Broadband Aeronautical Experiment," International Mobile Satellite Conference, IMSC '93, June 18, 1993.

[11] J.S. Levine ed., Global Biomass Burning - Atmospheric, Climatic, and Biospheric Implications, MIT Press 1991.

[12] J.A. Brass, "Fires and Global Change: Perspectives for Remote Sensing", World Resources Review, In press. 1995.

[13] H.H. Biswell, Prescribed Burning in California Wildlands Vegetation Management, Univ. of California Press, 1989.

[14] J.A. Brass, V.G. Ambrosia, P.J. Riggen, J. Myers and J.C. Arvesen, "Aircraft and Satellite Thermographic Systems for Wildfire Mapping and Assessment", AIAA 25th Aerospace Sciences Meeting, Reno NV, paper 87-0187, 1987.

Satellite Telemetry and Return Link (STARLink)

Andrew Roberts
NASA - High Altitude Mission Branch
MS 240 - 6
Moffett Field CA 94035
USA
(415) 604 - 5621
(415) 604 - 4987 FAX

Claude Hashem
Unisys-Government Division
640 N. 2200 W
Salt Lake City UT 84116
USA
(805) 594 - 7026

ABSTRACT

The High Altitude Missions Branch of NASA's Ames Research Center has been pursuing methods and communication architectures to decrease processing time and shorten the dissemination paths of the data from scientific experiments on board the high altitude ER-2 aircraft.

The Satellite Telemetry and Return Link (STARLink) is an innovative approach for providing real-time data from existing experiments and allows for highly interactive future experiment systems on the ER-2. The concept involves placing an advanced wideband data link system on the ER-2 (and future NASA aircraft) for communicating to the NASA Tracking Data and Relay Satellite System (TDRSS) and its designated ground station. The emphasis is on providing full duplex real-time data between the ground station hub (and its remote nodes) and the on board experiments, allowing real-time processing and alteration to the experiments. This paper defines the concept, goals, multiplexing and data transmission system architecture, current capabilities, and future plans of the STARLink and its ability to provide a distributed interactive gateway node between the aircraft and various scientific centers worldwide.

ACKNOWLEDGMENT

The following are a few of the individuals whose efforts have made STARLink a reality:

Gia Tran, STARLink Project Engineer, ATAC - Ames Research Center
Eugene Ferrick, Director, Space Network Division, NASA HQ
John Arvesen, Chief, High Altitude Missions Branch, NASA-ARC
Jim Barrilleaux, ER-2 Pilot, High Altitude Missions Branch, NASA-ARC
Allan Cartledge, Science Coordinator, High Altitude Missions Branch, NASA-ARC
Dr. Michael L. Ownby, Senior Staff Engineer. UNISYS Communication Systems, Government Systems Group.
Dr. LaMar K. Timothy, Senior Staff Engineer. UNISYS Communication Systems, Government Systems Group.
Mr. Robert E. Anderson, Staff Engineer. UNISYS Communication Systems, Government Systems Group.

ACRONYMS

ADR	Airborne Data Recorder
AGC	Automatic Gain Control
AMA	Airborne Modem Assembly
ARC	Ames Research Center
BER	Bit Error Rate
CVSD	Continuous Variable Slope Data
dB	decibels
deg	degree
DomSat	Domestic Satellite
EIRP	Effective Isotropic Radiated Power
ER-2	Earth Resources -2 Aircraft
G/T	Gain / Temperature
HVPS	High Voltage Power Supply
IF	Intermediate Frequency
K°	Kelvin
Kbit	Kilobits
KSA	Ku-band Single Access
LAN	Local Area Network
Mbit	Megabits
Mhz	Megahertz
NASA	National Aeronautics and Space Administration
NASCOM	NASA Communication
NCC	Network Control Center
O-QPSK	Offset Quadro Phase Shift Keyed
PI	Principle Investigator
POCC	Payload Operations Control Center
RF	Radio Frequency
s	seconds
STARLink	Satellite Telemetry and Return Link
STATMUX	Statistical Multiplexer
STGT	Second TDRSS Ground Terminal
TDRS	Tracking Data and Relay Satellite
TDRSS	Tracking Data and Relay Satellite System
TWTA	Traveling Wave Tube Amplifier
WAN	Wide Area Network
WSC	White Sands Complex

DESCRIPTION

The Satellite Telemetry and Return Link (STARLink) is an information system that is being integrated onto the NASA ER-2 aircraft located at Ames Research Center. This paper is designed to present an overview of the entire STARLink system.

STARLink system enables multiple instruments on board an ER-2 aircraft to continuously transmit the data being generated from each individual instrument to its respective Principle Investigator (PI), located anywhere Internet or telephone systems are present. STARLink also is capable of allowing the PIs who receive data to connect with the airborne instrument and control its functions or fine tune its data acquisition. Should it become necessary for the flight path or cockpit control of the instrument to be modified, a voice channel exists between the ground and the pilot. STARLink has the potential to create a telepresence system for the PIs who use the ER-2 aircraft.

ER-2 aircraft fly four basic missions: disaster response, stratospheric in-situ measuring, tropospheric meteorological studies and earth resource remote sensing. The requirements for STARLink are real-time data transfer and display, continuous coverage, and to provide command uplink. The real-time data transfer and display will be used for disaster situation monitoring such as fires, floods, hurricanes and earthquakes. These disasters currently take a few hours after landing to get the data to the appropriate disaster control agencies. Through STARLink the data can be transmitted instantaneously. This real-time data transfer and display will also support telepresence and telescience requirements of the stratospheric, tropospheric and earth resource science communities to maximize the data return from the missions. Continuous coverage for all these missions will normally be 4 to 6 hours, but could be up to 8 hours during extended missions. The coverage will need to be sustained over the entire 5000 km range of the ER-2 aircraft. The command link will also allow the PI to use the instrument in the teleoperate mode over the entire range of the ER-2 aircraft.

CONFIGURATION

The STARLink architecture is made up of three major elements; 1) the Airborne Element, 2) the TDRSS Elements, and 3) the Ground Station Element at Ames Research Center (See Figure 1).

Figure 1 - STARLink Elements

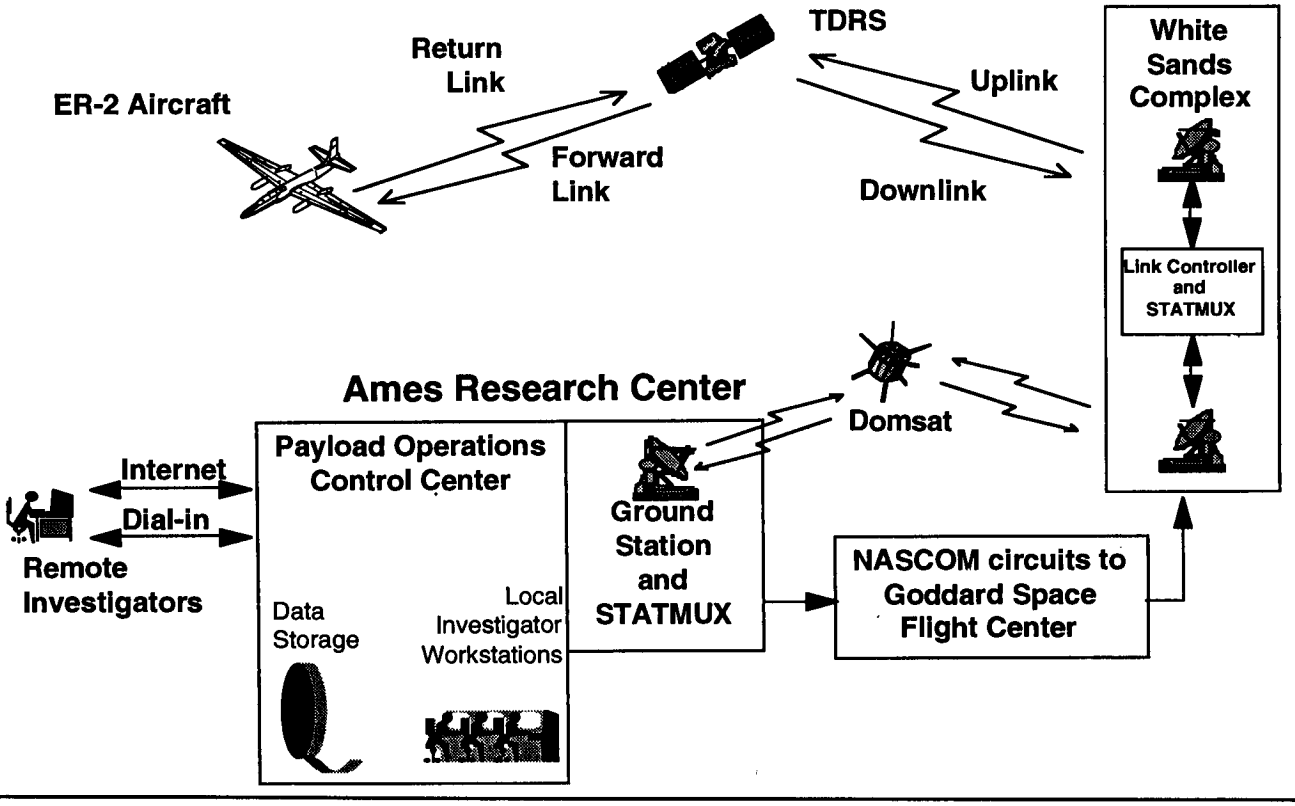

AIRBORNE ELEMENT

The Airborne Element consists of an Airborne Data Recorder (ADR) used as temporary buffer and storage for digital data channels from onboard experiments. The ADR interfaces to the Airborne Modem Assembly (AMA). The AMA provides multiplexing and demultiplexing of the various channels, modulates the aggregate return link I and Q channels, consisting of 137 Mbit/s each, and demodulates the forward link channels, consisting of 200 Kbit/s. Both the return and forward link Intermediate Frequency (IF) of 1700 Mhz are passed to the transceiver for conversion and amplification to the TDRSS Ku-band frequencies. The return link is transmitted to the satellite via a 400 watt Traveling Wave Tube Amplifier (TWTA) and a 30-inch steerable parabolic antenna.

Figure 2 - Link Capacities

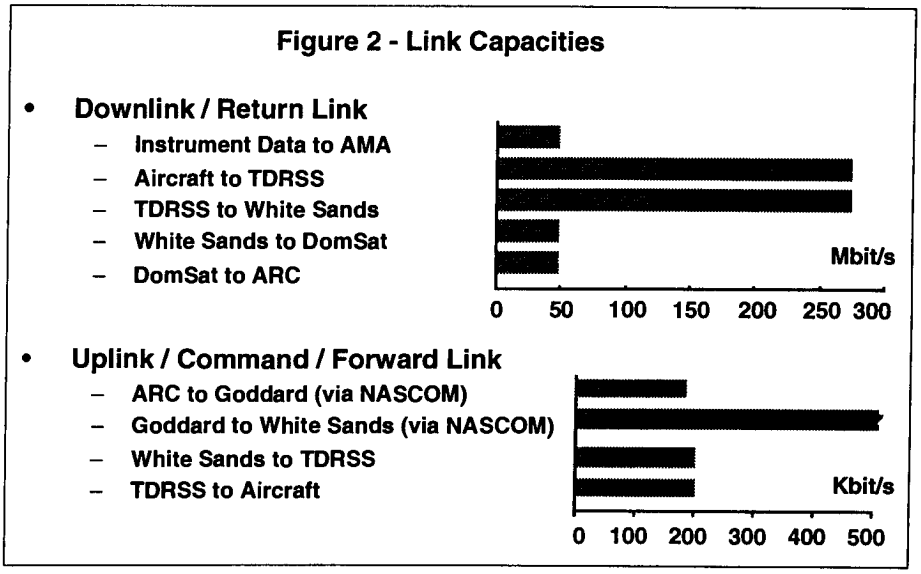

TDRSS ELEMENT

The TDRSS Element consists of the TDRSS constellation and the designated Second TDRSS Ground Terminal (STGT). The Ku-band Single Access (KSA) transponder of the TDRSS is utilized to receive the ER-2 RF return link of 274 Mbit/s with Offset Quadro Phase Shift Keyed (O-QPSK) modulation and relay the RF energy to one of the three designated STGT antennas at the White Sands Complex (WSC). The signal is then routed to the RF baseband equipment where it is demodulated and converted. The aggregate 137 Mbit/s channels are demultiplexed by the link controller into a combination of 42 Mbit/s, 21 Mbit/s, 6 Mbit/s, and 1.5 Mbit/s channels. A combined 48 Mbit/s (4 channels) is routed to the WSC Statistical Multiplexer (STATMUX) and to an existing Domestic Satellite (DomSat) earth station node for transmission to Ames Research Center.

GROUND STATION ELEMENT

The Ground Station Element center at Ames allows investigators to use telephone modems, Internet or a private on-site Local Area Network (LAN) for access to their data. This data distribution center will also coordinate all command link activity to send information back to the aircraft from the wide or local area networks. All the multiplexing and demultiplexing activity is performed in this control center. A full duplex voice channel is embedded within the architecture employing Continuous Variable Slope Data (CVSD) algorithm and allows constant communication with the ER-2 pilot. The ground station also performs all the necessary scheduling and coordination activity with the TDRSS Network Control Center (NCC) at Goddard Space Flight Center, Greenbelt, MD. both in advance of the mission and during flight operations.

LINK CAPABILITIES

The aircraft to White Sands maximum data transfer capability is 274 Mbit/s. The White Sands to aircraft data transfer capability is 200 Kbit/s. These are the maximum data transfer rates the STARLink system is anticipated to attain.

There are several link limitations that currently exist, but may be improved upon as the national information highway is upgraded. (See Figure 2.) STARLink, when using the STATMUX system developed for the Space Shuttle, limits the downlink through the DomSat to Ames at 50 Mbit/s. This downlink limit should be eliminated in the future to capitalize on the full data rate transfer capabilities that exist between White Sands and the aircraft.

The Ames to Goddard NASCOM data rate limit is 170 Kbit/s. In addition to the NASCOM limit, there is 20 Kbit/s of digital voice and 10Kbit/s of overhead transmitted through Goddard to WSC. The combined uplink can thus utilize the full 200 Kbit/s capability of the TDRSS system.

ENVIRONMENTAL QUALIFICATIONS

The STARLink installation onboard the ER-2 aircraft is an unpressurized environment operating at the aircraft mission altitude of 70,000 feet. The system is qualified to a full MIL-Spec range for temperature, altitude, and vibration experienced by the ER-2. One critical element is the High Voltage Power Supply (HVPS), which weighs less than 75 pounds, occupies 1.1 cubic feet, and employs encapsulation for isolation between high voltages exceeding 12K volts.

ANTENNA PERFORMANCE

A challenging element of the STARLink is its requirement to constantly track the TDRSS throughout the various aircraft maneuvers and attitudes. The tracking subsystem of STARLink is described below:

OPEN-LOOP VS. CLOSED-LOOP TRACKING

The term "open-loop" implies that the antenna receives no feedback from the satellite as to whether it is pointed correctly. The pointing accuracy depends entirely on a number of independent parameters, such as the accuracy of the on board Inertial Navigation System (INS), the correctness of the expected location of the satellite target, the precision of the antenna mounting relative to the INS, the resolution of the control computer and synchros, the deflection of the radome, and the bending of the aircraft.

In closed-loop operation, the antenna boresight is intentionally deflected slightly away from the assumed target location, while maintaining RF link. Using the Automatic Gain Control (AGC) signal to determine the relative strength of the return RF signal in the neighborhood of the target direction, the control system determines where the actual peak RF is and tracks the target via feedback loops.

ADVANTAGES OF CLOSED-LOOP TRACKING

With closed-loop tracking, specifications on sources of pointing error can be relaxed, since the tracking system compensates for unknown errors during operation. If the unknown errors are fixed (e.g. mounting misalignments), closed-loop tracking need only be used initially to determine the fixed errors after which open-loop pointing will successfully maintain the RF link. If the errors are varying (e.g. different RF beam deflections in each section of the radome), then closed-loop tracking must operate continually.

THE STARLINK SELF-SCAN (STEP-TRACK) SYSTEM

A common way of achieving intentional deflection of the RF beam to achieve closed-loop tracking is to use a separate scanning device which rotates continually. The Unisys-proprietary "self-scan" (step-track) system does not require a separate scanning device; rather it relies on mathematical procedures to estimate the shape of the beam peak, determine the peak RF location, and develop offsets which cancel other pointing errors that are present.

THE STAR LINK ANTENNA PEDESTAL

The Unisys pedestal for this application uses high-torque AC motors which can slew either antenna gimbal at 60 deg/s. Aircraft maneuvers as large as 12.5 deg/s velocity and accelerations of 6 deg/s^2 are readily handled at elevation angles as large as 85 deg.

ANTENNA BEAMWIDTH

The antenna beam has a 3-dB beamwidth of 1.9 deg and a 1-dB beamwidth of 1.12 deg. Assuming the allowable link margin loss due to mispointing is 1 dB, the amount of mispointing allowed is one-half the 1-dB beamwidth, or 0.56 deg.

INERTIAL NAVIGATION SYSTEM ACCURACY

The pitch, roll, and yaw (attitude) outputs of the INS are combined with the latitude, longitude, and altitude estimates of both aircraft and satellite target (ephemeris) to produce open-loop azimuth and elevation commands to the antenna gimbals. INS attitude inaccuracies enter directly into the pointing error budget in a purely open-loop system. Since pointing error must be controlled to within ±0.56 deg, the INS attitude inaccuracy can only be a small fraction of this total.

With step-track closed-loop operation, the INS accuracy and specifications on other components can be relaxed. Under the assumption that the RF link can at least acquire (but not perform with specified bit error rate) if the antenna beam is mispointed 3 dB, combined pointing errors (including the INS) as large as 0.95 deg (one half of 1.9 deg) can be tolerated. Closed-loop step-track operation then develops offsets to cancel the errors and bring the bit error rate within specification.

ACQUISITION

Unisys has successfully operated systems whose INS, physical alignment, bending, and radome inaccuracies cause mispointing as great as 6 deg. In this case, an initial acquisition mode is necessary, because the data link may not acquire when pointing errors contribute more than 3 db loss of link margin. The Unisys acquisition mode involves a spiral scan search beginning at the open-loop pointing direction, continuing at ever-increasing radial distances until RF is acquired. Although 30 seconds are required to complete the full spiral (6 deg deflection from the center point), RF is typically acquired much sooner, as total pointing error is seldom worst case. After acquisition, closed-loop operation cancels the INS, physical alignment, bending, and radome errors.

Whenever the spiral acquisition mode is invoked, or whenever the step-track algorithm determines that pointing error exists, it is clear that the current azimuth and elevation commands are not quite correct. Accordingly, azimuth and elevation offsets are generated which, when added to the open-loop commands, point the antenna correctly.

STARFISH SCAN PATTERN

The Unisys closed-loop step-track algorithm commands small deviations of the RF boresight away from the assumed peak target location using the available azimuth and elevation gimbal drive motors—hence the name "self-scan." The small deviations, typically 0.28 deg, are commanded simultaneously in azimuth and elevation. After approximately 300 msec, the mechanical motion and AGC signals have stabilized at the new conditions, and 100 AGC samples are taken in rapid order. These samples are subsequently averaged in order to produce an AGC reading as noise-free as possible. The gimbals are then commanded back to the assumed peak target location for another 100 AGC samples. By reversing the sign of only one azimuth or elevation command at a time, a four-legged "starfish" scan pattern is executed, which consists of 8 different AGC measurements (4 at the center, and 4 at the legs). Thus, the antenna spends most of its time pointing in the assumed target direction. (See Figure 3.)

Figure 3 - Starfish scan pattern

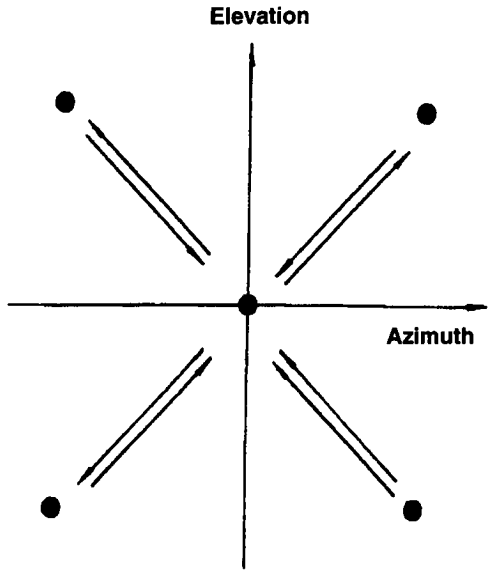

AZIMUTH AND ELEVATION OFFSETS

After a sufficient number of AGC measurements have been taken, least squares estimation algorithms are invoked to estimate two parabolas, representing the beam shape in both azimuth and elevation directions. If the peak of either parabola is not centered at the assumed target direction, then the algorithm assumes that the offsets which are applied to the processed outputs must be adjusted to maintain optimal tracking. (See Figure 4.)

The step-track algorithm then converts the apparent azimuth and elevation offsets into a set of roll, pitch, and heading offsets which, when applied to the INS outputs, produce the optimal RF boresight attitude. The advantage here is that the required azimuth or elevation offset can reverse sign when the aircraft reverses direction, while the roll, pitch, and heading offsets do not need to be re-estimated.

Figure 4 - Parabolic estimate of beam shape

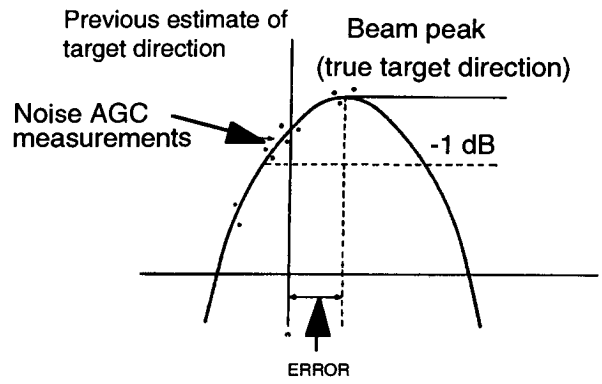

RF PERFORMANCE

The STARLink is a full duplex data link combining transmit and receive RF energy through a single antenna. The Effective Isotropic Radiated Power (EIRP) of the STAR Link is over 60.0 dBw. This is accomplished by utilizing a 400 Watt TWTA in conjunction with a 30 inch parabolic reflector achieving over 55 percent efficiency. The construction of the reflector and yoke system is of light weight composite material achieving a total antenna subsystem weight of less than 35 pounds. The receiver total Gain Over Temperature (G/T) is 10 dB/K°. The link quality is measured at 10E-8 Bit Error Rate (BER) for both the return and forward link with an uncommitted link budget of 3 dB and 10 dB, respectively.

INTERFACE TO STARLINK

There are two primary interfaces that an investigator needs to be concerned with. These interfaces are the Payload Hardware Interface and the Payload Operations Control Center.

PAYLOAD HARDWARE INTERFACE

The Payload Hardware Interface is shown in Figure 5a. The current aggregate transmission to the AMA cannot exceed 48 Mbit/s. This interface can be accomplished through several methods. For high data rate systems, 1.5 - 22 Mbit/s, there are three SCSI lines available. Any combination of data transmission between the high and low SCSI limits can be used (not to exceed the aggregate limit). The low data rate multiplexer contains seven bi-directional RS-232, 9600 baud lines and the inclusion of a NTSC video and aircraft navigation data broadcast. The low data rate multiplexer cannot exceed 1.5 Mbit/s. The forward command links to the instrument payloads have a current aggregate rate of 170

Airborne Element Interfaces

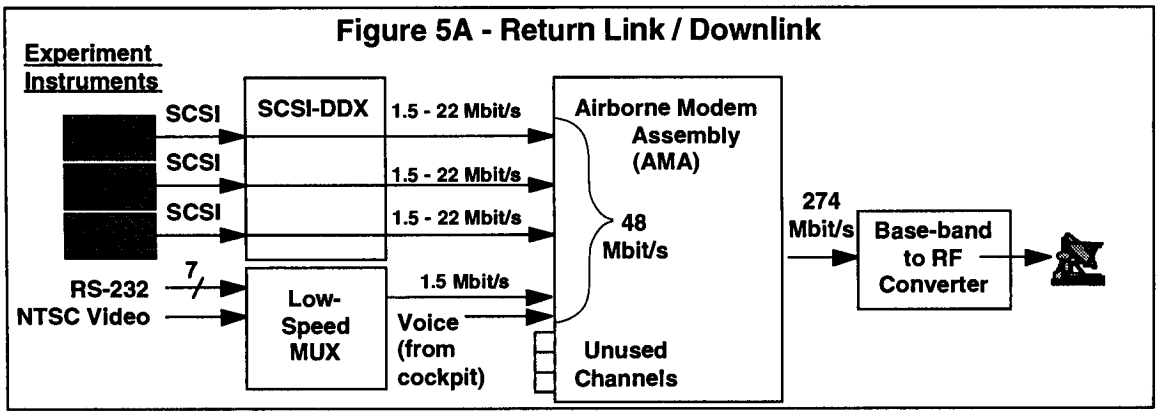

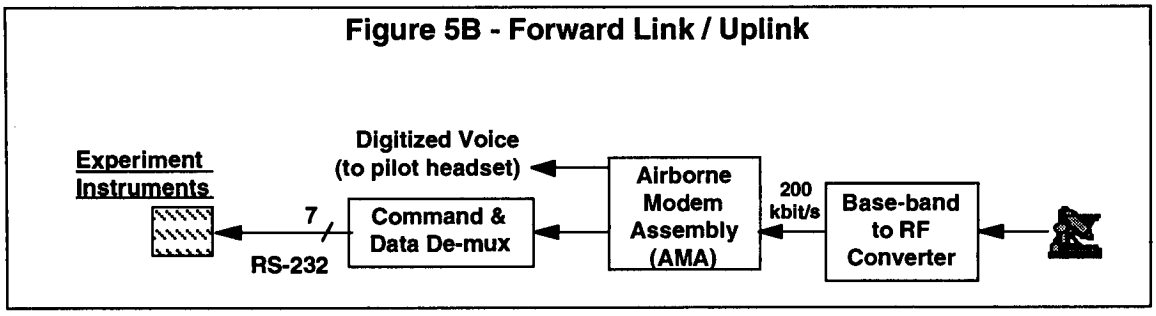

Kbit/s. Seven RS-232 lines are available at 9600 baud to teleoperate the instrument payload, (see Figure 5b). 30 Kbit/s of uplink bandwidth is reserved for digital voice and overhead functions.

PAYLOAD OPERATIONS CONTROL CENTER

The investigator has several methods available to access their data through the Ames Payload Operations Control Center (POCC). The slowest, but most available, will be

Figure 6 - Ground Station / POCC Interfaces

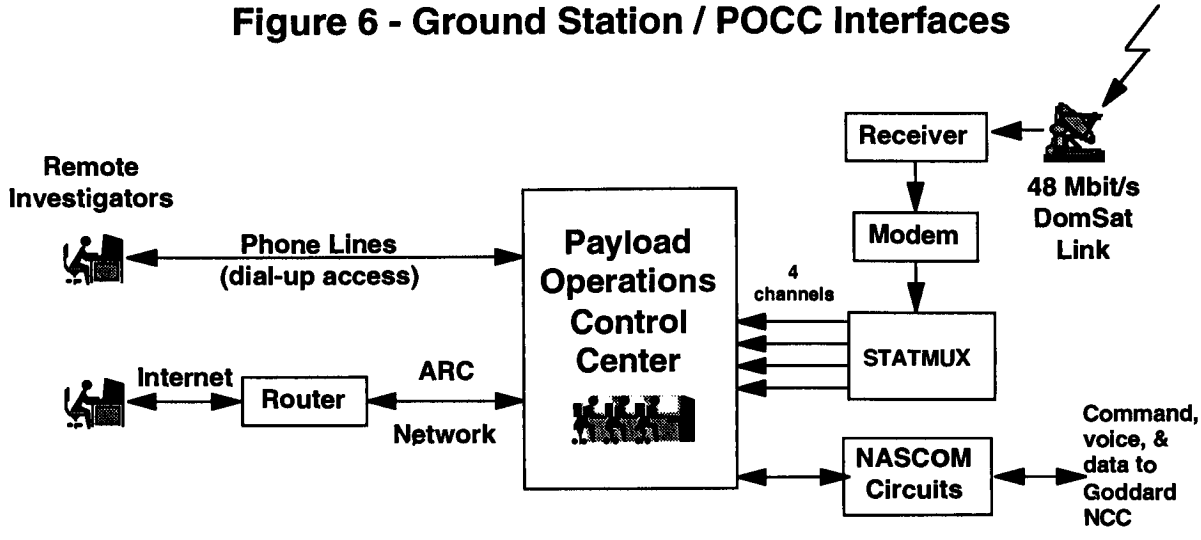

- **Basic POCC Services**

	On-site	Remote access
– Instrument command generation	√	√
– Data reduction, analysis, & display	√	√
– Data archival	√	√

through phone lines via a modem. The next fastest system will be through the Internet (Wide Area Network - WAN). The final and quickest real-time view and teleoperate capability will be at the STARLink facility at Ames Research Center which is directly tied to the POCC via a "private" Local Area Network (LAN). (See Figure 6.)

FLIGHT PLANNING AND CONTROL

Some operational considerations have been addressed regarding the use of the STARLink system as it applies to the flight operations:

1) All interaction with the pilot flying the ER-2 will be accomplished through a second pilot on the ground.
2) Use of the voice channel will be coordinated with the pilots prior to the mission
3) The type of commands sent by the investigators to teleoperate the instruments must be approved by the pilots prior to the mission.
4) The airborne pilot retains responsibility for the safe operation of the aircraft and conduct of the mission.

These operational considerations are necessary so that commands to the aircraft do not jeopardize ER-2 flight safety.

SUMMARY

STARLink is scheduled to be operational in late 1995. The initial STARLink utilization is in support of forest fire observations, by providing real-time imagery from the ER-2 scanner systems. The ER-2 operating at or below 70,000 feet, will transmit real-time data for worldwide dissemination over various LAN and WAN distribution systems. STARLink support of ongoing and future global research demonstrates NASA's continuing commitment to maximizing scientific return from its airborne programs. The STARLink architecture enhances current experiment capabilities by allowing real-time data dissemination, system monitoring and on-the-fly reconfiguration. It designed to allow for added growth capability, accommodating high resolution sensors and high data rate throughput. The programmability of the multiplexers and demultiplexers allows channel allocation to all on board experiments with a planned capability of up to the 274 Mbit/s TDRSS data rate capability.

REFERENCES

1) Prime Item Development Specifications (PID) for STARLink Communication Subsystem. UNISYS part number 8100114.

2) Interface Control Document (ICD) between the STARLink project and the Second TDRSS Ground Terminal -Draft- November 1994. 530-ICD-STGT/STARLink
NASA Goddard Space Flight Center. Greenbelt MD. 20771

3) Interface Control Document (ICD) between the STGT and Ground Communications Facilities - December 1987. STD No. 220.30 Goddard Space Flight Center. Greenbelt MD. 20771

4) **TDRSS Support Study for NASA Research Aircraft.** NASA Goddard Space Flight Center. Greenbelt MD. 20771 - September 1993- Stanford Telecom.

5) **Tracking and Relay Satellite System (TDRSS) Users Guide** - STDN No. 1001.2 Rev. 6

6) **TDRSS Orientation and System Data Flow** - Course 880, Student Workbook Rev. 12, 500-1151.4 NASA Goddard Space Flight Center. Greenbelt MD. 20771 - September 1993

7) **TDRSS Constraints and Scheduling Procedures** - Course 882, 500-NTTF-882.4 NASA Goddard Space Flight Center. Greenbelt MD. 20771 - February 1993

8) **TDRSS Ground Operations/Fault Isolation Procedures Student Workbook** - Course 883, 500-NTTF-883.4 NASA Goddard Space Flight Center. Greenbelt MD. 20771 - March 1993

ACTS Aeronautical Terminal Experiment: System Description and Link Analysis

Philip Sohn and Charles Raquet
NASA Lewis Research Center, 21000 Brookpark Rd, MS 54-6, Cleveland, OH 44135

Richard Reinhart, Analex Corporation, Brookpark, OH

and

Dan Nakamura, Jet Propulsion Laboratory, Pasadena, CA

ABSTRACT

During the summer of 1994, the performance of an experimental mobile satellite communication system was demonstrated to the industry and government representatives by the NASA Lewis Research Center (LeRC) and the Jet Propulsion Laboratory (JPL). The system was based on the Advanced Communications Technology Satellite (ACTS) and consisted of an K-/Ka-band active MMIC phased array antenna system, ACTS Mobile Terminal (AMT) and Link Evaluation Terminal (LET). A LeRC research aircraft, Learjet Model 25, was outfitted with the active MMIC phased array antenna system and AMT and served as the experimental 20/30 Ghz aeronautical terminal. The LET at LeRC in Cleveland, OH was interfaced with portions of fixed-AMT equipment and together provided the gateway station functions including ACTS satellite interface and Public Service Telephone Network (PSTN) interface. The ACTS was operated in its Microwave Switch Matrix (MSM) mode with a spot beam for the Learjet and another spot beam dedicated to the LET. The Learjet was flown over several major cities across the US and demonstrated the feasibility of full-duplex compressed voice link for an aeronautical terminal through the 20/30 Ghz ACTS satellite channel. This paper will present a technical description of the system including the MMIC phased array antenna system, AMT, Learjet, LET and ACTS satellite. The array antenna system consists of a 30 Ghz transmit array (LeRC/Texas Instruments) and two 20 Ghz receive arrays (USAF Rome Lab/Boeing and Martin Marietta), each one very small with sufficient performance for satellite voice link. The AMT consists of 2.4/4.8/9.6 Kbps voice coder/decoder, modem, PSTN interface and RF/IF converters. Link analysis will be presented and compared to the actual performance data collected during the demonstration flights.

SYSTEM DESCRIPTION

The overall system setup for the ACTS Aeronautical Terminal Experiment (AEROX) is illustrated in Figure 1. The system consisted of the ACTS satellite at 100°W in geosynchronous orbit, the Fixed Terminal (FT) located at the NASA LeRC in Cleveland, OH, and the Learjet aeronautical terminal (LJ) visiting several metropolitan areas in the United States.

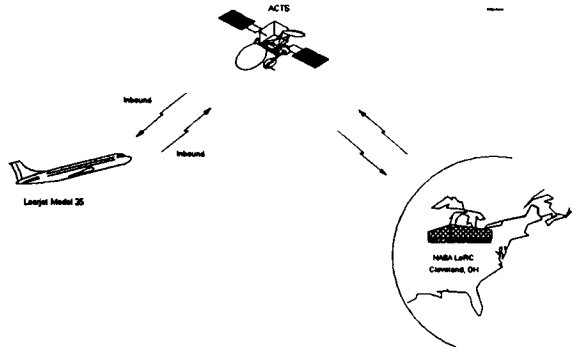

Figure 1: System Setup

The system demonstrated full-duplex voice at 4.8 Kbps between the FT and the LJ. Since the FT equipment included Public Service Telephone Network (PSTN) interface, many attendees at the various demonstration sites were able to experience the quality of seamless voice calls made from the LJ telephone handset.

ACTS Satellite

The ACTS is a proof-of-concept 30/20 Ghz satellite that was developed by Géneral Electric - now Martin Marietta - under contract to NASA and launched by the Space Shuttle Discovery (STS-51) in September, 1993. It was designed to validate key technologies such as 1) satellite Multibeam

Antenna (MBA) which produces multiple high gain spot beams that can be rapidly hopped, scanned or fixed; 2) Baseband Processor (BBP) which demodulates, routes individual circuit-switched messages and re-modulates; and 3) Microwave Switch Matrix (MSM) which handles up to 900 Mhz bandwidth signals and provides rapidly reconfigurable connectivity between the spot beams.

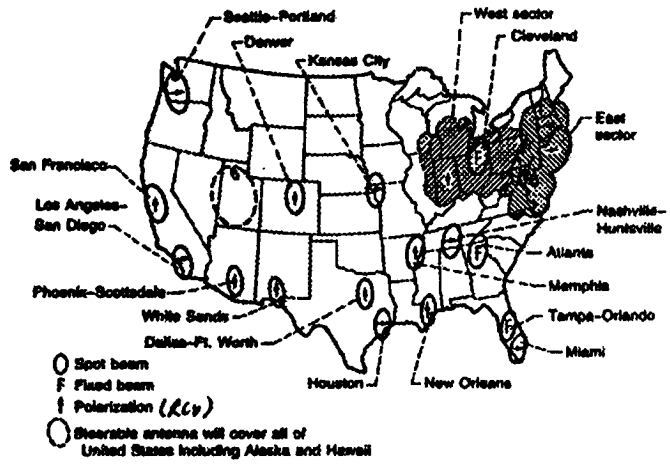

Figure 2: ACTS Satellite Coverage

Table 1: ACTS Transponder Characteristics

	G/T	EIRP
Cleveland	23.10	69.49
Dayton WS19	20.06	65.11
Washington DC	20.40	65.34
Boston, ES4	20.40	65.49
Dallas	22.31	67.77
Los Angeles	21.06	65.34
Seattle	21.16	65.54
Baltimore ES12	20.63	65.34

The MBA uses offset-fed cassegrain configuration with 2.2 meter and 3.3 meter main reflectors for the receive and transmit beams, respectively. The coverage afforded by this antenna technology on ACTS is illustrated in Figure 2. As evident in the figure, sixteen isolated metropolitan areas and two contiguous sectors - East and West - are covered in the CONUS. In addition, ACTS provides a mechanically steerable 1.1 meter antenna which produces a relatively larger spot beam for coverage anywhere on earth visible from its orbital position.

The West scan sector was used during the first phase of AEROX when Learjet flew between Cleveland and Chicago to checkout the system. The West scan sector is divided into twenty-two spot beam locations and "scanning" effect can be achieved by sequentially illuminating the adjacent spots. As Learjet flew between the two cities, it transversed three spot beam locations and the MBA and MSM configurations had to be controlled in real-time to track the Learjet by using this scanning capability.

Following the first phase of AEROX, the LJ and AEROX team members visited eight cities - Cleveland, Dayton, Washington DC, Boston, Dallas, Los Angeles, Seattle and Baltimore - and gave demonstrations to well-attended audiences which consisted of industry and government representatives. The relevant ACTS transponder characteristics for these cities are presented in Table 1.

Fixed Terminal (FT)

The FT was constructed by interfacing portions of NASA LeRC Link Evaluation Terminal (LET) with portions of JPL fixed-AMT. A block diagram is presented in Figure 3.

The LET was developed by NASA LeRC to evaluate the performance of ACTS satellite in MSM mode of operation. For this purpose, LET includes Serial Minimum Shift Keying (SMSK) modem, custom bit error rate test unit for data rates ranging from 1.25 to 200 Mbps, adaptive uplink power control capability to test rain fade compensation algorithms, and easily accessible IF interface which allows unique IF and baseband equipment to be tested over the ACTS satellite channel. The LET RF components used in the AEROX are 4.7 meter antenna, 30 Ghz transmitter based on a 60 Watt Traveling Wave Tube Amplifier (TWTA) and 20 Ghz low noise receiver. The LET is also responsible for generating the computer commands that control the ACTS satellite configuration for MSM mode of operation - specifically choosing the spot beams and the connectivity of the MSM.

The AMT was developed by NASA at the JPL to demonstrate the viability of speech (at 2.4, 4.8 and 9.6 Kbps) and data transmission (at 2.4, 4.8, 9.6 and 64 Kbps) in the 30/20 Ghz mobile satellite communications environment. The AMT components used at the AEROX FT are speech coder/decoder (CODEC), modem, IF Converter (IFC), Terminal Controller (TC), and data acquisition system (DAS).

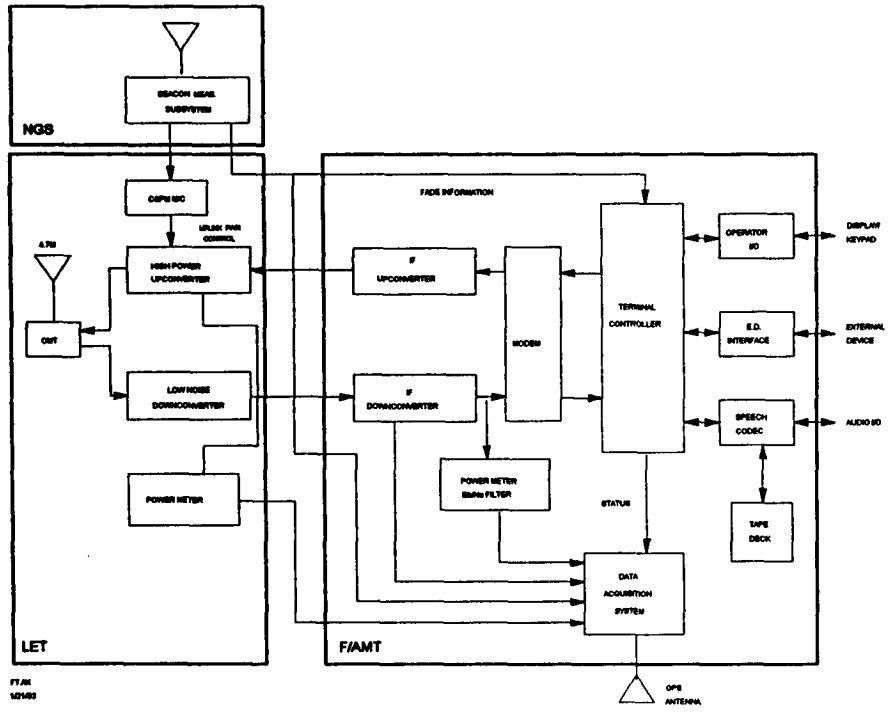

Figure 3: Fixed Terminal

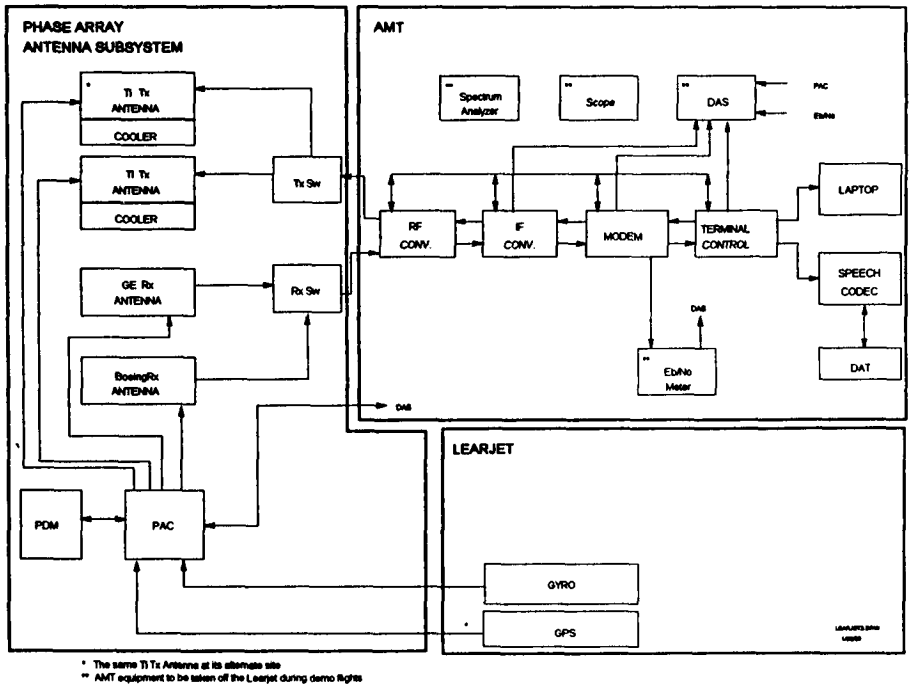

Figure 4: Learjet Terminal

The speech codec provided the audio user interface into the AEROX system. It converts analog speech input to a compressed digital representation at output data rates of 2.4, 4.8, or 9.6 Kbps using the government standard LPC-10, the proposed CELP government standard, or the MRELP (Motorola's proprietary algorithm), respectively. Data rate is controlled by the TC, either automatically (based on a rain fade compensation algorithm) or manually. For AEROX, data rate was fixed at 4.8 Kbps. The speech codec also provides interface into the PSTN. When the mobile user at Learjet enters a phone number on his handset, the FT speech codec receives the connection request and the phone number, takes its phone line off hook and generates the required dialing tones to initiate the call through the PSTN.

The modem implements a simple but robust Differential Phase Shift Keying (DPSK) scheme with rate 1/2 convolutional coding and interleaving. This scheme was chosen to minimize the effects of environmental shadowing and phase noise in the ACTS. The modem BER performance at 9.6 Kbps in AWGN has been measured to be 1E-3 at an Eb/No of 6.6 dB. The modem is designed to handle a frequency offset of +/- 10 Khz with a slew rate of 250 Hz/sec. The performance curve of the modem with respect to a fixed frequency offset is flat in the range of +/- 10 Khz and the degradation is less than 0.5 dB for offsets of +/- 20 Khz.

The IFC is responsible for the first stage of frequency translation from 70 Mhz to 3.373 Ghz on the uplink and 3.373 Ghz to 70 Mhz on the downlink. The IFC, under TC control, implements selection of transmit and receive frequency channels. The IFC also provides transmit and receive rotary attenuators which allow the operator to set transmit and receive RF power levels within 0 to 60 dB range with 1 dB precision.

The DAS is responsible for recording all actions and data taken by the terminal for postanalysis. The data is stored using two 8mm tape drives for 8 hours of continuous recording. Each DAS has a GPS receiver which it uses to continually update the internal clock for accurate time stamping of the data. For accurate measurement of received power, DAS provides three easily accessible bandpass filters. Each filter noise bandwidth has been measured and the operator can make the selection based on the data rate.

Learjet Aeronautical Terminal (LJ)

The Learjet model 25, a NASA LeRC research aircraft, served as the aeronautical mobile platform containing the aeronautical part of the AEROX communications electronics. A block diagram is presented in Figure 4. The major communications gear consisted of the NASA LeRC 30/20 Ghz phased array antenna system and the JPL AMT.

The phased array antenna system [3] consisted of one transmit array antenna and two receive array antennas. The antennas were mounted inside the Learjet looking out the standard plexiglass windows. Both receive array antennas were mounted, one on each side of the fuselage. The transmit array antenna had to be moved from side to side - depending on LJ flight profile. These array antennas incorporated individual GaAS MMIC devices for the individual radiating elements for electronic beam steering and distributed power amplification. An open loop antenna controller developed by the NASA LeRC used information from GPS and aircraft gyroscopes to electronically steer the array beams toward ACTS during flight.

The set of AMT equipment used in LJ was identical to that in the FT with the addition of RF Converter (RFC). The RFC translates the output of the IFC from 3.383 Ghz to 29.644 Ghz for transmit and the 19.904 Ghz receive signal to 3.363 Ghz.

LINK ANALYSIS

In the outbound direction, the FT transmitted a modulated carrier at 29.644 Ghz; the ACTS transponder received this carrier, translated it in frequency and downlinked it to the LJ at 19.924 Ghz. In the inbound link, the LJ transmitted its modulated carrier at 29.624 Ghz; ACTS transponder received this inbound carrier and downlinked it to the FT at 19.904 Ghz. Nominal data rate of 4.8 Kbps was chosen for AEROX. The modem - implementing DPSK technique with rate 1/2 convolutional coding and interleaving - required input C/No to the demodulator to be greater than 46.3 dB-Hz to ensure a link performance of 1E-3 or better in terms of the end-to-end Bit Error Rate (BER).

Table 2: Outbound Link Budget

FT Uplink Frequency	29.644	GHz
LET EIRP	53.80	dBW
LET Pointing	-0.80	dB
LET Pol Mismatch	-0.13	dB
Path loss	-213.45	dB
Atmosphere loss	-0.364	dB
Rain loss	0.00	dB
ACTS Cleveland G/T	23.10	dB/K
Antenna Gain	52.90	dBi
ACTS Beam Contour	0.00	dB
Uplnk C/No	90.75	dB-Hz
Uplnk CNR	-0.04	dB
Effective BW	1200	MHz
Limiter Effect	0.00	dB
Eff Uplnk CNR	-0.04	dB
Eff Uplnk C/No	90.75	dB-Hz
Downlink to LJ Frequency	19.924	GHz
ACTS Seattle EIRP	65.54	dBW
ACTS S/(S+N)	-3.03	dB
ACTS Beam Contour	-1.00	dB
Path loss	-210.11	dB
Atmosphere loss	-0.502	dB
Rain loss	0.00	dB
LJ G/T	-17.20	dB/K
LJ Pointing Error	-0.50	dB
LJ Pol Mismatch	-0.85	dB
Dwlnk C/No	60.94	dB-Hz
Outbound Link		
Achieved C/No	60.94	dB-Hz
Required C/No	46.31	dB-Hz
Bit Rate	4.80	Kbps
AWGN Eb/No req	6.00	dB
Modem Implem	1.00	dB
FreqOffsetPhaseNoise	2.50	dB
Performance Margin	14.62	dB

Outbound and inbound link budgets [1] are presented in Tables 2 and 3, respectively. Link margins are calculated with Learjet at 5 dB contour of the ACTS spot beam over Seattle, WA. The ACTS transponder is a highly non-linear hard-limiting channel and degrades carrier-to-noise

ratio by about 1 dB for small signals such as the one in the AEROX inbound link [2].

Table 3: Inbound Link Budget

LJ Uplink Frequency	29.624	GHz
LJ EIRP	23.40	dBW
LJ Pointing Loss	-0.50	dB
LJ Window Loss	-2.22	dB
LJ Pol Mismatch	-0.85	dB
Path loss	-213.56	dB
Atmosphere loss	-0.364	dB
Rain loss	0.00	dB
ACTS Seattle G/T	21.16	dB/K
Antenna Gain	50.80	dBi
ACTS Beam Contour	-5.00	dB
Uplink C/No	50.67	dB-Hz
Uplink CNR	-40.13	dB
Effective BW	1200	MHz
Limiter	-1.05	dB
Eff Uplink CNR	-41.18	dB
Eff Uplink C/No	49.62	dB-Hz
Downlink to FT Frequency	19.904	GHz
ACTS Cleveland EIRP	69.49	dBW
ACTS S/(S+N)	-41.18	dB
ACTS Beam Contour	0.00	dB
Path loss	-209.99	dB
Atmosphere loss	-0.502	dB
Rain loss	0.00	dB
LET G/T	27.48	dB/K
Antenna Gain	57.56	dBi
LET Pointing Loss	-0.50	dB
LET Pol Mismatch	-0.13	dB
Dwlnk C/No	73.26	dB-Hz
Inbound Link		
Achieved C/No	49.60	dB-Hz
Required C/No	46.31	dB-Hz
Performance Margin	3.28	dB

In the outbound link, the FT was configured with an EIRP of about 53.8 dBW and the calculated link margin was in excess of 10 dB. Since FT was capable of up to 70 dBW EIRP, this outbound link had significant reserve margin. In the inbound link, however, the maximum EIRP which the LJ TI array antenna could afford was measured to be 23.4 dBW. After quite significant loss through the standard plexiglass window in the Learjet - measured transmission efficiency of about 60% - and with an estimated combined total of about 1.4 dB for pointing error and polarization mismatch, the calculation shows a margin of about 3.3 dB for inbound link. The inbound link was completely uplink-limited.

Link Performance Data

The inbound carrier and noise in the receiver chain at the FT was measured by HP power meter via a calibrated 31.8 Khz bandpass filter in the DAS. A personal computer controlled the power meter - and a spectrum analyzer - and recorded power measurements about every 2 seconds. This data was processed to separate the power in carrier from that in noise. Since the rotary attenuator in the FT downconverter had to be changed several times during the demonstration, data processing involved subtracting out the effects of the changes made to the downconverter and determining noise reference by using data when the LJ was not transmitting.

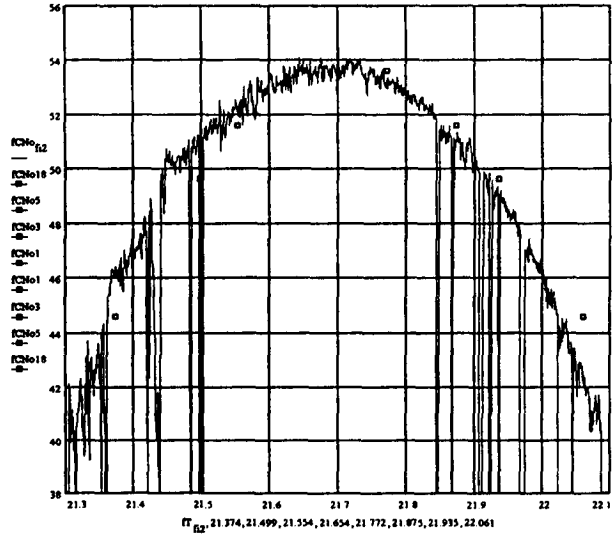

Figure 5: Inbound Link C/No vs. GMT

The inbound link carrier-to-noise density ratio, C/No, recorded during the Seattle demonstration flight on August 4, 1994 is plotted with respect to Greenwich Mean Time (GMT) in Figure 5. Also plotted in Figure 5 are the rectangular symbols representing the calculated C/No values.

The Learjet flight path corresponding to this data is plotted in Figure 6 along with the 10, 5, 3 and 1 dB contours of the ACTS uplink spot beam for Seattle. The Learjet flight

path is obtained from a notebook computer which recorded GPS coordinates and time. The ACTS beam contours are predictions based on pattern measurements before launch of ACTS satellite.

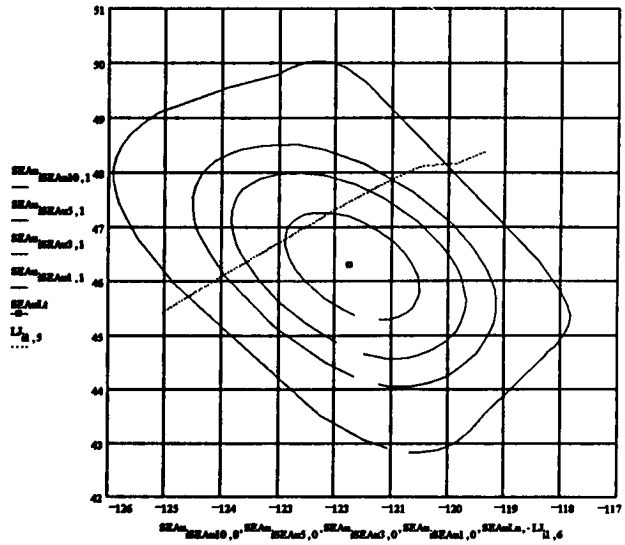

Figure 6: Seattle Beam Contours and Learjet Trajectory

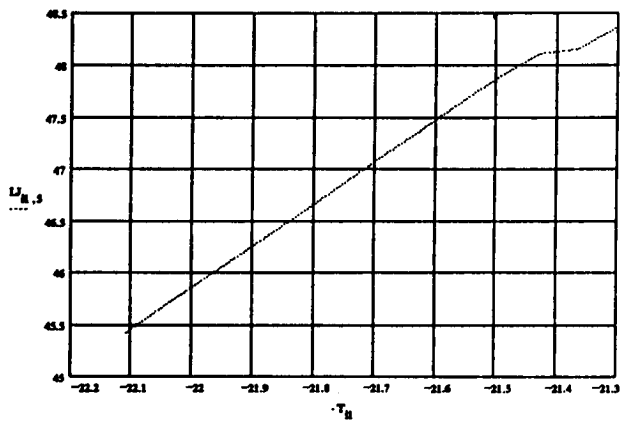

Figure 7: Learjet Latitude vs. GMT

To correlate Learjet movement with time, the Learjet latitude coordinates are plotted with respect to negative values of GMT in Figure 7. The Learjet flew south-west at an altitude of about 43,000 ft and crossed 48.15N, 47.87N, 47.66N, 47.26N, 46.78N, 46.36N 46.12N and 45.62N latitude lines at about 21.37, 21.50, 21.55, 21.65, 21.77, 21.87, 21.93 and 22.06 GMT, respectively. According to the data, these coordinates and times correspond to Learjet entering (and subsequently exiting - in reverse order) 10, 5, 3 and 1 dB contours. The inbound link budget calculation predicts C/No to be 44.6, 49.6, 51.6 and 53.6 dB-Hz for LJ at 10, 5, 3 and 1 dB contours, respectively. As shown in Figure 5, measured performance supports these predictions very closely. The data does suggest that the spot beam position is shifted - relative to the prediction - toward east by a small amount.

Good quality full duplex voice communication with LJ and FT/PSTN continued until about 22.0 GMT. Afterwards, the voice quality degraded rapidly and flight was aborted at about 22.1 GMT with the LJ well outside the 10 dB contour.

Outbound link parameters were recorded at the LJ but could not be processed due to a number of complications. For example, an accurate assessment of the FT EIRP could not be made - the rotary attenuator in the FT transmit chain was found to be faulty and the transmit power was not recorded in real-time.

CONCLUSION

The AEROX program provided an opportunity to showcase many proof-of-concept technologies found in the ACTS satellite, active phased array antennas and AMT. System description and link budget for Learjet in Seattle, WA have been presented. Actual data recorded at FT during the Seattle demonstration flight has been presented.

REFERENCE

1. Philip Sohn, Khalid Dessouky, Robert Zakrajsek, "Link Analysis for ACTS Baseline Aeronautical Experiment," NASA Lewis Research Center, ACTS Project Office, Interoffice Memorandum, February 19, 1992.

2. J. J. Jones, "Hard-Limiting of Two Signals in Random Noise," IEEE Transactions on Information Theory, January, IT-9, pp 34-42, January, 1963.

3. C. Raquet, R. Zakrajsek, R. Lee and J. Turtle, "Ka-band MMIC Arrays for ACTS Aero Terminal Experiment," 43rd Congress of the International Astronautical Federation, August 28-September 5, 1992.

ACTS Broadband Aeronautical Terminal

M.J. Agan, A.C. Densmore

Jet Propulsion Laboratory, California Institute of Technology
4800 Oak Grove Drive
Mail Stop 238-420
Pasadena, California 91109
Phone: (818) 354-3426 FAX: (818) 354-6825 E-mail: agan@bvd.jpl.nasa.gov

ABSTRACT

This paper discusses the design of, and experiments with, the ACTS Broadband Aeronautical Terminal. As part of the ongoing effort to investigate commercial applications of ACTS technologies, NASA's Jet Propulsion Laboratory and various industry/government partners are developing a broadband mobile terminal for aeronautical applications. The ACTS Broadband Aeronautical Terminal is designed to explore the use of K/Ka-band for high data rate aeronautical satellite communications. Currently available commercial aeronautical satellite communications systems are only capable of achieving data rates on the order of tens of kilobits per second. The broadband terminal, used in conjunction with the ACTS mechanically steerable antenna, can achieve data rates of 384 kilobits per second, while use of an ACTS spot beam antenna with this terminal will allow up to T1 data rates (1.544 megabits per second). The aeronautical terminal will be utilized to test a variety of applications that require a high data rate communications link. The use of the K/Ka-band for wideband aeronautical communications has the advantages of spectrum availability and smaller antennas, while eliminating the one major drawback of this frequency band, rain attenuation, by flying above the clouds the majority of the time.

INTRODUCTION

Since shortly after the launch of the ACTS in September, 1993 the NASA/JPL developed ACTS Mobile Terminal (AMT) has been conducting land-mobile satellite experiments in conjunction with a variety of industry partners[1]. Much has been learned about this communications channel as a result of these experiments [2]. A natural extension of these experiments was to investigate the K/Ka-band aeronautical communications channel by installing and testing the AMT in an aircraft [3]. Building on these aeronautical experiments the ACTS Broadband Aeronautical Terminal was designed to operate at higher data rates (≥384 kbps vs. 4.8 kbps), and without restrictions on the flight path or aircraft dynamics.

The specific experimental objectives with this terminal are to: (1) demonstrate and characterize the performance of high data rate aeronautical Ka-band communication (2) characterize the propagation effects of the communications channel during take-off, cruise, and landing phases of flight, (3) provide the systems/technology groundwork for an eventual commercial Ka-band aeronautical satellite communication system.

USE OF ACTS

ACTS is an experimental K/Ka-band satellite launched by NASA to explore advanced communication satellite technologies [4]. Positioned in geosynchronous orbit at 100° W longitude, ACTS transmits at 20 GHz and receives at 30 GHz. This experiment requires ACTS to operate in the baseband processor mode, in which it behaves as a bent-pipe transponder. The ACTS LA/San Diego spot beam will be used to establish the communication link between the fixed terminal at JPL and ACTS. The ACTS 1 meter diameter mechanically steerable dish antenna will be used to establish the link between ACTS and the aircraft.

The use of the ACTS steerable dish distinguishes this experiment from the previous ACTS land mobile and aeronautical mobile experiments in that the previous utilized an ACTS spot beam to illuminate the mobile terminal. The benefit of using the steerable antenna is that it removes the restriction that the flight path be within geographically fixed spot beam contours, allowing the aircraft to fly anywhere in the Western hemisphere. The drawback of using the ACTS steerable antenna is that it is smaller and thus has lower gain than the spot beam antennas, approximately 10 dB less on transmit and 7 dB less receive. This decrease in satellite antenna gain was in part overcome by designing a higher gain antenna on the aircraft.

Use of the ACTS steerable antenna introduces the additional complication of requiring the antenna to continuously track the aircraft. The ACTS steerable antenna has a 3 dB contour of 280 miles, which coupled with a maximum aircraft ground speed of 700 mph, results in a low dynamic tracking requirement. This tracking is accomplished by multiplexing aircraft positioning information (GPS latitude and longitude) with the data stream transmitted from the aircraft to the fixed terminal located at JPL. At the fixed terminal the positioning information is then demultiplexed and transmitted via the public switched telephone network (PSTN) to the ACTS control station, where the ACTS is then commanded to point the steerable antenna to the aircraft location.

TERMINAL DESIGN

A block diagram of the aeronautical mobile terminal is presented in Figure 1. The terminal development leverages off the technologies developed under the AMT project at JPL. As such the RF converter, IF converter, and Data Acquisition System (DAS) subsystems have been adapted from their AMT land mobile designs to operate in the higher dynamic aeronautical environment. The antenna, power amplifier, modem, and video codec were designed/specified specifically for this aeronautical application. The JPL fixed terminal equipment is essentially equivalent to that in the aircraft with the exception of the 2.4 meter ground antenna.

The link budgets for the forward link (JPL fixed terminal-ACTS-aircraft), and the return link (aircraft-ACTS-JPL fixed terminal) are given in Table 1. Not shown in the link budgets for simplicity is the forward link pilot signal. The pilot is transmitted from the fixed terminal to the aircraft as an aid in antenna tracking, Doppler compensation, and link characterization. More detailed descriptions of the subsystems follow.

Video Codecs

The commercial video codec will compress/decompress full motion video in real time as well as multiplex the aircraft position information into the data stream which is then passed to the modem. The video codecs are existing (off-the-shelf) codecs. In an effort to select an appropriate video codec for the aeronautical mobile satellite communication environment, codec requirements were specified, an exhaustive survey of video codec manufacturers was performed, and trials of three codecs were conducted at JPL. A summary of the codec requirements is given in Table 2. The surveyed video codec manufactures included: Compression Labs, VTEL, NEC, British Telecom, Panasonic, ABL, Hitachi, PictureTel, Mitsubishi, Horizons, UVC, and a variety of compression board manufacturers. A crucial part of this survey was attending the annual Video Telecommunications Conference (VTC) to make qualitative evaluations of the video quality at the data rates of primary interest. Circumstances were such that after the list of candidates was narrowed, actual laboratory tests and satellite experiments were performed with the ABL, CLI, and NEC video codecs.

The ideal video codec for aeronautical mobile applications has characteristics that are not necessarily important when the codecs are utilized in their traditional role of fixed site video teleconferencing. The aeronautical mobile satellite communications channel may have periods of signal outage due to aircraft structure shadowing or the antenna tracking keyhole effect (e.g., keyhole is symptomatic of 2-axis tracking mechanisms, when the tracking angle closely approaches one of the mechanisms rotational axes). Signal outages necessarily require the video codec to regain synchronization rapidly when the signal returns. The best outage recovery performance that could be had with existing video codecs was on the order of three seconds after the codec started receiving valid data. The mobile satellite communications channel typically has a higher bit error rate than do the communication channels which the video codecs typically encounters. As a result it is critical that the codec degrade gracefully in the presence of high bit error rates and, and again recover rapidly from these errors. Some video codecs were found to have a tendency to "hang" or freeze in the presence of high bit error rates, requiring the power to be cycled.

Other required codec features that are not as important in fixed site applications are that the codec be small in size, light in weight, somewhat rugged in construction, and capable of multiplexing multiple external data sources with the compressed video data stream.

In evaluating the codec video quality the performance at data rates from 128 kbps to 384 kbps was deemed to be most important for the planned mobile SATCOM experimental applications. Most video codecs were found to provide very good quality video at data rates approaching T1 (1.544 Mbps), but there were significant differences in quality at the data rates of interest. Quality varied significantly, primarily in image resolution, but also in motion handling capability. All the video codecs had their own advantages and disadvantages, but on the whole the NEC video codec was determined to be the currently available codec most appropriate for the aeronautical experiments.

Modem

The modem was designed to counteract the peculiarities of the K/Ka-band aeronautical communications channel, including varying frequency offsets, phase noise, and signal outages. BPSK modulation is combined with coherent demodulation, and error correction coding is provided by a concatenated code, a convolutional inner code (rate 1/2, constraint length 7) and a Reed-Solomon outer code (rate 239/256). A bit error rate of 10^{-6} is achieved at an E_b/N_o of 3.0 dB.

Operation at higher bit rates, compared to the AMT, allows the use of coherent differential detection because the high close-in to the carrier phase noise can be tracked out by the wider bandwidth of the tracking loop. The receiver loop parameters also had to be optimized to allow Doppler frequency offsets of up to 30 kHz, varying at 900 Hz/sec to be tracked. Additionally the synchronization algorithms (carrier, bit, and decoder) had to be optimized to allow recovery synchronization within one second of signal presence. Commquest Technologies, Inc. modified a commercial satellite modem to meet these aeronautical requirements for JPL.

RF Electronics

The IF up/down converter translates between 3.373 and a lower 70 MHz IF at the output/input of the modem. A key function of the IF converter is pilot tracking and Doppler pre-compensation. The down-converted pilot is tracked in a phase-locked loop and used as a frequency reference in the mobile terminal. The loop is capable of tracking out 39 kHz of Doppler varying at 900 Hz/sec. The tracked pilot is also processed in analog hardware and mixed with the up-converted data signal from the modem to pre-shift it to offset the Doppler on the return link. The IF converter provides the DAS and antenna subsystem with a report of pilot signal strength for link characterization and antenna pointing operation respectively.

Preceding (or following) the antenna the RF up (down) converter will convert an IF around 3.373 GHz to (from) 30 (20) GHz for transmit (receive) purposes. The RF converter interfaces directly to the antenna on the receive side of the link. On the transmit side the RF converter 30 Ghz signal goes to the traveling wave tube amplifier (TWTA). The TWTA supplies 100 Watts of 30 Ghz transmit power to the reflector antenna.

Antenna

The high gain aeronautical antenna will employ an azimuth and elevation pointing system to allow it to track the satellite while the aircraft is maneuvering. The aeronautical antenna and radome are developed by EMS Technologies, Inc. The EMS antenna design utilizes a slotted waveguide array, is mechanically steered in both azimuth and elevation, and is designed to enable mounting on a variety of aircraft. The radome is shaped with a peak height of 6.7" and a 27.6" diameter; roughly the size of the SkyRadio radome currently flying on United Airlines and Delta Airlines aircraft. Figures 2 and 3 show the antenna and installed radome respectively. Antenna installation requires a 3.5" diameter protrusion into the fuselage to allow the necessary signals to pass to and from the antenna.

The antenna is capable of tracking a full 360° in azimuth and -5° to zenith in elevation. The antenna RF requirements include that it maintain, in flight, a minimum transmit gain of 29 dBi and a minimum receive sensitivity of 0 dBi/°K. Circular polarization is utilized and there exists the capability to transmit up to 120 Watts through the antenna. The actual dimensions of the combined transmit and receive array apertures, shown clearly in Figure 2, are less than 16 inches wide, and less than 4.5 inches in height.

The transmit array 3 dB beamwidths are 5° and 2.5° in elevation and cross-elevation respectively. The receive array 3 dB beamwidths are 7° and 4° in elevation and cross-elevation respectively. The antenna tracking mechanism is required to maintain pointing within 0.5 dB of beampeak throughout all phases of flight. This is accomplished through a tracking algorithm that utilizes three sources of information, an inertial 3-axis rate sensor, the aircraft Inertial Navigation System (INS), and pilot signal strength feedback from a circular dithering of the beam. The rate sensor provides the primary information for accurately pointing the antenna, with the INS and the dithering mechanisms being used to adjust for long term drift of the rate sensor.

DAS

The DAS performs continuous measurement and recording of a wide array of propagation, communication link, and terminal parameters to aid in the characterization of the communication channel (e.g., pilot and data signal conditions, noise levels, antenna direction, aircraft velocity, pitch, roll, yaw, etc.). The DAS also provides real-time displays of these parameters to aid the experimenters in the aircraft and in the fixed terminal.

Terminal Development Status

The aeronautical terminal is currently undergoing integration and testing in preparation for experiments that will commence in June 1995. The terminal is being integrated into the JPL land mobile van to allow convenient testing of subsystem interconnectivity and overall system performance prior to aircraft integration.

EXPERIMENTS

The initial two experiments to be conducted with the aeronautical terminal are shown in the accompanying Figures 4 and 5. The NASA Ames Research Center will be flying the terminal in the Kuiper Airborne Observatory (KAO) to transmit imagery from the aircraft for an educational broadcast and to conduct remote tele-science. Rockwell/Collins is working with JPL to develop the terminal and integrate it into a Rockwell Saberliner aircraft to demonstrate the transmission of compressed video both to and from the aircraft. Beyond these two experiments, several additional experiments with industry and government partners are in various stages of planning.

KAO/ACTS Experiment

JPL, working cooperatively with NASA Ames, will be conducting a series of experiments on the KAO that will utilize the ACTS. These experiments will take place from June through September 1995. The JPL developed ACTS Broadband Aeronautical Terminal will be installed in the KAO C-141 aircraft to allow the establishment of a full-duplex 384 kbps satellite communications link between the aircraft and the ground, and extend Internet into the aircraft. There are currently four planned components of this experiment. These are:

1) Television broadcast/interactive classroom - a PBS produced live television broadcast entitled "Live from the Stratosphere". As part of the broadcast, students watching the live video transmitted from the aircraft

will be able to ask questions via voice link to the aircraft.

2) Video downlink to the San Francisco Exploratorium and Adler Planetarium in Chicago.

3) Telescience demonstration of remote control of scientific instruments onboard the KAO via an extension of Internet connectivity to onboard the aircraft.

4) System Health Monitoring demonstration of a system that remotely monitors scientific instruments onboard the KAO via Internet.

Rockwell/Collins Experiment

Rockwell International/Collins Corporation Commercial/ Government Aeronautical Services Experiment

Rockwell and JPL are currently working together on an experiment design that will investigate the feasibility and limitations of airborne Ka-band satellite communications. This experiment involves the installation of the Broadband Aeronautical Terminal into Rockwell's Saberliner 50 aircraft for a series of demonstration flights. The specific objectives of this experiment are to:

1) Determine the feasibility of high data rate communications, in particular compressed full motion video, to and from an airborne platform under varying weather conditions.

2) Determine the feasibility of slaving the steerable satellite antenna to an onboard aircraft Global Positioning System (GPS) receiver in order to automatically follow the flight path of the aircraft, allowing the highest possible data rate channel for critical applications.

This experiment has applications to both commercial aviation and government airborne services. Commercial airlines wish to offer live video and high bandwidth multimedia services to passengers, but currently do not have the necessary bandwidth capacity to/from the aircraft. Various government entities have mission requirements to transmit and receive real-time video between airborne mobile terminals and fixed earth terminals. This experiment is slated to take place during the latter part of 1995.

Additional Experiments

Presently two experiments are planned to follow the above two experiments. The first of these is a Wildfire Research and Disaster Assessment experiment that is described elsewhere in these proceedings [5]. Another currently planned experiment is with Vigyan, Inc. to transmit real-time graphical map information to the cockpit of an aircraft in flight. Additional experiments being discussed involve aeronautical remote sensing applications for fixed wing and rotary wing aircraft, and military aircraft applications.

SUMMARY

JPL, working with its industry partners, has undertaken the development of a pre-commercial broadband aeronautical terminal to explore new applications and uses of K/Ka-band satellite communications. Actual flights and experimental results will be generated starting in June 1995 and made available to any parties interested in advancing the commercialization of the technology. Planned commercial satellite systems with which the equipment described in this paper could be utilized include the K/Ka-band systems proposed by Hughes (Spaceway), Teledisic, and Norris Communications.

REFERENCES

[1] K. Dessouky and T. Jedrey, "The ACTS Mobile Terminal", Proceedings 14th AIAA Conference, March 22-26, 1992, Washington, DC.

[2] B. Abbe, and D. Pinck, "ACTS Aeronautical Terminal Experiment System Description and Link Analysis", International Mobile Satellite Conference, IMSC'95, June 6-8, Ottawa.

[3] P. Sohn, C. Raquet, R. Reinhart, D. Nakamura, "ACTS Aeronautical Terminal Experiment System Description and Link Analysis", International Mobile Satellite Conference, IMSC'95, June 6-8, Ottawa.

[4] E. Elizondo, J. Balcewicz, A. Stern, O. Regalado, T. Drackett, and S. Chulik, "Operational Satellites Using ACTS Technology," AIAA-94-0939-CP, Proceedings of the 15th International Communications Satellite Systems Conference, February 1994, San Diego.

[5] L. Shameson, J. Brass, J Hanratty, A. Roberts, and S. Wagener, "Satellite Communications Provisions on NASA Ames Instrumented Aircraft Platforms for Earth Science Research/Applications", International Mobile Satellite Conference, IMSC'95, June 6-8, Ottawa.

[6] A. Densmore, M. Agan, H. Prather, M. Guler, M. Moody "An Aeronautical Mobile Terminal for High Data Rate 20/30 Ghz Satcom," to be published.

ACKNOWLEDGMENTS

The research described in this paper was carried out by the Jet Propulsion Laboratory, California Institute of Technology, under contract with the National Aeronautics and Space Administration.

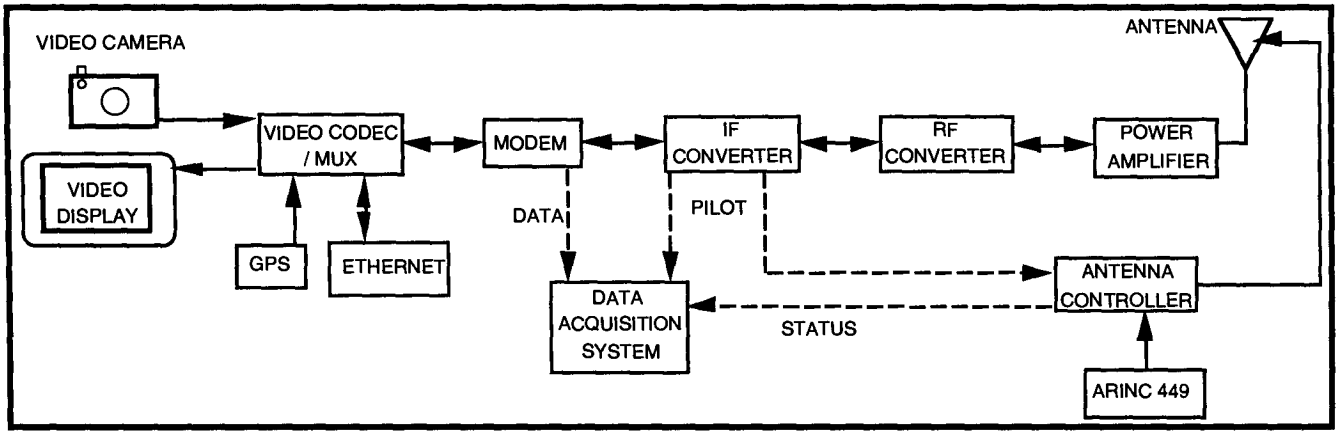

Figure 1 Block Diagram of the Broadband Aeronautical Terminal

Table 1 Link Budgets

RETURN (JPL-TO-ACTS-TO-AIRCRAFT) LINK BUDGET

UPLINK: AIRCRAFT-TO-ACTS

TRANSMITTER PARAMETERS	
TRANSMIT POWER, DBW	20.0
BPF & WG LOSSES, DB	-3.8
ANTENNA GAIN (W/RADOME), DBiC	29.0
EIRP, DBW (NOMINAL)	45.2
POINTING LOSS, DB	-0.5
POL. LOSS: CIRC. W/2DB AXIAL RAT., DB	-4.1
PATH PARAMETERS	
MAX. SPACE LOSS (AT 10° ELEVATION ANGLE), DB	-214.6
(FREQ., GHZ	29.6
RANGE, KM)	42800
ATMOSPHERIC ATTN, DB	-0.4
RECEIVER PARAMETERS	
G/T: STEERABLE BEAM PEAK, DB/K	14.5
POINTING LOSS(EDGE OF BEAM), DB	-0.5
BANDWIDTH, MHZ	900
RECV'D C/NO, DB.HZ	68.3
TRANSPONDER SNR IN, DB	-21.3
LIMITER SUPPRESSION	0.0
TRANSPONDER SNR OUT, DB	-21.3

DOWNLINK: ACTS-TO-JPL

TRANSMITTER PARAMETERS	
EIRP (EOC), DBW	41.1
POINTING LOSS, DB	-0.2
PATH PARAMETERS	
SPACE LOSS, DB	-210.0
(FREQ., GHZ	19.9
RANGE, KM)	38000
ATMOSPHERIC ATTN, DB	-0.5
RECEIVER PARAMETERS	
POLARIZATION LOSS, DB	-0.1
G/T, DB/K	25.7
POINTING LOSS, DB	-0.5
DOWNLINK C/N0, DB.HZ	84.1
OVERALL C/N0, DB.HZ	68.2
REQ'D EB/N0 (AWGN--SIMULATION), DB	3.0
MODEM IMPLEMENT. LOSS, DB	1.0
LOSS DUE TO FREQ. OFFSETS/DOP.,DB	1.0
REQUIRED EB/No, DB	5.0
LOSS DUE TO ACTS PHASE NOISE,DB	1.0
DATA RATE, KBPS	384
REQ'D EFFECTIVE C/N0,DB.HZ	61.8
HARDWARE PERFORMANCE MARGIN, DB	6.3

FORWARD (JPL-TO-ACTS-TO-AIRCRAFT) LINK BUDGET

UPLINK: JPL-TO-ACTS

TRANSMITTER PARAMETERS	
TRANSMIT POWER, DBW	16.7
WAVEGUIDE LOSS, DB	-8.5
ANTENNA GAIN, DBi	54.7
AVAILABLE EIRP, DBW	62.9
PERCENTAGE OF EIRP IN DATA SIGNAL, %	91.0
EIRP, DBW	62.5
POINTING LOSS, DB	-0.8
PATH PARAMETERS	
SPACE LOSS, DB	-213.5
(FREQ., GHZ/MHZ	29.6
ACTUAL RANGE, KM)	38000.0
ATMOSPHERIC ATTN, DB	-0.4
RECEIVER PARAMETERS	
POLARIZATION LOSS, DB	-0.1
G/T (EOC), DB/K	17.9
POINTING LOSS, DB	-0.1
BANDWIDTH, MHZ	900.0
RECV'D C/NO, DB.HZ	94.1
TRANSPONDER SNR IN, DB	4.5
EFF. LIM. SUPPRESSION, DB	-0.2
HARD LIM. EFF. SNR OUT, DB	4.3

DOWNLINK: ACTS-TO-AIRCRAFT

TRANSMITTER PARAMETERS	
STEERABLE BEAM MINIMUM PEAK EIRP	55.7
EIRP, DBW	54.0
POINTING LOSS (EDGE OF BEAM), DB	-0.5
PATH PARAMETERS	
MAX. SPACE LOSS (10° ELEVATION), DB	-211.1
(FREQ., GHZ	19.9
MAX. RANGE (AT 10° ELEVATION ANGLE), KM	42800.0
ATMOSPHERIC ATTN, DB	-0.5
RECEIVER PARAMETERS	
POL. LOSS: CIRCULAR W/2DB AXIAL RAT., DB	-4.1
G/T (W/RADOME), DB/K	0.0
POINTING LOSS, DB	-0.5
DOWNLINK C/N0, DB.HZ	65.9
OVERALL C/N0, DB.HZ	65.9
REQ'D EB/N0 (AWGN--SIMULATION), DB	3.0
MODEM IMPLEMENT. LOSS, DB	1.0
LOSS DUE TO FREQ. OFFSETS/DOP.,DB	1.0
REQUIRED EB/N0, DB	5.0
LOSS DUE TO ACTS PHASE NOISE,DB	1.0
DATA RATE, KBPS	384.0
REQ'D EFFECTIVE C/N0,DB.HZ	61.8
PERFORMANCE MARGIN, DB	4.0

Table 2 Video Codec Specifications

weight	<40 lbs.
height	<7"
compressed video rates	56 kbps to 2.048 Mbps
compressed audio rates	16 kbps to 64 kbps
image quality	high compressed image quality at all data rates
voice quality	high compressed voice quality at all data rates
power consumption	<300 Watts
BER performance	operate without degradation at 10^{-6}
operating temperature	typical of aircraft environment
operating humidity	typical of aircraft environment
clocking	independent transmit and receive data rates
broadcast capability	must be capable of transmitting while the receive is disabled, must be capable of receiving while the transmit is disabled
RS232 data ports	minimum of two ports
video format	NTSC
line interface	RS449 line interface
mounting scheme	rack mount hardware required

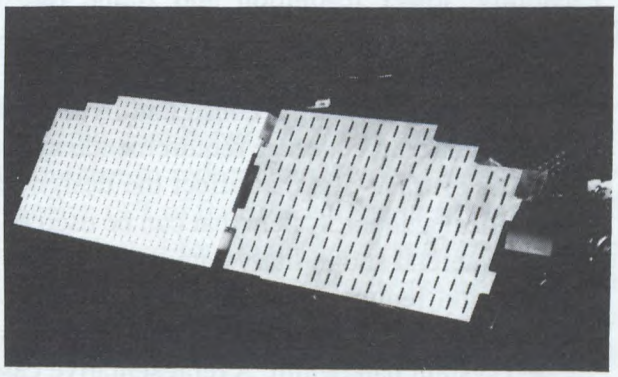

Figure 2 Slotted Waveguide Antenna

Figure 3 Aeronautical Radome on Rockwell Saberliner 50

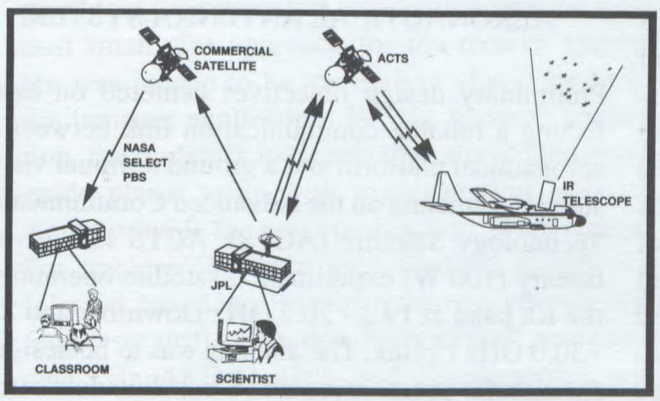

Figure 4 KAO Experiment

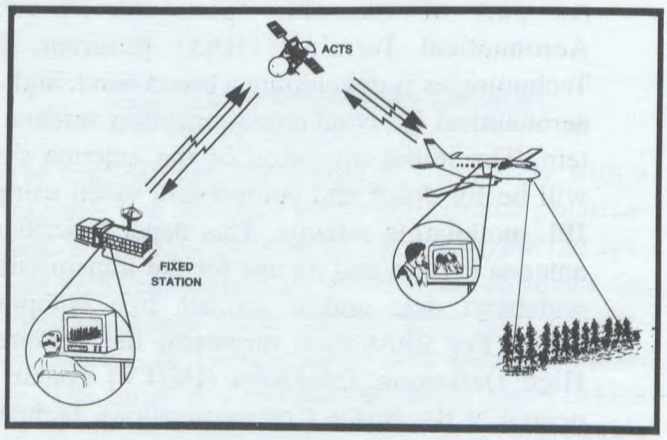

Figure 5 Rockwell/Collins Experiment

Aeronautical Applications of Steerable K/Ka-Band Antennas

Henry Helmken*, Horton Prather**

*Florida Atlantic University
777 Glades Rd
Boca Raton, FL 33431
Phone: 407-367-3452 FAX: 407-367-2336

**EMS Technologies, Inc.
660 Engineering Drive
Norcross, GA 30091-7700
Phone:404-263-9200 FAX: 404-263-9207

ABSTRACT

The expected growth of wideband data and video transmission via satellite will press existing satellite Ku-band services and push development of the Ka-band region. Isolated ground based K/Ka-band terminals can experience severe fading due to rain and weather phenomena. However, since aircraft generally fly above the severe weather, they are attractive platforms for developing commercial K/Ka-band communication links.

INTRODUCTION

As part of the JPL sponsored Broadband Aeronautical Terminal (BAT) program, EMS Technologies is developing a broad band, high gain aeronautical Ka-band communication antenna system. The initial operation of the antenna system will be for voice and compressed video using the JPL modulation scheme. This paper describes the antenna system and its use for the transmission of wideband data and/or artifact free compressed video. For illustration purposes, the compressed High Definition Television (HDTV) system pioneered at the Space Communications Technology Center (SCTC) at Florida Atlantic University will be used as the baseline video system. In this system, full HDTV transmission requires 6 Mbit/sec capability; lower resolution and frame rate and smaller picture sizes require corresponding less.

Depending on the satellite constellation (e.g. LEO, GEO) and aircraft coverage requirements, there are a number of trade-offs that affect the design of an aeronautical antenna system that can be used to satisfy commercial and military data and HDTV video transmission requirements. Multilevel modulation techniques can be used to fit high bit rates within a limited system bandwidth. A representative case of an aeronautical-geostationary satellite communication system will be considered.

AERONAUTICAL ANTENNA SYSTEM

Preliminary design objectives centered on establishing a reliable communication link between an aeronautical platform and a ground terminal via the steerable antenna on the Advanced Communication Technology Satellite (ACTS). ACTS is a geostationary (100 W) experimental satellite operating in the Ka band at 19.2 - 20.2 GHz Downlink and 28.9 - 30.0 GHz Uplink. The antenna was to be designed for circular polarization and a baseline data rate of 384 kbs. The basic link budget is shown in Table 1. Initial tradeoff studies were based on a receive G/T

Peak ACTS EIRP	54.1	dBW	Frequency	20000.0	MHz
Pointing Loss	0.5	dB			
Free Space Loss	211.1	dB			
Atmosphere Loss	0.5	dB			
Rain Fade	0.0	dB			
Receiver Characteristics (2.5 dB Noise Figure LNA)					
Polarization Loss	4.1	dB	Sky Temperature	50.0	K
Antenna Directivity	30.0	dB	Ant Eff Noise Temp	115.2	K
Ohmic Losses	1.4	dB	Receiver Noise Temp	362.9	K
Non-Ohmic Losses	1.6	dB	System Eff Noise Temp	350.1	K
Pointing Loss	0.5	dB			
Received Signal	-133.1	dBW	Receive Terminal G/T	1.6	dB/K
Downlink C/No	67.6	dB	Data Rate	384.0	kHz
Required C/No	61.8	dB			
Performance Margin	5.7	dB			

TABLE 1 SATELLITE DOWNLINK BUDGET

ranging from 0 dBi/K to +3 dBi/K and a range of transmit gain between 28 dBi and 32 dBi. In order to minimize radome heights to less then 7 inches, receive G/T of 0 dBi/K and transmit gain of 29 dBi was selected for final system performance. Single and dual axis electronic and/or mechanical steering options were considered. Tradeoffs indicated that a microstrip planar array or slotted waveguide planar array with mechanical two axis mechanical steering provided the best combination of performance and cost advantage. Further tradeoff studies indicated that the microstrip array might provide a low cost small size approach for the receive aperture but was judged to be too high in ohmic losses for the transmit application. For the transmit application, the tradeoffs indicated that the slotted waveguide planar array with a meanderline polarizer would provide the best combination of advantages. For tracking, an open loop tracking system was selected based on inertial reference sensors with long term drift correction from aircraft navigation data (via ARINC 429), and supplemented with slow rate mechanical dither (conical scan).

The Airborne Antenna System requires suitable radome for protection while remaining transparent to microwaves. The radome is intended to be top-mounted to the outside surface of an aircraft. The baseline design was primarily driven by array performance, satellite look angle, and the airborne environment. A low profile (6.6 in.) design, symmetrical about the azimuth axis (27.7 in. dia.) was selected. This design is largely insensitive to incidence angle variation and was designed for dual band operation. Figure 1 shows the overall system block diagram. Figure 2 is a CAD display of the antenna system.

TRANSMIT ANTENNA DESIGN

The transmit antenna design is a slot array with a meander line polarizer to provide circular polarization. It has directivity of 34 dB to provide the system gain requirement of 29 dB when all losses are included. These losses include array feed, polarizer, radome, two rotary joints, and waveguide losses. The array is a lightweight single piece design using EMS Technologies' multilayer waveguide construction techniques. It measures 4.5 by 9.5 by

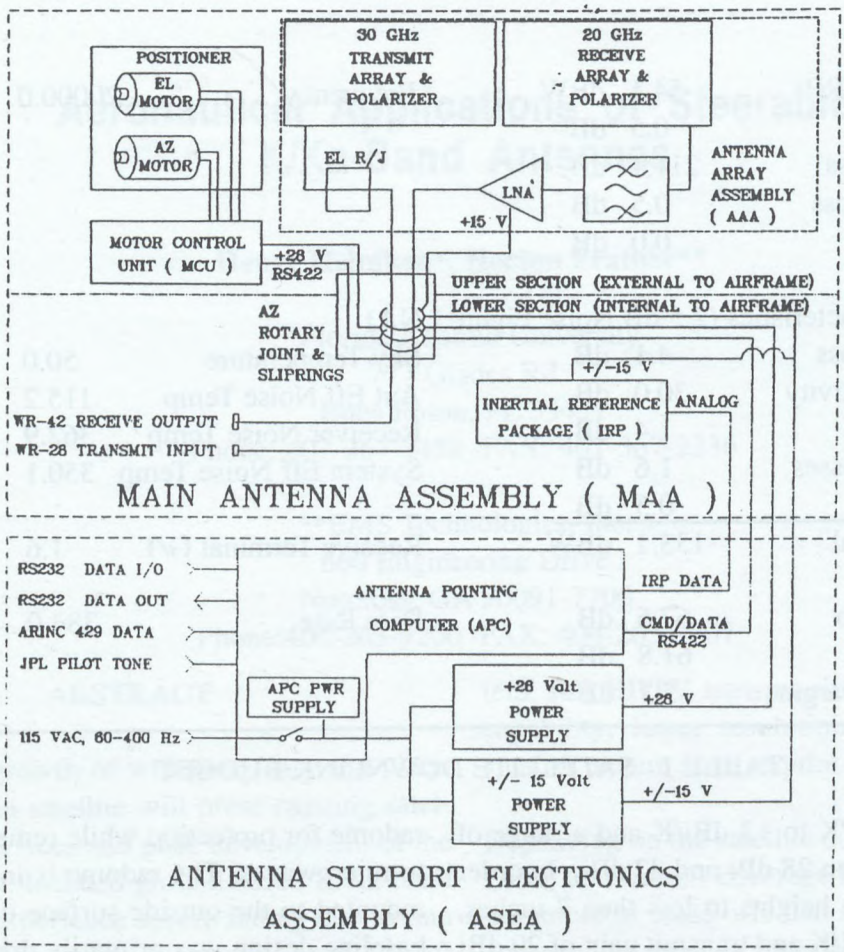

FIGURE 1. AERONAUTICAL ANTENNA SYSTEM BLOCK DIAGRAM

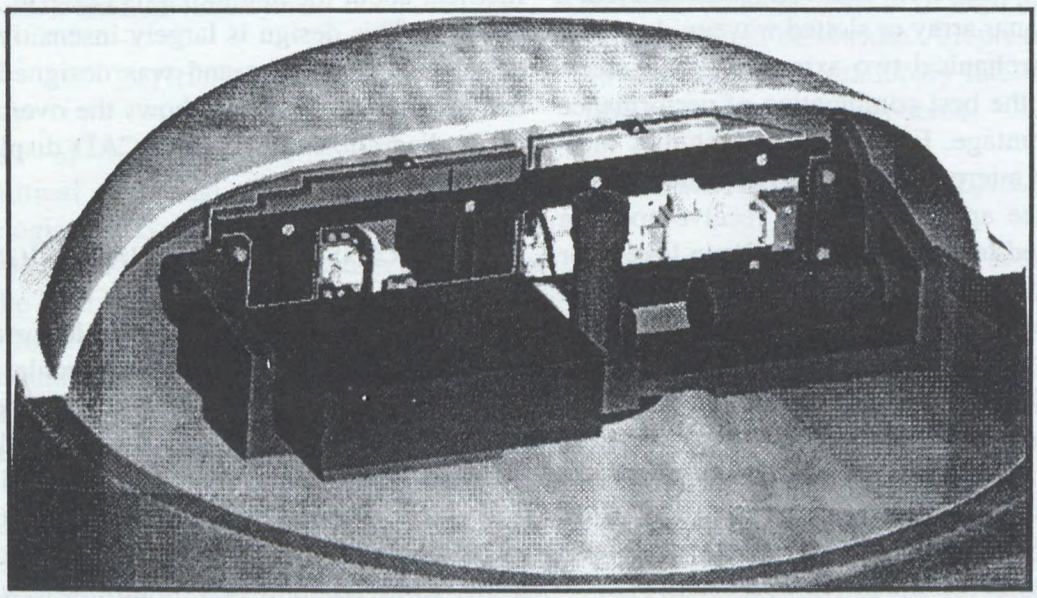

FIGURE 2. AERONAUTICAL ANTENNA SYSTEM ILLUSTRATION (EXTERNAL VIEW)

0.5 inches and weighs 0.85 pounds. The array uses uniform illumination and has first sidelobe levels of less than -12 dB.

RECEIVE ANTENNA DESIGN

The receive antenna is also a slot array with meanderline polarizer. It has a directivity of 30 dB to provide the system G/T requirement of 0 dB/K with some margin, when losses for the radome, polarizer, array, receive filter and waveguide are included. A GaAsFET low noise amplifier with a maximum noise figure of 2.5 dB at room temperature, and 32 dB gain is mounted to the back of the array. The array measures 4.6 by 8.0 by 0.5 inches and weighs 0.58 pounds. This array also has uniform illumination and sidelobe levels below -12 dB. Receive and transmit antenna specification are summarized in Table 2.

TRACKING ASSEMBLY DESIGN

A high accuracy, elevation over azimuth positioner provides mechanical 2D tracking of the antennas. The control system measures aircraft roll, pitch and yaw rates using quartz inertial sensors. These measurements are used to predict the pointing vector to the satellite and command the positioner. ARINC 429 navigation data is used to correct long term drift of the sensors, and a slow rate conical scan is used with a received pilot tone to provide correction of other fixed and time varying errors.

VIDEO TRANSMISSION

With NASA support, the Space Communications Technology Center at Florida Atlantic University has pioneered low cost HDTV video compression technology. Designed to match the characteristics of human vision, this compression technology uses 3-D subband coding in a pyramid design along with entropy coding and error correction[1-2]. A real time system , with a maximum of 100 millisec processing time delay, is currently operational at FAU. The technology is in the process of being transferred to ASIC hardware and will offer a very low cost alternative to JPEG and MPEG coder-decoder chip sets. Figure 3 shows a block diagram of the subband compression system.

Under CCDS sponsorship, a test of real time compressed image transmission to an aeronautical platform is being proposed. A full 525 line transmission, corresponding to the CCIR 601 standard,

	Receive Array		Transmit Array	
Frequency Range	19.2 - 20.2	GHz	28.9 - 30.0	GHz
Aperture Size	4.6 x 8.0	in.	4.5 x 9.5	in
Number of Elements	161		366	
Directivity	30.1	dB (19.2 GHz)	33.9	dB (28.9 GHz)
	30.6	dB (20.2 GHz	34.3	dB (30.0 GHz)
Azimuth Beamwidth	4.1	Deg (19.2 GHz)	2.6	Deg (28.9 GHz)
	3.9	Deg (20.2 GHz)	2.5	Deg (30.0 GHz)
Elevation Beamwidth	7.4	Deg (19.2 GHz)	5.1	Deg (28.9 GHz)
	7.0	Deg (20.2 GHz)	4.9	Deg(30.0 GHz)
Azimuth and Elev. sidelobes	12	dB Max (0 to 30)	12	dB (0 to 30)
	20	dB max (> 30)	20	dB (>30)
Taper and Ohmic Loss	0.9	dB	1.3	dB
VSWR	1.5:1		1.5:1	

TABLE 2 BASELINE TRANSMIT AND RECEIVE ANTENNA PARAMETERS

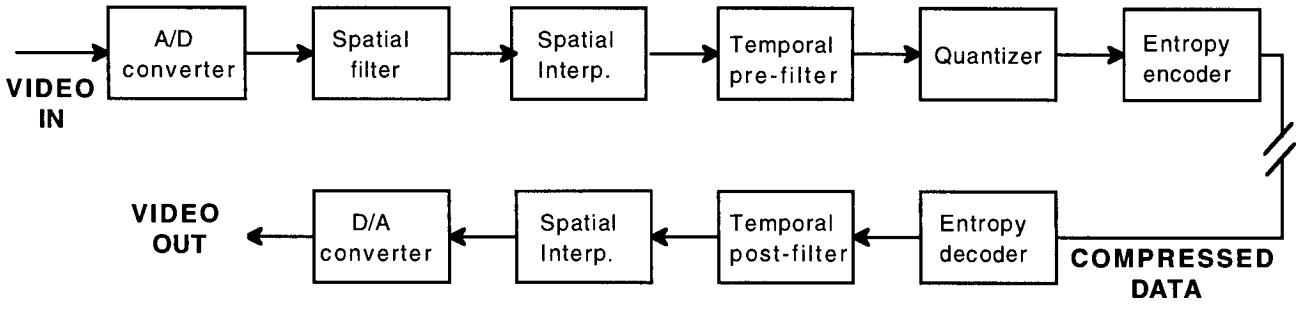

Figure 3. Block diagram of subband coding compression system

requires a 6 Mbit/sec rate to achieve artifact free NTSC transmission. At this rate, the received signal can be displayed on a NTSC monitor and will be better than broadcast quality. However, an aeronautical platform offers several bit rate trade-offs that depend upon video usage. For video entertainment, the viewer screen can be very close to the viewer and hence a full sized NTSC monitor is not required. By using half (CIF) and quartersize (QCIF) displays, the bit rate can be reduced by 1/4 and 1/16 respectively and still preserve a quality image. Since the FAU video compression system is microprocessor controlled, it can be reprogrammed to run at a slower rate. In laboratory tests, the processor has been run as low as 250 kb/sec. A test of the QCIF case is planned and fits within the current design envelope of the K/Ka band antenna system. Alternatively, if aeronautical video is to be used for video conferencing where motion is slower, frame difference techniques can be used to reduce bit rate. The current FAU processor is a full motion, (60 fields/sec) system but can be reprogrammed to run at lower rates.

For purposes of testing alternative modulation techniques, use will be made of a hardware in-the-loop simulator developed at FAU[3]. This system is based on communication model development and simulation via Signal Processing Workshop (SPW) software from the ALTA group of Cadence Design Systems, Inc. Candidate I & Q baseband signals for a selected modulation scheme are download into an arbitrary waveform generator and fed directly into a vector modulator. The IF output from the generator is upconverted to the transmitted frequency. Similarly, the received signal is downconverted to baseband I & Q signals and captured via an A/D converter to a high speed, high capacity Redundant Disk Array (RAID) system. Signals are subsequently analyzed with SPW software to determine optimum receiver design.

CONCLUSIONS

An aeronautical K/Ka band antenna system suitable for testing with ACTS has been designed and constructed. Preliminary analysis indicates that it can support a data rate of 384 kB/sec with a 5.7 dB performance margin. The antenna system was originally designed for installation on aircraft for voice and data transmission, however, using video compression technology developed at FAU, it will be used to test video transmissions suitable for commercial on board entertainment or real time military surveillance.

REFERENCES

[1] **W.E. Glenn**, "Digital Image Compression Based on Visual Perception and Scene Properties", SMPTE Journal, May, 1993 pp 392-396.

[2] **W.E. Glenn, W.E., Marcinka and R. Dhein**, R. ,"Simple Scalable Video Compression Using 3-D Subband Coding", Proc. of SMPTE Conference, San Francisco, February 1995, In press.

[3] **H.F. Helmken**, "Hardware Verification of Communication System Simulations", RF EXPO East Conference, October, 1993, pp 319-321.

A Satellite Based Telemetry Link for a UAV Application

Anthony Bloise
Hummingbird Aviation Inc.
871 Old Connecticut Pass, Framingham MA, USA
Tel: 508-877-2667

ABSTRACT

The requirements for a satellite based communication facility to service the needs of the Geographical Information System (G1S) data collection community are addressed in this paper. GIS data is supplied in the form of video imagery at sub-television rates in one or more spectral bands / polarizations laced with a position correlated data stream. The limitations and vicissitudes of using a terrestrial based telecommunications link to collect GIS data are illustrated from actual mission scenarios. The expectations from a satellite based communications link by the geophysical data collection community concerning satellite architecture, operating bands, bandwidth, footprint agility, up link and down link hardware configurations on the UAV, the Mobile Control Vehicle and at the Central Command and Data Collection Facility comprise the principle issues discussed in the first section of this paper. The final section of the paper discusses satellite based communication links would have an increased volume and scope of services the GIS data collection community could make available to the GIS user community, and the price the data collection community could afford to pay for access to the communication satellite described in the paper.

Paper not available for publication

Mobile Terminal Antennas

Session Chairman: **Yoshihiro Hase,** Communications Research Laboratory, Japan
Session Organizer: **René Douville,** Communications Research Centre, Canada

Topic Introduction: In mobile satellite communications systems, the most critical component in the communications link is the vehicle antenna. To support voice and medium speed data communications, a directional antenna is usually required. This implies a mechanical or electronic antenna steering subsystem to keep the antenna directed at the satellite through various movements of the vehicle. In all cases small size and low cost are the important features. The first group of papers in this session is focused on Ku or Ka-Band antenna developments, including two aeronautical applications. The second group of papers deals with low-profile L-Band antennas designed to work with current and planned geostationary systems. An overview of these issues is given in the fifth paper of this session. For personal satellite communications, the last paper presents two hand-held antenna designs, one applicable to GEO satellite systems, the other to MEO and addresses head-antenna interactions.

cont'd

Boeing Satellite Television Airplane Receiving System (STARS) Performance

Edward J. Vertatschitsch and George W. Fitzsimmons,

Boeing Defense & Space Group

INTRODUCTION

Boeing Defense and Space Group is developing a Satellite Television Airplane Receiving System (STARS) capable of delivering Direct Broadcast Satellite (DBS) television to an aircraft in-flight. This enables a new service for commercial airplanes that will make use of existing and future DBS systems. The home entertainment satellites, along with STARS, provide a new mobile satellite communication application. This paper will provide a brief background of the antenna issues associated with STARS for commercial airplanes and then describe the innovative Boeing phased-array solution to these problems. The paper then provides a link budget of the STARS using the Hughes DBS as an example, but the system will work with all of the proposed DBS satellites in the 12.2-12.7 GHz band. It concludes with operational performance calculations of the STARS system, supported by measured test data of an operational 16-element subarray.

Although this system is being developed for commercial airplanes, it is well suited for a wide variety of mobile military and other commercial communications systems in air, on land and at sea. The applications include sending high quality video for the digital battlefield and large volumes of data on the information superhighway at rates in excess of 350 Mbps.

BACKGROUND

Communication phased-array antennas are not new to the mobile SATCOM environment. However, an antenna, that enables simultaneous reception of 75 channels of TV on an airplane, would establish a new benchmark — particularly if the antenna were light weight, low drag and affordable.

Voice capable INMARSAT phased-array antennas are employed on airplanes today that are either top mounted (e.g., by Canadian Marconi, Tecom, etc.) or dual-side mounted (i.e., Ball Aerospace, etc.) [1]. These antennas contain transmit/receive (TR) elements (active TR modules and radiating elements) that are phase controlled to steer the antenna pointing toward the desired INMARSAT relay satellite. These relatively low-gain antennas are used for much lower bandwidth applications up to 21 kbps.

A new broadcast service direct from satellite to consumers began in the United States in April 1994 that can be received with a reflector antenna that is effectively 18" in diameter when pointed directly at the satellite(s). A pair of satellites (DBS-1 & DBS-2) at 101.2 degrees West Longitude is visible throughout all of the 48 contiguous United States (CONUS) with a maximum angle from gravitational normal of approximately 60 degrees as shown in Figure 1. Each satellite contains sixteen 120-watt transponders spaced from 12.2 to 12.7 GHz. DBS-1 broadcasts left-hand circular polarization while DBS-2 is right-hand circular. The 500 MHz instantaneous bandwidth means each satellite can provide approximately 640 Mbps of data encoded to provide from 350 to over 475 Mbps of transmitted information.

Level Flight Scan Angle Requirements

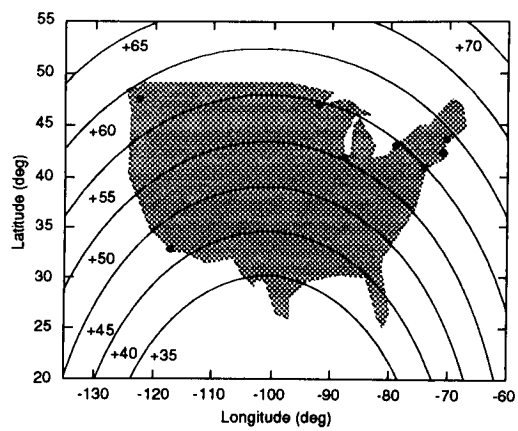

Figure 1: Contours of constant scan angle from airplane zenith to the DBS-1 satellite (101.2 W Longitude) when the airplane is in level flight.

There are substantial advantages of phased-array antennas over mechanical antennas for mobile

SATCOM applications. One obvious one is the drag cost associated with the frontal area of a mechanically steerable antenna under a radome. Even hybrid mechanical designs in which the antenna is rotated in azimuth and scanned from broadside electronically tend to require 4"-6" of height above the center spine of the aircraft. Boeing's innovative phased-array technology will permit design of an antenna that is less than 1.2" thick and protrudes approximately 1.5" above the center spine. Estimates of the relative cost of ownership, including weight plus drag penalties, result in significant savings. Another advantage to the cost of ownership is in the maintenance costs for an antenna with no moving parts over mechanical or hybrid designs. Properly designed, a phased array will last the life of the aircraft with no anticipated maintenance other than periodically coating the top surface of the antenna. The phased array includes more elements than the minimum required to receive DBS signals. This allows for failure of some elements over a 20-year lifetime without repair. Compared to mechanically pointed antennas, a phased array is certainly the low-maintenance cost option.

Until now, wide application of high-gain phased arrays has been precluded by high manufacturing cost. Using a conventional phased-array packaging architecture, an antenna with sufficient elements is not affordable for commercial applications. Recent developments at Boeing that address this problem are reported here.

BOEING PHASED-ARRAY ANTENNA RESEARCH

Boeing has been conducting company-funded and contracted research on microwave communication phased-array antennas since 1986 with an emphasis on affordability. Boeing phased arrays have been used to demonstrate high-quality video to aircraft platforms in tri-service mobile SATCOM demonstrations and for the Army MASCOM program in 1994. Two antennas completed and demonstrated for Air Force Rome Laboratory in 1993 exemplify the architectural approach, Figure 2, [2,3]. Each of these patented antennas (receive at 20 GHz, Transmit at 44 GHz) contain 91 individual "in-line" modules that are radiation coupled to a highly efficient open-ended waveguide receive or transmit element, [4]. Each waveguide radiator protects static sensitive semiconductors from potentially damaging environmental and lightning induced currents. A wide angle impedance matching (WAIM) radome-cover optimizes the antenna performance over scan angles in excess of 65 degrees from broadside, [5]. The interconnects to the antenna modules for dc and control signals are achieved using flexible elastomeric connectors that reduce assembly cost and improve reliability, by accommodating thermal-induced expansion and contraction. The antenna assembles without heat or solder using only fourteen screw fasteners. The architecture is as easy to service to the module level as it is to assemble. Each of the antennas shown in figure 2 may be taken apart easily and reassembled.

EHF Active Phased-Array Antennas

SATCOM-on-the-Move Antennas
- Low manufacturing & maintenance cost
- Scan coverage to ±70°
- Rugged architecture
- Integral semiconductor shielding
- Simple repair to the module level
- Ready for full-scale development

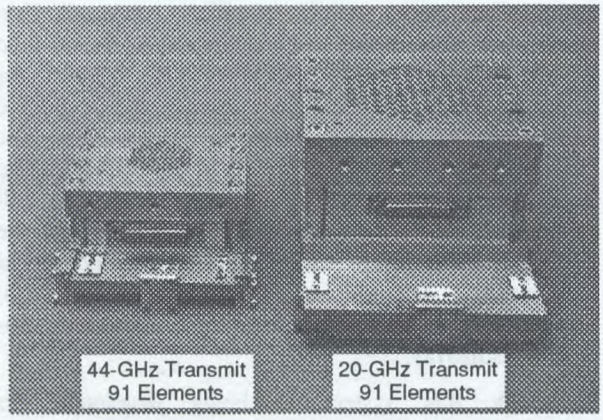

Figure 2: Photographs of ICAPA arrays

To keep costs low, the antenna uses a single module per radiating element keeping it simple and providing high-yield parts with no rework. Its waveguide radiator protects static sensitive low-noise amplifier semiconductors in each module from environmental and lightning induced currents. Scan angles up to 70 degrees are achievable. Using solderless connections means the antenna assembles and disassembles quickly and easily, entirely with mechanical fasteners.

The STARS antenna for 12 GHz takes advantage of all the features discussed above for the 20 GHz and 44 GHz antennas except that the long "in-line" module has been changed to a shorter, planar structure. The lower frequency permits wider spacing between antenna elements. This, in turn, provides more room to install phased array functions like RF signal summing, and dc and logic distribution while still leaving room for the semiconductors - enabling a substantially thinner antenna profile. Besides offering greatly reduced

antenna thickness, the planar architecture will be substantially less expensive to produce than its in-line predecessor.

Projected cost of the higher-frequency "in-line" module is $130.00 each. The new planar 12 GHz module target cost in volume production is approximately $25.00. In order to achieve the lower cost projection, it was necessary to reduce (1) the cost of the module package, and (2) the size and hence cost of the GaAs MMIC semiconductors. The module package is made of low-cost components and is designed to accommodate automatic manufacture using equipment common to the semiconductor industry. After assembly, modules will be automatically DC and RF tested, and failed units will be discarded. Defective modules will not be reworked.

The receive module contains two semiconductor chips which perform the functions: low-noise amplification (LNA), polarization switching, and phase shift. In addition, a single silicon CMOS logic ASIC chip is used to buffer the beam steering control commands, Figure 3. We have been able to reduce the total GaAs MMIC chip area to approximately four square millimeters ($4mm^2$). As an example of miniaturization, the four-bit phase shifter function occupies $1.23mm^2$, less than ¼ the size of standard designs.

Ku-Band Module Block Diagram

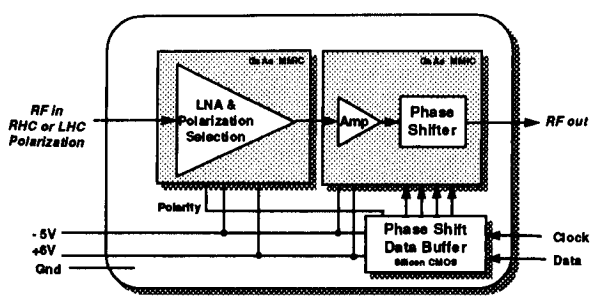

Figure 3: Electrical Block Diagram of the 11.7-12.7 GHz Module.

The RF power from each module is summed in a microstrip and waveguide feed network. The completed antenna thickness, including the protective WAIM-cover is on the order of 1.2". The antenna is mounted on an adapter plate that is customized for aircraft mounting. A transition fairing and skirt surround the antenna/adapter plate assembly to create a low-drag contour. The entire planar assembly is mounted external to the airplane, rises 1.5" above the center line and contains no moving parts. The antenna is ventilated to the atmosphere and is conduction cooled to the airplane skin. The antenna is connected to the supporting equipment inside the airplane via a cable assembly that enters the airplane through a single penetration hole that is sealed to prevent air leakage.

The planar architecture is cost competitive with more conventional, mechanically scanned and hybrid (mechanical/electrical) scanned designs. Using a module cost target of $25.00, internal studies reveal that phased-array antennas lower the cost of ownership over mechanical alternatives by a factor of two or more. Fly-away cost is comparable with other approaches, and projected operating cost is substantially lower.

THE MOBILE SATCOM LINK

STARS Components

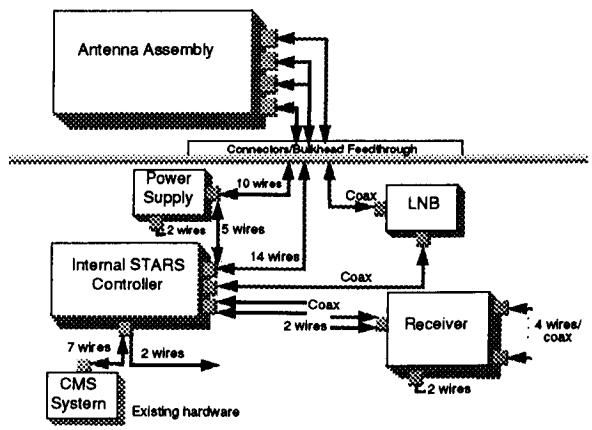

Figure 4: STARS line replaceable units with wire harness layout.

A block diagram of the STARS system is given in Figure 4. The antenna has no moving parts and the beam is electronically scanned. All acquisition and tracking functions are implemented without interfacing to the inertial reference systems of the airplane. Figure 5 contains an example link budget for a 1500-element array under worst-case flight conditions in the Seattle area. The primary performance metric is the carrier-to-noise-plus-interference (C/(N+I)) ratio. For an acceptable bit error rate of 10^{-10}, this value must exceed 4.9 dB for 23 Mbps operation.

The effective isotropic radiated power (EIRP) of the satellite accounts for both the satellite transmitted power and the downlink gain. The EIRP will vary with latitude and longitude and the broadcast beam is designed to maximize power in the area of interest as

well as to observe international boundaries and transmission agreements.

The antenna designer has control over the G/T, interference with other DBS systems through the sidelobes, and, the cross-polarized signals through the cross-pol isolation. For our phased-array design all of these parameters are functions of the scan angle.

Satellite EIRP - Seattle,dBW	50.4
Downlink Path Loss, dB	-205.9
Downlink Atmospheric Loss (STARS-10,000'), dB	-0.1
Weather Impact (STARS - 10,000'), dB	-0.5
Poiniting Loss, dB	-0.8
G/T @ peak of beam, dB/K	8.2
Bandwidth , dB-Hz	-73.8
Boltzmann's Constant, dBW	228.6
Downlink C/N (thermal)	6.1
Uplink C/N (thermal)	24.6
Crosspol Interference	12.6
Adjacent Satellite Interference	20.8
Total C/(N+I)	**5.1**
Required C/(N+I) for 10^-10 BER	**4.9**

Figure 5: Example link budget for the worst case conditions of STARS.

As can be seen from the example link budget, the G/T is the dominant limitation of operation. In this calculation we have placed the sun in the peak sidelobe and have rolled the antenna 6° away from the satellite. Also, the calculation includes the loss of elements expected over 20 years. Worst-case alignment of satellite and STARS polarization ellipses was assumed.

The relative sidelobe levels in the direction of other geo-synchronous DBS satellites will be held to better than -20 dB since these satellites are spaced at 9-degree centers. Cross-polarization interference will be a strong function of scan angle. We will be capable of maintaining better than 12 dB worst-case rejection out to 66 degree scan angles.

PERFORMANCE PREDICTIONS

The STARS will work with the Hughes DBS system in cruise conditions for all CONUS operations. It also will operate on the ground at any US airport under reasonably clear weather conditions. One needs to add the maximum roll/pitch angle of the airplane to the scan angle in-flight shown in Figure 2. For the Hughes DBS system, this shows scan angles of up to 66 degrees would cover CONUS. Our system is being designed to operate with at least 6 degrees of roll/pitch angles.

The antenna cover provides both an environmental cover as well as a wide-angle impedance match (WAIM) optimizing performance for the larger scan angles. The performance analysis of the antenna includes modeling of the active impedance between elements.

The 16-element subarray, shown in Figure 6, with a full set of modules containing the GaAs and CMOS semiconductors currently is being tested. The subarray includes the RF combining, DC power and data distribution networks. With an optimized WAIM, the subarray was scanned and the patterns compared to predicted values. Figure 7 is a plot of the measured and predicted antenna patterns at 12.7 GHz. Since this subarray is very small we would expect some inaccuracy because of edge effects. The elements will not be identical to the embedded elements of a large array, but agreement was still very good. We have already demonstrated our approach to acquisition and tracking of DBS signals with the subarray. This reduction to practice gives us great confidence in moving forward to build the full-size antenna of 1500 elements in the fourth quarter of 1995.

16-Element Ku-Band Subarray

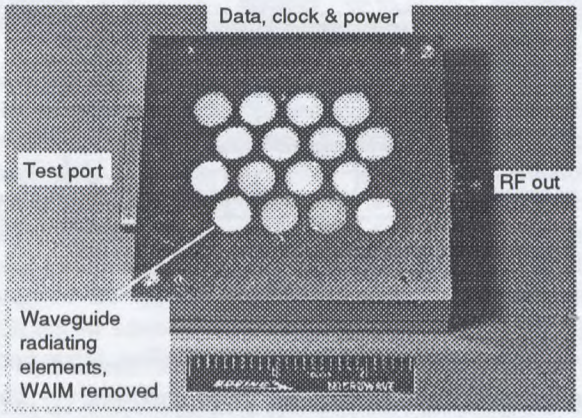

Figure 6: Photograph of the tested 16-element Ku-band subarray.

Subarray Performance

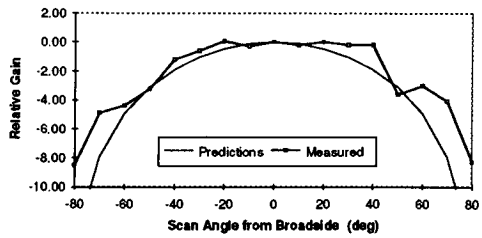

Figure 7: Measured gain of the 16-element subarray at various scan angles compared to full array predictions.

Combining the models for all of the elements in the link budget, a simulation was performed indicating the threshold of operation over CONUS and is presented in Figure 8. This is the point at which the margin in C/(N+I) is 0 dB. We show the contours for both the worst case flight conditions as described in the previous section as well as for the nominal cruise conditions of level flight. Clearly we continue to receive high-quality signals during cruise operations even under these worst-case conditions. This same chart is applicable to performance on the ground under reasonably clear-weather related attenuation of up to 0.5 dB.

Proposed Geographic Boundaries for STARS with DBS-1

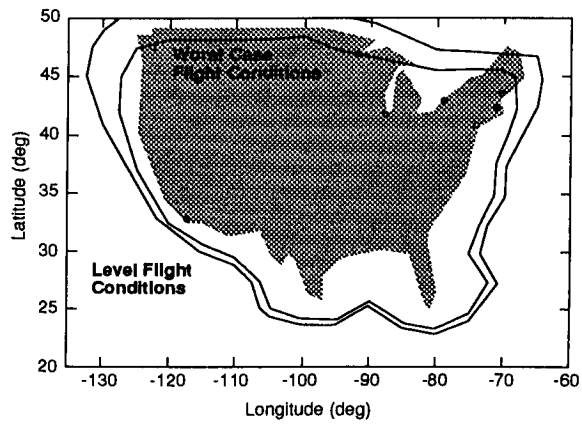

Figure 8: Contour of constant bit error rate in a) nominal level flight and b) worst case (6° roll away) operation that meet DBS requirements.

In conclusion, based on our detailed link analysis, laboratory measurements, and, our subarray demonstrations, we feel confident in claiming significant benefits to using Boeing's phased array as an antenna for the STARS. Further, our detailed cost of ownership analysis indicates STARS could be a cost- effective DBS receiving system installed on commercial airplanes.

REFERENCES

[1] *"Cabin Management Market Growing,"* Aviation Week & Space Technology, August 15, 1994.

[2] *"Integrated Circuit Active Phased-Array Antenna (ICAPA),"* Final Technical Report No. F19628-90-0168, Rome Laboratory, John P. Turtle, Technical Monitor/EEAA, Boeing Defense & Space Group, R&E Programs, March 1994.

[3] G.W. Fitzsimmons, B.J. Lamberty, E.J. Vertatschitsch, D.T. Harvey, D.E. Reimer, *"Packaging Architecture for Phased Arrays,"* US Patent Number 5,276,455, January 4, 1994.

[4] G.W. Fitzsimmons, B.J. Lamberty, D.T. Harvey, D.E. Riemer, E.J. Vertatschitsch, J.E. Wallace, *"A Connectorless Module,"* for an EHF Phased-Array Antenna, Microwave Journal, January 1994.

[5] B.J. Lamberty, W. P. Geren, S. H. Goodman, G. E. Miller, K. A. Dallabetta, *"Wide-Angle Impedance Matching Surfaces for Circular Waveguide Phased Array Antennas with 70-Degree Scan Capability,"* Proceedings of the 1992 Antenna Applications Symposium, Allerton Park, Monticello, Illinois, 23 - 25 Sept. 1992.

A Ka-band Helical Antenna

Michel de Léséleuc and Dan Hindson
Communications Research Centre
3701 Carling Avenue, P.O. Box 11490, Station "H"
Ottawa, Ontario, Canada K2H 8S2

ABSTRACT

A number of Ka-band satellite systems have been proposed to provide wide band personal communications services to terminals employing small antennas. Work has been performed looking at the use of helical antenna elements to provide an efficient low-cost antenna at these frequencies. Although helices are not planar, at Ka-band they are less than 2.5 cm in height and thus are suitable for these applications.
This paper describes the design and development of a broadband helical antenna element. The work performed on: feed configurations, matching techniques, ground plane structures, broadbanding, and the effects of dielectric loading are discussed. Experimental measurements performed during the development of the helical antenna element are presented.

I. INTRODUCTION

Although the helical antenna is not a new type of antenna, its design criteria, use and application at EHF have not yet been well established. The objective of the development work was to design a wide band helix, operating from 19 to 30 GHz, having at least 15 dB return loss, around 10 dBi gain(linear pol.) and less then 2 dB on axis, axial ratio throughout the band.

The work of Kraus [1] amongst others, formed the basis of the development work done on this EHF helix. The geometry used was a multi turn, monofilar, axial-mode, peripherally fed helical antenna. The basic geometry and associated design parameters of the helical antenna are shown in Fig. 1.

The helices designed and tested during development were made for $0.8<C/\lambda<1.2$, $0.005<d/\lambda<0.05$, $12^{\circ}<\alpha<14^{\circ}$ and $n>5$. The diameter "D" of the helix was changed accordingly depending on the required frequency of operation.

The next section establishes a proper coaxial ground plane/feed configuration. Then a variety of matching networks are examined and test results of matching the helical antenna to its 50Ω coaxial feed are presented. A series of modifications is then discussed and test results on a variety of helices to improve various parameters like gain, axial ratio, sidelobe level and bandwidth are presented.

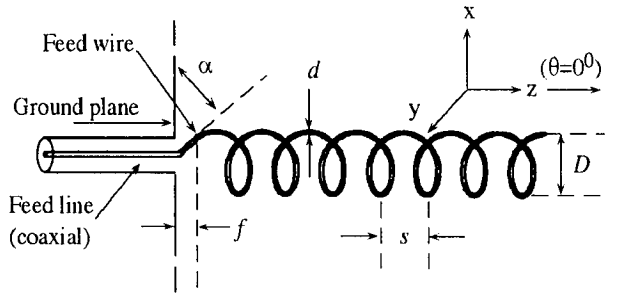

where D = diameter of helix (centre to centre)
C = circumference of helix = πD
S = spacing between turns (centre to centre)
α = pitch angle = $\arctan(S/\pi D)$
n = number of turns
d = diameter of helix conductor
f = spacing of helix from ground plane

Fig. 1. The helical antenna.

II. THE GROUND PLANE/FEED CONFIGURATIONS

The preferred approach in feeding a helix is by using a coaxial feed line, as shown in Fig. 1. This simple assembly eliminates transitions and connections, and removes unnecessary discontinuities. In our case, by using a 0.012" to 0.015" conductor, the helix could be "plugged" directly into the centre conductor of a K[1] connector. A "direct" type feed, shown in Fig. 2, has been designed incorporating a matching network in the ground plane.

III. THE MATCHING NETWORKS

A. The λ/4 Transformer.

The hole diameter "D" and thickness "T" in Fig. 2 were designed to match (geometric mean) the 50Ω K connector coaxial line to the helix terminal impedance.

therefore $$Z = \sqrt{50\Omega \times Z_{helix}} \qquad (1)$$

where $Z_{helix} = R = \dfrac{150}{\sqrt{C/\lambda}}$ (Eq. (3) of [2]) (2)

and $$D = d \times 10^{\left(\frac{Z}{138}\right)} \text{ (for air coaxial line)} \qquad (3)$$

[1]The K connector is a trademark of the Wiltron Company, Morgan Hill, California.

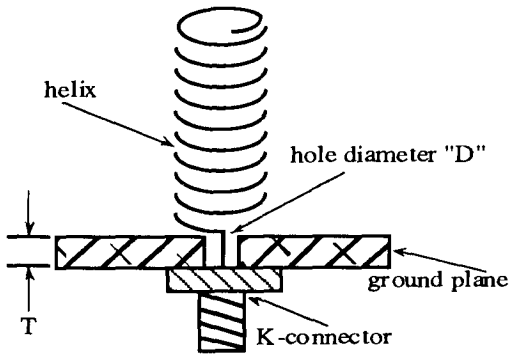

Fig. 2. Direct feed and λ/4 transformer.

and $$T = \lambda/4 \quad (\lambda \text{ @ centre frequency}) \qquad (4)$$

The match is optimized by simply adjusting the height of the helix over the ground plane. Although limited in bandwidth, it is a quick simple and effective design for narrow band applications. Fig. 3 shows the return loss response of a 23 GHz helix made with a 0.012" conductor, @ D=0.159", C/λ=0.98 and α=12.5°. The resulting bandwidth is about 29% @ 15 dB @ 21 GHz.

C. The Broadband Impedance Matching Section.

Baker et al, describe in [2], the precise design of a broadband matching network that is incorporated directly into the first turn of the peripherally fed helical antenna, to convert the input impedance to 50Ω. Also described, is a simple termination for the free end of the helix, in the form of a planar Archimedes spiral. Fig. 4 shows the coordinate system of the impedance matching section and the termination at the free end. This matching section is based on the Hecken [3] taper. The impedance matching section is a continuous transmission line (formed by the conductor-ground plane combination) of variable impedance which transforms the helix impedance, Z_2, to the line impedance, Z_1. At any point along the tapered line, the desired impedance at that point, $Z_c(s)$, is specified by (Eq. (29) of [3]):

$$\log_e Z_c(s) = \frac{1}{2}\log_e(Z_2 Z_1) + \frac{1}{2}\log_e\left(\frac{Z_2}{Z_1}\right) G(B,s) \qquad (5)$$

where s is twice the length of the matching section and G(B,s) is the taper function as described in [3].

The impedance change along the tapered line remains gradual and at any point along the line the impedance may be approximated by the characteristic impedance of a circular wire above a ground plane [4] as;

$$Z_c(s) = \frac{60}{\sqrt{\varepsilon_r}} \cosh^{-1}\frac{2h}{d} \qquad (6)$$

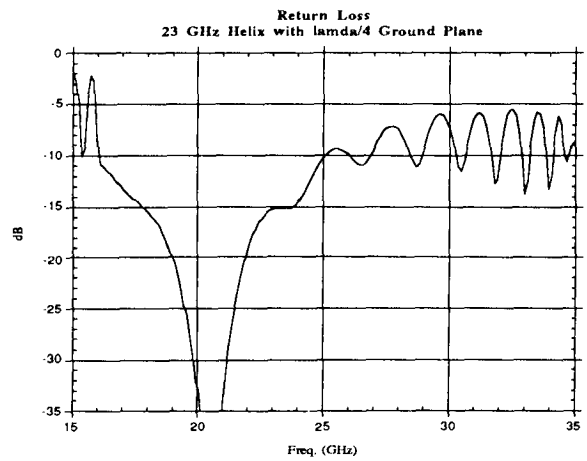

Fig. 3. Return loss, 23 GHz helix via λ/4 transformer ground plane.

where ε_r is the relative dielectric constant, d is the diameter of the circular conductor and h = h(s) is the spacing between the ground plane and the centre of the conductor (see inset in Fig. 4). Finally the design requires that the minimum length of the impedance taper be 0.44λ at the lowest operating frequency.

The matching section design and profile is computed from equation (6) as

$$h(s) = \frac{d}{2}\cosh\left(\frac{\sqrt{\varepsilon_r} Z_c(s)}{60}\right) \qquad (7)$$

A matching section was computed for a 23 GHz helix having d=0.012", C=0.507", α=12.5° and n=10. The helix has a cutoff frequency of C/0.7 = 16.296 GHz. In this case the lowest operating frequency is 19 GHz and therefore the matching section must be at least 0.44λ at 19 GHz, or 0.273" which is 0.532λ @ 23 GHz, therefore extending slightly more then 1/2 turn. The resulting height profile of the impedance matching section is shown in Table I.

Table I results are based on an example from [2] where the function G(B,s) in Eq. (5) was selected for a design which requires a maximum reflection coefficient of -21 dB at the 50Ω input connector to the helix (this corresponds to the first column of values in Table 1 of [3]). Notice that the conductor lies quite close to the ground plane over the first half of the taper (especially in this case). Also note that the impedance at the midpoint of the matching section is the geometric mean of Z_1 and Z_2.

At the free end, the helix is terminated by the addition of two or more turns in the form of a planar Archimedes spiral lying in the plane perpendicular to the helix axis (see Fig. 4).

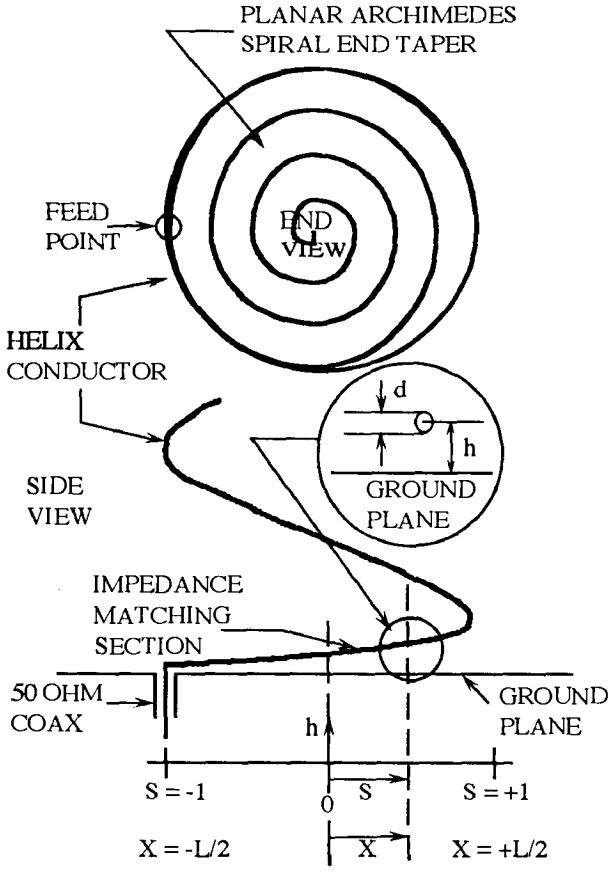

Fig. 4. Schematic diagram of a peripherally fed helical antenna illustrating the matching section coordinates and the termination of the helix at the free end.

This simple termination removes the resonant region ($C/\lambda>1.1$) found in the completely uniform helix and improves performance at the high-frequency end. The planar Archimedes spiral also gives significant improvement in axial ratio provided there are more than two turns and the minimum radius of the spiral is less than about D/6. This of course is dependent on the helix and conductor diameter, which are quite small at these frequencies but nevertheless not impossible to work with.

This helix was made as specified above and assembled on a new ground plane/feed assembly. The main difference with this new assembly is that the K connector centre conductor is now flush with the ground plane surface, thus eliminating the quarter wave transformer previously formed by the ground plane thickness. This is an even more "direct" type feed and ensures 50Ω impedance at the connector interface.

This new ground plane/feed assembly gives credit to the "Baker" type matching network. After a bit of tuning (manually adjusting height profile of matching section), the helix tuned to better then 15 dB return loss @ over 60% bandwidth @ 23 GHz. Fig. 5 shows the resulting match. Notice how the helix cut-off frequency agrees with the calculated value.

TABLE I
Characteristic impedance, $Z_S(s)$, and conductor spacing, h(s), as a function of distance, s, along the impedance matching section.

s	$Z_c(\|s\|)$ Ω	h(|s|) mm	h(|s|)mm -1/2 of d
-1	50.00	0.008	0.002
-0.5	64.54	0.010	0.004
0	86.60	0.013	0.007
0.5	116.20	0.021	0.015
1	150.00	0.037	0.031

Fig. 6 shows the radiation pattern of this 23 GHz helix @ 25 GHz. The field pattern exhibits only about 1 dB axial ratio, approximately 30 deg. beamwidth and the first sidelobes are about 10 dB. This helix featured these parameters or better from 18 to about 26 GHz. Field pattern testing reveals that although a helix is well matched over a very wide band, its axial mode of radiation bandwidth is limited to $0.7\leq C_\lambda \leq 1.3$ when $\alpha=12.5$ deg. (Fig. 7-10 of [1]). Beyond these limits, the radiation patterns look distorted and asymmetric, and the axial ratio increases.

The height profile of the matching section reasonably agrees with the design values. In reality, it's difficult to measure with any amount of reasonable precision the height profile of the matching section. Using a feeler gauge, the matching profile height was set as close as possible to the design values. At this point the helix was well matched (10 to 15 dB @ approximately 50% BW) but not optimum. The match is optimized manually by adjusting the height profile of different sections of the matching network. Once optimized, the matching section height profile was remeasured, but no appreciable differences could be accurately resolved. The fact is, as mentioned in [2], the match at the high-frequency end is very sensitive to deviations from the desired matching section profile over the first half of the matching section, and at these frequencies we are dealing with very small dimensions and adjustments.

Similar helices were designed for operation at other frequencies and were proven to be as good or better. The resulting match of a 24 GHz helix with and without the Archimedes end spiral is shown in Fig. 7. Notice the resonance reduction and the extension of the high frequency end of the helix with the Archimedes spiral.

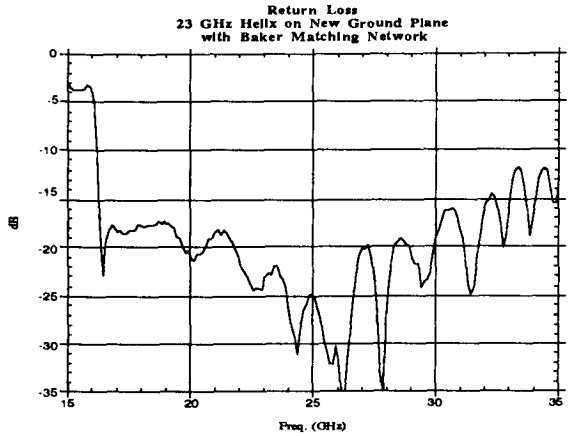

Fig. 5. Return loss of 23 GHz helix with "Baker" type matching section, assembled on new 50Ω ground plane/feed assembly.

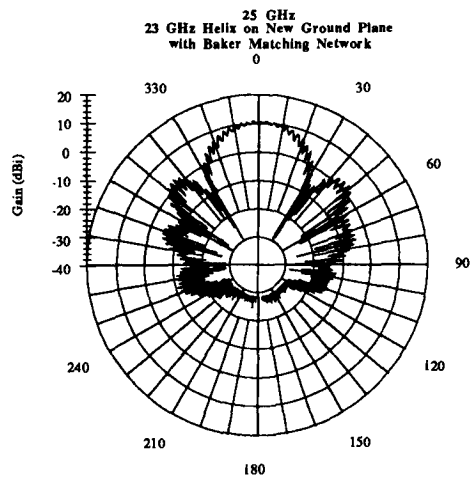

Fig. 6. Radiation pattern of above 23 GHz helix @ 25 GHz.

IV. HELIX OPTIMIZATION

Many modifications can be applied to the helical antenna to improve its performance. Test results obtained with some of these modifications are now presented.

A. Ground plane structures.

So far, although the ground plane/feed assembly has gone through many modifications, it has remained a flat ground plane. Modifications to the ground plane, as shown in Fig 8, can improve sidelobe levels and vary beamwidth.

The new 50Ω ground plane/feed was used to assemble and test the different ground plane configurations. Tested for comparison were a flat ground plane, 3 cupped ground planes were b=a/2, λ/2 and 3/4λ, and the deep conical ground plane designed as shown in Fig. 8.

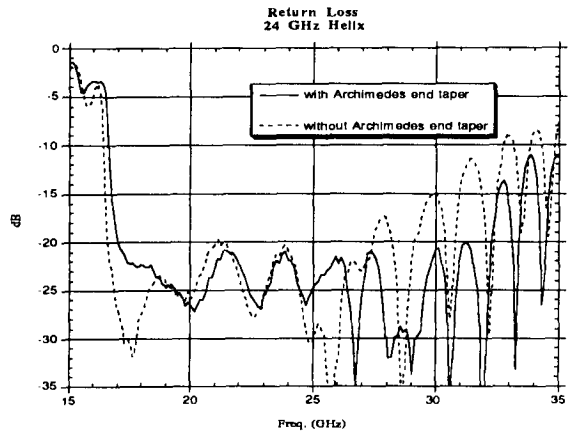

Fig. 7. Return loss of 24 GHz helices with "Baker" type matching section, with and without the Archimedes end taper spiral, assembled on the new 50Ω ground plane/feed assembly.

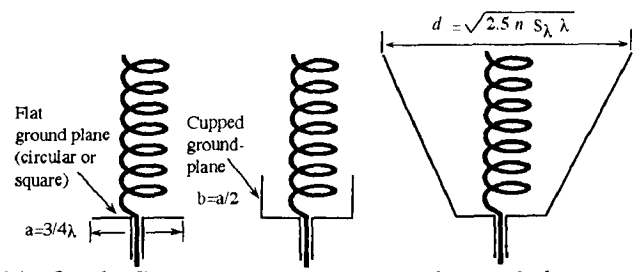

Fig. 8. The flat, cupped and deep conical ground plane.

Figures 9, 10, and 11 are the radiation pattern test results of a 23 GHz helix tested @ 23 GHz on a flat, cupped @ a/2 and conical ground plane respectively. Also tested were match, gain and axial ratio.

This helix was tested from 19 to 33 GHz. At most frequencies, as the height of the cupped ground plane was increased, the sidelobe levels decreased, however the beamwidth increased and the gain decreased. Throughout the band of interest, the conical ground plane decreased sidelobe levels, decreased the beamwidth by 5 to 20 deg. and increased gain by up to 3 dB. The different ground plane configurations had no effect on match but the conical structure did slightly increase the axial ratio variations vs frequency.

No single ground plane structure can be considered better or worse than the other. These different ground plane configurations simply offer a means to vary and control certain parameters of the helix, (i.e., gain, beamwidth and sidelobe level). This makes it easier to integrate and accommodate the helix to different system requirements and configurations.

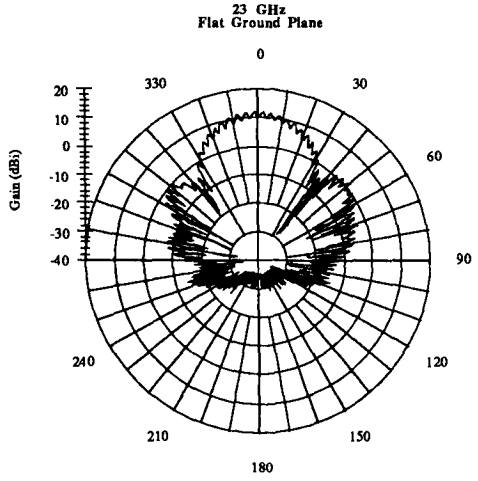

Fig. 9. Radiation pattern @ 23 GHz of helix on flat ground plane.

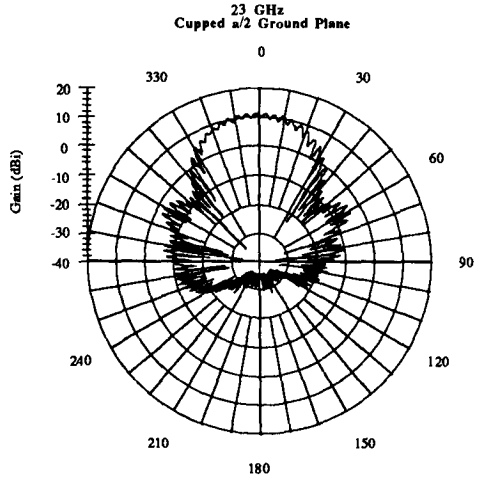

Fig. 10. Radiation pattern @ 23 GHz of helix on b=a/2 cupped ground plane.

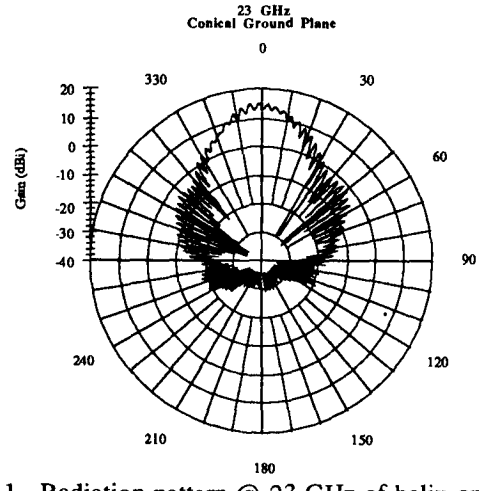

Fig. 11. Radiation pattern @ 23 GHz of helix on conical ground plane.

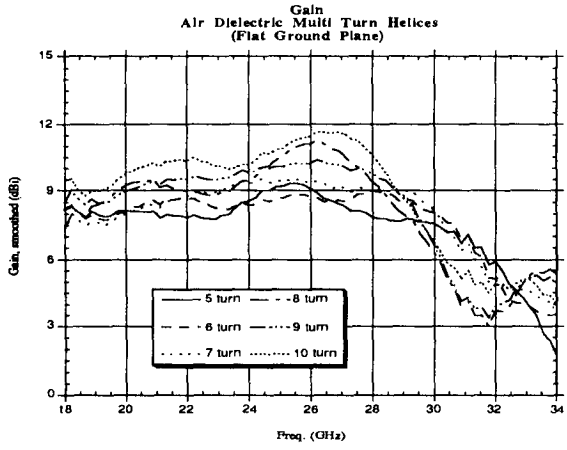

Fig. 12. Gain variation vs frequency for helices of different turns.

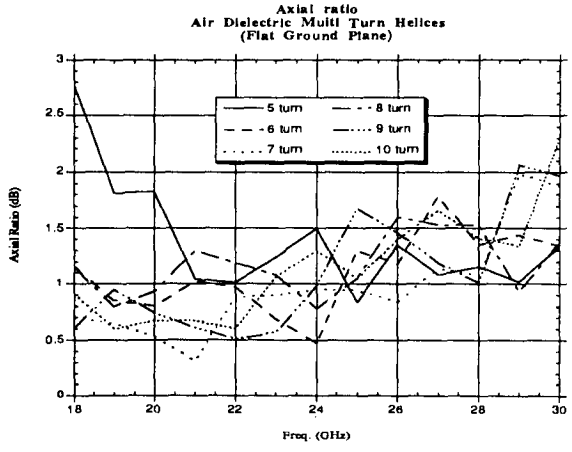

Fig. 13. Axial ratio variation vs frequency for helices of different turns.

B. The number of turns; helix length.

The previously mentioned design refinements were performed on 10 turn helices. Five, 6, 7, 8 and 9 turn helices were also tested and compared to the 10 turn helix. All the helices were identical and incorporated the "Baker" type matching network, and Archimedes end taper spiral. The effects on match, gain, axial ratio and radiation patterns were examined.

Figures 12 and 13 show the variations over frequency of gain and axial ratio vs the number of turns. Note that although a 10 turn helix offers more gain at first, it drops of fairly quickly and does not offer the best gain flatness. Axial ratio follows the same trend for all helices, except the 5 turn helix. Variations are about ±0.5 dB, but on average, the 8 turn helix seems to offer better axial ratio with less variations.

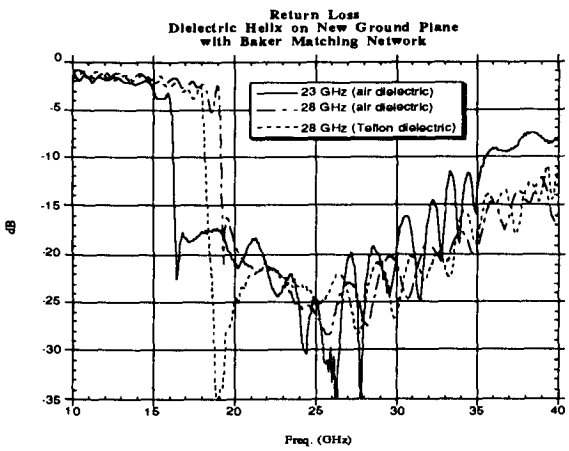

Fig. 14. Wideband return loss response of a 23 and 28 GHz helix with and without dielectric loading.

Another observation is that a 5 turn helix will have wider beamwidth and lower sidelobes than a 10 turn helix for the same frequency point. For example, a 5 turn helix has 46 deg. beamwidth and 11 dB first sidelobe level, compared to 36 deg. beamwidth and 9 dB first sidelobe level for the 10 turn helix, @ 25 GHz. Shorter helices also seem to have an extended high frequency end compared to longer helices.

The number of turns did not have a major effect on match, although helices with fewer turns were easier to "tune-in" and resulted in a slightly better match.

C. Dielectric loading.

Helices at these frequencies are very small and fragile and require some support for mechanical rigidity. One method to strengthen the structure is to wind the helix on a rigid dielectric tube of appropriate circumference. Tests have been done on a variety of helices were the helix is wound on a Teflon[2] tube. The design of the matching section in [2] can also be applied to helices supported on dielectric tubing. The downward shift, filling factor and effective dielectric constant are predicted to recompute from equation (7), with the appropriate value of ε_r, the new value of h(s).

This has been applied to a 28 GHz helix. The wideband return loss of this helix with and without a dielectric Teflon support tube is shown in Fig. 14. It is compared to a 23 GHz air dielectric helix. Notice the downward shift in the frequency response caused by the dielectric loading. Fig. 15 shows the radiation pattern of the 28 GHz Teflon dielectric helix @ 28 GHz. The measured field patterns of the 28 GHz Teflon helix revealed that the insertion of the dielectric support does not degrade the helix performance.

[2] Teflon is trademark of E.I. du Pont de Nemours & Co., Inc., Wilmington, Delaware.

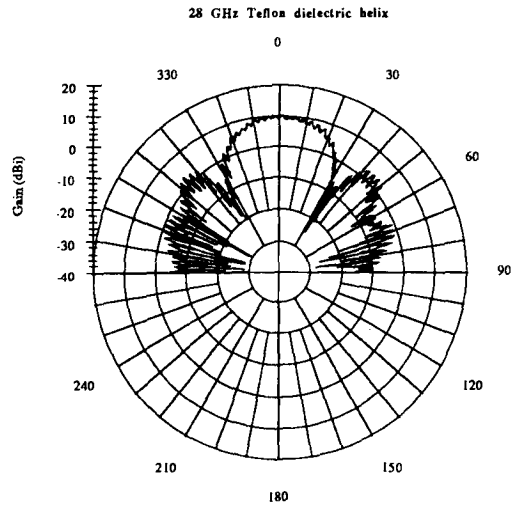

Fig. 15. Radiation patterns of 28 GHz Teflon dielectric helix @ 28 GHz.

V. CONCLUSION

The original design objective was achieved. An EHF helical antenna with better than 15 dB return loss, over 19 to 30 GHz, with 10 dBi gain and less then 2 dB axial ratio was designed using the general design practices of the monofilar, axial mode, peripherally fed helical antenna. Tests have shown that the EHF helix can be coaxially fed and properly matched over its entire usable bandwidth. Ground plane variations have demonstrated control over the beamwidth and sidelobe level. The matching section in [2] was proven very effective and has also indicated some control over axial ratio. Tests have shown that dielectric loading only causes a downward shift in frequency.

VI. REFERENCES

[1] Kraus, John D., "Antennas", Second Edition, 1988, McGraw-Hill, chapter 7.

[2] Baker, Dirk E., "Design of a Broadband Impedance Matching Section for Peripherally Fed Helical Antennas", The 1980 Antenna Applications Symposium, University of Illinois, Allerton Park Monticello, Illinois, September 1980.

[3] R.P. Hecken, "A near-optimum matching section without discontinuities", IEEE Trans. Microwave Theory and Tech., vol. MTT-20, pp. 734-739, November 1972.

[4] M.A.R. Gunston, Microwave transmission-line impedance data. London: Van Nostrand Reinhold, 1972, Ch. 2.

Ka-Band MMIC Array System for ACTS Aeronautical Terminal Experiment (Aero-X)

Charles A. Raquet, Robert J. Zakrajsek, Richard Q. Lee, and Monty Andro
NASA Lewis Research Center, 21000 Brookpark Rd., MS 54-8, Cleveland, OH 44135

and

John P. Turtle
USAF Rome Laboratory, RL/ERAA, 31 Grenier St., Hanscom AFB, MA 01731-3010

ABSTRACT

During the summer of 1994, the Advanced Communication Technology Satellite (ACTS) Aeronautical Terminal Experiment (Aero-X) was successfully completed by the NASA Lewis Research Center (LeRC) and the Jet Propulsion Laboratory (JPL). 4.8 and 9.6 Kbps duplex voice links were established between the LeRC Learjet and the ACTS Link Evaluation Terminal (LET) in Cleveland, Ohio, via the ACTS. The antenna system used in this demonstration was developed by LeRC and featured LeRC and US Air Force experimental arrays using GaAs MMIC devices at each radiating element for electronic beam steering and distributed power amplification. The antenna system consisted of three arrays mounted inside the LeRC Learjet, pointing out through the windows. An open loop tracking controller developed by LeRC used information from the aircraft position and attitude sensors to automatically steer the arrays toward ACTS during flight. JPL ACTS Mobile Terminal (AMT) system hardware was used as transceivers both on the aircraft and at the LET. The single 32 element MMIC transmit array developed by NASA / LeRC and Texas Instruments has an EIRP of 23.4 dBW at boresight. The two 20 GHz MMIC receive arrays were developed in a cooperative effort with the USAF Rome Laboratory/Electronic System Center, taking advantage of existing USAF array development contracts with Boeing and Martin Marietta. The Boeing array has 23 elements and a G/T of -16.6 db/degK at boresight. The Martin Marietta array has 16 elements and a G/T of -16.1 db/degK at boresight. The three proof-of-concept arrays, the array control system and their integration and operation in the Learjet for Aero-X are described.

INTRODUCTION

Figure 1 presents an overview of the ACTS Aeronautical Terminal Experiment, showing the Learjet on which the MMIC array antenna system was located, the ACTS, and the Link Evaluation Terminal in Cleveland. The block diagram in Figure 2 shows the interconnection of the arrays, the array controller, the aircraft position and attitude sensor systems, the data display and recording systems, and the JPL AMT [1]. The following sections describe the three MMIC arrays, the array controller and the data display and storage system. A

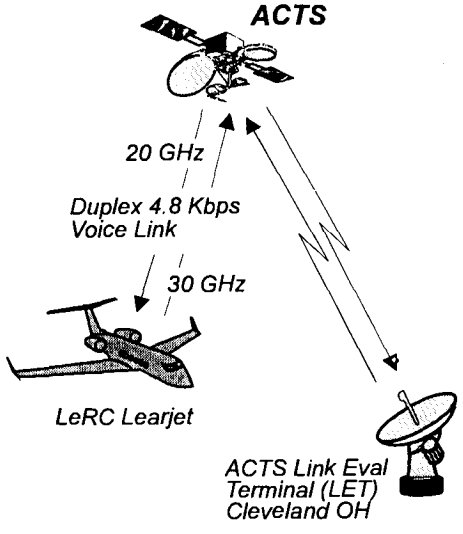

Figure 1. Aero-X Overview

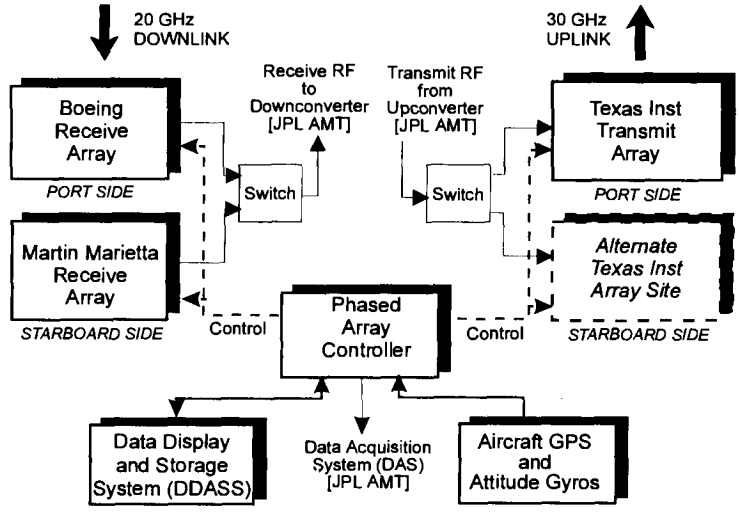

Figure 2. Antenna System Block Diagram

section on the integration of the array system on the Learjet follows, and the paper concludes with a brief discussion of system performance. Reference [2] provides additional system description and link analysis information.

MMIC ARRAYS

Three MMIC arrays were demonstrated in Aero-X. The single 20 GHz transmit array was developed by NASA/LeRC and Texas Instruments. The two 20 GHz receive arrays were developed in a cooperative effort with the US Air Force Rome Laboratory/Electronic System Center, leveraging existing Air Force integrated circuit active phased array (ICAPA) development contracts with Boeing and Martin Marietta. Table 1 summarizes the characteristics of the three proof-of-concept active arrays. In Figure 3, the radiating element geometry of each array is show to scale. Each array is electronically steerable, incorporating a MMIC amplifier and MMIC phase shifter at every radiating element.

As Table 1 and Figure 3 show, the three arrays represent three distinctly different approaches to MMIC integration. The successful performance of these arrays indicate that MMIC integration at 20 and 30 GHz is indeed feasible. It is important to note that these are experimental, proof-of-concept arrays. Continuing development efforts are required in MMIC integration technology and in thermal and mechanical packaging to bring the technology to operational readiness at acceptable cost.

30 GHz Transmit Array

Texas Instruments - The Texas Instruments (TI) 30 GHz transmit array [3] of 32 elements, shown in Figure 4, consists of two 16 element 4 x 4 modules mounted in an protective experimental housing. The TI approach features a thin "tile" architecture in which the components are mounted in a plane perpendicular to the antenna boresight. Each of the two 16 element subarray modules is 3.2 cm x 3.2 cm x 0.75 cm thick. Array element spacing of 0.8λ supports scanning to ±30°

Table 1. MMIC Array Characteristics

MMIC ARRAY	NASA / LeRC Texas Instruments	USAF / Rome Lab Boeing	USAF / Rome Lab Martin Marietta
TYPE	Transmit	Receive	Receive
FREQUENCY (GHz)	29.6	19.9	19.9
No. of ELEMENTS	32	23	16
ARRAY CONFIG	Tile	Brick	Brick
ELEMENT CONFIGURATION	Square Grid	Triangular Grid	Square Grid
ELEMENT SPACING (CM)	0.82 (0.80λ)	0.81 (0.53λ)	0.84 (0.55λ)
RADIATING ELEMENTS	Aperture Coupled Circular Patch	Dielectrically Loaded Circular Waveguide	Printed Circuit Endfire Dipole
POLARIZATION	Linear	Linear	Linear
PHASE SHIFTER BITS	4	4	3
SCANNING RANGE (deg)	+/- 30	+/- 60	+/- 60
EIRP at BORESIGHT (dBW)	23.4	N/A	N/A
G/T at BORESIGHT (dB/degK)	N/A	-16.6	-16.1
COOLING	Thermoelectric and Fan	None	Fan

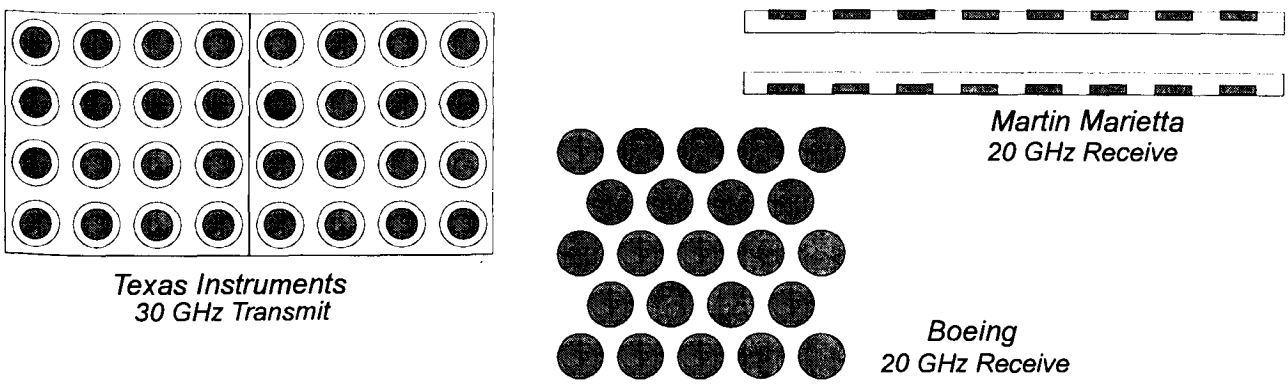

Figure 3. Array Radiating Element Geometry - Actual Size

without grating lobes. The thin profile is achieved via a multilayer construction approach involving vertical interconnections between different functional layers. The module design is based on a hybrid integration approach in which conventional wire bonding is used for interconnecting devices to the signal distribution layers. Devices are mounted on carrier plates and fully tested before insertion into the module, thus facilitating rework or device replacement. Furthermore, the "tile" construction allows use of semi-conductor batch processing techniques offering potential for reduced cost, size and weight.

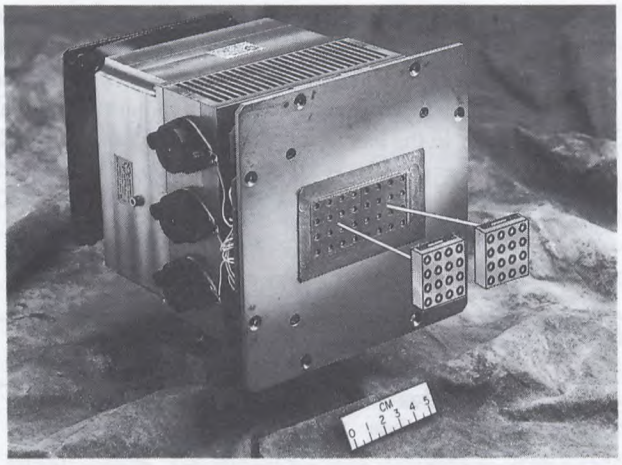

Figure 4. Texas Instruments 30 GHz Transmit Array

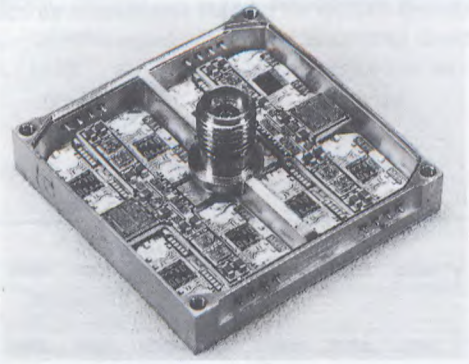

Figure 5. Texas Instruments Module - View From Back With DC/Logic Distribution Boards Removed

Figure 5 shows an inside back view of the 16 element subarray module. RF power is supplied via a coaxial connector (K series) and distributed to each radiating element through a sixteen way microstrip power divider network. Each of the sixteen RF lines feeds a 4-bit MMIC pin diode phase shifter of switched line length type and a three-stage PHEMT power amplifier and is electromagnetically coupled to a cavity backed, aperture coupled circular patch element. Logic commands for selection of individual phase bits and amplifier drain bias control (on/off) are transmitted via a serial data bus to a custom application specific integrated circuit (ASIC) which converts the serial data to parallel data for simultaneous control of the MMIC devices. DC bias and logic signals are supplied via individual pins and routed via a multilayer thin film network to provide gate and drain bias for the amplifier, ASIC power, and phase shifter bias control. Thermal stability is provided by a thermoelectric cooler and a small fan in the experimental housing.

Measured data for the 4-bit phase shifter shows an average insertion loss of 4.5 dB and phase accuracy of ± 10% of the selected phase state. The measured output power for the MMIC power amplifier was approximately 100 mW with 20 dB gain , and the insertion loss for the RF feed network at 30 GHz was approximately 5 dB. For the subarray module, the roll-off in gain as a function of scan angle was measured to be less than 3 dB over a 30° scan angle. The measured EIRPs of the two modules were 60 and 53 watts. The module DC power consumption was 10 watts and the RF power input to the radiating elements (sum of the individual amplifier outputs) was 1.6 watts, resulting in a 16% DC to RF efficiency. The two module array used in the Aero-X experiment has a measured EIRP of 23.4 dBW at boresight.

20 GHz Receive Arrays

The two 20 GHz receive phased arrays were provided through a joint effort of the Air Force Rome Laboratory Electronic System Center and NASA LeRC. In 1990 Rome Laboratory awarded contracts to Boeing and Martin Marietta to design full scale (approximately 4000 elements) integrated circuit active phased array (ICAPA) antennas for airborne satellite communications terminals. These contracts included the fabrication and delivery of 100 element proof-of-concept 20 GHz MMIC receive arrays. A subtask was added to each contract to deliver small (approximately 20 element) receive arrays suitable for the ACTS Aeronautical Experiment downlink. This was possible without incurring the cost of new MMICs because the ICAPA array design frequency of 20.2-21.2 GHz is sufficiently close to the ACTS downlink frequency of 19.9 GHz. These arrays were jointly sponsored by NASA LeRC and the Air Force.

Although the two designs involved fundamentally different packaging concepts, both the Boeing and Martin use a "brick" architecture in which the active components are mounted in modules parallel to the boresight of the radiating elements. The radiating elements have a nominal $\lambda/2$ separation allowing scanning to ±60° without grating lobes. As configured for ACTS Aero-X, both the Boeing and Martin arrays are linearly polarized.

Martin Marietta Array - The 20 GHz receive array built by Martin Marietta for Aero-X, shown in Figure 6, consists of 16 dipole antenna elements arranged on a 2 x 8 rectangular grid with half wavelength separation. The array is formed by two plug-in cards or trays each having 8 active receive channels. Each active channel consists of a printed circuit end-fire dipole antenna connected by microstrip to a PHEMT low noise amplifier and a GaAs 3-bit phase shifter. Each channel has a logic chip for phase shifter control. The overall gain of each channel is 23 dB with a noise figure of 3 dB. The RF output of the 8 channels is combined in a 8:1 beamformer and amplified by a follower amplifier. The RF output of each tray is combined in a 2:1 beamformer. Each tray is approximately 6.5 cm x 6.5 cm x 0.25 cm thick. As seen in Figure 6, the active elements are the two center rows separated by the air cooling channels (black squares).

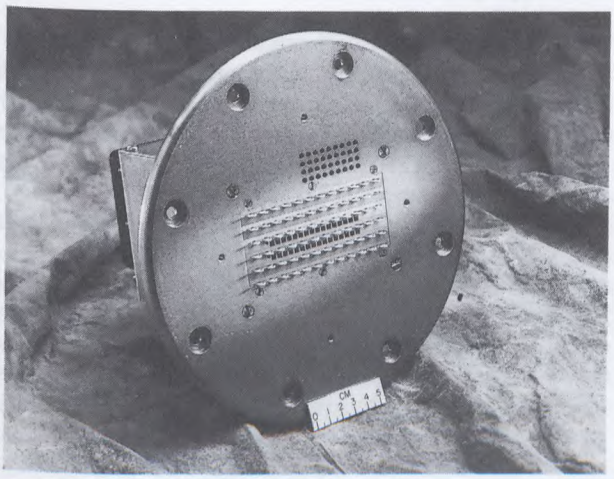

Figure 6. Martin Marietta 20 GHz Receive Array

Two rows of passive elements surround the 16 active elements to mitigate the edge-element pattern degradation associated with small arrays. The array was cooled by a fan. The overall gain of the array from the array face to the final beamformer was measured to be 42 dBi. The measured G/T of the array is -16.1 dB/degK at boresight.

Boeing Array - The 20 GHz receive array built by Boeing for the Aero-X is also of a "brick" architecture, but uses a different design concept. As illustrated in Figure 7, the array consists of a cluster of 23 active channels on a triangular grid with a half wavelength separation. Each channel is a separate dielectrically loaded circular waveguide into which a MMIC LNA and 4 bit phase shifter are integrated. The LNA and phase shifter are mounted in a ceramic module (4 cm x 0.5 cm x 0.3 cm thick) with a waveguide-to-microstrip transition at each end. The LNAs have a gain of 18 dB and a noise figure of 9 dB. In addition to the active components, each module has DC circuitry and a logic chip for phase shifter control. In the array developed for Aero-X, the RF output of the 23 channels is combined in a multi-mode space feed. A wide angle impedance matching (WAIM) layer is mounted in front of the receive aperture (not shown in Figure 7) to provide low VSWR over the 60° scan angle and 3% bandwidth. No active cooling was provided. The measured G/T of the array is -16.6 dB/°K at boresight.

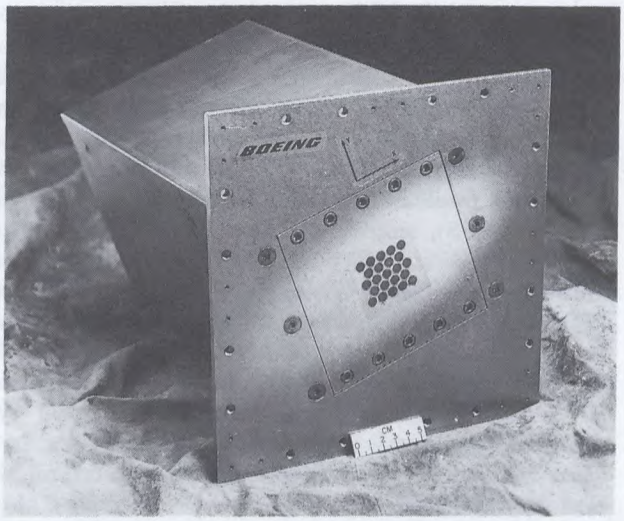

Figure 7. Boeing 20 GHz Receive Array

PHASED ARRAY CONTROLLER

The phased array controller (PAC), shown in Figure 8, is the subsystem that controls the steering of the three arrays and provides for the interface to the Learjet navigation system.

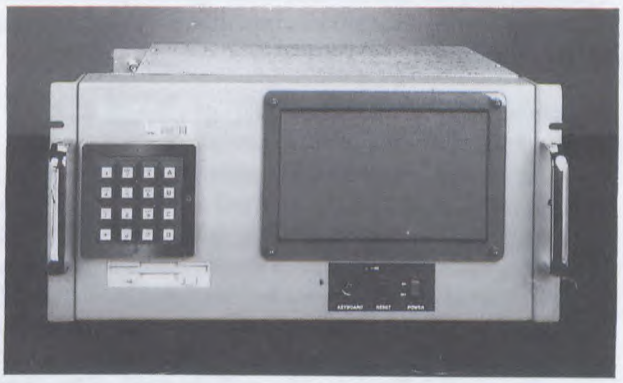

Figure 8. Phased Array Controller

Typically one transmit array and one of the two receive arrays would be automatically selected under program control to be active depending on the current aircraft flight path (orientation relative to ACTS). The controller consisted of a commercially available 486, 33 MHz processor board and expansion slots to accommodate I/O cards integrated into a single chassis with

an LCD flat panel display, keypad and 400 Hz power supply. Both custom and commercial I/O expansion cards were required to satisfy the various array interface requirements, Learjet navigation interfaces, solid state disk program storage requirements and inter-subsystem communication interfaces.

The PAC control software is written in the C language, running under the DOS standard personnel computer operating system. DOS, although not a real time operating system, provides a stable and standard platform in which to create the open loop steering algorithm for the arrays. Open loop steering was chosen after careful consideration of the antenna beam widths in combination with gyro accuracy, and restricting the Learjet rate of attitude changes to a maximum of 5 to 10 degrees/second. A single software control loop processes position updates from the global positioning satellite (GPS), received once per second under interrupt control, and current gyro attitude (roll, pitch, yaw) measurements via an analog to digital converter board. Combining the GPS position information, current attitude information and the known position of the ACTS satellite, the proper steering angles are calculated and antennas steered. The main control loop processes new GPS and gyro information and continuously updates the antenna steering as fast as the CPU speed will allow. This tight control loop demonstrated that antenna updates occurred from 0 to 18 times per second under flight conditions while maintaining acceptable link performance.

Increasing the main loop execution speed to provide faster updates to the antennas was the prime goal in maintaining acceptable link performance under aircraft attitude changes. The use of custom antenna interface boards reduces the CPU processing requirements. Also, all data communication between the PAC and the aircraft navigation systems and the data recording systems are interrupt driven to maximize main CPU utilization.

DATA DISPLAY AND STORAGE

Two data acquisition systems were used during Aero-X. During the verification flights in April and May, the JPL Data Acquisition System (DAS) of the ACTS Mobile Terminal (AMT) was used. The Aero-X demonstration flights in July and August use the data display and storage system (DDASS) developed by LeRC. This system, also used in the earlier verification flights, provides the flight system operator a complete visual indication of the in-flight status of the overall antenna system and aircraft flight parameters. Further capabilities allow for manual control of the various subsystems and archiving of data for later analysis of the flight. The DDASS is implemented with a 486 laptop computer with color LCD display and disk storage system. The DDASS interfaces with the PAC subsystem via a serial communication port for real time command and status information. Custom software written in QuickBASIC provides for the overall control of the DDASS.

Primary functions of the DDASS include data archiving of all aircraft attitude information and antenna pointing at one second intervals; a graphic map indicating the current aircraft position overlaid with spot beam patterns from the ACTS satellite; and display of the currently active spot beam based on current position.

AIRCRAFT INTEGRATION

Before installation in the Learjet, all three arrays were tested in the LeRC Near-Field Facility to confirm beam pattern and steering performance. The arrays were found to understeer slightly (a normal characteristic) so correction factors were chosen empirically and then used to modify each array's steering algorithm. A discrepancy with the TI antenna's beam pattern was noted at this time. This was compensated by the controller and later resolved when a hardware error was corrected.

The arrays were installed in the pressurized cabin of the Learjet, each looking out though a side window (Figure 9).

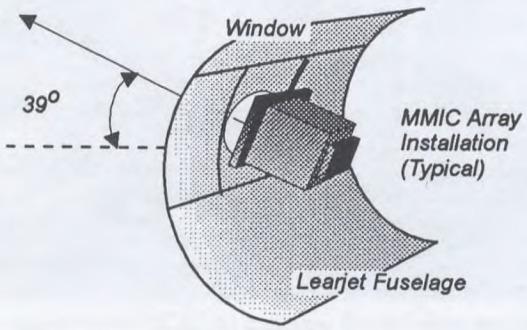

Figure 9. Array Mounting Detail

Originally, there were concerns that the loss through the acrylic aircraft windows would compromise the link margin. A procurement action to replace the acrylic window with a "radome type" window was instituted, but delivery delays and some hairline cracks in these windows caused enough concern that it was decided to continue using the acrylic windows in spite of the higher RF loss at high steering angles.

The arrays, controller and the JPL AMT were then installed in the Learjet and integrated with the aircraft avionics during the month of April 1994. The Martin Marietta and Boeing receive arrays were installed on the starboard and port sides of the Learjet, respectively, boresighted approximately 39 degrees up from the horizon. This elevation is appropriate for linking flights through the West Scan sector beams of the ACTS from Chicago, IL to Washington, DC. The Texas Instruments antenna was provided with mounting housings on both sides

of the Learjet; this enabled demonstration of the duplex communication link with the ACTS with either of the receive arrays just by moving the antenna from one side of the aircraft to the other. The Martin Marietta and the Texas Instruments arrays were used in the link during eastbound flights, while the Texas Instruments and Boeing arrays were demonstrated on westbound flights.

The installation of all of the special racks and system hardware, including the AMT, in the Learjet required a major effort. Because the existing experimental hardware was relatively large, space was limited. During the demonstrations flights in July and August the AMT DAS was removed to allow an additional passenger in the Learjet. The tight space made it difficult to get at the Boeing array to change its linear polarization axis relative to ACTS as required for some of the ACTS beams.

SYSTEM PERFORMANCE

The antenna system performed well during the technology verification flights after initial adjustments in level settings were determined and some residual controller software issues were resolved. Both 4.8 and 9.6 Kbps duplex voice links between the LeRC Learjet and the HBR LET were achieved. The 4.8 Kbps link was chosen for the demonstration flights as this rate was more robust and allowed the link to be maintained further down the taper of the ACTS beam, permitting longer test times. Lockup of the duplex link was typically achieved for periods of approximately 15 minutes, corresponding to the time of transit of the Learjet through a beam. Bit error testing at the signal levels achieved during these flights would require hours of continuous data. The short contact times precluded performing bit error rate tests. Consequently the E_bN_o values were used as an indication of the link quality.

During the early flights, conducted at varying times of day and evening, diurnal variations in the west sector scan beam pointing caused problems. Until this was understood, the operators on the aircraft could not be certain whether loss of link was due to system problems or drop off in beam gain. Another satellite beam pointing issue which became understood after several flights, was that the ACTS transmit and receive beams were not always co-located Since the modems and codecs for the transmit and receive sides of the link must communicate with each other, a viable link was only established where the two ACTS beams were co-located. This had the effect of reducing the time the link could be maintained..

Overall the antenna arrays were able to track the ACTS over the range of aircraft orientations for which ACTS was within the array scanning range. The measured performance of the system in the Seattle beam, for example, agreed with the predictions at both the -0.8 dB and -5 dB ACTS beam pattern contours. The ability of the array system to track the ACTS during an aircraft turn was demonstrated on several occasions.

The transmit antenna was the limiting factor in terms of link margin and scanning range. Nevertheless, on at least one occasion, a 9.6 Kbps link was established at a scan angle of 44°, well beyond the 30° at which grating lobes begin to appear. Other than a driver amplifier failure which was quickly repaired by Texas Instruments, the antenna system performed reliably throughout the program.

SUMMARY

Three different Ka-band electronically steerable MMIC arrays developed by NASA Lewis Research Center and the Air Force Rome Laboratory, an array control system and their integration and operation in the LeRC Learjet for the ACTS Aero-X have been described. Duplex voice links at 4.8 and 9.6 Kbps between the Learjet and the LET through ACTS were successfully demonstrated using the array system during flight when the Learjet was within an ACTS main or scanning spot beam and the ACTS was within the scanning range of the arrays. This is the first time an electronically steered Ka-band MMIC array system has been demonstrated in an aeronautical terminal link with a satellite.

The verification and demonstration flights provided opportunities to evaluate the performance of all system components. The successful results of this program provide a basis for the design of arrays, controllers and transceivers for future airborne satellite communications systems.

REFERENCES

1. **K. Dessouky and T. Jedrey,** "The ACTS Mobile Terminal", SATCOM Quarterly No. 8, Jet Propulsion Laboratory, Pasadena CA, January 1993

2. **P. Sohn, C. Raquet, R. Reinhart and D. Nakamura,** "ACTS Aeronautical Terminal Experiment System Description and Link Analysis", in Proceedings of International Mobile Satellite Conference - IMSC '95, Ottawa, Canada, June 6-8, 1995

3. **S. Sanzgiri, D. Bostrum, W. Pottenger and R. Lee,** "A Hybrid Tile Approach for Ka-Band Subarray Modules", to be published in a special packaging issue of the IEEE Trans. AP-S, 1995

Novel Low Profile Antenna Candidates for EHF Portable Terminals

D. Roscoe, L. Shafai*, A. Ittipiboon, M. Cuhaci, and H. Moheb**
Communications Research Centre
3701 Carling Ave., Ottawa, Ont. K2H 8S2

*Department of Electrical and Computer Engineering
University of Manitoba
Winnipeg, Manitoba, R3T 2N2

**InfoMagnetics Technologies Corporation
11-1329 Niakwa Road E., Winnipeg, Manitoba, R2J 3T4

ABSTRACT

This paper presents three low profile antenna candidates for EHF portable communication terminals. The first structure is a planar, multilayer microstrip antenna utilizing electromagnetic coupling to minimize the complexity and losses associated with the feed network. The second candidate is a medium gain (15dB) radiating cavity antenna utilizing a thick metallic ground plane. This element is amenable to device integration because a heat sink is incorporated and an area is available for fastening modular RF components. Thirdly, as an alternative to microstrip antennas, dielectric resonator antennas (DRAs) are presented. A broadband (28%) DRA is discussed. Experimental measurements are presented for all three antenna candidates.

INTRODUCTION

A wide variety of antenna candidates are being proposed for application to the portable personal communication terminal operating at 20 GHz (receive) / 30 GHz (transmit). These candidates range from an array of printed dipoles to a deployable reflector system. The antenna array approach is preferred to the reflector approach for two reasons. Firstly, low to medium power amplifiers can be distributed and integrated within an array to yield a more efficient antenna structure as compared to using a single power amplifier (as required with a reflector). Secondly, an integrated antenna array would be low profile, compact, and less obtrusive as compared to a deployable reflector. Efficient, low profile antennas are ideal candidates for portable communication terminals. For high gain antennas, the standard approach is to use an array of microstrip patch antennas. Although these antennas have attractive physical features, the feed network required is lossy at EHF. This in turn degrades the G/T of receive antennas and the efficiency of transmit antennas. This paper is subdivided into three sections and presents three novel antenna configurations suitable for portable terminals; i) a multilayer electromagnetically coupled microstrip patch configuration (Quad EMC patch), ii) a cavity type element, and iii) dielectric antennas. Each element has favourable characteristics for the specific application at hand.

SECTION I : QUAD EMC PATCH

The Quad Electromagnetically Coupled (EMC) patch is a multilayer microstrip patch configuration first presented in [1]. The element was developed to reduce the number of feed points required within an array. A 4:1 reduction has been achieved. As an example, an array of 128 microstrip patch antennas requires 128 feed points, however, using the Quad EMC patch would reduce the number of feed points to 32. The reduction simplifies and reduces the required feed network, and hence reduces the feed network losses. A slot coupled fed element was developed [2] and is presented in Fig. 1. The slot coupled feed is the preferred method of excitation as the common ground plane separates the radiating element from the feed network and no additional mechanical intervention is required (as compared to excitation with a probe). Isolating the feed network from the radiating element reduces the interaction of spurious feed network radiation with the element radiation pattern. This implies that a low cross polarization field component is expected. The Quad EMC patch is a three layer structure where energy is coupled through the slot from the feed line (feed layer) to the single patch on the first layer of the antenna. This patch then distributes the energy to the four patches above on the second layer of the antenna (electromagnetic coupling is utilized throughout).

Results :

A single slot-coupled Quad EMC patch designed for 20 GHz operation was fabricated using the materials presented in Fig. 1. The computed and measured radiated patterns (E- and H-plane) are presented in Fig. 2 and 3 respectively. The measured gain of this single element is approximately 10.75 dB if one subtracts the feed network losses. The measured cross-pol. component is approximately -40 dB below the co-pol. component at boresight. The input impedance bandwidth (VSWR 2:1) was measured to be 4.5%. It is evident that the antenna performance corresponds with that predicted.

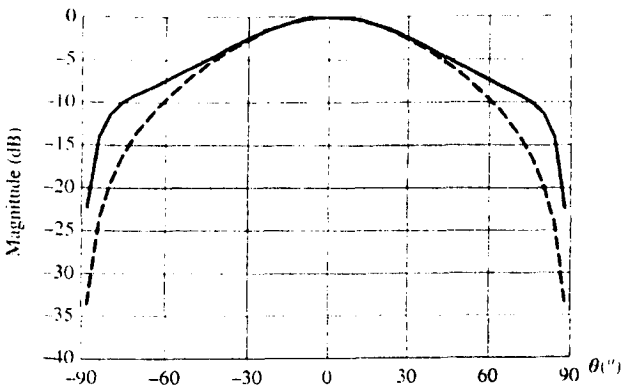

Fig. 2 : Computed far field pattern of the slot-coupled Quad EMC patch, E-plane ———, H-plane - - - - - -.

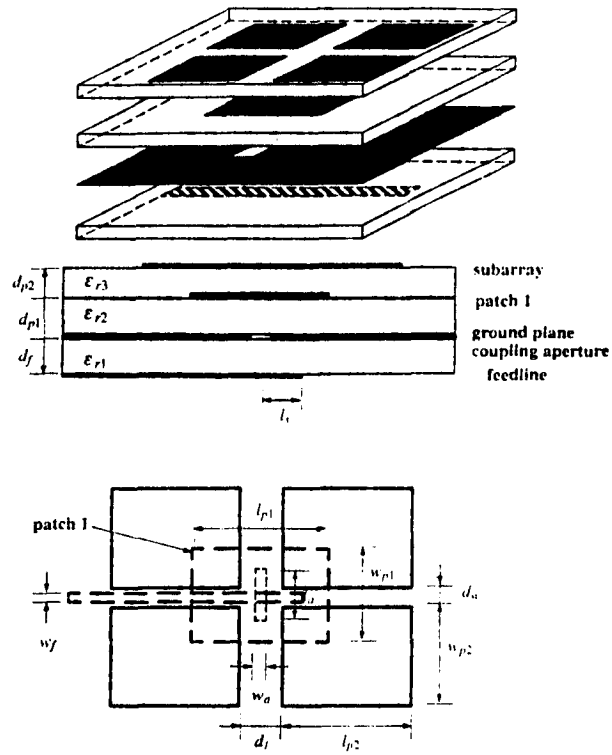

ε_{r1} = 10.2, df = 0.254 mm, ε_{r2} = 2.94, dp_1 = 0.254 mm, ε_{r3} = 2.94, dp_2 = 0.381 mm

Fig. 1 : Slot-coupled multilayer Quad EMC microstrip patch antenna.

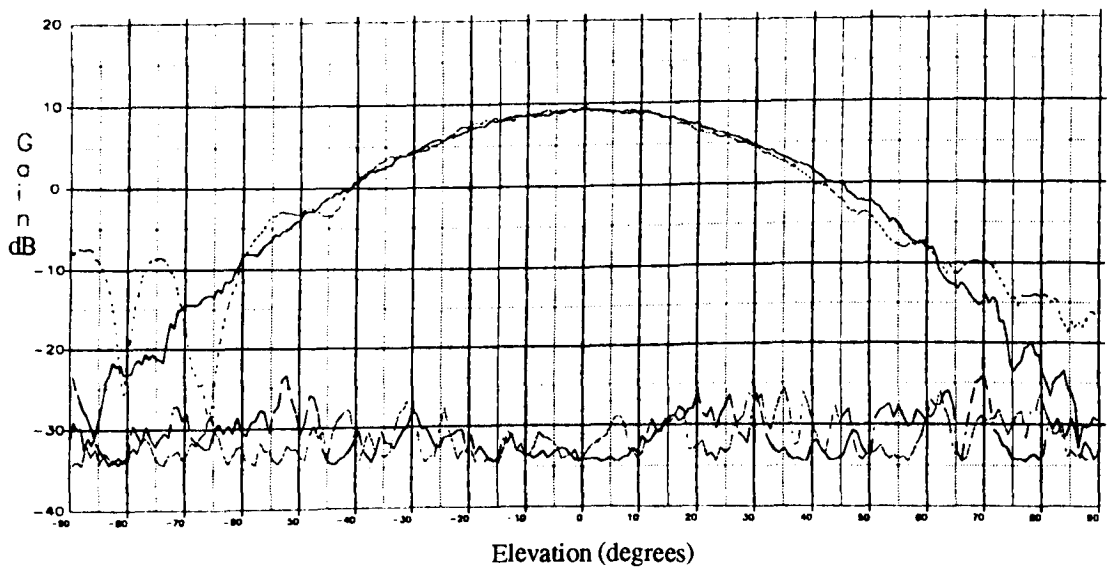

Fig. 3 : Measured far field pattern of the slot-coupled Quad EMC patch, E-plane - - - - - -, H-plane ———.

SECTION II : HIGH EFFICIENCY RADIATING CAVITY (HERC) ANTENNA ELEMENT

This antenna candidate is an efficient radiator and is amenable to device integration. With this configuration, a thick metallic ground plane is available for fastening modular RF components. The element is depicted in figure 4 [3]. The cavity is formed from a thick ground plane where a microstrip element is used to feed the cavity. Hence, coupling from the feed line occurs through a thin ground plane within the cavity, while device integration can be done using the thick ground plane outside the cavity. The passive antenna element is designed to yield gains of approximately 15 dBi. In addition to the mechanical advantages, the high gain obtained from this element is well suited for the application of a fixed beam or limited scan array for the personal communications terminal since fewer elements are required in comparison to an array using solely microstrip patches. This in turn reduces the size of the feed network and the required electronics.

The effective aperture area of this antenna is outlined by the circumference of the cavity. The achievable gain is a function of the cavity diameter. Hence the cavity diameter is not limited to a specific size, but is typically $> 1.5\lambda_0$. The patch within the cavity is the feed for the cavity and is not the primary radiator. The result is a relatively electrically large aperture area excited by a single point feed.

Results :

A passive cavity element was fabricated and measured. The structure is similar to that shown in Fig. 4. The cavity diameter was milled from a block of aluminum (thickness<1cm). The feed patch was etched on substrate material; relative permittivity 2.55, t=0.8mm. The computed radiation pattern for this element is presented in Fig. 5. The expected gain (no feed network losses) of this single element is 15.32 dB. The measured radiation pattern for the fabricated cavity element (fc = 17.3 GHz) is presented in Fig. 6. The peak gain (including feed network losses) is 14.5 dB and the measured input impedance bandwidth (VSWR 2:1) is 18 %. The return loss measurement is presented in Fig. 7. The measured results indicate that with a single point feed, a large aperture area can be efficiently excited. Results for the active integrated HERC element will be presented at the conference.

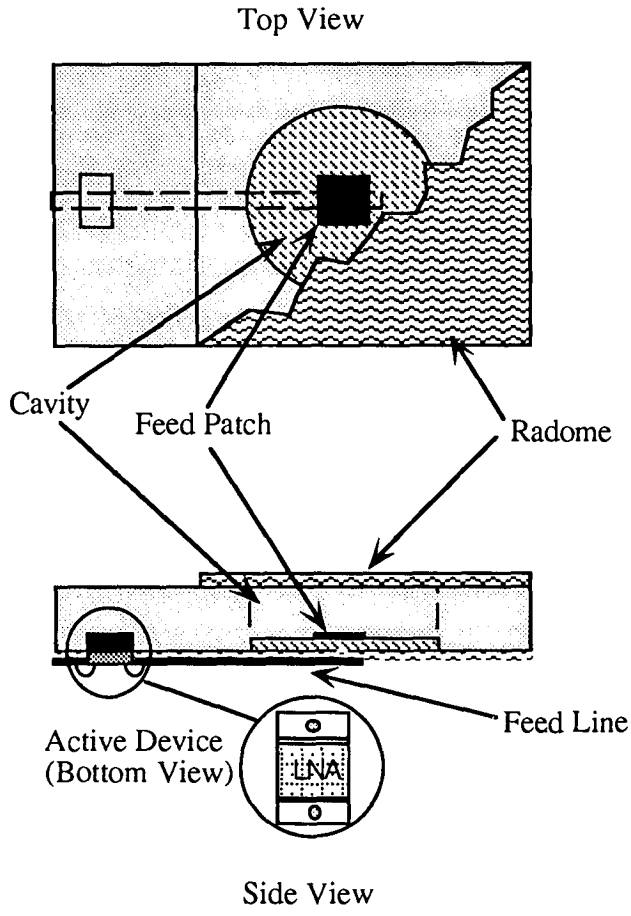

Fig. 4 : High efficiency radiating cavity antenna element amenable to device integration.

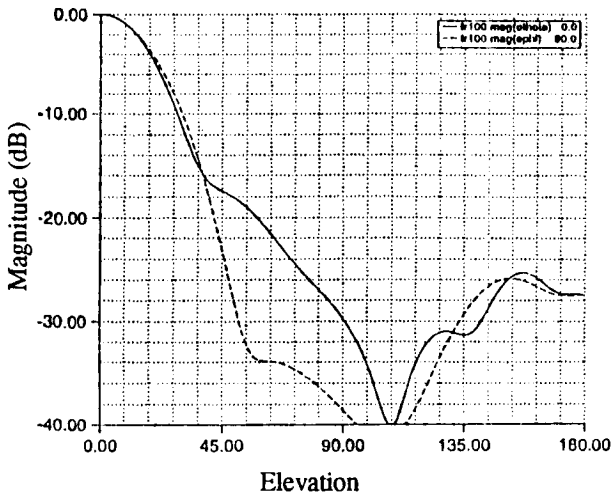

Fig. 5 : Computed far field patterns,f=fc,
E-plane - - - - - - -, H-plane ———.

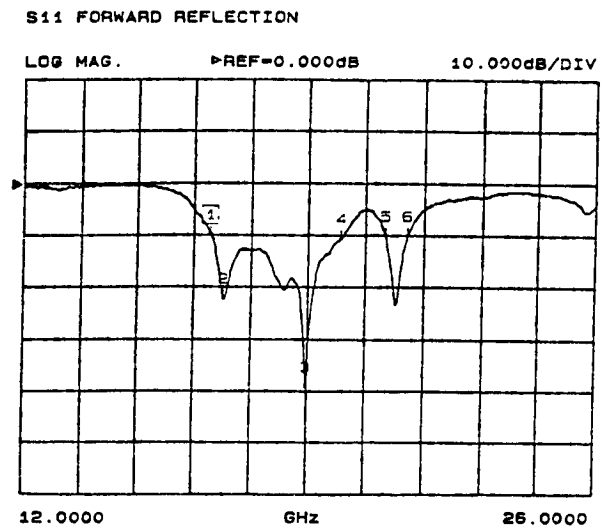

Fig. 7 : Measured return loss.

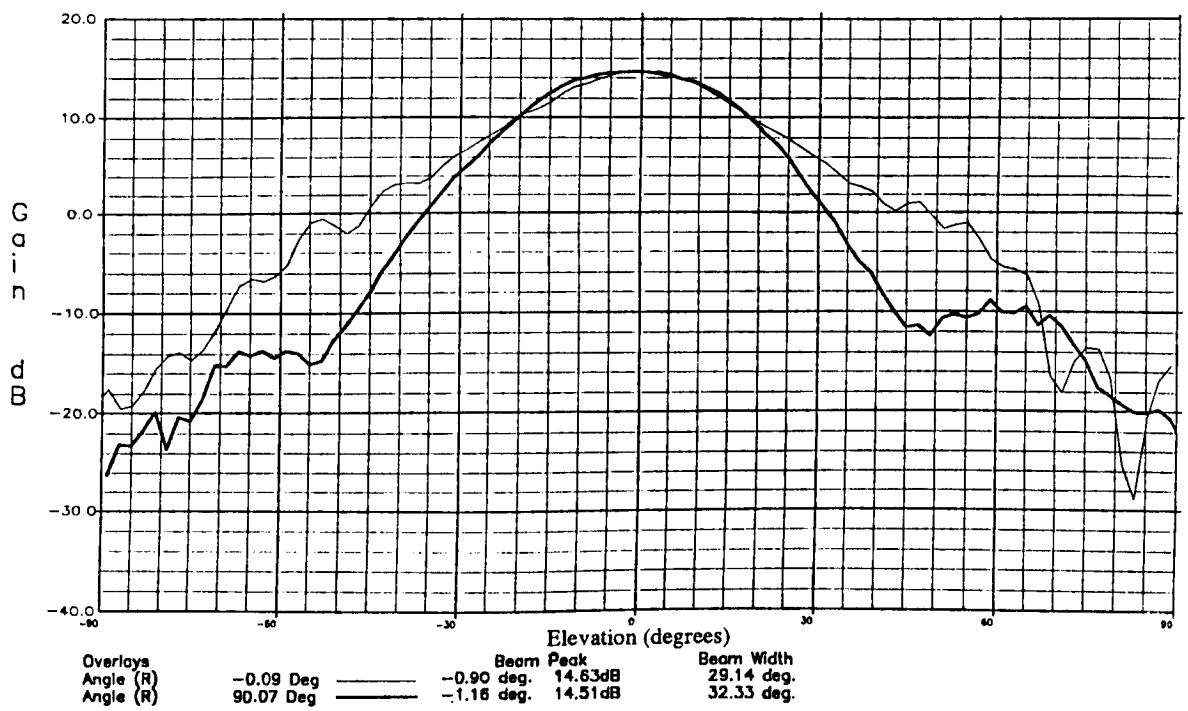

Fig. 6 : Measured far field pattern of the HERC antenna element, E-plane ———, H-plane ———.

SECTION III : DIELECTRIC RESONATOR ANTENNAS (DRAs)

Dielectric resonator antennas (DRAs) are presented as an alternative to microstrip antennas. These elements possess superior radiation efficiency [4] and bandwidth performance as compared to a microstrip patch. In addition, DRAs are amenable to numerous feed mechanisms (e.g. slot, probe, microstrip). These features are particularly attractive for EHF applications. A typical slot fed rectangular DRA element is presented in Fig. 8. The antenna is usually fabricated from medium to high dielectric constant material. The bottom layer is a microstrip line feed layer. A signal is coupled to the antenna through a narrow rectangular slot, perpendicular to the feed line, in the common ground plane between the antenna and the microstrip line. This antenna behaves like a short magnetic dipole aligned parallel to the axis of the slot with the maximum radiation in the boresight direction. The dimensions are frequency and material dependent. Thus the height of a typical DRA element is 1-3 mm at EHF. The operational bandwidth of the standard rectangular DRA is approximately 10%. However, this DRA can be designed to produce a much wider operational bandwidth than previously reported. Design and geometric details of the broadband element are not provided in this paper (patent in progress), however, the measured antenna performance is presented.

Results:

Several samples of the rectangular broadband DRA were fabricated from RT/duroid 6010 with a dielectric constant of 10.8. It should be noted that the operating frequency in this study was arbitrarily chosen for the convenience of the measurement. In general, the geometric shape is rectangular in nature having a length of 10 mm and height of 3 mm. In this experiment, the slot dimensions and the matching stub length were optimized so that the samples had a good match to the feed line. The measured return loss of several samples are shown in Fig. 9. The results show the characteristic of a double tuned resonant circuit. When the two frequencies are located closer to each other, the antenna has a broad operating bandwidth. When the two frequencies are farther apart, the antenna can be utilized in a dual band mode of operation. For the samples studied in this paper, it is found that the bandwidth of the modified rectangular DRA can be increased to 28% as compared to 10% of the standard rectangular element. The measured radiation patterns of this antenna varied only slightly over this broad impedance bandwidth, as shown in Fig. 10. Hence, it is clear that the operating bandwidth of this DRA is 28% which is a significant improvement over the single microstrip patch element (a few percent bandwidth). It should be noted that the cross-polarization level of this antenna is 20 dB lower than the peak co-polarization level over the same frequency band.

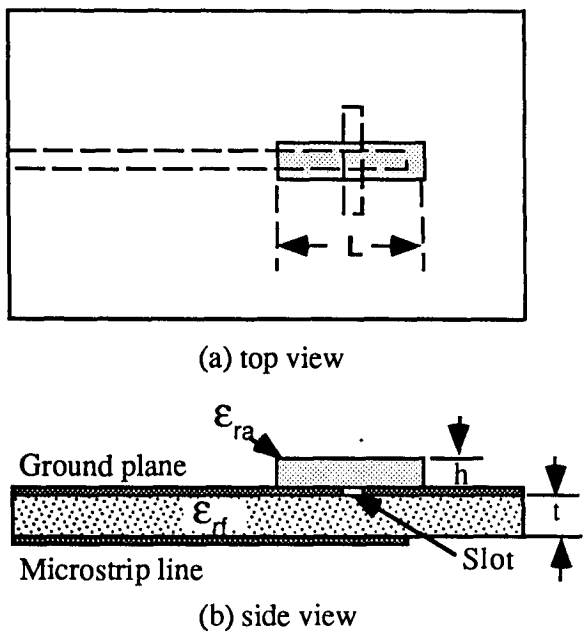

Fig. 8 : A rectangular slot-coupled dielectric antenna.

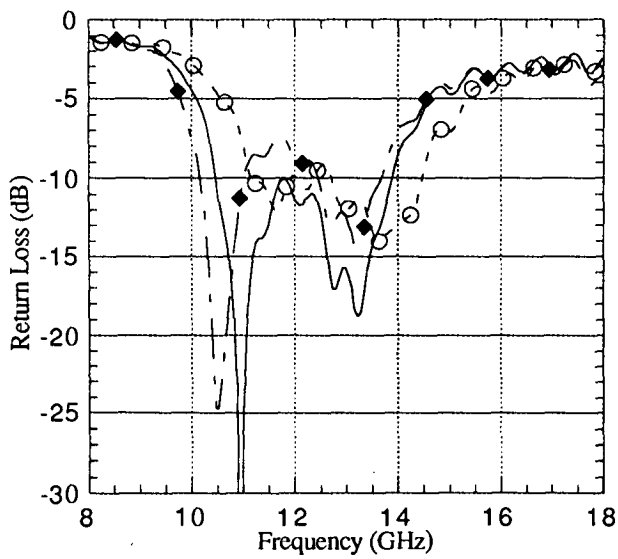

Fig. 9 : Measured return loss of several broadband dielectric resonator antennas.

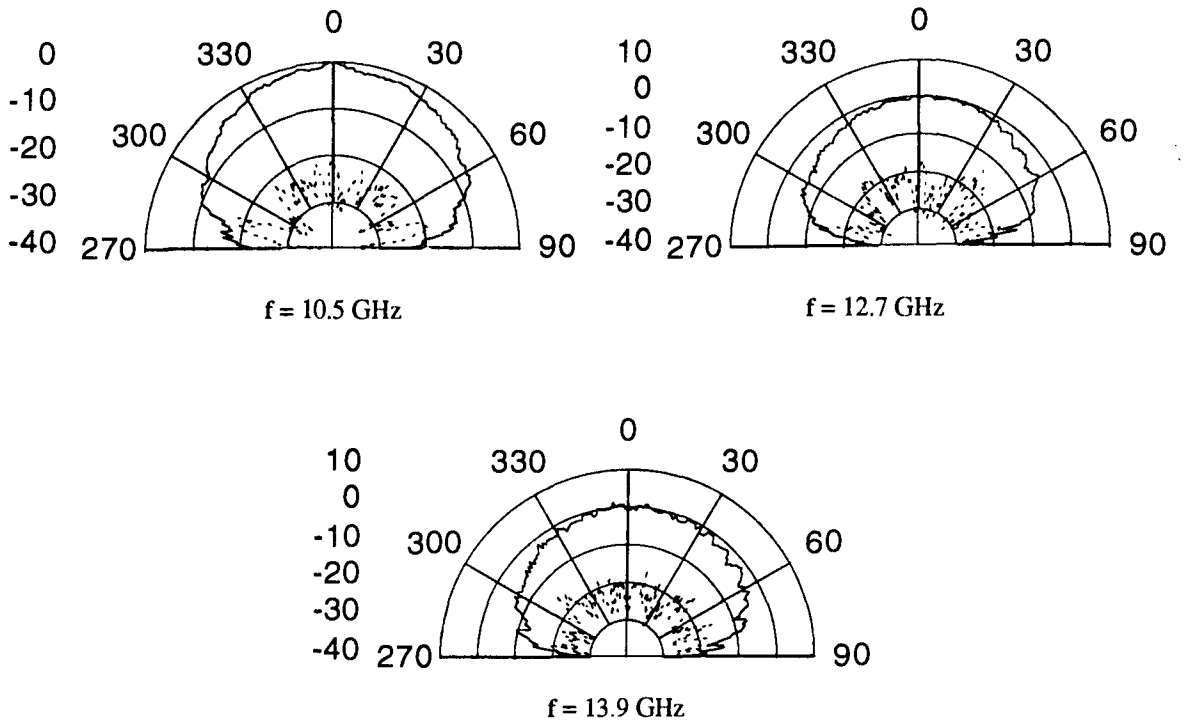

Fig. 10 : Measured H-plane co- and cross-pol. radiation patterns for the broadband rectangular dielectric resonator antenna.

CONCLUSIONS

Three low profile antenna candidates have been presented along with experimental measurements. The elements are well suited for low profile array applications and each antenna element has attractive characteristics.

The Quad EMC microstrip patch produced a peak gain of approximately 10.75 dB with a 4.5 % bandwidth. Although the bandwidth is narrow as compared to the other two elements, the antenna is a planar structure which minimizes the complexity of the feed network.

The high efficiency radiating cavity antenna element had a measured gain of 14.5 dB with an impedance bandwidth of 18%. This antenna element is particularly attractive for integrated array applications. The mechanical structure functions as a heat sink as well as providing an area for fastening modular RF components. Out of the three candidates presented, this structure is the best suited for an active integrated array.

The use of dielectric resonators as antenna elements is a relatively new field of study. Results to date are very promising and show their applicability to EHF arrays. The DRA element presented had a bandwidth of 28%. Although it is a low gain antenna element (-4dB), superior efficiency and bandwidth characteristics lend themselves to array applications.

REFERENCES

[1] H. Legay, L. Shafai, and J.S. Wight, "*Study of Integrated Antenna Concepts for Small EHF Terminals*", DSS Contract #36001-2-3532, Communications Research Centre, 1992.

[2] InfoMagnetics Technologies, "*Feed Distribution Studies of Integrated Antenna Arrays for Small EHF Terminals*", DSS Contract #36001-3-3651, Communications Research Centre, 1994.

[3] InfoMagnetics Technologies, "*Study of Thick Ground Plane Antenna Element for Small EHF Terminals*", DSS Contract #36001-3-3651, Communications Research Centre, 1994.

[4] R.K. Mongia, A. Ittipiboon, and M. Cuhaci, "*Measurements of Radiation Efficiency of Dielectric Resonator Antennas*", Microwave and Guided Wave Letters, Vol. 4, pp. 80-82, March 1994

Mobile Antennas for COMETS Advanced Mobile Satcom Experiment

Yoshihiro Hase, Masato Tanaka and Haruo Saito
Communications Research Laboratory
4-2-1 Nukui-Kitamachi, Koganei, Tokyo 184, Japan
Phone : +81-423-27-7506 Fax : +81-423-27-6825

ABSTRACT

Advanced mobile satellite communication experiments in the Ka-band and the mm-wave will be carried out using the COMETS satellite, which is scheduled for launch in 1997. Mobile antennas will play a much more key role in high frequency systems such as COMETS than in conventional L-band mobile systems. This paper describes three types of antennas which are now being developed by the CRL for the COMETS mobile experiments. One is a mechanically steered waveguide slot array antenna, another is an electronically steered active phased array antenna, and the third is a mechanically steered torus reflector antenna. The first two antennas will be used in the Ka-band, while the latter will be used in the mm-wave.

INTRODUCTION

COMETS[1] is an engineering test satellite for advanced mobile satellite communications, advanced satellite broadcasting and inter-orbit communications in much higher frequency bands than conventional ones. The satellite will be launched into a geostationary orbit of 121° east in 1997. Experiments on mobile communications and broadcasting will be carried out mainly by the Communications Research Laboratory (CRL), while an inter-satellite communication experiment will be conducted by the National Space Development Agency of Japan (NASDA).

The objectives of COMETS mobile satellite communications experiments are to develop basic technology, and to assess the feasibility of future mobile and personal satellite communications in the Ka-band (31/21GHz) and the Q-band (47/44GHz). This paper focuses on mobile terminal antennas which will be key elements in the COMETS mobile satellite communication system.

MOBILE EXPERIMENT SYSTEM

On-board transponders of COMETS have advanced features such as signal processing with SCPC/TDM regenerative modems[2], and an inter-beam connection capability using an IF filter matrix. The SCPC/TDM regenerative transponder will be the first of its type in the world, and

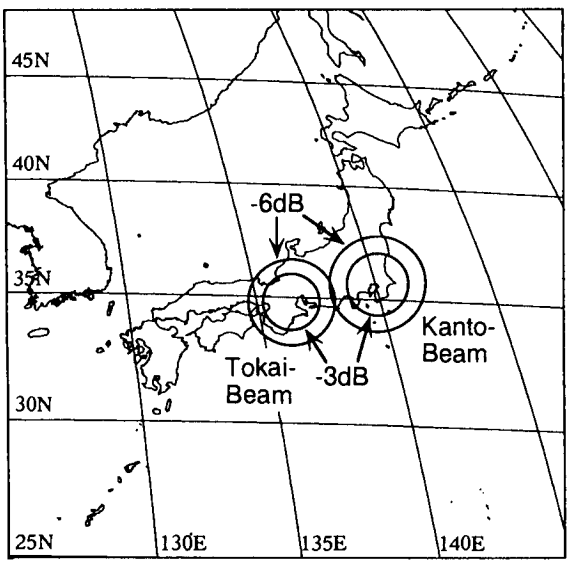

Figure 1. Beam Coverage in Ka-band

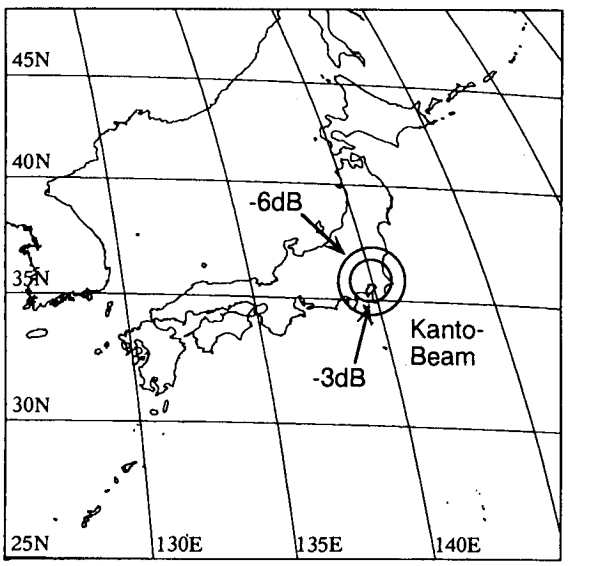

Figure 2. Beam Coverage in Q-band

is especially suitable for mobile/personal systems with many small earth stations. The on-board dual band multi-beam antenna has 2 spot beams for the Ka-band and one beam for the Q-band. The beam coverage of the antenna is shown in Figures 1 and 2.

Two hub stations with command and control functions will be set up at the CRL's Kashima Space Research Center in Kashima, Ibaraki, and at CRL's main site in Koganei, Tokyo. Each of them has a 1.8mϕ antenna for the Ka-band and a 1.2mϕ antenna for the Q-band.

The transmission rates used in this system will be from 4.8kbps to 640kbps depending on the type of information to be transmitted; video, voice, messages and so on. The modems used by the regenerative transponder links, however, must be a combination of a 24kbps BPSK modulator and a 192kbps demodulator, or a combination of a 4.8kbps modulator and a 38.4kbps demodulator. In the case of automobile terminals, the normal transmission rate will be 24kbps. Table 1 shows an example of the link budget using a Ka-band transponder with a 24/192 kbps modem, and a rate-1/2 FEC codec.

MOBILE ANTENNAS

Overview

Mobile antennas are key and technologically challenging components in the system. We intend to develop at least two types of antenna systems in the Ka-band and one in the mm-wave.

Table 1. Example of link budget in Ka-band

Transponder Type	Repeater Mode		Regenerative Mode	
Information Rate	12.0	kbps	12 / 96	kbps
Modulation Rate	24.0	kbps	24 / 192	kbps
Required C/No	47.4	dB·Hz	47.4 / 55.4	dB·Hz
(Up-link Path)	30.8	GHz	30.8	GHz
Mobile EIRP	24.0	dBW	24.0	dBW
Path Loss	214.1	dB	214.1	dB
Satellite G/T	16.9	dB/K	16.9	dB/K
Up-link C/No	55.3	dB·Hz	55.3	dB·Hz
(Down-link Path)	21.0	GHz	21.0	GHz
Satellite Tx Power	0.0	dBW	9.0	dBW
Satellite EIRP	44.0	dBW	51.0	dBW
Path Loss	210.8	dB	210.8	dB
Mobile G/T	-6.0	dB/K	-6.0	dB/K
Down-link C/No	55.8	dB·Hz	64.8	dB·Hz
Total C/No	52.5	dB·Hz		
Margin	5.1	dB	7.9	dB

As an automobile has a relatively small movement range, and the inclination of major roads is small (up to several degrees), the elevation angle toward the satellite can be regarded as almost constant, and for COMETS it is about 45° in the Tokyo area. If an antenna with a fairy wide beam in the elevation plane is used, a tracking function in the elevation direction can be omitted.

From the example link budget of Table 1, it can be seen that the G/T of the mobile stations must be greater than -6dB/K, allowing for an appropriate link margin. Considering a system noise temperature of about 500K (25dBK), the Rx antenna gain must be greater than 21dBi. The Tx antenna gain would be 24dBi, assuming the same aperture as that of the Rx antenna.

Waveguide Slot Array Antenna

The mechanically steered waveguide slot array antenna system is in its last stage of development. Its configuration consists of separated Tx and Rx antennas because a 10GHz difference between Tx and Rx frequencies is too large for this type. Although both antennas are mechanically independent, the Tx antenna is always controlled in exactly the same direction as the Rx antenna.

Figure 3 shows a picture of the Rx antenna system. The system was designed with an emphasis on low profile and light weight. In order to achieve a low profile, the beam direction of each antenna is tilted by 45° to the normal. This allows the antennas to be put on a rotating platform with no inclination. The gain of the antennas is 23.6dBi for the Rx and 26.4dBi for the Tx. The 3dB beamwidth in the elevation plane is 17° for the Rx and 10° for the Tx, and is a little wider than that in the azimuth plane. The radiation patterns are shown in Figures 4 and 5.

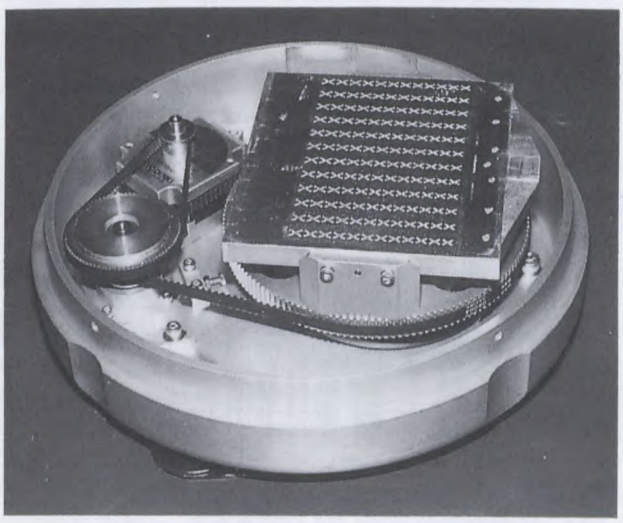

Figure 3. Waveguide Slot Array Antenna (Rx)

The antenna tracking method is a combination of closed loop tracking (step tracking) and open loop tracking (gyro tracking). The closed loop is controlled by detecting a CW pilot carrier. Although the terminal usually controls the antenna system with the closed loop, it changes to the open loop when the received level of the pilot carrier becomes lower than a threshold level, or when the automobile makes a quick turn.

Although the configuration of the separated Tx and Rx antennas has the disadvantage of a large overall size, it has the following advantage for the case of packet communications. Let us suppose that the Rx antenna is installed at the front of a car, and the Tx antenna at the rear with a distance d between them, and that the car is running at a speed v. A terminal can always recognize the shadowing condition at the Rx antenna position from the received signal level. This means that the terminal can predict the condition at the Tx antenna position a little earlier (d/v) than the actual shadowing event. For example, if v is 10m/s (36km/h) and d is 2 meters, the prediction is possible 0.2 second in advance. Thus the terminal can always avoid shadowing and choose a good Tx window if the packet length is less than d/v in time scale.

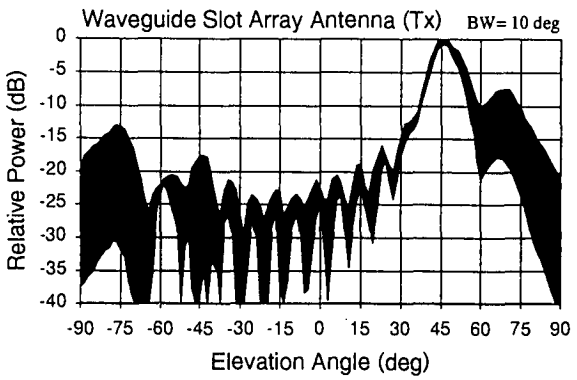

Figure 4. Radiation Pattern of WG Slot Array Ant.(Tx)

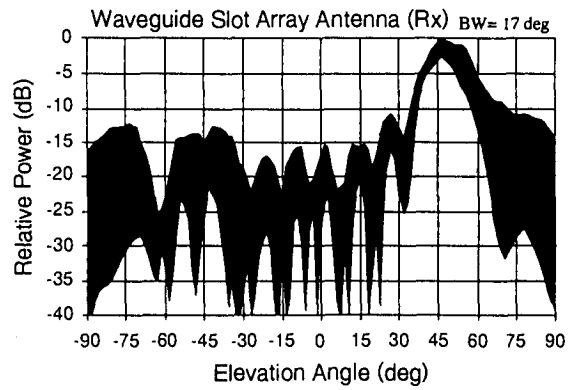

Figure 5. Radiation Pattern of WG Slot Array Ant.(Rx)

Active Phased Array Antenna

An active phased array antenna system in the Ka-band is a fully electronically beam scanning antenna system. It is one of the most technically challenging components in the COMETS system development.

Although we need to employ a duplex configuration using separated Tx and Rx antennas because of the same previously mentioned reason, current budget conditions do not allow for the development of both antennas, and so we are developing only the Rx antenna at this time.

We are going to adopt a higher-mode microstrip ring patch shown in Figure 6 as an element antenna rather than a fundamental-mode disc patch. This is because the antenna gain of the higher-mode patch is greater than that of the fundamental-mode patch in the 46° scanning direction, which corresponds to the elevation angle toward the COMETS satellite from Tokyo.

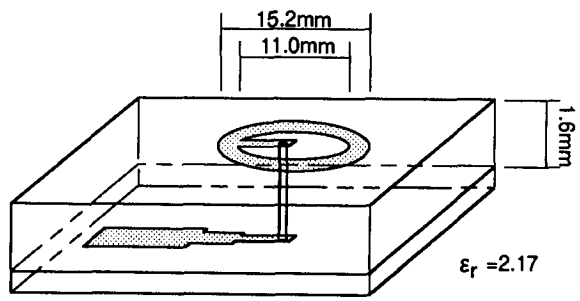

Figure 6. Higher-mode Ring Patch Element

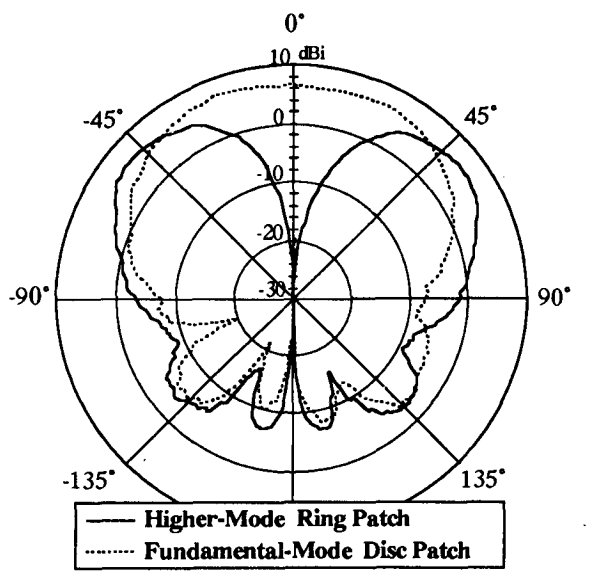

Figure 7. Radiation Pattern of Higher-mode Ring Patch

Figure 7 shows our experimental result of the radiation pattern of the higher-mode ring patch element compared with the pattern of the fundamental-mode disc element. This result, however, was obtained using scale models of the 10GHz patch elements.

About 40 elements are required to obtain more than 21dBi, considering about 5dBi element gain including feed loss. Although an element spacing of the array should be less than about 0.53λ in order to avoid grating lobes when scanning, the diameter of the higher-mode disc patch element is normally greater than 0.53λ. To overcome this difficulty, we are going to adopt a high εr (dielectric constant) substrate and a ring patch configuration, which has the advantage of decreasing its diameter to 60-80% of a disc patch.

A low noise amplifier (LNA) and phase shifter (PS) are installed just behind each element and the beam direction is controlled by adjusting each PS. The LNA and PS are under development using MMIC technology.

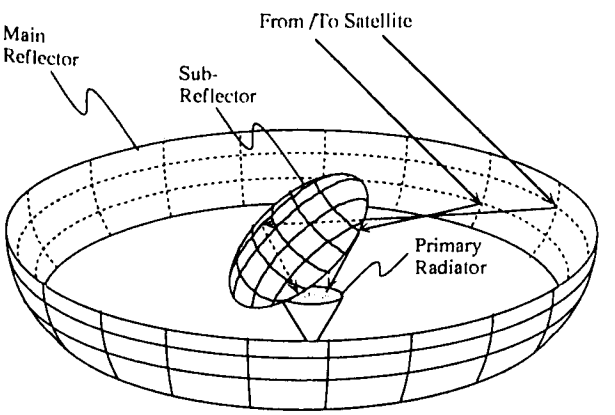

Figure 8. Concept of Torus Reflector Antenna

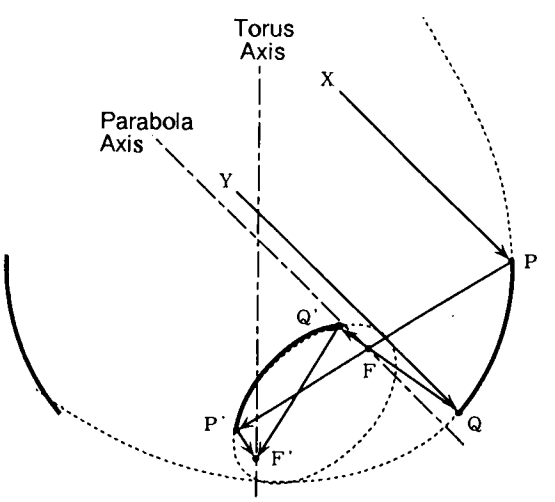

Figure 9. Vertical Section of Torus Reflector Antenna

Torus Reflector Antenna

As the development of thin array antennas is not cost effective in Q-band, even with state-of-the-art technology, we have chosen a reflector antenna for the mm-wave experiment.

The concept of a torus reflector antenna is shown in Figure 8. The main reflector has a torus shape whose surface in a vertical section is a parabola, while the sub-reflector is an ellipsoid. The tracking mechanism is very simple, merely revolving the sub-reflector around the central axis of the torus. It has a tracking function only in the azimuth direction, like the waveguide slot array antenna. The primary radiator does not move during tracking, and is fixed on the axis and points upwards. This configuration ensures a simple and low-cost antenna since an expensive rotary joint to feed RF signals is not required, and the moving portion of the antenna is small as the main reflector and the primary radiator do not move. The bandwidth of the antenna is wide enough to cover both the Tx and Rx frequencies because a horn antenna can be employed as the primary radiator.

The vertical section with projected radio wave paths is shown in Figure 9. The main reflector is a parabola whose focus is F, just the middle between the center and the main reflector, and the sub-reflector is an ellipse. A plane wave from the satellite is reflected by the main reflector and converted to a spherical wave. It focuses on F, and re-spreads to the sub-reflector. As one of the two elliptical sub-reflector's focuses is set at F and the other at O on the axis of the torus, the re-spread wave is reflected by the sub-reflector and finally concentrates at O. This configuration is the same as an offset Gregorian antenna.

As for the horizontal section, the main reflector is a circle. As a small part of an arc is approximate to a parabola whose focus is just on the middle of the radius, the spherical wave reflected at the main reflector focuses on F. From our calculations, if the arc PQ subtends an angle of 20 degrees or less, the aberration created by the main reflector is negligible.

CONCLUSION

The development of COMETS mobile antennas, currently under design or manufacture, has been described. The antenna gain must be more than 21dBi for Rx and 24dBi for Tx to satisfy the requirements of the link budget. All the antennas have a limited tracking function in the azimuth direction only using a fairly wide beam in the elevation plane. This allows the configurations and control circuitry to be simple and low-cost. The CRL will

continue to develop these antennas for the COMETS experiments and also develop terminal equipment. The key point in terminal development will be to overcome much larger frequency drifts than with other mobile systems.

ACKNOWLEDGMENT

The authors wish to thank Toshiba Corporation for the development of MMICs and Nippon Steel Corporation for the development of the waveguide slot array antenna system.

REFERENCES

[1] **S. Ohmori, S. Isobe, M. Takeuchi and H. Naito,** *Advanced Mobile Satellite Communications Using COMETS Satellite in MM-wave and Ka-band,* IMSC '93, p.549, June 1993.

[2] **S. Isobe, F. Kawamata, H. Naito, N. Hamamoto and S. Ohmori,** *Regenerative Transponder of COMETS for Advanced Mobile Communications Experiments,* ICUPC '93, p.309, October 1993.

Performance and Operational Considerations in the Design of Vehicle Antennas for Mobile Satellite Communications

R. Milne
Mobile & Personal Communications
Communications Research Centre
3701 Carling Avenue, P.O. Box 11490, Station H
Ottawa, Ontario, K2H 8S2
phone # (613) 998-2434, fax # (613) 990-0316

ABSTRACT

This paper examines the vehicle antenna requirements for mobile satellite systems. The antenna parameters are discussed in the light of the requirements and the limitations in performance imposed by the physical constraints of antenna and by vehicle geometries. Measurements of diffraction and antenna noise temperature in an operational environment are examined, and their effects on system margins. Mechanical versus electronic designs are compared with regards to performance, cost, reliability and design complexity. Comparisons between open-loop and close-loop tracking systems are made and the effects of bandwidth, sidelobe levels, operational constraints, vehicle angular velocity and acceleration, are discussed. Some consideration is given to the use of hybrid systems employing both open and closed-loop tracking. Changes to antenna/terminal specifications are recommended which will provide greater design flexibility and increase the likelihood of meeting the performance and operational requirements.

INTRODUCTION

The Inmarsat world-wide maritime mobile satellite system was inaugurated in 1979. The receiving terminals employed mechanically steered reflector antennas with diameters of 1 metre, gains of 20 dBic and beamwidths of 20°. In the early 90's, a second generation of higher powered satellites was launched. The higher power and improved modulation techniques permitted a reduction in minimum gain to 12 dBic with a corresponding reduction in physical size. The introduction of regional satellite service permits a further reduction in minimum antenna gain to between 7-8 dBic. The Australian OPTUS system has been in operation for over 1 year. The North American MSAT system is scheduled to be in operation by the fall of '95 and Inmarsat is planning to launch in 1997 a third generation of satellites using spot beams.

The reductions in physical size of the antennas and the associated reduction in cost open up large new consumer markets involving private vehicles, small aircraft, and small vessels. The use of low gain antennas, however, introduces problems not previously encountered using higher gain antennas. The following discussions relate to low profile antennas with the emphasis on electronic array design and land vehicle applications. The antennas have a diameter of less than 2 wavelengths and an overall height of less than 0.25 wavelengths.

OPERATIONAL CONSIDERATIONS

System Margin

Mobile satellite systems, in general, are designed for "line of sight" operation, i.e. the system margins can accommodate reductions in signal strength due to reflections and diffraction from the host vehicle and surrounding terrain, and due to attenuation of the signal in inclement weather. The margins are, however, not sufficiently large to overcome the direct blockage of the signal by buildings, trees and terrain. An antenna elevation angular coverage from 15° to 70° would satisfy almost all of the land mobile requirements. It is however at the lower elevation angles where the degrading effects due to multipath, signal blockage, and antenna noise temperature are the most pronounced. The realizable antenna gain also decreases in the direction of the horizon. The system will therefore be over designed at the higher elevation angles unless the angle subtended by the satellite at the user terminal is known, and the EIRP at the satellite and at the user terminal is changed accordingly.

Antenna Noise Temperature

As a result of improvements in LNA and diplexer design, it is possible to achieve terminal noise temperatures of less than 200°K under "line of sight" conditions. The antenna noise temperature is a significant contribution and is determined by

the RF losses and directivity of the antenna, and the nature of the surrounding terrain. A series of measurements were conducted in an operating environment with a low profile antenna mounted on the roof of a vehicle, the antenna beam pointing at right angle to the direction of the vehicle. The antenna had negligible RF loss, beamwidths of 50°, and could be switched in elevation. The antenna noise temperatures, under "line of sight" conditions, at boresight elevation angles of 30°, 45°, and 60° were respectively 50°K, 30°K, and 30°K. In the presence of woods, subtending an angle of 15° above the horizon at the vehicle, the temperatures were 85°K, 50°K and 50°K respectively.

Antenna /Vehicle Interactions

Antenna radiation patterns are affected by reflections and diffraction from the vehicle structure. Low gain antennas have relatively large beam- widths and are more sensitive to their environment than their higher gain counterparts. The effect is characterized by a ripple in the elevation radiation pattern which progressively decreases with increasing elevation angle and is a function of the curvature and effective ground plane size presented by the roof of the vehicle. The height of the antenna above the ground plane also has a significant effect. There is, in addition, a degradation in antenna axial ratio at lower elevation angles. The signal strength will vary as the antenna pointing changes relative to the vehicle. Measurements indicate that variations in signal strength of ± 1.5 dB are typical. In some configurations, use can be made of the ground plane to increase the effective antenna gain at low elevation angles.

Multipath

The communications signal is also affected by the presence of natural and man-made objects in the vicinity of the vehicle. It is the sum of the direct signal from the satellite and the signals scattered by objects within the antenna beam-width and involves both copolarization and cross-polarization signal components. Vehicle motion changes the relative phase between the direct and scattered signals resulting in a fluctuating signal with doppler components. Measurements of the received signal from an Inmarsat satellite were made with a low profile antenna mounted on the roof of a vehicle. The antenna had a 3 dB beamwidth of about 50° and was aligned to the satellite at an elevation of 35° and fixed relative to the vehicle. The signal fluctuated ± 1 dB under "line of sight" conditions with the vehicle in motion.

PERFORMANCE CONSIDERATIONS

Fundamental Limitations

A design objective is to maximize antenna performance for the given antenna geometry. Ignoring the effect of diffraction from the edges of the array, the gain of a low profile antenna will vary as the projected area of the array in the direction of the satellite i.e. as the sine of the elevation angle. The electrical boundary conditions imposed by the array do not permit a circularly polarized signal to be transmitted close to the horizon. Low profile antennas are characterized by a rapid drop-off in gain and increased axial ratio at low elevation angles. A low profile antenna with a diameter of 2 wavelengths has a maximum achievable gain of 7 dBic at 15° elevation and an axial ratio of about 11 dB.

Antenna RF Loss

It is possible to achieve a terminal noise temperature of less than 200°K. The measured black body noise temperature contributed by the operating environment with the presence of low angle shadowing by trees, varies between 50°K and 85°K. A diplexer loss of less than 1 dB and a LNA noise figure of less than 0.8 dB are achievable. To eliminate the effect of RF cable losses, the diplexer and LNA must be an integral part of the antenna or located in close proximity. Antenna RF losses have the affect of attenuating the signal and increasing noise temperature. A 0.5 dB RF loss raises the terminal temperature by 20°K with a corresponding reduction in G/T of 0.9 dB.

Antenna Design

There are two distinct categories of antennas, namely, those that track the satellite by mechanical means and those that do so electronically. The majority of low profile antennas that have been developed to date are mechanically steered and are similar in concept to the early low profile antennas designed at JPL [1]. The antenna consists essentially of a planar array of microstrip elements mechanically steered in azimuth by a low profile stepper motor. It satisfies the low profile requirement and it is likely to be inexpensive to manufacture. The antenna beam is fixed and shaped in the elevation plane. A major advantage is that the antenna electrical performance need be only optimized for

one set of antenna angular co-ordinates. Electronically steered designs on the other hand, present a formidable design challenge in that the performance has to be optimized for every switched beam position within the specified angular coverage. The advantages of the design are the high speed of operation, adaptability, inherent reliability, and low power consumption.

Vehicle Dynamics

The antenna has to acquire and track the satellite under all dynamic conditions of the host vehicle. Tests were conducted to determine the maximum angular velocities and accelerations likely to be encountered. It is possible to achieve a maximum angular velocity of 60°/sec by driving as fast as possible a compact car in a minimum turning circle of 40' diameter. Under normal driving conditions, an angular velocity of 20-30°/sec would be more typical. Rapid changes in direction can generate almost step functions in angular velocity with corresponding spikes in angular acceleration exceeding $50°/sec^2$.

Acquisition/Tracking

A design goal is to acquire and track the satellite with a minimum loss in signal strength. The bandwidth of the tracking system must be small enough to minimize pointing errors and large enough to follow rapid changes in angular velocity. An electronic antenna array has an azimuth 3 dB beamwidth of about 50° at 15° elevation. To keep the signal loss to within 0.5 dB the pointing error must be less than ± 10°. At an angular velocity of 60°/sec, the antenna pointing must be updated at a minimum rate of 6Hz. As the antenna beamwidth, when expressed in terms of azimuth angular rotation, varies as the secant of elevation angle, the pointing accuracy and sampling rate requirement can be relaxed at the higher elevation angles.

A close-loop tracking system uses the received satellite signal to track the satellite. There are a number of ways of implementing a close-loop tracking system. A simple method is to switch the antenna beam about the satellite position and select the beam position with the strongest signal. The tracking system always maximizes the received signal and is likely to provide superior performance compared to open-loop tracking systems. The principle disadvantages are that the terminal receiver is part of the tracking loop and a continuous received carrier is required for continuous tracking operation.

Open-loop tracking systems use external sensors such as a flux-gate compass or gyroscope to point the antenna. The sensors are not as affected by terminal or systems design considerations. The principal disadvantages are that the tracking system requires a knowledge of the user terminal location vis à vis the satellite, and that there is an additional cost and reliability penalty in the use of an external sensor.

The weakness of both tracking systems, as dictated by the current system and terminal requirements, could be addressed in a hybrid system employing both open and close loop tracking.

SYSTEMS CONSIDERATIONS

A minimum value of antenna gain is required to exceed a specified carrier to noise ratio [C/No]. This ratio determines communications performance as defined by voice quality or bit error rate. In any link calculation, a link margin is budgeted to accommodate, in part, the effects of multipath, fluctuating noise temperature, and partial shadowing by the terrain. The required system margin is not independent of antenna design and is determined, in part, by the antenna directivity. This would apply to both the transmit and receive communication links. Gains in excess of the required minimums permit a reduction in satellite and terminal EIRP.

The antenna design is governed by a mix of system, terminal, and specific antenna requirements. Axial ratio, directivity and sidelobe levels are specific examples. Axial ratio requirements in particular can have a major impact on antenna design and it is not always evident why a requirement is needed given also the fundamental limitations which exist. The parameter, axial ratio, is commonly used to specify a polarization requirement off-axis. A more precise definition is ellipticity ratio and a more useful measure of performance is the corresponding relative cross-polarization level. An increase in design flexibility is achievable if the terminal performance specifications are expressed in terms of system requirements, C/No rather than G/T, intersatellite isolation rather than antenna directivity etc. There will always be some uncertainty in the predicted performance which can only be resolved by conducting field trials in an operational environment.

ADAPTIVE ARRAY ANTENNAS

Operation

Earlier higher gain versions of an adaptive array antenna were described in a paper presented at IMSC '90. [2] The antenna [Fig. 1] consists essentially of a driven element mounted on a ground plane surrounded by concentric rings of switchable parasitic elements. Using high speed digital switching electronics an antenna beam can be steered in both the azimuth and elevation planes. The antenna is designed to operate between 15° and 70° in elevation, and 360° in azimuth. The electronics incorporates a microprocessor which permits close-loop tracking of the satellite using a control signal derived from the terminal receiver. The microprocessor can also conduct self diagnostics, and measure the satellite elevation and azimuth angles relative to the user terminal. In any given operating environment, the microprocessor can be programmed to optimize antenna performance.

Electrical Design

The antenna provides continuous operation between 1525 and 1660.5MHz but is optimized for the receive band between 1525 and 1560MHz.

It can generate up to 32 beams in azimuth and 3 beams in elevation. The current switching speed is less than 30 microseconds. The antenna has a nominal beamwidth of 55° in azimuth and 50° in elevation. The front to back ratio of the antenna is greater than 13 dB in the receive band. A high ratio is required during close-loop tracking to prevent the antenna locking on to the satellite via a back-lobe.

The antenna gains in the receive band, measured in an anechoic chamber at angles corresponding to elevations of 15, 30, 45, 60, and 70° are 7, 9, 10, 9 and 7 dBic respectively. The transmit gain can be up to 1 dB lower than the receive gain over the specified angular coverage. There is a trade-off between the achievable gains at the

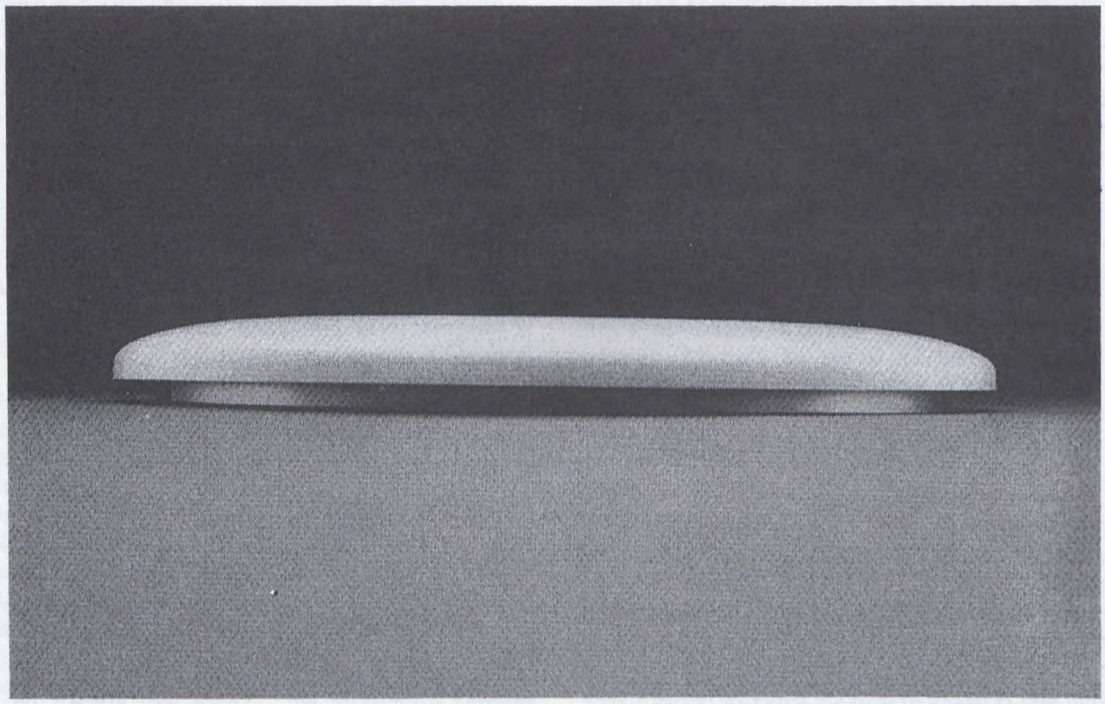

[Fig. 1] Adaptive Array Antenna

lower and upper angular limits. Use can be made of the ground plane presented by the roof of the vehicle to increase the gain at the lowest elevation angles. The maximum return loss is -13 dB (VSWR = 1.6) in the transmit and receive bands for all antenna beam positions.

The antenna has negligible RF loss and has an antenna noise temperature of less than 50°K under "line of sight" conditions. The antenna design has been tested up to 100 watts of RF power. An increase in noise temperature of 20°K was noted in the receive band. At 5 watts, the increase in noise temperature will be negligible. The antenna consumes less than 10 watts at +12 volts.

Mechanical/Thermal Design

The antenna has a diameter of 36 cm and an overall height of 4 cm with a weight of less than 2 kg. It can be designed to meet military shock and vibration specifications (MIL-STD-810D). The antenna is insensitive to temperature. The antenna components operated well within their design limit in an operational environment. No noticeable shift in antenna boresight or change in return loss has been noted during solar simulation tests. The antenna has been tested in an operational environment with ambient temperatures between -30°C and +30°C.

Acquisition and Tracking

The antenna has the capability of tracking the satellite in a close-loop or open-loop mode of operation. In the close-loop mode, a control signal proportional to the received RF signal is derived at the terminal receiver. The satellite is initially acquired by stepping through the antenna beam positions and selecting the beam with the strongest signal. The speed of operation is determined by the terminal C/No and the signal-to-noise requirement in the control loop. Currently It takes between 0.1 and 0.3 seconds to acquire the satellite after initial phase lock. The satellite is subsequently tracked by periodically switching on either side of the current beam position and selecting the beam with the strongest signal. This is accomplished in less than 15 msec and in normal vehicle operation occurs four times a second. The maximum phase transients when tracking in azimuth and elevation, are less than 5° and 20° respectively. In an open-loop mode, the control signal to point the antenna beam at the satellite, is obtained from an external sensor such as a flux-gate compass or gyroscope. The tracking systems have been extensively tested and two way full duplex voice communication successfully demonstrated in an operational environment via an Inmarsat satellite.

Manufacture

Antenna cost is the most significant factor affecting the commercial viability of an antenna for land mobile applications. Electronic array antennas have been mainly used in applications where cost is not the dominant consideration. The adaptive array antenna design lends itself, however, to the high volume, low cost production. The electronic components are low cost and readily available. The digital switching concept ensures a high level of repeatability and simplifies testing procedures. It is anticipated that the manufacturing processes will be automated and much of the expensive testing associated with conventional phased array technology can be eliminated. Preliminary studies indicate that the antenna could be manufactured and sold for less than $300 US in quantities of 10,000/year over a 5 year period.

ACKNOWLEDGEMENTS

The author is grateful for the support provided by Martial Dufour and Bert Schreiber of the Communications Research Centre in designing the tracking software, the antenna electronics and flux gate compass.

REFERENCES

[1] **Woo, K. et. al.**, 1990. "*Performance of a Family of Omni and Steered Antennas for Mobile Satellite Applications*", Proceedings of 1990 International Mobile Satellite Conference.

[2] **Milne, R.**, 1990. "*An Adaptive Array Antenna for Mobile Satellite Communications*", Proceedings of 1990 International Mobile Satellite Conference.

Low Profile Antennas for MSAT Applications

L. Shafai and H. Moheb
Dept. of Electrical and Computer Engineering
University of Manitoba
Winnipeg, Manitoba, CANADA, R3T 5V6
Phone: 204-474-9615 Fax: 204-261-4639
e-mail: shafai@ee.umanitoba.ca

W. Chamma and M. Barakat
InfoMagnetics Technologies Corporation
11 - 1329 Niakwa Road East
Winnipeg, Manitoba, CANADA, R2J 3T4
Phone: 204-989-4631 Fax: 204-989-4640
e-mail: walid@panda.infomag.mb.ca

ABSTRACT

For MSAT applications, a number of different antennas have been designed and investigated. They include low gain omnidirectional antennas and medium gain to high gain directional antennas. The latter include both portable and vehicular antennas. While portable units are desirable to be low profile and low cost, the vehicular antennas have proved to be the most challenging antenna types for the mobile satellite application. The results of our efforts in design of such antennas are described briefly.

Low profile designs are emphasized in most cases, and microstrip type radiators are therefore selected. The single radiator provides low gain omnidirectional patterns and is optimized for low cost applications. It provides low gains around 2 - 6 dBic and is useful mostly for the data transmission.

Medium to high gain antennas are developed as arrays of omnidirectional elements. Again, different designs are optimized to meet the needs of different applications. For portable units, the array configuration can be flexible and is optimized for maximum broadside gains. For vehicular units, however the configurations are desirable to be low profile, or compact, and have means for scanning the antenna beam. For simplicity, fixed beam antennas with mechanical beam scan are selected. For these antennas, as well, different designs, having low profile or compact size, are selected and optimized to meet the MSAT gain and G/T requirements.

OMNIDIRECTIONAL ANTENNA

Microstrip patch antennas operating at higher order modes radiate conical patterns with a null at the boresight. They can therefore be used as possible candidates for mobile satellite signal reception at low elevation angles. However, for conventional substrates and large ground planes their E- and H-plane patterns are not identical and result in poor axial ratios at the pattern peaks.

The difficulty with inequality of principal plane patterns can be overcome by selecting a lower dielectric permittivity for the substrates. In practice this can be achieved by stacking dual patch configurations that is usually used for broadbanding microstrip antennas. In such cases, and provided the spacing between the patches is left open, the effective dielectric constant of the structure becomes small and the radiation pattern symmetry improves becoming acceptable for circular polarization. This solution, however, is not ideal and raises the pattern peaks to higher elevation angles.

The TM_{31} mode of circular microstrip patch antennas generates radiation patterns that are suitable for MSAT applications in North American elevations. Samples of the measured patterns over the MSAT bands are shown in Fig. 1 and Fig. 2. This antenna operates at the TM_{31} mode and is fed by a branch line hybrid at two adjacent points, at phase quadrature. The slight asymmetry of the pattern is due to the excitation of lower order TM_{21} and TM_{01} and possibly TM_{11} modes. For more symmetric radiations a multiple feeding method may be

used. Nevertheless, even with a single feed technique the pattern axial ratio seems acceptable.

DIRECTIONAL ANTENNA

In an earlier papers a directional antennas based on multiple modes of multi-arm spiral antennas was reported [1] - [3]. In this paper an alternative design is investigated. It is based on the dominant mode spiral, i.e. n = 1 mode, that radiates on the broadside. This mode corresponds to the first active zone of spiral antennas, and radiates from a circle of circumference equal to one wavelength. The antenna element is therefore small and can be used to form a planar array [4]. For efficient radiation, however, the spiral element must be raised above the ground plane. A number of arrays of small spirals were investigated, to determine their scan gain and axial ratio in the MSAT band, and sample results are provided below.

For a 9-element array, i.e. 3 x 3 rectangular grid shown in Fig. 3, the computed data are shown in Figs. 4 - 9, for the MSAT receive and transmit bands. In these figures the element heights above the ground plane is 0.15 wavelength and the array element separation is 0.457 wavelength. Within each band, three sets of results are provided that correspond to different inter-element phase shifts of 150°, 155° and 160°, to scan the beam to a lower elevation angle. In the lower band the beam scans to around 47 - 48° from broadside and the axial ratio is relatively insensitive to the phase shift, and the computed peak circularly polarized gain is about 13dBic. In the transmit band the beam gain rises slightly to 14dBic and the axial ratio improves. But, the back lobe level deteriorates, rising quickly with frequency. Other phase shift values, or, inter-element separations provide different beam characteristics, but are omitted for brevity.

With the above element separation the array size is limited to less than 26cm x 26cm and can be accommodated within a circle of 35cm. Increasing the element separation improves the array performance, both in reducing the mutual coupling and in increasing the gain. However, the inter-element phase shift must be modified, i.e. increased, to lower the array beam to lower elevation angles. Unfortunately, both these parameters of increased element spacing and excessive beam scan generate grating lobes and raise the sidelobes. For these reasons, the above small inter-element spacing of 0.457 wavelength was selected for the array implementation.

Note that in generating the above results for 3 x 3 arrays, shown in Figs. 4 - 9, the mutual coupling between the array elements were included in the computation. Thus, the computed gains and axial ratios are realistic values. However, the mismatch and distribution losses in the feed network are not included. The measured gains would include such effects and therefore expected to be somewhat smaller. Nevertheless, in comparison with microstrip arrays the above spiral array yields higher gain values. For MSAT applications, 19-element microstrip arrays were commonly used in earlier studies [5] - [7]. Their gain at the broadside is expected to be higher. However, at low elevation angles the pattern role offs for microstrip antennas are higher and their gain drops rapidly away from the boresight. The above small arrays of spirals therefore yield higher gains at lower elevation angles. Of course, this is achieved due to high profile of spirals, which was selected to be about 0.15 wavelength.

The performance of the antenna was also tested experimentally. For the single element the gain pattern and axial ratio remains nearly constant over a wide frequency hand, and a sample at the lower band is shown in Fig. 10. The asymmetry of the pattern around 60° off the broadside is due to the interaction of spiral with its support over the ground plane.

A linear array of 3-elements was also tested for scan characteristics. Its result is shown in Fig. 11, which is similar to the computed ones. The feed network for this measurement had a

loss of about 3.5dB, giving the array peak gain of 10dBic. This linear array may be used as a single element for medium to small gain antennas in MSAT applications, or as an array to yield larger gains. Its feed network was not optimized for low loss, but used only to examine the pattern shape, beam scan characteristics and axial ratio.

The 9-element array, 3 x 3 array with a rectangular grid, was also tested. This test is very preliminary and the feed network has not been optimized yet. The preliminary results are, however, included to indicate the performance. They are shown in Figs. 12 and 13. In Fig. 12 the array is mounted on a small 1.5 ft. x 1.5 ft. ground plane, and the beam scans to lower elevation angles. In Fig. 13 the array is over a 3 ft. x 3 ft. ground plane and beam rises slightly. The measured peak gain is about 10.5dBic, and the axial ratio is dependent on the ground plane size. The feed network loss for this antenna was about 2dB. The array therefore performs similar to the computed ones. The optimization of the feed network for a lower loss, is currently under investigation.

REFERENCES

[1] L. Shafai and M. Barakat, "Low Cost Antennas for MSAT Vehicular Applications", Int. Mobile Satellite Con., IMSC 93, pp. 557-562, Pasadena, June 1993.

[2] L. Shafai, "Linear-Sum Mode Arrays and Beam Forming", Symposium on Ant. Tech. and Appl. EM., ANTEM 92, pp. 57-62, Winnipeg, August 1992.

[3] L. Shafai, "Design of Multi-Arm Multi-Mode Spiral Antennas for Directional Beams Using Equivalent Array Concept", Electromagnetics, Vol. 14, pp. 285-304, 1994.

[4] H. Nakano, "A New Trend in Microstrip and Low Profile Antennas", Symposium on Ant. Tech and Appl. EM., ANTEM 92, pp. 117-122, Winnipeg, August 1992.

[5] K. Woo, J. Huang, V. Jamnejad, D. Bell, J. Berner, P. Estabrook and A. Densmore, "Performance of a Family of Omni and Steered Antennas for Mobile Satellite Applications", Proc. Int. Mobile Satellite Conf., IMSC 90, pp. 540-546, Ottawa, 1990.

[6] S. Ohmori, K. Mano, K. Tanaka, M. Matsunaga and T. Suchiya, "A Phased Array Tracking Antenna for Vehicles", Proc. Int. Mobile Satellite Conf., IMSC 90, pp. 519-522, Ottawa, 1990.

[7] K. Sato, K. Kishikawa and T. Hirako, "Field Experiments of Phased Array Antenna for Mobile Satellite Vehicle Application", Proc. Int. Symposium on Antennas & Propag., Vol. 3. pp. 653-656, Sapporo, 1992.

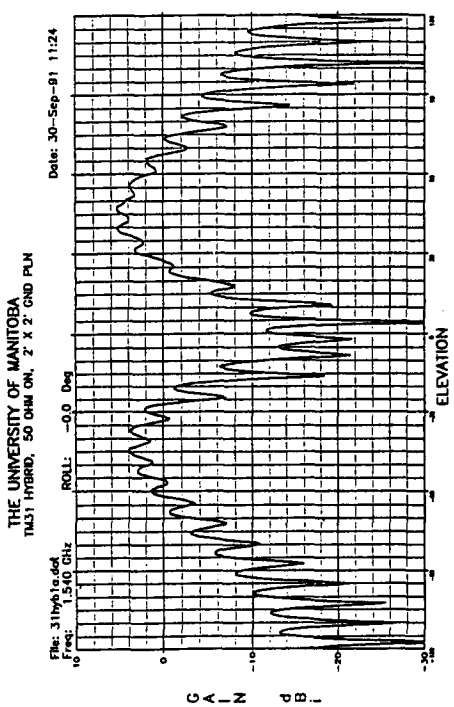

Fig. 1 Measured pattern of the TM_{31} omnidirectional antenna at the lower band, circularly polarized gain = 7.53dBic.

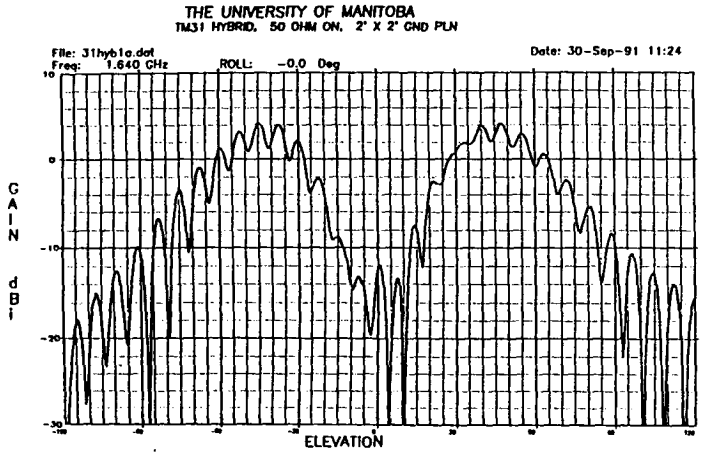

Fig. 2 Measured pattern of the TM_{31} omnidirectional antenna at the upper band, circularly polarized gain = 5.81dBic.

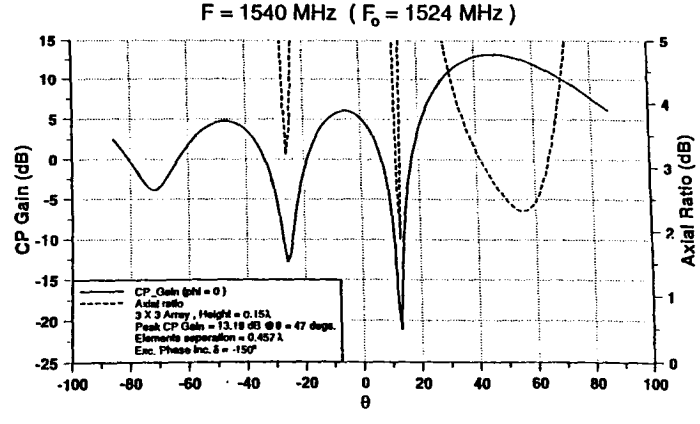

Fig. 4 Computed circularly polarized and axial ratio patterns of a 3 x 3 spiral array, phase shift = -150°, lower band.

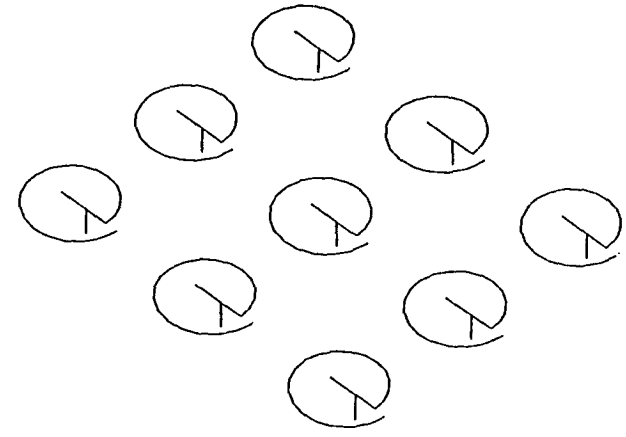

Fig. 3 Geometry of 3 x 3 spiral array.

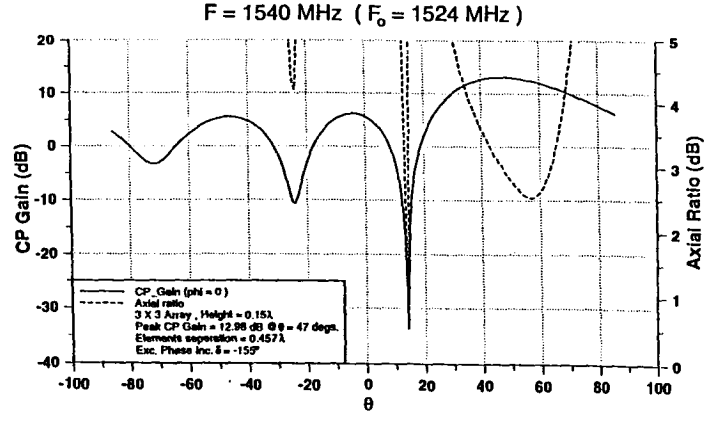

Fig. 5 Computed circularly polarized and axial ratio patterns of a 3 x 3 spiral array, phase shift = -155°, lower band.

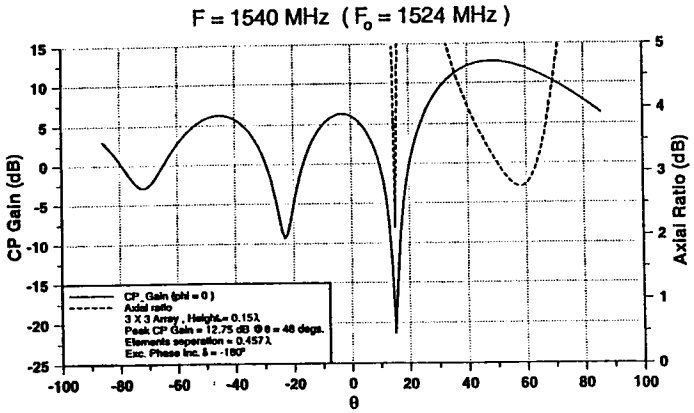

Fig. 6 Computed circularly polarized and axial ratio patterns of a 3 x 3 spiral array, phase shift = -160°, lower band.

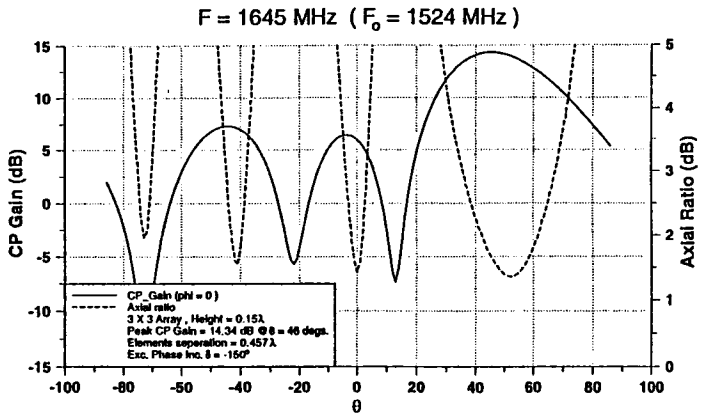

Fig. 7 Computed circularly polarized and axial ratio patterns 3 x 3 spiral array at the upper band, phase shift = -150°.

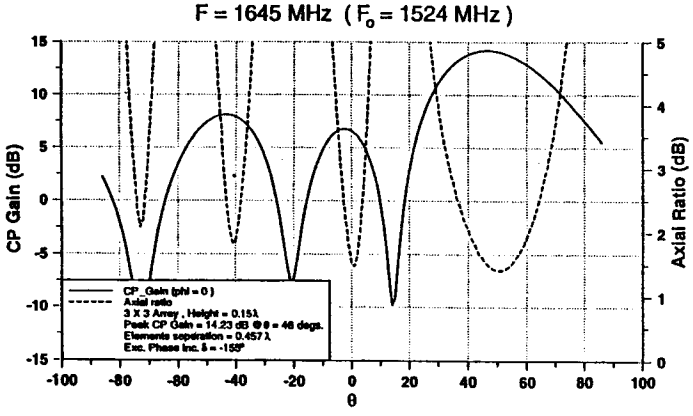

Fig. 8 Computed circularly polarized and axial ratio patterns of 3.3 spiral array at the upper band, phase shift = -155°.

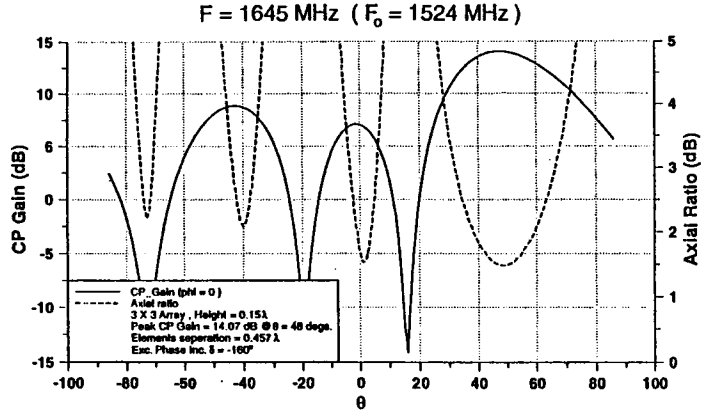

Fig. 9 Computed circularly polarized and axial ratio patterns of 3.3 spiral array at the upper band, phase shift = -160°.

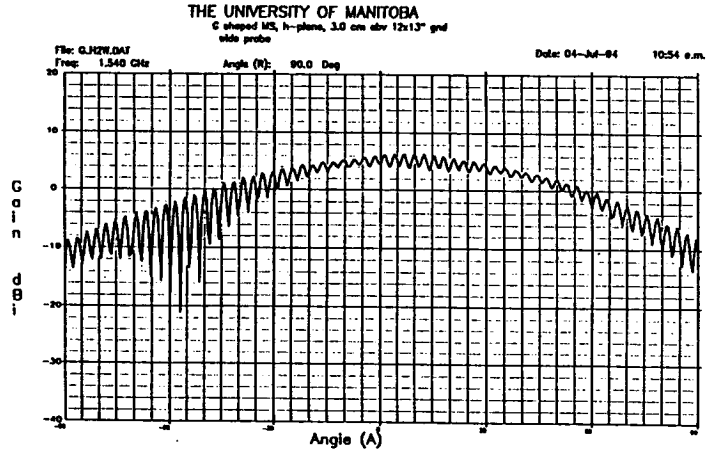

Fig. 10 Measured pattern of the spiral array element, circularly polarized gain = 8.18dBic.

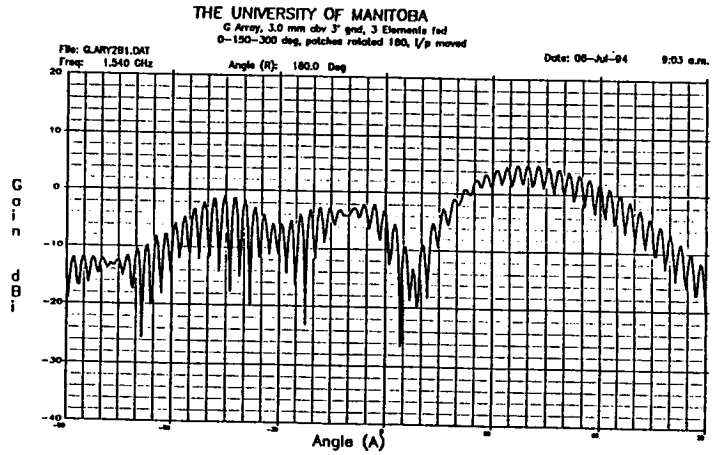

Fig. 11 Measured pattern of a 1 x 3 spiral array at the lower band, circularly polarized gain = 6.47dBic.

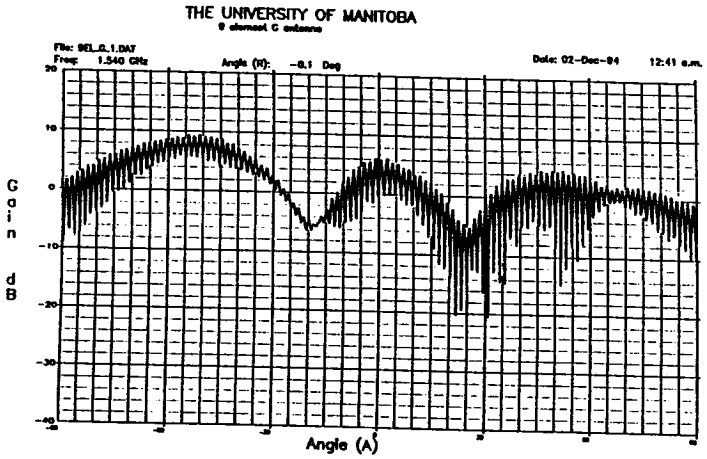

Fig. 12 Measured pattern of 3 x 3 spiral array over a small 1.5 ft. x 1.5 ft. ground plane, circularly polarized gain = 10.60dBic.

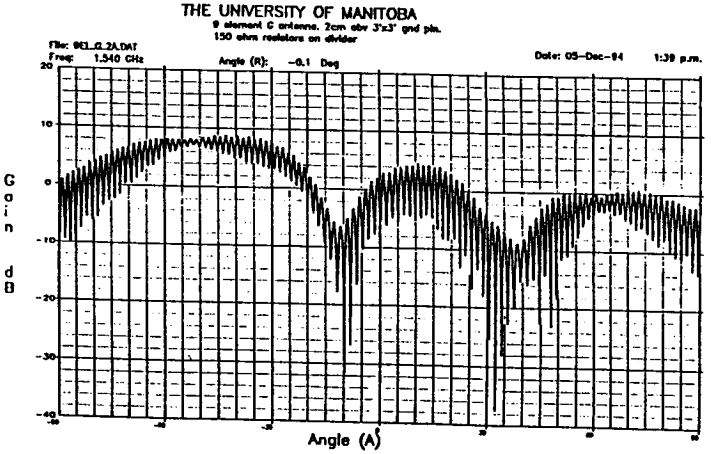

Fig. 13 Measured pattern of 3 x 3 spiral array over a 3 ft. x 3 ft. ground plane, circularly polarized gain = 10.29dBic.

Compact, Low Profile Antennas for MSAT and Mini-M and Std-M Land Mobile Satellite Communications

P.C. Strickland
CAL Corporation
1050 Morrison Dr.
Ottawa, Ontario, K2H 8K7

ABSTRACT

CAL Corporation has developed a new class of low profile radiating elements for use in planar phased array antennas. These new elements have been used in the design of a low cost, compact, low profile antenna unit for MSAT and INMARSAT Mini-M land mobile satellite communications. The antenna unit which measures roughly 32cm in diameter by 5cm deep incorporates a compact LNA and diplexer unit as well as a complete, low cost, beam steering system. CAL has also developed a low profile antenna unit for INMARSAT-M land mobile satellite communications. A number of these units, which utilize a microstrip patch array design, were put into service in 1994.

INTRODUCTION

Conformal phase scanned microstrip patch arrays have been in use for several years on aircraft for satellite communications over INMARSAT satellites. These arrays achieve very low drag but unfortunately suffer from high noise temperature due primarily to losses in the phase shifters. Phase scanned arrays are also very expensive due to the large number of PIN diodes or other control elements used and the use of multiple layers of PTFE based or other low loss substrate material. In order to achieve a required system gain to noise temperature ratio the aperture of the phase scanned array must be larger than that of a low loss mechanically steered antenna [1,2]. The aperture area is of minor importance on large aircraft provided that the antenna is conformal. On land vehicles however, it is likely to be an important concern. Similarly the need for reliable communications on large aircraft may justify the expense of phase scanned arrays whereas the land mobile market demands much less expensive antenna configurations.

ARRAY DESIGN

The principal challenge in designing a low profile phased array for the land mobile satellite communications application is achieving adequate gain at low elevation angles. Radiating elements with broad beamwidth are required allowing the beam peak to be formed at low elevations while maintaining low sidelobes near zenith. The element must be compact allowing close element spacing in order to avoid grating lobes.

The new radiating element developed for the Mini-M and MSAT application achieves a much larger beamwidth than microstrip patches allowing high gain to be achieved

at lower elevation angles. The array area occupied by the element is also much smaller allowing an increased packing density and facilitating the use of separable sub-arrays in cases where this is not possible using microstrip patches. The new element would typically occupy 1/16 of a square wavelength versus roughly 1/4 of a square wavelength required for a microstrip patch. The element in each case is assumed to be supported by a substrate of mostly air.

The new radiating element has been used in the design of a compact, low profile antenna for use in MSAT and Mini-M applications. A planar array of nine elements produces a broad beam in the elevation plane and a narrow beam in the azimuth plane. This array is mechanically scanned in azimuth by means of a pancake style stepper motor. The RF connection is made via a high reliability, low cost, miniature rotary joint. The outside dimensions of the radome which encloses the antenna and drive are approximately 32cm wide by 41cm long and 5cm deep. This array configuration is illustrated in figure 1.

Radiation patterns corresponding to the initial prototype of the MSAT/Mini-M antenna are given in figures 2 and 3. This initial version of the antenna has been optimized for southern MSAT coverage. A second version is under development which will satisfy the combined requirements for northern and southern MSAT coverage. The peak antenna gain is approximately 12dBic.

INMARSAT-M

The radiating element used in the Standard-M antenna is illustrated in figure 4. This element consists of two microstrip resonators stacked, one on top of the other. The centre frequencies of the resonators differ slightly to provide operation in the receive and transmit bands. The stacked structure maintains the advantage of the low profile offered by microstrip antennas while increasing the bandwidth above that of conventional microstrip radiators of the same thickness. The total combined thickness of the two substrate layers in only 4.7mm. Microstrip elements on thick honeycomb or polystyrene foam substrates could provide adequate bandwidth from a single resonator but would have insufficient beamwidth for coverage to within 14 degrees of the horizon.

Only the bottom resonator of the stacked resonator element is directly fed using microstrip transmission lines while the top resonator acts as a parasitic element. The result is a low cost structure in which the entire feed network is etched onto a single layer. The upper patches are simply bonded to the lower element, thereby minimizing the number of solder connections required. Both the lower layer, which includes the feed lines and the bottom radiator, and the upper layer use polyolefin (Polyguide 165) as a substrate. This material has a dielectric constant of 2.32 and is very low cost. The input impedance to the stacked resonator element can be varied to achieve an impedance match in the required frequency bands by introducing an offset between the centres of the resonators.

Circular polarization is achieved by feeding the element on adjacent sides with a 90 degree electrical phase difference between the feed points. A Wilkinson power splitter/combiner has been employed to balance the power levels appearing at the two feed points. The frequency bandwidth is sufficiently narrow that the variation in the performance of the Wilkinson splitter over the frequency band is negligible. A return loss of better than 14dB is

achieved from 1525MHz to 1660.5MHz at the input to the splitter with the radiating element connected. The radiation pattern of an individual element measured in the diagonal plane with a circularly polarized source is given in figure 5. A 3dB beamwidth of approximately 75 degrees is achieved. At our minimum elevation angle of interest, 14 degrees, the gain is approximately 15dB below that at the peak.

Twelve radiating elements are used which are layed out within the disc as illustrated in figure 6. The lower resonator of each element is incorporated onto the same substrate as the microstrip feed. Each of the twelve upper resonators are bonded separately into place. The microstrip feed network was designed using the Touchstone/Academy software tools.

The overall array diameter excluding radome is 47cm. It is interesting to note that the number of radiating elements required to fill this aperture without grating lobes is considerably lower than the 16 required if the array was phase scanned in two planes. The array configuration described here also has a lower noise temperature and higher gain for a given aperture area.

Typical azimuth and elevation radiation patterns for the Standard-M array are given in figures 7 and 8 respectively. The peak gain of this array is approximately 13dBic.

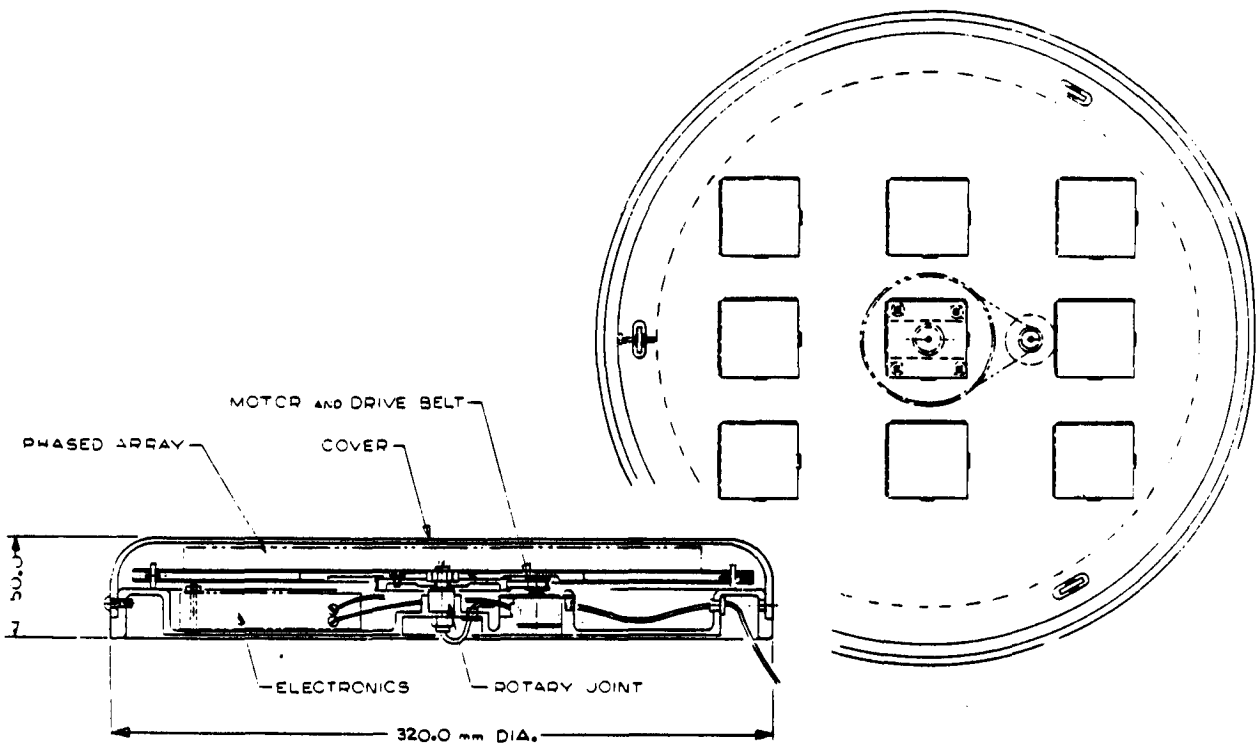

Figure 1
MSAT/Mini-M Antenna

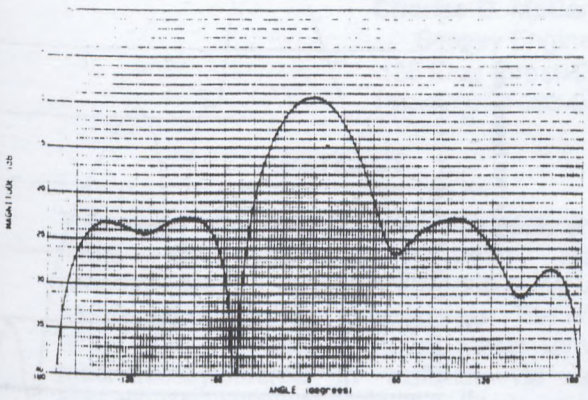

Figure 2
MSAT/Mini-M Azimuth Pattern

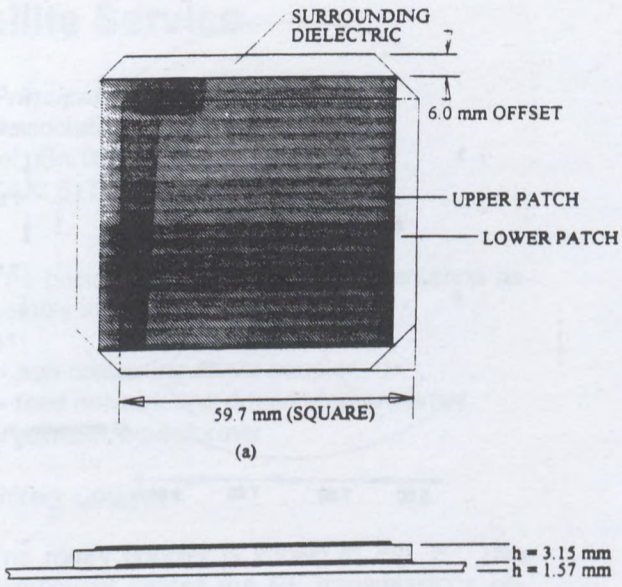

Figure 4
Standard-M Radiating Element

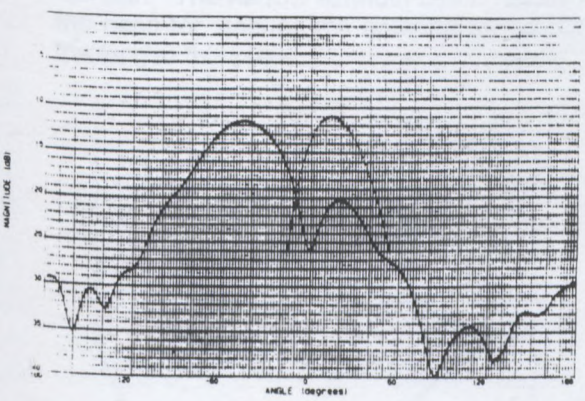

Figure 3
MSAT/Mini-M Elevation Pattern

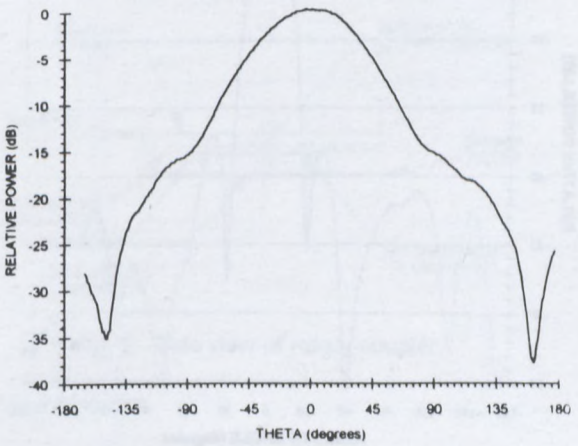

Figure 5
Standard-M Element Pattern

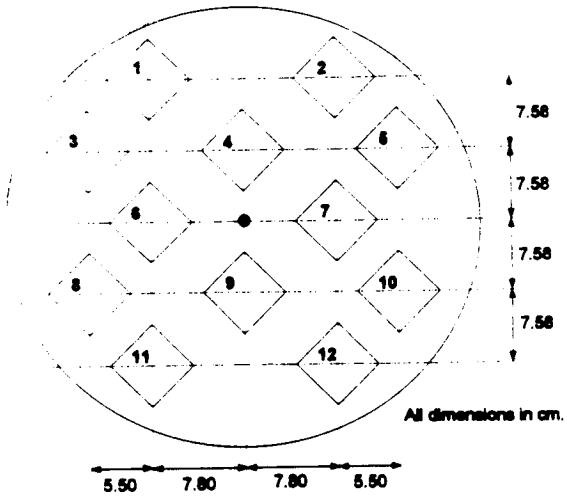

Figure 6
Standard-M Array Layout

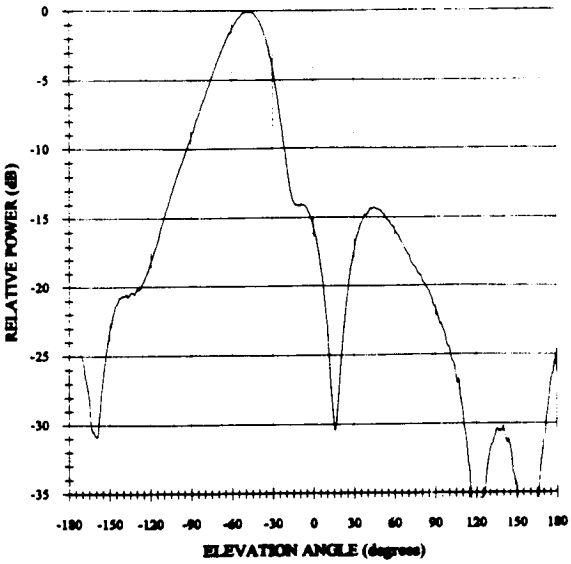

Figure 8
Standard-M Elevation Pattern

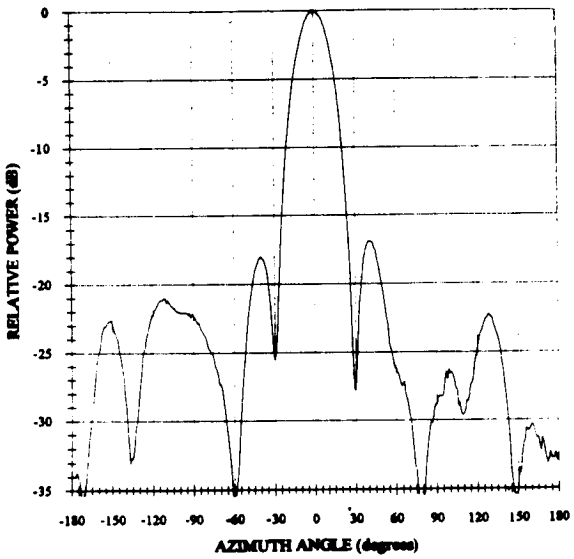

Figure 7
Standard-M Azimuth Pattern

Mechanically-Steered Disk Antenna For Mobile Satellite Service

Charles D. McCarrick, *Principal Engineer*
Seavey Engineering Associates, Inc.
135 King Street•Cohasset, MA 02025 USA
Phone: 617-383-9722 FAX: 617-383-2089

ABSTRACT

This paper describes a low-profile disk antenna for vehicular mounting that accommodates L-Band (1525-1660.5 MHz) mobile satellite service requirements. The antenna uses a rotatable printed circuit array mechanically-steered in azimuth via an external tracking system. A shaped elevation beam inherent to the antenna design provides continuous coverage with a minimum gain of 9 dBic between elevation angles of 25-degrees and 60-degrees measured above the horizon. A brief background on the theory, design, and performance for this antenna is discussed.

LOW-PROFILE DISK ANTENNA

The disk antenna uses a printed circuit type of construction abling it to fit within a radome of approximately 1-inch in height, as outlined in *Fig. 1*. A beamforming array of parasitic elements is utilized to shape the beam in elevation while producing a directive beam in azimuth. The narrow azimuth beam results in the need for steering the antenna for satellite tracking in this plane.

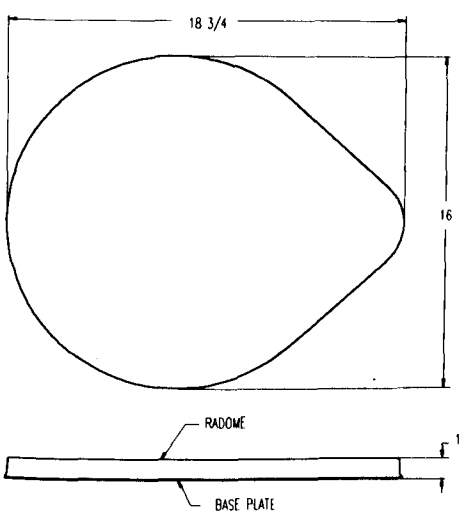

Fig. 1. Outline drawing of disk antenna.

The basic RF components of the antenna assembly include the following:

- non-contacting rotary coupler
- feed network and driven element array
- parasitic beamformer

Rotary Coupler

The rotary coupler is shown in *Fig. 2*. This component carries the RF transmissions between the antenna and terminal equipment while permitting continuous 360-degree rotation of the antenna circuitry relative to a stationary platform, such as a vehicle. It operates in principle as a parallel plate capacitor, electro-magnetically coupling RF energy between its electrodes. A short tuning stub is etched with the feed network to match the series reactance produced by the coupler for in band operation. A Teflon bearing maintains the coupling gap and facilitates smooth rotation.

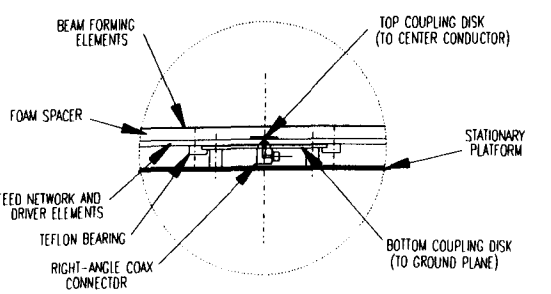

Fig. 2. Side view of rotary coupler.

Feed Network

A feed network using a microstrip medium is etched on a Teflon-fiberglass substrate (ε_r= 2.5) of 0.125-inch thickness and 15.5-inch diameter (*Fig. 3*). The network distributes uniform power and equal time delay between four driven microstrip elements. A rudimentary 90-degree reactive hybrid at each element excites the TM_{11} mode for circularly-polarized response. Total feed losses at the

output of the rotary coupler are estimated at 0.6 dB.

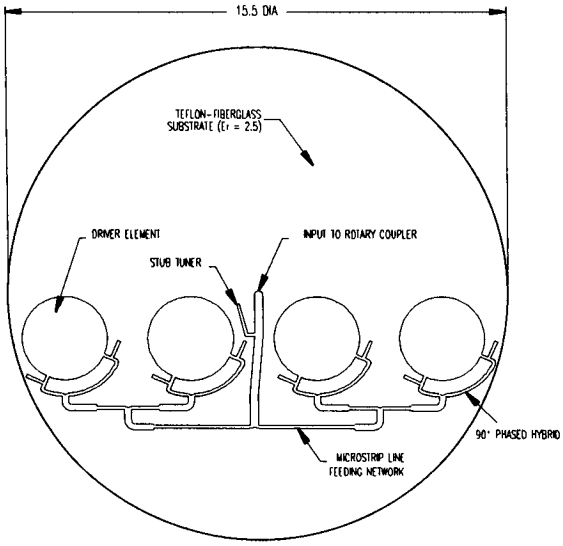

Fig. 3. RF combiner/driver element circuit.

Parasitic Beamformer

An array of 8 elements in a 2x4 configuration are etched on a 15.25-inch diameter sheet of Mylar film (*Fig. 4*). Each row, consisting of a 1x4 array of elements, is etched on the opposite side of the Mylar to the other to permit slight overlap without physical contact. These elements are located above the driver element circuit [1] by a spacing of 0.25-inches with a Styrene foam layer to create a parasitically-coupled beamformer for directing the elevation beam from zenith (broadside) to a lower intermediate elevation angle.

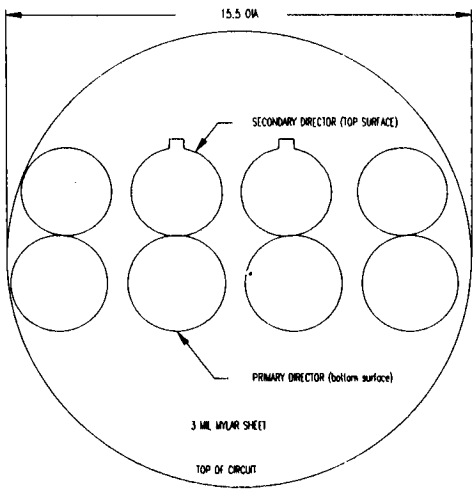

Fig. 4. Beamforming circuit.

The principle behind this scanning concept is similar that used on the JPL Microstrip Yagi array and described by Huang [2], in which parasitic director and reflector elements are excited in classic Yagi fashion to squint the beam in elevation. In the present study, the each pair of overlapped parasitics behave as two-element with a phase differential of 180-degrees between them. The position of the primary parasitics above the driving elements plays a role in suppressing the backlobe. It was demonstrated that moving these forward (in the direction of the beam squint) from complete overlap by about one-third the diameter of the driving element gave best results. In the JPL design, the parasitics are printed coplanar to the driven elements, with the feed network on a separate circuit board loacated beneath the array.

Benefits of using the EMC beamformer include reduced sensitivity to frequency, increased control for beam shaping, and simplification of the feed network. The down side of this antenna and all antennas with scanned radiation beams is an absence of vertical aperture near horizon, requiring the presence of a ground plane at least twice the diameter or length of the array. This is one reason that this antenna is best suited to vehicular mounting.

STEERING MECHANICS

The function of the steering mechanics are to rotate the disk antenna in azimuth on demand via control signals provided by tracking electronics. Basic components used to steer the azimuth plane include the following:

- stepper motor
- friction drive assembly
- support bearing assembly

These items are indicated in *Fig. 5.*

Stepper Motor

A stepper motor is chosen over a conventional analog type for its ability to accelerate and decelerate within in a short period of time. Also it is simple to control using a microprocessor, which can be an advantage for implementing a tracking system. The motor selected for the disk antenna is the low profile Series 80000 "pancake" motor with an overall height of 5/8-inch, designed and manufactured by Haydon Switch and Instrument, Inc. It operates with a 12VDC supply and is

capable of producing a 20 oz-in holding torque.

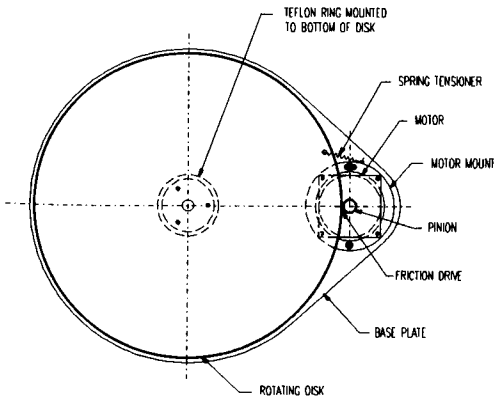

Fig. 5 Configuration of steering mechanics.

A separate controller board is supplied with the motor to interface with the satellite tracking processor. Headroom beneath the 1-inch high radome is maximized by locating the stepper motor at the perimeter of the disk antenna instead of beneath. The result is a "teardrop" shape as illustrated in previous Fig. 5.

Friction Drive Assembly

The disk is rotated using a friction wheel on the motor pinion which is spring-tensioned against a neoprene band that has been bonded along the disk perimeter. Tension on the friction wheel is must be set to reduce slippage without applying an additional load on the motor. This arrangement is simpler to implement than a belt and pulley drive and uses less parts. Also, since the motor load is reduced by the relatively large drive ratio [3], it is possible to use a smaller motor. The drive ratio is approximately 25:1 with a turning response capable of at least 45 degrees/sec.

Support Bearing Assembly

Mechanical support of the disk is facilitated by a bearing assembly which functions as a spindle and also incorporates the rotary RF coupler (*see Fig. 2*). A Teflon ring is attached to the antenna disk and acts as a bushing to the bottom coupling disk. The support and motor assemblies are mounted to a base plate having the shape of the antenna. A thermoformed radome of UVEX plastic seals the antenna from the environment. The RF connector and controller inputs exit the side of the radome so that drilling holes through the vehicle body is an option but not required.

MEASURED RESULTS

Measured results for the disk antenna are summarized in *Table 1*. Elevation and azimuth patterns at 1525, 1600, and 1661 MHz are shown in *Figs. 6-14*. These patterns were taken in a 30-foot indoor anechoic chamber with the disk antenna mounted on a 3-foot square ground plane and centered on an el-az test pedestal. For *Figs. 6-11* a RHCP transmitting source antenna was used. In *Figs. 12-14* a rotating gain horn was used to measure axial ratio in the elevation plane.

Table 1 Measured data of disk antenna.

Frequency (MHz)	1525	1600	1661
Gain (dBic)			
@ 25° Elevation	9.0	9.4	9.7
@ 45° Elevation	12.2	12.8	12.7
@ 60° Elevation	11.9	11.7	11.5
Elevation Backlobe (dB)	-10.2	-7.2	-7.0
3 dB Beamwidth			
Azimuth	27°	25°	23°
Elevation	46°	42°	42°
Axial Ratio (dB)	4.5	5.0	5.7
VSWR	1.62	1.65	1.45

REFERENCES

[1] **T. Hori and N. Nakajima**, *Broadband Circularly Polarized Microstrip Array Antenna with Coplanar Feed*, Electronics and Commun. in Japan, Part 1, Vol. 69, No. 11, 1986, pp. 76-83.

[2] **J. Huang, A. Densmore and D. Pozar,** *Microstrip Yagi Array for MSAT Vehicle Antenna Application*, in Proceedings of the Second IMSC, 1990, pp. 554-559.

[3] *Concepts and Cost-Tradeoffs for Land-Vehicle Antennas Satellite Mobile Communications*, JPL MSAT-X Report No. 102, 1984, ch. 4, pp. 1-12.

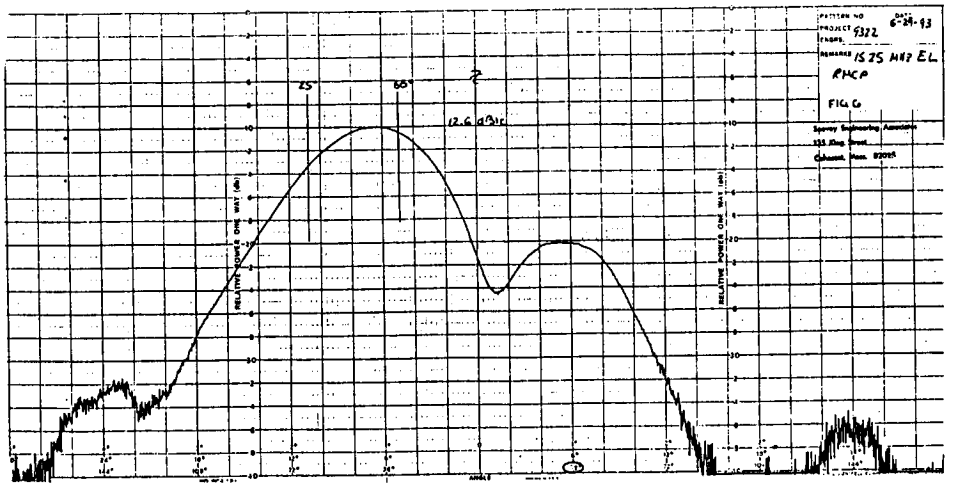

FIGURE 6
ELEVATION CUT AT 1525 MHz, RHCP SOURCE

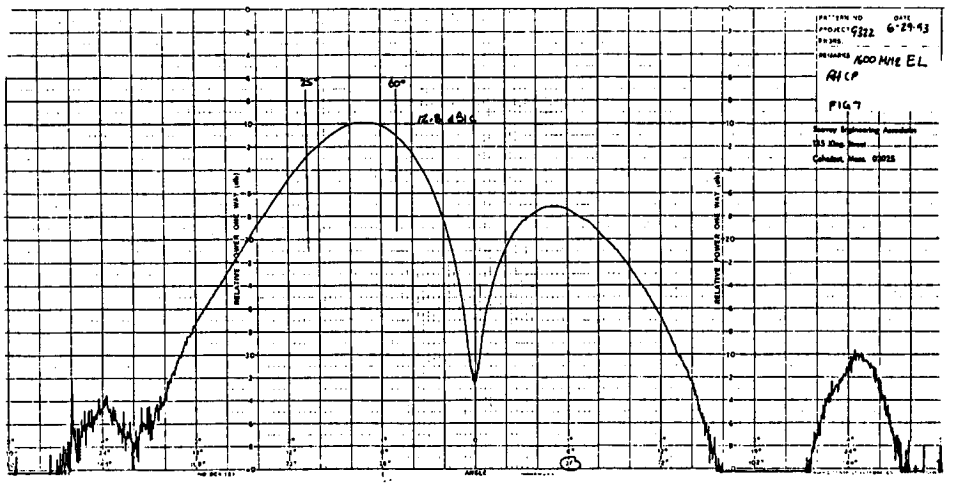

FIGURE 7
ELEVATION CUT AT 1600 MHz, RHCP SOURCE

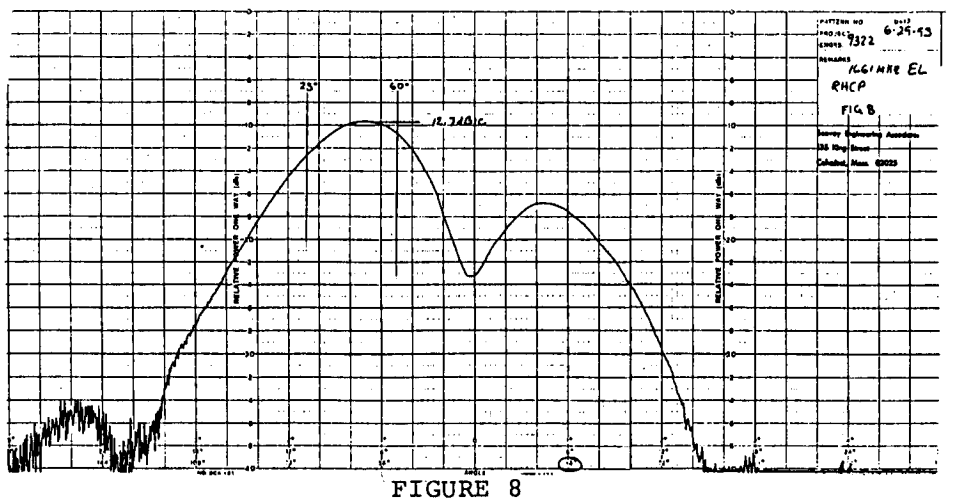

FIGURE 8
ELEVATION CUT AT 1661 MHz, RHCP SOURCE

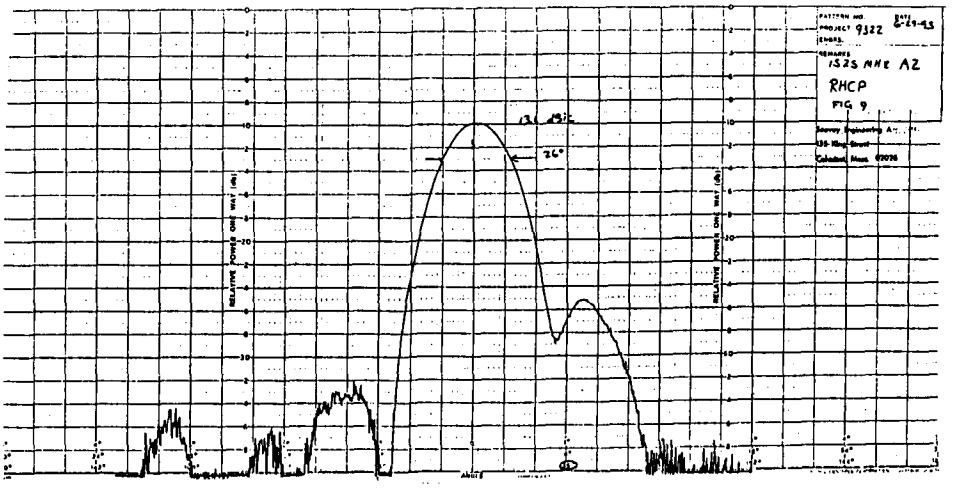

FIGURE 9
AZIMUTH CUT AT 1525 MHz, RHCP SOURCE

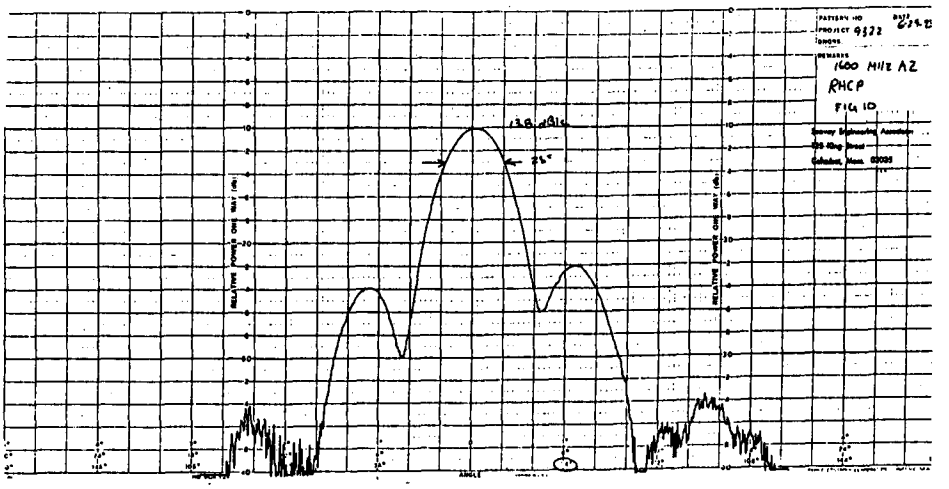

FIGURE 10
AZIMUTH CUT AT 1600 MHz, RHCP SOURCE

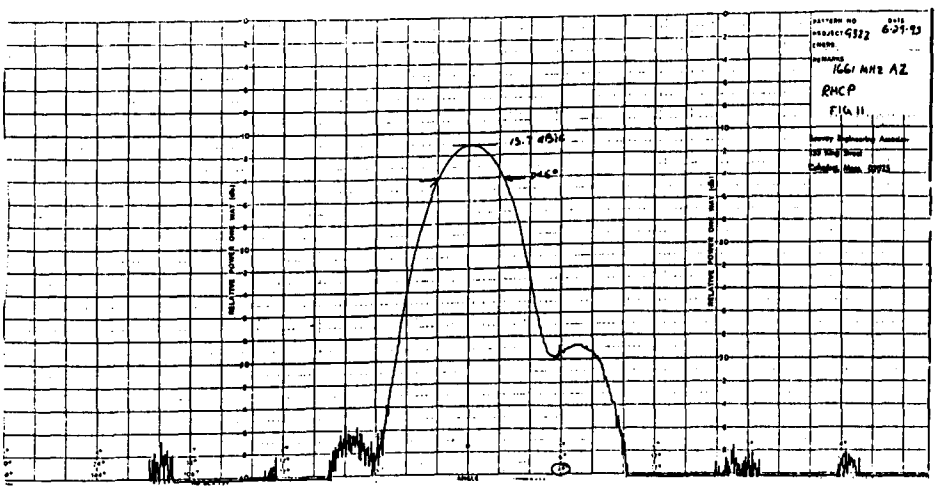

FIGURE 11
AZIMUTH CUT AT 1661 MHz, RHCP SOURCE

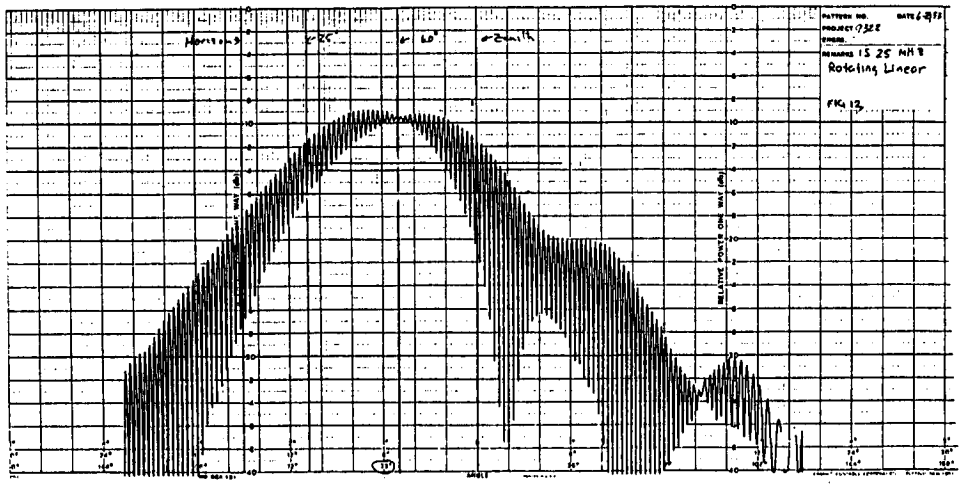

FIGURE 12
ELEVATION CUT AT 1525 MHz, ROTATING LINEAR SOURCE

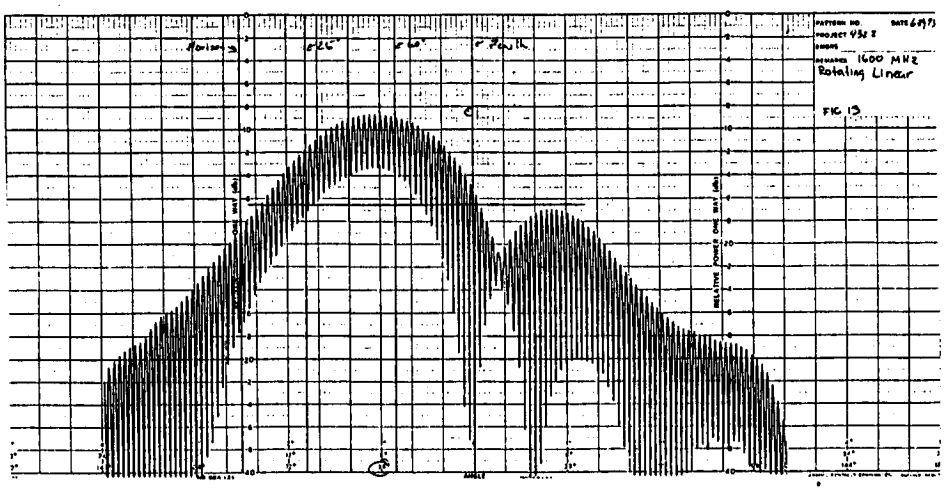

FIGURE 13
ELEVATION CUT AT 1660 MHz, ROTATING LINEAR SOURCE

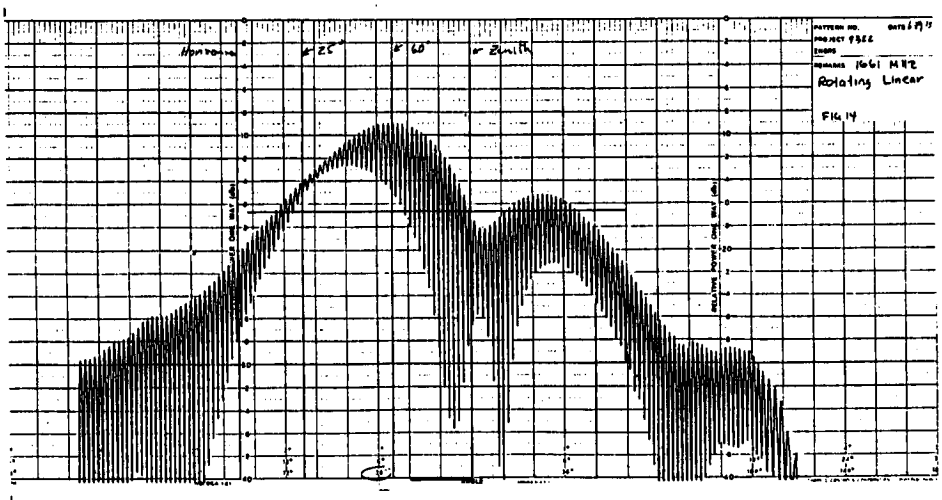

FIGURE 14
ELEVATION CUT AT 1661 MHz, ROTATING LINEAR SOURCE

Hand-Held Terminal Antennas for Personal Satellite Communications

J.E. Caballero, J. Badenes, M^a. J. Fernández, C. Martín-Pascual, and F. Municio

DETyCOM A.I.E.. C/. La Laguna, 7; 28220 Majadahonda, Madrid (Spain)
Phone: 34-1-638-6412, FAX: 4-1-638-6099

ABSTRACT

This paper deals with two hand-held antenna types operating with Geostationary (GEO) and Medium Earth Orbit (MEO) satellite systems. They could be applied to the Low Earth Orbit (LEO) and Highly Elliptical Orbits (HEO) ones respectively doing the appropriate frequency scale designs.

The first one is a $\lambda/2$ (½ turn) quadrifilar helix (quasi-hemispherical coverage), and the second one is a self-diplexed antenna made of a circular patch and a short-circuited ring patch in stacked configuration (zenithal coverage).

INTRODUCTION

Global personal communication systems are being developed in order to satisfy the unceasing demand of small and hand-held portable units to communicate with anyone, anytime and anywhere on the Earth [1,2].

To implement antennas that are simple, small size, light weight and low cost requires omniazimuthal coverage in circular polarization.

The specifications for the hand-held terminal antenna operating with the GEO satellite system are right-hand circular polarization (RHCP), omniazimuthal coverage for elevation angles between 10° and 90°, axial ratio better than 5 dB, VSWR better than 2:1 and gain of 0 ± 1 dB inside both Tx/Rx GEO frequency bands (1626.5 - 1660.5 MHz / 1525.5 - 1559 MHz) and coverage. The same performances have been also specified for the hand-held terminal antenna operating with the MEO satellite system but with omniazimuthal coverage for elevation angles between 30° and 90° at Tx/Rx MEO frequency bands (1616.5 - 1626 MHz / 2483.5 - 2500 MHz) [3].

HAND-HELD ANTENNA FOR GEO SATELLITE SYSTEM

After a review in the literature about quadrifilar helices [4], it has been found that the most suitable to fulfill the required specifications mentioned in the previous section is a $\lambda/2$ (½ turn) quadrifilar helix which has an axial length between 0.4 - 0.5 λ in air. The chosen antenna has already been developed in the PROSAT and PRODAT systems for aircraft antenna applications [5]. This antenna prototype is fed at the top by means of semi-rigid coaxial cables used as one of the elements of each bifilar helix. All the wires are rolled up around a Teflon substrate and short-circuited at the bottom of the antenna. This configuration operates as a balun which does not cause impedance transformation. A quadrature hybrid is needed to produce the 90° relationship between bifilar helices.

Due to cost reasons, an alternative feeding arrangement has been found when the antenna is fed from bottom part.

The computed radiation pattern for both isolated antenna designs can be seen in figure 1. They are modeled in air by using a wire-grid model and the Moment Method [6].

When the antenna is fed from bottom part, the four wires are short-circuited at central top part of the antenna.

The antenna is balanced by means of a Roberts balun [7] which has been found mechanically easier to manufacture than others like the split-coaxial balun or the folded balun [8]. The folded balun is a bifilar line which is short-circuited at $\lambda/4$ from the base of the antenna, while the Roberts balun is a version of it with an added coaxial line in series at the base which is open at $\lambda/4$ from it. When both bifilar line and coaxial line are done in the same medium such as Teflon, the feeding cables form this balun without the need to cut them. Furthermore, the balun has a reduced size and it is shielded to avoid radiation from the cables.

The antenna needs a matching circuit which has been developed in two steps:

- A $\lambda/4$ transformer between the input impedance (50 Ω) and the impedance at the base of the antenna (of the order of 10-14 Ω).

- A circuit with two parallel stubs.

The first one is done by means of 25 Ω coaxial input cables and the second one is photoetched on Epsilam-10 next to the 90° hybrid.

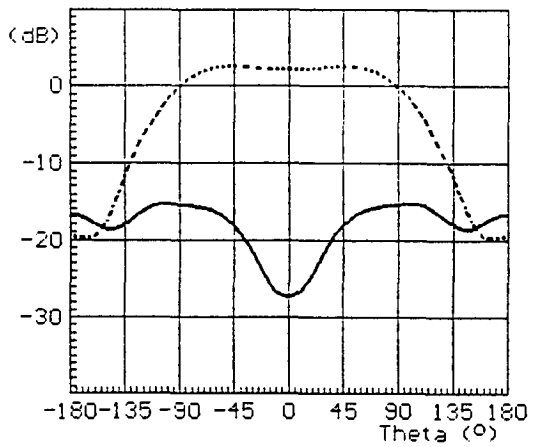

(a) Feeding from top part

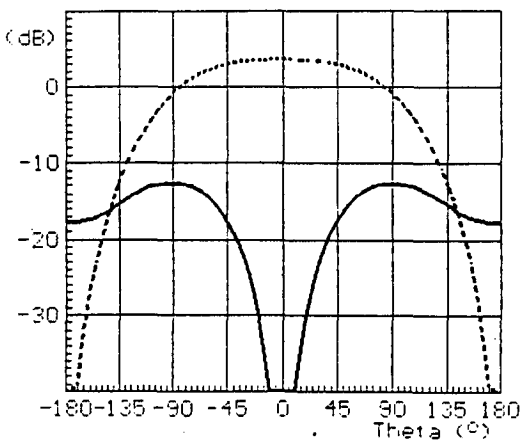

(b) Feeding from bottom part

Figure 1. Computed meridian cut of the radiation pattern for a $\lambda/2$ (½ turn) quadrifilar helix at 1.6 GHz. RHCP (- - -), LHCP (—).

A drawing of the antenna is shown in figure 2. The total height (including balun and matching circuit) is 155 mm and the external diameter is 24 mm (radome is not included).

The reflection coefficient at input antenna port is shown in figure 3 and a meridian cut of the radiation pattern at central Tx/Rx GEO frequencies can be seen in figure 4. The axial ratio for the same cut at these frequencies is also shown in figure 5.

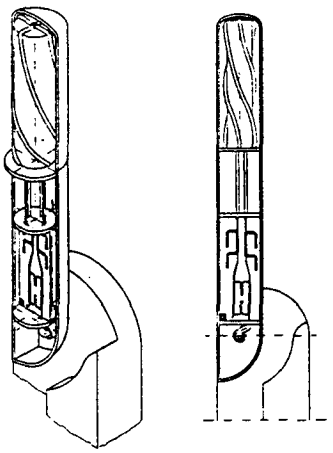

Figure 2. Drawing of the hand-held terminal antenna for GEO satellite system.

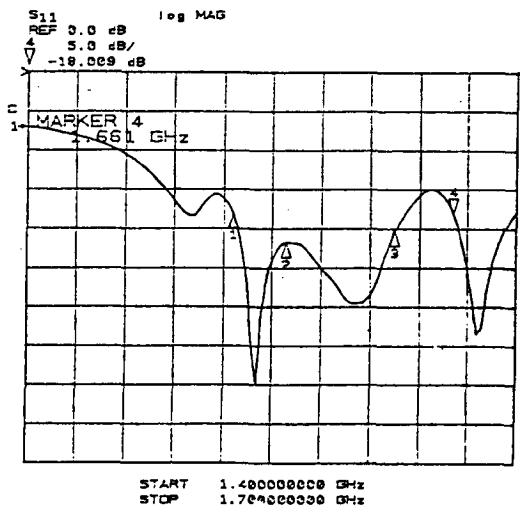

Figure 3. Measured reflection coefficient at input port of the antenna prototype for GEO satellite system.

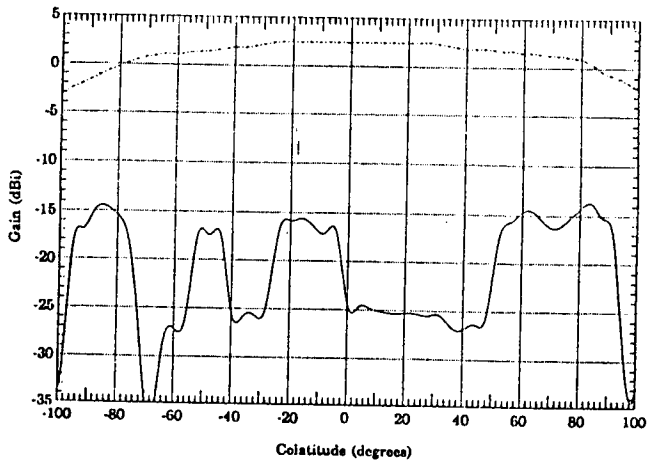

(a) 1542.5 MHz

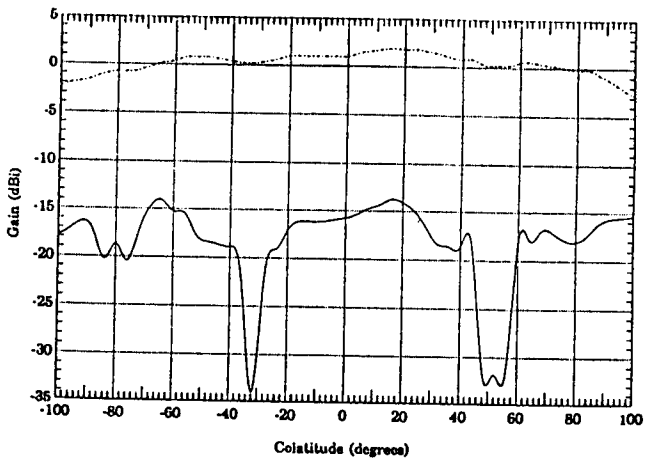

(b) 1643.5 MHz

Figure 4. Measured Meridian cut of the radiation pattern (co and cross polar) at central Rx (a) and Tx (b) GEO frequencies. RHCP (---), LHCP (—).

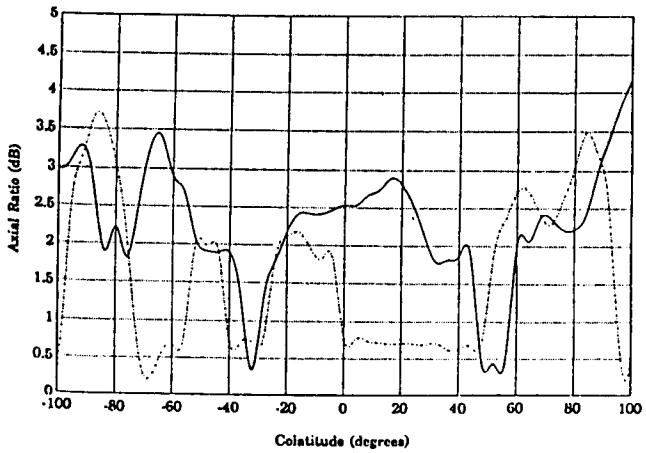

Figure 5. Measured axial ratio vs colatitude for the same cut as in figure 4. 1542.5 MHz (---). 1643.5 MHz (—).

HAND-HELD ANTENNA FOR MEO SATELLITE SYSTEM

This antenna is based on the design of a patch on a short-circuited ring at its inner radius [9] as can be seen in the scheme of figure 6.

In order to feed each antenna with a single port, circular polarization is obtained by using perturbations. From our experience, both a notch type perturbation for the ring and a central slot for the circular patch have been selected.

In order to adjust the whole antenna to a hand-held terminal, the ring patch is designed with a very small ground plane (0.43λ at 1621.25 MHz). The substrate chosen for the whole antenna is Cuclad-2.55.

It has experimentally been found that the stacked configuration does not have a serious effect neither in the reflection coefficient nor in the axial ratio of both patch antennas. But it is important to note that the increase in the ground plane of the patch when it is stacked makes the central slot not be optimum in this situation. Furthermore, a good electrical contact between the ground plane of the patch and the radiating face of the ring must be guaranteed.

The optimization of the slot for the circular patch has been done employing a simple model of the equivalent circuit of the patch with a perturbation [10] whereas the optimization of the rectangular notches for the ring has been experimentally obtained.

Due to the small bandwidth required at the Tx/Rx frequency bands (approximately 0.6 %), the influence of a radome must be taken into account in the final design of the antenna. This effect moves the frequencies of operation to lower values. This is not important for the circular patch but its influence on the short-circuited ring is decisive (see figure 7). For a Nylon radome, the reflection coefficient of the patch is shown in figure 8. A meridian cut of the radiation pattern at central Tx/Rx MEO frequencies is shown in figure 9 and the axial ratio for the same cut is illustrated in figure 10 at the same frequencies.

Finally, a self-diplexed antenna with more than 30 dB of isolation has been obtained. (see figure 11).

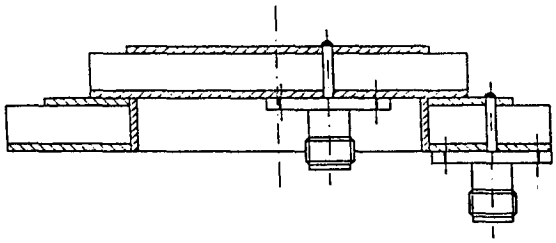

Figure 6. Scheme of the stacked patch antenna.

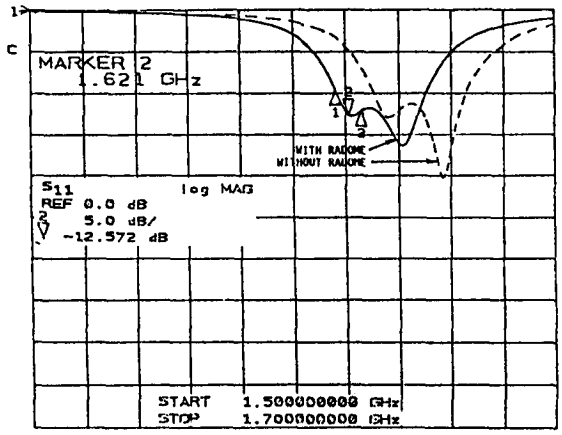

Figure 7. Measured reflection coefficient for the short-circuited ring in stacked configuration. (The effect of Nylon radome is also shown).

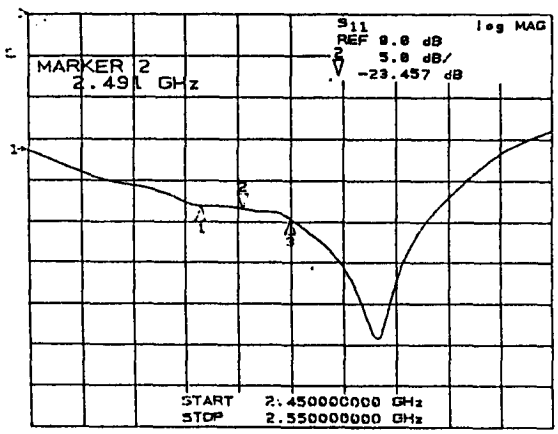

Figure 8. Measured reflection coefficient for the circular patch in stacked configuration.

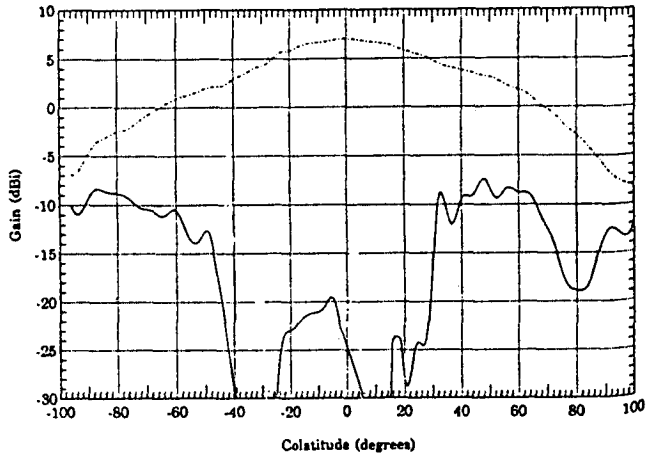

(a) 1621.5 MHz.

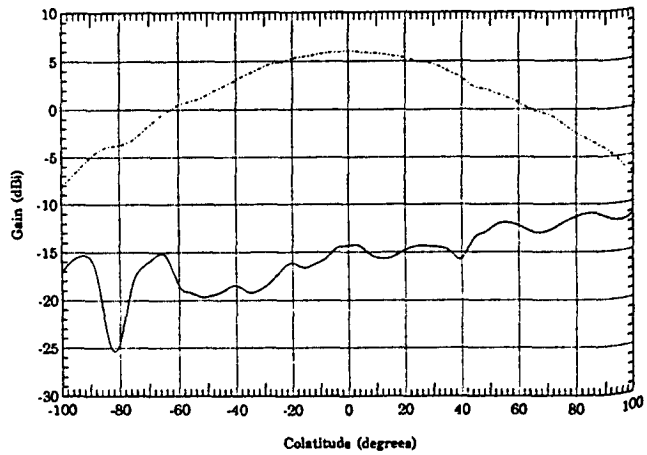

(b) 2491.75 MHz.

Figure 9. Measured Meridian cut of the radiation pattern (co and cross polar) at central Tx (a) and Rx (b) MEO frequencies. RHCP (---), LHCP (—).

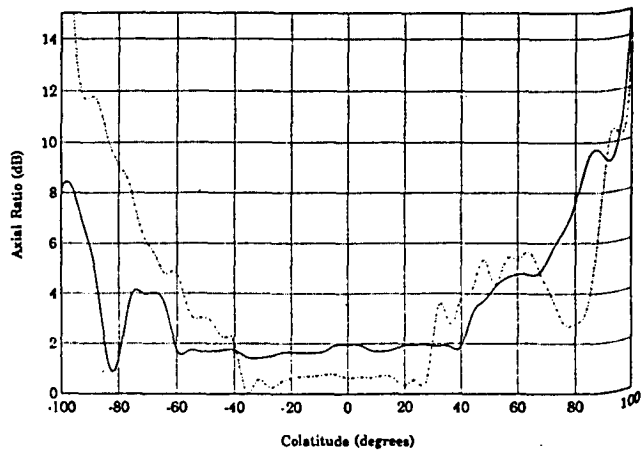

Figure 10. Measured axial ratio versus colatitude for the same cut as in figure 9. (---) 1621.5 MHz, (—) 2491.75 MHz.

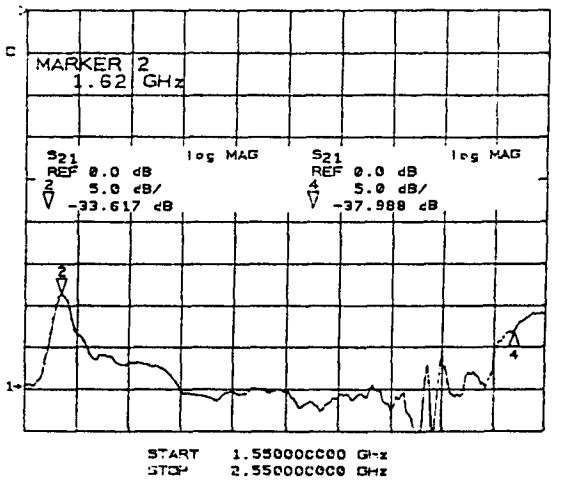

Figure 11. Isolation between frequency bands for stacked patch antenna.

ACCOMMODATION STUDY IN THE HAND-HELD TERMINAL

From the point of view of the accommodation of the antenna in the hand-held terminal the major impact for the " in use " behavior is the effect of the user head.

Recently some interesting models of head-antenna interaction have been done at frequencies between 800-1600 MHz [11] , GSM (900 MHz) and DECT (1900 MHz) bands [12]. In all these papers important distortions of the radiation pattern appear due to the presence of the head of the user. The results exhibit 10 dB or more of decay of the pattern in the directions covered by the head. For instance, if a 840 MHz dipole antenna is placed in front of the head at a distance between 5-1 cm, the radiated power into free space is only about 72-29 % of the antenna input power respectively.

These aspects lead to the key idea of having the antenna above the top of the head. This accommodation is much simpler than any other, reducing the problem to the design of a deployment mechanism. An accommodation design for each antenna is illustrated in figure 12 and 13. showing also both deployment and "in use" aspects.

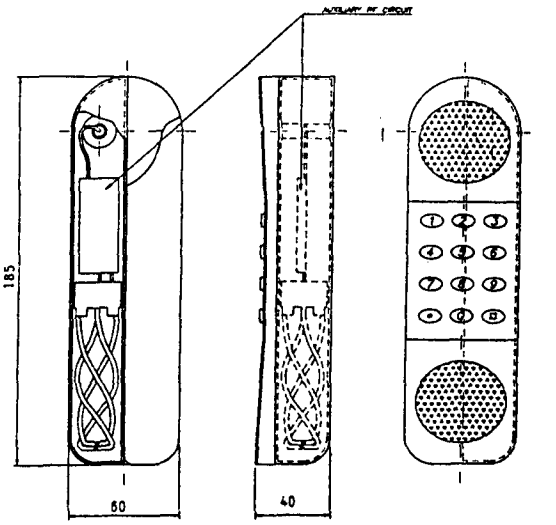

(a) Accommodation.

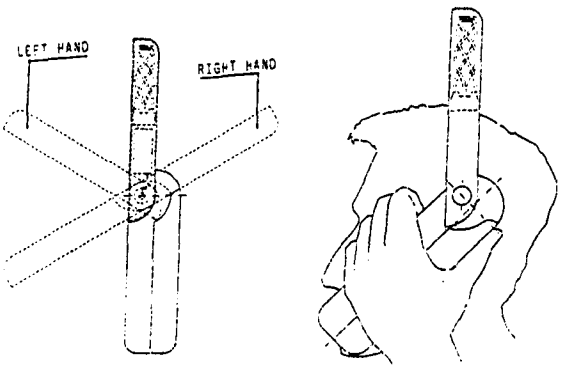

(b) Deployment and "in use" aspects.

Figure 12. Accommodation design of a $\lambda/2$ (½ turn) quadrifilar helix on a hand-held terminal.

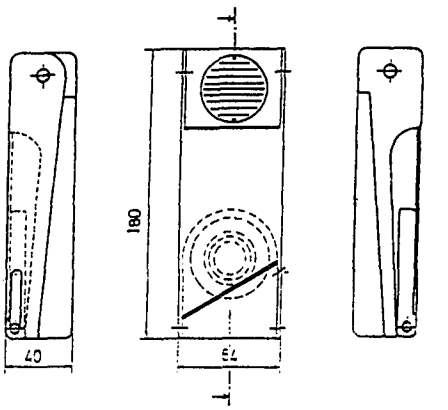

(a) Accommodation.

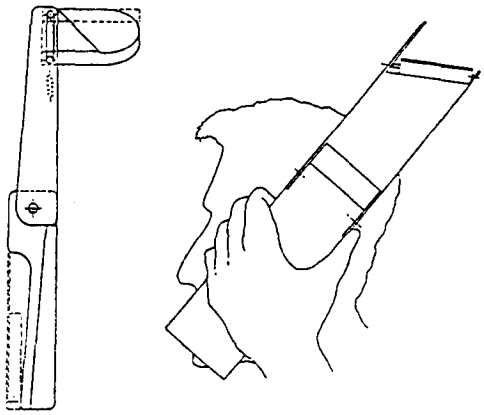

(b) Deployment and "in use" aspects.

Figure 13. Accommodation design of a stacked patch antenna on a hand-held terminal.

CONCLUSIONS

A quadrifilar helix and a self-diplexed stacked patch antenna for hand-held terminals operating with both GEO and MEO satellite systems respectively have been introduced.

The first one fulfills all the required specifications although in the upper edge of Tx band the gain inside coverage is in the limit of specifications.

The second one has an excellent compliance with the complete specifications.

A study of accommodation of each antenna in the terminal has been also presented giving a reasonable compact terminal design.

ACKNOWLEDGEMENT

This work has been carried out under a contract with European Space Agency (ESA-ESTEC). The authors wish to acknowledge to Mr. A. Jongegans and Mr. P. Rinous (ESTEC technical managers) for their very useful comments and suggestions.

REFERENCES

[1] J. Benedicto, J. Fortuny and P. Rastrilla. "MAGSS-14: A Medium Altitude Global Mobile Satellite System for Personal Communications at L-band". Vol. 16, pp..117-133, ESA Journal 1992.

[2] G.Solari, R. Viola. "M-HEO: The Optimal Satellite System for the Most Highly Populated Regions of the Northern Hemisphere". ESA Bulletin No. 70. May 1992.

[3] DETyCOM Final Report on "Antennas for New Applications on Personal and Mobile Communications". ESTEC Contract No. 10142/92/NL/RE, July 1994.

[4] C.C. Kilgus, "Resonant Quadrifilar Helix Design". Microwave Journal. pp. 49-54. Dec. 1970.

[5] J. Barbero et al, "Low Gain Antennas for Land-Mobile Terminals". Proceedings of ESA Workshop on Land-Mobile Service by Satellite. ESTEC, June 1986.

[6] J.H. Richmond, "Computer Program for Thin-Wire Structure in a Homogeneous Conducting Medium", Report 2902-12. the Ohio State University Electroscience Lab.; prepared for N.A.S.A.. June 1974.

[7] W.K. Roberts, "A New Wide-Band Balun". Proc. of the IRE. pp. 1628-1631. Dec. 1957.

[8] J.D. Kraus, "Antennas" McGraw-Hill Co., Chapter 31. 1950.

[9] M. Nakano et al, "Feed Circuits of Double-Layered Self-diplexing Antenna for Mobile Satellite Communications" IEEE Trans. on AP., Vol. 40, No. 10, pp.1269-1271, October 1992.

[10] J. Barbero, H. Lazo and F. Municio, "Model for the Patch Radiator with a Perturbation to achieve Circular Polarization". IEE Colloquium on "Recent Developments in Microstrip Antennas". London. Feb. 1993.

[11] H.R. Chuang "Human Operator Coupling Effects on Radiation Characteristics of a Portable Communication Dipole Antenna". IEEE Trans. on AP, Vol. 42, No. 4, pp. 556-560, April 1994.

[12] J. Toftgard, S.N. Horusleth and J.B. Andersen, "Effect on Portable Antennas of the Presence of a Person". IEEE Trans. on AP, Vol. 41, No. 6, pp. 739-746, June 1993.

Mobile Terminal Technology

Session Chairman: **Mukhtar Rahemtulla,** TMI Communications, Canada
Session Organizer: **Thomas Jedrey,** Jet Propulsion Laboratory, USA

Topic Introduction: At the heart of any mobile satellite communications system are the technologies utilized in the terminal design. These technologies range from baseband components to RF components. The proliferation of mobile satellite communications systems at multiple frequency bands has led to great diversity in terminal design and terminal technology development. The papers presented in this session review the current designs of two terminals for use with the AMSC system, design issues for user terminals operating with HEO satellites, an RF package design for use with DSCS and other satellite systems, and a technique for direct modulation using low cost components.

+Enhanced Performance of the Westinghouse *Series 1000* Mobile Satellite Telephone System

Richard E. Martinson
Westinghouse Electric Corporation
P.O. Box 746, MS 8419
Baltimore, Maryland 21203 USA
Phone: +1-410-993-8255 Fax: +1-410-765-5073

ABSTRACT

The Westinghouse *Series 1000* Mobile Satellite Telephone System is designed for land mobile, maritime and fixed site land applications. The product currently operates on the Optus Mobilesat® system in Australia and will operate on American Mobile Satellite Corporation's (AMSC) Skycell service in the U.S. and TMI Communications' (TMIC) MSAT service in Canada. The architecture allows the same transceiver electronics to be used for diverse mobile applications. Advanced antenna designs have made land mobile satellite communications a reality. This paper details the unique high performance product and its configuration for the vehicle mounted land mobile application.

THE *SERIES 1000* PRODUCT OVERVIEW

The *Series 1000* is modular designed to meet diverse land mobile, maritime and fixed site applications. The product consists of four units:

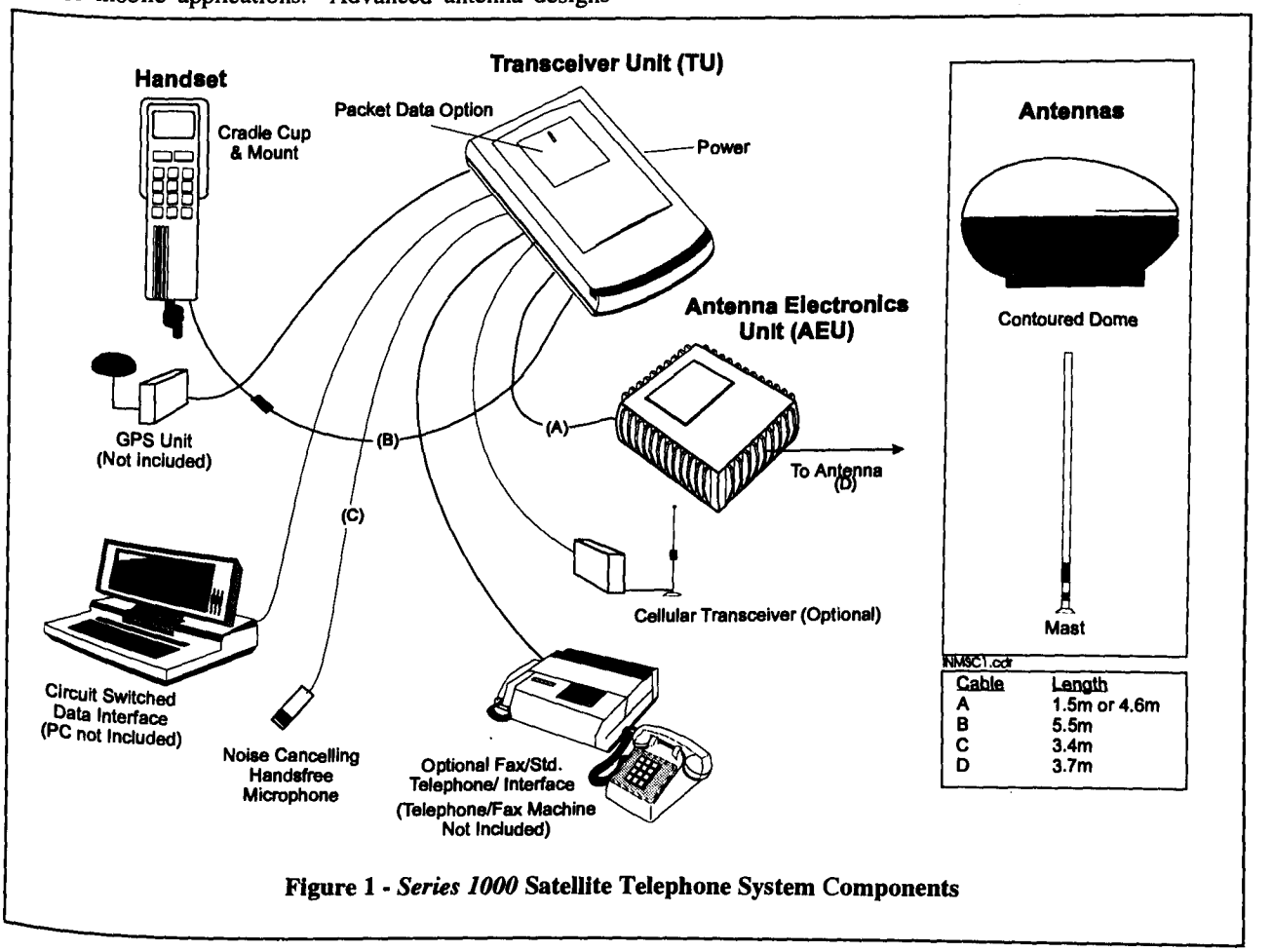

Figure 1 - *Series 1000* Satellite Telephone System Components

- the Transceiver Unit (TU) which holds all digital and most RF hardware;
- the Antenna Electronics Unit (AEU) which contains the transmitter, LNA and diplexer;
- the handset which provides the interface to the user; and,
- the antenna which size and shape is dependent on the application

Figure 1 details the TU, AEU and antennas and their interconnections. Mounting accommodations, power and cooling requirements, inter-unit cable lengths, shock and vibration requirements, and choice of options such as cellular and packet data are all tailored for installation and operation for land mobile applications. Westinghouse offers a three-box TU-AEU-Antenna product to reduce the size, weight and power requirements of the externally mounted antenna and the ability to re-use the TU and near identical AEU for maritime, fixed site and aeronautical applications. By placing the transmitter, LNA and diplexer in a separate unit from the antenna, the land mobile antenna can be significantly reduced in size and weight, therefore making more installations possible. The TU, AEU and antennas have been tested to meet the demanding environments from the frozen Canadian North to the hot dusty Australian outback.

Transceiver Unit (TU)

The TU contains the low power RF electronics incorporating the synthesizer, modulator, and receiver (except the LNA), digital signal processor, operational software, and the main power supply. It provides the central interface for other system components and the system intelligence. The TU can be mounted in any position and a variety of locations. Westinghouse has designed the TU for compatibility with a number of outboard commercially available GPS products from Garmen, Trimble, and other GPS manufacturers that meet NMEA-0183 interface standards.

The TU shown in Figure 2, is 5.4 cm x 17.8 cm x 30.5 cm size and weighs 3.2 Kg. The TU contains electrical connections for the handset, Group III Fax/standard telephone, short messaging and circuit switch data, and power to/from the AEU as shown in Table 1. The TU has passed the Australian AUSTEL certification for conducted and radiated EMI. The power dissipation of the Transceiver is 23 watts and is cooled by conduction of heat from circuit boards to chassis and free convection to the ambient air. The chassis is constructed to support free convection cooling, so cooling fans are not required.

The TU is not weatherproof, therefore must be protected from the outside environment. Recommended placements for TU include: under the passenger/driver seats; under the rear shelf or in the trunk of automobiles; and behind the rear seats in light trucks.

Ease of serviceability has also been designed into the product. A low cost RF loop-back and power test set is available to diagnose the input and output of the TU and AEU. This device supplements the RF portions of the *Series 1000* to provide more detailed performance infor-

Table 1 - TU Interfaces

Interface	Description
Handset Interface	Handset control, voice band audio, and power connections to/from the handset through the RJ-45 port.
Fax/Phone Interface	Standard RJ-11 phone jack for the connection of a Group III fax at 2400 BPS, or standard tone telephone/STUIII or small PBX switch.
DB-24 Data Port	Connection to external Data Terminal Equipment (DTE) such as a notebook PC or ruggedized mobile data device. Supports standard Hayes circuit switched data and synchronous and asynchronous Packet Assembler/Disassembler (PAD) packet data.
DB-15 GPS/Test/Control	Provides interface to an external NMEA standard GPS module, connection to a system test set and to an external DTE for remote control of the *Series 1000*. The product can also be controlled by a DTE in place of the handset for asset remote control and monitoring.
Power	Connector for 12V nominal prime power, ground, horn alert and ignition sense is provided.
AEU Interface	Integrated interface assembly that consists of the receive/transmit RF cable, AEU and antenna control, monitor functions and DC power and ground.
Handsfree Mic Port	Connection port for a vehicle mounted handsfree microphone.
Remote Speaker Port	For applications requiring a speaker in a different location than the back of the handset.
Cellular Interface	For connection to optional cellular module. Same number satellite/cellular interoperable service is available with AMSC's SKYCELL service.

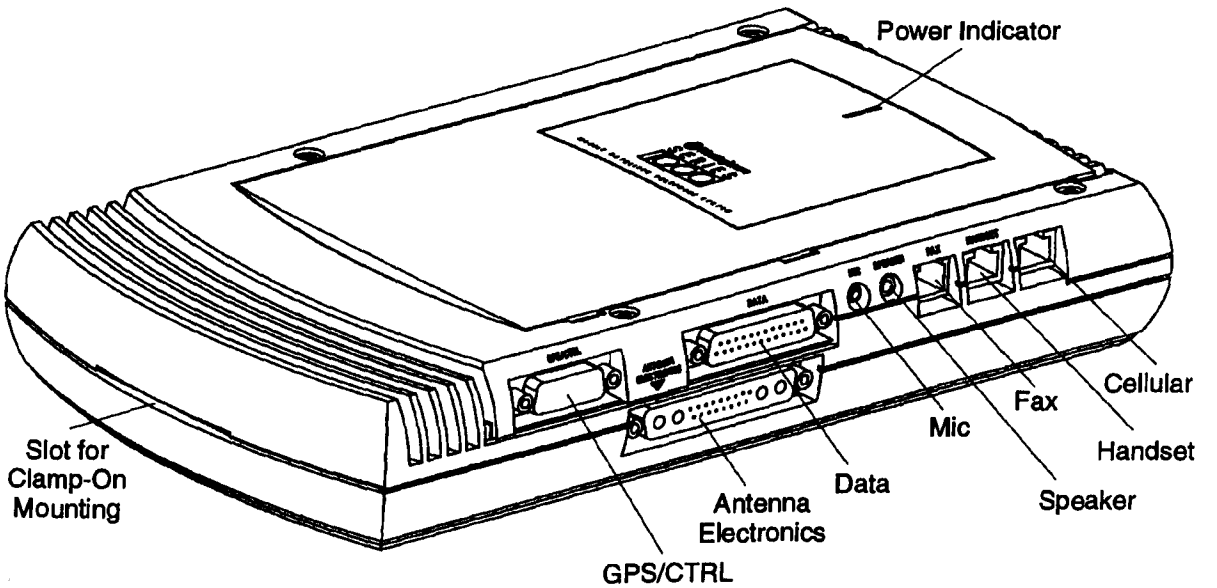

Figure 2 - *Series 1000* Transceiver Unit

mation. This information will allow authorized service centers to quickly and accurately diagnose faults and isolate failures to a single replaceable unit.

Antenna Electronics Unit (AEU)

The Antenna Electronics Unit (AEU) shown in Figure 3 is an FCC (USA) and AUSTEL (Australia) qualified full duplex, satellite transceiver amplifier. The AEU amplifies the receive and transmit signals which are processed by the TU. The AEU contains a linear amplifier in the transmit chain, a low loss diplexer for isolation and an ultra-low noise amplifier for the receive chain. To minimize installation time, the AEU uses only three external electrical connections. The Antenna RF Interface provides the RF drive from the High Power Amplifier (HPA) to the antenna. The Antenna RF Interface also delivers the receive signal to the Low Noise Amplifier (LNA). The Antenna Data Interface provides the control, power, and monitor functions for the automatically steered contoured dome antenna. The TU Interface handles the RF, power, monitor and control line communications between the TU and the AEU.

The amplifier is configured to deliver 5 watts in the transmit band. The amplifier contains a rugged, gain stabilization loop which maintains the output power within a narrow window. The AEU is designed to be cooled by free air convection. The AEU LNA is a mature GaAs design which has been used in Inmarsat applications. The low noise figure allows the mobile terminal to receive satellite signals at fringe locations regardless of temperature and external noise sources. The diplexer enables the LNA to operate in the presence of strong interfering signals in addition to the transmit signal without any degradation in Bit Error Rate (BER) performance. The AEU contains a microcontroller which performs several housekeeping functions. The microcontroller converses with the TU via RS-422 EIA bus. Via this bus, the TU can

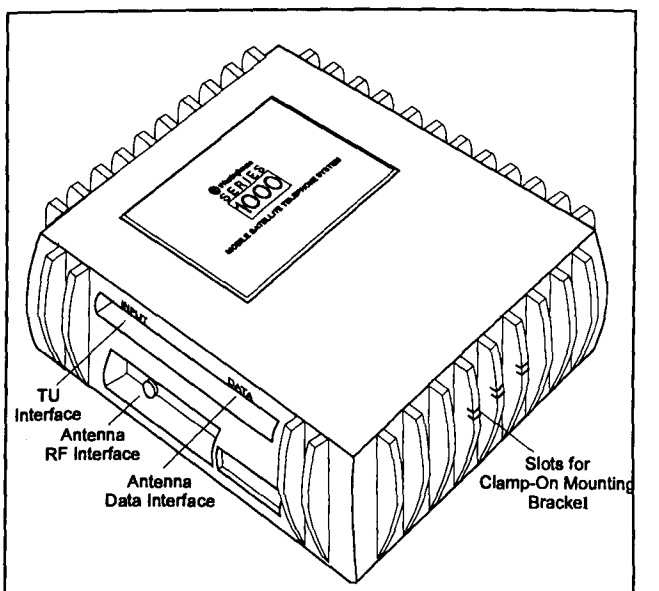

Figure 3 - *Series 1000* Antenna Electronics Unit

program the AEUs output power, turn the RF on and off and monitor the health of the AEU.

Like the TU, the AEU must be protected from the outside environment. The unit provides the RF amplification necessary to transmit signals to the satellite, and therefore generates a great amount of heat which must be dissipated. Therefore, the AEU must be mounted in an area that will allow sufficient ventilation for the unit. Recommended placements for AEU include: under the passenger/driver seats; under the rear shelf or in the trunk of automobiles; and behind the rear seats in light trucks.

Multi-Function Handset

The common handset to all *Series 1000* configurations is shown in Figure 4. The multi-function handset mounts in a location convenient to the operator. It is designed to be similar to standard cellular telephone handsets in size and function with the additional capabilities unique to satellite communications. It supports advanced features expected of a top-of-the-line cellular mobile phone such as 99 number memory, one touch dialing, no-touch answer, speed dialing and a multi-tiered menu system. The control panel for the handset consists of a multi-function key pad and addressable display. The handset is easily and smoothly docked with a cradle which attaches to any flat surface. The coil cord provided with the handset is approximately 2 meters when fully extended, and .5 meters when in the resting position. A built-in back-of-handset speaker emits a ringing tone, DTMF tones and voice conversation for hands free mode. For vehicle handsfree operation, a special noise cancellation microphone is used to mitigate the effects of background noise.

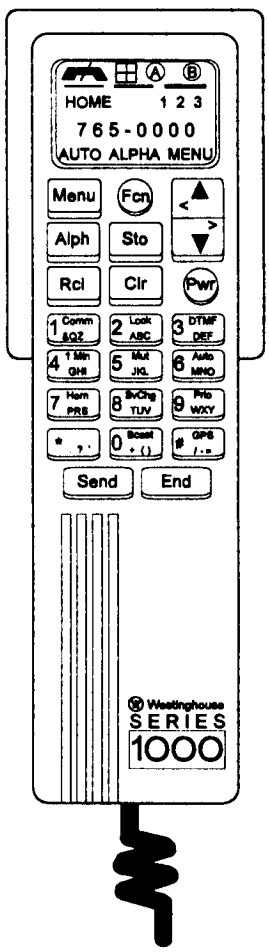

Figure 4 - Multi-Function Handset

The user and service/installer can use the handset to accomplish commissioning, setup of communications defaults, and product operation control. The distinction between these three tasks is in the interface required to effect control. Commissioning is conducted at that point-of-sale. Setup of communication defaults is conducted from an advanced menu system. Mode control is initiated by using the keypad, discrete function keys, and combinations of function key and keypad sequences.

WESTINGHOUSE LAND MOBILE ANTENNAS

Vehicles moving and turning at highway speeds and rapidly varying signal amplitudes caused by multi-path reflections impose stringent requirements on antenna steering design. In addition, the land mobile market demands low cost antenna solutions. These considerations argue for a mechanically simple mast and low cost compact dome that require minimum platform stabilization.

Mast Antenna

The Westinghouse mast antenna illustrated in Figure 5 is superior to standard mobile satellite mast antenna designs. Other mast antennas that provide steering in elevation suffer from two limitations. First, because of mechanical instability in the antenna elements, they are subject to large transmit gain variations in the horizontal pattern when subjected to vibration. Second, because the antenna response in the elevation plane is frequency sensitive, the transmit and receive peak gain responses do not occur at the same angle of elevation. This results in a

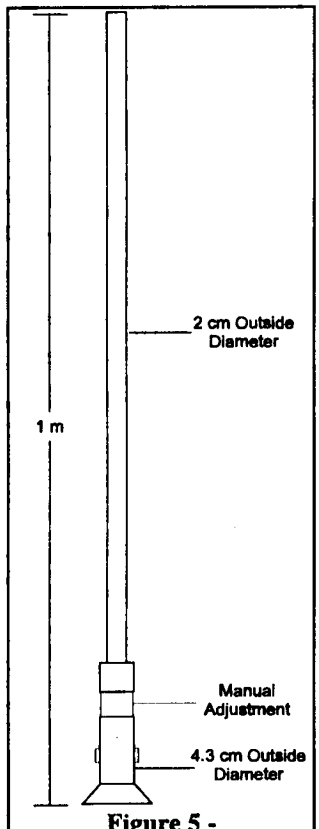

Figure 5 - Westinghouse Non-Squinting Mast Antenna

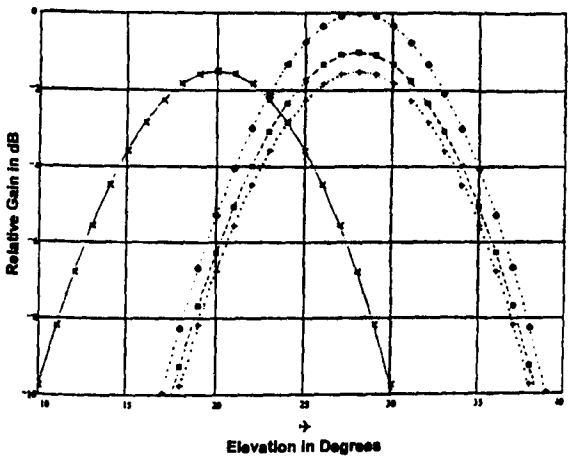

Figure 6 - Comparison of Westinghouse Mast to Common Mast Antenna Performance

frequency dependent "squinted beam" pattern as illustrated in Figure 6. Represented in this figure are the nominal relative gains of a standard mast antenna and the Westinghouse mast antenna. The curves labeled "Common Receive" and "Common Transmit" show the response of available mast antenna designs. Note that the peak response at the transmit frequency is displaced from the response at the receive frequency. This makes it impossible to orient the antenna optimally for both transmit and receive. Since the loss in transmit can be made up with more gain in the HPA, one adjusts the antenna for peak response in reception. This leaves a narrow range of acceptable elevation angles which in turn requires frequent adjustment of the antenna when traveling over long distances toward or away from the satellite.

The curves labeled "Westinghouse Transmit" and "Westinghouse Receive" show that the responses of the Westinghouse design for both the transmit and receive frequencies are centered at the same elevation angle. This significantly reduces signal loss going up and down hills and allows the vehicle to drive further without readjusting the mast antenna. In addition, the Westinghouse design provides exceptional mechanical stability and symmetry of the radiating elements minimizing gain variation caused by vehicle vibration. The mast antenna requires occasional adjustment of the beam pointing angle in elevation when traveling over long distances; therefore an easy to reach elevation adjustment is provided at the antenna base.

Contoured Dome Antenna

As shown in Figure 7, the Westinghouse contoured dome antenna is less complex and lower in cost and much smaller than existing Inmarsat Standard-M maritime antennas. This proprietary approach is simpler than the usual approach which requires inclinometers and expensive compasses in addition to multiple rate sensors to steer in both azimuth and elevation. The simple mechanization is possible in part because the antenna beamwidth from 15° to 60° elevation is sufficient to preclude the need for pitch and roll stabilization on land mobile platforms and in part because of a sophisticated steering algorithm. Great emphasis has been placed on reducing the size, weight, and cost of the antenna by putting the sophistication in the beam steering software rather than hardware. The beam steering controller accommodates vehicular turn rates of 60 degrees/second and acceleration of 20 degrees/sec/sec. Thus, the satellite acquisition can be accomplished in less than 6 seconds. Once the satellite is acquired, the tracking mode will maintain antenna pointing accuracy to the satellite. The antenna has two major control loops, one for stabilization due to vehicular motion and the other to perform acquisition and long term tracking of the satellite.

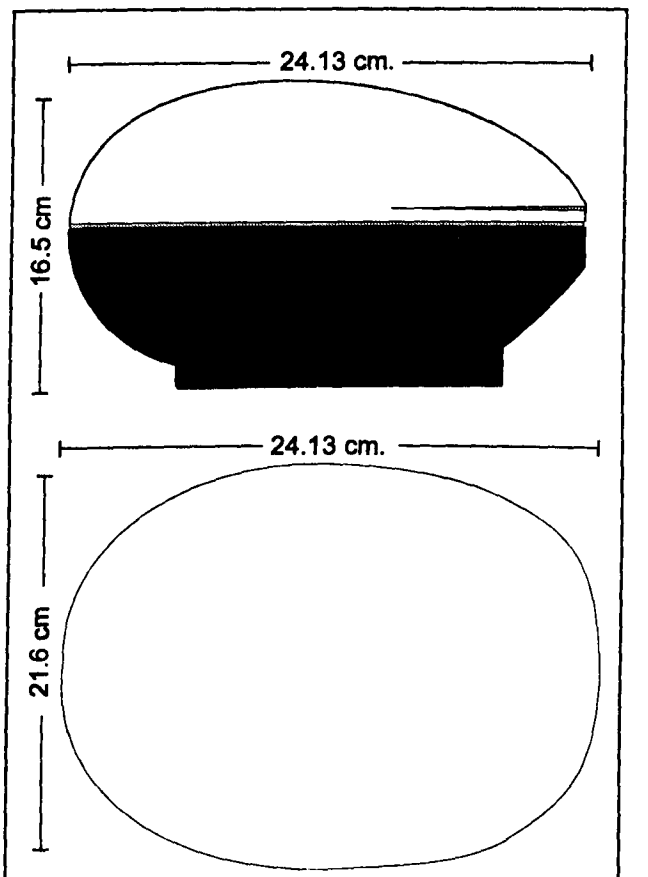

Figure 7 - Westinghouse *Series 1000* Contoured Dome Antenna

SERIES 1000 LAND MOBILE PRODUCT CONFIGURATION

The vehicle configuration is installed on an automobile as illustrated in Figure 8. The contoured dome antenna can be mounted either on the roof, the trunk, or the rear window and is ideal for light trucks and passenger vehicles. It may be mounted either on the quarter panel at the edge of the trunk lid or on the trunk lid near the center. Similarly, it may be mounted on the roof near the center or side. For temporary mounting, a magnetic mount is available such that no hole has to be drilled in the roof of the vehicle. The antenna cable may be routed over the outside of the vehicle to a door or trunk lid where it enters by compressing the weather stripping. Mast antennas may be mounted on the rear quarter panel, trunk lid, or on the vehicle roof.

The TU may be mounted in the trunk of automobiles or under the front seat. In pick-up trucks it may be mounted behind the seat. Orientation is not critical but some space for convection airflow is required. The AEU mounts up to 3.7 meters away from the contour dome and mast antennas to limit cable losses between the antenna and the LNA/HPA. The AEU mounts adjacent to the TU with a 1.5 meter cable connecting the two units. Optionally, a 4.6 meter cable is available for installations where the AEU and TU are mounted in separate locations in the vehicle. The handset is mounted near the driver's position within easy reach and attach to the TU through a 5.5 meter cable in addition to the coil cord. A hands-free microphone is provided to pick up the driver's voice and is typically installed on the sun visor.

OTHER APPLICATIONS

Because of its modular design, the *Series 1000* may also be used for diverse applications such as maritime, aeronautical and fixed site. The same TU, and similar AEU may be applied in each diverse application. Only the antenna configuration changes. Several of the products are being configured in conjunction with firms that are expert in the perspective market. In addition, a battery powered transportable product is planned that will enable communications any place, at any time, without external power.

SUMMARY

The *Series 1000* Mobile Satellite Telephone System is truly a revolutionary land mobile phone that brings reliable, low cost voice and data communications for the first time to all of Australia ***today*** and soon to North America. By placing most of the electronics inside the vehicle, the antennas become lighter, more aesthetically pleasing and may be installed in a variety of locations. The modular product design allows installation flexibility in all types of vehicles and hardware re-use for diverse applications.

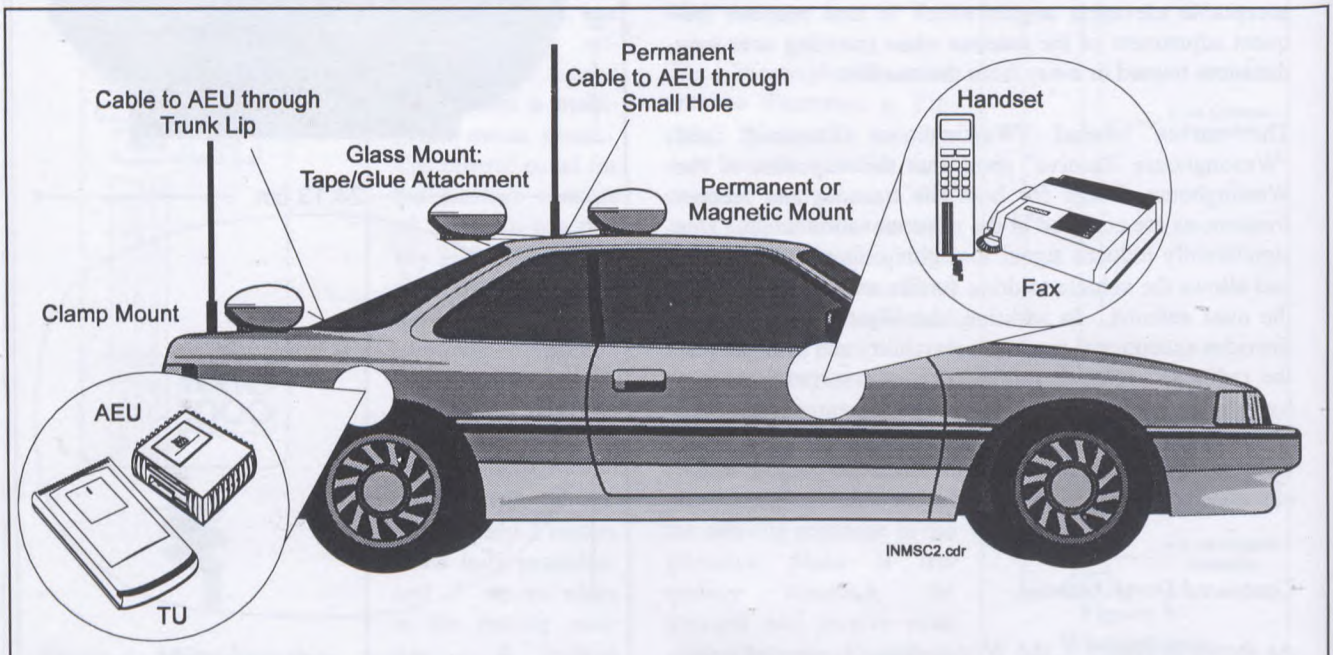

Figure 8 -Land Mobile Installation

Design and Performance of Mobile Terminal for North American MSAT Network

Tsuyoshi Fuji, Makio Tsuchiya, Yoji Isota and Katsuhiko Aoki
Mitsubishi Electric Corporation MSAT Strategic Business Development Center
1-1, Tsukaguchi Honmachi 8-Chome, Amagasaki-City, Hyogo, 661, JAPAN
Phone : +81-6-497-6206 FAX : +81-6-497-6381

ABSTRACT

The Mobile Terminal (MT), which can be selected for various applications, i.e. Land mobile, Transportable, Fixed site and Maritime use, has been developed. Two types of antennas are available i.e. medium gain and high gain antenna. The MT can support circuit switched voice and data service. Additionally, cellular roaming service, Net Radio and Group 3 facsimile services are optionally provided. A Mitsubishi handheld portable phone can be used as a stand-alone portable cellular-only phone or it can provide MSAT voice service when connected to MT.

The MT which operates in L-band (1.5GHz/1.6GHz) satisfies EIRP of 12.5dBW minimum and G/T of -16dB/K minimum for medium gain system and -12dB/K for high gain system. The excellent performance of transmit phase noise and bit error rate is achieved by using new technologies.

INTRODUCTION

North American Mobile Satellite Communication System using mobile satellite (MSAT) which has been developped by American Mobile Satellite Corporation (AMSC) and TMI Communications is scheduled to go into service in 1995. This system provides voice, data and facsimile communications services in North American territory [1]. Mitsubishi Electric Corporation (MELCO) has developed mobile terminals (MTs) for this network. This paper describes the outline, design and performance of Mitsubishi's MTs.

OUTLINE OF MT

Mitsubishi's MT can support circuit switched (CS) voice and data service (2.4kbps, 4.8kbps).

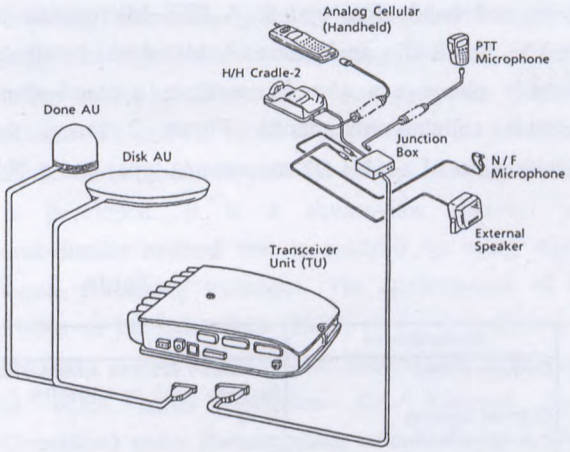

Figure 1
Configuration Drawing of MELCO CS MT

Figure 2
Outside View of AU (Upper) and TU (Lower)

Additionally, cellular roaming service, Net Radio and Group 3 facsimile services are optionally provided. A typical configuration of the MT consists of an Antenna unit (AU), a Transceiver unit (TU) and a Handheld phone. A plane handset can be used instead of a handheld phone. Several types of MTs are designed for various applications, i.e. Land mobile, Transportable, Fixed site and Maritime use. Figure 1 shows typical configuration drawings of MELCO CS MT with Net Radio and hands free option. A PTT Microphone is used in Net Radio application. A Mitsubishi handheld portable phone can also be used as a stand-alone portable cellular-only phone. Figure 2 shows the outside view of an AU (Dome antenna type) and a TU.

The principal performance of the MT is shown in Table 1. In this table there are five types of anntenas. Disk and Dome antennas are medium gain while others are high gain antennas. Power consumption is the maximum value in the case of transmitting L-band carrier. Disk and Dome antennas are mainly used for Land mobile use and mounted on the roof of the vehicle. Transportation antenna is used for transportation trucking use. Fixed site antenna is used for fixed site telephony applications. Transportable antenna is installed within the brief-case cover. In the case of Transportable MT, a TU and a Handset also installed in the brief-case.

Table 1 Principal Performance of the MT

Nomenclature	Performance Specificaiton
Frequency Band	Transmit 1,626.5 to 1,660.5MHz Receive: 1,525 to 1,559MHz
Channel 5pacing	6kHz
Tuning Increments	0.5kHz
Channel Rate	6.75Kbit/s
Modulation	QPSK 60 percent cosine rolloff
Scrambling	PN code (15 stages, CCIR Report 384-5)
FEC Encoding	Convolution Code. Rate 1/2 and Rate 3/4 punctured code (K = 7)
FEC Decoding	Viterbi decoding
Signalling Channel	Outbound : TDM6,75Kbit/s, DQPSK Inbound : Random Access 3.375Kbit/s. DBPSK TDMA 3.375Kbit/s. DBPSK
Data Rate	2,400 bit/s or 4,800 bit/s
Communication Interface	Handset Interface (Voice) : 4-W with serial async keypad and LCD signals Data Interface : RS232 C (CCITT V.24 or V.28) Facsimile Interface : CCITT Group 3, 2400 bit/s Voice band signal IB Interface : CCITT X.25
Power Supply	12DVC normal (11 to 16V range) Current : approx. 6A
Size/Weight (Approx.)	Antenna : see below Transceiver Unit : 12"(D) x 8"(W) x 2"(H) 5 lbs

Type of Antenna	Disk Antenna	Dome Antenna	Transportation Antenna	Fixed Site Antenna	Transportable Antenna
Size/Weight (Approx.)	13.7" (ϕ) x 1.9" (H) 5.3 lbs	6.8" (ϕ) x 6.6" (H) 3 lbs	11.5" (ϕ) x 7.2" (H) 5.5 lbs	19.7" (W) x 19.7" (D) x 2" (H) 14 lbs	14" (W) x 14" (D) x 4.3" (H) 20 lbs (Total amount of MT)
Maximum Transmit EIRP	16.5dBW	16.5dBW	16.5 dBW	16.5 dBW	16.5 dBW
Received G/T (θ: Elevation angle)	-16dB/K ($25° < \theta \leq 60°$)	-16dB/K ($15° < \theta \leq 60°$)	-13 dB/K ($25° < \theta \leq 60°$)	-10 dB/K ($5° < \theta \leq 90°$)	-12 dB/K ($15° < \theta \leq 90°$)

AU DESIGN

Figure 3 shows a block diagram of medium gain Dome AU [2]. This AU consists of an axial mode helical antenna on an inclined ground plane, RF components (a rotary joint, a diplexer, an LNA and an HPA) and tracking components (a motor, gears and driving circuits). The size of this antenna is around 170mm diameter and 170mm height. Weight is about 1.3kg. For this medium gain antenna, the gain more than 8dBi is obtained in the coverage area of 15 degrees to 60 degrees in elevation angle. Performance of G/T $\geqq$ -16dB/K and transmit EIRP $\geqq$ 12.5dBw can be achieved using an LNA with 1dB noise figure and an HPA with 4w output power (average).

Another antenna having higher gain has a performance of G/T $\geqq$ -12dB/K and ransmit EIRP $\geqq$ 12.5dBw using the same LNA, HPA and antenna with gain of 12dBi .

TU DESIGN

The TU is designed to be common to all types of MTs. It contains frequency converter, baseband processor, logic & signaling processor and power supply. Figure 4 shows the block diagram of TU. An echo canceler is adopted in the case of hands free option. The frequency converter adopts a dual tuning type PLL synthesizer driven by DDS (Direct Digital Synthesizer) to achieve low spurious and phase noise characteristics [3]. Figure 5 shows a typical data of phase noise characteristics of 1.6GHz output.

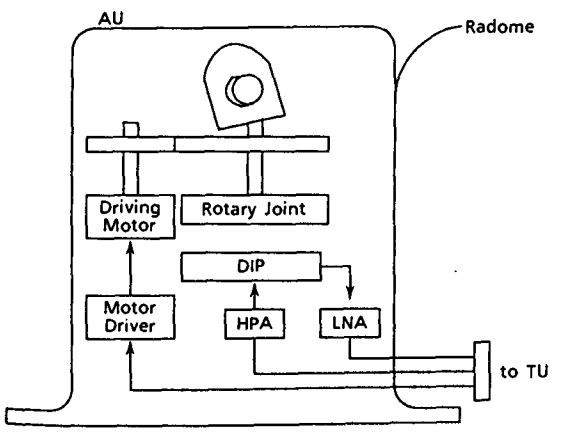

Figure 3 Block Diagram of Dome AU

Transmit phase noise is less than -70dBc at 1kHz offset. The frequency converter is able to cover from 1626.5MHz through 1660.5MHz for transmit band and from 1525MHz through 1559MHz for receive band in 500Hz step.

Baseband processor mainly performs the function of QPSK modulation/demodulation and framing/deframing. It is composed of a DSP (Digital Signal Processor). Demodulator adopts a differential detection with the technique of maximum likelyhood sequence estimation (MLSE) using Viterbi algorithm [4],[5] to cope with Ricean fading channel, which is called multiple differential phase detection (MDPD) scheme. To achieve rapid acquisition of the bit timing in the burst mode, the new bit timing recovery method is developed. It is a square-law detector and tank-limiter method that is realized by using digital signal processing technique. The performance of the Eb/No vs Bit Error Rate (BER) of the demodulator is shown in Figure 6. This figure shows BER in the case of voice mode operation (No Forward Error Correction) under Ricean fading with K-factor = 10dB and fading bandwidth of 100Hz. In this figure white circle indicates experimental result. BER is better than 1.0×10^{-2} at Eb/No = 9.0dB. Carrier detection and acquisition AFC which is accomplished by an accumulation of differentially detected signals is also newly developed to cope with large receive frequency offset [5].

The logic & signaling processor is the central controller of the MT. It includes network access and control functions too. Also, the logic & signaling processor includes the IMBE (Improved Multi Band Excitation) voice codec which proceed 6.4kbps voice data. Two custom LSIs are used in the TU to reduce H/W size and power consumption.

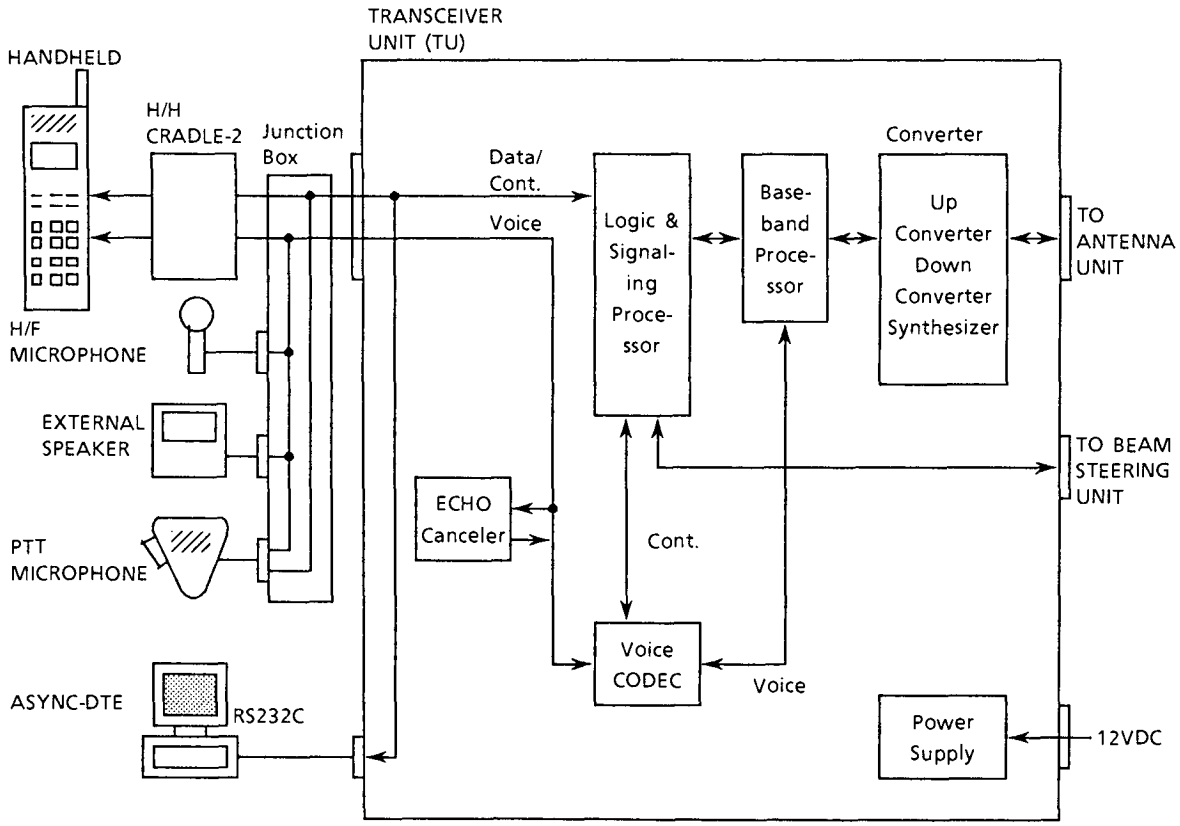

Figure 4 Block Diagram of TU

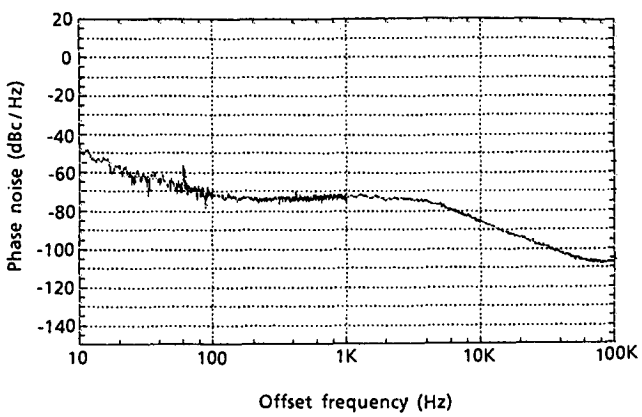

Figure 5 Transmit Phase Noise

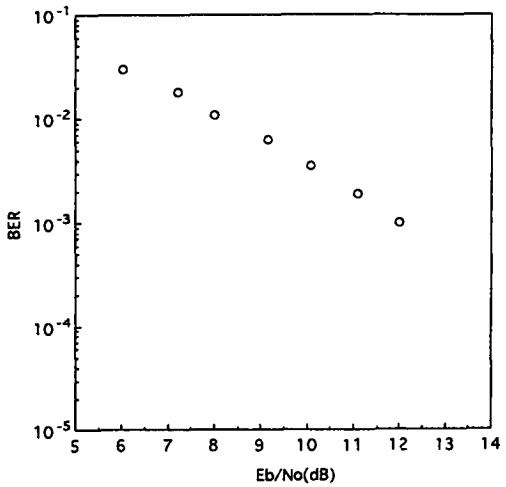

Figure 6
BER Performance in Voice mode
(K=10 dB, Fadking BW=100 Hz)

CONCLUSIONS

The outline, design and performance of MTs for North American MSAT Network are presented. This MT can be used for various applications. New method of demoduration and bit timing recovery are developed to cope with severe Ricean fading channel conditions. And a new PLL synthesizer is developed to achieve low spurious and phase noise characteristics. As a result, the excellent performance has been verified. Key technologies of this MT can also be used for other mobile satellite systems.

REFERENCES

[1] J.Lunsford, R.Thorne, D.Gokhale, W.Garner and G.Davies, "The AMSC/TMI mobile satellite services (MSS) system ground segment architecture", 13th AIAA Intl. Commun. Sat. SYS. Conf. Digest, pp.405-426 (Feb. 1992).

[2] M.Matsunaga, Y.Konishi, M.Ohtsuka and E. Morimoto, "Vehicle antennas for L-band mobile satellite communication systems using MSAT", ICPMSC'94 Digest, pp. 298-301 (Oct. 1994).

[3] K.Itoh, K.Tajima, S.Nishimura and A.Iida, "Dual Tunable Type Low Spurious PLL Synthesizer Driven by DDS with Frequency Converter", IEICE Technical Report, MW94-156 (Feb. 1995).

[4] T.Kojima, M.Miyake and T.Fujino, "Differential Detection Scheme for DPSK Using Phase Sequence Estimation", Trans. of IEICE, Vol.76-B-Ⅱ, No.10, pp.783-792 (Oct. 1993).

[5] T.Kojima, F.Ishizu, M.Miyake, K.Murakami and T.Fujino, "Design of an Anti-Rician-Fading Modem for Mobile Satellite Communication Systems", Proceedings of IMSC'95 (Jun. 1995).

Key Design Issues for User Terminals Operating with HEO Satellites

I. Stojkovic, J. E. Alonso

European Space Agency - ESTEC
Keplerlaan 1, P.O. Box 299
2200 AG Noordwijk
The Netherlands
Tel. +31-1719-86555
Fax. +31-1719-84596

ABSTRACT

Coverage of high-latitude areas in the northern hemisphere using geostationary satellites can not be achieved with good elevation angles, and highly inclined elliptical (HEO) orbits present one possible way to overcome this problem. The high elevation angles they achieve and the relative motion of the satellites across the sky, including satellite hand-over, present a specific set of requirements for the design of user terminals, be they for communication or broadcast-reception purposes. This paper reviews key design issues for user terminals operating with satellites in highly inclined elliptical orbits. While all aspects of user terminal design are broadly covered, special emphasis is given to the antenna and RF front-end design.

The types of terminals discussed include communications terminals: the hand-held, the notebook and the vehicle-mounted types, as well as the vehicle-mounted digital audio broadcasting (DAB) receiver terminal.

A number of solutions are outlined, based on trade-offs with respect to the most significant system interface parameters such as G/T and EIRP. Candidate antenna and front-end configurations were studied, in particular patch and helical antennas with the principal aim of deriving low cost, yet effective solutions.

Issues related with achieving best EIRP for the communications terminals are presented, taking into account radiation safety limits. The differences in the design of receive only versus receive/transmit RF front-ends for HEO system terminals are highlighted and solutions for both proposed.

This paper summarises the results of internal ESTEC studies and external ESA-sponsored work, concerning major user terminal parameters and design aspects, performed to size Archimedes - a HEO satellite constellation based multimedia broadcasting and communications system.

HEO SCENARIO AND ARCHIMEDES SYSTEM

A major drawback of geostationary satellite based communications and broadcasting systems for mobile users in the highly industrialised northern latitude regions (Europe, Canada and the US or Japan) is the severe propagation impairment due to shadowing (blocking) and fading of the signal, which is augmented by the low elevation angles at which the satellite is seen in these areas. While high elevation angles present a clear advantage for communications terminals, they are a necessity for satellite broadcasting to mobile terminals.

A possible way to overcome the problem of low elevation angles is to use constellations of satellites in highly elliptical orbits (HEO), which can provide high elevation angles to northern latitude regions, always in excess of 40°, and most of the time above 55°. This can provide an improvement in the required system and propagation link margins of between 5dB and 10dB. Other advantages of these constellations are the very good coverage achieved with a relatively low number of satellites, slow relative motion of the satellite across the sky, low rate of handovers and simple networking.

ESA has conceived a broadcasting and communications satellite system based on a HEO constellation, called ARCHIMEDES, and has carried out several system studies (Phase-A) to define a preoperational mission intended to demonstrate the feasibility and introduce digital audio broadcasting (DAB) and personal communications services by HEO satellites, Ref. [1]. The baseline system design was selected a multi-regional constellation (the 8-hour M-HEO constellation), the main system parameters of which are listed in Table 1.

Each satellite has a 3 to 5 beam coverage pattern. The beams are highly overlapped over the European region (allowing good broadcasting coverage) and they are re-pointed slowly, compensating for the satellite motion. A representative 4-beam coverage over Europe is presented in Figure 1.

Table 1. Archimedes system parameters	
Orbit (Archimedes)	M-HEO-8 hr
Coverage (potentially)	Europe, Canada, Far East
Min. elevation for coverage	40° (in most areas > 55°)
Number of satellites	5 or 6
Apogee altitude	26,800 Km
Perigee altitude	1,000 Km
Orbit inclination	63.4°
Comm's frequencies	S- and/or L- band
Downlink frequencies, DAB	1452.0MHz - 1492.0MHz
Voice activation factor	50%
Propagation margin comm's	6 dB
System margin comm's	3 dB
Required Eb/No, Comm's	2.8 dB
System and prop. margin DAB	6 dB
Required Eb/No DAB	6.8 dB

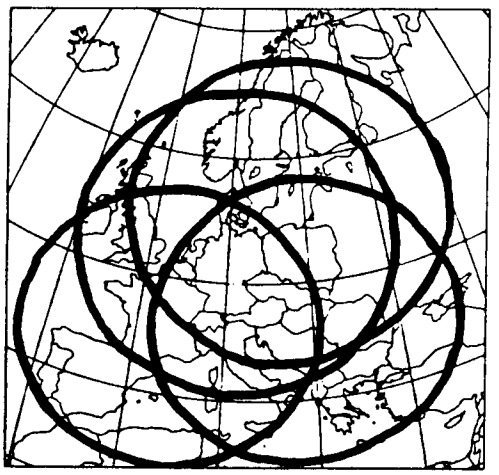

Figure 1 *HEO coverage of Europe from apogee for broadcasting (DAB) services.*

The selected HEO constellation influences a number of system parameters which affect the design of user terminals, such as the Doppler shifts and delay variations due to satellite motion, jumps in Doppler shift and propagation delay during inter-satellite handovers, which possibly have to be compensated at the terminal, the variation of path losses that define the type of power-level control needed, and elevation angles that influence the antenna design and offer reduced signal shadowing and fading.

SERVICES AND TERMINALS

The services that have been considered in the Archimedes system are primarily Digital Audio Broadcasting (DAB), but also personal (to hand-held phones and notebook sized terminals) and mobile (to vehicle-mounted terminals) voice communications. The option to provide interactive multimedia entertainment and information broadcasting is currently considered the baseline for DAB, although the services have yet to be fully defined. Multimedia satellite broadcasting in general, and in particular to mobile terminals, is considered by market studies as a very promising service. In the present paper we concentrate on DAB and personal communications services, as they were studied in the phase-A of the Archimedes project.

Satellite DAB is seen as a future service with very high potentials. It is intended to be delivered to fixed (home-installed) and vehicle-mounted terminals, the system design driver being the vehicular terminals. As presently foreseen, the DAB terminals perform only the receive function, so it is possible to achieve acceptably low cost and significantly better G/T performance. The interactivity, for those services that require it, could be achieved through alternative means of communication, such as cellular telephony.

With respect to communication services, currently there are several satellite personal communications systems in the procurement phase, and the market forecasts for them are bright. The services to be offered are telephony and low-rate data to users on the move. The improvement that HEO based PCSS could offer is the increased service availability due to the higher elevation angles. The user terminals considered for these services are hand-held (at the 2GHz FPLMTS band), vehicular and note-book types (at both L and FPLMTS bands).

The most significant user terminal issues, critical to the success of the offered services are considered to be:

- Cost of the terminals;
- Terminal user-interface;
- Cost of the service (tariffs and fees);
- Ability to offer dual-mode operation, with local terrestrial systems;
- Physical issues, such as mass and size;
- Autonomy of operation (stand-by and talk-time);
- User co-operation requirements (antenna pointing).

The expected charges from the satellite operator to the service provider for the leasing of satellite channels is a major parameter influencing the cost of the service. Most of the other issues listed are dependent on and defined by the user terminal manufacturer and the overall system parameters.

KEY TERMINAL DESIGN PARAMETERS

The two main terminal design parameters, which represent the interface with the satellite communications system are the G/T and EIRP of the terminal. In the case of the receive-only DAB terminals it is solely the figure of merit - G/T, which has to be considered.

The G/T depends primarily on the achievable antenna gain and the noise figure of the receiver. Terrestrial (cellular) system's terminals operate in a system-controlled C/I dominated environment, where the major performance limiting factor is the co-channel interference, which is defined, created and controlled by the system. On the other hand, satellite terminals operate in a C/N dominated environment in which the primary limitation is presented by the thermal and environmental noise present at the receiver input, regardless of the definition of the system. Therefore the significance of high G/T in terminals for use with satellites far outweighs that of comparable terrestrial terminals, and the possibility of achieving some gain (however small) at the terminal antenna, as a consequence of high satellite elevation angles, presents a considerable advantage.

Due to the high elevation angles offered by HEO satellites, antennas could be designed to provide an upward quasi-hemispherical radiation pattern allowing a small gain, in the region of 2 to 3 dBi for hand-held terminal and 4 to 5 dBi for DAB/Vehicular terminals, at the edge of coverage (at approximately 55° of elevation). The terminal G/T directly impacts the required transmitted satellite RF-power per channel and thus, ultimately, the cost of service.

The EIRP of communications terminals is determined by the terminal antenna gain and the transmitted RF power, which is in turn limited, especially for hand-held units by safety regulations. The growing concern of the public about possible adverse health effects arising from the use of mobile communications equipment, in particular hand-held telephones, is becoming a serious problem for the industry. Various research programs are now specifically addressing this topic, both independently and at the industry's behest, with the aim of eventually establishing a baseline for standardisation, but there is not, as yet, a world-wide accepted standard regulating this matter. However, in 1993, the FCC proposed to begin using the newly revised guidelines developed by the IEEE (C95.1-1991) and adopted by ANSI, for evaluating exposure to RF radiation. These guidelines incorporate generally stricter criteria for evaluating portable devices in terms of allowable specific absorption ratio (SAR) and radiated power, meaning that in the future these devices will be subject to more stringent evaluation, such as evidence of compliance with SAR limits, before an authorisation can be granted.

The introduction of satellite based personal communications systems may be even more vulnerable to the RF radiation safety aspects, not least because, unlike terrestrial cellular communications based on ever larger numbers of ever smaller operational cells (resulting in the desirable high frequency re-use and hence high system capacity), satellite based personal communications are critically dependant on user terminal EIRP and power, as any decrease in terminal EIRP directly impacts the required satellite on-board receiving antenna gain and hence its size and mass.

For vehicular terminals the transmitted power is mainly limited by EMC and interference issues, and to a lesser degree by safety aspects, as the user is, typically, well screened by the vehicle's metal roof construction.

Table 2 presents the expected G/T and EIRP values for the different types of terminals considered. They represent the ESTEC requirements, as refined during the phase-A study contracts.

Table 2. User terminal types

	Communications Terminals (TDMA)		
	hand-held	**notebook**	**vehicle**
Size	pocket	A-4 case	antenna + DIN
G_{ANT} @ EoC	1 ~ 2dBi	+8.5dBi	+4dBi
Tx av. Power	< 500mW	250mW	2.5W
EIRP (peak)	+7dBW	+8.5dBW	+17dBW
G/T @ EoC	-22.5dB/K	-15dB/K	-19.5dB/K
	DAB Receiving Terminals (COFDM)		
		fixed	**vehicle**
G_{ANT} @ EoC		+11dBi	+4dBi
G/T @ EoC		-12dB/K	-18dB/K

Battery capacity of the terminals and dc-power consumption (during stand-by, as well as during activity) determine the autonomy of operation, but the autonomy of operation has to be traded with the terminal size and weight, all of which are significant market-success factors. In particular, hand-held terminals require good stand-by performance and therefore the battery is foreseen as a major area of importance. To extend stand-by and talk-time there are two lines of action - improvement of the batterie's capacity by using new technologies and improvement of the efficiency of the RF and digital components. Special attention has to be given to the power amplifier design, as it has the greatest impact on the power consumption during talk-time and the selection of the number of cells in the battery.

Two most popular battery types presently used in hand-held terminals are the NiCd and the NiMH. The higher capacity and environmental-friendliness of the latter make it presently the most suitable candidate for satellite hand-held terminals, despite the higher cost. A standard 500mAh 6-cell battery could provide in the order of 1 hour talk-time and 24 hours of stand-by time.

The Doppler shift and delay compensation, as well as power level control can be implemented in the terminals. These require specific algorithms in the terminal controller, and hardware provisions at digital and RF component level. It would also be possible to make these compensations partially either on-board the satellite or at

the feeder Earth station. Power level control schemes are needed due to the path propagation loss variations that occur between satellite apogee and handover positions. They are based on received signal quality measurements in the terminals. In DAB, high quality service without interruptions is required. To achieve this, even in heavily shadowed areas, a gap-filler concept has been proposed, based on low-power terrestrial repeaters of the satellite signal placed in areas where direct line of site is not possible.

Key terminal design issues are size, mass and cost. Manufacturers minimise them by increasing the integration and miniaturisation of the components, as well as taking advantage of economies-of-scale in the production lines. In addition, for vehicular terminals, ease of installation is an important design driver. Latest trends in car electronics, such as provision of standard factory-fit integrated antennas (for VHF/FM, GPS, GSM etc.), introduction of standard data-bus systems and the general increase of value of electronic equipment within a vehicle, form a good basis for the introduction of new broadcasting and communications systems for vehicles. Market studies established that a vehicular DAB receiver price should be set at approximately 300 US$.

DAB TERMINAL DESIGN AND TECHNOLOGY

In the context of the Archimedes phase-A contracts preliminary designs of DAB terminals have been carried out by several European and Canadian manufacturers. Here we present the main results of these contracts.

Having only the receive function (a return service channel to provide interactivity within the broadcasting services is being considered, but it will not be treated as an integral part of the terminal), DAB receivers are able to achieve improved G/T values because they do not need a diplexer or a switch at the RF input. The vehicle DAB receiver terminal is thus both the system and the market driver, due to the sheer size of the expected market (40M in Europe alone). The main tasks in the development of these terminals are the hardware design and the vehicle installation strategy. ESA is presently conducting two contracts aimed at establishing technological feasibility and building critical components of the terminals.

In the RF front-end design the critical components were found to be the antenna and the LNA. Important issues in the antenna design are the achievable gain, the vehicle installation problem and the technology employed. The high elevation angles achievable with HEO systems will permit a certain antenna gain, and hence improved G/T, unlike other systems, such as LEO or MEO in which low gain, quasi omni-directional antennas would be necessary. There are, basically, two car installation options, which in turn imply different technological solutions. These are the roof-mounted flat antenna (ideal to be factory-installed as a standard), based on microstrip patches, and the quadrifilar helical antenna (which can, possibly, be integrated with the VHF antenna and suitable for retro-fit solutions).

Figure 2 shows a car roof-mounted antenna structure developed by the industry, and Figure 3 presents its calculated performance, Ref. [3, 7]. The antenna is composed of circular patch (TM_{11} mode) and an annular patch (TM_{31} mode) in a co-planar arrangement, allowing switched operation between the two patches and thus extending its performance over elevation angles to 40°. It is breadboarded in MHIA technology - active antenna, discrete front-end GaAs FET and encapsulated MMIC amplification stages. Its physical features are circular shape of approximately 20cm, height of approximately 2.5cm, and a mass of around 0.5 kg.

An important feature to implement in the terminal would be to have adaptive switched antennas to allow multimode operation of the receiver, i.e. either satellite or terrestrial/gap-filler DAB reception, depending on the current environmental conditions.

The other critical component, due to its large influence on the terminal G/T, is the input RF low noise amplifier (LNA). Today's HEMT technology permits LNAs with noise figures as low as 0.5dB with discrete input transistors (somewhat worse performance with full MMIC implementation), making the input stage's internal noise comparable with the received environmental noise. In general, extensive use of MMIC technology is required for the RF front-end in order to reduce size and improve overall performance.

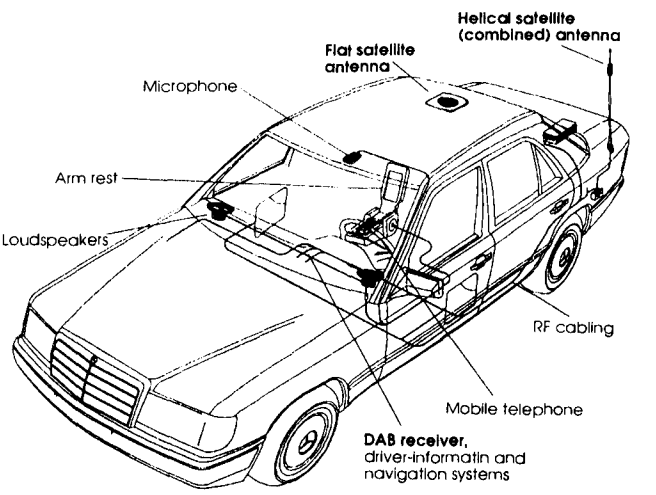

Figure 4 *Terminal integration options in a car*

The baseband module comprises analog front-end, digital signal processing chips (performing COFDM demodulation and channel decoding) and a main controller. The module will be based in VLSI technology.

As a reference, the European manufacturers that are engaged in R&D of terrestrial or satellite DAB user terminal equipments are Nokia in Finland, Bosch and Grundig in Germany, Thomson in France and Philips in the Netherlands.

With respect to the installation strategies of the terminal, consultations to the car manufacturing industry have resulted in a preliminary integration scheme. The two basic antenna options, flat antenna roof-mounted, or helical antenna that result in two different installations. are shown in Figure 4.

PCSS TERMINALS DESIGN AND TECHNOLOGY

Two parameters are of paramount importance when designing the mobile terminal for a given user application: the antenna (gain and profile) and the transmitted RF power. The antenna radiation pattern (and gain) has to be adapted to the problems of user mobility and hence possible degree of co-operation in pointing towards the satellite. The antenna profile and size is crucial to the terminal integration in a vehicle, notebook-sized case, or for an ergonomic hand-held design. The transmitted RF power will have an effect on the DC power demand and therefore the size of the batteries required (transportability). In addition to that are the short and long term safety aspects for the user related to the biological effects of the radiated fields, especially for a hand-held type terminal. Among the defined terminal types, the hand-held, vehicular and the notebook type, we focus here on the hand-held terminal, as it presents the biggest challenge for the designer, as well as being the communications system driver.

In the RF front-end the most critical unit is the diplexer that isolates the transmission and reception chains. Either operating in CDMA or in TDMA, the implementation of a diplexer to isolate transmission and reception chains in the terminals is a must. If a TDMA access scheme is used, and transmission and reception are not simultaneous, interference problem considerations imply that it can not be a simple switch. The losses of the diplexer are expected to be between 1dB and 1.5dB, Ref. [3, 4]. The antenna was selected as azimuth omni-directional zenith-pointing antenna, and from the technological point of view a quadrifilar helix antenna design is the most attractive approach, achieving a gain of 2dBi at edge of coverage. The amplifiers (LNA and PA) are based on MMIC technology and it is expected that the complete RF stage could be integrated in a single MMIC.

The design and production of these terminals will have many similar problems to those encountered and solved in GSM. Miniaturisation requires highly integrated ASIC chips, while DC-power constraints will require digital technologies based on 3.3V power supply. Extensive experience of the European manufactures and foundries in production of highly integrated low power consumption VLSI chips for GSM or DECT applications will be crucial for these new terminals.

Figure 5 shows a possible practical implementation of the RF front-end and base-band modules for a hand-held terminal, Ref.[5].

The power supply subsystem is another key design issue of the terminal. It is evident that future improvements of battery technology are required and will present a clear benefit, especially in improving the talk-to-stand-by-time ratio.

CONCLUSIONS

The main advantages of a HEO based satellite system to provide DAB and personal communications have been outlined and the ESA Archimedes system introduced.

Key terminals design issues were presented and the technical feasibility of the user terminals required for a satellite DAB service in Europe was shown through the results of several industrial contracts. Main outcomes from these contracts have been presented. Communication terminals served by HEO systems were also analysed in these contracts and principal results presented.

ACKNOWLEDGEMENTS

The authors are grateful to the many colleagues, in industry and in ESA-ESTEC, who have supported this work and in particular to colleagues in Nokia Research Center and DETyCOM A.I.E. for their valuable inputs, and Messrs W. Greiner and F. Petz for their comments.

REFERENCES

[1] G. Solari, R. Viola, *M-HEO: The Optimal Satellite System for the Most Highly Populated Regions of the Northern Hemisphere*, ESA Bulletin, May 1992, No. 70.

[2] D. Bell, K. Dessouky, P. Eastbrook, M.K. Sue, M. Bobb, *MSat-X Antennas: Noise Temperature and Mobile Receiver G/T*, MSAT-X Technical Feature Article, JPL, No. 16, August 1988.

[3] *Final report of Archimedes Phase-A ESTEC study contract with* Matra Marconi Space (and Detycom and Wavecom on user terminal issues), 1994/95.

[4] *Final report of Archimedes Phase-A ESTEC study contract with* British Aerospace Space Systems (and Nokia on user terminal issues), 1994/95.

[5] *Final report of Archimedes Phase-A ESTEC study contract with* Daimler-Benz Aerospace (and Alcatel Radiotelephone and Dornier on user terminal issues), 1994/95.

[6] *Final report of Archimedes Phase-A ESTEC contract with* SPAR (and CRC on user terminal issues), 1994.

[7] L. Garcia, F. Municio, J.E. Caballero, C. Martin-Pasqual, *Active Antennas for DAB Receivers*, IMSC'95, June 6-8, 1995, Ottawa, Canada.

ANNEX

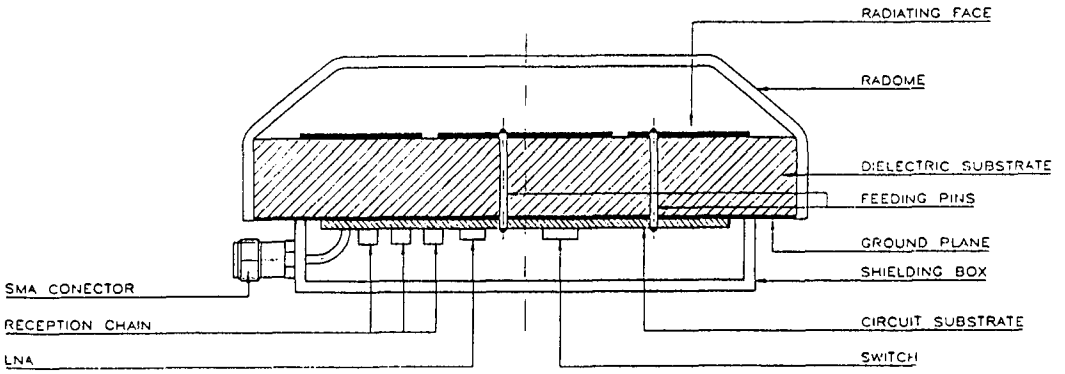

Figure 2 *DAB vehicle-mounted terminal antenna*

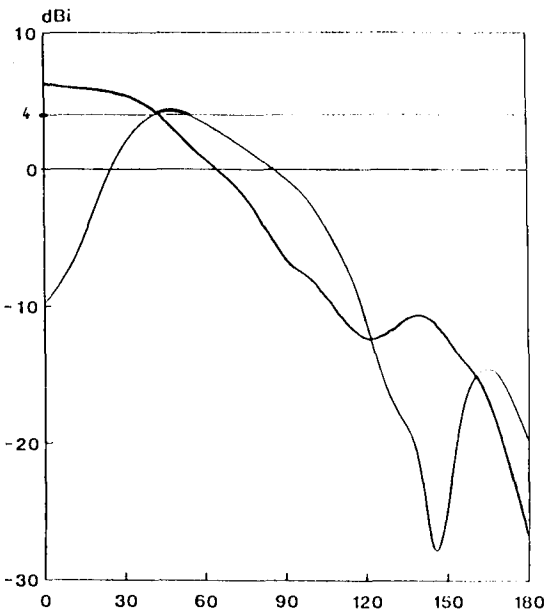

Figure 3 *Gain radiation patterns for circular patch (TM_{11}) and ring patch (TM_{31}) on Cu-clad with ε_r=2.55 and h=6mm.*

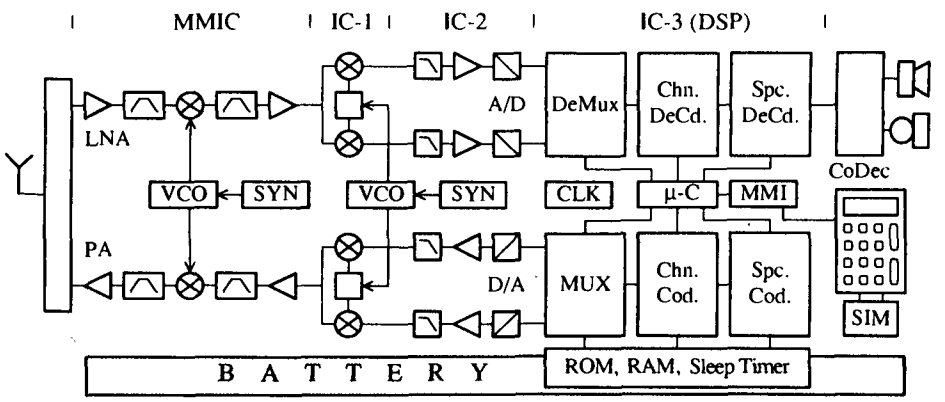

Figure 5 *Practical implementation of a handheld terminal as proposed by manufacturers.*

A New RF Package Suitable for Aeronautical Commercial and DSCS Satellite Applications

Robert J. Hamilton, Jr.
SSE Technologies, Inc.
47823 Westinghouse Drive
Fremont, California 94539 USA
Phone: 510-623-6081 FAX: 510-490-5891

ABSTRACT

Higher levels of integration through the use of GaAs and Silicon MMIC devices, a die-cast housing, and the reduction of the number of subassemblies has enabled a large reduction of the size and weight of the electronics package for commercial and military satellite communications. This paper presents an electronics architecture and hardware that utilizes many new integrated circuits, design techniques, and allows flexibility for future satellite frequency changes and expansion.

Key Features of the radio are as follows:

- Extended C-Band, InSat, DSCS, Ku-Band coverage options
- 70 (or 140MHz) transponder bandwidth or L-Band Block bandwidth IFs
- Integrated RS-232 control through local hand-held terminal or remote computer; remote control of crystal reference oscillator for aging and temperature compensation
- Integrated 2 or 5 watt SSPA; optional, integrated solid state booster amplifiers to 40 watts; optional external amplifiers 100 watts
- Integral beacon tracking with second integrated downcoverter for antenna positioning
- Radio, including LNB and SSPA, weighs 8.5 kg; measures 32 x 23 x 16.5 cm
- Environmentally ruggedized: -40 to +60 deg C; O-ring sealed for waterproofing, passive (convection) cooling
- Simple cabling and installation: single cable between radio and LNB; two cables between radio and IF interface

The small size and light weight of the radio make it ideal for mounting on stabilized antenna platforms (gyroscopic or servo). Several input power options (110, 220 VAC, +48, +12, -24 VDC) facilitate operation on multiple platforms.

INTRODUCTION

Commercial equipment designed for fixed site or transportable commercial C- and Ku-Band, and military X-Band satellite communications has not been easily adaptable for mobile satcom applications whether terrestial, marine, or aeronautical in nature. The size and weight was generally too high; environmental ruggedness, particularly in the areas of shock and vibration was too low; and reliability, while adequate for terrestrial applications, needed to be higher since servicing was more difficult and equipment redundancy not practical. Also, equipment mechanical designs did not lend themselves to adaptation for stabilized antenna configurations. Finally, the number of opportunities for mobile equipment application has generally been low when compared with terrestrial opportunities.

The "radio" function of a satellite earth terminal is generally to take the intermediate frequency analog data stream (usually 70 or 140 MHz), upconvert it to the satellite uplink frequency, and amplify it to a level commensurate with the signal bandwidth. On the receiving side, the "radio" amplifies the low level signal from the satellite downlink and converts it to the intermediate frequency. The radio may also provide a stable reference oscillator (for locking the various fixed and variable frequency local oscillators) and allow receive and transmit gain or transmit power level adjustment.

SSE Technologies, which to date has primarily focused on the commercial , terrestrial marketplace, undertook a new radio development program with prime focus on cost reduction through the use of concurrent mechanical design, commonality of functional blocks between satellite bands, and high levels of electrical integration. An additional emphasis was on simple testing and simple operator setup and control of the radio. During the course of design reviews with customers, it became apparent that the new design also addressed some of the previous limitations of commercial microwave terrestrial satcom equipment for mobile satellite applications.

DESIGN PHILOSOPHY

In an effort to reduce radio cost and size, the design approach minimized the number of printed circuit board assemblies to six and these were contained in four integrated mechanical housings. Of these six, four circuit assemblies (contained in two mechanical housings) were common across all satellite frequency bands. Thus only two functional blocks (or assemblies) need to be substituted to change the band of operation. A functional block diagram of the radio is shown in Figure 1. As detailed in the figure, only the Low Noise Block Converter (LNB) and the High Power Upconverter (HPC) are band-specific: The IF Converters, Sources Assembly, Monitor & Control (M & C), and Power Supply functions are universal for all bands.

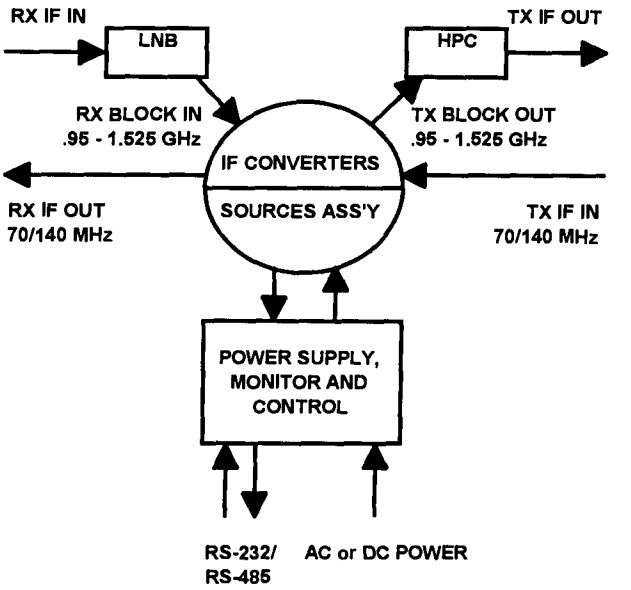

FIGURE 1. Integrated Radio Basic Block Diagram and Interfaces

Designs currently in production include:

C-Band: 3.625 to 4.200 GHz RX
5.850 to 12.750 GHz TX

Ku-Band: 10.95 to 12.750 GHz RX
14.000 to 14.500 GHz TX

Designs scheduled for release to production this fall include:

InSat: 4.500 to 4.8 GHz RX
6.700 to 7.000 GHz TX

X-Band: 7.250 to 7.750 GHz RX
7.900 to 8.400 GHz TX

Ku-Band: 13.750 to 14.500 GHz TX

The means to achieve the reduction in printed circuit board count and size came from three main directions: use of monolithic microwave integrated circuit (MMIC) devices, use of low cost surface-mount ceramic filters, and use of advanced PCB materials and technologies. Included in all RF and microwave circuits are components designed and produced for the wireless and cellular telephone products. These included silicon MMIC devices, gallium arsenide MMIC devices and ceramic filters. The MMIC devices greatly reduce the physical size of the circuit by reducing the number of component parts required for a particular function, and increase the reliability due to the part count and interconnection reduction. They also increase repeatability of circuit performance and reduce labor required for alignment due to discrete part variations.

The surface mount ceramic filters greatly reduce the size of the filtering function by providing high Q resonators with performance equal to cavity or mechanical filters but with at least a seventy percent reduction in size as compared to air dielectric filters. The cost of these filters has also been driven lower due to volume cellular telephone and wireless applications.

The single printed circuit board (PCB) approach has been enhanced through the use of multiple layer boards with combinations of dielectric materials on various layers. As an example, the Sources Assembly PCB is a four-layer board consisting of a sandwich of a low cost, high stability fiberglass board (FR-4 material) bonded to a high performance, high dielectric microwave board (RO 3003 material) with integral plated-through holes for interconnections between trace layers. A cross-sectional view of this approach is presented in Figure 2. The microwave devices are soldered on the top of the microwave board; a solid ground plane is used on the backside of this board. A two sided DC and control board is then bonded to the groundplane side of the microwave board with DC and control components subsequently soldered to the bottom surface. Finally, plated-through via holes are utilized to provide interconnections between the RF traces and the two DC and control layers as well as provide RF grounding on the top surface of the microwave circuit board.

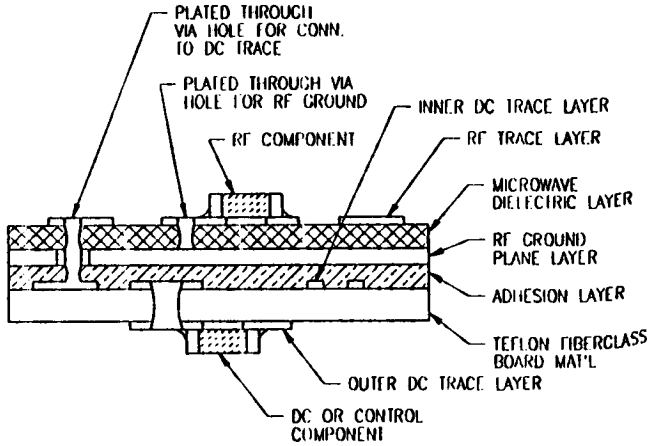

FIGURE 2. INTEGRATED, MULTI-LAYER CIRCUIT BOARD APROACH

Performance levels for the LNB and HPC functional blocks are contained in the following tables:

TABLE I. LNB PERFORMANCE

BAND	NOISE TEMP	BANDWIDTH
C-Band	45 deg. K	3.625 to 4.200 GHz
InSat	55 deg. K	4.500 to 4.800 GHz
X-Band	65 deg. K	7.250 to 7.750 GHz
Ku-Band	85 deg. K	10.95 to 11.200 GHz (Intelsat Lowband)
		11.450 to 11.950 GHz (Intelsat Highband & PanAmSat)
		11.70 to 12.200 GHz (NORAM)
		12.250 to 12.750 GHz (AusSat & Eutelsat)
Gain:		50dB min. @ 25 deg. C

Gain Flatness:	+/- 2.5 dB over temp and frequency
Reference Input Freq.	10MHz
IF Output Freq.	950 to 1525 MHz
Phase Noise & Spurious	Intelsat and Eutelsat complaint

TABLE II. HPC PERFORMANCE

Band	Power Levels	Bandwidth
C-Band	2 and 5 Watts	5.850 to 6.425 GHz
InSat	5 Watts	6.700 to 7.000 GHz
X-Band	5 Watts	7.900 to 8.400 GHz
Ku-Band	2 and 4 Watts	13.750 to 14.250(Eutelsat)
	2 and 4 Watts	14.000 to 14.500(all others)
Gain		43 dB in (or 46/47 dBm min for higher power units)
Gain Flatness		+/- 2 dB over temperature and frequency
Reference Input Freq.		5MHz and 210 MHz
IF Input Frequency		950 to 1525 MHz
Phase Noise and Spurious		Intelsat and Eutelsat complaint
Harmonics		Intelsat and Eutelsat complaint
Intermodulation Products		Intelsat and Eutelsat complaint

Figures 3 and 4 present the IF Converter and Sources Assembly functional block diagrams.

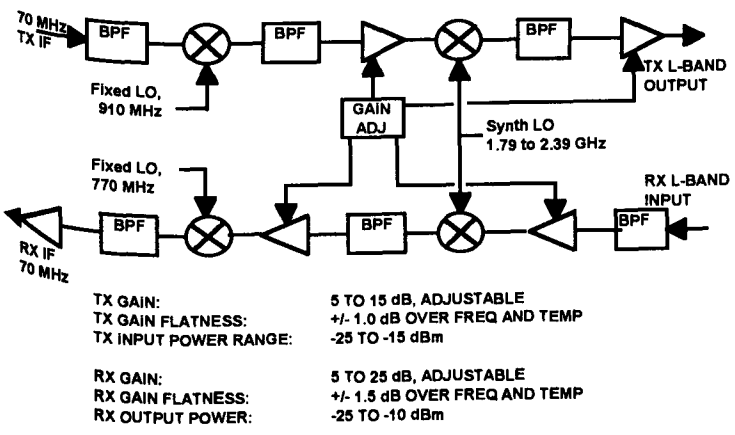

FIGURE 3. IF CONVERTER FUNCTIONAL BLOCK DIAGRAM

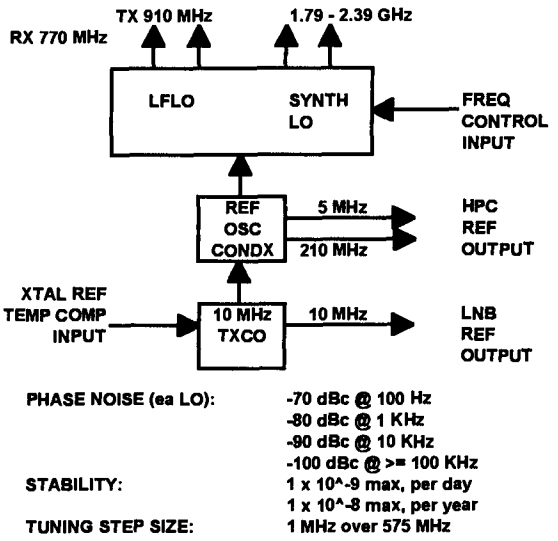

FIGURE 4. SOURCES ASSEMBLY FUNCTIONAL BLOCK DIAGRAM

MECHANICAL DESIGN APPROACH

A concurrent mechanical and electrical design approach was utilized for this radio, a departure for a traditionally electronics technology driven industry. The housings are all of diecast aluminum construction and are intended to form the internal enclosure for the electronics as well, eliminating the need for sub-packaging. The castings include chambers and channels for isolation of the various signal paths and holes for direct feedthrough of signals (eliminating the need for some coax cables). An exploded view of the radio is shown in Figure 5. Each of the three mechanical subassemblies can stand on its own from both an electrical function and mechanical standpoint. Thermal dissipation has been taken into consideration such that any combination of subassemblies will maintain the same case temperature in a given ambient. The thermal design is such that the internal temperature rise of any component or semiconductor is a maximum of 20 degrees C above ambient.

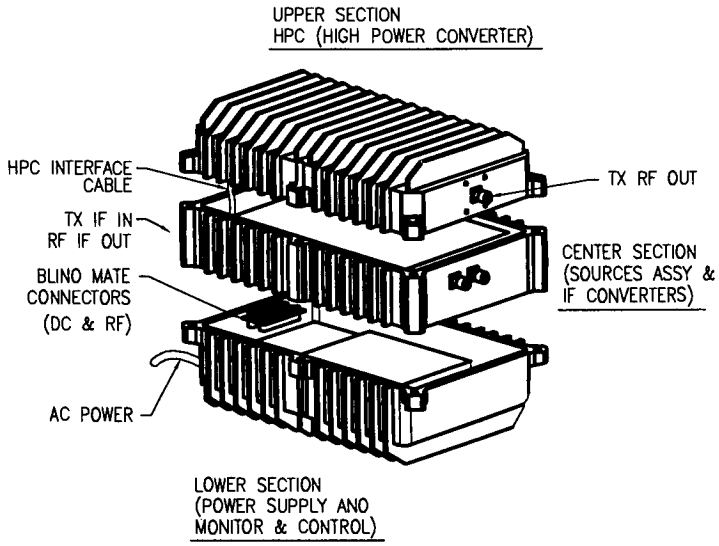

FIGURE 5a 2 OR 5 WATT CONFIGURATION

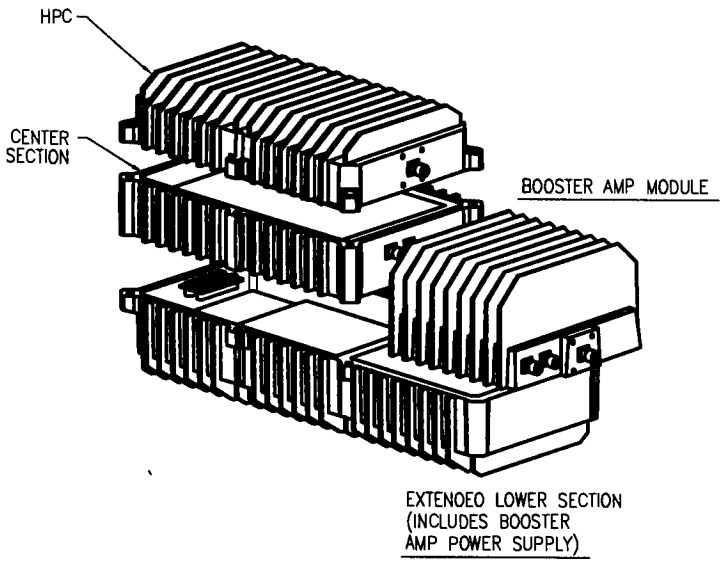

FIGURE 5b BOOSTER AMP

The modularized mechanical and electrical design philosophy allows for a wide variety of radio configurations depending upon platform and application. Figure 6 presents several configuration options that allow a variety of installation options and interface types. The basic configuration, shown in Figure 6A, is a typical terrestrial, fixed site configuration although it may be appropriate for some mobile platforms. In Figure 6B, a second IF converter and LO assembly is added for beacon signal reception. This output can be used to drive antenna positioning equipment and does not require another LNA or separate receiver. If the antenna or platform required a very low mass installation, a configuration like Figure 6C might be selected. In this case, only the L-Band block up and down conversion portions of the radio are mounted on the antenna: the IF converters are mounted at the base of the antenna or elsewhere on the platform. Finally, if physical volume is really at a premium, an integrated modem can be added to the configuration allowing direct connection to a digital signal stream, eliminating any physical separation between radio and modem. This approach is shown in Figure 6D.

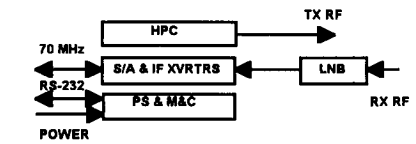

FIGURE 6A. BASIC CONFIGURATION

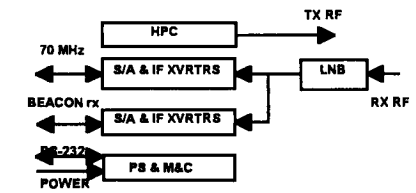

FIGURE 6B. BEACON RX CONFIGURATION

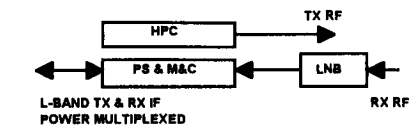

FIGURE 6C. L-BAND INTERFACE CONFIGURATION

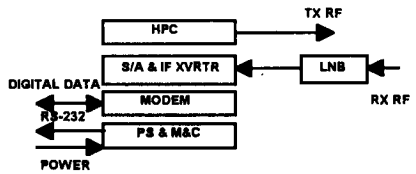

FIGURE 6D. INTEGRATED MODEM CONFIGURATION

FIGURE 6. RADIO CONFIGURATION OPTIONS

RADIO PERFORMANCE

The radio has been tested in a variety of environmental and operational conditions to insure full Intelsat compliance. Key performance specifications include phase noise, spurious, intermodulation products and harmonics. Careful attention has been paid to the frequency conversion architecture to insure minimum spurious signal generation. Likewise, the signal levels in the amplification process have been carefully adjusted to minimize harmonic and intermodulation product generation. Figure 7 presents two of the key performance levels measured on the radio: Phase Noise and Intermodulation Products.

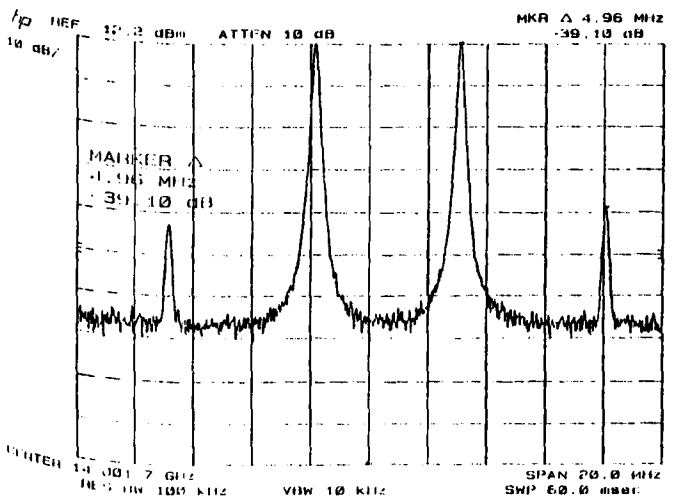

Figure 7a. Intermodulation Performance of Ku-Band, 2W Radio. Measured with two carriers each at +24dBm output, 30KHz separation. Intermods are -39dBc.

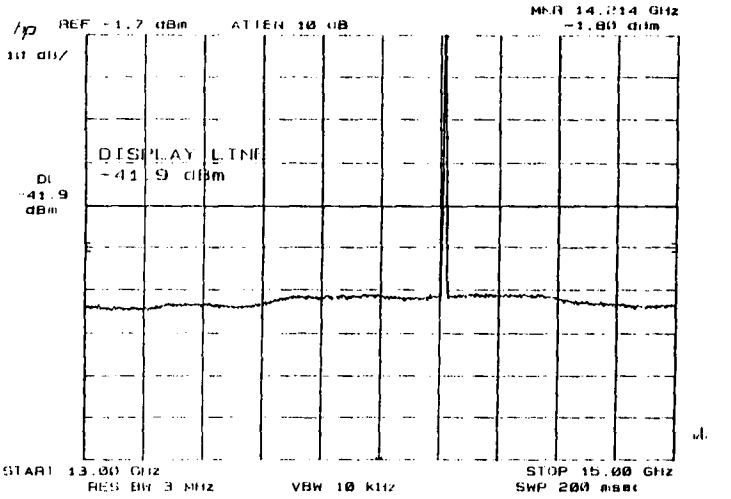

Figure 7b. Spurious Signal Performance of Ku-Band, 2W Radio. Measured with single carrier at +27dBm, 13 to 15 GHz sweep.

Specifications compliance is guaranteed over a -40 to + 60 degree C ambient temperature range. Gain compensation accomplished electronically with stored look-up table data in an EEPROM. The monitor and control circuitry evaluates hardware temperature at several locations in the radio, and after reading operating frequency, applies a correction through several variable gain/loss circuit elements. Table III summarizes operating specifications for the radio. The housing is assembled with O-Ring seals between sections insuring a weatherproof enclosure.

TABLE III. RADIO PERFORMANCE SPECIFICATIONS

Receive:		
Input level:	-127 to -80	dBm nominal
Output level:	+18	dBm min. P-1dB
Intermods:	-35	dBc max, 2 tones, -89 dBm ea.
Gain:	85	dB nominal
Gain Stability:	+/- 1.0	dB max, ref to +25 deg C
Gain Flatness:	+/- 1.0	dB max, any 36 or 72 MHz
	+/- 0.5	dB max, any 4 MHz
IF Bandwidth:	36 or 72	MHz min
Noise Temp.:	45 (80)	deg K max, C-(Ku-) Band

Transmit:		
Input level:	-30	dBm nominal
Output Power:	+33	dBm min, (+37 dBm optional)
Gain:	63	dB nominal
Gain Stability:	+/- 1	dB max, ref to +25 deg C
Gain Flatness:	+/- 1.0	dB max, any 36 or 72 MHz
Harmonics	-60	dBc max
Spurious	-80	dBm max, ref to RF output
Intermod Prod.:	-33	dBc max,
Synthesizers:		
Step Size:	1.0	MHz
Stability	1 x 10 ^9	max per day
	1 x 10 ^8	max per day
Phase Noise	-90	dBc max, 100KHz from carrier
Offset:	Fixed	(or variable with dual synthesizers)

Clearly, a wide variety of application and platforms can be addressed by the radio. One installation is presented in Figure 8 which shows the radio mounted on a servomotor stabilized antenna platform. The antenna size is 0.8 m, with an antenna of this size, data rates of up to 128 kbps can be transmitted while complying with Intelsat requirements for sidelobe performance.

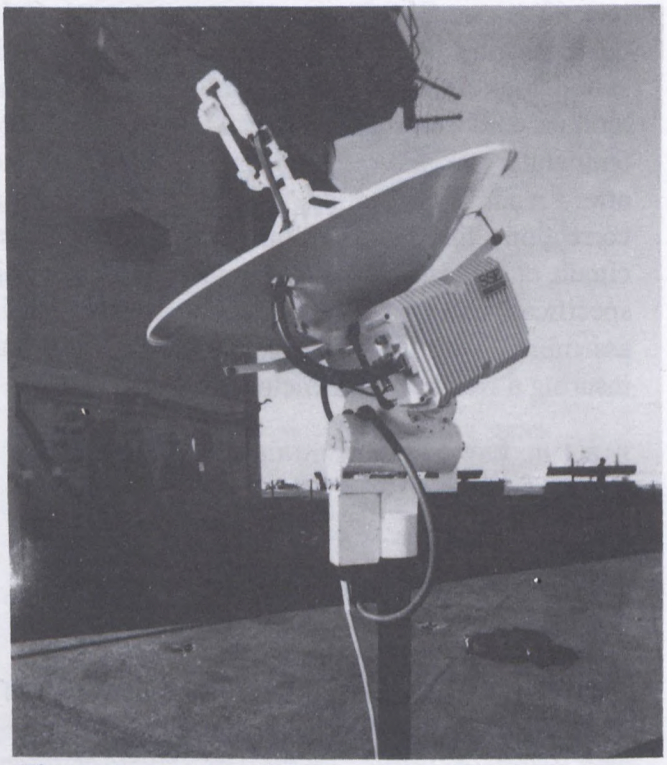

Figure 8. Ku-Band Integrated Radio mounted on servo-stabilized 0.8m antenna platform.

CONCLUSIONS

A highly flexible, small, modularized radio design has been presented which while allowing full Intelsat compliant performance, provides flexibility of physical and electrical configuration. This flexibility allows integration on a variety of mobile platforms and antennas in rugged environments. Use MMIC devices, new microwave and RF filter structures, multifunction circuit boards, and integral mechanical design has allowed reduced size and weight as well as cost savings over previous designs.

Direct Modulation at L-Band using a Quadrature Modulator with Feedback

Ravi Datta and Stewart N. Crozier

Communications Research Centre, 3701 Carling Ave., P.O. Box 11490, Station H,
Ottawa, Ontario, Canada, K2H 8S2, ph: 613-998-9262, fax: 613-990-0316

Abstract

This paper describes how a high quality modulated signal can be generated directly at the frequency of transmission, using a standard quadrature modulator and other commercially-available, low-cost building blocks. The method uses a feedback technique for automatic correction of carrier leakage, differential gain and phase mismatch errors in the quadrature modulator, and other building blocks, by providing guidance to the digital baseband portion of the modulator. Experimental results are presented for direct modulation at 1.65 GHz.

Introduction

There has always been a keen interest in direct modulation at the frequency of transmission, in order to reduce component count, increase reliability, and reduce power consumption and cost. When the modulator specifications require all transmit spurii, including local oscillator (LO) leakage and image spectra, to be less than 50 dBc, the conventional technique of a multi-stage up-converter is commonly used. Each stage requires an LO, a stable bandpass filter, and a mixer, along with associated components. The number of stages of up-conversion is usually a function of the transmit frequency. For example, at UHF/VHF frequencies, two stages of up-conversion are typically required. At L-band, three stages of up-conversion are often necessary to permit the use of inexpensive filters after every stage of up-conversion.

The tremendous demand for portable, mobile and personal communication systems has created a need for simplicity, unprecedented accuracy, and economic performance of front-end circuits operating in the gigahertz range. In this paper, it is shown that a high-quality modulated signal can be generated at the frequency of interest using an off-the-shelf quadrature modulator with a simple feedback circuit and digital baseband precompensation algorithms.

Direct Modulation Approach

Figure 1 shows the block diagram of the direct RF modulator under consideration. The system consists of a digital signal processor (DSP), digital-to-analog converters (DACs), direct quadrature modulator, and a feedback circuit. The feedback circuit can be implemented using an AM detector, baseband amplifier, and a single analog-to-digital converter (ADC). For baseband sample rates of 50 kHz or less, the two transmit DACs, feedback ADC, and all associated low-pass-filters (LPFs) can be provided by a single 16-bit stereo chip.

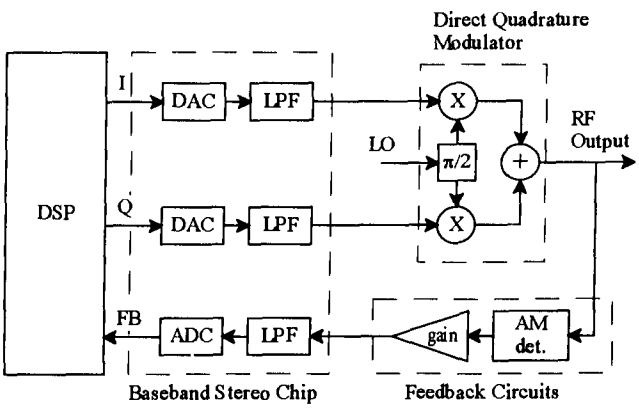

Fig. 1: Block diagram of direct quadrature modulator with feedback.

The problems associated with quadrature modulators are well documented and understood [1, 2, 3]. The main problems are quadrature phase and differential gain errors between the inphase (I) and quadrature (Q) channels, LO leakage, and third order intermod (IM3) products. These parameters vary with time, temperature, the LO frequency, the applied LO level, and the applied signal level, often making readjustment necessary. For many short time-duration applications, initial calibration is all that is required. For TDMA and voice-activated systems, intermittent recalibration or tracking is also easily performed. Continuous time tracking is also possible but

is beyond the scope of this paper. One tracking approach is presented in [3].

In addition to the inaccuracies of the quadrature modulator, phase and gain imbalances can also arise from other circuits used to implement a system. For example, inaccurate transmission lines at RF, DC offsets in the I and Q DACs, and baseband amplifiers can all cause distortion.

One way of solving most of the above problems is to use expensive components; having accurate $\pi/2$ phase shift networks and transmission lines, and other components with matched gain and very accurate DC offsets. Not only is this costly but also time consuming. On the other hand, accurately measuring the phase, amplitude, and DC offset errors of the quadrature modulator, or some related parameters, and providing the required precompensation, permits the use of off-the-shelf components. As shown in Figure 1, for the system under consideration, the feedback loop extracts the AM error component, which is subsequently digitized and processed by the DSP to adjust the I-Q transmit vectors. In our design, the phase can typically be corrected to within 0.001 radians and gain to within 0.01 dB, thereby yielding a very high performance RF modulator at low cost.

Quadrature Modulator Model

The standard quadrature modulator model is shown in Figure 2. It is characterized by I and Q DC offset errors, a_I and a_Q, I and Q gains, g_I and g_Q, and phase shift error, θ. Using equivalent baseband matrix notation and dropping the time dependence, as in [3], the quadrature modulator output is given by

$$w = Mv + Ma \tag{1}$$

where

$$M = \begin{bmatrix} g_I & g_Q \sin(\theta) \\ 0 & g_Q \cos(\theta) \end{bmatrix} \tag{2}$$

and

$$w = \begin{bmatrix} w_I \\ w_Q \end{bmatrix}, \quad v = \begin{bmatrix} v_I \\ v_Q \end{bmatrix}, \quad a = \begin{bmatrix} a_I \\ a_Q \end{bmatrix} \tag{3}$$

The two elements of each input and output vector correspond to the signals I and Q parts.

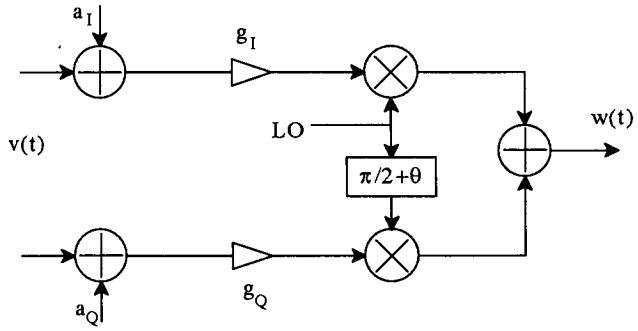

Fig. 2: Quadrature modulator model.

Quadrature Modulator Correction

The impact of quadrature modulator errors can be corrected by precompensating the original input signal vector, u. If the model error parameters are known, the precompensated signal is given by [3]

$$v = Cu + b \tag{4}$$

where

$$C = M^{-1} = \frac{\sec(\theta)}{g_I g_Q} \begin{bmatrix} g_Q \cos(\theta) & -g_Q \sin(\theta) \\ 0 & g_I \end{bmatrix} \tag{5}$$

and

$$b = -a \tag{6}$$

Figure 3 shows the corresponding precompensation circuit.

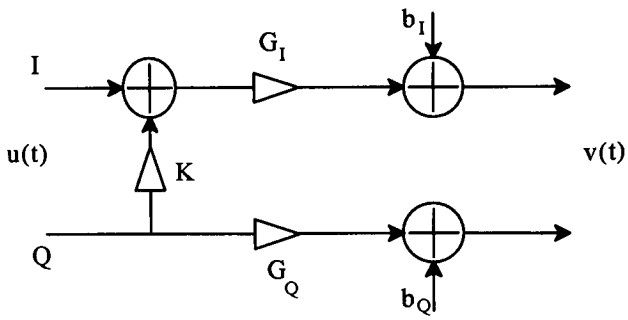

Fig. 3: Quadrature modulator precompensation circuit.

From (4), (5) and (6), the compensation parameters should be set to

$$G_I = \frac{1}{g_I} \quad (7)$$

$$G_Q = \frac{\sec(\theta)}{g_Q} \quad (8)$$

$$K = -\tan(\theta) \quad (9)$$

$$b_I = -a_I \quad (10)$$

$$b_Q = -a_Q \quad (11)$$

Calibration Approach

One approach to calibration, as suggested in [1], is to correct one parameter at a time by selecting appropriate DC test vectors and calculate the correction parameters. With this approach the feedback circuit must be very linear, or at least calibrated. An alternate approach, also suggested in [1], is to use DC test vectors to perform a linear search for the correct parameter values. With this approach there is no need for the feedback circuit to be linear or calibrated. However, the feedback circuit must still be accurately biased in order to pass a reliable low-level DC feedback signal. The linear search procedure is also very time consuming.

A different approach is presented here. A single complex calibration tone is used, instead of a number of different DC test vectors. With this approach, the feedback circuit does not need to be linear, calibrated, or accurately biased. As opposed to deriving the quadrature modulator model parameters and then calculating the various correction parameters, the four parameters G_Q, K, b_I, and b_Q are adjusted directly, with G_I fixed, as shown in Figure 3. An efficient binary search technique is used to minimize the feedback power associated with each parameter, as described below.

Calibration Tone

Calibration is performed by using the DSP to generate a single complex (I+jQ) calibration tone at frequency f_{cal}. For convenience, this frequency is selected to be exactly 1/8 the baseband sample frequency, f_s. This permits the tone to be generated using a simple table look-up of 8 values. The two transmit DACs and feedback ADC, shown in Figure 1, are assumed to operate with this common sample frequency.

Figure 4 shows a typical RF spectrum obtained before precompensation. The strong upper sideband (USB) corresponds to the desired calibration tone at RF. The lower sideband (LSB) is an image signal due to the gain and phase mismatch errors between the I and Q channels, and can be controlled with the Q gain, G_Q, and cross-talk parameter, K. The LO leakage is effectively due to the incorrect DC bias levels into the mixers, and can be controlled with the two bias levels, b_I and b_Q.

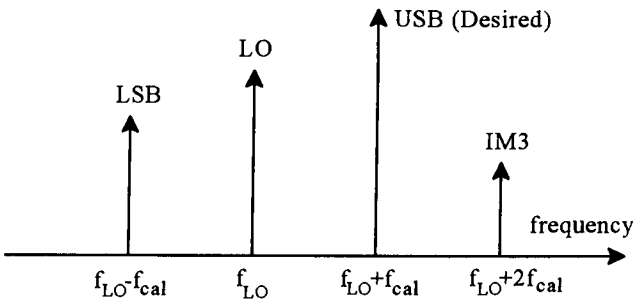

Fig. 4: Typical RF spectrum before precompensation.

In practice, a number of intermodulation products are also present due to non-linearities in the mixers, summer and other related circuitry. The dominant intermodulation product tends to be a third order intermod (IM3) just above the desired USB at a frequency of $f_{LO} + 2f_{cal}$. The easiest way to reduce this intermod is to back off the I and Q input levels. Theoretically IM3 drops by 2 dB for every 1 dB the input levels are lowered. Of course the LO leakage does not drop and, if not handled properly, can prevent the feedback circuit from working as desired. If a lower IM3 level is desired, the solution is to calibrate with high input levels and then recalibrate with lower input levels. This approach ensures that the feedback circuit behaves predictably.

The feedback circuit, shown in Figure 1, mixes all of the tones shown in Figure 4 together. The resulting baseband feedback tones are dominated by the mixing of the USB and the other tones. Figure 5 shows a typical baseband feedback spectrum. There is a DC component due to all components mixing with themselves. The DC component is not used in this approach and is easily removed with AC coupling prior to the feedback ADC. The tone at f_{cal} is primarily a result of the LO leakage but IM3 is also present since it is also f_{cal} away from the USB. The tone

at $2f_{cal}$ is primarily due to the LSB. Other miscellaneous products are also present at $3f_{cal}$.

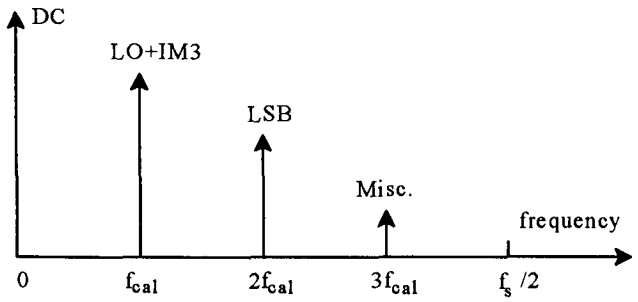

Fig. 5: Typical baseband feedback spectrum before precompensation.

The baseband feedback signal is sampled by the feedback ADC and passed to the DSP for processing. The objective is to minimize the power of the two feedback tones at f_{cal} and $2f_{cal}$ by adjusting the four parameters mentioned above.

The power of each tone is measured separately by complex down-converting to DC, averaging over the measurement time, and computing the squared-magnitude of the resulting complex sample. Averaging over an integer number of cycles of the calibration tone ensures that the two feedback tones can be separated using a simple rectangular window time average. An efficient binary search technique was used to adjust the parameters and minimize the feedback power. This is described in more detail below.

Figure 6 shows the expected RF spectrum after precompensation. The LO can typically only be driven down as far as IM3. This is because the feedback circuit cannot distinguish between the LO and IM3 tones, which can add destructively at baseband. The LSB feedback signal does not have this restriction. It is easily driven down 60 dB, as shown in the experimental results which follow. This implies that the phase error can be corrected to better than 0.001 radians and the I and Q gains can be balanced to better than 0.01 dB.

A two-stage calibration process may be appropriate for some operating scenarios, depending on the desired IM3 level. The feedback strategy assumes that the USB is the dominant RF tone. During initial startup, the gain of the calibration tone may be increased above the nominal operating point to ensure that the USB dominates the LO leakage. The LO can then be driven down to the initial IM3 level. Once this is accomplished, the input gain can be reduced to drive IM3 down to the desired operating point. This now allows the LO to be reduced further to the lower IM3 level.

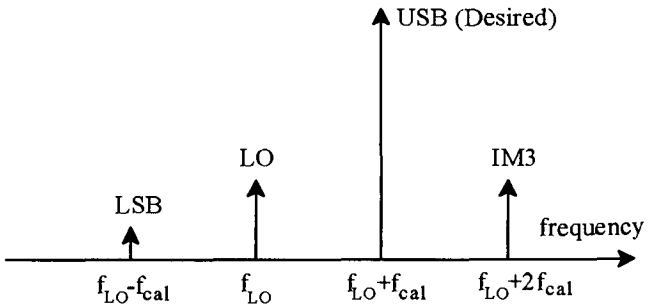

Fig. 6: Typical RF spectrum after precompensation.

Binary Search Technique

An efficient multi-stage binary search technique is used to adjust the correction parameters. A binary search is applicable at each stage because the feedback power is a quadratic (symmetric) function of each correction parameter. Multiple stages are required because each feedback tone is controlled by two parameters, and the two parameters are not independent. The number of stages required depends on the original uncertainty ranges for each parameter and the amount of correction desired. Four stages is usually sufficient, but more stages may be required for severely degraded systems.

Figure 7 shows the basic binary search concept, where x is the control parameter and y is the symmetric feedback value to be minimized. For example, x could represent the I bias parameter, b_I, and y the measured power in the LO feedback tone. The initial range of uncertainty is $[x_1, x_2]$ and the initial or default x value is in the middle of this range at x_3. The first two measurements are taken with x at x_1 and x_2. Since y_2 is greater than y_1, the minimum must lie to the left of x_3. It is only necessary to assume that the feedback is symmetric and monotonically increasing away from the minimum. Thus, the initial range of uncertainty is cut in half with only 2 measurements. The new nominal x value is at x_4. Note that measurements have not yet been taken at x_3 or x_4, and the search could terminate at this point, if desired. The second step is to take a measurement at x_3 and compare it to the previous measurement at x_1. Since y_3 is less than y_1, the minimum must lie in the range

$[x_4, x_3]$. The new nominal x value is in the middle of this range at x_5. Note that the previous range of uncertainty was cut in half with only 1 new measurement. Continuing this process, by taking measurements at x_4 and x_5, cuts the range of uncertainty in half two more times, and gives the final x value indicated. In general, N+1 measurements are required to take N steps and cut the range of uncertainty in half N times. This implies a 6 dB improvement in the range of uncertainty, and corresponding worse case RF distortion, with each step.

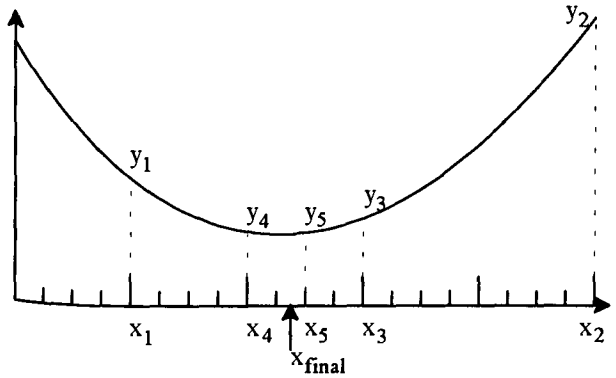

Fig. 7: Binary search technique.

The above procedure minimizes the feedback power with respect to a single parameter. However, the power in each feedback tone is a function of two parameters and these parameters are not independent, although they are typically close to being independent. For example, the power in the LO feedback tone, neglecting the quadrature gain imbalance and IM3, is given by

$$P_{LO} = (A_I + A_Q \sin(\theta))^2 + A_Q^2 \cos^2(\theta) \qquad (12)$$

where

$$A_I = a_I + b_I, \qquad A_Q = a_Q + b_Q \qquad (13)$$

and θ is the error in the $\pi/2$ phase shifter. The LO power is controlled by the I and Q bias parameters, b_I and b_Q. Minimizing (12) with respect to b_I only, gives an error of $-A_Q \sin(\theta)$ from the optimum value of a_I. Note that A_Q is the initial error in the Q bias. As an example, if $\sin(\theta)=1/8$, which corresponds to a reasonable maximum phase error of about 7 degrees, then at most three steps of the binary search technique should be used to estimate b_I before switching to work on b_Q. Improving the estimate of b_Q reduces A_Q, which then allows b_I to be improved further in a following stage. A similar argument can be made for the two parameters which control the LSB feedback tone.

The ability to separate the LO and LSB feedback tones allows two parameters to be adjusted at the same time. For example, the Q bias and Q gain parameters, b_Q and G_Q, can both be adjusted at the same time, and the I bias and cross-talk parameters, b_I and K, can both be adjusted at the same time. This leads to the following specific four-stage algorithm, which was used for the experimental results presented in the next section.

The first stage of the search uses 4 measurements (3 steps) to reduce the uncertainty ranges of b_Q and G_Q by 18 dB. The second stage repeats this process, with another 4 measurements, for parameters b_I and K. Now the uncertainty ranges are doubled to account for the potential bias errors caused by the correlation between parameters. The third stage uses 5 measurements (4 steps) to reduce the uncertainty ranges of b_Q and G_Q by another 18 dB. The fourth stage repeats this process, with another 5 measurements, for parameters b_I and K. The total number of measurements is 18. The total improvement in LO and LSB distortion at RF is expected to be about 36 dB. If appropriate, the I and Q input levels may both be lowered between stages 2 and 3 to reduce IM3.

Severely degraded systems, or systems with very large uncertainty ranges, will require additional stages with fewer measurements per stage, but a higher total number of measurements. Recalibration, or tracking, typically requires fewer measurements because the uncertainty ranges are much smaller.

Experimental Results

In the experimental setup, the averaging time per power measurement was 0.67 msec, which corresponds to 4 cycles of a 6 kHz calibration tone, or 32 samples at a 48 kHz sample rate. The time required for each parameter adjustment to propagate through the system, including the feedback ADC, was approximately 0.7 msec. The total time required per measurement, including processing, was about 1.4 msec. A four-stage binary search was used, as described above, requiring a total of 18 measurements. Thus, the total calibration time was about 25 msec.

Experimental results are presented for an RF frequency of 1.65 GHz. Figure 8 shows the RF spectrum of the calibration tone, before precompensation. The LO and

LSB tones are seen to be down about 17 dB and 26 dB, respectively. Figure 9 shows the corresponding RF spectrum after precompensation. The LSB is now down more than 60 dB. The LO leakage has been driven down to the IM3 level, which is down about 55 dB for this setup.

Figure 10 shows a 12 kbps QPSK signal, with 60% roll-off root-raised-cosine filtering, generated directly at 1.64 GHz, with precompensation. As expected, there is no sign of the LO leakage. Any quadrature distortion is in-band and cannot be seen with modulation present. The small amount of sidelobe distortion is due to IM3.

Conclusions

This paper highlights that direct modulation at RF frequencies is feasible. The inherent simplicity and precision of the system design has shown that a high performance direct modulator can be implemented using low-cost commercially available components. It is expected that third order intermodulation performance can also be improved using similar feedback and precompensation techniques. Further research is being conducted in this area.

References

[1] M. Faulkner, T. Mattsson, and W. Yates, "Automatic adjustment of quadrature modulators", Electron. Lett., Vol. 27, No. 3, pp. 214-216, January 1991.

[2] S. Crozier, R. Datta and J. Sydor, "Direct Digital RF Synthesis and Modulation for MSAT Mobile Applications", 3rd International Mobile Satellite Conference (IMSC'93), Pasadena, California, pp. 399-403, June 16-18, 1993.

[3] D. Hilborn, S. Stapleton, and J. Cavers, "An Adaptive Direct Conversion Transmitter", IEEE Transactions on Vehicular Technology, Vol. 43, No. 2, pp. 223-233, May 1994.

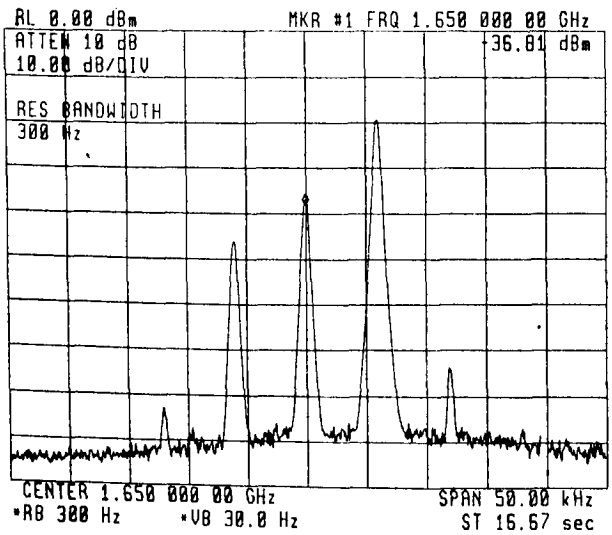

Fig. 8. RF spectrum of calibration tone at 1.65 GHz, without precompensation.

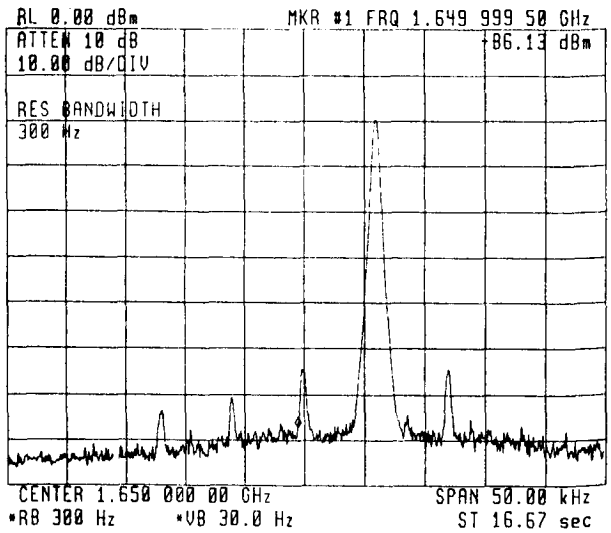

Fig. 9. RF spectrum of calibration tone at 1.65 GHz, with precompensation.

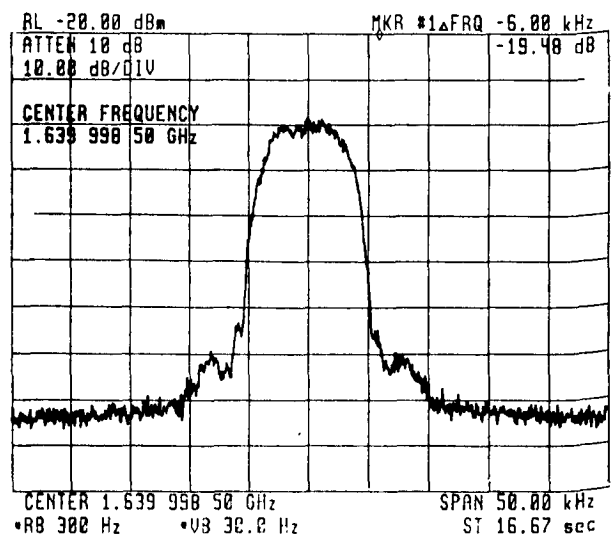

Fig. 10: RF spectrum of 12 kbps QPSK modulated signal at 1.64 GHz, with precompensation.

Current and Planned Systems

10

Session Chairman: **Hans-Christian Haugli,** VISTAR Communications, Canada
Session Organizer: **Brian Abbe,** Jet Propulsion Laboratory, USA

Topic Introduction: The past several years has seen a vast expansion in the number and types of mobile satellite services being offered to users. New services have arisen as a result of the new commercial satellite systems being launched. The papers in this session describe some of these new systems and services. GEO, MEO, and LEO systems that provide satellite coverage over North America, Europe, and Australia are represented through papers about Euteltracs, ORBCOMM, MSAT, MobileSat, and Ellipso. The last paper in the session introduces a top level Risk Taxonomy in order to assess the technical and programmatic risks of LEO and MEO mobile satellite systems.

New Applications for the Euteltracs Service

Jean-Noël COLCY and Laurent VANDEBROUCK

EUTELSAT
Tour Maine-Montparnasse - 33, avenue du Maine, BP 19 - 75755 Paris Cedex 15, France
Phone: +33 1 4538 4786 - Fax: +33 1 4538 4798

Summary

The EUTELTRACS two-way Mobile Satellite Messaging and Automatic Satellite Position Reporting (ASPR) service is Europe's first commercially operated Mobile Satellite Service. It was introduced by the European Telecommunications Satellite Organization (EUTELSAT) for commercial service in 1991. The system is based on a centralized network architecture organized around a single Hub station operated by EUTELSAT [1]. Initially the system was designed with a close user group architecture enabling a mobile to communicate exclusively with its own Headquarters. This paper describes the new applications (design and tests prior to their introduction into service) especially developed for the European market and particularly the Double Hop Services opening the system to authorized external entities. In addition, the European Commission (EC) pilot demonstrations in which the EUTELTRACS system is involved, are described.

COMMERCIAL SITUATION AND DEVELOPMENT OF EUTELTRACS IN EUROPE

Although EUTELSAT is run on a commercial basis, it is established as an International Organization and regulated by an Intergovernmental Convention, just like INTELSAT. The Organization was created in 1977, and formally established on 1 September 1985. Membership of EUTELSAT is open to any recognized European State which is a member of the International Telecommunications Union (ITU). The original membership of 17 countries has new risen to 44. Today, EUTELSAT manages eight telecommunication satellites. On behalf of its members (Signatories), EUTELSAT develops, manages and promotes satellite networks and services for:

- TV and radio broadcasting;
- Public telephony;
- Business services (VSAT networks, leased lines by satellites, video-conferencing.)
- Mobile services.

EUTELTRACS, is EUTELSAT's integrated mobile communications system especially conceived, designed and developed for the European transportation industry. With over 100 000 trucks equipped worldwide 7000 of which in Europe, EUTELTRACS is today the leader in mobile satellite communication systems.

EUTELTRACS provides simultaneously the following services throughout Europe, the Mediterranean Basin and the Middle East [2]:

- Location of a mobile by its base with an accuracy of 80 meters (depending on the current EUTELTSAT satellites used);
- Communication between mobiles and their base through a messaging service with a transmission of up to 1900 characters per message;
- Data collection and transfer from vehicles to base such as cargo and engine status, detection of door opening, etc.

Through the provision of these services and their integration within the client's information system, EUTELTRACS provides a real management tool for the improvement of carrier productivity.

Over the last two years, EUTELTRACS' commercial growth has almost reached 100% per year with several hundred transport companies as clients in Europe. This is thanks to:

- Improved and excellent reliability, quality and rapidity of the network (for instance, a message is transmitted and delivered in less than 30 seconds);
- A new application software product range fully oriented towards real time management and adapted to each market segment (HG transport, Security, Refrigerated Transport,...) rather than software merely oriented towards general communication management;
- Our 17 service providers in Europe acting in 20 countries in Europe, for the most specialized in the trucking industry, dealing with clients for one stop-shopping, and integrating the EUTELTRACS software into clients' information system;
- The development and commercialization of new tailor-made functionalities designed to meet client's needs such as the Double Hop or the Fast MIPR service: Double Hop not only enables a third party to receive specific authorized messages transmitted by equipped vehicles but also solves the problems of connection for clients located in remote places. This is achieved by using EUTELSAT's satellites and a EUTELTRACS terminal as a VSAT station rather than using obsolete PSTN or non-existent X25. The Fast MIPR on the other hand enables clients in the security market to continually track valuable goods and to beat crime.

One key strength of the system is also the large number of countries now authorizing the free circulation and use of EUTELTRACS in their territories. EUTELSAT has already successfully negotiated such licenses with 35 countries in Europe.

Through the use of EUTELTRACS, road transport companies in Europe have increased their productivity by around 15% thanks to a real time management of their drivers, vehicles and cargo, gaining in flexibility, seizing new opportunities, improving their client service and thus becoming more competitive. Furthermore, the current cost of hardware and service allows a return on investment in less than 12 to 16 months, depending on the country. This is the reason why large fleet operators in Europe such as Westerman in Germany (400 trucks), JP Vincent in France (125) or Harry Vos in the Benelux (600) have recently decided to use EUTELTRACS to manage their entire fleet, gaining substantial productivity gains in their overall management process.

With the excellent results from such a highly reliable network and system, EUTELSAT, has now decide to enter onto the maritime market, although the trucking industry remains our main and first market.

One of our first aims in the maritime sector has been to address the market for the fishing vessel operation control in EU waters initiated by the EC and now managed by the Fishery Authorities in each EU country. To do so, EUTELSAT has approached the EC to demonstrate the advantages of the system. The results of the demonstration were presented to the last IMSC Conference [2]. EUTELSAT then developed a dedicated technical offer including hardware, application software and a network to meet the exact requirements of the national Authorities. The aim of these bodies is to control the operation of their own vessels as well as those from the other EC countries operating in their territories while also meeting the needs of the ship owners. The characteristics of such a network and dedicated hardware are described below. Thanks to the success of this demonstration phase and offer evaluation EUTELSAT was selected as one of the potential systems to bid for the projects of fishing vessel operation control in the EU.

EUTELSAT then decided between June and September 1994 to bid for the competitive invitations to tender from the Ministries of Fishery in France, Germany, UK and Spain to control the activities of fishing vessels in their territories. EUTELSAT has successfully negotiated three of these contracts in which the entire hardware and software packages developed by EUTELSAT for this application have been selected by the Authorities of France, Spain and UK. This not only means that vessels from these countries will use EUTELTRACS on-board terminals on an operational basis but also that Control Centers from these countries will control the vessel operations by using our own software platforms and applications.

Furthermore, information such as vessel position reports will be automatically rerouted from our Hub station in France to the different control centers in the EU using the EUTELSAT satellites.

Such a commercial penetration of the maritime business also requires a careful examination of security issues. This work is in process including discussions, negotiations and tests with the International Maritime Organization (IMO), in order to make EUTELTRACS functionalities and performance compliant with Global Maritime Distress Satellite Services (GMDSS) standards. In 1995, only 100 vessels will be equipped with EUTELTRACS in Europe. However, a potential market of several thousand vessels will be open to us provided EUTELSAT 's marketing and testing of the system and value added services are successful. This will be helped by EUTELSAT 's current support of the creation and promotion of BOATRACS EUROPE, a subsidiary of BOATRACS Inc. in the US, to commercialize turn key solutions and added value services to the maritime community throughout Europe .

Besides vehicle fleet management and marine activities, EUTELTRACS is also active in the DGPS field (Differential GPS). EUTELSAT manages a DGPS network based on EUTELTRACS enabling oil platforms and vessels to receive accurate position data (3 to 5 meters) every 5 seconds using a EUTELTRACS terminal in receive only mode. The Differential Data and the terrestrial reference stations are managed by Fugro whereas EUTELTRACS is used to transmit in real time the data to vessels and platforms subscribing to the FUGRO service. 45 vessels are already using this service in the North Sea and it is expected that a total of 80 vessels will be equipped by year end.

With regard to EUTELTRACS' commercial goals in Europe, EUTELSAT aims to have :

- 10 000 trucks equipped by year end and 30 000 in 1998;
- 45 countries allowing the Free Circulation and Use of EUTELTRACS in their territories;
- 22 service providers dealing with final users.

EUTELSAT is also taking part in three Consortia for the 4th Framework Program of R&D of the EC (95-98) which will use EUTELTRACS to demonstrate the benefits of Telematic tools for improving the productivity, security and quality of transport by road, rail and sea in Europe.

These consortia, called HAZTRAK (for the control and monitoring of Hazardous Goods in Europe), MAXIM (for the improvement of efficiency of the transport in a multimodal environment) and MULTITRACK (to improve the productivity of transport in a multimodal environment for Just in Time applications), will take the benefits of the new functionalities EUTELSAT just developed including the Double Hop (also called SDS for Satellite Dispatch Service) and Fast MIPR (Mobile Initiate Position Report).

SDS is described below as well as its current use within the Pilot Projects for the control of fishing vessels operations in the EU waters sponsored by the EC and carried out by the Ministries of Fishery in France, UK and Spain. The results of the Frame project of the EC in which EUTELTRACS contributed for the monitoring and control of Hazardous Goods in Europe are also examined.

DOUBLE HOP SERVICE (OR SDS)

Background

This feature was developed to enable a mobile to send or to receive messages and/or position reports from another mobile or to provide a link with the Hub station to a Dispatch Center located in an area without any convenient terrestrial communication means.

A Routing Station (RS), located as close as possible to the Hub station analyzes the received message before sending it back to the relevant recipient according to a routing matrix under the control of a third party (connected either via terrestrial line or via an EUTELTRACS link).

SDS network architecture

In addition to the mobiles in the field which use standard Mobile Communication Terminals (MCTs) the following elements can be highlighted in the SDS network architecture (see Figure 1):

i) The Routing Station (RS) which is the node of the SDS network. It is linked to the Hub station and forwards incoming messages from mobiles or from Satellite Dispatch Center (SDC) connected by satellite to final recipients (single or multiple), based on an addressing matrix. The routing station should normally be a fault-tolerant machine (PC-LAN) in order to provide continuity of service.

ii) The Satellite Dispatch Center (SDC) comprising a PC connected to one or two MCTs via an RS-232C serial port. The proprietary Mobile Interface Protocol (MIP) is used to communicate between the PC and the MCT(s). The dialogue is always initiated by the PC, which requests the status of outgoing or incoming messages stored in the MCT(s).

iii) A Fix Dispatch Center (FDC) is an option which may be available within an operational SDS network. This station could receive a copy of any messages exchanged (allowing SDC stations to converse with FDC station) and could also identify the position of all mobiles. It could also manage the addressing matrix for mobiles to one or more SDC stations and the pre-formatted messages definition.

Functional description of the SDS system

The SDS system is designed to utilize message handling, position reporting and mapping display working stations derived from the stations already used for fixed bases in the EUTELTRACS environment. The PC software is enhanced for SDC application and offers new features required for use in such configuration. One of the main enhancements to the standard software is communication between the SDC station and the message server in Paris, which is no longer via modem and public switched network but via EUTELTRACS terminals. In this application, the MCT is used as a very low bit rate VSAT station.

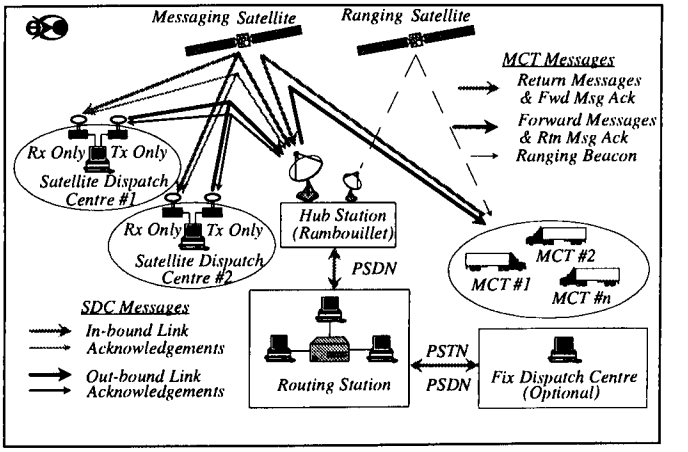

Figure 1 - SDS Network Architecture

The EUTELTRACS system was not designed in such a way that a mobile may transmit a message while receiving one. This event, highly unlikely during "normal" use of the EUTELTRACS system, generates a conflict between reception and transmission functions within the MCT. This conflict generally results in the impossibility of sending or receiving acknowledgments required by the transmission protocol, which therefore results in the retransmission of messages. For an operational SDS system, where the traffic on MCT communications links used in the SDC station may be high at times (or even saturate), this type of event could be frequent and could spark off an avalanche effect, whereby transmission speed for the user would virtually drop to zero. For this reason, at least two MCTs are needed for the SDC station, respectively specializing in message reception functions (only sending acknowledgments) and in message transmission functions (only receiving acknowledgments). This configuration would also secure links between SDC stations and Routing Station.

Messages from mobiles are extracted from the Hub station mailbox by the RS. The messages are analyzed to determine routing according to the current organization of the network stored in the RS, or additional information entered by the originator in the message header. The mobile position issued by the EUTELTRACS system with the message is added to the

data block. The new message is sent to the Hub station via a X.25 link for transmission. It is then sent to the SDC station MCT and received on the PC software to be decrypted and submitted to the recipient in the same way it would via a standard telephone connection.

SDC station messages follow the opposite route. They are sent to the RS , whoever the final recipients may be. The message passes through the Hub station and is then retransmitted by the RS to the recipient(s) specified in the header.

Connectivity and Performance

Any type of connectivity can be handled by the SDS network i.e. MCTs can be connected to the FDC station, to several SDC stations and even to other MCTs via the RS.

Based on the current operational EUTELTRACS system message size and generation rate statistics, a load test field trial showed that a SDC station equipped with two MCTs could manage the traffic generated by up to 150 MCTs.

E.C. PROJECTS

Fisheries Enforcement Project in the European Waters

Background

The European Commission (EC) is currently testing and evaluating a Vessel Monitoring System (VMS) via satellite in the European waters for the control and management by National Authorities of the fishery vessels with different control centers located in European countries. The proposed service is based on the EUTELTRACS system covering the Mediterranean Basin and the North Atlantic Sea.

The EUTELSAT VMS is designed to provide secure, 2-way messaging between EUTELTRACS equipped fishing vessels and a Fishing Monitoring Center (FMC) operated by the National Authority. Additionally, selected positioning and fishing information is relayed via the EUTELTRACS System to remote Fishing Monitoring Centers (rFMC) located in other foreign coastal countries with jurisdiction over specific fishing areas.

As shown on the Figure 2, the network is based on PCs located in the FMC and in rFMCs at each foreign site running proprietary software and connected to EUTELTRACS terminals.

FMC and rFMCs can communicate with the vessels and among themselves by using the services of a PC-LAN based Routing Station (RS) located in Paris. The software supplied as part of the service to operate the VMS can be customized to proved any type on connectivity between the various entities involved (software defined network).

VMS Network configuration

To meet the system requirements, a fully satellite based network was selected to offer the best response time for the least cost.

It consists of:

i) A PC-LAN based RS on EUTELSAT premises in Paris where leased lines to the Hub station and 24 hour operator services are available. The RS receives all messages and positions by querying the VAX computers located at the Hub station. Positions and messages can be retransmitted as needed either to a single addressee i.e. FMC, or to multiple addressees i.e. FMC and a rFMC(s).

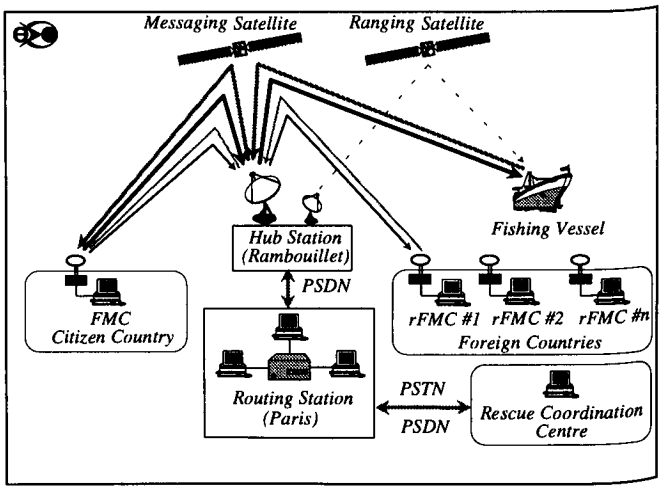

Figure 2 - VMS Network Architecture

ii) A PC based FMC software which can transmits/receives messages and positions to/from vessels via its attached EUTELTRACS terminal. Those messages are always picked up by the RS in Paris which retransmits them as needed either to a vessel, or to a foreign rFMC.

iii) Any number of PC based rFMCs, located in the Fisheries Control Center of other Coastal States. They are also attached to EUTELTRACS terminals which they use to communicate with the FMC.

Mobile unit

The communication equipment onboard the fishing vessel consists of a standard EUTELTRACS MCT equipped with a 4 buttons box with fixed/flashing red/green LEDs to be used by the fishermen primarily for reporting their fishing status as follows:

1. start fishing;
2. stop fishing;
3. (not yet assigned);
4. emergency/distress message.

Start and stop fishing LEDs are coupled by software so that it is always clear to the fishermen whether the current status is "fishing" or 'not fishing".

- *Vessel position data*

Each message transmitted by a EUTELTRACS terminal is automatically prefixed with a phase measurement header (inaccessible to the user) used together with the round trip delay (Hub to vessel and vessel to Hub) measured directly by the Hub station to compute the location of the vessel by dual satellite triangulation [2] [3]. The fact that the position is not generated in the vessels by some black box but is computed at the Hub station precludes any tampering with position data. From an engineering standpoint, even with access to significant equipment and talent, it is difficult to imagine a method for "faking" the EUTELTRACS position. Normally, the Hub station polls each vessel in the fleet which has neither sent nor received a message during the last 60 minutes. In response to the poll, the EUTELTRACS terminal on the vessel returns the information used by the Hub station to compute its position. This regular position reporting can be modified from the FMC in several ways. The FMC operators can (via the RS):

i) Issue an immediate poll to a specific vessel,
ii) Poll the vessel every "n" minutes,
iii) Change the Mobile Initiated Position Reporting (MIPR) parameter in the vessel's EUTELTRACS terminal to "n" minutes (down to 1 minute) which causes that terminal to send an unsolicited position report if it has not heard from the HUB during the last "n" minutes.

- *Maritime distress call*

By pressing the distress switch on the four-button fishing report box (hood-protected button requiring two sequential actions before an emergency message can be sent), the crew can cause a high priority emergency message including current position to be sent by the MCT to the Hub station (for maritime applications the message delivery time is equal to 30 seconds as average). That message causes an alarm to sound in the 24 hours a day EUTELTRACS control center where operators can relay the message to an appropriate Rescue Coordination Center (RCC).

In addition, this emergency message is also picked up by the routing station which can relay the priority message and position report to one or more RCCs based on the location of the distress call. Furthermore, both the FMC and the rFMC can relay emergency information messages which are picked-up by the RS and retransmitted selectively to all the vessels located within a specified area. It should be noted that the above features are as critical steps toward making the EUTELTRACS System GMDSS compliant.

Freight Management in Europe (FRAME) Project

- *Background*

The European Commission (EC) implemented within the DRIVE program, from early 1993 to end 1994, a pilot system called FRAME. The project was managed by an independent consortium appointed by the EC and provided to its users the capability to monitor, manage and control the transport of Hazardous Goods (HG) through European countries. Its implementation requires that the vehicles carrying HG be equipped appropriately with communication terminals in order to provide position determination, cargo manifest data, and a direct link between the vehicle driver, the freight office, the control administration and the emergency services [4].

- *FRAME Network Architecture*

As shown in Figure 3 the FRAME system comprises the following components:

i) a standard Personal Computer (PC) User Terminal (UT) running the relevant software to provide all the necessary functions to the user i.e. message transfer, position reporting and mapping capabilities;

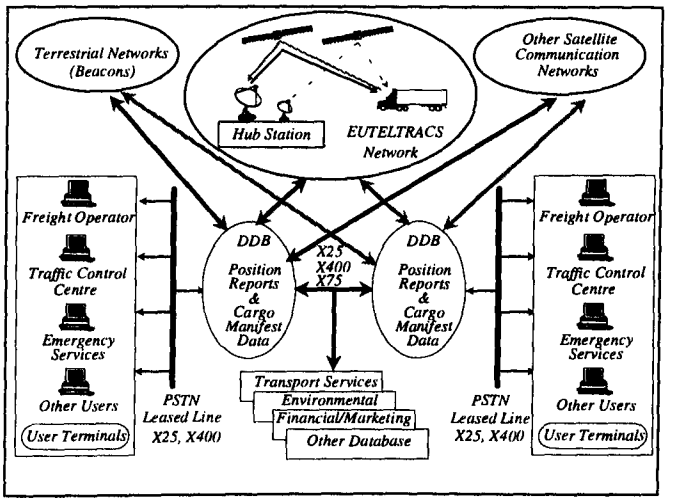

Figure 3 - FRAME Network Architecture

ii) Communication equipment (terrestrial and satellite via the Hub station);
iii) Distributed Data Base (DDB) facilities;
iv) In-vehicle communication equipment (EUTELTRACS or Inmarsat C/GPS).

- *Objectives of the Pilot*

The main objectives of the field trial were the following:

i) To demonstrate the feasibility of implementing a FRAME system with a pan-European coverage, multimodal and inter-modal transports (road, rail, sea, inland waterways);
ii) To evaluate the technical performance of the system;
iii) To provide all the necessary information to perform a detailed socio-economic evaluation of the FRAME system i.e. quantitative assessment of the impacts and benefits arising form the pilot system use, as well as calculations of incurred cost;

iv) To demonstrate to the users involved in HG transport the potential of advanced telematics in improving HG monitoring, management and control both form the commercial and administrative points of view;

v) To assess current procedures and legislation regarding the transport of HG and to provide feedback information and recommendations to legislative bodies.

❑ *Comparison of Alternative Technologies*

During the pilot trials the technologies used were EUTELTRACS and Inmarsat C with GPS. The comparison of technologies utilizes the results of the technical and user-acceptance analysis.

	Position Accuracy	Message Accuracy	Delay Time	Reliability
	c1 = 100 m	c2 = 100%	c3 = 420sec	c4 = 96.1%
Function	1 - 0.001 c1	c2	1 - 0.001 c3	c4
Criterion	u1 = 0.90	u2 = 1.00	u3 = 0.58	u4 = 0.96
Weights	w1 = 0.2	w2 = 0.2	w3 = 0.2	w4 = 0.4
Weighted	w1 u1 0.180	w2 u2 0.200	w3 u3 0.116	w4 u4 0.384
Weighted Sum for Inmarsat C with GPS: 0.880				

Table 1 - Inmarsat C with GPS performance

The indicators are:

i) Position reports accuracy;

ii) Message accuracy (the messages through the systems);

iii) Average message delivery delay time;

iv) Continuity of the service (system reliability).

	Position Accuracy	Message Accuracy	Delay Time	Reliability
	c1 = 80 m	c2 = 100%	c3 = 90 sec	c4 = 100%
Function	1 - 0.001 c1	c2	1 - 0.001 c3	c4
Criterion	u1 = 0.92	u2 = 1.00	u3 = 0.91	u4 = 1.00
Weights	w1 = 0.2	w2 = 0.2	w3 = 0.2	w4 = 0.4
Weighted	w1 u1 0.184	w2 u2 0.200	w3 u3 0.182	w4 u4 0.400
Weighted Sum for EUTELTRACS: 0.966				

Table 2 - EUTELTRACS performance

The comparison is based on the utility value analysis concept [5] consisting to transform the system-dependent indicators into dimensionless value quantities using a "value function". The weight normally amounts to 1.

The choice of the weights and the value functions is subjective and depends on the preference of the decision maker (independent body appointed by the EC in this case).

Tables 1 and 2 present both satellite systems under test performances.

CONCLUSION

These new functionalities will give EUTELTRACS the edge to enter rapidly into new markets such as Eastern Europe and the CIS via their transport agencies who are connected to the network using the EUTELSAT satellites and EUTELTRACS terminals in fixed configuration. This will also allow us to introduce the system throughout Europe with greater speed and flexibility. In addition, EUTELSAT is now in a position to penetrate new application markets such as data collection and transfer at low bite rates for fixed applications (e.g. environmental monitoring network for public organizations) requiring rapid simultaneous data dispatch to several destinations in complete confidentiality.

For this reason EUTELSAT expects a revenue increase of around 25% in 1995 thanks alone to the launch of these new functionalities along with a rapid growth in the maritime business, representing 5% of the total number of active terminals by the end of 1996.

References

[1] **J-N Colcy & R. Bardelli (EUTELSAT)**, *Traffic Control and Monitoring in the EUTELTRACS System*, in Proceedings of the 1992 International Conference on Digital Satellite Communications (ICDSC'92), Copenhagen, Denmark, pp 323-328

[2] **J-N Colcy & R. Steinhauser (EUTELSAT)**, *EUTELTRACS The European Experience on Mobile Satellite Services*, in Proceedings of the 1993 International Mobile Satellite Conference (IMSC'93), Pasadena, California, pp 261-266

[3] **J-N Colcy & J. Dutronc (EUTELSAT), W. G. Ames (Qualcomm Inc.)**, *The EUTELTRACS Position Reporting System - Characteristics and Performance*, in Proceedings of the 1990 Conference of the Royal Institute of Navigation (NAV'90), Warwick, U.K., Paper N° 24

[4] **Dr. A. P. Leros**, *European Commission DRIVE II Project V2034 FRAME*, Deliverable 16 - WP 5, December 1994

[5] **Rupert Bobinger et. al.**, *Evaluation Process for Road Transport Informatics - EVA Manual*, EVA 1036 project report, December 1991.

ORBCOMM - Initial Operations

David Schoen, Paul Locke
Orbital Communications Corporation
21700 Atlantic Boulevard, Dulles, Virginia, 20166-6801
Tel: 703-406-5000 Fax: 703-406-3504

INTRODUCTION

ORBCOMM, a subsidiary of Orbital Sciences Corporation (OSC), has developed the ORBCOMM System over the past 5 years. Working with OSC, a leading developer of small satellite technology and the low-cost launch systems (the air launched booster Pegasus), ORBCOMM has designed a system to provide low-cost mobile two-way data communications for worldwide commercial markets. The primary application areas are data communications and messaging. The project was fully funded when in 1993 ORBCOMM and Teleglobe (Canada), the world's fifth largest international telecommunications firm, entered a financing and marketing strategic alliance.

ORBCOMM
SYSTEM OPERATIONAL CONCEPT

The ORBCOMM System has been designed so a user can compose, transmit and receive messages, control and monitor assets and collect data on hand-held Subscriber Communicators (SCs). The user can send a query from his operational center or his/her personal SC to an asset or program the asset to send data on the occurrence of an event. With a constellation of 36 LEO satellites and terrestrial facilities, users in the temperate climate zones around the world will have a satellite in view continuously over 98% of the time, and will have to wait less than two minutes the rest of the time to directly access a satellite. A message transmitted from a SC and received by the satellite is relayed down to a regional Gateway Earth Station (GES). The GES then transmits the message via fiber land-lines to the Network Control Center (NCC). The NCC then determines the location of the recipient of the message and routes the message accordingly. The message can be routed back to a GES and relayed via satellite and then down to the addressee of the message. The NCC can also receive and transmit messages from terrestrial networks via X.400 and X.25 gateways. The NCC is in essence a X.400 backbone messaging system. The NCC can translate messages from widely used e-mail systems such as Internet, cc:Mail and Microsoft Mail into X.400 messages for transmission to and from ORBCOMM SCs.

ORBCOMM
SYSTEM COMPONENTS

The ORBCOMM System consists of three main components, the space segment, the ground segment, and the subscriber terminals or SCs. Currently, for coverage of North America., there are four unmanned Gateway Earth Stations (GES) located in the four corners of the U.S., one Network Control Center (NCC) and the constellation of LEOs. The system is designed to meet the following system performance objectives:

- 98% availability of spacecraft above 5 degrees elevation to the horizon,
- 99% of outages (satellite not in view) < 5 minutes,
- 98% of outages (satellite not in view) < 2 minutes.

As the network expands, countries around the world will have their own regional NCC and GES (the number of GESs being dependent on the size of the country). Twenty-two organizations covering thirty-nine countries have signed candidate licensee agreements with ORBCOMM to procure ground segments and provide service by the end of 1998. The satellites are "re-used" by each country as they pass overhead.

Space Segment

The ORBCOMM System's most unique characteristic is the use of low-Earth orbit satellites. The space segment will be comprised of 36 small communication satellites, each weighing less than 95 pounds, in orbit 775 km above the earth. LEO satellite systems provide the following advantages:

- Lower launch costs (approximately $15 million for one Pegasus launch) to place up to 8 small satellites in orbit,
- Minimal satellite transmission time delays with a LEO satellite versus GEO satellite,
- Availability of Doppler shift in signal for integrated position determination,
- Use of proven inexpensive VHF electronics, shared omni-directional VHF antennas,
- Excellent overall link availability independent of local terrain features.

Satellite Constellation

The ORBCOMM System uses a constellation of 36 satellites. The first two satellites deployed are in near-polar orbit inclined 70 degrees at the equator. They were launched on April 3 of 1995. Starting in mid-1996, the remaining 24 satellites will be launched in three groups. They will be placed in three orbital planes, each containing eight equidistantly spaced satellites in circular orbit inclined 45 degrees at the equator, spaced 135 degrees apart. The 26 satellite constellation will be deployed by the end of 1996. An additional 8 satellite plane, plus two more in polar orbit are being planned for deployment starting in 1997 to provide increased coverage and capacity. The satellites will be deployed eight at a time using OSC's Pegasus launcher.

The ORBCOMM satellites are very simply designed spacecraft whose main function is to complete the link between the SCs and the NCC. The satellites are constantly scanning the 148.0-150.05 MHz band in 2.5 KHz steps looking for open channels to assign to the SCs when they signal a transmission request.

The ORBCOMM satellites have the following characteristics:

Mass - 95 pounds
Solar Array Power - 160 watts (orbit average)
Transmitters
- VHF (users links) 2
- VHF (feeder links) 1
- UHF (beacon) 1

Receivers
- VHF (users links) 7
- VHF (feeder links) 2

Propulsion - GN2
Attitude Control - Autonomous/GPS
Design Lifetime - Four years
Cost less than $2 Million

Robustness and redundancy of the ORBCOMM System is attained by the number of satellites. The failure of any one satellite will not adversely affect the system. The satellites can be re-positioned within their plane to compensate for a single satellite failure. Up to four satellites can be lost without significant degradation to the capacity of the system. An entire plane of eight satellites can be replenished with one Pegasus launch.

Ground Segment

The ground segment is comprised of the NCC, SCC and unmanned GESs. The ground segment contains most of the "intelligence" of the ORBCOMM System. This approach avoids having expensive spacecraft in orbit that cannot be repaired.

Each country around the world that uses the ORBCOMM System will have their own NCC and GES. Initially, there will be four GESs located in the four corners of the U.S. with unobstructed views of the horizon. Each GES has redundant VHF antennas that track the satellites as they cross the sky. The GES and the satellites provide transparent access from the SC to the NCC.

Network Control Center

The NCC provides message routing and customer services. The NCC routes messages to the addressee(s) of the message. The NCCs are owned and operated by ORBCOMM in the U.S. and by each licensee in their individual territory.

The NCC is comprised of dual Hewlett-Packard computers with automatic switchover and mirrored disks. The NCC is connected to each GES by leased lines and the public data network, future plans call for VSAT backup at each GES to the NCC. The NCC also provides connections to customers operation centers over leased lines and the public data network.

The NCC provides the following functions:

- Message handling - Management of the delivery of data messages within and in/out of the ORBCOMM System,
- Network management - Statistics, diagnostics, and con figuration control,
- Message transfer - Delivery of data messages,
- Message gateway - Conversion to and from other message delivery/receipt formats,
- Customer Service.

Satellite Control Center

There is only one SCC co-located with the NCC in Dulles, Virginia and is solely owned and operated by ORBCOMM. The SCC serves two functions:

- Satellite Control - Telemetry collection and analysis, commanding of satellites, and
- GES Control and Monitoring - Commanding the GES, tracking a specific satellite, and GES telemetry collection and analysis.

Gateway Earth Station

The GES provides the link between the ground segment and the space segment. The unattended GESs have redundant power and communication links. They are monitored 24 hours per day by the NCC/SCC. The GES provides the following functions:

- Acquire and track satellites based on orbital elements received from the NCC,
- Transmit to and receive from the satellites,
- Transmit to and receive from the NCC,
- Monitor status of local GES hardware/software,
- Monitor the system level performance of the satellite "connected" to the NCC.

The GES has two steerable high-gain VHF antennas that track the satellites as they cross the sky. The GES transmits to the satellite in the 148.0 - 150.05 MHz range at 56.7 Kbps at 250 watts. The GES receives 5 watt transmissions from the satellite in the 137.0 - 138.0 MHz range.

Subscriber Communicator

The initial SCs are compact, weigh approximately 16-20 ounces, transmit at 5 watts and can use either internal or external power sources. A variety of SC models are being planned and manufactured by Panasonic, Tadiran/Elisra and Torrey Science under a licensing agreement with ORBCOMM. As part of this agreement ORBCOMM provides the communications operating software to the manufacturers that enables the SCs to communicate with the ORBCOMM network. ORBCOMM also type certifies that the SCs will operation the network in accordance with ORBCOMM's FCC license. The first production units will be data communicators and will function as a radio modem. They will have product features that will allow for external power, RS-232 interface and external antennas. Future units will have keypads, integrated GPS receivers, encryption capability and LCD screens and will be smaller in size. Many will have a variety of interfaces. Data transmissions can be encrypted by the application software using standard Digital Encryption Standard (DES) computer chips using the same methodology that is used by STU-IIIs to encrypt classified conversations.

The SCs have the following RF characteristics:

Transmit	
• Data rate	2400 baud
• Frequency	148 - 150.05 MHz
• Modulation	SDPSK
• Power	5 watts
Receive	
• Data rate	4800 baud
• Frequency	137 - 138 MHz
• Modulation	DPSK
• G/T	-28 dB/∫K

Each SC has a unique manufacturer's ID and is assigned a unique X.400 address at the time it is activated onto the ORBCOMM System. The ID and the X.400 address are cross referenced and verified by the NCC to ensure that the message sender and recipient are valid.

Commercial SCs designed for tracking and monitoring applications are expected to retail for approximately $700. Units purchased in quantity will have significant price reductions. Units with additional features such as GPS, encryption, and different antenna configurations will cost more.

The ORBCOMM System will provide a geo-location capability that combines the Doppler frequency shift available from a LEO satellite with the satellite on-board GPS receiver to calculate position within 500 meters

Mission Applications

The ORBCOMM System can readily satisfy many current and planned Asset management and logistics requirements. Many users will be able to adopt the ORBCOMM System for a variety of applications that:

- Track the position of logistics throughout shipment with SCs integrated into the asset,
- Remotely interrogate electronic tags and manifests,
- Collect crucial environmental data located anywhere in the battlespace,
- Monitor the status of remote sensors from the U.S. or field command posts,
- Interrogate beyond line-of-sight assets without terrestrial repeaters, or relays,
- Query the status of rapidly moving weapon systems and supplies,
- Retrieve messages at any time,
- Provide global coverage for downed pilots.

Asset Monitoring

Currently, there are no means by which a user can readily and inexpensively monitor remote assets. The ORBCOMM system offers a wide variety of methods for monitoring remote assets both manned and unattended regardless of the geographic or environmental conditions. SCs can either be integrated into the existing sensor units, such as is being done in a number of commercial environmental applications, or stand alone and simply be connected via the RS-232 port, using its own power source or sharing the asset's power source. The user can use a PC or another SC to query the asset on a random basis, poll the asset on a pre-determined schedule, or the user can program the application so that the asset sends a message based on an event. In those areas where a GES is not in the same footprint as an NCC, the satellite can store and forward the message from the asset until the appropriate GES comes into view. The reverse can be done when interrogating the asset from a sustaining base. Operational requirements, not the communications system, dictate the method of monitoring the equipment and sites.

Logistics

The ORBCOMM System will provide the users the ability to continuously track any shipment from the sustaining base, across the sea, at the port, and through the various depot levels. The user can interrogate electronic manifest tags remotely to determine the contents and condition of the container or exact coordinates of any portion of a logistics shipment. The only requirement is to interface an ORBCOMM SC to the electronic tag interrogator via the RS-232 port to provide the necessary communications link. All that the user needs to do is write an application program interface, allowing the SC to pass data to and from the tag interrogator. ORBCOMM provides software support for developing application interfaces as standard business policy. Then from an operational center the user can query via a PC or another SC the current location and status of his or her supplies directly while they are underway. ORBCOMM simply provides an inexpensive communications link to the shipment.

MSAT Broadcast Voice Services

John W. Jones, P.Eng.[1]
TMI Communications
1601 Telesat Court
P.O. Box 9826
Gloucester, Ontario K1G 5M2
Phone: (613) 742-0000 Fax: (613) 742-4100
E-mail: j.jones@tmi.telesat.ca

ABSTRACT

Later this year the MSAT satellite network will be delivering mobile and remote communications throughout North America. Its services include a family of Broadcast Voice Services, the first of which will be MSAT Dispatch Radio, which will extend the features and functionality of terrestrial Specialized Mobile Radio (SMR) to the entire continent. This paper describes the MSAT Broadcast Voice Services in general, and MSAT Dispatch Radio in particular, and provides examples of commercial and government applications.

MOTIVATING EXAMPLE – EXTENDING THE PUBLIC SAFETY NET

For public safety agencies that need to provide services in non-urban areas, the cost of mobile communications can be prohibitive. For this reason many agencies have areas of responsibility (sometimes large) which are off net — no coverage available. When emergency response personnel are dispatched to an off net scene there is no way to provide them with additional information or redirect them to a more urgent incident, and there is no way for these emergency response personnel to request backup assistance. This lack of coverage costs lives and money, but providing universal coverage by terrestrial means is not financially feasible.

This was one of the prime motivations for the creation of MSAT. The MSAT satellite provides universal coverage throughout North America. Cellular-like and broadcast voice. Async and X.25 data. Facsimile and GPS. From a single radio. With the launch of the MSAT satellite later this year, today's limitations in providing mobile communications will be left behind — the "public safety net" will be extended to cover the entire continent.

MSAT NETWORK OVERVIEW

Later this year TMI Communications will be offering services on its MSAT satellite communications network. The MSAT satellites are the most powerful mobile communications satellites ever built, using advanced technology new to commercial satellites. Two initial satellites, one owned by TMI Communications and the other by American Mobile Satellite Corporation (AMSC), will each provide full North America-wide coverage (including Alaska, Hawaii, Mexico and the Caribbean) with 6 L-Band beams.

The Communications Ground Segment will also be the most advanced ever developed for a commercial satcom system, allowing TMI Communications to offer a wide selection of advanced mobile and remote communications services.

The MSAT Network supports the following types of services:

- Telephony
- Circuit switched async data
- Facsimile
- Broadcast Voice Services (including Dispatch Radio)
- Packet Switched Data

Subscribers place and receive calls through terminal equipment known as Communicators.

[1] On secondment from the MSAT Program Office, Industry Canada, 300 Slater Street, Ottawa, Ontario K1A 0C8.

Since the MSAT Network is interconnected to public telephone and data networks, MSAT subscribers can always be reached from anywhere.

MSAT COMMUNICATORS

TMI Communications licences manufacturers to use the MSAT Network specifications to make MSAT Communicators (also called Mobile Terminals). Currently, Westinghouse Electric Corporation [3] and Mitsubishi Electric Corporation [1] have been licenced to produce Communicators. The manufacturers will compete for market share through different product features and prices. Since both manufacturers will employ a modular design, subscribers can begin with a basic product and purchase additional Communicator features as they wish to use additional MSAT capabilities.

A basic MSAT Communicator supports telephone and circuit switched data communications. Communicators can be upgraded to support cellular networks, G3 fax, Broadcast Voice Services and packet switched data communications. The Communicators have also been designed to support peripheral equipment such as Global Positioning System (GPS) devices, laptop computers, etc.

Additionally, a specialized MSAT Communicator that is designed to serve the niche SCADA (Supervisory Control And Data Acquisition) industry is available from Narrowband Telecommunications Research Inc. of Burnaby, B.C. This Communicator is intended for packet switched data communications across the MSAT Network. The design of the Narrowband Communicator is optimized for low power full duplex packet data communications and can operate unattended in remote locations with solar cells and rechargeable batteries.

BROADCAST VOICE SERVICES

The MSAT Broadcast Voice Services allow MSAT subscribers to carry out push-to-talk group voice conversations, called conferences. (In other published papers the MSAT Broadcast Voice Services are referred to as Net Radio [1], Trunked Radio [2] and Private Voice Network Service [4]. These terms all refer to the same functionality.)

These conferences take place within closed user groups of MSAT Communicators, called Talk Groups. Each Communicator can be a member of up to 15 Talk Groups, but can participate in only one conference at a time.

A conference typically begins when the first participant presses his push-to-talk, causing the MSAT Network to assign a channel to the Talk Group. A conference ends once the channel has been idle for a certain length of time. This length of time is called the Hangtime and is configurable.

In normal operation, when someone pushes-to-talk, no one else can speak until the current speaker releases their push-to-talk. All Talk Groups (except Broadcast Mode) and Communicators that support Voice Broadcast Services have a feature called Priority 1 Interrupt that permits a user in an emergency situation to interrupt another user or to contact the dispatcher.

There are three types of Talk Groups: Normal Mode, Private Mode, and Broadcast Mode. For Normal Mode, any number of participants who have access to the Talk Group can have a push-to-talk conversation. For Private Mode, two subscribers can have a private, push-to-talk conversation that no one else can listen to. For Broadcast Mode, subscribers who have access to a Broadcast Mode Talk Group can listen to the voice or audio broadcast, but cannot reply.

A Talk Group can be configured to allow a variety of different types of dispatcher access. A Talk Group can be configured to allow only subscribers using MSAT Communicators to participate. Alternatively, a Talk Group can allow someone with access to the PSTN to dial a phone number that connects them to the Talk Group; this is called Dial In Dispatch. A Talk Group can allow a Communicator subscriber to dial out to a pre-determined PSTN phone number to allow someone with PSTN access to participate in the conference; this is called Dial Out Dispatch. Talk Groups can also be configured to allow both Dial In Dispatch and Dial Out Dispatch (but not simultaneously). Finally, a Talk Group can be configured to automatically include a dispatcher via a leased voice line and a TCP/IP data connection; this is called Full Service Dispatch.

The MSAT satellite has 6 L-Band beams covering all of North America, with 4 of them covering all of Canada. There are three Talk Group configurations for determining which beams to include in a conference. First there is the Single Beam configuration, where only a single pre-determined beam is used; this beam will cover one quarter of the continent. Secondly, there is a Fixed

Multiple Beam configuration, where from 2 to 6 pre-determined beams are always used. Finally, there is a Dynamic Multiple Beam configuration, where from 2 to 6 pre-determined beams are allowed to be used, but whenever a conference is initiated the only beams included are those necessary to cover the geographic distribution of the Communicators that belong to the Talk Group.

Because MSAT is a satellite-based system, with propagation times inherent in satellite communications, "message" trunking mode is used for MSAT Broadcast Voice Services. This means that the channel will remain up between speakers in a conference as long as the delay between speakers is less than the Hangtime. The Hangtimer can be set to zero for "transmission" trunking.

Equipment Configurations

All MSAT Communicators manufactured by Mitsubishi and Westinghouse support Broadcast Voice Services. For the Mitsubishi Communicator, an external speaker and special PTT handset (with PTT and emergency interrupt buttons) are used.

A subscriber with a Westinghouse Communicator uses the regular mobile phone handset, and pushes-to-talk by pressing DTMF '1' or '3'. Emergency interrupt is also via the DTMF key sequence '*99'.

Dial In and Dial Out Dispatch

MSAT Broadcast Voice Service has features that allow someone from the PSTN to dial into the MSAT Network to establish a conference on a Talk Group, or for a Talk Group participant to have someone at the other end of a pre-assigned PSTN phone number join the conference. These are optional features subscribed to on a Talk Group basis.

There are two ways the PSTN dispatcher can speak to the Talk Group participants. One method is to briefly press the DTMF tone '1' to emulate PTT Transmit, speak, and press '3' to emulate PTT release. The second way is a hands-free mode — whenever no one else is pushing-to-talk the voice of the dispatcher is carried over the Talk Group.

Computer Aided Dispatch

A dispatch interface allows a subscribing organization to provide computer aided dispatch for MSAT Broadcast Voice Service, or to interface MSAT Broadcast Voice Service with their terrestrial trunked radio system. This interface consists of a voice line and a TCP/IP data line that provides information on the traffic (start and stop time of each conference, current speaker, conference parameters, call failure reasons) and allows the dynamic changing or disabling of hangtimers.

DISPATCH RADIO

TMI Communications is following a strategy of phasing in the services we are offering through our Service Providers. Our first service will be MSAT Phone, followed by MSAT Mobile Phone. We will then introduce MSAT Dispatch Radio, which offers some of the Broadcast Voice Service features described in the preceding section. Following the introduction of MSAT Dispatch Radio, we will roll out other, more complex, Broadcast Voice Services.

MSAT Dispatch Radio is a two-way push-to-talk voice service that enables subscribers to bring all the members of a group together, where each has the ability to speak to all the rest.

MSAT Dispatch Radio subscribers typically use Normal Mode Talk Groups, with Private Mode being available for private conversations between two subscribers.

Dispatch Radio is intended for applications where the dispatcher uses a Communicator, either in a mobile or fixed configuration. Therefore the Talk Groups do not support Dial In Dispatch, Dial Out Dispatch, or Full Service Dispatch.

Dispatch Radio Talk Groups are initially available only in Single Beam configuration. The Hangtimer is set at 6 seconds.

MSAT Dispatch Radio transcends distance and weather conditions to provide affordable, private, and secure communications. It bridges the communication gaps existing in isolated locations, as well as on all of Canada's busy highways and waterways.

DISPATCH RADIO APPLICATIONS

- Forestry companies work in constantly changing, remote wooded areas and require group communications in the harvesting of

MobileSat®
A characteristically Australian MSS

Dr Michael Wagg, Michael Jansen
Optus Communications Pty Ltd
PO Box 1, North Sydney 2059, NSW, Australia
Phone: 61-2-342-7823 Fax: 61-2-342-7803

ABSTRACT:

Optus launched its Mobile Satellite Telephone Service MobileSat® in August 1994. This provided Australia and its neighbouring waters with nation-wide mobile telephone coverage and still is the world's only domestic Mobile Satellite telephone system.

This paper provides details of Optus' experience in developing and launching the MobileSat service, including:

i) a retrospective of the issues that have waxed and waned in importance during the development and implementation phases, and

ii) the strategy for future activities based on the experience gained in the development phase.

INTRODUCTION

Australia's mobile satellite service had its beginning in late 1986 when Aussat Pty Ltd took the decision to develop and provide a mobile satellite service using an L Band package on its B series of satellites due for launch in 1992. Optus Communications Pty Ltd, Optus, continued with the project following their purchase of Aussat in late 1991 as part of being granted Australia's second general and mobile telecommunications carrier licence.

Optus employs over 3000 staff, has monthly revenues in excess of A$100M, a wireline customer base of over 1.4 million and mobile customer base of over 600,000. Optus is owned by a mix of Australian and international companies including Cable and Wireless and Bell South with 24.5% each, Mayne Nickless with 25% and other Australian investors with the remaining 26%.

Optus' MobileSat service is operated in conjunction with its mobile cellular services (digital GSM system and resale of analog AMPS system). It shares infrastructure including customer service, billing systems etc and provides a means for Optus to provide mobile communications services beyond the 85% population coverage reach of cellular. More importantly MobileSat gives Optus 100% coverage of the Australian land mass whereas the cellular coverage is only around 5%.

SERVICE OVERVIEW

MobileSat is a mobile telephone service providing the primary service features of voice, fax and dial up data. Each Mobile Telephone is assigned three telephone numbers in the Australian number range:

01451ABCDE is the voice number,
01452ABCDE is the fax number, and
01453ABCDE is the dial up data number.

The network and MobileSat telephone automatically routes the call to the appropriate port.

Ancillary features include call forwarding, voicemail and a short messaging capability for value added services such as a message waiting indicator for voicemail and the relay of GPS data and status messages as part of a fleet management package.

MobileSat provides coverage to all of Australia and its neighbouring waters. In addition the spread of the satellite beam has enabled operation and implementation of limited services in neighbouring countries such as Papua New Guinea, New Zealand and Indonesia.

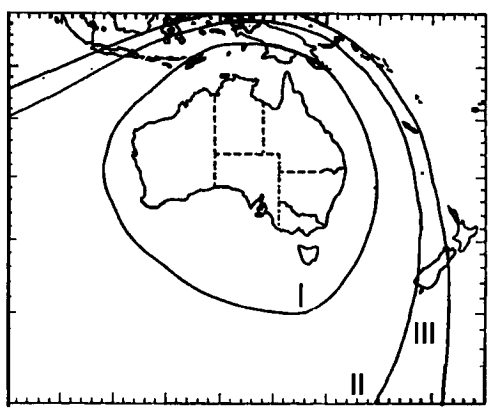

MobileSat Coverage

I: Limits of Mobile Service, II: Limit of Standard Fixed
III: Limit of High Performance Fixed Antenna

NETWORK OVERVIEW

Space Segment

The MobileSat Service uses an L/Ku Band package on board each of the two Optus B series satellites located at orbital locations 156 and 160 degrees east. The package represents around 15% of the satellite resource with nominally 150 Watts of L Band transmit power per satellite in a beam with a usable EIRP of 47dBW over Australia. The previous diagram shows the extent of the satellite coverage for different antenna configurations.

Ground Infrastructure

The MobileSat service is configured with a redundant Network Management System, NMS, with the primary site in Sydney and the back-up site in Perth. Access to the public switched telephone network, PSTN, is via a gateway station which is controlled by the NMS and interfaces into a network switch via Primary Rate Access , PRA, ISDN links in blocks of 30 channels. The switches used are Northern Telecom DMS100/200 switches which are used primarily in Optus' provision of Long Distance telephony throughout Australia. The network has been initially configured with 60 channels in each of Sydney and Perth with growth capability at each location to 900 channels. The total network capacity is nominally 1000 channels supporting 50,000 users with a call set up rate of 17 calls per second. The configuration of the MobileSat network is summarised in the following diagram:

MobileSat Ground Network

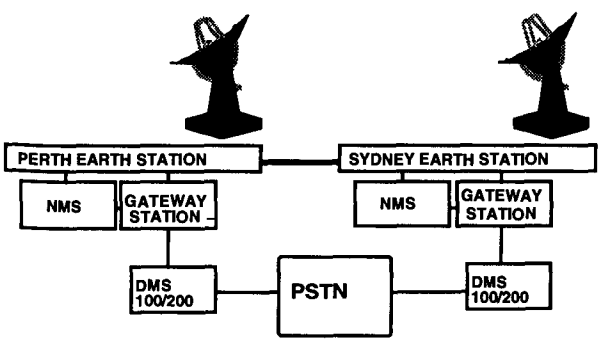

The MobileSat ground network was supplied to Optus by NEC Australia in a contract that commenced in December 1990. CSC Australia provided all the software for the network as a major subcontractor to NEC.

MobileSat Telephones

Optus has two Supply Agreements for the provision of MobileSat Telephones. NEC Australia have supplied their 'S1' telephone since the introduction of the service in mid 1994. Westinghouse are currently testing their 'Series 1000' telephone with full availability scheduled for May 1995. The technical specifications for the NEC and Westinghouse MobileSat telephones are summarised below:

	NEC	Westinghouse
Frequency TX	1646.5 to 1660.5 MHz	
RX	1545 to 1559 MHz	
Voice Coding	4200bps IMBE	
Channel	6600bps $\pi/4$ QPSK	
Antenna/ G/T	Mast/ -18 dB/K	
Transceiver mm	315x350x122	305x180x60
Antenna Unit	N/A	230x180x75
RF Output	3 Watts nominal	
Fax G3 2400bps	External Modem	Optional Card
Data 2400bps	External Modem	Integral

Photos of the NEC and Westinghouse equipment are given below:

NEC S1 Transceiver

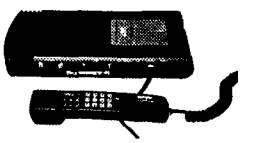

Westinghouse Series 1000 Transceiver and Handset

The telephones are available as either an in-vehicle version or a fixed/transportable version. The in-vehicle version has a cellular like handset in the cabin of the vehicle connected to the transceiver. The predominant antenna is a rod which fits on the vehicle ('bull' bar or 'kangaroo' bar is a popular location), is around one meter in height and is around two centimetres in diameter. The transportable version is packaged in a brief case and uses a planar antenna that may be located in the lid of the brief case or externally.

A variety of specialist applications are also being addressed including an aeronautical telephone for general aviation, low profile antennas for train use and maritime antennas to suit the environment, including salt water spray and pitch and roll of commercial and leisure boating.

COMMERCIAL OVERVIEW

Market

The Optus MobileSat service is targeted at supporting a total user population of nominally 50,000 users by the year 2000. The current take-up of the service will see over 5000 customers by the end of 1995. The early users are dominated by those industries operating in Australia's Rural and Remote areas, including:

Mining and Exploration
Emergency Services (eg Police, Ambulance and Fire)
Marine (Fishing)
Government (Defence, Customs, Social Services)
Transport (Railways, Trucking)
Support Services (Mining, Agricultural)

Support

Optus has integrated its MobileSat servicing into the teams supporting the other businesses throughout the company. This includes a 24 hour toll free access for all customer enquiries, distribution and servicing of equipment as well as billing. In addition, a dedicated service team is on hand to provide specialist advice and to handle all commissioning and decommissioning activities. Optus, its MobileSat telephone suppliers together with the Optus dealer network will provide a network maintenance and support service throughout the country.

Sales

Optus has set up two key channels for the sale of the MobileSat service. The main channel is a dealer network of over 50 outlets covering all the main centres throughout the country. The dealers are expected to sell around 80% of all MobileSat telephones with the remaining phones to be sold through Optus' direct sales force which in the main will target major corporate and Government organisations throughout Australia.

Service Fees

Optus offers its Australian customers a number of rate plans with the primary plans being:

VoicePlan:	A$100 (US$75) Connection fee A$45 (US$34) Monthly Service Fee A$0.90 (US$0.67) per 30 seconds Call Fee
DataPlan:	A$100 (US$75) Connection fee A$45 (US$34) Monthly Service Fee A$0.24 (US$0.18) per 6 seconds Call Fee

The Voice Plan is used primarily by those customers using the telephone for voice or fax calls, whereas the DataPlan is targeted at customers requiring dial up data access for short data transfer

RETROSPECTIVE OF DEVELOPMENT PROCESS

The development for the MobileSat service began in the late 1980s. At that time a number of the key technologies were still in their formative stages so the early work involved significant research, both directly and in conjunction with other parties, in order to develop a baseline product description. As well a range of market research activities were undertaken to identify the market requirements for the service and the implications for the service design.

Technology

The key technology elements considered during the developmental phase were:

L Band propagation,

Antennas and

Voice Encoding.

Propagation: The subject of propagation was vital to the determination of the link budget and the design of the signalling system. Extensive testing using the fortuitously available ETS-V L Band Satellite provided sufficient data to design a robust signalling channel and to settle on an appropriate link budget for the mobile operation. The testing concluded that a repeat strategy was optimum for the signalling channel and that only a small margin (~4 dB) was necessary in the communications channel. The work undertaken indicated that a prohibitive margin would be necessary to support applications such as in building coverage for handheld units.

Antennas: The availability of a low cost high performance mobile antenna was and, to some extent, still is the key challenge for the MobileSat service. In the late 1980s, due to the research programs within the US, Canada and Japan , there were a number of prototype antennas that were within a few steps of becoming a commercial reality. However, it could be argued that since then the antenna area has taken a few backward steps. The delay in the implementation of the North American services and their market potential can to some extent explain this hiatus.

The MobileSat system is predominantly using an adjustable mast that is omnidirectional in azimuth and has an adjustable elevation with a beam width of around 10 degrees. This antenna is the most cost effective available and has the advantage that it is easy to mount and is familiar to remote area users being similar but smaller that an HF whip antenna. However, the antenna does have the disadvantage of requiring user intervention,

degraded performance at low elevation angles and requires a stable platform to maintain pointing. Also the early promised performance of the mast was reduced somewhat due to the realities of practical implementation. This required adjustment in the overall system link budget and highlighted the need to have a tight overall control on all the implementation issues.

It should be noted that the user acceptability of the mast antenna has been good (a number of inventive users even achieving successful operation on fishing vessels using a counterweight to maintain the antenna vertical).

Tracking antennas are split between the mechanical and electronic versions. The mechanical antennas are still largely confined to maritime use with vehicle mounted versions still to enter the market place. An electronically switched antenna has been introduced into the Australian marketplace, but currently has a significant cost disadvantage compared to the alternatives.

The key development issues at present being the introduction of a cost competitive tracking antenna and a mast antenna without the squint between the transmit and receive beams (a number of versions are currently in prototype form).

Voice Encoding: The implementation of an efficient voice coding scheme, along with a low cost antenna, constituted the 'Holy Grail' of the development of land mobile satellite services. Early work involved the consideration of analog systems such as ACSSB, but an evaluation conducted some five years ago settled on the IMBE digital encoding scheme from DVSI. The practical implementation of this system has been highly successful with user acceptability being very good. In fact the vocoder is just one part of the overall implementation of a quality voice service. The primary issues in setting up the network being the maintenance of the signal level and the elimination (or minimisation) of echo. In fact the digital nature of the vocoder has not been an issue with the most noticeable features being clipping due to voice activation and variable signal levels from the PSTN and the 'satellite' delay compared to standard circuits.

Service Implementation:

The original concept for the MobileSat service was a feature rich product providing a diverse range a applications to the market place. However the practicalities of developing and launching a new service has resulted in the adoption of a 'vanilla' service, mobile telephony at launch with applications such as fax, data and messaging being added in a phased approach following the service launch. Value added features such fleet management, closed user groups (Radio), etc are being implemented based on specific market demands.

This approach has resulted from a mixture of delivery constraints and ease of marketing. Mobile Telephony has always been the single biggest market sector and represents the easiest sale in that only a single telephone sale is necessary to secure the customer. Value added applications such as fleet management, closed user networks and SCADA all require a significant upfront commitment from either the customer or service provider in development of the application and generally require a large user base to ensure commercial viability, which also requires a large commitment to achieve the sale.

A strategic decision was implemented within Optus some two years prior to the service launch to concentrate the available resources on launching the MobileSat telephony product. This was also based on market research at the time which highlighted that potential customers with large fleet or network requirements were likely to adopt a phased growth of the product. This was largely due to a conservative approach within the potential customer base to new products and new technology.

Ground Infrastructure:

The implementation of the ground infrastructure for the MobileSat service highlighted the conflict between needing to cement specifications at the beginning of the development stage (some two to three years prior to service) and to adapt to the requirements of the market place as it progressed towards adopting the service. This conflict was managed by including within the baseline specifiation all the necessary hooks to implement specialised services, but only implementing the 'vanilla' service features.

The program for developing, integrating and testing the service ground infrastructure did not involve any 'breakthrough' technologies, but did highlight the impact that seemingly small issues can have on a complex development program. The key issue being that early resolution and cementing of the specification for all elements and interfaces is necessary to avoid problems during the development stage.

Mobile Telephones:

The development of the mobile telephones were dominated in the early stages by the issues of antennas and voice encoding. However, the key driver when aiming for commitments in terms of price and delivery has been the take-up profile and the level of the total global market for the product. In a market such as Australia, this is an important issue as its size is not sufficient to independently kick start a mobile satellite telephone industry. Both suppliers, NEC and Westinghouse, have used commonalty with other products, namely INMARSAT and MSAT to support overall economies of scale. This has required a certain amount of movement in the telephone specifications (and

consequently the system) to accommodate the best possible combination from a price and performance perspective.

The key implementation issue with the MobileSat telephones has been the time frame to stabilise the software within the telephones and particularly the implementation of the user friendly features such as handset display and commands, handsfree operation and audio level/quality. This has been an iterative process which continues even into the delivery of the service. The mobile satellite telephone is compared by the users to an in car cellular telephone and they expect features comparable to those available on the cellular services.

THE FUTURE

The MobileSat service provides Optus with the capability of serving the total area and population of Australia and neighbouring regions with a mobile telephone service. The experience , expertise and general knowledge obtained through the development and implementation of this service provides a sound base for Optus, its customers and suppliers to profit from the developing market needs as the industry matures.

In particular over the last few years there has been a good deal of attention focused on the hand-held global mobile satellite services, be they LEO, MEO or GEO. The market demands in terms of service and support features for future services will be able to be evaluated and responded to from experience gained from the provision of the MobileSat service. Areas such as those outlined below will need to be reviewed:

Handheld telephones:- Is the market demand there or can it be supported by a cordless extension to a vehicular or transportable telephone?

Cellular Interoperability:- Does the user require features such as seamless handover and a dual capability handset? Will the user be willing to pay a premium for this feature or will they be willing to use two handsets and call forwarding?

Pricing:- Is the customer willing to pay a premium for specialised features such as global versus regional coverage and hand portability of equipment?

The current generation of Optus satellites are due to operate to after 2005. However, Optus is undertaking a continuous evaluation of its future options to maintain the provision of services to rural and remote area Australia. This includes review of the following options:

- global mobile satellite systems,

- Optus owned follow on satellite capacity and

- shared satellite capacity with regional/international operators.

SUMMARY

Australia's MobileSat service was launched in August 1994 heralding the first land mobile satellite telephone service throughout the world. The program has required implementation of technologies at the peak of the development scale in areas such as antennas and digitised voice, but in the main has been a balancing act between achieving customer expectations and managing a complex development and supply program.

The rural and remote area customers utilising the service now have features and capabilities only previously experienced by their urban cousins. Their demand and usage of the service promise that it will achieve the expectations of the team that first started the journey in late 1986.

The Ellipso™ Mobile Satellite System

Dr. David Castiel
President and CEO

John E. Draim
Advisor, Constellation Design

Mobile Communications Holdings, Inc.
Suite 460, 1120 19th Street, Washington, DC, USA
Tel: 202-466-4488

With the advent of Ellipso™, people in every country seizing this unprecedented opportunity will for the first time find the resources to stay in touch with the world regardless of their location or movement. A new approach to using satellites, coupled with user terminals small enough to be placed in a pocket, erases distance or mobility as barriers to communications. Ellipso™ was conceived as an innovative, satellite-based solution to extend and complement existing commercial terrestrial mobile and rural fixed telecommunications services.

Present mobile services, such as cellular telephone, have in practice only a very short radio propagation range, only a few kilometers, within which good service is available. Many expensive ground cell sites are needed for wide area coverage. Terrestrial mobile system operators are reluctant to expand coverage over areas that cannot themselves yield an economic return on the necessary investment. As a consequence, many rural areas are not served by cellular telephone. Furthermore, it is simply infeasible to offer terrestrial mobile services to some remote areas or areas where infrastructure is nonexistent, many of which have significant populations.

In addition, the mobile telephone user finds that other regions he visits often do not use the same cellular standards as the service he subscribes to. As a result, he is often out of touch when he roams abroad. In addition to the gaps in mobile telephone coverage, many rural areas of the world remain unserved by any type of telephone service at all. Many countries have not been able to afford the costs for installing the relatively expensive rural phone lines to serve the more dispersed customer base in those areas. As a result, without telecommunications, economic growth and prosperity has lagged, awaiting a solution to what has been so far a problem too costly for many administrations to bear.

With the arrival of the Ellipso™Mobile Satellite System, all this now changes. Using a constellation of medium earth orbiting satellites linking small, portable user ground terminals located anywhere in a country or region to the existing telecommunications networks, distance, isolation, or remote mobility no longer constitute a barrier to communications. People anywhere will be in touch with the world at low terrestrial network prices. This new telecommunications access in turn becomes an economic multiplier, empowering a country to harness and activate its resources for greater domestic and international strength.

Ellipso™ System is conceived to extend telecommunications services throughout the world to users that are not well, or not at all served by existing mobile or fixed telephone systems. Unlike cellular telephone, Ellipso™ offers fully nationwide service to every served country, thereby providing service to users located anywhere within the national boundaries, no matter how isolated or remote. With Ellipso™, a user in the middle of a wilderness area will have the same mobile telecommunications service available to him as a user in a major metropolitan area. The subscriber only requires a clear view of a serving satellite to achieve a connection and to connect to anyone else served by the national telecommunications system. Subscribers within view of two or more satellites will benefit from an automatic improvement in service quality, benefiting from Ellipso™'s unique satellite diversity processing, using all available satellites simultaneously to optimize circuit quality.

Ellipso™ uses medium earth orbiting (MEO) satellites and an efficient system design to reach its subscribers directly and at a price that is competitive with terrestrial cellular telephone service, that is, around $US 0.50 per minute and $US 35 per month. Ellipso™ will not only offer the user mobile telephone services, but can offer other digital services as well, such as data transfer, facsimile, paging, voice mail, and messaging. Ellipso™ will also offer geopositioning service to users upon request. Ellipso™ will not bypass existing telephone systems in offering these services, rather Ellipso™ will extend them. Figure 1 illustrates the Ellipso™ System.

The Ellipso™ Business Plan

Building to a viable and flexible business plan remains the most important aspect of the Ellipso™ system design. The market potential for mobile satellite services remains tentative. Therefore, Ellipso™ is intentionally designed to be capable of offering a profitable, economical service to a conservatively sized market, in order to succeed and grow while hedging market risks. Furthermore, the Ellipso™ design contains built-in flexibility for tailoring best its geographic coverage to market success.

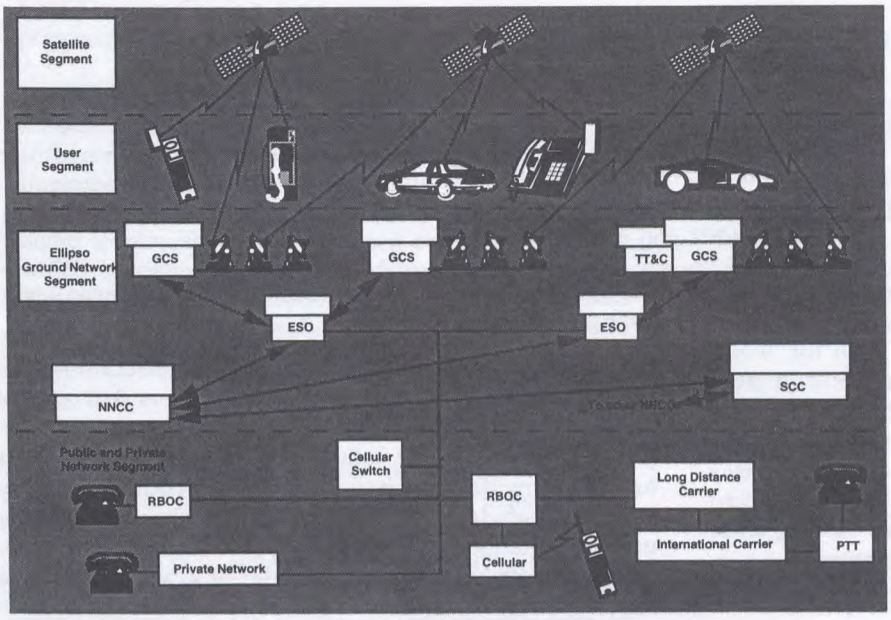

Figure 1: The Ellipso™ System

The Ellipso™ System will profitably operate serving a conservative initial market size of less than 1,000,000 subscribers throughout the world. Ellipso™'s unique and proprietary MEO constellation of satellites assures not only an even Ellipso™ coverage around the earth for each latitude, but coverage over the entire populated earth tailored in capacity to the earth's population by latitude. Ellipso™ is initially targeting 400,000 subscribers in the United States and 600,000 subscribers in other areas of the globe.

The Ellipso™ Constellation

The Ellipso™ system is unique in that it divides its global coverage into two zones, each served primarily by its own constellation of satellites. The earth's distribution of land and population by latitude serves as the basis for the overall Ellipso™ constellation design. Most noteworthy regarding the distribution of the world's landmasses is that the northern hemisphere contains many times more land mass north of 40°N than the southern hemisphere has south of 40°S. Virtually all of Europe is north of 40°N, almost one half of the United States and all of Canada lie north of 40°N, and all the CIS and part of Japan lie north of 40°N. Among these are some of the largest countries on earth.

In contrast, the southern hemisphere contains much less land mass at high latitudes than the Northern hemisphere. For example, continental Australia reaches south only to 39°S, Tasmania to 43°S, New Zealand to 47°S. South Africa to 35°S, and continental South America to 52°S. Moreover the amount of land south of 40° is very small in global terms, comprising only southern New Zealand, Tasmania, and the southern half of Argentina and Chile south of areas containing most of the populations. All areas south of 40°S are relatively sparsely populated. In short, almost all the earth's populated land mass lies north of 40°S.

In light of this asymmetry in populated landmasses, any satellite system offering worldwide coverage of populated landmasses must provide extensive coverage to northern latitudes. To do so requires inclined orbits for all low and medium earth orbit satellite systems. But if circular orbits are used, the inclined orbits mean that equal coverage is also given to the far southern latitudes, where it is largely wasted.

The Ellipso™ system is designed to match its capacity and resources more closely to the distribution of populated landmasses than would be possible using any constellation of satellites in circular orbits. It does so using two complementary and coordinated constellations of satellites, Ellipso™-Borealis™ and Ellipso™-Concordia™.

The Ellipso™-Borealis™ Constellation primarily serves areas in the northern temperate latitudes, while the Ellipso™-Concordia™ Constellation serves areas in the tropical and southern latitudes. Each constellation has been carefully conceived to complement the other, so as together to offer the most effective and efficient solution to worldwide coverage possible. The Tropic of Cancer roughly divides the service areas of the two constellations, although there is a wide band of latitudes that can be served by either or both constellations. Ellipso™ can adjust the deployment schedule and capacity of each of these two zones to optimize global coverage to investment and demand as necessary.

Ellipso™-Borealis™

The Ellipso™-Borealis™ Subconstellation provides coverage of the northern temperate latitudes. This subconstellation uses 10 satellites in elliptical orbits in two planes. Borealis orbits are inclined at 116.5 degrees in order to prevent movement of the apogee around the orbital path. They have apogees of 7,846 kilometers, perigees of around 520 kilometers, and a three-hour orbital period. The apogees are near the northern extremity of the orbits.

The Borealis elliptical orbits act to concentrate most of the deployed satellites to the north of the equator at any

one time[1]. Consequently, they can furnish northern service for a greater percentage of their orbits than if the orbits were circular. The elliptical orbits also require less launch energy than a circular orbit of similar northern coverage. Finally, these satellites are mostly quiescent when below the equator, when batteries are recharged. These factors translate into a requirement for fewer, smaller satellites having lower launch costs than would be needed using circular orbits. In fact, four Borealis satellites in elliptical orbit can provide service equivalent to six satellites placed in a circular orbit.

Furthermore, the Borealis™ orbits are carefully configured to be sunsynchronous. That is, the orientation of the orbital plane remains fixed relative to the direction to the sun throughout the year. Being sunsynchronous, each orbital plane can be adjusted to optimize the time of day at which the greatest satellite coverage occurs. This is achieved by carefully choosing the orientation of the orbital plane relative to the sun and by tilting the line of apsides (the line connecting the apogee and perigee) of the orbit so that the apogee is placed over the desired northern region at the desired time of day. For example, orbital planes that are edge-on to the sun have their apogee tilted toward the sun in order to increase system capacity in daylight hours over that at night. This favoring of one time of day over another will be true at all longitudes around the earth. Ellipso™ will exploit design flexibility like this, which are only possible with elliptical orbits.

ELLIPSO™-CONCORDIA™

The Ellipso™-Concordia™ Constellation provides corresponding coverage to the tropical and southern latitudes. These satellites need not provide high capacity at high latitudes, since there is very little land in the southern hemisphere at high latitudes, and northern high latitudes are already covered by Ellipso™-Borealis™. This permits tailoring an economical orbital configuration for Ellipso™ -Concordia™ coverage that focuses greater capacity at tropical and near-tropical latitudes than does Ellipso™-Borealis™.

Present planning calls for an initial complement of six Concordia™ satellites to be deployed in an circular equatorial orbit at an altitude of 8,040 kilometers. This constellation configuration will provide continuous coverage of all tropical latitudes plus all temperate latitudes to 47 degrees South (extending to 55 degrees South with reduced capacity). An additional complement of four satellites in a complementary elliptical Concordia™ orbit dramatically increases daytime capacity.

An important Ellipso™ system design objective is to offer at least dual satellite coverage to every served point on the earth above around 40 degrees South latitude, with single satellite coverage to 55 degrees South latitude. This redundant coverage enables Ellipso™ to exploit path diversity to overcome the effects of shadowing, blockage, and multipath fading on otherwise marginal links. Figure 2 illustrates the overall appearance of the initial Ellipso™ constellation, showing two planes of satellites in inclined Borealis™ orbits and a third equatorial orbital plane for the Concordia™ satellites.

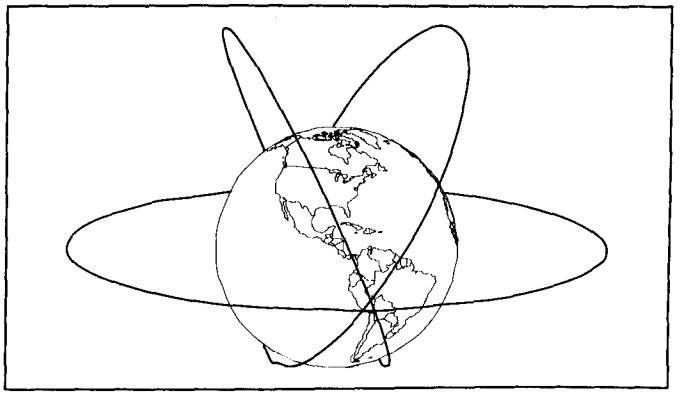

Figure 2: The Ellipso™ Orbits

THE ELLIPSO™ SATELLITES

Ellipso™ uses relatively simple transponder satellites. These satellites use proven, space-qualified components and spacecraft designs to the maximum extent possible. Their primary function is to interconnect the Ellipso™ subscriber with Ellipso™ Ground Control Stations, from where the subscriber connects with the existing national telecommunications network or to another Ellipso™ subscriber via satellite. Most electronic processing functions take place in the Ellipso™ System earth stations. This reduces satellite size, weight, and cost (satellite-based processing is much more expensive than equivalent ground-based processing) and permits greater processing flexibility. Such flexibility may be necessary to implement future system improvements or to tailor Ellipso™ better to the specific technical characteristics of each region's infrastructure.

The Ellipso™ satellite is a 3-axis stabilized design using solar wings and body-fixed antennas. The satellite's user link antennas divide the visible earth into 61 adjoining areas, each served by its own beam. These beams are arranged in a circularly symmetric manner. Figure 3 shows a conceptual drawing of the Ellipso™ satellite, and figure 4 illustrates the layout of the 61 user link beams.

[1] Since satellite angular velocity is dependent on satellite altitude, satellites in elliptical orbits pass rapidly through their perigees and travel more slowly through their apogees.

Each beam over the same 12 megahertz within the Mobile Satellite Service (MSS) band. This eliminates the need for users to switch frequencies as the beam or satellite serving them changes during a call. The signals in each mobile user beam are translated to a separate frequency and polarization assignment for transmission between the satellite and the Ground Control Station over the feeder links. The satellite transmits and receives from the Ground Control Stations in the corresponding feeder link bands using an earth coverage beam antenna,

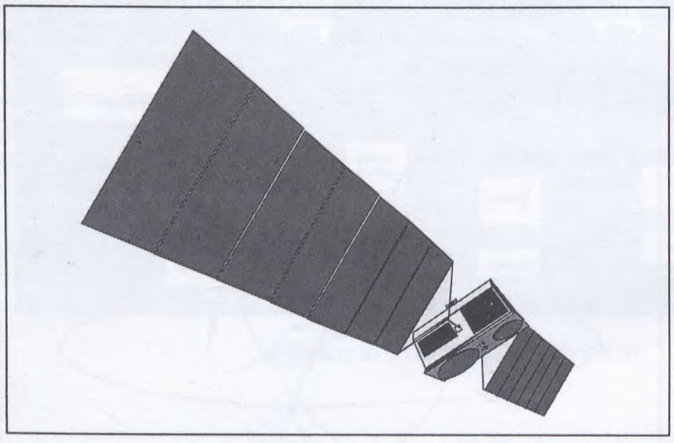

Figure 3: The Ellipso™ Satellite

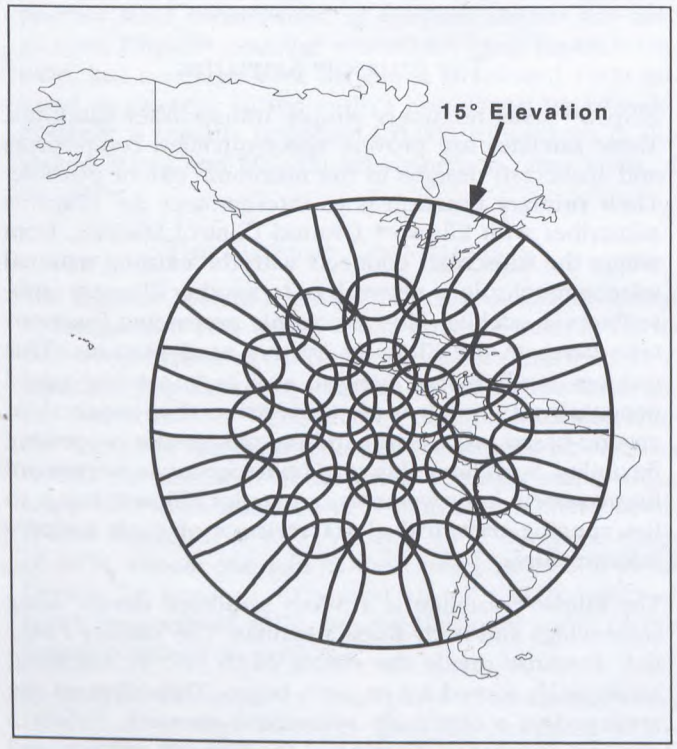

Figure 4: The Ellipso™ Mobile Service Beam Array Concordia Example

Figure 5 illustrates the manner in which user link beams are mapped to feeder link bands.

The satellite uses reaction wheels and thrusters for attitude control and station keeping. The satellites will contain enough battery reserve to allow full eclipse operation. The satellite is specified to have a five year mean life.

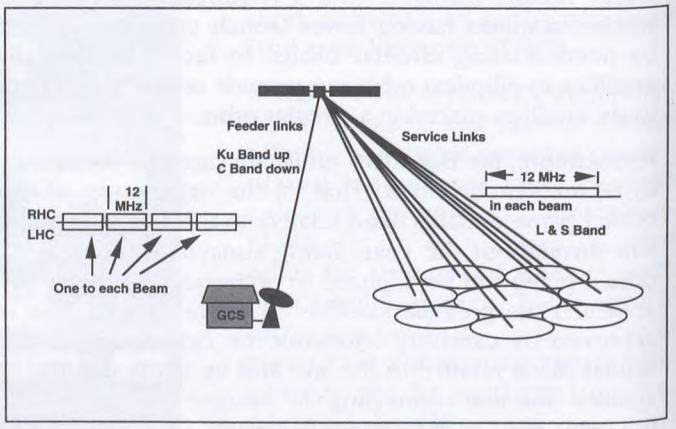

Figure 5: Mapping of service link beams into the feeder link

Ellipso™ Satellite Deployment

Here too the Ellipso™ design offers flexibility. Ellipso™ will introduce marketable services in phases, corresponding to its level of deployment. The Ellipso™ satellites will begin deployment in 1997.

Ellipso™ satellites may be launched up to six at a time while building the constellation, depending on the booster used. Constellation replenishment will use smaller boosters to launch one or two at a time. Ten satellites in two inclined planes will initiate full northern hemisphere Borealis™ service above the Tropic of Cancer. Six Concordia™ satellites will provide complete and continuous coverage of the tropical and southern latitudes. As a consequence of Ellipso™'s unique design, full time, fully capable service can begin for broad areas of the earth with only a partial deployment of the global Ellipso™ complement of satellites.

Additional Ellipso™ satellites will add capacity to those regions of the globe having additional demand as the need arises. They can be deployed in any of several combinations between Borealis™ and Concordia™, depending on the distribution of demand. Indeed, Ellipso™ is free to adjust the timing of the introduction of northern versus southern capacity depending on the demand in each region.

Ellipso™ User Terminals

The Ellipso™ user terminal will be very similar in form and operation to those used for cellular telephony.

Ellipso™ signal parameters have been selected to correspond closely to anticipated terrestrial CDMA cellular designs of the future.

There will be three primary types of Ellipso™ user terminals, mobile or portable, fixed, and handheld. Mobile terminals are designed for vehicular use and will be optimized for high quality service from moving vehicles. Fixed terminals are designed for public or private installed use. While they do not need to cope with the challenges of a constantly changing mobile environment, they are optimized for excellent service and high system capacity. Handheld Ellipso™ terminals resemble present cellular pocket phones in size, radiated power, battery life, weight, and operation.

Both the mobile and handheld terminal types use antennas having hemispheric coverage. Fixed terminals use more directive antenna designs for greater efficiency. In many cases, Ellipso™ terminals will be dual mode terminals, capable of operating selectively in the Ellipso™ system or in the local terrestrial cellular system, depending on service availability and pricing for the call.

Ellipso™ will also support other, more specialized terminal designs. These include data-only terminals, personal digital assistants, and paging/polling terminals. Value Added partners may develop a vertically integrated terminal package including specialized applications and features for specialized markets, such as fisheries or trucking Indeed, variations on user terminal design and packaging are only limited by the design ingenuity of terminal suppliers. Ellipso™ services will also integrate very well with the new personal communications services proposed by some as the next generation in public telecommunications.

It is expected that Ellipso™ user mobile terminals should cost around one thousand US dollars within one to two years of service initiation. Eventual Ellipso™ terminals costs should reduce to around five hundred dollars US.

The Ellipso™ Signal
Ellipso™ Services and Signals

It is anticipated that the primary service Ellipso™ will support will be voice telephony. To support this service, Ellipso™ will use a state-of-the-art digital voice encoding technique, known as the Code Excited Linear Predictive (CELP) algorithm, for carrying high quality voice efficiently, using a 4.15 kilobits per second digital rate. Testing has shown that this voice algorithm yields natural sounding, high quality voice reproduction. Ellipso™ will offer even higher grades of voice service during off-peak hours or to subscribers who request it.

Ellipso™ will also use its basic digital transmission capability to support various kinds of digitally-based services, such as Hayes modem data, facsimile, message forwarding, paging, and geolocation information. These services will be available at various data rates from 300 to 9600 bits per second.

For greater robustness, the user's signal is encoded using a powerful convolutional error correcting code, and interleaved to randomize errors. Before transmission, the user signal is multiplied by a high speed digital direct sequence spreading code, a random-like but reproducible digital sequence running at a rate around a thousand times faster than the user signal to be spread. This has the effect of spreading the signal's energy, which formerly occupied only several kilohertz, over several megahertz of bandwidth. After spreading, the resulting signal is transmitted using a power-efficient modulation technique.

Ellipso™ signals are transmitted in two types, a three megahertz wide band and a 7.5 megahertz wide band, depending on service type and operational conditions. Usually, mobile and handheld users will be assigned to the wide band, while fixed users are assigned to the narrow band.

When active, Ellipso™ user terminals monitor one of several packet based signaling channels for monitoring system status and availability, monitoring for incoming call alerts, and maintaining synchronization. Calls in either direction are handled over the signaling channel through a series of information packets exchanged between the user terminal and the Ground Control Station. Once the parameters for the call and the call connection have been established, the GCS assigns a call spreading code key to the user terminal and the user terminal and the GCS transition to this "code channel" for the call itself.

During the course of the call there is occasional need for control information, such as for power control settings, to be passed between user terminal and GCS. This information is inserted among the data bits pertaining to the call itself in a manner that is invisible to the user. Some functions, such as simple requests for position determination, and some types of short messages, such as for paging, are handled uniquely over the signaling channels. Ellipso™ will handle advanced signaling and call services available through the public switched telephone network. In all respects Ellipso™ will offer the modern call features that many users have come to expect from a telecommunications service.

Ellipso™'s Approach to Multiple Access: CDMA

Ellipso™ has chosen to use Code Division Multiple Access (CDMA) to permit multiple simultaneous access by many subscribers to Ellipso™ resources. CDMA has shown itself to be ideally suited for the mobile satellite environment, combining superior capacity, robustness, and flexibility when compared to system designs using other multiple access techniques.

Most mobile satellite systems will want to support many users simultaneously (permit "multiple access") in order to serve many subscribers and use system resources efficiently. There are several fundamental approaches for doing this. Each involves dividing up a resource and allocating a portion to each active channel.

The oldest multiple access technique divides up the frequency band to be shared into portions having a differing frequency and allocates a portion to each signal. The AM and FM broadcast bands use this technique to permit many radio stations to operate at once. This technique is known as Frequency Division Multiple Access (FDMA).

A second technique is to assign to each user the same frequency and allocate to each a different time to transmit. This is known as Time Division Multiple Access (TDMA). A conference call or a voice radio network are older examples of this approach. Digital techniques have refined this technique so that turns can be taken so quickly that it appears to each user that he has a full-time channel. The new digital GSM cellular standard is a modern application of TDMA.

The newest multiple access technique to come along is Code Division Multiple Access (CDMA), the technique Ellipso™ has chosen. Here each user is allocated the same band, in its entirety on a continuous basis. Each user is assigned a unique spreading code for spreading his signal to fill the band. The spreading code has a "processing gain" associated with it, which translates into an ability to recover the desired signal in an environment of strong interference. The greater the processing gain, the greater the permissible interference. Since each user's signal accounts for a portion of the total interference present, CDMA can be described as a means for dividing up a total permissible interference budget among simultaneous users.

How CDMA Works

The signal spreading process, using a high speed digital pattern known to both the transmitter and receiver, is the basis for CDMA. The transmitter spreads its signal using a code assigned to it by a code management function. The receiver multiplies everything received in the desired band (including the desired signal, noise, and other signals in the same band) by a synchronized copy of the spreading code used to spread the desired signal. This process has the very useful effect of causing only that signal that was spread with the same spreading code to collapse to the relatively narrow bandwidth it occupied before it was spread at the transmitter. This reconcentrates the signal's energy into its original narrow band.

But any signal at the receiver that was not originally spread by the same synchronized spreading sequence will be spread across the entire band by the same process that de-spreads the desired signal. This is true regardless of the nature of the interfering signal or noise. Consequently the signal energy from other signals in the band and from noise is made dilute in frequency, while the desired signal is concentrated (by a ratio equal to the ratio of the spreading code symbol rate to the de-spread signal symbol rate, which is the processing gain). Receivers can thereby pick out individual, weak signals that are otherwise lost under interference from a much stronger composite of many other signals and noise in the same band, when the receiver knows the appropriate spreading code, and when the code in use has adequate processing gain.

CDMA's Advantages

CDMA's characteristic of apportioning total aggregate interference confers a number of advantages that in turn translate into remarkable advantages in efficiency, robustness, and flexibility when compared to other techniques.

Frequency Re-use in Every Beam and Every Satellite.

FDMA and TDMA signals are prone to catastrophic disruption by interference. Therefore FDMA or TDMA systems must ensure that no such interference occurs by 1) ensuring that no other systems or sources interfere significantly, and 2) ensuring that neighboring cells, beams, or satellites within the same system are isolated from each other by using different times or frequencies for them and commanding user terminals to switch frequencies or time slots when the cell or beam providing service changes. This switching requirement can cause brief disruptions or delays to service and complicates user terminal design.

CDMA systems, on the other hand, can accept interference. They are built to do so. The degrading effect of interference on system performance is more than compensated for by the lack of any requirement for isolating neighboring cells, beams, or satellites. As a consequence, CDMA enables a system to reuse all available time and frequency resources in every beam and in every satellite. This in turn permits hand-offs from beam to beam and satellite to satellite, even potentially from satellite to terrestrial CDMA systems, that do not require any frequency or time adjustment at the user terminal (known as "soft hand-offs"). All hand-off processing can be handled solely at the Ground Control Station.

Path Diversity

Frequency reuse in every beam also permits a second very important performance advantage, that of path diversity. Every Ellipso™ satellite in view will receive the Ellipso™ subscriber's transmitted signal and relay it to the Ground Control Station. The Ground Control Station will combine all received signals to create a composite signal

that is better than that from any single path. In this way, if the signal over one path fades due to shadowing or blockage, the Ground Control Station will automatically adjust by using the signal carried by another path. In this way the incidence and depth of fading is greatly reduced over that encountered in systems that do not use path diversity. This process also automatically compensates for any failures in individual satellites. Observations of signal strengths in the subscriber-to-Ground Control Station direction can be used in turn for selecting the best path for signals to the subscriber. TDMA or FDMA systems cannot use path diversity without complex switching techniques designed to keep interference at a minimum.

TDMA and FDMA system's inability to use path diversity forces such systems to use a brute-force technique for combating fading: ensuring that enough signal power will be available the one link that serves each subscriber to overcome most signal strength losses from fading and shadowing. This dramatically increases total satellite power requirements and consequent cost. It also causes difficulties in meeting regulatory limits[2].

Soft Capacity Limit

CDMA systems have a "soft" capacity limit that automatically adapts to changes in system characteristics. Specifically, the addition of a user above the nominal capacity limit degrades the signals of all user's sharing the spectrum slightly rather than degrading the signals of a few other's catastrophically. In a pinch (for example, to handle an unforeseen peaking of demand), a slight degradation in everyone's signal quality can be traded for more capacity, if desired.

In contrast, TDMA and FDMA systems have hard capacity limits. It is not possible to exceed the capacity limit as the attempt causes the complete loss of an equal number of existing user channels. Once all the frequency or time slots are occupied, capacity is exhausted.

Easier, More Flexible Sharing Among Multiple Systems

Rather than segmenting the MSS band and assigning a segment to each MSS system, as is normal practice, CDMA MSS systems can all share the same complete band by assigning a maximum interference budget to each. In fact, since thermal noise is an important contributor to total interference, CDMA systems actually lose less capacity by sharing the complete band with each other than by segmenting the band and assigning a non-shared segment to each.

Full-band sharing also facilitates adjustment in the apportionment of band resources if the number of active systems changes (activation of a new system or withdrawal of an existing system). Instead, each system merely readjusts power commensurate with its new interference allocation.

In addition, full band interference sharing requires no wasted guard times or frequencies to ensure that no adverse bleed-over of power from one system to another occurs.

Additional Capacity by Voice Activation

When a speaker on a voice circuit is listening, his terminal can power down to conserve power and reduce interference to others. This is called voice activation. This action automatically makes room for other users. Since the only factor of importance in a CDMA system is the total interference, if the number of users is large, voice activation permits an increase in the total number of simultaneous users. Unlike TDMA systems, which sometimes also dynamically reassign channels based on user pauses, CDMA systems do not require complex switching capabilities to implement voice activation.

Resistance to Fading

Spread signals have better resistance to multipath fading. Multipath reception (a situation where signals from the transmitter arrive at the receiver over more than one path due to signal reflections) causes frequency selective fading of the received signal (that is, portions of the signal at different frequencies fades at different times). The broad bandwidth of the spread CDMA signal averages much of the frequency-selective fading, resulting in substantially reduced fading levels compared to more conventional narrowband signals, which are not generally wideband enough to permit useful frequency averaging.

Precise Relative Time Measurement

The same spreading code that reduces the effect of multipath fading also gives the signal a much higher resolution in time. This high resolution enables more precise time of arrival measurements, which in turn translate into improved geolocation measurements. The Global Positioning System (GPS) uses spreading codes for this same purpose.

---

[2] For these reasons, for example, Iridium chose to use the Mobile Satellite Service uplink band for their downlinks, since Iridium's high downlink signal strength requirements exceeded international limits in the Mobile Satellite Service downlink band, and since the uplink band has no downlink limits (downlink service in the MSS uplink band is permissible on a secondary, non-interference basis). (ref: Motorola Inc. "Why the Iridium System Cannot Use the 2483.5 2500 Band for its Space-to-Earth Link", Feb 4, 1993, document IWG1-28, MSS above 1 GHz Negotiated Rulemaking Proceedings, United States Federal Communications Commission.)

Privacy and Covertness

CDMA signals also lend themselves to communications security and privacy. The presence or absence of a signal destined for a particular user in the midst of interference from many users is very difficult to detect without knowledge of that user's spreading sequence. Likewise, the range at which a user terminal's CDMA emissions can be detected is smaller than for other types of signals, since the user's signal power is spread so widely (i.e., diluted) in bandwidth. It would be a simple matter to use spreading sequences that are very resistant to defeat or decoding for further enhancing signal security.

Ellipso™ Ground Network Highlights

The Ellipso™ ground segment must successfully accomplish a number of functions in order to offer a coherent, durable, flexible, and broadly capable mobile telecommunications service to its subscribers. These functions include:

- Subscriber record keeping and verification and vali dation,
- Call connection through the Ellipso™ satellite path from the mobile Ellipso™ subscriber to the GCS,
- Selection and maintenance of the optimum mobile satellite ground path for the call,
- Configuration of the mobile-satellite-GCS path to yield optimum signal quality, coordination of call ser vices and features,
- Interconnection of the call to the public telephone network as necessary, proper signalling coordination with the network,
- Geo-location of users, derivation, maintenance, and transfer of user location and status information around the network as needed,
- Ellipso™ transaction accounting at national, regional, and global levels,
- Creation and maintenance of an optimum network configuration for efficient Ellipso™ network opertion,
- Efficient Ellipso™ resource allocation,
- Maintenance of Ellipso™ system health, and
- Ellipso™ system planning.

In the Ellipso™ System, these functions are distributed among several functional elements of the Ellipso™ ground segment. They include the Ground Control Stations (GCS), the National Network Control Centers (NNCC), Ellipso™ Switching Offices (ESO), the System Coordination Center (SCC), and Tracking, Telemetry, and Command Centers (TTCC).

A primary objective of the Ellipso™ System is to minimize development time and costs of the system. In order to do this Ellipso™ has chosen, insofar as possible, to use as much of the equipment, procedures, and interfaces of existing cellular systems as possible. Indeed, some service providers may wish to integrate Ellipso™ and cellular facilities and actions as a cost effective and sensible approach to an overall telecommunications package for the consumer. Ellipso™ has chosen to use the GSM model, equipment, and standards for its ground network.

As a second objective, the Ellipso™ ground network will intemperate with modern switching and trunking facilities and with the CCITT and ANSI Signalling System 7. Ellipso™ is expected to support many of SS7's advanced features.

The Ellipso™ ground system is designed to offer the same kinds of features subscribers seek in an advanced mobile system. These will include many of the CCITT Signalling System 7 features, such as call forwarding and caller identification. Ellipso™ will automatically support domestic and international subscriber roaming for incoming and outgoing calls, and call handoffs in order to optimize routing and minimize costs for the call.

The Ground Network Elements

These component elements of the Ellipso™ System operate together to enable the placement of a call through the Ellipso™ system between an Ellipso™ subscriber and any other caller, regardless of the callers connection or his location around the world.

The **Ground Control Station** acts as the ground to satellite interface point for the Ellipso™ ground network. It handles the actual connections to the satellite, including the functions of satellite acquisition, tracking, handoffs, signal modulation and multiplexing. The GCS is essentially a ground entry point for the system. Each GCS typically tracks and uses two satellites while acquiring a third. The GCS exchanges user traffic channels and signalling information with an Ellipso™ Switching Office and control and status information with the NNCC for the area. The GCS also determines the position of subscriber terminals using various techniques over the GCS satellite-terminal path. The GCS interfaces to the Ellipso™ Switching Office and to the NNCC. Functionally it is analogous to a cellular system cell-site controller. Its interface to a Ellipso™ Switching Office will emulate that of a cell site controller as closely as feasible in order to simplify development and integration.

The Ellipso™ **Switching Office** includes a fault-tolerant, redundant switch together with a data processing system and subscriber and network data bases for managing subscriber affiliation, call placement, and network connectivity. The ESOs handle all the real-time switching and routing functions for the Ellipso™ portion of the ground network. ESOs may be collocated with the GCS or with the NNCC, may be collocated with or may be physically a part of the Mobile Switching Center serving a cellular system within an area, or may be remotely sited to serve one or more GCSs, depending on network requirements. The ESO interfaces in turn to the local PSTN in much the

same way a cellular Mobile Telephone Switching Office does and uses essentially the same interface standards and protocols. ESOs will accommodate X.25 and SS7 network interfaces. ESOs will also interconnect with the Ellipso™ NNCC for the served region for control and status purposes and for transfers of call record and subscriber information. Each ESO will interconnect with other ESOs within the region served by the supervising NNCC. ESO interconnections will include dedicated signalling and traffic trunks for accommodating handoffs.

Each Ellipso™ market is controlled by a **National Network Control Center.** The NNCC is the central network planning, management, and accounting facility for the market. It handles subscriber affiliation, record keeping, and validation, transaction accounting, roamer call routing, GCS management, satellite and network resource management for its market, time management, and system performance monitoring and maintenance. The NNCC interfaces to the market's GCSs and ESOs, as described earlier, and to the Ellipso™ SCC for transaction reporting, global roaming management, and system resource management.

The Ellipso™ **System Coordination Center** handles global level Ellipso™ functions. Overall Ellipso™ global system planning and allocation is handled here. The SCC is the central clearinghouse for Ellipso™ call transactions worldwide. It maintains a consolidated data base of all Ellipso™ subscribers and associated data, together with their present status and market location, and coordinates routing for internationally roaming subscribers. The SCC also manages worldwide Ellipso™ network management and system health and status. The SCC interfaces with the NNCCs for each of the Ellipso™ markets, and with the Ellipso™ TTCC for Ellipso™ satellite segment health, status, and management. Separate SCCs may be established for the Borealis and Concordia subconstellations.

The Ellipso™ **Tracking, Telemetry, Command Center** is the operational control center for the Ellipso™ satellites. At least two TTCCs will oversee the Ellipso™ satellites; each will be located where together they can see each satellite on every revolution. The TTCC oversees launch, orbital insertion, and satellite commissioning in conjunction with the satellite and launch providers. The TTCC continues to monitor and control the function and integrity of the satellites and their orbits and payloads. The TTCCs will also determine accurate satellite ephemeris information for use in geolocating subscriber terminals and managing satellite allocation and handoffs at the NNCC level.

Figure 6 illustrates the interconnections and hierarchy of the various Ellipso™ Ground Network elements.

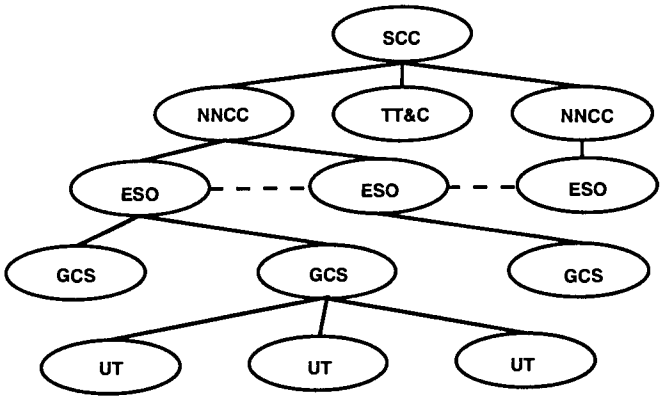

Figure 6: The Ellipso™ Ground Station Hierarchy

Ellipso™ Ground Network Deployment

The deployment of Ellipso™ Ground network resources (GCSs, ESOs, and the NNCC) within a market will be very significantly affected by conditions in the market. Significant factors include population and population distribution, demand for Ellipso™ services, the availability, nature, and economics of the existing telecommunications infrastructure, the geographic location of the market, and the Ellipso™ subconstellations used for service.

The Ellipso™ satellites operate at medium earth orbit (MEO) altitudes. As a consequence, each satellite is capable of seeing a much larger area than low earth orbiting (LEO) satellites can see. This significantly reduces the number of ground entry stations the Ellipso™ System requires in order to maintain good joint visibility statistics between the subscriber and the ground entry station, in comparison to a LEO system (conceivably, if territorial interests and the availability and cost of trunking were not factors, Ellipso™ could operate well with only fourteen Ground Entry Stations strategically located around the world). LEO systems must either use a larger number of more closely spaced ground entry stations, more ground entry station handoffs, or intersatellite links in order to prevent poor service (satellite having difficulty seeing both the user and the ground entry station).

As with other satellite systems, Ellipso™'s requirement for the number and location of GCSs is first and most importantly determined by common visibility requirements from the satellite to both the subscriber and the GCS. In many areas of the world, geographically small markets (less than 1,000 kilometers in extent) with undemanding network requirements may be adequately served by a single Ellipso™ GCS, ESO, and NNCC. A second may be desirable for redundancy purposes. Markets having significant geographic extent like the United States, Canada, Australia, Indonesia, China, and so on will require more than one GCS in order to ensure adequate satellite joint visibility statistics. Generally, GCSs should be located

near the extremes of travel of the satellite sub-points as the satellites travel over the market area, with additional intermediate GCS locations if the market extent warrants it. For example, in an area the size of the United States, two GCS locations would satisfy joint visibility requirements for Borealis.

As a market grows, the local Ellipso™ operator may wish to install more GCSs in order to provide better service at lower cost. For example, siting GCSs near important centers of population may offer favorable trunking economies for completing calls to ground telephone users.

Status and Summary

In summary, Ellipso™ is designed to succeed with a minimum required system financial investment and low cost to the user. It is structured so that it can begin earning revenues early in its deployment phase. Ellipso™ will offer an unprecedented degree of deployment flexibility and is able to tailor its geographic coverage in response to demand and investment. Ellipso™ uses innovative technical features in seeking optimum system efficiency. These features include efficient elliptical orbits for better satellite utilization, and CDMA for maximum spectrum efficiency. Ellipso™ provides an attractive service to the user, one having a low per-minute cost and non-disruptive seamless service transitions and link hand-offs. And Ellipso™ s system characteristics permit adjustment to suit technical and market conditions in each of the regions it serves.

Ellipso™ represents the optimum business and technical approach to introducing new mobile satellite services to users throughout the world. The Ellipso™ project is proceeding rapidly to detailed system engineering and construction.

Non-GEO Mobile Satellite Systems: A Risk Assessment

Leah M. Gaffney
404-592-1681
lgaffney@mitre.org

Neal D. Hulkower
617-271-6959
hulkower@mitre.org

Leslie Klein
617-271-6128
lklein@mitre.org

The MITRE Corporation
202 Burlington Road Bedford, MA 01730-1420 USA

ABSTRACT

Since 1991, The MITRE Corporation has performed several independent evaluations of proposed mobile satellite service (MSS) systems that would operate from low Earth orbit (LEO) or medium Earth orbit (MEO), also known as intermediate circular orbit (ICO). This paper introduces a top level Risk Taxonomy tailored to summarize the technical and programmatic risks that MITRE has identified. In general, as risks are identified and addressed, a system's technical characteristics, cost and schedule are affected. This paper traces changes in three key parameters – satellite launch mass, system cost, and system schedule – for each of the five original non-GEO MSS systems for which license applications were made to the U.S. Federal Communications Commission (FCC) from November 1990 until June 1991. Finally, specific risk areas are identified using the Risk Taxonomy as a framework for discussion.

Full text of the paper is in the Appendix page A-23

Direct Broadcast Satellite

11

Session Chairman: **Don Messer**, Voice of America, USA
Session Organizer: **Gérald Chouinard,** Communications Research Centre, Canada

Topic Introduction: Broadcasting of sound programs directly to vehicular, portable and fixed receivers has gained much importance lately with the allocation of three frequency bands at 1.5 GHz, 2.3 GHz and 2.5 GHz specifically for the *Digital Audio Broadcasting Service (DAB)* at the WARC '92. Since then, more work has been done to refine the service concepts and the various technologies required. In particular, only advanced digital modulation schemes are now being considered along with channel coding and time interleaving to combat the transmission channel distortions. Although unidirectional in nature, this service is related to the other mobile satellite services covered in this conference due to the fact that it will operate in the same frequency range, encountering similar propagation conditions for the mobile vehicle reception.

In this session an examination of the propagation aspects related to direct reception of sound broadcasting from satellite and an overview of mitigation techniques is presented. The need to achieve the use of a common frequency band and a common non-proprietary emission format is explored. A description of the Archimedes system is presented where HEO satellites would be used for broadcast services. The mixed concept where the same frequency band and a common emission format are used by both satellite and terrestrial broadcasting services is also presented. There is a description of the results of simulation studies and measured receiver performance from JPL. The session ends with an investigation of the merits of satellite spatial diversity.

Overview of Techniques for Mitigation of Fading and Shadowing in the Direct Broadcast Satellite Radio Environment

David Bell, John Gevargiz, Arvydas Vaisnys and David Julian
Jet Propulsion Laboratory
California Institute of Technology
4800 Oak Grove Drive
Pasadena, Ca. USA 91109
Telephone: (818) 354-3828
dbell@qmail.jpl.nasa.gov; gevargiz@semi.jpl.nasa.gov;
avaisnys@qmail.jpl.nasa.gov; djulian@nmsu.edu

Abstract - **The DBS radio propagation environment is divided into three sub-environments, indoor, rural-suburban mobile and urban mobile. Indoor propagation effects are in a large part determined by construction material. Non-metallic materials afford direct, albeit attenuated, penetration of the satellite signal with a minimum of multipath signal scattering. Signal penetration into structures using significant metallic materials is often indirect, through openings such as doors and windows and propagation will involve significant multipath components. Even so, delay spread in many situations is on the order of 10's of nanoseconds resulting in relatively flat fading. Thus frequency diversity techniques such as Orthogonal Frequency Division Multiplex (OFDM) and Code Division Multiple Access (CDMA) or equalization techniques do not realize their intended performance enhancement. Antenna diversity, directivity and placement are key mitigation techniques for the indoor environment. In the Rural-Suburban mobile environment with elevation angles greater than 20°, multipath components from the satellite signal are 15-20 dB below the line-of-sight signal level and often originate from nearby reflectors. Thus shadowing is the dominant signal impairment and fading effects are again found to be relatively flat for a large fading margin. Because receiver motion induces rapid variations in the signal level, temporal diversity techniques such as interleaving, channel coding and retransmission can be used to combat short intermittent fading events. Antenna diversity and directivity techniques are again useful in this environment. Finally, in the Urban mobile environment, slower vehicle speeds and blockage by buildings causes signal fades that are too long and too deep to combat with signal margin or time diversity. Land-based signal boosters are needed to fill in the coverage gaps of the satellite only broadcast scheme. On frequency boosters are suggested to conserve bandwidth yet these produce long delay multipath and create a frequency selective fading environment. Enter now OFDM, spread spectrum, equalization and other techniques that are capable of deconvolving the channel effects and effecting significant performance improvements by extracting the frequency diversity or time diversity components comprising the received signal.**

Introduction

Mobile radio propagation at L- and S-bands is hampered by signal shadowing and multipath from natural and man-made structures. The understanding of these effects and their mitigation are the subjects of many technical articles and books. A subset of these investigations are either applicable to or directly address Land Mobile Satellite Service (LMSS) configurations. We can further subdivide these into three propagation environments, indoor, rural-suburban mobile and urban mobile. Any Direct Broadcast Satellite - Radio, DBS-Radio, system design is based in large part on a thorough understanding of the propagation impairments and mitigation techniques associated with these environments.

The three following sections address these three environments. In each section we review important results from applicable UHF, L-band and S-band propagation measurements and discuss techniques to mitigate the LMSS signal impairments. In the sections covering indoor and rural-suburban mobile propagation, Satellite-only broadcast is assumed. In the urban-mobile section, it is noted from the outset that severe satellite signal shadowing requires some form of gap-filling technology. On frequency repeaters are suggested for reasons of bandwidth efficiency and discussion switches to a joint satellite ground transmission scheme and the associated propagation effects and mitigation.

Propagation for Indoor Portable Reception

One of the common environments for DBS-Radio will be the indoor home or business environment and listeners will expect adequate reception using only the antenna built into the receiver. Understanding the satellite to indoor propagation mechanisms is therefore of prime importance to the DBS-Radio system designer. In this regard there are many experimental results in the literature describing the propagation impairments associated with building penetration and indoor propagation at UHF, L-band and S-band frequencies. Table 1 summarizes some of these results that apply to DBS-Radio.

Spatial Variations

As expected, building structure and construction materials have a large impact on propagation effects. Non-metallic construction homes exhibit the lowest mean signal attenuation, 5-11 dB, with a standard deviation of 2-3 dB as the receiver is moved around inside the building, [2][3]. Signals penetrating office structures with some metallic construction materials experience larger mean signal losses of 5-14 dB. Reduction of the direct signal and increased multipath from the metallic materials raises the received signal standard deviation to 3-10 dB, [3][4][6]. An analysis of the spatial variations inside two office structures [6] showed close agreement with a Rician distribution having random/specular power ratio, K = -6.8 dB for one building and K= -11 dB for another. The spatial signal variations measured showed a quasi-periodic structure with trough-to-trough distances of 2-4 wavelengths for the satellite transmissions and 0.5 to 1.5 wavelengths for the low elevation angle transmissions. The reasons for this difference were not concluded.

Spectral Properties

ATS satellite tests [4] of signal penetration into single family non-metallic construction dwellings showed mean attenuation increasing by 2-3 dB per frequency octave over the range of 0.9 to

2.6 GHz. In particular they measured mean signal losses of 4.6 dB, 6.7 dB and 7.5 dB for 860, 1550 and 2569 MHz frequencies respectively. This same characteristic was corroborated by measurements reported in [3]. The opposite trend was observed for office buildings and semi to heavily metallic structures. Attenuation in these structures was observed to decrease by 2-5 dB per frequency octave, [3][7][8][9].

The following explanation seems reasonable. For the non-metallic structures, the primary signal penetration and propagation paths are through walls and ceilings. This mode favors lower frequencies. In the case of office buildings and other structures using metallic construction materials, the primary signal penetration and propagation paths are through openings such as windows, doors, etc. This mode favors higher frequencies.

Temporal Signal Variations

Even with the transmitter and receiver locations fixed, the signal level at the receiver can vary significantly according to changes in the environment that affect propagation paths. Low elevation angle, $\approx 0°$, experiments showed indoor temporal signal fading that was Rayleigh or Rician distributed with a dynamic range of 17-30 dB [6]. These variations resulted from the movement of outdoor traffic or people and doors inside the building which changed propagation geometries. In higher elevation satellite experiments [3] people moving near the receiver produced less than 0.5 dB signal variation. Presumably the higher elevation angle signal and its reflections encountered fewer moving objects in their path to the receiver, thus there was little to no change in the propagation paths. The exception to this was when a person blocked the direct transmission path, resulting in signal attenuation of 6-12 dB.

Elevation Angle Properties

Signal loss measurements made in [3] and [4] showed no dependence on elevation angles ranging from 12° to 55° for structures not blocked by external objects. Two different explanations accompany this result. First, for non-metallic structures where signal penetration is primarily though walls and ceilings, a signal arriving at an elevation angle greater than 10° will not encounter many movable obstacles and thus the signal variations were fairly similar over the test range of 12° to 55°. Second, for metallic structures were signal penetration is primarily through openings, the elevation angle of the direct signal has little to no impact on the entrance of the signal into the building and thus we would expect no dependence on elevation angle.

Delay Spread

In the articles that were reviewed, measured delay spread varied over a range of 10 ns to 350 ns. This corresponds to a coherence bandwidth range of 0.5 to 17 MHz. Thus we can say for most single channel per carrier DBS-Radio broadcast schemes, the indoor fading channel will look flat across the band.

Difficult Situations

There are many structures and situations were there is significant excess path loss. These include family dwellings and non-residential buildings using significant metallic construction including aluminum siding, corrugated steel, wire mesh screens, aluminum backed sheetrock, etc. The construction materials used in these buildings inhibits signal penetration through walls and entrance of the signal through openings such as doors, windows, etc. becomes the primary mode. The average path loss in these cases can be 10 to 20 dB more than the nominal 5 to 11 dB observed in structures making less extensive use of metallic construction materials.

Structures shadowed by trees, mountains or other buildings will experience excess loss if the obstruction blocks the satellite line-of-sight. During 1.6 GHz measurements on residential structures in Houston, TX [4] excess signal blockage from trees was measured at 12-15 dB. These blockage situations would increase in number and likely intensity as elevation angle decreases.

Signal Fading Mitigation for the Indoor Environment

Ten to fifteen dB fade margin will mitigate direct path signal attenuation in structures that make partial or no use of metallic construction materials. Additional techniques are needed for deep fades in bad locations or in difficult buildings making extensive use of metallic materials.

The spatial null separation measured in [3] and [6] suggests that a diversity antenna separation of 1 wavelength could put one antenna out of a null zone. Difficult structures may require the placement of an antenna external to the structure.

An alternative to antenna diversity is to use antenna element combining or switching to achieve signal directivity/nulling and thus reduce multipath fading.

The simplest mitigation technique is the listener's effort to place the radio or its antenna in a good signal location. This approach may be somewhat hampered by the proximity effect of the listener's body.

Spread spectrum, COFDM and equalization techniques can help in the office building environment where coherence bandwidth is smaller and standing wave signal levels had a measured standard deviation of 3-10 dB. These techniques will be less effective in residential structures where delay spread can be less than 10-20 ns. More discussion is given to these schemes later in this paper.

Propagation for the Rural and Suburban Satellite-Mobile Environment.

A significant body of measurement results and theoretical modeling exists on the LMSS channel. As part of this, important LMSS propagation tests were accomplished in the United States by Hess [11] and Goldhirsh, Vogel, et. al.[see Table 1.1 of Ref. 17 for list of 11 publications], in Canada by Butterworth [12][13], in Europe by Jongejans et al., [14], and Renduchintala et al., [15] and in Australia by Bundrock [16]. These tests included ATS-6, MARECS, INMARSAT, and ETS satellites as well as simulations of the LMSS channel using balloons, towers and aircraft. Results from these sources were distilled by Goldhirsh and Vogel in NASA Reference publication 1274, "Propagation Effects for Land Mobile Satellite Systems: Overview of Experimental and Modeling Results" and released in February 1992 [17]. The results of these and related studies are further distilled and summarized in table 2.

The coarse structure of the LMSS signal fading is dominated by the intermittent blockage of the line-of-sight by roadside objects such as building and trees. In the rural and suburban environment tree shadowing is the predominant LMSS signal impairment. In most situations in the Continental United States (CONUS) the elevation angle to a direct broadcast satellite would be above 20° with the result that the attenuation path is limited to 1 or 2 tree

canopies. The mobile antenna is often directive in elevation, discriminating low elevation signal scattering and multipath reflections from the ground. Thus signal absorption, scattering and re-radiation by the canopies of 1 or 2 nearby trees gives rise to the major attenuation components. Although omni-directional antennas are more susceptible to low angle multipath from surrounding signal scatters, it was found through measurements and modeling that even with these less directive antennas, the primary fading effects arise from the shadowing of the line-of-sight signal component.

Vogel and Torrence [18] simultaneously measured signal attenuation at 1600 and 2500 MHz of various tree types. Their results showed average fades of 4 - 9 dB with no measured dependence of fade level on frequency. Multipath components appeared at a level 15-20 dB below the unattenuated line-of-sight signal and thus the shadowed line-of-sight signal dominated the propagation statistics recorded. Results summarized in the NASA publication [17] showed similar fade levels with some tendency of increased signal impairment for increasing frequency. Of particular interest is the finding that signal absorption and scattering from branches is the main attenuation mode as opposed to the effects of leafy foliage. Goldhirsh and Vogel quantified the effect of full foliage as an increase of 35% in average signal attenuation over bare tree signal attenuation.

L-band measurements made by Vogel and Goldhirsh over 600 km of 2-lane and 4-lane highways and rural roads in Maryland using helicopter platforms and the MARECS-B2 satellite were used to derive an empirical "best fit" expression of cumulative fade distribution [17]. Data was taken at elevation angles of 21°, 30°, 45° and 60° and signal arrival was primarily perpendicular to the roadway, corresponding to maximum shadowing conditions. The dominant sources of shadowing were the roadside tree canopies with some shadowing from utility poles and only minor multipath. Roadside trees were primarily deciduous and resulted in 55% to 75% shading of the right lane in the direction of travel. Figure 1 from [17] plots some results of the cumulative fade model. Model agreement with the empirical distributions is within 1 dB for all four elevation angles measured.

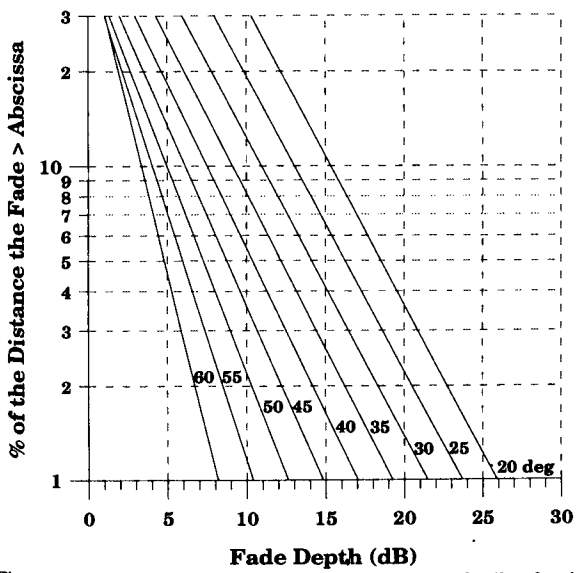

Figure 1: Cumulative fade distributions at 1.5 GHz for family of path elevation angles derived from the empirical Roadside Shadowing Model by Goldhirsh and Vogel [17].

Note the strong dependence of fading statistics on elevation angle. Combine these with figure 2 showing the elevation angle contours over North America resulting from a direct broadcast satellite favorably located at 100° west Longitude. Assuming similar ground environments, a user in rural Texas might see a 10 dB signal fade less than 2% of the time while a user in Washington state would experience a 10 dB fade 20% of the time. Similarly, if we choose a fixed fading percentage of 2%, the user in Texas requires only a 10 dB margin while the user in Washington state requires an 18 dB margin. One solution to this problem is to taper the satellite beam gain to direct more power toward regions with at elevation angles. Iridium satellite design uses this approach to provide 8 dB more gain to users at an elevation angle of 10° than users at an elevation angle of 50° [21]. Gaudenzi and Giannetti [25], emphasizing the desirability of high elevation angles, propose a constellation of satellites in Molniya type highly elliptical orbit (HEO) after a detailed orbit tradeoff study done by British Aerospace, et al. [26]. The proposed HEO constellation would provide the majority of Europe with a elevation angle greater than 60°.

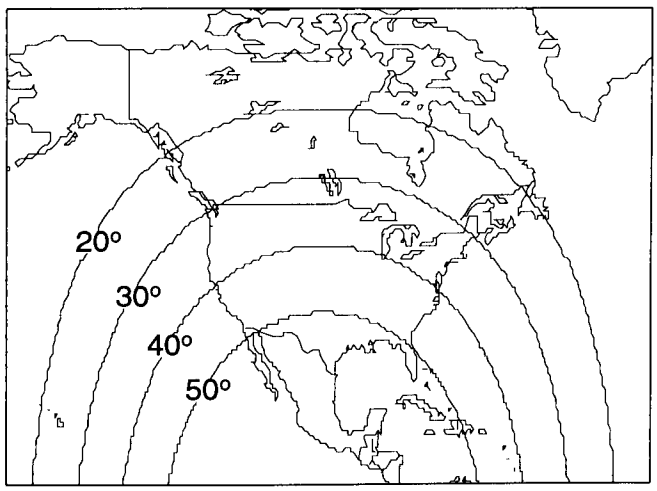

Figure 2: Elevation Angle Contours for direct broadcast GEO-stationary satellite favorably located at 100° west Longitude for North American Service.

While cumulative fade statistics are important they do not provide sufficient information to design fading counter measures. Additionally we need some measure of fade and non-fade durations. These depend on both the fading environment and the mobile speed through that environment. We should also consider signal phase fluctuation statistics to complete the picture.

Signal Margin and Time Diversity as Satellite Mobile Fade Mitigation Techniques

With the mobile environment comes rapidly time varying signal fading but also the possibility of combating the same with temporal diversity techniques. The effect of the LMSS shadowing environment is to knock out blocks of bits, block size varying with the fade duration. Time diversity techniques can be used to randomize the outage patterns through interleaving or repeat transmission so that some form of channel coding can reconstruct the original data in the decoding process. In the case of interleaving, block or convolutional error correcting codes are often applied before interleaving and the effectiveness of the decoding procedure in reducing bit error rate depends not only on

the average blocking percentage but on the ability of the deinterleaver to randomize the fading events chopping up long fades into smaller portions and redistributing them so that the error correcting code can handle them. In fact if a time diversity technique is unable to randomize a fading event (interleaving) or produce uncorrelated faded samples of the same symbol (repeat transmission) no reasonable channel coding technique will be capable of providing significant BER improvement on data sent over the LMSS channel. How does one predict the effectiveness of time diversity techniques and compare their effectiveness with other techniques such as simple addition of signal fading margin. This question will be addressed in this section by investigating an example time diversity strategy, i.e. repeat transmission.

The combination of fade and non-fade duration statistics are commonly used to characterize the temporal nature of signal fading in the mobile channel. In our investigations of repeat transmission we processed the signal level time history generating the related statistics, joint signal fading and fade autocorrelation, which more succinctly predict the effectiveness of a simple dual transmission scheme. We first generate the statistic $P_2(\tau,Z)$, the joint probability of fade at time (t) and (t+τ):

$$P_2(\tau,Z) = p(S(t) < -Z \text{ dB}, S(t+\tau) < -Z \text{ dB}) \quad (1)$$

where Z is the allowable fade margin and S(t) is the signal power time history normalized to the unobstructed line-of-sight signal power. If we define the hard limit inverting function H(x) as

$$H(x) = \begin{cases} 1; & S(t) < -Z \text{ dB} \\ 0; & S(t) >= -Z \text{ dB} \end{cases} \quad (2)$$

Then

$$E[H(S(t)H(S(t+\tau))] = p(S(t) < -Z \text{ dB}, S(t+\tau) < -Z \text{ dB}) = P_2(\tau,Z) \quad (3)$$

is the signal blocking percentage for single transmission diversity given a fade margin of Z dB.

Note that $P_2(0,Z) = p(S(t) < -Z \text{ dB}) = P_1(Z)$, (4)

Also note that fade autocorrelation, as we have defined it is:

$$R(\tau, Z) = \frac{P_2(\tau, Z)}{P_1(Z)} \quad (5)$$

Vogel and Torrence recently completed S-band mobile propagation measurements in and around NASA JPL [20]. The TDRSS satellite transmitted a 2050 MHz carrier only signal that allowed for 35 dB of measurable fading relative to the line-of-sight signal strength. Elevation angle to the S/C was 22°. The test course included several types of terrain, NASA JPL (12 minutes), Six Lane Freeway (6 minutes), Downtown Pasadena California (7 minutes) and Residential (20 minutes). Figure 3a shows the joint fading statistic $P_2(\tau,Z)$ averaged over the entire 45 minute run and parameterized on the allowed fade margin Z.

At a time offset equal to zero, the y-axis value is the overall sample probability, $P_1(Z)$, that the signal fade exceeds the fade margin. Assuming we have collected a sample of signal fade

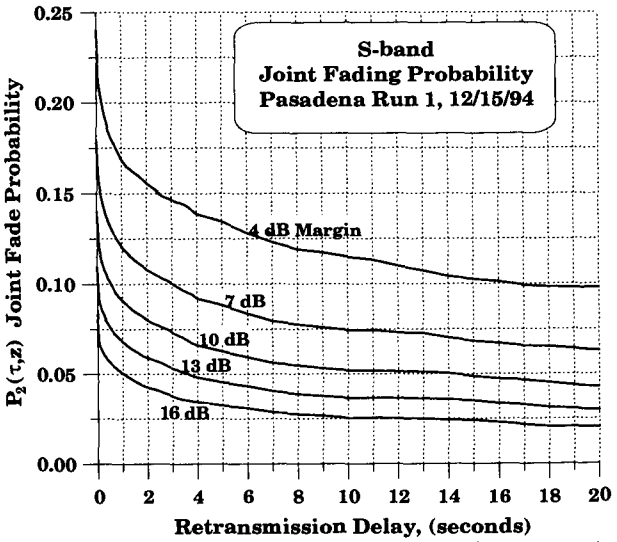

Figure 3a: Probability that Both Transmissions are Blocked; Statistic Averaged Over 45 minute Run through Various Terrains

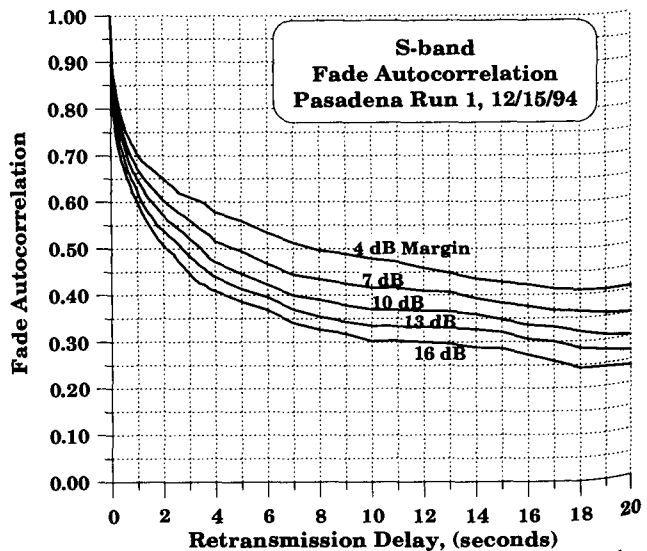

Figure 3b: Autocorrelation of Signal Outage Events; Statistic Averaged Over 45 minute Run through Various Terrains

statistics corresponding to typical mobile conditions, we now have a set of curves that at once indicate overall fade statistics and that decompose and display relative effectiveness of fade margin and time diversity in reducing the fraction of signal loss due to fading. For example, increasing the fade margin from 4 to 7 dB reduces fade time fraction from 24% down to 18%. A time diversity technique, such as retransmission, with a time delay of 0.6 seconds achieves the same effect. The sharp drop off of the joint fade statistic for short delays indicates that a significant amount of fading is short duration interspersed with non-faded times and can be mitigated with short delay retransmission or a combination of interleaving and coding.

Figure 3b is similar to figure 3a except all curves have been normalized to a value of 1.0 at a time offset of zero. The result is the conditional probability of experiencing a signal outage τ seconds in the future given that you are presently in the faded state, i.e. a true autocorrelation of the outage events. The curves show the increasing value of retransmission time diversity as the

fade margin increases. This is expected since higher fade margins eliminate many lower level fades opening up wide spaces of non-fade times that can be effectively utilized by time diversity techniques.

The results shown in 3a and 3b suggest combinations and trade-offs of fade margin and retransmission time delay that achieve some desired signal outage probability. In this capacity they are a tool to assist in communications system design.

We can extend this by parameterizing our analysis by terrain. Figure 4a shows the joint fading statistic $P_2(\tau,Z)$ as a function of terrain type for a fade margin of 10 dB. The Linda Vista residential roadway was lined with a canopy of leafless deciduous trees on both sides of the street presenting a roughly 60% tree shadowed environment. Note that the 33% fraction of time faded agrees well with the 30% value predicted from figure 1. Figure 4b, fade autocorrelation, shows how time diversity is more effective for some terrain types. Even though Linda Vista had twice the overall fading rate of Downtown Pasadena, a time diversity of less than 2.0 seconds is twice as effective at Linda Vista because the tree shadowing is characterized by many short duration outages while city driving results in longer periods of blockage due to larger blocking structures and slower mobile speeds. Not unexpectedly, time diversity is very effective in the freeway environment as higher mobile speeds result in shorter blockage times and the over all signal blocking percentage is lower.

This type of analysis can be extended to other time diversity schemes such as combined interleaving and coding, or multiple retransmissions. It could also be extended to antenna diversity.

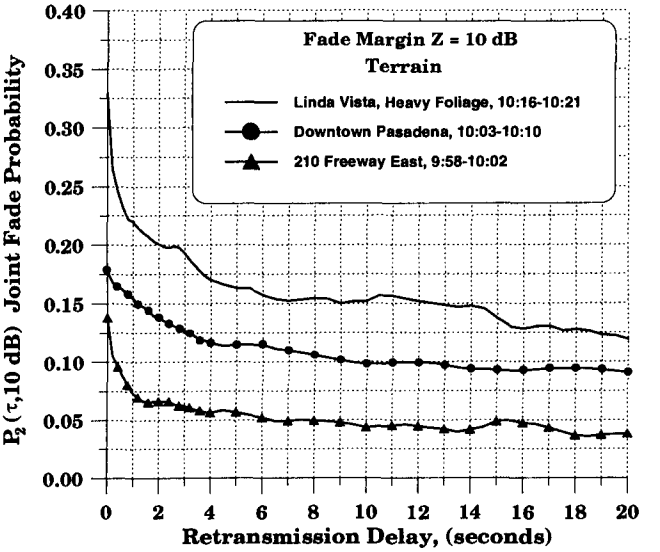

Figure 4a: Probability that Both Transmissions are Faded by More Than 10 dB; Parameterized by Terrain Type

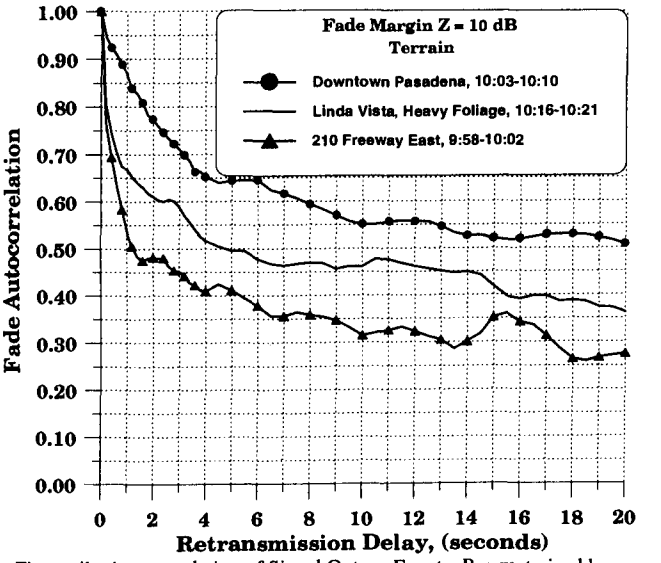

Figure 4b: Autocorrelation of Signal Outage Events; Parameterized by Terrain Type

Other Diversity Techniques For the Satellite Only DBS Radio Transmissions

As mentioned earlier, LMSS outdoor propagation effects are dominated by signal shadowing for the first 15 to 20 dB of fading. This limits the applicability of various diversity schemes. Frequency diversity or spread spectrum techniques are not effective because the shadowing effects are relatively flat across reasonable operating frequencies. Polarization diversity is limited because the shadowing can significantly diminish the polarization isolation. Measurements of tree shadowed signals reported in [18] showed cross-polarization levels 15-20 dB below co-polarization levels indicating that polarization isolation techniques have only marginal value.

Spatial antenna diversity is a scheme that can be effective for short distance outages such as those caused by tree branches. Consider a scenario of two spaced antennas atop a vehicle where each antenna feeds a separate receiver. If signal levels at the two antennas are even partially uncorrelated, selection of the higher level signal will result in some performance improvement. In fact if vehicle speed is recorded as part of a propagation test record, one can easily convert the fade vs. time data to fade vs. distance data and generate antenna diversity performance curves similar to figures 3a, 3b, 4a and 4b. As an example, the Linda Vista run of figures 4a and 4b included only one stop with average speed of about 12 meters/sec. Thus an antenna separation of 2 meters would be roughly equivalent to retransmission with a time diversity of 0.17 seconds. Based on the fade vs. time data such a two antenna diversity scheme would result in a 20% reduction in the time spent faded more than 10 dB. As vehicle speed decreases, time diversity becomes less effective whereas antenna spatial diversity maintains the same average performance enhancement regardless of vehicle speed.

Received Signal Phase Fluctuations

In brief, Vogel and Goldhirsh analyzed signal phase fluctuations recorded in "extreme" rural-suburban propagation environments, i.e., measurements made along roads having a "continuum of overhanging tree canopies where almost persistent shadowing occurred." They found that even in this worst case that for 98% of the time, measured phase fluctuation was no worse than +/-20° over a fading range of 2 to 8 dB. Based on this and results from more benign channels, they concluded that, "the influence of phase fluctuations on demodulation techniques at the elevation angle considered, (e.g. 51°), is minimal and that the LMSS channel characteristics can be estimated without considering phase." Recalling that multipath components were observed to be 15-20 dB below the line-of-sight signal level we may additionally conclude that phase fluctuations in the rural and suburban environment will not be significant except during deep fades. Conditions will worsen for lower elevation angles where deep

fades and multipath are more prevalent. A recent paper by Goldhirsh and Vogel investigates L-band amplitude and phase fluctuations for Satellite transmission scenarios at elevation angles ranging form 7° to 14° [28]

DBS-Radio Urban Propagation

Effectiveness of time diversity in all environments diminishes as the mobile speed decreases. When mobile speed is reduced to zero, i.e. stationary, time diversity is totally ineffective. This is particularly a problem in the city environment where traffic is stop and go and structures may completely block the line-of-sight signal. The ATS-6 satellite was used by Hess to measure UHF and L-band excess path losses in various cities [11]. As an example, in Denver, the satellite appeared to the southwest at 32° elevation. Streets running parallel to the satellite direction, i.e. NE/SW, experienced fades greater than 6 dB only 10% of the time, whereas streets running perpendicular experienced fades greater than 29 dB 10% of the time. This latter condition exceeds the mitigation capacity of any reasonable combination of fade margin and time diversity.

Urban Land-Based Gap Fillers

Land-based signal boosters have been suggested for this difficult urban environment. To minimize the spectrum requirements, we can further require the boosters to transmit the same program and signal structure as the satellite. The goal is to fill in the coverage gaps in the heavily shadowed city area. An unavoidable result of this scheme is the creation of severe multipath and intersymbol interference, ISI. Consider a DBS signal channel coded to a rate of 300,000 symbols/sec, (sps). One symbol time is equivalent to only 3.0 kilometers at the speed of light. Thus multiple symbol delays between booster signals are likely and the result will be ISI. Add to this the fact that low elevation angle mobile transmissions arrive at the mobile scattered by many intervening obstacles and you have at the receiver a combination of time delayed Rayleigh faded copies of the desired signal. Mutipath can be a desirable phenomena if we consider that it is equivalent to the repetitive transmission of the same signal. The signal from each source travels a different path to the receiver and thus experiences independent fading. This path diversity can be utilized if the modulation scheme is sophisticated, such as spread spectrum, or if the receiver has the sophistication to deconvolve the channel ISI effects, [22]. In further analysis we can consider the satellite as one of the boosters or if booster signal strength is overwhelming we can equivalently ignore the satellite signal.

Adaptive Equalization

Consider a single channel per carrier QPSK satellite system with on channel boosters in a metropolitan area. The requirement here is for an adaptive equalizer that can follow the phase and amplitude variations of the Rayleigh signal envelopes and deconvolve the combination of delayed signals were even the relative delays vary as the booster to mobile geometry changes.

This type of environment was investigated via computer simulation. Three Rayleigh faded copies of a QPSK 300,000 sps data stream are combined. Each signal is offset from the next by one symbol time delay and the average power of each component is equal. The Doppler spread of +/- 213 Hz on each signal is equivalent to a vehicle speed of 100 km/hr given a 2.3 GHz S-band transmission frequency. Signals plus white Gaussian noise (WGN) were applied to a Lattice Predictive Decision Feedback Equalizer, (Lattice PDFE) after Ling and Qureshi [23] and the resulting uncoded bit error rate was measured as a function of combined signal to noise ratio. Figure 5 shows the results for several different configurations. As part of JPL's DBS receiver development, we have used a Constraint Length =7, Rate = 1/2 convolutional code in conjunction with interleaving and a (160,140) Reed-Solomon code to combat short signal outages. An uncoded bit error rate, (BER), of 10^{-2} is needed to achieve 10^{-6} BER on such a concatenated coded channel assuming soft decision Viterbi decoding of the convolutional code. BER and Bit SNR values refer to information bits, i.e. results include the SNR cost of equalizer training symbol overhead.

The top curve indicates that the ISI and Rayleigh fading completely obliterate the normal QPSK signal structure with no chance of data recovery without equalization. The second curve shows the performance of a single diversity channel with one out of five symbols used for equalizer training/tracking. The third curve down is performance of the same equalizer structure but with one out of three symbols used for training. A bit SNR of 19 dB is reasonable in a ground transmission environment and thus our concatenated code performance of 10^{-6} is achievable.

The fourth curve displays the performance of a dual selection diversity system, where each receive string has a Lattice PDFE and the equalizer outputs are selected based on estimates of equalizer tracking error that are normally performed and available as part of the equalization process. The diversity gain is about 7 dB at the desired operating point. This is noteworthy for the DBS-Radio system designer.

The fifth curve down assumes a Rician channel where the unfaded signal, has a power equal to the average sum power of the two Rayleigh components. Diversity = 1 is also assumed. Note the improved equalizer performance for this Rician channel as compared to the Rayleigh channel even though both channels produce a 50% error rate without equalization.

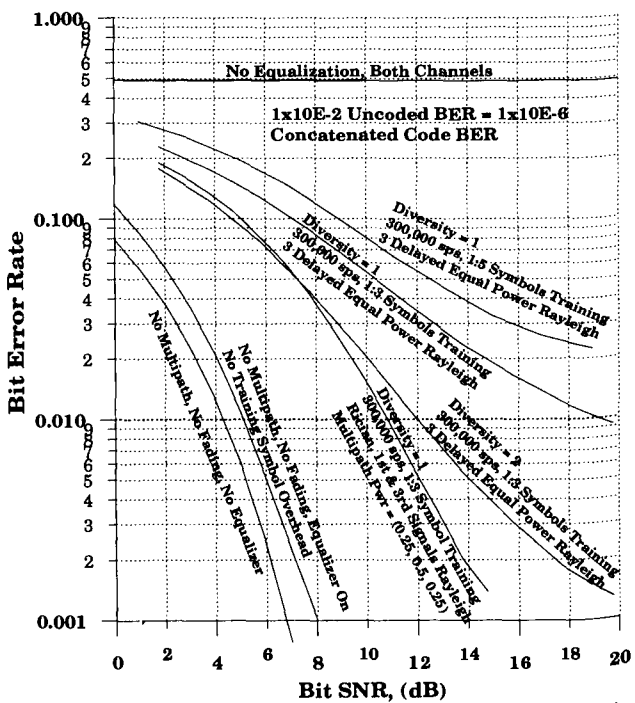

Figure 5: Lattice Predictive Decision Feed Back Equalizer Performance in Rayleigh and Rician Fading. Max. Doppler = 213 Hz, Equivalent Vehicle Speed = 100 km/h at S-band 2.3 GHz. Bit SNR Corrected for Training Symbol Overhead.

The sixth curve down shows performance of the Lattice PDFE in a white Gaussian noise only channel. Finally the standard theoretical performance of QPSK in a WGN channel is given as the last curve. The 1 dB performance penalty on the WGN channel is a consequence of adaptive equalizer attempts to track phantom channel variations caused by Gaussian noise.

Many different equalizer structures are possible but all at the expense of increased receiver complexity. The lattice PDFE was chosen because of it's adaptive ability, it's robustness to round-off errors and regular structure which lend it to VLSI implementation and its reduced computational complexity relative to other schemes. A more thorough description of the combined receiver-equalizer performance in the booster aided DBS environment is presented in another paper in this conference [29].

Coded Orthogonal Frequency Division Multiplex, (COFDM)

Coded Orthogonal Frequency Division Multiplex, (COFDM), is a technique useful in mitigation of frequency selective multipath fading and it is the basis of the Eureka 14.7 digital audio broadcast, (DAB), standard. The technique is particularly applicable to the on-frequency repeater transmission scheme. One or more high rate compressed and channel coded digital audio programs are transformed into N interleaved low-rate sub-streams and modulated onto separate subcarriers equally spaced 1/NT Hz, where T is the symbol timing. The number of carriers is chosen so that fading is flat across a single carrier but fading is independent among adjacent bits that have been assigned to diverse carriers and thus frequency interleaved. The channel effect on any particular carrier reduces to an amplitude scaling and a phase rotation. The use of a PSK signaling format then eliminates the need for amplitude correction and differential phase encoding at the transmitter allows differential phase correction at the receiver.

As with equalization techniques, COFDM diversity gains presume frequency selective fading across the signaling bandwidth. In rural and suburban environments and in the satellite broadcast environment the delay spread of the channel may be so short that fading tends to be flat or dependent across the channel. Typically the delay spread needs to be greater than the reciprocal of the program carrier spacing. When COFDM is working, subcarriers found in a spectral null will produce symbol errors at the detection stage, but these symbol errors are interleaved with correctly detected symbols from non-faded subcarriers and the channel coding scheme can effectively recover the lost information.

In an well written paper [27], Sari et al, show that OFDM is functionally equivalent to a single channel per carrier system employing frequency domain equalization. They further show that the two techniques with channel coding have essentially the same performance results in a frequency selective channel but that the single channel per carrier scheme has the advantage of low sensitivity to non-linear distortion, such as that found in a satellite transponder. The single carrier approach also alleviates the carrier synchronization problems associated with OFDM.

Antenna Directivity

This technique at once combats four propagation impairments. First, antenna directivity provides gain relative to an omni-directional antenna and can thus selectively enhance a desired signal and mitigate attenuation on that signal caused by shadowing. Second, antenna directivity reduces the number of multipath components by discriminating against much of the possible range of signal azimuth arrival angle. Third and forth, this same multipath discrimination also decreases Delay Spread and Doppler Spread in the booster assisted mobile environment where multipath signals with maximum delay and maximum Doppler offset often arrive at the mobile from nearly opposite directions [19]. If a sectored antenna is used with multiple receivers, (diversity), the effect is to flatten the channel response as seen by any one receiver. The challenge of this technique is to find a way to rapidly switch antenna gain pointing or antenna sector selection toward the best signal direction as it varies with receiver motion through the multipath environment. Yamao and Nagao [24] propose a predictive antenna selection scheme that could be combined with a azimuth sectored antenna such as the one described by Murata et al in [19]. Antenna directivity also combats co-channel interference and can be combined with antenna diversity.

Spread Spectrum

Spread Spectrum techniques employ a form of frequency diversity to combat fading in a frequency selective channel. As an example, Gaudenzi and Giannetti [25] describe a candidate direct-sequence spreading scheme for use in a combined satellite - ground based single frequency network. The PN sequence self-noise that typically limits the capacity of a CDMA system is overcome by appropriate phasing of Gold code spreading sequences. Code synchronization is possible because radio programs using different Gold codes are all transmitted together from the same sites. A Rake receiver structure is used to combine the three delayed signals with the largest signal powers, this includes both the satellite and booster signals. The system approach allows for data rate flexibility and distributed uplink. Finally VLSI CDMA receiver technology has been demonstrated by Qualcomm in their two-way digital radio design.

Summary

To properly design a DBS-Radio system it is imperative to understand the associated propagation impairments, their source, their nature and their extent. We have summarized these propagation effects in three generic environments, indoor, rural-suburban mobile, and urban mobile and in each case suggested several techniques to mitigate these effects. In addition, the references provide a wealth of more detailed information useful to the DBS-Radio system designer.

	Satellite/Simulated Satellite Propagation Tests	Other Indoor Radio Prop. Tests
Basic Test Conditions		
Frequency	[2,3] 0.7-1.8 GHz [4] 0.9, 1.6, 2.6 GHz	0.5 to 3.0 GHz
Elevation Angle to Xmitter	[2,3] 12° to 45° [4] 36° to 55°	≈ 0°
Spatial Signal Variations	Signal Loss	Signal Loss
Non-Metallic Residential	Mean = 5 - 11 dB, [2,3] Mean = 6 to 8 dB, Std Dev = 2-3 dB [4]	
Some-Metallic Office	Mean = 5-14 dB, Std Dev = 2-10 dB [2,3]	Mean = 10-15 dB, Std Dev = 3-6 dB [6] Mean Signal Attn. decreases by 1.5-2.0 dB per floor as one goes up in a multi-story building [7,8]
Null Spacing		
Non-Metallic Residential Some-Metallic Office	2 - 4 λ [2,3];	0.5 -1.5 λ, [6]
Cause	Standing Wave Pattern, Possibly, the higher elevation angle produces the different pattern.	Standing Wave Pattern
Frequency Variations		
Large Scale		
Non- and Some-Metallic Structure	2-5 dB attn. increase per octave [2,3] 2-3 dB attn. increase per octave [4]	
Office Buildings and Metallic	2-3 dB attn. decrease per octave [2]	1-3 dB attn. decrease per octave [7] 2-3 dB attn. decrease per octave [9]
Cause	Main Signal Penetration and Propagation Through walls and ceilings, favors lower frequencies.	Main Building Signal Penetration and propagation through openings, favors higher frequencies.
Small Scale	2-10 dB Signal Troughs 5-30 MHz Wide[3]	
Cause	Variations in Standing Wave Pattern with Frequency	
Temporal Variations	<0.5 dB unless antenna line-of-sight blocked by person, which causes fades of 6-10 dB. [3]	4 Hz BW, Rician K = -6 to -12 dB; Dynamic Range = 17-30 dB due to movement of people and doors inside and outside traffic. [6]
Cause	Main propagation through walls and ceilings and higher elevation angle signal encounters fewer moving reflectors and refractors	Main Propagation Probably through openings and Low Elevation angle. Result is standing wave pattern changes with changing pattern of reflectors.
Delay Spread		
Non-Metallic Single Story	≈10 - 30 ns Total, [3]	
Office Buildings and Metallic	≈100 ns Total, [3]	Rooms:≈200 ns Total, ≈50 ns RMS Hallways ≈350 Hallways; [5] 1.5 GHz
Difficult Structures		
Non-residential buildings	Loss: Mean = 20 dB, Std. 10 dB	
Buildings shadowed by trees, other buildings or mountains	12-15 dB Excess Loss due to Trees in Satellite Signal Path [4]	
Buildings with significant metal in construction elements	Metal Shack: Mean Loss = 9-11 dB; Mobile Home: Mean Loss = 20+ dB [3] 15-22 dB for houses with aluminum backed sheetrock; 24+ dB for mobile homes [4]	Metal Covered Roof, Walls and Mesh Screen on Windows and Doors. Median Attenuation = 26-32 dB, Rayleigh Distributed [10]

Table 1 - Summary of Reviewed Indoor Propagation Test Results that Apply to DBS-R.

	Rural and Suburban Satellite Mobile Fading
Basic Test Conditions	
Frequency	0.87 & 1.5 GHz, Some 2.6 GHz [17]; 1.6 & 2.5 GHz [18]
Elevation Angle to Xmitter	≥15°
Fixed Site Tree Attenuation 1 or 2 Trees, Roadside	**Signal Loss** Typical = 4-9 dB, Std Dev = 3-7 dB [18] Bare Trees = 5-14 dB, for Elev 40°-15°, ΔFade = 0.35 dB/°Elev, UHF 870 MHz [17] Full Foliage = 7-19 dB, for Elev 40°-15°, ΔFade = 0.48 dB/°Elev, UHF 870 MHz [17] Foliage Factor: Mean Fade Full Foliage (dB) = 1.35 x Mean Fade Bare Tree (dB)[17] UHF Fade = 1.3 dB/Meter of Canopy, L-Band Fade = 1.8 dB/Meter of Canopy [17] After 15-20 dB of Direct Signal Fade, Rayleigh multipath begins to dominate. Cross-Polarization signal level is 15-20 below Co-Polar Level. [18]
Spatial Auto Correlation S - L Fade Level Cross Correlation L-Band Fade Level Auto Correlation S-Band Fade Level Auto Correlation	 None Observed [18] Near 0 at lag of 10 λ [18]; Near 0 at lag of 1-2 meter @ 5-10 λ [17] Near 0 at lag of 20-30 λ [18]
Mobile - Spatial Variations **Source Perpendicular to Road** Cumulative Fade Stats vs Elevation Angle	**Main Signal Impairment is Tree Shadowing** See Figure 1 Tree Scattered Multipath Signals are 15-20 below the main signal so when main signal is faded by this amount the received signal becomes Rayleigh in nature. [18]
Source Parallel to Road Open Rural Road... No Trees Canyon Roads in Colorado	**Main Signal Impairment is Mutipath Fading** L-band, 3-5 dB... No Elevation Dependence between 30° and 60° [17] L-band, 2-8 dB... At Elevation Angle of 30° [18]
Frequency Variations Freq Scaling	 Same Mean Fade Level at L and S-band [18] [17], Observed Over UHF, L-band & S-band.
Polarization Effects	Cross Polarized Signal averaged 15-20 dB below Co-Polarized Signal Level [18] Unfortunately, Polarization Diversity degrades rapidly with increasing fade level e.g. at 5 dB fade level, polarization isolation is down to only 11 dB. [17]

Table 2 - Summary of Reviewed Rural and Suburban Propagation Test Results that Apply to DBS-R.

REFERENCES

[1] E. F. Schroeder, H. J. Platte, and D. Krahe, "MSC Stereo Audio Coding with CD- Quality and 256 kbit/sec", IEEE Transactions on Consumer Electronics, Vol. CE-33, No. 4, pp. 512-519, November 1987.

[2] W. Vogel and G. Torrence, "Signal Variability Measurements For Satellite Radio Broadcasting Into Buildings," Technical Report No. 9101, Electrical Engineering Research Laboratory, The University of Texas at Austin, January 1991

[3] W. Vogel, G. Torrence and N. Golshan, "Satellite Sound Broadcast Propagation Measurements and System Impairments," AIAA 14th Inter. Comm. Satellite Systems Conf. and Exhibit, March 1992, pp. 1461-1470.

[4] P. I. Wells, "The Attenuation of UHF Radio Signals by Houses," IEEE Tans. Veh. Tech. Vol. VT-26, Nov. 1977, pp. 358-362.

[5] A. Saleh and R. Valenzuela, "A Statistical Model for Indoor Multipath Propagation," IEEE Journal on Selected Areas in Comm., Vol. SAC-5, No. 2, Feb. 1987, pp. 128-137.

[6] R. Bultitude, "Measurement, characterization and Modeling of Indoor 800/900 MHz Radio Channels for Digital Communications," IEEE Communications Magazine, Vol. 25, No. 6, June 1987, pp. 5-12.

[7] A. Turkmani, J. Parson and D. Lewis, "Radio Propagation Into Buildings at 441, 900, and 1400 MHz," Proc. 4th Intl. conf. on Land Mobile Radio, Dec. 1987, pp. 129-138.

[8] A. deToledo and A. Turkmani, "Propagation Into and Within Buildings at 900, 1800 and 2300 MHz," 1992 IEEE Vehicular Technology Conf., pp. 633-636.

[9] A. Davidson and L. Marturano, "Impact of Digital Technologies on Future of Land Mobile Spectrum Requirements," Vehicular Technology Society News, Vol. 40, No. 2, May 1993, pp. 14-30.

[10] H. Hoffman and D. Cox, "Attenuation of 900 MHz Radio Waves Propagating into a Metal Building," IEEE Transactions of Antennas and Propagation, Vol. AP-30, No. 4, July 1982, pp. 808-811.

[11] G. Hess, "Land-Mobile Satellite Excess Path Loss Measurements," IEEE Transactions on Vehicular Technology, Vol. VT-29, No. 2, May 1980, pp. 290-297

[12] J. Butterworth, "Propagation Measurements for Land-Mobile Satellite Systems at 1542 MHz," Communication Research Center., Ottawa, Canada, Technical Note 723, August 1984.

[13] J. Butterworth, "Propagation Measurements for Land-Mobile Satellite Services at 800 MHz," Communication Research Center., Ottawa, Canada, Technical Note 724, August 1984.

[14] A. Jongejans, A. Dissanayake, N. Hart, H. Haugli, C. Loisy and R. Rogard, "PROSAT-Phase 1 Report," European Space Agency Technical Report ESA STR-216, May 1986.

[15] V. Renduchintala, H. Smith, J Gardiner, and I. Stromberg, "Communications Service Provision to Land Mobiles in Northern Europe by Satellites in High Elevation Orbits - Propagation Aspects," 40th International Conference on Vehicular Technology, May 6-9, 1990, pp. 706-713.

[16] A. Bundrock and R. Harvey, "Propagation Measurements for an Australian Land Mobile-Satellite System," Proceedings of Mobile Satellite Conference, 1988, pp. 119-124.

[17] J. Goldhirsh and W. J. Vogel, "Propagation Effects for Land Mobile Satellite systems: Overview of Experimental and Modeling Results," NASA Reference Publication 1274, February 1992.

[18] W. J. Vogel and G. W. Torrence, "Simultaneous Measurements of L-band and S-band Tree Shadowing for Space-Earth Communications," Univ of Texas Electrical Engineering Research Laboratory, Document #EERL-94-301, March 16, 1994.

[19] H Murata, S Yoshida and T. Takeuchi, "Adaptive Receiver Consisting of MLSE and Sector-Antenna Diversity for Mobile Radio Communications," IEICE Transactions on Communications, Vol. E-77-B, No. 5, May 1994, pp. 573-578.

[20] W. Vogel and G. Torrence, "TDRS Propagation Measurements at 2050 MHz in Pasadena, CA," Univ of Texas Electrical Engineering Research Laboratory, Document #EERL-95-B1, February 10, 1995.

Acknowledgments

The research described in this paper was carried out at the Jet Propulsion Laboratory, California Institute of Technology, and sponsored by the Voice of America (U.S. Information Agency) through an agreement with the National Aeronautics and Space Administration. The project was managed by Dr. H. Donald Messer of Voice of America.

[21] "An Evaluation of Selected Mobile Satellite Communications Systems and Their Environment," Prepared by MITRE corporation under contract to EST/ESTEC, document MTR 93B0000157, February 1994, pg. 75.

[22] S. Yoshida and M. Mizuno, "The Realities and Myths of Multipath Propagation," IEICE Transaction Communications, Vol. E76-B, No. 2 February 1993, pp. 90-97.

[23] F. Ling and S. Qureshi, "Lattice Predictive Decision-Feedback Equalizer for Digital Communication Over Fading Multipath Channels," Proceedings of Globecomm 86, December 1986, pp. 1050-1054.

[24] Y. Yamao and Y. Nagao, "Predictive Antenna Selection Diversity (PASD) for TDMA Mobile Radio," IEICE Transactions on Communications, Vol. E77-B, No. 5, May 1994, pp. 641-646.

[25] R. De Gaudenzi and F. Giannetti, "Analysis of an Advanced Satellite Digital Audio Broadcasting System and Complementary Terrestrial Gap-Filler Single Frequency Network", IEEE Transactions on Vehicular Technology, Vol. 43, No. 2, May 1994, pp. 194-210.

[26] British Aerospace et al., "Archimedes for BSS(S)," Final Study Report, Contract 8642/89/F/RD(SC), January 1991.

[27] H. Sari, G. Karam and I. Jeanclaude, "Frequency-Domain Equalization of Mobile Radio and Terrestrial Broadcast Channels," IEEE Globecomm '94 Conference Record, pp.1-5.

[28] W. Vogel and J. Goldhirsh, "Multipath Fading at L-band for Low Elevation Angle, Land Mobile Satellite Scenarios," IEEE Journal on Selected Areas in Communications, Vol. 13, No. 2, February 1995, pp. 197-204.

[29] J. Gevargiz, D. Bell, L. Truong, A. Vaisnys, K. Suwitra and P. Henson, "Performance of DBS-Radio Concatenated Coding and Equalization," International Mobile Satellite Conference, June 6-8, 1995.

Evolution of DAB by Satellite to Meet the Multi-media Challenge

K.P. Galligan, R. Viola
European Space Agency
P.O. Box 299, 2200 AG Noordwijk (NL)
phone: +31 71 653181/654513, fax: +31 71 654598

C. Paynter
Spar Aerospace Limited
21025, Trans-Canada Highway, Ste-Anne-de-Bellevue, Québec (CDN)
phone: +1 514 4572150 ext. 3832, fax: +1 514 4253041

ABSTRACT

This paper explores the various satellite and service components that will be significant in meeting the multi-media challenge of DAB in a satellite environment.

1. A POTENTIAL SYSTEM CONFIGURATION

1.1 Overview

It is useful to examine some of the potential configurations of a system of satellites to carry and distribute Digital Audio Broadcast (DAB) signals. In particular, this would allow a determination to be made regarding their suitability to offer services to European and North American communities is discussed.

1.2 Constellation

1.2.1 General

The concept of Digital Audio Broadcast (DAB) via satellite has been undergoing an evolution during the last few years. A part of this has resulted from the agreement of the international community, apart from the United States of America, to clear a band of frequencies in L-band for the exclusive use of the DAB/multi-media services that are currently being proposed world wide. Indeed, Canada has taken a lead in this in that the Canadian Broadcasting Corporation (CBC) has already installed an experimental network of terrestrial DAB transmitters in this frequency band, and is planning to start commercial broadcasting during the latter part of this year (1995).

DAB services could be provided by a Geostationary satellite. However, northern latitude countries, in particular Canada and most of Europe suffer from low elevation to the GEO orbit in terms of obstructions, as well as low antenna gains required in mobiles to provide omnidirectional azimuth coverage.

As a consequence, a set of constellation that has been under consideration for some years has begun to look increasingly attractive for these new services. One possibility is the proposed ARCHIMEDES constellation of satellites, using a Highly Elliptical Orbit configuration, similar to that of the established Molnyia orbits used for many years in the former Soviet Union.

A constellation of satellites using this orbital configuration would be ideally suited to transmit the proposed DAB services over continental

Europe, Canada and the USA and Eastern Asian countries.

1.2.2 HEO

The advantages of highly inclined (i=63.4°) orbits over others is that they provide a good coverage of the highly populated Northern Hemisphere, inclusive of the (less populated) polar regions, and have a relatively low cost launch per satellite. The disadvantages are the requirements of several satellites to form a constellation for continuous coverage of one hemisphere, and the need for satellite antenna pointing and satellite handover. At handover, the traffic routing through an outgoing satellite is replaced by an incoming satellite path.

The difference between an HEO orbit and the Molnyia orbits, is that the HEO orbit proposed for ARCHIMEDES will use an 8 hour orbit in the place of the Molnyia 12 hour orbit. This will result in the requirements for more satellites, 6 as opposed to 3, or 4, but will give the advantages of lower apogees, and therefore less path delay and losses. Additionally these orbits that allow the use of satellites for broadcasting over North America, Europe and the Far East from the one constellation.

HEO satellites may require two types of compensation, antenna zooming and Doppler shift compensation. Antenna zooming is used to compensate for the slant range loss variation (2.3 dB for an 8-hrs period) between apogee and handover. Doppler Shift compensation is the compensation for the Doppler frequency shift, due to the velocity of the HEO spacecraft relative to the earth's surface which is almost absent from the GEO configurations. The sign of the frequency shift is determined by the moving spacecraft direction. A change in the Doppler compensation needs to be performed at handover.

1.2.3 Archimedes

The ARCHIMEDES satellite constellation is based on Multiregional Highly inclined Elliptical Orbits (M-HEO) to cover defined service areas in the northern hemisphere. The primary service areas consist of Europe, Far East and North-America. The secondary service areas are all areas outside the primary service areas, which have a minimum elevation angle of less than 40 degrees.

The M-HEO constellation consists of six satellites in different orbital planes, each having an 8-hour period, with an operational orbit period of 4 hours. The apogee altitude is proportional to the orbit period. For this proposed orbit, the apogee and the perigee are respectively, 26786 kms and 1000 kms. At handover, the altitude will be approximately 20606 kms.

1.3 Ground Segments

1.3.1 Feeder Link Stations

A satellite system that is used to transmit DAB channels would benefit from the use of a minimum number of ground feeder link stations. This is especially true if the transmissions are using the currently preferred COFDM modulation technique, as there are requirements for the synchronisation of the signals that can only be met by using one transmitter per channel.

The HEO system of satellites results in one satellite being active over any one area at any one time. This situation results in the requirement for a "handover" of transmissions from one to another satellite every 4 hours. In order not to interrupt service whilst this is happening, two antennas will be required at the ground feeder link stations. Whereas it would be complicated to make the handover completely seamless, for a number of reasons, the worst case actual time

during which transmissions will be disturbed will last only a few milliseconds. Compensation that will have to be applied to the signals during the handover sequence will involve a change of Doppler Compensation and a correction for the time lag difference between the two satellites undergoing handover.

1.3.2 Doppler

The Doppler frequency shift will be a function both of time and location of Tx and Rx stations. The Table shows for a HEO/8 hrs satellite, the maximum Doppler frequency shift, spread over the coverage areas, for the up and down components of few forward and return links at selected frequencies. It should be noted that when the signal is undergoing handover from one satellite to another, the magnitude of the Doppler shift is doubled, as one of the satellites will be receding and the other will be advancing. That is, one of the shifts will be negative, and the other will be positive.

Doppler Compensation permits a reduction of the associated guard bands which would degrade the spectrum efficiently. The compensation procedure for the Doppler shift will be to correct for the Doppler shift at the middle of the coverage area for any one beam. This will require that there is some tolerance for the residual Doppler shift at the edge of any particular beam. Calculations show that this is well within reasonable tolerances of the buffer zone that would be required between channels.

Table Doppler Frequency Shift for a HEO/8hrs

Doppler Component	Maximum Expected Value (kHz)
Forward Link - C-Band	40.0
Up-Link - Ku-Band	87.5
Up-link - L-Band	10.5
Down-Link	
Return Link - L-Band	11.0
Up-Link - C-Band	26.5
Down-Link - Ku-Band	71.0
Down-Link	

2. INFLUENCE OF USER REQUIREMENTS

2.1 Audio Broadcasting

As the name suggests, DAB has its roots very firmly anchored in an audio broadcast environment, where broadcasting is accepted to mean unique and universal service to fixed and mobile users, not an adjunct to television directed at fixed installations. Clearly any new service has to offer a different "product" to that currently available and thus broadcasters' early thinking was directed at a CD quality service. These factors drove the development of audio compression and of COFDM, the latter being a multipath resistant digital transmission system. It is fortunate that in the development process a considerable amount of flexibility was incorporated in the transmission scheme.

In its first implementations, DAB will provide high quality audio programming. This need has been supported by market analysis[1], although

some of this work indicates that continuity of signals over long distances and a lack of extraneous noise are more important to listeners than CD quality itself.

However, as the functionalities in the COFDM system become better understood and the economics of a CD quality channel are better characterised, a number of broadcasters are considering lower bitrates. Whilst some of these have a world service vocation (RFI, VOA, etc.) others could have a service area which spread over a number of countries, but a financial regime that required only modest investment. Whilst standardisation of bitrates will be a policy issue for service providers (and perhaps regulators) it is clear that the audio broadcasting community will require a diversity of bitrate/quality offerings.

2.2 Other services

Alongside the exploitation of COFDM for audio applications, development of a framework for other non radio, databroadcast, services has been progressing.Such work is partly a result of transport development programmes such as the European Union's Drive activity. These developments are also a response to an increasing integration of electronics and communications in the car by car manufacturers. The facilities offered range from sophisticated cellular radio installations to rather simpler navigation aides.

There is also a growing realisation that whilst DAB multiplex rates are intermediate between the kilobit rate of cellular radio and the 100 Megabit rates of optical fibre, with its megabit rate it can provide for a number of multimedia applications, without the need for a special, hardline connection. Thus services can be offered ubiquitously, to users which would be prepared to pay for a near consumer priced personal computer extension card.

Taking advantage of another ubiquity, that of the telephone network, low rate interactivity can then also be provided.

Market investigations[2] have shown that a number of broadcast or broadcast with some interactivity services would be demanded by users. Their development is critically dependent on price of the consumer equipments. Indeed a number of the applications investigated in reference 2 were judged at the time to be inaccessible because of the cost of current VSAT terminals. It goes almost without saying that such services need a ready supply of material. It is believed that a major factor in the development of these services will be the active interest of organisations where vocation is the publishing of books and periodicals, since they will have the necessary infrastructures to produce services economically, probably at marginal cost.

3. STRATEGIC ALLIANCES

The digitalization of the broadcasting system worldwide requires a global approach. It would be unacceptable and a step back if the world would be split into areas with incompatible broadcast systems. Admittedly this is more difficult in a digital scenario rather than in a world of analogue systems.

Three main issues have to be pursued to commence the digital revolution, and, at least after a while, it has be to a revolution since there is no smooth transient from analogue to digital possible. These issues are:

- the provision of a globally assigned frequency band, to be commonly used by terrestrial and satellite services,
- an open, i.e. non-proprietary transmission standard and

- international strategic alliances among the main players, i.e. content provider, operator of broadcast transmission infrastructure, and, increasingly important, the equipment industry.

The first two issues have already been completed. The WARC'92 assigned the L-Band (1452-1492 MHz) and the R&D programmes Eureka 147 and Jessi AE13 created appropriate standard and key VLSI-components respectively. Now, the third element is required to ignite the process of implementation.

The global implementation of Digital Audio Broadcasting requires strategic alliances similar to those which are being established in the telecommunications area. These new alliances will comprise network operator, service and content provider (broadcaster) and will complement the "traditional" public operators. Since every player has to invest significant amounts, only the very powerful and visionary market leader can start such a revolution. Nevertheless all investors must make sure, that the other actors play their role.

The transmission medium now follows the example of the Compact Disc market. Within a relatively short time the CD overtook the entire analogue media range including the vinyl record, the magnetic tape and the cassette. The CD-Rom also introduced the missing link between audio and data storage, which in turn opened the new and innovative field of provision of multi-media services.

The very important element of the user terminal issue was solved with Personal Computer (Laptops) in the consumer market, whilst integrated in-car displays will also make their contribution.

Figure 1 illustrates the functionalities required in an international alliance for the operation of a satellite based DAB broadcasting system. The system should serve fixed and mobile subscribers in countries of northern latitudes and is based on use of highly-inclined elliptical orbits.

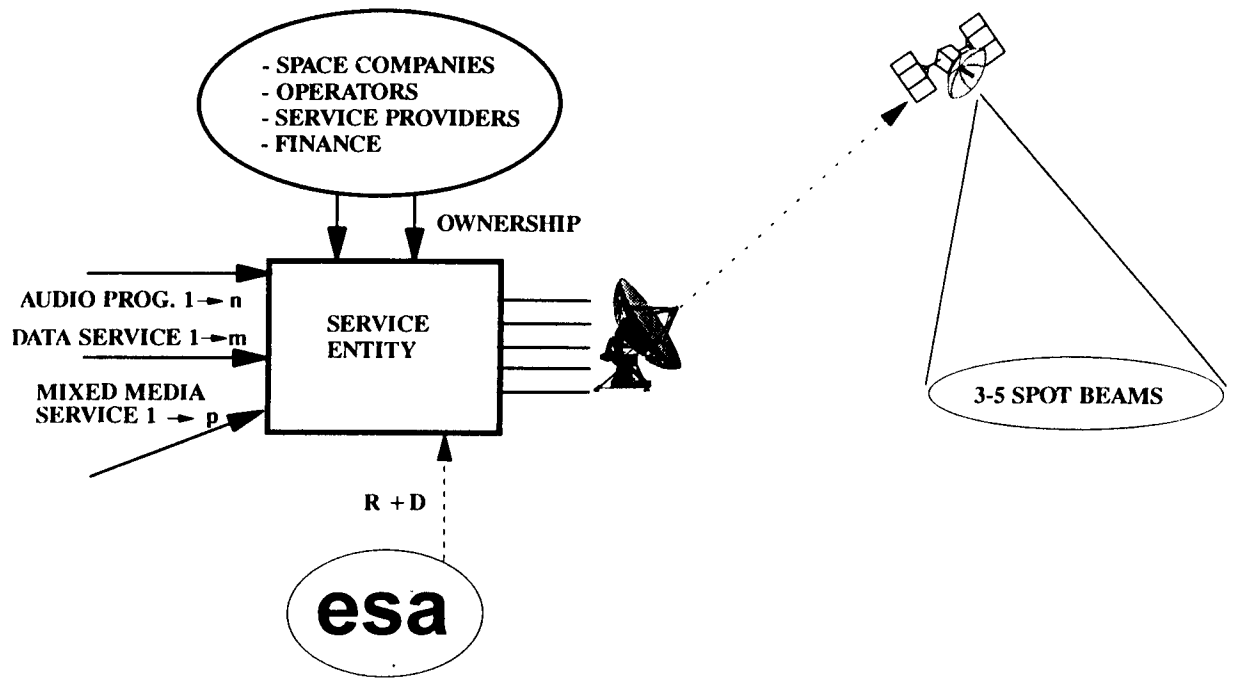

Figure 1: Structure of an internationally based satellite operator providing DAB services

4. MESSAGE SERVICES

Beside the provision of digital audio programmes the introduction of a new transmission infrastructure will offer flexibility for innovative data services. These data services can be characterised as high-rate and unidirectional serving mobile users in the first place. Since the reception in a mobile environment is the most critical it will equally well serve the fixed and portable users. The mobility component of the Eureka 147 is the unique advantage of this standard, since no other standard can provide this feature today.

Two groups of data in the DAB multiplex have to be considered. The first with programme associated data (PAD). This group comprises data information somehow connected to an on-going audio programme. It comprises information about station name, music or voice transmission, accompanied text or others. In addition, high rate and high volume data services in stream and packet mode can be transmitted in the body of the multiplex.

5. ANALYSIS

A number of important elements are needed to complete the evolution of DAB as an audio medium to the much larger field of a mixed media environment. These elements are evolving and could in the near future all be in place, thereby transforming the original vision of the early designers in DAB.

6. ACKNOWLEDGEMENTS

The authors acknowledge the contributions of all their colleagues, in particular those of the teams led by Daimler Benz Aerospace and Matra Marconi, who contributed to the development of the system and service concepts described above.

REFERENCES

(1) Touche Ross, Archimedes Market Study for DAB. Final Report December 1992.

(2) Racal Research Ltd., Economic Viability of Point to Multipoint Services via Satellite. July 1991.

Digital Radio Broadcasting Using The Mixed Satellite/Terrestrial Approach: An Application Study

Richard V. Paiement P.Eng., René Voyer Eng.
Radio Broadcast Technologies
Communications Research Centre
Ottawa CANADA K2H 8S2

Doug Prendergast P.Eng.
Prendergast Communications Inc.
Ottawa CANADA K1G 4B2

ABSTRACT

Digital radio broadcasting (DRB) is a new service that offers CD quality stereo programs to fixed, portable and mobile receivers. Terrestrial DRB in Canada is considered as a replacement technology for existing AM and FM services, and it is expected to start up in 1996. Canada currently favors Eureka 147 technology operating in the L-band, in the 1452-1492 MHz frequency band allocated during WARC'92 for DRB.

Terrestrial DRB delivery is appropriate for small to medium sized service areas, such as cities and their associated suburbs. For larger areas such as provinces, as well as for sparsely populated areas such as the regions in northern Canada, satellite delivery is more appropriate. The mixed approach is based on both satellite and terrestrial broadcasting services using a common frequency band. Spectrum efficiency is achieved through close coordination of both service types, to achieve proper frequency sharing and spectrum re-use. As well, use of a common transmission format by both types of services allows for a common receiver. This mixed satellite/terrestrial approach to DRB is being seriously considered in Canada and in other countries.

This paper studies the feasibility of such a mixed satellite/terrestrial DRB system. It looks at possible coverage scenarios for Canada, and at the satellite and receiver technology requirements.

INTRODUCTION

New digital radio broadcasting (DRB) services are being developed worldwide. In Canada, efforts are focused on a technology which should offer a reliable digital service to all Canadians. The objective is to deliver CD quality audio programs and data services to fixed, portable and mobile receivers, anywhere in the country.

The Eureka 147 technology [1] favoured in Canada uses advanced wideband digital channel coding which requires much less transmitter power than the current analog systems. As well, it features increased robustness to multipath interference during mobile reception. Distributed emission is possible with this technology, as opposed to the traditional single transmitter approach, and this leads to improved spectrum re-use. With gap fillers and coverage extenders, distributed emission allows for the gradual implementation of DRB services, with the possibility of filling coverage holes and shaping the coverage area. Future growth of the coverage area can also be easily accommodated.

DRB is expected to start up commercially in early 1996 in Canada, where it is considered a replacement for existing AM and FM systems. Services will be terrestrial, until DRB satellite technology is available. Once the required technology is designed and developed, sometime within the next ten years, satellite services will be brought on-line to complement the terrestrial services. Using a common transmission format for both types of service will mean a single receiver for consumers. A mixed system, with both satellite and terrestrial services in the same frequency band, offers great flexibility for delivering services to the whole Canadian population. The local terrestrial services will coexist with provincial or even national satellite services. Spectrum efficiency is achieved through frequency sharing as well as spectrum re-use between the various satellite and terrestrial services.

DIGITAL RADIO BROADCASTING

The Canadian DRB system is based on technology developed as part of the Eureka 147 project. This project was launched in 1987 in Europe, and the research efforts have yielded a universal digital sound broadcasting technology commonly referred to as the Eureka 147 DAB System, which was standardized in December 1994 by the European Telecommunications Standards Institute (ETSI). Also in December 1994, the International Telecommunication Union issued two draft recommendations to make this system a worldwide technical standard for satellite and terrestrial digital radio broadcasting.

To deliver CD quality audio services to fixed, portable and mobile receivers, the DRB system makes use of advanced source coding and channel coding techniques. The source coding uses Layer II from the ISO/IEC 11172-3 standard, also known as MPEG I. The system provides a 2304 kbit/s total capacity (without FEC) in a 1.536 MHz bandwidth. A typical rate 1/2 FEC offers a 1152 kbit/s data capacity that can be configured in a multitude of ways, for example as five CD quality stereo programs. Channel coding uses a wideband multi-carrier modulation scheme implemented as coded orthogonal frequency division multiplexing (COFDM) in conjunction with frequency and time interleaving [2]. When operating in Mode II, the 312.5 μs symbol includes a 62.5 μs guard interval. Multipath echoes received during this guard interval period are seen as constructive interference by the receiver. This results in robustness to multipath, which is critical in a mobile environment. It also makes distributed emission possible, where on-channel repeaters are used as gap fillers or coverage extenders, or in a single frequency network (SFN). The signal from these repeaters, considered as *active echoes,* are treated as multipath echoes in the receiver.

The DRB system can be operated at frequencies ranging from VHF to 3 GHz. At L-band, it is possible to use a mixed system, which includes both satellite and terrestrial services within the same frequency band. Higher frequencies limit terrestrial services to line-of-sight operation, while lower frequencies result in large satellite antennas. The DRB system supports transparent reception of either or both delivery systems by the receiver. The distributed emission concept mentioned above can be applied to satellite as well as terrestrial services: the hybrid approach uses terrestrial on-channel repeaters to fill shadowed areas of a satellite service.

Canada has been testing DRB systems since 1990, and currently has test installations in the Toronto and Montréal areas under the Digital Radio Research Inc. program. Currently, only test receivers are available, but commercial receivers are expected as early as September 1995. As well, the first licensed commercial DRB station in Canada is expected sometime in early 1996, using terrestrial delivery. These terrestrial stations will be able to cover the most densely populated areas of the country.

A satellite designed for DRB will permit the extension of coverage to reach remote areas, beyond the densely populated areas. It will link densely populated areas for highway motorists, and even offer province-wide or national services. The expected introduction of satellite delivery in the 2003-2007 time period will allow time for research, design and development of the required spacecraft technology. By that time, receivers bought for terrestrial services will be widely used, and the common transmission format of satellite and terrestrial services will provide instant access to a large audience for these new satellite services. This is true provided that early receivers are equipped with the proper receive antenna for satellite and terrestrial reception.

MIXED SATELLITE/TERRESTRIAL SYSTEM

A system with terrestrial transmitters can easily cover small or medium sized areas, corresponding to single cities and their associated suburbs. This is sufficient to reach most of Canada's population in densely populated areas. For larger areas, distributed emission can be used in an SFN configuration, with time synchronized on-channel transmitters; this approach increases in complexity as the size of the desired coverage area increases. Satellites provide a straightforward way of serving large areas such as provinces, and they address the need for coverage in remote or sparsely populated regions of the country, as well as along highways.

The mixed satellite/terrestrial concept [3] has both satellite and terrestrial services within the same frequency band, so services must be well coordinated. As part of WARC'92, a 40 MHz frequency band at L-band was allocated for satellite and terrestrial DRB services. Given a channel bandwidth of 1.536 MHz, a maximum of 26 channels (one channel provides the equivalent of five CD quality stereo programs) can be allocated within this band, depending on the guard band requirement.

Spectrum efficiency in this 40 MHz band is achieved through spectrum re-use. Satellite channels can be re-used as satellite or terrestrial channels at distances such that the interference becomes negligible, or at least acceptable. This is subject to limitations on the co-channel separation distance, dictated by the robustness of the transmission format. Certain trade-offs are possible in spectrum re-use [4]. The re-use distance can be decreased if the terrestrial power is increased, or if a reduction of the terrestrial coverage due to interference is acceptable. As an example, when using the RARC-83 co-polar reference pattern for the satellite antenna, the apparent noise increase in the receiver is less than 1 dB at a relative angle ϕ/ϕ_o of 1.4, where ϕ_o represents the half power beamwidth of the satellite antenna in the direction of interest, and ϕ is the off-axis angle at the satellite. The relative angle becomes 3 dB at $\phi/\phi_o = 1.2$, and 7 dB at $\phi/\phi_o = 1.0$. In Canada, for a satellite service with a 1° beam serving Eastern Quebec and the Maritime provinces, $\phi/\phi_o = 1.2$ corresponds to about

1100 km of separation, such that a terrestrial service in Toronto would be possible with no more than a 3 dB increase in apparent noise.

Channels not assigned to satellite services can be used for terrestrial services, subject to limitations on the adjacent channel separation distance that is dictated by the receiver design, including filter rejection and front-end linearity.

COVERAGE SCENARIOS

Initially, the DRB services in Canada will be provided terrestrially, limited to local services covering densely populated regions, including the urban areas. A few of the channels would be reserved for future satellite use. Remaining channels could be assigned to terrestrial services, subject as mentioned previously to the adjacent channel separation distance. Terrestrial services will be able to use gap fillers to fill shadowed regions, as well as coverage extenders to shape or extend the coverage as required. Such shaping can serve to cover highly traveled highways, such as the 401 that links the Windsor/Toronto/Montréal corridor. SFNs can be used for services that would include the urban area and associated suburbs, and possibly more.

The satellite services will serve to consolidate existing terrestrial services into larger service areas, including provincial and national services. As an example, one operational plus one spare channel, each providing the equivalent of five CD quality stereo programs, could be available in a given area. An initial assumption is that eight beams would be needed to cover the whole of Canada, organized as one beam per province, except for Alberta and Saskatchewan that are combined in one beam, as are the Yukon and NorthWest Territories, and the Maritime provinces.

SATELLITE TECHNOLOGY

A Canadian DRB service must offer high reliability for all reception conditions, including rural, suburban and urban environments. However, the L-band land mobile satellite channel suffers from propagation anomalies due to shadowing, multipath and Doppler. This results in signal fading, and the satellite design must include a downlink margin to overcome it. The fading is mostly a function of the reception environment and the satellite elevation angle. As the elevation angle increases, the fading becomes less important. However, at angles close to 90°, tree shadowing reappears, and building penetration becomes more difficult. Figure 1 presents fade margin requirements for various service availabilities and elevation angles [4]. Note that these results are applicable to narrowband systems operating at 1.5 GHz in suburban environments.

The elevation angle is a function of the service location on Earth, but also of the satellite orbit. A commonly used orbit for communication satellites is the circular geostationary orbit (GEO), which can provide elevation angles of 55° and more at latitudes between 20° South and 20° North, depending on the relative satellite longitude. According to Figure 1, a fade margin of less than 3 dB is required to offer a 90% location service availability at elevation angles of 55° and more.

For services at latitudes below 20° South or above 20° North, the fade margin requirement is much greater. For example, services in Canada achieve elevation angles ranging from a high of 42° in Windsor (with a satellite

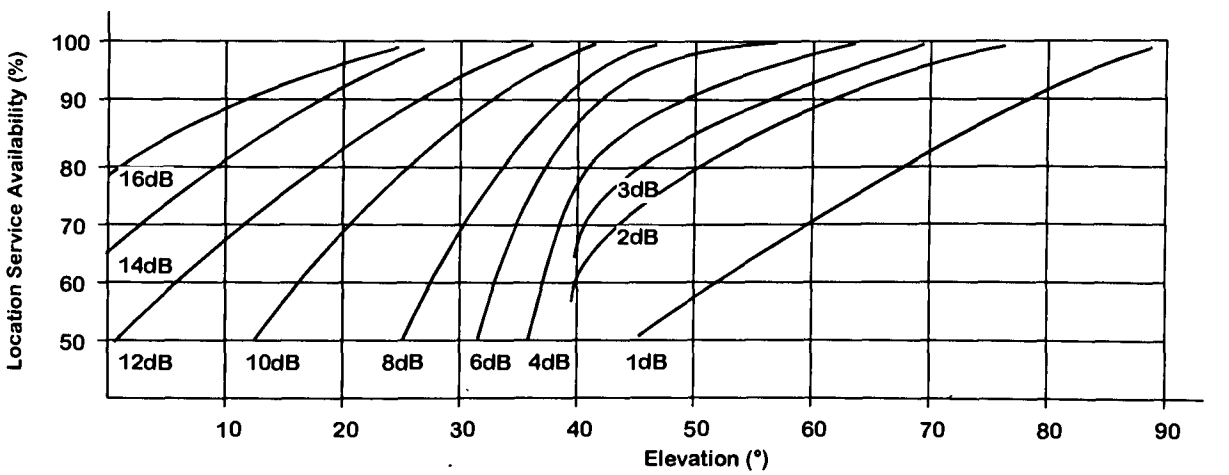

Figure 1: Fade margin requirement as a function of service availabilities and elevation angles, in a narrowband system operating at 1.5 GHz in a suburban environment [4].

positioned at 82.5° longitude) to below 10° in Yukon. Figure 1 shows that with elevation angles ranging from 15° to 35°, a fade margin of between 9 and 15 dB is required to achieve a 90% service availability.

To reduce this margin requirement, higher elevation angles can be achieved by using highly inclined elliptical orbits (HEO) instead of GEO. In Europe, where HEO systems are being studied as part of the Archimedes program, elevation angles of 55° and more are possible. A multi-regional HEO system with 8 hour elliptical orbits requires six satellites, and this can be shared by three areas of the globe, including Canada. Unfortunately, our country is physically wider than Europe, and while elevation angles of more than 55° would be achieved in Western and Central Canada, some eastern sections would have less than 40° elevation angles. A somewhat modified orbit could improve this situation, but it would probably worsen things elsewhere, namely in Europe.

This discussion has so far considered suburban reception, but other environments can not be ignored. For open rural reception, the elevation angle has little impact on fading, since line-of-sight reception is normally achieved. This is not the case for urban reception, where shadowing and multipath are worse than in suburban environments. A downlink margin of as much as 25 dB [5 , 6] could be required to overcome fading in urban environments. Such a margin is not realistic, and the hybrid approach is useful to address the problems of urban reception. A hybrid satellite service [7] uses terrestrial on-channel repeaters to fill coverage holes due to shadowing of the satellite signal. This is part of the Canadian approach to DRB, so that the downlink margin for a DRB satellite service can be specified based on suburban reception.

Fading studies presented in the literature are mostly concerned with narrowband systems and carrier wave measurements. However, the Canadian DRB system is expected to be wideband, and the channel impulse response must be evaluated to fully characterize wideband system performance. It is not yet well established if the use of a wideband system as opposed to a narrowband system would lead to a marked reduction of the required downlink margin.

The advanced channel coding scheme implemented in the Eureka 147 system provides robustness to multipath, as mentioned previously and demonstrated during various terrestrial measurements. This leads to a reduction in the required downlink margin: from the 9 to 15 dB suggested in Figure 1 for a narrowband system, about 6 dB is expected to be sufficient for reliable DRB coverage in Canadian open rural and suburban environments, from a GEO satellite. Inevitable shadowing in urban environments is resolved with local on-channel repeaters (hybrid system).

A downlink budget is presented in Table 1 based on a hypothetical DRB satellite service described in the ITU-R Report 955 [4] and ITU-R DRB Handbook [8] where a discussion of each item is presented. Based on more recent considerations applicable to the Canadian scenario, a receiver antenna gain of 4 dBic and a receiver noise figure of 2 dB are used. As well, a 6 dB fade allowance is used to account for lower elevation angles in Canada. This budget suggests that 62.5 dBW of on-axis EIRP is required from the satellite for each 1.536 MHz channel which contains the equivalent of five CD quality stereo programs.

Based on the information presented here for the mixed service, it is possible to sketch the profile of a DRB satellite. It is interesting to look at the MSAT satellite for comparison, because it has many of the features and attributes which are likely to be found on a DRB satellite. The MSAT satellite is a GEO satellite providing sufficient EIRP to serve narrowband mobile receivers at L-band. Also, its antenna reflector is the largest ever flown on a commercial satellite.

SYSTEM		
Operating frequency	1.472	GHz
Polarization	circular	
Channel error protection	conv.	(R=1/2)
Useful bit rate per 1.536 MHz channel	1152.0	kbit/s
Required Eb/No	8.0	dB
(Theoretical) downlink C/N_o	68.6	dBHz
System implementation margin	1.0	dB
Hardware implementation margin	0.5	dB
Degradation due to uplink	0.4	dB
Interference allowance	2.0	dB
Required downlink C/N_o	72.5	dBHz
RECEIVER		
Receiving antenna gain	4.0	dBic
Antenna noise temperature	90	K
Coupling and filter losses	1.0	dB
Receiver noise figure	2.0	dB
Receiver figure of merit	-21.8	dB/K
PROPAGATION		
Fade allowance	6.0	dB
Line-of-sight PFD at -3 dB contour	-103.5	dBW/m^2
Spreading loss @ 17° elevation	163.0	dB
SATELLITE		
On-axis EIRP per 1.536 MHz channel	62.5	dBW

Table 1: Satellite DRB downlink budget.

Using the initial assumption of eight satellite beams mentioned previously, a hypothetical DRB satellite payload is now considered. Each beam provides two DRB channels, one of which is a spare for future growth. A dedicated DRB satellite could therefore provide 16 DRB channels in all. The downlink budget shows that an on-axis EIRP of 62.5 dBW is necessary per 1.536 MHz channel. Since COFDM is a multi-carrier modulation with a non-constant envelope, output back-off is necessary to avoid excessive out-of-band intermodulation products. Operating with a back-off means that the SSPA will be slightly overscaled relative to the normal transmitted power, and the lower SSPA efficiency results in increased DC prime power requirements. A back-off on the order of 4 dB appears to be a good trade-off between SSPA efficiency and complexity of the output multiplex filter. The effect of in-band intermodulation was found to be negligible with such a back-off. The EIRP at 4 dB output back-off is 62.5 dBW per channel, or 65.5 dBW per beam. This EIRP consists of a combination of antenna gain and raw SSPA output power. Therefore, a configuration for proper partitioning of RF power and antenna gain is necessary to satisfy this EIRP requirement.

The MSAT 6m X 5m elliptical antenna can provide a half power beamwidth of approximately 2.4°, providing a gain of about 37 dBi. However, the Canadian plan includes beams as small as 1.4°. To generate the required shapes and sizes needed, it may be necessary to generate a number of 1.4° spot beams which are combined to provide the proper shape with the required power. Such small beams can be obtained with a 10 m parabolic reflector. This larger reflector would provide 41 dB of gain, with a resulting minimum amplifier requirement of 24.5 dBW or 280 Watts per DRB spot beam. Considering this finding, several possible arrangements could be investigated to identify the best approach.

Spectrum re-use distances can be improved by making the satellite footprint shaped as closely as possible to the service area. This could be achieved with multiple element feeds and a large reflector, or with a single element feed horn and a shaped reflector. Another benefit of the multi-element feed antenna approach is to provide rapid gain roll-off beyond the edge of coverage.

These techniques are used at frequencies of 12 GHz, but it is uncertain if they can be successfully applied at 1.5 GHz. The larger physical dimensions of the components (i.e., reflector, feeds, supports, etc.) at this lower frequency make their implementation more difficult. The excessive dimension of the main reflector would still be the prime limitation. Another concept that could help decrease the required separation distances between two adjacent co-channel satellite beams is polarization discrimination. The receiver is equipped with a circularly polarized antenna for the satellite service. The co-channel interference can be significantly reduced by using alternate polarization (RHCP and LHCP) in adjacent beams. The practicality of such polarization discrimination is under investigation.

Receiver Technology

The mixed system requires that the receiver operate with both the satellite and the terrestrial services in a manner transparent to the user. The satellite service assumes a circularly polarized receive antenna with typically 4 dBic of omnidirectional gain (i.e., a non-steerable antenna) at the elevation angles found in Canada, while the terrestrial service assumes a vertically polarized antenna with 0 dBi of gain [9]. This particular requirement can be accommodated with a receive antenna system that incorporates two distinct antennas and their respective LNAs, as presented in Figure 2. Such a system has been developed at the CRC [10] and will be tested in 1995. It consists of a bifilar helix and a quarter wavelength monopole mounted on the same base plate. Other approaches being evaluated include a microstrip patch and a loaded annular ring. The interest would be to integrate the two receive antennas and LNAs in the same package, in order to reduce to a

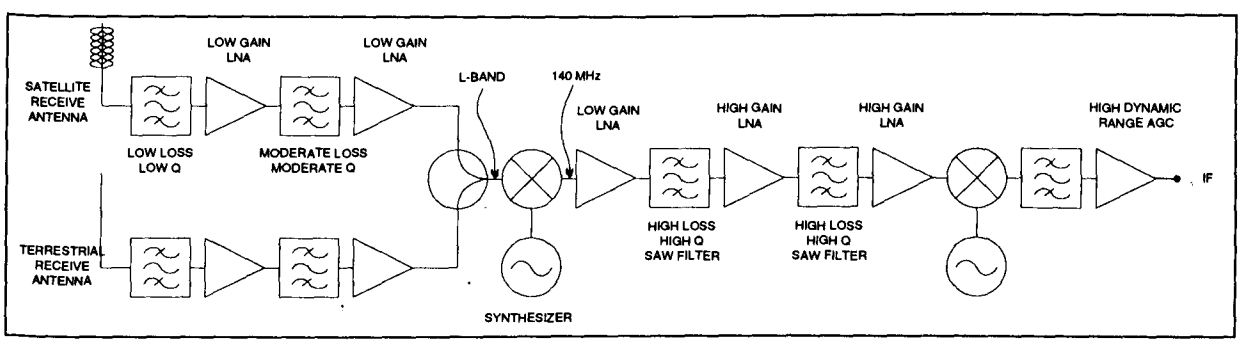

Figure 2: Mixed DRB receiver block diagram.

minimum the cost difference of the RF front end of a mixed service receiver as compared to a terrestrial only receiver.

The coexistence of the two services in the same band also implies that at many locations in a given service area, the receiver will be exposed to strong terrestrial signals neighboring relatively weak satellite signals. The front end must have the capability to select any of the 1.536 MHz wide DRB channel blocks present in the 40 MHz wide DRB frequency band, and to reject the potentially very strong neighboring DRB channel blocks. One proposed approach to achieving these objectives is shown in Figure 2. Each segment of the receive antenna (one for satellite reception and one for terrestrial reception) has its own LNA and set of filters. The large disparity in signal levels suggests the requirement for a high dynamic range on all components preceding the channel selection filter. This is achieved by a relatively low gain LNA with a high compression point but at the price of a higher noise figure. After the first amplification stage, filtering is applied again to eliminate dominant out-of-band signals. Then the two branches are combined into one single wideband signal that is applied to the channel selector. The channel selection is performed by the combination of a down conversion and a filtering process. Once converted from L-band to 140 MHz IF, the wideband signal is amplified again and then the selected channel is filtered with a cascade of SAW filters interleaved with amplifiers having a gain in the same order as the SAW filter insertion loss. The proper selection of these components is the key to a good rejection of the strong adjacent signals. Such a receiver configuration has been used at the CRC to develop an experimental receiver front end that will be evaluated in future DRB field trials.

CONCLUSIONS

The DRB system being implemented in Canada, based on Eureka 147 technology operating at L-band, supports a mixed approach which offers both satellite and terrestrial services to a common mobile receiver unit. Coverage requirements in Canada suggest such a mixed approach if services are to be available to the whole population. With the hybrid satellite approach, where on-channel repeaters serve to fill shadowed coverage in urban environments, it is possible to reduce the required satellite downlink margin to suburban and open rural reception conditions.

Research at the CRC is looking at certain issues presented in this paper, including wideband land mobile satellite channel characterization, satellite orbit, satellite antenna configuration, linearity and intermodulation, RF power requirements, polarization discrimination, as well as receiver antenna and front end configuration.

REFERENCES

[1] EBU/ETSI JTC, "Radio broadcast systems: digital audio broadcasting (DAB) to mobile, portable and fixed receivers," Final Draft prETS 300 401, European Telecommunications Standards Institute, Nov. 1994.

[2] Le Floch B., Halbert-Lasalle R., Castelain D., "Digital sound broadcasting to mobile receivers," *IEEE Trans. on Consum. Electron.*, vol. 35, no. 3, pp. 493-503, Aug. 1989.

[3] Chouinard G., Voyer R., Paiement R., "Coverage concepts for digital radio broadcasting at 1.5 GHz," *Proc. of 2nd Int'l Symp. on DAB,* pp. 157-181, March 1994.

[4] ITU-R WP10-11S, "Report 955: Satellite sound broadcasting to vehicular, portable and fixed receivers in the range 500 - 3,000 MHz," International Telecommunications Union - Radiocommunication.

[5] Vogel W.J., Goldhirsh J., "Propagation limits for land mobile satellite service," *Proc. of 13th AIAA Int'l Commun. Sat. Sys. Conf.,* pp. 564-574, 1990.

[6] Smith H., Gardiner J.G., Barton S.K., "Measurements on the satellite-mobile channel at L & S bands," *Proc. of the Third IMSC,* pp. 319-324, June 1993.

[7] Canadian Contribution, "Study of the hybrid coverage concept at 1.5 GHz," *ITU-R Document 10-11S/70-E,* Nov. 1994.

[8] ITU-R WP10-11S, "Special publication on digital sound broadcasting," International Telecommunication Union - Radiocommunication.

[9] Shafai L., Moheb H., Ittipiboon A., "Antenna candidates for digital radio broadcast," *Proc. of IEEE MTT-S Symp. on Technologies for Wireless Applications,* pp. 155-159, Feb. 1995.

[10] Wight J.S., "Versatile, high dynamic range receiver front end for digital radio broadcast and M-SAT reception," *Proc. of IEEE MTT-S Symp. on Technologies for Wireless Applications,* pp. 161-166, Feb. 1995.

Performance of DBS-Radio using Concatenated Coding and Equalization

J. Gevargiz, D. Bell, L. Truong,
A. Vaisnys, K. Suwitra and P. Henson

Jet Propulsion Laboratory
California Institute of Technology
4800 Oak Grove Dr.
Pasadena, CA 91201
gevargiz@semiramis.jpl.nasa.gov

ABSTRACT

The Direct Broadcast Satellite-Radio (DBS-R) receiver is being developed for operation in a multipath Rayleigh channel. This receiver uses equalization and concatenated coding, in addition to open loop and closed loop architectures for carrier demodulation and symbol synchronization. Performance test results of this receiver are presented in both AWGN and multipath Rayleigh channels. Simulation results show that the performance of the receiver operating in a multipath Rayleigh channel is significantly improved by using equalization. These results show that fractional-symbol equalization offers a performance advantage over full-symbol equalization. Also presented is the base-line performance of the DBS-R receiver using concatenated coding and interleaving.

1 -- Introduction

The Direct Broadcast Satellite-Radio (DBS-R) receiver is a flexible system for receiving digital audio and ancillary data in an indoor, outdoor, or mobile environment [1]. Figures 1 and 2 illustrate a typical mobile environment and the receiver's detail block diagram, respectively. The major building blocks of this receiver are: 1) a QPSK demodulator, 2) lattice predictive decision-feedback equalizer (LPDFE), 3) interleaver and de-interleaver and 4) Viterbi and Reed-Solomon encoders and decoders. The receiver operates in two modes: (a) Open loop or (b) Closed loop. The open loop mode is selected when the receiver operates in the presence of multipath. While in the open loop mode, the carrier and symbol loop. Numerical Controlled Oscillators (NCO) are initialized and updated using estimated or predicted carrier and symbol rate frequencies. When no multipath is detected, the receiver tracking loops are closed, and the equalizer is bypassed.

Figure 3 illustrates a simplified block diagram of the equalizer [2]. This equalizer utilizes a training sequence as one of its inputs for adjusting its coefficients. The training sequence is also used by the receiver for: 1) resolving QPSK I and Q ambiguity, 2) frame synchronization of the deinterleaver and Reed Solomon decoder and 3) determining the presence of multipath. The training sequence used in this article is set to a ratio of one third (1/3).

Section 2 presents the performance analysis. Section 3 briefly describes the multipath Rayleigh model. Section 4 presents the results of the performance analysis of the DBS-R receiver. Section 5 presents the summary an conclusions.

2 -- DBS-R Performance Analysis

The receiver depicted in Figure 2 is modeled using a combination of both analytical and simulation techniques. Analytical models are used for developing the receiver's matched filters. Simulation models are used for developing the receiver's tracking loops, equalizers, encoders, decoders, interleaver and deinterleaver.

To optimize the receiver's simulation algorithm and reduce simulation time, the Rayleigh propagation coefficients and the encoded data streams are generated only once before the receiver's simulation begins.

From Figure 2, the output of the matched filters can be expressed as,

$$IDF_I(k) = \sum_{i=1}^{N_{sym}^{NCO}} R_I(iT_s) \quad k = 1,2,\cdots \qquad (1)$$

$$IDF_Q(k) = \sum_{i=1}^{N_{sym}^{NCO}} R_Q(iT_s) \quad k = 1,2,\cdots$$

where,

$$r(t) = S_I(t)\cos[\omega_o t] + S_Q(t)\sin[\omega_o t]$$

$$R_I(t) = S_I(t)\cos[\Delta\omega t] - S_Q(t)\sin[\Delta\omega t]$$

$$R_Q(t) = S_I(t)\sin[\Delta\omega t] + S_Q(t)\cos[\Delta\omega t] \qquad (2)$$

for

$S_I(t) = \pm 1$, *I phase symbols*

$S_Q(t) = \pm 1$, *Q phase symbols*

and,

N_{sym}^{NCO} = number of samples per symbol

k = kth detected symbol

$\Delta\omega$ = carrier freq. error

ω_o = Input carrier frequency

By modeling the receiver at symbol rate as opposed to sample rate [3 and 4], significant computation time is saved. In a symbol rate simulation, there is one simulation cycle per symbol as compared to N_{sym}^{NCO} simulation cycles per symbol.

The receiver depicted in Figure 2 operates in an open loop, as well as in a closed loop mode. In the open loop mode, the free running frequency of the carrier and symbol tracking NCOs are initialized and updated using the predicted values computed using an FFT algorithm. In this mode, even though the receiver is open loop demodulating the QPSK signal, the detection is coherent. This is because the residual frequency and phase errors are resolved by the equalizer.

In the closed loop mode, the receiver uses the QPSK Costas and symbol transition loops for acquisition and tracking. The operational mode can be determined by an algorithm that utilizes the detected unequalized symbols and the training sequence.

The algorithm for the receiver's performance analysis provides the capability of studying: (1) acquisition, (2) tracking, (3) cycle slip, and (4) bit-error-rate performance.

3 -- Multipath Rayleigh Model

Figure 1 depicts the mobile environment. The terrestrial rebroadcast channel model includes multiple transmitters which results in signal components containing the same information at the mobile receiver [5]. However, the received signals have different time delays along with different Doppler and phase shifts. A worst case scenario involves the blockage of all direct signals, leaving only scattered energy from each rebroadcast site. The model for this is a multipath channel with time delays on each signal [5]. Time delays may be one or more symbol time, which may introduce Intersymbol Interference (ISI). Each delayed signal component is in itself a combination of scattered signals resulting in a Rayleigh distributed signal envelope. Thus, the signal component from each broadcast site arrives at the mobile receiver as a Rayleigh faded signal. The fading statistics on any pair of signals are independent.

Reference 6 describes several means of generating Rayleigh random processes. The technique that is used here simulates N multipath components, each arriving at an azimuth angle of $2\pi/N$ apart. If N is large the superposition sum is complex Gaussian process with a Rayleigh fading envelope, random phase modulation, and a nonrational spectra.

This technique approximates the Doppler spectral characteristics of scattered signals that arrive at a uniformly distributed angle relative to the motion of the mobile receiver.

In this article, the following parameters are used for generating the Rayleigh I and Q sample data:

- Number of oscillators =3202
- Doppler = $\pm 213\ Hz$ This corresponds to a driving speed of 100 km/h
- Symbol rate = 300,000 QPSK symbols per second

From Reference 6 and Equation 2, $R_I(t)$ & $R_Q(t)$ for the Rayleigh channel are expressed as,

$$R_I(t) = S_I(t)Ray_I - S_Q(t)Ray_Q$$
$$R_Q(t) = S_I(t)Ray_Q + S_Q(t)Ray_I \quad (3)$$

Where Ray_I & Ray_Q are the I phase and Q phase components of the Rayleigh channel.

4 -- Analysis Results and Summary

The performance of the receiver described in Figure 2 is analyzed for both AWGN and multipath Rayleigh channels, using open carrier and symbol tracking loops. Figure 4 illustrates the analysis results for the uncoded data using equalization for an AWGN channel. These results show the degradation due to the equalization. Shown in this figure are the BER results for the following cases:

- Without equalization, and no frequency and phase errors
- Using equalization, and no frequency and phase errors
- Using equalization, with a 10 Hz carrier frequency error, and no symbol frequency and phase error
- Using equalization, with a 10 Hz carrier frequency error, and 30% ($\tau = 0.3$) symbol phase error

It can be concluded that, in an open loop operation, the equalizer degrades the receiver performance between 1 to 2 dB for an AWGN channel. This figure also shows that the receiver's performance fails without equalization.

In this article, the multipath Rayleigh channel is modeled as three equally powered Rayleigh signals arriving at the receiver with τ_1, $(T+\tau_2)$, and $(2T+\tau_3)$ symbol delays (see Section 3 for details). In the above T is the symbol duration and τ_i is the fractional symbol phase delay for the i^{th} multipath. Figure 5 presents the BER results for the receiver described in Figure 2 using open carrier and symbol tracking loops. The results in this figure are presented for the following cases:

- Split symbol equalization
- Full symbol equalization
- Receiver's performance with no equalization

As shown by Figure 5, in a multipath Rayleigh channel the receiver without equalization fails, whereas the receiver using equalization operates at an acceptable uncoded BER. The results in Figure 5 also show that the fractional (half symbol) symbol equalizer outperforms the full phase equalizer.

To further optimize the performance of the receiver in an environment with one strong signal component, the acquisition and tracking algorithm may bypass the equalization and close the tracking loops. Through this optimization, a minimum of 1 dB gain in the receiver performance is achieved. This improvement is a result of bypassing the equalizer (see Figure 4.)

The base-line performance results of DBS-R using concatenated coding are presented in Figure 6. These results assume perfect carrier and symbol acquisition. The performance of convolutional and Reed Solomon coded and uncoded data is presented using interleaving. Figure 6 also shows that the simulation results fall within a small margin of their theoretical and measured counterparts.

5 -- Summary and Conclusions

A DBS-R receiver has been developed for operating in a multipath Rayleigh environment. The receiver's architecture utilizes both open loop and closed loop acquisition and tracking techniques. The receiver is modeled using a combination of analytical and simulation techniques for performance analysis.

The performance of this receiver is presented for both AWGN and multipath Rayleigh channels. The receiver uses a split symbol lattice predictive decision-feedback equalizer for acquisition and tracking in a multipath Rayleigh environment.

The results of the analysis have shown that this receiver can operate at an acceptable BER under a multipath Rayleigh channel.

References:

[1] A. Vaisnys, D. Bell, J. Gevargiz, N. Golshan, "Direct Broadcast Satellite-Radio, Receiver Development," In Proceedings of 1993 International Mobile Satellite Conference pp 21-26

[2] F. Ling and A. Quereshi, "Lattice Predictive Decision-Feedback Equalizer for Digital Communication Over Fading Multipath Channels," 1989 GLOBECOM pp 1050-1054

[3] J. Gevargiz and L. Truong, "Modeling Digital Receivers for Performance and Interference Analysis," Submitted to JPL/NASA Telecommunication and Data Acquisition Progress Report 1995

[4] J. Gevargiz, "Performance Analysis of an all Digital BPSK Demodulator," In Proceedings of 1993 GLOBECOM Conference pp 1670-1676

[5] D. Bell, J. Gevargiz, A. Vaisnys and D. Julian, "Overview of Techniques for Mitigation of Fading and Shadowing in the Direct Broadcast Satellite Radio Environment," In Proceedings of 1995 International Mobile Satellite Conference

[6] W. C. Jakes, " Microwave Mobile Communication," 1974 ATT, Reprint 1993, IEEE Press.

Acknowledgment

The work presented in the article was carried out at the Jet Propulsion Laboratory, California Institute of Technology, under a contract with the National Aeronautics and Space Administration. The technical support of F. Davarian, P. Robbins, and Kentom Widyono in the development of this analysis is gratefully acknowledged. The project was managed by Dr. H. Donald Messer of Voice of America.

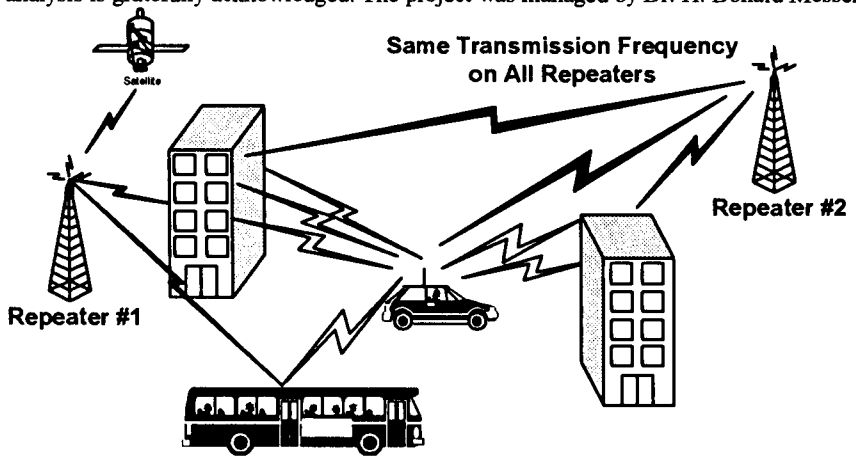

Figure 1. DBS-R Operational Scenario

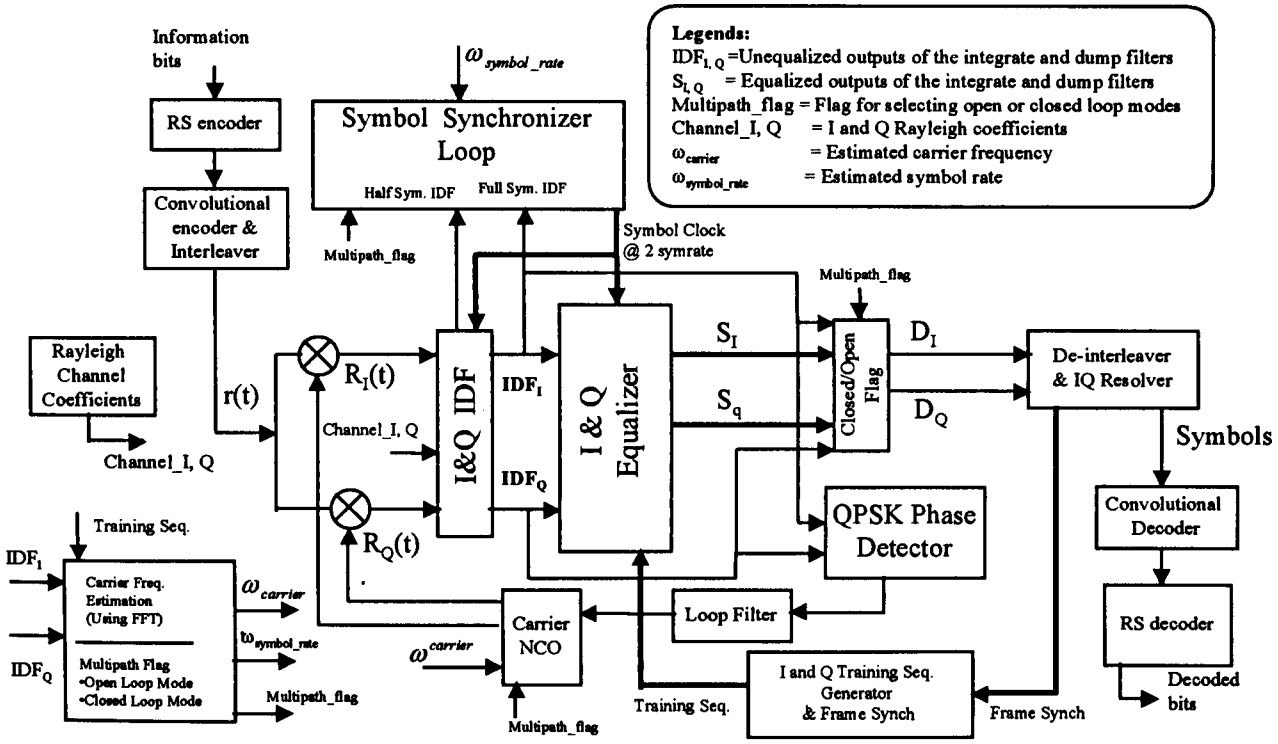

Figure 2. DBS-R Receiver Detail block Diagram

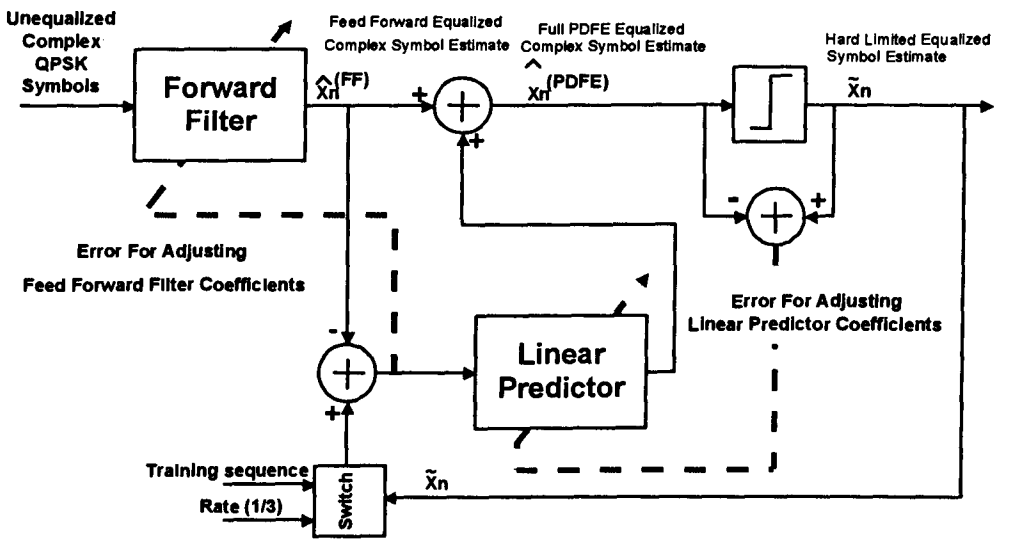

Figure 3. Decision-Feedback Equalizer Block Diagram

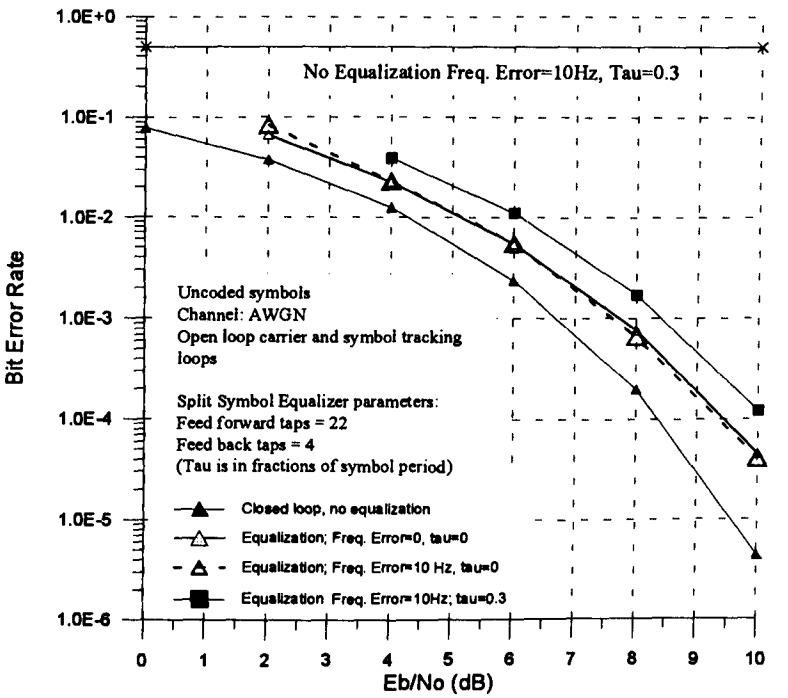

Figure 4. BER Results Using Equalization for AWGN Channel

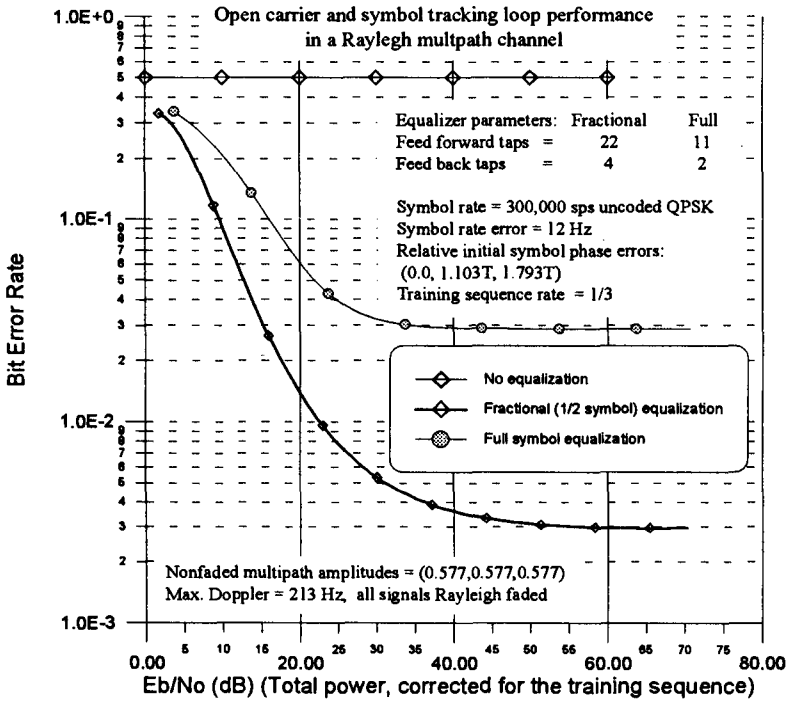

Figure 5. BER Results Using Equalization for a Multipath Rayleigh Channel

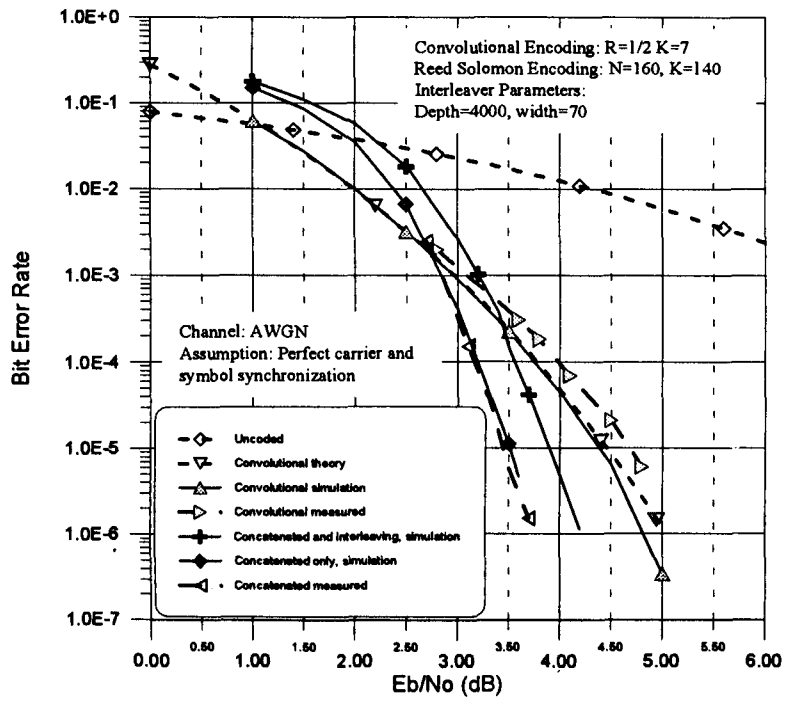

Figure 6. BER Results for AWGN Channel Using Concatenated Coding and Interleaving

NASA and CD Radio's TDRSS Industrial Test Program

Robert D. Briskman - CD Radio Inc.
1001 22nd Street, N.W.; Wash, DC 20037 USA
Phone: 202-296-6840 Fax: 202-296-6265

James E. Hollansworth - NASA Lewis Research Center
Cleveland, OH 44135 USA
Phone: 216-433-3458 Fax: 216-433-8705

ABSTRACT

The National Aeronautics and Space Administration (NASA) has embarked on a joint test program with CD Radio Inc. The program will demonstrate spatial diversity techniques in support of industrial development of a new satellite direct-broadcast national radio service called Satellite Radio. Satellite Radio will operate in the FCC approved frequency band 2310-2360 MHz which is close to NASA's Tracking and Data Relay System (TDRSS) satellites' high power transmit frequency near 2110 MHz. The cooperative test program in which NASA provides use of a TDRSS satellite and CD Radio provides the measurement equipped vehicle is described as well as its current status. Some initial measurement data are presented.

INTRODUCTION

Direct broadcast of radio programming from satellites to listeners in mobile vehicles, primarily automobiles and trucks, and in homes will be available before the end of the century. The service is called Satellite Radio and will operate in the Federal Communications Commission's approved frequency band 2310-2360 MHz. The service will provide listeners with diversity of radio programming, particularly in rural areas; niche programming, including foreign language and ethnic channels; and educational and cultural opportunities on a nationwide basis. Technical development, manufacturing and industrial benefits are also foreseen. Providing high quality Satellite Radio service to mobile vehicles requires that service outages, which are primarily caused by multipath and physical blockage be made extremely infrequent. CD Radio. intends to accomplish this by use of satellite spatial diversity in conjunction with other outage mitigation methods. Additional measured data on satellite spatial diversity at S-band frequencies would be useful, and a cooperative program with the National Aeronautics and Space Administration (NASA) was derived using the government's Tracking and Data Relay Satellite System, whose satellites can transmit with reasonable power at S-band (approximately 2110 MHz). The industrial test program is described in the following material.

SYSTEM/EXPERIMENT DESCRIPTION

The long range program is the accumulation of data on satellite spatial diversity performance for mobile reception in automobiles over a wide range of environments and conditions. This includes the various terrains throughout the country, operation in suburban/urban areas, effects of elevation angle to the satellites, and of trees, etc. The data will take the form of service outage occurrences and the length of such occurrences as a function of the previously mentioned conditions. The duration of the experiment is expected to be lengthy for several reasons, one of which is that measurements can only be performed when the TDRSS satellites are not being used for government purposes or for other experiments and as a function of the satellites' orbital locations.

The first phase of the experiment program has been initiated and will be described in the following material. The objective of the first phase was to characterize precisely the TDRS-to-automobile path in a mobile environment. The goal is to obtain field strength and polarization characteristics of the path over the eastern half of the contiguous United States. This can be done from the TDRS-East at elevation angles of interest (i.e., 20°-35°).

The measurement system utilizes a NASA

uplink which generates a Ka-band carrier to the TDRSS satellite sufficient to saturate the satellite's S-band transmitter. NASA also positions the satellite antenna beam to the portion of the eastern half of the U.S. where measurements are to be made that day. The S-band carrier is transmitted from the satellite using right hand circular polarization (RHCP). The measurement vehicle was developed, instrumented and operated by CD Radio. It is a passenger automobile with an instrument pod mounted on the roof containing a RHCP receiving antenna, a LHCP receiving antenna, and a Global Positioning System (GPS) antenna with the preamplifiers, detectors and a data acquisition system inside the car. Figure 1 is a simplified system depiction and Figure 2 shows a typical TDRS satellite downlink antenna coverage. Essentially, the amplitude of the received right and left hand polarized satellite transmissions are measured as a function of the automobiles physical location and time.

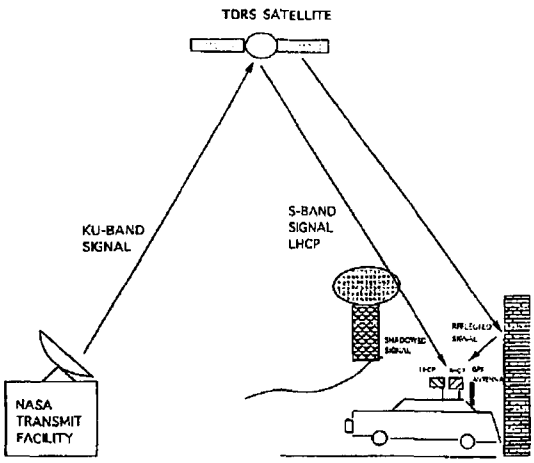

Figure 1 - System Configuration

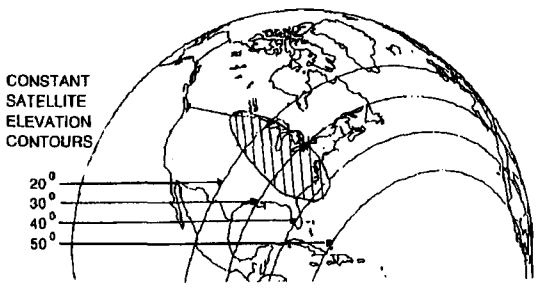

Figure 2 - S-Band Beam from TDRS at 45 Degress West

The link budget is based on a satellite beam center EIRP of 46.4 dBW (i.e., a flux density of -116 dBW/m^2/4kHz). A nominal path loss of -190.5 dB, a receiving beam center car antenna gain of 3.5 dBi and losses of 1.2 dB result in a received power of -141.8 dBW. The receiver noise power in its 1 kHz detection bandwidth is -176.3 dBW. Assuming good measurement precision at a C/N of 8 dB and averaging over 200 samples, fading of 26 dB can be accurately measured. The TDRS antenna's maximum axial ratio over the 3 dB beamwidth is 1.5 dB and the automobile antennas are similarly specified. An axial ratio of 1.5 dB reflects a cross-polarization rejection of 21 dB. However, since most measurements were made closer to beam center where axial ratios are better, the total polarization isolation is estimated as 25 dB $\pm$ 5 dB.

The following sections describe in more detail the space segment, the measurement vehicle and early measurement results.

SPACE SEGMENT

The NASA/CD Radio TDRSS Industrial Test program is based upon the Space Act of 1958 (42 U.S.C. 2451 et seg.) sections 203(c)(5)and 203(c)(6) and as implemented by NASA Management Instruction (NMI)1050.9A. The purpose of the Space Act Agreement is to conduct joint experimental programs between NASA and U.S. Industry for public benefit, U.S. manufacturing and obtaining technical data and development. There are two general types of Space Act Agreements called for (1) Reimbursable and (2) Non- Reimbursable.

NASA's Space Act Agreement with CD Radio is Non-Reimbursable and calls for the obtaining of technical data regarding satellite reception of digital audio radio at S-band on mobile platforms. The experimental program includes the testing of polarization isolation, diversity reception techniques and advanced automobile antennas at S-band.

The NASA satellite constellation that is being used for the CD Radio Industrial Test is the Tracking and Data Relay Satellite System (TDRSS) as shown in Fig.3. This system operates at both S-band (2025-2300 MHz) and at Ku-band (13.7-15.3 GHz). Single-access services in the S-band and Ku-band ranges use the umbrella-shaped, steerable 4.9-meter parabolic dish antennas to communicate with one user at a time. Operating in the S-band and Ku-band frequencies, the TDRSS can handle up to 300 million bits of information each second from a user, the

equivalent of the material in a 20 volume encyclopedia.

Tracking and Data Relay Satellites communications is controlled from two ground terminals located at White Sands, New Mexico. This site was chosen for its low geographic latitude within the United States, affording a clear view of the satellites, and because service interference caused by weather was minimal. The terminals are responsible for maintaining such functions as transmitting commands to the spacecraft, receiving the user data returned through each TDRSS, and keeping track of system status.

Under normal operations all uplink and downlink communications between a TDRSS satellite and the Earth (White Sands, NM) pass through the satellite's 2-meter parabolic dish antenna near the hexagonal satellite body. The NASA/CD Radio Test Program utilizes the same White Sands Uplink but uses the 4.9 meter parabolic dish antenna to transmit digital audio signals to the test vehicle on the ground see Fig 1.

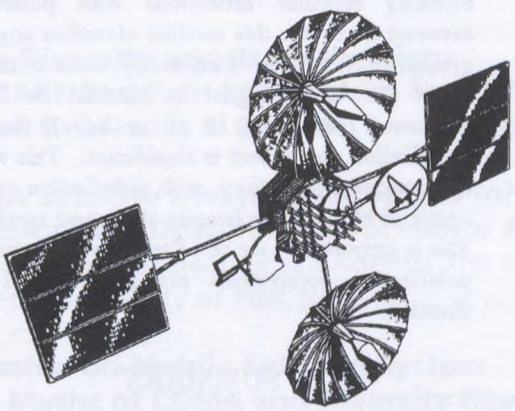

Figure 3 - Tracking and Data Relay Satellite System (TDRSS)

EARTH SEGMENT

The automobile used for the initial measurement phase is shown in Fig. 4 and its equipment block diagram in Fig.5. The LHCP and RHCP antennas are quadrifilar helices. The instrument pod contains microwave S-band absorber material to prevent reflection from the automobile rooftop from affecting the transmission path characterization. The data acquisition computer records the data in blocks, each block having a time stamp (6 bytes), vehicle location, speed and compass heading from the GPS (17 bytes) and the two signal amplitudes (4 bytes). An additional field is to be added allowing vehicle operator insertion of terrain/environment codes. By use of the vehicle tire rotation detector, it is possible to measure data only when the vehicle is in motion. Various equipment calibration and self-test features have been incorporated particularly to keep the receiving system gain, noise temperature and center frequency within required tolerance.

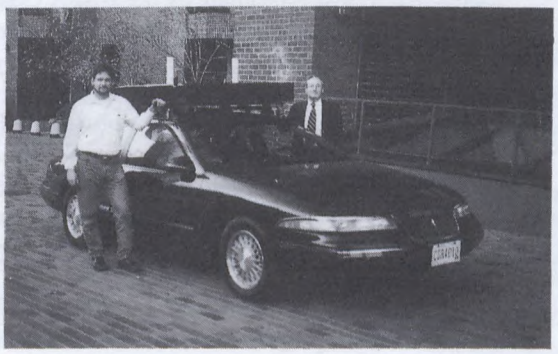

Figure 4 - Measurement Automobile

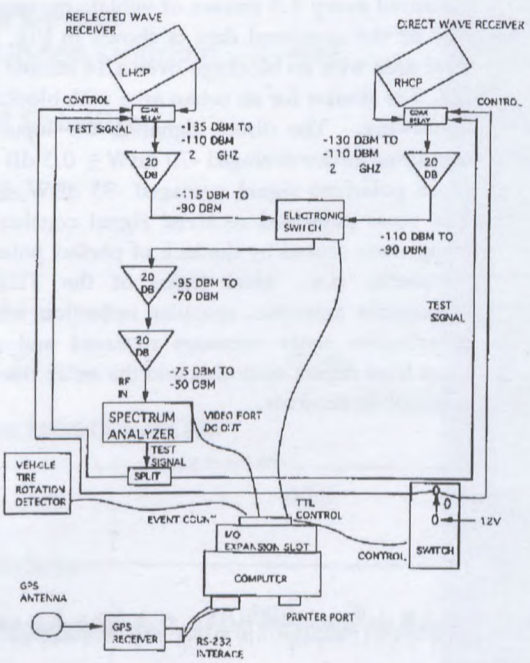

Figure 5 - Test Receiver

EARLY MEASUREMENTS

Several measurement sessions were conducted late last year. The initial one was static for equipment performance and calibration. This was followed by short mobile measurements both to characterize equipment performance in the automobile and to make routine the TDRS scheduling by the NASA Goddard Space Flight Center (GSFC). These tests detected leakage paths in the automobile measuring equipment which were rectified by additional shielding and changes in cable runs and minor software defects. The scheduling by GSFC was handled in an extremely efficient and professional manner. As earlier mentioned, besides finding convenient holes in the busy TDRS schedule, GSFC provides the up-link satellite signal and frequency clearance of the high flux density TDRS down link signal so no interference is caused to other government users of this radio frequency.

Two long duration measurement runs were made on October 30 and 31, 1994 each of several hours. Many hundreds of kilometers were covered including areas of downtown Washington, DC, suburban Virginia and rural Virginia. Data points were measured every 1.5 meters of vehicle movement. A plot of the measured data is shown in Fig. 6 for a rural area with no blockage over a 14 minute period. Fig. 7 is similar for an urban area with blockage and shadowing. The direct signal at the input of the measuring device averaged -70 dBW $\pm$ 0.5 dB and the cross polarized signal averaged -95 dBW $\pm$ 5 dB. The cross polarized received signal consists of the components caused by the lack of perfect polarization circularity (i.e., axial ratio) of the TDRS and automobile antennas, specular reflection where the polarization sense becomes reversed and residual noise from diffuse scattering and the noise floor of the automobile receiver.

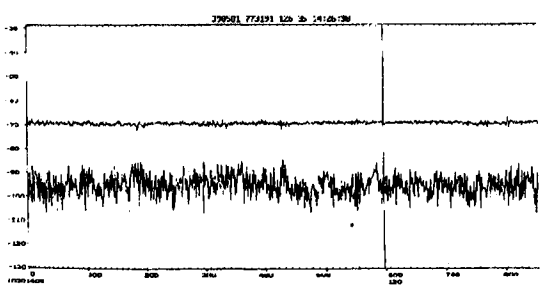

Figure 6 - Measurement Data (Rural)

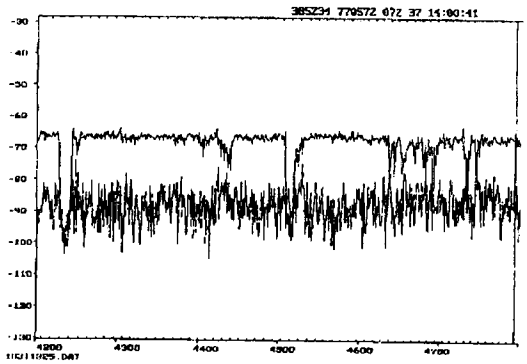

Figure 7 - Measurement Data (Urban)

Preliminary partial analysis of the data indicates relatively few occasions that a significant cross polarization component occurs under non-blockage/shadowing conditions of the direct signal. Significant is meant herein as where the cross polarized component is -12 dB or more with respect to the direct signal. This implies that few non-blocking specular reflections with polarization reversal occur for this satellite elevation angle and ground environment. Conversely, most of the time when the direct signal is blocked or heavily shadowed (attenuated 15 dB or more), the cross polarization component is significant. This implies that specular reflections with polarization reversal occur in blockage or heavily shadowed conditions. This is supported by the fact that the significant cross polarization components are generally of short duration.

SUMMARY

At the conclusion of testing, CD Radio will reduce the data obtained and issue a formal report summarizing the results of the testing. Copies of this report will be made available to NASA and the Federal Communications Commission. This type of cooperative government industry test program has been initiated by NASA and CD Radio Inc. to derive useful data on satellite spatial diversity in connection with the development of a new broadcasting service in the United States which will benefit the public, technology development and manufacturing.

The Use of CDMA for LEO and ICO Mobile Satellite Systems

Session Chairman: **Peter McLane**, Queen's University, Canada
Session Organizer: **John Lodge,** Communications Research Centre, Canada

Topic Introduction: CDMA is becoming an increasingly popular choice of multiple access scheme for mobile and mobile satellite systems. For the future mobile satellite systems for personal communications, the potential advantages of CDMA are sought after by some (e.g., Globalstar and Odyssey), while others remain skeptical and prefer to use a combination of FDMA and TDMA (e.g., Iridium and Inmarsat-P). Of the potential benefits of CDMA, none has been more controversial than that of path diversity. Questions that arise include; "How much performance can be gained and at what cost (e.g., extra feeder link bandwidth and power)?", and "Can similar gains be achieved without the use of CDMA (i.e., for FDMA/TDMA schemes)?"

This session is comprised of six papers all focusing on the above theme, but presenting widely varying views. Some of the papers include propagation data to fortify their conclusions. The diversity of opinions expressed in these papers exceeds the path diversity by a substantial margin!

Satellite Diversity and its Implications on the RAKE Receiver Architecture for CDMA-Based S-PCNs

P. Taaghol, A. Sammut, R. Tafazolli, B. G. Evans
Mobile Communications Research Group
Centre for Satellite Engineering Research, University of Surrey
Guildford, Surrey GU2 5XH, England
Tel: +44 1483-25 9808, Fax: +44 1483-25 9504
E-mail: P.Taaghol@ee.surrey.ac.uk

Abstract- *In this paper we examine the applicability of RAKE receivers in a mobile LEO satellite channel and identify the potential problem areas. We then proceed to investigate the possibility of a coherent combining architecture (downlink) in the presence of satellite diversity. We closely examine the path delay difference statistics of a diversity channel and propose a delay compensation scheme for the downlink in order to reduce the complexity of the user terminal. Finally, the required modifications to the conventional RAKE receiver are proposed and discussed.*

I. Introduction

Recently there has been great interest in the employment of CDMA for Satellite Personal Communications Networks (S-PCNs) in search of capacity improvements, and easier frequency resource management, over conventional TDMA and FDMA. Although the advantages of CDMA are clear in terrestrial cellular networks, its effectiveness when employed for mobile satellite communications is not yet clear.

One of the most important advantages of the terrestrial cellular CDMA system is the capability of constructively combating multipath through RAKE receivers. In a mobile satellite environment this is not as straightforward due to small delay spreads associated with such environments. However, the use of satellite diversity to introduce multipath has been suggested in [1] and [2]. In this paper we closely look at some of the practical issues involved in coherently combining the two diversity paths using RAKE receiver architecture. The paper is organised as follows, in section-I we briefly discuss the differences between the mobile terrestrial and satellite wideband channel characteristics and their implications on the receiver architecture. In section-II we discuss a particular LEO satellite constellation and examine the availability of dual satellite diversity for a range of latitudes. We then proceed in section-III to investigate the statistics of path delay difference in a dual diversity scheme for a series of different gateway positioning scenarios, the results of which will provide a valuable source of information for the design of RAKE receivers. And finally in sections-IV and V, we discuss the required modifications to both the overall structure and various elements of the conventional RAKE receiver.

II. Multipath Diversity

In relatively narrowband communication systems, the existence of multipath causes severe fading. In wideband CDMA systems, however, the multipath environment can be exploited through RAKE receiver architecture, allowing signals arriving with different propagation delays to be independently received and combined to provide an additional gain. This is a unique feature of the DS/CDMA referred to as *Multipath Diversity* which is essentially another space diversity technique.

It is known that if the chip rate $1/T_c$ (where T_c is the chip duration) is higher than the channel coherence bandwidth ($B_c \approx 1/T_d$, where T_d is the delay spread), fading tends to be frequency selective. Because there are many propagation paths with different delay times, the transmitted signal components corresponding to these propagation paths arrive at the receiver at different times [3]. If T_c is smaller than all of the differences in propagation delay time, each of the signal components corresponding to the propagation paths can be resolved and combined in the despreading process using RAKE receivers.

The use of RAKE receivers in terrestrial suburban and urban environments proves to be very effective due to the sufficient delay spread associated with such channels, as shown in Table-1.

Table(1): Distribution of delay spread in different terrestrial environments [4]

Type of Terrestrial Environment	*Delay Spread (Δ)*
Suburban area	0.5 μs
Urban area	3 μs

However, it has been demonstrated in the recent wideband channel measurement campaigns [5], [6] that in low-earth altitude satellite channels the delay spread has an average of about 100ns. Hence any CDMA system designed to effectively make use of the spreading to combat multipath would have to be spreading by at least an amount greater than the coherence bandwidth, i.e. 10MHz or more [2]. The available spectrum resources do not allow this since in WARC '92 a total of 16.5MHz band has been allocated to Mobile Satellite Services (MSS).

Although it appears that CDMA loses its most important advantage, i.e. the capability to resolve and combine the different paths when applied to the mobile satellite channel, it should be realised that independent fading paths with sufficient path delays can be introduced in the form of *satellite diversity*. This would ensure that the difference in the arrival times of the signals from the two satellites, transmitting to any given mobile, is greater than the duration of one chip of the spreading sequence, allowing effective employment of RAKE combining architecture.

III. Satellite Diversity in a LEO Constellation

The design of the 48 satellite Globalstar-like constellation ensures that dual diversity is offered only at a restricted range of latitudes. The minimum elevation angle to both the user terminal and the gateway station has been specified as 10°, although this may differ in a real system, i.e. the gateway station may be able to operate a link to satellites at a lower elevation angle. The following diagram illustrates the variation of dual satellite visibility potential with latitude to ground and mobile stations at a minimum elevation angle of 10°. The longitude of the ground station has negligible effect on visibility over time.

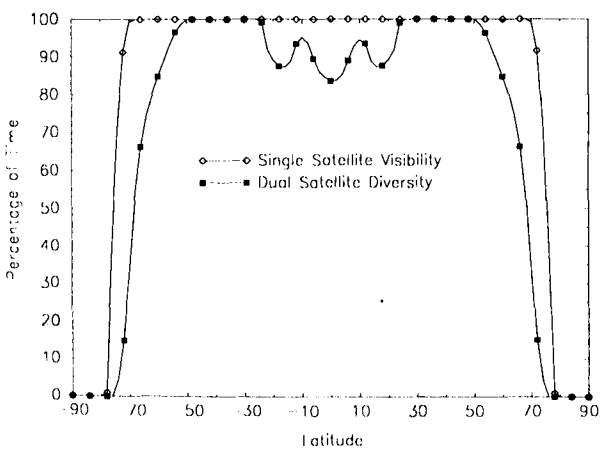

Figure-1. Dual diversity variation with latitude

As far as applicability of RAKE to a dual satellite diversity scenario is concerned, the mobile user must experience a dual satellite diversity which is also common to a suitable gateway station as shown in Figure-2. In the downlink the gateway station transmits information to the appropriate two satellites which then relay the traffic to the user using two different spreading code sequences. The User Terminal (UT) delays the signal received from one path with respect to the other, despreads the two signals, and sums the results using a RAKE combiner. In the uplink the user terminal transmits only one signal which is relayed by both satellites to the gateway station which can then resolve the signals.

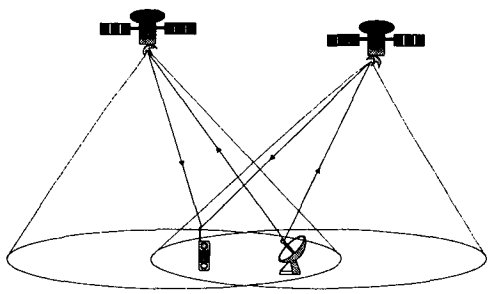

Figure-2. The dual diversity scenario

Hence, in order to be able to design and analyse the optimum receiver architecture for such an environment, path delay statistics are of great interest.

IV. Constellation Simulation and Gateway Positioning

One consideration that has to be made within such a system design is the availability of an appropriately positioned Land Earth Station (LES), capable of communicating with the same satellites as the mobile user. Since the availability of this mutual dual diversity also depends on the position of the mobile user, we have considered four scenarios in which the user terminal is positioned around London with the position of the serving gateways at: Paris (France), London (England), Cornwall (England) and Frankfurt (Germany).

a) Simulation Results

The availability of the mutual dual diversity for different scenarios are as follows:

Table-2: Dual diversity availability

Case	*UT*	*LES*	*Mutual Dual Diversity Availability (% time)*
1	London	Paris	99.53
2	London	Cornwall	99.45
3	London	London	99.61
4	London	Frankfurt	94.73

The Globalstar constellation provides 100% dual diversity down to 10° minimum elevation angle only in the regions ±26° to 50° latitude. As the simulations are partly performed outside this range some of the non-availability is due to this fact, but most of the non-availability can be attributed to the absence of a common gateway station to both the satellites and the UT. The distributions of the difference in delay between the two paths were obtained through a series of simulations for locations in Table-2 over a 24 hr period with steps of 1 second. Note that in our simulations the user terminal always selects the two satellites with the highest elevation angle. The process of handover from one satellite to the other is assumed to be instantaneous in order to have the worst case sudden changes in the path delays.

The distribution of the path delay differences throughout the simulations for different gateway locations were found to be similar, thus we only concentrate on case 1 of Table-2 as a representative case (Figure-3).

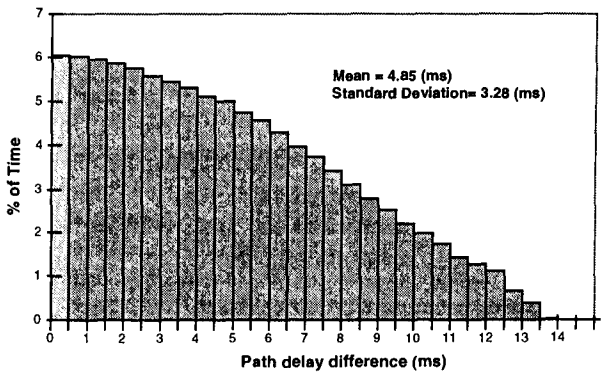

Figure-3. Path delay difference distribution for case(1); LES in Paris and UT in London

As illustrated above, the path delay difference is greater than a *chip* duration for most of the time (assuming a chip rate of about 1 Mchips/s). It is also evident that this path delay difference is much larger than a *bit* duration for a large percentage of time and could be as high as 13.5ms.

In order to reduce the user terminal complexity, it is possible in the downlink to compensate for long path delays at the gateway transmitter. The gateway can estimate the path length to the centre of each spotbeam[1] since it is aware of:

1. The spotbeam from which the user terminal is communicating.
2. The elevation angle of the gateway to the satellite.

Hence the gateway can delay one path with respect to other before transmission to decrease the wide range of this delay variation as shown in Figure-4.

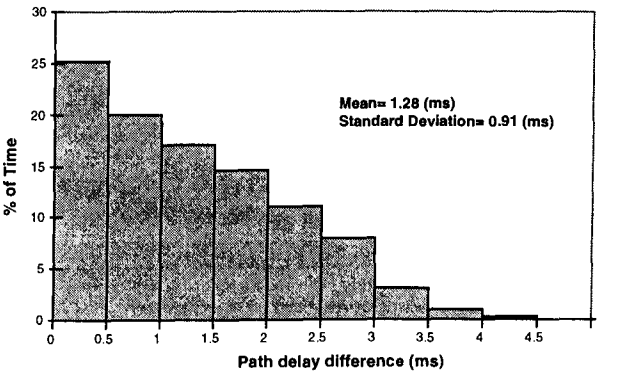

Figure-4. Compensated path delay difference distribution, case(1); LES in Paris, UT in London

Figure-5 shows the cdf of the received path delay differences of both the uncompensated and the compensated case.

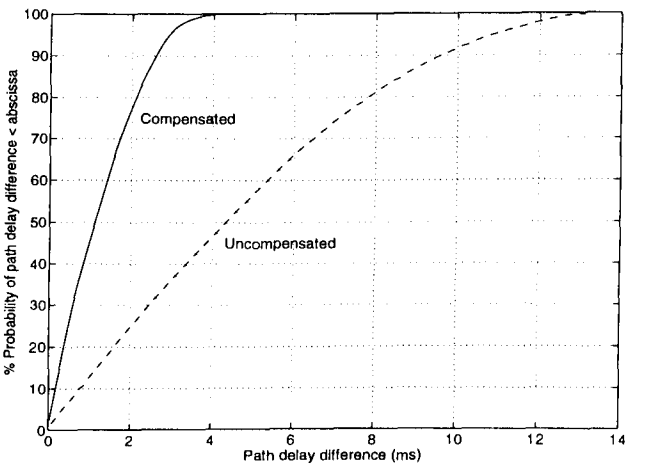

Figure-5. cdf of the received path delay differences for both the compensated and uncompensated case

As illustrated above, in the compensated case no delays (relative delays) greater than 4.2ms are experienced and for about 80% of the time delays are less than 2ms. In comparison, delays of up to 13.5ms are experienced and delays of less than 2ms are encountered for only 25% of the time in the uncompensated case.

From the code acquisition and tracking point of view it is very important to know how fast these delays change in such dynamic constellations. In our simulations we have closely looked at these changes. The variations in the path

[1] A 19 cell honeycomb beam-formed cell structure is assumed here.

delays as the satellites move over will be of the following three natures,

1. The gradual movement of the satellites hence changes in the slant path.
2. Satellite handover as higher elevation angle satellites become available.
3. Spotbeam handover as the spotbeams move with respect to the UT (position only in the compensated case).

Figures 6 and 7 show the distribution of these changes per second for both the uncompensated and the compensated case.

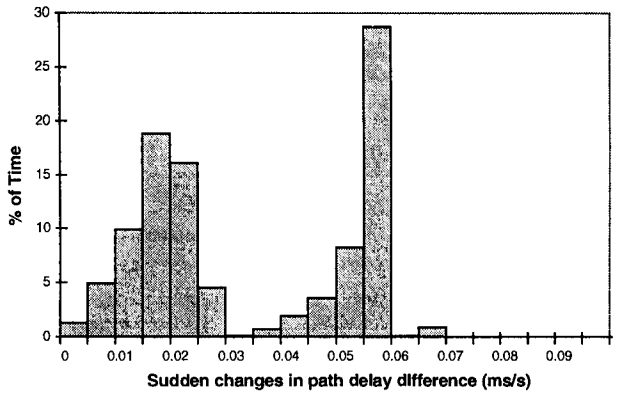

Figure-7. Distribution of the rate of change in the path delay difference in ms/s for the uncompensated case.

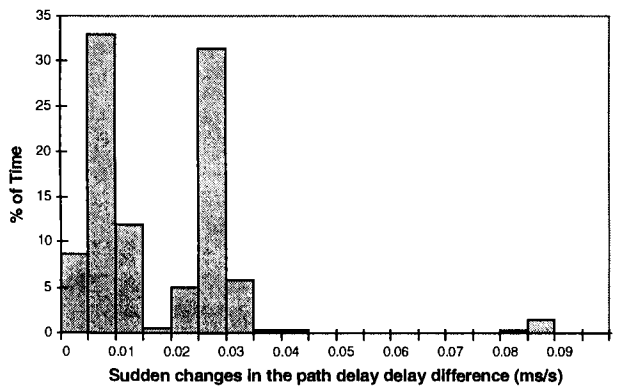

Figure-8. Distribution of the rate of change in the path delay difference in ms/s for the compensated case.

From above it is evident that the rates of change (change in the path delay difference/second) are generally smaller for the compensated case. This information could be later used to determine the rate by which the taps of the RAKE should be updated.

Figure-6 shows the cdf of sudden changes in delay difference between the two paths. Note that the shape of the cdf depends not only on the constellation but also on the position of UT and LES. However, in all the simulated cases of Table-2 the range of rate changes were very similar (between 0 - 0.1 ms/s) .

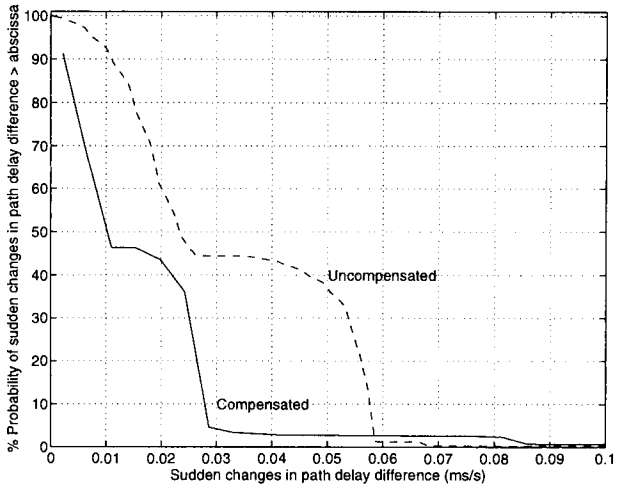

Figure-6. cdf of the changes in the delay difference between the two paths.

Note that from the above diagrams large sudden changes caused by satellite or spotbeam handovers are not clearly represented since compared to the gradual changes they do not occur very often as shown below,

	Probability of change > 0.1 ms/s
Uncompensated	0.61 %
Compensated	1.19 %

V. Implications of the Diversity Channel on the RAKE Receiver Architecture

In this section we concentrate on the implications of the dual diversity channel on the RAKE receiver architecture in the downlink.

a) Modified RAKE architecture

As mentioned before, the gateway will transmit through two satellites to the UT using two separate spreading sequences in order to avoid channel estimation complexity. This implies that two independent channel estimators should be used to provide the delay and the weighting factors for each RAKE arm as shown in Figure-9.

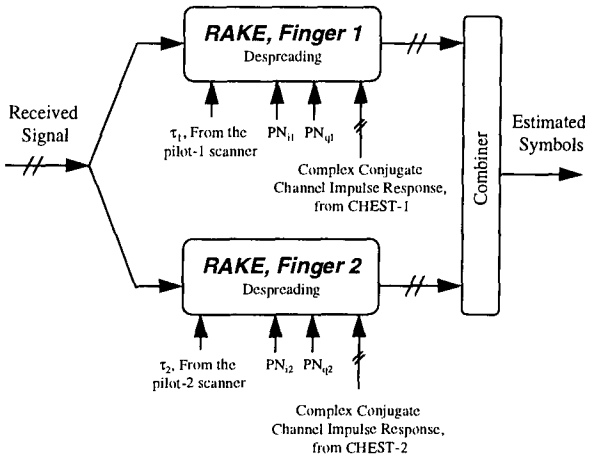

Figure-9. The two arm RAKE receiver

Where τ_1 and τ_2 are the estimated delays of each path, PN_i and PN_q are the locally generated inphase and quadrature spreading sequences respectively and CHEST is the channel estimator.

b) Channel Estimation (CHEST)

The downlink channel estimation schemes are all reference based due to the existence of the pilot channel. The downlink channel estimation can be performed on the pilot channel, an information-free channel transmitted by the gateway station.

In the case of *unsynchronised* gateway stations there is no clock distribution and consequently the spreading sequences used will have short periods. In practice the period of the pilot channel has to be of adequate length in order to able to provide different addressing codes for different gateway-spotbeam-satellite links. The shorter the period of the code, the shorter the acquisition time. On the other hand, the sequence has also to be long enough in order to be able to determine the relative delay of one path with respect to the other. In fact, the code length must be greater than twice the maximum path delay difference (d_{max}),

$$Code\ Period\ (s) > 2.d_{max}\ (s)$$

As shown in Figures 3 and 4 the maximum path delay difference is 13.5ms for the uncompensated and 4.5ms for the compensated case. This implies that the code period must be greater than 27ms and 9ms respectively.

In the case of the *synchronised* gateway stations, all the gateways share a common clock distribution, for example, through the Global Positioning System (GPS). In such a scenario, pilot channels could have very long spreading sequences which are offset in time from other pilot channel sequences. The time offset between the different code sequences must similarly be greater than twice the maximum path difference delay for the channel estimator to be able to estimate the relative delay between the two paths. Given a PN code sequence of finite length, the larger the offset time the fewer the number of usable codes. Hence the delay compensation technique discussed in section-IV is of vital importance in order to reduce the required offset time between the PN sequences of different pilot channels, and to avoid user terminal complexity. Note that the scenario discussed in this paper can be categorised as synchronised without the need for global synchronisation between the gateway stations, since the UT communicates through two satellites using the same gateway station.

c) Delay Adaptation Rate

Once the pilot scanners have estimated the path delays of the two links, the adaptation algorithm will update the programmable delays in each RAKE arm directly. It should then update the delay to keep up with the changing path delays. Figures 6, 7 and 8 illustrate the statistics of these changes. It can be seen that the changes in the path delay difference for more than 95% of the time are less than 0.1ms/s. Hence, knowing the maximum rate of change in the path delay difference and the chip duration, the rate of delay updating algorithm can be determined.

d) Satellite/Spotbeam Handover

In order to be able to provide seamless handover with no degradation in the quality of service a third RAKE finger with a different channel estimator and pilot channel scanner is required. The scanner continuously looks for another pilot channel code. Once a strong pilot channel is identified, taps of the third finger will be set and the channel impulse response from the CHEST will be fed into the RAKE. Finally when the handover takes place the 3rd RAKE will replace either of the other two arms.

VI. DISCUSSION AND CONCLUSIONS

We have demonstrate that the delay between two paths in a dual diversity scenario is large enough for employment of combining receiver architecture such as RAKE. However, since the difference in the path delay between the two satellites could be as large as 13.5ms, it is very important to employ a delay compensation technique at the gateway station to reduce the complexity of the user terminal and in particular the code acquisition and channel estimation algorithm.

We also propose the necessary modifications to the conventional RAKE architecture. That is, in order to take advantage of this diversity each RAKE finger at the user

terminal must carry out independent delay and channel impulse response estimation through employment of independent channel pilot scanners and channel estimators. As far as the acquisition time is concerned it is important to keep the length of the pilot channel's spreading code to a minimum. This implies that the path delay difference at the UT must also be as low as possible. The delay compensation technique discussed here is very simplistic. A more accurate delay compensation technique (UT positioning technique) would reduce the range of difference in the path delays which in turn improves the acquisition time.

It is also important to point out that such a system would introduce an extra delay equivalent to the difference in the path delay, which may affect the quality of service (longer end to end delays).

REFERENCES

[1] B. R. Vojcic, L. B. Milstein, and R. L. Pickholtz, "The Effect of Dual Satellite Diversity on the Total Capacity of Multiple Band-shared CDMA LEOS System", *New Orleans: ICC'94,* vol. 2, pp. 1141-1144, May 1994.

[2] B. R. Vojcic, R. L. Pickholtz, and L. B. Milstein, "Performance of DS-CDMA with imperfect power control operating over a low earth orbiting satellite link," *IEEE Trans. Select. Areas Commun.,* vol. 12, no. 4, May 1994.

[3] A. Higashi and T. Matsumoto, "Combined Adaptive RAKE Diversity and Coding for DPSK DS/CDMA Mobile Radio", *IEEE Jnl. Selct. Areas Comms.,* vol. 11, no. 7, pp 1076-1083, Sept 1993.

[4] W. C. Y. Lee, "Mobile communications design fundamentals," *Second Edition*, pub. John Wiley & Sons, 1993.

[5] E. Lutz, D. Cygan, M. Dippold, F. Dolainsky, and W. Papke, " The land mobile satellite communication channel-recording, statistics, and channel model," *IEEE Trans. Vehicular Technol.,* vol. 40, no. 2, May 1991.

[6] N.Kleiner, W.J.Vogel, "Impact of Propagation Impairments on Optimal Personal Mobile Satellite Communication System Design", November 1992, Australia.

DS-CDMA Satellite Diversity Reception for Personal Satellite Communication: Downlink Performance Analysis

Riccardo De Gaudenzi *, Filippo Giannetti **

* European Space Agency,
European Space Research and Technology Centre,
P.O. Box 299, 2200 AG Noordwijk, The Netherlands,
Phone: +31-1719-84227, Fax: +31-1719-84956,

** University of Pisa,
Dipartimento di Ingegneria della Informazione,
Via Diotisalvi 2, 56126 Pisa, Italy
Phone: +39-50-568548, Fax: +39-50-568522

Abstract

The downlink of a satellite-mobile personal communication system employing power-controlled Direct-Sequence Code Division Multiple Access (DS-CDMA) and exploiting satellite-diversity is analyzed and its performance compared with a more traditional communication system utilizing single satellite reception. The analytical model developed has been thoroughly validated by means of extensive Monte Carlo computer simulations. It is shown how the capacity gain provided by diversity reception shrinks considerably in the presence of increasing traffic or in the case of light shadowing conditions. Moreover, the quantitative results tend to indicate that to combat system capacity reduction due to intra-system interference, no more than two satellites shall be active over the same region. To achieve higher system capacity, differently from terrestrial cellular systems, Multi-User Detection (MUD) techniques are likely to be required in the mobile user terminal, thus considerably increasing its complexity.

1. Introduction

A number of personal communication systems based on Low and Medium Earth Orbiting (LEO, MEO) satellite constellations have been proposed and are under development. Direct-Sequence Code Division Multiple Access (DS-CDMA) is frequently selected as access scheme because of its noteworthy low power flux density emission, time-domain signal discrimination and interference resistance. Although the DS-CDMA multipath fading mitigation capabilities over the satellite mobile channel are still matter of contention for signal bandwidth up to a few MHz, it is well recognized its potential advantage when exploiting satellite-diversity reception. So far, the scarce quantitative results published about the link performance analysis for LEO/MEO satellite-mobile communication systems exploiting path-diversity reception, deal mainly with the inbound (mobile-to-gateway) link [1] and assume a simplified fading channel model to ease analytical derivations.

Diversity techniques in conjunction with DS-CDMA have been proved to be very effective for terrestrial cellular systems [2], [3], where the line-of-sight (LOS) signal is normally absent and lognormal-Rayleigh fading is experienced [3]. Furthermore, terrestrial system capacity is generally interference-limited. On the contrary, satellite systems are typically power-limited and consequently "forced" to exploit the LOS signal. Additionally, the peculiar satellite fading channel characteristics render impossible any accurate prediction of the diversity benefits by means of a straightforward extrapolation of the results obtained for the terrestrial cellular environment. This paper intends to offer an insight on the practical advantages in terms of link performance, when the satellite-diversity reception is exploited utilizing a Rake receiver [4] on the user side. The focus is on the downlink because it is often more demanding in terms of required spacecraft EIRP per channel compared to the uplink. The technique presented is of general applicability, whereas the numerical results reported are representative of typical LEO working conditions.

2. System Outline

The scenario to be analyzed is depicted in Fig. 1-a. It is assumed that one mobile user is simultaneously receiving the signals from N_s satellites in visibility. The signals are uplinked from the same gateway station equipped with the necessary antenna and facilities required to independently track the N_s satellites, each generating N_b spot beams toward the Earth surface. Throughout the paper the beam numbered as *one* will be the reference beam where the user is supposed to be located, and i will denote the location of the user within the reference beam. The user is seen by the l-th beam pertaining to the k-th satellite with an antenna angle $\theta^{(k,l,i)}$ with respect to the centre of beam (COB) direction. To provide soft hand-off and to make diversity reception possible, every satellite spot beam re-uses the same carrier frequency. Orthogonal DS-CDMA is adopted for each CDM multiplex transmitted from the gateway station to the satellite to eliminate the intra-beam self-noise effect [5]. No time-synchronization among the different satellite signals is assumed, thus after despreading CDM signals coming from different satellites generate asynchronous CDMA self-noise at the demodulator side. The power-control system is supposed to keep constant the average signal-to-noise plus interference ratio at the receiver side, but it is not capable to counteract the fast shadowing components. As shown in [13], the maximum shadowing speed which can be tracked by a closed-loop power-control system is estimated in less than 1 Hz for a LEO system orbiting at 1400 Km altitude. The demodulator is assumed to be a

conventional Rake receiver [4], [6] performing coherent combining of the N_c most powerful rays ($1 \leq N_c \leq N_s$). Based on satellite pilot broadcasting hypothesis, perfect signal carrier phase and amplitude estimation will be assumed.

3. Channel Model

The satellite-mobile channel model for the k-th satellite link is shown in Fig. 1-b. The model presupposes flat fading and closely follows the one recently devised by [7] for mobile satellite systems. The model, which applies to each satellite to mobile terminal link, has found very good matching with experimental data collected in Canada [8] and in Europe by the European Space Agency in several test campaigns embracing open and suburban environments with satellite elevation up to 80°. The flat fading assumption for chip rates below 2 Mc/s has been confirmed by several wideband test campaigns recently conducted in Europe [9], Japan and USA [10]. In Ref. [3] a flat fading channel was also retained for the performance analysis of a mobile satellite system utilizing DS-CDMA whereby the signal bandwidth was not in excess of 1.5 MHz. For a given propagation environment, the channel parameters are clearly dependent on the actual elevation angle $\psi^{(k,i)}$ of the k-th satellite as it is seen by the user in the i-th location. The fading process bandwidth is mainly related to the relative speed of movement between the satellite and the mobile user. In the above block diagram, $\xi_L^{(k,i)}(t)$ is a lognormal real process with bandwidth $B_L^{(k,i)}$ characterized by the following parameters $E\left\{10\log_{10}\left[\xi_L^{(k,i)}(t)\right]\right\} \triangleq \mu_L^{(k,i)}$ and $E\left\{\left(10\log_{10}\left[\xi_L^{(k,i)}(t)\right]-\mu_L^{(k,i)}\right)^2\right\} \triangleq \left[\sigma_L^{(k,i)}\right]^2$, which takes into account the effects of signal shadowing. The signal $\tilde{\beta}_R^{(k,i)}(t) \triangleq \beta_c^{(k,i)}(t) + j\beta_s^{(k,i)}(t)$ is a complex Gaussian process with independent unit-power I-Q components having bandwidth $B_R^{(k,i)}$ which represents multipath effects, while the parameter $R^{(k,i)}$ is the so-called Rice factor. Each channel is further characterized by the average carrier-to-multipath ratio $[C/M]^{(k,i)}$ for the k-th satellite link, defined as the ratio between the line-of-sight and the multipath power, i.e. $[C/M]^{(k,i)}$ [dB] $= 10\ \log_{10}\left[R^{(k,i)}\right]$, and the LOS power loss, given by $[\Delta P]_{LOS}^{(k,i)}$ [dB] $= \mu_L^{(k,i)} + \left[\sigma_L^{(k,i)}\right]^2/(20\log_{10}e)$. In general, there will be some degree of correlation among the shadowing processes affecting the different satellite links, chiefly related to the geometrical separation among the actual orbital positions of the satellites. Analytically, this can be formulated by decomposing each lognormal process in two independent components, $\zeta(t)$ representative of the common user near-field and $\zeta^{(k,i)}(t)$ pertaining to the particular satellite link, so that $10\log_{10}\left[\xi_L^{(k,i)}(t)\right] \triangleq 10\log_{10}[\zeta(t)] + 10\log_{10}\left[\zeta^{(k,i)}(t)\right]$ with $E\{10\log_{10}[\zeta(t)]\} = 0$, $E\{(10\log_{10}[\zeta(t)])^2\} = \sigma_\zeta^2$, $E\{10\log_{10}\left[\zeta^{(k,i)}(t)\right]\} = \mu_L^{(k,i)}$, $E\{\left(10\log_{10}\left[\zeta^{(k,i)}(t)\right]-\mu_L^{(k,i)}\right)^2\} = \sigma_{\zeta^{(k,i)}}^2$ and $E\{10\log_{10}[\zeta(t)]\cdot 10\log_{10}\left[\zeta^{(k,i)}(t)\right]\} = 0\ \forall\ k,\ i$. We define the following variances of the common and path-dependent lognormal shadowing processes, respectively, $\sigma_\zeta^2 \triangleq \rho^2\left[\sigma_L^{(k,i)}\right]^2$, $\sigma_{\zeta^{(k,i)}}^2 \triangleq \left(1-\rho^2\right)\left[\sigma_L^{(k,i)}\right]^2$ so that $\left[\sigma_L^{(k,i)}\right]^2 = \sigma_\zeta^2 + \sigma_{\zeta^{(k,i)}}^2$ with the parameter ρ representing the shadowing correlation coefficient evaluated for the best path, i.e. the path having the lowest shadowing. Channel parameters are derived from the experimental data fitting described in [7] that will be utilized for the numerical performance evaluation outlined in Section 5. A zero shadowing correlation factor will be used in the sequel considering that, generally, the spatial separation among satellites is large enough to provide mutually independent satellite-to-terminal shadowing/fading processes[1] and that the slow shadowing components due to near-field LOS signal obstruction will be in large part compensated by the power-control system. The zero shadowing processes correlation assumption corresponds to the best case from the diversity gain point of view. The parameters from [7] correspond to typical conditions foreseen for a system operating with omnidirectional hand-held antenna in a rural tree-shadowed environment with different satellite elevation angles.

4. Performance Analysis

As mentioned before, QPSK-based Orthogonal CDMA (O-CDMA) with pilot transmission is considered for the outbound link [5]. As discussed in [11], results are also applicable to the QO-CDMA signalling format described in Ref. [12]. A more detailed description of the signal format for both, O-CDMA and QO-CDMA is provided in [11]. To abbreviate the analysis according to the system functional diagram depicted in Fig. 1-c, we will start straight from the power associated to the samples at the symbol matched filter of the demodulator, corresponding to the traffic and pilot signal, respectively, evaluated at time $t_m = m\,T_s$, being T_s the symbol duration, given by

$$p_T^{(k,l,n,i)}(m) = P_0\,\alpha_V^{(k,l,n)}(m)\,\gamma_T^{(k,l,n,i)}(m)\left[a^{(k,i)}(m)\right]^2 g(\theta^{(k,l,i)})$$
$$p_P^{(k,l,i)}(m) = P_0\,\gamma_P\left[a^{(k,i)}(m)\right]^2 g(\theta^{(k,l,i)}) \qquad (1)$$

where k points out the satellite index, l is the satellite antenna beam index, n identifies the active carrier index, i indicates the user location, and $g(\theta^{(k,l,i)})$ is the the l-th normalized beam gain in the direction $\theta^{(k,l,i)}$ ($g(0) = 1$). The symbol P_0 stands for the nominal power received at the satellite antenna beam centre under unobstructed multipath-free conditions. The receiver antenna is assumed to be omnidirectional. The parameter $\alpha_V^{(k,l,n)}(m)$ takes into account the effect of the voice-activity detection (VAD) on the transmitted power per carrier, according to the following notation

$$\alpha_V^{(k,l,n)}(m) = \begin{cases} 0 & \text{if no voice} - \text{activity detected} \\ 1 & \text{if voice} - \text{activity detected} \end{cases}$$
$$E\{\alpha_V^{(k,l,n)}(m)\} \triangleq \bar{\alpha}_V \quad \forall\ k,l,n \qquad (2)$$

[1] The orbital parameters are commonly selected to optimize the Earth coverage by minimizing the number of satellites, thus maximizing their spatial separation.

Finally, $\gamma_T^{(k,l,n,i)}(m)$ and γ_P denote the power margin for the traffic and the pilot, respectively. Clearly, the pilot margin is fixed for all beams while, as discussed in [13], the traffic carrier power margin is slowly adapted in closed-loop fashion according to the average shadowing experienced by the user. Let now introduce the following arrays :

$$\begin{aligned}
\underline{p}_T^{(l,n,i)}(m) &\triangleq \left[p_T^{(1,l,n,i)}, \dots p_T^{(N_s,l,n,i)}\right]^T, \\
\underline{p}_P^{(l,i)}(m) &\triangleq \left[p_P^{(1,l,i)}, \dots p_P^{(N_s,l,i)}\right]^T, \\
\underline{a}^{(i)}(m) &\triangleq \left[a^{(1,i)}, \dots a^{(N_s,i)}\right]^T, \\
\underline{\alpha}_V^{(l,n)}(m) &\triangleq \left[\alpha_V^{(1,l,n)}, \dots \alpha_V^{(N_s,l,n)}\right]^T \\
\underline{\gamma}_T^{(l,n,i)}(m) &\triangleq \left[\gamma_T^{(1,l,n,i)}, \dots \gamma_T^{(N_s,l,n,i)}\right]^T, \\
\underline{g}^{(l,i)}(m) &\triangleq \left[g(\theta^{(1,l,i)}), \dots g(\theta^{(N_s,l,i)})\right]^T
\end{aligned} \tag{3}$$

The Rake demodulator performs the sorting of the signal powers. The sorted powers can be indicated as

$$\begin{aligned}
\underline{\hat{p}}_T^{(l,n,i)}(m) &= \mathbf{H}^{(1,i)}(m)\, \underline{p}_T^{(l,n,i)}(m), \quad \underline{\hat{p}}_P^{(l,i)}(m) = \mathbf{H}^{(1,i)}(m)\, \underline{p}_P^{(l,i)}(m) \\
\underline{\hat{a}}^{(i)}(m) &= \mathbf{H}^{(1,i)}(m)\, \underline{a}^{(i)}(m), \quad \underline{\hat{\alpha}}_V^{(l,n)}(m) = \mathbf{H}^{(1,i)}(m)\, \underline{\alpha}_V^{(l,n)}(m) \\
\underline{\hat{\gamma}}_T^{(l,n,i)}(m) &= \mathbf{H}^{(1,i)}(m)\, \underline{\gamma}_T^{(l,n,i)}(m), \quad \underline{\hat{g}}^{(l,i)}(m) = \mathbf{H}^{(1,i)}(m)\, \underline{g}^{(l,i)}(m)
\end{aligned} \tag{4}$$

where the $N_s \times N_s$ sorting matrix $\mathbf{H}^{(1,i)}(m)$ is obtained as a permutation of the identity matrix so that the following relation is verified :

$$\hat{p}_P^{(k,1,i)}(m) \geq \hat{p}_P^{(k+1,1,i)}(m) \quad \forall\ m,\ 1 \leq k \leq N_s - 1 \tag{5}$$

By defining the equivalent number of active carriers as

$$\begin{aligned}
N_{eq}^{(k)}(m) \triangleq\ & \frac{(1+\chi_p)}{2} \sum_{l=1}^{N_b(k)} \hat{g}(\theta^{(k,l,i)}) \\
& \left[\gamma_P + \sum_{n=1}^{N(k,l)} \hat{\alpha}_V^{(k,l,n)}(m)\, \hat{\gamma}_T(m)^{(k,l,n,i)}\right]
\end{aligned} \tag{6}$$

after some manipulation one can find [13] :

$$\begin{aligned}
\left[\frac{E_b}{N_0 + I_0}\right]^{(i)}(m) \simeq\ & \left\{ \left(\left[\frac{E_b}{N_0}\right]_{LOS} \cdot \sum_{r=1}^{N_c} \left[\hat{a}^{(k,i)}(m)\right]^2 \right)^{-1} \right. \\
& \left. + \gamma_A \frac{\sum_{r=1}^{N_c} \sum_{k=1, k\neq r}^{N_s} N_{eq}^{(k)}(m) \left[\hat{a}^{(r,i)}(m)\, \hat{a}^{(k,i)}(m)\right]^2}{\sum_{r=1}^{N_c} \left[\hat{a}^{(k,i)}(m)\right]^2} \right\}^{-1}
\end{aligned} \tag{7}$$

$$\left[\frac{E_b}{N_0}\right]_{LOS} \triangleq \frac{P_0}{N_0 R_b}, \quad \left[\frac{\overline{E}_b}{N_0}\right]^{(k,i)}_{LOS} \triangleq \left[\frac{E_b}{N_0}\right]_{LOS} \cdot 10^{\frac{[\Delta P]^{(k,i)}_{LOS}\ [\mathrm{dB}]}{10}} \tag{8}$$

where $N_b(k)$ is the number of beams for the k-th satellite, $N(k,l)$ is the number of active carriers for the l-th beam, χ_p is the resulting cross-polar isolation factor at the user side[2], $G_p \triangleq R_c/R_b$ is the so-called processing-gain, R_c and R_b are the chip and bit rate, respectively, m/p is the rate of the error correcting code and M is the size of the M-ary PSK constellation used. Moreover, $\gamma_A \triangleq 2m/(p\, G_p R_b \log_2 M)$, $\left[\overline{E}_b/N_0\right]_{LOS}$ represents the ratio between the average energy per bit and the noise density received at the centre of the beam in the presence of the sole LOS component. Equation (6) represents the equivalent average number of traffic carriers, useful for interference computation, seen by the i-th user from the k-th satellite. Its value is clearly dependent on the traffic distribution among the spot beams and on the satellite antenna design. The equivalent number of active carriers $N_{eq}^{(k)}(m)$ is a random variable depending on the power margins assigned to the individual traffic carriers by the power-control system to counteract the non uniform propagation conditions encountered by the traffic channels in the different beams. In the derivation of eqn. (7) the effect of the asynchronous CDMA interference coming from the different satellites in visibility has been approximated by additional AWGN of equivalent power spectral density [3], [11]. Each satellite beam has up to L orthogonal signatures available to be used for the spreading of the traffic channels. To perform a full reuse of the orthogonal signatures each beam superimposes to the traffic channels a different long pseudo-noise (PN) sequence. Therefore, an user located within the reference beam that is receiving the n-th carrier from the k-th satellite, sees the signals coming from the remaining $N_b(k) - 1$ beams of the same satellite as non-orthogonal interferers, due to the superposition of the PN sequence. Since, the capacity of the system turns out to be rather modest as it will result from the following numerical results, the total number of traffic carriers transmitted by every satellite is assumed to be less than L. In this case no reuse of orthogonal signatures among beams is required and therefore the same PN sequence can be superimposed.

If the bit error rate is related by a known expression $f(\cdot)$ to the bit energy-to-noise density ratio $\phi^{(i)} \triangleq \left[E_b/(N_0 + I_0)\right]^{(i)}$, the average probability of error for the signal is given by

$$\overline{[P_b]}^{(i)} = \int_0^{+\infty} f\left(\phi^{(i)}\right) p_\Phi(\phi^{(i)})\, d\phi^{(i)} \tag{9}$$

where $p_\Phi(\phi^{(i)})$ is the equivalent bit energy to noise density PDF, derived from eqn. (7). In absence of diversity reception, the probability of error can still be computed through eqns. (7) and (9) by setting $N_c = 1$ and disabling the sorting mode of the Rake demodulator based on signal power estimation, i.e. letting $\mathbf{H}^{(1,i)}(m) = \mathbf{I}\ \forall i,\ m$, being $\mathbf{I}$ the identity matrix. The link outage probability [7] is simply computed as

$$P_{out}(\phi^{(i)}_{nom}) = \int_0^{\phi^{(i)}_{nom}} p_\Phi(\phi^{(i)})\, d\phi^{(i)} \tag{10}$$

where $\phi^{(i)}_{nom}$ is the value of $\phi^{(i)}$ corresponding to the maximum BER.

Let now suppose that every satellite has the same number of beams N_b and that the voice-activity factor can be replaced by its average value. We also suppose that the power margin of a generic traffic channel can assume only values belonging to a finite set $\gamma_T^{(s)}$, $1 \leq$

[2] In the sequel when $\chi_p < 0$ dB, equal sharing of the left and right satellite antenna circular polarization is assumed among the active user's population. $\chi_p = 0$ dB corresponds to the case of no polarization reuse.

Case No.	Sat. 1 Elevation	Sat. 2 Elevation	Sat. 3 Elevation
1	30°	30°	30°
2	30°	40°	50°
3	20°	40°	-

Table 1: Multi-satellite configurations

$s \leq S$, with probability $\lambda^{(s)}$, each corresponding to a specific environment. Over a large population of users we can assume that the associated probabilities $\lambda^{(s)}$ are time invariant so that eqn. (6) can be reformulated as

$$N_{eq}^{(k)} \simeq \frac{(1+\chi_p)}{2} \sum_{i=1}^{N_b} g(s^{(k,l,i)}) \left[\gamma_P + N(k,l)\,\overline{\alpha}_V \sum_{s=1}^{S} \lambda^{(s)} \gamma_T^{(s)} \right] \tag{11}$$

where by definition $\sum_{s=1}^{S} \lambda^{(s)} = 1$. Equation (11) includes most of the system dependent parameters, thus decoupling the time consuming numerical evaluation of the equivalent signal-to-noise ratio PDF given by eqn. (7) from detailed system design issues such as satellite antenna gain shape, cross-polar isolation factor and link margin statistical distribution.

5. Numerical Results

According to eqn. (9), the average bit error computation requires the derivation of the PDF of the energy per bit to noise plus interference ratio. Looking at eqn. (7), a computer simulation approach seems to be the only viable solution. The N_s independent fading and shadowing processes have been simulated together with the Rake sorting functionality and combined according to eqn. (7). An histogram of the PDF of $\phi^{(i)}$ has been derived and the result has been used to numerically evaluate the integral described by eqn. (9). Two cases, corresponding to the different satellite configurations listed in Table 1, have been examined assuming $G_p = 64$, $m = p = 1$, $M = 4$. Figure 2-a reports the bit error rate results for an uncoded coherent DS-QPSK system, similar to the the one described in Ref. [5]. Continuous line curves correspond to the Case 1 of Table 1 for $N_s = 3$ satellites in simultaneous visibility and $N_c = 2$ signals combined by the Rake receiver. The calculation has been performed for several $[\overline{E}_b/N_0]_{LOS}$ and for different beam loading conditions. $N_{eq}^{(k)} = 0, 10 \ldots 60\ \forall k$. In order to perform a fair comparison, in the case of diversity reception the $[\overline{E}_b/N_0]_{LOS}$ corresponds to the cumulative $\overline{E}_b/N_0$, where the energy-per-bit is comprehensive of all the LOS paths received from the N_s satellites. In the specific case ($N_s = 3$), $[\overline{E}_b/N_0]_{LOS}$ for the diversity reception is 4.77 dB higher than the individual link $\overline{E}_b/N_0$. Error-counting computer simulations have been successfully compared with the semi-analytical bit error rate derivation based on equations (7), (9). The simulation model used is representative of the system discussed in Fig. 1. Similarly to the analysis, the asynchronous CDMA interference has been represented by an equivalent AWGN process to make the simulation manageable both, in complexity

Beam No. [l]	Norm. distance from COB $r^{(k,l,i)}$	Norm. antenna gain $g(r^{(k,l,i)})$ (dB)
1, 2, 3	1	-1
4, 7, 10	2	-10
5, 6, 8, 9, 11, 12	$\sqrt{7}$	-15

Table 2: Satellite antenna characteristics

Index [s]	Propagation environment	Probability of occurrence $\lambda^{(s)}$	Link margin $\gamma_T^{(s)}$ [dB]
1	Open	0.3	3.0
2	Light shadowing	0.6	6.0
3	Medium shadowing	0.1	12.0

Table 3: Power margin distributions

and time. Such assumption has already been extensively validated in Ref. [11]. As expected, the large performance advantage provided by satellite-diversity reception under light spot beam traffic loading conditions ($N_{eq}^{(k)} \leq 10$) is attenuated when the beam traffic capacity is augmented. However, it should be reminded that the system performs a full frequency reuse in all satellite beams, therefore to achieve the same overall efficiency of TDMA-FDMA systems a lower individual spot beam loading is required. Although a limited diversity gain persists at high E_b/N_0, a BER floor due to the asynchronous CDMA interference caused by the co-frequency emission from the other satellites, limits the minimum uncoded BER attainable. Figure 2-b is representatives of a double satellite visibility case indicated as Case 2 in Table 1. Simulation results indicate the need to avoid more than two satellites active over the same geographical region reusing the identical frequency band. It is also interesting to analyze how the bit error rate modifies with the number of Rake fingers for a given number of satellites in visibility. Numerical result presented in [13], show that the additional gain provided by the third Rake finger ($N_c = 3$) is marginal compared to a two fingers receiver ($N_c = 2$). Considering that many satellite constellations provide $2-3$ simultaneous satellites in visibility for most Earth locations, a two-finger Rake receiver appears to be a good trade-off between complexity and performance advantage. The above results are of general validity for the propagation environment and the satellite constellations described by Table 1. Let now derive some numerical results for the equivalent number of active carriers in a study case by introducing the following simplified hypotheses : uniform traffic distribution in the different beams i.e. $N(k,l) = N\ \forall\ k,\ l$, equal number of beams for all the satellites, i.e. $N_b(k) = N_b\ \forall\ k$, worst-case user location (beam crossing point), satellite antenna pattern as in Table 2, cross-polar isolation $\chi_p = -8$ dB when polarization reuse is applied, $\chi_p = 0$ dB otherwise, average voice-activity factor $\overline{\alpha}_V = 0.4$, pilot margin $\gamma_P = 6$ dB, power margins distribution according to Table . Under the above assumptions, it follows that [13]

$$N \simeq \frac{1}{\overline{\alpha}_V \sum_{s=1}^{S} \lambda^{(s)} \gamma_T^{(s)}} \cdot \left[\frac{2\,N_{eq}}{(1+\chi_p) \sum_{l=1}^{12} g(r^{(k,l,i)})} - \gamma_P \right] \simeq \begin{cases} 0.19\,N_{eq} - 2.18 & \text{without polarization reuse} \\ 0.33\,N_{eq} - 2.18 & \text{with polarization reuse} \end{cases} \tag{12}$$

Const. Case	Max. N_{eq}	N/beam no polar. reuse	N_{max}/beam with polar. reuse
1	5	0	0
2	11	0	1.43
3	18.5	1.34	3.93

Table 4: System capacity not exploiting diversity for $\overline{P}_b = 3 \cdot 10^{-2}$, $[\overline{E}_b/N_0]_{LOS} = 15$ dB

Constellation Case	Max. N_{eq}	N/beam no polar. reuse	N_{max}/beam with polar. reuse
1	19.0	1.44	4.06
2	18.1	1.27	3.77
3	48.1	7.02	13.69

Table 5: System capacity exploiting diversity for $\overline{P}_b = 3 \cdot 10^{-2}$, $[\overline{E}_b/N_0]_{LOS} = 15$ dB, $N_c = 2$

Using the previous simulation results the capacities presented in Tables 4, 5 are derived for an uncoded average bit error rate of $3 \cdot 10^{-2}$. The total system capacity can be easily computed by multiplying the beam capacity shown in Tables 4, 5 by the product $N_b \cdot N_s$ representing the total number of system beams. The numerical results demonstrate the advantage provided by diversity and polarization discrimination to enhance up to three times the total system capacity. Table 5 shows the capacity advantage provided by diversity but does not highlight the related quality of service improvement. While Table 5 results on one side confirm the "low-capacity" hypothesis used in deriving eqn. (7), on the other side are quite disappointing in terms of system capacity except maybe of the Case No. 3 where only two satellites are active over the same region. Numerical results show that a double satellite diversity combined with polarization reuse are a must to achieve acceptable performance both on terms of capacity and quality of service. Countermeasures to attenuate the intra-system interference effect appears unavoidable to achieve a consistent system capacity improvement. Adaptive CDMA interference cancellation at the demodulator side appears to be the solution imposing the less constraints on the system itself. Following [14], the intra-system interference for LEO-MEO satellite personal communication systems is not peculiar of CDMA. On the contrary, the problem affects even more seriously conventional access techniques such as FDMA and TDMA.

6. Summary and Conclusions

An analytical model capable of illustrating the instantaneous signal energy-to-noise plus interference density ratio in the satellite downlink has been devised for DS-CDMA systems exploiting diversity reception. It turns out that satellite-diversity jointly with polarization reuse is indeed effective to improve the outbound link performance, provided that the satellite spacing is large enough to generate independent shadowing processes in the different links. However, the diversity usefulness weakens as the channel loading of the spot beam increases because of the BER floor generated by the asynchronous CDMA interference. The diversity reception appears less effective when at least one satellite is seen by the user with a high elevation angle. A two-finger Rake receiver results sufficient to exploit the bulk of diversity advantage in several situations. Being the asynchronous interference the major system capacity limiting factor, the use of some kind of Multi-User Detection techniques to reduce co-channel CDMA interference appears to be a necessary solution provided that the receiver complexity increase is affordable.

Acknowledgement The authors gratefully acknowledge the support provided by the ESTEC colleagues, Mr. S. Badessi for the satellite antenna modeling and by Mrs. M. L. De Mateo for reviewing the manuscript.

References

[1] B. R. Vojcic, R. L. Pickoltz, L. B. Milstein, *"Performance of DS-CDMA with Imperfect Power Control Operating over Low Earth Orbiting Satellite Link,"* IEEE Journ. on Sel. Areas in Comm., Vol. 12 , No. 4, May 1994, pp. 560-567.

[2] J. S. Lehnert, M. B. Pursley, *"Multipath Diversity Reception for Spread Spectrum Multiple Access Communications,"* IEEE Trans. on Comm., Vol. COM-35, No. 11, November 1987, pp. 1189-1198.

[3] K.S. Gilhousen, I. M. Jacobs, R. Padovani, A. J. Viterbi, L. A. Weaver Jr., and C. E. Wheatley III, *"On the Capacity of a Cellular CDMA System,"* IEEE Transactions on Vehicular Technology, Vol. 40, No. 2, May 1991, pp. 303-312.

[4] R. Price and P. E. Green, *"A Communication Technique for Multipath Channels,"* Proc. IRE, Vol. 46, pp. 555-570, March 1958.

[5] P. Monte, S. Carter, *"The Globalstar Air Interface"*, In the Proceedings of the AIAA 1994 Satellite Communication Conference, San Diego, California, USA, March 1994, pp. 1614-1621.

[6] U. Fawer, *A Coherent Spread Spectrum Diversity Receiver with AFC for Multipath Fading Channels,"* IEEE Trans. on Comm., Vol. COM-42, No. 2/3/4, February, March, April 1994, pp. 1300-1311.

[7] G. E. Corazza, F. Vatalaro, *"A Statistical Model for Land Mobile Satellite Channels and Its Application to Nongeostationary Orbits,"* IEEE Trans. on Vehicular Technology, VOL. VT-43, No. 3, August 1994, pp. 738-742.

[8] C. Loo, *"A Statistical Model for a Land Mobile Satellite Link,"* IEEE Trans. on Vehicular Technology, VOL. VT-34, No. 3, August 1985, pp. 122-127.

[9] Axel Jahn (DLR), *"Propagation Data and Channel Model for LMS Systems,"* ESA Study No. 141742, Final Report, December 1994.

[10] ITU-R Study Group, Doc. WP 10-115/USA-[C], *"Channel Fading for Mobile Satellite Communications Using Spread Spectrum Signalling and T-DRSS,"* Oct. 7, 1994.

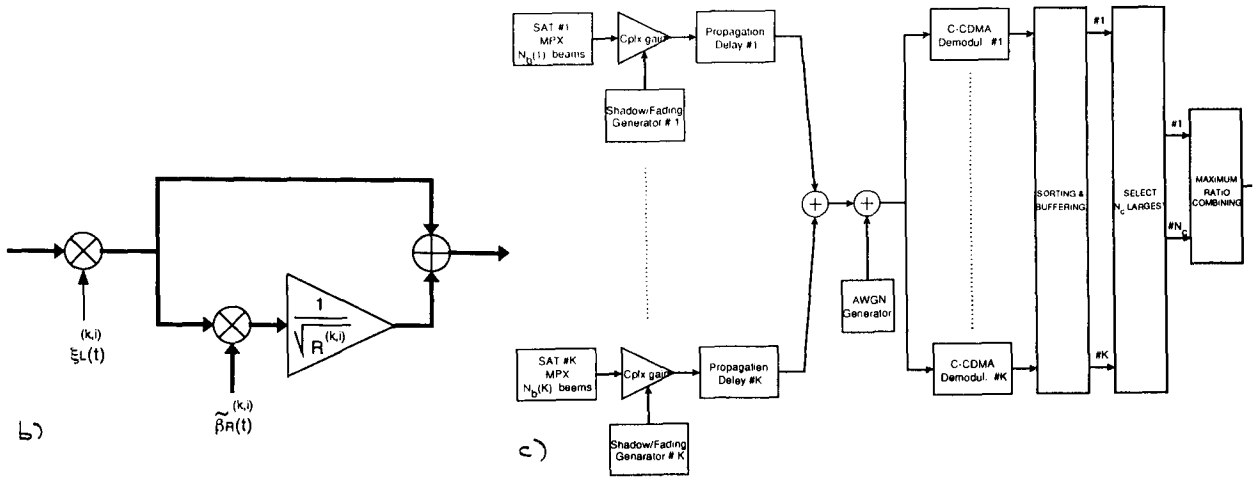

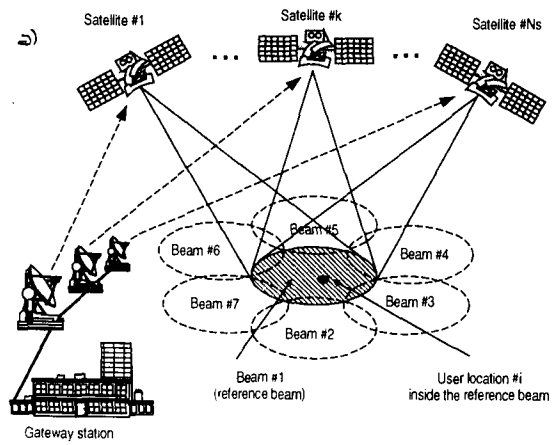

Figure 1: System and channel models

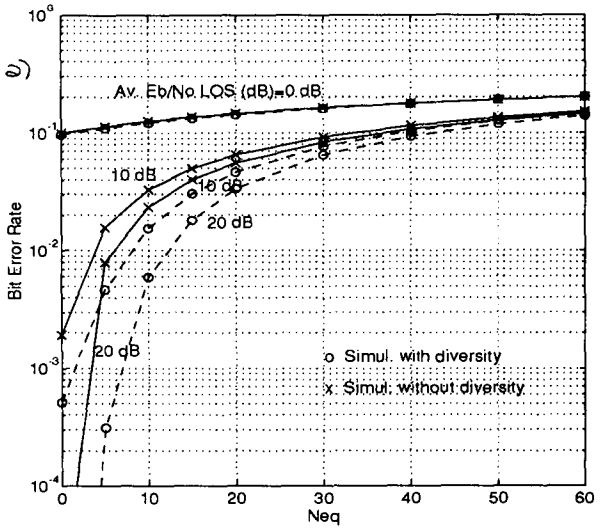

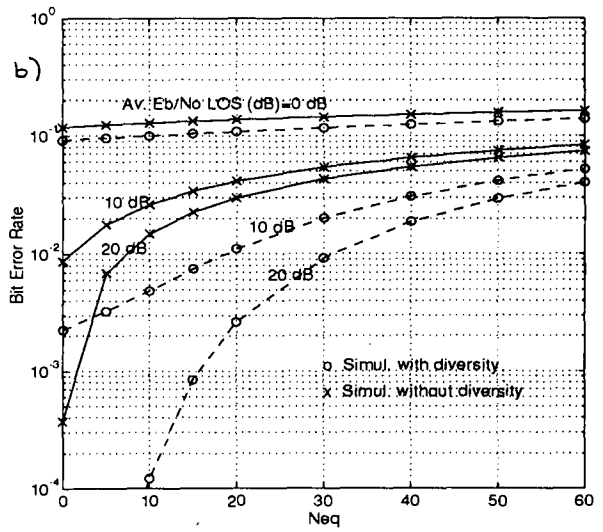

Figure 2: Average BER versus beam loading : a) case 2, b) case 3

[11] R. De Gaudenzi, T. Garde, F. Giannetti, M. Luise *"Orthogonal CDMA Transmission for Satellite-Based Mobile Communications Radio Networks"*, In the Proceedings of IEEE GLOBECOM '94, S. Francisco CA, November-December 1994.

[12] R. De Gaudenzi, C. Elia, and R. Viola, *"Bandlimited Quasi-Synchronous CDMA: A Novel Satellite Access Technique for Mobile and Personal Communication Systems"*, IEEE Journal on Selected Areas in Communications, Vol. 10, No. 2, February 1992, pp. 328-343.

[13] R. De Gaudenzi, F. Giannetti, *"DS-CDMA Satellite Diversity Reception for Personal Satellite Communication : Downlink Performance Analysis"*, Submitted to IEEE Trans. on Vehic. Technol., January 1995.

[14] F. Vatalaro, G. E. Corazza, C. Caini, C. Ferrarelli, *"Analysis of MEO, LEO and GEO Global Mobile Satellite Systems in the Presence of Interference and Fading,"* To appear on the IEEE Journal on Sel. Areas in Comm., First quarter 1995.

A Discussion on Mobile Satellite System and the Myths of CDMA and Diversity Revealed

Nicholas Hart
Inmarsat,99 City Road
London EC1Y 1AX,UK
Phone: +44 71 728 1407
Fax: +44 71 728 1702
Email:
Nicholas_Hart@inmarsat.org

Thomas Goerke
Inmarsat,99 City Road
London EC1Y 1AX , UK
Phone: +44 71 728 1704
Fax: +44 71 728 1702
Email:
Thomas_Goerke@inmarsat.org

Axel Jahn
DLR, P.O. Box 1116
82330 Wesslong, Germany
Tel: +49 81 53 282847
Fax: +49 81 53 28 1442
Email: Axel.Jahn@dlr.de

ABSTRACT

The paper explores the myths and facts surrounding:

- link margins and constellation designs;
- the use of satellite diversity in a mobile satellite channel;
- Trade-offs in multiple access technique.

Different satellite constellations are presented, which are comparable with those used by the big LEO proponents, with the associated trade-offs in the system design. Propagation data and results from various narrowband and wideband measurement campaigns are used to illustrate the expected differences in service performance.

1.0 INTRODUCTION

A number of communication networks have been proposed recently, to provide global handheld mobile satellite telephony services. The design concept for most of these systems is based on the use of non-geostationary satellite orbits. However, each of these programmes propose different system designs including orbit constellation, satellite design, multiple access scheme and mobile link margin. This paper reviews some differnet system designs considered by Inmarsat and provides an insight into their service performance and associated system design trade-offs in three key areas:

- Orbit constellation and satellite design
- Diversity and link margin handoffs
- Multiple access technique.

However, before analysing these different technical parameters it is worth considering and defining how these may impact the overall service performance.

2.0 SERVICE PERFORMANCE

In order to analyse the service performance it is necessary to define a few general terms:

- Service availability
- Call completion probabilities

Service availability is a measure of how often, or the percentage of locations from which, the service is available to a particular user. For a good system design which has sufficient network capacity and a high equipment availability this is dominated by the availability of the radio link between the mobile terminal and the satellite, termed the "mobile link". This link which uses a frequency 1.5 to 2.5 GHz may be subject o sever signal fading due to multipath fading and/or shadowing effects, as described in section 4. The mobile link availability is a function of the number of satellites potentially in view to the mobile terminal and, their associated elevation angles and link margins.

The call completion probabilities indicate the probability of a certain length call being successfully completed. Theoretically, with all the non-geostationary systems, satellite handover can be supported whereby a mobile terminal is switched or handed over to different satellites as required during a call. However, in practice as with terrestrial cellular systems, any handover process may fail which will result in the call being dropped. In this case the user may be stationary and the satellites moving. If the satellites are moving rapidly, the call completion probabilities will normally decrease as the satellite handover process will occur more frequently.

The service performance will also be affected by the environment and the actions of the user before and during a telephone call. Inmarsat has considered in detail the overall service performance in various rural, suburban, urban and in-building "real life" situations. It is clear from these analyses that service performance varies greatly with different satellite constellations.

3.0 CONSTELLATION CHOICE

The constellation choice depends upon the requirements of the system design. Generally, non-geostationary orbits are preferred for handheld mobile satellite services as they allow the overall telephony service end to end delay to be significantly reduced. Also, they provide a global service coverage, with a good overall service availability, at even high latitudes, by supporting either medium/high link margins or satellite spatial diversity and/or high elevation angles to mobile terminal.

Inmarsat considered a number of different orbit constellations before selecting the Intermediate Circular Orbit (ICO) around 10,000km, with a system baseline of 10 operation satellites. For illustrative purposes this paper also considers two LEO orbits one based on 66 satellites in polar orbits (800 km) and another using 48 satellites in an inclined orbit (1400km).

A simple method to review the relative performance between these different constellations is to consider the elevation angle statistics. Figure 1 shows the average elevation angle for the highest satellite over a range of latitudes. Figure 2 illustrates the elevation angle Probability Density Function (PDF) of the highest satellite in view for a user at 35 degrees latitude. It is clear that the ICO provides the highest elevation angles at all latitudes and has a minimum elevation angle at 35 degrees latitude of 30 degrees, with an average elevation angle well in excess of 50 degrees.

Figure 3 illustrates the probability of both one and two satellites in view for the ICO-10 and LEO48 constellations both of which are designed to provide satellite spatial diversity. Both constellations generally provide in excess 80% probability of at least two satellites in view. However, the LEO48 performance degrades rapidly above 60 latitude. Also the ICO constellation balances the statistics with the number of satellites in view against the high elevation angles for the different latitudes. The satellite spatial diversity and the high elevation angles both minimise the probability of signal shadowing due to both the local environment and head shadowing effects.

However, for most environments there is a not only high degree of correlation in the probability of being shadowed as a function of elevation angle but also as a function of azimuth angle. For example, a row of trees beside a road or street surrounded by buildings both have a similar correlation in shadowing probability as a function of azimuth angle. For example, the azimuth correlation of blocking for an urban areas is given in Figure 4. Clearly, it is not sufficient to only consider elevation statistics, in determining the relative performance of the different constellations. Inmarsat has analysed the relative performance of the ICO constellation and shown that it also has very goo azimuth decorrelation.

The speed at which the satellites move is very important in determining the call completion probabilities for stationary users. The faster the satellites move relative to the mobile terminal, the less chance there is of the call completing successfully. On average the LEO satellites move at about 15° per minute, compared to about 1° per minute for the ICO. For a call duration of 5 minutes the LEO satellites have moved through approximately 75° arc whereas the ICO satellites have only moved through 5°. This quasi-stationary feature of the ICO constellations also allows the user to move to acquire the service. For example, by crossing from one side of the street to the other a user may bring a satellite into view which then remains available for the duration of the call.

Inmarsat have analysed a number of Walker orbits before selecting the 10/2/0 constellation which has the following attributes:

- Altitude - 10350 km (6 hours)
- 10 operational satellites in two orthogonal planes
- Each orbital plane inclined at 45° to equator
- Offset between planes 0°

Figure 5 illustrates the relative satellite phasings for the constellation and Figure 6 provides a snapshot of the coverage areas from each satellite with a 10 degree cut-off angle. This shows the satellite footprinting giving continental type of coverage areas.

The baseline system was selected to provide the necessary service performance and initial capacity with the minimum number of satellites. However, the system performance and capacity can be increased further if more satellites are launched. This is easily accomplished with the ICO constellations where additional satellite planes can be introduced during the lifetime of the system.

In summary, the ICO-10-2P constellation provides very good service performance due to its high elevation angles and relatively slow satellite motion. However, clearly the LEO orbits minimise the path

distance between the mobile terminal and the satellite so potentially enabling the system link margins to be increased. The impact of link margin on the service performance is described in the next section.

4.0 PROPAGATION MEASUREMENTS

For any mobile communication network to provide a good quality service it is essential that the system design support adequate link margins. For handheld mobile satellite systems the link margin on the return link is critical as the handset radiated power is limited by radiation safety limits. There fore once the satellites are deployed the return link margin is fixed for the lifetime of that constellation.

Inmarsat has undertaken, with its Signatories, many propagation campaigns to determine and verify the minimum link margins. Narrowband (CW) studies were performed using helicopters and light aircraft to mimic moving satellites. In addition geostationary satellite propagation measurements and voice trials have been used to cross check the propagation results. More recently wideband propagation campaigns and voice demonstrations simulating satellite diversity have been performed using light aircraft to verify the link margin strategy.

This propagation data has enabled Inmarsat and its contractors to simulate the impact of different link margins, and multiple access schemes in conjunction with the different orbital configurations. Theoretical modelling of the different channel impairments using propagation tools was also essential to continually cross check both the theoretical and practical measurements to prove their validity and accuracy.

A brief review of the narrowband and wideband results are giving in this paper and more detailed analyses are given in the references.

Narrowband Measurements

The different environments that were surveyed for the narrowband campaign included rural, suburban, urban, in-building and in vehicle. Propagation effects for voice and signalling channels were characterised in each of the environments.

From the campaigns it was found that an excess link margin of 7dB was sufficient to support voice transmissions if a Line Of Sight (LOS) link was available to the satellite. The excess link margin included the loss due to coupling and shadowing associated with the users head. If a LOS link was not available the link margin required to support voice depended upon the obstruction. The margin required ranged from 10-35dB for tree clutter and 20-30dB for building clutter.

Wideband Measurements

To understand the possible benefits of the use of spread spectrum in the mobile satellite channel, Inmarsat in conjunction with DLR conducted a series of wideband trials [1,2]. The wideband measurements used a PN sequence with length 511 and a signal bandwidth of 30 MHz. The satellite transmitter was simulated using a light aircraft.

The measured data proved that the wideband characteristics of the LMS channel are completely different from the terrestrial channel. Only a few echoes with very small delays (in general less than 500 nsec) appear. The echo amplitude is fairly suppressed by 15...25 dB. These results have also been reported by [3].

From the measured data the Channel Transfer Function (CTF) has been derived. Fig. 7 gives the CTF for various environments. All figures are shown for a handheld with RHCP-antenna. In the open environment (a) the CTF is flat over the total system bandwidth of 30 dB. This is an example of the ideal channel behaviour. In the urban environment (c) there is also a frequency-flat channel for the line-of-sight (LOS) conditions. Only a small undulation of about ± 1.5dB indicates a number of small echoes. The delay spread is approximately 200 nsec corresponding to a frequency selectivity of 5 MHz. In shadowed conditions in the rural (b) and urban (d) environment, the CTFs and attenuated by 5 dB, but the channel becomes frequency-selective just above 5 MHz.

Using a spread spectrum signal and with a RAKE receiver architecture a system can benefit from the echoes. The theoretical gain corresponds tot he difference between the minimum and the maximum of the CTF $\max(CTF(f)) - \min(CTF(f))$ when all echoes are detected and combined. Then the system bandwidth should be at least $f_{\max} - f_{\min}$. A CDMA system without RAKE-receiver will even perform worse than a narrowband TDMA since the channel power is now obtained by the integration over the CTF for a given bandwidth which yields to smaller values. From the results shown above it is obvious that the satellite CDMA systems proposed so far can only benefit from the channel echoes since the system bandwidth is far too small.

Two main advantages are claimed for the CDMA technique: the fading resistance and the spectral efficiency. We could show with the wideband data that the fading resistance can not be obtained in the satellite LMS channel with a bandwidth of less than 5 MHz. In [4] it is also shown the spectral efficiency can be better achieved with a narrowband TDMA system.

5.0 DIVERSITY

Most environments suffer from some form of blockages, i.e. trees and buildings. To provide a service within these environments requires the system to provide

1. sufficient link margin to operate off reflections, or;
2. sufficient link margin to power through the obstructions, or;
3. continual LOS connections

To facilitate the first method requires large link margins which are normally associated with terrestrial cellular. The second method can only feasibly be used to combat light tree shadowing unless an unlimited link margin is available. The 3rd method uses the smallest link margin but requires sufficient satellites to be available to clear any obstructions.

From the measurement campaigns conducted by Inmarsat it has been able to compare methods 2 and 3. Table 1 illustrates the link margin required depending upon the number of satellites visible to a user in a given environment.

	Rural	Urban
One Satellite	16.5 dB	23.5dB
Two Satellites	7dB	8dB
Three Satellites	5dB	8dB

Table 1 Diversity Improvement with Multiple Satellites

There are multiple types of diversity including:

- Time diversity
- Frequency diversity
- Spatial diversity

Time diversity uses interleaving and repeat procedures. Due to the delay in the satellite system it is not possible to use time diversity for speech but it can be used for signalling. Frequency diversity is beneficial if the channel exhibits any form of frequency selective fading. From measurement campaigns it has been found that there is minimal frequency selective fading for most environments. Spatial diversity employs the characteristics of two different channels. In a satellite system these are provided using different radio links to each satellite. From analysis of propagation data and environments it is clear that spatial diversity offers a significant improvement in service performance.

To take advantage of the improvement that diversity offers requires a system design that can support transmissions from more than one satellite. There is an additional link margin gain if it is possible to combine the two transmissions. The gain for two guassian channels is 3dB, but for fading channels can be significantly greater.

The method of combining the signals can be :

- Maximal ratio combination
- Equal gain combination
- Selection combination

It is important to consider both the forward and return link as it may be possible to use different schemes on each link. For example the return link is power limited due to safety constraints and battery life whereas the forward link can make use of higher powers when the satellite is not fully loaded.

If there are two channels available to the user terminal then as one becomes faded, the other remains providing a seamless of 'soft' handover. If both channels are partially shadowed then a maximal ratio combination of the two channel may provide a reliable link where one was not possible on either.

A common fallacy is that CDMA is the only multiple access scheme in which spatial diversity can be achieved. It is not an intrinsic property of CDMA and nor is it necessarily the best technique for exploiting spatial diversity. A discussion on link margin in [3] specifics how CDMA and satellite diversity can be used to reduce margins. However, TDMA may also simply support diversity and is not constrained by many of the negative aspects of CDMA which are outlined in section 6. The Inmarsat-P system uses TDMA, and benefits from both soft handover and the link margin gains arising from satellite diversity.

6.0 MULTIPLE ACCESS METHOD

Inmarsat has undertaken a number of studies, in conjunction with industry, to evaluate the benefits of TDMA and CDMA. Theoretical analyses and simulations using realistic channel models and recorded propagation data were used to determine the

performance of the two multiple access techniques. All the studies have indicated that TDMA is favoured for the Inmarsat-P system and a summary of the main conclusions are given below.

most importantly satellite systems are generally power limited instead of interference limited as in terrestrial cellular networks. Narrowband TDMA signals are orthogonal in time and frequency apart from some minimal losses due to adjacent channel interference. Whereas non synchronised CDMA system become generally interference limited when approaching maximum capacity so reducing the system link margins. If orthogonal CDMA were to be used then the amount of interference would be reduced, however it is difficult to achieve signal orthogonality with satellite path diversity due to differential path delays.

In a TDMA system it is possible to arrange for the transmit and receive burst to occur at different times, thereby eliminating the requirement for a diplexer in the mobile terminal. Since CDMA is continuous (except for voice activation) in both directions a diplexer is required which will increase the front end losses in the terminal so reducing its sensitivity.

If a system is to use non-orthogonal CDMA then power control needs to be very accurate for CDMA otherwise the capacity will be significantly reduced. This is normally possible in terrestrial cellular due to small propagation delays but it may not be feasible in a satellite system which inherently have delays of up to 40ms even in LEO systems.

CDMA can handle modest interference gracefully if the interferer is in the same order as the signal. If the interferer is large it can wipe-out the entire multiplex. The wide bandwidth of CDMA is open to interference whereas narrowband TDMA can easily avoid interferers by assigning new time slots of frequencies.

The major claimed advantage of CDMA in terrestrial cellular systems is that frequencies can be reused between cells due to the statistical interference effects. Indeed the "size" of the terrestrial cells varies so as to try to maintain an even number of users in each cell, with, for example, rural cells being much larger than the urban sized cells. In any mobile satellite system the frequency "cells" are fixed by the spot beam size which are given by the satellite antenna aperture. For example, with the ICO satellite the spot beam footprint is around 800 km and there will be over 100 beams within the satellite footprint. Only a small fraction of these beams will be supporting any significant traffic density. TDMA enables the peak capacity within a beam to be increased and switched so as to cover real life traffic distributions.

A clear benefit of CDMA is the reduced power in the return link when compared to the high peak power requirements associated with the TDMA bursts. The differences can be minimised by using non-linear amplifiers in the TDMA mobile terminal, whilst CDMA terminals require linear amplifiers.

Finally any interference generated by one CDMA system will reduce the capacity of another CDMA system operating in the same frequency band. To reduce the interference between different systems requires very careful co-operation between system operators. With TDMA, agreements for splitting the available spectrum between different systems is easily negotiated between different systems.

7.0 CONCLUSIONS

This paper has provided a brief review of the work undertaken by Inmarsat in selecting the ICO/TDMA system to provide handheld mobile satellite services. The ICO constellations provide good service performance due to their high elevation angles and good satellite diversity properties. Whilst TDMA enables power efficient modulation schemes and peak traffic capacities to be supported.

References:

[1] **Axel Jahn**: *Narrowband and Wideband Channel Characterisation for Land Mobile Satellite Systems: Experimental Results at L-Band.* ISMC Ottawa 1995

[2] **Axel Jahn and Erich Lutz**: *DLR channel measurement programme for low earth orbit satellite systems.* In Proc. Int. Conf. on Universal Personal Communications ICUPC'94, pages 423-429, San Diego, 1994

[3] **Norbert Kleiner and Wolfhard Vogel**: *Impact of propagation impairments on optimal personal communication systems.* Workshop, Adelaide, Australia, Nov. 1992

[4] **Reuven Meidan**: *To spread or not to spread, this is the question.* In Proc. Int. Vehicular Technology Conf. VTC'94, pages 56-59, Stockholm,1994

[5] **Douglas G. Dwyre**: *Link Margin Isn't Eveyrthing* Global Mobile, Paris, October 1994.

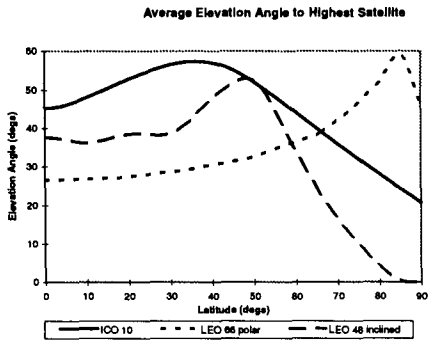

Figure 1 Average Elevation Angle to Highest Satellite

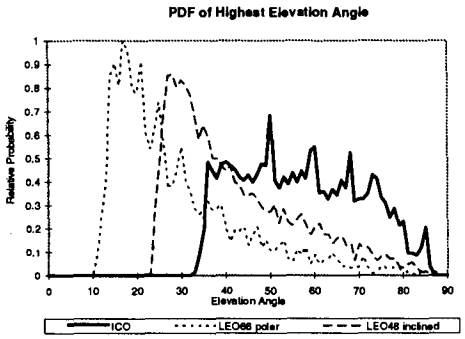

Figure 2 PDF of Highest Elevation Satellite

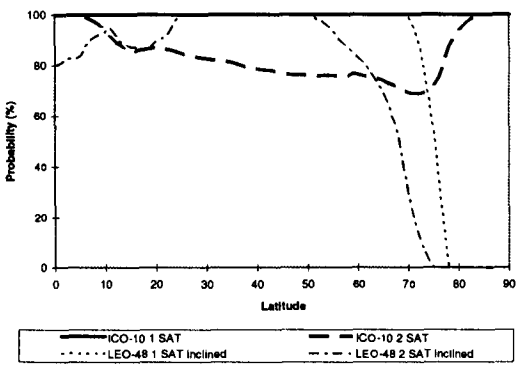

Figure 3 Probability of Satellites in View vs Latitude for Systems which use Diversity

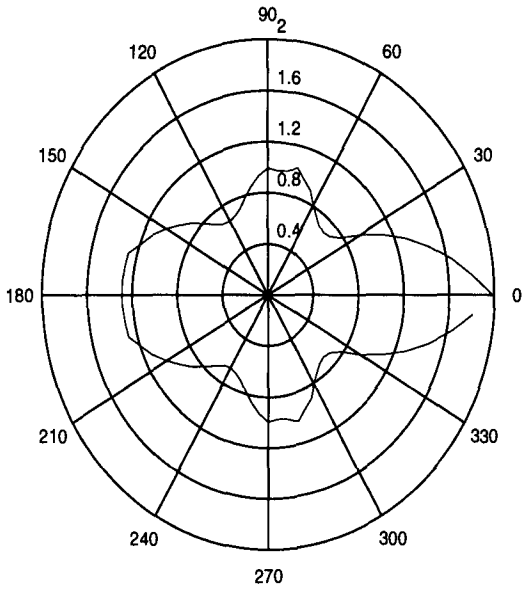

Note: 2 corresponds to correlation coefficient of +1
0 corresponds to correlation coefficient of -1

Figure 4 Azimuth correlation for an urban area

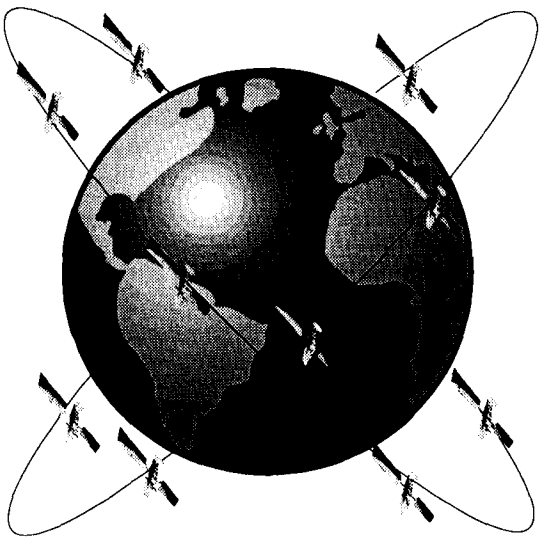

Figure 5 ICO-10 constellation

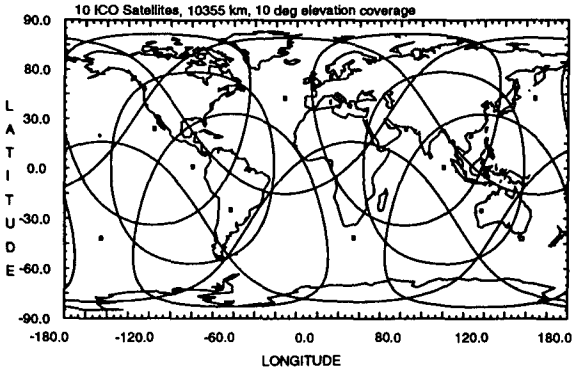

Figure 6 Snapshot of ICO-10 Constellation Coverage

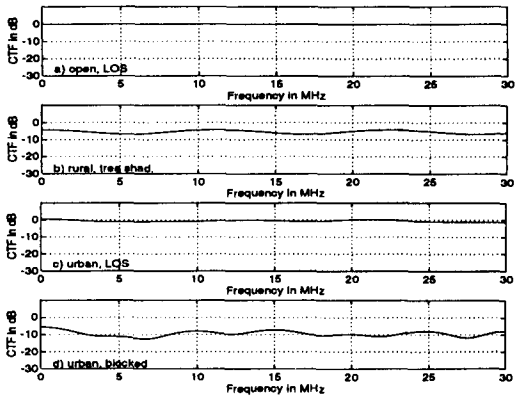

Fig. 7: Channel Transfer Function for different environments

a) open environment, LOS
b) rural environment, tree shadowing
c) urban, LOS
d) urban shadowed

Mobile User Environment and Satellite Diversity for NGSO S-PCNs

Markus Werner Hermann Bischl Erich Lutz

German Aerospace Research Establishment (DLR)
Institute for Communications Technology
P.O. Box 1116
82230 Wessling, Germany
Tel: +49 8153 28-{2826,2884,2831}
Fax: +49 8153 28-1442
E-mail: {Markus.Werner,Hermann.Bischl,Erich.Lutz}@dlr.de

ABSTRACT

The performance of satellite diversity under the influence of the mobile user environment is analysed. To this end, a digital channel model is presented which takes into account the elevation angle as well as the user mobility in a given environment.

For different LEO and MEO systems and for varying mobile user environments, some crucial benefits and drawbacks of satellite diversity are discussed. Specifically, the important GW service area concept is introduced.

The conclusions are validated by numerical results from computer simulations. Globalstar (LEO) and Inmarsat (MEO) are compared in terms of visibility, service availability, and equivalent handover complexity for different environments and user mobility.

1 INTRODUCTION

Recently, satellite diversity has been discussed as an efficient countermeasure against QOS deterioration due to shadowing effects in non-geostationary satellite systems for personal communications. Moreover, with satellite diversity the number of critical handover procedures can significantly be reduced.

Proposals like Globalstar [1] and Inmarsat-P [2] include the use of satellite diversity as fundamental system characteristic, and intensive evaluation work has already been done based on propagation data from channel measurement campaigns [3]. Besides the strong direct use of analog propagation data the work done so far is also closely related to the CDMA/Rake scenario.

In this paper we present an approach that aims at the evaluation of satellite diversity at a higher level on the one hand, i. e. focussing on the statistical exploitation of multiple satellite visibility rather than on lower level operational aspects. Our approach assumes these operational issues to be solved, however. Secondly, we base our evaluation on a simplified digital channel model; this is directly motivated by the "digital" behaviour of the mobile user link channel in LEO/MEO satellite systems and a shadowing environment.

Numerical results throughout this paper are given for two constellations, Globalstar and Inmarsat, also serving as representatives for the LEO and MEO system classes. Relevant parameters of both systems are given in Table 1.

	Globalstar	Inmarsat-P
Orbit altitude	1400 km	10354 km
Orbit period	113 min	360 min
Number of satellites	48	10
Number of orbits	8	2
Inclination	52°	45°
Min.user elev.angle	20°	20°
Footprint diameter	4760 km	10850 km
Max. footpr. pass. time	14 min	97 min

Table 1: Parameters of the considered constellations.

2 SATELLITE DIVERSITY

2.1 *Terminology*

In the course of the following considerations, a clear and consistent terminology is very important.

We consider a gateway earth station *GW* which is responsible for all communication needs of mobile users (MT) in its *service area SA*. The MT location is referred to as *user position UP*. An important distinction

has to be made between the terms *visibility* and *availability*. We call a satellite *visible* from a UP or GW, respectively, if it has an elevation angle $\varepsilon \geq \varepsilon_{\min}$. With this definition, visibility of a satellite does not necessarily mean clear line-of-sight (LOS) as common sense may expect; the clear LOS condition is rather denoted as *availability*, visibility thus being a precondition for availability. Consequently, a shadowed satellite with $\varepsilon \geq \varepsilon_{\min}$ is *visible*, but not *available*. Extending these considerations to the satellite diversity scenario, the simultaneous visibility of n satellites from a certain UP is called *n satellites visibility*, whereas the simultaneous visibility of satellites to both, UP and according GW, is denoted as *mutual (n) satellite(s) visibility*. In the case of n satellite diversity, *availability of service* to a UP is given whenever at least one out of these n satellites is available to UP (it can be assumed that the link between GW and serving satellite(s) is never shadowed and thus permanently available if visible). The "digital" channel behaviour on the mobile user up/downlink, which implicitly underlies the above definitions, is motivated by results from several measurement campaigns [4] [5] and further discussed in Section 3.

2.2 *Satellite Diversity Concept and Operation*

Satellite diversity is a concept that provides communication links between a MT and a serving GW via more than one satellite, generally to a changing extent over time. It can be regarded as a fundamental countermeasure for the signal deterioration through shadowing and blocking in the mobile user environment, thus providing the possibility of availability enhancement.

Recently, great interest has raised in the capabilities and approaches to compensate for multipath fading in terrestrial mobile communication systems, as represented by the CDMA Rake receiver technique. Here the predominant principle is to combine the signals from several indirect paths with varying delay, whereas the signal component from the line-of-sight path is generally not available. It is now worth emphasizing that the satellite scenario shows some important difference: Due to large free space loss as well as power and antenna size limitations, personal communication via a satellite link essentially depends on clear line-of-sight conditions. Therefore, satellite diversity is a kind of artificially introduced multipath (especially for CDMA systems also providing the appropriate path delays) [6] in order to increase the probability of having a satellite with clear LOS available.

In the investigations underlying this paper, we presuppose that the implementation of satellite diversity reception is given by means of separate parallel receivers within the MT and GW, respectively. Based on that, we specify the following baseline for operating satellite diversity (cf. Fig. 1): A GW selects up to three satellites visible with an elevation angle $\varepsilon \geq \varepsilon_{GW}$. Then all MTs which are in the coverage area of at least one of these satellites, i.e. $\varepsilon \geq \varepsilon_{MT}$, communicate with the GW via *all* mutually visible satellites. In the case of Fig. 1, only single mutual visibility is given for MT A and B, respectively. Considering a handover (HO) system in comparison with the diversity system, it is obvious that the resulting availability is the same assuming both, perfect diversity and handover schemes. The latter means that at every instant of time, when a serving satellite is no longer available, a perfect switching to an available successor is performed, if there is any; generally, such HO actions lead to a significant amount of signalling. A comparison of diversity and equivalent HO operation is therefore interesting in order to specify the signalling complexity reduction properties of a diversity system.

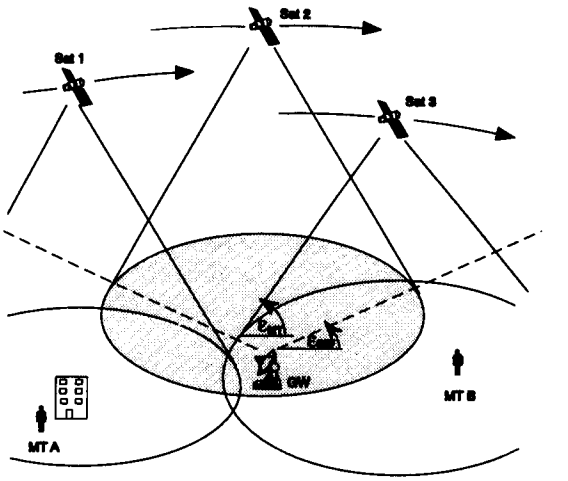

Figure 1: 3 satellite diversity scenario.

3 Mobile User Environment and Digital Channel Model

Satellite communications with land mobile or personal terminals suffer from strong variations of the received signal power due to signal shadowing and multipath fading.

Shadowing of the satellite signal is caused by obstacles in the propagation path, such as buildings, bridges, trees, etc. The percentage of shadowed areas on the ground, as well as their geometrical structure critically depends on the type of environment, e.g. urban, suburban, rural, etc. For low satellite elevation the shadowed areas are larger than for high elevation. Especially for streets in urban and suburban areas, the

percentage of signal shadowing also depends on the azimuth angle of the satellite.

Multipath fading occurs because the satellite signal is received not only via the direct path but also after being reflected from objects in the surroundings.

Measurements at L-band with the MARECS satellite [4] have shown that signal shadowing dominates the propagation behaviour. To a first approximation, the communication channel can be considered as being interrupted (bad channel state) if there is no line-of-sight to the satellite. Vice versa, the channel can be approximated as being ideal (good channel state) if a line-of-sight connection is present.

Due to the movement of the non-geostationary satellites, the geometrical pattern of shadowed areas is changing with time. Similarly, the movement of a mobile/personal user translates the geometrical pattern of shadowed areas into a time-series of good and bad channel states. In [4] it has been shown that the time-varying channel behaviour can be approximated by a two-state Gilbert-Elliott model with the mean durations in the good and bad state, respectively, depending on the type of environment, satellite elevation, and mobile user speed, Fig.2.

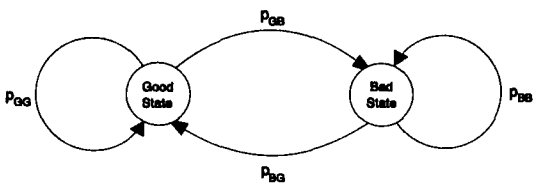

Figure 2: Digital channel model.

For the purpose of this paper, a separate and independent channel model was considered for each of the satellites visible to an investigated user position. Possible dependencies on the azimuth angle have been neglected. For different elevation angles, statistical values for the time-share of shadowing, A, and for the mean extent (in meters) of the good and bad channel state, D_G and D_B, have been taken from [4]. In order to derive a channel model taking into account the satellite elevation, the channel parameters have been fitted over the elevation angle. As limiting cases, for 90° elevation $A = 0$ was assumed and $A = 1$ was used for 0° elevation. Table 2 shows the approach with a finite number of discrete elevation areas used as input for computer simulation.

Elevation area	Elevation range	{environment}, {velocity}	
1	0...5°	$p_{GB}(1)$	$p_{BG}(1)$
⋮	⋮	⋮	⋮
n	⋮	$p_{GB}(n)$	$p_{BG}(n)$
⋮	⋮	⋮	⋮
18	85...90°	$p_{GB}(18)$	$p_{BG}(18)$

Table 2: Elevation areas.

4 Numerical Evaluation

4.1 Simulation Approach

For both systems, Globalstar and Inmarsat, our goal was to evaluate satellite diversity in terms of visibility, availability, and equivalent HO rates. Considering the satellite dynamics and the diversity scheme as presented in Section 2.2, we performed extensive simulations for one GW at (-100° W / 40° N) and 400 UPs in its SA, which was assumed to be a circle with radius r_{SA} around the GW. The UPs are equally distributed within SA; more specifically, they are located on concentric circles, thus providing the possibility to derive all relevant statistics as a function of distance between UP and GW. As r_{SA} is obviously a crucial parameter, it has to be chosen reasonably. From the system implementation viewpoint, the SA should be as large as possible to reduce the required number of GWs, but from the QOS point of view, the SA is clearly limited, especially if one wants to exploit satellite diversity. In order to guarantee quite a fair comparison between the LEO and MEO system, in a preceding visibility analysis we extracted the maximum possible r_{SA} for both systems such that mutual visibility of at least one satellite is 100% over time for all UPs in SA; consequently, all UPs outside this SA are assumed to be served by a neighbouring GW. Specifying $\varepsilon_{GW} = 5°$, the results for two considered MT elevation angles are as follows:

	Globalstar	Inmarsat-P
$\varepsilon_{MT} = 20°$	$r_{SA} = 970$ km	$r_{SA} = 2600$ km
$\varepsilon_{MT} = 10°$	$r_{SA} = 1880$ km	$r_{SA} = 3680$ km

From here, the simulation approach is as illustrated in Fig. 3. Both constellations are simulated over a whole day (1440 min) with a time step of 1 minute. Once the satellite selection has been performed by the GW for the actual instant of time, all 400 UPs can be investigated in terms of visibility. Then the channel model is simulated for each UP/Sat pair independently (cf. Section 3). The according time step is dynamically adapted such that the channel function

is called at least 10 times within the minimum of the mean channel state durations, thus minimizing quantization errors. The diversity evaluation concludes with the calculation of mean values for statistics.

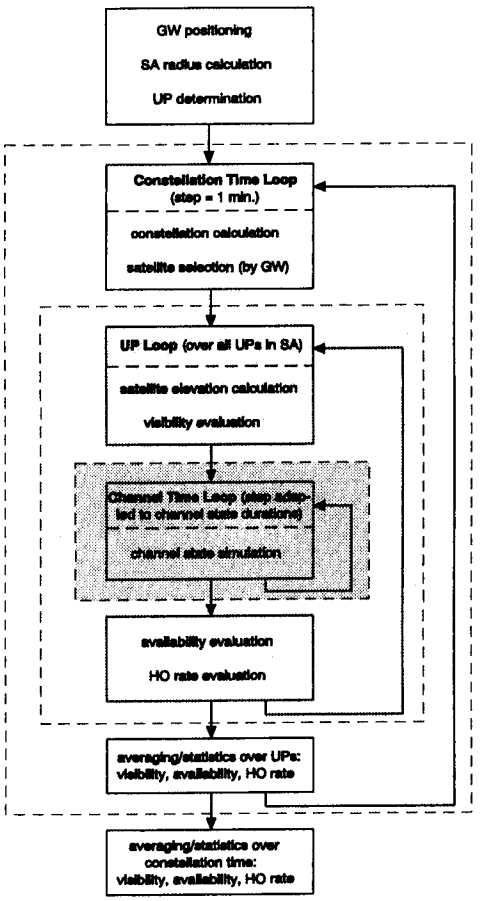

Figure 3: Generalized flow chart of diversity evaluation program.

4.2 Numerical Results

The visibility as well as the availability in a highway and an urban scenario, respectively, are compared for both systems in Figs. 4 and 5. The elevation angle ε_{MT} is 20°. The mutual dual satellite visibility turns out to be significantly higher for Globalstar than for Inmarsat. The availability curves, on the other hand, show that the strengths of diversity are nearly completely exploited in the dual satellite diversity scenario. Consequently, the diversity gain is higher for Globalstar. However, in both environments the absolute availability figures in the diversity case are nearly the same for both systems, with even slight advantages for Inmarsat. The reason is, that the first visible satellite in the Inmarsat system obviously has a better elevation angle distribution, inherently providing higher availability in the case of no diversity. Comparing the two environments, one might conclude that – no matter which system implementation – reasonable satellite PCN seems to be very well possible in rural areas, whereas in urban areas the satellite component will of course not be more than a complementary or backup solution for terrestrial systems.

All the simulations underlying Figs. 4 and 5 were also run for $\varepsilon_{MT} = 10°$. The extension of the SA due to the lower elevation has already been discussed above. As a second effect the improvement of mutual dual and triple satellite visibility can be seen. As one expects, this translates into higher availability, and again the diversity gain is more distinct for Globalstar. For comparison with the 20° situation, respective results are depicted for the availability in both environments for Globalstar, Fig.6. It seems however, that the overall benefit of lower user elevation angle, as far as diversity is concerned, is more the SA expansion than the availability gain improvement.

Finally, in Fig. 7 some interesting numerical results are given for equivalent HO rates. Fig. 7(a) shows a comparison of Globalstar and Inmarsat for three different scenarios. The influence of environment and mobile user velocity on the absolute HO figures is obvious. The discrepancy between HO requests and successfully performed handovers is much higher in unfavourable urban environments. Fig. 7(b) finally shows a HO rate comparison between the two considered elevation angles for Globalstar. Generally, the rate of performed handovers increases with lower elevation due to the enhanced availability of alternative satellites.

5 Conclusions

The performance of satellite diversity under the influence of the mobile user environment has been analysed. Different environments have been characterized by a unique digital channel model which takes into account the elevation angle as well as the user mobility. Based on a specific diversity operation scheme, reasonable service area sizes have been derived.

Generally, the availability gain through use of satellite diversity is to a major part determined by the improvement of mutual dual satellite visibility. The effects are more distinct in the Globalstar (LEO) system than in the Inmarsat (MEO) system, whereas the absolute availability figures in the diversity case are nearly the same in both systems.

As an overall conclusion, the operation of satellite based PCNs under reasonable QOS constraints seems to be realistic in rural areas, whereas in less favourable environments they should not be the solution of choice.

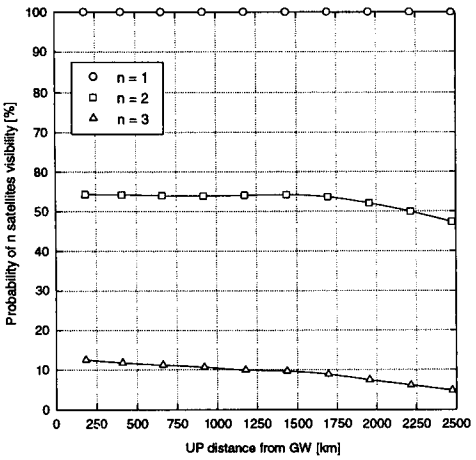

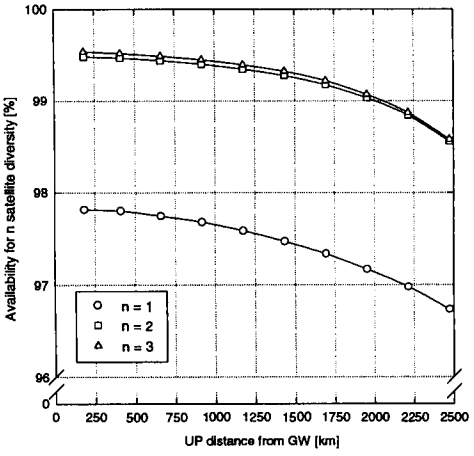

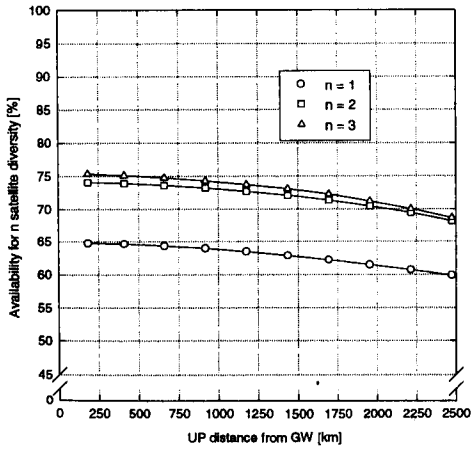

Figure 4: Inmarsat, $\varepsilon_{MT} = 20°$: (a) visibility, (b) availability in highway environment, (c) availability in urban environment.

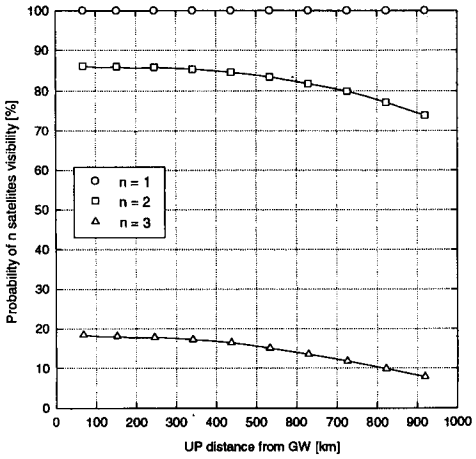

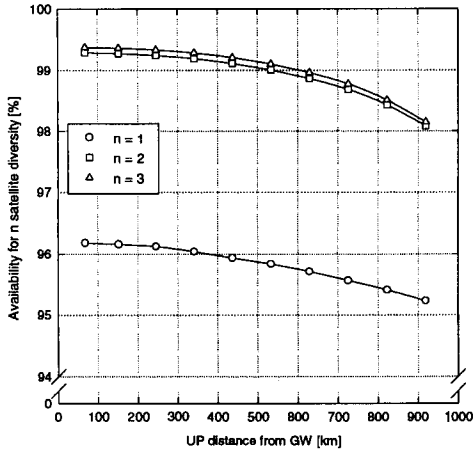

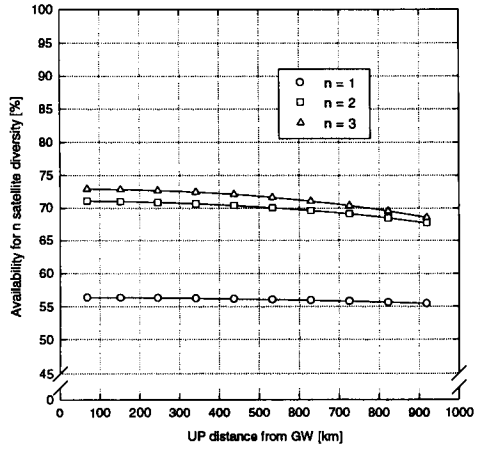

Figure 5: Globalstar, $\varepsilon_{MT} = 20°$: (a) visibility, (b) availability in highway environment, (c) availability in urban environment.

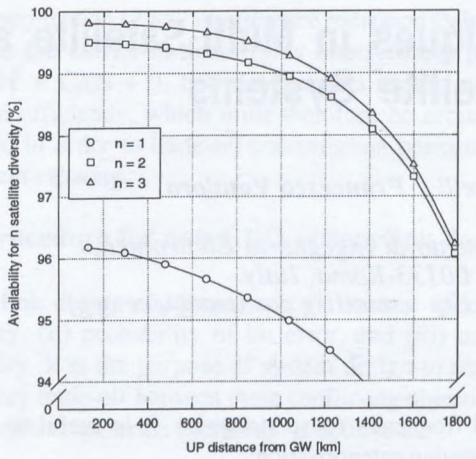

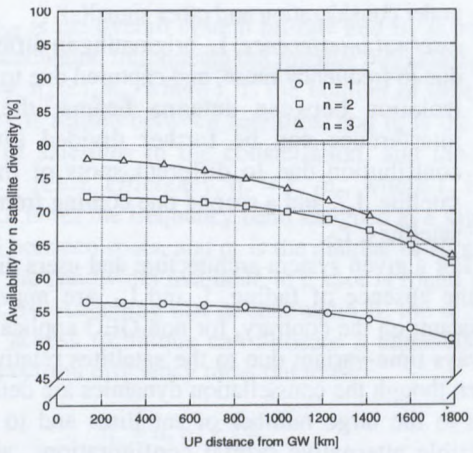

Figure 6: Globalstar, $\varepsilon_{MT} = 10°$: (a) availability in highway environment, (b) availability in urban environment.

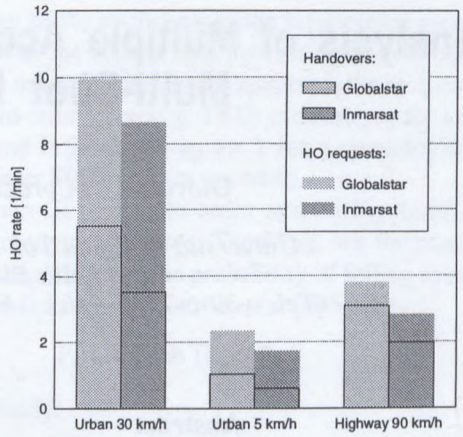

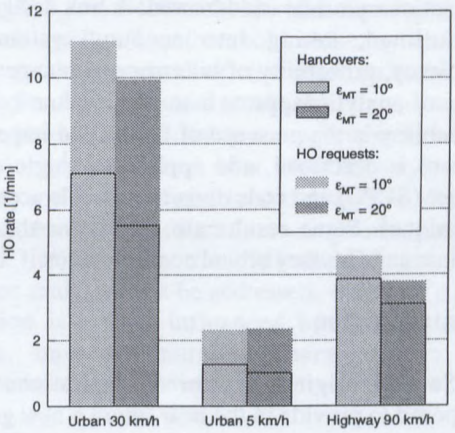

Figure 7: Equivalent HO rates for different environments: (a) comparison Globalstar and Inmarsat, (b) comparison $\varepsilon_{MT} = 20°$ and $\varepsilon_{MT} = 10°$ for Globalstar.

References

[1] R. A. Wiedeman, A. J. Viterbi, "The Globalstar mobile satellite system for worldwide personal communications," in *Proc. 3rd Int. Mobile Sat. Conf., IMSC '93*, Pasadena, CA, June 1993.

[2] "Inmarsat-P The world in your hand." Inmarsat brochure, Summer 1994.

[3] "Impact of propagation impairments on the design of CDMA-based LEO/MSS systems that employ satellite diversity," ITU Doc. 8D/TEMP/63 (Rev.2)-E, Annex II, ITU, Nov. 1993.

[4] E. Lutz et al., "The land mobile satellite channel - recording, statistics and channel model." IEEE Trans. on Vehicular Technology VT-40 (1991), pp. 375-386.

[5] A. Jahn et al., "Narrow and wideband channel characterization for land mobile satellite systems: Experimental results at L-band," in *Proc. 4th Int. Mobile Sat. Conf., IMSC '95*, Ottawa, Canada, June 1995.

[6] A. Sammut et al., "Multipath by satellite diversity for CDMA based S-PCN," COST Doc. 227TD(94)36, 11th COST 227 Management Committee Meeting, Aveiro, Portugal, Sept. 1994.

Analysis of Multiple Access Techniques in Multi-Satellite and Multi-Spot Mobile Satellite Systems

Giovanni E. Corazza , Carlo Ferrarelli , Francesco Vatalaro

Università di Roma Tor Vergata, Dipartimento di Ingegneria Elettronica,
Via della Ricerca Scientifica, 00133-Roma, Italy
(Tel. +39-6-7259-4453 Fax: +39-6-2020519 e-mail: g.corazza@ieee.org)

Abstract

In this paper the analysis of mobile satellite systems adopting constellations of multi-spot satellites over non-geostationary orbits is addressed. A link design procedure is outlined, taking into account system spectrum efficiency, probability of bit error and outage probability. A semi-analytic approach to the evaluation of outage probability in the presence of fading and imperfect power control is described, and applied to single channel per carrier (SCPC) and code division multiple access (CDMA) techniques. Some results are shown for the Globalstar, Iridium and Odyssey orbital configurations.

I. Introduction

Several original system configurations have been proposed to provide in the near future a new generation of mobile and personal satellite services (e.g. Globalstar [1], Iridium [2], Odyssey [3]). All proposals aim at offering a basic set of global communication services by means of large constellations of small-to-medium sized non-geostationary (non-GEO) satellites. System designers are facing the difficulties arising from the many technical alternatives in orbital choices, satellite configurations, payload and on-board antenna architectures, multiple access, modulation and coding. Optimum blend of these and other technical aspects is very important, since it eventually determines the systems effectiveness in terms of cost/circuit.

This paper concentrates on the design procedure for non-GEO systems, with particular emphasis on the trade-off in the area of multiple access techniques, which is one of the most controversial and critical issues for these multi-satellite and multi-spot systems where a very large capacity is required and, consequently, high interference levels must be tolerated. The interference contributions depend on many interlaced system aspects, such as: satellites constellation (number of satellites, orbit type, orbital height, etc.); on-board antennas (number of spots per satellite, shape and pointing direction of mainlobes, sidelobe levels, cross-polar characteristics, etc.); coverage and frequency reuse strategies. It is useful to adopt the following categorisation:

- *internal interference*, I_i, originating within the serving spot due to lack of orthogonality between the signal under consideration and other signal(s);
- *external interference*, I_e, originating in different spots due to frequency reuse, and captured due to imperfect isolation between antenna beams; the external interference can be further divided into a first contribution due to different spots of the serving satellite, I_{e1}, and a second one coming from different satellites, I_{e2}.

For a given system architecture and users distribution, in the absence of fading, I_i and I_{e1} are approximately constant; on the contrary, for non-GEO applications I_{e2} is always time-variant due to the satellites relative motion. Even though the constellation dynamics are deterministic, due to the large number of satellites and to the many possible alternative orbital configurations, an analytic evaluation of I_{e2} is hardly achievable. Our preferred approach has been to evaluate the above-mentioned interference contributions, and as a consequence the carrier-to-interference power ratio, $C/I = C/(I_i + I_e)$, through a time-domain simulation [4]. In general, it is necessary to introduce one or a combination of interference reduction techniques, such as:

A. *spot clusters*, for which, similarly to the terrestrial cellular case, frequency subsets are assigned to spots in a cluster according to a regular structure and the total bandwidth assigned to the satellite transponder is reused in different clusters;
B. *spot turn-off*, for which one of two spots belonging to different satellites is shut-off when, due to the satellites motion, the main beam footprints are superimposed by a certain degree;
C. *inter-orbital plane frequency division*, for which the overall service bandwidth is segmented between different orbital planes;
D. *beam hopping*, which is dual to technique A in the time domain;
E. *orthogonal spot polarization*, which uses right and left circular polarizations in different spots.

The application of any interference reduction technique improves the carrier-to-noise (plus interference) power ratio C/N' = C/(N + I), but also impacts on the system spectrum efficiency, which must therefore be accurately evaluated in order to trade-off transmission performance and system capacity.

II. A procedure for non-GEO system link design

The link design objectives are: (i) system spectrum efficiency, (ii) probability of bit error, and (iii) outage probability. It is the purpose of system design to reach a satisfactory trade-off between these conflicting objectives.

The *system spectrum efficiency* is defined as:

$$\eta \triangleq \frac{R_{bT}}{B_T} \tag{1}$$

where R_{bT} is the overall system bit-rate and B_T is overall needed bandwidth. Introducing the *satellite frequency reuse efficiency*, $\eta_s = f_s/n_s$, where f_s is the number of times the frequency is reused between satellites, and n_s is the total number of satellites in the constellation, and the *spot frequency reuse efficiency*, $\eta_c = f_c/n_c$, where f_c is the number of times the frequency band assigned to a satellite is reused between spots, and n_c is the number of spots per satellite, the bandwidth available to a spot is found to be $B_c = \eta_s \eta_c B_T$. Assuming that in bandwidth B_c the selected multiple access technique can allocate k channels, the system spectrum efficiency turns out to be:

$$\eta = n_s\, n_c\, k \frac{R_b}{B_T} \tag{2}$$

where R_b is the individual user information bit-rate.

The *probability of bit error*, P_e, is the usual parameter to assess link quality (and availability) of a digital system. For a given modulation and coding technique, a specification on P_e translates into a minimum bit energy-to-noise power spectral density ratio, $\mathcal{E}_b/\mathcal{N}_0$, related to the carrier-to-noise power ratio, C/N', through:

$$\frac{C}{N'} = \eta_m \frac{\mathcal{E}_b}{\mathcal{N}_0'} . \tag{3}$$

In (3) we denote with η_m the modulation and coding spectrum efficiency, which for a quadrature carrier modulated system is

$$\eta_m \triangleq \frac{R_b}{B} = \frac{\log_2 M}{g_p(1+\beta)} \tag{4}$$

where B is the single-user signal bandwidth, M is the number of modulation symbols (e.g. M = 2 for BPSK, M = 4 for QPSK, etc.), g_p is the processing gain, and $\beta \geq 0$ is the spectrum roll-off factor. The processing gain in (4) is defined as $g_p = R_p/R_b$, i.e. the ratio of the bit rate at the input of the modulator to the information bit rate at the output of the source. The processing gain is equal to one for an uncoded modulation system, is the reciprocal of the forward-error correcting (FEC) code rate, r_c, for a coded system, and is generally $g_p >> 1$ for a spread-spectrum system (either FEC-coded or uncoded).

In a non-GEO mobile radio system P_e, $\mathcal{E}_b/\mathcal{N}_0'$, and C/N' are random processes. Therefore, we introduce the *outage probability*, i.e. the probability of failing to meet a given specification, P_{th}, for the error probability:

$$P_{out} = \text{Prob}\,\{P_e > P_{th}\} \tag{5}$$

or equivalently:

$$P_{out} = \text{Prob}\left\{\frac{\mathcal{E}_b}{\mathcal{N}_0'} < \left(\frac{\mathcal{E}_b}{\mathcal{N}_0'}\right)_{th}\right\} \tag{6}$$

where $\left(\mathcal{E}_b/\mathcal{N}_0'\right)_{th}$ is the threshold value for $\mathcal{E}_b/\mathcal{N}_0'$ that corresponds to P_{th}. The threshold value is set by the choices in modulation, coding, and diversity techniques, along with fast fading channel conditions.

Fig. 1 shows the relationship among main elements in the link design procedure of a non-GEO system. A preliminary orbital analysis is necessary, to evaluate geometrical characteristics such as coverage area, handover time, and link absence time [4]. Subsequently, the interference analysis must be addressed, which for a given constellation is mainly influenced by multiple access technique, on-board antenna characteristics, and interference reduction techniques.

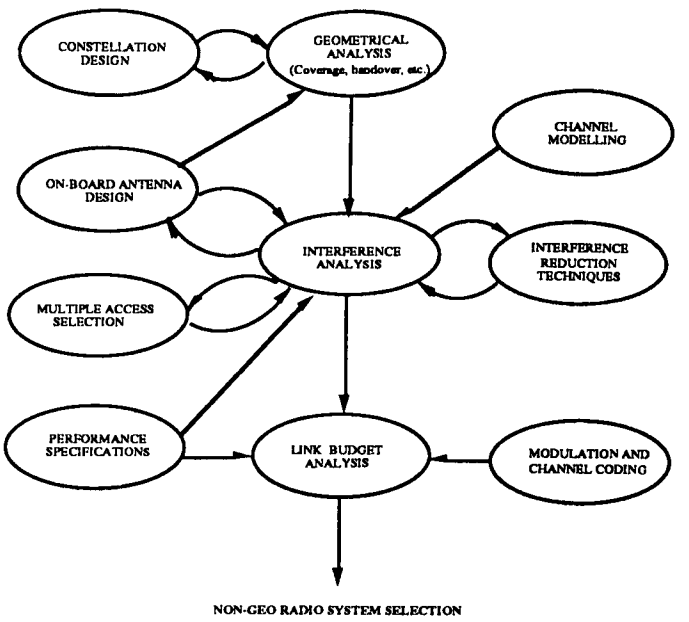

Fig 1 - Non-GEO link design procedure

In general both the desired signal and interfering signals are affected by multipath fading and shadowing, which may be taken into account through appropriate channel modelling. Having evaluated the effects of interference under different system configurations, the link budget analysis may be addressed.

III. Outage in the presence of fading

Personal satellite systems must be able to operate in the presence of multipath fading and shadowing effects, which may be taken into account by means of a Rice-lognormal (RLN) model with parameters matched to the elevation angle, α [5]. The RLN model parameters are the Rice factor, K, the mean attenuation, μ, and the dB-spread, σ^2, and the functions $K(\alpha)$, $\mu(\alpha)$ and $\sigma(\alpha)$ have been derived according to a third-order polynomial model fitted to an ESA measurements data-base [6]. According to our model, the fading envelope r is written as r = RS, where R is a Rice random variable (r.v.) which accounts for multipath effects and S is a lognormal r.v. which accounts for shadowing. Due to the inherent delay in the satellite link, the power control procedure cannot follow fast fading variations; the presence of Rice fading is reflected into the value for $\left(\mathcal{E}_b/\mathcal{N}_0'\right)_{th}$. Conversely, power control can follow slow power level fluctuations due to shadowing.

A distinction must be made for interferers in the area of coverage of the satellite serving the desired user and those served from other satellites. For interferers in the first category, shadowing in the link toward their serving spot-beam and the interfered spot-beam is perfectly correlated, and ideal power control compensates for both. For the second set of interferers, shadowing in the two links can be modelled as statistically independent; therefore, power control cannot compensate for shadowing in the link toward the interfered spot-beam, which can lead to very large interference contributions at times. To include a further refinement to our modelling, we do not assume perfect power control, but we take into account a lognormal fluctuation, ε, around the nominal transmitted level, with variance σ_ε^2. The bit-energy to noise power spectral density in the desired user link can be written as:

$$(7) \qquad \frac{\mathcal{E}_b}{\mathcal{N}_0'} = \frac{1}{\eta_m}\frac{C\,\varepsilon}{N+I} = \frac{C/N}{\eta_m}\frac{\varepsilon}{1+\frac{C/N}{C/I}}$$

where C/N is the nominal carrier-to-noise power ratio, and C/I is the carrier-to-interference power ratio, a r.v. due to constellation dynamics, shadowing, and imperfect power control. The outage probability can be shown to be:

$$(8) \qquad P_{out} = \int_0^\infty p_\varepsilon(\varepsilon)\, F\left[\frac{\eta_m\left(\mathcal{E}_b/\mathcal{N}_0'\right)_{th}}{\varepsilon - \frac{\eta_m}{C/N}\left(\mathcal{E}_b/\mathcal{N}_0'\right)_{th}}\right] d\varepsilon$$

where $p_\varepsilon(\varepsilon)$ is the lognormal probability density function (pdf) of the power control error variable, and

$$(9) \qquad F(x) \triangleq \begin{cases} P_{C/I}(x), & x \geq 0 \\ 1, & x < 0 \end{cases}$$

where $P_{C/I}$ is the cumulative distribution function (cdf) for C/I, evaluated through time-domain simulation.

IV. Analysis of SCPC and CDMA techniques

For interference and link analyses we assumed the orbital parameters of the Globalstar, Iridium, and Odyssey constellations. In all cases, we considered an on-board antenna with $n_c = 49$ spots, which have different radiation functions to compensate for the different angles of incidence and free space losses. The spot radiation functions have been modeled through suitable masks enveloping the maxima of the generic tapered-aperture antenna radiation pattern [4]. While system spectrum efficiency is a global figure of merit, outage probability is evaluated locally. As an example, we considered a rural tree-shadowed environment in Rome (41.9° N, 12.5° E), where the serving satellite is seen most frequently in the range 45° - 50°. As a preliminary approach, we considered imperfect power control in the desired user link only.

IV.1 *SCPC Systems*

For a SCPC system we refer to an ideal cellular arrangement, where the $n_c = 49$ spots are distributed in seven clusters (technique A with $f_c = 7$, $\eta_c = 0.143$). Letting B be the signal bandwidth plus any required guardbands, it holds $k = \eta_s\eta_c B_T/B$, and the system spectrum efficiency results in:

$$(10) \qquad \eta_{SCPC} = n_s\, n_c\, \eta_s\, \eta_c \frac{R_b}{B} = \eta_0\, \eta_m$$

where $\eta_0 = f_s\, f_c$, and η_m derives from (4) with $g_p = 1/r_c$. According to (10), the effects on spectrum efficiency of interference reduction techniques (acting on η_0), and modulation and coding (acting on η_m) are decoupled. For a given service area, η_{SCPC} increases proportionally with η_m, with the spot frequency reuse factor, and with the satellite frequency reuse factor. A larger constellation of satellites therefore leads to higher system capacity, although system cost increases. When spot turn-off is used f_c and η_{SCPC} are average figures. Table 1 shows η_0 for different constellations and interference reduction techniques (assumed area of service is globe excluding polar regions, i.e. latitudes over ±70°).

Technique	Iridium	Globalstar	Odyssey
A	462.0	336.0	84.0
A+B	430.7	224.8	50.6
A+C	77.0	42.0	28.0

Tab. 1: SCPC system spectrum efficiency for different interference reduction techniques ($\eta_m = 1$)

The local carrier-to-interference ratio cdf, $P_{C/I}(C/I)$, can be derived through time-domain simulation for given constellation, on-board antenna characteristics, and a particular interference reduction technique (i.e., η_0). As an example, Fig. 2 reports $P_{C/I}$ for the Globalstar constellation. Using technique A alone, the outage probability is unacceptably high. Adding inter-orbital plane frequency division (tech. C) yields drastical improvements, but it is also detrimental to spectrum efficiency (see Tab. 1). Spot turn-off (tech. B) appears to achieve a reasonable compromise between transmission performance and spectrum efficiency, at the expense of system complexity. Assuming technique A+B, the outage probability has been evaluated for $\eta_m = 1$, C/N = 18 dB and different values of the power control error standard deviation in a rural-tree shadowed environment [5], and the results are reported in Fig. 3.

IV.2 *CDMA Systems*

For a CDMA system it holds $g_p >> 1$, so that the modulation and coding spectrum efficiency for a single user is generally very small; therefore we can assume M = 2 and $\beta = 0$ in (4), and therefore $\eta_m = 1/g_p$, which shows that η_m is not affected by FEC coding for any practical value of r_c. Differently from SCPC, an asyncronous CDMA system is essentially interference limited. In this case, the evaluation of the number of channels per spot, k, cannot be carried out without an interference analysis. Under the hypothesis of ideal power control, in [7] we showed that:

$$(11)\quad \eta_{CDMA} = n_s n_c \frac{1}{a_f(1+F)} \frac{R_b}{B_T} \left(\frac{C}{N'}\right)^{-1} =$$

$$= \frac{f_s f_c}{a_f(1+F)} \eta_m \left(\frac{C}{N'}\right)^{-1} = \frac{\eta_0}{a_f(1+F)} \left(\frac{\mathcal{E}_b}{\mathcal{N}_0'}\right)^{-1} .$$

where $a_f < 1$ is the voice activity factor, F is the *other-cell interference factor*, i.e. the ratio between external and internal interference power. We again note that η is proportional to $\eta_0 = f_s f_c$: however, due to the properties of CDMA, it is possible to have $f_s = n_s$, and $f_c = n_c$, i.e. it may not be necessary to adopt techniques A, B, or C. Contrary to SCPC, CDMA spectrum efficiency does not directly depend on η_m, and reduction of $\mathcal{E}_b/\mathcal{N}_0'$ specification proportionally reflects on spectrum efficiency increase.

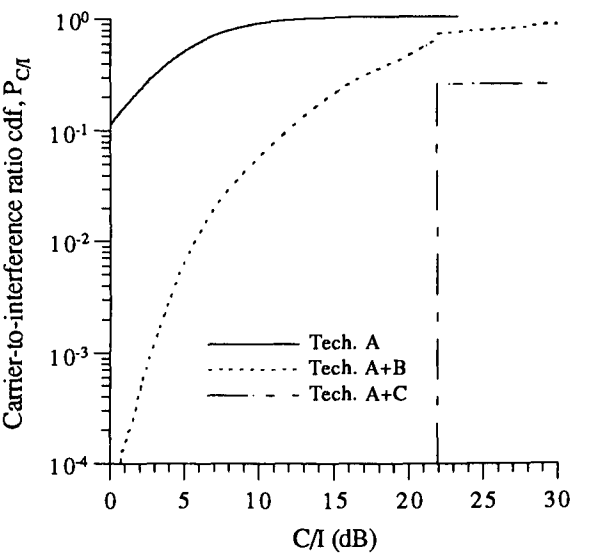

Fig. 2 - Cumulative distribution function of the carrier-to-interference power ratio for SCPC and different interference reduction techniques

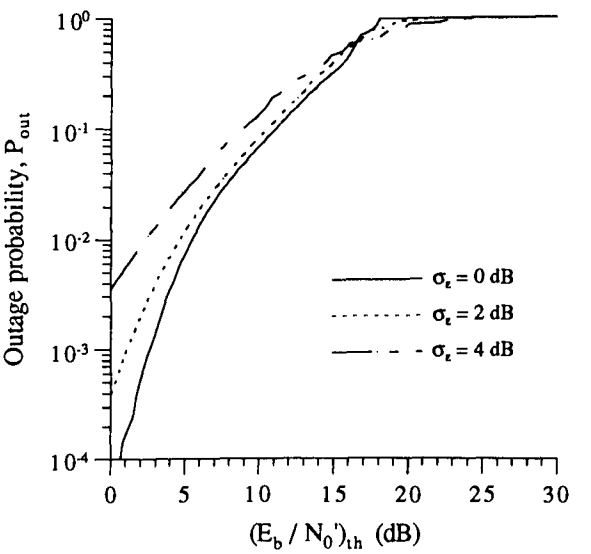

Fig. 3 - Outage probability for SCPC with techniques A+B and different values for the power control error standard deviation

This confirms that for a CDMA system FEC coding is certainly beneficial, since it improves both transmission performance and η_{CDMA}. Interference from other spots contributes to reduction of efficiency through F. The other-cell interference factor is a function of time which

we are able to estimate through time-domain simulation. The result is dependent on the system architecture and on the adopted interference reduction techniques. The system designer may decide for an availability specification, say 99%: the other-cell interference factor not exceeded for 99% of the time for different system architectures and interference reduction techniques is reported in Tab. 2. The values for CDMA system spectrum efficiency have been plotted in Fig. 4 for the Globalstar constellation. Techniques B, E (cross-polarization: -10 dB), and D (1 over 7 spots active at all times) are considered.

When shadowing and imperfect power control are considered, a simple formula as (11) does not hold. Given the number of users per spot (assumed constant), we must again find the cdf $P_{C/I}$ and use it in (8) to find outage probability. The results for Globalstar constellation with shadowing (rural tree-shadowed environment), g_p = 24 dB, C/N = - 6 dB, a_f = 0.4, are shown in Fig. 5 for different interference reduction techniques and k = 50, and in Fig. 6 as a function of the number of users per spot and with the standard deviation of the power control error variable as a parameter.

Technique	Iridium	Globalstar	Odyssey
Full reuse	5.5	5.8	2.9
E (orth. polariz.)	3.4	3.7	2.0
D (beam hopping)	0.8	1.1	0.8
D+E	0.6	1.0	0.7
B (spot turn-off)	2.6	2.2	1.3
B+E	1.6	1.4	0.9
B+D	0.4	0.4	0.3
B+D+E	0.3	0.3	0.2

Tab. 2: Other-cell interference factor not exceeded 99% of the times, $F_{99\%}$, for different constellations.

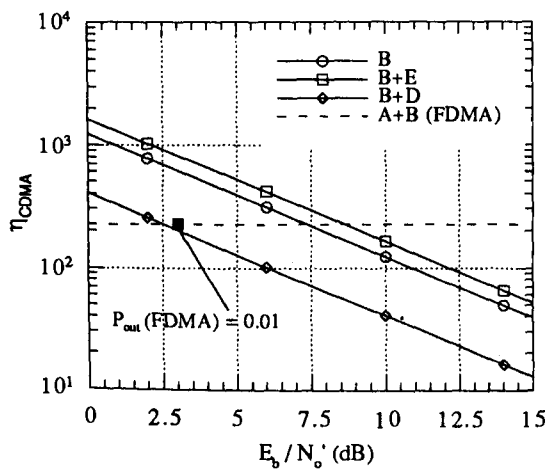

Fig. 4 - Spectrum efficiency for a CDMA system using different interference reduction techniques and the Globalstar constellation.

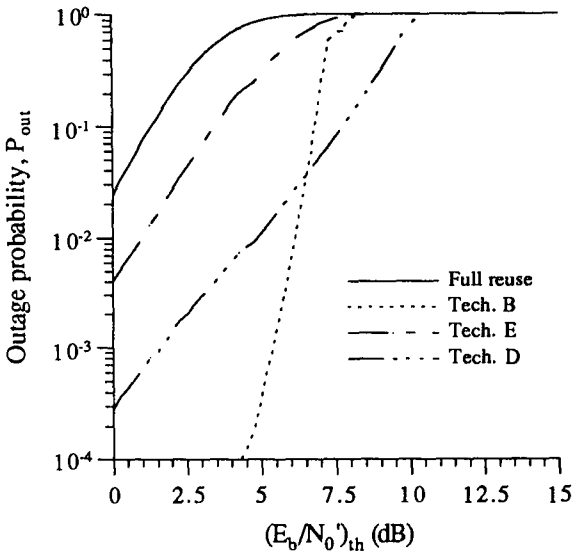

Fig. 5 - Outage probability for CDMA with ideal power control and different interference reduction techniques.

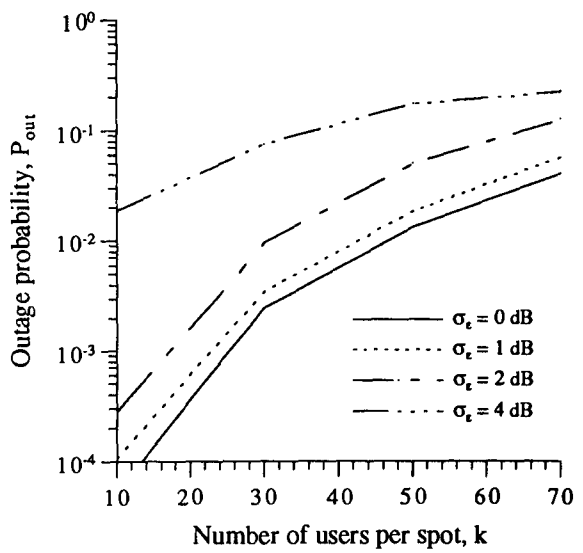

Fig. 6 - Outage probability for CDMA with technique D (beam hopping) as a function of the number of users per spot and with σ_ε as a parameter.

V. Conclusions

This paper considered the analysis of multiple access techniques for non-geostationary satellite systems in the presence of interference, shadowing and imperfect power control on the desired user link. The proposed procedure is based on combination of analysis and time-domain simulation. Due to the constellation dynamics, multiple access interference is a random process having statistics difficult to be evaluated analytically. However, the cdf of the carrier-to-interference power ratio may be evaluated through time-domain simulation for different interference reduction techniques which are characterised by different degrees of complexity and different values of spectrum efficiency. Both SCPC and CDMA techniques have been considered in the paper. In particular, system spectrum efficiency and outage probability have been evaluated in some significant cases, showing that the compromise between these two conflicting objectives is particularly troublesome for these systems.

References

[1] R.A. Wiedeman, and A.J. Viterbi, "The Globalstar mobile satellite system for worldwide personal communications," Proc. 3rd Int. Mobile Sat. Conf., IMSC'93, Pasadena, pp. 291-296, June 1993.

[2] J.E. Hartleid, and L. Casey, "The Iridium system personal communications anytime, anyplace," Proc. 3rd Int. Mobile Sat. Conf., IMSC'93, Pasadena, pp. 285-290, June 1993.

[3] C.J. Spitzer, "Odyssey personal communications satellite system," Proc. 3rd Int. Mobile Sat. Conf., IMSC'93, Pasadena, pp. 297-302, June 1993.

[4] F. Vatalaro, G.E. Corazza, C. Caini, C. Ferrarelli, "Analysis of LEO, MEO, and GEO Global Mobile Satellite Systems in the Presence of Interference and Fading", *IEEE Journ. of Sel. Areas in Commun.*, Feb. 1995.

[5] G.E. Corazza, F. Vatalaro, "A statistical model for land mobile satellite channels and its application to non-geostationary orbit systems", *IEEE Trans. on Veh. Technol.*, vol. 43, N.3, pp.738-742, Aug. 1994.

[6] G.E. Corazza, A. Jahn, E. Lutz, F. Vatalaro, "Channel characterization for mobile satellite communications", Springer Verlag: Proc. 1st European Workshop on Mobile/Personal Satcoms (EMPS'94), Frascati, Oct. 13-14, 1994.

[7] G.E. Corazza, F. Vatalaro, "Aspects for System Trade-Off in Mobile and Personal Satellite Communica-tions", Proc. IEEE MTT-S Europ. Topical Symp. on Tech. for Wireless Appl., Turin, pp. 19-24, Nov. 2-5, 1994.

Use of CDMA Access Technology in Mobile Satellite Systems

Jay Ramasastry
Qualcomm Incorporated
1233 20th Street NW, Suite 202, Washington 20036
Tel: 202-223-1720 Fax: 202-833-2161

Bob Wiedeman
Globalstar L. P.
3200 Zanker Road, PO Box 640670, San Jose CA, 95164-0670
Tel: 408-473-6201 Fax: 408-473-5548

Abstract

Use of Code Division Multiple Access (CDMA) technology in terrestrial wireless systems is fairly well understood. Similarly, design and operation of Power Control in a CDMA-based system in a terrestrial environment is also well established. Terrestrial multipath characteristics, and optimum design of the CDMA receiver to deal with multipath and fading conditions are reliably established. But the satellite environment is different. When the CDMA technology is adopted to the satellite environment, other design features need to be incorporated (for example; interleaving, open-loop and closed-loop power control design, diversity characteristics) to achieve comparable level of system performance. In fact, the GLOBALSTAR LEO/MSS system has incorporated all these features. Contrary to some published reports, CDMA retains the advantages in the satellite environment that are similar to those achieved in the terrestrial environment. This document gives a description of the CDMA waveform and other design features adopted for mobile satellite applications.

1. Background

Satellites inherently represent an ideal medium for multiple access wireless networks. This document illustrates how Code Division Multiple Access (CDMA) technology can be applied to mobile satellite networks. A major consideration in multiple access satellite technology is interference. Due to the advances in signal processing and VLSI technologies, interference in wireless communication can be suppressed fairly well by a combination of two techniques: spread spectrum modulation and multiple element antenna arrays. Spread-spectrum techniques use a wideband carrier, which appears random to the interferer but which is known or can be reconstructed by the intended receiver. The Pseudo-random" carrier demodulation process spreads the hostile interference signal over a larger bandwidth and makes it appear like white noise of thermal origin.

With multiple access to one or more satellites by a large population of users, some interference is unavoidable even with a high degree of coordination among users and satellites. The nature or source of this interference falls into one or more of the following three categories:

- *spatial overlap* - neighboring satellites with small arc separation interfering with, or receiving interference from, small user terminals with relatively large antenna beamwidths
- *spectral overlap* - diverse users in adjacent frequency bands with spectral spillover due to inadequate filtering or to cross-products of non-linear amplifier origin; possibly also due to polarization overlaps
- *temporal overlap* - intersymbol interference caused by mismatched filters and by multipath effects.

One effective multiple access technique is to use a power controlled spread spectrum signal for all users and to share the frequency allocation. The multiple access application of spread spectrum is referred to as Code Division Multiple Access (CDMA). CDMA makes every user's signal, including that of overlapping satellite beams, appear as wideband noise to every other user's receiver. Wideband noise is the natural environment of a satellite receiver, and the signal processing receiver technology that works well in power-limited applications will work equally well in a heavily user-loaded system, thereby providing bandwidth efficiency. Techniques such as power control are utilized to achieve the objective of equal user power.

MSS satellite transponders can either be used as "bent-pipe" repeaters, or as "intelligent switches" with special on-board processing. In this paper, application of CDMA in MSS systems utilizing bent-pipe configuration is discussed. Spatial diversity (through multiple satellites in view, and intelligent combining of multiple signals using a RAKE receiver), power control, reuse of all spectrum in all beams and all satellites, and soft-handoff, are techniques available in MSS CDMA systems. Mobile users typically access the satellites using the MSS service link frequencies (for example, 1610-1626.5 MHz for the uplink and 2483.5-2500 MHz for the downlink). User signals are connected to the terrestrial PSTN via satellite gateway stations generally operating in a separate higher frequency band assigned to MSS feeder-links. The MSS gateways acquire satellites newly appearing above their horizon and uplink signals through them. The user terminal with omnidirectional antenna will communicate with all the satellites in view without knowledge of the satellites' positions or ephemeris.

This document describes a particular CDMA channel and signal format derived from recent U . S . technology developments, and appropriately modified for MSS applications. The CDMA waveform format described in this document has been adopted in the design of the GLOBALSTAR system, which is a LEO/MSS (also known as NGSO-MSS) system that has been licensed in the United States. However, the general techniques discussed in this paper are applicable to other CDMA channel and signal formats.

2. The CDMA Waveforms

2.1 Forward Link CDMA Waveform (Gateway to Handset)

The example used in this annex is based on a forward link CDMA waveform [1] that uses a combination of frequency division, pseudorandom code division, and orthogonal signal multiple access techniques. Frequency division is employed by dividing the available spectrum into Bw (nominal 1.23 MHz) bandwidth channels.

All gateway stations transmit on the same frequency. Pseudo-random noise (PN) binary codes are used to distinguish between the signals from different beams, different satellites and different gateway stations. Each gateway transmits the same code, but with a different time offset to each beam of each satellite in its view. Since the correlation of the code with a time shifted version results in a small random number relative to the peak correlation (unshifted version), when the average is done over many chips, signals from other beams of the same satellite or other satellites in view appear as noise. Time shifts are assigned to beams in a manner such that the codes do not overlap in the same coverage area.

Quadriphase or biphase PN modulation can be used which leads to one or two PN sequences. The PN chip rate is CR megachips per second, or exactly CR/IR times the peak information transmission rate, IR Each PN sequence is a maximal length sequence of length 2L 1 augmented with a 0 to obtain a sequence of length 2L.

The signals are bandlimited by a digital filter that provides a very sharp frequency roll-off, resulting in a nearly square spectral shape that is Bw MHz wide at the 3 dB point. All signals transmitted from a single antenna on a particular CDMA radio channel share a common PN code phase. They are distinguished at the handset by using a binary orthogonal code based on Walsh

functions (also known as Hadamard matrices). The Walsh function is (Code Rate)* (CR/ IR) or 2w PN code chips long and provides 2w different orthogonal codes called code channels. Orthogonality provides perfect isolation between the multiple signals transmitted by the gateway. However, orthogonality is not maintained between multipath components resulting in some mutual interference between code channels.

The handset receives two code channels, the Pilot Channel, described later, and an information bearing "traffic" channel. Information bits transmitted on the traffic channel are convolutionally encoded to provide forward error correction. The code has a constraint length of K and a code rate of FR. When transmitting at the full IR bps rate, this provides a code symbol rate of IR/FR symbols per second. When the gateway is transmitting at a lower rate, the code symbols are repeated to obtain a constant symbol rate. The code symbols are interleaved and each symbol is covered with the Walsh function resulting in a CR megachips per second stream. This stream is BPSK modulated and covered with the PN code(s) described above. To provide communications privacy, each traffic channel is scrambled with a user addressed long code PN sequence. Thus, a "channel" on the Forward link of the CDMA system consists of a signal centered on an assigned frequency, quadriphase or biphase modulated by PN code(s) with an assigned time offset, biphase modulated by an assigned orthogonal Walsh function, and biphase modulated by the encoded, interleaved, and scrambled digital information signal. In an MSS system, gateways may precorrect time and/or frequency in their transmitted waveform.

An important aspect of the Forward link design is the use of the Pilot Channel that is transmitted by each gateway to each beam. The Pilot Channel is a code channel that is unmodulated by information and is assigned the zero Walsh function (which consists of 2w zeros). Thus, the signal simply consists of the PN code(s). The handset obtains the first level of synchronization without prior knowledge of the gateway's identity, or the transmitting satellite's position by searching for this PN code. The handset performs a correlation to collect a sufficient amount of energy to detect the signal's presence. The largest of the correlations corresponds to the desired signal path (gateway-satellite combination). The Pilot Channel is also used for time tracking and as a coherent carrier phase reference for demodulating other code channels transmitted by the gateway.

Once the handset acquires the Pilot Channel, it starts demodulating the synchronization channel (Sync Channel). The synchronization channel's framing is time aligned with the pilot PN code, and uses a preassigned Walsh function. The synchronization channel conveys time-of-day and the time offset of the pilot PN code for the gateway relative to true time. This allows the handset to move its timing from that aligned with the pilot PN code to the true time which is the same for all gateways. Once time has been adjusted, the handset receives one of the paging channels which conveys other system information, pages, and responses to accesses. Figure 1 shows an example of the signals transmitted by a gateway. Out of the 2W-1 code channels available for use, the example depicts seven paging channels (the maxi-

mum number allowed), one synchronization channel, and 2W-9 traffic channels.

Figure 1 illustrates the case of 128 Walsh codes, 1.23 MHz spread bandwidth, 4.8 bps information rate.2.2 Reverse Link CDMA Waveform (Handset to Gateway)

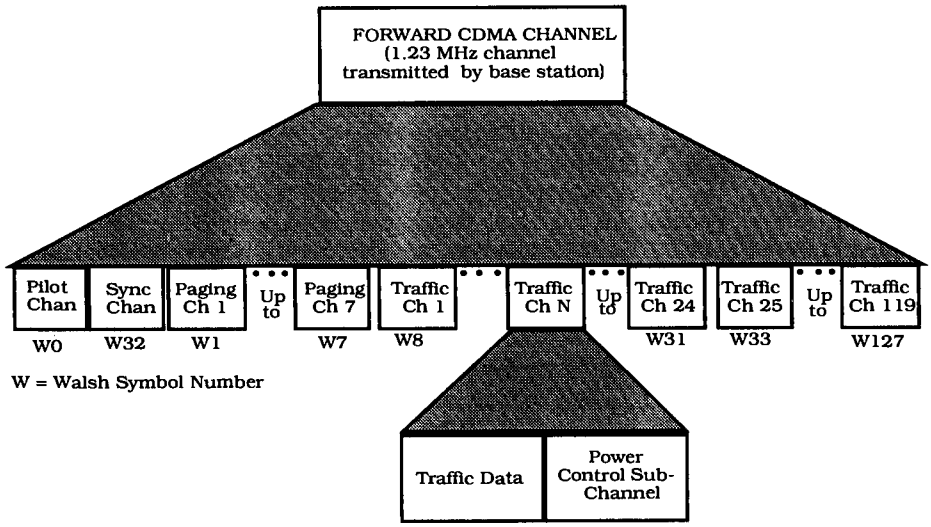

Figure 1: Example of the Code Channels Transmitted by a Gateway

The Reverse CDMA Channel example also employs PN modulation using the same 2L length binary sequences that are used for the Forward CDMA Channel. Here, however, a fixed code time offset is used. Signals from different handsets are distinguished by the use of a very long (242 - 1) PN sequence whose time offset is determined by the user address. Because every possible time offset is a valid address, an extremely large address space is provided. This also inherently provides a high level of privacy.

The transmitted digital information is convolutionally encoded using a rate RR (RR<FR) code of constraint length K. The encoded information is grouped in w symbol groups or code words. These code words are used to select one of 2w different orthogonal Walsh functions for transmission. The Walsh function chips are combined with the long and short PN codes. Note that this use of the Walsh function is different than on the Forward CDMA Channel. On the Forward CDMA Channel, the Walsh function is determined by the handset's assigned code channel while on the Reverse CDMA Channel the Walsh function is determined by the information being transmitted. The use of the Walsh function modulation on the Reverse CDMA Channel is a simple method of obtaining 2W-ary orthogonal modulation, which can be demodulated by a Fast Hadamard Transform. The Fast Hadamard Transform is similar to a Fast Fourier Transform except that it requires only additions and subtractions and thus simplifies demodulator implementation. Also note that on the Forward CDMA Channel, the Pilot Channel signal is shared among all the handsets and is used as a reference for coherent demodulation of essentially a BPSK signal. The Reverse CDMA Channel uses orthogonal modulation with non-coherent demodulation. A "channel" on the Reverse CDMA Channel consists of a signal centered on an assigned frequency, offset modulated (quadriphase or biphase) by PN code(s), biphase modulated by a long PN code with address determined code phase, and biphase modulated by the Walsh encoded and convolutionally encoded digital information signal. Figure 2 shows an example of all of the signals received by a gateway.

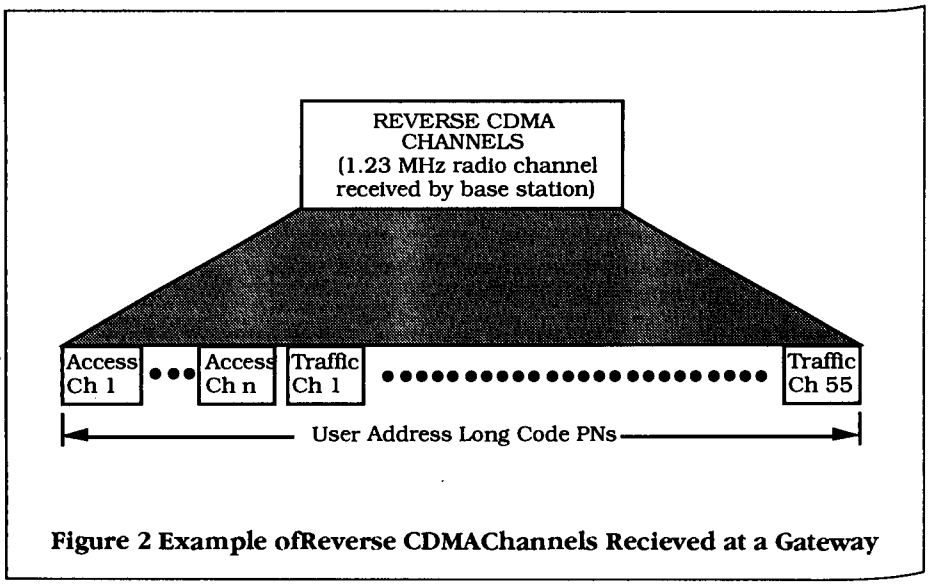

Figure 2 Example ofReverse CDMAChannels Recieved at a Gateway

3. Power Control

3.1 Reverse Link Power Control

To maximize the example system capacity, it is required that the received Eb/No from all handsets are similar at the gateway. Wireless handsets transmitting more power than nominal create more interference which reduces capacity. To resolve this problem, the example system proposes to use dynamic power control on the Reverse Traffic Channel.

Two types of power control are used: open loop and closed loop. For open loop power control the handset adjusts its transmitted power based on the power received on the forward link. For closed loop control, the gateway compares the received power from the handset to a threshold and sends out a command to have it increase or decrease its transmitted power.

The open loop power control mechanism is designed to respond quickly (for example, when a user is emerging from shadow, such as from behind a large building). Open loop control requires some correlation between the forward and return link signal attenuation, which is the case in blocking situations such as passing behind a building. Multipath fades are largely uncorrelated at S- and L-bands, but may be better correlated at 2 GHz MSS frequencies. Thus, open loop power control may not be effective in S- and L-band MSS operations.

The closed loop power control counteracts errors from the open loop power control process and sets the long-term average. Closed loop power control is slightly slower, with loop response times closer to the round-trip delay to the satellite (about 40 msec). It should be noted that power control is not meant to correct fast fades (on the order of milliseconds). Fast fades are more effectively dealt with through proper interleaving, efficient error-correcting codes, and utilizing satellite diversity paths.

3.2 Forward Link Power Control

It is also desirable to control the relative power used for each code channel on the Forward CDMA Channel. The primary reason for such power control is to minimize the amount of satellite power devoted to static link margin. To achieve this objective, the handset measures the received signal quality and periodically transmits the results of the measurements to the gateway. In addition, if the quality is less than a desired minimum value, which may depend upon system load, then the handset immediately transmits the results of the measurement. When the gateway receives a report of poor quality, it evaluates the power needs of all the handsets using the gateway and decides whether to increase the code channel power to the handset. The gateway can either increase its total transmit power, which has the disadvantage of increasing interference to handsets using other satellites or beams, or the gateway can redistribute power from handsets with good quality to the disadvantaged handset. Note that in all of these cases, the gateway must work within the constraints of the available downlink satellite power.

4. Diversity Archetecture in CDMA

Achieving spatial and temporal diversity is a critical objective of CDMA system design. The objective is to take advantage of alternate satellite path signals to improve link performance and availability, and to achieve soft handoff. In some situations, useful multipath signals may be present.

4.1 Rake Receiver Concept

The example system handset utilizes the RAKE receiver to process multiple components of the transmitted signal. These components are intentionally created diversity paths through alternate beams or satellites. Multipath signals of over a chip duration and of sufficient strength may also be available in some situations. Each received component can be differentiated by its time offset from the others. The handset utilizes a single RF front end, but multiple RAKE "fingers" in the digital hardware. Another demodulator continuously searches for additional signal paths. After the modulation process, the output signals are coherently combined to achieve the maximum signal to noise ratio.

4.2 Soft Handoff

In the example system, a CDMA Channel uses the same frequency assignment in adjacent beams and satellites. When a handset enters the region providing reasonable coverage by another beam or satellite, the handset detects the Pilot Channel of the overlapping beam or satellite, and reports it to the gateway. The system assigns a modulator and demodulator at the gateway and notifies the handset that a soft handoff is in progress. The gateway transmits the same information to both beams or satellites on the code channels assigned to the call. The handset combines the transmitted signals. Likewise, the multiple signals that are demodulated at the gateway are combined. When the handset fully moves into the coverage area of the new satellite, the handset reports that the old satellite's Pilot Channel has dropped below threshold level. The system then tears down the soft handoff.

Soft handoff is truly a "make before break" type of operation. The additional diversity of the second satellite maintains higher signal quality in the handoff region and results in a smaller probability of a dropped call. Moreover, the additional diversity may reduce the amount of power radiated by a handset.

4.3 Exploitation of Multipath

A capability of direct sequence CDMA is the exploitation of multipath to provide path diversity. The wide bandwidth PN modulation allows different propagation paths to be separated when the difference in the path delays for the various paths exceeds the PN chip duration. This is because the PN sequence has essentially zero correlation for time offsets greater than one chip time.

If two or more paths from a single satellite exist with greater than one chip differential path delay, as may be the case with very low elevation angle satellites, multiple PN receivers can be employed to separately receive the multiple path signals. The number of signal paths that can be received is equal to the number of PN receivers that are used. If these signal paths exhibit independence in fading, i.e., if they don't fade together, the outputs of the receivers can be diversity-combined so that a substantial loss in performance only occurs when all paths being received experience fades at the same time. This type of diversity not only mitigates fading but also overcomes blocking of the signal path by physical obstructions. A one chip path delay corresponds to a differential path distance of 250 meters. Signals arriving with larger than a chip delay spread will likely also arrive from different directions. Signals coming from different directions will be affected differently by obstructions in the immediate physical environment of the handset.

4.4 Path Diversity

In many MSS environments, the differential path delays are often less than one chip, or the reflected paths are greatly attenuated, and cannot be recovered by the rake receiver in the handset. Useful path diversity can be created in the MSS environment by utilizing multiple satellites or beams with overlapping coverages but with different slant angles to the user. This design approach will assist in achieving improved performance in fading and blocking environments.

Experiments have shown that diversity reverse channel reception is a key ingredient in obtaining satisfactory reverse channel performance. Note that handsets naturally create this effect, since their near-omnidirectional antennae can see several satellites/beams if orbits are chosen properly. The gateway can demodulate as many of these signal paths as it chooses to observe. On the forward link, the gateway can choose the optimum transmission path. Using multiple transmit paths does not require additional power, since the power sent through each path is reduced - the total level at the receiver remains constant. Indeed, average power is reduced due to the reduced fading and blocking levels that diversity brings.

5. Link and System Margins in a MSS CDMA System

Statistically speaking, not all users in any beam require large margins simultaneously. Each link is designed with available dynamic power range to assure a certain performance and availability. The system allocates power up to that dynamic range limit to those users that require it at any instant of time through the use of power control.

Not all users will be using the maximum of their dynamic power range (for example, 10 dB) at the same time, which translates into a much smaller overall system power margin. To calculate the average margin for the entire system, the statistics of individual users (both in space and time) must be used. At any given time, the fraction of users that require extra power is dependent on many factors, such as terrain, number of diversity paths available, user calling patterns, etc.

System capacity depends on this average power of all users. In the forward link, the important parameter is the total satellite power used. In the return link, the important parameter is the aggregate of mutual interference of all users. The system power requirement is averaged over all users in a beam. It is possible to share power between beams. The system margin in a CDMA MSS system is also referred to as "Capacity Margin" It means that the system design can trade margin for capacity. Conversely, one can increase margin by lowering the capacity. There is no "brick wall" in capacity in a CDMA system. Thus, the quality of individual links must be estimated using the maximum available dynamic range, while the overall capacity is based on the average.

6. System Capabilities of Multiple MSS CDMA Systems

Multiple CDMA MSS systems can share the same spectrum. There will be a loss of capacity in each system as compared to the achievable system capacity in the absence of other systems. The total net capacity of multiple CDMA systems operating co-coverage, co-channel, is significantly higher than the capacity achieved by segmenting the available bandwidth among different systems. This is one of the major advantages of systems based on CDMA modulation/access scheme. In order to achieve this advantage, the systems must conform to the following: (a) constant uplink areal power spectral density at the satellite; (b) constant downlink power flux density. This will create a situation, that within a fixed beam coverage area, each of the systems will contribute the same amount of interference into others, and receives the same amount of interference from others.

7. REFERENCES

[1] *Methodology for Calculation of Interference between Multiple CDMA MSS Systems operating Co-frequency,* ITU-R 8D/TEMP/12 (Rev. 1), December 5, 1994, International Telecommunications Union.

[2] *Impact of Propagation on the Design of Non-GSO Mobile-Satellite Systems that Employ Satellite Diversity,* ITU-R 8D/TEMP/9, December 5, 1994, International Telecommunications Union.

[3] **E.G. Tiedeman, A. Salmasi, and K.S. Gilhousen,** *Tithe System & Development of a Code Division Multiple Access (CDMA) System for Cellular and Personal Communications,* Proceedings of the 1991 IEEE International Symposium on Personal, Indoor and Mobile Radio Communications, London, U.K., September 23-25, 1991.

[4] **N. Ransom,** *Bell South Perspectives in Personal Communications,* Globecom' 91 Workshop on Personal Communications Services, Phoenix, AZ, USA, December 6, 1991.

Hybrid Networks - II

Session Chairman: **Richard Wolff,** Bellcore, USA
Session Organizer: **Polly Estabrook,** Jet Propulsion Laboratory, USA

Topic Introduction: This session is the last of two sessions to explore the challenges facing the integration of satellite and terrestrial networks. The session begins with an overview of the network reference models being drawn up for Personal Communications Services networks and a discussion of the possible incompatibilities of interconnecting satellite PCS networks with terrestrial PCS networks operating according to these reference models. Network design issues for the IRIDIUM system are then detailed in the following paper. The next two papers present traffic models: the first for a second generation mobile telecommunication system comprised of interconnected satellite and terrestrial networks; the second for a LEO satellite system possessing land and aeronautic mobile users. The last two papers in the session characterize the performance of protocols, designed for operating over wireline channels, when used over a satellite channel: the first paper details the PCS applications field trials conducted over terrestrial wireless and satellite channels; the second discusses the use of a popular protocol for multi-media applications, Asynchronous Transfer Mode, over satellite links.

13

Issues in PCS Interoperability and Internetworking

Richard A. Dean
National Security Agency
9800 Savage Road
Ft. Meade, MD 20755-6000
(301) 688-0293
radean@alpha.ncsc.mil

Polly Estabrook
Jet Propulsion Laboratory
4800 Oak Grove Drive
Pasadena, CA 91109-8099
(818) 354-2275
Polly.Estabrook@jpl.nasa.gov

ABSTRACT

This paper is an expansion of an earlier paper on Satellite/Terrestrial PCS which addressed issues for interoperability that included Networks, Services, Voice Coders and Mobility/Security. This paper focuses on the narrower topic of Network Reference Models and associated interfaces and protocols. The network reference models are addressed from the perspective of the User, the Cellular Carrier, the PSN Carrier, and the Radio Vendor. Each perspective is presented in the way these systems have evolved. The TIA TR46/GSM reference model will be reviewed. Variations in the use of this model that are prevalent in the industry will be discussed. These are the North American Cellular networks, the GSM networks, and the North American Carriers/Bellcore perspective. The paper concludes with the presentation of issues that develop from looking at merging satellite service into a world of many different networks.

NETWORK PERSPECTIVES

How we view the network models and interfaces will vary in accordance with the perspectives we bring. Figure 1 illustrates four such perspectives. The user doesn't see the complexity inherent in the networks. The user's expectations are that the networks are simply universally available infrastructure that support services transparently in many different environments. PCS has largely been marketed with this vision and users pretty much expect this to be the case. One wonders what surprises are in store for the users!

North American Cellular networks have evolved as a privately operated access network. Cellular systems are loosely coupled into the public networks and look much like a Private Branch Exchange with many proprietary features. This loose connection with the network may complicate the delivery of some services such as data, and may inhibit the user's vision of highly integrated networks.

North American Carriers look at PCS networks as an extension of the core network with wireless access. Wireline carriers want to project the wired network model out to the radio components and accommodate multiple radio technologies independently.

Finally, Radio Vendors look at the network models as a mix of standard and proprietary networks each with a unique set of protocols and features. Integrating a new radio system into PCS means accommodating technology insertion into different points in different networks in order to accommodate the legacy components in the carriers networks and to support different strategies each carrier might have taken. This perspective might best fit the way a satellite vendor might look at integrating satellite systems into the emerging PCS networks.

PCS REFERENCE MODELS

The simplified TR46 model shown in Figure 2 is a good common reference point from which to begin. This model with minor variations is used by GSM, existing North American cellular systems in TR45, and proposed PCS systems in TR46. It is important to point out however that, even though there is a common reference model, there are considerable differences in the interfaces and protocols, and the extent to which they have been accommodated in practice. The model shows several major components that are emphasized here.

The radio components includes the Air Interface (Um) and the Radio System (RS). The Um interface includes the physical layer and access meth-

ods as well as the traffic and control link protocols. The Radio System includes the transceiver (BTS) and the channel control (BSC) subsystems.

The network components includes the Personal Communications Switching Center (PCSC) and its associated interconnection (E) with other PCSC's, and Mobility Managers (C), the Home and Visitor Location Registers (HLR/VLR). The C interface is typically internal to a PCSC.

Connections into other networks includes standard interfaces and interworking functions.

The North American (N.A.) carriers and the Bellcore vision of PCS is characterized in the model shown in Figure 3 as presented by Campanella [2] at the ICUPC94 conference. This model is known as the generic C model. This model shows PCS services integrated into the wireline networks using ISDN services and Intelligent Network technology. In this case the radio technology is isolated from the network technologies. It allows prospective PCS carriers to use PSN switched and Intelligent Network services to support access and personal mobility.

NETWORK PROTOCOLS

While reference models may appear the same or similar, major differences can be found in the protocols used in the systems. A comparison of protocols for North American (IS41), GSM, and the Bellcore generic C network models are presented in Figure 4 for comparison. Protocols are presented in a layered fashion but do not rigorously correspond to the seven ISO layers.

IS41 based systems use a custom set of messages with the TCAP messaging structure from SS7 standards. They use X.25 message protocol structure for the intersystem messages on top of an arbitrary (TBD) physical layer of the E interface. Note that the A interface between the radio system and the switch is not defined. This reflects the practice of using proprietary cellular switches and interfaces at the mobile telephone switching office. Typically the A interface carries compressed voice multiplexed over one or more links for efficient back haul on leased lines.

GSM uses many PSTN conventions in their structure and protocol [3]. They use a custom set of messages built on SS7 protocols. They however define both the physical layer and the link layers at the A interface and the E interface consistent with PSTN conventions for T1 and SS7 standards. As GSM was developed by the European PTT's the emphasis on efficient back haul is absent. The A interface is completely defined.

The Bellcore generic C system [2] uses the IS41 like message structure and develops the remaining network elements on existing wireline conventions for SS7 and ISDN. The strategy used by Bellcore is not unlike the GSM approach in that the A interface looks and behaves like a telephone interface.

Another feature presented by these models is the network boundary (this is a conceptual fabrication of this presentation). Both the IS41 and the GSM models connect the PCS system to the network beyond the PCS switch. The Bellcore model however pulls the network into the PCS system to include PCS elements virtually in the network.

FUNCTIONAL ALLOCATION

The allocation of functions in the reference model is critical to the differences seen in the GSM and North American Digital Cellular (NADC) models. Differences in the allocation of functions across the Radio System and PCS switch boundary are presented in Table 1.

Table 1: GSM/IS41 Function Location

Function	Radio System	PCSC
Voice Coder	GSM	NADC
Encryption	GSM	NADC
Interworking	GSM	NADC

The location of the voice coding and encryption differ from GSM to N.A. and has been the subject of controversy in the standards bodies. This follows mostly from the decision by N.A. cellular providers to bring the compressed and encrypted payload back to the switch for reasons of efficiency. The location of the data interworking also follows from this strat-

egy. Interworking is performed by GSM systems at the radio system so that the physical and link layers coming to the PCSC appear in standard wireline format. NADC systems bring the radio link layer format back to the PCSC.

OPERATION AND SERVICES

All of the network models have to function to support a variety of services. Three functions that are integral to PCS operation will be shown here to highlight potential interoperability issues. Call Origination is an essential PCS function. Figure 5 shows the interaction among network elements to support Call Origination. These elements are present in all network models with appropriate variations in terminology. Of special importance in this operation is the activity across the network elements to support access over the radio links, authentication of the user, and development of the service profile and privileges. These are accomplished with a well defined set of functional entities and protocols across the network. It also highlights the complications that will arise when differences exist among the network models. If, for example, the serving PCS provider and the Home PCS provider have differences in authentication algorithms or in protocol, translations will have to be accomplished (where possible) to support service.

Handover, shown in Figure 6, is another function that emphasizes the complexity of functions and protocols involved in supporting a wireless connection. Considerable variations in this process exists across the networks and access technologies.

Operation in traffic, shown in Figure 7, likewise demonstrates the complexity of PCS systems. After an initial connection, a home PCS system service is typically extended to a another serving PCS system as the user migrates beyond the range of the originating (anchor) system. In North America connection to the PSTN at the home system is "anchored" and extended to adjacent switches during the call to support transparent operation.

ISSUES

For Satellite operation with terrestrial PCS the challenge is to create a strategy that will accommodate integration of services into mixed networks. Any successful strategy will have to address the following questions:

- What are the advantages and disadvantages of each existing network model?
- What networks will satellite systems have to accommodate nationally and internationally?
- Is is possible to select a single network strategy for interconnection?
- If multiple network interfaces and protocols are required, how will conversions be accomplished and what will be the impact of these?
- At what point in the network should satellite systems interconnect with terrestrial networks: at the PSTN?, at the BSC? at the PCSC? What are the implications of each of these decisions?
- Can the functions and protocols of the HLR/VLR for mobility and security be shared for satellite and terrestrial systems?
- How will these decisions affect the complexity of the dual mode handset?

Summary

Those who would integrate Satellite services with terrestrial systems face considerable challenges. The diversity of existing systems and the failure of standards bodies to unify network models requires Satellite developers to make hard choices. Some decisions might affect the future of the satellite component of the PCS industry, others might adversely affect user services or transparency. Open discussion of these issues by the industry is recommended.

REFERENCES

[1] **R.A. Dean**, *Satellite Terrestrial Interoperation in Personal Communications Networks*, Presented at IEEE ICUPC'94, San Diego, CA, Nov. 1994

[2] **P.A. Campanella**, *Radio System to PSTN Network System Interfaces and Services*, Presented at IEEE ICUPC'94, San Diego, CA, Nov. 1994

[3] **M. Rahnema**, *Overview of the GSM System and Protocol Architecture*, IEEE Communications Magazine, April, 1993

Figure 1 Four Perspectives of PCS Networks

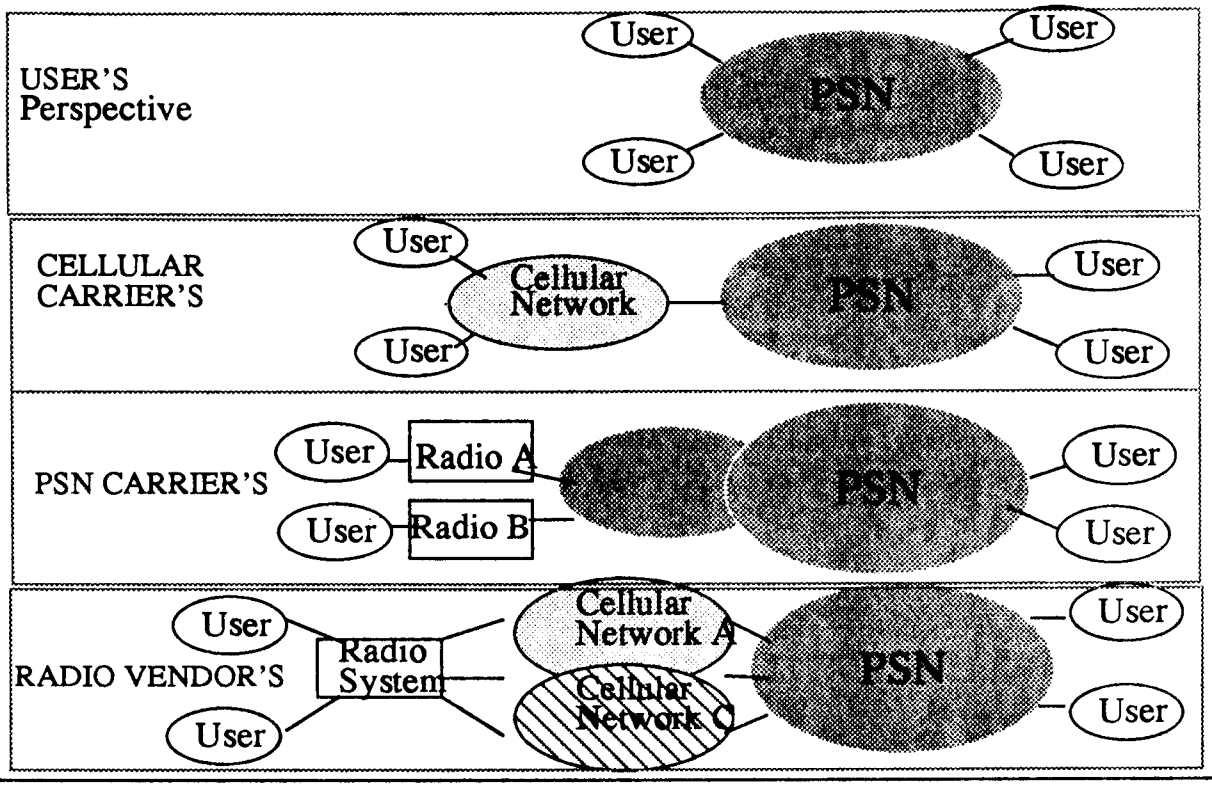

Fig. 2 Simplified TR46 Reference Model

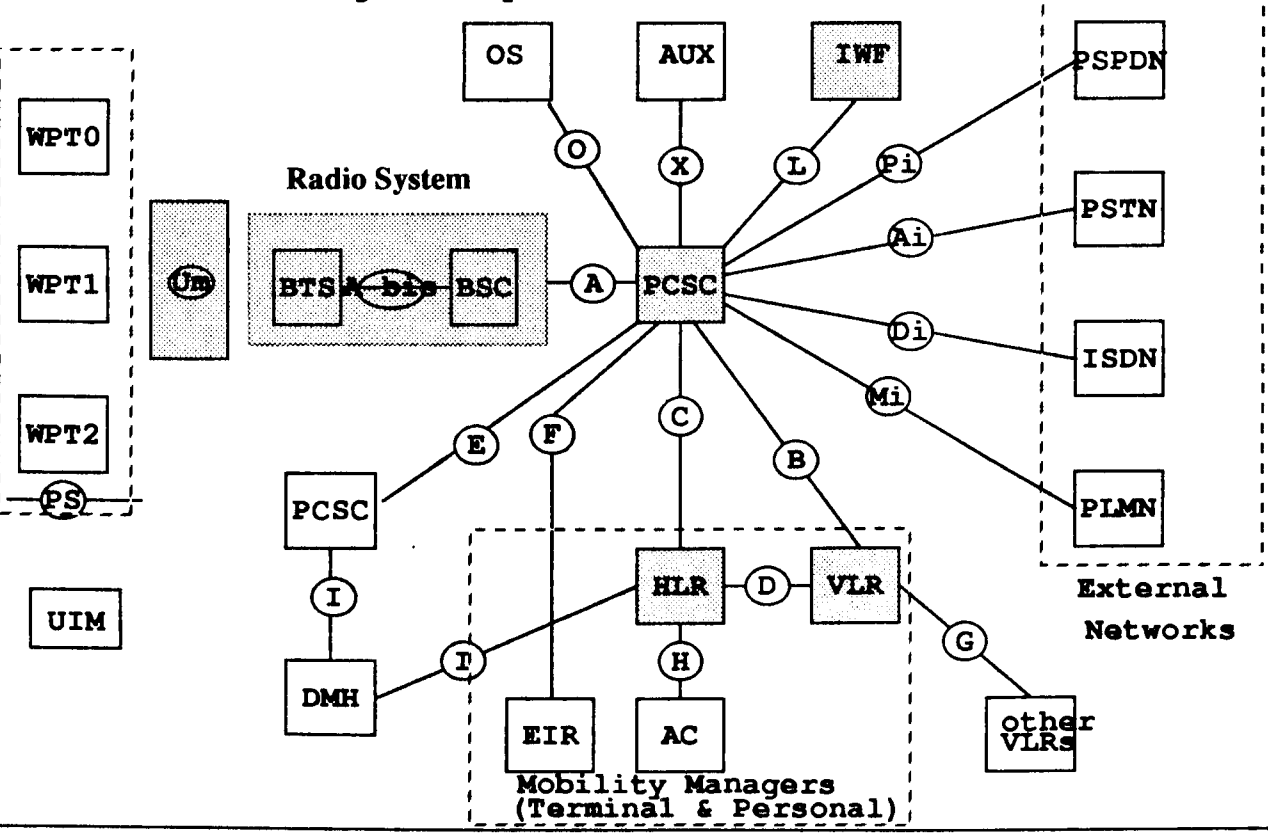

Figure 3 Bellcore PCS Architecture

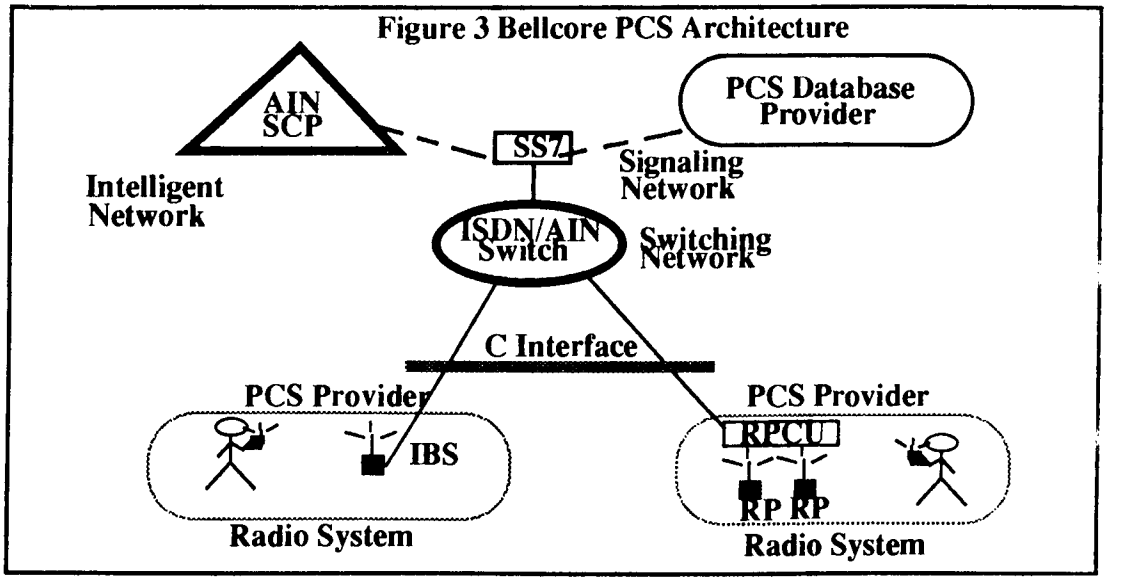

Figure 4 Comparison of Protocol Structure

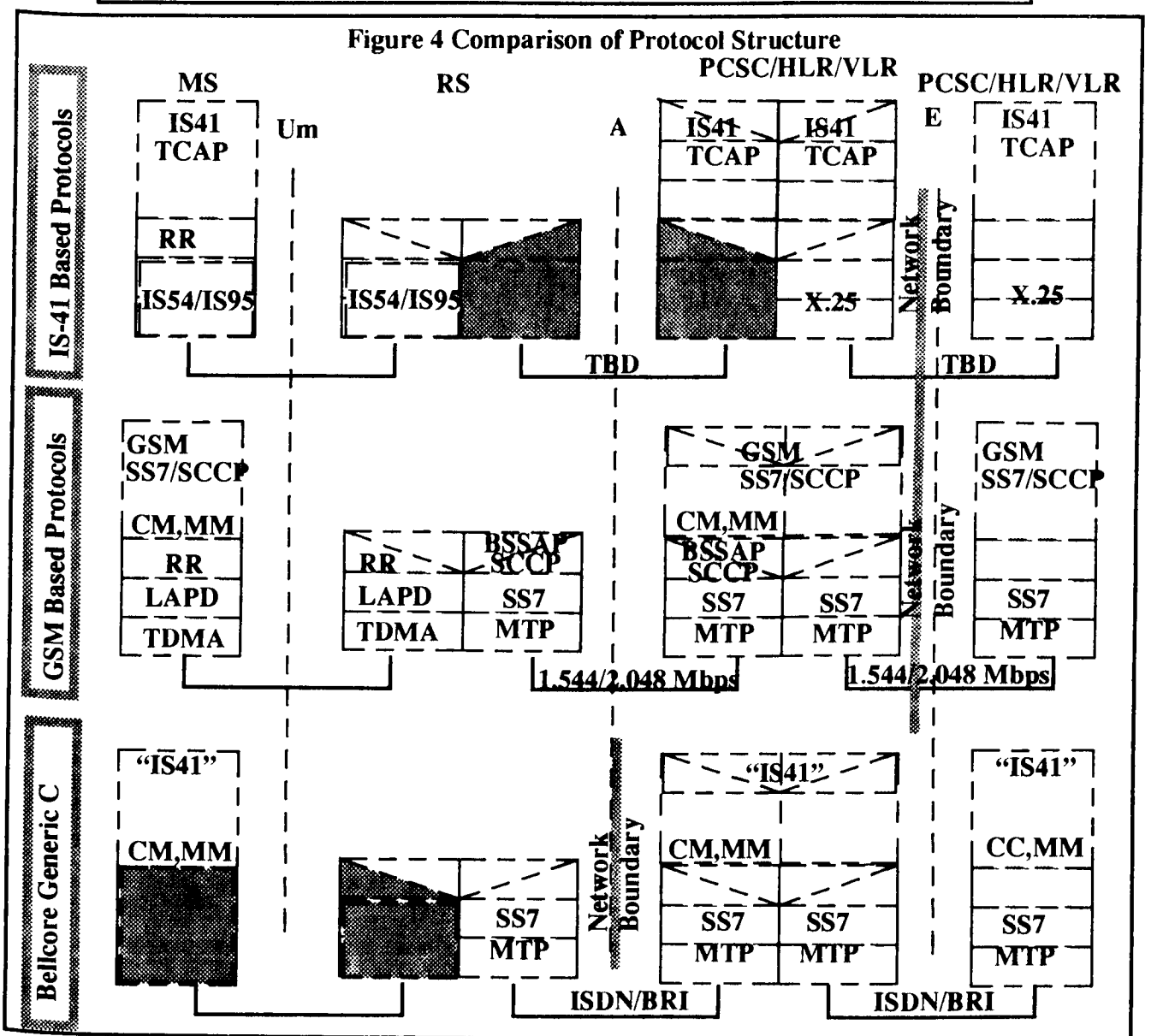

Figure 5 Call Origination Connection Diagram

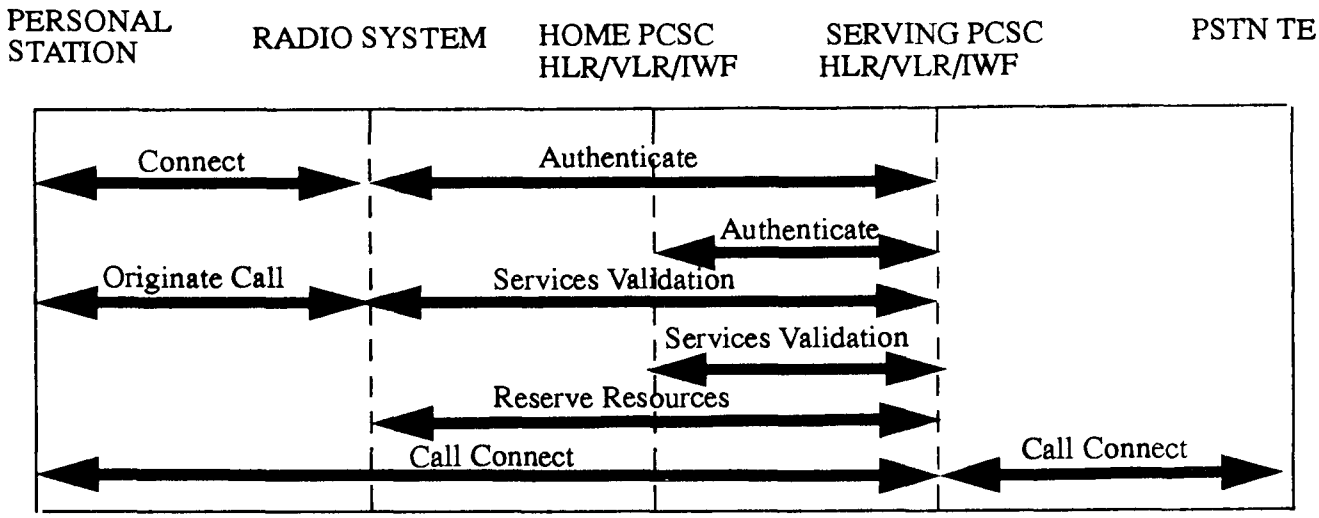

Figure 6 Hand Off Connection Diagram

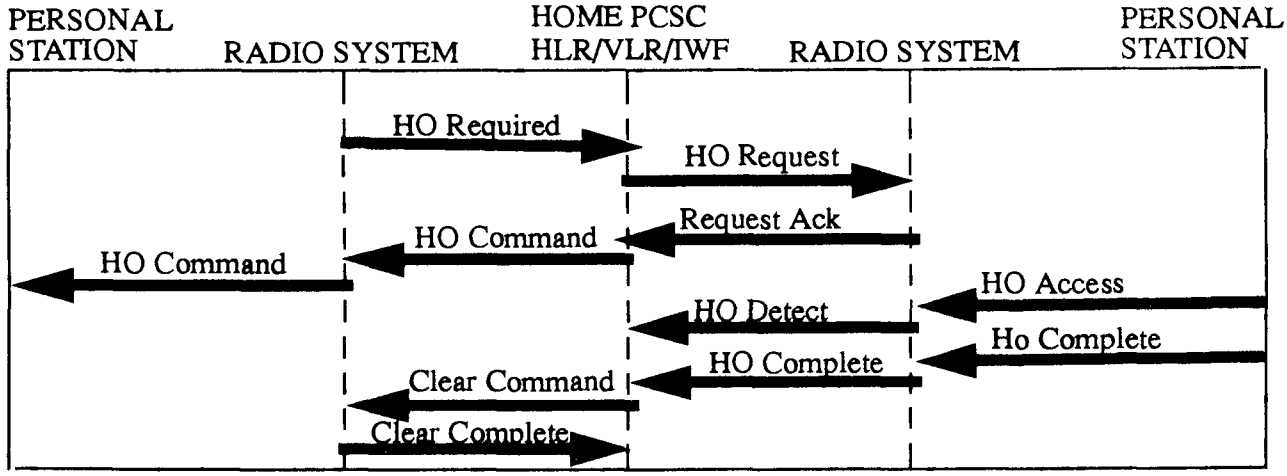

Figure 7 Traffic Flow - Normal and Handoff

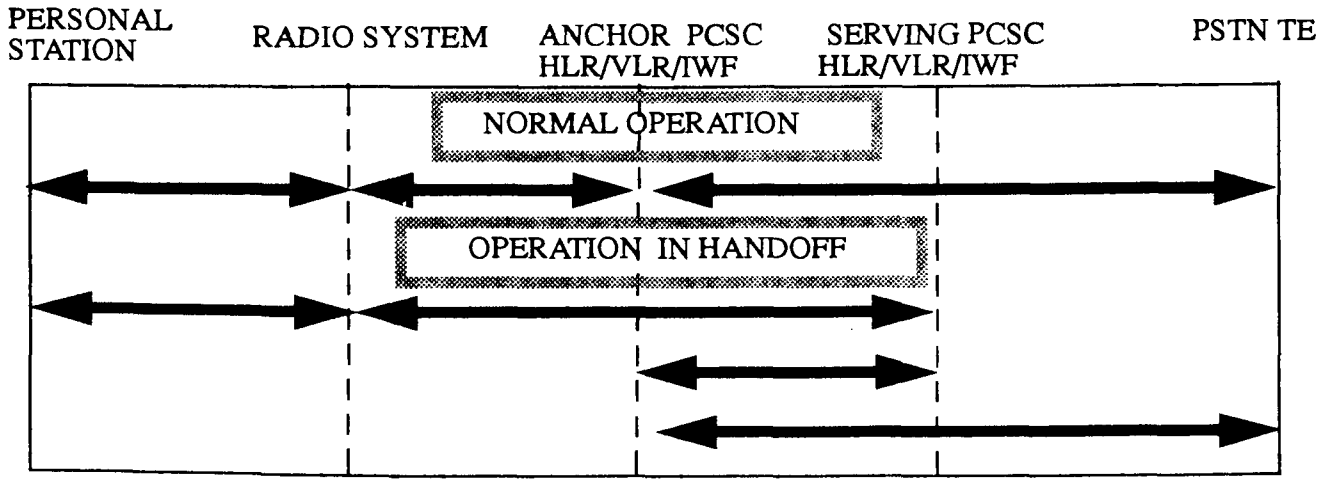

Network Flexibility of the IRIDIUM® Global Mobile Satellite System

Jonathan Hutcheson and Mala Laurin
Engineering & Product Services
Motorola Satellite Communications
2501 S. Price Rd., Chandler AZ, 85248, U.S.A.

ABSTRACT

The IRIDIUM[1] system is a global personal communications system supported by a constellation of 66 low earth orbit (LEO) satellites and a collection of earth-based "gateway" switching installations. Like traditional wireless cellular systems, coverage is achieved by a grid of cells in which bandwidth is reused for spectral efficiency. Unlike any cellular system ever built, the moving cells can be shared by multiple switching facilities. Noteworthy features of the IRIDIUM system include inter-satellite links, a GSM-based telephony architecture, and a geographically controlled system access process. These features, working in concert, permit flexible and reliable administration of the worldwide service area by gateway operators. This paper will explore this unique concept.

INTRODUCTION

The world has witnessed an explosive growth in wireless personal communications over the past decade. In the early 1980's, cellular telephone service was offered only in a few major cities in the world. By the year 1990, most medium to large cities throughout the world offered cellular service. These days, cellular service has also appeared in many select rural corridors between cities. Despite the phenomenal growth in wireless personal communications, incompatible standards exist, and vast areas throughout the world do not offer wireless service at all. Today's society has asked for wireless personal communications for anyone, anytime, anyplace. To meet this demand, the IRIDIUM system for global personal communications is now being developed.

The IRIDIUM system is first and foremost a global communications system. What distinguishes the IRIDIUM system from all other personal communications systems is its unique constellation of 66 low-earth-orbit (LEO) satellites. These satellites are arranged in six polar orbital planes 780 kilometers above the planet, each containing 11 satellites as depicted by Figure 1. This configuration offers low path delays and global coverage. No matter where a subscriber is standing on the planet, a satellite is always visible at least eight degrees above the horizon.

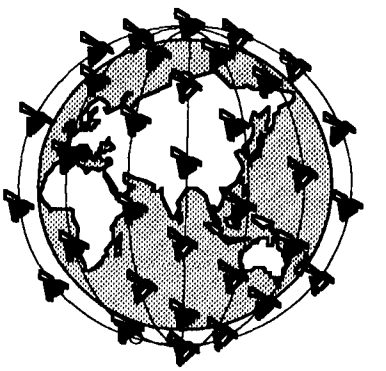

Figure 1. The IRIDIUM Constellation

The constellation of satellites of the IRIDIUM system comprise the L-band "cell sites" through which subscribers obtain mobile wireless service. However, to work as a complete personal communications system, several ground components are involved, as depicted by Figure 2.

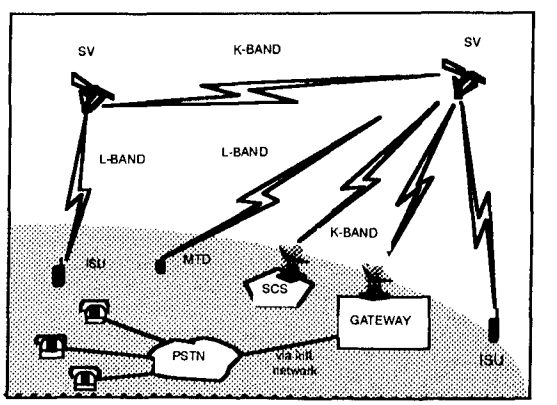

LEGEND:
ISU – IRIDIUM® Subscriber Unit
PSTN – Public Switched Telephone Network
SCS – System Control Segment
MTD – Message Termination Device
SV – Space Vehicle

Figure 2. IRIDIUM System Overview

1. IRIDIUM is a registered trademark and service mark of Iridium, Inc.

The constellation of satellites is controlled by the System Control Segment (SCS). This is a ground station which handles satellite commands and telemetry. In addition to maintaining proper satellite orbits, the SCS also computes and loads the satellites with frequency planning and routing information.

Connection between the land public switched telephone network (PSTN) and the constellation is achieved by gateway (GW) installations. Connection to the constellation is done using high gain parabolic tracking antennas operating at K-band frequencies. Connection to the PSTN is via lines to an international switching center (ISC) using PCM transmission and SS7 or Multi-frequency Compelled Response (MFCR2) signaling.

IRIDIUM Subscriber Units (ISUs) and Message Termination Devices (MTDs) comprise the ground subscriber equipment. An ISU is a hand held phone which communicates to the satellite using an L-Band link. An MTD is a pocket-sized "beeper" unit capable of receiving short alphanumeric messages, also sent using an L-Band link.

CROSSLINKS -- THE KEY TO GATEWAY PLACEMENT FLEXIBILITY

Figure 3 depicts the intersatellite links employed by the IRIDIUM system. These K-band crosslinks provide reliable, high-speed communications between neighboring satellites, forming a robust information network in the sky.

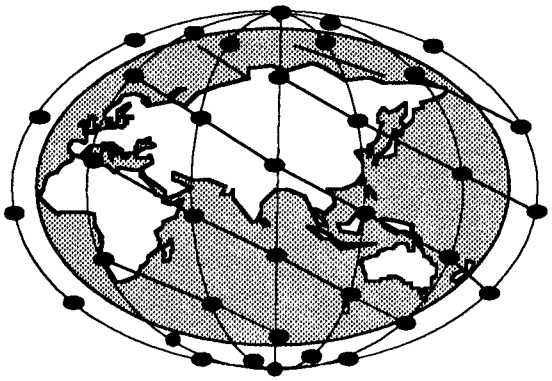

Figure 3. IRIDIUM SYSTEM INTERSATELLITE CROSSLINKS

Figure 4 shows a "close-up" view of this network over a typical part of the world. The clusters of 48 hexagons beneath each satellite represent the cells formed by phased-array L-band antennas aboard the satellite. Two gateways are also depicted on this diagram.

Crosslinks provide the flexibility to place gateways virtually anywhere. Consider a subscriber standing in one of the cells depicted in Figure 4. Even though there is not a gateway shown within any of the pictured hexagons, the crosslinks provide multiple possible paths between the subscriber and the gateway which "lands" his conversation. These multiple possible paths offer the IRIDIUM network additional robustness and reliability. It should be also noted that the crosslinks make it possible for even one Gateway to provide connectivity to all users throughout the planet.

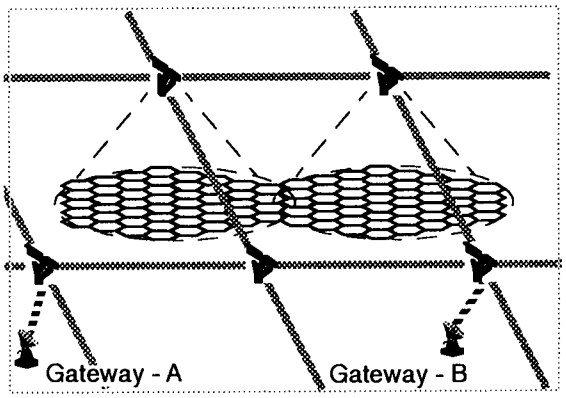

Figure 4. Close-up Depicting Individual Cells

Individual L-band cells and channels are not "owned" by any particular gateway. Consequently, calls can be routed to whichever gateway that makes sense. This flexibility therefore permits efficient call delivery and an extra measure of system reliability.

THE IRIDIUM GATEWAY AND THE GSM STANDARD

The call processing architecture of the IRIDIUM system is patterned after the GSM (Global System for Mobile Communications) standard. GSM is a popular digital cellular standard which offers a wealth of features to subscribers, and is continuously being enhanced with new features. By adopting this standard, IRIDIUM subscribers will benefit as advances in the GSM standard are transferred to the IRIDIUM system.

Unlike GSM, however, the Gateway must also manage the effects of the dynamic nature of the satellite constellation, thus while the majority of the Call Processing functions are identical between GSM and the IRIDIUM system, many of the lower level hardware and software functions of GSM have IRIDIUM-specific modifications.

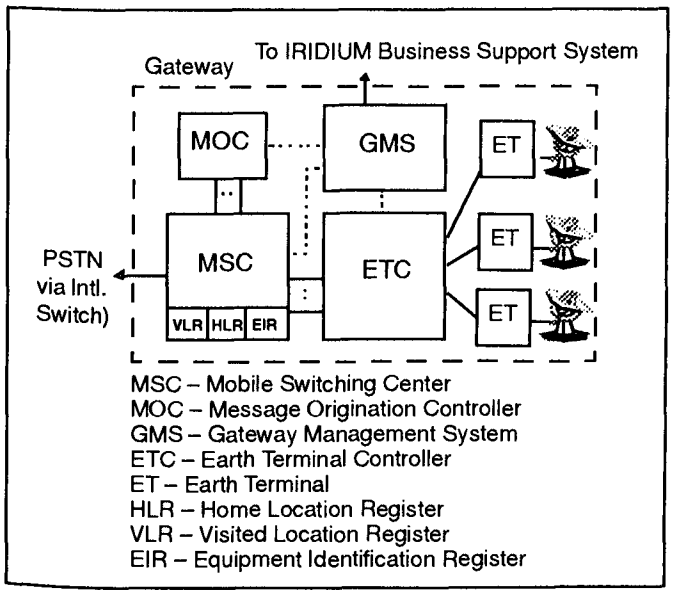

Figure 5. Gateway Block Diagram

Figure 5 shows a block diagram of an IRIDIUM gateway. At the heart of the gateway is the mobile switching center (MSC), a GSM switch. The MSC has two "sides": a land side which connects to the telephone network, and a mobile side which connects across an "A" interface to an Earth Terminal Controller (ETC). The ETC is analogous to the Base Site Subsystem (BSS) of a terrestrial GSM system, and it controls a set of Earth Terminals (ETs) which communicate with the constellation using K-band radio links, also called the Feeder Links. Since the Gateway/Constellation interface must be maintained continuously, the Gateway is constantly establishing a new connection with the rising SV before dropping its connection with the setting SV. Each Gateway includes three ETs, one maintains the active, traffic-bearing connection to the SV passing overhead, another prepares to acquire the next rising SV, and the third provides redundancy in case of ET hardware or software failure, and, depending on its separation from the other ETs rain diversity. Information for subscribers is kept in the Visited and Home Location registers (VLR and HLR). Information for physical subscriber equipment is kept in the Equipment Identification Register (EIR).

The gateway Message Origination Controller (MOC) supports a variety of messaging services, such as direct messaging to Message Termination Devices (pagers). The Gateway Management System (GMS) provides Operations, Administration, and Maintenance support for each of the gateway subsystems.

The IRIDIUM Business Support Subsystem is responsible for collecting, consolidating, and wholesale rating all of the usage on the IRIDIUM system, and creating settlement statements between Iridium, Inc. and the Gateway operators. The Call Detail Record (CDR) information is sent over an ethernet connection from the GMS to the IBSS.

GEOGRAPHICALLY CONTROLLED SYSTEM ACCESS AND GATEWAY ROLES

Each IRIDIUM subscriber is assigned a "Home Gateway". A permanent record of subscriber information is kept at this Home Gateway in the HLR. IRIDIUM subscribers may be identified by any of the following numbers:

- MSISDN - The Mobile Subscriber ISDN number, the number which a land party would dial to reach an IRIDIUM subscriber.
- TMSI - The Temporary Mobile Subscriber ID, the number that is normally sent over the airwaves when a mobile is placing or receiving a call. The TMSI is changed periodically to protect subscriber confidentiality.
- INSI - The IRIDIUM Network Subscriber ID, a permanent number stored in the subscriber unit which is sent over the airwaves only when a valid TMSI is not available.

Irrespective of where a subscriber is, the home gateway can be determined by examining the "Geopolitical Entity/Service Provider" (GESP) fields which are common to each of the listed subscriber number representations. Figure 6 shows the structure of an MSISDN number, and its associated GESP fields, which is based on the ITU-T standard E218 numbering scheme. The IRIDIUM country code will be assigned by the ITU organization.

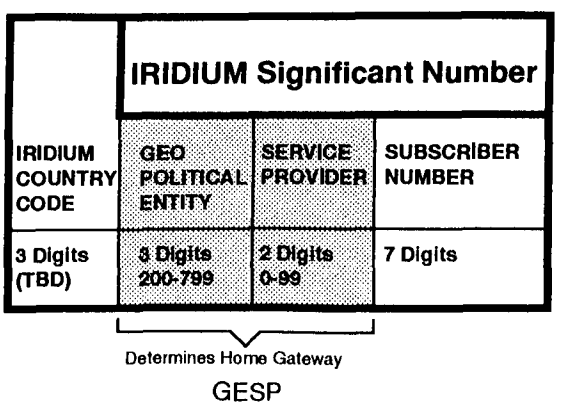

Figure 6. MSISDN Number Structure

The Home Gateway is responsible for granting system access. Whenever an IRIDIUM subscriber places or receives a call, the IRIDIUM system will determine the subscriber's location. The home gateway will receive and evaluate this location information to determine whether it is permissible for the call to proceed. This feature is essential to help ensure compliancy with calling restriction laws in nations where such laws exist.

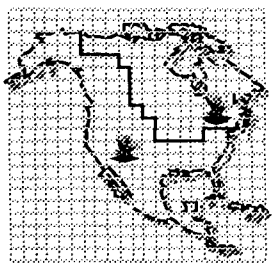

- LAC Define Service Area of a Gateway
- 2047 LACs available/GW
- Square Shapes Recommended
- During Network Access, Home GW selects a serving gateway based upon which LAC the mobile unit is found
- All Gateway's worldwide know which LACs belong to which Gateway.

Figure 7. Visited Gateway Assignment

The Home Gateway is also responsible for the assignment of a Visited Gateway as part of the system access process. Subscriber location information is used to index into a map of the world kept at the home gateway. This map determines a Location Area Code (LAC) which is in turn used to identify a visited gateway which will serve and control the call. Figure 7 depicts a hypothetical map demonstrating the LAC concept.

The visited gateway receives the subscriber information using SS7 transaction capability (TCAP) and keeps its own copy of the information in its VLR. This information stays with the visited gateway until the subscriber "roams" into a new visited gateway area. Note that when a subscriber is at "home", the visited gateway and home gateway become the one and the same.

The visited gateway "controls" the mobile subscribers it serves, and is responsible for all aspects of mobile call processing: setup, maintenance, tear-down, and management of supplementary services such as call waiting or call forwarding. From a regulatory viewpoint, this visited gateway concept permits sovereign authority by the gateway operator within his service territories.

In addition to being a "home" or "visited" gateway, a gateway may serve as a "PSTN connecting" gateway. The IRIDIUM system is designed to accept incoming PSTN calls at any gateway. Even if this gateway is neither the home nor visited gateway of the called subscriber, the visited gateway may be identified and connected by querying the home gateway.

For mobile originated calls, the visited gateway will determine a "PSTN connecting" gateway based upon the digits dialed by the mobile subscriber. Also in this case, the "PSTN connecting" gateway could differ from the visited gateway, in which case a transit link is established between them. Again, thanks to the intersatellite links of the IRIDIUM constellation, this approach to efficient call delivery becomes possible.

FLEXIBLE GATEWAY SERVICE TERRITORIES

Flexibility to add new gateways to the system and/or repartition service areas is an important feature of the IRIDIUM system. Again, this flexibility is possible thanks to the constellation crosslinks, the GSM telephony architecture, and the system's geographically controlled system access process. This flexibility is essential to support equitable business arrangements among gateway operators. It also permits "backup" arrangements between gateways to safeguard against catastrophic events, such as earthquakes or fires.

One aspect of this flexibility is the independence between home and visited gateway territorial assignments. In most cases, a gateway operator will keep these one and the same. However, as depicted by Figure 8, it is possible to partition these areas differently, if desired.

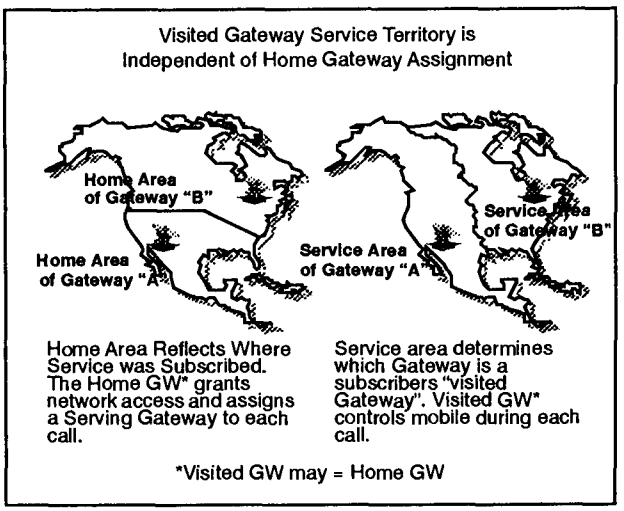

Figure 8. Independent Home & Service Areas

This independence is possible because home gateway assignment depends only upon the MSISDN number assigned to a mobile subscriber, whereas visited gateway territory also depends upon the subscriber's location.

Basing the home gateway assignment on the MSISDN number is of special advantage to a gateway operator who chooses to establish multiple gateways. Under this arrangement, he is free to partition home gateway assignment on whatever criteria suits his business arrangement best, whether it be subscriber mailing address, retail outlet, or any other factor.

New gateways are easily added to the system. Blocks of new or existing subscriber numbers may be added to a new home gateway by simply instructing the system to "point" the number blocks to this new home gateway. Visited gateway territories for newly added gateways can be established simply by reprogramming the maps used in the geographically controlled access process. If desired, geographic regions can even be configured to be a shared visited gateway territory between multiple gateways. This is possible because each gateway has its own set of maps used for the geographically controlled system access process.

As the number of IRIDIUM subscribers grows worldwide, it is anticipated that more and more gateways will be added to address the growing demand. It will be exciting to observe how the roaming and calling patterns of IRIDIUM subscribers evolve. The gateway operators will need to keep pace with the direction established by the worldwide subscriber population. Consequently, the gateway operators will need the flexibility to modify service territory, routing, and traffic loading strategies to accommodate this dynamic market. The IRIDIUM system will provide the gateway operators with this needed flexibility.

TRANSIT TRUNKS & CALL CUT-THROUGH FEATURE

We have seen that in the IRIDIUM system, mobile subscribers will be controlled by a visited gateway which is assigned based upon where the subscriber is standing. We have also seen that connection to the PSTN could occur at any gateway, depending upon the location of the land party. In many cases, especially international calls, these two gateways may differ. To connect these gateways together, the IRIDIUM system supports transit trunks via the cross-linked constellation of satellites.

Figure 9 depicts a visited/serving gateway providing a transit connection to a PSTN connecting gateway. In this figure, dotted lines represent signaling paths, and solid lines represent the voice path. The top edge of each MSC represents its "mobile" side, and the bottom edge represents the "land" side. The top edge of each ETC represents its K-band constellation link side, while the side and bottom edges represent transit and mobile trunk connections respectively. In situations where speech must pass through the serving gateway, for example when using certain supplementary services, the transit connection between the two gateways is achieved by "looping" both the signaling and speech path back into the constellation via a transit connection destined for the PSTN connecting gateway.

However, in most cases, it is not necessary for the speech path to pass through the serving gateway once a transit connection is established. Recognizing this, the IRIDIUM system offers a special feature called "Cut-Through". When the "Cut-Through" feature is used, Figure 9 does not apply, instead, the system will arrange for speech to pass directly to the PSTN connecting gateway as depicted by Figure 10.

Note that although the voice path will bypass the serving gateway, the signaling path continues to flow through the serving gateway, permitting it to maintain control of the call. The voice connection through the MSC is maintained, although voice does not pass through the connection after doing a cut-through. Consequently, the serving gateway can "pull" back down the speech path at any time if needed, for example, if a call-waiting call comes in for a mobile subscriber.

Although the "Cut-through" feature was designed for improved performance for land-to-mobile and mobile-to-land calls involving two gateways, it may also be advantageously invoked for mobile-to-mobile calls.

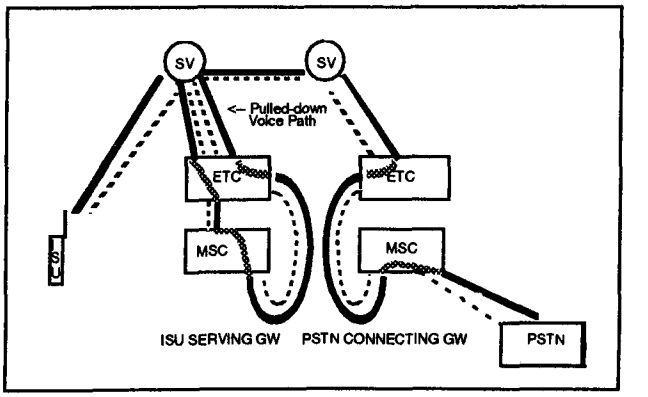

Figure 9. Mobile-Land Call, No Cut-Through

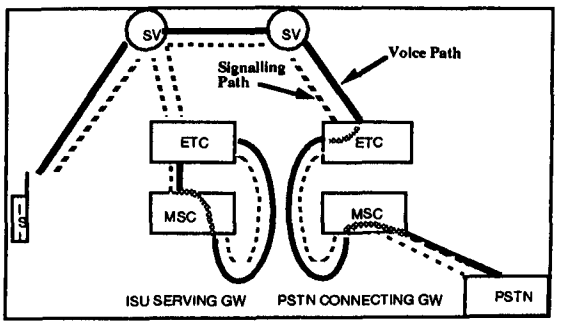

Figure 10. Mobile-Land Call, Cut-Through

We see "Cut-through" refers to voice path bypass around the ISU serving gateway. This feature offers benefits to both the subscriber and the system. Call delivery becomes even more efficient, and the voice path delay is reduced. Also, loading on the gateway K-band feeder link to the constellation is reduced, allowing the link to be used more efficiently.

SUMMARY AND CONCLUSIONS

The IRIDIUM system is a global personal communications system which offers hand-held wireless telephony to anyone, anytime, any place. It achieves world wide wireless coverage through a network of 66 satellites in low-earth-orbit and a collection of ground based "gateway" installations.

The IRIDIUM system is characterized by several distinguished attributes: the intersatellite links of its constellation, its GSM-based telephony architecture, and its geographically controlled system access process. These features, working together, create a flexible, reliable network which provides efficient call delivery. The benefits are shared by both the IRIDIUM subscribers and gateway operators alike.

The introduction of the IRIDIUM system will be a key milestone in the history of telecommunications. Mankind's unrelenting quest for more ways to communicate with one another is advancing another step.

Traffic Model For The Satellite Component Of UMTS

Y.F. Hu and R.E. Sheriff
University of Bradford, Richmond Road
Bradford, West Yorkshire, BD7 1DP,
United Kingdom
Phone: +44 1274 384031, +44 1274 484053 Fax: +44 1274 391521
e-mail: y.f.hu@bradford.ac.uk r.e.sheriff@bradford.ac.uk

ABSTRACT

An algorithm for traffic volume estimation for satellite mobile communications systems has been developed. This algorithm makes use of worldwide databases for demographic and economic data. In order to provide for such an estimation, the effects of competing services have been considered so that likely market demand can be forecasted. Different user groups of the predicted market have been identified according to expectations in the quality of services and mobility requirement. The number of users for different user groups are calculated taking into account the gross potential market, the penetration rate of the identified services and the profitability to provide such services via satellite.

Keywords: Satellite mobile communications systems, traffic volume, gross potential market, penetration,

INTRODUCTION

The definition of third generation mobile telecommunication systems is now in progress. In Europe, activities are concentrating on the standardisation of the Universal Mobile Telecommunication System (UMTS). Under the European Community's RACE II programme, a number of projects are addressing UMTS, one of which is SAINT - Satellite Integration in the Future Mobile Network. SAINT, which commenced in January 1994, is focusing specifically on the requirements of the satellite component of a 3rd generation mobile network. Satellites can play an important role in the development of the future mobile network. For example, satellites can be used to provide coverage to areas where the terrestrial network is unable to provide coverage.

One of the tasks of SAINT is to define a traffic model suitable for the dimensioning of the satellite component of UMTS. Before traffic can be determined, the Gross Potential Market (GPM) must first be calculated. The GPM is dependent on a number of parameters including demographic and economic factors.

This paper reports on the development of this model.

SATELLITE-MOBILE TRAFFIC MODEL

When considering satellite-mobile traffic modelling, it should be noted that there is very little publicly available information; and what is available is sparse in its content. Probably the most up-to-date available information was that produced during the European Commission's recently sponsored study 'Satellite Personal Communications'[1]. This study was performed for the European Commission by KPMG Peat Marwick et al. KPMG's approach to predicting the market for future satellite services has been used as a basis for the development of the traffic model presented in this paper.

The first step in the dimensioning of a SPCN (Satellite Personal Communications Network) service is to identify potential user groups. Three categories of services/users identified by KPMG were used, namely, cellular in-fill users, rural fixed users and international business travellers. Demand for voice services is assumed to outweigh that for data and paging. The algorithm for each category of service is as follows:

Cellular in-fill services

In order to estimate the size of this market, the gross potential market (GPM) has to be identified. The GPM for the cellular in-fill market is defined as the number of people residing outside of the cellular terrestrial coverage. To determine the GPM, a population density threshold, DEN_{thres}, has been introduced in the traffic models of KPMG. This is defined as the threshold of the population density above which the implementation of a terrestrial cellular system is profitable. Conversely, the use of satellites for the provision of mobile services is preferable. DEN_{thres} is related to GDP per capita and is defined in Table 1 [1].

Thus, if the population density in a region is lower than DEN_{thres}, there is a market for SPCN services. The number of subscribers, $N_{cellular}$, in this case is:

$$N_{cellular} = Pop_{region} \times Pr_{cellular}(t)$$

where $Pr_{cellular}(t)$ is the penetration of the cellular services at year t and is a function of relative tariff of the SPCN

Country GDP per capita	Year 2010
High GDP (> US$20000 per capita)	DEN_{thres} < 3 people/km^2
Mid GDP (between US$6000 and US$20000 per capita)	DEN_{thres} < 30 people/km^2
Low GDP (< US$6000 per year)	Cities < 1 million people

Table 1 Population Density Thresholds

services. Relative tariff is defined as the ratio of GDP per capita of the region to the tariff of the SPCN services per user. Figure 1 shows the relationship between $Pr_{cellular}$ and the relative tariff. In predicting the penetration of cellular in-fill services, the historical growth of existing cellular mobile communications systems is assumed.

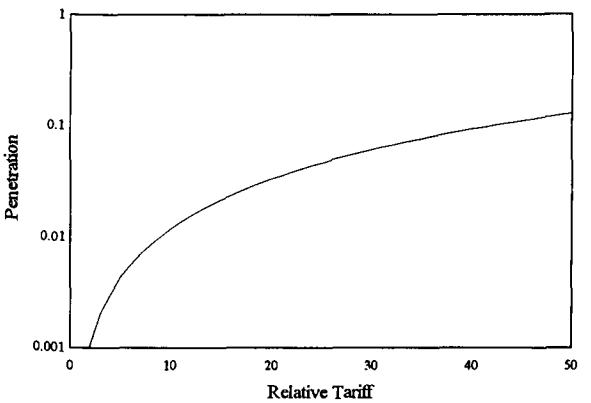

Figure 1 Relationship between penetration of cellular in-fill services and relative tariff

Rural fixed services

As in the cellular in-fill service, the first step in estimating the number of rural fixed service users is to identify the GPM. According to KPMG, the GPM for fixed rural service is defined as the number of households minus the number of telephone mainlines, to give the number of households without a mainline. However, the number of telephone mainlines includes also the telephone mainlines in business environment. In order to provide a more accurate estimate to the market, the GPM of the rural fixed service is modified as follows:

$$GPM = N_{household} - T_{residential}$$

where $N_{household}$ is the number of households and $T_{residential}$ is the number of telephone mainlines in residential areas. This would give the true number of households without a telephone mainline.

Having determined the GPM, the penetration of the fixed rural service has to be determined. The penetration, $Pr_{fixed}(t)$, is defined as the expected number of telephone lines per household at year t. Figure 2 shows the relationship between Pr_{fixed} and relative tariff. Assuming that it is more economical to provide fixed services via satellite, the total number of subscribers, N, for the rural fixed services is:

$$N_{fixed}=(N_{household} - T_{residential}) \times Pr_{fixed}(t)$$

In predicting the penetration rate of the rural fixed services, the historic growth of telephony services is applied.

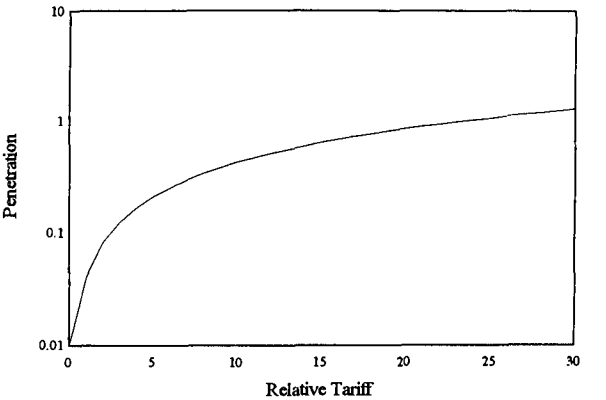

Figure 2 Relationship between fixed service penetration and relative tariff

Satellite services for international business travellers

The methodology adopted in deriving the traffic model for international business travellers is the same as the cellular in-fill model. The gross potential market for this group of users is defined as the number of outbound airline travellers, $N_{air\ travellers}$, per annum. In determining the penetration of provision of SPCN services to this group of users, the subscriber payment per call minute is set three times higher than that in the cellular in-fill model[1]. The number of subscribers, N_{IBT}, for this user group can be predicted as follows:

$$N_{IBT} = N_{air\ travellers} \times Pr_{IBT}(t)$$

where Pr_{IBT} (t) is the penetration of SPCN services for international business travellers in year t.

DATA

Any forecasting model is subject to uncertainty. One of the contributions to this uncertainty is the scarcity of data. Most of the data obtained to date are mainly from the United Nations[2,3], the ITU[4] as well as from the EU's databases[5]. Table 2 identifies the data used for the prediction of traffic for each user group.

Although the number of countries used in each set of data is high, the mapping of one data set onto another to generate a complete set of data remains difficult.

RESULTS

It is of interest to consider the distribution of traffic throughout the world. Figures 3a-3c show the traffic distribution for different user groups over 7 regions of the globe. Figure 4 shows the total traffic distribution. It can be seen that among these regions, Asia has the biggest potential market.

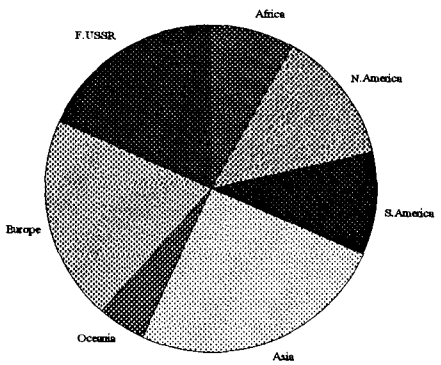

Figure 3a Distribution of traffic for cellular in-fill users

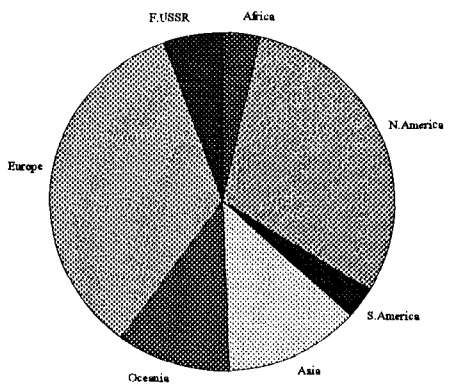

Figure 3b Distribution of potential subscribers for international business travellers

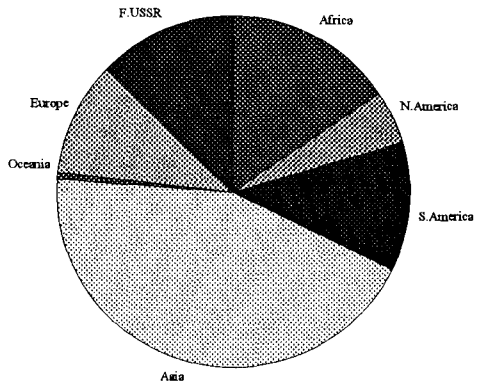

Figure 3c Distribution of potential subscribers for rural fixed users

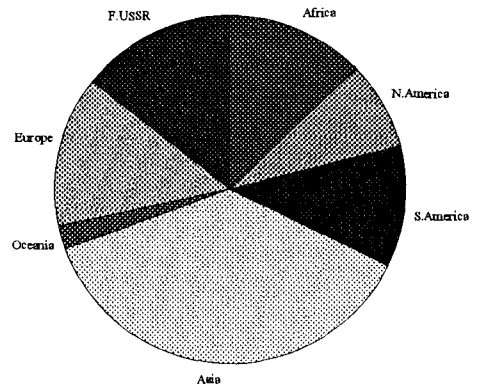

Figure 4 Total distribution of potential subscribers

Potential satellite traffic has been predicted for over 210 countries, from which a 36 x 72 traffic grid has been generated.

The prediction of traffic volume enables the determination hourly traffic in Erlang. Table 3 shows the hourly traffic generated per user, as used in the model.

Time period	Traffic per user (mErlang)
Office Hour	10
Travelling Hour	4
Evening	0.75

Table 3 Hourly traffic generated per user

Assuming that the call duration is 120 s, Figure 5 shows the traffic variations along the longitude line at 6:00 GMT and 18:00 GMT.

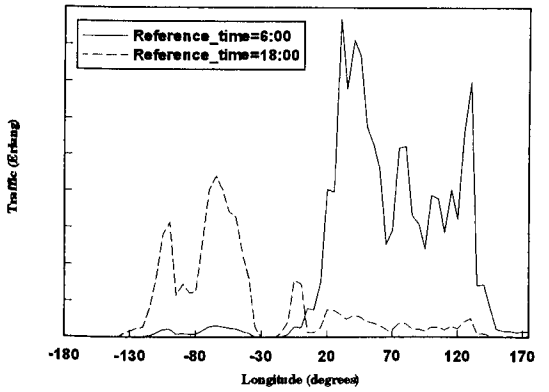

Figure 5 Traffic variation along longitude line

CONCLUSION

The traffic capacity for the satellite component of UMTS has been predicted. The traffic model has incorporated dynamic traffic variation over a 24 hour period. This enables equipment and circuit provisions to be planned in the most optimum manner.

ACKNOWLEDGEMENTS

The authors would like to thank the European Commission for funding this project, Project No. R2117. The authors would also like to thank SAINT partners for their comments and contributions during the development of this model.

REFERENCES

[1] "Satellite Personal Communications and their consequences for European Telecommunications Trade and Industry" Report to European Commission, KPMG, March 1994.
[2] Statistical Yearbook, 38th Issue, UNESCO.
[3] Demographic Yearbook, 42nd Issue, UN.
[4] ITU Statistical Yearbook, 1994.
[5] Eurostat Data, European Commission.

User group	Data for prediction of the number of potential subscribers	Number of Countries Used
Cellular in-fill	1) Population	225
	2) Rural area population %	225
	3) Gross domestic product (GDP)	225
	4) Surface area of the region	225
	5) Number of mobile communications subscribers	216
	6) Population of cities over a million	58 (limited to low GDP countries)
Rural fixed services	1) Number of telephone mainlines	218
	2) % of residential telephone lines	199
	3) Number of occupants/household	225
	4) GDP	225
International Business travellers	1) Number of outbound airline travellers per annum	146
	2) GDP	225

Table 2 Data Used for Traffic Capacity Prediction

Low Earth Orbit Satellite Traffic Simulator

John Hoelzel
System Engineer and Deputy Program Manager for E-Systems
(System Integrator for the LEO Constellation System)
E- Systems, Inc. Garland Division, P. O. Box 660023,
Dallas, Texas, 75266-0023
Tel: 214-205-4895 Fax: 214-205-7180
SatCom11@aol.com

Abstract

This paper describes a significant tool for Low Earth Orbit (LEO) capacity analysis, needed to support marketing, economic, and design analysis, know as a Satellite Traffic Simulator (STS). LEO satellites typically use multiple beams to help achieve the desired communication capacity, but the traffic demand in these beams in usually not uniform. Simulations of dynamic, average, and peak expected demand per beam is a very critical part of the marketing, economic, and design analysis necessary to field a viable LEO system. An STS is described in this paper which can simulate voice, data and FAX traffic carried by LEO satellite beams and Earth Station Gateways. It is applicable world-wide for any LEO satellite constellations operating over any regions. For aeronautical applications to LEO satellites, the anticipated aeronautical traffic (Erlangs for each hour of the day to be simulated) is prepared for geographically defined "area targets" (each major operational region for the respective aircraft), and used as input to the STS.

The STS was designed by Constellations Communications Inc. (CCI) and E-Systems for usage in Brazil in accordance with an ESCA/INPE Statement Of Work, and developed by Analytical Graphics Inc. (AGI) to execute on top of its Satellite Tool Kit (STK) commercial software. The STS simulates constellations of LEO satellite orbits, with input of traffic intensity (Erlangs) for each hour of the day generated from area targets (such as Brazilian States), accumulated in custom LEO satellite beams, and then accumulated in Earth Station Gateways. The STS is a very general simulator which can accommodate: many forms of orbital element and Walker Constellation input; simple beams or any user defined custom beams; and any location of Gateways.

The paper describes some of these features, including Manual Mode dynamic graphical display of communication links, to illustrate which Gateway links are accessible and which links are not, at each "step" of the satellite orbit. In the two Performance Modes, either Channel capacity or Grade Of Service (GOS) for objects (Satellite beams, Gateways, and an entire satellite) are computed respectively by standard traffic table capacity lookup and blocking probability equations. GOS can be input, with number of channels calculated, or number of channels can be input, with GOS calculated. Also described are some of the STS Test Procedure approach and results. AGI plans to make the STS features available through their normal commercial STK products.

E-Systems is a co-developer, tester, and user of the STS. The Test Procedure for the STS was prepared by E-Systems, as an independent tester for CCI, to support the CCI delivery of the STS to ESCA, for their customer INPE.

Low Earth Orbit Satellite System Overview

On November 16, 1994 six Low Earth Orbit (LEO) Satellite applicants submitted their amended applications to the Federal Communications Commission (FCC) for authority to construct, launch and operate respective LEO Satellite Systems in the FCC U.S. jurisdiction, including CONUS, Alaska, Hawaii, Puerto Rico, and the U.S. Virgin Islands. Three of these applicants complied with all the FCC Report and Order requirements and were awarded a license in early 1995 and two licenses were deferred for up to one year for completion of the required financial statements: Loral/QUALCOMM Partnership (GLOBALSTAR System); Motorola Satellite Communications, Inc. (IRIDIUM System); TRW Inc. (Odyssey System); deferred: Constellation Communications, Inc. (Constellation System); Mobile Communications Holdings, Inc. (Ellipso System).

These "Big LEO" systems differ somewhat in their service, business, and coverage focus. In general they provide worldwide "wireless" mobile and fixed voice, data and FAX communication service via LEO satellites. It is the voice service that primarily distinguishes "Big LEO" from "Little LEO" systems.

Low Earth Orbit Aeronautical Services

The LEO mobile voice, data and FAX services can be applied to the aeronautical community. Commercial and General Aviation markets are within the technical and economic capability of the Big LEO systems. However the costs and procedures of qualifying LEO services for

commercial airline applications , compared to those for General Aviation may tend to favor application of LEO services to General Aviation in the aeronautical community.

Economic, Capacity, and Coverage Analysis for LEO Systems

For aeronautical and land-based fixed and mobile users of LEO services, complex economic, capacity, and coverage analysis is needed to support marketing, economic, and design decisions. LEO satellites typically use multiple beams to help achieve the desired communication capacity, but the traffic demand in these beams in usually not uniform. Traffic demand in LEO satellite beams is a function of the user density covered by each beam, and the "time-of-day" traffic demand for that geography/coverage. Simulations of dynamic, average, and peak expected demand per beam is a very critical part of the marketing, economic, and design analysis necessary to field a viable LEO system. A Satellite Traffic Simulator (STS) is described below which can simulate voice, data and FAX traffic carried by LEO satellite beams and Earth Station Gateways to provide this type of critical and complex analysis. It is applicable world-wide for any LEO satellite constellations operating over any regions. For aeronautical applications to LEO satellites, the anticipated aeronautical traffic (Erlangs for each hour of the day to be simulated) is prepared for geographically defined "area targets" (each major operational region for the respective aircraft), and used as input to the STS.

Satellite Traffic Simulator Background

The STS was designed by Constellations Communications Inc. (CCI) and E-Systems for usage in Brazil in accordance with an ESCA/INPE Statement Of Work, and developed by Analytical Graphics Inc. (AGI) to execute on top of its Satellite Tool Kit (STK) commercial software. AGI plans to make the STS features available through their normal commercial STK products. E-Systems is a co-developer, tester, and user of the STS. The Software Test Procedure for the STS was prepared by E-Systems, as an independent tester for CCI, to support the CCI delivery of the STS to ESCA, for their customer INPE.

Satellite Traffic Simulator Description

The STS simulates constellations of LEO satellite orbits, with input of traffic intensity (Erlangs) for each hour of the day generated from area targets (such as Brazilian States), accumulated in custom LEO satellite beams, and then accumulated in Earth Station Gateways. The STS is a very general simulator which can accommodate: many forms of orbital element and Walker Constellation input; simple beams or any user defined custom beams; and any location of Gateways. The STS features include Graphics Mode dynamic graphical display of communication links, to illustrate which Gateway links are accessible and which links are not, at each "step" of the satellite orbit. This Graphics Mode provides a stepping through of access successes and failures for single and double hop (Subscriber-to-Subscriber) situations, displaying corresponding link (Subscriber-to-Satellite Beam-to-Gateway) color codes for each step of satellite motion. In the two Performance Modes, either Channel capacity or Grade Of Service (GOS) for objects (Satellite beams, Gateways, and an entire satellite) are computed respectively by standard traffic table capacity lookup and blocking probability equations. GOS can be input, with number of channels calculated, or number of channels can be input, with GOS calculated.

Aeronautical Simulation Approach

STK supports non-orbital simulations which can be used to simulate aircraft. These Great Arc simulations support specification for each flight of start and end latitude, longitude, altitude, and time, as well as the aircraft rate. This STK simulation support, or independent means, can be used to map aircraft locations (and associated traffic intensity) versus time-of-day into tables of traffic density (for each hour of the day). STS calls the traffic density tables "Area Target" Tables, selected to represent sectors of aeronautical routes to be simulated. After the aeronautical traffic tables are prepared, the STS simulation can be run in the same manner, regardless of whether it is simulating aeronautical traffic or terrestrial-based mobile and fixed traffic through the LEO system.

STK and STS Conventions and Nomenclature

The following convention and nomenclature description is very important to efficiently and unambiguously define STK access computations via the STK "Chains" features. The six conventions to observe in defining Chains for use by the STS are listed below. Chain accesses are computed in a "top-down" order. Therefore the following is a complete chain order that supports the more complex "virtual link" (double hop). All 6 of the following objects are Constellations (STK term within the Chains features).

1 - target Constellation (typically area target for Performance; Point target for Graphics)
2 - vehicle + custom sensor Constellation (to represent subscriber uplink)
3 - vehicle with min. elevation angle constraint (to represent G/W down-link) Constellation
4 - Facility Constellation (to represent G/Ws)

5 - Vehicle with elevation angle constraint Constellation (to represent 2nd hop uplink rom G/W)
6 - Facility (subset to represent only Destination G/Ws)

STS Test Description; An Aid To Understanding STS Functionality

The following highlights from the Software Test Procedure for the STS, Reference [6], are presented as an aid to understanding the STS functional and performance capability as specified in the STS Program Requirements and Development Plan.

The following STS Requirements Verification Traceability Matrix (RVTM) from the STS Test Plan, Reference[1], provides a road map for Test Cases A-G, which reference the Functional and Performance Spec. paragraphs in the STS Program Requirements and Development Plan, Reference[2].

	Test Case Title	STS RVTM **Functional Spec. Capability Reference** (ID's below are from Ref. [2], Appendix A)
* A	Input Validation	Validate Operator Input Error Messages & Input Logic Checks
* B	Algorithm Test	2.4-3; 3.2-1
* C	Simple Demo	2.0-1; 2.1-1; 2.4-1; 3.2-1; 3.2.1-1; 3.2.1-2
* D	G/W Placement	1.2-1; 1.2-2; 2.2-1; 3.1.1-1
* E	Instantaneous Traffic Analysis	2.1-2; 2.2-2; 2.4-2; 3.1.2-3; 3.2.2-1
* F	Detailed Traffic Analysis	1.2-3
* G	STS Changes	3.1-1; 3.1-2; 3.1.2-1; 3.1.2-2; 3.1.3-1

NOTE: Functional Spec. IDs above use the Reference [2] Functional Spec. requirement paragraph number, followed by a dash, and a section number written in the left margin of the respective paragraph.

Selected Test Case B, D, E, F and G summaries of the entire Test Procedure which was executed at AGI, are presented below as an aid to understanding major STS functions. The STS Test Procedure supplied by E-Systems and the Users Guide supplied by AGI can be used for more detailed understanding of STS functionality and details of each test case outlined in the RVTM. Three STS Scenarios (named Graphics, PerfA, and PerfB) specified in the detailed test steps were used to execute these tests.

Test Case B: Algorithm Analysis

The following algorithm verification description is presented as an aid to understanding STS computations. Service of subscribers is supported by the "closest Gateway algorithm" for non-"long distance" and non-"mobile-to-mobile" users. This algorithm was checked by comparing the test scenario configuration with the output data file results for several steps.

Channel capacity and Grade Of Service (GOS) for objects (Satellite beams, Gateways, and an entire satellite) are computed respectively by standard traffic table capacity lookup and blocking probability equations. The output channel capacity values from a GOS Performance Mode simulation were input into a capacity Performance Mode simulation to provide a "self-consistency check," per respective test scenario steps. Additionally specific values were used to verify these calculations, including:

Equation & Table Verification:

INPUT	OUTPUT
Capacity = 24 channels Traffic Demand = 15 Erlangs	Pb = Blocking Probability = .0084 GOS = 100(1 - Pb) = 99.16%
GOS = 99.16% Traffic Demand = 15 Erlangs	Capacity Required = 24 Channels

Self-consistency check:

INPUT	OUTPUT
Grade Of Service Mode:	
GOS = **99.0000** %	Max. Facility (G/W) Traffic Demand at BRA =367.449 Erlangs; Requires **392** channels for the Brasilia G/W. Max. vehicle/sensor (Beam) Traffic Demand at S/C a3, beam a10 = 329.753 Erlangs; Requires **354** channels per beam.
Capacity Mode:	
Channels per G/W = **392**	GOS = **99.0004** % for BRA G/W;
Channels per beam = **354**	GOS = **99.0269** % for S/C a3, beam a 10

This self-consistency test showed inverse equation and table lookup calculations have a GOS precision within 0.0269 %. This procedure is much more precise than traffic loading can be estimated, so the self-consistency error is insignificant.

The distribution of area target traffic demand over respective satellites and beams, and per cent coverages, were also spot checked for consistency.

Test Case D: Gateway Placement Demonstration

This Test Case demonstrated a variety of Subscriber-to-Satellite-to-Gateway links which include both successful and failed accesses. Hand-offs to the next satellite are also included. Typical STK features are supported under STS, which include: Mouse clicking in the map window to specify the geographical location of a point target subscriber and a gateway, and constraints such as facility (Gateway) minimum elevation angle.

Test Case E: Instantaneous Traffic Analysis

This test represents the "quick look" approach to performance analysis done after the Gateway locations were configured in the Graphics Mode. It is recommended to use only 2 or 3 adjacent equatorial plane satellites for about a 30 minute simulation run to detect peak or "worst case loading conditions for further analysis.

This Test Case tested the capability of the STS to compute the traffic offered from Area Targets [e.g. 3 Brazilian States (AZ (Amazon), SP (Sao Paulo), and BA (Bahias) are in the PerfA Scenario] and to allocate it to satellite beams and gateways [e.g. 3 Brazilian Gateways (BRA (Brasilia), (MAN (Manaus),and SAL (Salvador) are in the PerfA Scenario] as the satellites move over the country. This includes hand-offs to the next satellite. Although slight satellite-to-satellite beam overlap is designed to support "make-before-break" satellite hand-off, STS satellite footprints are typically made to "just touch" to provide full coverage.

Test Case F: Detailed Traffic Analysis

This test demonstrated the STS capability to provide a long performance simulation analysis done after the Gateway locations were configured in the Graphics Mode. It is NOT recommended to make such long runs because of the compute time and the tendency of so much output data to obscure appropriate thinking and analysis. The amount of detailed data can be overwhelming. Note that the Object Maximums and the Individual Object Maximums are also printed for long simulations, so these may be useful to assure data agreement with a more thoroughly analyzed shorter STS run.
This Test Case tested the capability of the STS to compute the traffic offered from 27 Area Targets and to allocate it to satellite beams and 8 gateways as the satellites move over the country. This includes hand-offs to the next satellite.

AGI ran STS on a DEC Alpha for a 12 hour simulation without experiencing any memory or timing difficulties.

Test Case G: STS Object Changes

This test demonstrated the STS capability to support changes to STK/STS objects, including the new polygonal area target files. The STK Tutorial illustrates how to load, unload, and create new objects such as satellites, sensors, facilities, and targets. Each area target file is a text file to be edited by any text editor. Similarly the STS Traffic Data Table formats are illustrated in Tables 1-3. Recall that Test Case A verified the STS input and logic checks to assure that the STS Traffic Data File format is correct (including free from editing errors which might produce incorrect format), prior to executing the STS simulation.

AGI made many of each of the above type of STS object and file changes during STS development. Also during Test Case A, changes with deliberate errors were introduced to STS to evoke/clear the associated error message to/from the STS operator.

Recommended STS Tool Usage

The STS/STK tool supports essential and powerful analysis of LEO coverage and capacity as they affect business plan economics. Much attention should be given to collecting and documenting the driving economical and associated traffic load data which will drive STS simulations from its Traffic Data File. These tools have already been used to show that users along the southern border of the Constellation L/S rectangular (23 degrees south latitude) satellite beams can receive 100 % coverage by using just 2 Gateways in Brazil, Manaus and Brasilia. The Graphics Mode of this tool is an excellent way to explore various Gateway location alternatives to providing required services.

Once Gateway selection is firmed up, modest length of STS Performance Mode simulations can then be used to investigate the worst case loading periods. Then even shorter runs can be used to focus on critical time periods. Typically half or full day runs can be avoided, or used only to assure that their statistics are consistent with shorter, more focus simulation periods and analysis. Obviously the driving economical and associated traffic load data in the STS Traffic Table can represent many types of situations, including: various economic class penetration rates, various time-of-day peak and usage profile curves, time-phased growth of terrestrial infrastructure whereby "double hops" are primarily required to connect 2 CCI users, time-phased growth of demand for CCI services, and finally, use of empirical traffic data once LEO systems are in orbit and starting their respective ramp-up periods.

TABLE 1
STS Interface Traffic Data File Format

Traffic Table Name: (name that appears in browser window)	AAA...AAA
Number of Major Cities:	NN
For Each Major City:	
Name:	AAA...AAA
Coordinates:	XX.XX XX.XX
Global Scale Factor:	XX.XX
Number of Economic Reporting Areas:	NN
For Each Economic Reporting Area:	
Name:	AAA...AAA
Hour Offset:	NN
%Local Traffic:	XX.XX
%Mobile-Mobile Traffic:	XX.XX
Erlangs Hour 00-01:	XX.XX
Erlangs Hour 01-02:	XX.XX
Erlangs Hour 23-24:	XX.XX
Major City 1 Name:	AAA...AAA
%Long Distance Traffic to Major City 1:	XX.XX
Major City 2 Name:	AAA...AAA
%Long Distance Traffic to Major City 2:	XX.XX
Major City n Name:	AAA...AAA
% Long Distance Traffic to Major City n:	XX.XX

where n is maximum size of set of city names

TABLE 2
Market Data Table Format

Market Segment Name:	AAA...AAA
ßvoice:	XX.XX
ßdata/fax:	XX.XX
ßpaging:	XX.XX
For Each Economic Reporting Region:	
Name of Region:	AAA.AAA
Demographic Vale:	XX.XX
Penetration Rate:	XX.XX
%Local Traffic:	XX.XX
%Mobile-to-Mobile Traffic:	XX.XX
Daily Minutes/User - Voice:	XX.XX
Daily Minutes/User - Data/Fax:	XX.XX
Daily Pages/User:	XX.XX
Name of Traffic Distribution Table:	AAA...AAA

REFERENCES

[1] *"STS Test Plan"* prepared by E-Systems In Support Of ESCA-INPE Satellite Traffic Simulator Contract with CCI, Presented at the Customer Design Review at AGI, 15 August 1994.

[2] *"STS Program Requirements and Development Plan"* prepared by CCI In Support Of ESCA-INPE Satellite Traffic Simulator Contract with CCI. This document is included in Appendix A for functional and performance requirement reference, and to show very slight "as built" changes.

[3] *"STS Statement Of Work"* prepared by ESCA for INPE This document was updated by CCI to provide consistency with the STK baseline which STS is built upon.

[4] *"Satellite Tool Kit Tutorial"* prepared by AGI as part of their commercial customer support documentation. This was delivered along with the original STK installation in Brazil.

[5] *"Satellite Traffic Simulator Users Guide"* prepared by AGI as part of their delivery and installation of STK in Brazil.

[6] *"Software Test Procedure for the STS"* prepared by E-Systems In Support Of ESCA-INPE Satellite Traffic Simulator Contract with CCI; Used by E-Systems to execute STS Tests September 14-15, 1994 at Analytical Graphics, Inc., in King Of Prussia, PA.

CO-DEVELOPERS:

Frank Linsalata
Analytical Graphics Inc. P. O. Box 61206
King of Prussia, PA. 19406
Tel: 215-337-3055
Fax: 215-337-3058

Ron Lepkowski
Constellation Communications Inc.
Suite 200, 10530 Rose Haven Street,
Fairfax Virginia, 22030
Tel: 703-352-0300
Fax: 703-352-9297

TABLE 3. DAILY TRAFFIC DISTRIBUTION TABLE FORMAT

HOUR	VOICE	PAGES	DATA/FAX
00-01			
01-02			
02-03			
03-04			
04-05			
05-06			
06-07			
07-08			
08-09			
09-10			
10-11			
11-12			
12-13			
13-14			
14-15			
15-16			
16-17			
17-18			
18-19			
19-20			
20-21			
21-22			
23-24			

Satellite-Enhanced Personal Communications Experiments

Deborah S. Pinck & Loretta H. Tong
Jet Propulsion Laboratory,
California Institute of Technology, M/S 161-241,
4800 Oak Grove Drive, Pasadena, CA 91109
Phone: +1-818-354-8041, Fax: +1-818-393-4643,
e-mail: pinck@zorba.jpl.nasa.gov

Anthony J. McAuley & Michael Kramer
Bellcore (MRE 2N263)
445 South Street, Morristown, NJ 07960-4698
Phone: +1-201-829-4698, Fax: +1-201-829-2504,
e-mail: mcauley@bellcore.com

Abstract

As an initial step in exploring the opportunities afforded by the merging of satellite and terrestrial networks, Bellcore and JPL conducted several experiments utilizing Bellcore's experimental Personal Communications System, NASA's Advanced Communications Technology Satellite (ACTS) and JPL's ACTS Mobile Terminal. These experiments provided valuable information on the applications, interfaces, and protocols needed for seamless integration of satellite and terrestrial networks.

1 Introduction

Users of future generation wireless information services will have diverse needs for voice, data, and potentially even video communications in a wide variety of circumstances. For users in dense, inner-city areas, low power PCS should be ideal. Vehicular-based users traveling at high speeds will need high power cellular networks. Packet data networks provide an excellent solution for users requiring occasional small messages, while circuit switched networks provide more economical solutions for larger messages. For users in remote or inaccessible locations, or for applications that are broadcast over a wide geographic area, a satellite network would be the best choice. To provide ubiquitous personal communications service, it is necessary to integrate all these networks into one seamless internetwork, using the strength of each network.

As an initial step in exploring the opportunities afforded by merging various networks, Bellcore and JPL conducted a series of experiments [1] to demonstrate the joint use of satellites and terrestrial networks in the delivery of personal communications services.

This paper describes results from several field trials conducted during August 1994 and January 1995 in Los Angeles, CA and Morristown, NJ. During these trials, applications communicated over various combinations of networks including satellite, wireless packet data, the wired Internet, and the wired Public Switched Telecommunications Network (**PSTN**). Section 2 describes the experiments, Section 3 presents the results, and Section 4 provides an analysis of the data collected.

2 Experiment Description

This section describes the satellite-enhanced personal communications experiments. The goals of the experiments are listed first, followed by a description of the experiment configuration. Next, the satellite and terrestrial protocols are explained, and lastly, each of the applications is described.

2•1 Experiment Goals

The experiment goals fell into three categories: a) demonstrate the delivery of personal communications applications via satellite, b) demonstrate interoperability of satellite and terrestrial networks, and c) evaluate protocol mechanisms and parameters that make efficient use of wireless links. This work is important because:

- Applications currently planned for terrestrial PCS need to be demonstrated on the satellite network to determine their behavior, and consequently their commercial viability, in a satellite-enhanced personal communications network.
- Various terrestrial wireless networks, including packet data and cellular networks, need to be integrated with the satellite network to evaluate overall end-to-end system performance.
- The protocol mechanisms (e.g., selective vs. cumulative acknowledgments) and parameters (e.g., packet size) developed for terrestrial PCS need to be tested and optimized for use over satellite and integrated terrestrial/satellite networks.

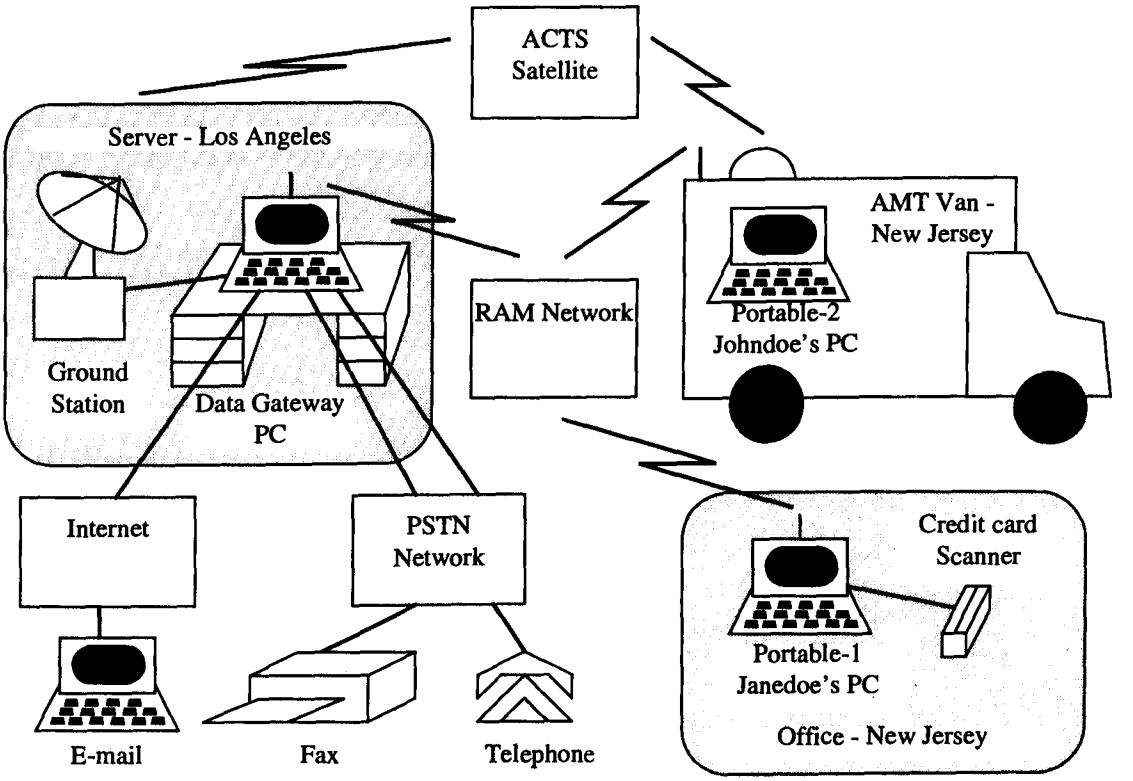

Figure 1 Satellite-enhanced PCS Experimental Setup

2•2 *Experiment Configuration*

These experiments utilized Bellcore's Experimental Personal Communications System (**BEPCS**), NASA's Advanced Communications Technology Satellite (**ACTS**), and JPL's ACTS Mobile Terminal (**AMT**). Figure 1 shows the experimental configuration involved in this series of experiments.

BEPCS consists of a Data Gateway PC located at the satellite ground station, the portable PCs (one belonging to the hypothetical Johndoe and the other belonging to the hypothetical Janedoe), the credit card scanner, the prototype application software (see 2•4), and an experimental transport protocol TPE (see 2•3). All the BEPCS hardware uses standard commercial components with custom applications and protocols. The Data Gateway has multiple serial ports allowing it to route all five connections simultaneously: ACTS Satellite link, RAM wireless packet data network, Internet, PSTN to any fax, and PSTN to any telephone. The portable PCs, however, have only a single serial port, so during internetworking experiments the RAM modem was directly connected to the satellite equipment, bypassing Johndoe's PC.

ACTS is an experimental K/Ka-band satellite developed by Martin Marietta Astro Space under contract to NASA. The satellite, launched into geostationary orbit at 100 degrees west longitude in September 1993, operates in a virtually untapped frequency spectrum in the K- (20 GHz) and Ka-bands (30 GHz).

The AMT [2] is a proof-of-concept K/Ka-band mobile communications terminal intended to demonstrate the system techniques and high risk technologies needed to accelerate the commercial use of land-mobile systems at K/Ka-band. One such technique is the ability to integrate the mobile terminal for satellite communications with terrestrial personal communications equipment. To support this integration, the AMT Terminal Controller provides a digital interface between the portable PCs and the AMT. The data signal is then up/downconverted to the satellite frequencies for transmission over the K/Ka-band channel. The baseline AMT can support up to 128 kbps full-duplex communications; for this experiment, a 9.6 kbps link is used. A sophisticated Data Acquisition System (DAS) has been developed to provide real-time monitoring and data collection for the AMT system. For land-mobile experiments, the AMT is mounted in a customized Ford Econoline 350 van. The fixed station, located at JPL,

utilizes a 2.4m antenna and a 10W high power amplifier (HPA).

Figure 1 shows the communication channels. The primary channel used for evaluation and measurements was that between Johndoe's PC and the Data Gateway via the satellite channel. The most demanding configuration was the connection from Janedoe's PC located in New Jersey, via the RAM network, via the AMT van (effectively acting as a mobile base station), over the satellite, through the Data Gateway located in Los Angeles, and back over the Internet to a user back in New Jersey.

2•3 Protocol Description

An important question related to satellite-terrestrial interoperability is whether the data communications protocols can operate efficiently across multiple channels. Most protocols in use today (e.g., TCP/IP) have been optimized for wireline channels; their use over wireless networks presents significant new challenges. The radio and free space channels characteristic of these networks introduce noise, multipath interference, shadowing, and weather effects that can cause higher bit error rates and longer periods of increased bit errors than their wireline counterparts. Host motion creates time-varying communication paths that can cause packet delay, misordering, duplication and loss. In addition, the satellite-link channel can add significantly to the round-trip packet delay, especially when geostationary satellites are used. As currently envisaged, both terrestrial and satellite systems will operate in bandwidth limited channels where efficient use of the spectrum takes on great importance.

These experiments used two independent protocols: the AMT communications protocol for the satellite link, and TPE located in the end systems.

2•3•1 AMT Communications Protocol Description

The AMT provided the satellite communications between terrestrial devices including the Data Gateway, the portable PCs, and the RAM modem. These devices interfaced with the AMT system by sending packets through a standard asynchronous RS232 serial port. However, the AMT system is based on synchronous data transmissions, with specially designated signals to control data flow.To minimize development time and costs, the discrepancies in data flow between the devices and the AMT system were handled by modifying the existing open-ended, unacknowledged, full-duplex AMT communications protocol (similar to that used for a voice link).

This modified AMT protocol maintained a link at all times (circuit connection); any data received was immediately transmitted over the satellite link with minimal buffering. In order to maintain the communications link during periods when there was no data from the device, the protocol transmitted uniquely identifiable "fill" bytes. On the receiving end, the protocol removed the fill bytes, passing only data bytes to the receiving device.

A satellite fill pattern was chosen that could not occur in the Serial Line Internet Protocol (SLIP) [3]. As SLIP uses an escape byte of 0xDB (i.e., 11011011), with escape-end being 0xDBDC and escape-escape being 0xDBDD, we chose the uniquely identifiable fill pattern of 0xDBDE.

2•3•2 Wireless Protocol (TPE) Description

For error control an experimental transport protocol, called **TPE**, was used that was optimized for wireless networks. The main objective was to understand the types of mechanisms and parameters desirable on wireless networks (we did not address where the error control should be located). This section gives an overview of TPE, more details can be found in [4].

TPE uses the following message framing mechanism:

- Framing into **chunks** that fit inside a network packet.
- Transport Protocol Data Units (**PDUs**) made up of an integer number of chunks.
- Signaling to reduce the chunk header size.

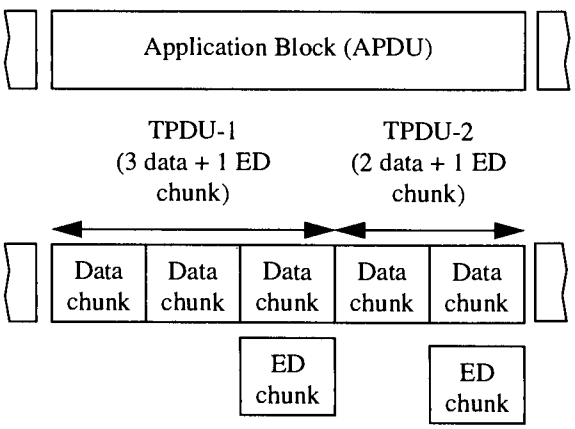

Figure 2 Segmentation of an application block into data and error detection (ED) chunks

Figure 2 shows an example of how TPE segments an application PDU (**APDU**) into 5 data chunks. In addition, TPE adds 2 error detection (**ED**) chunks, because the application block was split into 2 Transport PDUs (**TPDU**s). TPE moves chunks directly to and from main memory - application data is never copied at the level of APDU or TPDU. In the field trials, TPE added 8 bytes/ packet for chunk header, put exactly one chunk into every packet.

The TPE's error control mechanisms operate on the TPDUs. The main mechanisms are:

- Error detection using a powerful 32-bit code.
- **ARQ** (Automatic Repeat reQuest) with selective acknowledgment and retransmission.
- Combining data from multiple transmissions.

TPE sends a 4 byte error detection parity per TPDU, encoded using the Weighted Sum Code. The Weighted Sum Code has similar error detection properties to the CRC, but can be calculated faster.

TPE corrects errors by retransmission. TPE uses a computationally demanding form of ARQ: using selective-acknowledgments (receiver sends a list of correctly received TPDUs) and selective retransmission (transmitter only resends those TPDUs that are unacknowledged).

TPE combines chunks from multiple partially received TPDUs to make up a complete TPDU. Thus, when a TPDU is retransmitted, the receiver only processes the missing chunks (eliminating duplicate chunks).

TPE uses timer based connection management that allows connections to be set-up without a three way handshake. Reliable sessions are established on top of these unreliable connections.

2•4 Applications

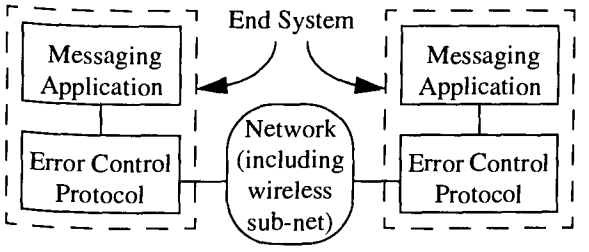

Figure 3 Logical Network Architecture

For these trials, four messaging applications designed to suit mobile users were developed. Figure 3 shows the relationship among the applications, the wireless networks, and the error control protocol. All the application and protocol software executes on PCs running UNIX[1]. The server applications ran on the Data Gateway, and the client applications on the two portable PCs. The applications on the portable PC's had an X-windows[2]/Motif interface. The four messaging applications were: a) E-mail, b) Fax, c) Call Command and d) Credit Card Verification.

1 Unix is a registered trademark of Novell. Inc.
2 X-Windows is a trademark of MIT.

The E-mail application allows mobile users to exchange text messages with any machine on the Internet. The Fax application sends and receives standard Group III faxes between a mobile user and any standard fax machine connected to the PSTN. Both the E-mail and Fax application servers reduce bandwidth on the wireless link by sending only a small mail/fax header automatically to the mobile user. The user is informed of the incoming message and can decide whether to request delivery of the (potentially large) body of the message.

Call Command [5] is a personal telephone management application that enables users to redirect telephone calls in real time. If someone calls Janedoe, the Call Command server (the Electronic Receptionist) tells the caller to wait while Janedoe is contacted. The Call Command server sends information about the incoming call to Janedoe's portable PC. Upon receiving the notification, Janedoe can route the call directly, either to any local phone, to voice mail, or to another person.

The Credit Card Verification application was designed for field service and sales people submitting charges for equipment or services anywhere within the radio coverage area. The user scans a credit card, causing a window to pop-up (on the portable PC) with the information on the card. When the user enters the amount of the transaction, it sends a message to the credit card server. A database at the server (the Data Gateway for this case) stores valid credit card numbers and available credit line. After checking the database, the server sends a message back either authorizing or rejecting the transaction.

2•5 Experiment Procedure

During the Los Angeles and Morristown field trials, experiments were conducted under varying channel conditions in order to characterize hybrid satellite-terrestrial personal communications. Both stationary and mobile tests were conducted at various signal strength levels.

For the stationary tests, the bit signal-to-noise ratio (E_b/N_0) was varied from as low as ~5dB to as high as ~14dB. The E_b/N_0 was measured by filtering the received signal with a known noise equivalent bandwidth (BW) filter and feeding that output into a power meter. Using an initial noise power only reading plus the filter BW, and bit rate, the DAS was capable of calculating the E_b/N_0.

For the mobile tests, the E_b/N_0 was set at a high level (~13dB) to allow characterization of shadowing and fading events. Tests were run in both clear weather (LA in August) and inclement weather (New Jersey in January). In addition, runs were taken on roads with clear line-of-sight (LOS) to the satellite as well as roads with foliage and/or buildings that disrupted the clear LOS to the satellite.

Each of the four messaging applications was tested under the various field conditions. These applications were used to determine the behavior of wireless messaging applications in a mobile satellite environment. In order to characterize the protocol, a simple file transfer application was used which sent a 100 kilobyte file from the portable PC to the Data Gateway and vice versa. By sending the same file, we were able to gauge the relative signal strength at the various locations. TPE was instrumented to collect statistics at the transmitter and receiver as they affected packets and TPDUs.

Normally terrestrial radio errors are presented in terms of bit error rates; however, we were interested in the error control mechanisms that work at the packet and TPDU level. These error control mechanisms are complementary to mechanisms that reduce the bit error rate. Although the results presented here are not exhaustive, they lead to some interesting initial findings about a) the characteristics of radio networks as seen from the level of packet and TPDU, and b) the performance of different ARQ mechanisms in reducing packet and TPDU retransmissions.

3 Experiment Results

This section summarizes the results from the field trials. All the quantitative results presented below were obtained by sending the same 100 kilobyte file (see Section 2•5).

3•1 Characterizing the radio networks

The error distribution for the mobile runs differed substantially from the error distribution for the stationary runs. Figure 4 shows that for the mobile tests, corrupted TPDUs often needed several retransmissions, while Figure 5 shows that for the stationary tests, most corrupted TPDUs only required a single retransmission.

To investigate the error distribution further, the distribution of packet errors within a TPDU was graphed. Figure 6 and Figure 7 show results from experiments where each TPDU was composed of 5 small (24 or 32 byte) packets and statistics were collected on how many of these 5 packets were destroyed within corrupted TPDUs. Figure 6 shows that for the mobile test, most corrupted TPDUs had all 5 packets destroyed. For the stationary test, Figure 7 shows that most TPDUs lost only a one or two packets. In stationary tests with larger (128 and 256 byte) packets (not shown), most TPDUs lost only a single packet.

3•2 Error Detection

The satellite-enhanced PCS trials did not utilize link error control; therefore there were many packets with bit errors. However, all errors were detected by the powerful 32-bit TPDU error detection parities.

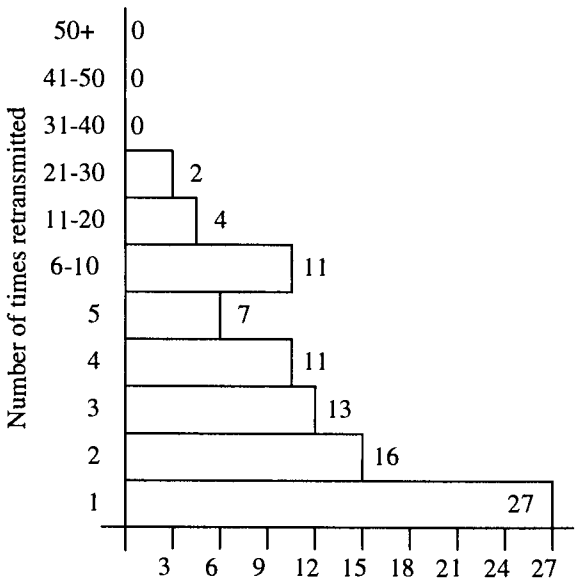

Figure 4 TPDU retransmissions for mobile tests with the satellite (~15,000 192 byte TPDUs sent)

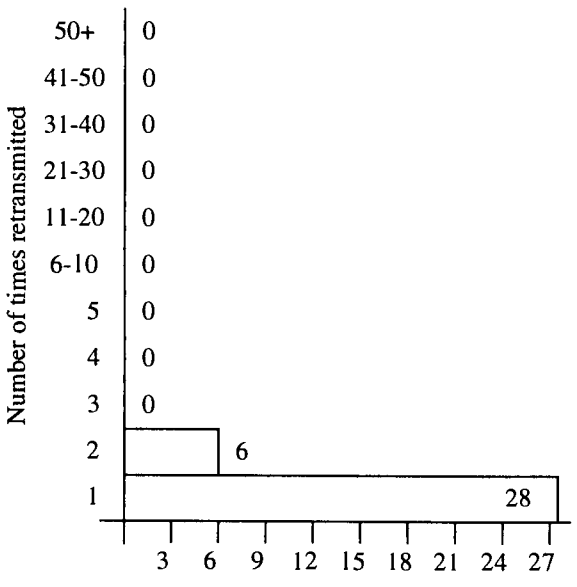

Figure 5 TPDU retransmissions for stationary tests with the satellite (~15,000 192-byte TPDUs sent)

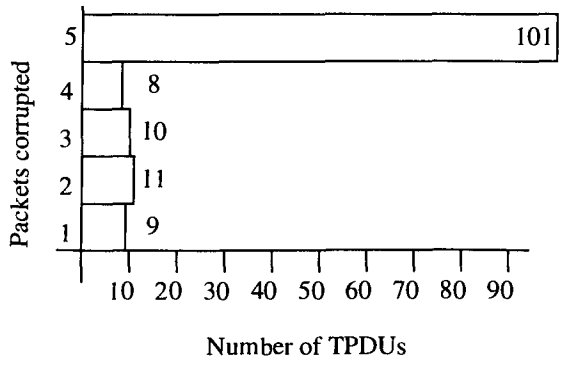

Figure 6 Distribution of packet errors within a 5-packet TPDU for Mobile Test (with ~8000 TPDUs using 24-bytes/packet)

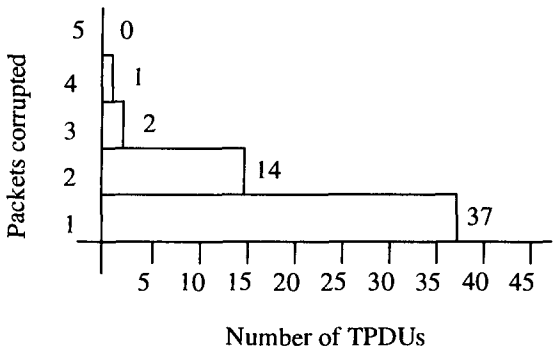

Figure 7 Distribution of packet errors within a 5-packet TPDU. Stationary Test (with ~8000 TPDUs sent using 32 byte/packet)

3•3 Packet Size

For the satellite tests, the results on ARQ mechanisms and TPDU sizes were similar to that for terrestrial experiments conducted previously [4]. For the satellite tests we also measured the transmit time for a 100 kilobyte file with various packet sizes.

Under good conditions (with high bit signal-to-noise ratios), the use of larger packets reduced the time needed to send the 100 kilobyte file as it lessened per-packet processing overhead. For example, it took approximately half the time to send the file using 256 bytes per packet as it did using 32 bytes per packet. Under poor conditions (with lower bit signal-to-noise ratios), however, the larger packet size often took much longer than using smaller packets, and in extreme cases would result in no useful throughput.

4 Analysis

4•1 AMT system

The modified AMT protocol has several shortcomings:

- An operator is required to establish and terminate the satellite portion of the communications link.
- The satellite communications link is always maintained (circuit connection) even when no application data is being transmitted
- Frequent bit errors over the satellite link increase demands upon the end-to-end protocol.
- Corruption of the "fill" bytes into a start of frame marker caused frequent corruption of the first packet within a burst.

Although these shortcoming were acceptable for this experiment, it is evident that a more efficient protocol would be beneficial.

As a result of our experiments, a new AMT communications protocol is being proposed that eliminates the above shortcomings. The key change is that when no data is present, the new protocol leaves the satellite link idle. By maintaining an appropriately sized data buffer, the protocol has time to resynchronize the connection. Although the added buffering delay is unacceptable for real time voice or video applications, it is acceptable for most messaging applications, such as those used in our experiments, that can tolerate some delay.

4•2 Error Conditions

As our results confirmed, the radio propagation environment is well modeled by a time-share between Rician and Rayleigh fading. It is critical, therefore, that wireless error control schemes work efficiently under both types of fading conditions. Mechanisms and parameters that work well under only one scenario will not provide robust service and will limit the range of useful operations.

4•3 Error Control Mechanisms and Parameters

The results confirmed earlier observations on the power of error control mechanisms such as selective acknowledgment and chunk combining [4]. The results also demonstrate that dynamic algorithms are required to change the error control parameters. For example, as the bit signal-to-noise ratio decreases so should the packet size.

Results obtained here also provide new insights into the possible use of packet Forward Error Correction (FEC) in a wireless environment. Although no experiments were performed with FEC, the results represented in Figure 6 and Figure 7 show that a packet FEC scheme, such as that described in [6], would have worked well for stationary tests, but would have been ineffective where errors were

dominated by long periods of fading. The number of packets of overcode should vary depending on the packet size. For example, two overcode packets per TPDU would be necessary to ensure the most TPDUs with small packets got through; while, with larger packets, a single overcode packet would have been sufficient.

4•4 Applications

The four messaging applications consistently performed well in stationary tests. More surprising, however, was that the applications maintained reasonable performance in mobile tests, even when voice connections were unintelligible (messaging applications are tolerant of wide delay variation).

5 Conclusion

This paper describes results from satellite-enhanced personal communications field trials using the ACTS satellite with various wireless and wireline terrestrial networks. The interconnectivity among multiple wireless communications services shows how a mobile user can have personal services available even while outside the coverage area of a single communications provider.

The results of packet and higher layer block loss show that, even within a single wireless network, conditions vary dramatically depending on whether Rayleigh fading or Rician fading dominate the errors.

In order to deal with the varying radio conditions, we believe an efficient general wireless error control protocol requires powerful error control mechanisms and sophisticated dynamic control algorithms. With the correct block and packet sizes, a selective ARQ protocol can provide efficient error control under virtually any radio condition. Also, with the correct packet overcode parameter, an FEC scheme could provide efficient low latency error correction under some radio conditions.

Acknowledgments

The research described in this paper was carried out at the Jet Propulsion Laboratory, California Institute of Technology, and was sponsored by Bellcore and the National Aeronautics and Space Administration.

References

[1] R. Wolff & D. Pinck, "Internetworking Satellite and Local Exchange Networks for Personal Communications Applications," International Mobile Satellite Conference, Pasadena, CA, June 1993.

[2] K. Dessouky & T. Jedrey, "The ACTS Mobile Terminal," SATCOM Quarterly, JPL, Pasadena, CA, No. 8, January 1993.

[3] J. Romkey, "A Nonstandard for Transmission of IP Datagrams over Serial Lines: SLIP," Internet RFC 1055, June 1988.

[4] A. J. McAuley, "Error Control for Messaging Applications in a Wireless Environment," INFOCOM 95, Boston, MA, April 2-6, 1995.

[5] M. Kramer, G. Ramirez, D. Turock, R. S. Wolff, "Use of Two-Way Wireless Messaging for Personal Telephone Management," 2'nd Universal Personal Communications Conference, Ottawa, Canada, 1993.

[6] A. J. McAuley, "Reliable Broadband Communication Using a Burst Erasure Correcting Code," Proceedings of ACM SIGCOMM, pp. 287-306, September 1990.

Using ATM Over SATCOM Links

Gary M. Comparetto
Principal Engineer
The MITRE Corporation
1259 Lake Plaza Dr
Colorado Springs, CO 80906

ABSTRACT

The Asynchronous Transfer Mode (ATM) protocol is studied from the standpoint of determining what limitations, if any, exist in using it over satellite links. It is concluded that, while there is nothing intrinsic about ATM that would generally preclude its use over satellite links, there are, however, several intrinsic characteristics of satellite links, as well as some satellite system configuration-specific issues, that must be taken into account.

INTRODUCTION

ATM represents an emerging technology that is becoming pervasive in almost every aspect of local and wide area networks. The purpose of this paper is to investigate the use of ATM techniques over satellite links. The need to integrate satellite links into ATM-based networks may be required for a variety of reasons including long-haul extension of ATM-based local area networks (LANs), delivery of ATM-based traffic into geographically remote areas having little or no existing telecommunications infrastructure, and utilization of legacy satellite systems to augment/extend ATM-based networks and services.

A brief overview of ATM is first presented that addresses the key characteristics of ATM and touches upon current market trends as well as the degree of maturity of ATM-related standards. A more detailed analysis of ATM over SATCOM links follows that is divided into two primary areas: general or non-configuration-specific and configuration-specific.

DISCUSSION

Overview ATM is a telecommunications protocol that supports the transfer of information using fixed size, 53 byte cells. ATM is connection oriented meaning that the end-to-end path is set up prior to data transmission. Finally, ATM utilizes the concept of statistical multiplexing which is a method that allows a larger transmission bandwidth to be allocated than is actually available based upon the assumption that not every user will have a requirement to simultaneously use their allocated bandwidth.

ATM Interface ATM interfaces with higher level protocols via one of four ATM adaptation layers [1]. AAL 1 supports constant bit rate (CBR) voice, video, and data services, via connection-oriented services, and is currently available as a standard. AAL 2 is not currently available; however, it will support compressed video, variable bit rate (VBR) traffic, and connection-oriented services. AAL 3/4 and AAL 5 support variable bit rate, data-only traffic and both are currently available as standards.

PVCs and SVCs The physical medium on which ATM resides is described in terms of permanent virtual circuits (PVCs) and switched virtual circuits (SVCs). PVCs requires a pre-established virtual channel connection between source and destination nodes, creating a network of fixed grids or connectivities, and require a dedicated, pre-

established committed information rate (CIR) and quality of service (QOS). PVCs are best applied to support communications among a fixed group of users where traffic levels are reasonably predictable.

SVCs allow user-initiated connectivity, between any source and destination pair, without pre-established virtual channel connections. SVCs use switched access lines which are set up at the initiation of each session and released upon completion and allow the CIR and QOS to be negotiated at the start of each session. SVCs are necessary to support true real-time bandwidth-on-demand applications.

Standards The development of ATM standards has been an ongoing activity over the last several years. A variety of ATM services are currently offered; some of these services adhere to national and/or international standards while others are based upon proprietary solutions. While significant progress had been made in the ATM standards arena, several key deficiencies exist.

First, there is a need for a private network/network interface (PNNI) standard. This standard will govern ATM switch/switch compatibility amongst multiple vendors and is essential to ensure network/network interoperability [2]. Second, there is no standardized international ATM tariff structure. Third, there is a need for "usage-based" cell monitoring by ATM switches to support real-time bandwidth-on-demand applications. Fourth, there is no network management standard which is needed to support network configurations, fault isolation, user reconfigurations, etc. Fifth, there is no congestion/flow control standard. And, sixth, there are no signaling standards which are needed to support the introduction of SVCs.

Current Market Trends Only PVCs are currently being offered by most service providers since the standards needed to ensure interoperability amongst integrated suites of vendor-unique equipment have not yet been developed. Most ATM equipment supports data-only traffic versus a mix of data, video, and voice. ATM ports are typically ≥ T1. If the incoming traffic stream is comprised of lower data rate users, some type of multiplexing or traffic concentration would be necessary in order to efficiently utilize the available ports. Fourth, the number of ports per ATM switch is typically ≤ ~32. In summary, the market condition indicates a trend in available ATM equipment and services toward high data rate users needing fixed long-haul connectivities to support a relatively small number of users.

General Areas The general areas to consider when transmitting ATM traffic over satellite links include bit error rate (BER), capacity, and delay.

ATM was developed assuming SONET-based fiber would be the transport medium. Fiber generally supports data transfer at achievable BERs on the order of 1E-9 to 1E-11. The supportable transmission capacity or bandwidth is on the order of several GHz and the end-to-end delay is typically less than a few 10s of milliseconds. On the other hand, achievable satellite BERs for current satellite systems are normally in the 1E-5 to 1E-7 range. The supportable capacity is generally on the order of 10s of MHz and the one-way source-to-destination delay can be as high as ~.25 seconds for a geostationary satellite system. The result of the above is that modifications must be made to either the satellite system or the ground system in order to ensure an efficient coupling and integration of the two transport mechanisms.

BER Two approaches are available to address the fact that satellite links generally have poorer BERs than fiber links: improve

the achievable satellite link BER to the 1E-9 to 1E-10 level and/or utilize a cell re-transmission protocol that efficiently accommodates cell errors.

Improve BER The achievable satellite link BER can be improved via the introduction of forward error correction (FEC) techniques utilizing concatenated coding schemes. In concatenated coding schemes, the data is initially encoded using a convolutional encoding scheme. The data is then re-encoded using a Reed-Solomon (RS) encoding scheme. The net effect is a very low achievable BER at reasonable received signal-to-noise ratios (SNRs). The drawback to using FEC coding includes an increase in both the channel bandwidth requirement and modem complexity.

Another way to improve the achievable BER is to increase the transmit EIRP and/or the receive terminal G/T. The drawback to this is an increase in the required size and complexity of the transmit and/or receive terminals.

Improve Protocol The re-transmission of errored cells would be accomplished by higher level protocols in an ATM network and is normally based upon one of several automatic repeat request (ARQ) techniques. A widely used protocol that supports data re-transmissions is transport control protocol/internet protocol (TCP/IP). TCP/IP uses a go-back-N ARQ technique. Go-back-N was developed for use in ground-based networks and utilizes a sliding-window approach toward data delivery. This protocol has been shown to be quite inefficient in applications having large delays and/or relatively poor BERs which is the case with satellite links [3]. Figure 1 shows the achievable link utilization of a satellite link using TCP/IP as a function of the achievable BER [4].

One alternative to TCP/IP is to use a protocol based upon a selective repeat ARQ scheme in which only the errored packet or cell is re-transmitted. One example is the Service Specific Connection Oriented Protocol (SSCOP) [3]. The drawback in using selective repeat ARQ schemes is the fact that the destination node must now have the capability to re-sequence the packets or cells that it receives.

Capacity Satellite link capacity can be addressed by limiting the in-bound or out-bound traffic to/from the ATM switch.

Limit In-Bound Traffic The simplest solution is to throttle down the in-bound traffic arriving at the ATM switch by limiting it to CBR traffic at rates less than or equal to the link capacity. This solution; however, defeats the intent of ATM to be able to support VBR traffic which more efficiently utilizes limited bandwidth and is required to support bandwidth-on-demand applications.

Limit Out-Bound Traffic The second solution involves throttling down the out-bound data leaving the ATM switch. One way of accomplishing this is via the use of a traffic priority protocol in which higher priority data is sent first, followed by lower priority data that was buffered until bandwidth became available. This second option requires the use of a higher level protocol and may result in data loss depending upon the traffic statistics.

Delay There really is no way to directly address the problem of larger satellite link delays relative to fiber unless we increase the speed of light! This problem is less impacting for low earth orbit (LEO) satellite systems; however, most current systems in existence today are geostationary (GEO) systems with an ~.25 second one-way source-to-destination delay. In effect, the larger delay degrades the achievable throughput by exacerbating the problem of

cell re-transmissions. Consequently, the same techniques identified above to address the BER mismatch between satellite systems and fiber systems would be applicable to address the delay mismatch as well.

Configuration-Specific Areas Several ground segment and space segment configurations are investigated below including point-to-point, point-to-multi point, and multiple point-to-point links for the ground segment (shown in Figure 2), and GEO and LEO satellite constellations for the space segment.

Point-to-Point The point-to-point configuration includes two large, fixed, high capacity terminals that maintain connectivity over long periods of time. Each ground terminal can support the transmission of single or aggregated user traffic. In studying the point-to-point configuration, it was determined that there were no additional concerns in using ATM over such a configuration other than the general considerations discussed in the previous section.

Point-to-Multi Point In the point-to-multi point configuration, data transmission is one-way from a single transmitter to multiple receivers. The data is received simultaneously by each receiver that is within the satellite footprint. The source or destination ground terminals can accommodate single user traffic or aggregated multi-user traffic. Point-to-multi point or broadcast communications is a key feature of satellite systems.

ATM is basically a point-to-point connectivity protocol. This requires that a satellite system supporting multiple ATM users be designed to support a series of point-to-point links which defeats the broadcast nature of SATCOM. ATM does support a concept referred to as multi-cast in which a cell entering an ATM switch is replicated and sent to multiple destinations; however, without the existence of an ATM switch on-board the satellite, this capability could not be utilized. The result is that ATM is precluded from being used for typical SATCOM broadcast applications.

Multiple Point-to-Point The multiple point-to-point link configuration can be viewed as an attempt to mimic ground-based communications or local area networks over long distances. There are a variety of sources and destinations, each with direct satellite access and the ability to communicate with one another. The transmitted traffic may represent aggregate streams from multiple users or may only represent local traffic from the source/destination node. The users may each reside in different satellite beam coverage areas or multiple nodes may reside within the same beam. The satellite transmissions are not broadcast in the sense discussed on the previous slide. That is, while multiple nodes may reside in the same beam, they do not receive the downlink transmission simultaneously.

For the multiple point-to-point configuration, connectivity becomes a challenge. Figure 3 depicts two connectivity schemes that are in common use today including full-mesh connectivity and hub-spoke connectivity.

In a full mesh connectivity scheme, each of N terminals can communicate with one another. In figure 3, the lines going from ground terminal to ground terminal, through the satellite, represent the logical communication channels. The available single user bandwidth, assuming equal apportionment of the available bandwidth to the users, will vary as ~ $1/N^2$ squared. Within the context of supporting ATM traffic, the impact is that this will drive a requirement for low rate ATM output ports for the ATM switches. Secondly, the number of required satellite accesses varies as ~ N^2. The number of

satellite accesses will drive the number of ports required for each switch. As N increases, a full mesh connectivity network will require ATM switches with many ports, with each port supporting relatively low transmission rates. Both of these requirements are against current trends in ATM switch production which was shown earlier to be favoring a small number (i.e., ≤ 32) of high rate users.

In the hub spoke connectivity scheme, all of the transmissions go through a hub terminal. Hub spoke connectivity results in fewer required satellite accesses. In fact, the number of satellite accesses varies as N versus N^2 as in the full mesh connectivity option. Also, the available single user bandwidth varies as 1/N. Both of these characteristics are positive within the context of current ATM product capability trends. However, the primary drawback of the hub spoke connectivity scheme is that a double hop is required for each source-to-destination transmission (i.e., source to hub and hub to destination). The result is an increased delay with larger buffers at the transmitting terminal.

The section above addressed configuration-specific issues from a ground segment standpoint . The next section addresses the satellite segment.

GEO Satellite Systems A GEO satellite has an altitude of ~19,322 nmi and is positioned on the equator (nominally). The satellite appears to be fixed relative to the user resulting in static communication links. This is a common space configuration for most current satellite communications systems. It was stated earlier that ATM is a connection-oriented protocol. Consequently, static links are "ATM-friendly", so to speak. As a result, the transmission of ATM traffic can be readily supported over a GEO satellite system as long as the general satellite-related considerations discussed earlier are addressed (i.e., BER, capacity, and delay).

LEO Satellite Systems LEO satellite systems require continual user/satellite reconfiguration since the satellites are constantly moving into and out of the user's field of view. The use of LEO satellites appears to be the current evolution path for some systems including Orbcomm, IRIDIUM, Globalstar, Odyssey, and Teledesic to name a few The satellite visit times for LEO systems are on the order ~10 minutes. Consequently, during a single ATM session, a LEO satellite system may require several reconfigurations. This is not "ATM-friendly" since ATM is connection-oriented. That is, ATM requires the re-establishment of the end-to-end path for each re-configuration which will impact the choice and operation of higher level protocols.

One way around this problem is to "fool" the end-to-end path into believing that a re-configuration never occurred. Two possible options are shown in figure 4 and are referred to as "make-before-break" and "buffer during change over".

In the "Make-Before-Break" approach, connectivity is achieved with the next satellite arriving over the horizon prior to breaking contact with the current satellite. This requires the use of additional ground terminal equipment, accurate synchronization during terminal change over, and may require a small amount of buffer capability during the change over period.

In the "Buffer During Change Over" approach, a buffer is used to store the ATM traffic while connectivity is broken with the current satellite and re-established with the next satellite arriving over the horizon. This can require the use of a large buffer, depending upon the transmission rate, and may result in cell loss in the event that the buffer size is exceeded or the satellite link

capacity is not large enough to make up for the interruption in service. Additionally, no traffic can be transmitted during the change over process which may also add unacceptable end-to-end delays.

Whatever solution is chosen, the requirement to continually re-configure the space/ground link in LEO satellite-based configurations will introduce key challenges that must be addressed in order to support the transmission of ATM traffic.

SUMMARY

The overall finding is that there is nothing intrinsic about ATM that would generally preclude its use over satellite links. However, having said this, it must be noted that satellite systems do have intrinsic characteristics that must be taken into account if ATM is going to be used successfully. These include the generally poorer BER, capacity, and delay characteristics of satellite links relative to fiber.

Also, it is clear from this analysis that each SATCOM application must be studied individually in order to determine any specific limitations and/or modifications that are required in using ATM over a SATCOM link.

The future market direction is still unclear; however, one thing is certain: ATM technology is pervasive in the telecommunications industry, appears to be here to stay, and, as a result, must be considered in the development of future communications architectures.

REFERENCES

[1] *B-ISDN ATM Adaptation Layer (AAL) Specification*, ITU-T Recommendation I.363, Mar 1993.

[2] **G. Swallow**, *PNNI: Weaving a Multivendor ATM Network*, Data Communications, pp. 102-110, Dec 1994.

[3] **P. Chitre**, *Demonstration of ATM via Commercial Satellite*, COMSAT Report, 25 Oct 1993.

[4] **S. Smith, J. Marshall**, *System Trade-offs and Design for Integrated ATM/SATCOM Networks (Draft)*, MITRE WN 94W175, Sept 1994.

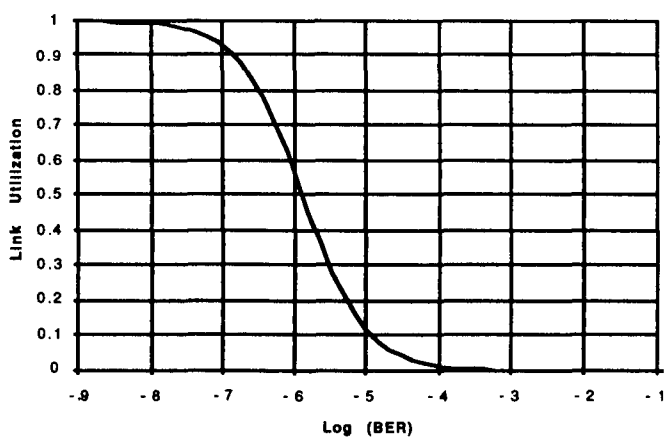

Figure 1: Link Utilization as a Function of BER Using TCP/IP

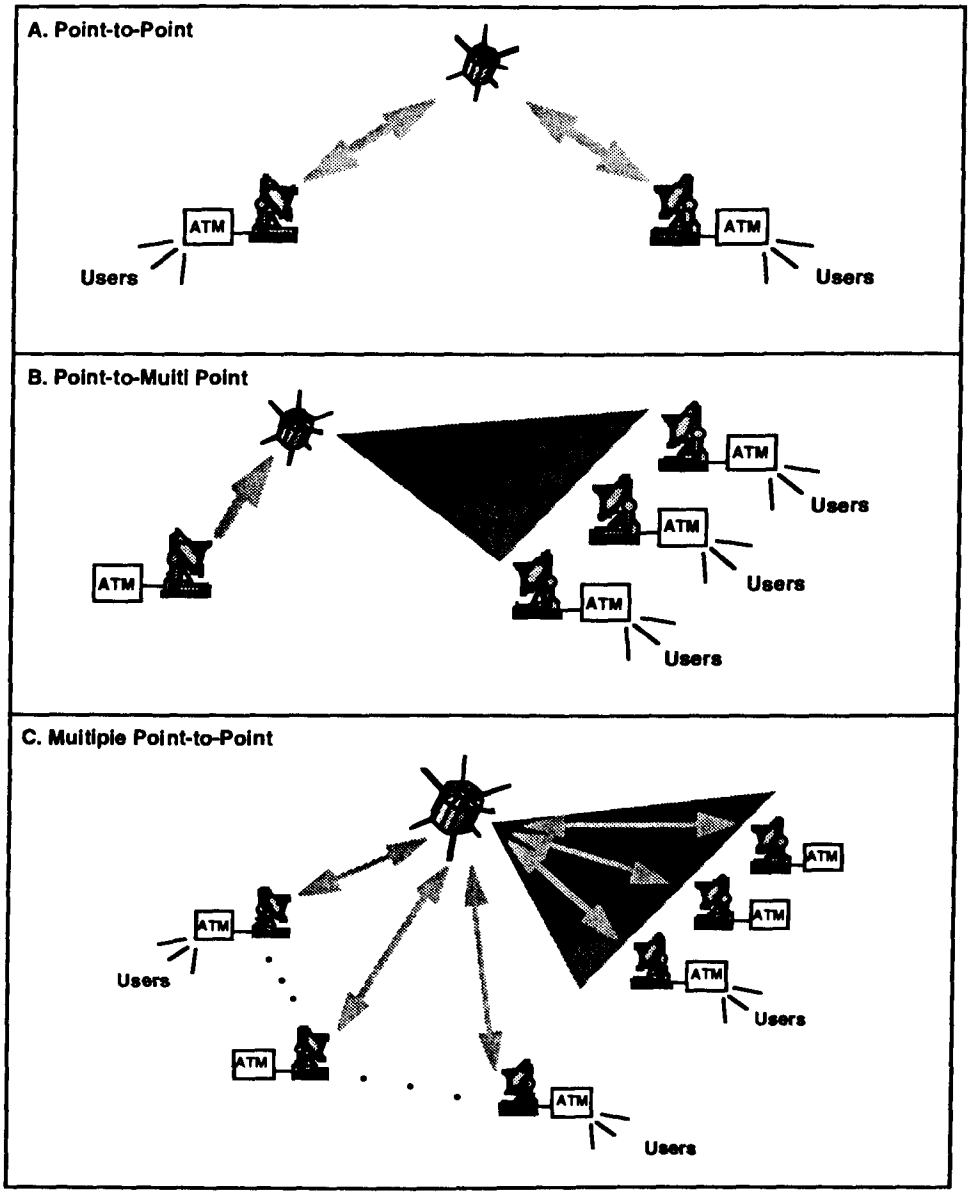

Figure 2: Several Common Ground Segment Configurations

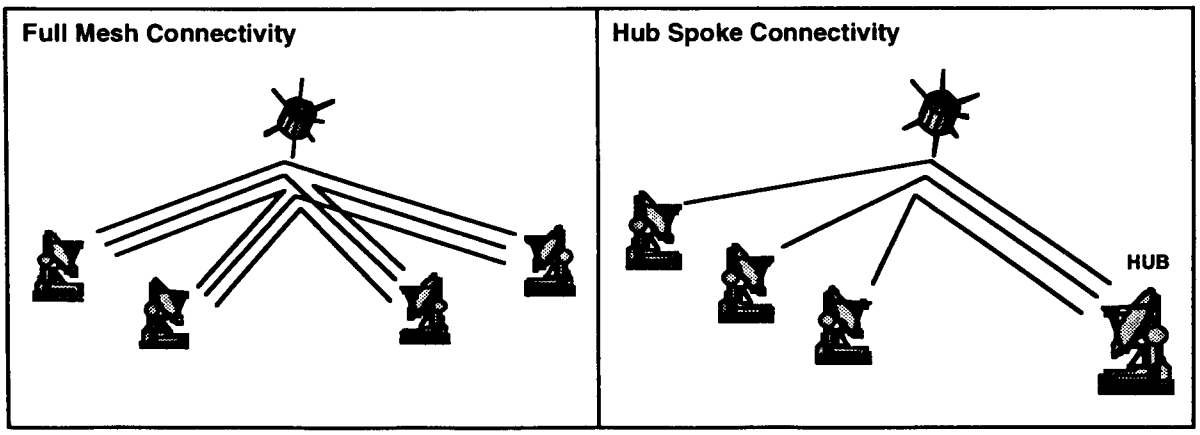

Figure 3: Two Options to Support the Multiple Point-to-Point Configuration

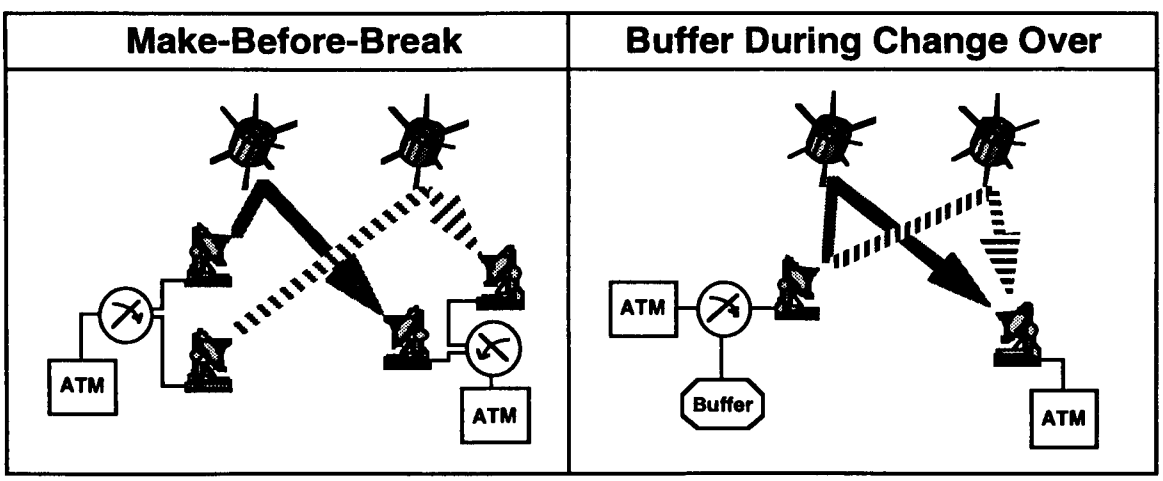

Figure 4: Two Options to Support ATM Traffic Over LEO Configurations

Applications and Experiments - II

Session Chairman: **Michael Wagg,** Optus Communications, Australia
Session Organizer: **Brian Abbe,** Jet Propulsion Laboratory, USA

Topic Introduction: Many new mobile satellite systems and services are currently being developed for deployment around the world. This session describes some of mobile satellite services which may be offered by first and second generation systems. The session begins with a description of the Private Voice Network capabilities of the newly launched MSAT satellite for the American Mobile Satellite Corporation (AMSC). The Russian mobile satellite system - comprised of satellites in geostationary and highly elliptical orbits - is detailed in the subsequent paper. A novel use for Globalstar satellites is proposed in the third paper. Low data rate services, such as intelligent road traffic management and Private Mobile Radio networks, to be offered by the European Mobile System are discussed in the following paper. The session concludes with an assessment of the market opportunities for the delivery of multi-media services in rural and small urban areas of Canada at Ka-band.

14

Description of AMSC's North American Private Voice Network (PVN) Service

C. E. Sigler
N. H. Magliato
American Mobile Satellite Corporation (AMSC)
10802 Parkridge Blvd.
Reston, Virginia,
USA, 22091
Tel: 703-758-6000
Fax: 703-758-6111

ABSTRACT

This paper provides both a technical description of the American Mobile Satellite Corporation (ASMC) Point-to-Multipoint Voice service and initial service offering descriptions. AMSC has selected the term Private Voice Network (PVN) for this service. The PVN service has been designed to take advantage of AMSC's continent-wide coverage.

Thus PVN provides a service not currently found in the mobile communications marketplace: seamless 2-way point-multlpoint voice communications across North America. This paper describes the PVN system within terms of physical components and configurations overall PVN system capabilites and initial PVN product offerings.

Paper not available for publication

Russian Mobile Satellie Communication Program

Igor S.Tsyrlin, Vladimir B.Tamarkin
Joint – Stock Company INFORMCOSMOS
ul Kazakova,16, Moscow, 103064, RUSSIA
Phone:7–095–261–1371 FAX:7–095–261–0090

The Russian MARATHON Program is a program for the development of technical facilities and systems to be used for communications with mobile and remote objects via satellites.

Reliable efficient communication links over the whole territory of the country are of vital importance because they are an essential element in the development of a civilized market and in the implementation of economic reforms in Russia.

It is evident that at present communication services and, in particular, mobile satellite communications are inadequate in Russia and, moreover, in some large remote areas such as Siberia, the Far East, Kamchatka, Tyumen and others, they are, in fact, lacking.

That is why the Ministry of Telecommunications of the Russian Federation and the Russian Space Agency worked out a Program for the Development of Satellite Communication and Broadcasting Systems in Russia that was approved by the Government. The Program has defined strategies for a development of the Fixed Satellite Service (this system called Express is based on an orbital cluster consisting of the new Express satellites at over a dozen positions in the geostationary satellite orbit), the Mobil Satellite Service (the Marathon system will use the Arcos satellites to be launched to five geostationary slots and four Mayak satellites at a highly elliptical orbit) and the Broadcasting Satellite Service (this system called Gals will include Gals type direct broadcasting satellites to be launched to more than five geostationary slots).

At the same time the Government issued a decree on the Government support and funding of the space activities in the Russian Federation which, inter alia, provides for a shared government financing of the Arcos and Mayak satellites in the Marathon system as well as the Gals satellite.

The INFORMCOSMOS Stock Company Limited is a prime contractor for the above systems and is responsible for:

- building the Express, Gals, Arcos, Mayak spacecraft, their launches, testing and operation;
- building earth segments for the fixed (Express), mobile (Marathon), communication and broadcasting (Gals) satellite systems and for the provision of communication and braodcasting services.

INFORMCOSMOS Ltd. was incorporated in 1991 by the leading Russian enterprises in the space and RF technology industries, namely: the Scientific and Production Association of Applied Mechanics, the Russian Scientific and Research Institute of Space In truments, the Radio Research and Development Institute and the Russian Space Communications Company.

Informcosmos Ltd. was established at a time when, on the one hand, the government appropriations to space contracts were sharply reduced and, on the other hand, the Gorizont satellites which are a basis of the public satellite communication system in this country failed to meet modern requirements.

During three years since the Informcosmos establishment a few members of the staff were able to retain the existing subcontractors including satellite communication research institutions and manufacturers and, by raising credits and investments, to build and in 1994 to launch the new Express (14 deg. W) and Gals (71 deg. E) satellites. These satellites operate very effectively now.

In 1993 Informcosmos Ltd. proceeded with the Marathon Program.

As far back as 1988 the Government of the former Soviet Union announced for the first time that a mobile satellite communication system should be developed. However, the work only

started in 1991 by the Marathon Inter-Department Association. In 1993 it was resolved that with a view to speeding the Marathon Program realization and integrating the potential of missile and space industries in the framework of a single national program for the development of communication and broadcasting satellite systems in Russia any further work on the mobile satellite system should be conducted by the Informcosmos Stock Company Limited.

The Marathon satellite system designed for communications with mobile and remote terminals will handle voice, facsimile, telegraphy, telex, E-mail and data between mobile or remote users, i.e. in such an environment where there is either no other means of communication (cable, microwave, troposcatter) or it is inadequate, and terrestrial international, trunk, local public switched networks and dedicated (overlay and private) systems through the Marathon fixed earth stations having an access to these terrestrial lines.

The Marathon system is being developed based on the Arcos cluster in the geostationary orbit that will provide global service areas and the Mayak satellites in a highly elliptical orbit that will render communication services in the Earth's Arctic areas (above 70 deg. N) and will provide a "single-hop" data transfer between users in the Eastern and Western hemispheres. The Arcos and Mayak satellites use multi-beam antennas which will allow both global and regional communication networks to operate through the Marathon system. Consequently, it is expected that mobile satellite communication services will be furnished to users in Russia and in the NIS countries.

The Marathon system includes:

- a space segment consisting of 5 Arcos satellites in the geostationary orbit, 4 Mayak satellites in a highly elliptical orbit and spacecraft control centers (a mission control center and ground satellite TT&C stations;
- an earth segment including fixed stations (both hubs and base stations), mobile and transportable terminals (user's terminals) which can be mounted either on mobile vehicles or in remote areas and may be distinguished by their service capabilities;
- network support systems, traffic control and management, customer services including coordination stations, an operation control center, a charging and settlement office, a type approval center.

The Arcos and Mayak satellites operate in two frequency ranges through 3 trasponders:

- from the C-band to the C-band (C/C);
- from the C-band to the L-band (C/L);
- from the L-band to the C-band (L/C).

The C/C transponder is used for communications between fixed stations where a primary circuit operates at the 64 kbit/s rate.

The C/L and L/C transponders are designed for communications between fixed stations and user's terminals. Each C/L or L/C transponder has a filter matrix the filters of which are capable of being switched over the full mobile bandwidth. The filter matrix control (its switch-on, switch-off, adjustment) is performed be a command from the Earth.

In the L-band the Arcos and Mayak satellites use phased antenna arrays to form a multi-beam steerable system in which the beam shape can be changed in response to traffic requirements.

The use of change-over filter matrix capabilities and multi-beam antennas will ensure some flexibility in coping with EMC problems that may arise with other mobile satellite communication systems.

The basic Arcos satellite characteristics are given below:

- orbital slots - 40.0 deg.E, 90.5 deg. E, 145.5 deg. E, 160.0 deg. W, 13.5 deg. W;
- station-keeping: N/S +-0.1 deg.
  E/W +-0.1 deg.;
- service life: 7 years to be operationally developed up to 10 years;
- frequency range:
  - mobile terminal-to-satellite
    1631.5 MHz to 1660.5 MHz
  - satellite-to-mobile terminal
    1530.0 MHz to 1559.0 MHz
  - fixed station-to-satellite
    6355.0 MHz to 6420.0 MHz
  - satellite-to-fixed station
    4030.0 MHz to 4095.0 MHz
- type of antennas to be used:
  - in the C-band: 5deg. x 11deg. parabolic
  - in the L-band:
    a phased array which provides
    - a global 17geg.x17deg. beam
    - steerable spot beams the patterns of which can be changed from 5deg.x6deg. to 8deg.x8deg.
- off-axis e.i.r.p.:
  - in the C-band:
    32 dBW for the 5deg.x11deg. beamwidth;
  - in the L-band:

41 dBW for the 5deg.x6deg. beamwidth;
35 dBW for the 17deg.x17deg. beamwidth with a powerback-off capability;

- off-axis G/T:
  - in the C-band:
  minus 8.5 dB/T for the 5deg.x11deg. beams;
  - in the L-band:
  minus 5.0 dB/T for the 5deg.x6deg. beams;
  minus 12 dB/T for the 17deg.x17deg. beams.

The basic Mayak satellite characteristics are as follows:

- orbit inclination: 64.0deg. -84.5deg.;
- period: 11.96 hours;
- service life: 7 years to be operationally developed up to 10 years;
- frequency range:
  - mobile terminal-to-satellite: 1631.5 - 1660.5 Mhz;
  - satellite-to-mobile terminal: 1530.0 - 1559.0 Mhz;
  - fixed station-to-satellite: 6355.0 - 6420.0 MHz;
  - satellite-to-fixed station: 4030.0 - 4095.0 MHz;
- types of antennas to be used:
  - in the C-band: 12deg.x12deg. parabolic;
  - in the L-band: phased antenna array which provides:
    - a 12deg.x12deg. zone beam;
    - steerable 6deg.x6deg. spot beams;
- off-axis e.i.r.p.:
  - in the C-band:
  30 dBW for the 12deg.x12deg. beam;
  - in the L-band:
  40 dBW for the 6deg.x 6deg. beam;
  33 dBW for the 12deg.x12deg. beam with a back-off capability;
- off-axis G/T:
  - in the C-band:
  minus 6.0 dB/T for the 12deg.x12deg. beam;
  - in the L-band:
  minus 5.0 dB/T for the 6deg.x deg.6 beam;
  minus 10.5 dB/T for the 12deg.x12deg. beam.

The fixed station has a module design with the following characteristics:

- antenna system: a 4.8 m parabolic dish;
- antenna G/T: 22 dB/T;
- voice channels: from 4 to 12;
- on-axis e.i.r.p.: 71 dBW;
- channel type: depending on standards to be used.

The Arcos and Mayak transponder performance and the fixed earth station characteristics make it possible to set up communication circuits that fully meet the requirements specified for the A, B, M, C and Aero Inmarsat standards as well for as the European land mobile satellite (Prodat) standard. At present the terminal capabilities of the North-American standards are being studied.

The first Arcos launch is expected at the end of 1996 or at the beginning of 1997 primarily due to financing difficulties.

The Program is presently financed, on a shared basis, by the Russian Space Agency and Informcosmos Ltd. from their internal funds and by raising capital in non-government organizations.

Informcosmos Ltd. is convinced that this Project will result in a qualitative enhancement of the communication infrastructure in Russia and in the NIS countries; moreover, it will also facilitate the development of regional (national) mobile satellit systems. Reliable communications between mobile and remote users will make a major contribution to:

- the introduction of new advanced economics and production management concepts;
- a higher efficiency and safety of transportation;
- environment-freindly production processes;
- a continuous environment monitoring;
- setting up readily-accessible reliable communication circuits through regional terrestrial stations Uhterfacing international terrestrial public switched networks.

The social benifits of the Marathon system are also of great importance because it will enable the space and RF technology industries to retain thousands of jobs which are to be released under the conversion programs.

The Telestation
A Product For Distributed Data Gathering and Operations

Robert R. Cleave, Christopher F. Hoeber
SPACE SYSTEMS/LORAL
3825 Fabian Way
Palo Alto, CA 94303-4604, U.S.A.
Phone: 415-852-6212 FAX: 415-852-5008

ABSTRACT

Advances in computer, navigation and wireless telecommunication technologies are enabling better electronic devices at reduced costs. Individually, these devices have been applied to increase the performance of many common systems, such as desktop computers, surveying equipment, and modems. However, we believe the convergence of these three technologies will create a product that simultaneously lowers life cycle costs while increasing operational effectiveness. Space Systems/Loral (SS/L) is developing portions of this product, known as the Telestation, for both terrestrial and orbital applications. The Telestation consists of an advanced microprocessor for command and data handling; a GPS receiver for position, time, and attitude information; and a Globalstar Transceiver for two-way digital communications. The Telestation provides the user with real-time command and control of globally distributed hardware elements. This capability can be applied terrestrially for gathering information (e.g., science, environmental, etc.) in remote or inhospitable locations, or where logistical support is inadequate. An in-orbit version can be used for spacecraft or payload operations, allowing principal investigators instant access to their payloads during all phases of a mission. This paper describes some cost effectiveness metrics of the Telestation, its development status, and its utility in both terrestrial and orbital applications.

INTRODUCTION

Great mechanical and scientific achievements have been made in planetary exploration, earth observation, and other domains of space travel, using custom equipment, and without a space communications and navigation infrastructure. These achievements were very expensive due to the recreation of this infrastructure for each mission. In these times of fiscal pressures, public and private entities are searching for methods to reduce operational costs. SS/L recognizes this need, and believes the combination of maturing space assets with increasingly sophisticated ground systems now enables greater strides in space exploitation at far less cost.

The particular space assets that have reached maturity are space-based navigation and communication systems. The Global Positioning System (GPS) became fully operational in June, 1993, allowing for the first time complete coverage of the earth with an average of eight spacecraft. This allows any GPS receiver to gather precise time and position information anywhere on the planet.

The planned Big LEO satellite networks comprise the second asset, and many of these systems will become fully operational by the turn of the century. The FCC-approved Big-LEO players are Globalstar, Iridium, and Odyssey, and are located in both low- and medium-earth orbits. In essence, these systems provide global connectivity with hand-held devices for two-way digital voice and data transfer.

Along with these space-based assets are equally impressive advances in ground-based applications. For instance, Hertz offers rental cars with digitized city maps and GPS receivers on-board, providing drivers essential information needed to navigate the streets of an unfamiliar city or region. Another example is the tour bus company, who can replace their tour guides with a CD-ROM activated video display system residing within the bus. As the bus travels around a city, the software in the CD-ROM causes various multimedia "shows" to play based upon inputs from the GPS receiver.

Independently, these technologies are very impressive. Collectively, they can yield incredible results. It is the collective sense which forms the basis for the Telestation, whose name is derived from the notions of telepresence and remote station.

TELEPRESENCE

Telepresence is the ability to non-physically extend ourselves to another location in real time. For years the science community has envisioned telepresence in planetary exploration, whereby the scientists can operate their instruments from the safety of an orbiting space station. With this capability, the robotic payload sent to the planetary surface is smaller and less complicated than that payload containing life support equipment. Further, the scientific instrument need not operate autonomously since a human is "in the loop". As a result, science can be collected with simpler and less costly designs.

A number of applications on Earth exist which require gathering information in remote and/or inhospitable locations. The accuracy of the information becomes even more critical when policy is formulated based on the data collected. And being able to operate payloads remotely increases the systems' cost effectiveness, simply because one is now able to extend himself to multiple locations simultaneously.

TELESTATION TECHNOLOGIES

The three elements central to the Telestation concept are navigation, communication, and computer technologies. Each technology is briefly described below.

GPS Receivers

GPS is already widely used in commercial industries, and has recently become fully operational. As a result, hand-held GPS receivers can provide precise position location and time references. Attitude knowledge is also available with software proprietary to SS/L, in a product known as Tensor. Technological advances continue to bring the size of these receivers down. Currently, Rockwell-Collins boasts the smallest GPS receiver in existence today — the size of a computer chip.

Wireless Communications

Operational in December 1998, the 48 satellite constellation comprising SS/L's Globalstar will provide real-time communications over 90% of the surface of the earth. This system enables users to call nearly anywhere in the world at any time. CDMA technology makes maximum use of limited bandwidth while increasing the quality of information transmitted. The envisioned dual-mode (cellular and Globalstar) handsets are digitally controlled, and require very little power.

Computer Systems

The third converging stream comprising the Telestation can be found at the heart of personal computers currently in production. Advances in the computing industry are yielding processors which can outperform most mainframes built in the late 1980's, at a fraction of the cost, mass, and power. The number of transistors in a chip doubles every 18 months (Moore's Law) and Loral Federal Systems has the ability to manufacture these processors in radiation hardened form for space applications, virtually eliminating the technology gap which has existed between space and ground processor hardware.

TELESTATION HARDWARE DESCRIPTION

Central to the communications system is the Globalstar transceiver being developed by Globalstar Limited Partners. The transceiver will interconnect the user and the equipment on the Telestation in a manner analogous to a modem operating at 4.2 kbps. This modest data rate is more than adequate for many instruments existing today, and advanced compression algorithms, such as Fractals, will ease bandwidth requirements in the future.

For terrestrial applications, the GPS receiver provides an added value in position and time determination. The orbital application requires information from GPS to determine the Doppler correction required, and to adjust the signal strength for operation through Globalstar.

Command and Data Handling (C&DH) electronics are required to operate the instrumentation and process the data for subsequent return. A microprocessor, such as the RISC 6000, lies at the heart of the C&DH, providing users with 32-bit addressing and 27 MIPS at under 15 Watts of power. An optional data recorder can be used to ensure no information is lost.

The addition of a standard AC or DC power supply completes the system, allowing emplacement anywhere on or around the earth.

All hardware components with the exception of the Globalstar transceiver exist today. Shown below is a functional block diagram of the Telestation (see Figure 1).

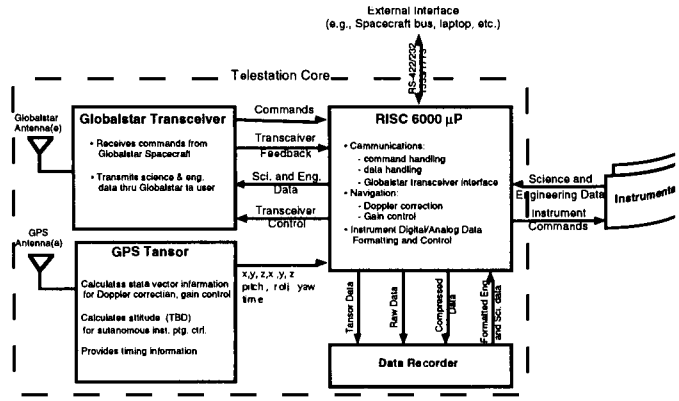

Figure 1: Telestation Functions Are Clearly Defined.

Rough estimates concerning the terrestrial Telestation form factors are provided below in Table 1 (costs are recurring).

Table 1: Telestation Hardware is Inexpensive and Light Weight.

Item	Mass (kg)	Power (W)	Cost ($)
GPS Rcvr	*0.5*	*2*	*500*
Globalstar Trcvr.	*0.4*	*2*	*1000*
RISC proc.	*0.5*	*3-15*	*1000*
Data recorder	*0.5*	*0.1*	*500*
Batteries	*3*	*N/A*	*100*
Solar Array (opt.)	*1*	*N/A*	*100*
Total	***< 6***	***7-21***	***3,200***

OPERATIONAL CONCEPTS

Once a Telestation is in place, its operation depends entirely upon user requirements. Two scenarios are presented: one driven by events, and one for continuous operations. In both scenarios, the Telestation is free to move.

Scenario 1: Event Driven

The Telestation is passively waiting for an event to occur, and is simply monitoring the environment at a low level and low frequency. When an event occurs, the C&DH activates the system, logs the time and position at which the event occurred, and begins collecting data. It also initiates a phone call notifying the user that an event occurred. Examples include unpredictable events such as tectonic movement, volcanic eruptions, encounters with wildlife, or a dynamic change in a given parameter beyond a predetermined threshold.

Scenario 2: Continuous Operations

In this scenario, the user is continuously monitoring and downloading data from the Telestation. The user initiates communications with a coded command set, which either turns on/off the instrument, adjusts the control parameters of the instrument (gain, S/N, frequency, etc.), and requests data to be fed into the bit-stream back to the user.

In both scenarios, the Telestation communicates with a Globalstar platform in either S- or L-band (forward- or return-link, respectively). The Globalstar routes the data to a Gateway, which uses the Public Switched Telephone Network to further route the information to the user. The exact routing is transparent to the user. Figure 2 represents the operational construct for the terrestrial version, which may be on the ground, in the water, or on an aircraft.

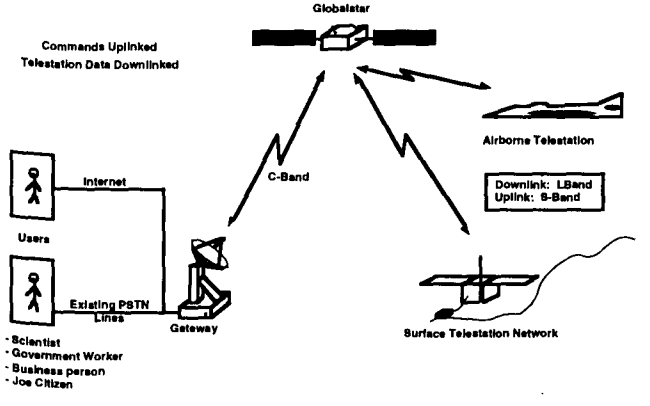

Figure 2: Terrestrial Operations Take Maximum Advantage of Existing Infrastructure

TERRESTRIAL APPLICATIONS

The following sections discuss some terrestrial applications of the Telestation. These applications are broken into three groups: Science/Education, Civil/Governmental, and Entertainment

I. Science/Education

The Telestation could be useful for a variety of science disciplines, as well as fostering education in a multitude of categories.

Seismology. Currently, limited capability exists for transmitting seismic data to a central processing site. Typically data transfer is accomplished via strip charts mailed to the USGS in Colorado Springs, which is time consuming and not very useful for predicting or mitigating seismic events.

Ideally, seismometers are positioned in order to triangulate and derive the source and magnitude of tectonic activity. These long-lived, passive instruments remain dormant over great periods of time, and become active once an event occurs. The placement of these instruments is primarily driven by the tectonic features of the planet, such as near faults. But accessibility secondarily drives their placement, since the instruments require moderate maintenance for data retrieval and power regeneration/replacement.

The use of a Telestation would greatly simplify the operational requirements while providing a potential for increased science return and prediction capability. When an event occurs, the Telestation can be configured such that it calls the scientist at his/her location with information on the magnitude, duration, and frequency of tectonic activity. Further, the scientist could adjust the instrument parameters in real-time, perhaps capturing secondary transients and increasing the value of data. Solar cells on the Telestation provide the requisite power for a long life, negating the need for battery maintenance. The RISC processor compresses the data by a factor of 10 to minimize bandwidth requirements, while an on-board data recorder stores the raw data. No restrictions on the number of seismic Telestations employed exist, thereby allowing for finer resolution. And two seismic Telestations can be collocated to sample different wavelengths without interference (see Figure 3).

Meteorology. Meteorological science requires a network of stations longitudinally spaced to provide ground truth for remote sensing satellites. Currently, physical constraints limit the number of meteorology stations. Most cities possess meteorological instrumentation, but a widely distributed set of instruments enables a finer resolution to ascertain the micro climates and transient events associated with the Earth's weather. The wide distribution of meteorological Telestations could be shared amongst many entities (e.g., governments, news groups, etc.), to provide data to anyone who has access.

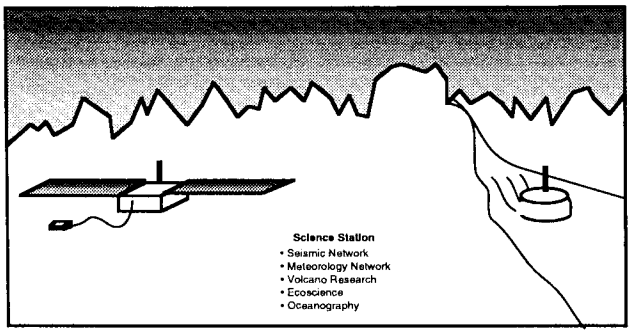

Figure 3: The Telestation Offers Increased Science Return and Educational Awareness.

The meteorological Telestations would contain instruments to determine temperature, humidity, wind speed and direction, and barometric pressure. The RISC processor provides an ability for post-processing to either minimize bandwidth requirements, or to provide the data in a user friendly format, such as automatically graphing the information. This processing capability is further enhanced by the on-board data recorder, which could couple prior bits of information to ascertain weather patterns.

Because the oceans have a significant impact on our weather, these Telestations can be placed on buoys to deliver the same type of data. Currently, buoys are placed close to land masses, and are serviced once a year. Furthermore, there is method to transmit the data to a ground station for continuous monitoring.

Volcanology. An imaging system and other instrumentation can be mounted to the Telestation and placed at areas known for volcanic activity, to be commanded when a volcano erupts. Or, a Telestation can be air-dropped nearby a volcano once an eruption has occurred. The information a Telestation can provide is useful in understanding the processes involved with an eruption, while removing the observer to a safe distance from the hazards. Most likely, the volcano will engulf the Telestation, allowing measurements to be taken until the last possible moment without the threat to human life, as occurred during the Mt. St. Helens eruption, when one noted volcanologist decided to stay until the last possible moment and unfortunately made the ultimate sacrifice for the sake of science.

Other examples abound: oceanography (ocean current/ temperature/ wave monitoring); fishing (photoplankton assessment); ecology (wetlands/ desert/forest monitoring and management), etc.

II. Civil/Government

Many of the civil/governmental applications are concerned with resource monitoring and management. The following examples illustrate some applications of the Telestation to these fields.

Hazardous Spills. Instrumented Telestations can be dropped in the vicinity of carcinogenic oil spills to determine the hazardous fallout. The buoy and oil will travel with the currents, leading researchers and policy makers to take evasive action ensuring minimal environmental damage.

City Pollution Monitoring. The Telestation can be equipped to monitor air pollution with a consistent sampling methodology. The EPA is currently modifying the rules and regulations which cities must adhere to. Cities exceeding the pollution control limits established by the EPA will pay stiff fines, and repeated violators will require local industries to modify their production operations.

Snow Depth/Stream Gauges/Lake Buoys/Rainfall Gauges/Flood Assessments. As our awareness of our environment increases, we are cognizant of the importance of streams and lakes. The level of fresh (or frozen) water provides an indication of the area's ecological wellness. Furthermore, the struggle continues between farmers who need fresh water and environmentalists who are concerned about the projected level of fresh water, thereby increasing the politician's need for accurate information.

Currently in situ measurements are physically taken, logged, and relayed to central data bases. By using the GPS receiver and equipping the Telestation with some instrumentation, these in situ measurements can be taken remotely and with greater frequency. This results in better assessments on the ecological soundness of our environment, which equates to better policy. Furthermore many mountainous summits are inaccessible during the winter; an air dropped Telestation could relay more accurate information than visual inspection or extrapolation.

Tagged Wildlife. Currently, tagged wildlife are manually tracked and their motions logged. This tedious process could be simplified with an SS/L Telestation. A microminiaturized beacon device would be attached to the tag, which would set off an alarm on a Telestation. When the animal is within close proximity, the beacon on the animal triggers the Telestation, which then notes the tag's identifier and time. This data is then automatically logged and transmitted via Globalstar to the scientist, who then can determine the animal traffic and other physiological features.

Wildfires. Similar to the pollution monitoring, Telestations can be deployed to detect wildfires in bush country. Many fires occur in these remote areas, and often go undetected for some time, allowing the fire to grow. These Telestations would most likely be consumed in the ensuing blaze.

Iceberg Monitoring. Attaching the Telestation to an iceberg allows scientists and ocean-going vessels to monitor the paths of icebergs. The path of an iceberg is

important to the military as well, since they pose a danger to submarines.

Military Communications. During war games, the Telestation can be attached to various vehicles, which can then relay battlefield information back to the commander. A UHF-based system, also built by Loral, known as TAPER exists today, and it provides a similar capability with limited coverage.

Another example is the Remotely Piloted Vehicles (RPV's), which are limited in range because they must remain within the line-of-sight of the tower-based pilot. With Globalstar and a GPS Tensor, RPV's can be flown nearly anywhere in the world with the pilot safely at some fixed location. The Tensor system also eliminates the beacon interferometry currently used by RPV's.

Illegal Drug Traffic. A Telestation with Infrared motion detectors can be located near borders to notify law enforcement officials when motion is detected, such as when a small plane flies overhead. Tens of these small, inconspicuous Telestations can be deposited, with the possibility that a few fail or become discovered and destroyed. An imager can be integrated and commanded to turn on when motion is detected. The imagery can then be used to capture suspects in our war on drugs.

III. Entertainment

Finally, the Telestation could be used in entertainment, as the following fanciful example explains.

Tourism. Telepresence can also be sold as a means to take a vacation without physically traveling to the location. The cost and time away from the office are greatly reduced, although the aura and feeling would possibly be missing. However, the feeling could be simulated through heat lamps, Tiki torches, and Mai Tais. Virtual Reality technology could also be applied to increase the return.

In addition, some of the scientific measurements discussed earlier are important to tourists as well. For example, before planning next spring's vacation, a user could tap into the meteorological Telestations at various destinations to determine if the weather patterns are suitable. Or a traveler could use the same Telestations to determine how to pack for impending business trips.

ORBITAL TELESTATION

The orbital Telestation operates similarly to the terrestrial version. The payload on the spacecraft becomes just another node on a computer network. Instrument commands are uplinked through the Telestation to the instrument, and data collected is returned to the user (See Figure 4) which eliminates the need for a dedicated communications link and supporting ground infrastructure for many potential payloads. Continuous payload monitoring can be eliminated, as the payload will have the ability to call the principal investigator, at home if necessary, when an event of temporal significance occurs.

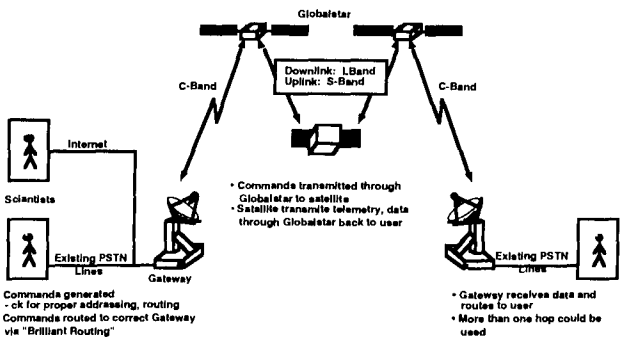

Figure 4: Operational Concept for Orbital Telestation.

Currently in the U.S.A., either the Air Force Tracking Network or NASA's TDRS system is used to satisfy these requirements. Both systems are expensive to use, and both have priority missions to support, which implies an inability to transfer data and/or commands upon demand for every user. Not only does the Telestation allow an investigator to more readily capture episodic events, but the orbital Telestation can offset operational expenses by reducing ground support requirements, evolving the investigator into spacecraft operator.

As an example, presented in Figure 5 is one cost effectiveness metric for three different systems. This metric is one of the more significant commodities on-board a spacecraft. TDRS is NASA's Tracking and Data Relay Satellite, a geosynchronous spacecraft designed in the 1980's to provide two-way communications between NASA spacecraft and earth.

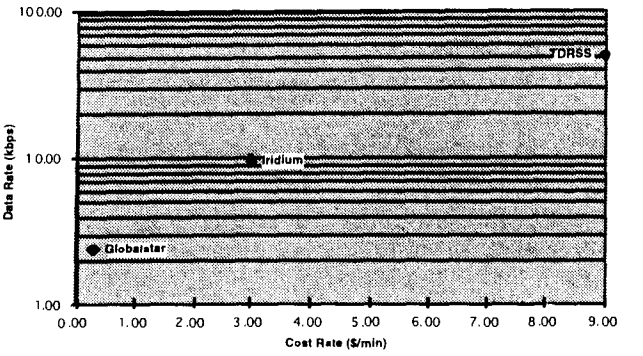

Figure 5: Cost Effectiveness of the Telestation.

As shown, the Telestation's modest bandwidth is in fact more cost effective than several other existing and planned systems. Furthermore, bandwidth requirements continue to drop with advances in compression techniques.

Globalstar's 4.2 kbps data rate is more than adequate for commanding an instrument, which typically contains only a dozen instructions totaling 1-2 kilobits. This data rate does not meet all return data rate requirements, but is adequate to provide a preview of an instruments' data (metadata files), which is sometimes essential to successful operations. In this case, the investigator would continue to use the existing infrastructure for downlinking the payload data.

Figure 6 shows the downlink requirements for several payloads proposed for NASA's Earth Observation Satellite (EOS) program, more commonly referred to as Mission to Planet Earth.

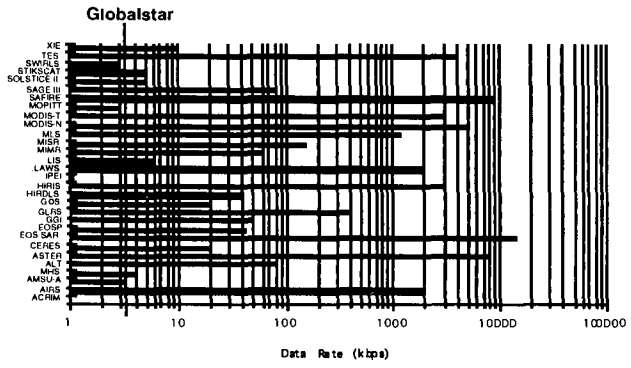

Figure 6: Downlink Data Rate for Several Payloads Proposed for NASA's Mission to Planet Earth Program.

The major limitation for in orbit operations is the payload orbital altitude must be several hundred kilometers below the planned altitude of Globalstar (1400 km altitude). Note that Globalstar is several hundred kilometers higher than Iridium's planned orbit. If either of the proposed intermediate orbit systems (TRW's Odyssey or Inmarsat's P-21) become reality, this limitation will disappear with their transceivers.

DEVELOPMENT STATUS

The Telestation is a concept which takes maximum advantage of existing and planned infrastructure. Space Systems/Loral is developing portions of the system, and is considering to produce the entire device. The development status for the Telestation is shown in Figure 7 below.

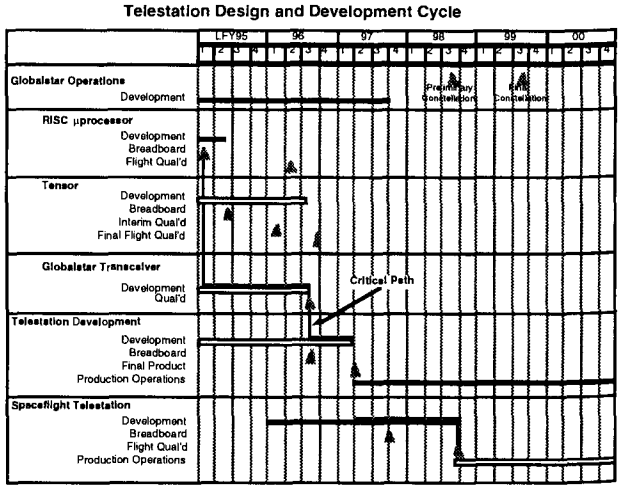

Figure 7: Development Time Line for the Telestation.

CONCLUSION

Technologies at Space Systems/Loral enable a telepresence capability for both ground application and in low earth orbit, which will revolutionize many industries. This enables the ability to gather more data, with finer spatial and temporal resolution, to better support technical or political activities. The Telestation is affordable, with costs comparable to high-end personal computers on the market today. Operating these Telestations can provide operational cost savings with a significant improvement in the knowledge base provided by each instrument.

European Mobile Satellite Services (EMSS) a Regional System for Europe

C. Loisy, P. Edin and F. J. Benedicto
European Space Agency, Directorate of Telecommunications Programs
ESTEC-TSM, Postbus 299, 2200 AG Noordwijk, The Netherlands
Phone: +31-1719-83155, FAX: +31-1719-84598

ABSTRACT

The European Space Agency is presently procuring two L-band payloads in order to promote a regional system for the provision of European Mobile Satellite Services (EMSS). These are the EMS payload on the Italsat I-F2 satellite and the LLM payload on the ARTEMIS satellite. Telecommunication system studies have been concentrating on mobile applications where full European geographical coverage is required. Potential applications include high priority Private Mobile Radio networks requiring national or European coverage, such as civil security, fire brigades, police and health services, as well as a dedicated system for provision of Air Traffic Services to the civil aviation community. A typical application is an intelligent road traffic management system combining a geographically selective traffic data collection service based on probe vehicles with a geographically selective traffic information broadcast service. Network architectures and bearer services have been developed both for data only and voice/data services. Vehicle mounted mobile transceivers using CDMA access techniques have been developed. The EMSS operational phase will start with the EMS payload in orbit in 1996 and continue with the LLM payload in 1997.

1 INTRODUCTION

The business of Mobile Satellite Communications started close to twenty years ago with the introduction of a system for the provision of a maritime service with worldwide coverage using initially three geostationary satellites. An aeronautical system was later defined, based on the same space segment, in order to provide civil aviation with a public telephony service as well as safety communications. It is however expected that it is in the area of land user applications that the greater part of the mobile satellite communication market will materialise in the years to come.

The development of the overall mobile communication market is fast, particularly since the advent of the digital cellular networks which now allows a large utilisation for personal communication. Although the major part of this market will effectively be served by terrestrial systems, satellites will also be used in many areas to supply the service, due to their inherent economic superiority to terrestrial infrastructure where user density is low.

The satellite systems which are now being considered for the provision of services on land are significantly different from the initially developed maritime and aeronautical systems and may use satellites, besides the geostationary ones, either on highly inclined, intermediate or low Earth orbits. The present paper reports on developments carried out in Europe for the introduction of services based on geostationary satellites, but with a coverage optimised for the European region. Indeed, this configuration has appeared to carry significant advantages for some types of services.

Advantages associated with the operation of a regional coverage combined with the utilisation of a flexible feeder link access system are first discussed and the limits of the approach are indicated. The various elements of the European Mobile Satellite Services with their main characteristics are then introduced. Typical applications which take maximum advantage of these characteristics are finally presented.

2 RATIONALE FOR A REGIONAL SYSTEM FOR EUROPE

Reducing the coverage area of a geostationary global beam satellite automatically brings the advantage of a reduction in beam solid angle. This directly translates into an increase in satellite antenna gain. In the case of the European coverage shown in figure 1, the resulting extra link margin is in the order of 8 dB. For a given communication system, in the forward (fixed to mobile) link, this extra margin will directly determine an equivalent reduction in satellite EIRP and/or mobile station antenna gain. Similarly, in the return (mobile to fixed) link, the extra link margin can be shared between mobile station antenna gain and RF power. In all cases, very significant cost savings are generated.

The choice of the frequency band to be used for the feeder

links has a considerable impact on the cost of the fixed user stations. Typically if Ku-band is selected as opposed to C-band, it allows RF front ends of the fixed stations to be in the VSAT range i.e. with antennas smaller than 2 m diameter. As a consequence of the smaller fixed user stations, optimisation of network architectures as well as user costs becomes feasible, through bringing the satellite access points closer to and even at the fixed user sites.

Finally, in order to take full advantage of the possibility of installing a high number of fixed Earth stations, it is important to implement communication systems which allow multiple access from the fixed side while requiring minimum overhead for the management of the communication capacity. This is indeed a key to the provision of independent low capacity satellite networks, which can thus effectively share a common satellite resource at minimum costs.

These considerations have been the basis for the definition of the European Mobile Satellite Services, which are using a single Regional coverage beam from a geostationary satellite. This type of system is probably not appropriate for all mobile applications since, in particular, due to the minimum performances which are required from the mobile stations, "hand held" equipment tend to be excluded. As a consequence, a significant part of the potential personal communication market will be dependent on other solutions, typically based on smaller spots or lower orbits.

However, with the practical example of the coverage indicated in figure 1, it can be shown that a telephony service based on a 4.8 Kb/s vocoder can be operated with adequate margins through a 7 dB gain antenna at the mobile; this corresponds to a one element directional antenna at the mobile, steered around a vertical axis. The outer dimensions of the corresponding radome are typically 25 cm diameter and 25 cm high, which is compatible with an installation on road vehicles from smaller vans upwards. If only low rate data is required, a flat isotropically radiating antenna with a 9 cm diameter and a 2 cm height is sufficient; that antenna can be integrated into the roof of a private car.

For numerous applications, vehicle mounted and/or portable equipment is adequate and a simple, flexible and inexpensive "single cell" network with a wide gap-free coverage is the right answer to the communication problem. This is further discussed in chapter 4, and chapter 5 introduces examples of typical applications.

3 THE EUROPEAN MOBILE SATELLITE SYSTEM

The European Space Agency undertook years ago the development and promotion of Regional Mobile Satellite Systems with the goal of optimising the communication system design, the space segment and the user stations for operations within Europe. To this end, space segment at L-band over Europe is being procured and dedicated communication system developments have been made with the goal of optimising the overall design for the contemplated services. These activities have already been reported in earlier publications [3], [4], [5], [6] and the present chapter only provides a summary and the present status of activities.

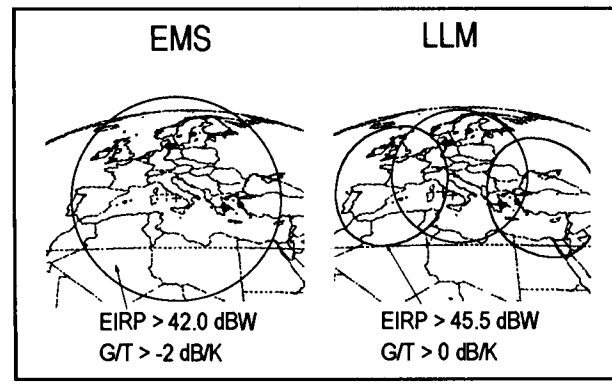

Figure 1: Regional European Coverage of EMS and LLM

3.1 Payload Characteristics and Coverage

Two satellite payloads are being procured for the early implementation of EMSS over Europe. The EMS payload is to be carried in orbit as from 1996 by the ITALSAT 1-F2 satellite of the Italian Space Agency and the LLM payload of the ARTEMIS satellite of ESA will be launched in 1997.

3.1.1 EMS/Italsat 1-F2

The EMS payload includes two transparent transponders, one from Ku-band (14 GHz) to L-band (1.5 GHz) for the implementation of the fixed to mobile (or forward) link and one from L-band (1.6 GHz) to Ku-band (12 GHz) for the mobile to fixed (or return) link; it will be in geostationary orbit at 10.2 degrees East. The antenna at L-band has been optimised for European coverage (see figure 1) and exhibits a minimum edge of coverage gain of 26 dB. A total bandwidth of 12 MHz distributed in three segments of 4 MHz is available in each of the two transponders.

Main characteristics are:

Total L-band EIRP:	42.5 dBW
L-band G/T:	-2 dB/K
Ku-band G/T:	-1.4 dB/K

3.1.2 LLM/Artemis

The LLM payload also includes two transparent transponders

with frequency bands identical to EMS; it will be in geostationary orbit at 16.4 degrees East. The antenna at L-band has been optimised for European coverage (see figure 1); it features three spots with a minimum edge of coverage gain of 29 dB and a Eurobeam which is the combination of the three spots. A total bandwidth of 15 MHz distributed in three segments of 4 MHz plus three segments of 1 MHz is available in each of the two transponders; all 6 segments are separately tunable over the whole Mobile Satellite Service band. Main characteristics are:

Total L-band EIRP (Spot):	45.5 dBW
L-band G/T (Spot):	0 dB/K
Ku-band G/T (Spot):	-1.4 dB/K

3.2 Satellite Access Schemes

Satellite access schemes have been studied considering both the fixed Earth station technology and the satellite capacity sharing technique. The contemplated types of applications do require network architectures based on numerous fixed Earth stations; this has a bearing both on the allowable unit cost of the Earth station and on the satellite capacity apportionment scheme, which must be kept efficient also with low capacity networks. Using frequencies higher than C-band for the feeder links has a favourable impact on the Earth station antenna size; Ku band was selected as a good compromise between antenna size and component costs. The fixed Earth stations of EMSS are VSATs with 1.8 m diameter non tracking antennas.

The satellite capacity apportionment among the various networks or Earth stations in EMSS is implemented using CDMA multiple access techniques, which, under certain conditions, may allow to simplify or even sometimes dispense from explicit channel allocation procedures. In order to maximise efficiency, a Quasi Synchronous CDMA system has been developed which dramatically increases the maximum number of simultaneously operable channels in a given bandwidth, taking advantage of the considerable improvement in orthogonality of synchronous spreading sequences.

3.3 Communication System Developments

The EMSS applications and service demonstrations will be partly based on two developments of mobile satellite communication system made by European Industry under sponsorship of ESA; PRODAT is a store and forward and MSBN a real-time voice and data communication system.

3.3.1 PRODAT

The PRODAT system has already been presented in various publications and this is only a brief summary of its characteristics. The basic PRODAT architecture is presented in figure 2.

PRODAT was conceived as a low data rate messaging system which operates through a rather compact and low cost mobile terminal equipment. The mobile antenna has an isotropic coverage and can be realised either as a quadrifilar helix 120 mm high or, for satellite elevations greater than 20 degrees, as a printed antenna of 90 mm diameter and 20 mm thickness. The other characteristics are as follows:

- 10 W RF power
- TDM / BPSK 1500 b/s receive
- CDMA / OQPSK 600 b/s transmit
- Adaptive ARQ based block coding

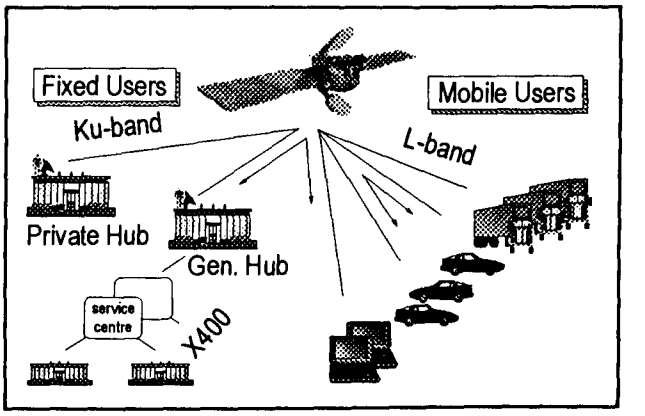

Figure 2: PRODAT System Architecture

PRODAT will often be used as a mobile extension to terrestrially based messaging services; it was designed along the X400 ITU-T standard and provides service compatibility with established messaging services. The PRODAT hub-station is both the interface point to the terrestrial networks and the centralised access point to the satellite; it controls the mobile network. Messages are transmitted between the hub and the mobiles in both directions. The system has been extensively tested and has proven a remarkable robustness to adverse propagation conditions in land mobile environment. The transmission delays are particularly short compared to competing satellite systems.

3.3.2 Mobile Satellite Business Network (MSBN)

MSBN was designed for vocoded voice and real time data transmission services with particular emphasis on decentralised, low capacity, applications. The system allows for a wide range of network architectures and can be tailored to the particular applications. A typical application is shown on figure 3. The main design feature is the possibility of decentralised satellite access from the fixed side, while maintaining overall efficiency even in low traffic networks; it

is based on the use of low cost VSAT stations operating at Ku band and of a CDMA multiple access scheme.

MSBN is now in the prototype stage and the achievements to date are reported in [2]. The QSCDMA concept can be considered validated and ready for the implementation of applications.

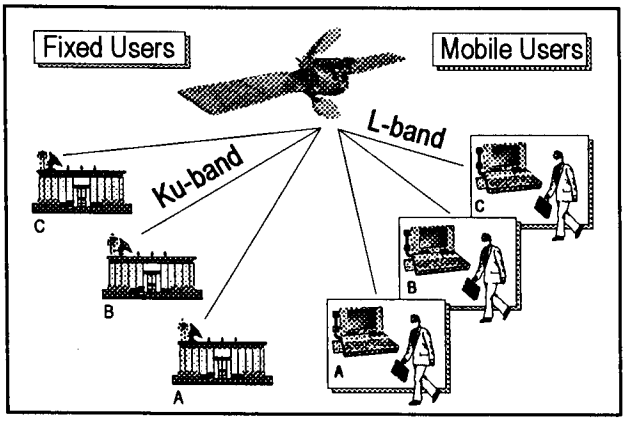

Figure 3: MSBN System Architecture

4 TYPICAL EMSS APPLICATIONS

EMSS intend to cover applications which are not expected to be adequately supported by the existing or emerging mobile networks, whether terrestrial or using satellites. The present mobile satellite services are essentially extensions of public network services to mobiles, which is also true for terrestrial mobile networks such as GSM. With these infrastructures, private networks may be implemented through Closed User Group application on public networks. This however only covers a part of the potential applications of mobile communications since the service requirements will often significantly deviate from what is available on public networks. Typically, performances relating to effective coverage, availability, network architecture flexibility and mobility may not be satisfactorily met. This is the gap that EMSS aims at bridging.

4.1 Key Features

EMSS development activities have focused on features which although fundamental for some services, will not generally be available in public mobile networks.

4.1.1 Coverage

Many applications require a continuous gap-free coverage over extended service areas; this is typically in Europe the complete territory of one or several countries. For satellites, the antenna footprint should be tailored to the required service area in order to be economically competitive. For terrestrial systems, there are economical trade-offs in the implementation of cellular systems which will always tend to exclude areas where user density is low and/or radio wave propagation is difficult.

4.1.2 Service Availability

Some potential users of mobile communications have very high service availability requirements; this typically applies when safety of life is involved. Traditionally these users have enjoyed private usage of dedicated communication resources where service availability is not dependent on the traffic of other users. This is not easy to achieve when sharing a public network infrastructure; besides some services are required to operate at times when basic infrastructures may have been damaged (natural disasters and emergencies in general).

4.1.3 Flexibility and Independence

Mobile services provided by means of extensions to the basic infrastructure are by definition dependent on this infrastructure not only in terms of availability, but also in terms of physical connections. In some cases mobility of the operational centres within the service area may also be required. A complete independence of the mobile communication network from the fixed infrastructure will be an asset for many applications and a mandatory feature for some.

4.1.4 Specific Functionalities

Some mobile communication users may require dedicated functionalities within their network which do not easily map on the standard networking functions of the basic infrastructure, which are essentially end-to-end connections. A typical example is a fleet surveillance system where position data have to be collected from the various mobiles within strict time delay constraints. An efficient system will use specific low level communication protocols involving all mobiles concerned in the same transaction (e.g. polling) which cannot easily be supported by a connection oriented network.

5 SERVICE DEMONSTRATIONS

The EMSS space segment has been optimised for European services with a transparent L-band capacity compatible with a range of communication systems. In relation to existing and currently planned GEO systems, the optimised coverage will offer competitive advantages for a range of European applications regardless of choice of communication systems.

Specific communication system developments have been made, taking full advantage of space segment performance, to promote European commercial services for applications such as transportation fleet management and business traveller communications. These well known applications, having already been proven and being ready for implementation, will not be further expanded upon in this context. The unique features of EMSS and its dedicated communication systems also offer an opportunity for demonstrations of improved and new services which will be discussed in more detail.

5.1 Aeronautical Satellite Data Link System

An Aeronautical Satellite Data Link System for civil aviation specifically devoted to the communications associated with Air Traffic Control (ATC), known as Air Traffic Services (ATS), is one of the candidate applications for EMSS.

An original system concept was developed within ESA, based on the capability for flexible architectures of EMSS. Indeed a decentralised architecture can precisely map the management organisation of airspace, through providing a local "private" network for each ATC centre or even each controlled sector of airspace. The major advantage is the higher robustness to equipment failures of a distributed system compared to a centralised one and its independence from other infrastructure for the safety critical communications. Very significant implementation cost savings are anticipated, when compared to centralised solutions, particularly in view of the exceptionally high service availability which is required. A feasibility study has now been commissioned to Industry and the status of the work is presented in [1]. A detailed design study is planned to follow with production of prototypes in order to demonstrate in-flight performance.

5.2 Regional Emergency and Priority Services

EMSS allow the implementation of independent European mobile emergency and priority communications networks. User and applications will typically include civil protection agencies, disaster response efforts, law enforcement, fire fighting and tele-medicine. High reliability services and low system and service costs are foreseen which can economically enable greatly increased usage amongst non-commercial and government oriented users.

In case of disasters, the public telephony network cannot be relied upon to provide adequate service. This is primarily due to potential damages to local infrastructure and to system overloads likely to be caused by this type of event. This justifies a private and independent architecture for exclusive use by professionals with limited or no need for public network access. The ability to communicate while moving, such as in the case of emergency transports, may greatly increase the efficiency of relief efforts and victim survival. The geographical location of the disaster will also, in many cases, exclude digital cellular or private trunked terrestrial radio systems for coverage reasons. This makes the case for a private mobile satellite services network with primary requirements on rapid deployment and simple data messaging or voice/fax service.

A characteristic that greatly increases the political and practical feasibility of any international network of this type, is the ability to cater for national independence while enabling sharing of resources. Flexibility of the network architecture and independent, but resource sharing, private networks are keys to success.

EMSS with a capacity to support private networks with low cost hub stations offers each national civil agency, or equivalent, independent control of its communications network. Further separation within each country for distinct services such as disaster response and fire fighting is also feasible. Expensive resources such as space segment are shared amongst all users and identical terminal technology ensure international compatibility and low manufacturing cost. While separate networks ensure independence, the sharing of resources and network flexibility enable efficient cooperation when so required, such as for major disasters involving more than one national service or several nations.

5.3 Road Traffic Monitoring and Information System

This application addresses the communications between road traffic control centres and vehicles on the road which are required for the implementation of a Dynamic Road Traffic Management System. The system performs a selective collection of motion and other data from "probe vehicles" in order to generate statistical road surveillance data. In addition, advisory data targeted at road users are assembled and selectively broadcasted to suitably equipped vehicles. A system overview is presented in figure 4.

The system is based on the combined usage of a positioning (e.g. GPS) and a two-way data communication system on board vehicles. Positioning is required since it is the core of the surveillance data, but is also essential in the implementation of the communication system. A specific feature is that the basic communication function does not address individual vehicles but rather geographical cells, and this in both directions. The positioning function allows to relate vehicles to cells and thus enables selective addressing. For the data collection function this guarantees the wanted distribution of data reports over the cells and for the data

broadcast, the selective filtering of the information of interest. The Dynamic Road Traffic Management system only requires a few percent of vehicles on the road to be equipped for data collection. Data reception, however, is potentially of interest for all users.

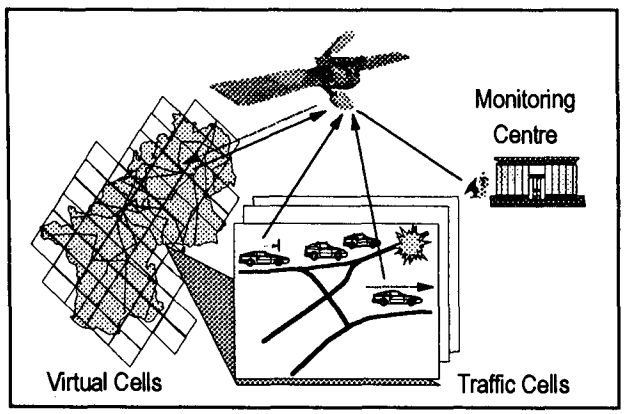

Figure 4: Road Traffic Monitoring and Information System

An initial dimensioning study concluded that a two-way satellite data communication system based on EMSS using low data rate would be totally adequate for this application. Transmit/receive stations are only required by the vehicles which contribute to the data collection; these stations could also be used concurrently for private messaging. Significantly cheaper receive only stations would be used for sole reception of broadcast data.

The multiple access feature of EMSS allows the combined operation of a number of such networks in the same transponders and with a common user base. This is particularly well suited for Europe, where road management authorities are likely to remain organised on a national basis, while a significant number of users will roam between various countries.

The implementation of similar systems using terrestrial cellular infrastructure is being studied elsewhere. It is however anticipated that the regional satellite system will demonstrate its superiority, at least in economical terms, which will result from the exploitation of the specific features of the satellite based networks. This system has been proposed for demonstration within the Telematics Applications of the Fourth Framework R & D Programme of the European Union.

6 CONCLUSION

The rationale for the introduction of regional European Mobile Satellite Services (EMSS) concurrently with the existence and advent of other systems has been presented. Examples of important applications for which regional European as well as national coverage will be required and for which the EMSS concept is particularly relevant have been introduced. These applications represent a sizable market already today. The European Space Agency has funded a space segment at L-band to support the initial operations of EMSS as from 1996. Part of the capacity available will be used to demonstrate and evaluate, in a user environment, emerging services for which usage of regional satellite networks are likely to favourably compare with other competing solutions.

REFERENCES

[1] A. Delrieu et al, *Aeronautical Satellite Data Link System for High Density Air Traffic Areas*, Proceedings of the IMSC conference, June 1995.

[2] M. L. de Mateo et al, *Mobile Satellite Business Networks: A Part of the European Mobile System*, Proceedings of the IMSC conference, June 1995.

[3] A. Jongejans, R. Rogard, I. Mistretta, F. Ananasso, *The European Mobile System*, Proceedings of the IMSC conference,1993.

[4] R. Rogard, *LMSS: From Low Data Rate to Voice Services*, Proceedings 14th International Communication Satellite Systems conference AIAA, Washington DC, March 1992.

[5] S. Barberis et al, *MHS Concepts and Services in a Land Mobile Satellite System*, Proceedings of the IMSC conference, June 1990 .

[6] R. Rogard, A. Jongejans and C. Loisy, *Results of field trials with the PRODAT system*. ESA Journal - 1989 Vol 13.

Market Opportunities in Canada for Multimedia Residential Services in Rural and Small Urban Areas

Dr. Mehran Shariatmadar, Program Manager, Telesat Canada
1601 Telesat Court, Gloucester, Ontario, Canada K1B 5P4
Phone: 613-748-0123 FAX: 613-748-8712

Ms. Vasantha Narasimhan, Marketing Consultant, Simhan Research Associates Inc.

ABSTRACT

This paper reviews the studies which were undertaken jointly by Telesat and Industry Canada to provide an estimate of the market opportunities for residential multi-media services in the rural and small urban areas of Canada.

This study is part of the Advanced Satcom program, a Ka-band satellite system proposal which is currently in the implementation proposal phase by the government and the Canadian space industry of which Telesat is an active member.

Advanced Satcom extends the reach of terrestrial information highways to the remote and sparsely populated parts of the country in a cost-effective manner and thus provides a ubiquitous coverage of the information highways to all Canadians. Therefore, the rural and small urban markets are believed to be good opportunities for the Advanced Satcom. Although the results are primarily intended for fixed residential applications, they can also be used as input to market opportunity studies for wideband mobile applications. Consideration of the market potential for other services (not addressed in this paper) such as education, health care, government, and business services within the rural and small urban areas is also being pursued by Telesat in support of the Advanced Satcom program.

INTRODUCTION

The study follows two complementary approaches in Module 1 and Module 2. Module 1 is an in-depth analysis of Statistics Canada's database of facilities, equipment and income of households in rural and small urban locations with populations less than 30,000. The key considerations in Module 1 include:

- Characteristics that relate to the adoption of various information and entertainment (infotainment) equipment such as VCRs, camcorders, satellite dishes, and personal computers.
- Potential number of households most likely to adopt infotainment services on the electronic superhighways.

Module 2 is a primary research study based on analyses of responses to a telephone survey of 1,000 households. The statistical sample of 1,000 households for the survey is considered to be representative of different types of rural and small urban locations across Canada with populations less than 30,000. The specific areas considered in Module 2 include:

- Awareness and interest of households in the generic concept of the home infotainment services.
- Perceptions of households with respect to the usefulness of various infotainment services including educational, transactional, and home business services.
- Affordability range for terminal equipment and monthly charges to be connected to these services.
- Potential of households to subscribe to these services, and the relationship between interest in infotainment services and the adoption of other household innovations.
- Segmentation of the market via statistical analysis and comparison of the projection of potential households obtained via Module 2 analysis with those of Module 1.

An urban population of 30,000 is taken to be the cut-off point for areas included in the study in order to ensure that only locations with potential for achieving economic advantages, in being served by an Advanced Satcom instead of fibre or terrestrial wireless facilities, are considered for the analysis.

MODULE 1
SECONDARY SOURCE ANALYSIS

Distribution of Households by Province and Area Type

The analysis of rural and urban locations with population less than 30,000 was performed using the Census Subdivision (CSD) as the geographic unit of analysis. CSD is a term applying to municipalities or their equivalent and includes six area types:

- Very Small Rural: Pop. < 2,500
- Small Rural: Pop. 2,500 to 29,999
- Very Small Urban: Pop. < 2,500
- Small Urban: Pop. 2,500 to 29,999
- Very Small Mixed: Pop. < 2,500
- Small Mixed: Pop. 2,500 to 29,999

The distribution of households by province and area type is shown in Table 1.1 and Fig. 1-1. There are 5,501 CSDs with populations less than 30,000 containing 3.9 million households. The table of distribution by province and area type shows that the largest number of households is found in small urban areas, followed by small mixed areas, very small rural areas, and finally small rural areas. The rural only portion is approximately 40% and the remaining small urban and mixed areas is 60% of the total 3.9 million households. The fact that there are approximately 1.5 million households in the rural areas is encouraging in that these areas could be best served by the Advanced Satcom.

The table of distribution also shows that the number of households within the CSDs with population less than 30,000 is the highest in Quebec (31.7%), followed by Ontario (26.3%) and British Columbia (11.4%), therefore indicating that about 70% of the target population reside in these three provinces. This is an important factor to be taken into account from a capacity distribution standpoint in a multi-spot beam satellite communications system such as the Advanced Satcom. Such a non-uniform population distribution will have a significant impact in the utilization of the total capacity if no capacity distribution capability is factored into the design of the payload.

Adoption of Infotainment Equipment and Facilities by Province, Area Type, and Income Level.

The adoption of infotainment equipment and facilities by households has been derived from the facilities database of Statscan. Please note that this database has 19,817 records that represent 3.12 million households in rural and small urban areas as opposed to the 3.9 million households represented in the CSD database. Tables 1.2, 1.3, and 1.4 illustrate the significant impact of area type and income level by province on the adoption of infotainment facilities:

- Radios connected to cable and cable TV are available in a higher percentage of households in small urban areas than in rural areas. For example, 81.8% of small urban households have cable TV as compared to 32.3% in rural households.
- Satellite dishes are available in 8.7% of households in rural areas, 3.5% in very small urban areas and 1.9% in small urban areas.
- The percentage of households with CDs, VCRs, camcorders, and home computers increases significantly from the low income to the very high income households.

Table 1.1 Percentage Distribution of Households by Province and Area Type
(based on CSD Database of 3.9 Million Households)

Prov	V. Small Rural	Small Rural	V. Small Urban	Small Urban	V. Small Mixed	Small Mixed	*Total %*
PQ	7.9	2.6	1.0	10.2	0.6	9.4	31.7
ON	3.7	6.2	1.1	6.6	0.1	8.6	26.3
BC	0.8	2.3	0.4	3.7	0.1	4.1	11.4
AB	1.0	2.6	0.5	3.0	0.02	0.3	7.4
NS	0.1	2.3	0.2	1.5		1.5	5.5
SK	3.0		0.7	1.0	0.03		4.8
NB	1.7	1.2	0.2	1.5		1.5	4.6
MB	1.5	0.9	0.2	0.7	0.05	0.2	3.5
NF	1.5	0.3	0.1	0.3	0.1	1.1	3.4
PE	0.6		0.1	0.4			1.1
NT	0.2					0.2	0.4
Total	21.9	18.3	4.5	28.0	1.0	26.2	100.0

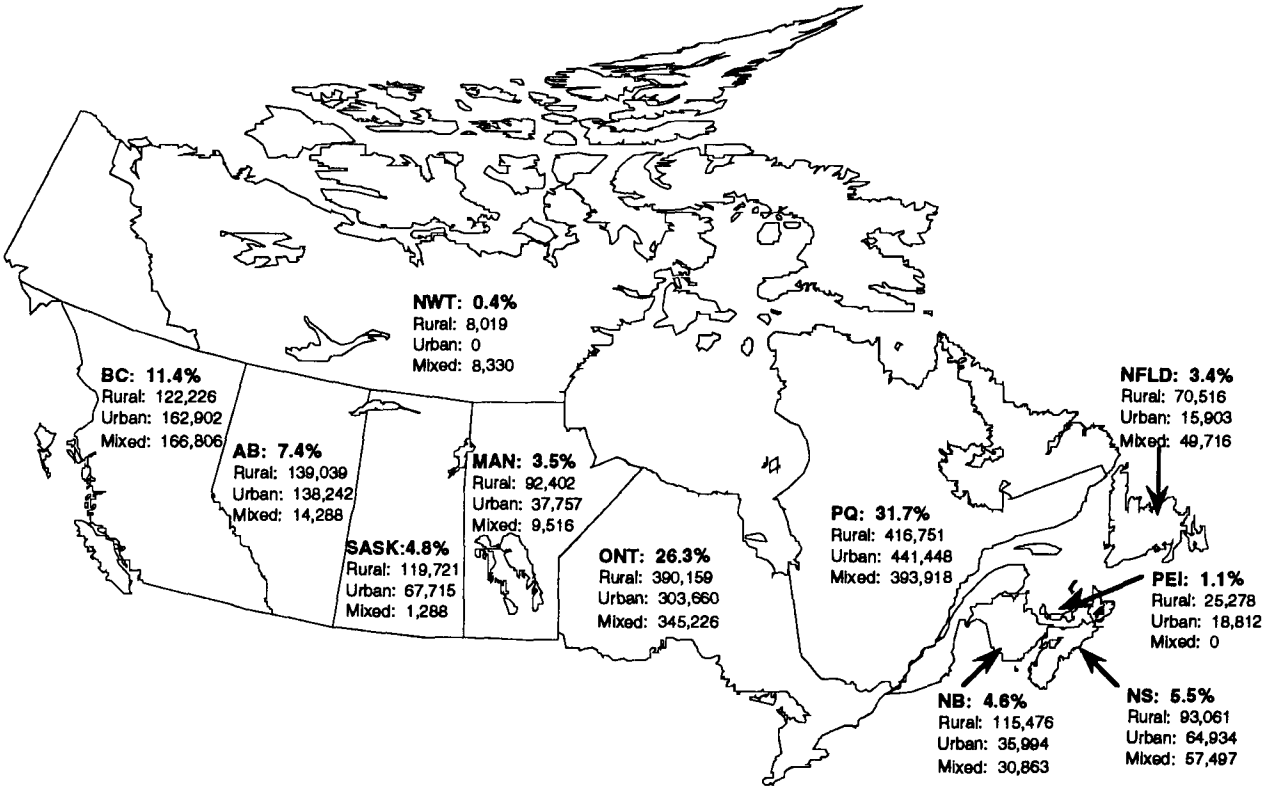

Figure 1-1 Percentage Distribution of Households by Province and Area Types

Table 1.2 Percentage Distribution of Infotainment Equipment and Facilities by Province
(based on Statscan Facilities Database of 3.12 Million Households)

Equipment	NF	PE	NS	NB	PQ	ON	MB	SK	AB	BC	TOTAL
Radios	98.7	99.1	99.5	98.8	99.1	98.3	98.6	98.4	99.0	98.9	98.8
Telephones	97.6	97.3	97.9	98.2	98.8	99.2	98.2	98.0	98.0	98.3	98.5
Colour TVs	97.1	98.2	97.4	97.7	99.2	98.2	96.4	97.7	98.1	96.5	98.0
VCRs	76.6	73.6	75.5	76.9	75.6	78.6	70.4	66.9	82.1	76.9	76.5
Cable TV	75.5	65.4	61.8	60.2	52.6	49.8	39.4	40.9	40.9	67.3	53.4
Cable Radio	72.6	61.9	57.6	55.0	42.7	40.6	35.9	37.8	34.8	48.6	44.8
CD Players	26.2	25.7	22.6	25.1	22.6	28.0	24.3	20.9	30.4	31.8	26.2
Home Computers	14.1	12.5	13.2	12.6	12.7	21.3	16.6	19.5	24.7	22.7	18.0
Camcorders	11.9	8.6	9.4	10.3	11.7	12.4	11.1	10.9	15.6	15.3	12.3
Sat. Dishes	1.7	3.9	5.2	6.7	2.9	6.8	6.1	9.7	9.1	6.5	5.8

Table 1.3 Percentage Distribution of Infotainment Equipment and Facilities by Area Type
(based on Statscan Facilities Database of 3.12 Million Households)

Equipment	V. Small Urban	Small Urban	Rural	Total
Radios	99.0	98.8	98.7	98.8
Telephones	98.4	98.3	98.7	98.5
Colour TVs	98.2	98.3	97.8	98.0
VCRs	76.2	76.6	76.4	76.5
Cable TV	70.6	81.8	32.3	53.4
Cable Radio	60.7	67.3	27.8	44.8
CD Players	24.5	29.0	24.6	26.2
Home Computers	16.5	17.6	18.4	18.0
Camcorders	10.8	12.3	12.6	12.3
Sat. Dishes	3.5	1.9	8.7	5.8

Table 1.4 Percentage Distribution of Infotainment Equipment and Facilities by Income Level
(based on Statscan Facilities Database of 3.12 Million Households)

Equipment	Low	Medium	High	Very High	Total
Radios	98.6	98.7	99.3	99.6	98.8
Telephones	97.8	99.8	99.8	99.9	98.5
Colour TVs	97.3	99.0	99.2	99.3	98.0
VCRs	68.0	86.9	91.6	93.6	76.5
Cable TV	50.3	56.1	58.9	60.6	53.4
Cable Radio	44.2	47.1	46.5	44.5	44.8
CD Players	18.5	31.0	37.9	47.2	26.2
Home Computers	11.0	19.6	29.7	38.8	18.0
Camcorders	7.8	16.6	20.5	22.5	12.3
Sat. Dishes	4.7	7.9	6.6	8.4	5.8

Statistically Significant Characteristics Related to the Adoption of Infotainment Equipment

Cross-tabulations, regression, and segmentation analyses were performed to examine the significant relationships of household characteristics such as total income, age and education to the "potential" of the household, a variable which was derived by adding the number of infotainment equipment and facilities in each household. Three groups of potential have been defined:

- Low: 0-7 equipment and facilities.
- Medium: 8-11 equipment and facilities.
- High: 12 and more equipment and facilities.

Regression and segmentation analyses are powerful statistical techniques used to identify the variables that contribute the most to explaining the variance in the potential of households and are used in the development of the forecast model.

Cross-Tabulation Analysis: Cross-tabulation analysis looks at the potential of households by income level and area type. Total income level is a variable which contributes significantly to a household's likelihood of purchasing infotainment facilities. Table 1.5 shows the distribution of the 3.12 million households of relevance by four income categories:

- Low: under $45,000
- Medium: $45,000-$54,999
- High: $55,000-$69,999
- Very High: $70,000 and above

Table 1.5 Distribution of Potential by Income

Total Income	Potential (%)			
	Low	Medium	High	Total
Low	23.9	27.0	12.0	62.9
Medium	1.9	5.2	4.6	11.7
High	1.3	4.6	6.0	11.9
Very High	1.0	4.4	8.1	13.5
Total	28.1	41.2	30.7	100.0

This table indicates that high potential households are also found in the low income group. For example, 12% of households have high potential despite low income. This is a key factor which has been used in the development of the forecast model.

Area type also has a statistically significant relationship with the household's purchase potential for infotainment equipment and facilities. Table 1.6 provides a distribution of the 3.12 million households into potential groups by the three area types. It shows that although small urban areas have a higher proportion of high potential households, in terms of total households rural areas have a relatively higher percentage in the high potential category.

Table 1.6 Distribution of Potential by Area Type

Area Type	Potential (%)			
	Low	Medium	High	Total
Small Urban	8.4	14.7	13.1	36.2
V. Small Urban	2.3	3.6	2.6	8.5
Rural	17.4	22.8	15.1	55.3
Total	28.1	41.1	30.8	100.0

Regression Analysis: Regression analysis confirms that, when measured simultaneously, variables such as education, area type, number of persons in the household, age, professional occupation, number of adults, and income level have a significant relationship with the potential of households to purchase infotainment equipment and facilities.

Segmentation Analysis: CHAID (Chi-squared Automatic Interaction Detector) is used for segmentation modeling. This is a relatively new statistical application that is useful in dividing a population, e.g., households, into segments that differ with respect to a criterion, which herein is the potential of households to purchase infotainment equipment and services. CHAID divides the population first on the basis of a variable that best predicts low, medium, and high potential. It then subdivides each of these segments based on other predictors.

Based on CHAID segmentation modeling, **income** is the first best predictor variable that would be used to divide the population of households into high, medium, and low potential. Within the four income groups, the next best predictor variables are identified as follows:

- high income: **age;**
- medium income: **number of adults;**
- low income: **number of persons.**

Forecast Model

Having carried out cross-tabulation, regression, and segmentation analysis, we can now choose the most significant variables in the development of the forecast model. Among all the variables listed earlier, "potential" and "income" are chosen as the basis of the forecasting model as shown in Figure 1-2. The adoption levels have been derived using the adoption pattern of the most relevant infotainment equipment such as home computers.

Although analysis has shown that "age", "number of adults", and "number of persons" in the household can be used as predictors and bases for further segmentation, they were not directly used in the forecasting model as their impacts were secondary. The forecast for Module 1 is based on past purchase behaviour of infotainment equipment and facilities only. No information is available in the secondary source with respect to consumer behaviour variables such as interest, awareness, innovation, perceived usefulness of superhighway services, willingness to try services at a reasonable price, etc. Therefore, because of the lack of information on consumer disposition to superhighway services (only in the case of Module 1), the explanatory variable income, which is highly related to the past purchase behaviour, is used to predict the early adopters and innovators.

Estimate of Market Opportunity

Table 1.7 shows an estimate of the market opportunity based on the analysis presented earlier.

Of the 3.12M households, 960,000 are considered high potential which includes 440,000 in the high to very high income category (innovators) and 520,000 in the medium to low income category (early adopters).

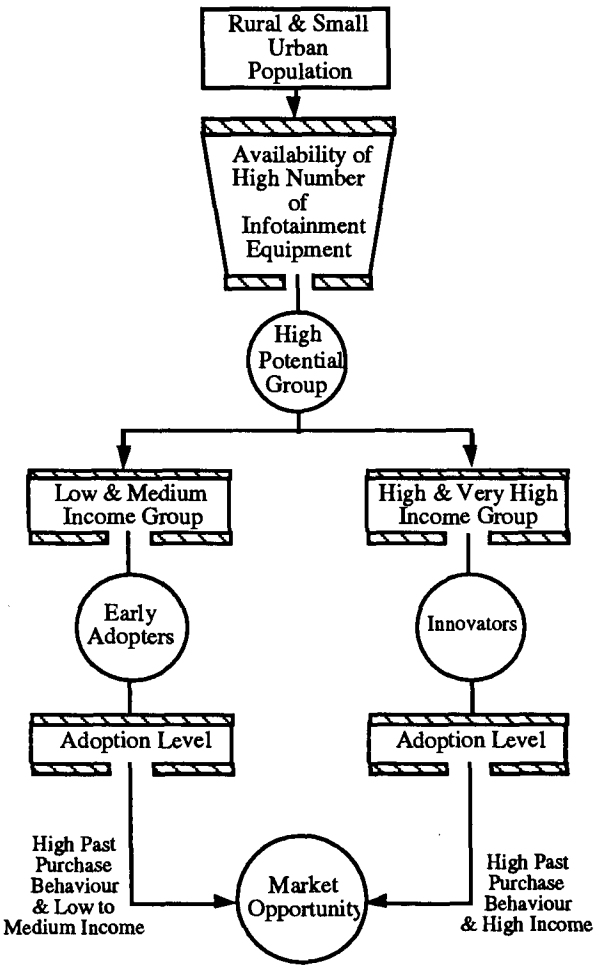

Figure 1-2 Forecast Model 1

Database analysis on the adoption levels of the innovators for relatively recent infotainment innovations such as the home computer and CD players indicates that it is reasonable to assume that 60% (under scenario 1) of the 440,000 innovators, and 40% (under scenario 1) of the 520,000 early adopters will subscribe to the multimedia services, thus amounting to an estimated total of 472,000 households under scenario 1.

Scenario 1 assumes a merging of various technologies and service providers in order to fulfill the needs of the information environment in total. It also assumes that information services to the home are well linked with entertainment services and are affordable.

The forecast under scenario 2 is 236,000 households. Scenario 2 assumes a 30% adoption level for the innovator group and 20% for the early adopter group. Scenario 2 assumes that the information service providers are not united in a single strategic vision and, therefore, products are not as affordable as in Scenario 1 services. Also, the link between information and entertainment is not fully established to provide a total interactive environment.

Sensitivity Analysis: As shown in Table 1.8, sensitivity analysis addresses the extent to which the market opportunity forecasts would change if only rural markets or rural markets with no cable televisions are to be considered. It is noted that in Module 1 the rural markets with no cable TV includes households which do not have cable television either because they do not subscribe to it or because there is no cable television in the area.

Table 1.7 Market Opportunity Estimate

Area Type	High Potential Group	Innovator Group (I)	Early Adopter Group (E)	Adoption Level	Total Market Opportunity
Rural and Small Urban	960,000	440,000	520,000	60%(1)-30%(2) (I) 40%(1)-20%(2) (E)	472,000 (1) 236,000 (2)

(1) = Scenario 1, (2) = Scenario 2

Table 1.8 Market Opportunity Estimate (Sensitivity Analysis)

Area Type	High Potential Group	Innovator Group(I)	Early Adopter Group(E)	Adoption Level	Total Market Opportunity
Rural	471,791	212,812	258,979	60%(1)-30%(2) (I) 40%(1)-20%(2) (E)	230,000(1) 115,000(2)
Rural with no cable	250,837	112,508	138,329	60%(1)-30%(2) (I) 40%(1)-20%(2) (E)	122,000(1) 61,000(2)

(1) = Scenario 1, (2) = Scenario 2

MODULE 2
PRIMARY RESEARCH

Survey Methodology

A stratified sampling plan was developed so that all the provinces and the six area types were represented. The sample was weighted so that each response could be appropriately extrapolated to the number of households that it represents in the CSDs relevant to the study. In other words, once the sample was weighted, the distribution within each area type in a province became identical to that of the distribution of households in the population of 3,956,653 households in the relevant CSDs.

Awareness and Interest

Awareness of the infotainment superhighways to the home was found to be significantly related to education, province, and income levels. The overall survey response rate for all of Canada was 31.8%. Of the 1,007 respondents:

- 54.9%: aware of developments
- 51.1%: moderately to greatly interested.
- 44.4%: very interested.

Perceived Usefulness of the Services

The respondents were asked their opinion on how useful the future infotainment services appeared to their household. The results, reflecting the useful and very useful responses, are:

- Combined services 65.3%
- Information services 64.0%
- Transactional services 61.1%
- Home business services 46.6%
- Entertainment services 41.3%

Table 2.1 shows that the interest in the home business services is at higher levels in those households with a home office and is at the highest levels in households with a home business. Of the 1,007 households surveyed, it is noted that 8.4% had a home office and 13.0% had a home business.

Table 2.1 Usefulness of Home Business Services

	Not Useful	Somewhat Useful	Useful	Very Useful	Total
No H-Off./ Bus.	34.1	22.9	21.0	22.0	100.0
H-Office	9.7	26.8	27.5	36.0	100.0
H-Bus.	7.2	20.1	35.1	37.6	100.0

Affordability as Perceived by Consumers

Monthly Charges: In order to arrive at an understanding of what consumers consider to be a reasonable price for the infotainment services to be delivered on the electronic superhighway, questions pertaining to a household's chance of trying the described services under four different price scenarios were asked. Responses were rated based on percentages of people with medium (3-7) to high (8-10) grouped chance scores, as well as average scores of all respondents, on a 10 point scale where 0 stood for no chance and 10 stood for a 100% certainty of trying the service as shown in Table 2.2.

Table 2.2 Chances of Trying the Services

Price Scenarios	Percentage	Average Scores out of 10
The right price	80.7 %	5.5
$40 per month	71.0%	5.3
$60 per month	52.5%	3.4
$100 per month	not well received	1.8

Tables 2.3, 2.4, and 2.5 provide a distribution by grouped scores representing the low, medium, and high chances of trying the services for various price levels and Figure 2-1 provides the average chance of trying the service calculated among all respondents.

Table 2.3 Chances of Trying the Services at a Reasonable Price

Chances of Trying	Numbers	Percent
Low (0-2)	185	19.4
Medium (3-7)	494	51.7
High (≥8)	277	29.0

Table 2.4 Chances of Trying the Services at $40 Per Month

Chances of Trying	Numbers	Percent
Low (0-2)	270	29.0
Medium (3-7)	336	36.1
High (≥8)	326	34.9

Table 2.5 Chances of Trying the Services at $60 Per Month

Chances of Trying	Numbers	Percent
Low (0-2)	446	47.5
Medium (3-7)	354	37.7
High (≥8)	138	14.8

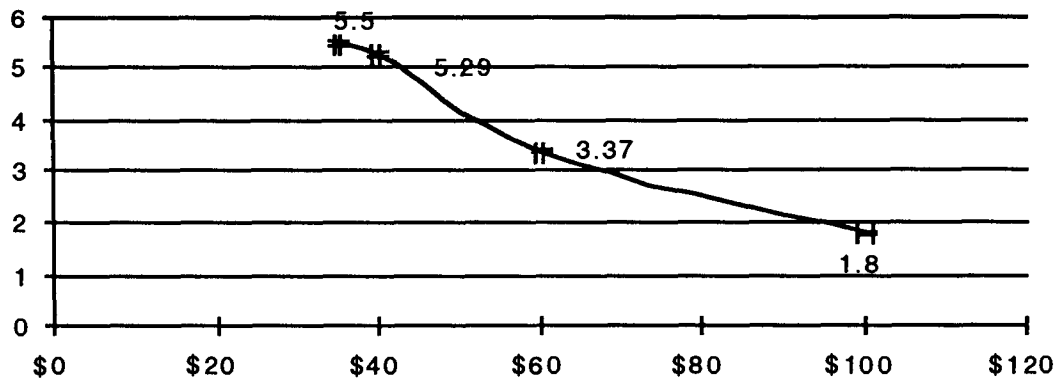

Figure 2-1 Comparison of Average Chances of Trying at Different Price Points

An average monthly charge of $33.50 was deemed reasonable by the respondents. Based on the responses, it is concluded that $35-$40 per month would be affordable by consumers in the rural and small urban areas of Canada. In both cases, respondents wanted the monthly charge for the infotainment services to cover cable television charges. The price point of $100 per month was not well received. Assuming an average monthly charge of $25 for cable television, representing entertainment services, a monthly charge of $10-$15 for the information services seems affordable.

Satellite Dish: The respondents were asked to consider a situation wherein they had to purchase a satellite dish to obtain the services. 48.3% of the respondents found a satellite dish between $1,000 and $1,400 as acceptable.

Potential of Households to Subscribe to the Infotainment Services

A variable which is herein termed ***potential*** was created by adding the responses measuring awareness and interest of respondents, perceived usefulness of each of the four types of infotainment services, perceived chances of the households trying the service at a monthly charge of $35-$40, and the innovativeness level of the respondents measured subjectively through the respondents' perception of how readily they buy or try high technology equipment and services. Based on the scores obtained, respondents were grouped into three potential categories:

- Low: score of 0-13.
- Medium: score of 14-20.
- High: score of 21 and above.

Table 2.6 provides a distribution of respondents by potential.

Table 2.6 Distribution of Respondents by Potential

	Potential to Subscribe			
Respondent	Low (0-13)	Medium (14-20)	High (21 & ab)	Total
Numbers	247	466	294	1007
%	24.5	46.3	29.2	100

The relationship between potential as defined in Module 2 (a measure of future disposition) and the availability of infotainment equipment in the household (a measure of past purchase behaviour) is especially important. The latter refers to items such as VCRs, colour television sets, large screen televisions, compact disk players, camcorders, laser video disk players, radios, radios hooked to cable, home computers, number of telephones, satellite dishes, cable television outlets, and pay movie channels. The numbers provided for the items listed above were added and the respondents were divided into three groups:

- Low: 0-8 equipment and facilities.
- Medium: 9-13 equipment and facilities.
- High: 14 and more equipment and facilities.

The distribution of households by the infotainment equipment and facilities groups and the potential to subscribe are shown in Tables 2.7 and 2.8. Table 2.8 shows that of the households with a high number of equipment and facilities available, 47.2% have high potential and only 11.5% have low potential. By contrast, of the households with a low number of equipment and facilities, 41.3% have low potential and only 13.9% have high potential. Again, this is a key factor that is used in the development of the forecast model.

Table 2.7 Total Distribution of Potential by Infotainment Equipment Availability

	Potential to Subscribe (%)			
Infotainment Equipment	Low (0-13)	Medium (14-20)	High (21 & ab)	Total
Low	11.2	12.2	3.7	27.1
Medium	10.1	22.6	12.4	45.1
High	3.2	11.5	13.1	27.8
Total	24.5	46.3	29.2	100

Table 2.8 Row Distribution of Potential by Infotainment Equipment Availability

	Potential to Subscribe (%)			
Infotainment Equipment	Low (0-13)	Medium (14-20)	High (21 & ab)	Total
Low	41.3	44.8	13.9	100
Medium	22.4	50.2	27.4	100
High	11.5	41.3	47.2	100
Total	24.5	46.3	29.2	100

Table 2.9 indicates that the highest number of high potential households are located in small urban areas, followed by small mixed areas, small rural areas and very small rural areas. It is important to note that 11.8% of the 3.9 M households are in rural areas and have high potential.

Table 2.9 Percentage Distribution of Potential by Area Type

Area Type	Low (0-13)	Medium (14-20)	High (21 and ab)	Total
Very Small Rural	5.9	10.3	5.8	22.0
Small Rural	4.3	8.0	6.0	18.3
Very Small Urban	1.4	2.7	0.4	4.5
Small Urban	7.0	12.5	8.5	28.0
Very Small Mixed	0.2	0.6	0.2	1.0
Small Mixed	5.7	12.2	8.3	26.2
Total	24.5	46.3	29.2	100

Regression Analysis: The results of the regression analysis were similar to those of Module 1 indicating that there is a significant relationship between the potential of households to subscribe to infotainment services and the availability of infotainment equipment, education, age, and income level.

Segmentation Analysis: A CHAID segmentation analysis was undertaken to segment the low, medium and high potential respondents by significant predictor variables relating to demographic characteristics. The analysis indicated that age, education, current infotainment available to the household, and occupation were significant parameters which influenced the development of the forecast model.

Forecast Model: Among all the variables listed earlier, "potential" (i.e., future disposition to superhighway electronic services), and "availability of medium (early adopters) to high (innovators) number of infotainment equipment in the household", are chosen as the basis of the forecasting model as shown in Figure 2-2. Adoption levels are as defined in Module 1.

The forecast for Module 2 defines early adopters and innovators on the basis of primary information on consumer disposition to future infotainment services as well as their past purchase behaviour with respect to infotainment equipment and facilities. Information pertaining to the future purchase decisions of consumers with respect to infotainment services has been obtained through primary research, e.g., interest, awareness,

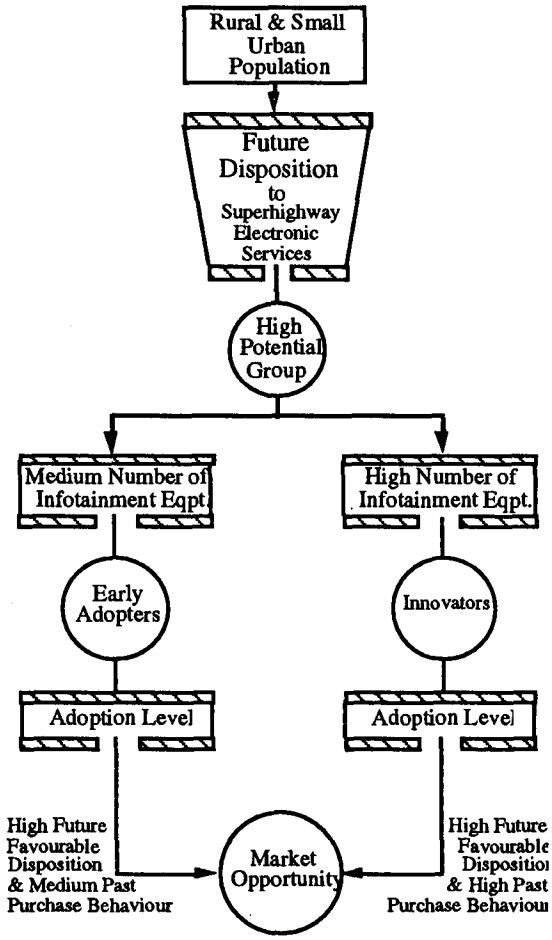

Figure 2-2 Forecast Model 2

innovativeness, perceived usefulness of superhighway electronic services, willingness to try services at a reasonable price, etc. Given a complete profile of past and possible future behaviour, the forecasting model has no need for independent variables to define early adopters and innovators. For example, age and education, which are significant explanatory variables for future consumer disposition, are not directly used in the forecasting model. Similarly, income, which is a significant explanatory variable for past purchase behaviour, is not directly used in the forecast model.

Estimate of Market Opportunity

Table 2.10 shows an estimate of the market opportunity based on primary research studies.

The market opportunity estimates presented in Module 2 are further enhancements to the estimates made in Module 1. Of the 1,156,352 households with high favourable future disposition, 517,000 have high past purchase behaviour (innovators), and 490,000 have medium past purchase behaviour (early adopters). Considering adoption levels of 60% for the innovator group and 40% for the early adopter group leads to a total market opportunity of approximately 500,000 households under scenario 1. Taking 30% and 20% adoption levels for innovators and early adopters respectively gives a market opportunity of approximately 250,000 households under scenario 2. Scenarios 1 and 2 are as defined in Module 1.

As shown in Table 2.11, the sensitivity analysis indicates the extent to which market opportunity forecasts would change if only rural markets or rural markets with no cable television are to be considered.

Table 2.10 Market Opportunity Estimate

Area Type	High Potential Group	Innovator Group (I)	Early Adopter Group (E)	Adoption Level	Total Market Opportunity
Rural and Small Urban	1,156,352	517,000	490,000	60%(1)-30%(2) (I) 40%(1)-20%(2) (E)	506,200(1) 253,100(2)

(1) = Scenario 1; (2) = Scenario 2

Table 2.11 Market Opportunity Estimate (Sensitivity Analysis)

Area Type	High Potential Group	Innovator Group (I)	Early Adopter Group (E)	Adoption Level	Total Market Opportunity
Rural	467,411	191,524	275,887	60%(1)-30%(2) (I) 40%(1)-20%(2) (E)	225,300(1) 112,600(2)
Rural with no Cable TV	151,337	58,024	93,313	60%(1)-30%(2) (I) 40%(1)-20%(2) (E)	72,100(1) 36,000(2)

(1) = Scenario 1; (2) = Scenario 2

Conclusion

Based on both the secondary and primary research studies, the potential market opportunity for the multimedia residential services in the rural and small urban areas is estimated to be about 500,000 households. This is an indication of a sustainable market that can be served by the Advanced Satcom if it were used by telcos as a cost-effective extension to their terrestrial fibre optics system.

It is assumed that Advanced Satcom will be cost-effective and competitive with cable for low density areas. It is also assumed that information services are well linked in an affordable manner with entertainment services in a merging of various technologies and service providers in order to fulfill the needs of information environment in total.

As stated in the Abstract section of this paper, the potential market opportunity for the Advanced Satcom in the rural and small urban areas is not just limited to residential services. The potential market can also include (although not addressed in this paper) wideband mobile, distance education to schools, health care, government, and business services.

In addition to the potential for a sustainable market in the rural and small urban areas, the Advanced Satcom can also offer directly to end users in urban areas a full range of interactive multimedia services by means of small, low-cost consumer terminals. Advanced Satcom can be offered on a temporary basis to urban areas which are not yet fully served by fibre.

Acknowledgement

The authors wish to acknowledge the contributions of their colleagues at Telesat, and the support and encouragement that was provided by colleagues at Industry Canada, the Communications Research Center, and Spar Aerospace. Ms. Vasantha Narasimhan conducted the research and prepared the study reports.

Appendix Index

K/Ka-Band Channel Characterization for Mobile Satellite Systems

Deborah S. Pinck (pinck@zorba.jpl.nasa.gov)
Michael Rice (mdr@ee.byu.edu)
Jet Propulsion Laboratory/California Institute of Technology
4800 Oak Grove Blvd.
Pasadena, CA 91109
PHONE: (818) 354 - 8041 FAX: (818) 354 - 4643

ABSTRACT

NASA's Advanced Communications Technology Satellite provides an ideal spaced-based platform for the measurement of K- and Ka-band propagation characteristics for land mobile satellite applications. This paper reports and compares results from pilot tone tests at both K- and Ka-band in three environments: lightly shadowed suburban, moderately shadowed suburban, and heavily shadowed suburban. The results show that K- and Ka-band pilot tones experience significant multipath and fading effects with similar characteristics. Thus, both K- and Ka-band channels would require substantial coding or diversity techniques to realize reliable land mobile satellite communications in the suburban environment.

1. Introduction

Mobile satellite systems allow truly ubiquitous wireless communications to users anywhere and anytime. A mobile terminal is affected by shadowing and multipath interference caused by roadside obstacles and terrain conditions. The degree of shadowing depends on the length of the path which intersects the roadside obstacles. Many parameters effect the intersecting path including: elevation angle, nature and geometry of the obstacle (e.g., tree, utility pole), distance between the road and the obstacle, lane and direction of travel, and road surface conditions (e.g., rolling/flat, straight/curved). In addition, the antenna pattern, the environment, the season, and the carrier frequency also affect the degree of shadowing.

Propagation experiments at UHF (850 MHz) and L- (1.5 GHz) bands have quantified the shadowing and multipath interference effects [1, 2, 3] for these bands. NASA's Advanced Communications Technology Satellite (ACTS) provides a stationary platform ideally suited to the measurement of mobile propagation effects at K-(20 GHz) and Ka-(30 GHz) bands. Field tests conducted during the first 7 months of 1994 using JPL's ACTS Mobile Terminal (AMT) provide channel characterization data for these channels. Recently published results from AMT experiments [4, 5] and from the ACTS Mobile Propagation Campaign [6, 7] have provided insight into the K-band mobile satellite channel. This paper reports on the results of AMT experiments at Ka-band.

2. Experimental Aspects

1. *System Configuration*

The system configuration is illustrated in Figure 2. The basic features of the system include

- The fixed station or Link Evaluation Terminal (LET) located at the NASA Lewis Research Center in Cleveland, Ohio.
- ACTS, operating in the microwave switch matrix mode (MSM), i.e., as a bent pipe repeater, connects the fixed station with the mobile unit. The satellite was configured to provide two way communication between Pasadena, California (in the Southern California spot beam) and the LET (in the Cleveland spot beam).
- The AMT, a breadboard mobile terminal designed as a testbed for proof-of-concept designs using ACTS (see [8] for a detailed description).

The *forward channel* originated at the fixed station with a 29.634 GHz pilot tone. This pilot tone was received by ACTS, mixed to the downlink frequency of 19.914 GHz, and transmitted on the Southern California spot beam. The forward channel offered a composite C/N_0 of 55.63 dB-Hz and was the basis for the K-band results reported in [4, 5]. The *return channel* originated at the AMT with a 29.634

GHz pilot tone which was uplinked to ACTS, mixed to 19.194 GHz, and downlinked to the fixed station. The available C/N_0 on the return channel was 53.58 dB-Hz. The return channel formed the basis for the Ka-band results reported in this paper.

Typical Doppler shifts at this frequency (due to car motion) can be as high as 3kHz, with a rate up to 250 Hz/sec. In addition, uncertainties on the various oscillators along the link can accumulate about 2 kHz of frequency offset. The Doppler and frequency uncertainties can therefore be a large fraction of the data rates. In the AMT, the Doppler shift present on the pilot was tracked at the mobile terminal, translated in frequency, and used to pre-compensate (appropriately pre-shift) the data channel on the return link.

2. Antenna Tracking System

The AMT is equipped with a small, high gain reflector antenna which tracks the satellite signal in azimuth for a fixed elevation angle[1] [9]. The antenna is mechanically steered and acquires/tracks the satellite signal over the entire 360° of azimuth with a pointing error less than 0.2°. Vehicle turn rates of up to 45 degrees/second can be accommodated. The antenna provides an uplink EIRP of 22 dBW over a bandwidth of 300 MHz. The 3 dB beamwidth is ±9° in elevation and ±6° in azimuth. The reflector resides inside an ellipsoidal water-repelling radome with an exterior base diameter of 9 inches and a height of 3.5 inches.

The antenna pointing system enables the antenna to track the satellite for all practical vehicle maneuvers. The antenna is mated with a simple, yet robust, mechanical steering system. The antenna is smoothly dithered about boresite by one degree at a rate of 2 Hz. The pilot signal strength measured through this dithering process is used to compliment the inertial information derived from a simple turn rate sensor. This combination maintains the antenna pointing at the satellite even if the satellite is shadowed for up to ten seconds.

3. Data Acquisition System

Both the AMT and the fixed station were equipped with identical data acquisition systems (DAS). The DAS continuously recorded parameters important for link characterization. At the AMT, the DAS recorded forward channel parameters. The measurements included IF pilot tone level, noise calibration levels, mobile velocity (speed and direction), antenna pointing direction, mobile location, time, video images of the ACTS-AMT link, and an audio record documenting the test runs. At the fixed station, the DAS recorded return channel parameters such as the IF pilot tone level and noise calibration levels.

The IF pilot tone used to characterize the channel was filtered using a 17 kHz bandpass filter as shown in Figure 1. The filtered IF pilot tone was processed by a phase-locked loop and non-coherent power detector. The phase-locked loop generated in-phase and quadrature-phase voltage levels in a 1.5 kHz bandwidth. The non-coherent power detector generated voltage levels proportional to pilot power in a 100 Hz bandwidth. These signals were sampled at a rate of 4000 samples/second and were recorded on 5 Gbyte Exabyte tapes for off-line evaluation.

The time, vehicle velocity, and position were derived from an on board GPS system and updated at 10 Hz (time) and 100 Hz (velocity and position).

3. Test Runs

The configuration used for these experiments was slightly different from typical mobile propagation experiments. Normally, the transmitter is stationary while the receiver is mobile. In this case, the transmitter was mobile while the receiver was stationary. Data was collected solely from the return channel. The fact that the transmitter was mobile had no impact on the results of the experiment. All ACTS propagation results reported to date have been for the K-band link (19.914 GHz); in this case, the results are for Ka-band (29.634 GHz). As will be seen in later sections, results indicate that K- and Ka-band experience almost identical effects.

Data was collected in a variety of locations which may be broadly classified in three categories: lightly shadowed suburban, moderately shadowed suburban, and heavily shadowed suburban. These categories are somewhat subjective; however, the criteria used to label the road were as follows: 1) lightly shadowed roads had infrequent, partial blockage to the satellite, 2) moderately shadowed roads had occasional, complete blockage to the satellite, and 3) heavily shadowed roads had frequent, complete blockage to the satellite.

All tests were conducted in Southern California

[1]The elevation angle for experiments in the Pasadena area is 46°.

which does not experience large seasonal variations. Therefore, the propagation effects due to foliage do not change throughout the year.

1. Lightly Shadowed Suburban Environment

Orange Grove Boulevard in Pasadena, California, is a broad, level thoroughfare with trees lining both sides of the road. The trees lining this route are primarily Southern Magnolia with Fan Palm and Date Palm trees spaced 50 meters apart. The road is laid out in a north-south direction. With the satellite to the south-east, the western most lane (right-hand, south bound lane) presented the best look-angle to the satellite. In this lane, the AMT antenna boresite to the ACTS line-of-sight path just barely skirted the tops of the Palm trees on the east side of the road and, generally did not intersect the foliage of the Magnolia trees. This environment is characterized as lightly shadowed. A representative time series of the pilot power transmitted by the AMT and received at the fixed station is shown in Figure 3. The solid line represents the one second average of the 4000 samples. In addition, vertical dashed lines are displayed which connect the maximum and minimum values of the pilot power during the one second interval.

The statistics of the shadowing/fading are summarized by a histogram of the cumulative distribution of the pilot power received at the fixed station. The histogram of the run shown in Figure 3 is represented by the solid line in Figure 4. Also shown is the histogram of the cumulative distribution of the pilot power received by the AMT (at K-band) at the same time (this is the dashed line). The solid line models the 30 GHz land mobile channel where it is seen that the 1% fade level for Ka-band is 8 dB. In other words, 1% of the time the pilot signal is worse than 8 dB below the reference level. This is essentially equal to that at K-band.

2. Moderately Shadowed Suburban Environment

The center lanes of Orange Grove Boulevard represent a moderately shadowed suburban environment. Figure 5 shows the time series for a test run on the eastern center lane (left-hand, north bound lane). In this case, significant shadowing resulted from the intersection of the line-of-site path between AMT and ACTS by the Magnolia trees on the eastern side of the road. In addition, periodic blockage by the trunks of the Palm trees was observed. The statistics of the shadowing/fading are summarized by the histogram in Figure 6 where it is seen that the 1% fade level for Ka-band is 26 dB which is 1 dB better than the land mobile satellite channel at 20 GHz.

An interesting observation here is different lanes on the same road exhibit different fading levels. In this case, the difference in 1% fade levels is 18 dB which represents a remarkably wide variation due to lane diversity.

3. Heavy Shadowed Suburban Environment

To obtain results from a heavily shadowed suburban environment, a route along Grand Avenue in Pasadena, was selected. Grand Avenue is a narrow two lane road with many turns and runs in a generally north-south direction. The road is lined with a heavy mixture of Coastal Live Oak, Southern Magnolias, and Holly Oak. In many places along the route, the tree canopies completely covered the road blocking any direct line-of-site path between AMT and ACTS. This environment is creates severe shadowing/fading as illustrated in Figure 7. The statistics of the shadowing/fading are summarized by the histogram illustrated in Figure 8 where it is seen that the 1% fade level for Ka-band is well in excess of 30 dB (perhaps even as high as 45 dB). Results for the simultaneous return channel at K-band are also shown and are essentially equivalent.

4. Analysis

Each of the histograms illustrated in Figures 4, 6, and 8 displays the same characteristic shape. The slope between the reference level (0 dB) and 2 dB below the reference level is steep. This is characteristic of Ricean fading which occurs when reflected copies of the transmitted pulse accompany the line-of-sight signal. This steep curve is followed by a "knee" which forms the transition between the Ricean characteristic and the shadowed fading characteristic. Shadowed fading contributes a shallower characteristic to the curve which indicates that the combination of signal blockage (shadowing) and multipath interference (shadowed fading) is severe. The combination of these two characteristics suggests a "time share" between Ricean fading and shadowed fading as observed at L-band [1, 2] and K-band [4, 6, 7].

A summary of the results for all runs conducted on 9 July 1994 is included in Table 1.

5. Conclusions

The results of the AMT Ka-band mobile propagation field tests show that the shadowing and fading processes are essentially identical for both K- and Ka-band frequencies and for the mobile transmitter and receiver. As such, the conclusions and results for K-band apply to Ka-band frequencies as well.

It may be possible to design link margins to provide reliable service for the lightly shadowed suburban environment at Ka-band. However, for areas with moderate and heavy shadowing, the link margin required to realize reliable communications with 99% availability is excessive (26 dB for moderate shadowing, and greater than 30 dB for heavy shadowing). An alternate approach would be to use shadowing/fading countermeasures (e.g., interleaved error control coding and antenna diversity). Such mitigation techniques, necessary for reliable Ka-band mobile communication within a suburban environment, are currently being considered within the NASA program.

6. Acknowledgments

The authors are grateful to Mr. Jim Mosa, Forestry Inspection Foreman of the City of Pasadena, and Mr. Steve Jessup, C.G.C.S. Brookside Golf Course, for their assistance in identifying the foliage along the experiment routes.

The work described in this paper was carried out at the Jet Propulsion Laboratory, California Institute of Technology, under contract with the National Aeronautics and Space Administration.

References

[1] E. Lutz, D. Cygan, M. Dippold, F. Dolainsky, and W. Papke. The land mobile satellite communication channel — recording, statistics, and channel model. *IEEE Transactions on Communications*, COM-40:375–386, May 1991.

[2] J. Castro. Statistical observations of data transmission over land mobile satellite channels. *IEEE Journal on Selected Areas in Communications*, 10:1227–1235, October 1992.

[3] H. Hase, W. Vogel, and J. Goldhirsh. Fade-durations derived from land-mobile-satellite measurements in Australia. *IEEE Transactions on Communications*, COM-39:664–668, May 1991.

[4] M. Rice and D. Pinck. K-band mobile satellite propagation characteristics using ACTS. In *Proceedings of the URSI National Radio Sciences Meeting*, page 207, Boulder, CO, January 1995.

[5] D. Pinck and M. Rice. K/Ka-band channel characterization for mobile satellite systems. In *Proceedings of the IEEE Vehicular Technology Conference*, Chicago, IL, July 1995.

[6] J. Goldhirsh and W. Vogel. ACTS mobile propagation campaign. In F. Favarian, editor, *Proceedings of the Eighteenth NASA Propagation Experimenters Meeting (NAPEX XVIII)*, pages 135–150, Vancouver, British Columbia, 1994. NASA, Jet Propulsion Laboratory. JPL Publication 94-19.

[7] J. Goldhirsh and W. Vogel. ACTS 20 GHz mobile propagation measurements. In *Proceedings of the URSI National Radio Sciences Meeting*, page 206, Boulder, CO, January 1995.

[8] K. Dessouky and T. Jedrey. The ACTS mobile terminal (AMT). In *Proceedings of the AIAA Conference*, Washington, DC, November 1992.

[9] A. Densmore and V. Jamnejad. A satellite-tracking K- and K_a-band mobile vehicle antenna system. *IEEE Transactions on Vehicular Technology*, VT-42:502–513, November 1993.

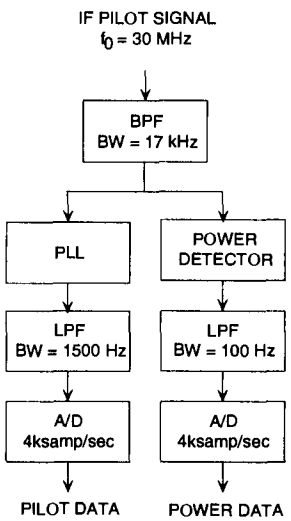

Fig. 1. Pilot Tone Signal Processing

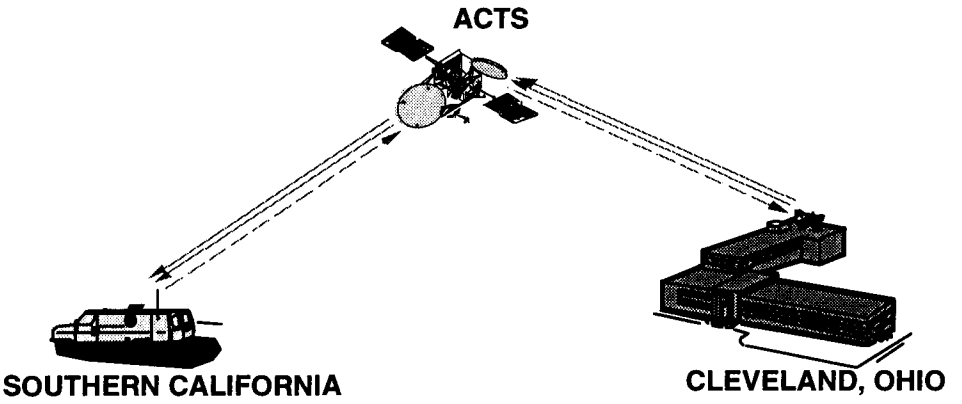

Fig. 2. System Configuration for AMT Propagation Experiments

Table 1. Summary of AMT Test Runs 9 July 1994 (Category 1 = lightly shadowed suburban environment, Category 2 = moderately shadowed suburban environment, Category 3 = heavily shadowed suburban environment).

		1% FADE LEVEL		3% FADE LEVEL		5% FADE LEVEL	
ROUTE	CATEGORY	K-band	Ka-band	K-band	Ka-band	K-band	Ka-band
Orange Grove Blvd. south bound	1	8 dB	9 dB	1 dB	1 dB	1 dB	1 dB
Grand Ave. north bound	3	>> 30 dB	>> 30 dB	>> 30 dB	>> 30 dB	>> 30 dB	>> 30 dB
Orange Grove Blvd. north bound	3	>> 30 dB	>> 30 dB	>> 30 dB	>> 30 dB	> 30 dB	> 30 dB
Grand Ave. south bound	3	> 30 dB	> 30 dB	26 dB	26 dB	19 dB	19 dB
Orange Grove Blvd. north bound	2	27 dB	26 dB	17.5 dB	17.5 dB	12.5 dB	12.5 dB
Arroyo Blvd. south bound	3	>> 30 dB	>> 30 dB	>> 30 dB	>> 30 dB	>> 30 dB	>> 30 dB
Arroyo Blvd. north bound	3	>> 30 dB	>> 30 dB	>> 30 dB	>> 30 dB	>> 30 dB	>> 30 dB

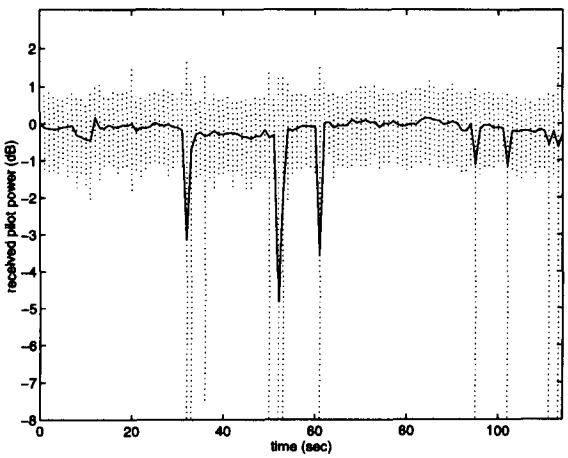

Fig. 3. Pilot Power (dB) vs. Time For A Lightly Shadowed Suburban Environment

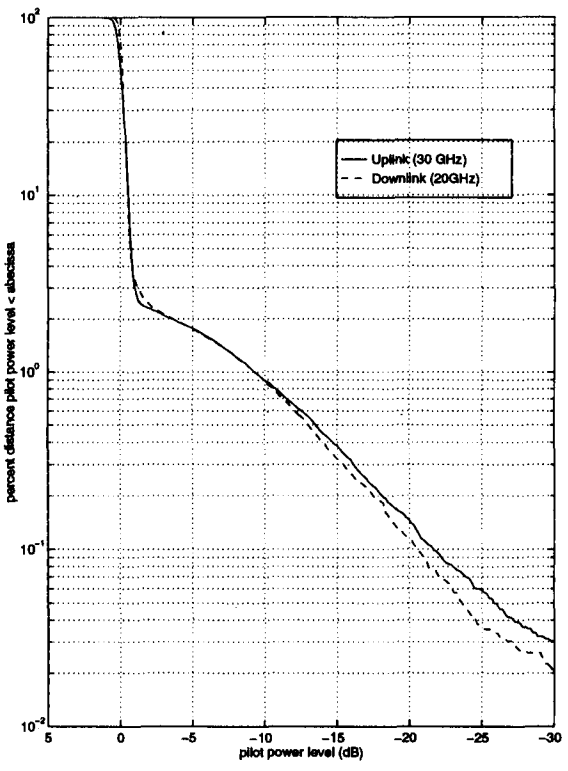

Fig. 4. Histogram of the Cumulative Distribution of the Pilot Power for a Lightly Shadowed Suburban Environment

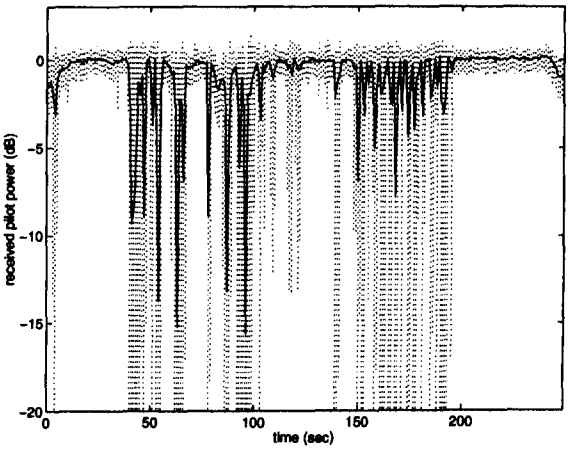

Fig. 5. Pilot Power (dB) vs. Time For A Moderately Shadowed Suburban Environment

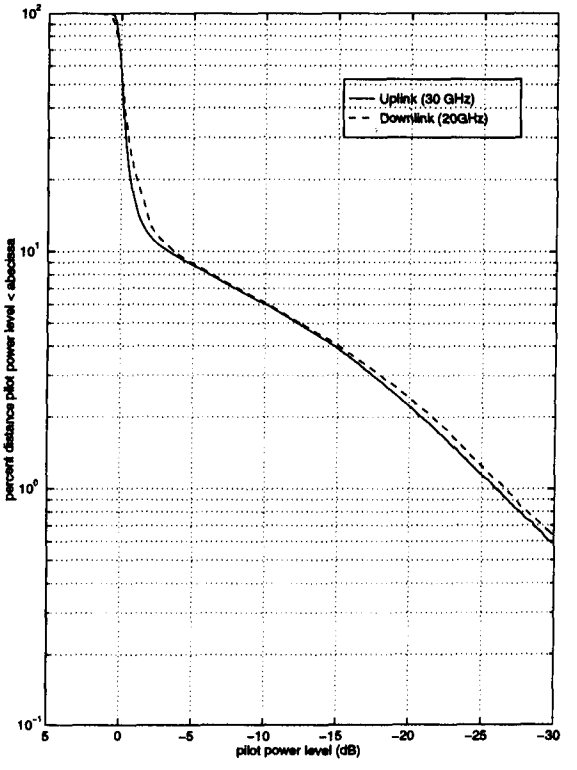

Fig. 6. Histogram of the Cumulative Distribution of the Pilot Power for a Moderately Shadowed Suburban Environment

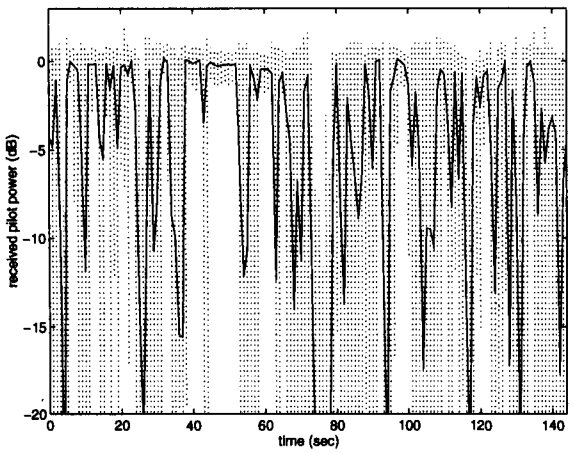

Fig. 7. Pilot Power (dB) vs. Time For A Heavily Shadowed Suburban Environment

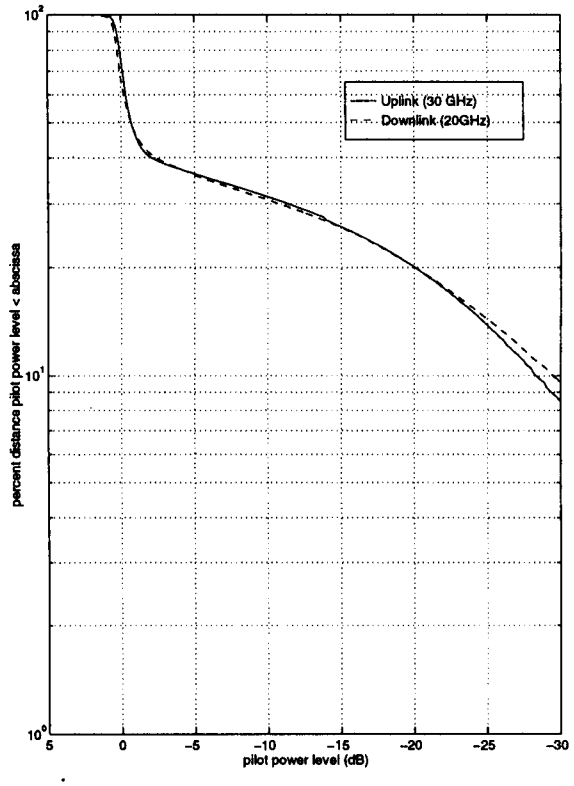

Fig. 8. Histogram of the Cumulative Distribution of the Pilot Power for a Heavily Shadowed Suburban Environment

Concept and Implementation of the Globalstar Mobile Satellite System

Dr. Joel Schindall
Globalstar L.P., San Jose, California,USA Tel: 408-473-6201, Fax: 408-473-5040
Based in part on earlier papers by
Ming Louie, Anthony Navarra, Bob Wiedeman and Paul Monte, Globalstar L.P.;
and Klein Gilhousen, Andrew Viterbi, Steve Carter and Len Schiff, Qualcomm;
and Denis Rouffet, Alcatel

Abstract

Globalstar is a satellite-based mobile communications system which provides quality wireless communications (voice and/or data) anywhere in the world except the polar regions.

The Globalstar system concept is based upon technological advancements in Low Earth Orbit (LEO) satellite technology and in cellular telephone technology, including the commercial application of Code Division Multiple Access (CDMA) technologies.

The Globalstar system uses elements of CDMA and Frequency Division Multiple Access (FDMA), combined with satellite Multiple Beam Antenna (MBA) technology and advanced variable-rate vocoder technology to arrive at one of the most efficient modulation and multiple access systems ever proposed for a satellite communications system. The technology used in Globalstar includes the following techniques in obtaining high spectral efficiency and affordable cost per channel:

1. CDMA modulation with efficient power control.
2. High efficiency vocoder with voice activity factor
3. Spot beam antenna for increased gain and frequency reuse
4. Weighted satellite antenna gain for broad geographic coverage
5. Multisatellite user links (diversity) to enhance communications reliability
6. Soft hand-off between beams and satellites.

Initial launch is scheduled in 1997 and the system is scheduled to be operational in 1998. The Globalstar system utilizes frequencies in L-, S- and C-bands which have the potential to offer worldwide availability with authorization by the appropriate regulatory agencies.

1. Introduction

The Globalstar system consists of three major segments: space segment, ground segment, and user terminal segment. Space Systems/Loral, with a number of overseas partners, is responsible for the space segment. Qualcomm is responsible for the major part of the ground and user segments. Each segment incorporates recent technological innovations, and the segments work together to achieve superior system performance.

The space segment consists of 48 satellites that act as "bent pipes" to relay the telephone signal to a local terrestrial gateway. From there, the signal is carried over existing telephony channels.

The ground segment can be thought of as a cellular telephone base station which utilizes the satellite relay to greatly extend its coverage area. CDMA technology is used to maximize the system capacity. The ground segment also includes satellite monitoring and control functions.

The user terminal segment involves the design and manufacture of fixed and mobile user handsets. Dual-mode handsets, which combine the local cellular standard with a Globalstar capability, will also be developed.

2. Basic Concepts

A number of very basic principles form the foundation of the Globalstar approach.

1. Keep it simple (and affordable!)
2. Minimize risk — use proven technologies, minimize satellite hardware
3. Combine technologies synergistically so the whole is greater than the sum of its parts
4. Maximize spectral efficiency
5. Utilize existing communication infrastructure and service providers as much as possible

"Keep it simple (and affordable!)" permeates the design. Perhaps it's a bit difficult to think of a 48 satellite system with multibeam antennas and sophisticated CDMA modulation as "simple." However, Globalstar has been configured to employ proven concepts and straightforward implementation. For example, the satellite orbits are chosen to minimize the number of satellites required by distributing the coverage proportional to population density of the earth. The "bent pipe" transmission path

allows the switching and routing to take place on the ground which reduces satellite weight, risk and cost. Reduced satellite weight, in turn, lowers launch costs. Interface with existing terrestrial telephony systems avoids the need for independent long distance routing and utilizes existing infrastructure for billing and customer support.

"Minimize risk" means sticking to proven technologies and keeping as much hardware and software as possible on the ground. Note that use of proven technologies doesn't mean that the most modern technologies are not used. In fact, some very advanced technologies are key to the system design. Each of them, however, has been deployed and proven. For example, the satellite uses sophisticated multibeam antennas to provide isoflux coverage of the earth below, but they are based on proven Space Systems/Loral (SS/L) designs. The RF communication link is based on Qualcomm CDMA designs which have a long heritage in government and satellite communication systems and have been deployed in over a dozen cities.

"Combine technologies synergistically" is mentioned as a basic design principle because Globalstar is truly a system where the whole is greater than the sum of its parts. For example, the rake receiver developed to handle multipath in terrestrial CDMA is utilized at no extra "cost" in Globalstar to implement simultaneous links to the user through multiple satellites. This significantly improves link reliability. Another example is that the multibeam antenna, developed by SS/L for other applications, not only provides increased antenna gain, but it also significantly increases system capacity by allowing 16X frequency reuse by each satellite.

"Maximize spectral efficiency" is vital because RF spectrum is a limited resource. It is expected that demand for LEO satellite communications will quickly exceed capacity, and the limitation on capacity boils down to the number of calls that can fit into the assigned spectrum. The CDMA modulation approach with power control provides the highest efficiency possible, offering *and demonstrating* ten to twenty times the capacity of conventional FDMA systems. The frequency reuse provided by the multibeam satellite antenna (mentioned above) further increases the spectral efficiency. In addition, Qualcomm's design utilizes a highly efficient vocoder to minimize the spectrum required for each conversation.

"Utilize existing infrastructure" is an important decision that was made early in the program. The world already has in place a very efficient, very redundant terrestrial communication infrastructure. There is no need add cost, complexity, or risk to the system in order to duplicate an infrastructure that already exists. The single function of Globalstar is to enable anyone, anywhere, to link into that existing infrastructure. In addition, sticking with existing service providers permits utilizing existing customer service and billing procedures.

Now let's look at how all of these principles are implemented in the Globalstar system.

3. Space Segment

The Space Segment is comprised of 48 Low Earth Orbit (LEO) satellites. The satellites are organized in a 48/8/1 Walker constellation (8 satellite planes with 6 satellites per plane), with 1414 km altitude and 52 degrees inclination. Orbital period is 114 minutes. The Walker constellation simplifies orbital control and concentrates the satellite density over the more highly populated temperate zones. The altitude is chosen to be below the Van Allen Belt, above the "debris" belt, low enough to minimize space loss and transit delay, and high enough to permit broad (5760 km) beam coverage and thus reduce the number of satellites required. The orbital inclination is chosen to provide 100% coverage from 70 degrees south to 70 degrees north (and intermittent coverage as far as 80 degrees north and south).

The straightforward "bent pipe" approach allows a relatively simple, modest sized, economical satellite. The satellite measures 1.78x0.96x0.58 meters and launch mass is 390 kg. The envelope shape allows "packing" satellites so that 8 or more can be orbited on a single commercial launch vehicle. Alternately, one to three satellites can be launched by the emerging class of smaller launch vehicles.

Fortuitously, it turns out that the satellite size and altitude, when chosen to meet the criteria above, are just about perfectly matched to the physical antenna design realities. The satellite is just large enough to support antenna geometries which can provide the required ground coverage from the desired altitude.

Globalstar's operational altitude is sufficiently high that no compensation for atmospheric drag is required. Further, the overlap of individual satellite coverage patterns allows relatively relaxed orbit control requirement. As a result, orbit control requirements are modest, allowing use of the simple, economical and highly reliable hydrazine monopropellant propulsion system, with significantly fewer parts than bipropellant systems.

The satellite bus uses technologies that are well developed for communications satellites. The silicon solar cell array continuously points toward the sun to provide maximum electrical power for the number of cells.

Nickel-hydrogen battery cells, used on all SS/L communications satellites for more than a decade, provide electric power storage for use during solar eclipse and during peak power periods. All satellite components are designed to support an on-orbit longevity of 7.5 years.

Global Positioning System (GPS) receivers on the satellite are used to provide position and attitude control. This greatly simplifies orbit maintenance, and also furnishes a timing and frequency reference for the satellite payload.

The satellite receives user signals at L-band (1610 - 1626.5 MHz). It amplifies the signal, converts it to C-band, and relays it to a gateway. This is called the reverse link. The signal from the gateway, also in C-band, is received by the satellite, amplified, converted to S-band (2483.5 - 2500 MHz), and transmitted to the user. This is called the forward link. The allocated bandwidth is divided into thirteen 1.25 MHz channels.

The L- and S- band antennas use a sophisticated phased array design to divide the user coverage into 16 beams that collectively fill the 5760 km diameter circle on the Earth visible to an individual satellite. The beams form a honeycomb pattern with one beam in the center, surrounded by a circle of six beams, which are in turn surrounded by a circle of 9 beams. The antenna gain is shaped to be isoflux. That is, the antenna gain increases toward the outside of the circle to compensate for the increased range, thus providing constant power throughout the operating region.

The multibeam antenna design serves two critical functions. First, the individual beams provide higher gain than a single antenna spanning the entire coverage. Second, the entire L- and S-band frequency band allocated to Globalstar is used in each of the 16 beams. Since spectrum is "scarce," this re-use significantly increases system capacity.

The gateway links, in C-band, operate through satellite antennas that use a single beam to cover the 5760 km satellite coverage "footprint." The frequency spectrum from each of the beams is combined using FDMA into a single broad spectrum. Half of them are transmitted Right Hand Circularly Polarized (RHCP) and the other half Left Hand Circularly Polarized (LHCP), which reduces the total required bandwidth by half.

4. Ground Segment

4.1 Introduction

The Globalstar Gateway is owned and operated by the local Service Provider. It is similar to a CDMA cellular base station except that it links to the orbiting satellites and uses them as virtual "base stations in the sky." The gateways are linked through a dedicated digital network to the Ground Operations Control Center (GOCC). The GOCC allocates satellite capacity between gateways and collects operational and billing information. Some of the gateways incorporate equipment to send and receive satellite command telemetry data over separate C-band carriers. This data is relayed to the Satellite Operations Control Center (SOCC). The SOCC monitors and controls all satellite operations. Both the GOCC and the SOCC have geographically separated backup units .

The gateway is comprised of the RF section, the CDMA controller, and the switch.

4.2 Gateway RF Section

The RF portion normally incorporates four tracking antennas for the C-band satellite uplink and downlink. Four antennas are used because the satellite constellation is chosen so that three satellites are normally in view at a time. One antenna tracks each in-view satellite, while the fourth antenna is slewing to acquire the next satellite. Fewer antennas can be used when the service area is limited or at latitudes where only two satellites are normally in view at a time.

4.3 CDMA Controller

The CDMA controller discussion will be subdivided to discuss a number of important system design features. These include:

1. CDMA technology,
2. Frequency reuse
3. Power Control
4. Vocoder design
5. Multiple links to user terminals
6. Soft hand-off
7. Multipath performance

4.3.1 CDMA Technology

Qualcomm's CDMA technology is already developed, field tested, and codified in the U.S. EIA/71A IS-95 CDMA standard. The purpose of this discussion is only to examine certain aspects of that technology which are especially germane to the Globalstar system.

4.3.2 Frequency Reuse

CDMA achieves more effective frequency reuse than other techniques by its tolerance to co-channel interference.

In FDMA and TDMA systems, frequency reuse is limited by the necessity to attain an adequate Carrier-to-Interference (C/I) ratio. In a multibeam satellite system using TDMA or FDMA techniques, a major source of interference is signals from the adjacent beam(s). This interference essentially prevents frequency reuse within adjacent beams. It also imposes tight requirements on beam isolation between adjacent beams. A typical beam isolation required for FDMA or TDMA would be 18 dB or more. For example, in cellular systems, a frequency reuse of about one in seven is required for adequate performance. This means that a frequency used in a given call will not be reused in any neighbor cell, or in that of any neighbor's neighbor.

In CDMA, a large number of signals are co-channel users of a wide bandwidth frequency channel. Each signal generates noise in the receivers of the other signals. The C/I is determined by the ratio of the desired signal to the sum of all the co-channel signals (and thermal noise.). The system is designed so that there are a large number of co-channel signals. In that way, no one interferer dominates the situation. Instead, the average of all the interferer's signal power determines the C/I for each signal. In practice, this means that the spectrum can be reused in every cell (or in every beam), even with beam isolation as low as 2 or 3 dB.

The resulting increase in capacity over a current analog system is 10 to 20 times. Remarkably, because of digital modulation and error correction, this increase in capacity is accompanied by an actual increase in radio link quality.

4.3.3 Power Control

Power control is one of the key elements in the Globalstar system to achieve high spectral efficiency. Through power control, all signals (and interference) arrive at the CDMA receivers at about the same level, and no one interferer dominates the C/I. This is achieved by providing both closed-loop and open-loop dynamic power control for both the gateway stations and the mobile users. In addition, the multibeam antennas on the satellite, as described elsewhere, are designed to compensate for the difference of link losses between the near and far users.

Because the round trip delay in Globalstar exceeds that in terrestrial cellular, the closed loop power control operates with reduced bandwidth. This is acceptable because multipath fluctuations are much less than in terrestrial systems. Shadowing will be the primary cause of fluctuation. As in CDMA cellular, this will be accommodated by open loop power control where the remote increases its power when it detects a drop in received signal strength due to shadowing. Path diversity, described in Section 4.3.5, also acts to mitigate the power control requirements.

4.3.4 Vocoder Design

In a typical full duplex two-way voice conversation, the average duty cycle of each voice is typically only 35% to 40%. With the CDMA system, the transmitted data rate is reduced when there is less speech activity, allowing a corresponding reduction in transmitter power and thus substantially reducing interference to others. Since the level of other-user interference determines capacity, the capacity is increased by a factor or two or more and the energy efficiency is increased by a factor of three. Note that there is no equivalent to these improvements in FDMA or TDMA, where each signal operates in a separate frequency channel or a separete time slot, and reducing power in one channel or slot does not increase capacity in the others.

The vocoder design uses a 20 msec frame interval and produces four different data rates which can vary every 20 msec frame. The terrestrial rates are 9600, 4800, 2400 and 1200 bits per second (actual data transmission is slightly lower because of overhead bits). Preliminary results with an improved vocoder suggest that Globalstar may not require the 9600 bps rate. The average rate required is only 2400 bits per second.

The vocoder rate varies each frame in response to voice activity. When no activity is detected, the rate drops to 1200 bps. This is much superior to simply gating the channel off. Allowing the channel to continue with the low rate allows the background ambiance to be preserved.

The CDMA system automatically reduces transmitter power when lower rate vocoder frames are produced. This reduces average interference to others and allows proportionately higher capacity.

4.3.5 Multiple Links to User Terminals (Path Diversity)

A significant strength of the Globalstar architecture is that a gateway may communicate with a user through several satellites simultaneously. This is possible because of a unique advantage of the CDMA modulation: delayed signals using the same CDMA code can be separately demodulated by the user and combined to yield an improved S/N ratio. This feature is called *diversity*.

Diversity provides a significant improvement in communications reliability. The frequencies used in LEO systems are higher than existing cellular bands and power margins are more limited, so intermittent shadowing by trees, buildings or other objects is more of a problem.

With diversity, one takes advantage of the fact that simultaneous blockage of two or three satellites is much less likely than the probability that a single satellite path will be blocked. The user terminal uses what is called a rake receiver to track up to four signals at once. If a satellite path is blocked, the user terminal simply utilizes the signals from the other satellite(s) in view. Buildings and trees are very opaque at L- and S-band frequencies, so the improvement provided by diversity is much more significant than trying to "burn through" with additional power in the primary link.

As an aside: the rake receiver was actually developed for a different purpose, namely to handle the severe multipath situations that are common in terrestrial applications. In Globalstar, multipath will be uncommon because of the overhead satellite location. Conceptually, what the gateway does is to create "intentional multipath" by intentionally illuminating several satellites. In this manner, the multipath capability already built into CDMA is utilized to provide multi-satellite path diversity.

4.3.6 Soft Hand-off

In a terrestrial cellular system hand-off is somewhat the exception rather than the rule, since it is only required for users in motion who travel over cell boundaries. In an LEO system, however, it is as if the base stations themselves are traveling — at 429 km/minute! Depending on the geometry, this means a beam-to-beam hand-off (the RF equivalent to moving to another cellular base station) takes place every two to four minutes, or even faster when only the edge of a beam sweeps across the user. In normal cellular systems, every beam transition requires a commanded or "hard" switchover to a new frequency assignment, where the user terminal actually drops the only signal and blindly "switches" to the new. This causes data dropouts and sometimes results in lost calls.

This transfer is completely different in a CDMA system. When the gateway begins to "see" the return power from a user terminal coming up in an adjacent beam or cell, it begins transmitting a time-shifted copy of the same signal in the new beam. This causes the rake receiver in the user terminal to automatically perform a seamless or "soft hand-off". The rake receiver progresses from tracking one beam to tracking both the departing and the arriving beams, and then to tracking the new beam only (whereupon the original rake receiver channel automatically begins hunting for the next beam). Exactly the same soft hand-off is performed as the coverage moves from satellite to satellite (in fact, it is this hand-off that is intentionally maintained as long as possible to provide diversity, as described in the previous section). Except for routing details, it makes no difference to the gateway whether the user is shifting between beams or between satellites.

Another strength of the rake receiver approach is that the soft hand-off is semiautonomous This is important when one considers that every user terminal on the system is being handed off every four minutes or less. The gateway, by knowing the receiver location and/or by monitoring its return signal power picked up by adjacent beams, simply begins to transmit and monitor on the "approaching" beam in advance of the switchover. The rake receiver in the user terminal will autonomously begin to utilize both beams during the transition, and then automatically completes the changeover (and begins looking for the next beam) as the old beam moves out of range. This greatly reduces the load on the gateway.

4.3.7 Multipath Performance

This discussion is almost anticlimactic. In terrestrial cellular, multipath is a significant problem. In a CDMA system, the rake receiver actually *exploits* the multipath signal rather than being harmed by it.

In a satellite system, multipath is less of a problem but, should it occur, the rake receiver provides the same advantage. The point that has been made earlier, though, is that the ability of the rake receiver to exploit multipath is utilized in the Globalstar system, almost without modification, to provide soft hand-off between beams and satellites and to provide diversity of signal paths to the user terminal through multiple satellites.

5. User Terminals

There are three basic types of user terminals for the Globalstar system.

1. Fixed user terminals for residential and rural locations.
2. Portable units for mobile access to the Globalstar system.
3. Portable dual-mode units for mobile access to both a terrestrial cellular system and the Globalstar system.

The **fixed user terminals** incorporate a small fixed antenna and a nominal three watt PA to provide robust communication capability. They are similar in operation to a terrestrial cellular telephone, but they incorporate a microprocessor and software to handle Globalstar-unique functions such as satellite orbit data.

The **portable unit** will be only slightly larger than a conventional cellular telephone. A sophisticated antenna design has been developed to provide coverage from

horizon to horizon (with some overage to allow for head movement). The antenna projects slightly above the user's head to avoid blockage. Initial measurements suggest that the antenna can provide 1 to 1.5 dB of gain, which represents good performance given the coverage required and the design constraints. Output power will average in the milliwatts, with a peak power capability of 600 mw. Battery life will exceed 2 hours talk and 15 hours standby. Like the fixed terminal, the portable unit incorporates a microprocessor and software for Globalstar-unique functions, including a local earth model for use in position location)

The **dual-mode portable terminal** is essentially a portable Globalstar terminal added to a standard terrestrial cellular phone. Components will be combined between the two systems whenever possible. Performance of the Globalstar portion will be the same as the single-mode portable.

The philosophy of the dual-mode unit is that the Globalstar mode will "look and feel" very similar to the local terrestrial cellular operation. When roaming in territories served by other cellular standards, the user's home territory "look and feel" will be preserved as much as can be supported by the local network capability. In most locations, it is anticipated that the full capabilities of the home performance will be preserved. Considerable work is going on to maximize compatibility in this area.

Provision for a Subscriber Identification Module (SIM card) will be incorporated in the phone design, so a user can "roam" from phone to phone. At this time it is not certain whether a worldwide standard will evolve for such a card, or whether Globalstar will have to either select a particular standard or develop its own. Fortunately, the Globalstar consortium includes many key service providers throughout the world, so there is opportunity for considerable input and advice on the matter.

Note that all terminals have the capability to handle both voice and data (nominally to 9600 baud). Design of the portable units will include a "car kit" incorporating a power amplifier and an outside antenna.

7. Conclusion

Globalstar is a practical, realizable system that makes synergistic use of some powerful, but *proven* new technologies to yield a communications system well suited for the 21st century.

Appendix

Overall responsibility for the Globalstar system development rests with Loral Qualcomm Partnership L.P. Loral Corporation is the General Partner. Strategic Partners and investors include AirTouch Communications (USA), Alcatel and France Telecom (TESAM) (France), Alenia Spazio (Italy), Dacom (South Korea), Deutsche Aerospace (Germany), Hyundai (South Korea), Loral Corporation (USA), Qualcomm Inc. (USA), Space Systems/Loral (USA plus overseas partners), and Vodafone (Great Britain).

Primary hardware subcontracts are to Space Systems/Loral (SS/L) for the space segment and to Qualcomm for the ground segment and user terminals. SS/L in turn has placed significant subcontracts with Loral AeroSys, Alcatel, Alenia, Deutsche Aerospace, and others.

After satellite launch, Globalstar will maintain the space segment, the GOCC and the SOCC. The service providers, which include many of the strategic partners plus other providers who will be added, will own and operate their own gateways.

Acknowledgment

Acknowledgment and thanks are extended to many members of Loral, Globalstar and Qualcomm staff who provided information used to develop this paper. Acknowledgment is also extended to the entire Globalstar team, whose hard work is what has created this program and will make it successful.

Efficient Mobility Management in Intelligent Networks Using Satellite Wide Area Networks

K. M. Sundara Murthy[1]
Advanced Technology & Networks,
VISTAR Telecommunications Inc.
Ottawa, Ontario, Canada K1G 3J4
murthy@vistar.ca

Abstract

Currently proposed intelligent network & advanced intelligent network (IN/AIN) architectures envision using SS7 -based signaling network for exchanging mobility & related information between switches (SSP - MSC) and databases (SCP - HLR & VLR)[2]. In this paper we propose an efficient mobility management network architecture which will (i) reduce mobility management **cost**, (ii) increase network **flexibility,** (iii) increase service **coverage,** and (iv) improve **performance** (delay, differential delay, blocking, etc.). The proposed architecture has two important elements : (1) consider the mobility management network as a functionally separate entity and divide the databases into a two-tier systems, a low-tier system handling more frequent short-range mobility data typical of a metropolitan area, and a high-tier system handling wide area mobility data. (2) use a satellite-based network for the interconnection of DBs, particularly for the high-teir systems. The low-tier DBs can be linked using an appropriate satellite or terrestrial network. The proposed satellite approach is essentially applicable to IN/AIN segments of all types of mobile networks (e.g. GSM, IS-41, UPT, etc.) and is efficient when used in conjunction with (i) a two-tier DB system (also proposed in this paper), (ii) a centralized DB system and (iii) a fully distributed DB system. An example studied for location registration process in IS-41 show that the mobility traffic reduction of better than 4:1 is achievable.

1 Intelligent Networks & Mobility

Providing personal communications systems supporting full mobility require intelligent networks for tracking mobile users and facilitating outgoing and incoming calls over different physical and network environments. In realizing the intelligent network functionalities, databases play a major role. Databases store, update and transfer service and user related information among themselves and with the switches in order to establish, maintain and terminate calls.

Currently proposed network architectures envision using the SS7-based signaling network for linking these DBs and also for interconnecting DBs with switches. Thus, in the present IN/AIN architecture the SS7 forms the communication infrastructure which facilitates the transfer of messages between the databases and switches.

If the IN network has to support ubiquitous, seamless mobile services, then it has to support additionally mobile application parts, viz., mobile origination calls, mobile destination calls, mobile location updates and inter-switch handovers.

These functions will generate significant amount of data and require them to be exchanged between databases (HLR, VLR) and switches (MSCs) very efficiently. Such a transfer of messages should occur between DBs and Switches in order to track and serve the mobile user. As the number of mobile users and their mobility increase, the volume of mobility management traffic increase very rapidly.

In the future, the users (fixed or mobile) may use and communicate with sophisticated CPEs (e.g. multimedia, multipoint & multisession calls) which may require complex signaling functions. This will generate volumness service handling data and require efficient transfer of these messages between databases and switches. Consequently, the network providers would be able to add new services and capabilities to their networks incrementally, quickly and cost-effectively.

1 This paper was prepared under severe time constraints and readers are cautioned of possible discontinuity in text.

2 In IN terminology, a database (DB) is denoted as a service control point (SCP), and a stored program control switch is denoted as service switching point (SSP). When used in mobile network environment (e.g. GSM), the SSP could be a mobile switching center (MSC) and SCP could be either a home location register (HLR) or a visiting location register (VLR).

We propose that the DBs associated with IN which handle mobility management data are divided into two-tiers, viz., low-tier databases (LTDB) and high-tier databases(HTDB). The low-tier databases are destined to serve short-range, high density metropolitan mobile users with largely intra-metro traffic. The DBs are fully interconnected with high speed terrestrial networks (e.g. MAN, W-MAN) having some kind of bandwidth on demand (BOD) capability. The high-tier databases are destined to serve long-range, low density wide area mobile users with largely inter-metro traffic profile. The DBs are fully interconnected with medium/low speed satellite wide area network with bandwidth-on-demand capability and capable of handling broadcast protocols.

2 Mobility Management Network

2.1 User Expectations

The key user expectations from a mobility network services are given below : **(1) Quality**[*]: Users who are used to higher bit rate, higher quality wireline services would expect comparable or better **signal quality** in an end-to-end network in which the signal undergoes multiple conversions while passing through a cascade of vastly different network infrastructures. In addition to signal quality, the **service reliability** after connection is very important especially when the user is subjected to high levels of environmental noises, propagation impariments and mobility, **(2) Delay** [*]: Users may not tolerate unduely large service access delays (from call initiation to call connection), **(3) Blocking** [*]: Call blocking may occur due to a variety of reasons, viz, lack of resources, delays in DB searches, undue delays in signaling networks, unsuccessful hand-overs, etc. Users may not accept higher level of blocking, and **(4) Cost** [*]: A significant level of plant investment is required to develop network infrastructure & intelligence (up to 50% of existing PSTN plant cost ?). In addition, the overheads associated with multiple network operators, basic service providers, value added resellers, etc. will only help increase the overal service cost. The **users** cannot afford and/or accept any significant increase in cost as compared to corresponding wireline services.

The key factors determining the worldwide deployment of mobile/personal communications are : **(1) Cost** : the PCS users will be the most cost consience of all telecom users and therefore, the Standards bodies & network designers should strive to evolve most cost-effective solutions. e.g. (i) minimize database record sizes, (ii) minimize mobility management traffic by simplifying user tracking procedures, (iii) provide low bit rate transport, (iv) increase coverage by hybrid (satellite + terrestrial) networking, (v) define architectures which, if necessary, will allow separate operators to operate different segments of the networks (e.g. access, transport, SS7, DB networks, etc.), etc., **(2) Flexibility** : network should have high level of flexibility to accommodate nonhomogenous growth, full (personal, terminal, etc.) mobility, feature protability over a variety of networks and operators, etc.,and **(3) Performance** : overal network performance (quality of service) including signal quality, service access delays,blocking probability, etc.

[*] Unfortunately, these parameters have the so called "bottle-neck effect". i.e. The overal vaule could be degraded by the worst case value of one process or a segment of the network.

2.2 Classification of DBs

Separate DB Management Network: We propose to develop database management network as an independent entity/layer which will serve a variety of access, transport, signaling networks(AN, TN, SN) and PCS service providers(PSP). While the different network elements may access DBs using SS7 network(protocol), the DBs themselves may be interconnected with other networks having economic infrastructure, flexibile architecture and efficeint protocols. We propose to lassify DBs[3] into 2 Groups: Low-tier & High-tier:

(1) Low-tier DBs (LTDB) : The low-tier databases are destined to serve short-range, high density metropolitan mobile users with largely intra-metro traffic. The DBs are fully interconnected with high speed terrestrial networks (e.g. MAN, W-MAN) having data broadcast & BOD capability

(2) High-tier DBs (HTDB) : The high-tier databases are destined to serve long-range, low density wide area mobile users with largely inter-metro traffic. The DBs are fully interconnected with medium/low speed satellite wide area network (SWAN) having data broadcast & BOD capability. These DBs are

2.3 DB Interconnection Architectures

The DBs (HLR, VLR) can be interconnected in a number of ways and 3 possible architectures are shown in Fig. 1.

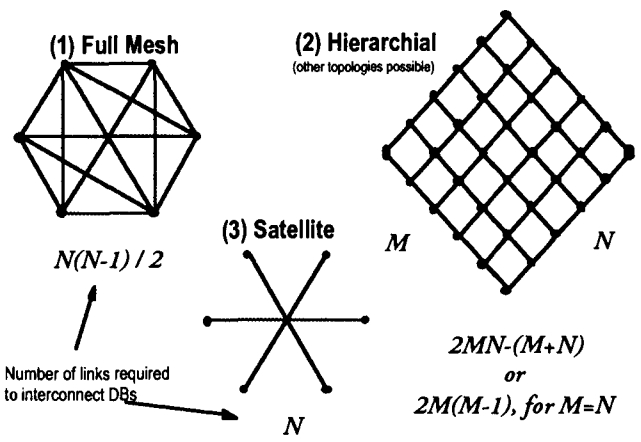

Fig. 1 DB Interconnection Architectures

Cases\1 & 2 are terrestrial-based connectivity and Case 3 is satellite-based.

3 Note that the proposed satellite interconnection is applicable to centralized & fully distributed DBs as well

The number of links required to interconnect all databases as a function of the number of databases for the three case are shown in Fig. 2

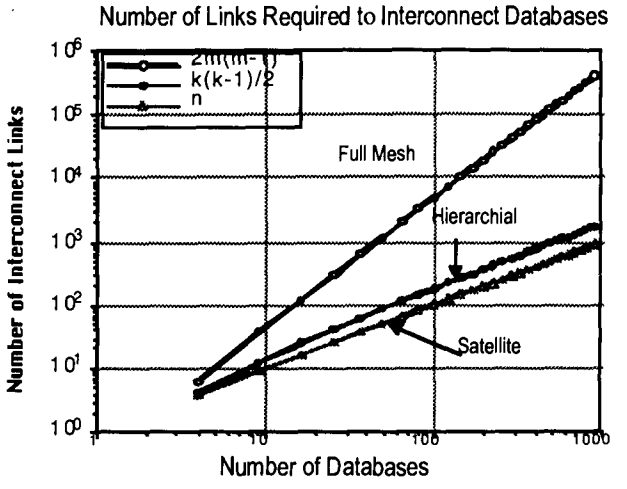

Fig. 2 No. of Links Required to Interconnect All DBs

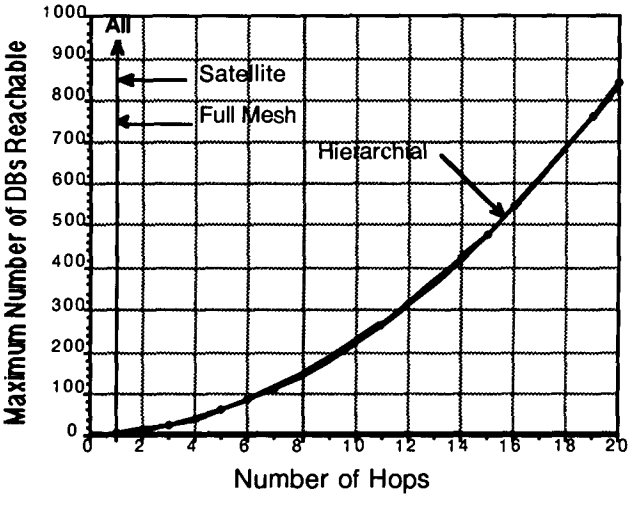

Fig. 3 Max. Number of DBs Accessable Within Specified Hops

In Fig. 3, the maximum number of databases reachable within the specified number of hops is given. In full mesh terrestrial and satellite cases, communications between any two databases can take place within a single hop.

2.4 Proposed Database Interconnection

The GSM & other systems conform to the IN architecture which uses SS7 for communications between and amongst switches and DBs. In our proposed approach the DBs are linked with a satellite wide area network(SWAN), and the link between a switches may still use SS7. In the proposed interconnection Option 1, all the DBs (LTDB & HTDB) are linked via a SWAN (see Fig. 4).

In Option 2, the LTDB are linked using metropolitan area network (MAN) and the HTDB are linked with SWAN as shown in Fig.5. The MAN may use conventional wireline or emerging wireless technologies.

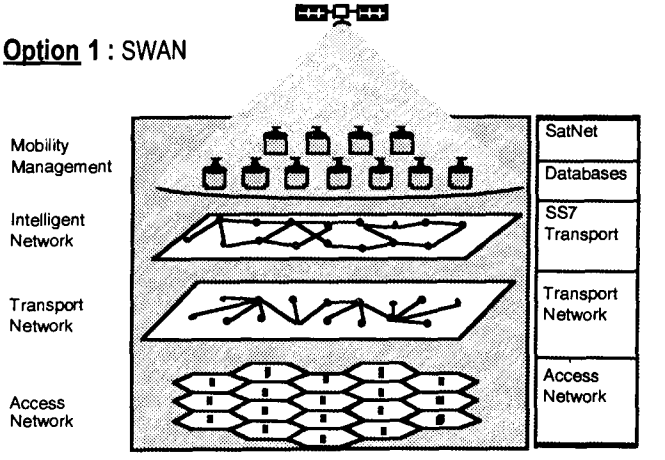

Fig. 4 DB Interconnection via SatNet

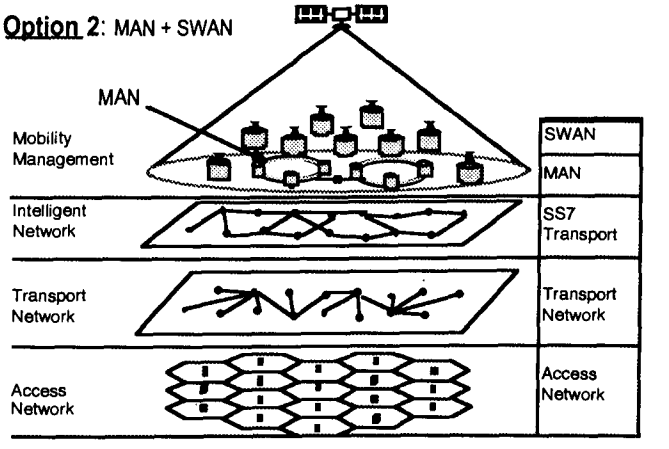

Fig. 5 DB Interconnection via SWAN/MAN

4 Application Case Study (GSM & IS-41)

4.1 Application

The proposed approach is essentially applicable to the intelligent network segment of all types of mobile networks (e.g. GSM, IS-41, UPT, etc.) either with centralized or fully distributed DB management systems. First, we illustrate the four basic GSM procedures which generate SS7 mobile application part (MAP) messages, viz., (i) mobile origination messages (MOM), (ii) mobile termination messages (MTM), (iii) location update messages (LUM), and (iv) inter-MSC handover messages (IHM). Then, for the case of IS-41, we show as how the proposed satellite-based DB interconnection technique could reduce the number of mobility messages to about one quarter of what is required using the most efficient terrestrial-based interconnection

mechanism. The proposed technique is also readily applicable to mobility management elements of GSM as well as other evolving networks such as UPT, etc. The proposed concept is not only an ideal solution for handling mobility management traffic of terrestrial-based systems but also a natural catalyst for the integration of terrestrial and satellite mobile personal communication systems.

4.2 GSM Procedures

Mobile Origination Messages : The protocol sequence and number of messages involved in a mobile origination call are shown in Fig. 6.

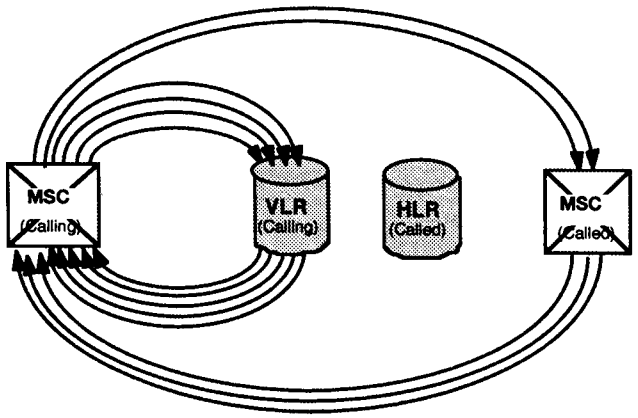

Number of messages	14
Total number of bytes (bits)	670 (5360)
Avg message length-bytes (bits)	48 (383)

Fig 6 Mobile Origination Messages

Mobile Termination Messages : The protocol sequence and number of messages involved in a mobile termination call are shown in Fig. 7.

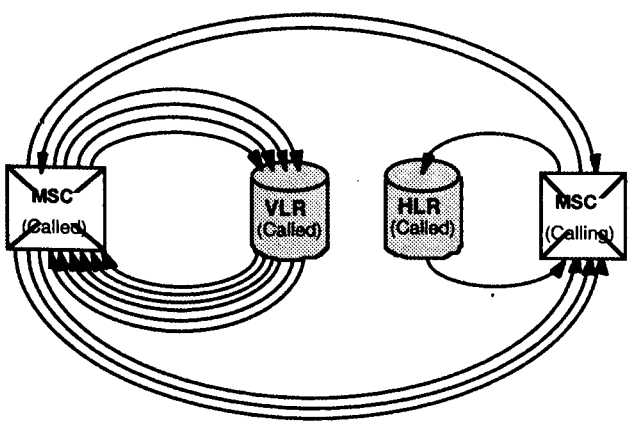

Number of messages	17
Total number of bytes (bits)	858 (6864)
Avg message length-bytes (bits)	50 (404)

Fig. 7 **Mobile Termination Messages**

Location Update (Registration) Messages : The protocol sequence and number of messages involved in a location registration process are shown in Fig. 8.

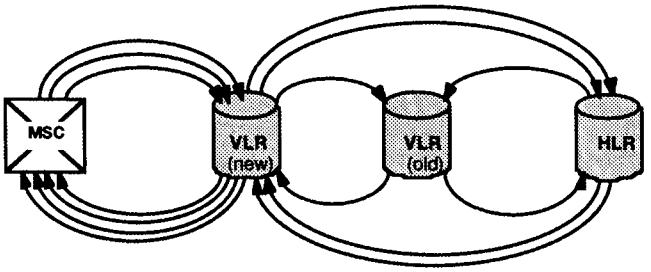

Number of messages	15
Total number of bytes (bits)	1210 (9680)
Avg message length-bytes (bits)	81 (645)

Fig. 8 Location Update (Registration) Messages

Inter-MSC Handover Messages : The protocol sequence and number of messages associated with an inter-MSC handover process are shown in Fig. 9.

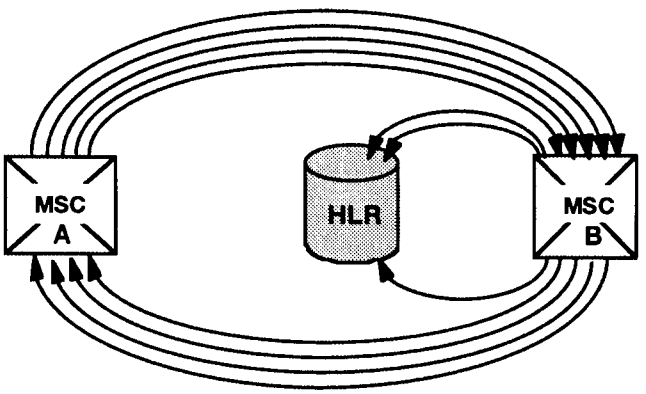

Number of messages	12
Total number of bytes (bits)	531 (4248)
Avg message length-bytes (bits)	44 (354)

Fig 9 Inter-MSC Handover Messages

4.3 Location Registration in IS-41

(a) Terrestrial Approach : We can look at the process of location registration in IS-41 employing the terrestrial approach illustrated in Fig. 10. When a user moves to a new serving area (NSA) from an old serving area (OSA), a sequence of 12 messages need to be exchanged between switches and DBs in order to complete a new location registration process. This is illustrated in Fig. 10. First, a registration request is sent to the new MSC (MSC-n) from the user terminal. The MSC-n generates an authentication request for its (new) VLR-n which is forwarded all the way to the HLR to which the user belongs to. The HLR verifies the user identification and sends back authentication

response to MSC-n via the VLR. The MSC-n then sends registration notification message to the HLR via VLR-n. The HLR then sends a user service profile to the VLR-n. The HLR also sends a registration cancellation message to MSC-o and the associated VLR-o of the so called old serving area (OSA). Thus, the location registration of a user in a NSA & the cancellation of the user's registration from an OSA require 12 messages communicated through SS7 signaling network.

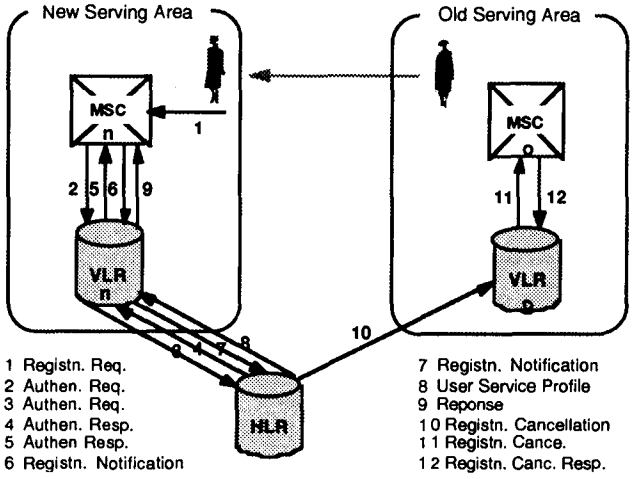

Fig 10 Location Registration in IS-41 : Terrestrial Approach

In the 12-message protocol sequence described above, three important events take palce: (i) MSC-n sends an authentication request to HLR, (ii) HLR sends authentication response & user service profile to MSC-n, and (iii) the HLR sends a registration cancellation to MSC-o. In the following, we describe how this 12-message process can be accomplished in using no more than 2 messages.

(b) Proposed SWAN Approach : In our proposed approach, the above mentioed 3 important events could be effected using only two messages as opposed to 12 for the case of terrestrial network described above.. As shown in Fig. 11, the MSC-n sends an authentication request which is received by all the network elements involved, viz., MSC-o, MSC-n, VLR-o, VLR-n, and HLR. While HLR is preparing for a response, others are advised of a registration transfer process underway. Once ready, the HLR sends a message which contains authentication response & user service profile. This message is received by all and enables MSC-n & VLR-n to complete registration process & at the same time helps MSC-o & VLR-o to complete registration cancellation process.

Thus the proposed approach reduces the 12 location registration messages into just 2 and the associated cost. In addition to cost the SWAN approach reduces the differential delay and associated blocking as well. It can be shown that the proposed approach brings about similar drastic reduction in message sequence in all types of mobility management processes. There are other advantages to the proposed approach, e.g. even the unregistered users could be paged & located nationally with the help of a single paging message.

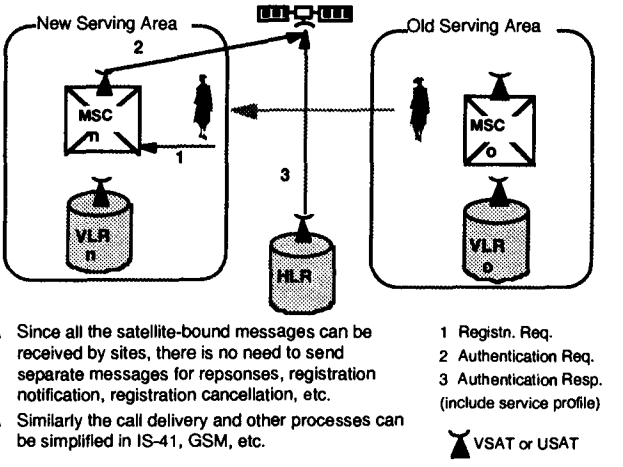

Fig 11 Location Registration in IS-41 : Using SWAN Approach

5 Advantages of Proposed Approach

Comparison of DB Management Techniques : The following table presents the relative merits of the of the (i) centralized, (ii) distributed, and (iii) proposed two-tier systems.

Table 1 Comparison of Database Management Techniques

Description	Centralized	Fully Distributed	Proposed Two-Tier
No. of DBs / network	one	many	many
DBs size (memory)	large	medium/ small	medium/ small
DBs processor size	large	small	small
DBs SW devlp cost	high	medium	medium
Total DBs cost	medium	high	medium
Interconnect cost	medium	high	low
Queuing delay at db	high	medium	low
Records search time	high	medium	low
Impact of differential delay	low	high	medium
Record duplication	low	high	medium
Paging cost/delay	N/A	high	low
Overal flexibility	low	high	high
Disaster recovery	slow	fast	fast
Overal reliability	low	high	high

Advantages of Satcom Network: The proposed two-tier DB management systems has several advantages over the others as mentioned in the table above. Further, these advantages are enhanced several fold by using a satellite-based wide area network to interconnect the high-tier gateway DBs. Several inherent strenghts of satellite

networks can be exploited in this application. Some of these include: (i) single network can handle singlecast, multicast, broadcast packets, (ii) can support all topologies in a single network if necessary, (iii) supports a wide range of bandwidths from a few bits per second to a few megabits per second, (iv) bandwidth on demand capability is available to meet instantaneous requirements, (v) wide area coverage, (vi) efficient centralized resource utilization (analogous to multiple queue single server case), (vii) uniform delay (min. differential delay), and (viii) fastest nationwide network deployment.

Benefits : If the satellite network is used in conjunction with the proposed two-tier DB interconnection method for the management of mobility & other related information in an IN/AIN network, the resulting benefits are many. Some of these include :

- significant reduction in mobility management traffic,
- reduction in DB record size,
- reduction in call blocking probability,
- reduction in delay (e.g. call setup time,..)
- simplification registration & service access processes
- increase in service coverage area
- decrease in deployment time frame
- highest efficiency in network resource sharing,
- highest flexibility in accommodating future, yet undefined services,
- act as a catalsyt for the evolution and introduction of terrestrial-satellite hybrid network to enable the availability of PCS services "anywhere" in its true sense,
- satellite terminals available from $2000 to $ 20,000 depending on their transmission capability.

Performance

The performance of the proposed technique is studied for different cases including the ones mentioned in this paper. The results may be presented in terms of improvements in number of messages, average message length, blocking probability, delay spread, etc. and compared with terrestrial mobility management systems taking into account a number of delay elements associated with public SS7 packet data network. These performance analyses are to be done using realistic mobility management traffic models. This quantitative performance result is not available at the time of this paper.

6 Conclusions

We have made two important contributions in this paper. **First**, we have proposed to separate the mobility management network (functionally or physically if necessary) entity from the signalling network (SS7) within IN/AIN environment. The DBs themselves can be classified into two type; a low-tier system handling more frequent short-range mobility data, and a high-tier system handling wide area mobility data.

Second, we proposed to use a satellite-based wide area network for the interconnection of DBs, particularly for the high-teir systems. The low-tier DBs can be linked using either wireless, wireline or satellite networks having some form broadcast protocol capability. While the DBs (SCP) could be interconnected using satellite networks, the SS7 network may be used for signaling communications between switches (SSP).

Finally, the proposed satellite network is not only advantageous for the two-tier DB interconnection environment but also equally efficient and applicable to a centralized or a fully distributed DBs interconnections.

Some of the merits of the proposed approach have been illustrated and comapred with conventional terrestrial-based approaches. For example, the proposed satellite approach could reduce the mobility management traffic to about one fourth as compared to the most efficient terrestrial-based system. In addition to the techno-economic benefits, the proposed concept could help the evolution of integrated terrestrial - satellite PCS network which is necessary to extend the service to "anywhere".

7 References

[1] K. S. Meier-Hellstern & E. Alonso, "Signalling System No. 7 Messaging in GSM", Technical Report WINLAB-TR-25, Rutgers University, New Jersey, Dec. 1991

[2] J. M. Duran & J. Visser, "International Standards for Intelligent Networks", IEEE Communications Magzine, February 1992, pp 34-42

[3] D.C.C.Wang, "A Survey of Number Mobility Techniques for PCS", IEEE Intl. Conf. Universal Personal Communications, Ottawa, 1993, pp 340-344

[4] B. Jabbari, etal., "Intelligent Network Concepts in Mobile Communications", IEEE Comm. Magz., Feb. 1992, pp64-69

[5] J. Homa, etal, "Intelligent Network Concepts in Mobile Communications", IEEE Comm. Magz., Feb. 1992, pp64-69

[6] K. M. S. Murthy, "Efficient Mobility Management in IN /AIN by Interconnecting Databases via Satellite", IEEE ITC Mini-Seminar on Mobility & Intelligent Networks, Montebello, Canada, Oct.17-19,1994

[7] S. Mohan & R. Jain, "Two User Location Strategiess for Personal Communications Services", IEEE Personal Communications, 1994, pp 42-50

[8] K. M. S. Murthy, "An Approach to Efficient Mobility Management in Intelligent Networks", IEEE Intelligent Network Workshop Proceedings, Ottawa, 9-11 May 1995

Non-GEO Mobile Satellite Systems: A Risk Assessment

Leah M. Gaffney
404-592-1681
lgaffney@mitre.org

Neal D. Hulkower
617-271-6959
hulkower@mitre.org

Leslie Klein
617-271-6128
lklein@mitre.org

The MITRE Corporation
202 Burlington Road Bedford, MA 01730-1420 USA

ABSRACT

Since 1991, The MITRE Corporation has performed several independent evaluations of proposed mobile satellite service (MSS) systems that would operate from low Earth orbit (LEO) or medium Earth orbit (MEO), also known as intermediate circular orbit (ICO). This paper introduces a top level Risk Taxonomy tailored to summarize the technical and programmatic risks that MITRE has identified. In general, as risks are identified and addressed, a system's technical characteristics, cost and schedule are affected. This paper traces changes in three key parameters – satellite launch mass, system cost, and system schedule – for each of the five original non-GEO MSS systems for which license applications were made to the U.S. Federal Communications Commission (FCC) from November 1990 until June 1991. Finally, specific risk areas are identified using the Risk Taxonomy as a framework for discussion.

INTRODUCTION

As part of its role as a general system engineering and integration organization, MITRE is concerned with early assessment and management of risk. To facilitate this critical activity, MITRE has undertaken the development of a Risk Assessment and Management Program (RAMP™ [1]). This tool collects and organizes "lessons learned" from a wide array of programs. A key feature of RAMP is a Risk Taxonomy, a classification of pertinent technical and programmatic risks. Just as a classic Work Breakdown Structure (WBS) is intended to ensure that the cost and schedule of every element of a system are addressed, a Risk Taxonomy is intended to ensure that every technical and programmatic issue that could adversely affect a system's performance, cost or schedule is considered.

Table 1 presents a high-level Risk Taxonomy tailored to non-GEO MSS systems. At the level presented here, the technical issues generally are the same for any kind of satellite communications system. Most of the elements would also appear in a WBS for a satellite communications system.

The Risk Taxonomy for programmatic issues is markedly different from a classic WBS for a non-GEO MSS system. Many of the elements are intangibles, which are not explicitly resourced. These could have a greater impact on a system's cost, schedule and viability in the marketplace than the elements appearing under technical issues.

Table 1. Risk Taxonomy

Technical Issues (inexhaustive)

- System engineering, including "ilities," system specifications and performance, interfaces (e.g. space-to-ground)
- Space segment, including software development, hardware design, development and production, integration and test, launch availability and reliability, operating environment, operations
- Ground segment, including software develop ment, hardware design, development, production or acquisition, operations
- External interfaces, including connections to public switched telephone network (PSTN), public land mobile network (PLMN), and private networks

Programmatic Issues (inexhaustive)

- Cost
- Schedule
- Regulatory issues, including worldwide spectrum allocation and assignment, export control laws, launch vehicle agreements
- Legal issues, including patent claims, product liabiity
- Attractiveness to investors and financing
- Contracting
- Program management
- Risk management
- Market issues, including pricing and packaging of services and user terminals, rate of penetration, competition

[1] RAMP is a trademark of The MITRE Corporation.

Evolution of Proposed Systems

Figures 1 through 3 compare the proposers' estimates of three significant parameters of their systems at three points in time. The first two dates shown correspond to the original release dates of MITRE's two studies for the European Space Agency [1, 2, 3]. The values plotted here are those in the MITRE reports and were taken from various open sources, including FCC filings and amendments, and literature from the proposers. Note that Constellation was not included in the February 1994 report. The latest estimates were taken from the most recent amended FCC filings.

Figure 1 illustrates the evolution of satellite launch mass, an important parameter to track since any growth is likely to increase the development and production cost, and could increase launch cost. It is not uncommon for systems that experience significant mass growth to be delivered late, as well. After the initial filing with the FCC, each of the proposers reexamined the availability of its system and decided to increase the number and gain of spot beams. Such changes resulted in a more massive communications payload, which in turn requires a more massive bus to support it. On the positive side, a higher grade of service can be expected.

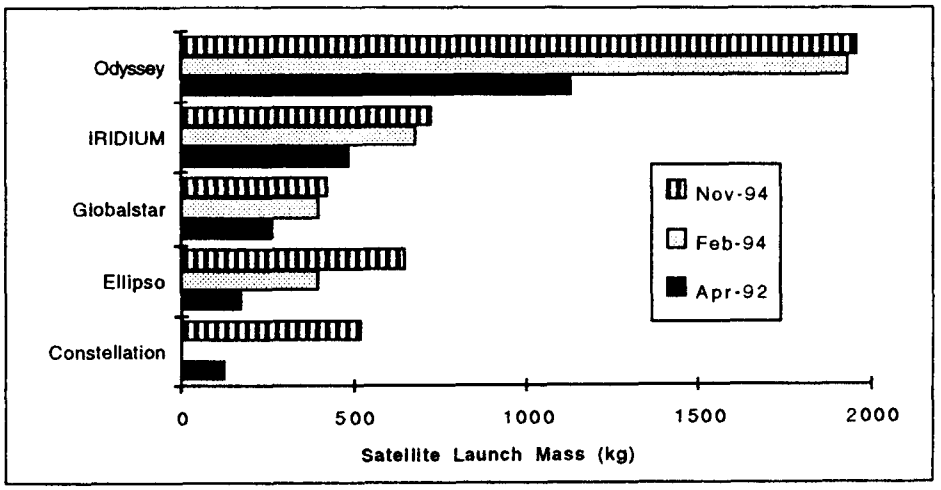

Figure 1. Satellite Launch Mass Evolution

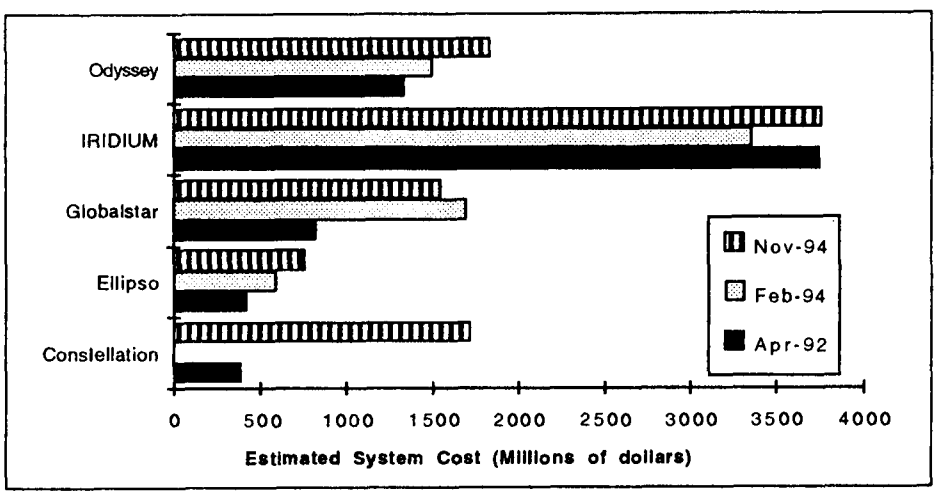

Figure 2. System Cost Evolution

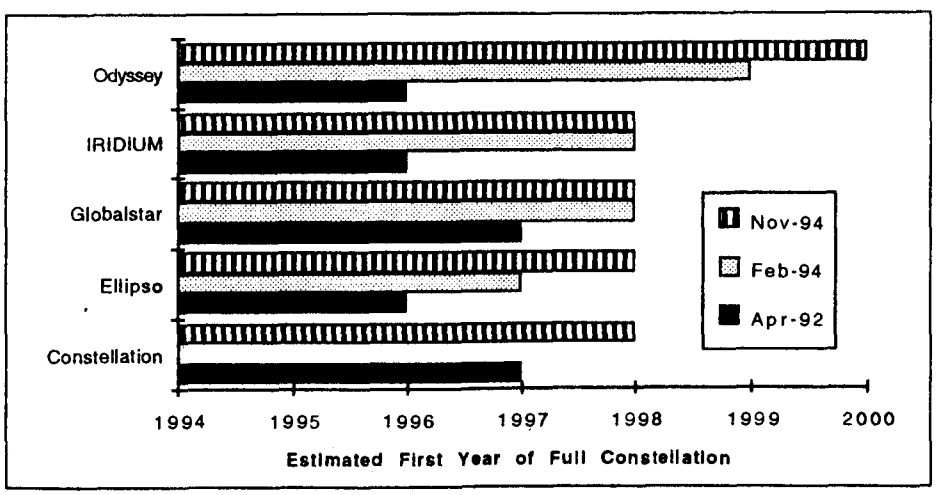

Figure 3. System Schedule Evolution

System cost is a critical programmatic issue affecting profitability and attractiveness to investors. Each of the proposers includes different elements within the estimates shown in Figure 2; therefore the reader is cautioned not to make comparisons across the systems without examining the proposers' detailed breakouts (provided in References 1 and 3). For all systems, the major cost elements are covered; all the estimates include the cost of designing, developing, producing and launching the satellites, as well as some amount for the ground segment. Other costs, such as operations for one or two years, are also included. These costs are presented in then or real year dollars. With the exception of Ellipso™ [2], for which the most recent estimate includes for the first time $200 million for the ground segment, one can assume that the cost elements included for each system remain the same.

Date of entry into the market is taken as the date the entire constellation is on orbit. This parameter affects system cost, attractiveness to investors and market penetration. Many of the schedule estimates shown in Figure 3 had to be computed from the proposers' schedules given in terms of months after FCC licensing. We computed the April 1992 dates for Constellation, Ellipso and Globalstar using an anticipated FCC licensing date of April 1993 (the date projected by Globalstar in its original filing). Otherwise, we used the proposers' dates. Schedule slippage illustrated in Figure 3 can be attributed largely to licensing delays which caused hesitation on the part of the proposers and potential investors.

Technical and Programmatic Issues

Using the Risk Taxonomy, the discussion that follows highlights several significant risk areas MITRE has identified during its independent evaluations. Not all of these apply to each system, but many do. The interested reader is referred to the MITRE reports for more detailed discussion. Summary comments follow.

System Engineering

Interference Control: It is not clear that procedures exist so that multiple systems can be coordinated to operate with acceptably low levels of inter-system interference. In addition, there is the question of interference from the earth stations of one system into the satellites of another system.

Improvement of Forward Error Correcting (FEC) Codes: The development of improved FEC codes would have a beneficial impact on link performance and availability, since these codes would enhance performance in the presence of fading or blockage, especially when combined with channel interleaving to randomize correlated errors. The proposed designs use convolutional codes and Viterbi decoding; they perform well and are inexpensive to implement. Improved codes optimized for the satellite-to-user terminal channel would enhance performance, but do not inhibit development of the current systems.

Speech Encoding Technology: The development of improved speech encoding algorithms is an important system driver. Speech quality is important because it affects user acceptance. From the system viewpoint, it is important to provide acceptable speech quality at the lowest possible bit rate and at relatively high bit error rates because these rates affect required link performance, and system capacity and availability.

Space Segment

Satellite Producibility: This is a manufacturing challenge for the three LEO systems, Constellation, Globalstar, and IRIDIUM™/SM [3], because of the large numbers of satellites required. Meeting published schedule milestones requires a serial production of satellites at rates never attempted before. This is a formidable manufacturing challenge. In addition, there is a risk that the manufacturing facilities may be underutilized after the initial deployments.

Spacecraft Antennas: The development of efficient spacecraft L-band and S-band multibeam antennas is a technological challenge. In order to operate with handheld terminals, large, complex antennas are required. The system proposers are considering different design approaches, including microstrip arrays and multiple-feed parabolic reflectors. In general, the antenna constitutes a major weight and cost driver for the spacecraft, and this aspect of the satellite has received considerable attention from the proposers. A second challenging aspect of the satellite antenna is that of pattern control, in particular control of the sidelobes and pattern rolloff. These are important in determining the level of beam-to-beam interference, which affects the frequency reuse capability and thus the capacity of the system. These antenna parameters are also of importance in complying with International Telecommunications Union-Radiocommunications (ITU-R) flux density limits.

On-Board Processing and Intersatellite Links: This issue affects only the IRIDIUM system. Although the on-board processing included in the design is of the simple

[2] Ellipso is a trademark of Mobile Communications Holdings, Inc.

[3] IRIDIUM is a trademark/service mark of Iridium, Inc.

demodulation/remodulation type, this has not been attempted before in commercial satellites and is only now being flown for the first time on NASA's Advanced Communications Technology Satellite (ACTS). Also new to this design, at least in a commercial application, is the use of Ka-band intersatellite links, requiring tracking antennas for communication with satellites in the adjacent orbits.

Operation in Radiation Belts: This problem primarily affects the two MEO systems, Odyssey™ [4] and Ellipso, although it could also affect Constellation, which would use a very high LEO. The satellites must be designed to withstand the large radiation dose of the Van Allen belts. This increases solar array size and forces the use of more expensive GaAs technology for solar cells in order to meet end-of-life power requirements, and requires shielding of the electronics or the design of radiation hardened components. There is clearly an impact on satellite size, mass and cost.

Ground Segment

Earth Station Technology: It appears to MITRE that the complexity of the earth stations has been generally underestimated by the proposers. This complexity involves the tracking, handoff and signal integrity for the multiple satellite constellations, and also involves the question of baseband interfaces and general access to the PSTNs with which these systems will operate. Experience with stations used with GEO satellites that provide some of the same services as the proposed systems indicates that these stations are quite complex and expensive. There is considerable general purpose software available for operation of networks connected to the public switched telephone environment, and generally for the telephony aspects of the system operation. The system proposers are planning on using as much of this commercially available software as possible; however, it is difficult to avoid the conclusion that the cost and complexity of these stations have been underestimated by the proposers. Furthermore, the maintenance of worldwide databases and the sharing of information among these databases is a problem that all proposers have recognized. However, details of procedures to identify terminals and their locations, verify credit, and so forth, have not been presented. These aspects also constitute a risk area with cost and schedule implications.

The other aspect referred to, namely the general requirements for tracking, handoff from satellite to satellite, and antenna to antenna, is straightforward in principle, but could be time-consuming and expensive to implement, so that the required system reliability is achieved. This aspect of the earth stations is more complex for those systems that have chosen Ka-band for the feeder link frequencies. Additional diversity antennas must be supplied in order to combat rain fading, and while this is also straightforward, there is little operational experience with such systems at Ka-band; most commercial experience with earth-station diversity operation has been at Ku-band.

Hand-held Terminal Antenna: A number of antenna types have been considered, including quadrifilar-wound helices, microstrip patches, and monopoles. Combinations of these and other elements have also been considered. The antenna gain and pattern are of concern because the patterns of most elements on a handset are difficult to control and stabilize. For a microstrip element or a monopole, or for unbalanced elements generally, a ground plane is necessary to stabilize the pattern, and it is not possible to provide this with a handset. Even a balanced helical element will excite currents on the unit when in proximity to the user, and this will alter the pattern and gain, although to a lesser extent than with some other element types. For inexpensive hand-held terminals, it is clear that only the simplest antennas are practical. System proposers and manufacturers have recognized this and have selected helices and monopoles, predominantly. Thus, the system must provide sufficient margin to achieve the target capacity and availability, taking into account the variability of practical antenna patterns of hand-held terminals. This margin adds power, mass, and cost risks.

Cost and Schedule

In its analyses, MITRE has found that some of the cost and schedule estimates for the satellites are optimistic. While MITRE recognizes that nontraditional methods are planned for building the satellites, such methods have not been demonstrated, and thus, cost overruns and schedule slippages remain possible. Schedule slippages were recently demonstrated with the much simpler, store-and-forward ORBCOMM system. An approximate one-year delay was experienced in the deployment of the first two ORBCOMM satellites, and subsequent delays are expected due to satellite malfunctioning problems.

Regulatory Issues

All of the proposed systems are seeking to provide service to the populated regions of the earth. To do so, they must obtain licenses to operate their systems on a country-by-country basis. In some countries, the user terminals will also require licensing. Spectrum must be

[4] Odyssey is a trademark of TRW, Inc.

allocated and assigned for feeder links as well. In some frequency bands (such as C-band, which two of the proposers have selected for their feeder links) the spectrum available is limited because of current allocations in the band for the fixed satellite service. While Globalstar, IRIDIUM and Odyssey have received licenses in the U.S., Constellation and Ellipso have not yet been licensed. The latter two systems have until January 1996 to demonstrate financial ability to field their respective systems. To the best of our knowledge, none of the proposers has received licenses elsewhere, although some can be expected soon. Regulatory delay has already pushed schedules out and unresolved issues remain.

Attractiveness to Investors and Financing

To date, none of the five proposed systems has raised more than about 45 percent of its estimated system cost, although two have attained their goals for equity funding. IRIDIUM has stated that it has completed its equity funding and will use debt financing for the remainder of its budget. Globalstar has raised nearly $0.5 billion in equity and plans to raise additional funding through debenture sales, vendor financing and prepaid franchise fees. Odyssey has under $200 million in equity funding from TRW and Teleglobe. The other two systems have not released details of their financing plans.

Market Issues

In its April 1992 report [2], MITRE explored the characteristics of an economically viable MSS system. We learned from the terrestrial cellular experience that to attract a large initial subscriber base, the cost of the handset must be set low. To retain this base, the cost of service cannot grow too high. We expect the market for MSS to behave similarly. Our analyses indicate that rapid market penetration will require an initial hand-held terminal price that is less than $1500 and a service price that is less than $1.50 per minute.

Non-GEO MSS systems face competition from a variety of sources, including terrestrial cellular and personal communications services (PCS) networks, little LEOs, and regional GEOs already in place. Two advantages of non-GEO MSS systems will be service to hand-held terminals (not yet available from GEO) and shorter propagation delay than from GEO. These advantages will ensure some market for the early entrants, but competition will already be in place for other services. While terrestrial cellular service will never be ubiquitous, it will cover increasing portions of the most highly populated regions. Since the hand-held terminals will operate in dual mode, first seeking a terrestrial cellular link, one can expect the spread of terrestrial cells to diminish the use of the satellite link. MSS to mobile and transportable terminals of briefcase or laptop computer size is already available from GEO satellites in some regions and will be available in North America later this year. A GEO MSS system capable of servicing hand-held terminals is being planned for Asia and the Pacific Rim. Many data services to be offered by the non-GEO MSS systems will already be offered by regional GEO satellites and by little LEOs like ORBCOMM. The latter will provide store-and-forward messaging to hand-held terminals at a low cost as early as this year.

Conclusions

Each system has undergone major changes since the initial filings with the FCC. While each of the proposed systems faces technical challenges, none appears insurmountable. Some have already experienced cost growth and schedule slip. The most critical risks are optimistic cost and schedule estimates, lack of full financing, interference control that could affect quality of service, earth station complexity and cost, and competition.

References

1. **Ciesluk, W. J., Jr., et al.,** *Survey of the Mobile Satellite Communications Industry,* MTR92B0000059, The MITRE Corporation, Bedford, MA, April 1992.

2. **Ciesluk, W. J., Jr., et al.,** *An Evaluation of Selected Mobile Satellite Communications Systems and Their Environment,* MTR-92B0000060, The MITRE Corporation, Bedford, MA, April 1992.

3. **Gaffney, L. M., et al.,** *A Reevaluation of Selected Mobile Satellite Communications Systems: Ellipso, Globalstar, IRIDIUM, and Odyssey,* MTR-93B0000157, The MITRE Corporation, Bedford, MA, February 1994.

Author Index

Author Index con't.

IMSC '95

INTERNATIONAL MOBILE SATELLITE CONFERENCE 1995

JUNE 6-8, 1995
OTTAWA, CANADA

JPL 95-12
CRC-CP-95-001